INFLUENCE OF REDOX PROCESSES ON COPPER (II) EXTRACTION BY DTPA

V.I. Kuz'min, O.A. Logutenko* and A.I. Kholkin**

Institute of Chemistry and Chemical Technology SB RAS, Krasnoyarsk, Russia
***Instutute of Solid State Chemistry and Mechanochemistry SB RAS, Novosibirsk, Russia**
****** Institute of General and Inorganic Chemistry RAS, Moscow, Russia**

The influence of redox and semi-association processes in the organic phase on copper (II) extraction by di(2-ethylhexyl)dithiophosphoric acid (DTPA) has been investigated. It was shown that the copper(II) di(2-ethylhexyl)dithiophosphate (CuA_2) which is formed in the extraction decomposes to copper(I) di(2-ethylhexyl)dithiophosphate (CuA) and the disulfide (A_2)- $(RO)_2PSSP(OR)_2$. CuA is polymerized with the formation of various linear and cyclic polymers. All constants of the redox and self-association reactions of the copper compounds have been calculated using the electronic, EPR spectra and isopiestic methods.

INTRODUCTION

Sulphur-containing acidic extractants are of considerable interest for the recovery of nonferrous metals because of their high selectivity, particularly over the alkaline earth metals and manganese. However processes using these extractants are complicated by the redox reactions that take place in the organic phase [1-4], These lead to changes in the kinetic and thermodynamic parameters of the extraction and can cause irreversible decomposition of the extractant.

Earlier it was shown [5], from consideration of the forward and back redox reactions in the extraction of copper by di(2-ethylhexyl)dithiophosphoric acid, that the copper(II) di(2-ethylhexyl)dithiophosphate (CuA_2) which is formed in the extraction, decomposes to copper(I) di(2-ethylhexyl)dithiophosphate (CuA) and the disulfide (A_2)- $(RO)_2PSSP(OR)_2$ by the reaction (1):

$$2CuA_2 \overset{Kred/ox}{\rightarrow} 2CuA + A_2 \qquad (1)$$

The formation of a tetramer, reaction (2), was established by an isopiestic method:

$$4CuA \sim (CuA)_4 \qquad (2)$$

At the same time, as further research work has shown, these processes do not provide a full description of the extraction reaction.

RESULTS AND DISCUSSION

The transformation of DTPA into a disulphide in the reaction with copper (II) is easy to prove taking into account the reversibility of this process in organic solutions. It has been shown that, after fast saturation of the DTPA solution in toluene with copper (II), the optical density of the extract gradually reduces over time to a constant value. On the other hand, on mixing a stoichiometric amount of colourless copper(I) di(2-ethylhexyl)dithiophosphate with a disulphide, re-formation of copper(II) di(2-ethylhexyl)dithiophosphate, accompanying by an increase in the optical density of the organic solution, is observed.

For equation (1), in the absence of additional interactions in the organic phase, the maximum of the copper (II) concentration on an isomolar curve should correspond to a ratio of CuA: A_2 = 2:1. In practice this ratio was found to be approximately equal to 2:3.

Various possible processes involving the interaction of the components which could explain this result are considered. It is shown that the shift in the maximum is caused by a high degree of self-association of the copper(I) di(2-ethylhexyl)dithiophosphate.

The self association of CuA is a unique property of this system. It was shown that, beginning from a certain level of CuA concentration (above 0,05-0,1 M), the equilibrium position of reaction (1) becomes practically independent of the total analytical concentration of copper (I) in the solution. At the same time, the influence of the second component of the reaction, the disulphide, corresponds to reaction (1) over a wide concentration range. In particular, Fig 1 shows the dependency of the CuA_2 concentration on the concentration of the disulphide at two fixed initial concentrations of copper(I) di(2-ethylhexyl)dithiophosphate. It is seen from the resulting data that an increase in the disulphide concentration leads to an increase in the equilibrium copper (II) concentration in solution, in full agreement with reaction equation (1), but at the same time these dependences for various copper(I) di(2-ethylhexyl)dithiophosphate concentrations coincide (within the limits of experimental error). At sufficiently high copper (I) concentrations in solution the system is quantitatively described by equation (3). [2]

$$C^2(Cu^2) > K \cdot C(A_2) \qquad (3)$$

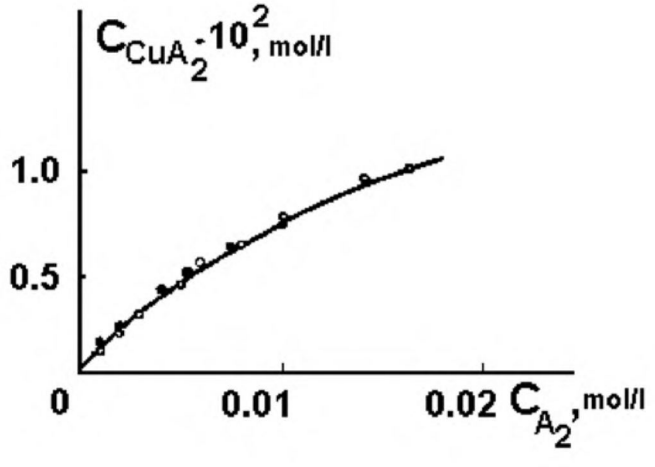


Figure 1. Influence of the initial disulfide and copper(I) di(2-ethylhexyl)dithiophosphate concentrations on the copper(I) di(2-ethylhexyl)dithiophosphate oxidation:

- *• - C(CuA) = 0.1 mol/l*
- *o - C(CuA) = 0.2 mol/l*

A thermodynamic analysis provides the explanation for why the equilibrium position of equation (1) is independent of the total analytical concentration of CuA when there is a high degree of polymerization of one of the components of the equilibrium system, in this case, copper(I) di(2-ethylhexyl)dithiophosphate.

Ignoring the possible structures of the associates formed, we note that intermolecular Cu-S bonds should lead to the formation of various linear and cyclic polymers. For a quantitative estimation of the formation of linear polymers we use the theory of ideal associated solutions [6]. In this case the formation process of the associates is described by the following equations (4):

$$\begin{aligned} &\text{CuA} + \text{CuA} \xrightarrow{P_2} (\text{CuA})_2 \\ &(\text{CuA})_2 + \text{CuA} \xrightarrow{P_a} (\text{CuA})_3 \\ &\cdots\cdots\cdots\cdots\cdots\cdots\cdots \\ &(\text{CuA})_n + \text{CuA} \xrightarrow{P_n} (\text{CuA})_{n+1} \end{aligned} \qquad (4)$$

It is accepted as a first approximation that the energy of addition of the CuA molecule to a polymeric molecule does not depend on the length of a polymer chain. It corresponds to a condition when $p \approx p_2 \approx p_3 \approx \ldots \approx p_n \approx \ldots$

Thus for the total analytical concentration of copper (I) in solution we find:

$$C_{CuA-(i)} = [CuA] + 2[(CuA)_2] + 3[(CuA)_3] + \ldots + n[(CuA)_n] + \ldots = [CuA] + 2p[CuA]^2 + \ldots + np^{n-1}[CuA]^n =$$

For this sequence

$$C_{CuA-(i)} = [CuA]/(1-p[CuA])^2 \qquad (5)$$

The total concentration of the linear polymers may be written:

$$T[(CuA)] = [CuA] + [(CuA)_2] + [(CuA)_3] + \ldots + [(CuA)_n] + \ldots$$

Accordingly we find

$$Z[(CuA)_n] = [CuA]/(1-p[CuA]) \qquad (6)$$

Then the average degree of polymerization of the linear associates will be equal (7)

$$\bar{n} = C_{CuA}/T[(CuA)_n], = 1/(1-p[CuA]) \qquad (7)$$

On analysis of equation (5) we find that when the copper (I) concentration in solution is increased, the [CuA] monomer concentration will increase also. However, the [CuA] concentration has a limit when $C_{CuA} \to \infty$ then $p[CuA] \to 1$. Thus, with increasing copper (I) concentration in solution, the concentration of the monomer and any other polymeric linear forms will tend to 1/p. Thus, on substitution of the monomer concentration in the equilibrium constant expression (8) for the redox reaction (1), we obtain an expression (9) from which it follows that the copper (II) concentration in a high copper (I) concentration solution depends only on the disulphide concentration and does not depend on the copper (I) concentration. [3]

$$K_{red/ox} = [(CUA)]^2 [A_2]/ [CuA_2]^2 \quad (8)$$

In the absence of self-association and solvation of both the disulphide and CuA_2 we accept, that

$[A_2]^* C(A_2)$; $[CuA_2] *C(Cu^{2+})$, respectively, then

$$K_{red/ox} = [CuA_2]^2 C(A_2)/C^2(Cu^{2+}) \text{ -»} 1/p^2 C(A_2)/C^2(Cu^{2+}) \quad (9)$$

In accordance with equation (9) the dependence of $C(A_2)$ on $C^2(Cu^{2+})$ is linear. From the slope of the straight line $p^2K_{red/ox}$ can be calculated:

$$P^2K_{red/ox} - 100+8.$$

It was shown that good agreement between the calculated and experimental data is achieved only at rather high concentration of the components. This is because the model under consideration does not take into account the formation of cyclic polymers in solution

$$(CuA)_{n\cdot(l)} \overset{K_n\text{-}©}{\sim} V (CuA)_n.© \quad (10)$$

Taking this process into consideration, the expression for the total analytical concentration of copper (I) in solution is

$$C_{CuA} = [CUA]/(1-P[CUA])^2 + C_{CuA\text{-}©} \quad (11)$$

In equation (11) the first term reflects the total analytical concentration of copper (I) in the linear associates (i.e. the sum of the row $i^nZnp'''^1[CuA]^n$), and the second term, $C_{CuA\text{-}©}$, reflects the total analytical concentration of copper (I) in the cyclic polymers.

As the stability of the cyclic polymers essentially decreases with an increase in n, that is the K_n-© value (equation 9) rapidly decreases with an increase in n at high copper (I) concentrations, the linear polymers predominate in the solution, and the system can be satisfactorily described within the framework of the theory of ideal associated solutions. On reduction of the copper (I) concentration in solution the fraction of cyclic polymeric molecules increases. Therefore it is impossible to neglect their contribution to the value of $C_{CuA\text{-}}$

For an estimation of the change in the amount of those or other associate forms that are dependent on the solution composition, the dependence of the monomer concentration of copper(I) di(2-ethylhexyl)dithiophosphate on the total analytical concentration of copper (I) was determined. The monomer concentration, more precisely the $[CuA]/VK_{red/ox}$ value, was calculated from spectrophotometric data using an expression for the equilibrium constant of the redox reaction (8, 12):

$$[CuA]/\sqrt{K_{red/ox}} = \sqrt{(C^2_{CuA2}/C_{A2})} \quad (12)$$

The dependence of this value on the CuA concentration is shown in Figure 2. [4]

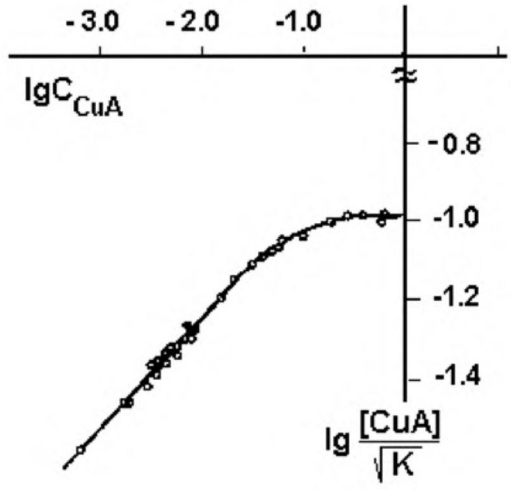


Fig. 2 Dependence of the copper(I) di(2-ethylhexyl)dithiophosphate monomer concentration on the total analytical copper (!) concentration in solution.

As can be seen from these data, at high copper (I) concentration (> 0,1M) the CuA value is practically constant and the slope of the line is close to zero thus testifying to the formation of very high molecular weight associates. At low copper (I) concentration the slope of the line is 0,25, i.e. the relation between the copper (I) concentration and the monomer concentration is as follows:

$$C_{CuA}=K[CuA]^4 \qquad (13)$$

From the resulting data it follows that, along with linear polymers in solution, very stable tetramers of copper(I) di(2-ethylhexyl)dithiophosphate are formed. The high stability of this form can be explained only by the formation of a cyclic structure. The formation of copper(I) di(2-ethylhexyl)dithiophosphate tetramers in solution has been shown earlier by an isopiestic method [5], Lawton et al. [7] also reported that Cu (I) complexes of 0,0-diisopropylphosphorodithioate are tetranuclear, of the form Cu4[(i-$C_3H_4$0)2PS2]4.

Taking into account the formation of stable cyclic tetramers, equation (11) becomes:

$$C_{CUA} = [CuA]/(1-p[CuA])^2 + 4\,K_n.©p^3[CuA]^4 \qquad (14)$$

From the experimental data all constants of the redox and self-association reactions of the copper compounds have been calculated (toluene was used as the diluent):

$$P = (1{,}72 \pm 0{,}03)\,10^3;\ K_n.© = 27.2 \pm 0{,}5;\ K_{red}/_0x = (3{,}38 \pm 0.21)\,10^5$$

Thus the total analytical concentration of copper (I) may be written as:

$$C_{CUA} = [CuA]/(1-1{,}72\ 1\ 0^3[CuA])^2 + 5.54\ 10\text{^}CuA]^4 \qquad (15)$$

Equations (8) and (15) satisfactorily describe the interactions in the organic phase for the extraction of copper (II) with DTPA. In Figure 3 the calculated curves of an isomolar series of the copper(I) di(2-ethylhexyl)dithiophosphate and disulfide interaction, and the corresponding experimental points are shown. As seen from the obtained data, the results coincide, thus showing that the "abnormal" position of the maximum of the curve is caused by the self-association of the product of the reaction - copper(I) di(2-ethylhexyl)dithiophosphate.

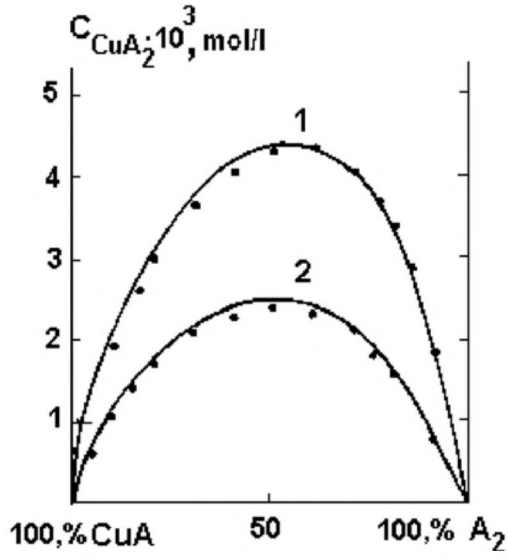


Fig. 3. Calculated curves and experimental points of the copper(I) isomolar series di(2-ethylhexyl)dithiophosphate and disulfide interaction.
1 - C(CuA)+ C(A_2) = 0,02 mol/l; 2 - C(CuA)+ C(A_2) = 0,01 mol/l

In Figure 4, the experimental data and calculated dependence of the amount of copper (II) in the organic phase on the total copper concentration in the organic phase is shown. This dependence also has an "abnormal" character. If only the redox reaction (1) is taken into account, then it may be concluded that, at increasing CuA_2 concentration, the amount of copper (II) relative to the total amount of copper in the organic phase will increase as reaction (1) will move to the left. In fact, the opposite phenomenon is observed - the fraction of copper (II) in the organic phase decreases rapidly with increasing total copper concentration. This is caused by the high degree of polymerization of copper(I) di(2-ethylhexyl)dithiophosphate.

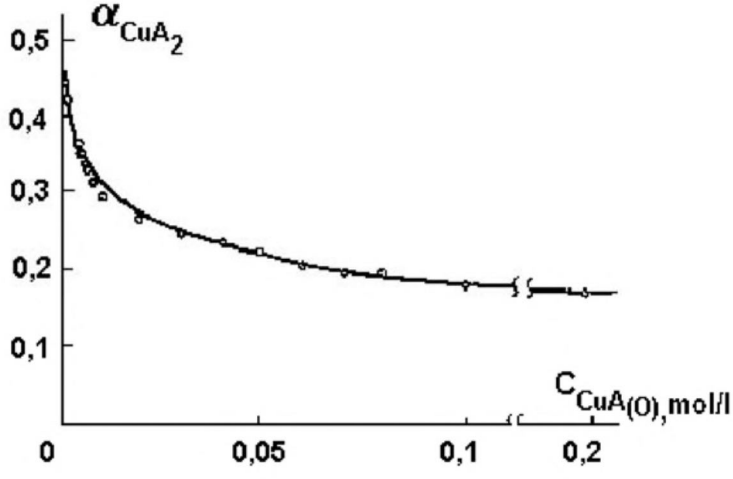


Fig. 4. Influence of total copper concentration in the organic phase on the amount of copper (II) in solution on extraction by DTPA in toluene
— calculated dependence
. . - experimental points

As the redox processes in the organic phase as well as self-association lead to a decrease in concentration of the extraction product - CuA_2, this results in an increase in the distribution coefficient of copper on extraction with DTPA or its salts.

Thus if the copper concentration in the organic phase is more than 0,1M, the shift in equilibrium is caused mainly by the self-association of the products of the redox reaction. So, the fraction of copper (II) in the total copper concentration in the organic phase, calculated from equation (8), without taking into account the process of self-association would be 0,88-0,99 for copper concentrations in the range 0,1-1 M. When self-association of the copper(I) di(2-ethylhexyl)dithiophosphate is taken into account it is actually, 0,2-0,07.

At a copper concentration of more than 0,1M

$$0CCuA_2 = CcuA2/\ Ccu(org) * 0.0707/"\backslash Ccu(o) \quad (16)$$

Taking this into account, at high copper concentration in the organic phase, the cation exchange extraction of copper (II) by DTPA (17) can be described by equation (18).

$$Cu^{2+}(aq)^+ 2HA(_{org}) \text{ ^} 2H^+_{(aq)} + CuA;_{(org)} \quad (17)$$

$$KCu^{2+}/H^+ * 0.0707\ V(D_{Cu}/CCu^{2+}_{(aq)})\ (a^2H^+(aq)/C^2HA(o)) \quad (18)$$

(without taking y+into account)

CONCLUSIONS

In summary it is necessary to note the efficiency of application of the theory of the ideal associated solutions for the description of self-association. Any restriction of the degree of self-association, artificial or otherwise, which is quite often used for simplification of the system description, actually complicates it. This does not now allow qualitatively examination of new properties of highly associated substances, in particular, the limit in the concentration value of any of the associate forms with increasing total concentration of the associated substance in solution.

Such correlations are simple and can be used to estimate the activity of the components in any description of the solvation processes for other multicomponent systems.

REFERENCES

1. T. H. Handley and J. A. Dean (1962), *Anal. Chem.,* 34, 1312-1315.
2. T. H. Handlev (1963), *Anal. Chem.. 35.* 991-995.
3. G. Cote and D. Bauer (1989), *Rev. Inorg. Chem.,* 10, 121-144.
4. K. C. Sole and J. B. Hiskey (1995), *Hydrometallurgy,* 37, 129-147.
5. V. I. Kuz'min, O. A. Logutenko, A. I. Kholkin and A. Yu. Erastov (1986), *Zh. Neorg. Khim.,* 31, 2613-2616.
6. I. Prigogin and R. Defay (1954), Chemical Thermodynamics, Longmans Green and CO, London - New York - Toronto, p. 510.
7. S. L. Lawton, W. G. Rohrbaugh and G. T. Kokotailo (1972), *Inorg. Chem.,* 11,612-618. 7



A FTIR STUDY OF THE PHASE TRANSITION of PLURONIC L64 IN NACL SOLUTION

Zheng Lily[1,2], Guo Chen[1], Wang Jing[1], and Liang Xiangfeng[1'2], Liu Hui-zhou[1]*

(1. Young Scientist Laboratory of Separation Science and Engineering, State Key Laboratory of Biochemical Engineering, Institute of Process Engineering; Chinese Academy of Sciences, Beijing 100080, China;

2. Graduate School of the Chinese Academv of Sciences. Beiiina 100039. China)

The micellization of the Pluronic L64 (from BASF, $EOI_3P03oE0_{13}$, mw PPO=1740, %PEO=40) in different concentration of NaCl solution was examined by Fourier transform infrared (FTIR) spectroscopy. The deconvalution method was used to obtain independent information to probe the temperature effect on the hydration of PO and EO blocks. The wavenumber shifts of the bands at 1080 and 11 OOcnrf[1] were studied as a function of temperature. For the Pluronic L64 in aqueous solultion and NaCl solution, the PO and EO blocks undergo the shifts abruptly at the same temperature, but the transition temperature in NaCl solutions is lower than that in the aqueous solution, this may indicates that the salt ion in the solution accelerates the dehydration of the EO and the PO blocks and effects the CMT of the aqueous solutions of triblock polymer.

INTRODUCTION

Polyethylene oxide-polypropylene oxide-polyethylene oxide (PEO-PPO-PEO) triblock copolymers are typical nonionic polymeric surfactants with potential applications in the pharmaceutical, textile and detergent industries [1-4], Strongly concentration- and temperature-dependent micellization has been observed for various Pluronics differing in molecular characteristics [5-12], The phase behavior of block copolymer in water and in salt solutions have been extensively studied [13-19], Alexandridis et al.[12] found that the presence of LiCl, KCl, NaCl, and NaBr decreased both CMT and cloud point (CP) in the order Cl" > Br" and Na* > K^+ > Li^+, while the presence of Nal decreased the CMT but increased the CP. Desai et al. [20] examined the micellization of Pluronic F127 in NaCl solution, and found that the addition of NaCl lowered the critical micelle concentration (CMC).Su et al. [21] investigated the effect of NaCl on the thermally induced behavior of Pluronic Pl03, and found that the standard enthalpy and entropy of micellization for Pluronic Pl03 in water increased with the presence of small amount of NaCl, but the further addition of NaCl decreased both standard enthalpy and entropy of micellization.

Fourier transform infrared (FTIR) spectroscopy has been applied to study the temperature-dependent micellization of Plutonics in aqueous solutions and in salt aqueous solution [21], Guo et al [22] studied the phase transition between unimer and micellar phases of Pluronic P105 in aqueous solutions by FTIR, suggesting that both the PEO and PPO blocks exhibit dehydration during the phase transition. Su et al [23] investigated the micellization of Pluronic [8]

F127 in salt solution by FTIR spectroscopy, and found that the proportion of anhydrous methyl groups was increased, while the proportion of the hydrated methyl groups was decreased during the micellization process. The purpose of this work is to further study detail information about the effects of the salt of different concentration on the temperature-dependent micellization of PEO-PPO-PEO block copolymers in aqueous solutions using FTIR spectroscopy, and give the mechanism of the salt effect on the phase transition of the block copolymer.

MATERIALS AND METHODS

Materials.

PEO-PPO-PEO block copolymers Pluronic L64 was donated by BASF Corp. and used as received. The copolymer has a nominal molecular weight of 2900 and approximately 40wt% PEO and can thus be represented by the formula $EO_{13}PO_{30}EOI_3$. The various salts used were of analytical grade or better, while the water was triple-distilled.

Fourier transform infrared (FTIR).

FTIR spectra were recorded on a Bruker Vector 22 FTIR spectrometer with a resolution of 2 cm^{-1} using a DTGS (deuteriotriglycine sulfate) detector. The temperature of the sample was measured by a thermocouple inserted into a stainless steel block containing the sample cell. This system was comprised of a Graseby-Specac temperature cell (P/N 21525), and the temperature measurement was accurate to 0.1 °C. The equilibration time for each measurement was 1 min. FTIR spectra of all samples were recorded from 2°C to 50 °C by scanning 64 times and using a BaF_2 cell. The OPUS spectroscopic software was used for data handling.

RESULTS AND DISCUSSION

The wavenumber shift of the bands at 1100cm^{-1} was investigated as a function of temperature, which was assigned to the C-O stretching mode for aliphatic ether. It is well known that the characteristic peak bands change abruptly at the CMT of the PEO-PPO-PEO block copolymer.

The changes of wavenumber of the C-O-C stretching vibration band of 10wt% Pluronic L64 in NaCl solution of different concentration are given in the Figure 1.

As is shown in Figure 1, the CMT of 10 wt% Pluronic L64 aqueous solution moved to lower temperature when salt is added, the more NaCl added, the lower the CMT of 10 wt% Pluronic L 64 aqueous solutions. The CMT of 10 wt% Pluronic L64 in aqueous solution, 0.5M NaCl solution, 1M NaCl solution, 1.25M NaCl solution, and 1.5M NaCl solution is 22.5°C, 20.5°C, 16°C, 14°C, and 2°C(or even more lower) respectively.

To probe the effect of salt on the PPO and PEO block during temperature-dependent micellization, the deconvolution method was used to obtain the independent information about the PPO and PEO block under a complex band profile in the C-O stretching region. In the deconvoluted spectra, the strong band in the 1200-1000 cm^{-1} region can be separated into two components, one around 1080 cm-1 and the other around 1100cm^{-1}, which are assigned as the C-O stretching vibration band of PEO block and PPO block respectively[21]. The frequencies of two bands of 10wt% Pluronic L64 in aqueous solution and in 1M NaCl solution versus temperature are plotted in Figure 2 which indicates that an increase in temperature leads to drastic changes in the frequencies of both the PEO and PPO bands. For the Pluronic L64 in the aqueous solution, the two bands show abrupt changes at the

same temperature, but the 1110 cm'1 band exhibits a larger wavenumber shift, and the 1080 cm- 1 band shows a smaller wavenumber shift; while that in the NaCl solution, the abrupt changes of the two bands occur at lower temperature, which are taken as the transition temperature of PEO ($T_{m(EO)}$) and PPO ($T_{m(PO)}$) blocks. When salt is added to the Pluronic L64 aqueous solution, both the $T_{m\ (EO)}$ and the $T_{m\ (PO)}$ decreased and the values of them decreased with the increase of the concentration of the NaCl solution, which is shown in Figure 3.

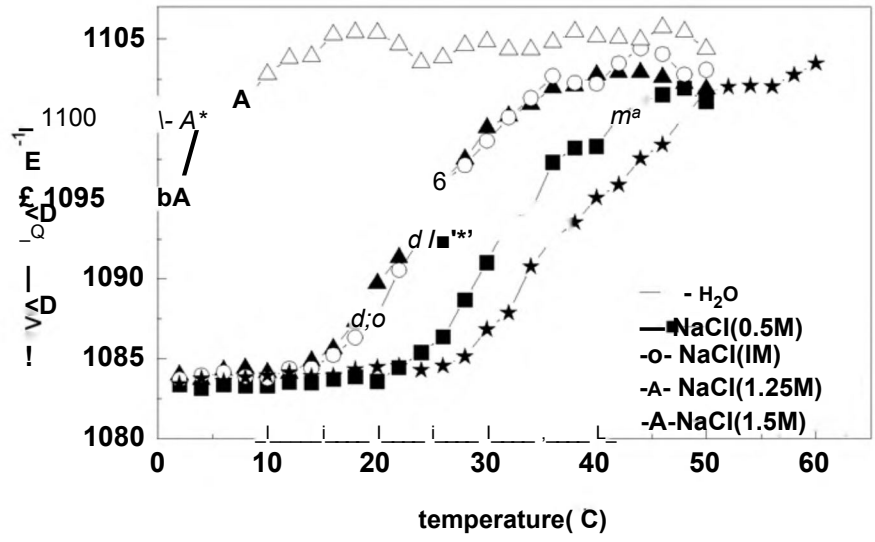


Figure 1 Changes of wavenumber of the C-O-C stretching vibration band of Pluronic L64 in different solutions as a function of temperature.

It is known that in the unimer phase, the copolymer dissolves in water as a molecular micelle, which forms a PPO hydrophilic core surrounded by the hydrophilic PEO blocks. The water molecules can bind to the hydrophobic EO blocks and could also penetrate into the hydrophobic PPO core. Therefore, at low temperature, the wavenumbers of the C-O stretching modes of the PO and EO blocks are both low. Upon adding salt in Pluronic L64 aqueous solution, the water is polarized by the ionic field that formed by the salt ion, resulting in a low free energy, while the water in the EO hydration shell or that in the hydrophobic PPO core is in a high free energy state because of unfavorable entropy contributions, so the water in the EO hydration shell or that in the hydrophobic PPO core tends to move to the bulk water. As the temperature increase, the water molecules are easier to removed from the EO and PO blocks than those in aqueous solution and the hydrogen bond between the water molecules and the block copolymers splits more easily, so the $T_{m(EO)}$ and $T_{m(PO)}$ of Pluronic L64 in the salt solution are lower than those in the aqueous solution, thus the CMT of the Pluronic L64 in salt solution moves to the lower temperature too. For the same copolymer, the tendency of the water moving from the EO hydration shell depends on the intensity of the ionic field, for the sodium chloride solution, it is obvious that the intensity of the ionic field is strengthened with the increase of the salt concentration, so the CMT of NaCl solution decreases with the increase of the salt concentration.

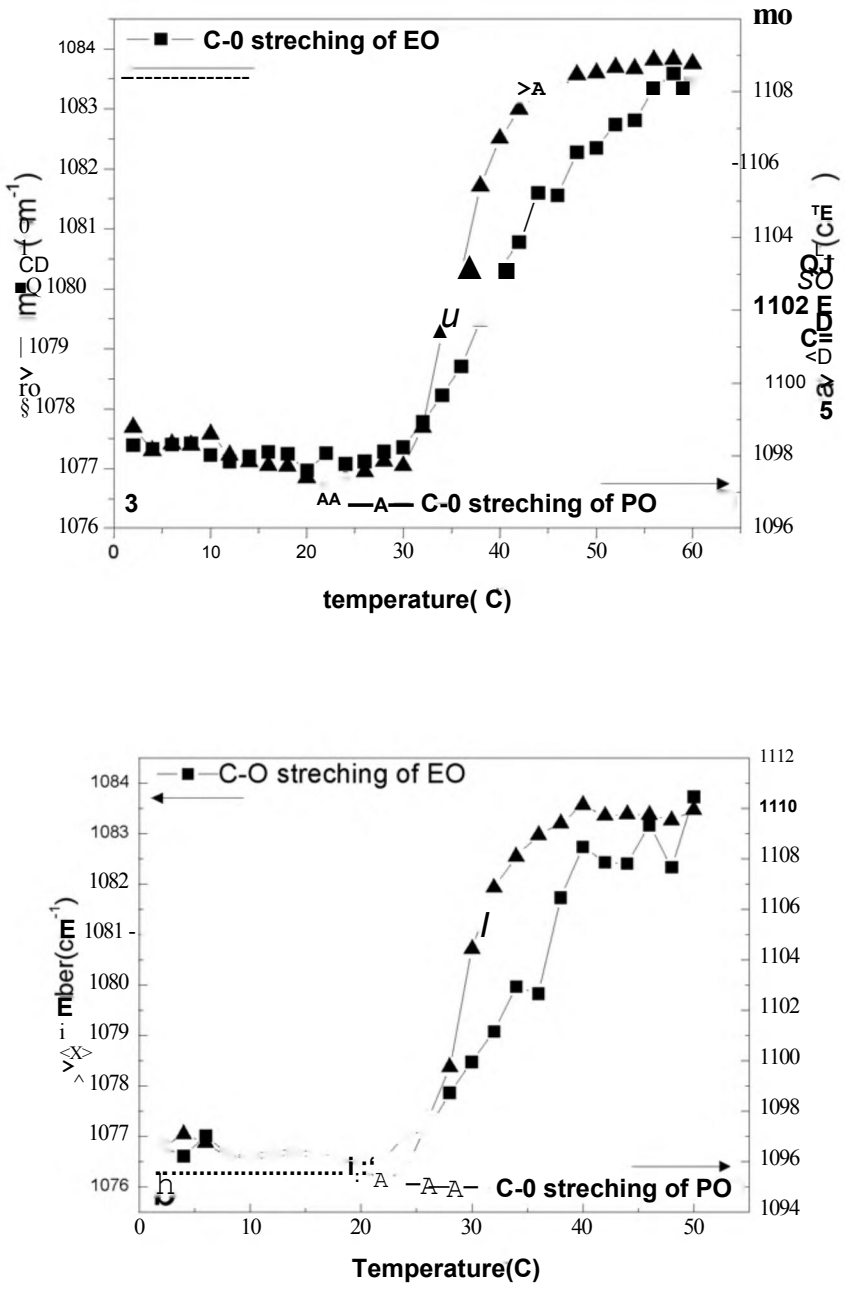


Figure 2. The temperature dependence of the frequency of the **C-0** *stretching mode of the PPO and PEO block in the infrared spectra of Pluronic L64 (a) in aqueous solution and (b) in 0.5M NaC! solution at a concentration of 10wt%.*

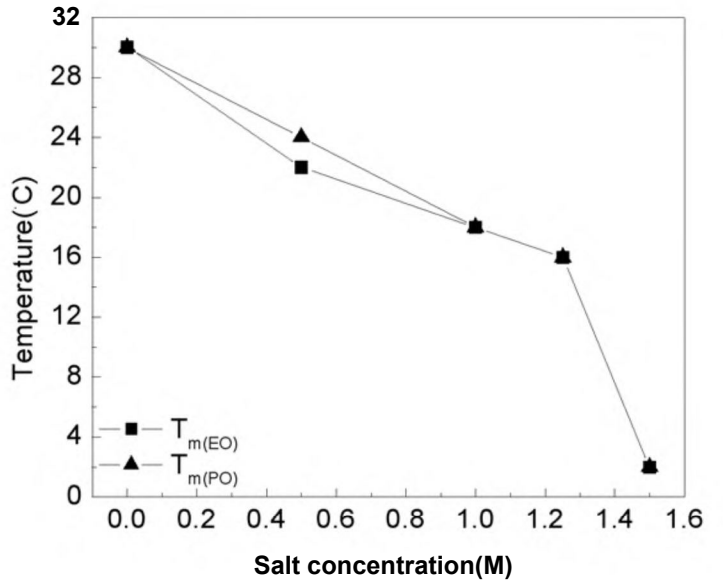


Figure 3. The $T_{m(E}$o> and $Tm_{(PO}$) vs. different concentration of sodium chloride salt.

CONCLUSIONS

Wavenumber shift of the C-O-C stretching vibration band Pluronic L64 in different concertration of NaCl solutions with the increase of the temperature was studied. The strong band near 1100 **cm"[1] was found to be separated into two components, one around 1080 and the other around 1100cm'[1], which were assigned to the C-O stretching vibration bands of the PEO block and PPO block respectively.**

The addition of salt distinctly decreases the CMT of the Pluronic L64 in aqueous solution. For the Pluronic L64 in NaCl solutions, the CMT of the triblock copolymer and the transition temperature of the EO and PO blocks move to lower as the increase of the concentration of the NaCl solutions. The addition of the salt promotes the dehydration of the EO and PO blocks and lowers the transition temperature of them, so the CMT of the triblock polymer moves lower.

REFERENCES

1. **I.R. Schmolka(1967),** *Surf. Sci. Ser.,* **1, 300-371.**
2. **R. H. Whiltmarsh(1996),** *Surf. Sci. Ser.,* **60, 1-30.**
3. **M.W.Edens(1996),** *Surf. Sci. Ser.,* **60, 185-210.**
4. **P. Alexandridis(1996),** *Curr. Opin. Colloid Interface Sci.,* **1, 490-501.**
5. **M.Malmsten, B.Lindman (1992),** *Macromolecules,* **25, 5440-5445.**
6. **M.Malmsten, B. Lindman (1993).** *Macromolecules,* **26, 1282-1286.**
7. **P.Alexandridis, U. Olsson, B.Lindaman (1995),** *Macromolecules,* **28, 7700-7710.**
8. **K.Zhang, B.Lindamn, L.Coppola(1995),** *Langmuir,* **11, 538-542.**
9. **P.Alexandridis, U.Olsson, B. J.Lindman (1996),** *J. Phys. Chem.,* **100, 280-288.**
10. **P.Holmqvist, P.Alexandridis, B.Lindman(1997),** *Langmuir,* **13, 2471-2479.**
11. **P.Alexandridis, U.Olsson, B.Lindman(1997),** *Langmuir,* **13, 23-34.**
12. **P.Alexandridis, J. F.Holzwarth (1997),** *Langmuir,* **13, 6074-6082.**

13. **Z.Chu, B.Chu(1987),** *Macromolecules,* **20, 3089-3091.**
14. **M.Almgren, J.Alsins, P.Bahadur(1991),** *Langmuir,* **7, 446-450.**
15. **E. B.Jorgensen, S.Hvidt, W.Brown. K.Schillen (1997),** *Macromolecules,* **30, 2355-2364.**
16. **J.K.Armstrong, B. Z.Chowdhary, M. J.Snowden, S. A.Leharne(1998),** *Langmuir,* **14, 2004-2010.**
17. **P.Bahadur, K.Pandya, M. Almgren, P.Li, P.Stilbs (1993),** *Colloid Polym. Sci.,* **271, 657-667.**
18. **P.Bahadur, P.Li, M.Almgren, W.Brown (1992),** *Langmuir,* 8**, 1903-1907.**
19. **M.Almgren, P.Bahadur, M.Jansson, P.Li, W.Brown, A. Bahadur(1992),** *J.Colloid Interface Sci.,* **151, 157-159.**
20. **P.R.Desai, N.J Jain, R. K.Sharma, P.Bahadur(2001),** *Colloid Surf. A.,* **178, 57-69.**
21. **Y. L.Su, X. F.Wei, H. Z.Liu(2003),** *J. Colloid Interface Sci.,* **264, 526-531.**
22. **C.Guo, H.Z.Liu, J.Y.Chen (1999),** *Colloid Polym Sci.,* **277, 376-381**
23. **Y.J.Su, H.Z.Liu, J.Wang, J.Y. Chen (2002),** *Langmuir,* **18, 865-871.**

SYNERGISTIC EXTRACTION OF ERBIUM BY MIXTURE OF CA-12 AND CYANEX272

X. B. Sun, X.Q Sun , D.Q. Li*

Key Laboratory of Rare Earth Chemistry and Physics,
Changchun Institute of Applied Chemistry,
Graduate School of Chinese Academy of Sciences, Changchun 130022, P. R. China.

The synergistic extraction of trivalent erbium (Er^{3+}) from chloride medium using mixture of bis (2,4,4-trimethylpentyl) phosphinic acid (Cyanex272,HL) and sec-octylphenoxy acetic acid(CA-12,HA) in heptane has been investigated. The synergistic enhancement factor was observed (R_E, = 7.04). The composition of the extracted species was determined as $ErH_6A_4L_5$ instead of $ErL_3$2HL, Er(OH)-, $_5$2.5HA, which were extracted by Cyanex272 and CA-12, respectively. The extraction of other heavier rare earths has been studied and the separation possibility between Er and heavier rare earths were discussed.

INTRODUCTION

Recently, numerous types of synergistic extraction systems have been applied to rare earth extensively [1-6]. Most of the synergistic systems are the combination of acidic extractants (e.g.(3-diketones, carboxylic and organophosphorus acids) with neutral extractants (e.g. organophosphorus esters, crown ethers, TBP, TOPO, Cyanex923 et al). Only a few papers have reported the synergistic systems composed of two acidic extractants, for example, Yuan and Rickelton[6] have reported the synergistic extraction using C274+Cyanex272 system to separate heavy lanthanides. Moreover, we have reported the synergistic extraction of lanthanide and Yttrium by the mixture of BTMPPA (Cyanex272) and 1-phenyl-3-methyl-4-benzoyl-pyrazalone-5 (HPMBP)[7].This prompted us to investigate new synergistic extraction systems involving CA-12 and Cyanex272.

Sec-octylphenoxy acetic acid (CA-12) is a novel organic carboxylic acid extractant developed by Shanghai Institute of Organic Chemistry, Chinese Academy of Sciences. Recently, the physicochemical properties of CA-12 and the extraction of rare earth ions have been investigated by our laboratory [8],

In this paper, we developed a new two acidic synergistic extraction system by CA-12 and Cyanex272, which has not been reported so far. The synergistic effect and the extraction mechanism of Er were studied thoroughly. And also, the extraction of other heavier rare

earths (HRE) was investigated and the separation possibility between Er^{3+} and HRE were discussed.

EXPERIMENTAL

Reagent and Apparatus

CA-12 and Cyanex272 was kindly supplied by Tianjin Biechen chemical Plant and the CYTEC Canada, Inc. CA-12 and Cyanex272 were used without further purification and dissolved in n-heptane to the required concentrations. Stock solutions of rare earths were prepared from their oxides (99.9%) by dissolving and diluting to required volume with. All extraction experiments were performed at constant ionic strength (NaCl=1 mol/l).

An orion model 720 pH meter made by Shanghai Rex Instruments Factory was used for pH measurement.

Solvent extraction procedure

Equal volumes (5ml) of aqueous and organic phases were mixed and shaken in equilibrium tubes for 30 min at 298±0.2K(except for the temperature experiments), which was sufficient for equilibrium attainment. The concentration of the metal ion left in the aqueous phase was analyzed by volume titrically using EDTA and that in the organic phase was obtained by mass balance. These concentrations were used to obtain the distribution ratio D.

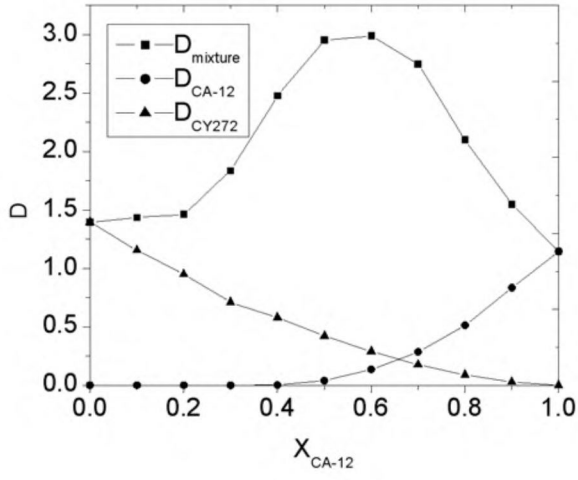
RESULTS AND DISCUSSION

The synergistic effect of Er^{3+}

The extraction of Er^{3+} from chloride solutions by Cyanex272, CA-12 respectively and their mixture is investigated. Figurel showed the obvious synergistic effect. The synergistic enhancement factor $R=D_{mixture}/(D_{Cyanex272}+D_{CA-12})$ was obtained following Xu et al[S| and the largest R, R_{max}, was obtained to be 7.04. These results demonstrate that a dramatic increase of the extraction ability for rare earths was observed in the CA-12 +Cyanex272 system.

Extraction equilibrium of Er with Cyanex272 and CA-12 respectively

The solvent extraction of rare earths by Cyanex272 has been studied earlier [10,11], but the extraction of Er^{3+} in chloride medium has not been discussed in detail. For demonstrating the extraction mechanism, the extraction of Er^{3+} with Cyanex272 or CA-12 in n-heptane as a function of pH and extractant concentration respectively has been studied (Figure2, Figure3). The relevant log-log plots were liner with a slope of 3 for Cyanex272 and 1.5 for CA-12 in Fig2, and in Fig3 the slopes are 2.5 for Cyanex272 and 2 for CA-12 respectively indicating the extraction complexes is ErL_3 2HL for Cyanex272. However, the extraction species of Er^{3+} with CA-12 is different from Cyanex272, it may be combined with OH' or Cl'. Based on the stability constants of Er with OH' or Cl', OH' is prone to take part in the extraction. Experiments confirmed the assumption for Cl' has almost no effect on the extraction of Er^{3+}, which means that OH' take part in the extraction and the similar result was obtained by Zhang et al [12],



Figurel. Extraction and synergistic extraction of Er³ by Cyanex272, CA-12 and Cyanex272+CA-12. [Er³*]=5.038x1O'³M, P-I.OM, pH=2.69. (•)-CA-12 system alone (A)-Cy272 system alone (m)-CA-12+Cy272 system, $[Cyanex272]_{(0)}$+$[CA-12]_{(o)}$=0.04M.*

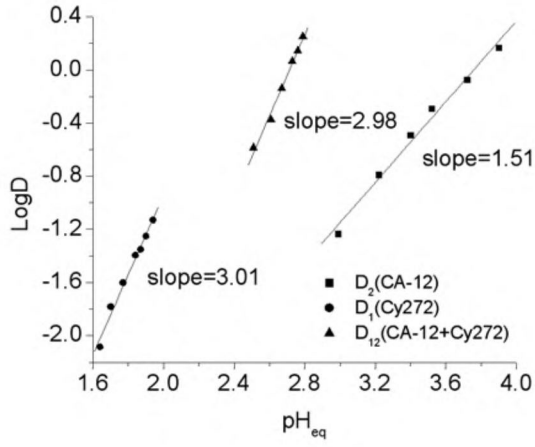


Figure2. Distribution ratio for Er³ as a function of pH in CA-12, Cy272 and their mixture systems. [Er³*]=5.038x10-³M, P =1.0M, $[Cyanex272]_{(o)}$=$[CA-12]_{(o)}$=0.02M.*

Therefore, according to the slope analysis, the extraction equilibrium of Er^{3+} from hydrochloride mediums with Cyanex272 (H_2L_2) and CA-12 (H_2A_2) can be expressed as follows,

$$Er^{3}_{a)} + 2.5H_2L_{2io)} \text{ <—^—>} ErL_3 \blacksquare 2HL \quad _{(o)} + 3H^{+}_{(a)} \qquad (1)$$

$$Er^{3}_{a)} + 1.50H\sim_W + 2H_2A_{2(o)} \text{ <-^} Er(OH),\ _SA,\ _5 \bullet 2.5HA_{(o)} + I.5H_{a)} \quad (2)$$

where "a" and "o" denote aqueous and organic phase respectively.

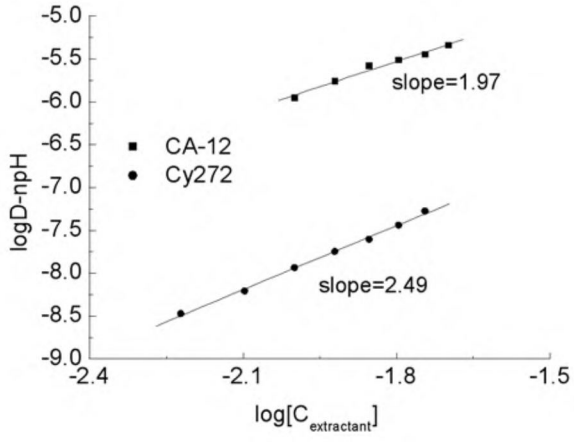


Figure 3. Effect of extractant concentration on the extraction of Et³ in Cyanex272 or CA-12 system alone, [Er³*]=5.038x10'³M, u =1.0M, pH=2.69.(m)-the relationship: logD-1.5pH vs. logC$_C$A-i$_{2,}$(*)-the relationship: logD-3pH vs. logC$_{Cy272}$-*

Synergistic Extraction of Er³* with the mixture of CA-12 and Cyanex272

If the synergistic extraction of Er³* by the mixture of CA-12 and Cyanex272 from chloride medium is expressed as

$$Er^{3+}_{(a)} + x(3-H_{(a)} + nH_2A_{2(0)} + mH_2L_2^{}_{0)} < \xrightarrow{K_{12}} * ErH_{2ll+2m-x}Cl_{2-x}A_{2n}L_{2m}^{}_0^{} + xH^{}_{a)} \quad (3)$$

Then the distribution ratio, D_{I_2} and the equilibrium constant, K_{I_2}, of the synergistic extraction reaction should be:

$$D_{U\backslash 2} \sim \overline{U}T\ D_{U\backslash U2} = D_{-} = \frac{[ErH_{2n,2m-x^{}h-x^2n^2n,\backslash o)}}{,,^{3+},\ \backslash .^{Er}\ \mathbf{I(-)}} \qquad {}^{/y1x}W$$

$$K_{12} = \frac{[^{}2n+2m-*C^3-x^2n^2m](o)[i/\ ]^{+\ x}_{(a)}}{\mathbf{[^{3+}]_{(a)}[c/-t7[//_2^{}_2]_{(}^{}{}_{0)}[//_2L_2]r_{0)}}} \quad (5)$$

Where, D_T denotes the total distribution of the mixture system, D-, denotes the distribution of Cyanex272, D_2 denotes the distribution of CA-12.

Taking logarithms:

$$\log D_n = \log K_n + xpH_{(a)} + n\ \log[H_2A_2]_{(o)} + m\ \log[H_2L_2]_{(o)} + (3-x)\ \log[C/\ ]_{(a)} \quad (6)$$

In order to determine the extracted complexes in the CA-12+Cyanex272 system, a series of experiments were carried out. As shown in Figure 2, the plots of LogDi$_2$ vs. pH (pH=2.5~3.1) at fixed concentrations of Cyanex272 and CA-12 give a straight line with a slope of about 3,

which suggests x=3. Similarly, at fixed aqueous acidity and concentration of the other extractant, the plots are liner with slopes of about 2.5 for Cyanex272 and 2 for CA-12 respectively, indicating that m=2.5, n=2 in the extracted complex of Er^{3+}.(Figure 4).

The synergistic extraction reaction, Eq.(3), can thus be rewritten as:

$$Er^{3}\backslash_{a)} + 2H_2A_{2(o)} + \mathbf{2.5}H\ {}_2L_{2(o)} \xleftrightarrow{K_{12}} ErH_6A_4L_{5(g)} + 3H^{+}_{(a)} \quad \textbf{(7)}$$

According to (4), (5) and (6):

$$\log\pounds_{12} = \log(D_r - D_l - D_2) - 3pH - 2\backslash og[H_2A_2]_{(o)} - 2.5\backslash og[H_2L_2\backslash_{o)} \quad (8)$$

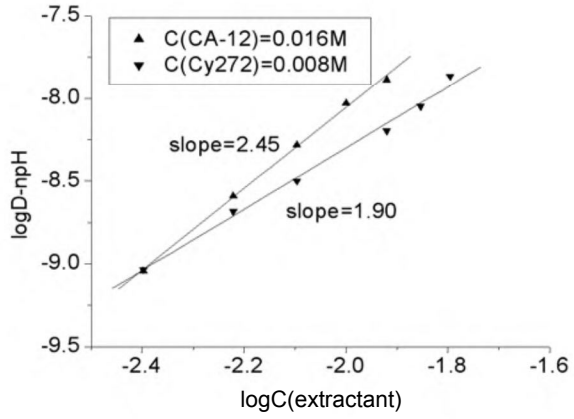


Figure 4. Relationship between distribution ratio $D_{12}$and equilibrium concentration of CA-12 and Cyanex272. [E^]=5.038x10^{3}M, v=1.0M, pH=2.69.

The synergistc extraction reaction is cation exchange mechanism and as ideal as suggested in the literature [13], the equilibrium constants are calculated logKi=-2.48, logK_2=-1.77 and logKi2=3.24 and follow the order K_I<K_2< Ki_{2I} therefore, the Cyanex272 +CA-12 system is more stable than Cyanex272 or CA-12 system alone, when Cyanex272 is mixed with CA-12, the synergistic reaction is more easier to be carried out.

Separation of Er^{3*} from heavier lanthanides by mixture of CA-12 and Cyanex272

The synergistic effects were also found for Tm^{3+}, Yb^{3+} and $Lu^{3+}$and the calculated R_{max} for Tm=7.50, Yb=13.12, Lu=17.58. Tablel gives the separation factors (SF) between Er and heavier rare earths with CA-12, Cyanex272 and Cyanex272+CA-12 system. The selectivities between Y and heavier lanthanides were found to be much higher than that of the CA-12 system and comparable to Cyanex272 system alone. The high selectivities can be explained that the synergistic effects increase with decreaseing ionic radii of heavy lanthanides while the synergistic effect of Er^{3*} is smaller than Tm^{3+} $Yb^{3+}$and Lu^{3+}. The CA-12+Cyanex272 system can be used to separate Er^{3+} from heavier lanthanides due to its increased extraction efficiency and improved selectivities.

Table 1. Separation factors of heavy rare earths by the Cyanex272+CA-12 system.

System	Tm/Er	Yb/Er	Lu/Er
CA-12	0.92	0.92	0.86
Cy272	3.73	3.89	4.55
CA-12+Cy272	2.98	3.75	13.41

CONCLUSIONS

The organophosphinic acid and carboxylic acid synergistic system is proposed. Mixtures of CA-12 and Cyanex272 exhibit evident synergistic effect when used to extract Er^{3+}. The synergistic enhancement factors and the extraction equilibrium were studied thoroughly. The separation factors between Er^{3+} and heavier lanthanide ions were calculated for Tm/Er=2.98, Yb/Er=3.75, Lu/Er=13.40 and superior to CA-12. The Cyanex272 +CA-12 system exhibits obvious synergistic effects, strong extraction ability, high selectivity, which can be used to separate Er^{3+} from heavier lanthanide ions.

ACKNOWLEDGEMENTS

The authors wish to thank Cytec Canada Inc. for supplying Cyanex272. This project was supported by the State Key Project of the Foundation Research (G1998061301) and National Natural Science Foundation of China (29771028, 29801004).

REFERENCES

1. **T. Sekine;.Y. Hasegawa, Adduct Formationos Metal Species Extracted With Acid Extractants, Solvent Extraction Chemistry;** *Marcel Dekker. inc:* **New York(1977);200pp**
2. **J. Ydberg, T.Sekine, Solvent Extraction Equilibria, In** *Principles and practices of Solvent Extraction,* **J. Rydberg, C. Musikas, G.R. Choppin (Eds.),** *Marcel Dekker, Inc.:* **New York (1992), 101pp.**
3. **J.N. Mathur(1983),** *Solvent Extr. Ion Exch.,* **1, 349-361.**
4. **M.L.P. Reddy, T.R. Ramamohan, C.S.P. Lyer (1998),** *Solvent Extr. Research and Dev.* **(Japan), 5,1-5.**
5. **M.L.P. Peddy, S.Sujatha, R.Luxmi Varma (1997)** *Talanta* **44, 97-85**
6. **Chengye yuan, Hengli Ma, W.A Rikelton. Synergistic extraction of Rare earths based on Cyanex272;** *ISEC'96,* **Voll, 733-738**
7. **J. sun, D.Q. Li (1994),** *Chinese journal of analytical chemistry,* **11,49-53**
8. **X.Y. Zhang, Q.B. Bo, D.Q. Li (2000), The mechenism of solvent extraction of rare earth (III) by Sec-octylphenoxy acetic acid,** *Chinese journal of applied chemistry,* **17(2), 198-200**.
9. **G.X. Xu, W.Q.Wang, J.G.Wu (1963),** *At. Engery Sci. Technol,* **7, 487-508.**
10. **X, Zhang, D.Q. Li (1993),** *Chinese journal of applied chemistry,* **10 (4), 72-74.**
11. **M.I. Saleh, Md. Fazlul (2002),** *Hydrometallurgy,* **63, 75-84.**
12. **X. Y. Zhang, G.Y. Yin, Z.G. Hu(2003),** *Talanta* **, 59, 905-912**
13. **Emmanuel O.out (1997),** *Solvent Extr. Ion Exch.,* **15, 1-13**

VIBRATIONAL SPECTRA OF 2- BUTYL- TETRAHYDROTHIOPHENE- 1- OXIDE AND ITS Pd (II) COMPLEX BY AB INITIO CALCULATIONS

Zhi-Guang Xu,[1] Guo-Bang Gu * \ Song-ping Wu \ Fei Yam [2], Hai-Yang Liu *[1]

1, Department of Chemistry, South China University of technology Guangzhou 510641, China

2, Department of Chemistry, The Hong Kong University of Science and Technology, Hong Kong, China

Vibrational Spectra of 2- Butyl- tetrahydrothiophene- 1- oxide (BTHTO) and Its three isomeric Pd (II) Complexes have been calculated by using ab initio RHF method with 6-31G* as the basis set (for metal Pd (II), LanL2MB basis set is used). The calculation result show that vibration v_s=o of sulfoxide will shift to higher wavelength number with S-coordinated, and it will shift to lower wavelength number with O-coordinated. The theoretical analysis of molecule energy by DFT method at B3LYP/6-31G* level (for metal Pd (II), LANL2DZ basis set is used) suggests, among three isomers, the most stable structure is one in which Pd(II) is coordinated by O atom of one BTHTO, and the S atom of the other BTHTO ligand.

INTRODUCTION

Sulfoxides are good extractants for precious metals, they form complexes via coordination interaction between S or O and the metal ions. IR spectra is quite useful in determining coordination mode between sulfoxide ligands and the metal ions. It was suggested that vibration $v_{s=0}$ of sulfoxide will shift to higher wavelength number when metal ion is ... coordinated by its S atom, and it will shift to lower wavelength number when metal ion is coordinated by its O atom[1]. So far, no systematic theoretical investigation is performed to elucidate this phenomena.

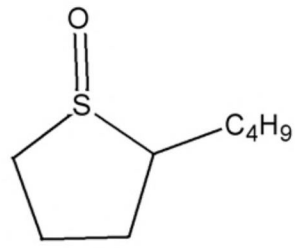


Figure 1. Molecular structure of BTHTO

We have prepared a cyclic sulfoxide derivative, 2- Butyl- tetrahydrothiophene- 1-oxide(BTHTO) recently[2]. The extraction ability of the cyclic sulfoxide is stronger than that of the linear one, and the compound also has the excellent ability to separate Au, Pd and Pt in extraction[3], In this paper, we wish to report the theoretical analysis on the IR spectra of 2- Butyl- tetrahydrothiophene- 1- oxide (BTHTO) (figure 1) and its Pd (II) complexes by using the ab initio RHF methods at 6-31G* level (for metal Pd (II), LanL2MB basis set is used).

COMPUTATIONAL DETAIL

Geometries of BTHTO were optimized at RHF/6-31G* and B3LYP/6-31G* level respectively. Three Pd (II) -BTHTO isomeric complexes A, B and C are constructed as model complexes (see figure 2). and geometries of Pd (II)-BTHTO complexes were optimized at RHF/6-31G* level (for metal Pd (II), LanL2MB basis set is used). The vibrational frequencies were calculated by the same method. Molecular energy of BTHTO and its Pd (II) complex were calculated by DFT method at B3LYP/6-31G* level (for metal Pd (II), LANL2DZ basis set is used). All calculations were performed on a P4 (2.8G) personal computer by using Gaussian 98 program [4],

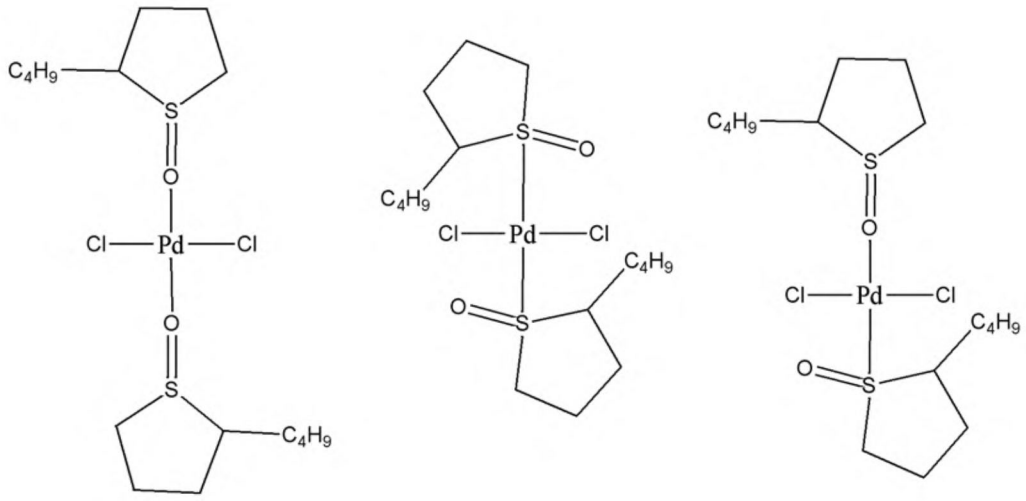


Figure 2. Molecular structures of BTHTO-Pd(II) complexes

RESULT AND DISCUSSION

Molecule Geometry

Geometries of BTHTO were optimized at RHF/6-31G* and b3lyp/6-31G* level. Selected geometry parameters are listed in table 1. Optimized geometrical structures

show carbons in the ring of the tetrahydrothiophene are not of a plane, and the ring is of a half-chair conformation. The bond lengths obtained by RHF/6-31G* are shorter than those by B3LYP/6-31G*. Bond lengths optimized at RHF/6-31G* is close to geometry of thirane oxide, and thus the geometries optimized at RHF/6-31G* level is preferable,

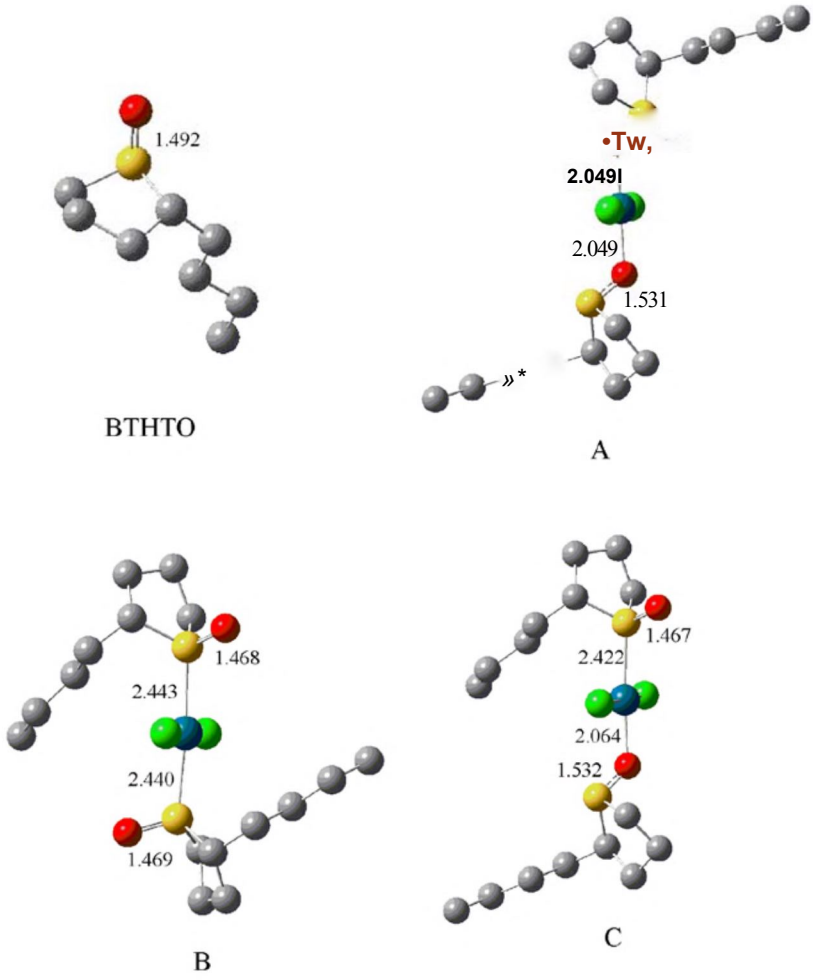


Figure 3. Optimized geometries of $PdCl_2$ • 2BTHT0 complexes at RHF/6-31G (for metal Pd (II), LanL2MB basis set is used)*

Table 1 Selected geometry parameters of BTHTO[3]

	Method	S-O	S-C2	S-C5	C2-C3	C3-C4	C4-C5	ZC2SC5	ZOSC2C3
	RHF/6-31G*	1.492	1.842	1.807	1.542	1.530	1.526	92.2	102.5
	B3LYP/6-31G*	1.518	1.899	1.856	1.541	1.535	1.528	90.6	105.9
Thirane oxide	Exp[b]	1.489	1.822	1.822					

a. distance in A and angle in degree; b. from ref.6.

The S-O bond distance (1.531 A) in complex A (figure 3) is considerably longer than that of free ligand BTHTO (1.492A). This suggests the coordination interaction between O and the Pd (II) metal ion will weaken the S=0 bonding of BTHTO. Contrary, the S-O bond length in complex B (1.468A) are considerably shorter than the S-O bond length (1.492A) in BTHTO, and this indicates its S=0 binding will be strengthened by S-coordination. Similar situations could be observed in model complex C too. Bond length of Pd-O is approximately 2.05 A (figure 3), which is in agreement with experimental data [5],

Vibrational frequencies

There are no imaginary frequencies in all optimized model complexes; this indicated optimized conformations are reasonable. The total energy of complex B (-956.5329 a.u.) is lower than that of complex A (-956.5322 a.u.), showing S coordination complex is little more stable than O coordination complex. The total energy of complex C reaches a minimum (-956.5346 a.u.). Complex C is the most stable among three model complexes.

The calculated $v_{s=0}$ of BTHTO is 995 cm'[1], corresponding to 1017 cm'[1] in experiment. In complex C, calculated v_s=o of O-coordination S-O and S-coordination S-O are 931cm'[1] and 1066cm'[1] respectively. This indicated when Pd(II) is coordinated by S atom of BTHTO, its S=0 binding will be strengthened (bond length = 1.467A), and when Pd(II) is coordinated by O atom of BTHTO, S=0 bonding will be weakened (bond length = 1.532A). In the experimental IR spectra of Pd (II)-BTHTO complex, both 1116 cm'[1] and 922 cm'[1] peaks which ascribed to v_s=o vibration were observed. This indicates the most possible structure of BTHTO-Pd (II) extraction adduct is complex C. [23]

Table 2. Calculated Vibration frequencies of BTHTO and $PdCl_2$ • 2BTHTO (Scaled factor: 0.8929)[a]

Normal mode	BTHTO		Pd (II) BTHTO complexes				
	Expt	Cal	Expt	Complex A	Complex B	Complex C	Approx. Mode descriptions
A	2955	**2915**	2956	**2913**	**2914**	**2911**	Yas -CH3
A	2929	**2897**	2926	**2897**	**2885**	**2897**	I/as -CH2-
A	2864	**2858**	2859	**2859**	**2855**	**2859**	*Vs* -CH2-
A	1458	**1468**	1458	**1468**	**1468**	**1469**	8 s -CH2-
A				**1078**	**1080**	**1080**	T -cH2-(cycle)
A	1017	**995**	1116		**1061**	**1066**	Vs-O
A			922	**925**		**931**	Vs-o
Total energy[6]				**-956.5322**	**-956.5329**	**-956.5346**	

a. Frequency in cm'[1]; b. By B3LYP/6-31G* (for metal Pd (II), LANL2DZ basis set is used)

CONCLUSIONS

The calculation results of BTHTO and its Pd(II) complexes showed vibration v_s=*o* of sulfoxide will shift to higher wavelength number by S-coordination, and shift to lower wavelength number by O-coordination. Model complex C is the most stable one among three possible isomeric BTHTO-Pd(II) complexes..

REFERENCES

1. **K. William, J. M. Christopher, D. David (1970),** *Inorganic Chemistry,* **9, 541-549.**
2. **S. P. Wu, G. B.Gu (2002),** *Precious Metals,* **23, 11-16.**
3. **S. P. Wu, G. B.Gu (2002),** *Chinese Journal of Rare Metals.,* **26,217-220.**
4. **M. J. Frisch, G.W.Trucks, H. B. Schlegel, et.al. Gaussian 98 (Revision A.7), Gaussian, Inc., Pittsburgh PA, 1998.**
5. **M. Calligaris, O. Carugo (1996),** *Coordination Chemistry Reviews,* **153, 83-154.**
6. **W. S. Jenks, N. Matsunaga, M. Gordon (1996),** *J. Org. Chem.,* **61, 1275-1283.** [24]

STUDY ON SURFACE PROPERTIES FOR PURE AND MIXED FLUIDS WITH DENSITY FUNCTIONAL THEORY

Lu Jiufang, Wu Wei, Liu Jinchen, Chen Jlan, and Li Yigui

State Key Laboratory of Chemical Engineering, Department of Chemical Engineering, Tsinghua University, Beijing 100084, China

The surface properties of pure and mixed non-polar fluids are studied by the density functional theory (DFT). A reasonable long rang correction is adopted to avoid the truncation of the potential. The perturbation theory is applied to establish the equation of state for the phase equilibrium, in which the hard-core chain fluid is used as the reference fluid and the Yukawa potential is used as the perturbation term. Three parameters, *elk, d* and m_s, are regressed from the vapor-liquid equilibria. The surface properties, including density profile, surface tension, local surface tension profile and thickness of the surface region, can be predicted for the pure non-polar liquids with these parameters, and the surface properties for mixed liquids can be calculated with two additional mixing parameter.

INTRODUCTION

The interface between two liquids is the way for mass transfer in the liquid-liquid extraction systems. The surface is the interface between the liquid and vapor faces, and the surface properties are much like the interface properties between the two liquids, so the study on the surface properties for liquids is important in liquid extraction technology. The interface is an inhomogeneous region with definite thickness, and there are continuous changes for the properties such as density and composition in this region. The density functional theory (DFT) [1,2] is one of the most popular approaches based on statistical mechanics for the inhomogeneous fluid, and it is widely used for the study on the interface properties.

Winkelmann *et al.* [3-5] did a systematic investigation about the application of density functional theory for the surface properties of simple liquids and their mixtures. According to their description, the intermolecular potential is cut-off which means the long-range interaction is truncated. Fu *et al.* [6] established a new method for the study of the surface properties of Lennard-Jones fluid by assuming that the density profile can be described as a hyperbolic tangent curve. Up to now there are a few papers published about the surface properties for mixed liquids.

THEORIES

The intermolecular potential used in this work is a hard sphere potential coupled with an attractive Yukawa potential:

$$u(r) = \begin{cases} \infty & r < d \\ -\varepsilon \dfrac{\exp[-z(r-d)/d]}{r/d} & r > d \end{cases} \quad (1)$$

where *r* is the distance between two molecules, *e* is the energy parameter representing the

minimum energy between two molecules, d is the hard sphere diameter, z_m is the Yukawa range parameter that attributes the rate of potential decay.

The grand canonical ensemble is applied in the density functional theory. As the external potential of free surface is zero, the grand potential functional Q[{p(r)}] is expressed as follows [1]:

$$\text{^\{Mr)\}] = } F_{mt}[\{p(r)\}]\text{-\}X[P(r)//,]dr \quad (2)$$

where r is a vector that refers to a position in the system, dr is the integration volume element, r is the phase space, {/?(r)} is the local number density of molecules, ^K/Kr)}]

is the 'intrinsic' Helmholtz free energy functional, the perturbation expansion of which is as the follows:

$$\text{^[\{p(r)\}]^}^{re/}\text{[\{p(r)\}] + F}^{P}\text{"[\{p(r)\}]} \quad (3)$$

where $I\text{-}^{ref}[\{p(r)\}]$ is the reference term, $F^{per}[\{/?(r)\}]$ is the perturbation term.

Ignoring the short-range correlation contribution to free energy of reference fluid according to the local density approximation (LDA) method, the reference item F^{ref} can be expressed with the local density:

$$F^{ref}\,[\{p\{r)\}]\backslash = \text{Jdr/}'^{r0}[\{p(r)\}] \quad (4)$$

where $/,^{0}[\{p(r)\}]$ is the Helmholtz free energy density of the homogeneous reference liquid whose density is $p(r)$.

The reference fluid is hard-core chain fluid, so the Helmholtz free energy density is as follows:

$$/r^{\circ}[\{p(r)\}] = /'^{d}[\{Mr)\}] + /^{hs}[\{p(r)\}] + /^{cha,n}[\{p(r)\}] \quad (5)$$

where $/^{ld}[\{/?(r)\}]$ is the term of the ideal gas with the same density and temperature as the real system, $/^{hs}[\{/?(r)\}]$ is the hard-sphere fluids term, which is obtained from Carnahan-Starling equation [7] for pure liquids, or from MCSL equation [8] for mixed liquids, $/^{chain}[\{p(r)\}]$ is the term of hard sphere chain formation which is obtained from the statistical associating fluid theory (SAFT) [9],

The mean field approximation (MFT) is adopted to simplify the calculation process, and the Dirac Delta function is introduced to express the radial distribution function at the contacting point.

$$8^{h}\backslash r) = \begin{cases} 0 & (r<d) \\ (o(r)S(r-d) & (r = d) \\ 1 & 0_{r>d}\ ) \end{cases} \quad (6)$$

The grand potential functional $fi[\{/?(r)\}]$ has a minimum at equilibrium. The density

distribution $p_0(r)$ can be obtained by minimizing Eq.(2). The necessary condition for functional £l[{p(r)}] attaining its minimum value is <$Q = 0, which is Euler-Lagrange equation. Thus the chemical potential expression is:

$$P = \frac{SF_{ideal}}{\delta\rho} = \frac{(df^{r0}\backslash SF^{1*''}}{1\,dp\;J_T\;5p} = \left(\frac{'df^{d'}}{<^{d}P,}\right)_T + \left(\frac{'df^{**''}}{,\,dp,}\right)_T + \left(\frac{^{f}Qjchain>}{\approx}\right) + \frac{SF^{per}}{6p} \qquad (7)$$

Then the chemical potential p in the system is obtained, and the density distribution in an equilibrium system can be calculated by solving the equations $p[p(z_1)] = p[p(z_2)]$, where z is the direction perpendicular to the surface.

For a system with plain surface, the grand potential functional Q is:

$$Q = /A\text{-}pV \qquad (8)$$

where p is the bulk phase pressure, which equals to the normal part of the pressure tensor in the surface, V is the total volume of the system. The 'local' surface tension $y(z)$ is defined as[10]:

$$r(z) = f[p(z)\backslash\sim pp(z) + p \qquad (9)$$

The surface tension is obtained as

$$r = \backslash \int_{-\infty}^{\infty} \gamma(z)\mathrm{d}z \qquad (10)$$

When p and p are obtained, both the profile of the density and local surface tension can be computed. These two parameters are solved from the vapor-liquid phase equilibrium.

CALCULATION

The vapor-liquid surface region with thickness of 60d along the z direction is divided into N layers, where d is the diameter of segment. With this treatment, the Adams-Moulton method is adopted to calculate the numerical integration. The ranges of integration in Eq. (9) are (-oo,+oo), the integration in the region out of the identification must be calculated additionally as a long-range correction (LRC). The thickness of surface region is several times of molecular diameter at normal temperature, so the range of 60d is enough for holding a complete surface region. The surface region is located at the middle, and the densities out of the range are the bulk densities.

The density profile, which makes the calculated chemical potential in every layer equal to one another, can be obtained with the above equations. In the computation process the criterion is that the maximum relative deviation of the calculated chemical potentials between two layers are less than 0.001%. Three molecular parameters, hard sphere diameter d, minimum potential energy s and segment number m_s, are needed for the pure non-polar fluid in this method. Two methods are used to obtain these three parameters, in the first method the parameters are regressed from vapor-liquid equilibrium data, in this case the surface tensions are predicted. In another method they are regressed from surface tensions data. The mixing parameter is needed for mixed liquids, which is regressed from surface tensions data.

For convenience, some reduced thermodynamic quantities are used, they are: $T^* = kT/s$, $z^* = z/d$, $p'' = pd^y$ and $y^* = yd^2/e$. [27]

RESULTS AND DISCUSSIONS

The reduced surface tensions for pure non-polar fluids with different segment number are computed, and the results are shown in Fig. 1. From this figure, it can be found that at the same reduced temperature *T, the larger m_s is, the greater 7* will be. With increasing/?^ , the decreasing rate of 7* with *T** rise will be reduced. It is because the attractive interaction is more affected by m_s than the repulsion, and the surface tension is derived from the intermolecular attraction directly. This figure shows also that the surface tension 7* reaches zero at the critical temperature. The profiles of the reduced density and the reduced chemical potential of one-segment molecule are given in Fig.2. The density profile shows that the region of the surface is expand when the temperature is up. The chemical potential profile represents that the chemical potential does not depend on the space position in a thermodynamic equilibrium, which is the prime criterion forjudging whether the iteration has finished successfully.**

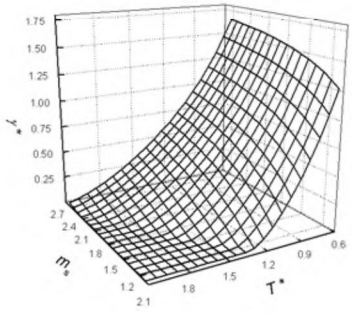


Fig. 1 Relationship between surface tension with segment number and temperature

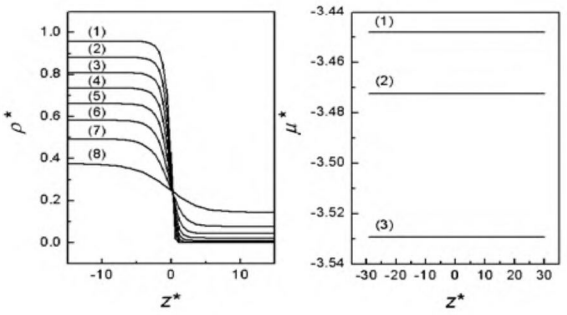


Fig. 2 Reduced density and chemical potential profile in different temperatures for one segment molecule
(1): **T*=0.5;** *(2): V=0.6; (3): T*=0 7; (4):* **T*=0.8,** *(5): T*=0.9; (6): T*=1.0; (7): V=1.1; (8): V=1.2.*

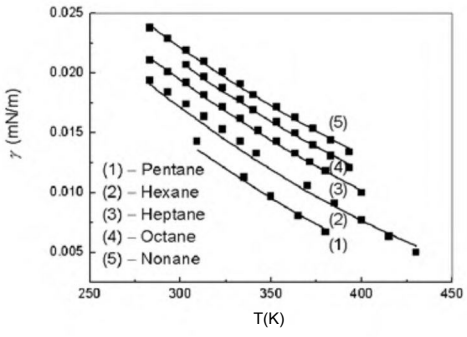


Fig. 3 Comparison of predicted surface tension with experimental data in different temperatures for multi-segment molecules

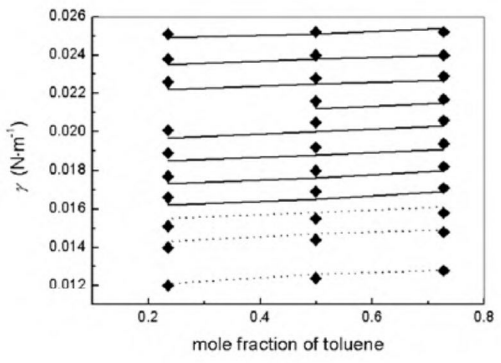


Fig. 4 Surface tension of toluene-benzene mixture at different temperatures
points: experimental data, solid line: regressed results, dot line: predicted results, the temperatures up to down are:323.15K. **333.***15K, 343.15K, 353.15K, 363.15K, 373.15K, 383.15K, 393.15K, 403.15K, 413.15K.423.15K.*

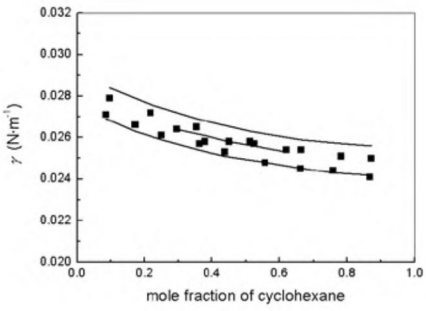


Fig. 5 Surface tensions of cyclohexane-benzene mixture at different temperatures (the temperatures from top to bottom are 293.15K, 298.15K, 303.15K)
• **experimental data, — regreesed results**

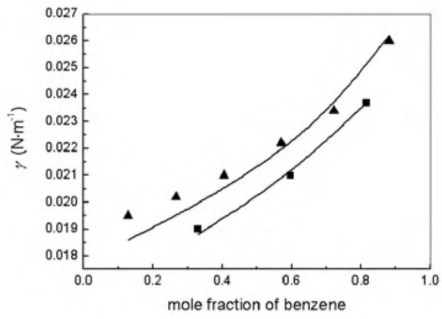


Fig. 6 Surface tensions of benzene-n-hexane mixture at different temperatures
points: experimental data, lines: regreesed results
▲ *293.15K, »303.15K*

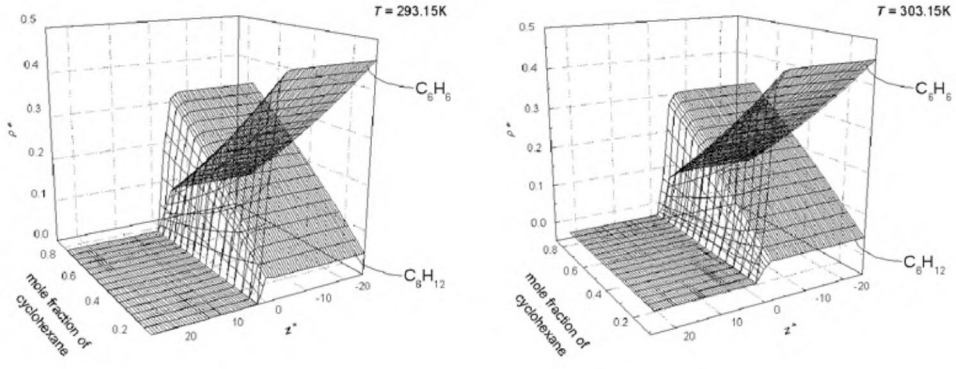


Fig. 1 Surface density profile of cyclohexane-benzene mixture

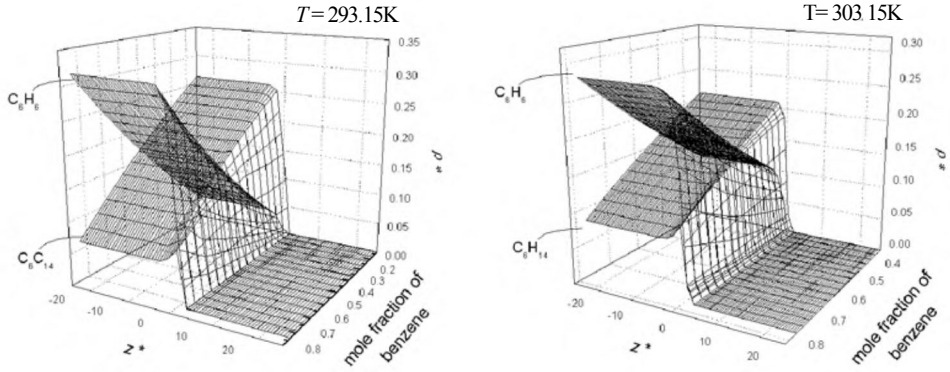


Fig. **7** *Surface density profile of benzene-n-hexane mixture*

The methane is chosen as the standard one-segment molecule, and then the best range parameter *z* is obtained from the regression of the methane VLE, which equal to 1.985.

For other compounds, only the molecular parameters, *d, e* and m_s are needed. The total average relative deviation (ARD) of saturated pressure is 6.69%, and the ARD of density is 3.29 %. These parameters are used to predict the surface properties of the same compound. The surface tensions for 16 pure non-polar liquids are predicted. The total ARD of *y* is 3.87%. The predicted results for some liquids are shown in Fig 3. It shows that the prediction for the surface tension is satisfactory.

The surface tensions of 6 **mixed liquids are calculated with the mixing parameter k_{tj}, which** [29]

are obtained from the experimental surface tension data at some temperatures, then the surface tension at other temperatures are predicted. The surface tension of toluene-benzene system is shown in Figs. 4~6. It shown both the regressed and predicted results are agreed with the experimental data. The density profiles of mixed liquids are shown in Fig 7 and fig 8. **The Fig 7 and Fig 2 show that the density distributions change monotonously for pure liquids and both components of some mixed liquids, but Fig** 8 **shows that it may have enrichment for the component with less surface tension in other mixed liquids. From Fig** 8 **it can be seen that when the temperature is higher, this kind of enrichment will be reduced. The above results show that the hyperbolic tangent function, which used to describe the density profile of pure liquids very often, may be unable to be used for mixed liquids.**

CONCLUSIONS

The density functional theory is applied to study the surface properties for pure non-polar fluids and mixed liquids. The surface properties for 16 pure liquids and 6 **mixed liquids are calculated. The calculated surface tensions agree well with the experimental data. The calculated local density profiles for binary mixtures show that the enrichment of the component in the surface may happen. The results show that the hyperbolic tangent function, which used to describe the density profile of pure liquids, may be unable to be used for mixed liquids.**

ACKNOWLELEGEMENTS

This work is supported by the National Nature Science Foundation of China (No. 20102007) and the Fundamental Research Fund of Tsinghua University of China (No. JZ2002003).

REFERENCES

1. **R. Evans (1979),** *Adv. Phys.,* **28, 143-200.**
2. **R. Evans (1992),** *Fundamentals of Inhomogeneous Fluids,* **edited by Henderson, D.Marcel Dekker: New York.**
3. **J. Winkelmann, U. Brodrecht, and I. Kreft (1994),** *Ber. Bunsen-ges. Phys. Chem.,* **98, 912-919.**
4. **J. Winkelmann (1994),** *Ber. Bunsen-ges. Phys. Chem.,* **98, 1308-1316.**
5. **J. Winkelmann (2001),** *J. Phys.-Condes. Matter.,* **13, 4739.**
6. **Fu D., Lu J.-F., Liu J.-C. and Li Y.-G. (2001),** *Chem. Eng. Sci.,* **56, 6989-6996.**
7 **N. E. Carnahan, K. E. Starling (1969),** *J. Chem. Phys.,* **51, 635-636.**
8. **G. A. Mansoori, N. F Carnahan, K. E. Starling and T. W. Leland (1971),** *J. Chem. Phys.,* **54, 1523-1525.**
9. **W. G. Chapman, K. E. Gubbins, G. Jackson and M. S. Radosz (1990),** *Ing. Eng. Chem. Res..* **29. 1709-1723.**
10. **B. D. Smith and R. Srivastava,** *Thermodynamic Data for Pure Compounds, Part A: Hydrocarbons and Ketones,* **Elsevier, Amsterdam-Oxford-New York-Tokyo, 1986** [30]

SEPARATIONS OF METAL IONS USING IONIC LIQUIDS: THE CHALLENGES OF MULTIPLE MECHANISMS

Violina A. Cocalia, John D. Holbrey, Keith E. Gutowski, Nicholas J. Bridges, and Robin D. Rogers*

**Department of Chemistry and Center for Green Manufacturing
The University of Alabama, Tuscaloosa, AL 35487, U.S.A.**

Ionic liquids are a distinct sub-set of liquids, comprising only of cations and anions, often with negligible vapor pressure. As a result of the low or non-volatility of these fluids, ionic liquids are often considered in liquid/liquid separations schemes where the goal is to replace volatile organic solvents. Unfortunately, it is often not yet recognized that the ionic nature of these solvents can result in a variety of extraction mechanisms, including solvent ion-pair extraction, ion exchange, and simultaneous combinations of these. Here we discuss current ionic liquid-based separations research where the effects of the nature of the solvent ions, ligands, and metal ion species were studied in order to be able to understand the nature of the challenges in utilizing ionic liquids for practical application.

INTRODUCTION

Ionic Liquids (ILs) are proving to be increasingly interesting fluids for application in soft-matter materials systems from electrochemistry to energetic materials, and are also studied as potential solvents in separations processes [1-19], Properties including low melting points, wide liquid ranges, and negligible vapor-pressure, have encouraged researchers to explore the uses of ILs to replace volatile organic solvents (VOCs).

Seddon [20] has remarked that over 10^{18} simple organic salts that might be potential ILs could be prepared by varying the substitution patterns and anion choices, even just within imidazolium and pyridinium systems. High symmetry pseudo-spherical, non-coordinating anions are commonly regarded as optimal for formation of ILs. Common examples of cations and anions which have been most widely investigated with regard to ionic liquid phase formation are shown in Figure 1. Common anions that yield ILs include hexafluorophosphate ($[PF_6]'$), tetrafluoroborate ($[BF_4]'$), bis(trifyl)imide ($[(SO_2CF_3)_2N]'$ or $[Tf_2N]'$), and chloride (Cl). [39]

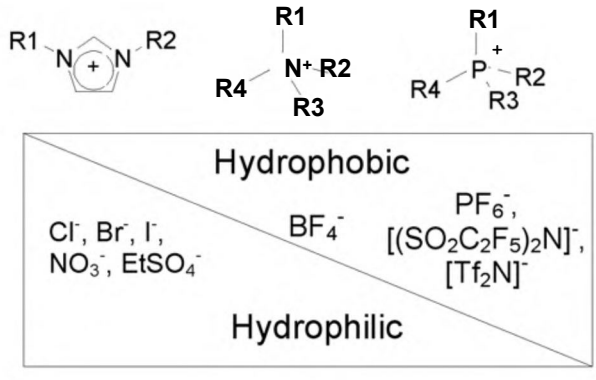


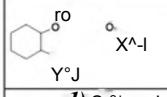
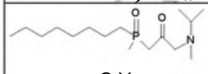
Figure 1. Examples of IL cations and anions.

Differences in solvent behavior of ILs and conventional organic solvents, especially for hydrophobic ILs, have been manifested in different and enhanced distribution of metal extractant complexes in two phase systems. The presence of two charged species from the ionic solvent itself, in an IL/aqueous biphasic system, makes metal ion separation a much more complex process than in traditional solvents. This doesn't necessary mean that ILs are not suitable for separation processes (although for some ILs that is the case), but one needs to find the right combination of IL and ligand to obtain similar behavior as in organic solvents or one needs to use the differences from organic solvents for achieving more advantageous separations.

The first investigations of metal ion extraction in IL/aqueous systems showed extremely high metal ion partitioning to the IL phase [8,16], It was the success of these initial studies that led to conjecture that ILs could also be used for the removal of hazardous actinide ions and fission products from aqueous media. Further studies of different IL-based separation systems followed to elucidate the cause of the very high distribution ratios for metal ions. Dietz showed that the high distributions in IL/aqueous systems were due to a change in extraction equilibria in comparison to the octanol/aqueous system [17], In octanol Sr^{2*} is extracted as a strontium nitrato-crown ether complex (Table 1, eq. 3), whereas in ILs the two axial bound nitrates are substituted with two water molecules bound to the metal ion and the charged $Sr(CE)(H_20)_2^{2+}$ species, where CE is dicyclohexano-18-crown-6-ether, is transferred to the IL phase [18], The neutrality of the system is maintained through the migration of two imidazolium cations to the aqueous phase for each extracted metal ion. The loss of the IL components in the aqueous phase would be a major limitation for practical applications of ILs in separations (Table 1, eq. 1).

Further investigations on the same system, but using the more liphophilic IL, $[C_{10}mim][Tf_2N]$, demonstrated that the extraction mechanism in ILs can be the same as in octanol (Table 1, eq. 2). However, the coordination environment of the metal ion was found to be different than that observed in 1-octanol/water biphasic systems with nitrate ions lying outside of the metal ion's inner coordination sphere [21], [40]

Table 1. Extraction mechanisms in IL/aqueous vs. organic/aqueous biphasic systems.

Equilibrium Reaction for M'' Separation in ILs*	*Equilibrium Reaction for NT* Separation in Molecular Solvents*
 £ = ***Dicyclohexyl-18-crown-6***	
1) $Sr^{2*}_{,,} + L_{,}L + 2[C_5mim]^*iL + 2H_20 \bullet => [(SrL)(H_20)_2]^{2*}_{iL} + 2[C_smim]^*_{,q}$ [17] *or* ***2)*** $Sr^{2*}_{,,} + 2N0^-_{3,q} + L_{iL}$ o [SrL] $(N0_3)_{2\ ,L}$ [21]	$S^Sr^{2*}_{,,} + L_{„}g + 2N03\ ^-_{„}C=.\ [Sr(N0_3)_2L]_0r_S$ [17]
 *L = CMPO*	
4) $U0_2^{2*}_{,q} + [C_{„}mim]Y + NO_{,,}^- + I_{_,L}$ <=> $[(U0_2)N0_3)L]^*_{iL}$ + $[C_nmim]$ aq [23]	***51*** $U0_2^{2*}_{,,} + 2N0_3^-{}_{„} + 2Ur_9$ ■=■ $f(U0_2VN0_3l_2L_2l_{„9}$ T231
 ***L „ HUa***	
6) $Ln^{3**}_{,} + 4HL_{,}L + [C_4mim][Tf_2N]iL$ o $[C_{„}mim]^*$ [LnUfii + $4H^*_{a„}$ + [Tf2Nr„ [22]	*7)* $Ln(H_20)_{„}^{3*}_{„} + 3HL_{„g}$« $[LnL_3(H_20)_{„\cdot 6}]_{org} + 3H^*_{,q} + 6H_2O_{lq}$ [22] *and* *8)* $Ln(H_20)_{n}^{3*}_{,q} + 4HL_{org}$ <=> $LnLj^*\ HL_{\ 0,q} + 3H^*_{,q} + nH_2O_{aq}$ [22]

The nature of the IL is not the only factor which determines the metal extraction pathway; ligand type also has a very important contribution. Lanthanide(III) salts were shown to follow an anion exchange mechanism (Table 1, eq. 6) when extracted in an IL/aqueous system using Htta; in contrast to the cation exchange observed in molecular solvents (Table 1, eqs. 7-8) [10], Here, changing the lipophilicity of the IL did not change the partitioning mechanism.

Another example of different behavior of metal ion extraction in ILs was observed by Visser, et al. who showed that the high extraction of $U0_2^{2+}$ with the well studied CMPO ligand to an IL phase, was due to a different mechanism (Table 1, eqs. 4-5) than observed in molecular organic solvents [23], Further, it was demonstrated that the metal ion coordination environment in the extracted species was also different than observed in organic solvents. The coordination environment of uranyl nitrate with CMPO and TBP in a series of hydrophobic ILs was probed using both UV/Vis spectroscopy and extended X-ray absorption fine structure (EXAFS) spectroscopy. Differences in UV/Vis peak location and intensity patterns (Figure 2) in ILs vs. dodecane illustrated their inequivalence. [41]

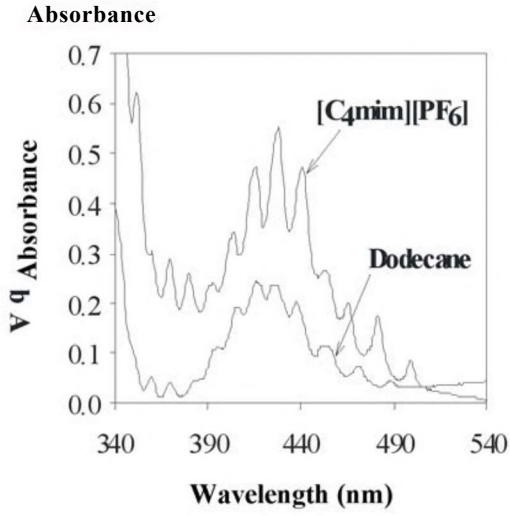


Figure 2. Absorption spectra of dodecane and [C4mim][PFe] solutions containing 0.1 M CMPO and 1 M TBP, after contact with 20 mM $U0_2(N0_3)_2$ in 1 M $HN0_3$ from ref. [23].

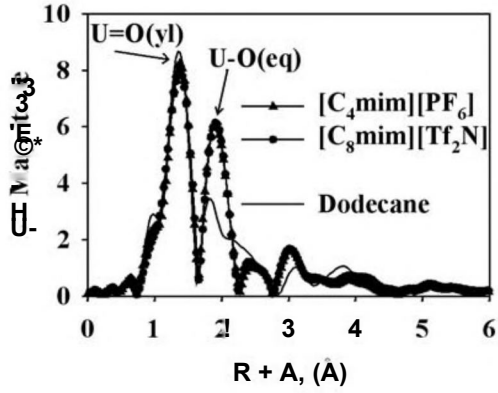


Figure 3. Fourier transform magnitude of the k^3 weighted L_3 EXAFS of the $U0_2^{2+}$ complexes in dodecane, $[C_4mim][PFe]$, and $[C_8mim][Tf_2N]$ from ref. [23],

The coordination environment around the metal ion in each instance was further clarified using EXAFS (Figure 3). The EXAFS data for the uranyl-CMPO complex in dodecane was consistent with a hexagonal bipyramidal $U0_2(N03)_2$(CMP0)2 complex, while the data in $[C_4mim][PF_6]$ and $[C_8mim][Tf_2N]$ suggested an average equatorial coordination number of 4.5, yielding a net stoichiometry of $U0_2(N0_3)(CMPO)^+$. The differences observed between the two types of solvents (ILs and molecular) illustrated the importance of elucidating the unique coordination interactions that occur in the ILs to optimize separations performance.

Clearly, coordination, speciation, and extraction mechanism can and do vary from those in conventional solvent systems. The challenge is now to use the differences from traditional solvents efficiently and develop unique and more advantageous separation schemes, or to find the combinations of ILs and ligands which behave in an identical manner to molecular organic solvents. In our current work we have studied a range of separation schemes in order to gain a better understanding of the relative roles and importance of complexant, metal, and IL ions to achieve these tasks. Here we review some of the preliminary data coming from these studies.

RESULTS AND DISCUSSION

Ligand assisted metal ion partitioning

We have investigated Cyanex-923 as an extractant for actinide ions in liquid/liquid separations using the hydrophobic IL $[Ci_0mim][Tf_2N]$ as the extracting phase. Cyanex-923 is a neutral complexant that is a mixture of tri-alkyl-phosphine oxides of varying chain lengths (hexyl- and octyl-) and has been used for actinide extraction into molecular solvents [12]. Distribution ratio measurements for Pu^{4+} and Am^{3*} showed little acid dependency ($HN0_3$) for Pu^{4+}, but strong acid dependency for the trivalent actinide. In addition, ligand dependency studies seem to support [42]

1:1 metal-to-ligand binding for Pu^{4+}, but significantly different binding ratios for Am^{3*}, again supporting the notion that ILs can provide different coordination environments.

The high distribution ratios for Pu^{4+} and lack of acid dependency (Figure 4) precludes stripping using a pH or concentration swing. Since oxalate has a high affinity for tetravalent actinides such as plutonium, forming hydrophobic anion complexes, the ability to strip extracted Pu^{4+} from the IL using oxalate as a stripping agent was investigated. The stripping of Pu^{4+} from Cyanex-923 from dodecane (85%) was more efficient that in the IL (70%) (Figure 5), although conditions were not optimized.

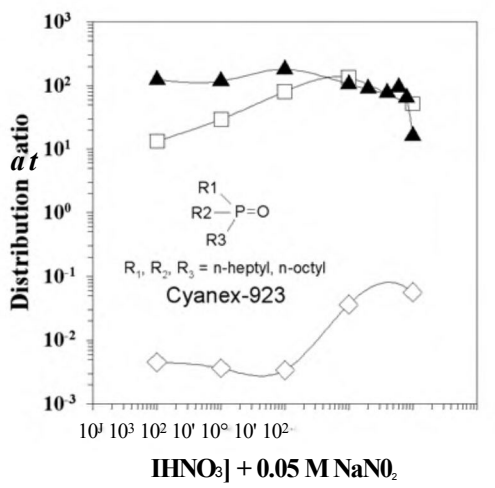


Figure 4. Distribution of Pu^{4*} to 0.10 M Cyanex-923 in [C_{10}mim][rf_2N] (a), 0.10 M Cyanex-923 in dodecane (A), and [C_{10}mim][Tf_2N] blank (0) versus [HNOJ.

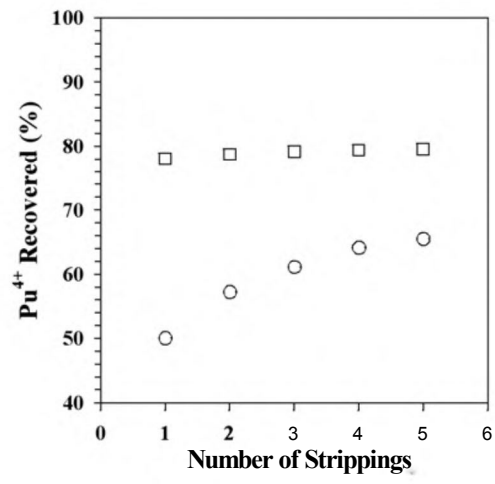


Figure 5. Pu^{4*} stripping from 0.1 M Cyanex-923 in dodecane (O) and [C_{10}mim][Tf_2N] (o).

A second class of complexants we are currently investigating are closely related to siderophores. Siderophores are molecules produced by bacteria to bind Fe^{3+} in iron-deficient environments. The binding constants for Fe^{3+}can be as high as 10^{52} in some cases and their relative affinities for a series of metals is based on charge-to-size ratio. Due to the similarities in charge-to-size ratio between Fe^{3+} and Pu^{4+}, siderophores can be highly effective sequestering agents for Pu^{4+} from solution. The siderophore-derived molecule, 1-hydroxy-6-/V-octylcarboxamide-2(1 H)-pyridinone (octyl-1,2-HOPO), has been studied by Raymond for the extraction of plutonium species from acidic media into octanol [13],

We have studied the partitioning of Pu^{4+} with octyl-1,2-HOPO in IL/aqueous systems incorporating the hydrophobic ILs [C_4mim][Tf_2N] and [C_8mim][Tf_2N] (Figure 6). Effects of cation hydrophobicity and lipophilicity (controlled by variation in the length of the alkyl-chain substituents) could be observed and can be related to changes in extraction mechanism following the observations made by Dietz, et al. [21], [43]

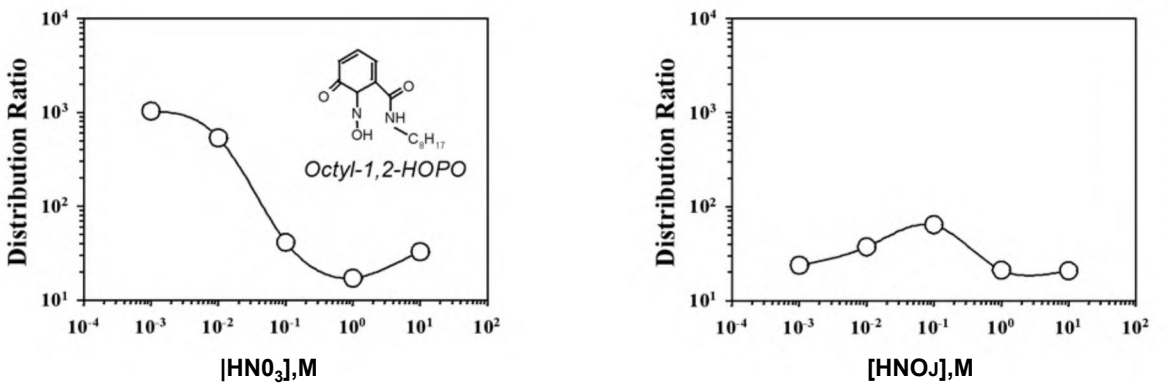


Figure 6. Pu[4] distribution ratios for 0.003 M octyl-1,2-HOPO in [C_4mim][Tf_2N] (right) and [$C_B$mim][Tf_2N (left) versus [HNOJ.*

Interestingly, the IL with the butyl chain (least lipophilic) resulted in Pu^{4+} distribution ratios which were nearly acid independent, whereas the IL with the octyl chain showed extraction behavior that was strongly acid dependent; the latter most closely paralleled the distribution ratios obtained from the octanol system. In both ILs, however, the ligand dependency observed was significantly different from those in octanol. In octanol, four octyl-1,2-HOPO ligands are bound to each Pu^{4+} ion in the extracting phase, whereas in the IL, a lower ligand:metal ratio was observed, with, presumably, nitrate anions filling the remainder of the plutonium coordination sphere.

Most importantly, it can be seen that the IL environment can greatly affect the degree to which an extractant molecule interacts with a metal ion, thus supporting the need for more targeted studies aimed at elucidating the nuances of IL coordination chemistry for the ultimate design of better, tailored ILs for application to more complex systems. These studies are now underway.

Hydrophilic ILs in liquid/liquid separation

Hydrophobic ILs are not the only choice for liquid/liquid IL-based separation of metal ions. We recently showed that hydrophilic ILs such as 1-butyl-3-methylimidazolium chloride ([C_4mim]Cl), can also be induced to form biphasic systems that are wholly aqueous in nature via the addition of concentrated aqueous solutions of water-structuring salts such as K_3P0_4 (Figure 7) [14], These aqueous biphasic systems (ABS) can be formed from a wide range of IL types, including imidazolium-, pyridinium-, phosphonium-, and ammonium-based salts, as well as, with a variety of inorganic salts including phosphates, carbonates, hydroxides, and sulfates. These systems contain two aqueous phases: the upper phase is more lipophilic (containing organic cations), whereas the lower, more dense phase consists of a concentrated inorganic salt solution. [44]

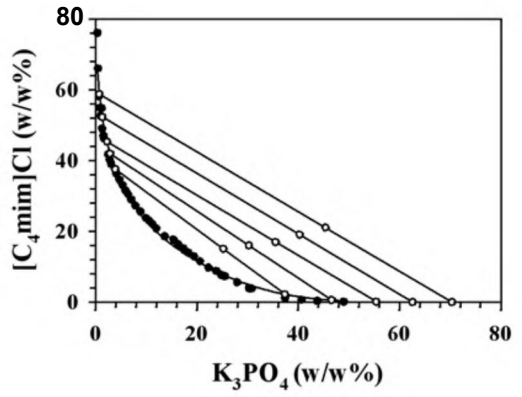


Figure **7.** *The mutual coexistence curve for the aqueous [C_4mim]Cl/K_3P0_4 system from ref. [26], System compositions below the binodal are monophasic, compositions above the binodal are biphasic.*

It is important to note that many of these inorganic salts are present in large amounts in nuclear tank wastes. As a result, these salt-salt biphasic systems are excellent models to critically investigate the behavior and sustainability of ILs with regard to stability and ion exchange under tank waste conditions. For example, it was found that distribution ratios for $Tc0_4^-$ from a concentrated K_3P0_4 solution to the IL-rich phase will exceed 700 and increase with increasing tie line length, without the need for an extractant. This is similar to polyethylene glycol-based aqueous biphasic systems where $Tc0_4$' was found to partition to the polyethylene glycol-rich phase [27], This offers the potential to remove $Tc0_4$' from tank waste using IL technology. In addition, further studies of the role of the IL anion and cation in these systems will aid in developing new ILs that are better suited for tank waste applications.

CONCLUSIONS

Separations utilizing ILs as the extracting phase are much more complex that those with simple molecular organic solvents. However, understanding the IL systems and choosing appropriate conditions to design targeted extractions is possible. One can either take advantage of the different extraction mechanisms which ILs afford, or one can find those separations, ligands, and ILs which afford identical behavior to molecular solvents. Our preliminary results, which will be presented at the conference, show that separation schemes in ILs can indeed utilize the same extraction mechanism while preserving the same metal ion coordination found in traditional solvents, but only when an appropriate metal ion/ligand/IL system is used. This argues once again, for a more complete fundamental understanding of IL systems in general.

ACKNOWLEDGEMENTS

This research is supported by the U.S. Department of Energy, Division of Chemical Sciences, Geosciences, and Biosciences, Office of Basic Energy Research (Grant DE-FG02-96ER14673), and Office of Environmental Management, Environmental Management Science Program (Grant DE-FG07-01ER63266). The authors thank Cytec Inc. and 3M for gifts of Cyanex (272® and 923) and Li[Tf_2N], respectively.

REFERENCES

1. **Ionic Liquids as Green Solvents: Progress and Prospects, R. D. Rogers, K. R. Seddon, (eds.), ACS** *Symposium* **Series 856, American Chemical Society:** *Washington, DC,* **2003.**
2. **Ionic Liquids: Industrial Applications to Green Chemistry; R. D. Rogers, K. R. Seddon (eds.), ACS** *Symposium* **Series 818, American Chemical Society:** *Washington, DC,* **2002.**
3. **T. Welton (1999),** *Chem. Rev.,* **99, 2071-2084.**
4. **J. D. Holbrey and K. R. Seddon (1999)** *Clean Prod. Proc.,* **1,223-236.**
5. **P. Wasserscheid and W. Keim (2000),** *Angew. Chem. Int. Ed.,* **39, 3772.**
6. **J. Dupont, R. F., de Souza, and P. A. Z. Suarez (2002),** *Chem. Rev.* **102, 3667-3692.**
7. **A. E. Visser, R. P. Swatloski, W. M. Reichert, S. T. Griffin, and R. D. Rogers (2000),** *Ind. Eng. Chem. Res.,***39, 3596-3604.**
8. **S. Chun, S. V. Dzyuba, and R. A. Bartsch (2001),** *Anal. Chem.,* **73, 3737-3741.**
9. **J. G. Huddleston, H. D. Willauer, R. P. Swatloski, A. E. Visser, and R. D. Rogers (1998),** *Chem. Commun.* **16, 1765-1766.**
10. **A. E. Visser, R. P. Swatloski, and R. D. Rogers (2000),** *Green Chem,* **1, 1-4.**
11. **A. E. Visser, R. P. Swatloski, W. M. Reichert, R. Mayton, S. Sheff, A. Wierzbicki, J. H. Davis, Jr., and R. D. Rogers (2001),** *Chem. Commun.,* **1, 135-136.**
12. **A. E. Visser, R. P. Swatloski, S. T. Griffin, M. P. Hartman, and R. D. Rogers (2001),** *Sep. Sci. Technol.,* **36, 785-804.**
13. **L. A. Blanchard, Z. Gu, and J. F. Brennecke (2001),** *J. Phys. Chem. B.,* **105, 2437-2444.**
14. **A. G. Fadeev and M. M. Meagher (2001),** *Chem. Commun.,* **3, 295-296.**
15. **L. C. Branco, J. G. Crespo, and C. A. M. Alfonso (2002),** *Angew. Chem. Int. Ed.,* **41, 2771-2773.**
16. **S. Dai, Y. H. Ju, and C. E. Barnes (1999),** *Dalton Trans.,* 8**, 1201-1202.**
17. **M. L. Dietz and J. A. Dzielawa (2001),** *Chem. Commun.,* **20, 2124-2125.**
18. **M. P. Jensen, J. Dzielawa, P. Ricket, and M. L. Dietz (2002),** *J. Am. Chem. Soc.,* **124, 10664-10665.**
19. **A. E. Visser, S. T. Griffin, D. H. Hartman, and R. D. Rogers (2000), J. Chromatogr. B:** *Biomed. Sci. Appl.,***743, 107-114.**
20. **K. R. Seddon (1999), The International George Papatheodorou Symposium: Proceedings; S. Boghosian, V. Dracopoulos, C. G. Kontoyannis, and G. A. Voyiatzis (eds.), Institute of Chemical Engineering and High Temperature Chemical Processes:** *Patras,* **p 131.**
21. **M. L. Dietz, J. A. Dzielawa, I. Laszak, B. A. Young, and M. P. Jensen (2003),** *Green Chem.,* **5, 682-685.**
22. **M. P. Jensen, J. Neuefeind, J. V. Beitz, S. Skanthakumar, and L. Soderholm (2003),** *J. Am. Chem. Soc.,* **125, 15466-15473.**
23. **A. E. Visser, M. P. Jensen, I. Laszak, K. L Nash, G. R Choppin, and R. D. Rogers (2003),** *Inorg. Chem.,* **42, 2197-2199.**
24. **Y. Zhu and R. Jiao (1994),** *Nuclear Technology,* **108, 361-369.**
25. **V. V. Romanovski, D. J. White, J. Xu, D. C. Hoffman, and K. N. Raymond (1999),** *Solvent Extr. Ion Exch.,* **17, 55-71.**
26. **K. E. Gutowski, G. A. Broker, H. D. Willauer, J. G. Huddleston, R. P. Swatloski, J. D. Holbrey, and R. D. Rogers (2003),** *J. Am. Chem. Soc.,* **125, 6632 -6633.**
27. **R. D. Rogers, A. H. Bond, C. B. Bauer, J. Zhang, S. D. Rein, R. R. Chomko, and D. M. Roden (1995),** *Solv. Extr. Ion Exch.,* **13(4), 689-713.**

STUDY ON PHASE EQUILIBRIUM FOR SEPARATION OF HEXENE ISOMERS USING IONIC LIQUIDS

Zhu Jiqin, Chen Jian and Fei Weiyang

Department of Chemical Engineering, Tsinghua University, Beijing 100084, China

The separations of olefin isomers are very important but difficult since their very close boiling points. Room temperature ionic liquids are green solvents and have good potential for the separation of hexene isomers by extraction or extractive distillation. Therefore, binary and ternary isothermal vapor-liquid and liquid-liquid equilibrium data of hexene isomers with different ionic liquids were measured by headspace gas chromatography method. The solubilities of hexene isomers in ionic liquids were determined experimentally. The NRTL model was used to correlate the binary vapor-liquid equilibrium data to obtain interaction parameters, and then to predict ternary data compared with experimental ones.

INTRODUCTION

Higher a-olefins, mainly 1-hexene, are useful co-monomers in the production of HDPE and LLDPE. One of the production methods for 1-hexene is the new ethylene recovery process developed by Lummus, which involves the separation of 1-hexene from 3-hexene. The separations of olefin isomers are very difficult for their low relative volatility [1],

Room temperature ionic liquids are new green solvents that interest many researchers in recent years for their wide ranges of liquid state, negligible vapor pressures, high temperature stability, and high dissolving ability for both polar and non-polar organic, inorganic and organometallic compounds [2-4], The separation of aromatic compounds from aliphatic hydrocarbons using ionic liquids has been investigated [5, 6], While the separation of hexene isomers using ionic liquids have not been reported. The polarity of ionic liquids is strong and they will have different molecular interactions with hexene isomers. Also olefins can form reversible TT-complexes with transition metals, such as Ag^+ or Cu^+. In general, a-olefins complex with transition metal more easily than internal or branched olefins of the same carbon number because of different steric hindrances at the double bond [7], If the transition metal salts are dissolved or suspended in ionic liquids, a more effective solvent system for the separation of olefin isomers is expected.

Accurate experimental data of vapor-liquid equilibria (VLE) and liquid-liquid equilibria are necessary for the design of a separation process involving ionic liquids [8, 9], Because ionic liquids are hardly volatile while hexene are low-boiling point liquids, the headspace gas chromatography method (HSGC) was used to determine phase equilibrium data for the system of hexenes with ionic liquids.

EXPERIMENTAL

Materials

1-Hexene and *trans*-3-hexene with 99.5% purity were purchased from Fluka. 1-methyl-3-butylimidazolium hexafluorophosphate ([BMIM][PF_6]) and 1-isobutenyl-3-methylimidazolium tetrafluoroborate ([iBeMIM][BF_4]) ionic liquids were obtained from Institute of Chemistry, Chinese Academy of Sciences, and were purified by vacuum evaporation. $AgBF_4$ was purchased from Galtchem, with purity>99.5%. The mixture of ionic liquid and $AgBF_4$ mixture were made by dissolving crystalline $AgBF_4$ into [iBeMIM][BF_4] until saturation at 283.15K.

Procedures

The HSGC system consists of a HP5890 gas chromatograph and a HP19395A headspace auto-sampler. A hydrogen flame ionization detector (FID) and HP Ultra-2 capillary column (25m x0.2mm x0.33|jm) were used for the analysis. Because ionic liquids are very viscous, an electronic balance with an accuracy of 0.0001 g was used to determine the concentrations of liquid mixtures. The glass vials with sample mixtures were placed in the thermostat for more than 6 h to reach equilibrium. Then a constant amount of headspace vapor was transferred and analyzed by GC. For the measurement below 293.15K, a low temperature thermostat bath with an accuracy of 0.1 K was used to equilibrate and a Hamilton airtight syringe was used to transfer the headspace vapor. Before and after sampling, the syringe was placed in an air bath with a temperature of 303.15K. It was necessary to flush the syringe several times with the vapor to ensure reproducibility.

RESULTS AND DISCUSSION

The isothermal vapor-liquid equilibriums of 1-hexene + [BMIM][PF_6], frans-3-hexene + [BMIM][PF_6], 1-hexene +the mixture of [iBeMIM][BF_4] and $AgBF_4$, frar?s-3-hexene + the mixture of [iBeMIM][BF_4] and $AgBF_4$ were determined at the temperature of 283.15, 293.15 and 303.15K by the HSGC method. The experimental results were shown in Figs. 1 —4.

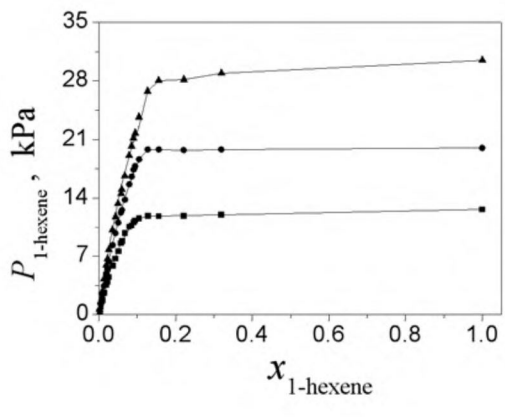


Figure 1. Experimental VLE data of 1-hexene in [BMIM][PF_6]. (■) 283.15K, (•) 293.15K, (A) 303.15K, (—) correlated with NRTL.

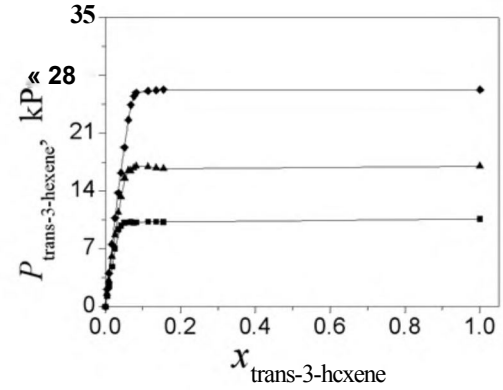


*Figure 2. Experimental VLE data of trans-3-hexene in [BMIM][PF_6]. **(a)** 283.15K, (•) 293.15K, (A) 303.15K, (—) correlated with NRTL.*

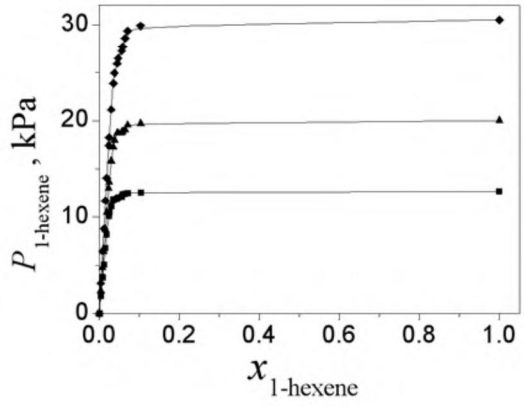


Figure 3. Experimental VLE data of 1-hexene in $AgBF_4$-[iBeMIM][BF_4]. (m) 283.15K, (•) 293.15K, (A) 303.15K, (—) correlated with NRTL.

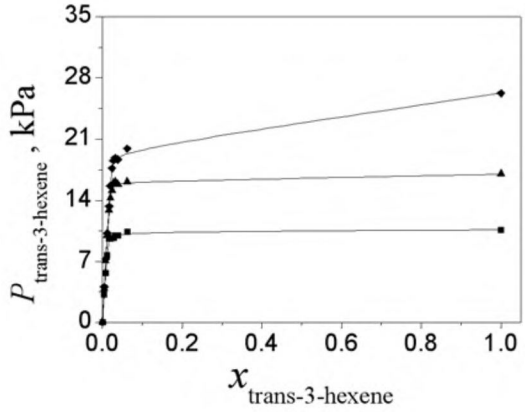


*Figure 4. Experimental VLE data of trans-3-hexene in [iBeMIM][BF_4]+ $AgBF_4$. (a) 283.15K, **(a)** 293.15K, **(A)** 303.15K, (—) correlated with NRTL.*

According to Figures 1-4, there are miscibility gaps for hexene isomers and ionic liquids. The observed larger miscibility gaps for frans-3-hexene compared to 1-hexene can be used for the separation of hexene isomers by liquid-liquid extraction. Using the method developed by Massaldi and King [10], the solubilities of hexene isomers in ionic liquids can be calculated and listed in Table 1.

Table 1. The solubilities of hexene isomers in ionic liquids

T, K	[BMIM][PF_6]		[iBeMIM][BF_4]+$AgBF_4$	
	•^1-hexene	•trans-3-hexene	•1 -hexene	trans-3-hexene
283.15	0.07888	0.03729	0.02616	0.01569
293.15	0.1008	0.05183	0.03168	0.01986
303.15	0.1189	0.06801	0.03473	0.02246

NRTL equation was used to correlate the VLE data and the interaction parameters Ty were obtained, where the non-randomness parameter a was set to 0.2. The correlated results were also shown in Figures 1-4. The binary VLE of 1-hexene + frans-3-hexene were measured and correlated with NRTL equation to get the binary interaction parameters.

Table 2. Experimental VLE data of 1-hexene+trans-3-hexene+[BMIM][PF_6]

*i	*2	yi		
		283.15 K	293.15 K	303.15 K
0.003465	0.03144	0.07435	0.07787	0.08154
0.006920	0.02791	0.1833	0.1894	0.1914
0.01039	0.02444	0.2870	0.2889	0.2920
0.01395	0.02110	0.3781	0.3816	0.3873
0.01717	0.01731	0.4641	0.4713	0.4811
0.02092	0.01406	0.5545	0.5701	0.5786
0.02444	0.01056	0.6457	0.6602	0.6740
0.02772	0.006986	0.7239	0.7342	0.7441
0.03110	0.003484	0.8046	0.8108	0.8111

Table 3 Experimental VLE data of 1-hexene+trans-3-hexene+ftBeWM][BF_4]+$AgBF_4$

*i	*2	yi		
		283.15 K	293.15 K	303.15 K
0.001860	0.01500	0.08858	0.09427	0.1012
0.002780	0.01402	0.1323	0.1386	0.1476
0.005580	0.01125	0.2693	0.2749	0.2921
0.008370	0.008439	0.4145	0.4188	0.4438
0.01119	0.005639	0.5739	0.5762	0.6015
0.01393	0.002808	0.7642	0.7651	0.7800
0.01488	0.001875	0.8285	0.8309	0.8369
0.01581	0.0009377	0.9063	0.9082	0.9085

Using NRTL equation with the interaction parameters fitted by binary VLE experimental data, the ternary VLE can be predicted. The comparisons of experimental and predictive data

by NRTL model at 283.15K were shown in Figs 5 and 6. In the two figures, the x (1-hexene) refers to its composition without the ionic liquids.

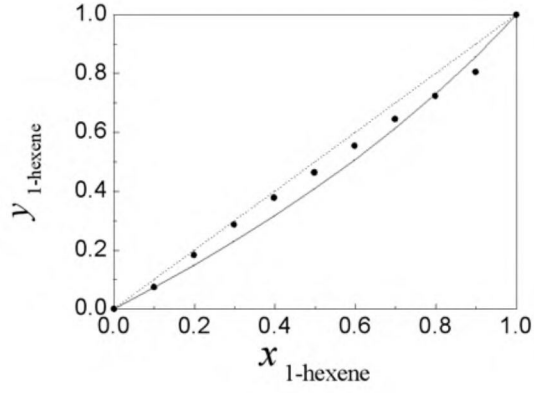


Figure 5. Experimental and predictive data of hexene isomers+[BMIM][PF_6] at 283.15K.

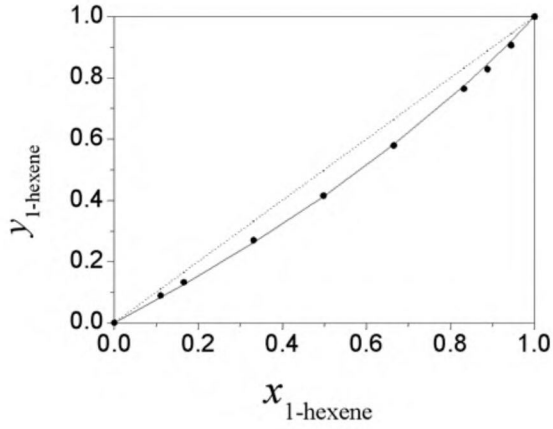


Figure 6. Experimental and predictive data of hexene isomers+silver [\BeWM][BF_A]+$AgBF_4$ at 283.15K.

Then the ternary VLE of 1-hexene (1) + *trans*-3-hexene (2) + [BMIM][PF_6] (3) and 1-hexene (1) + frans-3-hexene (2) + [iBeMIM][BF_4]+$AgBF_4$ (3) were measured by the same HSGC method at 283.15K, 293.15K and 303.15K. The results were listed in Tables 2 and 3.

It can be seen from Figs. 5 and 6 that the correlated NRTL parameters from binary experimental data can be used to predict the ternary VLE results. For the systems with [BMIM][PF_6] and [iBeMIM][BF_4]+$AgBF_4$, the overall average deviations for three temperatures are 9.97% and 2.34%, respectively.

CONCLUSIONS

The phase equilibria of hexene isomers and ionic liquids were studied. Ionic liquids are the potential solvents for extraction or extractive distillation of olefin isomers. NRTL model was used to correlate and predict the experimental data successfully.

REFRENCES

1. **A. E. Wentink, P. W. T. Krooshof, N. J. M. Kuipers, A. B. de Haan and H. Mulder(2002),** *Proc. ISEC'2002,* **1301-1306.**
2. **J. G. Huddleston, H. D. Willauer, R. P. Swatloski, A. E. Visser and R. D. Rogers (1998),** *Chem. Comm.,* **1765-1766.**
3. **A. Fadeev and M. M. Meagher (2001),** *Chem. Comm.,* **295-296.**
4. **A. E. Visser, J. D. Holbrey and R. D. Rogers (2002),** *Proc. ISEC'2002,* **South Africa.**
5. **M. S. Selvan, M. D. McKinley, R. H. Dubois and J. L. Atwood (2000),** *J. Chem. Eng. Data,* **45, 841-845.**
6. **T. M. Letcher and N. Deenadayalu (2003),** *J. Chem. Thermodynamics,* **35, 67-76.**
7. **W. W. S. Ho, G. Doyle and D. W. Savage (1988),** *Ind. Eng. Chem. Res.,* **27, 334-337.**
8. **S. P. Verevkin, T. V. Vasiltsova, E. Bich and A. Heintz (2004),** *Fluid Phase Equilibria,* **218, 165-175.**
9. **R. Kato, M. Krummen and J. Gmehling (2004),** *Fluid Phase Equilibria,* **224, 47-54.**
10. **H. A. Massaldi and C. J.King (1973),** *J. Chem. Eng. Data,* **18, 393-397.**



Solvent Extraction: Past, Present and Future (1975-2035)

M.H.I. Baird, McMaster University, Canada; and
T. C. Lo, T.C. Lo & Associate, U.S.A.

It is 30 years since the authors, with the inspiring collaboration of Professor Carl Hanson, began their editorial work on the Handbook of Solvent Extraction (Wiley-Interscience, 1983). We look back with gratitude to the leading personalities from industry and academia who contributed to the Handbook, and to the challenges which faced the researchers of those days.

We look at the sometimes unexpected ways in which the solvent extraction field has been evolving up to the present day, as reflected in the changes in the subject groups in the Proceedings of ISEC. For example, there has been a significant shift of interest towards the basic chemistry of new extraction system, along with a reduction in research in some fields such as nuclear extraction and the physics of equipment performance.

We venture to make a few predictions about the future of the field over the next 30 years. One of the most important challenges will be to keep track of the excellent work of the past which is still relevant to future developments.

In the coming years, solvent extraction will play an important role as the process industries changes and many challenges, especially with the growing use of new raw materials and lower grade ores as feedstocks, and the needs to save energy and to meet ever stricter environmental requirements.

THE EFFECT OF INTERFACIAL PROPERTIES ON THE KINETICS OF NICKEL(II) EXTRACTION BY LIX84 IN A n-HEPTANE/WATER SYSTEM

Dallas B. Warren, Franz Grieser", Jilska M. Perera and Geoff W. Stevens
Department of Chemical & Biomolecular Engineering, The University of Melbourne, Victoria 3010, Australia
'School of Chemistry, The University of Melbourne, Victoria 3010, Australia

This study examined the effects of changing interfacial properties on metal ion extraction kinetics in a two phase oil/water system. The reaction mechanism and rate constants for nickel(II) extraction by 2-hydroxy-5-nonylacetophenone oxime (active component of LIX84) was determined in a two-phase, n-heptane/water system. The addition of neutral surfactants, n-dodecyl-dimethyl-3-ammonio-1-propanesulfonate (DDSA) and octa-ethyleneglycol mono-n-dodecyl ether ($C_{12}E_8$), was performed to determine the effects of interfacial competition between the surfactants and extractant. Ionic surfactants, sodium dodecyl sulphate (SDS) and dodecyl trimethyl ammonium chloride (DTAC), were also used to determine the influence of interfacial electrostatic surface potential on reaction rate, in addition to competitive interfacial adsorption.

INTRODUCTION

Until recently the majority of metal ion extraction research was equilibria based. Most metal extractants utilised industrially are interfacially active with low aqueous phase solubility [1], therefore the reaction occurs in the interfacial region. The aim of this study was to quantify the effects of measurable interfacial physicochemical properties on metal extraction kinetics in a two-phase oil/water system. This study used the extraction of nickel(II) by 2-hydroxy-5-nonylacetophenone oxime (HNAPO) as the model reaction in a two-phase oil/water system.

EXPERIMENTAL TECHNIQUE

Investigation of the nickel/HNAPO extraction kinetics in a two-phase oil/water system was performed in a total internal reflectance static transfer cell (TIRSTC) [2], Light enters from the left side, through an optical fibre, into the organic phase, is totally internally reflected off the organic/aqueous phase interface, reflected back towards the interface by a parallel mirror and bounces once more before being collected at the other end of the cell. Neither phase was agitated and the UV-visible spectrum was monitored to follow the extraction reaction. The surfactants Ci2E_8, DDSA, DTAC and SDS were added to observe their effects, via surface competition and electrostatics, on the Ni(II)/HNAPO extraction reaction.

REACTION KINETICS

Apparent Initial Reaction Rate Equation

The apparent initial reaction rate equation was determined by varying the proton, nickel ion and HNAPO concentrations independently. Increasing the nickel ion concentration, pH or HNAPO (HR) concentration increases the rate of nickel/HNAPO complex (NiR_2) formation. The surface excess of HNAPO provides a better fit to the kinetic data, indicating that interfacial HNAPO is part of the rate limiting reaction step(s). Ionic strength was found to have no effect on the reaction rates. From the log R_{int} versus log concentration plots the initial reaction rate was found to be proportional to $[Ni^{2+}]^{10}$, $[HNAPO]^{1.0}$ and $[H^+]^{-0.9}$. Therefore, the apparent observed initial rate in the n-heptane/aqueous system is given by equation (1):

$$\frac{d[NiR_2]_{org}}{dt} (I \to 0) \quad \propto \quad \frac{[HNAPO]^2 [Ni^{2+}]}{[H^+]} \qquad (1)$$

This initial rate equation is consistent with the micelle phase [3], and for Ni^{2+}/Cu^{2+} extraction by HNAPO and other hydroxyoximes in two-phase systems [4-6]

Identification Of The Reaction Mechanism And Rate Constants

The proposed mechanism for the extraction of Ni^{2+} by HNAPO in a n-heptane/aqueous system is shown in equations (2) to (5), where *HR*= HNAPO, R=NAPO, k_1 and k_2 are forward reaction rate constants, k_{-1} and k_{-2} are backwards reaction rate constants and subscripts denote location; o/g=organic phase, ad=adsorbed at interface or ag=aqueous phase.

$$HR_{org} \rightleftharpoons HR_{ad} \qquad (2)$$

$$M^{2+}_{aq} + HR_{ad} \overset{k_1}{\underset{k_{-1}}{\rightleftharpoons}} MR_{ad}^{+} + H^{+}_{aq} \qquad (3)$$

$$NiR^{+}_{ad} + HR_{ad} \overset{k_2}{\underset{k_{-2}}{\rightleftharpoons}} NiR_{2\,ad} + H^{+}_{aq} \qquad (4)$$

$$MR_{org} \rightleftharpoons NiR_{2\,org} \qquad (5)$$

Using the steady state approximation for the intermediate species NiR^{+}_{ad} and if the reaction is not diffusion controlled (diffusion controlled would produce a log [NiR_2] versus log *t* line with gradient 0.5), then the initial reaction rate equation can be derived as equation (6). Linearising equation (6) to equation (7) enables the fitting of the experimental data.

$$\frac{d[NiR_2]_{org}}{dt} (I \to 0) = R_{ml} = \frac{k_1 k_2 [Ni^{2+}]_{aq} s\Gamma_{HR}^2}{k_{-1}[H^+]_{aq} + k_2 s\Gamma_{HR}} \qquad (6)$$

$$\frac{1}{R_{int}} = \frac{1}{k_1 k_2} X + \frac{1}{k_1} Y \qquad (7)$$

The two phase experimental data collected with varying concentrations of HNAPO, H^+ and Ni^{2+} was fitted using the equation $Z=a*X+b*Y$, where $z=1/R_{int}t$, $a=k_{-1}/k_1k_2$ and $b=1/k_1$. A plane [64]

with a=3.95x10'3 and 6=0.363 fitted the data with R^2=0.94. R_{int} was calculated for all the experimental conditions, using the fitted values of a and 6, and compared satisfactorily. The fitted values of a and *b* enable the determination of /cj=2.8 M'1 s'1 and *k.i/k*$_2$ as 1.1x1 O'2.

INTERFACIAL COMPETITION

Non-Ionic Surfactant

The addition of $C_{12}E_8$ has a dramatic effect on the rate of extraction, as shown in Figure *1.* With only 3.0x10'7 M $C_{12}E_8$ in the aqueous phase, it displaces the HNAPO from the free oil/water interface to such an extent that it essentially halts the reaction.

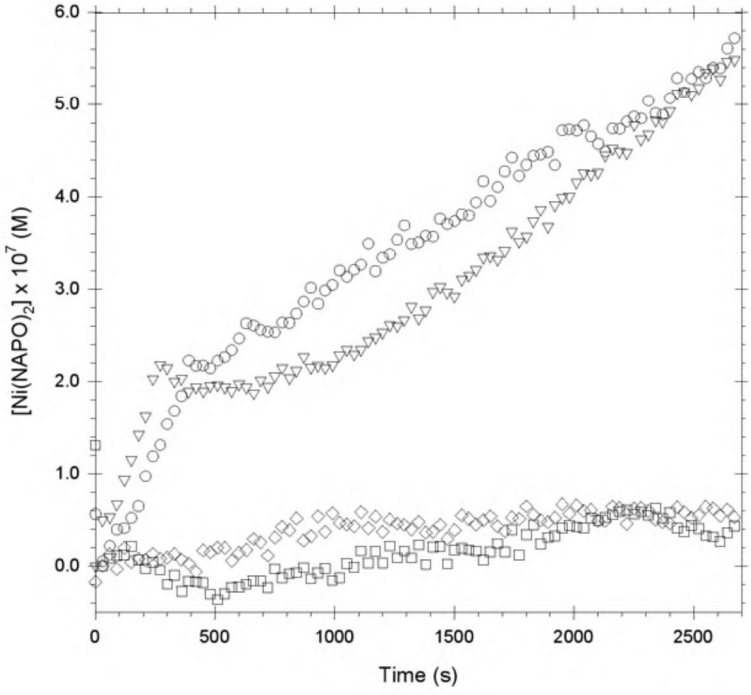


Figure 1. Effect of Cl_2E_8 on the kinetics of nickel extraction by HNAPO in the two-phase system. Aqueous phase of 0.01 M HClOytriethanol amine, 3.4 x 10'6 M $Ni(Cl0_4)_2$ and the approphate [$C_{12}E_8$] at pH 7.4. Organic phase of n-heptane containing 7.1 x 10'5 M HNAPO and

aqueous phase of (0) 0 M $C_{12}E_8$(u) 2.9 x 10'8 M $C_{12}E_8$, (U) 3.0 x

m7 M $C_{12}E_8$, and (0) 3.0 x 10 6 M $C_{12}E_8$

Zwitterionic Surfactant

The addition of the zwitterionic surfactant DDSA behaved in a similar manner to $C_{12}E_8$, halting the extraction reaction when sufficient surfactant was added. A concentration of 2.4x1 O'4 M DDSA completely inhibited the extraction reaction, which is three orders of magnitude higher than $C_{12}E_8$. This difference in concentration required to stop the extraction reaction is due to the higher surface activity of $C_{12}E_8$.

INTERFACIAL COMPETITION AND SURFACE POTENTIAL

The addition of charged surfactants has two different effects on the rate of extraction. Firstly, there is the competition for interfacial area as observed for neutral surfactants and secondly, the concentration of charged aqueous phase species at the interface is altered by the electrostatic surface potential generated by the charge surfactant [7,8],

Cationic Surfactant

The effect of DTAC on the extraction is shown in Figure 2. It is interesting to note that a similar concentration of DTAC (7x1 O'4 M) is required to halt the reaction as for DDSA (2x1 O'4 M). This similarity is accounted for by the fact that DTAC is not as interfacially active as DDSA. Therefore, DTAC does not displace HNAPO at the interface to the same degree as DDSA, with the positive electrostatic surface potential providing the additional impairment.

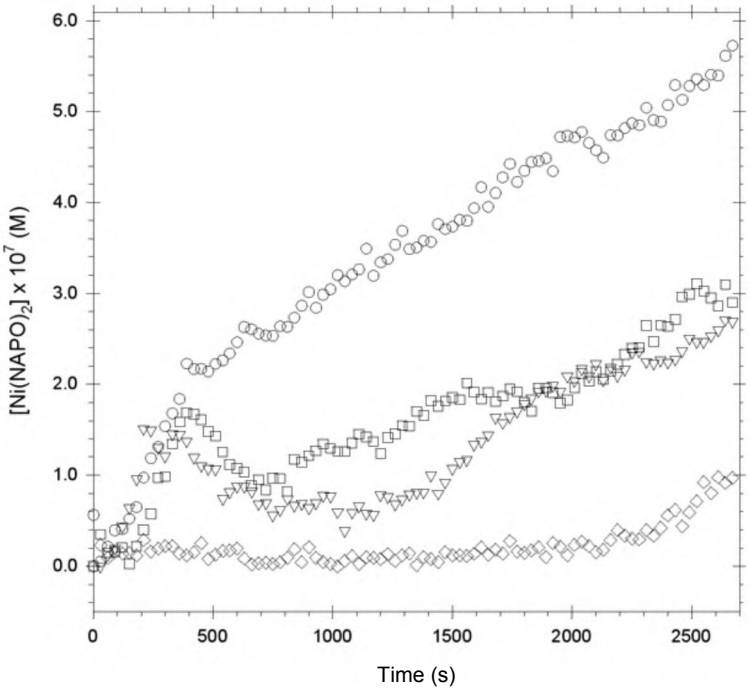


Figure 2. Effect of DTAC on the kinetics of nickel extraction by HNAPO in the two-phase system. Aqueous phase of 0.01 M HCIO^triethanol amine, 3.4 x 10'6 M $Ni(CI0_4)_2$ and the appropriate [DTAC] at pH 7.4. Organic phase of n-heptane containing 7.1 x 10'5 M HNAPO and aqueous phase of (o) 0 M DTAC, (u) 2.4 x 10'6 M DTAC, (U) 2.4 x 10A M, DTAC and (<>) 7.1 x 10A M DTAC

Anionic Surfactant

The addition of SDS was found to initially increase the rate of the extraction and then cause a decrease. This observed trend is a result of the competition between the two phenomena influencing the reaction rates: the enhancement from the negative electrostatic surface potential which increases the concentration of Ni^{2+} (and decreases $[H^+]$) at the interface, and inhibition due to displacement of HNAPO at interface by SDS. It is unlikely that SDS could halt the extraction if its concentration was high enough, as even if there is a very small concentration of HNAPO present at the interface, the rate of reaction is still significant due to [66]

the elevated concentration of Ni^{2+} cations at the interface. SDS concentrations above 7x1 O'4 M were not experimentally obtainable, due to water droplet entrainment in the organic phase, to enable full exploration of this phenomenon.

MODELLING OF INTERFACIAL COMPETITION AND SURFACE POTENTIAL

If the initial reaction rate for the systems containing the various surfactants is calculated using the reaction rate constants previously calculated, the results do not fit. The model used in this manner is insufficient to determine the value of R_{int} as it does not consider the change in concentration of reacting species at the oil/water interface.

Interfacial Competition

The interfacial concentration of HNAPO, with an additional surface-active species, can be calculated using a surface adsorption model [9], shown in equation (8). After correcting the value of THNAPO, recalculated R_{int} values provide a better fit for the zwitterionic DDSA. However, in the case of $C_{12}E_8$ the fitting is not as good. The initial reaction rate calculated is significantly higher than observed experimentally. It appears that $C_{12}E_8$ adsorbs at the interface more strongly, and therefore reduces the concentration of HNAPO more than the surface adsorption model predicts. Adjustment of the interfacial concentration of HNAPO only is insufficient when charged surfactants are involved. The R_{int} for DTAC is correctly over estimated, given that the actual interfacial concentration of Ni^{2+} will be lower due to the positive electrostatic surface potential and consequently a higher rate of reaction. The converse is true for SDS, $R_{in}t$ is under estimated as the increase in interfacial concentration of nickel(ll) owing to the negative electrostatic surface potential has not been considered.

$$0 = \frac{*,4(i-*>*\#,(1-4)}{(l - 4\,Xi - \phi_2) + K_1\phi_1(i - f^*_:)+K\#, (l - _<^*)} \quad (8)$$

where ^surface fractions of surface-active species, K=constant, ()>=volume fractions of the species in a bulk phase, and the subscripts are the surface-active species number.

Surface Potential

The concentrations of charged species at the oil/water interface can, in principle, be calculated using the Boltzmann distribution, this requires knowledge of the interfacial surface potential which can, in principle, be calculated using Gouy-Chapman theory, equation (9). In order to use Gouy-Chapman theory, a value for the surface charge density, a, is required and can be estimated using equation (10) if the degree of surfactant ionisation is known. At this stage it is not possible to calculate the electrostatic surface potential of the free oil/water interface reliably as the degree of surfactant ionisation is unknown for this system.

$$y = \frac{2kT}{ze}\sinh^{-1}\left(\frac{\sigma}{\sqrt{8\,£,.£_Q kTn_0}}\right) \quad (9)$$

$$\& = er_{„}a. \quad (10)$$

where e=electronic charge, fipaqueous dielectric constant, *so*= permittivity of free space, n_0= number volume density of background 1:1 electrolyte, /^surface excess in number area density, and cr_s=degree of surfactant ionisation. [67]

In order to determine if the Boltzmann distribution can account for the change in initial reaction rate, the electrostatic surface potential was adjusted so that the rate, R_{inl}, fitted the experimental value. The presence of DTAC requires a gain in the electrostatic surface potential of approximately +20 mV at 10^{-7} M DTAC. The behaviour of the electrostatic surface potential at higher concentrations is not observable, so it cannot be determined if it follows the same trend as SDS. SDS has a low electrostatic surface potential from a concentration of 0 M to 10^{-5} M, followed by a rapid increase. As the surface fraction of SDS approaches 1.0 then $R_{in}t$ remains approximately constant, implying that there may be an increasing surface potential increasing the interfacial concentration of Ni^{z+} to counteract the reduction in THNAPO **due to surface competition with the SDS.**

CONCLUSION

Nickel/HNAPO extraction kinetics within the two-phase system has been examined using the TIRSTC. A mechanism involving a two step reaction between the nickel ion and the extractant satisfactorily explains the observed initial reaction rate. From the initial reaction rate data, ki (forward reaction rate constant for formation of the 1:1 **complex) was determined as 2.8 M^{-1} s^{-1} and the ratio of k.i (backward reaction rate constant for formation of the 1:1 complex) to k_2 (forward reaction rate constant for formation of the** 1:2 **complex) as** 1.1 **x** 10^{-2}**. The value of k_{-2} (backward reaction rate constant for formation of the 1:2 complex) could not be calculated. The additional of neutral surfactants, non-ionic ($C_{12}E_8$) and zwitterionic (DDSA), decreased the initial reaction rate, which was modelled using a surface adsorption model to calculate the interfacial concentration of HNAPO. The presence of the anionic surfactant SDS accelerated and then decelerated the reaction rate, while the cationic surfactant DTAC caused a decrease. The effects of these charged surfactants can be accounted for using a surface adsorption model and the Boltzmann distribution of charged species. The electrostatic surface potential of the free oil/water interface required for agreement with the experimental R_{int} was calculated and found to be reasonable.**

ACKNOWLEDGEMENTS

Support from the Australian Research Council and Particulate Fluids Processing Centre is gratefully acknowledged and thanks to the Cognis Corporation for the LIX 84 sample.

REFERENCES

1. **D. S. Flett (1977),** *Accounts Chem. Res.,* **10, 99-104.**
2. **J. M. Perera, J. K. McCulloch, B. S. Murray, F. Grieser and G. W. Stevens (1992),** *Langmuir,* **8, 366-368.**
3. **D. W. Warren, G. Dyson, F. Grieser; J. M. Perera, G. W. Stevens and M. A. Rizzacasa (2003),** *Colloid. Surface. A,* **227, 49-61.**
4. **K. Inoue, S. Tomita, and T. Maruuchi (1985),** *J. Chem. Eng. Jpn.,* **18, 445-449.**
5. **Y. Miyake, Y. Takenoshita, and M. Teramoto (1983),** *J. Chem. Eng. Jpn.,* **16, 203-209.**
6. **H. Watarai, M. Takahashi, and K. Shibata (1986),** *Bull. Chem. Soc. Jpn.,* **59, 3469-3473.**
7. **J. Szymanowski, and C. Tondre (1994),** *Solvent Extr. Ion Exch.,* **12(4), 873-905.**
8. **Y. Miyake, Y. Imanishi, Y. Katayama, T. Hamatani and M. Teramoto (1986),** *J. Chem. Eng. Jpn.,* **19(2), 117-125.**
9. **D. W. Warren, F. Grieser; J. M. Perera, and G. W. Stevens,** *Langmuir* **(in press).** [68]



THE KINETICS OF COPPER (II) EXTRACTION BY LIX 84 IN MICELLAR SYSTEMS

Ying Pan, Geoff W. Stevens, Jilska M. Perera

Department of Chemical and Biomolecular Engineering, The University of Melbourne, Victoria, 3010, Australia

The extraction kinetics of copper(II)/LIX 84 in a micellar phase has been examined in detail. A mechanism involving a two-step reaction between the copper ion and the extractant LIX 84(HL) satisfactorily explained the phenomena. The reaction rate constants determined are ^=1.9x10^3 M'V^1, k_2=1.6x10^4 M'V^1, $k._1$=4.6x10^6 M'V^1, k_{-2}=2.2x10^3 M'V^1 .

INTRODUCTION

Solvent extraction is an important separation processes in the hydrometallurgical industry. It is used to purify a range of metals including copper, nickel and cobalt in Australia. In all of these cases there is a move to use short residence time low inventory equipment and in some cases the implementation of this is limited by the rate of extraction [1-2],

From a fundamental point of view, micellar media are very attractive because their microheterogeneous structure guarantees transparency. This property has invaluable advantages for physicochemical studies, especially for kinetic and mechanistic studies dependent on optical methods. Also from an applied point of view, it is possible to achieve metal ion extraction using solutions which are up to 99% aqueous, which, viewed from the environmental side, is also quite attractive [3],

The complete understanding of the mechanisms of reactions taking place at liquid-liquid interfaces is a difficult problem. A number of publications [4-7] have demonstrated that micellar media can provide convenient model systems for the study of the metal complexation reactions involved in solvent-extraction processes, since they possess microscopic interfaces separating a bulk aqueous phase and a hydrophobic environment that is capable of solubilizing lipophilic extractant molecules.

The aim of this study was to determine the extraction reaction mechanism and characterise the rate constants by simulation in a micellar system.

EXPERIMENTAL SECTION

Chemicals [69]

Cupric sulphate (copper II sulphate pentahydrate), $CuS0_4$-$7H_20$, AR. (Aldrich Chemical Company Inc., USA); sodium sulphate (anhydrous), Na_2S0_4, AR. (BDH Chemicals Australia); sulfuric acid, H_2S0_4, AR. (BDH Limited, England); sodium hydroxide, NaOH, AR. (Ajax Chemicals, Australia); acetic acid, HAc, CH_3COOH, AR. (Ajax Chemicals, Australia) and sodium acetate, NaAc, CH_3COONa, AR. (ICN Biomedicals, Inc. Ohio) were used without further purification. An industrial sample of LIX 84 (active ingredient: 2-hydroxy-5-nonylacetophenone oxime $C_9Hi9(C_6H60H)CCH3NOH$) courtesy of Cognis Australia Pty Ltd., was purified as described by Preston et al. [8], The surfactant used was poly-dispersed octa-ethyleneglycol mono-n-dodecyl ether, $G_{12}A_8$, (Huntsman Corporation Australia Pty. Ltd.).

Techniques

The stopped flow technique with optical detection was used for the kinetics measurements. Two reactant solutions were utilised, one solution containing the copper ion and the other containing the extractant (HL) in a micellar phase. The micellar phase consisted of 0.05 M $G_{12}A_8$, 0.2 M HAc-NaAc buffer solution. Details of the stopped flow equipment used have been previously updated [7],

EXTRACTION REACTION MECHANISM

LIX 84 (HL) and Copper (II)/LIX 84 complex (CuL_2) are oil soluble. They are assumed to be present near or in the core of micelles or the core of microemulsions [9], Neglecting the diffusion process [10], the controlling reaction mechanism is presented as equations (1) and (2). Equations (3) and (4) give the rate equation for the formation of the 1:1 intermediate and the 1:2 complex. Subscripts "m" and "aq" represent micellar phase and aqueous phase species.

$$C< + HL_m \overset{*1}{\underset{\wedge\text{-}1}{0}} CuL\wedge + H\wedge \qquad (1)$$

$$Cu_m^{+} + HL_m \overset{*2}{\underset{k_{-2}}{\Longleftrightarrow}} CuL_{2m} + H; \qquad (2)$$

$$\frac{d\backslash CuL_2\backslash}{dt} = /c_2[CuL^+]_m[HL]_m - k_{2}[CuL_2]_m[H]_{aq} \quad (3)$$

$$\frac{d[CuL^+]_n}{dt} = kt[Cu^{2+}UHL]_m - k_{-,}[CuL^+]_m[H^+]_{aq} \qquad (4)$$

where k-i ($M^{'1}$ $s^{'1}$) and k_2 ($M^{'1}$ $s^{'1}$) are the forward rate constants, k_i ($M^{'1}$ $s^{'1}$) and $k_{.2}$ ($M^{"1}$ $s^{'1}$) are the back rate constants.

MODELLING AND SIMULATING EXTRACTION KINETICS

The copper (II)/LIX 84 complex (CuL_2) concentration as a function of time collected from stopped flow experiments was fitted using the equation (3) and (4). Nonlinear [70]

fitting was used in the mathematica program to determine the four-reaction rate constants ki, M, k_2 and k_{-2}. These values of the rate constants were then used to simulate the full experimental kinetic extraction curves. The fitting achieved is shown in Figures 1-2.

The reaction simulation provides a concentration profile that agrees quantitatively with all the experimental data, following the same trends and curve shapes. The values of the rate constant used for the simulations are summarised in Table 1. It can therefore be concluded that the mechanism is valid for the extraction system under the range of conditions studied.

Table 1 Reaction rate constants (equation (3) and (4)) from reaction rate and mechanism simulation using Mathamatica modelling program

System	MM'1 s'1)	MM'1 s'1)	MM'1 s'1)	MM'1 s'1)
micelle	**1.9 x 10^3**	1.6 **x** 10^4	**4.6 x 10^b**	2.2 **x** 10^3

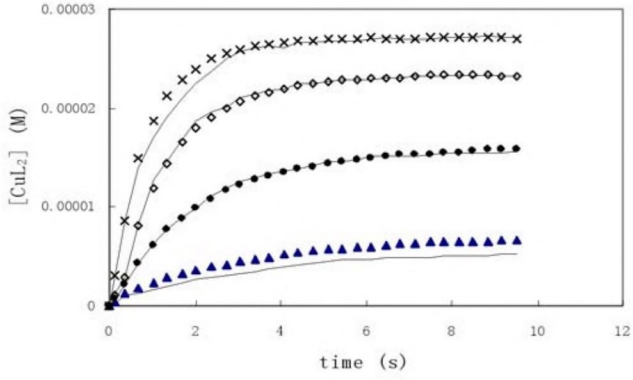


Figure 1. Effect of copper ion concentration on the kinetics of copper ion extraction by LiX 84 (symbols) and simulation (lines) in the micellar phase.
Micellar phase of 0.05 M $G_{12}A_8$ with 0.2 M NaAc-HAc at pH 4.85
0.0001 M LIX 84
A *0.0002 MCu²⁺*
• *0.001 M Cu²**
0 *0.003 M Cu²**
*x 0.005 MCU²**
— *Mathematica simulations* [71]

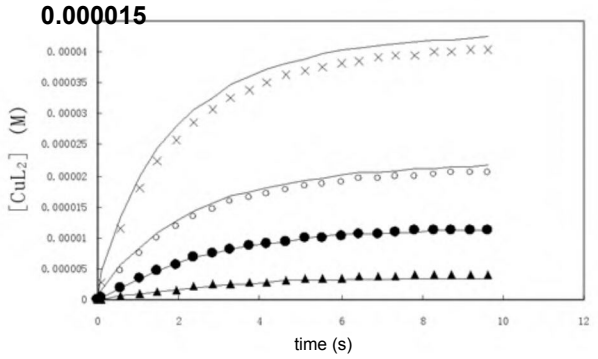


Figure 2. Effect of LIX 84 concentration on the kinetics of copper ion extraction by LIX 84(symbols) and simulation (lines) in the micellar phase.
Micellar phase of 0.05 M GnAg with 0.2 M NaAc-HAc at pH 4.85
0.001 MCu^{2+}

▲ *4.0x1 O'^{5} M LIX 84*
• *8.0x1 O'^{5} M LIX 84*
o *1.2x1 O'^{4} M LIX 84*
x 2.0x10^{4} M LIX 84
—) Mathematica simulations

CONCLUSION

The copper(ll)/LIX 84 extraction kinetics in a micellar phase has been examined. A mechanism involving a two-step reaction between the copper ion and the extractant satisfactorily explained the phenomena. The reaction rate constants determined are k!=1.9x 10^{3} M'^{1} s'^{1}, k_2=1.6 x 10^{4} M'^{1} s'^{1}, k.i=4.6 x 10^{6} M"^{1} s'^{1}, k.$_2$=2.2 x 10^{3} M"^{1} s'^{1} in micellar system.

ACKNOWLEDGEMENTS

This work was funded by an ARC grant. We acknowledge the support of the PFPC (The Particulate Fluids Processing Centre). We thank Huntsman Australia Pty. Ltd. for the surfactants samples and Cognis Australia Pty Ltd. for the LIX 84 sample. We also thank Dr. Y. Leong Yeow for his invaluable help with the Mathamatica program.

REFERENCES

1. **G. W. Stevens and J. M. Perera (1997),** *Min. Pro. Ext. Met. Rev.,* **17, 205.**
2. **G. W. Stevens, J. M. Perera and F. Grieser (1997),** *Curr. Opin. Colloid Interface Sci.,* **2, 629.**
3. **S. G. Son, M. Hebrant, P. Tecilla, P. Scrimin and C. Tondre (1992),** *J. Phys. Chem.,* **96, 11072.**
4. **C. Tondre and M. Hebrant (1992),** *J. Phys. Chem.,* **96, 11079.**
5. **J. K. McCulloch, J. M. Perera, E. D. Kelly, L. R. White, G. W. Stevens and F. Grieser (1996),** *J. Colloid Interface Sci.,* **184, 406.**
6. **A. Hokura, J. M. Perera, F. Grieser and G. W. Stevens (1998),** *Solvent Extr. Ion Exch.,* **16(2), 619.** 72

7. **D. B. Warren, F. Grieser, J. M. Perera and G. W. Stevens (2004),** *Colloids and Surfaces A: Physicochem. Eng.,* **243, 127.**
8. **J. S. Preston and R. J. Whewell (1977),** *J. Inorg. Nucl. Chem.* **39, 1675.**
9. **D. B. Warren, F. Grieser, J. M. Perera, G. W. Stevens and M. A. Rizzacasa (2003),** *Colloids and Surfaces A: Physicochem. Eng.,* **227, 49.**
10. **C. Tondre, M. Hebrant and H. Watarai (2001), J. Colloid Interface Sci., 243, 1** [73]

EXTRACTION OF SILVER FROM CHLORIDE SOLUTIONS - HOW TO ESTABLISH THE CHEMICAL REACTIONS?

A. P. Paiva

Departamento de Quimica e Bioquimica, Centro de Quimica e Bioquimica, Faculdade de Ciencias da Universidade de Lisboa, Rua Ernesto de Vasconcelos, Bloco C8 1749-016 Lisboa - PORTUGAL

The known Ag(I) extractive data from chloride media by organophosphorous sulphides (mainly) is reviewed in this work and critically discussed. In fact, the establishment of the Ag(I) chemical reactions based on the dependence of Ag(I) distribution coefficient on extractant and chloride ion concentrations, and on available Ag(I) speciation studies as well, is quite difficult to be achieved. Hence, different sorts of approaches are proposed and tentatively checked for their validity in contributing for a clarification of this interesting scientific challenge.

INTRODUCTION

Several works in literature point out to the development of liquid-liquid extraction systems for an efficient and selective Ag(I) recovery from concentrated chloride media, the most relevant information on the subject having been compiled in a rather recent review [1], Amongst the extractants most broadly studied, the neutral organophosphorous reagents deserve a special mention, since the best efficiency performances and selectivity factors towards Ag(I) have been found with this sort of organic compound [2], In fact, the traditional extractive affinity occurring between Ag(I) and ligands with sulphur atoms (as the only heteroatom) is not extensive to aqueous media in which Ag(I) is linked to complexing anions, and this is indeed the case of chloride media [3],

According to Marcus [4] and Fritz [5], increasing chloride concentrations in solution lead to the formation of anionic Ag(I) complexes of the type $AgCl_2'$, $AgCl_3^{2'}$ and AgCU$^{3''}$, those species being responsible for the solubility of silver chloride in chloride aqueous phases. Marcus presents a compilation of data based on solvent extraction and ion exchange experiments [4] and points out to the predominance of $AgCl_2$‘ in the 0.1 to 0.5M HCl range, whereas the principal species ascribed to 0.5M<[HCl]< 6M is $AgCl_3^{2'}$. $AgCl_4^{3'}$ is reported to be the main species for HCl concentrations above 6M [4], This data is roughly similar to the information published by Fritz [5], who presents the calculated distribution curves of dissolved AgCl as a function of NaCl concentrations at 25°C. Hence, Figure 1 summarizes his results for the relative percentages of the Ag(I) chlorocomplexes for NaCl concentrations between 1 and 5M.

Figure 1 puts in evidence that $AgCl_3^{2'}$ is always the predominant species for the considered chloride concentrations, although the contribution of $AgCl_4^{3'}$ becomes quite significant for 3M NaCl and higher concentrations. At 5M NaCl, the relative weight of $AgCl_4^{3'}$ to $AgCl_3^{2'}$ surpasses one third of the overall contributions [5],

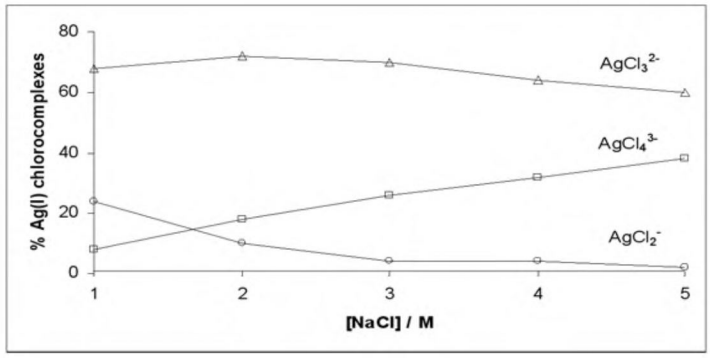


Figure 1. Relative percentages of the Ag(I) anionic chlorocomplexes found for Nad concentrations between 1 and 5M, calculated from Fritz diagram [5],

A more recent study [6], based on a potentiometric method used to determine hydrogen and chloride ion activities in HCl solutions, was extended to the exploitation of results obtained with the Ag / Ag^+ electrochemical system in HCl solutions from 3M to 9M. The data obtained seem to point out that $AgCl_4^{3-}$ species prevail in those media [6],

Amongst the neutral organophosphorous ligands that have been tested for Ag(I) extraction from chloride phases [1], the most adequate proved to be the trialkylphosphine sulphides, namely triisobutylphosphine sulphide (TIBPS) [2,7,8], and tributyl- and trioctylphosphine sulphides (TBPS and TOPS, respectively) [2], The general data achieved either for the efficiency of extraction or for Ag(I) selectivity when in presence of excess concentrations of some base metals denote a good compromise for all the extractants.

The establishment of the involved chemical reactions between Ag(I) and the above mentioned trialkylphosphine sulphides was also attempted [2,7,8] and the basis of interpretation has been the results obtained from the influence of the extractant, hydrochloric acid and chloride concentrations on the distribution coefficient of the metal ion. That information had obviously to be complemented with the data available on the Ag(I) speciation [4-6] in those aqueous media.

Based on all the information available, some difficulties have arisen to clearly interpret the Ag(I) extraction reactions by trialkylphosphine sulphides [2,7,8], In this work, the different sorts of approaches that have been proposed [2,7,8] - and also some newly ones - are presented and discussed, either for the general use of neutral organophosphorous reagents or even other extractants. All those assumptions will be tentatively checked for their validity in contributing for a clarification of this interesting scientific challenge.

SILVER (I)/NEUTRAL ORGANOPHOSPHOROUS SULPHIDES/CHLORIDE SOLUTIONS

The most relevant information regarding the establishment of the chemical reactions involved in Ag(I) extraction from chloride media by trialkylphosphine sulphides can be visualized in Table 1, in which parameters such as extractant and Ag(I) concentrations, HCl and total chloride contents in the aqueous solutions and the slopes obtained from the plots of log D *vs.* log [Cl^-], for each set of experiments, are detailed.

It should be emphasized that the [extractant] / [Ag(I)] ratio, determined from the slope of log D *vs.* log [L] (L being the extractant), gave systematically a proportion of 2 /1 for all cases. A thiophosphonate derivative (O.O-dibutyl-a-phenylamino-phenylmethanethiophosphonate, BATP) was also used for Ag(I) extraction from chloride media [9] and therefore its available

data is also included in Table 1. When BATP was used at concentrations lower than 0.01 M [9], a [L] / [Ag(I)] of 1 / 1 was obtained instead. However, the real problem in establishing the Ag(I) extraction reactions does not really come from the log D - log [L] plots but from the graphics of log D - log [Cl⁻] instead, as suggested by the solvent extraction data presented in Table 1.

Table 1. Data related with the most relevant parameters contributing to the establishment of the Ag(I) extraction reactions from chloride media by organophosphorous sulphide derivatives.

Extractant (L)	[L]/M	$[Ag^+]$/M	[HCl]/M	[CF] range / M (+ NaCl)	Slope Log D *vs.* log [Cl⁻]	Ref
TIBPS	**5x10"¹**	**5x10"⁵**	**1 -5.6**	----------	**-3.6**	**7**
	4.3x1 O'²	**4.6x1 O'⁴**	1	**2 - 5**	**-2.4**	8
	8.5x10"³	**9.2x10"⁵**	1	**1-5**	-2.1	8
	6x1 O'²	1.8x1 O'³	2	**3-5**	**-4.1**	10
TBPS	**6x1 O'²**	**1.4x10³**	2	**3-5**	**-4.0**	2
TOPS	6x10"²	**1.4x1 O'³**	2	**3-5**	**-4.1**	2
	2x10'²	**5.8x1 O'⁴**	2	**3-5**	**-4.0**	10
BATP	**5x10"²**	< 10"⁶	**0.5***	0.02-1	**-1.4**	**9**
	4x1 O'²	< 10"⁶	0.1 *	**0.03-1**	**-1.4**	**9**

** The ionic strength of the medium was maintained at 1M with ht, Cf and ClO_4'.*
Abbreviations: TIBPS: triisobutylphosphine sulphide; TBPS: tributylphosphine sulphide; TOPS: trioctylphosphine sulphide; BATP: 0,0-dibutyl-a-phenylamino-phenylmethanethiophosphonate.

Triisobutylphosphine sulphide (TIBPS) is the active ingredient of Cyanex 471X, commercially available from Cytec Canada Inc., this fact justifying its larger use when compared with those of the other organophosphorous sulphides. The first report that appeared in literature related with Ag(I) extraction from chloride media by TIBPS was published by Abe and Flett [7] who used a large excess of the purified organic compound (0.5M) to extract vestigial Ag(I) concentrations. Their results clearly demonstrate that the affinity of TIBPS to extract Ag(I) decreases with increasing chloride concentrations in the aqueous solution [7],

Additionally, they present three sets of Ag(I) extraction results [7]: different Ag(I) and increasing NaCl concentrations, different Ag(I) and increasing HCl concentrations, and finally a 5.35 mg/L Ag(I) and increasing HCl concentrations. Taking the results for a fixed Ag(I) concentration as a reference, it can be observed that at 1M HCl 5.25 mg/L Ag(I) are extracted, against 3.70 mg/L at 3.7M HCl and 2.35 mg/L at 4.8M HCl. These results suggest that even a great excess of TIBPS (a 10^4-fold concentration when compared to that of Ag(I)) is not able to quantitatively extract Ag(I) from above 2M Cl". Furthermore, above a total 2M chloride concentration, the results obtained from the plot of log D *vs.* log [L] lie on a straight [76]

line with a slope of ~-3.6.

Based on the overall results obtained, Abe and Flett concluded that the stoichiometry of the Ag(I) extracted species should be $(TIBPS)_2AgCl$, the negative effect on Ag(I) extraction by increasing chloride ion concentrations in the aqueous phase being explained by the existence of non-extractable anionic silver complexes [7], Therefore, if data of Ag(I) speciation in chloride media is taken into account [4-6], it seems reasonable to suppose that the extractant is able to interact with Ag(I) species until $AgCl_3^{2-}$ but TIBPS should leave $AgCl_4^{3-}$ behind. If one tries to write a chemical equation to express the phenomenon, that would be such as (1).

$$AgCl_3^{2-} + 2\ TIBPS \Leftrightarrow AgCl.\ 2\ TIBPS + 2\ Cl^- \qquad (1)$$

Taking into account the equilibrium constant of the reaction and the related Ag(I) distribution coefficient, a straight line with a slope of -2 would be expected from a plot representing log D *vs.* log $[Cl^-]$, In fact, a slope of about that value has been obtained from other data related with Ag(I) extraction by TIBPS [8] - see Table 1 -, therefore Ag(I) extraction by TIBPS has directly been expressed by equation (1). The slope values slightly higher than -2 were justified by the probable presence of Ag(I) chlorocomplexes to whom TIBPS had no affinity [8].

When the Ag(I) extraction performances of other trialkylphosphine sulphides were investigated, tributylphosphine- and trioctylphosphine sulphides (TBPS and TOPS, respectively), following experimental conditions a bit different from the previous ones [2], an unexpected result of about -4 for the slope analysis related to both TBPS and TOPS was found instead. Those results have tentatively been explained through the interaction of 2 $AgCl_3^{2-}$ moieties with 2 ligand (L) molecules, giving something of the type AgCl.2L.AgCl and releasing 4 Cl' for each Ag(I) species [2],

Afterwards, similar experimental conditions as those used for TBPS and TOPS were adopted to test TIBPS performance towards Ag(I) extraction [10] - Table 1 -, the slope analysis giving again -4.1. It can then be concluded that all trialkylphosphine sulphides give a coherent result for the slope from log D *vs.* log [Cf], at least for the adopted set of experimental conditions.

In order to broaden this discussion, a rough estimation can be useful: if one calculates the percentage of non-extracted Ag(I) from the D values obtained at the different chloride concentrations, for each trialkylphosphine sulphide tested, those results can directly be compared with those correspondent to the $AgCl_4^{3-}$ content in the aqueous solution, as determined by Fritz [5] - Figure 1. The former results that could be calculated for the Ag(I) content not extracted by TIBPS, TBPS and TOPS are plotted in Figure 2. [77]

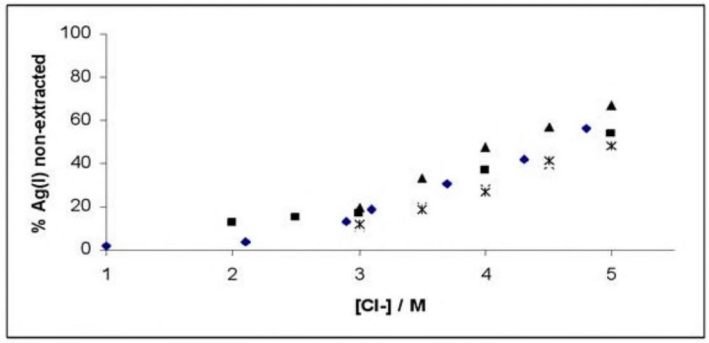


Figure 2. Dependence of non-extracted Ag(I) by TIBPS, TBPS and TOPS on the chloride concentration in the aqueous phase **(#- TIBPS [7], M - TIBPS [8], - TIBPS [10], x,+ - TBPS and TOPS [2].**

It can be concluded that the data calculated for the three sets including TIBPS, and also for TBPS and TOPS, are relatively close to each other, generally showing a quite similar pattern. Until 2M chloride, the Ag(I) percentage not extracted corresponds roughly to that of $AgCl_4^{3'}$, but from 3M until 5M chloride, Ag(I) contents left in the aqueous phase by the extractants are always higher than those previewed by Fritz [5] for the $AgCl_4^{3'}$ contribution. If one considers that $AgCl_4^{3''}$ is the predominant species for [HCl] higher than 3M, as stated by Sella and Bauer [6], then an attempt to interpret the interaction between these extractants and the Ag(I) chlorocomplexes is still more difficult.

One parameter that can surely influence the slope analysis results is the [L] / [Ag(I)] ratio. In fact, Abe and Flett [7] used a quite large ratio, as mentioned before, therefore the maximal extraction performance by TIBPS was not reached for sure. However, those ratios were 93 [8] and 33 [10] for TIBPS, and about 43 for TBPS and TOPS. TIBPS, when used under the conditions described in [10] - Table 1 - could probably be saturated, and this can be a justification for the higher percentages of Ag(I) left in the aqueous phase. However, saturation problems seem not to be the case for TBPS and TOPS, despite the 43 value for the [L] / [Ag(I)] ratio, their results being perfectly comparable with those of TIBPS from [7] and [8],

The data obtained for BATP [9], the thiophosphonate derivative, can be interpreted on the basis of the interaction of the extractant with the $AgCl_2'$ and $AgCl_3^{2'}$ species mainly, the correspondent Ag(I) extraction reactions justifying the slope value of -1.4 for the log D *vs.* log [Cl] plot-Table 1.

A hint for a better interpretation of the log D vs. log [Cl"] plots, for this particular case involving Ag(I) extraction from concentrated chloride media, could be the consideration of activity values instead of concentrations. Data published in literature by Sella [11] and Sella and Bauer [6,12,13] (establishing values for the individual activity of chloride ions for concentrations between 2M and 9M and the global activity coefficients of Ag(I) for each chloride media), can be collected and applied to the results obtained for Ag(I) extraction by TIBPS [10], Replacing the chloride concentrations by the correspondent activities, and considering the adequate Ag(I) activities before and after extraction by TIBPS in order to calculate the "corrected " D values, a new plot of log D *vs.* log aCF (activities of chloride ion) can be made. No significant changes were revealed for the slope of this alternative straight line, as the value obtained reduced to -3.77, against a former value of-4.1- Table 1.

Another value-adding that could help on the clarification of this extraction phenomenon could be the direct experimental determination of the stability constants of the Ag(I) [78]

chlorocomplexes for the "real" chloride solutions used in the extraction experiments reported. However, the conventional procedures [14] cannot be applied easily, since the chloride concentrations involved are quite high.

SILVER (I)/NEUTRAL NITROGEN-SULPHUR LIGANDS/CHLORIDE SOLUTIONS

Other extractants, in addition to the organophosphorous ones, have also been used for Ag(I) extraction from chloride media [15,16], Amongst those that were tested, dibutylthiourea (DBT) and tetraethylthiuram disulphide (*disulfiram*, DSF) deserve a mention. For these extraction systems, data on the dependence of Ag(I) extraction on chloride ion concentration in the aqueous phase can be observed in Table 2.

DBT is highly efficient for Ag(I) extraction, that is why a small [L] / [Ag(I)] ratio - about 22 - was employed. Regarding DSF, the first set of experiments seemed to point to a "normal" interaction with $AgCl_3^{2-}$ complexes, but the second set revealed once again an "anomaly". If the [L] / [Ag(I)] ratios are taken into account, this latter result can be partially explained by the unavailability of extractant concentration to recover Ag(I), since the [L] / [Ag(I)] ratio is less than a half of the one used in the former experiment set [15],

Table 2. Data related with the most relevant parameters contributing to the establishment of the Ag(I) extraction reactions from chloride media by nitrogen-sulphur extractant derivatives.

Extractant (L)	[L]/M	$[Ag^+]$/M	[HCl]/M	[Cl"] range / M (+ NaCl)	Slope Log D *vs.* log $[Cl^-]$	Ref
DBT	1x1 O^{-2}	4.6x10^{-4}	2	3-5	-1.7	15
DSF	6x10^{-2}	4.6x1 O^{-4}	2	3-5	-1.5	15
	8x1 O^{-2}	1.4x1 O^{-3}	2	3-5	-5.3	16

CONCLUSIONS

Data collected on Ag(I) solvent extraction from chloride media by adequate organic extractants, particularly that used to establish the Ag(I) extraction reactions, has been summarized and critically discussed. The treatment of those results allowed the highlight of a few parameters that are probably some of the most important in determining the occurrence and nature of the Ag(I) extraction reactions.

More important than a clear answer to a problem is perhaps the way the questions are addressed. One aim of this paper has clearly been to enrich the discussion around the "high" slope values obtained from the log D *vs.* log $[Cl^-]$ plots when Ag(I) is extracted from chloride media. A clear answer has not already been found, however, it is probable that a viable explanation could be based on the lack of affinity shown by the organic ligands to interact with the most charged anionic Ag(I) chlorocomplexes, namely $AgCl_4^{3-}$. Attempts to determine the speciation of the Ag(I) chlorocomplexes in different chloride solutions, either by a theoretical or experimental route, are currently in progress.

This topic obviously remains wide open to discussion within the chemical community.

REFERENCES

1. **A. P. Paiva (2000)** *Solv. Extr. Ion* **Exc/7.,18, 223-271.**
2. **R. S. Capela, A. P. Paiva (2002)** *Proc. ISEC 2002,* **K. C. Sole, P. M. Cole, J. S. Preston, 79**

D. J. Robinson (eds.), vol. 1, Cape Town, South Africa, pp. 335-340.

3. **A. P. Paiva, M. Lemaire (1993) Sep.** *Sci. Technol.,* **28, 2279-2283.**
4. **Y. Marcus (1967)** *Coord. Chem. Rev.,* **2, 257-297.**
5. **J. J. Fritz (1985)** *J. Solution Chem.,* **14, 865-879.**
6. **C. Sella, D. Bauer (1990)** *Hydrometallurgy,* **23, 353-364.**
7. **Y. Abe, D. S. Flett (1992)** *Proc. ISEC'90,* **T. Sekine (ed.), Elsevier Science Publishers, vol. 2, Tokyo, Japan, pp. 1127-1132.**
8. **A. P. Paiva, L. M. Abrantes (1994)** *Proc. EPD Congress, 123rd TMS Annual Meeting,* **G. Warren (ed.), San Francisco, USA, pp. 243-255.**
9. **D. Sevdić, H. Meider, D. Pavkovic (1990)** *Solv. Extr. Ion Exch.,* 8**, 643-658.**
10. **A. P. Paiva, unpublished results.**
11. **C. Sella (1989), Etude Analytique des Milieux Chlorure Concentres, Ph. D. Thesis, Université Paris VI, France.**
12. **C. Sella, D. Bauer (1990),** *J. Chem. Research (S),* **174-175.**
13. **C. Sella, D. Bauer (1990), J.** *Chem. Research (S),* **284-285.**
14. **G. R. Choppin (1992), Principles and Practices of Solvent Extraction, J. Rydberg, C. Musikas, G. R. Choppin (eds.), Marcel Dekker, New York, pp. 71-100.**
15. **A. P. Paiva (2001),** *Proc. ISEC 1999,* **M. Cox, M. Hidalgo, M. Valiente (eds.), vol. 1, Barcelona, Spain, pp. 399-404.**
16. **A. P. Paiva (2001),** *Proc. EPD Congress, 130th TMS Annual Meeting,* **P. R. Taylor (ed.), New Orleans, USA, pp. 665-673.** [80]



THE COUPLING OF TRANSPORT AND INTERFACIAL REACTION AS A NEW APPROACH TO THE KINETICS OF CHEMICAL EXTRACTION

W. Nitsch, R. Sacher

Department Chemie der Technischen Universität München, Lichtenbergstr. 4, 85747 Garching, Germany

ABSTRACT

For the extraction of zinc- and cadmium ions with dithizone as the chelating agent the borderline cases of transport- and interfacial kinetics are verified experimentally by variation of the ion concentration levels. For a general application of these concentration effects a model equation for the coupling of transport and interfacial reaction was derived, allowing the interfacial concentrations to be calculated.

Introducing the corresponding interfacial resistances the concentration dependency of rate limitation becomes accesible for the first time for any concentration level at all. The predicted interfacial resistances agree with corresponding experiments demonstrating a systematic behaviour of the different concentration dependencies.

INTRODUCTION

The technical application of chemical extraction is well known and important for the production of different metals, for the separation of heavy metals from waste water or for the recycling of nuclear fuel as examples.

In spite of the broad technological importance of such processes the knowledge about extraction is limited to the systematic treatment of equilibria [1]- In comparison a systematology of kinetic behaviour similar to the chemical gas absorption [2] is not recognizable until now because of the lack of suitable methods for the determination of concentrations at the interface and the surrounding. [81]

APPLIED METHOD

With the aim to identify the borderline cases of chemical liquid/liquid kinetics a special stirring cell was developed years ago [3], The apparatus characterized by axial convections as shown schematically in fig. 1, is distinguished by the possibility to identify the case of transport limitation: for the condition that the Reynold number in both phases are controlled by the stirring number n_w and n_s to the same value, the flux of mass transfer *h* is always proportional to the selected stirring number n_W-

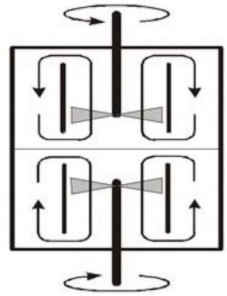


Fig. 1: Scheme of the convection flow in the applied cell

MODEL SYSTEMS

The efficiency of the applied stirred cell is demonstrated for the chemical extraction of aqueous zinc ions conducted with dithizone (HX) being exclusively soluble in apolar phases (CCl_4, $CHCl_3$ as examples). The plots in fig. 2 show the proportional relationship (h_{Zn}~ n_w) for transport limitation in the case of high zinc ion concentration.

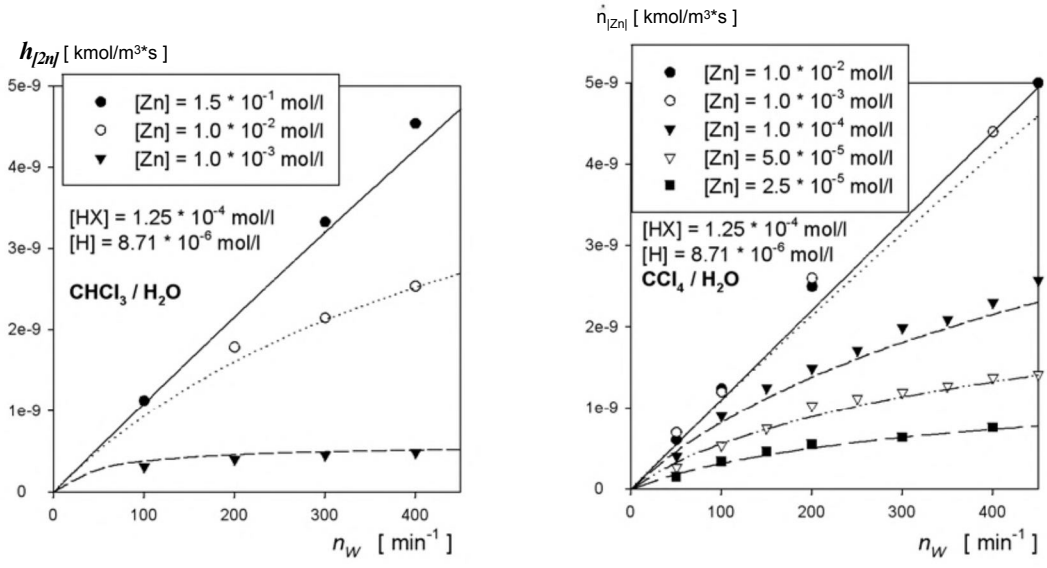


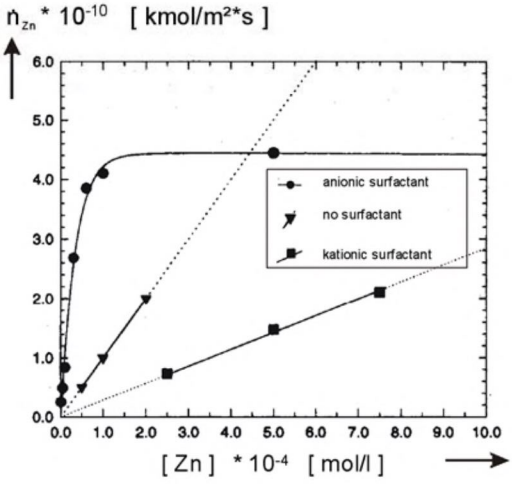
Fig.. 2: Flow dependency at various zinc levels in water/CHd_3 and water/CCl_4

Decreasing the ion concentration, the flow dependent fluxes h_{Zn} become more and more flow independent indicating the influence of chemical reactions for the rate determination [4], Evaluating the flow independent regions there results [82]

$$h_{Zn} \sim \underline{k}[ZnHHX] \cdot \frac{}{[H]} \qquad (1)$$

as the equation for the kinetically controlled mass transfer related to the direction of extraction.

The most important property for the selection of chemical extractions with dithizone is the interface as the provable locality of the chemical reaction. This statement is evident concerning the system behaviour in the presence of surfactants (fig. 3a). Especially the pronounced enhancement of the chemical reaction for anionic- and the inhibition for kationic surfactants [5] are strong arguments for the interface as a locality of the reaction. Another relevant argumentation concerns the time dependent coextraction of zinc- and cadmium ions distinguished by a maximum value for the cadmium concentration (fig. 3b). This experimental behaviour agrees quantitatively with the calculation based on the assumption of interfacial reactions related to the kinetic data for the both single extraction systems [6],



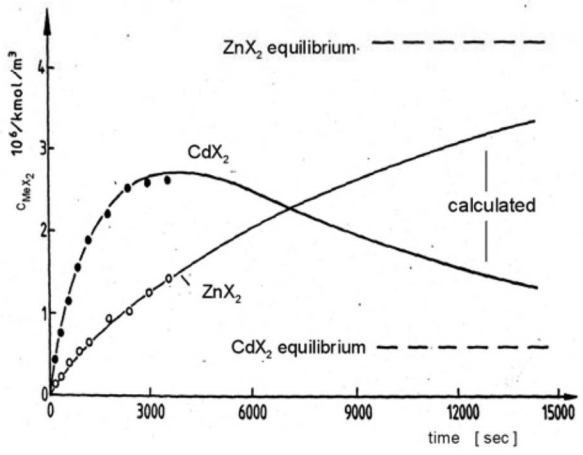


Fig. 3a: Charge effects of surfactants on the initial flux

Fig. 3b: Time dependent zinc and cadmium extraction coupled at the interface

Besides dithizone systems are suitable for systematic investigations because of the strong influence of the solvent phase and the broad variation of the rate constants for different kations. Finally it is remarkable that dithizone shows no interfacial activity which allows neglect of adsorption steps and hence simplifies the kinetic equations. Of course for experiments the absence of interfacial contaminations is very important because of the relevant sensitivity of the fluiddynamics and reactions at the interface.

PROBLEM

Directed to a contribution for further development in kinetics of chemical extraction a physical model should be derived for the coupling of flow dependent transport of species with the flow independent interfacial reaction related to measurements of the zinc/dithizone system in the special stirred cell.

The model should be able to facilitate for the first time the calculability of interfacial resistances (non equilibrium states at the interface) for any concentrations at all.
An alternative empirical approach to the concentration dependency of interfacial resistances is not realistic because of the number of variables and hence the large number of experiments being necessary. This fact is the reason for the usual uncertainty about the correlation of interfacial resistance and concentrations. [83]

COUPLING OF TRANSPORT AND INTERFACIAL REACTION

The model equation is based on the four equations for the species transport together with the measured kinetic equation for the microscopic step of complexation (1) at the interface. Introducing the equilibrium condition with the corresponding equilibrium equation (2)

$$K_{ex} = \frac{[ZnX_2]\cdot[H]^2}{[Zn][HX]^2} = \frac{\vec{k}}{\overleftarrow{k}} \qquad (2)$$

and with equation (1) it is possible to derive the kinetical equation for the microscopic step of reextraction (3) (c* indicate interfacial concentrations, K_{exCCU} =200, K_{exCHCh} = 4.4).

$$\overleftarrow{n}_{Zn} = \overleftarrow{k}\,[ZnX_2]\cdot\frac{[HV]^*}{[HX]^*} \qquad (3)$$

Applying the zinc ion transport

$$\dot{n}_{Zn} = \beta_{Zn}\,(Zn - Zn^*) \qquad (4)$$

as the corresponding expression for the transport process together with the two kinetic equations there results for stationary states the model equation (5)

$$\dot{n}_{Zn} = \beta_{Zn}\,([Zn] - [Zn]^*) = \vec{k}\,[Zn]\,\frac{[HXY]^*}{[H]^*} - \overleftarrow{k}\,\frac{[ZnX_2]^*\,[H]^*}{[HXV]} \qquad (5)$$

as the general expression for the coupling of transport and interfacial reaction. For the borderline case of transport limitation the four gradients are maximal (e g. [Zn]* * [Zn]*$_e$) and for chemical limitation the gradients can be neglected (e g. [Zn]* = [Zn]).

Applying the kinetic data the model system allows the iterative determination of the interfacial concentrations c$_i^*$. For simplification reasons the calculation runs with the assumption Pi = p for the four coefficents at equal Reynold numbers. This approach seems to be justified because of p ~ D^{0,5} (penetration theory).

CONCENTRATION DEPENDENCE OF RATE LIMITATION

Caused by the required large varation of concentrations related to the four different species it is necessary to operate with the interfacial resistance A_R

$$\Delta_R = \frac{[Zn]^* - [Zn]^*_e}{[Zn] - [Zn]^*_e} \cdot 100\ [\%] \qquad (6)$$

in order to get a suitable overview. The key value Zn* is caculated applying equation (5).

Of course, with two dimensional plots for A_r^* **= f** $([Zn]_H, Hx)$. f **($[HX]_{Zn,H}$) resp. f ($[H]_{ZniH}$x) a lot of paper is necessary to demonstrate the systematic behaviour of the interfacial resistances. Some typical dependencies are presented: in fig. 4a the influence of the selected solvent phase is demonstrated together with experimental results. The large difference of** A_R **for the same concentration levels in fig. 4a is caused by the rate constants (k_{ccu} «100 /$c_{CHC,3}$). The plot in fig. 4b shows the strong influence of the pH-value, with the possibility to discover the interfacial reaction with decreasing pH. The bell-shaped function in fig. 5a and 5b is characteristic for the variation of the H- resp. the HX-concentration. In both cases interfacial limitation is restricted to a more or less small variation. Again the agreement with experiments is quite satisfying. Summarising it is to state that high values of interfacial resistances can be realized with the component concentrations near the same order of magnitude approximately. Besides, the resulting different behaviour of** A_R **= f(c) are comprehensible interpreting equation (5).** [84]

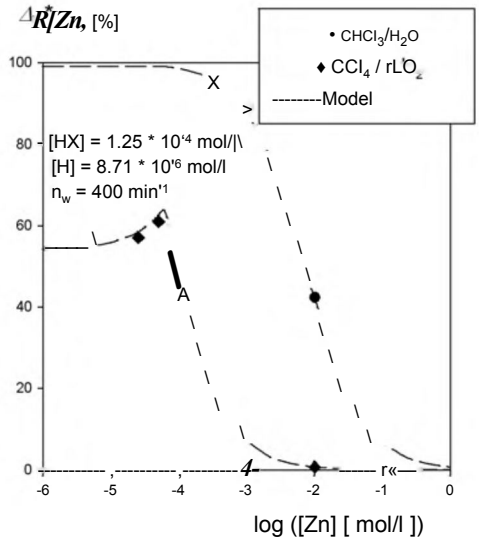


Fig. 4a: A_R = f ($[Zn]_H$.Hx), calculated and experimental data in CCl_4 and $CHCl_3$ system*

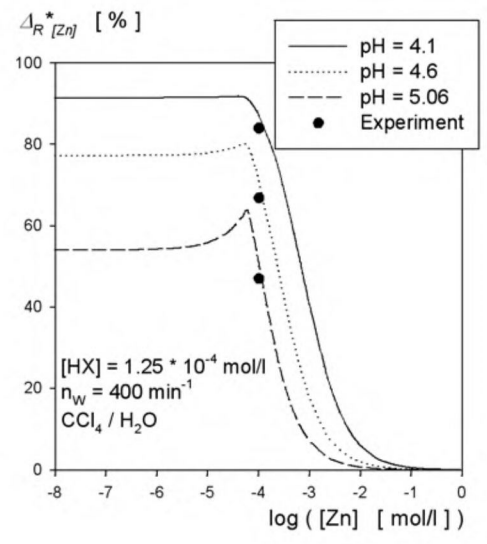


Fig. 4b: A_R = f ($[Zn]_H$.Hx), calculated at various phi value and experimental data in CCl_4 system*

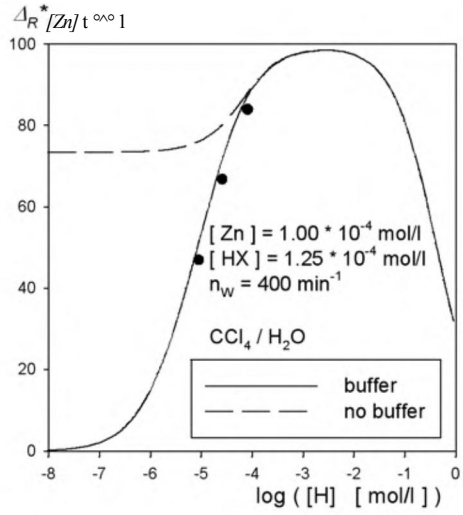


Fig. 5a: A_R = f ($[H]_{Zn}$,Hx) calculated and experimental data*

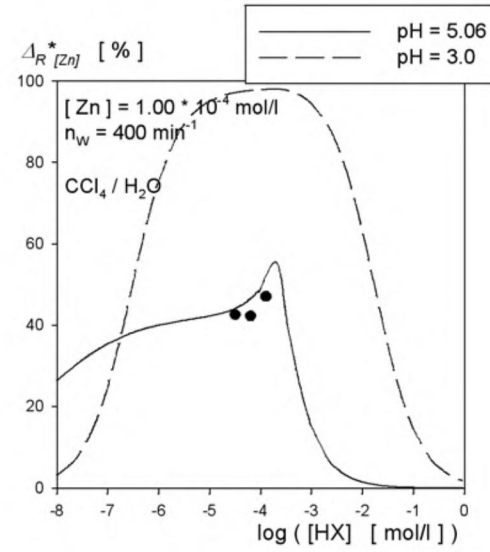


Fig. 5b: A_R = f ([HXJZP.H) calculated and experimental data*

REEXTRACTION

Because of the possibility to derive the kinetic equation for reextraction applying the kinetic equilibrium condition explizit measurements are not necessary. The justification for this procedure is demonstrated with the three fluxes calculated with equation (5) for different zinc ion concentrations. Comparing the data especially the differences between the both interfacial reaction terms the approach to equilibrium with increasing zinc concentration and degreasing A_R values is obviously. Because of the agreement between calculation and experiment (fig. 4a) it seems justified to operate with the kinetic equilibrium condition for the kinetics of interfacial reaction in general.

*Table 1: Initial fluxes and interfacial resistance in CCl_4 / water at stirring speed riR.wss = 400 min^{-1} and concentration conditiones [HX] = 1.25 * 10^{-4} mol/l and [H] = 1.00 * 10^{-5} mol/l*

	[Zn] [mol/l]	zinc flux [kmol/m^2*s]	flux extraction [kmol/m^2*s]	flux reextraction [kmol/m^2*s]	AR*[Zn] [%]
1	1.00* 10'^{6}	**3.0050* 10'^{11}**	**3.0051 * 10'^{11}**	**7.1667 * 10-^{16}**	**57.63**
2	1.00* 10'^{b}	**2.9001 * 10'^{10}**	**2.9002 * 10'^{10}**	**7.3506 * 10'^{1b}**	**59.11**
3	1.00* 10'^{4}	**2.0305* 10'^{9}**	**2.0306* 10'^{9}**	**8.8752 * 10'^{14}**	**53.86**
4	1.00* 10'^{3}	**4.0682 * 10'^{9}**	**4.0694* 10'^{9}**	**1.1719 * 10'^{12}**	**8.09**
5	1.00 * 10'^{2}	**4.3953* 10'^{9}**	**4.4076* 10'^{9}**	**1.2324 * 10 ”**	**0.80**
6	1.00* 10’^{1}	**4.4289* 10'^{9}**	**4.5499* 10'^{9}**	**1.2098 * 10–$^{1°}$**	**0.07**

FINAL COMMENT

For chemical extraction the model equation can be applied to calculate concentration profiles in columns provided that the interfacial kinetic is relevant and known. On the other hand with systematic variations of virtuell values for K_{ex} and $\vec{k}$ the relevant concentration regiones should be accessible for suitable measurements with kinetical control.
In addition the application of the model equation can be seem as relevant for heterogenous and homogenous catalysis as well as for carrier mediated membrane permeation especially concerning the metabolic membrane processes in biological systems.
Furthermore it is remarkable that very fast ion reactions are accessible caused by the interface as the locality of reaction accompanied by the coupled transport of educts and products.

REFERENCES

1. **Y. Marcus and A.S. Kertes (1969), Ion Exchange and Solvent Extraction of Metal Complexes, Wiley, London.**
   T. Sekine and Y. Hasegawa (1977), Solvent Extraction chemistry, Marcel Dekker.Inc., New York and Basel.
2. **P.V. Danckwerts (1970),** *Gas-Liquid Reactions,* **Me Graw Hill, New York.**
3. **W. Nitsch and J. Kahni (1980),** *Ger. Chem. Eng.,* **3, 96.**
4. **W. Nitsch and B. Kruis (1978),** *J. Inorg. Nucl. Chem.,* **40,857.**
5. **W. Nitsch and M. Weigl (1998),** *Langmuir,* **14 (23), 6709.**
6. **A. Hoffmann (1986), Die kinetische Behandlung chemisch gekoppelter Grenzflächen-reaktionen am Beispiel der Extraktion von Zink- und Cadmiumionen in Dithizon-beladene Solventphase, PhD Thesis, Technische Universitat Munchen.**

EXTRACTION KINETICS OF ACTINIDES AND LANTHANIDES TRIVALENT NITRATES BY DMDOHEMA MOLECULE

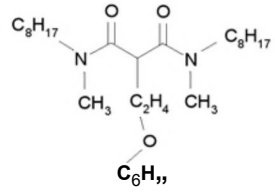
L. Bosland[(1)], J.M. Adnet[(1)], L. Berthon [(1)], D. Pareau [(2)], M. Stambouli[(2)]

[(1)] CEA/VALRHO/DEN/DRCP/SCPS/LCSE BP17171, Bagnols-sur-Cezè, France, 30207
[(2)] Ecole Centrale Paris, LGPM, Grande voie des vignes, Chatenay-Malabry, France, 92295

Nd(III) nitrate extraction kinetics by DMDOHEMA molecule was studied with the ARMOLLEX cell and the pendant drop technique, in nitric acid media. Transfer in ARMOLLEX cell seems to be diffusion controlled. Transfer in single drop technique might be controlled by both regimes: the diffusion and the chemical reaction. In order to understand the influence of the temperature on the extraction kinetics, the precise knowledge of chemical reaction is necessary at each temperature. So, the organic phase organization is studied by vapour pressure osmometry (VPO) in order to determine the average number of aggregation in the organic phase. Nitric acid has a strong influence on the aggregation of molecules in the organic phase. But at present, all species aren't well known. Other characterization techniques will be used in the future to have a better understanding of the influence of the aggregation on the kinetics.

INTRODUCTION

In the framework of nuclear waste reprocessing, separation process of minor actinide from the high level liquid waste by liquid-liquid extraction is developed by CEA. One separation strategy is based on a two-step process: this is the DIAM EX-SAN EX process. The first step consists in extracting trivalent minor actinides and lanthanides with a DMDOHEMA molecule (A*l*,A*l*-dimethyl *N,N*-dioctyl hexyloxyethyl malonamide (scheme 1):



Scheme 1. DMDOHEMA molecule

The second step consists of the separation of the actinides and lanthanides ions. As kinetics is an important parameter in an industrial process, we studied the kinetics of extraction of the trivalent Neodymium by DMDOHEMA molecule.

KINETICS STUDIES

Two techniques were conducted in order to measure the kinetics rates : a modified constant interfacial area cell of the Lewis type, namely ARMOLLEX cell, and the single drop technique. The chemical conditions are :

Aqueous phase: **$[HN0_3]$ = 3 mol.L^{-1} ; $[Nd(N0_3)_3]$ = 0.01 mol.L^{-1}**

Organic phase: **[DMDOHEMA] = 0.65 mol.L-1 in TPH (Hydrogenated TetraPropene, a branched aliphatic solvent), contacted with $[HN0_3]$ = 3 mol.L^{-1}.**

The effect of temperature is investigated in the range 5 - 35°C. Distribution coefficient D was found to be : 10.4 at 15 °C, 5.1 at 25 °C and 4.1 at 35 °C.

The ARMOLLEX Cell Technique

Description

Figure 1 shows a representation of the constant interfacial area cell. The interface is maintained between two grids in order to stabilize it [1], The stirring of the two phases is achieved by two independent impellers. Aliquots of aqueous phase are taken out from the cell with a syringe and analysed with an atomic absorption spectrophotometer. The knowledge of the interfacial area is necessary to obtain the value of the kinetics parameters.

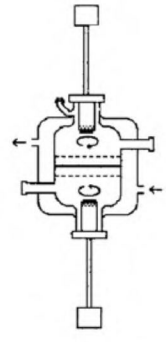


Figure 1: Schematic view of the ARMOLLEX cell

Experiments were conducted at the same Reynolds number in both phases to ensure the same hydrodynamic conditions [2],

Kinetics measurements

The global transfer coefficient E_A^g is obtained from equation (1) for ARMOLLEX cell technique:

$$\ln\left(\frac{Cf - C_a}{C_a^{eq} - c^0}\right) = -\frac{A}{V_a} E_a^g \left(1 + \frac{V_a}{V_G . D}\right) t \qquad \text{(D}$$

where :

C_a^{eq} : concentration (mol.L^{-1}) of the metal in the aqueous phase at the equilibrium

C_a : concentration (mol.L^{-1}) in the aqueous phase at time "t"

$C_a°$: initial concentration (mol.L^{-1}) of the metal in the aqueous phase

A : interfacial area (cm^2)

V_a (respectively V_G) volume of the aqueous (respectively organic) phase

E_a^g : global transfer coefficient relative to aqueous phase

D : distribution coefficient

The Single Drop Technique

Description

A drop of organic phase is injected through in a column filled with aqueous acid solution of Neodymium.

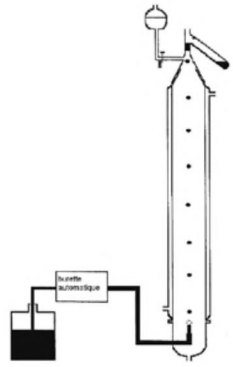


Figure 2 : Schematic view of the rising drop technique

Kinetics measurements

With the single drop technique, E_a[9] is given by the equation (2):

$$\ln\left(1 - \frac{C_o}{D.C_a^o}\right) = -\frac{6\text{-fif}}{d_{\text{„}}.D} J + \ln\left(1 - \frac{C_o^o}{D.C_a^o}\right) \qquad (2)$$

where:

d_p: drop diameter

C_0: concentration (mol.L'[1]) in the organic phase at time "t"

C_a°: initial concentration of the metal in the aqueous phase.

C_0°: initial concentration of the metal in the organic phase, when the drop starts to rise.

KINETICS RESULTS

The global transfer coefficient E_A[9] includes two contributions : the diffusion of the metal from the bulk to the liquid-liquid interface and the chemical reaction with the extractant at the interface. Thus, increasing Reynolds number would reduce the thickness of the diffusion films. When this latter is reduced to zero, only chemical reactions can be rate-controlling, and the rate of extraction becomes independent of the stirring rate. Figure 3 shows the results obtained with the same Reynolds number in both phases :

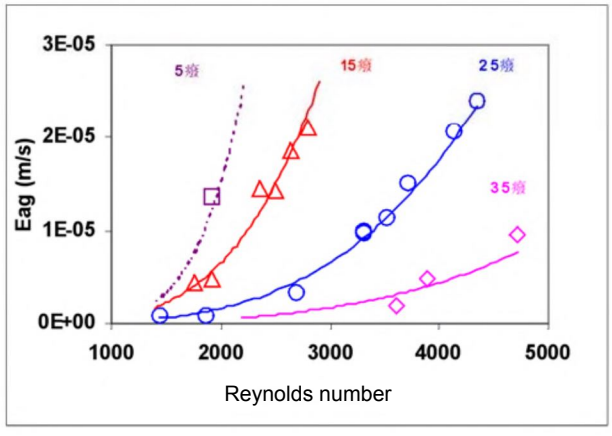


Figure 3 : Variation of E_a[9] versus Reynolds number in ARMOLLEX cell (DMDOHEMA 0.65 mol.L[1] in TP; $Nd(NQ_3)_3$ 0.01 mol.L[1] in nitric acid 3 mol.L[1])

As a matter of fact, the mass transport is totally or partially diffusion controlled for the whole range of the Reynolds number and all the temperatures investigated. M. Weigl [4] found the same trend with DMDBTDMA molecule, working with the same stirring rate. Moreover, kinetics rates are decreasing with increasing temperature, contrarily to what is usually expected.

Table 1 shows the results obtained with the single drop technique in the same chemical conditions, for Reynolds number range (100-450) :

Table 1: Variation of the global transfer coefficient versus temperature with single drop technique

Temperature (°C)	**15**	**25**	**35**
Global transfer coefficient E_a (x 10^5): (m/s)	**(4.0 ±0.7)**	**(3.7 ± 0.6)**	**(3.0 ± 0.6)**

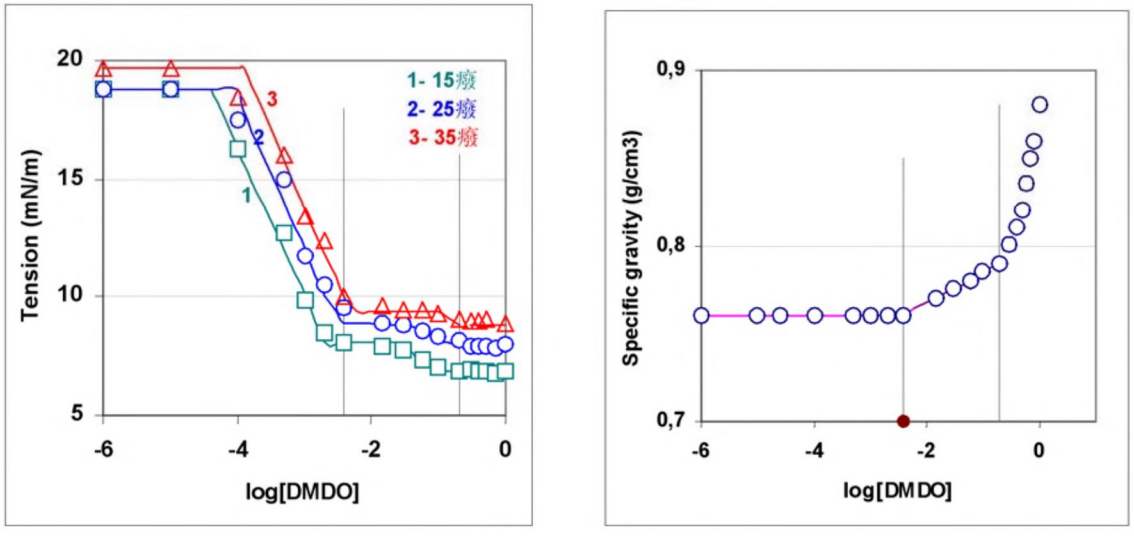
The fact that the values of the alobal transfer coefficient are hiaher than those obtained previously confirms the diffusional nature of the transfer regime in the ARMOLLEX cell. The surprising effect of temperture on kinetics is thoroughtly confirmed.
In order to better understand the surprising kinetics results, the knowledge of the organization of the organic phase is required.

ORGANIC PHASE ORGANIZATION

It had been shown that malonamide molecules organise themself in reversed micelles [4], Various techniques were conducted in order to better understand the organic phase organization (interfacial tension and osmometric measurements and organic species titration).

Determination of the Critical Micellar Concentration (CMC)

As the diamide is a strong surfactant and exhibits low solubility in water phase, CMC determination is achieved by specific gravity [6] and interfacial tension measurements.



Figures 4,5 : Interfacial tension (left) and Specific gravity (25°C) measurements of the organic phase versus DMDOHEMA concentration.

The interfacial tension measurements at different temperature show that an increase of the temperature leads to an increase of the CMC values, located around (CMCi = 5.10^{-3} mol.L^{-1}). Moreover, a change in the micellar solution organization is observed at higher concentration of diamide (C_2 = 0.1 - 0.2 mol.L^{-1}).

The measurements of the specific gravity of the organic phase at room temperature as a function of the diamide concentration clearly confirm the change in the micellar solution behaviour. The small reversed micelles formed at CMC, exhibit a new rearrangement leading to bigger micelles for extractant concentrations higher than at C_2. These processes depend significantly on temperature.

Nitric acid and water extraction

After contact of the organic phase with either pure aqueous solutions or containing nitric acid (3 mol.L^{-1}), the concentration of extracted water and nitric acid in the organic phase were measured by Karl-Fischer or acido-basic titration. Figure 6 shows the number of water molecule extracted by one molecule of extractant as a function of the extractant

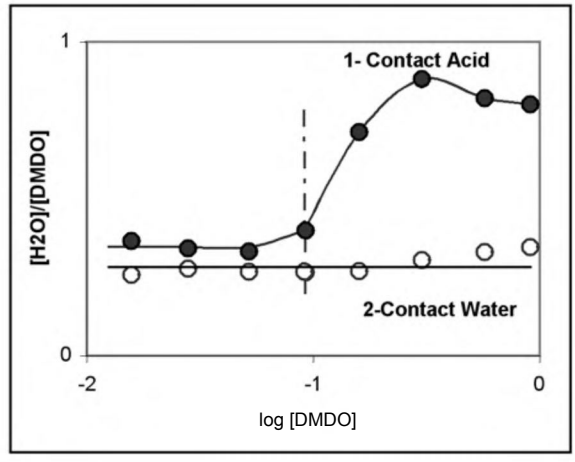


Figure 6: Extracted H_20 as a function of DMDO concentration (Diamide) after contact with pure aqueous solution (curve 2)or containing nitric acid (curve 1) at 23°C.

concentration.

Both water and nitric acid are extracted by the diamide. In the case of pure aqueous phase, the ratio [H_20]/[Diamide] is almost constant (1/ 3) whatever the diamide concentration. Nevertheless, when nitric acid is added (3 mol.L^{-1}), the amount of the co-extracted water per molecule of extractant increases strongly for DMDOHEMA concentration higher than C_2, i.e., when the rearrangement of the micellar solution occurs. Moreover, one molecule of water is co-extracted with one molecule of nitric acid.

Aggregation measurements

Aggregation measurements were achieved by Vapor Pressure Osmometry (VPO) technique [5], Appropriate technical modifications were brought allowing direct measurements in TPH solvent and temperature range (15-35 °C).

The organic phase was contacted with aqueous phase either pure or containing nitric acid (3 mol.L^{-1}). The average aggregation numbers were then deduced in each case. Experimental results are illustrated in figures 7-8.

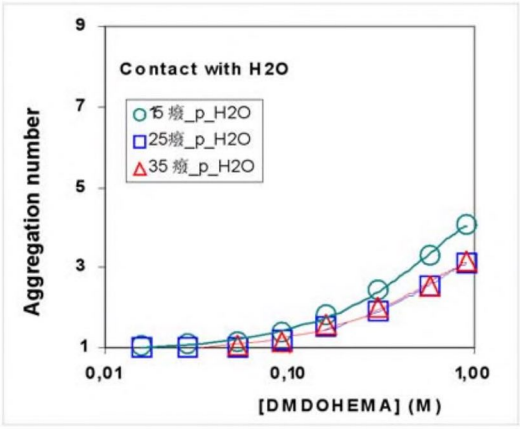


Figure 7

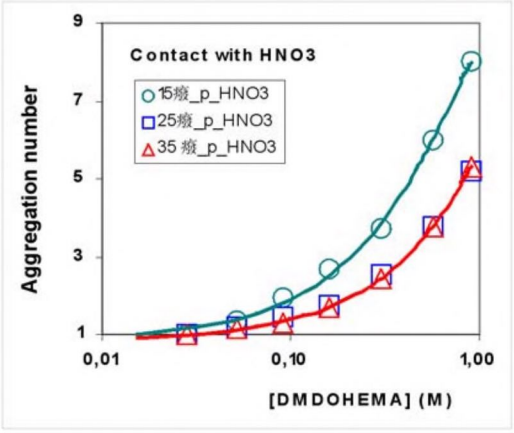


Figure 8

Figures 7,8 : Average aggregation number of the diamide (DMDOHEMA) in the organic phase after contact with pure water (figure 7) and nitric acid solution (figure 8).

In accordance with the different previous results, aggregation strongly increases when the rearrangement of the micellar solution occurs (i.e., > C_2). The extraction of nitric acid strongly favours aggregation in the range of temperature investigated. Curiously, while aggregation decreases when the temperature is increased from 15°C to 25°C, no significant effect is observed between 25°C and 35°C.

CONCLUSIONS

Kinetics studies conducted in either Armollex cell or single drop technique clearly show that the mass transport is totally or partially diffusion controlled for the whole range of the Reynolds number and all the temperatures investigated. Moreover, kinetics rates are decreasing with increasing temperature, contrarily to what is usually expected. This surprising phenomenon is related to the specific behaviour of the organic phase.

Specific gravity and interfacial tension measurements lead to the conclusion that the reversed micelles occurring at very small amounts of diamide (CMCi ≅ 5.10^{-3} mol.L^{-1}) exhibit a rearrangement at higher concentrations (C_2 > 0.1 mol.L^{-1}). Thus, only those bigger aggregates are able to extract water, acid and Neodymium. The aggregation process is highly dependent on temperature and acid co-extraction.

In order to complete the characterization of the organic phase, NMR measurements and small angle neutron scattering measurements are planned.

REFERENCES

1. **W. Nitsch and k. Hillekamp,** *Chem. Ztg.* **96, 254-261 (1972).**
2. **M. Dal Don,** *Thèse CEA-R-5839*, **1999.**
3. **M.Weigl, A. Geist, K. Gompper, J. Il Kim,** *Solv. Ext. & Ion Exch.* **19(2), 215-229, (2001).**
4. **C. Erlinger, L. Belloni, Th Zemb, C. Madic,** *Langmuir,* **15, 2290-2300 (1999).**
5. **A. Buch, thèse univ. Paris VI (2001).**
6. **A. Faure, A.M. Tistchenko, T. Zemb and C. Chachaty,** *J. Phys Chem.,* **89, 3373-3378 (1985)**

ISEC 05
Beijing

The extraction kinetics of Nickel(II) by a synergistic mixture of 2-ethylhexanal oxime and bis(2-ethylhexyl) phosphoric acid

A. Buch [2], M. Stambouli [r], D. Pareau [1]
[1]Ecole Centrale Paris/LGPM - Châtenay-Malabry, 92295 France
[2]NASA / Goddard Space Flight Center, Greenbelt, MD 20771, USA
' Corresponding author: stambouli@lgpm.ecp.fr

Extraction kinetics of Nickel(II) by a mixture of 2-ethylhexanal oxime and bis(2-ethylhexyl) phosphoric acid have been carried out on two complementary techniques, namely, an improved constant interfacial area cell and a highly stirred homothetic cell. The effect of different parameters have been investigated, such as the concentrations of both extracting reagents, nickel(II) and protons. Chemical reactions have proven to control the overall extraction kinetics in both techniques. The extraction rate was determined and a reaction scheme was proposed where the rate-determining step was assumed to be the interfacial reaction between one monomer of £>/s(2-ethylhexyl) phosphoric acid (HA) and the interfacial adsorbed complex $Ni(A)(H_20)^{+}_{5ad}$ according to :

$$Ni(A)(H_2O)^{+}_{5\ ad} + \overline{HA} \underset{k_{-2}}{\overset{k_2}{\rightleftharpoons}} Ni(A)_2(H_2O)_{4,ad} + H^{+} + H_2O$$

INTRODUCTION

In order to extract nickel from an acidic medium, mixtures of extractants such as hydroxyoxime and phosphoric or carboxylic acid have previously been used. Castresana et al. [1] used LIX 63 associated with carboxylic acid, but the best combination seems to be the association of LIX 63 with D_2EHPA [2, 3], Nevertheless that thermodynamic synergism goes with a kinetic antagonism. Indeed, kinetic extraction of nickel by the LIX 63/D_2EHPA system reaches equilibrium after 10 hours. For the LIX 63/carboxylic acid system, Flet et al. [4] assume that the the limiting step is the interfacial reaction between metal ion and the carboxylic acid. At low pH (<2), nickel(II) extraction by oxime is kinetically possible but very slow [5, 6, 7], But if extraction is performed using a mixture of 2-Ethylhexanal oxime (EHO) and D_2EHPA the kinetics of the reaction is greatly enhanced [8, 5]; equilibrium is reached in less than 5 min.
This work deals with the kinetic study of the EHO/D_2EHPA system and is an extension of previous work on the kinetics of the nickel(II) extraction by EHO alone [9],

EXPERIMENTAL

2-Ethylhexanal oxime (EHO) was prepared by reacting 2-ethylhexanal with hydroxyl ammonium chloride [7, 10], The measured EHO purity was 98.5%. Bis(2-ethylhexyl) phosphoric acid (Sigma, 95%) was purified by the copper(II) saturation method [11], The diluent used was dodecane (Aldrich 99%+). The aqueous solution was prepared by dissolving nickel nitrate salt (Fluka 99%) in water.

For both cells, 150 mL and 85 mL of aqueous nickel phase were contacted at 24°C, respectively in organic phase containing a mixture of EHO and D_2EHPA. The pH was controlled using a specific calomel electrode.
The metal contained in the organic phase was stripped with aqueous $HN0_3$. Ni concentrations in the aqueous phases were measured by atomic absorption spectrometry (AA300 Varian).

The kinetics study was performed using two complementary techniques : a modified constant interfacial area cell of the Lewis type (CIA-Cell), and a homothetic highly stirred cell of the Rushton type (HHS-Cell), designed in order to ensure good reproducibility of the experimental results.

KINETICS STUDY OF NICKEL EXTRACTION BY A MIXTURE OF EHO- D_2EHPA

Kinetics model

In a previous study [10] we demonstrated that nickel extraction could be achieved at low pH with the extracted complex are $Ni(Ox)_2(HOx)_2(HA)_2$ or $Ni(HOx)_4$ A_2, where HOx stands for EHO.
The kinetics model can be written as :

$$X(t) = Xeq + (X_c - X_{,q}).exp(-oc.t) \quad (1)$$

Where, $a=a.k_s^{\wedge L}$ $Va\ q$

- V_{aq} (respectively V_{org}) is the volume of the aqueous (respectively organic) phase,
- a is the specific interfacial area per unit of total volume V_{tot}, ($V_{to}t = V_{aq} + V_{org}$)
- k_g is the global transfer coefficient relative to aqueous phase,
- X(t) is the concentrations of aqueous Ni(II) at time t,
- X_0 and X_{eq} are initial and equilibrium Ni(II) aqueous concentrations.

Experimental results (Xj , t,) for both cells are fitted by an exponential curve according to equation (1) using Microcal origin®. Thus, the experimental value of the global volumetric transfer coefficient. $a.k_g$. is then calculated. In the onlv case of the Armollex cell, values of kg are then deduced since the interfacial area a is precisely known.

Influence of physical parameters

In order to make sure that diffusion was not the limiting step of the Ni(II) extraction reaction, the influence of both stirring rate and temperature was investigated for nominal chemical conditions (pH = 1.2 ; $[Ni(N0_3)_2]$ = 3.51 $O^{'3}$ mol/L ; [EHO] = 0.5 mol/L ; $[D_2EHPA]$ = 0.24 mol/L).

For a stirring rate higher than 200 rpm for CIA-Cell and 650 rpm for HHS-Cell, $a.k_g$ was proved to be constant at room temperature. On the other hand, the influence of the

temperature on a.k_g in the range 4 - 60°C was found to obey Arrhenius equation with an activation energy value as high as 52.5±5.5 kJ/mol.
Both experimental results show evidence to the chemical nature of Ni(ll) transfer regime.

Influence of chemical parameters
The influence of all the chemical parameters were then successively investigated by plotting the value of a.k_g as a function of one concentration among Ni(ll), EHO, D_2EHPA, and H^+ respectively, while the remaining chemical parameters fixed. The physical conditions considered to ensure chemical regime were : room temperature (24±1°C) ; stirring rates 270 rpm for CIA-Cell and 700 rpm for HHS-Cell. The nominal chemical conditions were : [$Ni(N0_3)_2$]=3.51 $O^{'3}$ mol/L, [EHO]=0.5 mol/L, [D_2EHPA]=0.24 mol/L.

(i) Influence of Nickel and nitrate concentrations :
At pH=1.0, the nickel concentration was varied from 325 mg/L to 622 mg/L. Either in CIA-Cell or HHS-Cell, the global volumetric transfer coefficient a.k_g was found to be independent on both nitrate and nickel concentrations. For the highly stirred cell, the experimental value was : (2.1 ± 0 .3).10^2 $s^{'1}$. Thus, both nitrate and Ni(ll) concentrations have no effect on the extraction kinetics.

(ii) Influence Oxime concentration :
At pH=1.1, a.k_g was found to be constant in the range 0.20 - 0.51 mol/L of EHO concentrations, with a value of (7.5 ± 0.8).$10^{'3}$ $s^{'1}$ for the HHS-cell.

(Hi) Influence of D_2EHPA concentration :
At a fixed pH and the concentration of D_2EHPA ranged from 0.10 mol/L to 0.58 mol/L, a.k_g was found to be globally a linear function of the monomer D_2EHPA concentration in a logarithmic plot.

(iv) Influence of pH:
The influence of pH in the range of 0.4 to 1.7 was also investigated. The global volumetric transfer coefficient is found to be thoroughly linear with respect to proton concentrations in a logarithmic diagram.

REACTION SCHEME

In a previous study [7] we demonstrated that nickel extraction could be achieved at low pH with the extracted complex: Ni. $(Ox)_2$. $(HOx)_2$. $(HA)_2$ or Ni. $(HOx)_4$. A_2. The following mechanism was proposed and its accordance with the experimental results was tested.

1) $Ni(H,0)g^{2+}$ + HA_{ad} =5?=* $Ni(A)(H_20)_{;ad+}$ H +H_20^+ **Rapid Ki**

2) $Ni(A)(H_2O)^+_{5\ ad} + \overline{HA} \underset{k\text{-}2}{\overset{k_2}{\rightleftharpoons}} Ni(A)_2(H_2O)_{4,ad} + H^+ + H_2O$ **Slow**

3)$Ni(A)_2(H_20)_{4ad+}$ $\overline{H0x}$ $\rightleftharpoons$ $Ni(A)_2(H0x)(H_20)_{3ad+}$ H_20 **Rapid K3**

4) $Ni(A)_2(HOx)(H_2O)_{3,ad} + \overline{HOx} \rightleftharpoons Ni(A)_2(HOx)_2(H_2O)_{2,ad} + H_2O$ **Rapid K_4**

5) $Ni(A)_2(HOx)_2(H_2O)_{2,ad} + \overline{HOx} \rightleftharpoons Ni(A)_2(HOx)_3(H_2O)_{ad} + H_2O$ **Rapid K_5**

6) $Ni(A)_2(H0x)_3(H_20)_{ad+}\overline{H0x} \rightleftharpoons Ni(A)_{;}(H0x)_{4ad+} H_20$ Rapid Kg

7) $Ni(A)_2(HOx)_{4\,ad} + \overline{HA} \rightleftharpoons \overline{Ni(A)_2(HOx)_4} + HA_{ad}$ Rapid K,

where the overbar represents a species in the organic phase, K's equilibrium constants and k kinetics constants.

The rate of the limiting step (reaction 2) is defined as :

$$R: = k:.\ [Ni(A)(H:0)s]ad\ .\ [\overline{HA}] - k\text{-}2.\ [Ni(A)_2(H20)4]ad.aH. \quad (2)$$

Activities were defined on the molarity scale, with reference to C_0=11 mol/L. The ionic strength of the organic phase was very low, so the activity coefficients were assumed constant.

$[Ni(A)(H_20)_5]_{ad}$ and $[Ni(A)_2(H_20)_4]_{ad}$ are replacing by their respective expression :

$$R: = Ki\ k2\ \frac{[\overline{HA}].[HA]_{ad}}{an\text{-}}\ x - k\text{-}2\frac{[HA]_{ad}.a_{H+}}{K_s.K4.K_s.K6.Kd.[HOx]4.[HA]}\ Y \quad (3)$$

With X = $[Ni^{2+}(H_20)_6]$ and Y=$[\overline{Ni(A)_2(HOx)4}]$

As pH was kept constant and HA and EHO were present in large excess : $[\overline{HA}]=[\overline{HA}]_{eq}$, $[\overline{HOx}]=|\overline{HOx}]$ and $a_{+}=a$. The mass balance of nickel lead to :

$$R2 = [Kik!PAUHA_{ii+\ k}\ \frac{}{an\text{-}}\ ^{-2}\ \frac{[HA]ad}{K.3.\ K_{4.}\ Ks.\ K\ e.\ Kd.\ [HOx]_4.\ [H\ A]}\ ] \bullet (X\ Xeq) \quad (4)$$

Thus, the global volumetric transfer coefficient is :

$$a.k_g = a.\vec{k}o.\frac{[\overline{HA}]}{[H]} + a.\overleftarrow{k}o\ .\ \frac{[H]}{[HA].[HOx]4} \quad (5)$$

where : $\vec{k}o=k_2.Ki.[HA]a,$ and $\overleftarrow{k}o=\frac{r\ k\text{-}2fHAlad}{K_3.K_4.K_5.K_6.Kd.}$

For this study we used the monomer concentration of EHO and D_2EHPA calculated using a model previously described [7, 12]. D_2EHPA is more surfactant than EHO. The interfacial liquid-liquid saturation will be achieved preferentially by the bis(2-ethylhexyl) phosphoric acid (HA). Then, the absorbed species concentration could be assumed constant, $[HA_{ad}]$ = cst.

EXPERIMENTAL VALIDATION

Experimental validation of the proposed reaction scheme is done graphically. In each case, expression (5) is rearranged leading to a linear form. The slope and the origin intercept of the best-fitted straight line were then calculated. Thus, the experimental

values of $a.\overleftarrow{k}_o$ and $a.\vec{k}_o$ were deduced for each cell. Specific interfacial area is known in the only case of the Armollex cell ($a_c$ic = 17.6 m'¹).

Validation for pH effect :

According to equation (5), plotting ($a.k_g.[H^+]$) versus $[H^+]^2$, at fixed [HOx] and [AH], would be linear with a slope equal to $\frac{a.\overleftarrow{k}_0}{[HA].[HOx]4}$ and $a.\vec{k}_o\overline{JHA]}$ as its origin intercept.

Experimental validation is illustrated in Figures 1.

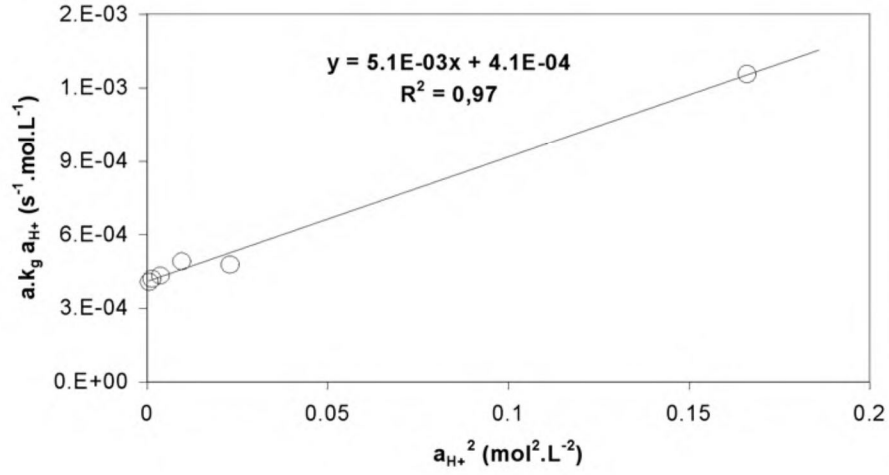


Figure 1. Variation of $a.k_g.an+$ versus $(a_{!!+})^p$ in the Homolhetic Highly Stirred Cell. ([EHO]=0.51 mol/L ; $fD_2EHPA/$=0.24 mol/L ; lNH_4NO_3]=0.2 mol/L ; 700 rpm).

Validation for [HOx] effect :

In the same way, plotting $a.k_g.\overline{[HOx]4}$ vs. $\overline{[HOx]4}$, at fixed pH and [AH], would be linear with a slope equal to $a.\vec{k}_n\frac{\overline{\wedge\wedge}}{[H^+]}$ and its origin intercept to $a.k_{(V}\text{-}t\overleftarrow{\wedge}\overline{L}_{[HA]}$ (Figure 2).

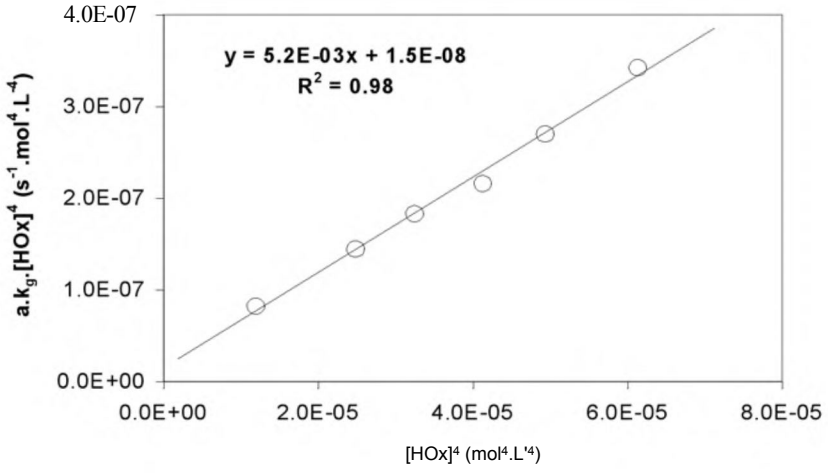


Figure 2. Variation of **$a.k_g.\overline{[HOx]}^4$ vs. $\overline{[HOx]}^4$** *for the Homothetic Highly Stirred Cell (pH=1.1; $[D_2EHPA]$=0.24 mol/L ; $[NH_4NO_3]$=0.2 mol/L ; 700 rpm).*

Validation for [AH] effect :

In the same way, plotting $a.k_g.\overline{[HA]} = f(\overline{[HA]}^2)$, at fixed pH and [HOx], would be linear with a slope equal to $a.\vec{k}_n$ and a k, $\frac{\vec{P}^*}{[H]^+}$ as its origin intercept (Figure 3).
$[HOx]^4$

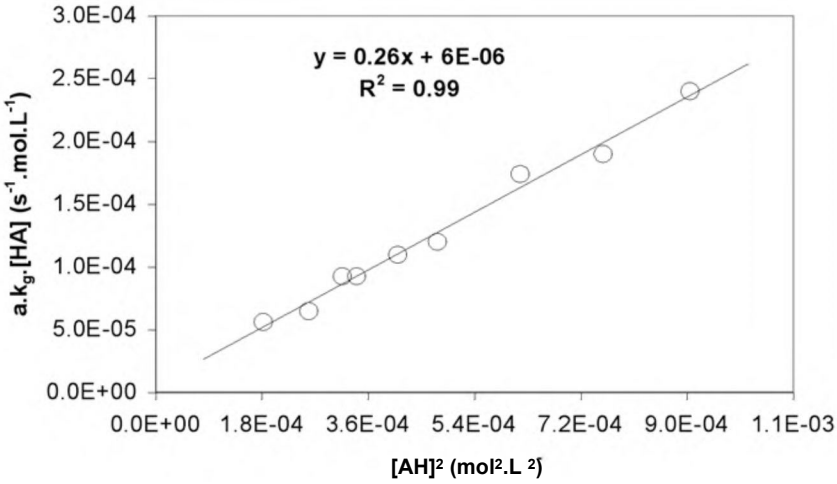


Figure 3. Variation of $a.k_g$. [HA] versus $[AH]^2$ in the Homothetic Highly Stirred Cell (pH=1.1; [EHO]=0.51 mol/L ; $[NH_4NO_3]$=0.2 mol/L ; 700 rpm).

Thus the mean experimental values of the kinetics constants deduced from the slopes and the origin intercepts are :

$a.\vec{k}_0 = (2.0 \pm 0.4).10^{-2}$ (s^{-1}) **$a.\vec{k}_{fi} = (5.0 \pm 0.6).10^{3}$ ($mol^4, m^{-4} . s^{-1}$)**

The same procedure was applied for the experimental results obtained with the Constant Interfacial Area Cell ($a_C$ic=17.6 m^{-1}). Good agreement was observed and kinetics constants deduced :

$\vec{k}_o$ **= (1.0 ± 0.5).10'6 (m . s'1)** $\overleftarrow{k}_o$**= (1.7 ± 1.6)10 1 (mol4 . nT3. s'1)**

As the chemical system in both cells was the same, it is easy then to estimate the value for the developed specific interfacial area into the homothetic cell (a_HHs **= 250 ± 70 cm'1). This result is in good agreement with those observed in similar conditions [13, 14],**

CONCLUSION

A kinetics mechanism proposed for the extraction of nickel by the synergistic mixture EHO- D_2EHPA was found to be consistent with experimental results. When D_2EHPA is introduced, the limiting step is not the reaction between the charged complex $Ni(Ox)^+$ and HOx, but between the adsorbed complex Ni(A)(H,0)^ $_{gd}$ and one D_2EHPA monomer.

While no extraction was observed with D_2EHPA in acidic media and very slow extraction kinetics with EHO alone, a significant enhancement of the extraction kinetics was observed with the mixture EHO- D_2EHPA, en relation with the easier exchange of the labile proton of the D_2EHPA.

ACKOWLEDGEMENTS

We gratefully acknowledge C. Leroi for technical help and for her confirmed assistance.

REFERENCES

1. **J. M. Castresana, M. P. Elizald, M. Aguilar, M. Cox (1988),** *Solv. Ext. Ion Exch.,* **6(2), 265-274.**
2. **M. P. Elizalde, M. Cox, M. Aguilar (1996),** *Solv. Ext. Ion Exch.,* **14(5), 833-848.**
3. **J.S. Preston (1982),** *Hydrometallurgy*, **9, 115-133, 1982.**
4. **D.S. Flett, M. Cox, J.D. Heels (1974),** *Proceedings ISEC'74,* **3, 2559-2575**
5. **L.D. Redden, R.D. Groves (1993),** *Sep. Sci. & Techn.,* **28, 201-225.**
6. **G.L. Pashkov, N.P. Bezrukova, V.N. Volk, I. Yu. Fletlich, N.I. Pavlenko, G.E. Seluti and E.D. Korniyets (1991),** *Solv. Ext. Ion Exch.,* **9, 549-567.**
7. **A. Buch, D. Pareau, M. Stambouli and G. Durand (2001),** *Solv. Ext. Ion Exch.,* **19, 277-299.**
8. **J.S. Preston (1983),** *Hydrometallurgy,* **10, 187-204, Extraction Conference, 3, 2559-2575,.**
9. **A. Buch, D. Pareau, M. Stambouli, G. Durand (2002),** *Proceedings ISEC'02, 262-* **267.**
10. **V.M. Peshkova, V.M. Savostina, E.K. Ivanova (1977),** *Oximes,* **Nauka, Moscow.**
11. **J.A. Partridge, R.L. Jensen (1969),** *J. Inor. Nucl. Chem.,* **31, 2587-2597.**
12. **A. Buch, D. Pareau, M. Stambouli, G. Durand (2002),** *Solv. Ext. Ion Exch.,* **20(1), 49-66.**
13. **C. Foulon (1997),** *Thermodynamique et cinetiqué de /'extraction du palladium(ll) pardes melánges d'extractants contenant la LIX 63,* **PhD Dissertation - Paris VI**
14. **J.B. Fernandes, M.M. Sharma (1967),** *Chem. Eng. Sci.,* **22, 1267-1282**

KINETICS OF Y(III) EXTRACTION WITH MIXTURES OF CYANEX 272 AND P507 AS AN EXTRACTANT

Ying Xiong, Shulan Meng and Deqian Li*

Key Laboratory of Rare Earth Chemistry and Physics,
Changchun Institute of Applied Chemistry, Chinese Academy of Sciences,
Graduate School of Chinese Academy of Sciences, Changchun, 130022, P R.China

The Yttrium(III) extraction kinetics and mechanism with the mixtures of Cyanex 272 and P507 dissolved in heptane have been investigated by constant interfacial cell with laminar flow. The stoichiometry of the extracted complex formation reaction is determined. The studies of effects of the stirring rate, temperature, specific interfacial area, hydrogen ion and extractant concentration on the extraction rate show that the extraction regime is dependent on the extraction conditions and the most probable reaction zone is at the liquid-liquid interface. The rate of mass transfer per unit area is found to be proportional to $[H_2A_2]_{(0)}^{\circ}$-17, $[H_2B_2]_{(o)}^{043}$ and $[H^+](a)\sim^{\circ 85}$ at the interface. The extraction rate constant, k_F, has been measured to be $10^{'372}$ m/s. The rate expression can be written as: $R_F = 10^{'3\cdot 72}[Y^{3+}]_{(a)}\ [H_2A_2]_{(o)}^{0}-17[H_2B_2]_{(o)}^{0,43}[H^+]\ (a)^{-085}$ kmol/m^{2}s. The synergistic effects for yttrium(III) extraction with the mixtures of Cyanex 272 and P507 has been discussed.

INTRODUCTION

There is a sharp rise in demand of yttrium (Y), due to the quick growth of advanced industries, such as electronics and new ceramics [1-2], For their application in high-tech fields, the purity of Y is strictly required, for example, the fluorescent grade Y_20_3 requires the content of relevant RE impurities should be lowed to 1x1 O'4 level or even lower. However, it is generally difficult to separate and purification of Y from relevant heavy rare earth because of the similarity in chemical properties of these elements. For the effective separation of Rare earth metals, various modification of the solvent extraction system have been reported, one of the most effective methods for improving the separation is to modify organic phase [3-4]

In earlier work, we reported the kinetics of Y(III) with Cyanex272 using constant interfacial cell with laminar flow developed by Zheng and Li [5-6], Studies indicate that the extractant has several advantages including high selectivity, low aqueous acidity in extraction and stripping and high separation factors of rare earth ions by contrast with P204 and P507. However, due

to the higher $pH_{1/2}$ value of Cyanex272, the extraction ability of rare earth ions with Cyanex272 is lower than that of latter. Therefore, we investigated the kinetics of Y(III) with the mixtures of Cyanex 272 and P507 (abbreviation as HDP) and found that it was different from the kinetics mechanism with Cyanex 272 (HA) or P507 (HB) alone. In this paper, the research results on the extraction kinetics of Y(III) with HDP dissolved in heptane using a constant interfacial cell with laminar flow have been reported.

EXPERIMENTAL

Reagent

P507 and Cyanex272 were kindly supplied by Shanghai Organic Chemistry Institute and CYTEC Canada Inc., respectively, and they were used without purification. Yttrium stock solutions were prepared by dissolving yttrium oxide (99.9%) in hydrochloric acid and standardized by EDTA titration using xylenol orange as an indicator. All other reagents were of analytical grade.

Procedure

In the kinetics experiments, the concentrations of Cyanex272, P507 and mixtures of Cyanex272 and P507 (at a ratio of 1 to 1) were all 3.0xl0'²mol L'¹, and when studying the effect of one extractant, concentration of the other extractant was 1.5 xicr²mol L'¹. The pH value of aqueous phase was kept at 2.10 (ionic strength 1 mol L'¹), and varied when the effect of pH was studied. The aqueous phases contained 3.1x1 O'³ mol L'¹ yttrium ion. The extraction kinetics was investigated using a constant interfacial area cell with laminar flow described previously [5],

Theoretical

Assuming that the mass-transfer process could be formally treated as a pseudo-order reversible reaction with respect to the metal cation [7], one can write the following equation:

$$\text{^(o)}^{0}\ Y_w \qquad (1)$$

The following equation of extraction can be obtained as described in Eq. (5):

$$R_{//} = -\frac{ct[Y]_{w}}{at} = k_F[Y]^{b}[H+Y[H^{\wedge}Y \qquad (2)$$

$$--^{\wedge} = -y(k_{m},[Y\backslash_{o)}-k_{ao}[Y]_{M}) \qquad (3)$$

$$\ln\left(1-\frac{[Y]_{(o)}}{P\%>,}\right) = -\frac{O}{V}(1+K_{,,})k_{o\alpha}t \qquad (4)$$

where “a” refers to the aqueous phase, “o” is the organic phase, “e” indicates the equilibrium

of extraction, "k_{ao}" and "k_{oa}" are the forward as well as backward pseudo-first-order rate constants, respectively, "k_F" is forward extraction rate constant, "K_d" represents the distribution constants, "Q" stands for the interfacial area and "V" is the volume of the aqueous phase or the organic phase.

The slopes of the plots $\ln(1-[Y]_{(0)}/[Y]_{(0)}^{e})$ vs. t have been used to evaluate k_{oa} and k_{ao}. All plots were straight lines in the work, indicating that above assuming was reasonable.

RESULTS AND DISCUSSION

Stoichiometry of the extracted complex formation reaction

The stoichiometry of the complex formation reaction between the yttrium ion and HDP in heptane has been carried out. As shown in Fig. 1, the plots of LogD versus pH at constant HDP concentration give a straight line with a slope of about 1.0. Similarly, at constant aqueous acidity and concentration of the other extractant, the plots are linear with slopes of about 1.0 **and 2.0 for $[Cyanex272]_{(0)}$ and $[P507]_{(O)}$, respectively (shown in Fig.2). Thus, the equilibrium equation can be proposed as follows:**

$$Y(OH)^{2+}_{(a)} + 0.5(H_2A_2)_{(O)} + 2.5(H_2B_2)_{(O)} = Y(OH)AB_5H_{4\,(0)} + 2H^{+}_{(a)} \qquad (4)$$

where H_2A_2 and H_2B_2 presents the dimmer of Cyanex272 and P507, respectively.

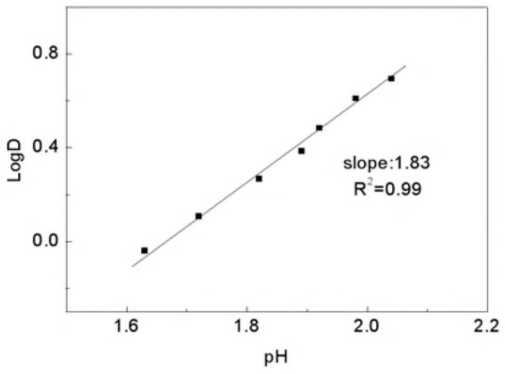


Figure 1. Dependence of distribution coefficient on equilibrium pH

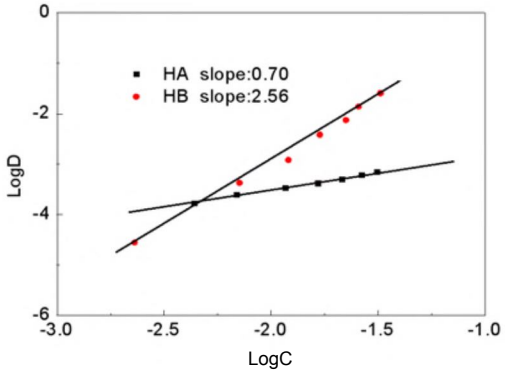


Figure 2. Dependence of distribution coefficient on extractant concentration

Extraction Regime

In extraction kinetics experiments, the criterion generally used to identify the extraction regime is the dependence of the extraction rate on the stirring speed in constant interfacial area cell. The influence of the stirring rate of the two phases on k_{ao} has been studied for Y(III) with HDP at constant chemical composition (shown in Fig.3). This theory has been reported in earlier work [8**], When the stirring speed is greater than 250r/min, a plateau region is reached, which indicates that the extraction rate with HDP and Cyanex272 [**6**] may be chemical controlled in** [110]

that zone, whereas the extraction rate with P507 is independent of the stirring rate indicates that it may be diffusion controlled in the range from 150 to 350 rpm. In addition, the data shown in Fig.3 elucidate that the extraction rate is neutralize with mixtures extractant of Cyanex272 and P507, a fact that has also been observed in the following experiments.

A further criterion that enables distinguishing between a diffusion-controlled and a kinetics regime is the experimental determination of the activation energy of the extraction process. The effect of temperature on the extraction rate with HDP has been studied in the temperature range from 293 to 313K and the results are given in Fig.4. Combining with the results that has been studied earlier [6], the apparent activation energy for Y(III) with Cyanex272, P507 and HDP are 45.62, 21.05 and 26.52 kJ mol"[1] in the temperature range of 293K to 303K. That is, the admixture of Cyanex272 and P507 neutralizes the activation energy, which is the reason why it can't accelerate the extraction rate of Y(III) with HDP.

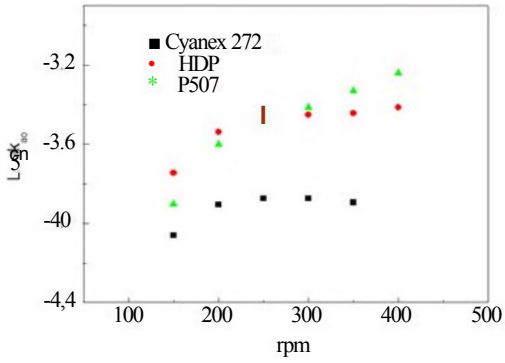


Figure 3. The effect of the stirring speed on the extraction rate

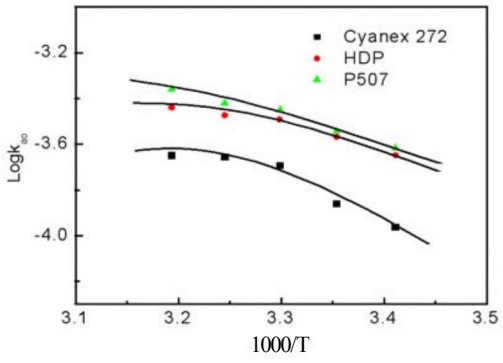


Figure 4. The effect of the temperature on the extraction rate

According the general theory [9], the obtained value of Ea of extraction suggests a possible mixed controlled regime for HDP, chemical controlled regime for Cyanex272 and diffusion controlled regime for P507. All other kinetics experiments are measured at 250 rpm/min and 303K in order to maintain the same hydrodynamic conditions.

Reaction Zone

An important criterion to determine whether the chemical reactions controlling the rate of extraction in a kinetic regime occur in the bulk phase or at the interface is the relationship between the extraction rate and the interfacial area. If the slow chemical reactions occur in the bulk phases, the initial rate will be independent of interfacial area. On the contrary, a reaction occurring at the interface will show a direct proportionality between the rate and the interfacial area and the plot will pass the origin [10], The effect of the specific areas Q/V (intcrfacial area / phase volume) on the extraction rate (k_{ao}) has been studied and a linear relationship (y = 0.0003x + 2E-06, R^2 = 0.98) is obtained, which is the characteristic of an interfacial reaction for Y(1II) extraction with HDR

Extraction Rate Equation [III]

The effect of pH on the extraction rate is given in Fig.5. From the slope of the plot (pH<1.9) [11] one can calculate that the order of hydrogen ion concentration is -0.85. The influence of extractant concentration on the extraction rate is given in Fig.6. A linear correlation between Logkao and LogC indicates that the orders of extractant for Cyanex272 and P507 are 0.17 and 0.43, respectively. Using the values of the intercepts in Figs.5-6, the forward extraction rate constant is evaluated (represented in Table 1). The estimated $Logk_F$ is -3.72 with a standard deviation of ±0.08. According to above results, the rate equation for HDP can be written as:

$$R_F = 10^{'3\ 72}[Y^{3+}]_{(a)}\ [H_2A_2]_{(o)}{}^{0\ 17}[H_2B_2]_{(o)}{}^{\circ\ 43}[H^+]_{(a)}{}^{\wedge 85}\ \text{kmol/m}^2\text{s} \qquad (5)$$

Comparing *the value of* k_F **shown in Table 2, it is clear that the mixtures of Cyanex272 and P507 exhibits no synergistic effects for yttrium(III) extraction for a certainty.**

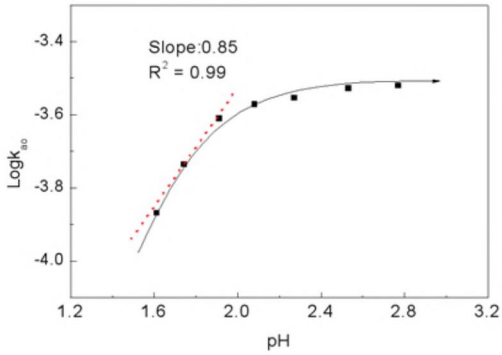


Figure 5. The effect of phi on the extraction rate

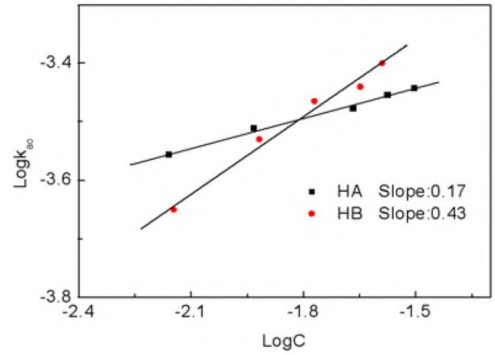


Figure 6. The effect of the extractant concentration on the extraction rate

Table 1 Evaluation of the value of forward extraction rate constant, k_F

Fig.	Variable	pH	$[H_2A_2]$ M	$[H_2B_2]$ M	Value of $Logk_F$	Mean $Logk_F$	Standard deviation of $Logk_F$
5	pH	**2.27** **2.53** **2.77**	**0.015** **0.015** **0.015**	**0.015** **0.015** **0.015**	**-3.56** **-3.65** **-3.71**		
6	**Cyanex272**	**2.18** 2.12 2.10	**0.024** **0.038** **0.058**	**0.015** **0.015** **0.015**	**-3.72** **-3.77** **-3.73**	**-3.72**	**±0.08**
	P507	**2.39** 2.12 2.10	**0.015** **0.015** **0.015**	**0.019** **0.037** **0.059**	**-3.81** **-3.75** **-3.80**		

Table 2. The value of k_F in the Y(III) extraction

Extractant	Cyanex272	P507	HDP
kF	$10^{-3.441}$ ±0.03	$10^{-3.360}$ ±0.02	$10^{-3.372}$ ± 0.08

CONCLUSIONS

The extraction of Y(III) with HDP is a complex kinetics process with interfacial reaction. The stoichiometry of the extracted complex is determined to be $Y(OH)AB_5H_4$. The extraction regime is diffusion and chemical controlled, moreover, it changes with the variation of conditions. The most probable reaction zone is at the liquid-liquid interfacial area based on the studies of specific area. The dependence of extraction rate on species concentration has been studied and the rate equation of extracting yttrium with HDP in heptane is: $R_F = 10^{-3.72}[Y^{3+}]_{(a)}\ [H_2A_2]_{(0)}^{0.17}[H_2B_2]_{(o)}^{0.43}[H^+]_{(a)}^{-0.85}$ kmol/m²s. The mixtures of Cyanex272 and P507 exhibits no synergistic effects for yttrium(III) extraction.

ACKNOWLEDGEMENTS

The authors wish to thank Shanghai Organic Chemistry Institute and CYTEC Canada Inc. for supplying the P507 and Cyanex272. This project is supported by the National Program entitled 'Basic Research of Rare Earths' (G1998061301), National "863" project (2002AA647070) and National Natural Science Foundation of China (20371046).

REFERENCES

1. **A. N. Turanov, V. K. Karandashev, A.V. Khaaritonov, A. N. Yarkevich and Z. V. Safronova (2000),** *Solv. Extr. Ion Exch.,* **18(6), 1109 -1134.**
2. **M. H. Chhatre and V. M. Shinde (1998),** *Talanta*, **47, 413-419.**
3. **Y.G. Wang, L. G. Wang and D. Q. Li (2003),** *Solv. Extr. Ion Exch.,* **38(10), 2291-2306.**
4. **J. S. Preston, J. H. Partrick and G. Steinbach (1994),** *Hydrometallurgy,* **43, 143-160.**
5. **Z. Zheng, J. Lu, and G. X. Ma (1998),** *Chem. Eng. Sci.,* **53(13) 2327-2333.**
6. **Y. Xiong and D. Q. Li (2004),** *Solv. Extr. Ion Exch.,* **22(5), 833-851.**
7. **P. R. Danesi and G. F. Vandergrift (1981),** *J. Phys. Chem.,* **85, 3646-3651.**
8. **P. R. Danesi and R. Chiarizia (1980),** *CRC Crit. Rev. Anal. Chem.,* **10, 1-126.**
9. **J. F. Yu and C. Ji (1992),** *Chem. J. Chin. Univ.,* **13, 224-226.**
10. **Dietz. M. L., Freiser, H. (1991),** *Langmuir,* **7, 284-288 .**
11. **R. K. Biswas, M. A. Hanif and M. F. Bari (1996),** *Hydrometallurgy,* **42, 399-409.**

Control Strategy of Rare Earth Countercurrent Extraction Process

Sheng Wu,[a,b] Chunsheng Liao,[ab] Jiangtao Jia,[ab] and Chunhua Yan[a]*

[a] **State Key Lab of Rare Earth Materials Chemistry and Applications, Peking University, Beijing 100871, China**

[b] **Beijing Institute of Founder Rare Earth Science and Technology Co., Ltd, Beijing 100871, China**

Countercurrent extraction (CCE) is the most important method for rare earth separation. In order to make the qualified products, it is necessary to achieve the automatic control of the CCE process. In this paper, the computer simulation and control strategy of rare earth separation process based on the model of real mixer-settler extraction cascade was studied. Since the data errors may occur during the purity measurement and the flow-rate control of different reagents in a real production line, the random noise was introduced to the input or output data in correspondence with the real case in the simulation. The software is running on a personal computer, and the calculated data can be transferred into the network database. Then the data are retrieved and analyzed using specific control algorithm, the diagnosis and control commands are obtained thereafter. Here, the simulated control experiments with different control algorithm are verified and optimized by comparing different control results.

INTRODUCTION

Rare earth (RE) elements play the crucial role in the functional materials and high-tech fields. In order to meet the requirements of the applications, the quality and the quality stability of the products have been improved rapidly during last two decades [1,2]. As an effective and powerful method, recently, the countercurrent extraction (CCE) is the mainly applied method for industrial RE separation, however, it is still necessary to establish a quality control system and optimize the adjustment strategy for the production lines. Compared with other chemical processes, the control system of the CCE for RE separation is more complicated due to the multi-parameter and serious hysteresis.

Based on our previous studies of the CCE for RE separation, we developed a control simulation system. In this system, a mixer-settler model is used to simulate the separation process, and random noise is introduced to simulate the flow-rate and purity measurement. Both the transfer of the detected purity data and the issue of the control command are realized *via* network database. With this software, a series of virtual control experiments were carried out to test and optimize various control algorithms.. Optimization for specific control algorithm is also achieved by comparing the corresponding results.

CONTROL SIMULATION SYSTEM

Virtual cascade: the simulation of CCE in mixer-settler process

A mixer-settler model has been used in the simulation to the CCE [3,4], Extractant and [122]

aqueous solution are mixed in the mixer, and separated in the settler. The key parameters, such as the volume of mixer and settler, flow-rates, RE concentrations in both aqueous and organic phases are taken into consideration to obtain an exact simulation to the real cascade.

The mixer-settler model of the simulation of CCE process is depicted in Figure 1. The aqueous solution and the organic extractant are fed into the mixer. After the mixing process was completed, the mixture was transferred into the settler and separated into two phases, organic and aqueous phases, which are led into the adjacent mixers, respectively. The mixer efficiency is applied to the simulation for the mixing process by solving the extraction equilibrium of multi-component RE system. The computation for every stage of the cascade is carried out repeatedly to perform the simulation. A virtual cascade is set up and the virtual experiments can be carried out.

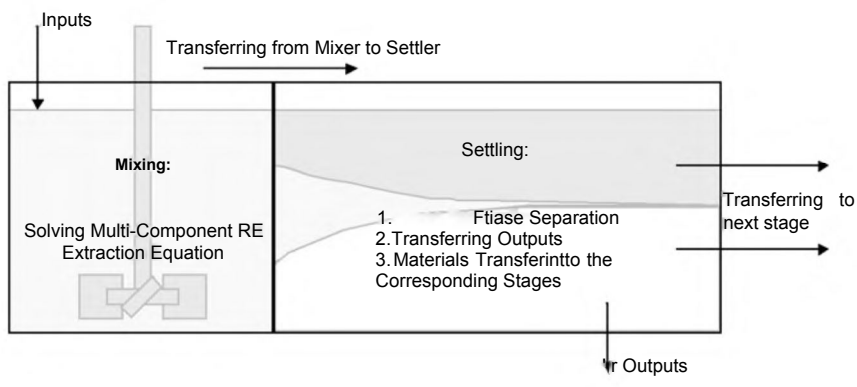


Figure 1. Mixer-settler model for RE countercurrent extraction simulation.

Data noise generation

Based on the product indexes (purity and recovery) and the process parameters (the stages of extraction, scrubbing, and stripping sections; the flow-rates, concentrations and composition of the feed, extractant and solvent, scrubbing and stripping solutions), the distributions of RE in each stage can be simulated. Compared with the control accuracy of the real process (10^{-1}~10^{-3}), the computational simulation accuracy is quite high ($\geq 10^{-6}$). To make the simulation more practicable, the random noise was introduced, and ±5% and ±10% random noises were applied to the flow-rates and RE composition, respectively.

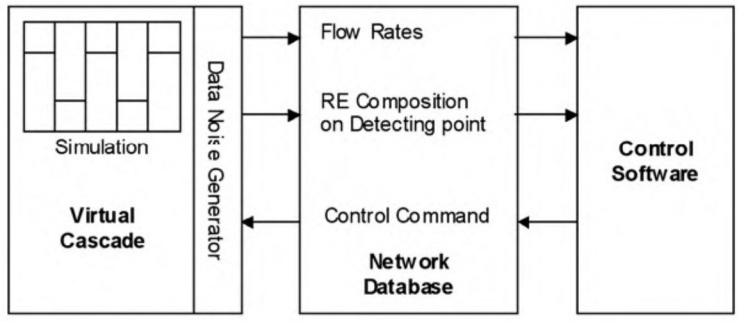


Figure2. Control simulation system construction

Control software

The control commands are issued *via* the control software. Control command is generated on the specific control algorithm based on the data analysis with the simulation software. Various control methods are programmed into the control software to achieve the control simulation. Control statistics analysis is then used to optimize the corresponding control algorithm. [123]

System construction

As shown in Figure2, the simulation system consists of 2 major parts: the virtual cascade and the control software.

The virtual cascade performs the control command, simulates countercurrent extraction, and provides RE composition data on specific stages for purity control. The control software analyzes the detected data and issues the control commands. The data are transferred through a network database where the data are stored.

VIRTUAL CONTROL EXPERIMENT

Control target

In this experiment, we simulate the Ce/Pr separation of certain extraction separation system. The configuration of the CCE separation is shown in Figure 3, and the RE distribution in balancing state is illustrated in Figure 4.

The Separation parameters are: $Pc_e/i_a=6$, $Pp_r/c_e=2$, $p_Nd/p_r=1\text{-}5$. **The feed composition is: La=30%, Ce=50%, Pr=5%, Nd=15%. Separation index for outlet A is: La+Ce<0.1%, Pr+Nd>99.9% separation index for outlet B is: La+Ce>99.9%, Pr+Nd<0.1%.**

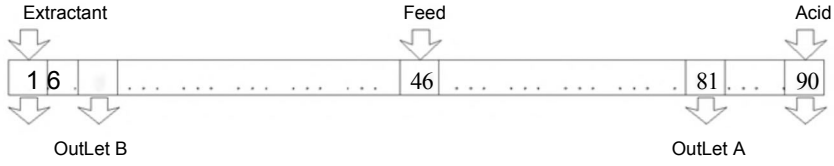


Figure 3. Configuration of experimental countercurrent extraction separation

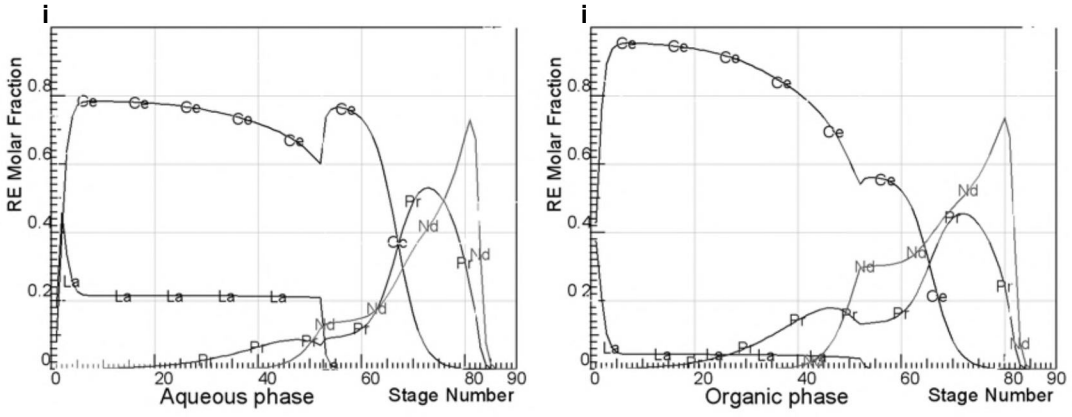


Figure4. RE distribution in balance state

In the control experiment, we choose the detecting point on stage 65, where the Ce concentration change is the most quickly in between the consecutive stages. The control target for Ce/RE at stage 65 is 40% in this virtual experiment.

Virtual PID control experiment

PID (Proportional-Integral-Diffractive) is a generic control algorithm, which is commonly used in many control fields[5]. We implemented the progressive PID in our control software to test the behavior of PID in countercurrent extraction control. PID algorithm can be expressed as the following equation in our experiment: [124]

$$m = K_p \cdot E(t) + K_r \int_{T=0} F(T)/t + K_d$$

To evaluate the control behavior of the algorithm, some parameters were introduced. I_a and I_s are the inaccuracy and the instability of control, respectively. P_a and P_b are the averaged purity in outlet stage 81 and 6, respectively. T_s is the sampling time, and it was fixed to 24 hour in this case, since it is the time taken by the off-line analysis in the common daily sampling practice.

For comparison, the simulated response without control is shown in Figure 6A. In the graph, F represents flow rate, and E represents Error at the detecting point. As the input and output flow rates are inaccurately measured, the separation system is unstable, and hence a control is necessary.

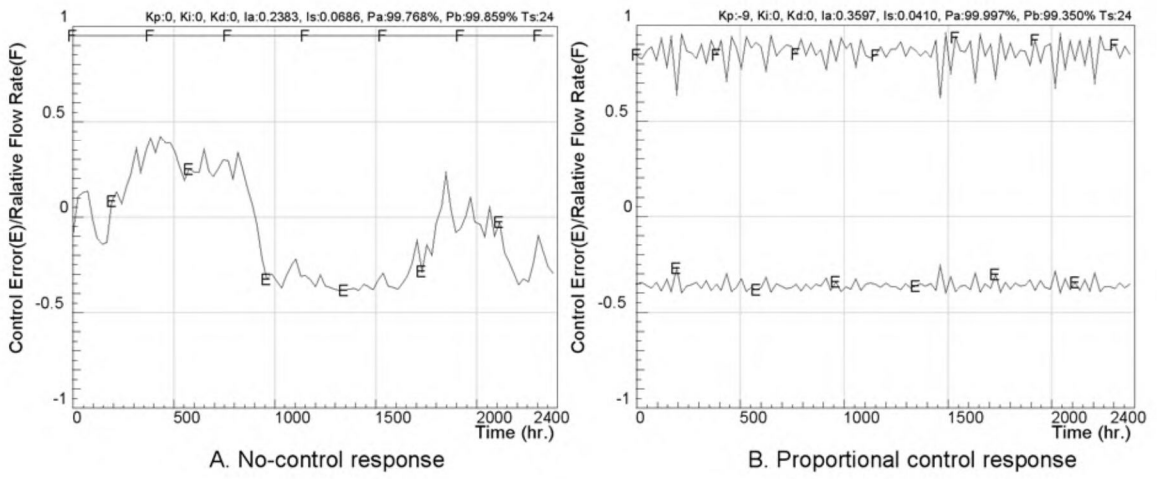


Figure 6. Simulated no-control and proportional control response.

It is the proportional control while the integral and diffractive factors, K; and Kd, were ignored. The experimental control response is shown in Figure 6.B, indicating that the proportional control is of a good stability, but of a bad accuracy. As a result, P_b is not satisfiable for the separation requirement. [125]

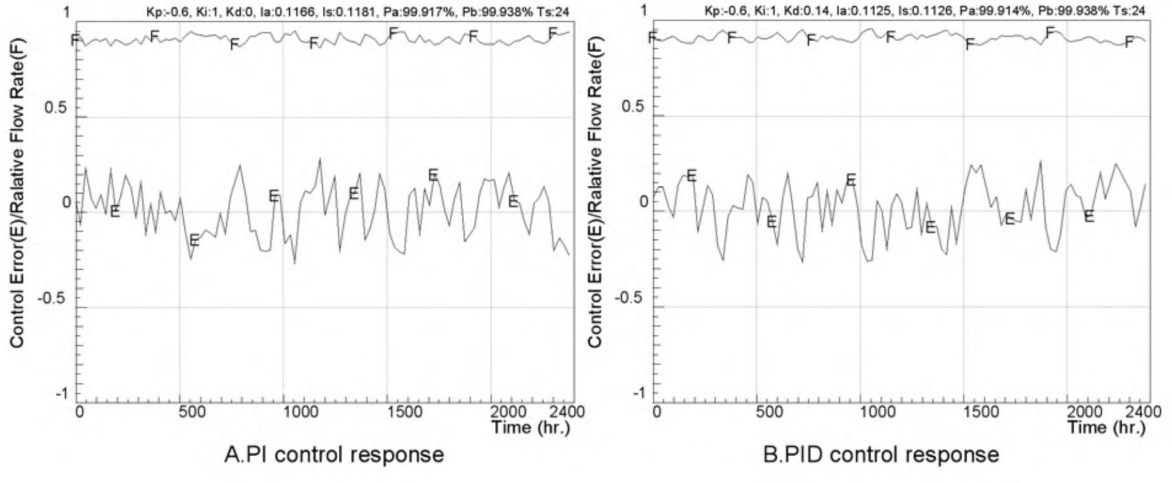


Figure 7. Simulated PI and PID control response

It is a PI control with the integral factor, Kj introduced.. While Kj was set to be 1, the integral

factor could automatically adjust the system to reach the E=0 state. Control response of PI is shown in Figure 7.A

Taking the Kd factor into account in the PI control, the control became a PID control. The control response is shown in Figure 7.B. Comparing with PI control response, the stability was improved, while the control accuracy remained at the same level.

Optimization of PID parameters

In order to have a good control performance, the control parameters of PID have to be optimized. The simulation provides an effective way for the variation of the parameters. By comparing the corresponding control results, the optimization can be achieved.

For each set of PID parameter, a 100-day virtual control experiment is performed. hQ was set to be 0 and the K_p as a variable. The results are shown in Figure 8A. Comparing with the control results, the optimized K_p was determined to be 0.6.

Then the Kj is varied. The result of the virtual control is shown in Figure 8.B. Comparing with the control results, we take optimized Kj as 0.14. The optimized control response was shown in Figure 7.

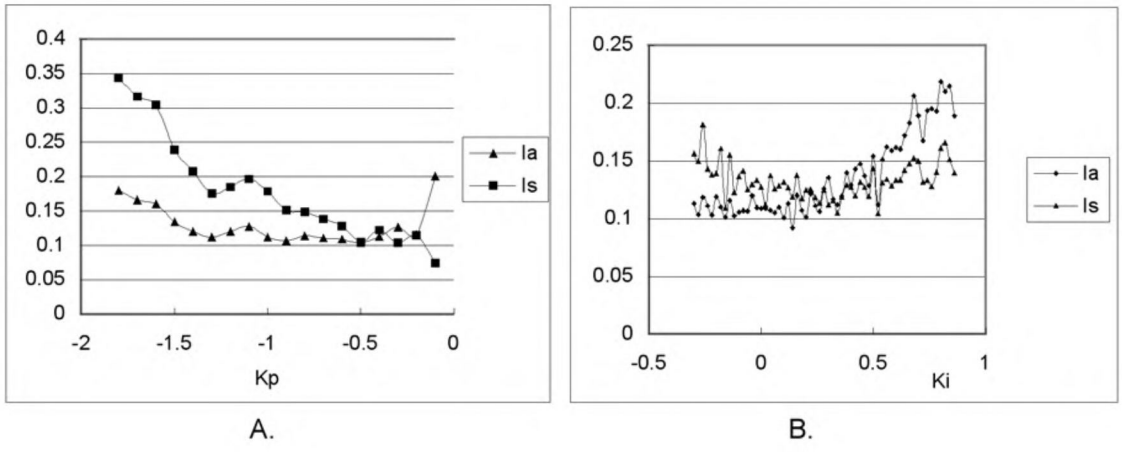


Figure 8. Optimization for K_p and K,

Sampling time

In real separation process, sampling to the cascade has to be set to a reasonable and practicable scheme. To test the control behavior with different sampling time, the sampling time was varied from 1 to 96 h. Shown in Figure 9 is the corresponding results. [126]

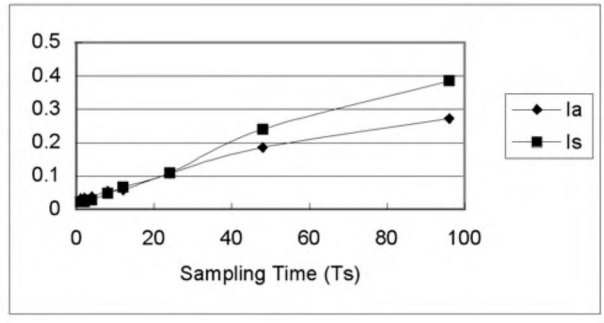
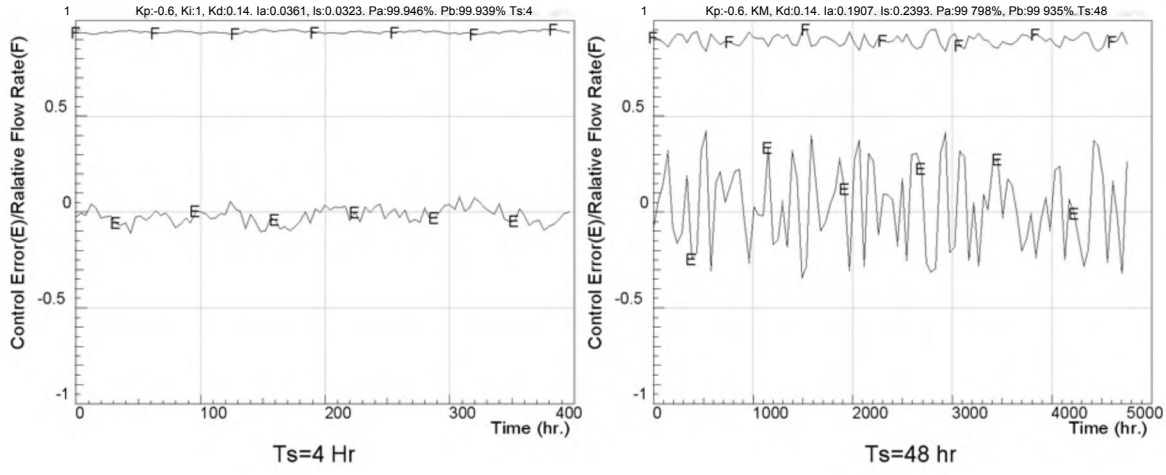


Figure 9. Simulated control influence of sampling time

Typical control result with T_s=4 and T_s=48 is shown in Figure 10. It can be conluded that the sampling time is an essential factor for the control of countercurrent extraction with PID algorithm. To get better control performance, the high sampling frequency is necessary.



FigurelO. Control response of Ts=4 and 48 (Hr)

CONCLUSIONS

In this paper, we developed a control simulation system for countercurrent extraction. With the mixer-settler model and introduction of random noise, the behavior of countercurrent extraction cascade can be simulated under specific control strategy.

The commonly used PID control algorithm was chosen in the simulation system. The PID parameters were optimized to improve the control performance. The sampling time play a key role in the PID algorithm in countercurrent extraction control. If the short sampling time is not available in practice, the control performance of the PID strategy will not expected to be satisfactory.

With this virtual control experimental platform, various control strategies can be tested and optimized. In fact, we are now developing control algorithm specific for countercurrent extractions, which is underway on this platform now. Relative works beyond this paper will be published elsewhere.

References

1. **P. Maestro, D. Huguenin (1995),** *J. Alloys and Compounds, 255,* **520-528.**
2. **D. Z. Wang, Q. Wan, Y. C. Yang (1996),** *J. Rare Earths, 14,***223-230.**
3. **J. T. Jia, S. Wu, C. S. Liao, et al. (2004),** *J. Rare Earths, 22,* **576-581.**
4. **J. T. Jia, C. H. Yan, C. S. Liao, et al. (2001),** *J. Rare Earths, 19,* **6-10.**
5. **D. F. Wang (2005),** *Acta Physica Sinica. 54,* **1495-1499** [127]



KINETIC STUDY OF CHROMIUM(III) EXTRACTION FROM AQUEOUS SOLUTIONS BY BIS(2ETHYLHEXYL)PHOSPHORIC ACID (DEHPA)

^eyna G. Turriza Cruz, [2]Dominique Pareau, [2]Gerard Durand, [2]Moncef Stambouli
Ricardo Navarro Mendoza, 'T. Imelda Saucedo Medina and ^ario Avila-Rodriguez"

^nstituto de Investigaciones Cientificas. Universidad de Guanajuato. Guanajuato, Mexico.
[2]Laboratoire de Genie des Precedes et Materiaux. Ecole Centrale Paris. Paris, Francia.

The results obtained from the kinetic study of extraction of chromium(III) with DEHPA are presented. This study has been performed in a stirred, temperature controlled and constant interfacial area Lewis Cell, in order to determine the regime controlling the mass transfer rate of chromium(III) from the aqueous to the organic phase. Control of the extraction rate may be originated from the diffusion of species in both phases or across the water/organic interface, and also from chemical reactions taking place in both phases or at the interface. The minimum rate of stirring of both phases necessary to reach the chemical regime (i.e., control of the rate by chemical reactions), was calculated from the product of the global mass transfer coefficient (*k*) by the interfacial area (*a*), at different stirring rates. The results obtained show that the chemical regime is reached when the stirring rate of the aqueous phase is 150 rpm. At slower stirring rates the mass transfer rate is controlled by diffusion. The same study for the variation of stirring rate in the organic phase confirms the previous results, i.e. the chemical regime is reached at 150 rpm in the aqueous phase.

INTRODUCTION

The tannery industry generates large amounts of residual waters with high levels of Cr(III) that negatively impact the environment. For example, Eisler [1] reports toxic effects of chromium in fish at 10 mg/L of Cr(VI) and 30 mg/L of Cr(III). In the case of birds, the harmful effects of chromium are observed at concentrations of 5.1 and 10 mg/L of Cr(VI) and Cr(III) respectively, by kg of diet [1], In spite of the existing controversy about Cr(III) toxicity, the high contents of this material in such effluents bring up the necessity to control this chemical species.

The liquid-liquid extraction is an alternative to lower the concentration of Cr(III) in aqueous solutions. Thus, the extraction of Cr(III) by di(ethylhexyl)phosphoric (DEHPA) acid has been studied by several authors [2-4], Pandey [2] studied the extraction of chromium (III) with mixtures of DEHPA, Cyanex and isodecanol in kerosene, reporting slow extraction kinetics. Islam and Biswas [3] studied the dependency of extraction equilibrium on acidity, the [128]

*** Corresponding author, e-mail: avilam@quijote.ugto.mx**

extractant's concentration, the temperature, and the nature of the diluent used. Mack and Hampe [4] focused on the study of chromium (III) extraction kinetics by DEHPA according to the diluents used, and report a slow chromium (III) extraction rate.

It is difficult to explain why the rate of mass transfer is slow in a liquid-liquid extraction system, because there are different factors than can control the extraction rate. However, it is pointed out that frequently, the reactions of complex formation in the aqueous phase or at the interface, and the sorption-desorption process at the interface can be slow enough to control the extraction rate [5], Because DEHPA has surfactant properties, it can be adsorbed at the interface. This phenomenon can play an important role in liquid-liquid extraction kinetics of Cr(III) and must be considered to understand the extraction mechanisms. However it is necessary, first of all, to determine if the transfer rate of Cr(III) is controlled by diffusion or by kinetics of chemical reactions.

We present here the results obtained in a systematic study of the extraction kinetics of Cr(III) usina DEHPA diluted in kerosene as an extractant, in order to determine the mass transfer system that controls the reaction rate of this metallic ion, from the aqueous phase to the organic phase.

EXPERIMENTAL

The kinetic study was done in a constant interfacial area Lewis cell. The aqueous phase was composed of different concentrations of $Cr(N0_3)_3$ (from 25 to 500 ppm of Cr^{3+}), depending on the experiment to be done. The organic phase had DEHPA extractant (kindly supplied by Albright and Wilson), diluted in kerosene with 10% of decanol. The pH of the solutions was 3. The temperature was 25°C, except in the activation energy determination, where temperature changed from 20 to 40 °C.

In order to determine the transfer regime, both phases were stirred in an interval of 70 to 200 rpm, at 25°C, and initial pH = 3. This experiment was repeated under the same conditions, maintaining one rotation speed constant and changing the other one in the interval of 70 to 200 **rpm.**

The concentration of Cr(III) in the aqueous phase was determined by Flame Atomic Absorption spectroscopy. The concentration of Cr(III) in the organic phase was determined by mass balance.

RESULTS AND DISCUSION

In order to determine the mass transfer regime of the Cr(III)/DEHPA system, we studied the variation of the concentration of Cr(III) in the aqueous phase, as a function of time. Figure 1 shows that the concentration of Cr^{3+} in the aqueous phase decreases as time increases, until it reaches a basically constant value at around 150 minutes; it is considered that in this period of time the equilibrium is reached.

Figure 2 shows the variation of the extraction percentage (%E) as a function of contact time and stirring rate. In all cases the extraction percentage increases as the contact time and the stirring rate increase. For stirring rates of 100 rpm and greater, the extraction percentage [129]

becomes practically constant at 150 min and above. However, at 70 rpm the behavior is different probably due to the very strong diffusion phenomena that arise at this stirring rate.

Transfer Regime Determination

In order to determine the mass transfer regime in the extraction of Cr(III) by bis(2-ethylhexyl)phosphoric acid, the product of the global mass transfer coefficient by the interfacial area, *ka* was calculated starting from a Cr(III) mass balance:

$$-VdX = ka(X - X^*)dt \qquad (1)$$

where:

V **= volume of the aqueous phase at a time t**

X **- concentration of the aqueous phase at a time t**

k **= global mass transfer coefficient of the aqueous phase**

a **= interfacial area**

dt **- time interval**

*X** **= concentration of the aqueous phase at equilibrium with the organic phase**

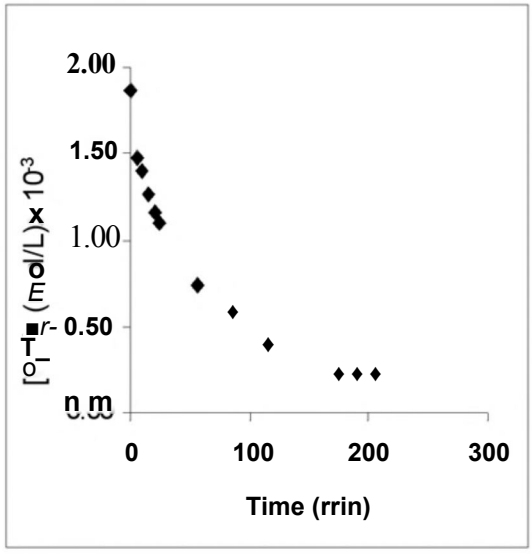


Figure 1. Variation of Cr(III) concentration in aqueous solution, as a function of time, [Cr^{3+} 7 = 100 ppm, [DEHPA]= 0.1 M in kerosene/10% decanol, T=25°C, pH=3, 150 rpm both phases.

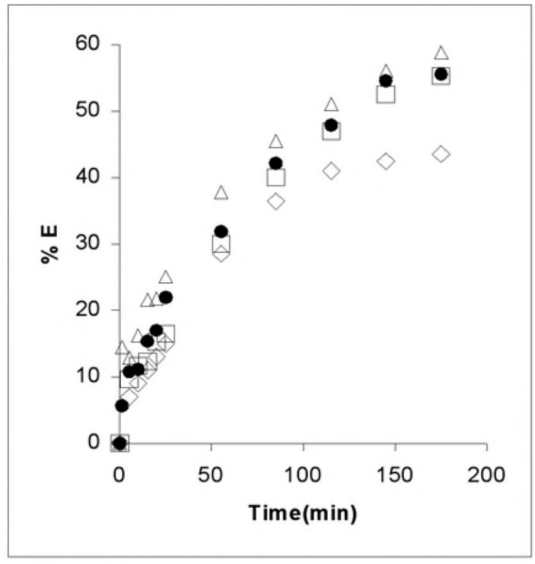


Figure 2. Influence of the stirring rate on the percentage of extraction of Cr(III) by DEHPA 0.1 M, as a function of time. (O) 70 rpm, (D) 100 rpm, (O) 150 rpm, (A) 200 rpm.

The difference in concentration *X-X can be approximated by a linear relationship of X:**

$$X\text{-}X^* = aX + p \qquad (2)$$

where:

a **and** *(5* **are constant.**

Due to the sampling method, the volumes of both phases decrease with time. Thus, between tj=i and tj, where V = V, one gets:

$$\ln\left(\frac{ccX, + p'}{pXt\text{-}x+P.}\right) = -kaa \qquad \frac{t_i - t_{i-1}}{V_i} \qquad (3)$$

An adequate handling of the above expressions yields:

$$\ln(aX + I?) - \text{-}kaa\text{—} + \frac{t}{V} cte \qquad (4)$$

which represents the equation of a straight line (vs *\N)* **with a slope of** *ka a.* **Using this equation and knowing the values of** *a* **and** *p,* **it is possible to obtain values of** *ka* **and to determine the mass transfer regime.**

The values of *a* **(1.0329) and** *p* **(-2.996) were obtained from the variation of** *X-X** **as a function of X (Figure 3).**

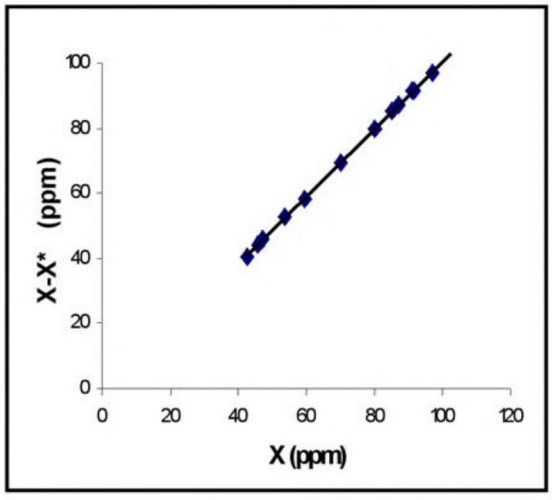


Figure **3.** *Variation of X - X* as a function of X. [DEHPA]= 0.1 M in kerosene/10% decanol,* $[C^]_o$*=100 ppm, T=25°C, 150 rpm.*

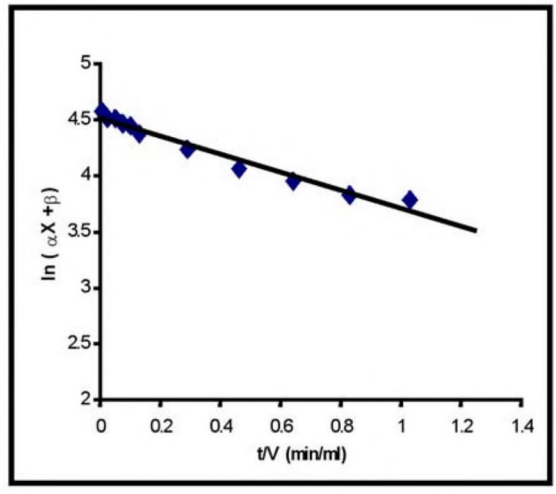


Figure 4. Variation of **ln***(ccX + p) as a function of t/V. DEFIPA 0.1 M in kerosene/10% decanol.fCr**I = 100* DDm. *150 rpm, T=25°C*

With the values of or and *p* **, using equation 4, the value of the** *ka* **product was obtained. Figure 4 represents the variation of ln** *(aX + p)* **as a function of** *\N.* **It can be observed that the experimental values are grouped on a line of slope = -0.8022, and thus** *ka* **= 0.7766.**

The study of *ka* **as a function of the stirring rate was done by stirring both phases at the same rate. In order to confirm the results, a constant-stirring phase was maintained, and the rate of the other one was varied (Figure 5). Two regions are observed in both curves. In the first one,** *ka* **varies linearly with the stirring rate. In the second one, from 150 rpm, a constant** [131]

extraction rate is reached; increases in the stirring rate do not have a significant influence on the extraction rate, which brings us to the conclusion that the chemical regime has been reached.

The curves obtained are very similar, and thus it is possible to say that at stirring rates over 150 rpm a chemical regime has been reached, and this has been corroborated by calculating the activation energy (see below).

Activation energy calculation

The Arrhenius equation relates the influence of temperature on the kinetic extraction constant, k.

$$k = k_0 e^{-\frac{E}{RT}} \quad \textbf{(4)}$$

By applying logarithms one obtains:

$$\ln k = -\frac{}{RT} + c. \quad \textbf{(5)}$$

With this equation it is possible to determine the activation energy, which is a criterion to confirm the nature of the mass transfer regime. When a process presents activation energy values under 20 kJ/mol, it is considered to be controlled by diffusion, while those activation energy values over 40 kJ/mol are attributed to processes controlled by chemical reactions.

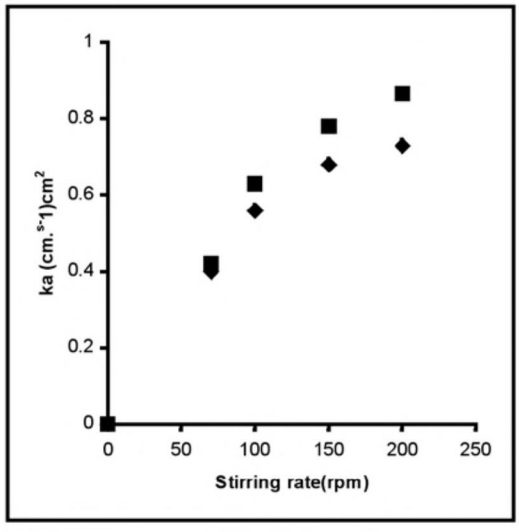


Figure **5.** *Variation of ka as a function of the stirring rate,* ***(m)*** *Same stirring rate in both phases;(*) Constant stirring rate into the organic phase. [DEHPA]= 0.1 M in kerosene/10% decanol, [Cr³*]= 100 ppm, T=25°C.*

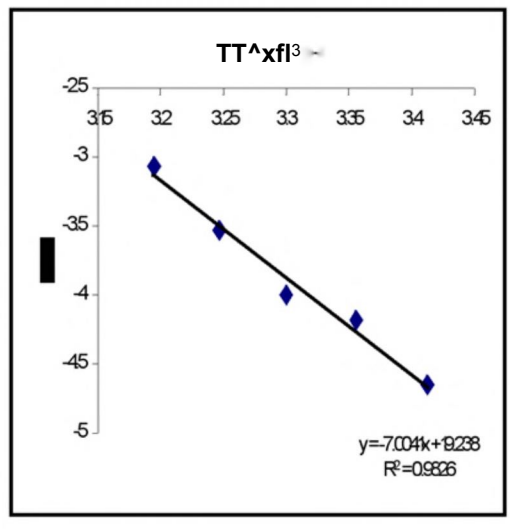


*Figure 6. Activation energy calculation. [Cr*³] = 100 ppm, [DEHPA] = 0.1 M, 150 rpm, variable temperature (20°C to 40 °C).*

From the analysis of the variation of ln k as a function of 1/T (Figure 6), an activation energy of 58.02 kJ was obtained. This value confirms that the chemical transfer regime has been reached at 150 rpm.

CONCLUSIONS

The results obtained in this study show that the extraction of Cr(III) by DEHPA is slow, reaching an equilibrium after 150 min of contact of the two phases.

On the other hand, when determining the regime that controls the extraction kinetics, it is concluded that at low stirring rates diffusion has an important role in the control of the extraction rate, while at rates over 150 rpm, the chemical system is the one that controls the mass transfer rate of Cr(III) in the organic phase.

The value calculated for the activation enerav of 58.02 kJ confirmed that the chemical mass transfer regime was reached.

The results from this study will allow in a future study the establishment of the extraction reaction mechanism.

ACKNOWLEDGMENTS

Authors would like to thanks financial support by CONACYT (Mexico) and ECOS (France) (projects CONACYT SEP-2003-C02-44768/A-1 and ECOS-ANUIES M01P04).

REFERENCES

1. **R. Eisler (1986), Contaminant Hazard Reviews. Report No.** 6. *Biological Report* **85(1.6). Fish and Wildlife. U.S. Department of the Interior.**
2. **B. D. Pandey, G Cote and D. Bauer (1996),** *Hydrometallurgy* **40(3), 343-57.**
3. **M. F. Islam and R. K. Biswas (1979),** *Journal of Inorganic and Nuclear Chemistry,* **41(2), 229-33.**
4. **C. Mack and M. J. Hampe (1999),** *Proceedings of International Solvent Extraction Conference*, **Barcelona, Spain. 1, 329-33.**
5. **P. R. Danesi (1992),** *Principles and Practices of Solvent Extraction.* **Ed by J. Rydberg, C. Musikas and G. R. Chopin Chap. 5. 157-206.** [133]

EXTRACTION OF MANGANESE FROM SOLUTIONS CONTAINING ZINC AND COBALT BY D2EHPA AND D2EHPA-CYANEX®272 OR CYANEX® 302 MIXTURES

D. Darvishi*, M. Teimouri, E. Keshavarz Alamdari**, D.F. Haghshenas*, S.K. Sadrnezhaad*, K. Nazri*****

'Center of Excellence for Advanced Processes of Production and Forming of Materials, Department of Materials Science and Engineering, Sharif University of Technology, Tehran, IRAN
**** Department of Mining, Metallurgy and Petroleum Engineering, Amirkabir University of Technology, Tehran, IRAN**
***** Atomic Energy Organization, Tehran, IRAN**

This paper presents the results of the studies carried out on the effect of pH on extraction of manganese from aqueous solutions containing zinc and cobalt at ambient temperature. Empirical data indicates that an increase in the ratio of Cyanex®272 (or Cyanex® 302) to D2EHPA shifts the extraction curve of zinc to the lower pH values and that of manganese to the higher pH values; but it does not affect on the cobalt extraction curve. Selectivity separation parameter ((3) obtained experimentally shows that the most suitable extractant for separation of zinc from manganese is a 0.3/0.3 mixture of D2EHPA with Cyanex® 302; while that for separation of manganese from cobalt is pure D2EHPA. The stoichiometric coefficients of the manganese and zinc extraction reactions were obtained to be 3 and 4, respectively.

Introduction

Liquid-liquid extraction is known as an efficient method for separation, removal and purification of the metallic ions that exist in aqueous media. Separation of manganese as a troublous ion from solutions containing cobalt and zinc has previously been investigated. Dhadke and Ajgaonkar carried out a quantitative study of the extraction of Mn(II) and Co(II) from sulfate solutions using Cyanex® 302 in toluene [1], They extracted Co(II) and Mn(II) in the pH range of 7.0 to 7.5 and 8.5 to 9.5 in presence of 0.1 M $(NH_4)_2S0_4$, respectively.

Extraction and separation of Mn(II) and Co(II) from sulfate solutions using sodium salts of D2EHPA, PC 88A and Cyanex®272 in kerosene have also been investigated [2], The most suitable extractant for separation of these metals have been found to be 0.05M NaD2EHPA present at an equilibrium pH of 4.45. Hoh et al. [3] have separated manganese from cobalt in sulfate solution by diluted D2EHPA in kerosene. The pH for aqueous and organic systems was controlled to be in the neighborhood of 4.2 and 2.0, respectively.

Mihaylov et al. [4] have carried out the simultaneous extraction of 0.6 gr/lit Co and 6 gr/lit Ni from sulfate solutions containing 3gr/lit Mn using 15% Cyanex®301 at A/O ratio of 2.5. Cobalt

and nickel were reported to extract at a pH of less than 2.0. Manganese did not leave the aqueous phase under these conditions. Separation of Mn(II) and Co(II) from ammoniacal solutions using versatic-10 acid was carried out by Woo and Cho [5], They found that the best condition for high degree of separation could be achieved with 0.5M $(NH_4)_2S0_4$ at a pH of 9.0 to 9.5. Devi et al. [6] showed that during study of divalent zinc and manganese solvent extraction from sodium salts of Cyanex® 272, the extracted species were $ZnA_2.3HA$ and $MnA_2.3HA$.

The purpose of this study is to determine the synergistic effect of increasing the Cyanex® 272 to D2EHPA ratio and Cyanex®302 to D2EHPA ratio in the extractant mixture on Mn(II) separation from Co(II) and Zn(II). The stoichiometric coefficient of the extractant in Mn(II) extraction equation is an important quantity [7] that has been determined in this work, too.

Experimental Procedure

Materials

All extractants and metallic sulphates (zinc, manganese and cobalt) were laboratory grade materials. Bis-2-ethylhexyl phosphoric acid (D2EHPA) was purchased from Sandong Chemical, Ghengdu, China and both di-2,4,4,-trimethylpentyl phosphinic (Cyanex® 272) and di-2,4,4,-trimethylpentyl monothiophosphinic (Cyanex® 302) acids were prepared from Cytec Netherlands. Tehran Refinery Company supplied kerosene as the diluent. Aqueous solutions having constant cobalt, zinc and manganese concentrations of 5gr/lit were prepared by dissolving metal sulphates made of Panreac Company of Spain in distilled water.

Experiments

All experiments were carried out at ambient temperature. The extractant concentrations were 0.6 mol/lit, in all cases. Equivolume (20 ml) aqueous-organic solutions were agitated for 30 minutes in order to reach equilibrium. Complete separation was then allowed. Ionic concentration of the aqueous phase was directly determined by titration with EDTA. Eirochromblack T was used as an indicator for zinc and manganese determination; while Muroxide was used for cobalt determination. Organic phase was stripped with 300gr/lit sulphuric acid and titration method was used to analyze the solution obtained.

Results and Discussion

Effect of pH

Experiments were carried out to investigate the effect of pH on the extraction of zinc, manganese and cobalt at the ambient temperature. Figure 1 shows the extraction curves of zinc, manganese and cobalt obtained with the use of D2EHPA and a mixture of D2EHPA and Cyanex® 302, as extractant. It can be seen that the increasing of Cyanex® 302 to D2EHPA ratio does not affect the position of the experimental data for cobalt; but it shifts the extraction curve of zinc to the left and that of manganese to the right. Similar results are obtained for D2EHPA-Cyanex®272 mixture. However, the figures are not the same. Table 1 summarizes the pH_{05} (pH at 50% metal extraction) and ApHo.s (pH_{05} differences of two metals) data for zinc, manganese and cobalt that were experimentally obtained.

Separation of zinc from manganese

Selectivity of the extractant with respect to zinc and manganese can be attributed to the difference between $pH_{0.5}$ values of the two metals, i.e. ApH_0.s. Figure 1 shows that the addition of Cyanex®302 to D2EHPA increases this value for zinc and manganese. According to the data summarized in Table 1, a 0.3-0.3 D2EHPA-Cyanex® 302 mixture is the most suitable extractant for separation of zinc from manganese.

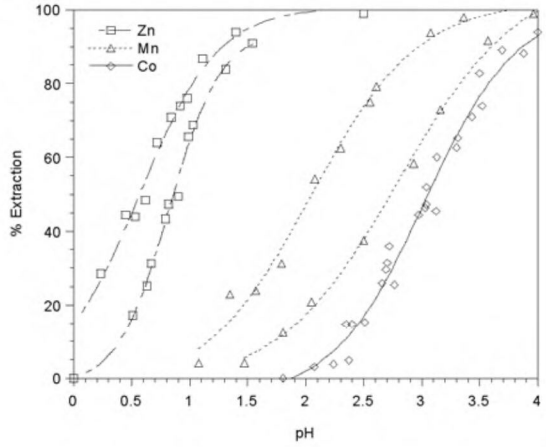


Figure 1. Variation of zinc, manganese and cobalt extraction percentages with pH. Hollow symbols correspond to 0.6 molar D2EHPA. Solid symbols correspond to 0.3 to 0.3 mixture of D2EHPA and Cyanex® 302, having a constant extractant concentration of 0.6 mol/lit.

Table 1. Values of $pH_{0.5}$ for different D2EHPA to Cyanex® ratio at 25 °C.

[D2EHPA]/[Cyanex®] ratio		PH_0,5				
		Zn	Mn	Co	Mn-Zn	Co-Mn
272	0.6:0.0	**1.30**	**2.05**	**3.04**	**0.75**	**0.99**
	0.5:0.1	**1.24**	**2.07**	**3.25**	**0.83**	**1.18**
	04:0.2	1.20	**2.28**	**3.39**	**1.08**	1.11
	0.3:0.3	**1.17**	**2.76**	**3.48**	**1.59**	**0.72**
302	0.6:0.0	**1.30**	**2.05**	**3.04**	**0.75**	**0.99**
	0.5:0.1	**0.70**	**2.18**	**3.11**	**1.48**	**0.93**
	0.4:0.2	**0.61**	**2.43**	**3.11**	**1.82**	0.68
	0.3:0.3	**0.57**	**2.74**	**3.13**	**2.17**	**0.37**

Separation of manganese from cobalt

Extractant condition for cobalt-manganese separation is different from that for zinc and manganese. Adding Cyanex® 302 to D2EHPA decreases, for example, the ApH_0.sof cobalt and manganese. For separation of cobalt from manganese, best results are obtained with a mixture of 0.5-0.1 D2EHPA-Cyanex®272. This corresponds with a $ApH_{0.5}$ value of 1.18 (see Table 1).

Effect of addition of Cyanex® 272 and Cyanex® 302 to D2EHPA on selectivity ratio of manganese

The ratio of the two distribution factors D_A and D_B is called separation factor (P): [136]

$$P_{A/B} = \frac{D_A}{D_B} \quad (0)$$

where D_A and D_B are the distribution factors of species A and B, respectively. The separation factor $P_{A/13}$ indicates how well the extractant can separate the species A from B. Variation of Pzn/Mn and PMn/Co versus pH are illustrated in Figure 2. As is seen in the figure, using a mixture of D2EHPA and Cyanex®302 instead of pure D2EHPA improves the selectivity of zinc in a solution containing manganese. Moreover, for separation of manganese from a cobalt containing solution, utilization of D2EHPA is advised.

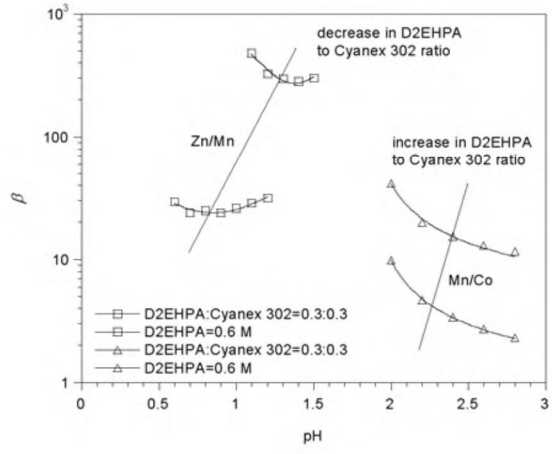


Figure 2. Effect of pH and D2EHPA to Cyanex 302 ratio on the amount of separation factor. Square symbols correspond to separation of zinc from a manganese containing solution. Triangle symbols correspond to separation of manganese from a cobalt containing solution.

Mechanisms of extraction of manganese and zinc

Mechanism of the manganese extraction depends on the stoichiometric coefficient n of the extraction reaction:

$$M^{2+} + nRH_0 \; MR_2(RH)_{n-2} + 2H^+ \quad (2)$$

Equilibrium constant of the reaction is evaluated from:

$$K = D_M \times \frac{[H^+]^2_{equ}}{[RH]^n_{equ}} \quad (3)$$

where D_M is the distribution coefficient defined by $\frac{[MR_2(RH)_{n\cdot 2}]}{[M^{2+}]}$

The following expression can thus be derived:

$$\log D_M = \log K + 2pH + n\log [RH]_{equ} \quad (4)$$

Considering the amount of the extracted manganese, concentration of the extractant at

equilibrium is given by:

$$[RH]_{equ} = 0.6\text{-}nx \quad \frac{\%ExC_0}{M_w \times 100} = 0.6\text{-}nfMl_{L\ J}org \qquad (5)$$

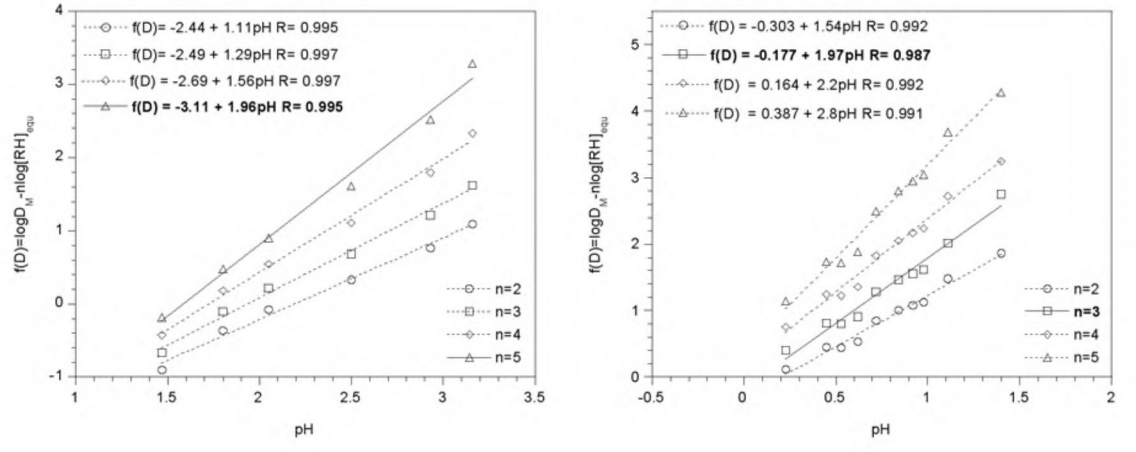
where
n = stoichiometric coefficient of the extractant
%E = extraction percentage
C_D= initial concentration of the element, gr/lit
M_w = molar mass of the element, gr/mol

Combining (4) and (5) gives:

$$\log D_M = n\log\left[0.6\text{-}nfMl_{L\ J_0}rg\right] + \log K + 2pH \qquad (6)$$

Stoichiometric coefficient of extractant, n, can be calculated by trial and error method. Plotting ($logD_M$ -nlog $[RH]_{y}$) against pH at different values of n, gives straight lines with

different slopes and intercepts (see Figure 3). The correct one for manganese or zinc extraction equation is the line with slope 2. The number replaced for n, is the stoichiometric coefficient of the extractant. The values of n in zinc extraction equation, using either D2EHPA or mixture of D2EHPA with Cyanex® 272/Cyanex® 302, were found to be 3. This value in manganese extraction equation, using either D2EHPA or mixture of D2EHPA with Cyanex® 272, was obtained to be 4. Using different D2EHPA to Cyanex® 302 ratios, the value of n was found to be 5. Darvishi et al. [7] found values of n in cobalt extraction equation, using either pure D2EHPA or mixture of D2EHPA with Cyanex® 272/ Cyanex® 302, to be equal to 4.



(a) *(b)*

Figure 3. Variation of $logD_M$ - nlog [RH ~\^$_u$ versus pH. The data obtained by extractant with ratio of D2EHPA to Cyanex 302 equal 0.3 to 0.3: (a) manganese and (b) zinc

Base on the results obtained from slope analysis, the extraction equation of manganese and cobalt can be represented as follows:

1. **With D2EHPA and mixture of D2EHPA with Cyanex® 272 used as extractant:** [138]

$$Mn^{2+}+4RHG \quad MnR_2(RH)_2 +2H^+ \qquad (7)$$

$$Zn^{2+} + 3RH \square \quad ZnR_2(RH) + 2H^+ \qquad (8)$$

2. **With mixture of D2EHPA and Cyanex® 302 used as extractant:**

$$Mn^{2+}+5RHD \quad MnR_2(RH)_3+2H^+ \qquad (9)$$

Zinc extraction equation at this stage is the same as the above.

Conclusions

The percentages of extraction of all three metals were increased with increasing of the pH of the solution. Zinc and cobalt were extracted at the lowest and highest equilibrium pH for all extractants, respectively. The mixture of D2EHPA with Cyanex®302 at the ratio of 0.3:0.3 was the most suitable extractant for separation of manganese and zinc. Due to the maximum value of ApHo.5, a solution containing 0.6 molar D2EHPA was the best extractant for separation of manganese from cobalt. Stoichiometric coefficient of extractant in the manganese extraction equation was 4 when D2EHPA was merely used as the extractant. Adding Cyanex® 302 to D2EHPA changes the stoichiometric coefficient of the extractant in manganese extraction equation from 4 to 5. However in the case of Cyanex® 272, no change was observed. The stoichiometric coefficient of the extractant in zinc extraction equation was found to be 3 with using either D2EHPA or a mixture of D2EHPA with Cyanex 272/Cyanex 302.

References

1. **P.M. Dhadke, H.S. Ajgaonkar (1996), Indian J. Chem.** *Technol.* **3 (**6**), 358-362.**
2. **N.B. Devi, K.C. Nathsarma, V. Chakravortty (2000),** *Hydrometallurgy,* **54, 117-131.**
3. **Y.-C. Hoh, W.-S. Chuang, B.-D. Lee, C.-C. Chang (1984),** *Hydrometallurgy*, **12, 375-386.**
4. **I. Mihaylov, E. Krause, Y. Okita, J.J. Perraud,** *CIM Bull.* **93 (1041), 124-130.**
5. **A.J. Woo, L.E. Cho,** *Nonglim Nonjip* **26 (1985) 119-128,** *CA* **105 (1986) 230345g.**
6. **N.B. Devi, K.C. Nathsarma, V. Chakravortty (1997),** *Hydrometallurgy,* **45, 169-179.**
7. **D. Darvishi, D. F. Haghshenas, E. Keshavarz Alamdari, S. K. Sadmezhaad, M. Halali, Synergistic effect of Cyanex 272 or Cyanex 302 on separation of cobalt and nickel by D2EHPA, Submitted for publication to** *Hydrometallurgy.* [139]

SYNERGISTIC EFFECT OF TBP ON SEPARATION OF ZINC AND CADMIUM WITH D2EHPA

E. Keshavarz Alamdari, D. Darvishi*, S.K. Sadmezhaad, D.F Haghshenas*

Dept. Mining, Metallurgical and Petroleum Eng; Amirkabir University of Technology, Tehran, IRAN
'Center of Excellence for Advanced Materials Forming Processes, Department of Materials Science and Engineering, Sharif University of Technology, Tehran, IRAN

This paper investigates TBP selectivity effects for extraction of zinc and cadmium. Empirical results show that existence of M2EHPA in D2EHPA causes extraction curve of zinc and cadmium to reach the same. Separating zinc from cadmium is encountered, therefore, with difficulty. Addition of TBP, as a modifier, to D2EHPA can improve undesirable separation conditions due to the presence of M2EHPA in D2EHPA. Results shows that up to 2 Vol.% of M2EHPA existing in D2EHPA decreases the value of the selectivity parameter, (3, to less than 10; while addition of up to 5 Vol.% of TBP to D2EHPA in presence of M2EHPA increases the value of (3 to nearly 30.

Introduction

D2EHPA as a general and practical extractant is widely used in solvent extraction of zinc [1-3], Almost all solvent extraction units of zinc utilize D2EHPA as the organic solvent [4], This compound is commercially supplied with an assay of near 95%. All impurities present in this compound, including M2EHPA, influence on separation of zinc from cadmium during the extraction process [4-5], Presence of M2EHPA as an impurity in D2EHPA yields an undesirable synergistic effect on co-extraction of zinc and cadmium [4],

Use of oxidizing agents such as $KMn0_4$ and a highly concentrated acid in stripping units provides the conditions for decomposition of D2EHPA to M2EHPA [4], It seems, therefore, that the concentration of M2EHPA will increase during the extraction cycle. TBP is utilized, therefore, as a most suitable modifier for solvent extraction of zinc [6-8], Adding of TBP to the organic phase improves the phase separation and decreases the viscosity of the organic phase. Previous studies showed that TBP yields a synergistic effect that decrease the unwanted synergistic effect of M2EHPA [4],

This paper tries to deal with properties of TBP as a modifier during zinc and cadmium separation when M2EHPA is present as an impurity in D2EHPA. Presence of the latter can be due to poor purification or due to hydrolysis of D2EHPA with M2EHPA. 140

Experimental Procedure

Materials and reagents

All used chemical reagent except kerosene were analytical grade. D2EHPA (Bis-2-ethylhexyl phosphoric acid) was prepared from Merck chemical company, Germany. TBP (tri-n-butyl phosphat) and M2EHPA (mono-2-ethylhexyl phosphoric acid), used as a mix of D2EHPA and M2EHPA, reagents were provided by Fluka, Swiss. The needed concentration of organic extractant with sum of D2EHPA and M2EHPA amounting to 20 vol% was prepared with diluting of the calculated amount of D2EHPA and Mix D2EHPA - M2EHPA in Kerosene. Kerosene was provided by Tehran Refinery Company, Iran. Organic phases containing D2EHPA and M2EHPA with ([M2EHPA]: [D2EHPA]) ratio 0, 0.1 land 0.25 as extractant plus 0%, 2.5%, 5% and 10% TBP as modifier were prepared by dissolving the materials into pure kerosene, respectively. Aliquot samples containing 5 g/L zinc or Cadmium in ionic form were prepared by dissolving analytical grade of zinc or cadmium sulfate made in Fluka AB, Switzerland, in distilled water. Sulfuric acid and ammonium hydrate (Ammonium solution) from Baran Chemical Company of IRAN was employed for adjusting pH of the system.

Experiments

Batch experiments were carried out in a flask containing equal volumes (20 ml) of both aqueous and organic phases. The mixture was agitated at a constant temperature with a mechanical shaker. The experiments were allowed to run for one hour in order to reach equilibrium. The samples were retained for three hours and the two phases were separated by passing through a separation funnel. The initial concentration of zinc or cadmium in the aqueous phase in all experiments was 5 g/L. Zinc or cadmium content of the aqueous phase was analyzed with titration method with EDTA at presence of Eirochromblack T as indicator. Zinc or cadmium concentration of the organic phase was determined through mass balance calculations.

Results and Discussion

Effect of M2EHPA on zinc and cadmium extraction

Extraction curves of zinc and cadmium obtained for 20 Vol.% D2EHPA and M2EHPA are illustrated in Figure 1. As can be seen from the figure, the presence of M2EHPA in D2EHPA causes the zinc and cadmium extraction curves to shift to lower pH values. The figure also shows that the cadmium ApH ($pH^{D2EHPA} - pH^{D2EHPA+M2EHPA}$) variation is more sensitive to increasing of M2EHPA Vol.% in D2EHPA than that of zinc. The values of ApH for cadmium and zinc are 0.58 and 0.14 unit pH, respectively. So it seems that separation of zinc and cadmium would not be simple. More scrubbing stages are necessary for a highly selective separation.

Effect of addition of TBP on zinc and cadmium extraction

As mentioned before, TBP is usually used as modifier in order to improve solvent extraction conditions. So experiments were carried out to find out the effect of TBP on zinc and cadmium extraction. Extraction curves of zinc and cadmium with respect to increasing of TBP, are shown in figure 2. As can be observed in figure 2-a, increasing of TBP up to 10 vol% has not affected on zinc extraction curve considerably, while the results of figure 2-b show that increasing of this compound to D2EHPA causes cadmium extraction curve shifts to right, vice versa of M2EHPA performance. In other words, presence of TBP in D2EHPA, [141]

including impurity as M2EHPA, could have a synergistic effect in order to modify the separation of zinc and cadmium. The values of $pH_0.5$ (the equilibrium pH value at which 50% extraction of metal occurs) for zinc and cadmium due to variation of M2EHPA and TBP are listed in Table 1.

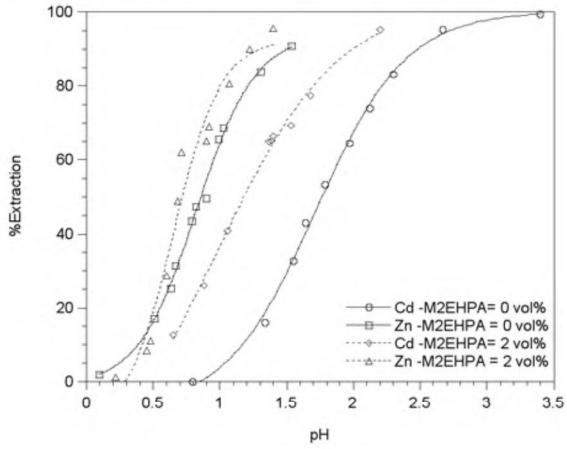


Figure 1. Variation of extraction percentages of zinc and cadmium versus pH,TBP Vol.% = 0.

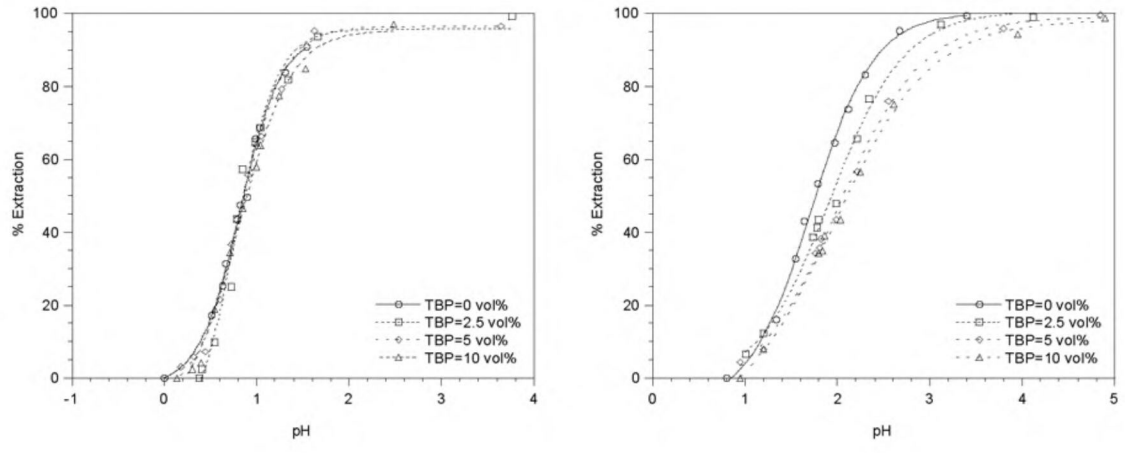


Figure 2. Variation of extraction percentages of zinc and cadmium versus pH, using 20 Vol.% D2EHPA as extractant (a) zinc and (b) cadmium.

Effect of addition of TBP on zinc and cadmium extraction in presence of M2EHPA

According to the results obtained from Figure 1, presence of M2EHPA, weather as an impurity or produced by D2EHPA decomposition under unsuitable stripping conditions causes the unsatisfactory separation of these two metals. Based on the data given in Figure 2 it can also be concluded that the presence of TBP would improve the separation conditions. Therefore, a number of experiments were carried out to determinate the effect of addition of TBP in presence of M2EHPA in separation process of zinc and cadmium.

As shown in Figure 3, addition of up to 5 Vol.% TBP can reduce the undesirable effect of increasing of M2EHPA up to 2 Vol.% (compare with Figure 1). The effect of TBP and M2EHPA on pH_0.s and ApH_0.s of zinc and cadmium are illustrated in Table 1. [142]

Table 1. Values of pH_0.s for zinc and cadmium due to variation of M2EHPA and TBP.

MEHPA Concentration (vol. %)	TRP Pnnr.pntrpfinn (Vol. %)	pHo.s		
		Zn	Cd	Cd-Zn
0	0	0.86	**1.76**	**0.90**
	2.5	0.86	**1.94**	**1.08**
	5	0.86	**2.04**	**1.18**
	10	0.86	2.11	**1.25**
9	0	**0.72**	**1.18**	**0.46**
	2.5	**0.72**	**1.31**	**0.59**
	5	**0.73**	**1.56**	**0.83**
	10	**0.80**	**1.64**	**0.84**
A	0	**0.60**	**0.90**	**0.30**
	2.5	**0.65**	**0.92**	**0.27**
	5	**0.73**	**1.13**	**0.40**
	10	**-**	**1.19**	**-**

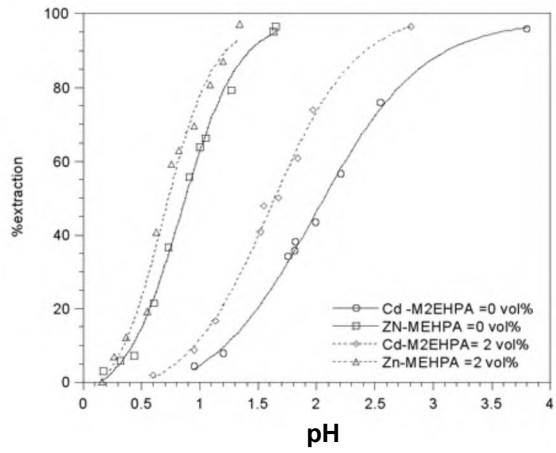


Figure 3. Variation of extraction percentages of zinc and cadmium versus pH, Vol.% of TBP = 5.

Effect of TBP and M2EHPA on zinc and cadmium separation

The separation factor (P) is a measure of selectivity in extraction of metals. In case of zinc and cadmium, this factor is defined as:

$$Pzn/Cd = \frac{D_{Zn}}{{}_{n}{}^{u}Cd} \qquad 0)$$

The existence of a tendency towards lowering of cadmium distribution factor indicates a better separation of zinc over cadmium. In other words, at a higher separation factor it is easier to perform a selective extraction procedure.

The values of Pzn/Cd are illustrated in Table 2. As is seen, values of Pzn/Cd decrease strongly when up to 2 Vol.% of M2EHPA exists as an impurity in D2EHPA, in which these values decrease to less than 10. Addition of up to 5 Vol.% TBP to D2EHPA in presence of

M2EHPA would improve the separation conditions in which the values of Pzn/Cd **increase to nearly 30. Based on these results, it can be concluded that TBP improves the selective separation parameter** Pzn/Cd **as we^ as purified D2EHPA, if the percentage of M2EHPA is less than 2 Vol.%.**

Table 2. Experimental results on distribution coefficient and separation factor of zinc and cadmium.

TBP Concentration (%Vol.)	pH	MEHPA Vol. % = 0			MEHPA Vol. % = 2		
		D_{Zn}	D_Cd	$\beta_{Zn/Cd}$	D_Zn	Dcd	Bzn/Cd
	0.5	0.20	0.00	∞	**0.23**	**0.05**	**4.44**
	0.7	**0.50**	0.00	∞	**0.94**	**0.18**	**5.33**
	0.9	**1.19**	0.01	**84.50**	**2.59**	**0.42**	**6.15**
0	1.0	**1.87**	**0.04**	**42.87**	**4.04**	**0.59**	**6.89**
	1.1	2.68	**0.08**	**33.92**	**5.67**	**0.79**	**7.15**
	1.3	**5.24**	**0.19**	**27.44**	**7.70**	**1.35**	**5.69**
	1.5	**8.57**	**0.41**	**20.71**	**17.02**	**2.42**	**7.04**
	0.5	**0.18**	0.00	∞	**0.28**	0.00	∞
	0.7	**0.47**	0.00	∞	0.86	**0.03**	**26.64**
	0.9	1.11	0.02	**54.40**	**2.19**	**0.09**	**23.99**
5	1.0	1.68	**0.05**	**35.70**	**3.42**	**0.14**	**24.58**
	1.1	**2.59**	**0.07**	**36.51**	**5.11**	**0.19**	**26.74**
	1.3	**5.68**	**0.14**	**39.58**	**12.04**	**0.35**	**34.03**
	1.5	**11.48**	**0.26**	**44.37**	**70.43**	**0.67**	**105.38**

Conclusions

Presence of M2EHPA in D2EHPA caused shifting of the extraction curves of zinc and cadmium to the lower pH values. The experimental data showed that with increasing Vol.% of M2EHPA in D2EHPA, the ApH (pH^{D2EHPA} -$pH^{D:EHPA,M:EHPA}$) of cadmium varies more than that of zinc. Increasing up to 10 Vol.% of TBP does not considerably affect the zinc extraction; while increasing of this compound to D2EHPA causes cadmium extraction curve to shift to the right. Addition of TBP in D2EHPA containing M2EHPA has a synergistic effect, which modifies the separation of zinc from cadmium. Existence of M2EHPA in D2EHPA causes the unsatisfactory separation of zinc from cadmium. Addition of up to 5 Vol.% TBP can reduce the undesirable effect of increasing of M2EHPA up to 2 Vol.%. Presences of up to 2 Vol.% M2EHPA decreases the values of Pzn/Cd **t0 'ess than 10. Addition of up to 5 Vol.% TBP to D2EHPA in presence of M2EHPA improves the separation conditions in which increases the values of** Pzn/Cd **to nearly 30.**

References

1. **George Owusu (1998),** *Hydrometallurgy,* **47(2-3), 205-215.**
2. **J. Aparicio and M. Muhammed (1989),** *Hydrometallurgy,* **21 (3), 385-399.**
3. **Ana Maria Sastre and Mamoun Muhammed (1984),** *Hydrometallurgy,* **12 (2), 177-193.** 144

4. **E. Keshavarz Alamdari, D. Moradkhani, D. Darvishi, M. Askari, D. Behnian (2004), J.** *Minerals Engineering.* **17, 89-92.**
5. **Y. Ramachandra Rao and Sridhara Acharya (1993),** *Hydrometallurgy,* **32, 129-135.**
6. **E. Keshavarz Alamdari, D. Darvishi, S. K. Sadmezhaad, Z. Mos'hefi Shabestari.A. O'hadizadeh and M. Akbari (2002), Proc. Int. Conf. Solvent Extraction, Cape Town, South Africa, pp. 1052-1057.**
7. **K. L. Nash and G. R. Choppin (1977),** *J. Inorganic and Nuclear Chemistry,* **39(1), 131-135.**
8. **V. M. P. Forrest, D. Scargill and D. R. Spickernell (1969),** *J. Inorganic and Nuclear Chemistry,* **(31 (1), 187-197. 145**

EXTRACTION OF CHLORIDES OF RARE EARTH METALS WITH BINARY EXTRACTANTS BASED ON DIALKYLPHOSPHINIC ACIDS

Vera V. Belova, Natalia S. Egorova, Anatoly I. Kholkin and Andrey A. Voshkin

Kurnakov Institute of General and Inorganic Chemistry of RAS, Moscow, Russia

Extraction of some rare earth metals from chloride solutions with binary extractants such as salts of trioctylmethylammonium and dialkylphosphinic, dialkylmonothiophosphinic, dialkyldithiophosphinic acids in toluene depending on compositions of the aqueous and organic phases was studied. The extraction isotherms and dependencies of the metal extraction on C_{ex} with trioctylmethylammonium bis(2,4,4-trimethylpentyl)phosphinate indicate a ratio of C_M : C_{ex} is close to 1 : 3 for all elements studied in the case of the loaded organic phase. Extraction power of binary extractants towards lanthanum chloride decreases in the series: dialkylphosphinate > dialkylmonothiophosphinate > dialkyldithiophosphinate of quaternary ammonium base (QAB). The effect of NaCl concentration on the lanthanum chloride extraction is different for the binary extractants studied. The concentration constants of the rare earth metals extraction and separation coefficients of some metal pairs were calculated using data obtained.

INTRODUCTION

Binary extractants based on organophosphorus acids have been widely studied for recovery and separation of several metals in acidic media [1-4], Particularly, enhanced separation of rare earth metal salts has been reported with dialkylphosphates of QAB [5], moreover, stripping of metals from the organic phase was possible with water. Dialkylphosphinic acids as well as dialkylphosphoric ones appear to be the effective extractants for the separation and recovery of rare earth metals from acidic solutions [6-8], However, binary extractants based on dialkylphosphinic acids have not been studied to date Therefore, we first have investigated distribution of some rare earth metals from chloride aqueous solutions with binary extractants such as salts of QAB and dialkylphosphinic acids.

EXPERIMENTAL METHODS

Aqueous solutions of rare earth metals were prepared by dissolution of their chloride salts into water. In some cases NaCl was added into an aqueous solution to support the constant ionic strength and Cl' concentration.

Solutions of trioctylmethylammonium bis(2,4,4-trimethylpentyl)phosphinate, bis(2,4,4-trimethylpentyl)monothiophosphinate, bis(2,4,4-trimethylpentyl)dithiophosphinate were used as extractants. The binary extractant, R_4NA, was prepared by mixing equimolar amounts of trioctylmethylammonium chloride (R_4NCl) and corresponding organic acid (HA) in toluene and with subsequent washing of an organic solution with 1 M NaOH for 10 min. The metal

extraction with equal of aqueous and organic phases was carried out at 20°C. Samples in glass-stoppered bottles were shaken mechanically for 15 min.

The concentrations of metals in aqueous solutions of their mixtures were determined on ICP-OES spectrometer model IRIS Advantage, Thermo Jarrel Ash. Studying the distribution of individual metal the concentration of metal in the aqueous solution was determined by EDTA titration using xylenol orange as the indicator. The differences in metal concentration between the initial and final aqueous solutions were used to calculate the concentrations of metals in the organic phase. All chemicals were of reagent grade.

RESULTS AND DISCUSSION

Extraction Isotherms

The extraction isotherms of rare earth metals were obtained in the extraction of each metal from 2 M NaCl aqueous solutions with a 0.05 M trioctylmethylammonium bis(2,4,4-trimethylpentyl)phosphinate solution in toluene separately (Figure 1). Data obtained show that under conditions of the loaded organic phases a ratio of the concentration of the binary extractant to the concentration of metal in the organic phase is close to 3 for all metals studied. The interface distribution of rare earth metals in binary extractant system can be represented as follows:

$$Ln^{3+}_{(a)} + 3\,Cr_{(a)} + 3\,R_4NA\,(_0) \;o\; 3\,R_4NCl\,(_0 j + LnA^{\wedge\,\wedge} \qquad (1)$$

with the concentration extraction constant of this process:

$$\overline{K}_{ex} = \frac{C^3_{R\,jNCl\,(0)}\; C_{Ln\,(0)}}{{}^{C}Ln_{(a)}\,{}^{C}Cl^{\wedge}{}_{)}\,{}^{Y}Cl_{(-)}\,{}^{CR}4NA_{(0)}} \qquad (2)$$

where C_{Ln} (a) and C_{Ln} <$_0$) are the analytical concentrations of lanthanide in the aqueous and organic phases respectively.

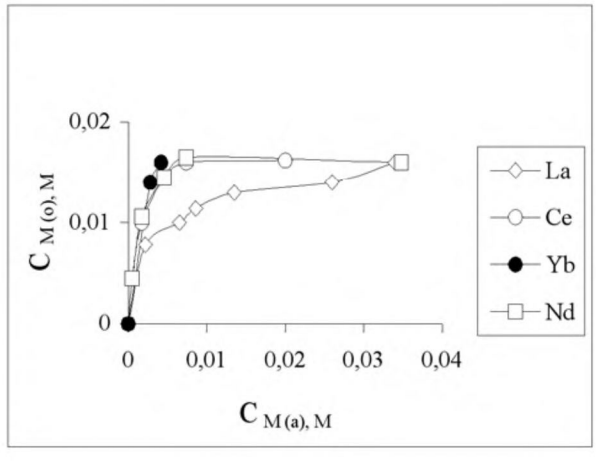


Figure 1. Isotherms for the extraction of rare earth metals with trioctylmethylammonium bis(2,4,4-trimethylpentyl)phosphinate in toluene (C_{ex} = 0.05 M, C_{NaCl} = 2 M)

Binary Extractant Concentration Effect

The effect of binary extractant concentration on the extraction of rare earth metals by trioctylmethylammonium bis(2,4,4-trimethylpentyl)phosphinate in toluene is shown in Figure 2. The extraction was occurred from aqueous solutions containing mixtures of metals such as La, Ce, Nd, Yb (Figure 2, a) and Er, Dy, Er, Gd (Figure 2, b). Logarithmic plots of the distribution coefficients for rare earth metals against the concentration of R_4NA show linear slopes close to 3 (the slopes vary over range of 2.7-3.2) and confirm stoichiometry of the equation (1). The slopes of these plots are consistent with the mechanism of binary extraction of metal salts in which two extracted species are formed in the organic phase. Extractability of metals in their common presence decreases in the series: La < Ce < Nd < Yb. Such metals as Gd, Er, Dy and Er differ in their distribution coefficients insignificantly under given extraction conditions.

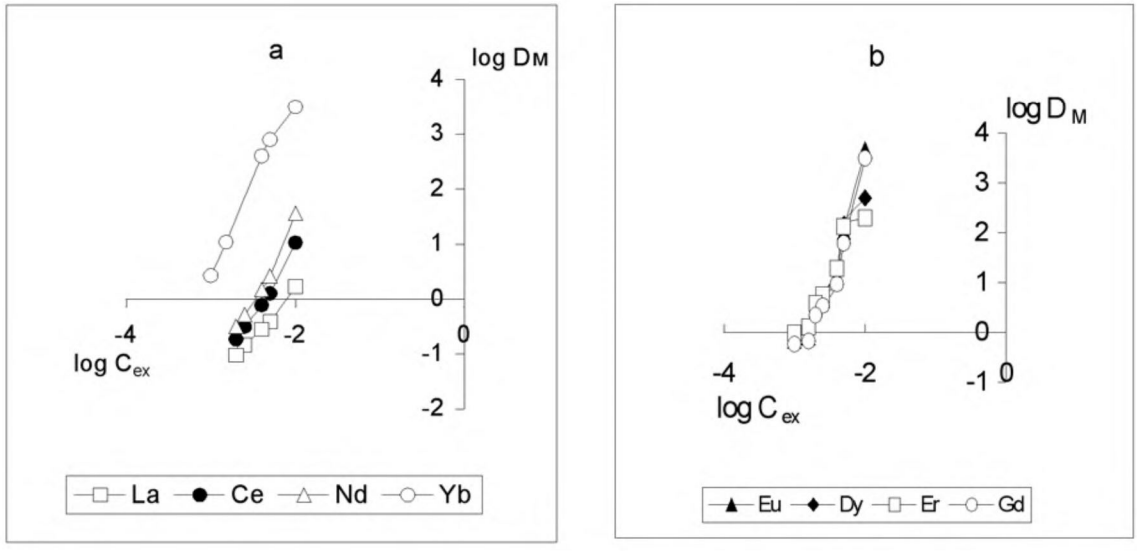


Figure 2. Dependencies of distribution coefficients on concentration of trioctylmethylammonium bis(2,4,4-trimethylpentyl)phosphinate for the extraction of rare earth metals from aqueous solutions ($C_{Ln\ (in}i_{t)}$ = 0.0002 M).

NaCl Concentration Effect

With respect to the mechanism of extraction of rare earth metals from chloride solutions, Figure 3 shows the distribution coefficients of lanthanum as a function of the concentration of NaCl in the aqueous phase in systems involving different binary extractants. It can be seen that the extraction of lanthanum is low from low NaCl concentration solutions, but is significantly enhanced in high concentrations of chloride sodium in systems involving bis(2,4,4-trimethylpentyl)phosphinate of trioctylmethylammonium accordingly to stoichiometry of the process (1). Because organophosphorus acids do not extract appreciable amounts of rare earth metals [9, 10], increasing additions of NaCl do not significantly improve the La extraction with binary extractants based on bis(2,4,4-trimethylpentyl)monothiophosphinic and especially bis(2,4,4-trimethylpentyl)dithiophosphinic acids. We have studied also the lanthanum extraction with solutions of bis(2,4,4-trimethylpentyl)phosphinic, bis(2,4,4-trimethylpentyl)monothiophosphinic and bis(2,4,4-trimethylpentyl)dithiophosphinic acids in toluene at $pH_{eq.}$ ~ 4 (Figure 4) and have found that dialkylphosphinic acid appeared to be the most effective extractant. Thus, the extraction power of binary extractants decreases in the series: bis(2,4,4-trimethylpentyl)phosphinate > bis(2,4,4-trimethylpentyl)monothiophosphinate > bis(2,4,4-trimethylpentyl)dithiophosphinate of trioctylmethylammonium. [148]

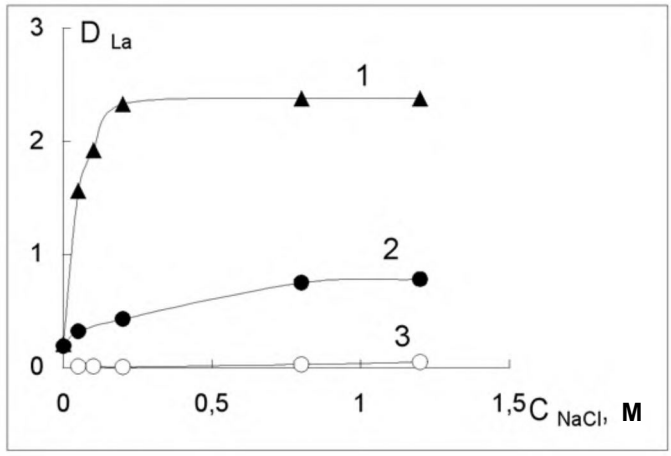


Figure 3. Dependencies of the lanthanum extraction on aqueous concentration of NaCl with 0.05 M solutions of bis(2,4,4-thmethylpentyl)phosphinate (1), bis(2,4,4-trimethylpentyl)monothiophosphinate (2), bis(2,4,4-trimethylpentyl)dithiophosphinate (3) of trioctylmethylammonium in toluene (C_{La}=0.02 M).

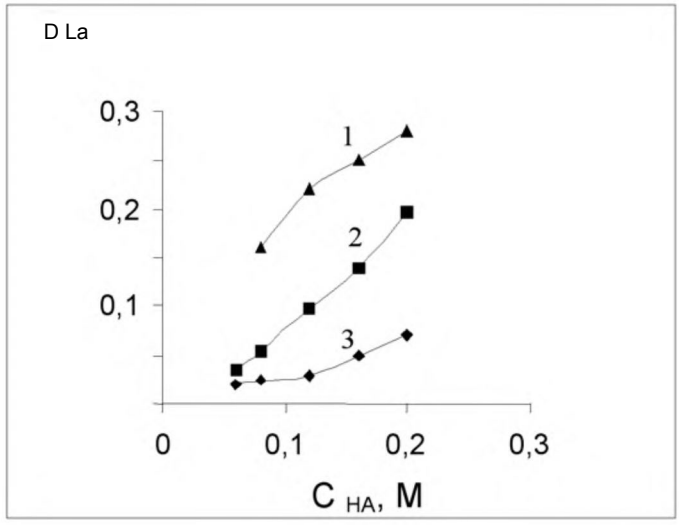


Figure 4. Dependencies of the lanthanum extraction on concentration of bis(2,4,4-trimethylpentyl)phosphinic (1), bis(2,4,4-trimethylpentyl)monothiophosphinic (2), bis(2,4,4-thmethylpentyl)dithiophosphinic (3) acids in toluene ($C_{La\ init}$= 0.021 M, pH^t ^ 4.0).

Extraction Constants

The data for the extraction of La, Ce, Nd and Yb depending on the binary extractant concentration (Figure 2) were used to determine the concentration constants of the extraction ($\overline{K_{ex}}$) accordingly to the Equation (2). The data on the concentration extraction constants related to the $LaCl_3$ extraction constant are given in Table 1, which confirm the extractability of rare earth metals in accordance with their positions in the raw of lanthanide. [149]

Table 1. Alteration of the extraction constants of rare earth metals (trioctylmethylammonium bis(2,4,4-trimethylpentyl)phosphina te system)

Element	La	Ce	Nd	Yb
$^{Al°}9\ ^{K}ex_{L}nCl_3/LaCl_3$	0	**0.46**	**0.75**	**2.70**

Separation of Rare Earth Metals

Experimental results obtained in the extraction of rare earth metals with trioctylmethylammonium bis(2,4,4-trimethylpentyl)phosphinate allow to calculate separation coefficients of these metals, which are represented in Table 2. The most high distribution coefficients towards rare earth metals are observed for ytterbium because of its position in the raw of lanthanide. It can be seen that the separation coefficients of elements decrease with decreasing concentration of the binary extractant owing to decreasing in their distribution coefficients.

Table 2. Separation coefficients of rare earth metals in trioctylmethylammonium bis(2,4,4-trimethylpentyl)phosphinate system

Cex, M	Element (Ln)	Separation coe fficients						
		Ln/La	Ln/Ce	Ln/Nd	Ln/Eu	Ln/Gd	Ln/Dy	Ln/Er
0.01	**Ce**	**6.4**						
	Nd	**21.4**	**3.3**					
	Yb	**600**	**92**	**27.6**				
0.001	**Ce**	1.1						
	Nd	1.1	1.0					
	Eu	**5.0**	**4.6**	**4.6**				
	Gd	**4.2**	**3.9**	**3.9**				
	Dy	**5.6**	**5.3**	**5.3**	1.1	**1.4**		
	Er	**6.9**	**6.4**	**6.4**	**1.4**	**1.7**	1.2	
	Yb	**19.2**	**18.0**	**18.0**	**3.9**	**4.6**	**3.4**	**3.9**

CONCLUSION

The extraction of rare earth metals from chloride solutions by binary extractants based on dialkylphosphinic, dialkylmonothiophosphinic and dialkyldithiophosphinic acids has been examined under different conditions. As a result, it is seen that the extraction of these metals occurs through the binary mechnism according to the Equation (1). The most effective extraction is observed in the system involving bis(2,4,4-trimethylpentyl)phosphinate of trioctylmethylammonium and recovery of rare earth metals enhances with increasing aqueous NaCl concentartion.

ACKNOWLEDGEMENTS

Financial support of Russian Foundation for Basic Research (grant N 04-03-32580) and the Russian President (grant N NSN-1577.2003.3) are gratefully acknowledged. [150]

REFERENCES

1. **A.I. Kholkin, V.V. Belova, G.L. Pashkov, I.Yu. Fleitlikh and V.V. Sergeev (1999),** *J. Mol. Liquids,* **82, 131-146.**
2. **V.V. Belova and A.I. Kholkin (1998),** *Solv. Extr. Ion Exch.,* **16, 1233-1255.**
3. **V.V. Belova, A.I. Kholkin and T.I. Zhidkova (1999),** *Solv. Extr. Ion Exch.,* **17, 1473-1491.**
4. **A.I. Kholkin, V.I. Kuzmin, G.L. Pashkov and et al. (1990),** *Izv. Sib. Otd. AN SSSR,* **5, 3-17.**
5. **S.N. Kalyakin and V.I. Kuzmin (2000),** *Mendeleev Commun.,* **1510152.**
6. **A. Hino, T. Hirai and I. Komasawa (1996),** *J. Chem. Eng. Jpn.,* **29, 1041-1044.**
7. **A. Hino, S. Nishihama, T. Hirai and I. Komasawa (1997),** *J. Chem. Eng. Jpn.,* **30, 1040-1046.**
8. **S. Nishihama, N. Sakaguchi, T. Hirai and I. Komasawa (2002),** *Hydrometallurgy,* **64, 35-42.**
9. **T.H. Handley (1965),** *Talanta,* **12, 893-901.**
10. **I.S. Levin, V.V. Sergeeva, V.A. Tarasova and et al. (1973),** *Zh. Neorg. Khim.,* **18, 1643-1649.** [151]

EXTRACTION OF RARE, NON-FERROUS AND ACCOMPANIED METALS WITH DIALKYLDITHIOPHOSPHATE OF TRIOCTYLMETHYLAMMONIUM

Anatoly I. Kholkin, Andrey A. Voshkin, Vera V. Belova and Tatiana I. Zhidkova*

Kurnakov Institute of General and Inorganic Chemistry of RAS, Moscow, Russia
'Institute of Chemistry and Chemical Technology of SB RAS, Krasnoyarsk, Russia

The extraction of of rare, non-ferrous and accompanied metals in their common presence with quaternary ammonium base (QAB) salt - trioctylmethylammonium di(2-ethylhexyl)dithiophosphate from chloride and nitrate solutions depending on concentration of the extractant was studied.

The extraction series obtained: $Re0_4'$ > $PtCl_6^{2'}$ > $M0O4^{2'}$ > $ZnCl_3'$ > $RhCl_6^{3'}$ > $FeCl_4'$ > $MnCl_4^{2'}$ coincides in common with the anion-exchange series for QAB involving mineral anions with the exception of iridium, which is reduced to Ir (III). Gold, palladium, zinc, iron and molybdenum can be combined into a group of metals, which are extracted forming complexes involving metals both into cation and anion parts of extracted species in the organic phase. Extractability of metals extracting preferably as salts of dialkyldithiophosphoric acid, MA_n, decreases in series: Cu (II) > Bi (III) > Pb (II) > Sb (III) >Sn (II) » Ni (II), Co (II), Y (III), La (III). This series coincides in common with the extraction series for di(2-ethylhexyl)dithiophosphoric acid in the extraction of metals from chloride solutions. Results on stripping of metals with using different reagents such as 0.05 M H_2S0_4, 0.3 M NH_4OH, 0.7 M thiourea solution are given.

INTRODUCTION

Dialkyldithiophosphoric acids possess high extraction ability [1-3], Being soft extractants according to the principle of hard and soft acids and bases they preferably extract soft and also middle metal ions in accordance with the Pearson's rule [4, 5], The main disadvantage of dialkyldithiophosphoric acids appears to be the high thermodynamic stability of some extracted species, which complicates stripping of these metals from the organic phase.

Utilization of binary extractants (salts of organic acids and organic bases) based on dialkyldithiophosphoric acids allows to get over these difficulties because the stripping in binary extractant systems is simplified [6, 7],

EXPERIMENTAL

Aqueous solutions of mixtures of metal salts (chloride or nitrate) in 0.1 M HCl or 0.1 M $HN0_3$ correspondingly were used for the extraction. Chloride solutions of bismuth (III) were prepared by dissolving bismuth oxide (Bi_20_3) in hydrochloric acid of selected concentration.

Compounds of rhenium and molybdenum such as, $KRe0_4$ and Na_2Mo0_4, were used for preparation of chloride solutions. Platinum metals and gold were employed as chlorocomplex acids, H_2PtCl_6, H_2IrCl_6, $H_2Rh(H_20)Cl_5$, $HAuCl_4$.

Solution of trioctylmethylammonium di(2-ethylhexyl)dithiophosphate was used as an extractant. The binary extractant, R_4NA, was prepared by mixing equimolar amounts of trioctylmethylammonium chloride (R_4NCl) and potassium di(2-ethylhexyl)dithiophosphate in toluene and with subsequent washing of an organic solution with 1 M NaOH for 10 min. The metal extraction with equal of aqueous and organic phases was carried out at 20°C. Samples in glass-stoppered bottles were shaken mechanically for 15 min. Stripping of metals from the organic phases was carried out with different solutions - 0.05 M H_2S0_4, 0.3 M NH_4OH and thiourea solution.

An initial chloride solution contained ~ 15 mg/l of each metal. The concentration of metals in aqueous solutions was determined on ICP-OES spectrometer model IRIS Advantage, Thermo Jarrel Ash. The differences in metal concentration between the initial and final aqueous solutions were used to calculate the concentrations of metals in the organic phase. All chemicals were of reagent grade.

EXTRACTION OF METALS FROM CHLORIDE SOLUTIONS

The extraction of 19 metals from hydrochloric acid solutions (0.1 M HCl, 1 M HCl) in their common presence with trioctylmethylammnium di(2-ethylhexyl)dithiophosphate depending on concentration of the extractant was studied. Data obtained (Figure 1) show a difference in metal distribution coefficients that provides a possibility of their separation.

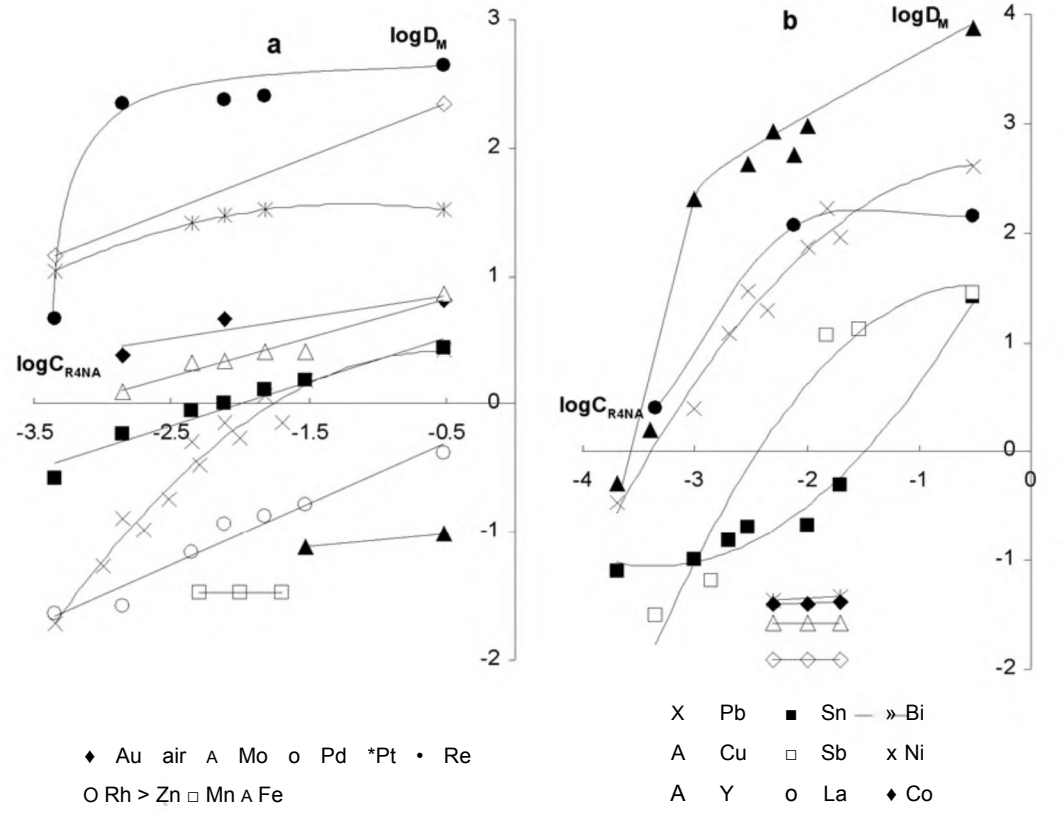


Figure 1. Extraction of metals from 0.1 M HCl solution with trioctylmethylammnium di(2-ethylhexyl)dithiophosphate in toluene. [153]

Under the experimental conditions metals are being in the aqueous phase as different cationic and anionic complexes, which composition and a ratio for different metals are determined by the constants of complex formation. As a result, the metals can be distributed into the organic phase in form of salts of di(2-ethylhexyl)dithiophosphoric acid as well as ionic associates involving QAB. In this connection elements studied should be divided into three conventional groups: the metals are mainly extracted as cationic and anionic forms as well as the metals are simultaneously extracted as both forms. Such division allows qualitatively to interpret the data obtained.

The experimental data for metals, which are effectively extracted with QAB salts are given in Figure 1 (a). Among these metals platinum, iridium and rhodium forming stable chlorocomplex anions are practically not extracted with dialkyldithiophosphoric acids, therefore, in binary extractant system they are mainly extracted as ionic associates, $(R_4N)_m$. $_nMCl_m$, in accordance with the equation of binary extraction of acids, $H_{m-n}MCl_m$'$^{(n,vn)}$:

$$(m\text{-}n)\ hr_{(a)} + MCl_m^{(m-n>}{}_{(a)} + (m\text{-}n)\ R_4NA_{(0)} \text{ o } (R_4N)_{m\cdot n}MCl_{m\ lo)} + (m\text{-}n)\ HA_{(0)} \qquad (1)$$

where n is an oxidation extent of metal, m is a coordination number. Obviously, Zn (II) and Fe(III) forming stable one-charged anions such as $ZnCl_3$' and $FeCl_4$' are also extracted through the same mechanism. Rhenium (VII) forms the stable perrhenate ion in aqueous solutions. Equilibrium for rhenium extraction can be described:

$$H^*(_a) + Re0_4\ (_3) + R_4NA\ (o) \text{ o } R_4NRe0_4\ (_0) + HA\ f_0j \qquad (2)$$

Apparently, molybdenum and manganese may by extracted as oxyanions. The extraction series obtained: $HRe0_4$ > H_2PtCl_6 > H_2Mo0_4 > H_2IrCl_6 > $HZnCl_3$ > H_3RhCl_6 > HFeCU > H_2MnCl_4 coincides in general with anion-exchanged series for QAB salts involving mineral anions. In common presence of different metals in an initial aqueous solution the extraction of complex anions with binary extractants accompanies the extraction of metal cations, therefore, a ratio of extracted species such as $(R_4N)m\text{-}_nMCl_m$ and HA can not necessarily correspond to stoichiometry. So far as effect of metal cation extraction on the distribution of anionic forms of different metals owing to decreasing HA concentration in the organic phase is similar, the extraction series can be written as that for binary extraction of acids. Analogues effect of the extraction of anionic metal complexes on the binary extraction of salts doesn't hinder to determine the extraction series for metal chlorides. Some peculiarities of the series obtained are explained by properties of dialkyldithiophosphate ion involving in the binary extractant. For example, Ir (IV) is extracted with QAB chlorides better than platinum [8] and in the extraction with binary extractant this metal is recovered much worse. It is accounted for by reduction of Ir (IV) to Ir (III) in systems involving dialkyldithiophosphoric acids [9] and three-charged chlorocomplexes, $IrCl_6^{3}$', are poor extracted by QAB salts [8], Some metals are extracted as both anions and cations that results in increasing distribution coefficients. Such metals as gold (III) and palladium (II) form stable anionic chlorocomplexes, which are extracted with QAB salts. At the same time, dialkyldithiophosphoric acids extract aold with hiah distribution coefficients, while Au (III) is reduced to Au (I) Ml. Earlier we have studied the extraction of palladium from chloride solutions with dialkyldithiophosphates of QAB and amines (Am) and have determined that palladium is extracted with these extractants with the formation of the complexes involving mixed ligands such as $(R_4N)[PdCl_2A]$ or $(AmH)[PdCl_2A]$ as well as palladium dialkyldithiophosphate, PdA_2, in the organic phase [10], Portions of these complexes depend on a ratio of concentrations of a binary extractant and palladium in the organic phase. Owing to this fact, palladium is extracted with the binary extractant much better than platinum.

Dialkyldithiophosphoric acids extract zinc from weak acidic chloride solutions [1, 3] and molybdenum in a wide range of aqueous acidity [1], Salts of amines and QAB recover anionic chlorocomplexes of zinc [11] and molybdate ions [12], therefore, one can suppose extraction of zinc and molybdenum occurs forming two extracted species such as salts of dialkyldithiophosphoric acid and trioctylmethylammonium involving complex anions. Thus, [154]

gold, palladium, zinc and molybdenum, apparently, can be indicated as a group of metals, which are extracted with the formation of extracted species, in which metals are present both in cationic part (dialkyldithiophosphates) and in anionic one (QAB salts). It should be noted a capacity of a binary extractant should increase compared to an initial organic acid or, for example, QAB chloride. It was shown using an example as the extraction of chlorocomplexes of palladium with dialkyldithiophosphate of tetraoctylammonium [10],

Figure 1 (b) shows distribution curves of metals, which are mainly extracted with the formation of salts of di(2-ethylhexyl)dithiophosphoric acid due to high thermodynamic stability of forming dialkyldithiophosphates of metals and low values of the stability constants of chloride complexes according to the binary extraction of salts, MCl_n:

$$M^{n+}_{(3)} + n\ Cl_{(a)} + n\ R_4NA_{(0)} <=> n\ R_4NCl\ _{(0)} + MA_{n\ (0)} \qquad (3)$$

Such metals as Y (III), Co(II), La (III) and Ni (II) are not practically extracted under the conditions of the extraction (D_M < 0.1). In accordance with the experimental data extractability of metals increases in the series: $CuCl_2$ > $BiCl_3$ > $PbCl_2$ > $SbCl_3$ > $SnCl_2$ » $CoCl_2$, $NiCl_2$, YCl_3, $LaCl_3$. This series of salt binary extraction coincides in general with cation-exchange extraction series for di(2-ethylhexyl)dithiophosphoric acid in the extraction of metals from chloride solutions [3],

EXTRACTION OF METALS FROM NITRATE SOLUTIONS

The extraction of metals from nitrate solutions containing as individual metals as well as their mixture with dialkyldithiophosphate of trioctylmethylammonium was investigated ($C_{HN}Q_3$ =

0.1 M). Experimental results showed Ca(II), Ga (III), Fe (III), Co (II), Ni (II) didn't practically transfer into the organic phase in the extraction of metals with 0.01 M solution of the binary extractant in toluene (C_M j_{njt} = (1 -5) $10^{'3}$ M). The data for the extraction of individual metals depending on concentration of the extractant are given in Figure 2. Extractability of metal nitrates decreases in the series: $Pb(N0_3)_2$ > $In(N0_3)_3$ > $Zn(N0_3)_2$ > $Cu(N0_3)_2$ > $Co(N0_3)_2$ > $Ni(N0_3)_2$. [155]

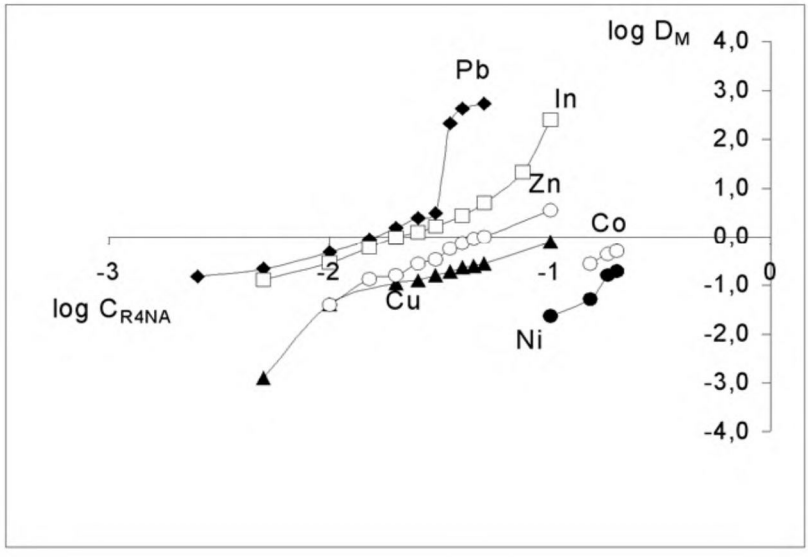


Figure 2. Extraction of individual metals from nitrate solutions with trioctylmethylammnium di(2-ethylhexyl)dithiophosphate in toluene. $C_{Minn.}$ **= 0.01 M,** $C_{HN}Q_3$ **=** *0.1 M,* $C_{KNO:j}$ **=** *1 M.*

Figure 3 shows the results of the metal extraction from nitrate solution containing their mixture with QAB dialkyldithiophosphate in toluene. An initial solution contained nitrates of Cu (II), Ag (I), Pb (II), In (III) and Bi (III). The data obtained indicate the extraction of metals decreases in the series: $AgN0_3$ > $Bi(N0_3)_3$ > $Cu(N0_3)_2$ >> $Pb(N0_3)_2$, $In(N0_3)_3$.

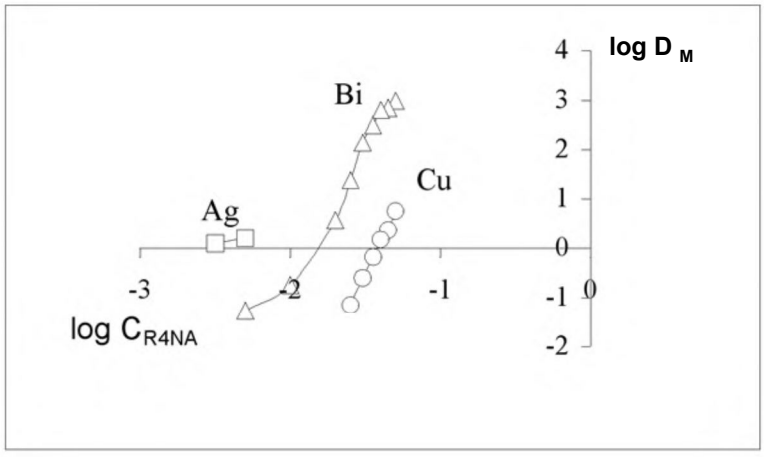


Figure 3. Extraction of metals in their common presence from nitrate solutions with trioctylmethylammnium di(2-ethylhexyl)dithiophosphate in toluene.

CM inn =0.01 M (Ag); 0.005 (Bi); 0.001 (Cu). **$C_{hnc,3}$ =** *0.1 M.*

Because in the extraction different metals form complexes of different structure and stability, for stripping metals from the organic phase we studied successively 0.05 M H_2S0_4 solution and solutions of complex formation agents - 0.3 M NH_4OH and 0.7 M thiourea (Table). An extract was obtained in the extraction of metals from an aqueous solution of their mixture in 1 **M HCl. An weak acid solution was used for the stripping to prevent hydrolysis of metals in the aqueous phase. Table reports the data on recovery of metals at each step of striping and also the common percentage of recovery of each metal from the organic phase after three steps of stripping with different reagents.**

Table. Results of stripping of metals from the organic phase with different reagents. [156]

Element	Concentration 10^4 (M)	Stripping, %			
		0.05 M H_2S0_4	0.3 M NH_4OH	0.7 M thiourea	Stripping after 3 steps
Co (II)	**0.39**	**13.4**	**0.06**	0	**13.5**
Cu (II)	**3.34**	0	0.02	**0.04**	**0.006**
Fe (III)	**1.54**	**19.2**	**0.06**	**0.06**	**19.3**
Pb (II)	**0.51**	**1.53**	0	**0.03**	**1.56**
Sn (II)	1.12	2.0	**23.4**	**5.4**	**30.0**
Zn (II)	2.22	**60.2**	**0.56**	**0.36**	**60.6**
Au (III)	**0.004**	**15.4**	**23.0**	**72.7**	**82.2**
Bi (III)	**1.09**	**0.25**	2.0	**0.75**	**3.0**
Mo (VI)	**1.08**	**3.0**	**51.5**	**26.1**	**65.2**
Pt (IV)	**0.28**	0	11.0	**0.41**	**11.3**
Re (VII)	**0.95**	0.11	**65.5**	**6.3**	**67.7**
Sb (III)	**0.24**	**0.59**	**82.2**	**33.6**	**90.2**

The results obtained allow to choice perspective systems for separation of metals and suggest possible ways of their stripping. For example, zinc is effectively stripped with 0.05 M sulphuric acid solution. Ammonia solution strips molybdenum, rhenium and antimony. Copper forming the most stable dialkyldithiophosphate was not practically recovered from the organic phase under the experimental conditions, because of low concentration of ammonia solution but with using 3 M NH_3 solution copper is completely stripped [13], With using solutions of thiourea stripping of Au, Mo and Sn can be achieved. Experimental data on distribution of metals from chloride and nitrate solutions in the binary extractant system allow to estimate behaviour of metals in their common presence both in the extraction and in the stripping of metals with solutions of different reagents.

ACKNOWLEDGEMENTS

Financial support of Russian Foundation for Basic Research (grant N 04-03-32580) and the Russian President (grant N NSN-1577.2003.3) are gratefully acknowledged.

REFERENCES

1. **T.H. Handley and J.A. Dean (1962),** *Anatyt. Chemistry*, **34, 1312-1315.**
2. **T.H. Handley (1965),** *Talanta*, **12, 893-901.**
3. **I.S. Levin, V.V. Sergeeva, V.A. Tarasova and et al. (1973),** *Zh. Neorg. Khim.,* **18, 1643-1649.**
4. **R.G. Pearson (1963),** *Amer. Chem. Soc.,* **85, 3533-3539.**
5. **B.Ya. Spivakov and O.M. Petrukhin (1980),** *Zh. Neorg. Khim.,* **25, 245-259.**
6. **V.V. Belova and A.I. Kholkin (1998),** *Solv. Extr. Ion Exch.,* **16, 1233-1255.**
7. **A.I. Kholkin, V.V. Belova, G.L. Pashkov, I.Yu. Fleitlikh and V.V. Sergeev (1999),** *J. Mol. Liquids,* **82, 131-146.**
8. **L.M. Gindin, S.N. Ivanova, A.A. Mazurova and et al. (1967),** *Izv. Sib. Otd. AN SSSR, 2,* **89-96.**
9. **N.A. Bortch, O.M. Petrukhin and Yu.A. Zolotov (1978),** *Zh. Ana/it. Khim.,* **33, 1120-1127.**
10. **V.V. Belova, A.I. Kholkin and T.I. Jidkova (1999),** *Solv. Extr. Ion Exch.,* **17, 1473-1491.**
11. **T. Sato, T. Nakamura and M. Kuwahara (1983),** *Solv. Extr. Ion Exch.,* **1, 453-462.**
12. **T. Sato, H. Watanabe and H. Suzuki (1986),** *Solv. Extr. Ion Exch.,* **4, 987-996.**
13. **A.I. Kholkin, V.I. Kuzmin, G.L. Pashkov and et al. (1990),** *Izv. Sib. Otd. AN SSSR,* **5, 3-17.** **157**

AGGREGATION IN ORGANIC PHASE AND THIRD PHASE FORMATION IN THE Zr-$HN0_3$ - TBP - ALKANE SYSTEM

Oksana A.Sinegribova, Ulyana V. Bortnikova, Yanis I.Baksha, Ekaterina A.Zherebieva
D.Mendeleyev University of Chemical Technology of Russia, Moscow, Russia

Aggregation in the organic phase and formation of a third organic phase in the extraction of zirconium from nitric acid solution by TBP in aliphatic diluents have been investigated. Lazer light scattering measurements on TBP solutions loaded with various amounts of $HN0_3$ and Zr revealed the presence of aggregates which sizes increase at higher concentration of metal but decrease when $HN0_3$ concentration increases. The third phase formation is a result of Zr extraction into organic phase where TBP is combined with $HN0_3$. Volume of the third phase depends on the original concentration of TBP in the organic solution. For 30 - 50% TBP concentration of TBP in the third phase is about 55% and molar ratio Zr: TBP is ≥ 0.1 : 1. Chemical analysis of the third phase saturated by Zr has shown that its composition is closed to $Zr(N0_3)_4 2TBP\ HN0_3$. The species size in such third phase is smaller than size of species presented in homogeneous organic phase with high concentration of Zr. Probably the determined hydrodynamic radius corresponds to size of water (or solvent) pockets dispersed in continuous highly structured medium.

INTRODUCTION

The phenomenon of third phase formation in solvent extraction of actinides or zirconium-hafnium from nitrate solutions by TBP is well known. These extraction systems have technological importance and in the beginning of development of extraction technology the task was to dissolve the third phase or to avoid its formation. The decision was found in addition of some modificators to organic phase or in application of aromatic instead of aliphatic diluent. The common conception obtained on the basis of technological experience was the following:

- **the high concentration of $HN0_3$ promotes the third phase formation;**
- **the high concentration of extractable compound in the organic phase precedes organic phase splitting;**
- **the aggregation in the organic phase leads to formation of large aggregates that are insoluble in the organic phase at high metal loading.**

The recent publications show revived interest in the third phase formation from the standpoint of its chemical composition and structural aspects especially due to the possibility to estimate the size of species formed in the organic phase. Chemical analyses, spectroscopic and EXAFS data indicated that the third phase speicies for U(VI) extraction by 20% TBP in n-dodecane had the composition $U0_2(N0_3)_2\ 2TBP.HN0_3$ [1], Addition of 1 molecule of $HN0_3$ to U(VI)-adduct leads to organic phase splitting. The similar composition of third phase was proposed in [2] for extraction not only U(VI), but Pu(IV) and Th(IV) by TBP. Small-angle neutron scattering (SANS) measurements on TBP- octane solutions of U [1] and Th [3] revealed the presence of ellipsoidal reverse micelle-like aggregates before phase splitting. The presence of hexameric aggregate of trisolvate $Th(N0_3)_4 3TBP$ before

splitting of organic phase (20% TBP - n-octane without $HN0_3$) was assumed in [3], Zirconium third phase formation was investigated for the 30%TBP-various diluent - $HN0_3$ system in [4] and the limiting organic concentration (LOC) - the most concentration without splitting - of Zr was determined. In [5] the third phase template with an optimized bi-continuous structure in extraction system *triaikyl phosphine oxide* **-** *kerosine/Zr(IV)* **-** *HCI* **was used for preparation of mesoporous $Zr0_2$.**

The objective of present work is the system *Zr* **-** *$HN0_3$* **-** *TBP* **-** *alkane*: **the conditions of third phase formation, its composition, the aggregation of extractable compounds in the homogeneous organic phase and in the third phase after organic phase splitting. In spite of technological application, very few detailed information was obtained about the state of extractable species in the organic phase for this extraction system. The main focus of this investigation was to reveal effect of various parameters - concentrations of $HN0_3$, TBP and Zr on structure formation in the organic solution and phase behaviour of extraction system. .**

EXPERIMENTAL AND PROCEDURE

The fulfilment of extraction experiments was routine. The organic solutions of extractant were preequilibrated with corresponding solutions of $HN0_3$ (phase ratio V_{org}:V_{aq} =1:5). After zirconium extraction, centrifugation and phase separation, aliquots of the phases were analyzed. Concentration of $HN0_3$ was determined by titration with standard base after zirconium complexation with F' -ion. Concentration of zirconium was determined by complexometric or by gravimetric methods. The TBP concentration in the heavy organic phase resulting from phase splitting was determined after contacting with $HCl0_4$ solution following a published method [6], Water concentration in third phase was determined by Carl Fisher titration.

Hydrodynamic radius of species in the organic phase was calculated from the data on diffusion coefficients. Diffusion coefficients were measured using a method of dynamic light scattering with He-Ne - lazer as light source. This method allowed to estimate the mean size of aggregates, probably hydrated in organic solution. Precision of method was low for ziconium concentration < 10 g/L (-20%), but it improved with increase of zirconium content up 5%.

RESULTS AND DISCUSSION

The values of Zr species radius for systems with 40% TBP and 70% TBP in n-octane and in toluene for comparison are presented in Fig.1 as a function of zirconium content for different nitric acid concentrations in equilibrium aqueous phase. As it seen from presented data, a size of Zr aggregate in the organic phase increases with increasing of metal concentration but decreases with increasing of $HN0_3$ concentration in equilibrium aqueous phase. In [7] the formation of extractable mixed compounds contained both zirconium nitrate and $HN0_3$ - $H_2Zr(N0_3)_4$2TBP - was assumed. In this case the results presented above show that hypotetic mixed extractable species is less capable to associate than $Zr(N0_3)_4$2TBP, the formation of mixed compounds begins apparently at acidity -4-5 M $HN0_3$ and in this interval the transition from more associated aggregates to less assosiated species takes place.

It should be noted that the difference in the size of extractable species for system with octane and toluene is visible only at low concentration of $HN0_3$. But it is known that the third phase formation is observed for alkane solvents of TBP, not for toluene. It means that the reason of third phase formation is not high aggregation of extractable metal compounds, leading to low solubility of these compounds in solvent. [159]

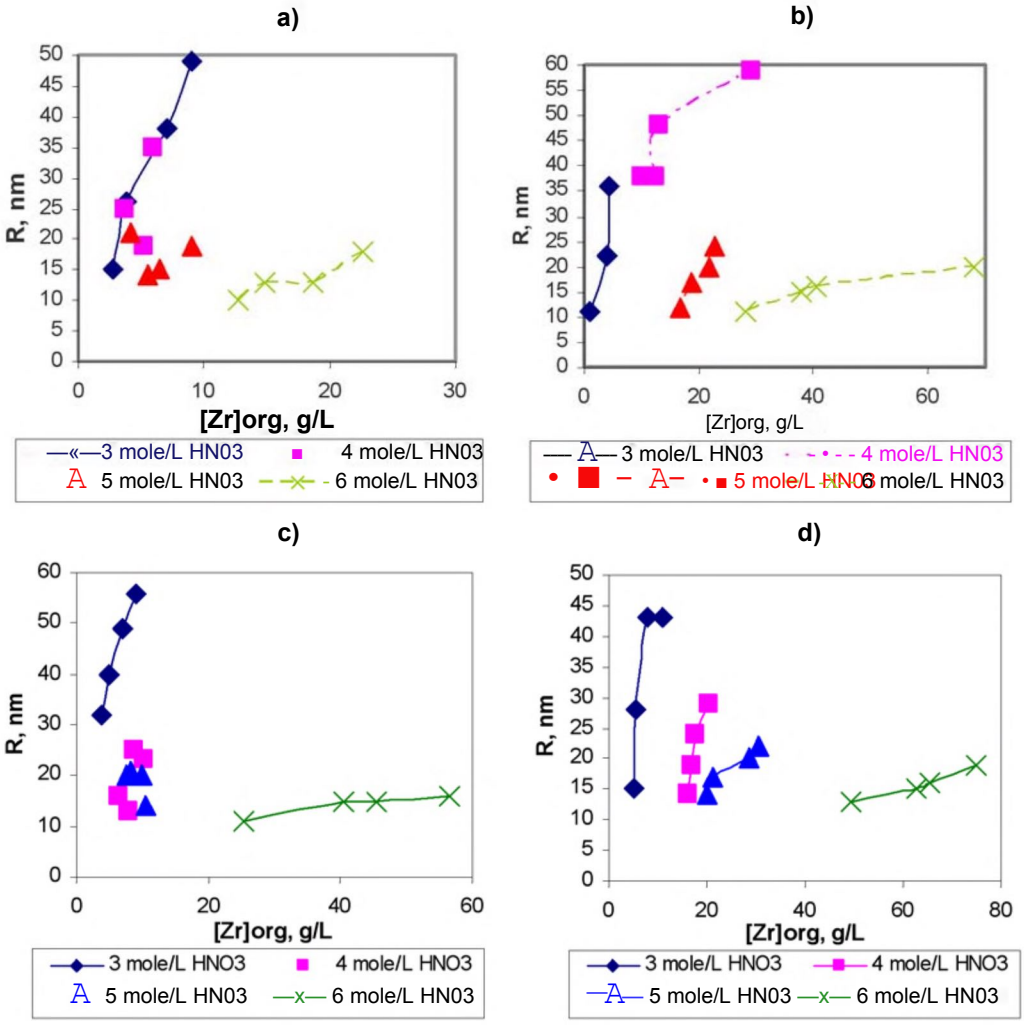


Figure 1. Effect of Zr concentration in the organic phase on species hydrodynamic radius, (a) 40% TBP-n-octane, (b) 70% TBP-n-octane, (c) 40% TBP-toluene, (d) 70% TBP-toluene

The alternative explanation can be given for the dependences presented in Fig. 1: the speices size is defined by polarity of organic phase. Its polarity increases up when concentration of solvate HNO_3TBP increases. But it should be noted, that at 6 mole/L HNO_3, when mixed extractable compounds predominate, the differences of aggregate hydrodynamic radius at the equal Zr concentration as for organic phase with 40% TBP or with 70% TBP, as for organic phase with octane and toluene, are neglectible. As far as in TBP solutions in toluene the third phase does not form, the reason of its appearance is not associacion of extractable compounds with formation of aggregates insoluble in organic phase.

Third phase formation in system *Zr - HNO_3 - 40%TBP - n-octane (n-decane)* **was observed for high equilibrium HNO_3 concentration (Table 1). It is reasonable to conclude that the third phase formation in system Zr - $HN0_3$ - TBP - alkane takes place when TBP is mainly combined with HNO_3, so free TBP is almost absent in the organic phase.** [160]

Table 1. Third phase volume at Zr extraction by 40% TBP in alkane

$[HN0_3]_{aq}$,, M	octane		decane		$[HN0_3]_{aq}$. M	octane		decane	
	$[Zr]_{org}$ M	V 3ph.,%	[Zf]org M	v_{3ph}.,%		[zr]orgM	V 3ph.,%	[Zrjorg. M	V 3ph.,%>
5.0	**0.31**	0	**0.35**	**50**	8.0	0.20	**67**	**0.17**	**63**
6.0	**0.30**	**60**	**0.25**	**55**		**0.59**	**56**	0.22	**63**
	0.50	**60**	**0.51**	**60**				**0.27**	**63**
7.0	0.20	**67**	**0.18**	**61**	**8.5**	**0.63**	**57**	**0.28**	**53**
	0.23	**62**	0.20	**57**				**0.38**	**51**
	0.30	**67**	0.22	**58**				**0.71**	**53**
	0.65	68	**0.34**	**57**	**9.5**	**0.57**	**58**	**0.18**	**63**
			0.37	**50**				**0.30**	**60**
			0.56	**51**				**0.33**	**60**

The data of Table 2 show that the third phase volume for 40% TBP is approximately constant (±10%), it does not depend on concentratios of $HN0_3$ and Zr. The volume is a little more for octane, than for decane. Increase of number of carbon atoms in linear hydrocarbon diluents up Ci_2 decreases volume of third phase (Table 2).

Table 2. Third phase volume in systems with different alkanes
Aq.phase: $[HN0_3]$=7.5 M; Org.phase: 40% TBP in alkane

Diluent	octane	decane	dodecane	Cl2 " C-14
$[Zr^{4+}]_{n}$ third phase* 9^-	20	68	**59**	**18**
Vthird phase, *k*	**62**	**52**	**45**	**44**

The volume of third phase depends on TBP concentration (Table 3).

Table 3. Volume of third phase at various TBP concentration

$[HNO_3]$ aqueous M	30% TBP		50% TBP		60% TBP
	octane	decane	octane	Decane	octane
6.0	20	**25**	88	**90**	0
7.0	**25**	**23**	**92**	**82**	**90**
8.0	20	**28**	**90**	**90**	**95**

In the extraction system with 70% TBP the splitting of organic phase was not observed.

In Table 4 the concentrations of Zr in the organic phase (calculated by deferences of initial and final aqueous concentrations) corresponding to the third phase appearance - minimum organic concentration (MOC) - are presented. In these experiments the third phase was attained by variation of Zr concentration in the aqueous phase and of V_0rg:V_aq with step 5%. [161]

Table 4. Minimum organic concentration of Zr for 3-rd phase appearance

[TBP],%	$[HN0_3]_{aq}$ M	octane				decane			
		$[Zr]_{aq}$ in.g/L	Vorg- V_{aq}	$[Zr]_{aq}$ fin.g/L	$[Zr]_{org}$ g/L	$[Zr]_{aq}$ in.g/L	Vorg ■ V_{aq}	$[Zr]_{aq}$ fin.g/L	$[Zr]_{org}$ g/L
30	6.0	**38.9**	**1 : 1.3**	**30.4**	**11.0**	**33.4**	1 : 1	**24.2**	**9.2**
	7.0	**15.6**	1 : 1.1	**6.4**	**10.1**	**18.9**	1 : 1.2	**9.8**	**9.1**
	8.0	**12.4**	1 : 1.1	**3.8**	**9.4**	**11.9**	**1 : 1.15**	**3.2**	**9.6**
40	6.0	**36.8**	1 : 1	**15.0**	**21.8**	**38.1**	**1 : 1.7**	**23,6**	**25.1**
	7.0	**23.4**	1 : 1.1	**6.4**	**18.7**	**25.4**	1 : 1	**7.6**	**17.8**
	8.0	**25.5**	1 : 1	**7.7**	**17.8**	**17.1**	**1 : 1.05**	2.1	**15.7**
	8.0					**4.4**	1 : 8	2.2	**17.0**
50	6.0	**57.8**	1 : 1.1	**34.2**	**26.0**	**56.4**	**1 : 1.3**	**35.9**	**26.7**
	7.0	**28.6**	1 : 1.1	6.8	**24.0**	**28.7**	1 : 1	6.8	**21.9**
	8.0	**25.6**	**1 : 1.15**	**5.4**	**23.2**	22.8	1 : 1.2	**5.0**	**21.7**

The data of Table 4 indicate that MOC $_{z'}$ depends mainly on TBP content in the organic phase. The values of MOC for 30% TBP are closed to LOC values for Zr in [4],

The third phases obtained at MOC $_{z'}$ and at Zr saturation were analyzed. Compositions of third phases are given in Table 5 and Table 6.

Table 5. Composition of third phases obtained at MOC_{Zr}

$[HN_{03}]_{aq}$ M	D"BP]org total		W $_3$ phase	[Zr] $_3$ phase	[TBP] $_3$ phase		$[HN0_3]$ $_{3\ ph}$ mole/L
	%	M	%	M	%	M	
7.0	40	1.46	61	0.30	58	2.14	1,7
	40	1.46	67	0.30	58	2.12	1,7
	50	1.83	82	0.29	60	2.19	1,9
8.0	30	1.11	28	0.18	54	1.97	1,9
	40	1.46	63	0.26	50	1.83	1,9

The results indicate that in these experements TBP concentration in the third phase is closed to ~2 M, the third phase appears at Zr concentration in 7-10 times lower than TBP concentration but whole TBP is combined with $HN0_3$ and Zr. Comparison of TBP concentrations in 3-rd phase, experimental and calculated from total TBP amount and 3-rd phase volume, shows that at low TBP initial concentration a part of TBP remains in light organic phase. For 30%TBP analysis of light phase gave ~17% TBP.

Table 6. Composition of third phase loaded by Zr (TBP - decane)

$[HN0_3]_{aq}$ M	[TBP] $_{or}$g total		[Zr] $_3$ phase M	$[HN_{03}]_3$ phase M	[TBP] $_3$ phase		$[H_2O]_3$ phase M
	%	M			%	M	
7.5	40	1.46	1.26	0.9	74	2.7	0.4
			1.37	1.0	79	2.9	0.5

The ratio Zr : TBP in third phase saturated by Zr is ~ 1:2 but $HN0_3$ presents in the third phase as well. It is poissible to suggest that the composition of species in this third phase (saturated by Zr) in [162]

general can be expressed as $Zr(N0_3)_4 2TBP\ HN0_3$ (neglecting water). This compound is similar to uranium compound in the third phase [1-2]. Interaction of Zr nitrate with $HN0_3$ probably is a result of transformation of bidentate nitrate ligand in Zr compound to monodentate with formation of strong hydrogen bond with molecules of nitric acid as it was supposed for uranium [1],

A size of species in third phase saturated by Zr was estimated through its hydrodynamic radius determined by method of dynamic light scattering. The results are given in Table 7.

Table **7.** *Hydrodynamic radius of species in the third phase*
Org.phase: 40% TBP in decane, V 3 phase ~ 50%

$[HN0_3]_{aq}$,M	$[Zr^{4+}]_{3\ ph.}$, M	R, nm
7,0	0,70	21,0
7,5	0,90	21,5
7,5	0,75	19,5
8,0	0,66	13,5
8,5	0,75	15,0

Comparison of these data with data of Fig. 1 shows, that a size of aggregates in the third phase is lower than a size of Zr aggregate in the organic phase without splitting at high Zr concentration.. It is reasonable to suppose that the aggregates in the third phase are dispersed pockets of water (or solvent) in continuous structure of extractable compounds.

CONCLUSIONS

In the system Zr - $HN0_3$ - TBP - alkane splitting of organic phase is observed when TBP is combined with $HN0_3$ and free TBP is almost absent. The molar Zr concentration in third phase at third phase appearance is 10-15% of molar TBP concentration in it. Volume of third phase depends mainly on original TBP concentration. The composition of third phase saturated by Zr is closed to $Zr(N0_3)_4$ 2TBP $HN0_3$. A size of species in the third phase loaded by Zr is lower than a size of species in the unpartitioned organic phase with high concentration of zirconium, so these aggregates probably are the pockets of water or solvent in continuous highly structured media.

REFERENCES

1. **M.P.Jensen, R.Chiarisia, J.R.Ferraro et al. (2002),** *Proc.ISEC 2002,* **Cape Town, 1137-1142.**
2. **S.Kumar and S.B. Koganti (2003),** *Solvent Extr. Ion Exch.,* **21, 547-557.**
3. **M.Borkowscy, R.Chiarisia, M.P.Jensen et al.(2003),** *Sep.Sci.Technol.* **38, 3333-3351.**
4. **M.J.Carrot, R.J.Taylor, I.S.Denniss, B.Ya.Zilberman (2001),** *Proc.int.Conf.* **Global'01, Paris, rep.FP-316**
5. **X.Fu, L.Yu, Lin Yu. et al. (2004),** *Solvent Extr. Ion Exch.,* **22, 885-895.**
6. **I.V.Shilin, E.M.Indikov, Yu.F.Zhdanov, D.G.Makarov (1958),** *USSR Patent* **114 186**
7. **G.F.Egorov, V.V.Fomin, Yu.G.Frolov, G.A.Yagodin (1960),** *Zhurn.neorgan.chim* **5, 1044-1050 (in Russian).** [163]

KINETICS OF AMERICIUM EXTRACTION WITH 2,6-Di(5,6-DIPROPYL-1,2,4-TRIAZIN-3-YL)PYRIDINE

Michael Weigl, Andreas Geist, Udo Miillich, Klaus Gompper

Forschungszentrum Karlsruhe GmbH
Institut für Nukleare Entsorgung
POB 3640, 76021 Karlsruhe, Germany
weigl@ine.fzk.de

A very promising extractant for the separation of minor actinides from high-level liquid waste is 2,6-di(5,6-dipropyl-1,2,4-triazin-3-yl)pyridine (n-Pr-BTP). n-Pr-BTP extracts trivalent actinides over lanthanides from 1-2 molar nitric acid with a separation factor of approx. 135. The dependency of americium extraction rates from stirring speed was measured in our special stirred cell. It was found that extraction rates are independent of stirring speed. This means that the mass transfer is limited by a slow chemical complexation reaction ("chemical regime"). Diffusion resistance is to be neglected, and the mechanism of the chemical reaction is accessible by a kinetic investigation.

INTRODUCTION

Partitioning & Transmutation is intended to reduce the long-term radiotoxicity of nuclear waste [1], Therefore plutonium and the minor actinides (neptunium, americium, curium) must be separated (Partitioning) from spent nuclear fuel. After this separation these long-lived radionuclides could be transmuted into stable or short-lived nuclides in dedicated reactors (Transmutation). The radiotoxcity of the remaining nuclear waste to be finally disposed would decay to the level of natural uranium within less than 1,000 years. In Partitioning, the separation of trivalent actinides (americium, curium) from the fission lanthanides is a key step. Due to the chemical similarity of the two groups of elements, this is a major challenge. To make this step process compatible, a feed acidity in the range of 0.1 to 1 kmol/m³ $HN0_3$ must be processed.

A very promising extractant for this difficult task is 2,6-di(5,6-dipropyl-1,2,4-triazin-3-yl)pyridine (n-Pr-BTP) (see Figure 1), a solvating extractant which was developed in our laboratory [2], It is able to extract trivalent actinides from up to 1 kmol/m³ $HN0_3$with usable distribution coefficient and an Am(III)/Eu(III) separation factor of approx. 135. The so-called *SANEX-III* process (selective actinide extraction) [3] is based on this extractant.

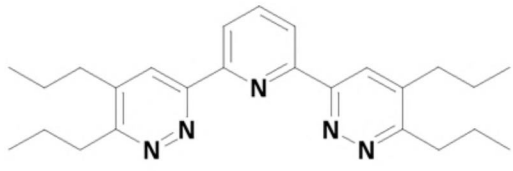


Figure 1. 2,6-di(5,6-dipropyl-1,2,4-triazin-3-yl)pyridine (n-Pr-BTP)

Furthermore, this extractant complies with the "CHON principle", consisting only of C, H, O, and N atoms, making it fully combustible to gaseous products. This extractant has already proven its potential in mixer-settler and centrifugal extractor battery tests performed in other laboratories [3],

This contribution focused on clearly identifying the kinetic regime (chemical or diffusional) of this extraction system. It is generally accepted that liquid-liquid interfacial kinetics are an important subject [4], Knowledge of the extraction regime is a pre-requisite for calculating extraction rates [5], Furthermore knowledge of the extraction regime leads to a better understanding of the physical and chemical fundamentals of an extraction system.

A kinetic investigation can conveniently be performed in a stirred cell of appropriate design [6, 7], The stirred cell we used was calibrated on a physical mass transfer system (toluene-water), showing a linear increase of mass transfer rate with stirring speed [6], Hence, we can be sure that, in a chemical mass transfer system, a linear increase of mass transfer rate with stirring speed indicates diffusional regime. Mass transfer rates independent of stirring speed indicate that processes other than transport (e.g., chemical reaction) control the mass transfer rate.

EXPERIMENTAL

Reagents and Solutions

n-Pr-BTP was synthesized according to [2], Melting point was in the range of 105-107 °C and NMR data confirmed the product's identity. A solution of n-Pr-BTP (0.01 to 0.04 kmol/m^3) in kerosene/1-octanol (70:30 vol.) was used in the kinetic study. Aqueous phase was a solution of trace amounts of ^{241}Am(lll) in 0.25 - 2.0 kmol/m^3 $HN0_3$ and 0.5 - 2.0 kmol/m^3 NH4NO3.

Kinetic Experiments

Kinetic measurements were performed in our special small stirred cell at 293 K. This cell has a half cell volume of only 6 ■ 10'^{5} m^3 (60 cm^3) and an interfacial area of 1.26 ■ 10'^{3} m^2 (12.6 cm^2). The stirred cell used is a scaled-down version of the Nitsch-type stirred cell. It is described in detail in [6], The stirred cell was filled with both aqueous and organic phases, and stirrers were started with the same speed in both phases ($n_{aq} = n_{org}$). All measurements were performed with ^{241}Am radiotracer. The course of mass transfer was detected by measuring the change in ^{241}Am activity over time in the aqueous phase. ^{241}Am activity was detected continuously in a by-pass with a well-type germanium detector (Canberra GCW2022). Measured activity was plotted vs. time and normalized initial metal fluxes were calculated using the following equation:

$$j_{t=0} / \left[Am^{3+} \right]_{t=0} = -\log \frac{\partial \left[Am^{3+} \right]}{\partial t} \frac{V}{F} \square 2.3026 \quad (1)$$

RESULTS AND DISCUSSION

The plot of normalized initial americium fluxes, $j_{t=0}/[Am^{3+}]_{t=0}$, over stirring speed (Figure 2) characterizes the kinetic behavior of Am(lll) extraction with n-Pr-BTP. The flow-independent (plateau) rates indicate that mass transfer is controlled by a slow chemical complexation reaction ("chemical regime"). Diffusion resistance is to be neglected, and the mechanism of the chemical reaction is accessible by a kinetic investigation. Therefore the dependency of extraction rates from the concentrations of all participating species (Am^{3+}, H\ $N0_3$', n-Pr-BTP) [165]

must be studied [7], This leads to the reaction orders of the reaction for each species. If the reaction orders are known a rate equation can be expressed.

For different initial americium activities in the aqueous phase (not shown), always the same normalized initial americium fluxes were measured. Therefore it is verified that extraction rate is first-order with respect to americium concentration.

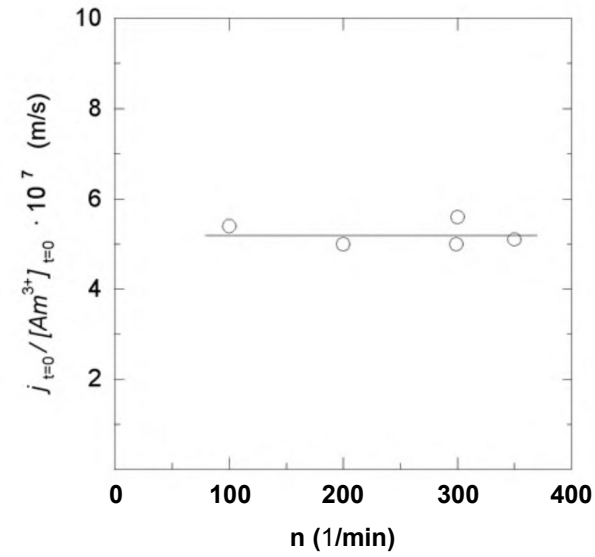


Figure 2. Stirring rate dependency of normalized initial flux. [Am] = 1 MBq/L, [$HN0_3$] = 1 kmol/m³, [NH_4NO_3] = 2 kmol/m³; [n-Pr-BTP] = 0.04 kmol/m³. Symbol: experiments; line: calculated average plateau rate.

Second the influence of the complexing agent concentration was studied. A linear dependency between normalized initial americium fluxes and n-Pr-BTP concentration was found, as shown in Figure 3. This indicates that the reaction is of first-order for n-Pr-BTP. This must not be confused with the third-order dependency of americium *distribution ratio* **on the extractant concentration [3].**

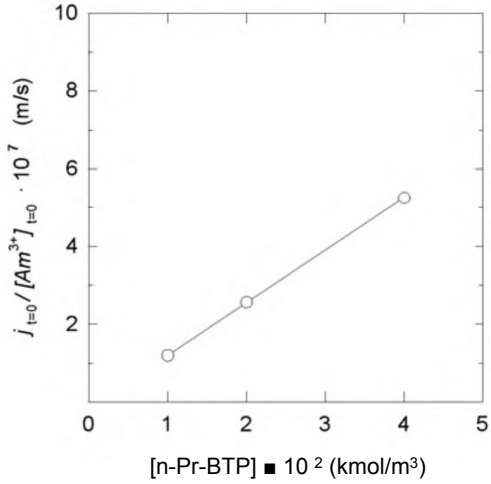


Figure 3. Dependency of normalized initial flux on n-Pr-BTP concentration at a stirring rate of n =300 (1/min). [Am] =1 MBq/L, [$HN0_3$] = 1 kmol/m³, [NH_4N0_3] = 2 kmol/m³. Symbol: experiments; line: regression. [166]

Initial nitrate concentration has no influence on the initial fluxes (Figure 4). This, again, must not be confused with the third-order dependency of americium *distribution ratio* **on the nitrate concentration [3],**

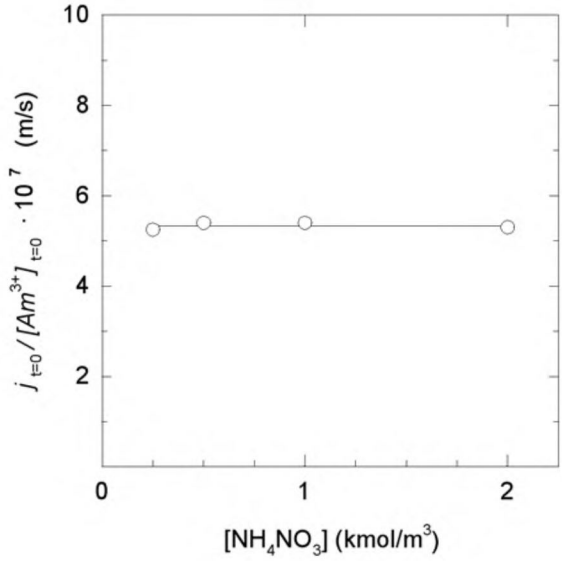


Figure 4. Dependency of normalized initial flux on ammonium nitrate concentration at a stirring rate of n =300 (1/min). [Am] = 1 MBq/L, [$HN0_3$] = 1 kmol/m³; [n-Pr-BTP] = 0.04 kmol/m³. Symbol: experiments; line: regression.

Results regarding the influence of aqueous nitric acid concentration on initial americium fluxes are presented in Figure 5, showing a decrease with increasing $HN0_3$ concentration. This can be explained considering results reported by Kolarik et al. [2], The amount of nitric acid co-extracted by n-Pr-BTP is increasing with initial aqueous nitric acid concentration and thereby the concentration of free n-Pr-BTP is lowered. [167]

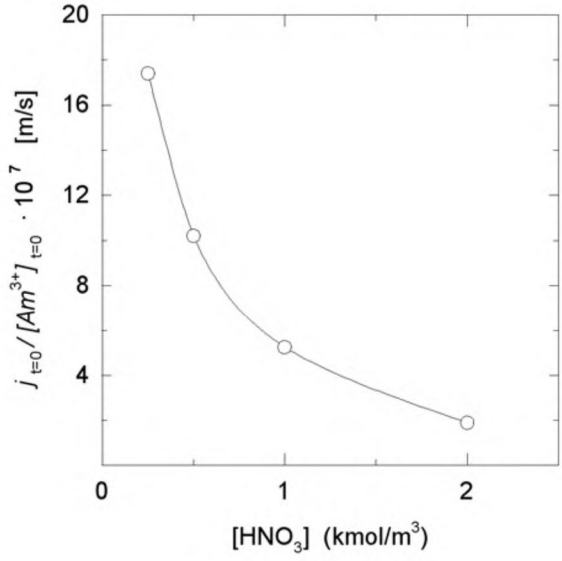


Figure 5. Dependency of normalized initial flux on nitric acid concentration at a stirring rate n =300 (1/min). [Am] =1 MBq/L, [NH_4N0_3] = 2 kmol/m³; [n-Pr-BTP] = 0.04 kmol/m³. Symbol: experiments; line to guide the eye.

From the results presented, the following rate equation for the kinetics of Am(III) extraction with n-Pr-BTP can be derived for a given aqueous nitric acid concentration,

$$j_{Am,0} = *\vec{\square}\ [Am]l_q\ U[n\text{-}Pr\text{-}BTP\backslash_{org}\ \square[A/0_3]^{\circ}{}_{(?}\ (2)$$

The forward rate constant $(\vec{k})$ for a nitric acid concentration of 1 kmol/m^3 calculated with this equation is $\vec{k} = 1.3\text{-}10^{-s}$[-].

CONCLUSION

Within the scope of this work it is shown that the presented extraction system is limited by the chemical reaction. Nitrate concentration has no influence on the kinetics and nitric acid concentration indirectly influence the extraction rate by lowering the concentration of n-Pr-BTP available for americium complexation. The complexation reaction between americium and n-Pr-BTP determines the extraction rate. Initial americium fluxes can be calculated for a given aqueous nitric acid concentration by using the presented rate equation.

ACKNOWLEDGEMENTS

The authors are grateful for the financial support from the Commission of the European Communities (project EUROPART, contract FI6W-CT2003-508854).

REFERENCES

1. Status and Assessment Report on Actinide and Fission Product Partitioning and Transmutation, *OECD-NEA* (1999) (www.nea.fr/html/pt/pubdocs.htm).
2. Z. Kolarik, U. Mullich, F. Gassner (1999), *Solvent Extr. Ion Exch.,* 17 (5), 1155-1170.
3. C. Madic, M.J. Hudson, J.O. Liljezin, J.P. Glatz, R. Nannicini, A. Facchini, Z. Kolarik, R. Odoj (2000), *New Partitioning Techniques for Minor Actinides,* EUR 19149, European Commission, Luxembourg, ISBN 92-828-9696-X.
4. G.W. Stevens, H.R.C. Pratt (2000) *Solvent Extr. Ion Exch.,* 18*(6),* 1051.
5. W. Nitsch (1984), *Faraday Discuss. Chem. Soc.,* 77, 85.
6. M. Weigl, A. Geist, K. Gompper, J.I. Kim (2001), *Solvent Extr. Ion Exch.,* 19, 215-229.
7. W. Nitsch, M. Weigl (1999), *Langmuir,* 14 (23), 6709-6715. 168

SYNERGIC EXTRACTION OF LANTHANIDES AND SELECTED ACTINIDES USING 2,6-BIS-(BENZOXAZOLYL)-4-DODECYLOXYLPYRIDINE AND 2-BROMODECANOIC ACID

Sofie Andersson, Klaus Eberhardt*, Christian Ekberg, Daniel Magnusson, Mikael Nilsson, Heino Nitsche***, Gunnar Skarnemark and Ralf Sudowe*****

Nuclear Chemistry, Chalmers University of Technology, Göteborg, Sweden
***Institut für Kernchemie, Johannes Gutenberg-Universität, Mainz, Germany**
‘‘Department of Chemistry, University of California Berkeley, Berkeley, USA
‘“Lawrence Berkeley National Laboratory, Berkeley, USA

The separation of actinides and lanthanides is an important factor in the design of novel extraction systems for alternative methods to treat spent nuclear fuel (e.g. partitioning and transmutation or conditioning). In this work the extraction behaviour of several lanthanides was studied to explore differences within the lanthanide group and in comparison with actinides (Am and Bk). The synergic extraction system used was 2-bromodecanoic acid and 2,6-bis-(benzoxazolyl)-4-dodecyloxylpyridine in ferf-butyl benzene. The aqueous phase consisted of trace amounts of metal ions and 1 or 5 M perchlorate ion concentration. Results indicate a decrease in extraction along the lanthanide series and a tetrad effect. The actinides (Am and Bk) show higher distribution ratios.

INTRODUCTION

Before a future transmutation process of long-lived element in the spent nuclear fuel can be realized, the separation of *eg.* lanthanides and actinides as well as the actinides themselves must become more feasible. Solvent extraction is a good technique to facilitate this partitioning because of its high efficiency and separation ability together with the knowledge already gathered by working with highly active waste streams from the reprocessing plants operating today. In many studies europium is used as a reference lanthanide together with americium as a representative of the trivalent actinides [1-2], but here all lanthanides have been included to see their different behaviour as a function of decreasing ionic radius along the series. Experiments have also been made with Am and Bk to have two actinides for comparisons.

The synergic solvent extraction system used consists of 2,6-bis-(benzoxazolyl)-4-dodecyloxylpyridine (BODO), see Figure 1, and 2-bromodecanoic acid (HA) in ferf-butyl benzene (TBB). Soft donor ligands (containing *e.g.* N and S) have the ability to bind more efficiently to actinides than lanthanides due to their differences in electron configuration between the 5f and 4f electron shells [3], The aromatic nature of the BODO rings with delocalised electrons, together with the inductive electron withdrawing effect of the oxygens within the five membered rings lower the affinity of the nitrogens towards protons [4], [177]

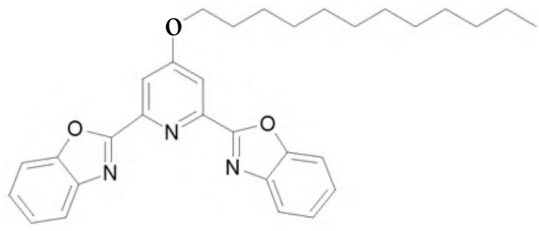


Figure 1. 2,6-bis-(benzoxazolyl)-4-dodecyloxylpyridine (BODO).

In this work the extraction behaviour of BODO and HA for the lanthanides and americium and berkelium has been studied at 1 and 5 M ionic strength (perchlorate medium) and 0.01 M hydrogen ion concentration. The same system has been used earlier to determine general extraction properties of BODO [5] and stability constants of the nitrate complex formation [6-8],

THEORY

The distribution ratio of a metal ion can be expressed as

$$D_M = \frac{[M]_{org}^{tot}}{[M]_{aq}^{tot}} \qquad (1)$$

Using equal phase volumes and radioactivity this equation is equal to the ratio of specific activities, which makes the determination of total concentrations much easier compared with other methods. The reactions that are assumed to occur can be described as

$$\overline{(HA)_2} \rightleftharpoons 2\overline{HA} \qquad (2)$$

$$\overline{(HA)} \rightleftharpoons H^+ + A^- \qquad (3)$$

$$M^{3+} + 3\,HA + 2\,\overline{BODO} \rightleftharpoons \overline{M(BODO) \sim A} + 3\,H^+ \qquad (4)$$

A mechanism parallel to that for 2,2':6',2''-terpyridine is used [9], The undissociated 2-bromodecanoic acid is known to dimerise in the organic phase [10],

EXPERIMENTAL

Materials

BODO was synthesized at the University of Reading. The diluent was TBB (Aldrich, 99 %), the BODO concentration was 0.01 M in all experiments and HA (Fluka, ~98 % purity) was used at a concentration of 1 M. In the aqueous phase sodium perchlorate (Merck, pro analysi, >99 % purity) was used to keep the ionic strength constant. The hydrogen ion concentration was 0.01 M.

For neutron activation of Dy (Dy_20_3, Fluka), Lu (Lu_20_3, Cerac), Er (Er_20_3, Light & Co, LTD Colubrook) and Nd ($Nd(N0_3)_3 \cdot 6H_20$, Fluka) aqueous solutions were irradiated in the TRIGA Mainz research reactor for one hour at a thermal neutron flux of $7x10^{15}$ m'V^1 to produce suitable amounts of tracer activities of ^{155}Dy, ^{176m}Lu, ^{171} Er and ^{149}Nd. Tracer activities of ^{140}La ($La(N0_3)_3 \cdot 6H_20$, Riedel de Haën AG), ^{142}Pr (Pr_6On, Cerac), ^{153}Sm (Sm_20_3, Kebo), ^{159}Gd (Gd_20_3, Fluka) and ^{166}Ho (Ho_20_3, Light & Co, LTD Colubrook) were produced at the TRIGA Mainz within an irradiation time of three hours applying the same neutron flux. Experiments ^{178}

with Pm were done with the same solvent extraction technique, but the radioactive nuclide (^{147}Pm from Amersham) was already available *i.e.* no irradiation of stable isotopes was needed. ^{141}Ce (Ce_2O_3, Sigma), ^{152}Eu (Eu_2O_3, ORNL), ^{160}Tb (Tb_2O_3, Fluka), ^{170}Tm (Tm_2O_3, Ventron) and ^{175}Yb (Yb_2O_3, Cerac) were produced at the Institutt for Energiteknikk in Kjeller, Norway (JEEP II reactor, 10^{17} rn'V[1] thermal neutron flux). ^{249}Bk was provided by Oak Ridge National Laboratory, USA, and is trivalent under the chosen experimental conditions [11],

Experiments and procedures

All experiments were done in duplicates or triplicates. 0.4 mL of each phase were contacted by vigorous shaking for five minutes and then allowed to settle. Samples (0.05 to 0.2 mL depending on the activity amount) were taken from both the organic and aqueous phases. All experiments were done at constant temperature (295 K). All lanthanides except Pm, Eu and Tb were measured using gamma spectrometry analysis and HPGe detectors with efficiencies between 17.7 and 29.2 % and resolutions of 1.69 - 1.8 keV (at ^{60}Co, 1332 keV), respectively. The organic and aqueous phases from the same shaking vial were always measured using the same detector. The measurement times were adjusted to minimise the influence of statistical uncertainties and at the same time take the number of samples into account, considering the half-lives of some of the nuclides. The gamma spectra (except Eu and Tb) were evaluated using Genie 2000 (Canberra) and its manual Peak Fit package. Eu and Tb were measured in a NaI(Tl) scintillation well detector connected to an Intertechnique model CG-4000 with automatic sample changing. Pm and Bk were measured using a liquid scintillation detector, LKB Wallac 1219 Rackbeta.

RESULTS AND DISCUSSION

In Figures 2 and 3 the results for 1 and 5 M ionic strength are shown, respectively. There is a clear trend in decreasing distribution ratios with increasing atomic number of the lanthanides. As expected, a significant difference between the actinides and the lanthanides due to their 4f and 5f electron interactions with the nitrogen donor groups of the 2,6-bis-(benzoxazolyl)-4-dodecyloxylpyridine is also shown.

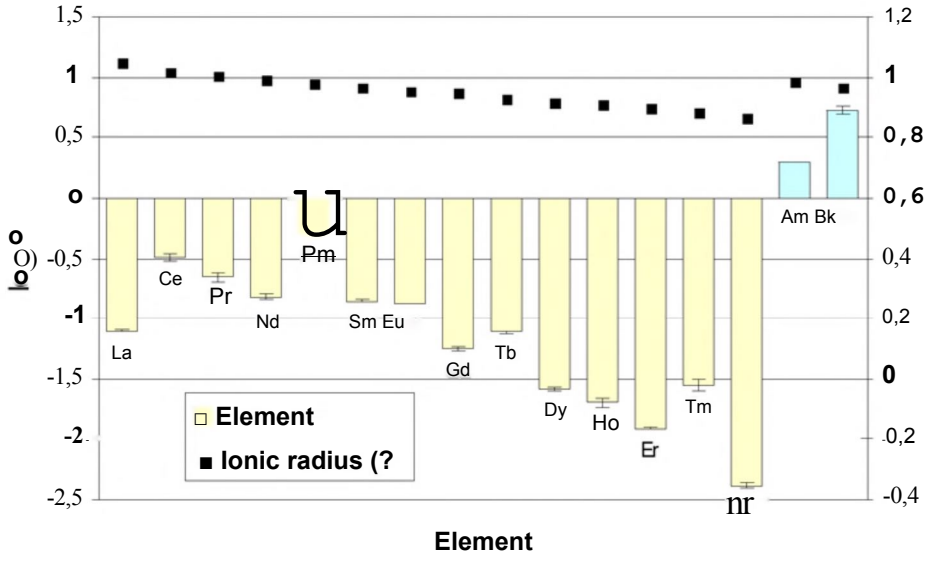


Figure 2. Distribution ratios for the lanthanides, americium and berkelium at 1 M ionic strength (perchlorate ions, 0.01 M hf, 295 K). Left axis: log D, right axis: ionic radius (coordination number 6). Uncertainties are included in the figure and are based on the standard deviation of the duplicate/thplicate samples.

The tetrad effect (or the double-double effect) has previously been described in the literature [12-18], It states that it is possible to group the lanthanide elements into four tetrads when plotting the logarithm of a certain parameter versus Z through the use of four smooth curves. The effect is explained by the stabilisation energy related to inter-electron repulsion energy for the 4f electrons. The gadolinium point is common to the second and third tetrad and can be explained by the extra stability in the $4f^7$ electron configuration. The two other break-points are located at 4^-4^ and $4f^{10}$-$4f^{11}$. Even though different methods are used to estimate the interesting parameter, the same patterns generally show up. Recently an alternative model was described where not only a maximisation of the stabilisation energy was taken into account but also a minimisation in the inter-electronic repulsion, related to the steric symmetry of the major axes of the electron clouds [19], Here the tetrad effect is more pronounced at higher ionic strength and is indicated in Figure 3 by lines.

The decrease in extraction along the series may also be explained with lanthanide contraction in ionic radius. The ionic radii for coordination number 6 **are shown in the figures. When the charge-to-radius ratio increases it will increase the reaction with the negatively charged 2-bromodecanoic acid anion, but at the same time decrease the BODO-metal interaction since the degree of covalency in the bonding decreases. This shows that the BODO-metal interaction is decisive for the distribution ratio.**

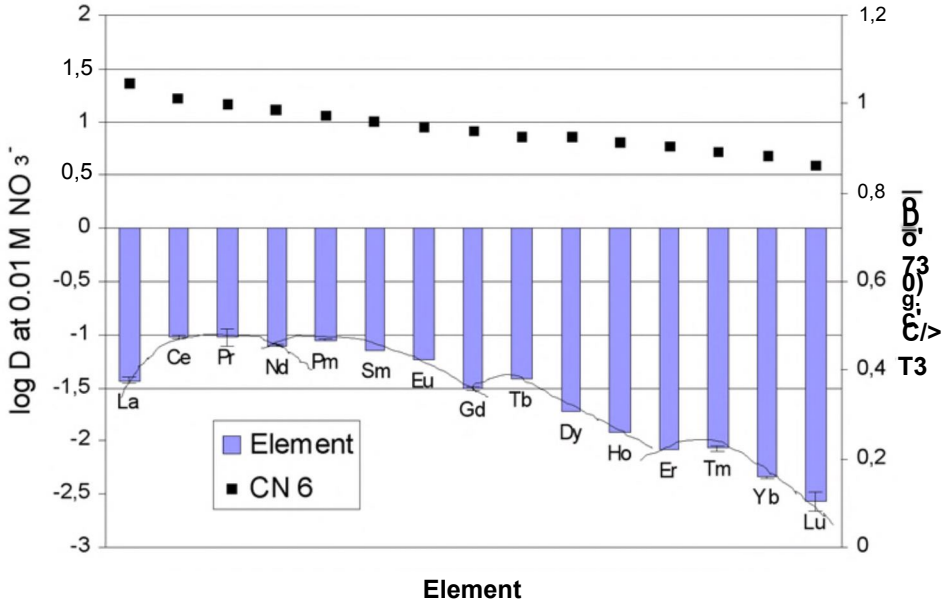


Figure 3. Distribution ratios for the lanthanides at 5 M ionic strength (4.99 M perchlorate 0.01 M nitrate, 0.01 M hF, 295 K) Left axis: log D, right axis: ionic radius (coordination number 6). Uncertainties are included in the figure and are based on the standard deviation of the duplicate/triplicate samples.

CONCLUSIONS

The distribution ratio for all lanthanides and the actinides americium and berkelium has been studied in the system 2,6-bis-(benzoxazolyl)-4-dodecyloxylpyridin and 2-bromodecanoic acid in ferf-butyl benzene at 1 and 5 M perchlorate ion concentration. There is a clear trend in decreasing distribution ratio along the series, which may be explained by increasing charge-

to-radius ratio and a decreasing covalency in the metal-synergist (BODO) interaction. The tetrad effect is especially clear at the higher ionic strength and show four groups with Nd, Gd and Er as the three dividing elements.

ACKNOWLEDGEMENTS

The authors are indebted for the use of Bk to the Office of Basic Energy Sciences, U.S. Department of Energy, through the transplutonium element production facilities at the Oak Ridge National Laboratory. We also would like to thank our colleagues at the University of Reading, U.K., for synthesising BODO. The Mainz TRIGA reactor crew are acknowledged for help with producing radioactive isotopes of the short-lived lanthanides. The European Union (PARTNEW project FIKW-CT2000-00087) and the Swedish Nuclear Fuel and Waste Management Co., SKB, are acknowledged for financial support. We are also indebted to the Royal Society of Arts and Sciences in Göteborg and the foundation Bengt Lundqvist Minne for financial support on Bk chemistry.

REFERENCES

1. **P. Y. Cordier, C. Hill, P. Baron, C. Madic, M. J. Hudson and J. O. Liljenzin,** *Journal of Alloys and Compounds* **(1998), 271-273, 738-741.**
2. **I. Hagström, L. Spjuth, A. Enarsson, J.O. Liljenzin, M. Skalberg, M. J. Hudson, P. B. Iveson, C. Madic, P. Y. Cordier, C. Hill and N. Francois (1999),** *Solvent Extraction and Ion Exchange***, 17(2), 221-242.**
3. **G. T. Seaborg and W. D. Loveland (1990), The elements beyond uranium, J. Wiley & Sons, New York.**
4. **T. L. Gilchrist (1992), Heterocyclic chemistry, Longman Scientific & Technical, Chapter** 8.
5. **S. Andersson, C. Ekberg, M. R. S. Foreman, M. J. Hudson, J-O. Liljenzin, M. Nilsson, G. Skarnemark, and K. Spahiu (2003),** *Solvent Extraction and Ion Exchange***, 21(5), 621-636.**
6. **S. Andersson, C. Ekberg, J.-O. Liljenzin, M. Nilsson and G. Skarnemark (2004), accepted for publication in** *Radiochimica Acta.*
7. **S. Andersson, K. Eberhardt, C. Ekberg, J-O. Liljenzin, M. Nilsson and G. Skarnemark (2004), submitted to** *Radiochimica Acta.*
8. **S. Andersson et. al. (2004), work in preparation.**
9. **L. Spjuth (1999), Solvent Extraction Studies with Substituted Malonamides and Oligopyridines, PhD Thesis, Chalmers University of Technology, Sweden.**
10. **T. Sekine, M. Isayama, S. Yamaguchi and H. Moriya (1967),** *Bulletin of the chemical society of Japan,* **40, 27-32.**
11. **A.J. Bard. R. Parson and J. Jordan (1985V Standard ootentials in aaueous solution, International Union of Pure and Applied Chemistry, New York, pp. 667-669.**
12. **I. Fidelis and S. Siekierski (1971),** *J. inorg. nucl. Chem.***, 33, 3191-3194.**
13. **D. F. Peppard, G. W. Mason and S. Lewey (1969),** *J. inorg. nucl. Chem.,* **31, 2271-2272.**
14. **D. F. Peppard, C. A. A. Bloomquist, E. P. Horwitz, S. Lewey and G. W. Mason (1970), J.** *inorg. nucl. Chem.,* **32, 339-343.**
15. **L. J. Nugent (1970),** *J. inorg. nucl. Chem.,* **32, 3485-3491.**
16. **C. K. Jorgensen (1970), J.** *inorg. nucl. Chem.,* **32, 3127-3128.**
17. **S. N. Limaye and M. C. Saxena (1990),** *J. Indian Chem. Soc.,* **67,** 66-68**.**
18. **S. N. Limaye, and A. A. Kopyrin (1991),** *J. Inst. Chemists (India),* **63, 215-216.**
19. **M. Minami and A. Masuda (1998),** *Journal of Magnetism and Magnetic Materials,* **177-181, 1021-1022.**

EXTRACTION CHEMISTRY OF SYNERGISTIC MIXTURES BASED ON CHLORINATED COBALT DICARBOLLYDE

V. A. Babain, I. V. Smirnov, V.N.Romanovskiy, M.Yu.Alyapishev, T.Todd*, R.S.Herbst*

Khlopin Radium Institute, St.-Petersburg, Russia, e-mail: babain@atom.nw.ru
*** Idaho National Engineering and Environmental Laboratory, Idaho Falls, USA**

In the oroDosed work the DroDerties of extraction svstems based on nitroaen-containina compounds for recovery of minor actinides, americium in particular, are considered. A new class of synergistic additions to CCD - diamides-2.6-pyridindicarboxylic (dipicolinic) acid is described. Synthesis of these compounds is simple and inexpensive. The extraction properties of the mixtures of CCD - diamides of dipicolinic acids are similar to those of the mixtures of CCD with carbamoylphosphinoxides. A new variant of UNEX-solvent wherein diamides are used as the synergistic addition instead of CMPO providing the extraction of actinides is put forward. The extraction of nuclides from simulated radioactive waste solutions is conducted.

INTRODUCTION

Radionuclides should be incorporated into strong matrices of glass type to afford their safe storage. Reduction of high-level waste volume should considerably lower the storage cost. For reducing the volume of resultant HLW the radwaste partitioning, i.e. radionuclide recovery, is required. The most practically acceptable method for reprocessing of liquid radioactive waste is liquid extraction. Many extraction systems are proposed for waste reprocessing. Extraction mixtures on the basis of chlorinated cobalt dicarbollyde (CCD) offer the greatest promise for radwaste reprocessing.

It is known that extraction properties of these systems strongly depend on properties of acomplementary co-extractant - so called "synergistic addition" to CCD. Polyethylene glycols are the first of the investigated additions. Addition of polyethylene glycols or crown ethers affords extraction of both cesium and alkali-earth-elements /review see 1**/.**

Mixture of CCD - polyethylene glycol has found practical application and is used for several years on industrial scale at Mayak PA (Ozersk, Russia). Bidentate organophosphorus compounds (carbamoylphosphonates, carbamoylphosphine oxides, phosphorylated polyethylene glycols, diphosphine dioxides), crown ethers, calixarenes, nitrogen-containing bidentate compounds were investigated as synergistic additions. The presence of bidentate organophosphorus compounds ensures extraction of trivalent actinide elements and REE *12,21.* **Although the conditions for Am/Eu separation were not established in this work, but the considered mixture of carbamoylphosphinoxide (CMPO) - dicarbollyde makes it possible to attain very high values of D(M^{3+}). It has been revealed that the synergistic effect of dicarbollyde towards Eu^{3+} shows up in weakly acidic medium.**

The mixtures of nitrogen-containing extractants with voluminous anions - CCD mixtures with

diamides of malonic acid and with phenanthroline, dibutylphosphoric acid (DBPA) with phenanthroline are investigated/4/. It is found that in extraction from 0.1M $HN0_3$ solution by mixture 0.05M $Na^+BCl'_6$ + 0.25M o-phenanthroline in nitrobenzene the high distribution coefficient D_{Am} (D_{Am} = 10.8) is attained with high separation from Eu^{3+} (D_{Eu} = 0.316, D_{Am}/ D_{Eu} = 34.1). The metals are extracted in the pH of equilibrium phase no less than 2. At higher concentrations of nitric acid in equilibrium aqueous phase no extraction takes place. Am and Eu cannot be separated by extraction with mixture of DBPA and o-phenanthroline.

A mixture is proposed for simultaneous extraction of cesium, strontium, and actinides from acidic solutions (UNEX-process) *151.* **Solution of 0.08 M CCD + 0.007-0.02 M PEG-400 + 0.02M diphenyl-N,N-dibutylcarbamoylphosphinoxide (CMPO) in phenyltrifluoromethylsulfone provides extraction of above elements from acidic solutions.**

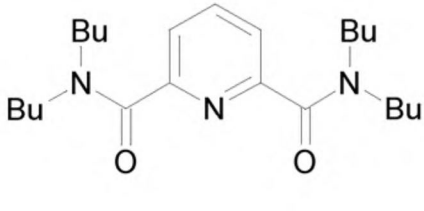
The prospects for using malonamides and picolinamides are considered as applied to americium and REE extraction from $HN0_3$ solutions/6/. Picolinamides are capable of extracting minor actinides from weakly acidic solutions.

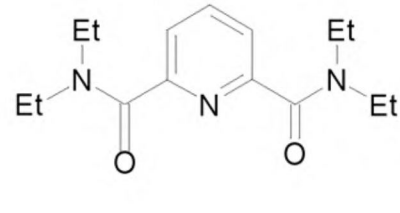
The extraction ability of mixtures of picolinic acid amides and anionic surfactant towards actinides is investigated *111.* **Sodium bis(2-ethylhexyl)sulphosuccinate is used as an anionic surfactant. It is shown that the introduction of voluminous anion into the system considerably increases its extraction ability and enables to extract trivalent metals from more acidic media. The best extraction properties are manifested by amides of picolinic acid containing a branched alkyl substituent in pyridine ring and amides substituted at amide nitrogen. However, even the mixture of picolinamide - anionic surfactant does not extract trivalent metals from $HN0_3$ solutions at its concentration above 0.2M. Most likely this fact may be explained by protonation of picolinamides in acidic medium. Picolinamide salt does not extract metal ions.**

The significant synergistic effect is detected in extraction of trivalent metals by mixtures of dipicolinic acid diamides with CCD/8/. Diamides of dipicolic acid are less basic compounds to compare with picolinamides, because the introduction of the second carbamide group into molecule further decreases nitrogen basicity in pyridine ring. Therefore, diamides of dipicolinic acid in pure form do not practically extract metals *151.*

EXPERIMENTAL

Materials and reagents





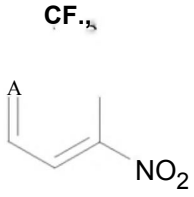
Figurel Tetrabutyldiamide of dipicolinic acid (TBDPA)

Figure 2. Tetraethyldiamide of dipicolinic acid (TEDPA)

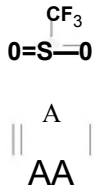
Tetraethyldiamide of dipicolinic acid (TEDPA, Mp = 82°C, yield 74%), was re-crystallized from hexane-benzene mixture. Tetrabutyldiamide of dipicolinic acid (TBDPA, 60%) - oil was purified by column chromatography on silica gel. Purity and structure of compounds were confirmed by NMR (^1H and ^{13}C) and mass-spectra.

Metha-nitrobenzotrifluoride (F-3), phenyltrifluoromethylsulfone (FS-13) and bis- tetrafluoro-

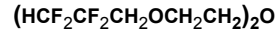
propyl ether of diethylene glycol (F-8) were used as diluents.



F-3



FS-13



F-8

CCD was produced by Kathem Co (Czechia). Other reagents of analytical grade were received from "Vekton" Co (St.Petersburg, Russia). Cs^{137}, Sr^{85}, Eu^{152} and Am^{241} isotopes of "Isotop" Co (St.Petersburg, Russia) were used.

RESULTS AND DISCUSSIONS

It was shown *191,* that diluent has the same influence on extraction properties of diamide-CCD-PEG extraction system. The results for metal extraction by 0.1M CCD + 0.05M TBDPA + 0.025M Slovafol-909 from 3M $HN0_3$ in different diluents are presented in Fig 3. TEDPA

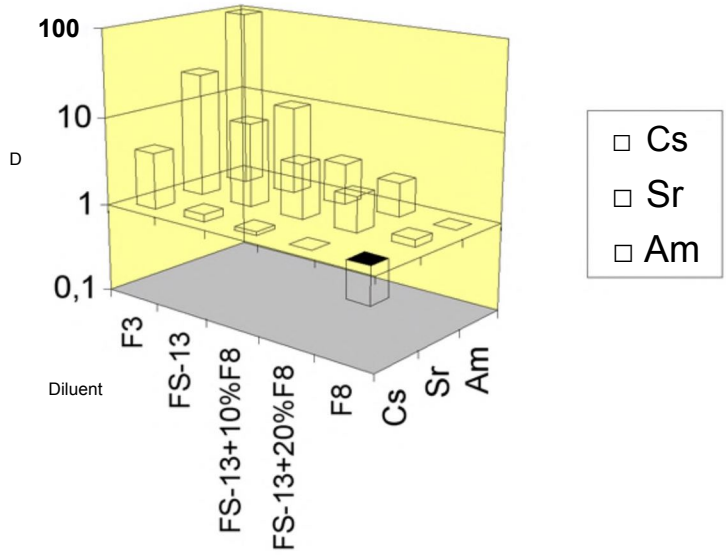


Figure 3. Extraction of metals by 0.1M CCD + 0.05M TBDPA + 0.025M Slovafol-909 in F-3 depending on diluents

It's seen from Fig 3, that it's possible to use F-3, FS-13 and mixtures of FS-13 and F-8 as diluents for simultaneous extraction of Cs, Sr and Am from acidic solutions.

Extractant capacity is of prime importance in extraction of minor actinides from solutions containing the high concentrations of REE. In order to determine the saturation limit of extraction mixture, some experiments on organic phase saturation by successive extraction were carried out. Composition of solution simulating Purex-process raffinate is given in Table 1. Eu or Am traces were added into solution. Experimental scheme is shown on Fig. 4; results obtained are presented in Table 2.

Table 1. Composition of simulated solution

Element	Content, mg/L	Element	Content, mg/L
Al	100	**Mn**	**150**
Ba	120	**Mo**	**970**
Ca	100	**Na**	**500**
Ce	2100	**Nd**	2100
Co	210	**Ni**	100
Cr	**140**	**Sr**	**230**
Cs	**350**	**Zr**	**820**
Fe	**480**	HNO_3	**2.9 M**

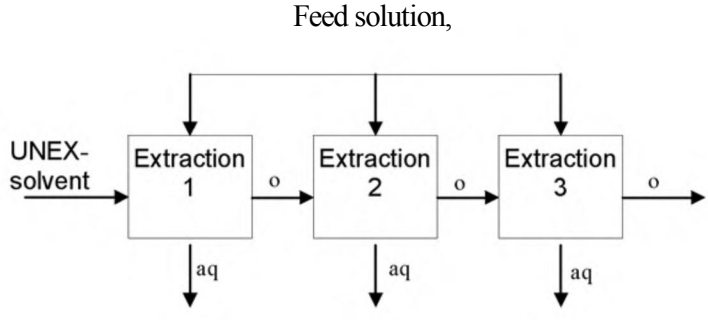


Figure 4. Flowsheet of experiment

Table 2. Extraction of metals from simulated solution with successive saturation of extractant

	D_{Cs-137}	D_{Sr-85}	D_{EU-152}
Extractant - 0.1 M CCD + 0.05 M TEDPA + 0.025 M Slovafol-909 in F-3			
1st **contact**	2.8	8.1	**50**
2nd **contact**	**2.4**	**7.5**	**3.8**
3d contact	**2.3**	6.6	0.01
Extractant - 0.08 M CCD + 0.06 M TEDPA + 0.01 M Slovafol-909 in F-3			
1st **contact**	**0.63**	1.8	**42**
2nd **contact**	**0.34**	**0.9**	**0.9**
3d contact	**0.17**	**0.36**	**<**0.01
Extractant - 0.08 M CCD +0.02 M TEDPA + 0.01 M Slovafol-909 in F-3			
1st **contact**	**7**	**9.2**	**1.4**
2nd **contact**	**7.6**	**3.8**	**<**0.01
3d contact	**7.5**	2.2	0.01
Extractant - 0.08 M CCD +0.02 M TEDPA + 0.01 M Slovafol-909 in FS-13			
1st **contact**	**2.4**	**3.5**	2
2nd **contact**	**2.7**	2.8	**<**0.01
3d contact	**2.7**	1.8	0.01

It is evident from Table 2 that the high concentration of diamide - no less than 0.05 M/L - is needed to provide the complete extraction of trivalent elements. However, even at such concentration the organic phase is almost fully saturated by REE after the third contact. Hence, it is necessary to bind Zr and Mo hindering the extraction process. To suppress the extraction process, 15%vol. of the solution containing 0.33 M oxalic acid and 0.67M D-mannitol was added. In the prepared solution the final concentration was 0.09 M D-mannitol

and 0.04 M oxalic acid.

Scheme of test with the prepared initial solution is shown in Fig. 5; the results obtained are presented in Table 3. Solvent composition 0.08 M CCD + 0.05 M TBDPA + 0.013 M (0.8% vol.) Slovafol-909 in F-3.

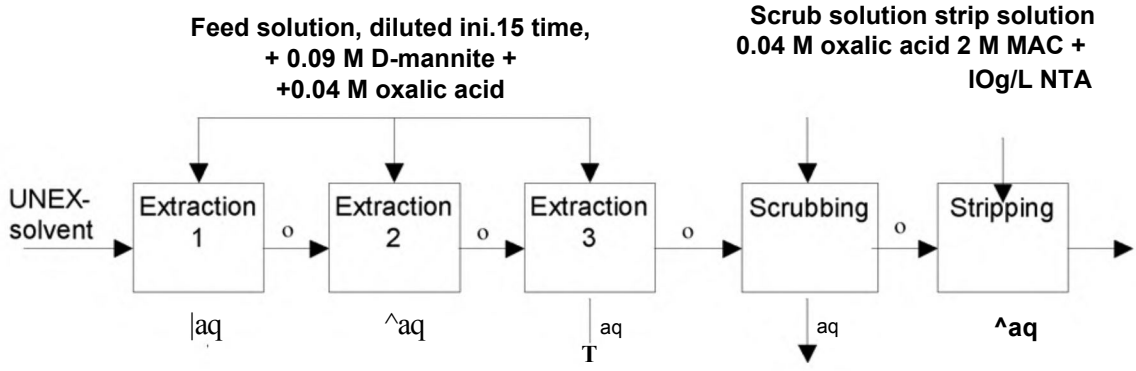


Figure 5 Scheme of test

Table 3. Distribution coefficients of radionuclides in static tests

Stage	Dcs-137	Usr-85	UAm-241
Extraction 1	**4.3**	**5.4**	**>** 100
Extraction 3	**4.0**	2.0	**14**
Stripping	**0.32**	**<**0.01	**<**0.01

It is evident that the recovery of Am, Cs and Sr from modified aqueous solution remains rather high even after three successive contacts with fresh aqueous solution. Sr, Am and REE are very efficiently stripped by both methylaminecarbonate (2.5 M MAC + lOg/L nitrilotriacetic acid) or guanidinecarbonate soluiton (180g/L guanidinecarbonate + 20g/L DTPA). Cesium is extracted to a lesser degree, but quite sufficiently for complete extraction.

CONCLUSIONS

The presented data indicate that diamides of dipicolinic acid are of considerable interest as synergistic additions to chlorinated cobalt dicarbollyde. The mixture of CCD - diamides of dipicolinic acid efficiently extracts trivalent metals from $HN0_3$ solution. Diamides are more easily to synthesize and they are much cheaper than carbamoylphosphinoxides; at the same time the extraction properties of the systems CCD - diamides of dipicolinic acid and CCD - carbamoylphosphinoxides are practically the same. Modified extraction mixture - CCD - tetraburyldiamide of dipicolinic acid - Slofavol was tested on simulated HLW solutions with high content of REE. The mixture provides recovery of Cs, Sr and minor actinides.

ACKNOWLEDGEMENTS

This work was carried out under financial support of the United States Department of Energy Environmental Management Science Program (EMSP Project 81995) and Rosatom.

REFERENCES

1. **E Makrlik,. P. Vanura, (1985),** *Talanta,* **32, 423.**
2. **J. Rais, S. Tachimori (1994)*// Extraction of Europium and Americium by a mixture of CMPO and dicarboilide** *// J. Radioanal. Nucl. Chem.,* **Letters 188 (2) 157 - 162.**
3. **J. Rais, S. Tachimori, P. Selucky, L. Kadlecova (1994)** *// Sep.Sci.&Technol.,* **29 (2), 261 - 274.**
4. **J. Rais, S. Tachimori (1994)** *// Sep.Sci.&Technol.,* **29 (10), 1347 - 1365.**
5. **V.N. Romanovskiy, I.V. Smirnov, V.A.Babain, T.A. Todd, R. S. Herbst, J.D. Law, K.N. Brewer (2001)*// Solv.Extr.Ion Exch.,* 19, 1-21.**
6. **M.J.Hudson, , L.Nigond, , P.Y Condamines,., J.Cordier, , C.Livet, , C.Madic, , C. Cuillerdier, and C.Musikas, (1995)*// Sep. Sci.& Technol.,* 30, 2075-2099.**
7. **P.Y.Cordier, H.Naganawa, S.Tachimori*//** *Proceedings of International conference Atalante-2000,* **http://www.cea.fr/conferences/Atalante2000/P3-28.pdf.**
8. **M.Yu. Alyapyshev, V.A. Babain, I.V. Smirnov (2004)** *// Radiochemistry (Radiochimiya),* **46, 270-271.**
9. **M.Yu. Alyapyshev, V.A. Babain, I.V. Smirnov T.A. Todd, R. S. Herbst, J.D. Law, (2004)*//** *Proceedings of XIII Russian extraction conference,* **Moscow, 19-24 September 2004,** v.1, **p.228-229.**

SYNERGISTIC EXTRACTION OF METAL IONS WITH NOVEL BIDENTATE NEUTRAL LIGANDS

Shigeo Umetani, Matsumoto Hirofumi and Kensuke Kurahashi

Institute for Chemical Research, Kyoto University, Uji, Kyoto 611-0011, Japan

Some novel neutral bidentate ligands such as 2-pyridyldiphenylphosphine oxide (1), 2-pyridylmethyldiphenylphosphine oxide (2) and bis(diphenylphosphinyl)ethene (3) have been synthesized. The former two ligands have pyridyl and phosphine oxide moieties which are neutral and possibly form an adduct with metal chelates. The last one has two phosphine oxide moieties and is also expected to work as an bidentate neutral ligand. The synergistic extraction of alkaline earth metal ions and lanthanide metal ions has been examined with these novel bidentate neutral ligands using 1-phenyl-3-methyl-4-benzoyl-5-pyrazolone (4) or 1-phenyl-3-methyl-4-trifluoroacetyl-5-pyrazolone (5) as an extractant. 1 and 2 were found to work as an bidentate neutral ligand in the synergistic extraction of alkaline earth metal ions and lanthanide metal ions and the extractions were surely enhanced. They are more powerful than the monodentate neutral ligand such as TOPO (tri-n-octyl phosphine oxide, 6), and less powerful than BDPPM (bis(diphenylphosphinyl)methane, 7) which has two phosphine oxide moieties. The synergistic effect with 3 was similar to that with BDPPM which is structurally analogous to 3. The separability of the metal ions was found to depend on the structure of the neutral ligand.

INTRODUCTION

It has been well-known that the addition of a Lewis base to the solvent extraction system with an acidic extractant not only enhances the extraction of metal ions but also makes it possible to extract metal ions such as alkali and alkaline earth metals which are usually unextractable owing to the low stability of the chelate and the remaining water molecules in the chelate [1], Many investigations have been made on the monodentate neutral ligands such as TOPO, tributyl phosphate and pyridine as well as on the bidentate ligands such as 1,10-phenanthroline [2, 3],

In our previous papers for the extraction of metal ions such as lanthanide metal ions [4] and group 13 metal ions [5] with modified (3-diketones, it was shown that the geometry of the donating two oxygens gave a significant effect to the extraction separability. The contribution of this geometry effect prompted us to consider that the similar modification to the bidentate neutral ligands would result in an interesting synergistic extraction of metal ions.

In the present paper, some novel bidentate neutral ligands have been prepared. The synergistic extraction of lanthanide and alkaline earth metal ions were examined and the results are discussed referring to those with mono and bidentate phosphine oxide ligands [6, 7].

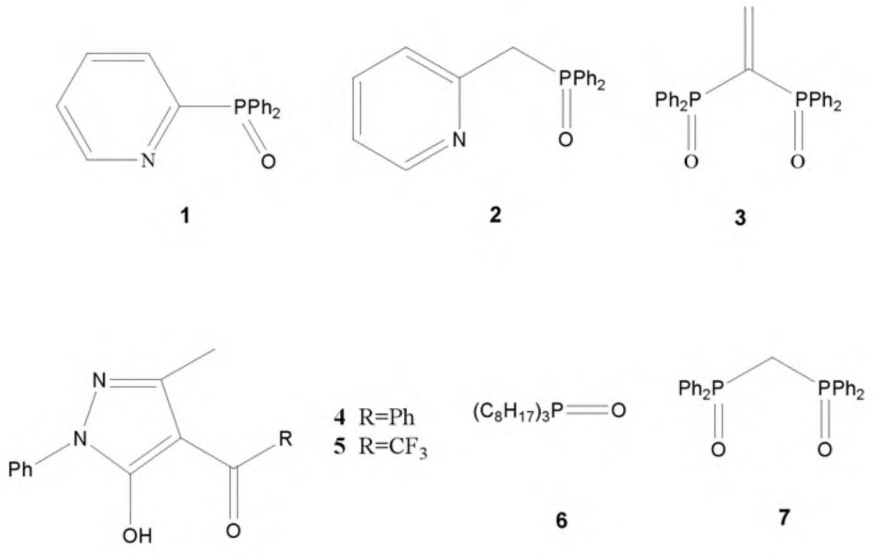
RESULTS AND DISCUSSION

Synthesis of the Bidentate Neutral Ligands

2-Pyridyldiphenylphosphine Oxide (1) was synthesized according to the literature [8], The crude compound was recrystallized from cyclohexane and dried in vacuo at 70 °C (51 % yield), m.p. 109.5 ~ 110.0 °C. ^-NMR (300 MHz, CDCL) : 5 7.34-7.53 (3,4,5-Ph-5, 5-Pyr-H, 7H), 7.79-7.89 (2,6-Ph-H, 4-Pyr-H, 5H), 8.28(3-pyr-H, t, 1H), 8.75(6-pyr-H, d, 1H). (Found: C, 72.82; H, 4.79; N, 4.84. Calcd. for $C_{17}H_{14}NOP$: C, 73.11; H, 5.05; N, 5.02 %).

2-Pyridylmethyldiphenylphosphine Oxide (2) was synthesized according to the literature [9], The crude compound was recrystallized from methanol and dried in vacuo at 80 °C (19 % yield), m.p. 130.0 ~ 132.8 °C. ^-NMR (300 MHz, CDCL) : 5 7. 3.91 (methylene-H, d, 2H), 7.04-8.36 (Py-H and Ph-H, m, 14H). (Found: C, 73.65; H, 5.67; N, 4.76. Calcd. for $C_{18}H6_4NOP$: C, 73.71; H, 5.50; N, 4.78 %).

Ethylene-1,1'-bis(diphenylphosphine oxide) (3) was synthesized oxidizing ethylene-1,1'-bis(diphenylphosphine) by hydrogen peroxide. Ethylene-1,T-bis(diphenylphosphine) is commercially available. (54 % yield), m.p. 196.8 ~ 1991.9 °C. ^{1}H-NMR (300 MHz, CDCl$_3$) : 57.620 - 7.694, 7.371 - 7.424, 7.221 - 7.324 (Ph-H, m, 20H), 6.85(ethylene-H, q, 2H). (Found: C, 72.75; H, 5.21. Calcd. for $C_{26}H_220_2P_2$: C, 72.89; H, 5.18 %).



Scheme 1. Neutral ligands and acylpyrazolones

Apparatus

Metal ion concentrations were measured with a Japan Jarrell Ash Model ICAP-500 inductively coupled argon plasma atomic emission spectrophotometer. pH measurements were made with a Hitachi-Horiba F-8L pH meter equipped with a glass electrode. ^-NMR spectra were measured with a Varian VXR-200 spectrometer (200 MHz) at 25 °C in CDCl3.

The extractions were performed in 30 cm^3 centrifuge tubes with the aid of Taitek Bio-shaker type BR-30L thermostated at 25 °C. Semi-empirical calculation was performed on fully optimized molecular geometries on a Cray T94/4128 using MNDQ94 (Cray Research, Inc.).

Extraction Procedures

A 10-cm^3 aliquot of an aqueous phase containing metal ion, 0.1 mol dm^{-3} sodium perchlorate and 0.01 mol dm^{-3} sodium acetate or MES as buffering component was adjusted to the desired pH with hydrochloric acid or sodium hydroxide solution. The aqueous phase was shaken with an equal volume of chloroform or benzene containing the required amount of ligand at 25 °C for one hour. The shaking time of 1 h was found to be long enough to reach equilibrium. After centrifugation, the pH of the aqueous phase was measured and taken as the equilibrium value.

The metal concentration in the aqueous phase was determined by inductively coupled plasma atomic emission spectrometry. That in the organic phase was measured in the same way after back-extraction by stripping with hydrochloric acid solution. The sum of the metal concentrations in the two phases agrees well with the initial concentration.

Data Processing

In the solvent extraction of metal ion (M^{n+}) with acylpyrazolone (HA), the extraction equilibrium and the extraction constant, K_{ex}, can be expressed as follows.

$$M^{n+} + nHA_0 = MA_n + nH^+ \quad (1)$$

$$K_{ex} = [MA_n]_o [H^+]^n / [M^{n+}][HA]^n_0 = D [H^+]^n / [HA]^n_0 \quad (2)$$

Where subscript o denotes the species in the organic phase and *D* is the distribution ratio of metal ions.

In the synergistic extraction of metal ions with the mixture of acylpyrazolone and the neutral ligand (L), **the extraction equilibrium and the extraction constant, K_{exs}, can be expressed as follows.**

$$M^{n+} + nHA_0 + sL_0 = MA_nL_{S0} + 2H^+ \quad (3)$$

$$K_{ex,s} = [MA_nL_s]_0 [H^+]^n / [M^{n+}][HA]^2_0 [L]^s_0 = D [H^+]^n / [HA]^2_0 [L]^s_0 \quad (4)$$

The adduct formation equilibrium in the organic phase and its stability constant, /3, are written as follows.

$$MA_n,0 + SL_0 \; MAnLg \; o \quad (5)$$

$$/3 = [MA_nL_s]_o / [MA_n]_0 [L]^s_0 \quad (6)$$

Dividing eqn. (4) by eqn. (2) gives eqn. (7).

$$P \sim K_{ex} s / K_{ex} \quad (7)$$

Synergistic Extraction of Lanthanide Metal Ions

The synergistic extraction of lanthanide metal ions (Ln^{3+}) with 1x10^{-2} mol dm^{-3} of 5 in the presence or absence of lxlO^{-3} mol dm^{-3} of 3 in chloroform had been examined. The extraction reactions were traced via the slope analyses. The logarithmic value of the distribution ratio of metal ions, log *D* (*D* = $[Ln^{3+}]_0$ / $[Ln^{3+}]$), is plotted against the pH of the aqueous phase. The plots are found to fall on straight lines. The slopes of the lines are close to three. In order to clarify the composition of the extracted species, the effect of $[HA]_0$ on log *D* was also examined. The slopes of the straight lines were found to be close to three,

indicating that the extracted species is LnA_3 and no self-adducts are observed. The log K_{ex} values are obtained by substituting the $pH_{1/2}$ values, the pH read from log *D vs.* pH plots at which half of the metal ion is extracted (log *D* = 0), in eqn. (2). Since the concentration of the lanthanide ion is much smaller than that of the extractant, the concentration of the extractant in the organic phase ($[HA]_0$ in equation (2)) can be considered equal to the initial concentration. The number of the neutral ligand in the chelate, s in eqn. (3) was determined analyzing the the plots of log D vs. $[L]_0$ at the constant pH and $[HA]_0$. The log K_{ex} values are obtained by substituting the pHi/2 values in eqn. (4). The results are shown in Table 1 together with those with 6, 7 and CMPO (n-octylphenyl-(N,N-diisobutylcarbamoyl-methyl)phosphine oxide, 8) [7], The number of the neutral ligand in the adduct (s) was found to be two for the monodentate neutral ligand (6) and one for the bidentate neutral ligand (3, 7 and 8) indicating that 3, 7 and 8 work as a bidentate ligand.

The log $K_{ex's}$ values for 7 having two P=0 groups are much larger than those for 8 having one P=0 and one C=0 groups. P=0 is known to be much stronger donating power than C=0. Although 3 has two P=0 groups, the log K_{exs} values for 3 are between those for 6 and 7. The electron densities (Mulliken charge) of the oxygen atoms obtained by PM3 semi-empirical molecular orbital calculation are -0.310 and -0.392 for 3, and -0.301 and -0.349 for 7, This results show that 3 is rather more powerful than 7. 3 is sterically restricted by the ethylene group. It could be considered that the coordination of 3 to the lanthanide acylpyrazolonate would be also restricted resulting in a smaller extraction constant as compared with 7.

It is interesting that the extractions with 3 or 7 do not follow the order of the atomic number but show a maximum at Eu. The adduct formation constants, /3, are calculated on the basis of eqns. (6) and (7). The adduct formation constants decease monotonically with atomic number, so that the extraction constants have a maximum at Eu.

Table 1. Extraction constants for lanthanide metal ions

L		La^{3+}	Pr^{3+}	Eu^{3+}	Her	Yb^{3+}
None	log K_{ex}	-6.18	-4.98	-3.78	-3.36	-3.15
3	log $K_{ex,s}$	2.34	3.54	4.38	4.23	4.02
	log/3	8.52	8.52	8.16	7.59	7.17
	s	1	1	1	1	1
6	log Kexs	4.20	5.19	6.06	6.08	6.36
	s	2	2	2	2	2
7[a]	log Kex s	3.81	4.89	5.64	5.52	5.34
	s	1	1	1	1	1
8	log K_{exs}	1.47	2.61	3.45	3.54	3.42
	s	1	1	1	1	1

$[5]_0$ = 1x10[2] mol dm[-3], $[L]_0$ = 1x10[3] mol dm[-3] in chloroform. $[NaClO_4]$ = 0.1 mol dm[-5], $[Ln^{3+}]$ = 2x10[-5] mol dm[-3].

[a] $[5]_0$ = 1x1 O[-3] mol dm[-3], $[L]_0$ = lxlO[-3] mol dm[-3]. $[NaClO_4]$ = 0, $[Ln^{3+}]$ = 2xl0[-5] mol dm[-3].

Synergistic Extraction of Alkaline Earth Metal Ions

The synergistic extraction of alkaline earth metal ions with 5x1 O[-2] mol dm[-3] of 4 in the presence or absence of 1x10[2] mol dm[-3] of 1, 2 or 3 in benzene had been examined. The log K_{exs} and log K_{exs} values are obtained in the similar manners mentioned in the lanthanide

extraction section. The results are shown in Table 2 together with those with 6 and 7 [6], The number of the neutral ligand for 2 in the Mg and Ca adduct could not obtained, thus only pH-i/2 values were given.

As shown in the table, s depends on the ionic radii of the central metal ions. Three molecules of the monodentate ligand (6) are allowed to attach to Ba chelate, whereas two to Mg, Ca and Sr chelates. One molecule of the bidentate ligand (3 and 7) is allowed to attach to Mg chelate, whereas two to Ca, Sr and Ba chelates. The extraction enhancement by 2 is weaker than 1, although two molecules of 1 attach to Mg chelate. In this case, 1 might work as a monodentate ligand leaving weak pyridyl moiety not coordinating to the Mg chelate.

The bidentate ligand (7) having two P=0 donating groups is most powerful analogous to the case of lanthanide metal ions. 3 was found to be weaker than 7, although 3 is expected to be more powerful than 7 speculated from the MO calculations as mentioned previously. Steric restriction would decrease the coordination ability of 3.

Table 2. Extraction constants for alkaline earth metal ions

L		Mg^{2+}	Ca^{2+}	Sr^{2*}	Ba^{2*}
none	log K_{ex}	-9.02	-10.26	-12.30	—
1	pHi/2	4.78	5.00	6.19	7.03
	1OQ K_{QX_s}	-2.95	-3.40	-5.78	-7.45
	s	2	2	2	2
2	pH-1/2	4.47	5.12	5.78	6.49
	109 ^ex,s	—	—	-4.96	-6.38
	s	—	—	2	2
3	pH-1/2	4.25	4.61	5.50	6.18
	log $K_e x$ s	-3.90	-2.62	-4.40	-5.76
	s	1	2	2	2
6	log $K_e x$ s	-1.44	-2.27	-5.02	-4.56
	s	2	2	2	2
7	log Kex s	-3.08	-1.92	-3.26	-4.11
	s	1	2	2	2

$[4]_0$ = 5x10 $^{-2}$ mol dm^{-3}, $[L]_0$ = 1x1 O^{-2} mol dm^{-3} in benzene.
$[NaClO_4]$ = 0.1 M, $[M^{2+}]$ = 1 × 10^{-5} M.

ACKNOWLEDGEMENTS

The authors are thankful to Prof. Shoko Yamazaki for helpful discussion and assistace with the synthesis of the neutral bidentate ligands.

REFERENCES

1. T. Sekine and Y. Hasegawa, *Solvent Extraction Chemistry,* Marcel Dekker, New York (1977).
2. S. Umetani, K. Sasayama and M, Matsui, "Solvent Extraction of Alkaline Earth Metals and Lithium with 1-Aryl-3-methyl-4-acylpyrazol-5-ones and Trioctylphosphine Oxide",

Anal. Chim. Acta, **134, 327-331 (1982).**

3. **S. Nakamura, N. Imura and N. Suzuki,** *Inorg. Chim. Acta,* **109, 157-162 (1985).**
4. **Q. T. H. Le, S. Umetani, M. Suzuki and M. Matsui, "a-Substituted (3-Diketones: Effect of the a Substituent on the Complexation and Selectivity for Lanthanides",** *J. Chem. Soc., Dalton Trans.,* **643-647 (1997).**
5. **Q. T. H. Le, S. Umetani, and M. Matsui, "Ion-size Recognition of Group 13 Metals (Al^{3+}, In^{3+}) with Modified 13-Diketones",** *J. Chem. Soc., Dalton Trans.,* **3835-3840 (1997).**
6. **S. Umetani and M. Matsui, "Solvent Extraction of Alkaline Earth Metals with 4-Acyl-5-pyrazolones and Polydentate Phosphine Oxides",** *Anal. Chem.,* **64, 2288-2292 (1992).**
7. **S. Umetani and H. Freiser, "Mixed Ligand Chelate Extraction of Lanthanides with 1-Phenyl-3-methyl-4-trifluoroacetyl-5-pyrazolone and Some Phosphine Oxide Compounds",** *Inorg. Chem.,* **26, 3179-3181 (1987).**
8. **G. R. Newkome and D. C. Hager, "Chemistry of Heterocyclic Compounds. 27. An Improved Preparation of Pyridyldiphenylphosphines", J.** *Org. Chem.,* **43, 947-949 (1978).**
9. **S. M. Nelson, M. Perks and B. J. Walker, "New, Ready Degradation Reactions of Biphosphines",** *J. C. S., Perkin Trans.* **1, 1205-1209 (1976).**

EFFECT OF P-ALKYL SUBSTITUENTS AT PHOSPHORYLATED CALIX[4]ARENES ON AMERICIUM AND EUROPIUM EXTRACTION

I. V. Smirnov, M. D. Karavan, V. A. Babain, E. S. Stoyanov',
S.A.Cherenok", V. I. Kalchenko"

Khlopin Radium Institute, St.-Petersburg, Russia
e-mail: igor_smimov@atom.nw.ru
' Boreskov Institute of Catalysis, RAS, Novosibirsk, Russia
** Institute of Organic Chemistry, NASU, Kiev, Ukraine

In contrast to common phosphine oxides, the length of alkyl substituent at phosphorus atom of the calixarenes containing four dialkylphosphine oxide groups at the macrocyclic upper rim strongly affects their extraction properties. With decreasing the alkyl length from butyl to methyl the extraction maximum is displaced into more acidic region. The main reason for such anomalous alkyl effect is unexpectedly high solubility of calix[4]arenes with methyl and ethyl substituents at phosphorus atom in diluted $HN0_3$. Drastic effect of the alkyl substituent length on americium and europium extraction is observed in calix[4]arenes functionalyzed at the upper rim with two methylenediphosphonate substituents $CH[P(0)(0Alk)2]_2$. The extractability is decreased in the following order: propyl » iso-propyl > methyl > ethyl > butyl. Difference in americium distribution coefficients in extraction by calixarene bis-phosphonates with propyl and iso-propyl substituents attains 3 orders. In this case the anomalous alkyl effect is not associated with elevated solubility of investigated extractants, electron factors or differences in composition of extractable solvates.

INTRODUCTION

Management of nuclear power waste remains one of the most complicated problems of radiochemical industry. Recovery of the most hazardous radionuclides from waste, their separate disposal or reprocessing (transmutation) will make it possible to increase significantly the ecological safety and efficiency of nuclear fuel cycle. A combined approach to reprocessing, i.e. the simultaneous recovery of several radionuclides in one extraction cycle, especially such radiotoxic ones as actinides, super long-lived technetium-99, and platinides being of commercial value appears to have considerable promise.

A very convenient platform for creation of extractants is calixarene molecule. Donor centers in substituted calixarenes may be best arranged around metal cation, considerably increasing the performance and selectivity of extraction. Previously we have already shown that phosphorylated calix[4]arenes, as distinct from extractants like POR and CMPO, provide joint recovery of REE, TPE, technetium and palladium from acidic HLW [1],
The complicated molecule geometry of functionalized calixarenes sometimes changes the properties of substituents very much. When studying Am and Eu extraction by phosphorylated calixarenes we found [2] that the substituents at phosphorus atom affect the extraction properties of calix-arenes similarly to conventional organophosphorus compounds and the extraction is impaired in the following rows of substituents: $(Alk)_2PO>AlkArPO>Ar_2PO$ and $(Alk)_2PO»(AlkO)_2PO$. However, transfer from phosphorylated calix[4] to calix[6]arenes, i.e. increasing the number of donor P=0 groups, does not practically affect Am and Eu extraction.

Calix[4]phosphinoxides with substituents $CH_2P(0)Bu_2$and $CH_2P(0)MetPh$ on upper rim extract Am and Eu about 100 times more efficiently than monophosphoryl analogs. By this is meant that it i s not a lways possible to p redict the e xtraction p roperties of phosphorylated calixarenes beforehand on the basis of the properties of phosphoryl substituents.

An interesting effect manifests itself in the row of phosphorylated calix[4]arenes containing dialkylphosphinoxide fragments (Fig. 1, R' = Pr, R = $CH_2P(0)Alk_2$) [3], In contrast to routine phosphinoxides, the length of alkyl substituent at phosphorus atom very strongly affects the extraction properties of calixarenes. With decreasing the length of alkyl in the row of dibutyl (C2), dipropyl (C67), diethyl (C45). dimethyl-(C57) phosphinoxide derivatives, the extraction maximum of europium and americium is shifted to more acidic region (Fig. 2).

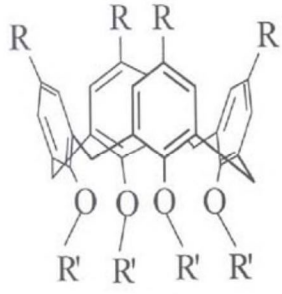


Figure 1. Phosphorylated calix[4]arenes.

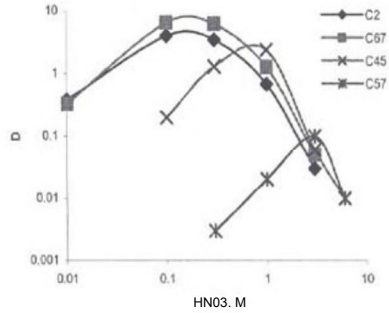


Figure 2. Extraction of europium by 0.01 M solutions of calixarenes in m-nitrobenzotrifluohde (NBTF) [1].

The main reason for such anomalous alkyl effect is unexpectedly high solubility of calix[4]arenes with methyl (C57) and ethyl (C45) substituents at phosphorus atom in diluted nitric acid [3]. In two-phase aqueous-organic systems C45 passes into aqueous phase to a considerable degree, its concentration in organic phase decreases, resulting in decrease of metal extraction from diluted acid. IR-spectrum of C45 solution in water exhibits anomalous decrease of v(P=0) frequency by 73 cm'[1]. Other frequencies of the spectrum, including v(COC), are retained identical to those of aqueous solutions. This is indicative of strong binding of water with C45. In strongly acidic solutions (3 M $HN0_3$) C45 is protonated by nitric acid to form water-insoluble non-hydrated complex [ClP-2H*][0_2N0-H-0N0J'[2], which does not practically transfer from organic into aqueous phase.

The objective of the present work is to investigate the alkyl effects in calix[4]arenes with methylenediphosphonate substituents of $CH(P(0)(0R)_2)_2$ type.

EXPERIMENTAL PROCEDURE

Phosphorylated calixarenes were synthesized at Institute of Organic Chemistry NAN Ukraine (Kiev) according to procedures [5, 6**],**

The m-nitrobenzotrifluoride (NBTF) made by "Rhodia" Co (France) was used as a diluent. Solutions of extractants were prepared by precise weighed portions. Other reagents were obtained from "Vekton Co", St. Petersburg. Isotopes ^{152}**Eu,**^{241} **Am, "Tc were received from "Isotop" Co, St. Petersburg.**

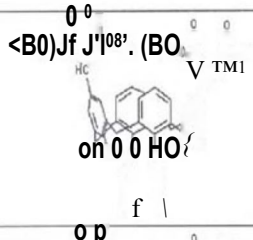
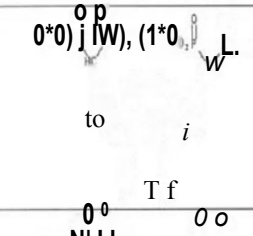
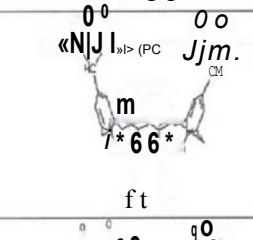
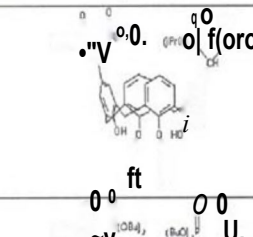
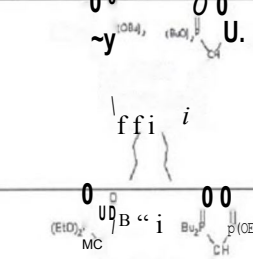
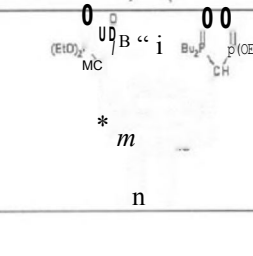
To determine the distribution coefficients of radionuclides, 1.5 ml of organic and aqueous phases each were poured into polypropylene test tube with a stopper, were stirred at 22-24°C for 5 min, the phases were separated by centrifuging and the content of elements in both phases was

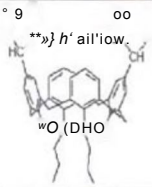
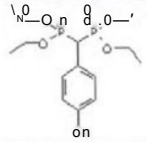
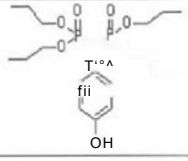
determined by radiometry with the use of scintillation y-spectrometer ((DeskTop InSpector» based on NaJ-detector of 51x51 mm made by «Canberra» Co. Measurement time of samples was chosen so that the error of radiometric measurements be no more than 15%.

RESULTS AND DISCUSSION

The data on extraction of americium, europium and technetium from $HN0_3$ solutions by the investigated extractants are given in Table 1.

Table 1. Extraction ofEu ([10~5 M]), Am (+10'5 M Eu) and Tc (traces) from $HN0_3$ by 0.01 M solutions of calixarenes in m-nitrobenzotrifluonde (NBTF).

Formula			[$HN0_3$] M:				
			0.1	0.3	1.0	3.0	6.0
C82		DEU	0.23	0.17	0.14	0.17	0.06
		OAIB	0.3	0.24	0.24	0.27	0.06
		DTC	0.46	0.40	0.21	0.03	<0.01
C83		DEO	0.86	0.50	0.20	0.08	0.01
		DAKI	1.02	0.55	0.22	0.07	0.01
		DTC	0.59	0.24	0.03	<0.01	<0.01
C84		DEU	>1000	350	25	4.7	0.61
		DAm	>500	300	30	4.6	0.47
		D T C	0.94	0.62	0.13	0.01	<0.01
C85		DEU	0.78	0.54	0.42	0.27	0.02
		DAm	1.05	0.77	0.56	0.33	0.02
		Die	1.6	0.94	0.35	0.01	<0.01
C86		DEU	0.01	0.01	0.06	0.18	0.06
		DAITI	0.01	0.02	0.11	0.27	0.05
		DTC	0.78	0.41	0.20	0.03	<0.01
C94		DEU	9.5	7.9	5.9	1.18	0.08
		DADI	11.2	9.0	8.0	1.45	0.06
		DTC	7.6	4.5	0.95	0.05	0.01

C95		DEU	**3.0**	**4.5**	**3.9**	**0.87**	**0.08**
		DAITI	**4.1**	**7.1**	**6.3**	**1.23**	**0.06**
		D_{Tc}	6.1	**3.9**	**0.76**	**0.03**	0.01
C87 0.2 **M**		DEU	**<**0.01	-	0.02	-	-
		DAIH	0.01	-	**0.03**	-	-
C88 0.2 **M**		DEU	**2.5**	-	**0.96**	-	-
		DARI	**3.7**	-	**1.65**	-	-

Extraction performance of americium and europium strongly depends on alkoxy substituent size at phosphorus atom and decreases in the row: propyl » iso-propyl > methyl > ethyl > butyl. Difference in the distribution coefficients of americium between calixarenes with propyl (C84) and iso-propyl (C85) substituents at phosphorus atom attains 3 orders. Technetium is extracted by calixarenes C82 - C86 **to the same degree, which points to the absence of difference in basicity of phosphoryl groups in these compounds. Thus, it is evident that this effect is not connected with differences in basicity of phosphoryl groups.**

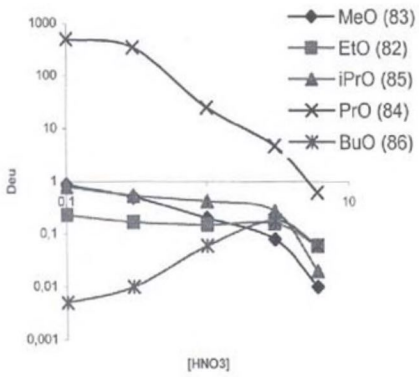
The effect cannot be also explained by higher solubility in water of some diphosphonate calixarenes, as in the case of dialkylmethylenephosphinoxide derivatives of calix[4]arenes [3]. As already noted, the effect is observed only in extraction of americium and europium, but is not detected in the case of technetium. Besides, diphosphonate with propyl (C84) substituents extracts europium considerably better than a more hydrophobic calixarene with butyl (C86**) substituents.**

The replacement of two alkoxyl groups in diphosphonates (C84 - C85) by alkyl ones (C94 - C95) leads to the expected growth of extraction ability of calixarenes, but no difference is observed in the properties of ethoxyl and propoxyl derivatives. Technetium is extracted by these calixarenes more efficiently than by diphosphonate calixarenes C82 - C86**.**

The significant decrease of europium distribution coefficients with increase of aqueous phase acidity observed in the case of C84 (Fig. 3) is characteristic of acidic extractants. It might be supposed that C84 contains an acidic impurity, but according to NMR data all the investigated calixarenes contain no impurity of acid.

It is seen from Table 1 that a similar alkyl effect is also observed in the row of conventional methylenediphosphonates. The compound containing propoxyl-groups at phosphorus atoms (C88**) extracts americium and europium much better than ethoxyl analog (C87). On the other hand, in the case of C87 the distribution coefficients of technetium are approximately an order lower than for C**88**, while the corresponding calixarene derivatives C82 and C84 extract it almost identically. This suggests that ethoxyl diphosphonate (C87) may dissolve in water and its reduced extraction ability is connected with partial transfer into aqueous phase. Therefore, further studies are needed to distinct clearly the contribution of structure of phosphoryl group and calixarene platform into anomalously strong extraction properties of propoxyl diphosphonate.**

An interesting effect is observed in europium extraction by calixarenes C82 - C86 **from lithium nitrate solution (Fig. 4).**



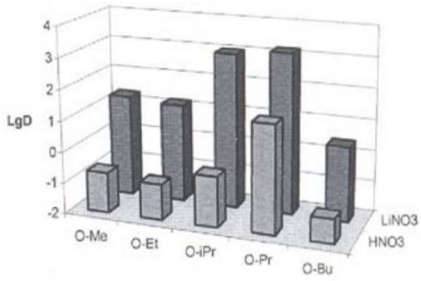


Figure 3. Extraction of Eu by 0.01 M solutions of CIP 82 - 86 in NBTF from $HN0_3$

Figure 4. Extraction of europium from 1 M $HN0_3$ and 3 M $LiN0_3$ by 0.01 M solutions of extractants in NBTF.

It is clear that in neutral medium the calixarenes containing propoxyl and iso-propoxyl substituents at phosphorus atom extract europium much better than other compounds.

The stronger extraction ability of phosphinoxides containing propyl substituents as compared to iso-propyl ones were known earlier. So, thorium and REE forming trisolvates with neutral organophosphorus compounds are worse extracted by extractants containing branched radicals at phosphorus atom (going from normal to iso- and then to secondary alkyls) [4], This fact may also explain an effect observed in the row of phosphorylated calix[4]arenes. On going from calixarene C67 (R' = Pr, R = $CH_2P(0)Pr_2$, Fig. 1) to C75 (R' = Pr, R = $CH_2P(0)i\text{-}Pr_2$), the distribution coefficients of europium decrease by two orders, those of technetium remain practically unaffected (Fig. 5).

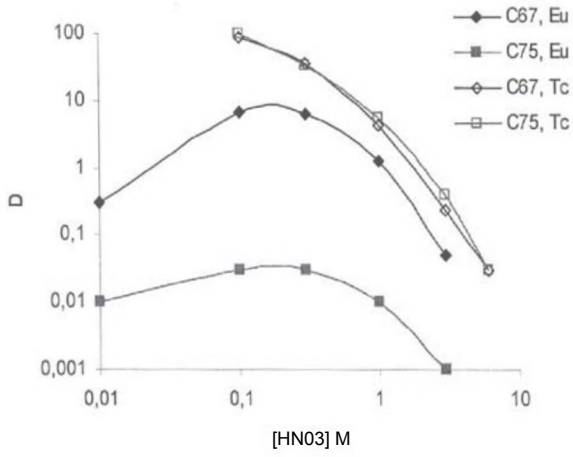


Figure 5 Extraction of europium and technetium from $HN0_3$media by 0.01 M solutions of calix[4]arenes C67 (R' = Pr,R = $CH_2P(0)Pr_2$, Fig. 1) and C75 (R' = Pr,R = $CH_2P(0)i$-Pr2) in NBTF.

At first glance there are the same regularities as in the row of diphosphonatate calixarenes C84 and C85. However, europium is also extracted from $LiN0_3$ solutions by calixarene C67 by two orders better than C75 (for 0.001 M solutions of C67 and C75 in NBTF and 3 M $LiN0_3$ D_{Eu} >500 and 20**, respectively. Besides, in the case of dialkylmethylenephosphinoxide derivatives of calix[4]arenes no differences are observed in extraction ability of dipropyl (C67) and dibutyl (C2)**

derivatives^]. Hence, the steric hindrances to formation of europium complexes with phosphoryl groups associated with volumetric iso-propyl radical cannot be considered as the main reason for anomalies in the row of diphosphonate calixarenes C82 - C86.

We have determined the solvate numbers of europium complexes with C84 and C85 by using the method of equilibria shift. In the case of extraction from 0.3 M $HN0_3$ these values are equal to 2.5 (C84) and 2.1 (C85), while in 3 M $LiN0_3$- 2.5 and 2.8, respectively. Thus, irrespective of composition of aqueous phase and calixarene type, europium is extracted in the form of di- and trisolvates. Such essential differences in extraction ability of C84 and C85 do not depend on differences in composition of extractable compounds.

CONCLUSIONS

The extraction of americium, europium and technetium by calix[4]arenes with diphosphonate substituents is investigated and the effect of anomalous influence of alkoxy radical structure at phosphorus atom on extraction properties is detected.

The extraction of americium and europium from acidic media decreases in the row of calix[4]arenes with the following substituents: propyl»iso-propyl - methyl - ethyl ~ butyl, and from neutral ones - propyl ~ iso-propyl» methyl - ethyl ~ butyl. Technetium is extracted by the investigated diphosphonates with much the same efficiency.

By the method of equilibrium shift it is shown that the diphosphonates containing both propyl and iso-propyl radicals at phosphorus atom extract europium in the form of di- and trisolvates, irrespective of aqueous phase composition.

It is suggested that the detected anomaly is not associated with different basicity of diphosphonate substituents and solubility in water of the investigated compounds or the presence of acidic impurities therein.

ACKNOWLEDGEMENTS

The work was carried out under financial support of ISTC, Project 2068 and USTC (Project RUS-09).

REFERENCES

1. **I.V. Smirnov, V.A. Babain, T.I. Efremova (2003),** *Proceedings of International conference Global-2003*, **New Orleans, USA, pp. 702 - 706.**
2. **I. Smirnov, V. Babain, T. Efremova, V. Kalchenko (2002),** *J. Nucl. Sci. & Technol., Suppl.* **3, p. 321-324.**
3. **I. V. Smirnov, M. D. Karavan, V. A. Babain, E. S. Stoyanov (2004),** *Extended Abstracts of Papers presented at the 6th Int. Conference on Nuclear and Radiochemistry (NRC6),* **Aachen, Germany, pp. 571- 573.**
4. **G.W. Mason, H.E. Griffin (1980),** *Proceedings ACS symposium 1979,* **Honolulu, Hawaii, "Actinide Separation", Ser 117, Washington DC, p.890**
5. **O. Klimchuk, L. Atamas, V. Miroshnichenko, V. Kalchenko, I. Smirnov, V. Babain, A. Vamek, G. Wipff (2004),** *J. Inclusion Phenom. and Macrocyclic Chem.,* **9, p. 47-56.**
6. **A.I. Vovk, V.I. Kalchenko, S.O. Cherenok, V.P Kukhar., O.V. Muzychka, M.O. Lozynsky (2004), J. Org. Biomol. Chem. In press.**



SOLVENT EXTRACTION SEPARATION AND DETERMINATION OF YTTRIUM WITH CYANEX272

Manjusha Karve* and Bhagyashree Vaidya
Dept, of Chemistry, Univ. of Mumbai, Vidyanagari
Mumbai 400 098, India

A simple and selective method for the liquid - liquid extraction of yttrium with Cyanex272 is presented. The influence of the pH of aqueous phase, concentration of extractant, nature of diluent, extraction time, type of stripping agent and stripping time were evaluated to optimize the conditions for quantitative extraction of yttrium. The effect of certain foreign ions on the extraction of yttrium was studied. Yttrium was quantitatively extracted at pH = 7.0 with 5 x 1CT^{4} M Cyanex272 in xylene. It was stripped from the organic phase with 4M nitric acid and determined spectrophotometrically with Arsenazo (III) at 650nm.

INTRODUCTION

Yttrium has applications in various fields ranging from metallurgy, catalyst to electronics. Liquid - liquid extraction has been the most commonly used technique for isolation of yttrium. The extraction of yttrium with various alkyl phosphoric acids such as mono - 2 - ethyl hexyl phosphoric acid [1] and bis - (2 - ethylhexyl) phosphoric acid (HDEHP) [2] have been well established. Its extraction with other organo phosphorus compounds like, 2 - ethylhexyl phosphonic acid mono - 2 - ethylhexyl ester [3] and mono-octyl phosphinic acid [4] was also studied. The addition of Cyanex923 (a mixture of four trialkyl phosphine oxdes) to Cyanex301 [bis (2,4,4 - trimethylpentyl)dithiophosphinic acid [5] or Cyanex272 [bis(2,4,4-trimethylpentyl)phosphinic acid)] [6] improved the extraction efficiency of yttrium. Its extraction was influenced by the aqueous phase acidity, concentration of extractant and nature of diluent using acidic organo phosphorus compounds as extractants [1, 2], The selective recovery of yttrium from associated elements was therefore achieved by the process of selective extraction. Due to the ever increasing demand for yttrium in industries, its separation and isolation for reuse has importance. Hence the recovery of yttrium needs to be explored for better extraction and stripping characteristics, using versatile extractants particularly for the practical applicability. Cyanex272 was selected as an extractant for yttrium due to its low water solubility and relatively lower acid strength (pKa = 6.4) [7] as the acidity of the extractant influences its extractability [4], Also the systematic studies of yttrium using Cyanex272 are lacking. Various parameters such as pH of aqueous phase, nature of diluents, extractant concentration and the equilibration time were studied in detail to optimize the conditions for the quantitative extraction of yttrium. The influence of different mineral acids as stripping agents for yttrium was studied to enable its easy recovery from the organic phase. The effect of diverse ions on yttrium extraction was also investigated.

EXPERIMENTAL

Materials

A Digispec 110 D spectrometer (Feedback, India Ltd.) with matched 10mm glass cuvettes, a digital pH meter (Elico Private Ltd., India) with a combined glass and calomel electrode (Toshniwal - Moller,India) and a Wrist Action Flask Shaker (General Trading Corporation, India) were used.

The stock solution of yttrium(III) was prepared by dissolving 0.2252 g of yttrium carbonate in 1.0 cm^3 nitric acid, evaporated completely and then treated with 10 cm^3 nitric acid and finally diluted to 100 cm^3 with distilled water. It was standardized complexometrically [8] and was found to contain 1.0010 mg/cm^3 yttrium. A solution containing 30 pg/cm^3 of yttrium was prepared by appropriate dilution. Cyanex272 [CYTEC Canada Inc.] received as a gift sample was used without further purification. A 0.1 % aqueous solution of Arsenazo(III) [Loba Chemie, A.R.] was used for spectrophotometric determination

General Procedure

An aliquot of solution containing yttrium (30 pg) was adjusted to pH = 7.0 with 0.1 M sulphuric acid or 0.1 M ammonium hydroxide and then equilibrated with 10 cm^3 of 5.0 x 10^{-4} M Cyanex272 in xylene. The phase volume ratio of aqueous to organic phase was maintained at 1:1. The equilibration was done on a wrist action flask shaker and the period of equilibration was 20 minutes. After allowing the two phases to settle and separate out yttrium from the organic phase was stripped with 10 cm^3 of 4.0 M nitric acid. Yttrium was estimated in the aqueous phase spectrophotometrically with Arsenazo(III) at 650 nm [9], The amount of yttrium was computed from the calibration curve. The distribution ratio (D) of yttrium was calculated from the ratio of percent of yttrium extracted in the organic phase to the aqueous phase. The extraction of yttrium carried out as per the general procedure for six replicate determinations had a relative standard deviation of 0.15.

RESULTS AND DISCUSSION

Effect of pH

Yttrium was extracted from pH = 1.0 - 8.0 with 5.0 x 10^{-4} M Cyanex272 in xylene. The extraction was quantitative at pH =7.0 with 5.0 x 10^ M Cyanex272 in xylene as shown in Fig. 1.0. Hence further studies were carried out by maintaining the pH of aqueous phase at pH = 7.0.

Effect of Diluents on Extraction

Various organic solvents were used as diluents for 5.0 x 10^{-4} M Cyanex272 (Table 1). The liquid cation exchangers undergo polymerization in non polar organic solvents. The extent of aggregation and hence the extractability is influenced by the nature of the organic solvent. Low dielectric constant solvents favour extraction as the extraction proceeds by ion pair formation. The increase in the aromatic character of solvent results in the decrease of extraction The interaction of the diluent with the extractant may inhibit extraction [10], The incomplete extraction of yttrium with chloroform may be due to its high dielectric constant. The observed trends in extraction using toluene, benzene and cyclohexane may be attributed to their aromatic character. However a particular physical property of the organic solvent cannot be correlated with the extent of extraction. Hence it was observed that yttrium was quantitatively extracted when xylene was used as a diluent for Cyanex272. Hence the organic phase used was 5.0 x 10^{-4} M Cyanex272 in xylene throughout the studies.

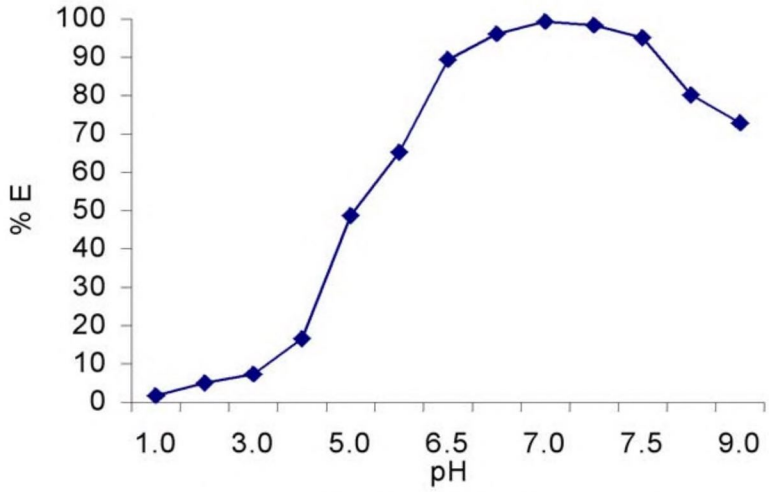


Figure 1. Plot of pH Vs % Extraction

Table 1 Effect of Diluents on Extraction

Diluents	Dielectric Constant €	Percent Extraction E	Distribution Ratio D
Benzene	2.20	**85.0**	**5.7**
Toluene	**2.24**	**74.5**	**2.9**
Xylene	**2.28**	**99.4**	**165.7**
Cyclohexane	2.02	**88.4**	**7.6**
Chloroform	**4.90**	**76.8**	**3.3**
Carbon Tetrachloride	2.20	**80.1**	**4.0**

Effect of Extractant Concentration

Yttrium was extracted from (0.9 - 5.0) x 10"4 M Cyanex272 in xylene. It was quantitatively extracted at 5.0 x lO^M Cyanex272 (Table 2). Hence further studies were carried out with 5.0 x 10'4 M Cyanex272 in xylene.

Table 2 Effect of Cyanex272 Concentration

Cyanex272 1 X 10'4M	Percent Extraction E	Distribution Ratio D
0.9	**82.3**	**4.6**
1.0	**88.3**	**7.5**
2.0	**94.0**	**15.7**
3.0	**95.0**	**19.0**
4.0	**98.3**	**57.8**
5.0	**99.4**	**165.7**

Effect of Stripping Agents

The influence of stripping agents was studied by stripping yttrium from the organic phase with (1 - 8**) M hydrochloric acid, (1 -** 8**) M nitric acid or (0.5 - 4 M)sulphuric acid (Table 3). The recovery of yttrium was incomplete with hydrochloric acid and sulphuric acid. However,**

it was quantitatively stripped with 4 M nitric acid. Hence the stripping agent used for all studies used was 4 M nitric acid.

Table 3 Effect of Stripping Agents

Stripping Agent	0.1	**0.5**	1	2	**3**	**4**	**5**	6	**7**	8
M										
					% Recovery					
HNO_3	**-**	**-**	**80.1**	**82.3**	**84.0**	**99.4**	**98.3**	**88.3**	**84.0**	**78.3**
HCl	**-**	**--**	**80.7**	**82.3**	**83.3**	**85.0**	**87.3**	**89.0**	**90.7**	**80.7**
H_2SO_4	**-**	22.2	**67.9**	**76.2**	**96.7**	**85.3**	**-**	**-**	**-**	**-**

Period of Equilibration and Stripping

The extraction of yttrium was studied for different periods of equilibration and stripping. The extraction was studied for 5.0, 10.0 15.0 and 20.0 minutes and the corresponding percentage extraction was 95.7, 97.3, 98.3 and 99.4 respectively. The stripping of yttrium was studied using different time periods. The percent recovery with 5.0, 10.0 15.0 and 20.0 minutes of stripping with 4M nitric acid as stripping agent was 85.7, 90.0, 93.3 and 99.3 respectively Hence the period of equilibration and stripping throughout the studies was 20 minutes.

Nature of Extracted Species

The nature of extracted species of yttrium with the extractant was ascertained by slope analysis [10]. A graph of Log [Distribution ratio] versus Log [Cyanex272] at fixed pH = 7.0 (Fig 2.) was a straight-line plot with slope = 1.7. Hence the probable stoichiometric ratio of yttrium with the extractant was 1 : 2.

Effect of Various Diverse Ions

The extraction of yttrium was studied in the presence of various diverse ions with 5.0 x 10^{-4} M Cyanex272 in xylene (Table 4). The tolerance limit was set as the amount of foreign ion which will cause $\pm$ 2% error in the recovery of yttrium. The alkali and alkaline earth metals were tolerated in ratios exceeding 1:150. Chromium(VI), manganese(II) and zinc(II) were tolerated in the ratio 1:16 while cobalt(II) and cadmium(II) were tolerated in the ratio 1:30. Various ions like nickel(II), zirconium(IV), scandium(III) and lanthanum(III) were tolerated at the ratios 1:1.6 , 1:3.3, 1:2.7 and 1:1 respectively. Cadmium(II) was tolerated in the ratio 1:33. Elements like vanadium(IV), vanadium(V), aluminium(III), thorium(IV) and some lanthanides interfered by co-extraction. The anions chloride, nitrate and sulphate were tolerated in ratios exceeding 1:150.

The separation of yttrium(III) from sodium(I), potassium(I), magnesium(II), calcium(II) and strontium(II) in binary mixtures was possible as these elements remained unextracted in the aqueous phase under the extraction conditions of yttrium. It was similarly separated from cerium(IV), lanthanum(III), zirconium(IV), cobalt(II) and nickel(II) as these elements were not extracted under the condition for extraction of yttrium. The elements after separation were determined spectrophotometrically with a suitable chromogenic ligand [9],

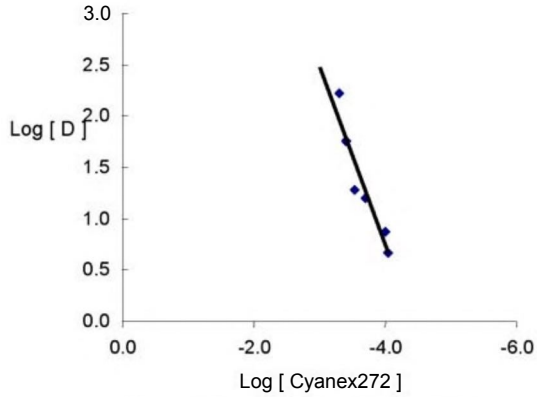


Figure. 2 Log [D] Vs Log [Cyanex272]

Table 4 Effect of Various Diverse Ions

Elements	Added As	Tolerance Limit fig
Na^{+}	NaCl	5000
K^{+}	KCl	5000
Mg^{2+}	$MgS0_4.7H_20$	5000
Ca^{2+}	$CaCl_2$	5000
$Sr^{2"}$	$Sr\ (N0_3)_2$	5000
La^{3+}	$La_2\ (C0_3)_3$	30
Cr^{6+}	$Cr\ (N0_3)_6$	500
Mn^{2+}	$MnSO_4.7H_20$	500
Co^{2+}	$Co(N0_3)_2.6H_20$	1000
Ni^{2+}	$(NH_4)_2\ S0_4.NiS0_4.6H_20$	50
Zn^{2+}	$ZnS0_4.7H_20$	500
Cd^{2+}	$3CdS0_4.8H_20$	1000
Ce^{4+}	$Ce\ (S0_4)_2\ 4H_20$	100
Zr^{4+}	$Zr(N0_3)_4.2H_20$	100
Mo^{6+}	$(NH_4)_5M0_7O_{24}.4H_2O$	500
Sc^{3+}	$Sc(N0_3)_3$	80
cr	NaCl	5000
NO_3^-	KNO_3	5000
$SO_4^{2'}$	K_2SO_4	5000

Conclusion

The method developed for the solvent extraction separation of yttrium is simple, rapid and reproducible. The concentration of extractant required for the quantitative extraction is very

low and the diluent used is non toxic in nature. Complete recovery of yttrium by nitric acid in a single stage will have potential for practical applicability. The method is selective for yttrium as most of the common elements are tolerated in high ratios during extraction of yttrium.

Reference

1. **D. F. Peppard, G. W. Mason and C. M. Andrejasich (1963),** *J.Inorg. Nucl. Chem.,* **25, 1175-89.**
2. **L.S. McCarty, G. W. Mason and D. F. Peppard (1978)** *J. Inorg. Nucl. Chem.,* **40, 1423 - 26.**
3. **Ma Enxin, Yan Xiaomin, Wang Sanyi, Long Haiyan and Yuan Chengye (1981),** *Sci. Sin.,* **24, 1237-47.**
4. **D. F. Peppard, G. W. Mason and C. M. Andrejasich (1966),** *J.Inorg. Nucl. Chem.,* **28, 2347 - 2359**
5. **M. L. P. Reddy, J. R. Bosco Bharathi, S. Peter and T. R. Ramamohan (1999) Talanta, 50, 79-85.**
6. **M. L. P. Reddy, T. R. Ramamohan and C.S.P. Iyer (1998) Solvent Extraction Res. Dev. Jpn., 5, 1 - 5.**
7. **American Cyanamid Company, Cyanex272, Cyanex302 and Cyanex301 Technical Brochures**
8. **F.J. Welcher (1961), The Analytical Applications of Ethylenediamminetetraacetic Acid, D. Van Nostrand Company, Inc.,** *New Jersey,* **pp 27.**
9. **F.D. Snell (1978),** *Photometric and Fluorometric Methods of Analysis,* **John Wiley and Sons, New York, Part (I & II).**
10. **T. Sekine and Y. Hasegawa (1972),** *Solvent Extraction Chemistry Fundamentals and Applications,* **Marcel Dekker Inc. (New York), pp 919.**



THERMODYNAMICS OF THE EXTRACTION OF BISMUTH WITH MONO-2-ETHYLHEXYL PHOSPHORIC ACID

Emmanuel O. Otu

School of Natural Sciences, Department of Chemistry, Indiana University Southeast
New Albany, IN 47150, USA

ABSTRACT

The extraction of Bi(III) from aqueous nitric, sulfuric and perchloric acid medium by mono-2-ethylhexyl phosphoric acid dissolved in o-xylene was studied in the temperature range 25 - 60°C. The extractions were investigated as a function of aqueous acid concentration and extractant organic phase concentration. The extractant aggregation and extraction stoichiometries did not change with temperature. The thermodynamics of the extraction process was studied by measuring extraction coefficients in this temperature range. The slopes of the extractant dependencies are unity and acid dependencies were negative three, the formal charge on Bi(III) at the acidities studied, indicating a micellar-type mechanism. In nitric and perchloric acids, the extraction was favored by entropy, whereas extraction from sulfuric acid was opposed by entropy.

INTRODUCTION

Organophosphorus reagents (neutral and acidic) have been developed as extractants for various metal ions from aqueous medium. Di-2-ethylhexyl phosphoric acid (HDEHP) is the most widely used and a vast amount of information has been established for the extraction of various metal ions in different media (aqueous and organic). In comparison, only very sparse information exists for the di-acidic analogue, mono-2-ethylhexyl phosphoric acid (H_2MEHP) [for example, 1-12].

Mono-2-ethylhexyl phosphoric acid (H_2MEHP) is a strong diprotic (hard) acid and as such has been used mostly for the extraction of hard (bases) metal ions (mainly the lanthanides and actinides). It has been shown to polymerize extensively in non-polar organic solvents and exists as monomers in polar organic solvents [13-15],

Khwaja et. al. have extracted Cr^{3+}, Fe^{3+}, Mg^{2+}, Mn^{2+}, Cu^{2+}, Co^{2+} and Ni^{2+} [1,3] with H_2MEHP. Demopoulos and Pouskouleli reported the extraction of Fe^{3+} [4], Bismuth is a green heavy metal that is being used as replacement for environmentally unfavorable metals. This report delineates the thermodynamic parameters accompanying the extraction of bismuth from nitric, sulfuric and perchloric acid medium using the dependence of the coefficient of extraction on temperature. The thermodynamic parameters will give insight into the mechanism of the process.

EXPERIMENTAL

Materials

Purified mono-2-ethylhexyl phosphoric acid (H2MEHP) was received from Argonne National Laboratory stock. The purity checked according to (16) was greater than 91%. Certified ACS grade o-xylene used as diluent was obtained from J.T. Baker (Phillipsburg, NJ). Bismuth nitrate pentahydrate, nitric, sulfuric and perchloric acids, potassium iodide, hypochlorous acid (all certified ACS grade) were obtained from Fisher Scientific (Fair Lawn, NJ). Deionized water was used to prepare the aqueous phase solutions.

Procedure

Extraction of metals

Stock solution of H_2MEHP in o-xylene was prepared by weight. Extractions were performed by mixing equal volumes (1 mL) of the organic and aqueous phases in a 13 x 100 mm Pyrex test tube, at the desired temperature. The aqueous phase contained 10^{-4} M Bi(III) ion and the organic phase contained 0.05 - 0.2 m H_2MEHP. Extractions at designated temperatures were performed by mixing the phases and allowing the test tubes to sit in a thermostated jacketed beaker. After temperature equilibrium was attained, the samples were mixed on a vortex mixer several times, placing them back in the thermostated beaker each time to attain temperature equilibrium. The phases were allowed to sit for phase separation. Before separation, the test tubes were centrifuged and placed back in the thermostated beaker for 0.5 hr. for temperature and chemical equilibrium to re-establish. This was sufficient time for attainment of chemical equilibrium [4], The aqueous phase was analyzed and quantitated using spectrophotometry as the yellow bismuth tetraiodo complex ion at 460 nm.

The concentration of bismuth ion in the organic phase was obtained by the difference between the initial and final aqueous phase concentrations. The distribution ratios, D, were determined as customary as the ratio of bismuth concentrations in the organic and aqueous phases. Duplicate extractions were performed at various temperatures and duplicate analyses were performed on the aqueous phases. These duplicate experiments were used to estimate the uncertainty levels in the distribution ratio measurements. The relative standard deviation of the D measurements was less than 10%. The measured molar D values were converted to molal values by multiplying them by the appropriate aqueous to organic phase density ratio.

RESULTS AND DISCUSSIONS

Extraction stoichiometry and Equilibrium constants

H_2MEHP has previously been reported as hexameric in o-xylene [13, 17], In a previous study, it was reported that this aggregation did not change with temperature [17], Hence, it is assumed that extraction stoichiometries under the conditions of this study remained the same. Therefore, it is valid to use the extraction coefficients as a function of temperature for the determination of thermodynamic parameters as in this study.

The slopes of the extractant dependency were unity in the temperatures range studied. This suggests that extraction of bismuth by H_2MEHP takes place through a micellar-type mechanism as previously reported (8,12,18), and similar to other highly aggregated extraction system such as dinonylnaphthalene- and didodecylnaphthalene- sulfonic acids (19-21) and quaternary alkylammonium salts (22), wherein metal ions are extracted into the core of the extractant

aggregate. The slopes of the acid dependencies were equal to -3, indicating that three protons are lost from the extractant upon extraction of the metal ions.

The extraction equation can therefore be written as:

$$Bi^{3+} + \overline{(H_2Y)}_6 \Longleftrightarrow \overline{Bi(H_gY_6)} + lH^+ \qquad (1)$$

where $(H_2Y)_6$ is the hexamer of H_2MEHP, species with overline exist in the organic and charged species exist in the aqueous phase. The thermodynamic equilibrium constant can be written as:

$$K = 6\frac{[\overline{Bi(H_9Y_6)}][H^{\pm}f\ rim,}{[\overline{\wedge}]_{c_{HiY}\ rt.BN}} \qquad (2)$$

where $Y_{\pm HN}$ and $Y_{\pm BN}$ are the mean molal ionic activity coefficients of $HN0_3$ and $Bi(N0_3)_3$, respectively, and C_{H2Y} is the molal analytical concentration of the extractant. At tracer metal ion concentration, if the extractant monomer concentration is negligible, the analytical concentration of the extractant can be expressed as $C_{HY_2} = 6[(H_2T)_6]$.

Activity coefficient of bismuth nitrate is available and allowed nitrate complexing in the aqueous phase to be taken into account as follows:

$$Br^{2-} + iNo; \text{ <- } \quad \overset{\beta i}{\text{---}} \wedge Bi(NO,)- \quad {}^{3-i}{}_{i} \qquad (3)$$

The total concentration of Bi(III) in the aqueous phase, $[Bi^{3+}]_{to}t$, can be shown to be

$$iBl\ Li.ao = IBl\ Ji^{1+}\left\{\frac{1 + \beta_1\gamma_{Bi^{3+}}[NO_3^-]\gamma_{NO_3^-} + \beta_2\gamma_{Bi^{3+}}[NO_3^-]^2\gamma^2_{NO_3^-} + \beta_3\gamma_{Bi^{3+}}[NO_3^-]^3\gamma^3_{NO_3^-}}{y\text{Bi(JVOj)}^{2*} \qquad y\text{B:(NO,)I} \qquad y\text{BKNO,),}}\right\} \qquad (4)$$

where p is the formation constant for the nitrate complexes. Recognizing that the distribution ratio, D, is the ratio of the concentration of metal in the organic phase and the total concentration of metal in the aqueous phase, the activity coefficient of neutral species is unity, and deriving mean molal activity coefficients of the species in Equation 4, Equation 2 can be expressed as:

$$K = 6\,D\frac{[H^+]^3\gamma^6_{\pm,HN}}{C_{..v.}}\left\{\frac{1}{\gamma^4_{\pm,BN}} + \frac{\text{ARIJP:}}{\gamma^3_{\pm,BN}}, \frac{\text{,r}}{\gamma^2_{\pm,BN}} + \beta_3[NO_3^-]^3\right\} \qquad (5)$$

The mean molal activity coefficients of the bismuth nitrates at the relevant ionic strengths were taken from (23). The following p values were taken from (24): 6i = 6.46, $t>_2$ = 7.98 and 63 = 5.01 for nitrate. The listed b values for sulfate were at concentrations higher than was used in this work. Therefore, similar treatment was not offered. Perclorate ion, at the concentration used, is non-complexing.

The values of the thermodynamic equilibrium constants calculated at different temperatures are given in Table 1. The influence of temperature on activity coefficient was neglected in these calculations (25). The indicated uncertainties are the average standard errors estimated from

statistical analysis of the logK data at each temperature for the different acid and ligand concentrations included in this study.

TABLE 1. Thermodynamic Equilibrium Constants

T,°C	log K		
	HNO_3	H_2SO_4	$HClO_4$
25	2.70 ±0.08	-3.83 ±0.17	3.36 ±0.01
30	2.80 ±0.07	-3.75 ±0.19	3.40 ±0.01
40	2.86 ±0.07	-3.54 ±0.11	3.45 ±0.02
50	2.95 ±0.09	-3.45 ±0.12	3.47 ±0.02
60	3.03 ±0.09	-3.37 ±0.12	3.52 ± 0.02

Free Energy, Enthalpy and Entropy Changes

The extractant and acid dependencies indicate that the extraction stoichiometry and equilibria did not change in the temperature range of this study. Therefore, the temperature coefficient method was used to determine thermodynamic parameters of the extraction. The thermodynamic parameters were calculated from the Gibbs-Helmholtz equation written in the form:

$$\log AT = \frac{A\ G^\circ}{2.303RT} = \frac{AH^0\ 1\ AS^0}{2.3037?\ T\ 2.3037?} + \text{—} \qquad (6)$$

where R (8.314 J/mol.K) is the gas constant. The enthalpy and entropy changes of the extraction processes were calculated from the slopes and intercepts of the plots of logK vs. $\frac{1}{T}$. The linear regression plots are shown in Figure 1, and each data point is the averaged value of logK for the different acid and extractant conditions employed in this study. The constancy of H° and aqueous phase activity coefficients over the temperature range of this study had been discussed in a previous report [25],

The enthalpy and entropy changes of the extraction processes calculated from the slopes and intercepts of the plots, and free energy calculated from *AG° = -2.303RT\ogK* are tabulated in Table 2. The uncertainties reported for AH^0 and AS^0 are the standard errors of the slopes and intercepts, respectively. Those for AG° were obtained from the uncertainties of logK shown in Table 1.

TABLE 2. Thermodynamic parameters

Acid	H° (kJmol'¹)	S° (JK¹ mol'¹)	,G° (kJ/mol'¹)
HNO_3	15.96 ±2.16	105.9 ±6.9	-15.4 ±0.3
H_2SO_4	25.16 ±2.66	-11.5 ±8.5	21.3 ±0.3
$HClO_4$	7.88 ±0.65	91.0 ±2.1	-19.2 ±0.2

In the extraction of a metal cation by a liquid cation exchanger, the net enthalpy and entropy

changes of the extraction are the result of several different processes. The dehydration of the metal cation generally involves a positive enthalpy change (AH > 0) as a result of the breakage of ion-water bonds, and a positive entropy change (AS > 0) due to an increase of disorder in the system by the release of coordinated water. The opposite will occur for the hydration of the proton(s) lost by the ligand. On the other hand, metal coordination by the organic ligand will result in a negative enthalpy change (AH < 0), as a consequence of replacing relatively weak hydrogen bonds (typical of organophosphorus acids) with stronger metal coordination bonds, and in a negative entropy change (AS < 0) due to the increase of order caused by the new bonds. The deprotonation of the extractant produces opposite effects.

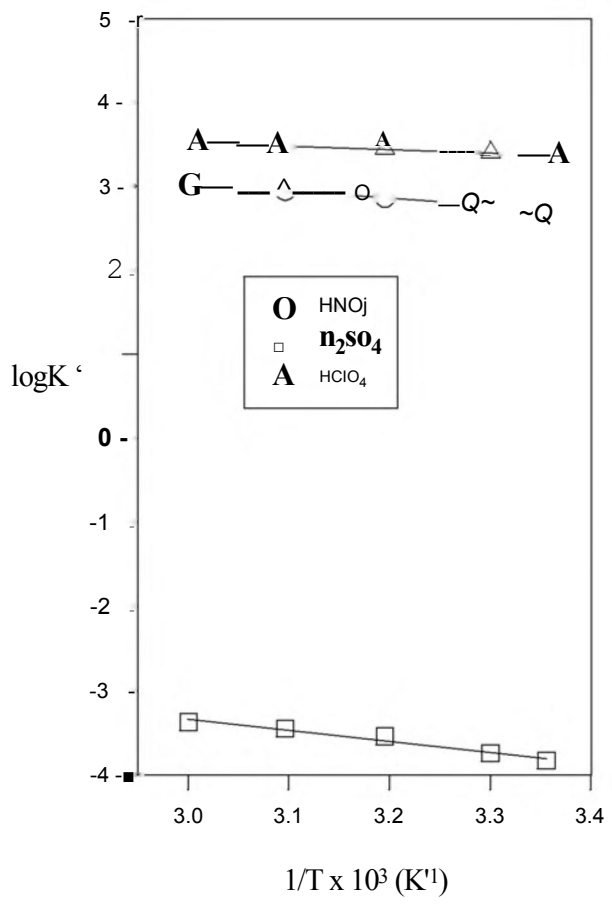


Figure 1. Variation of equilibrium constant with temperature in the extraction of Bi(III) from aqueous nitric, sulfuric and perchloric acids with o-xylene solution containing H_2MEHP.

The extractions from nitric and perchloric acids are (a) favored by entropy changes, and (b) the unfavorable enthalpic changes are also indicative of micellar extraction mechanism [25-27], The unfavorable entropy changes in aqueous sulfuric acid does not corroborate the micellar-like

extraction mechanism indicated by the extraction stoichiometry. Aqueous sulfuric acid is an inefficient extraction medium as indicated by the positive value of AG. The stronger water structure-making capability of the sulfate ion over nitrate and perchlorate ions [28] is manifested in the observed entropy changes of extraction.

ACKNOWLEDGMENT

Dr. Renato Chiarizia of Argonne National Laboratory provided the extractant used in this study. Melanie Huff performed some of the spectrophotometric analysis.

REFERENCES

1. **A.R. Khwaja, O.V. Singh and S.N.Tandon (2000),** *Sep. Sci. Technol.* **35, 447.**
2. **J.O. Asha, O.V. Singh and S.N. Tandon (1991),** *J. Radioanal. Nucl. Chem.* **147, 355.**
3. **S.K. Yadav, O.V. Singh and S.N. Tandon (1991),** *Indian J. Chem.* **30, 982.**
4. **G.P. Demopoulos and G. Pouskouleli (1989),** *Canadian Metallur.* **Quater. 28, 13.**
5. **T. Lee and G. Ting (1981), Sep.** *Sci. Technol.* **16, 943.**
6. **G. Ting and T. Lee (1981),** *Radiochimica Acta* **28, 103.**
7. **T. Lee and G. Ting (1981), Sep.** *Sci. Technol.* **16, 303, and references therein.**
8. **G.W. Mason, S. McCarty and D.F. Peppard (1962),** *J. Inorg. Nucl. Chem.* **24, 967.**
9. **R.D. Baybaz and R.E. Leuze (1961),** *Nucl. Sci, Eng.* **11, 90.**
10. **C.G. Warren and J.F. Suttle (1960),** *J. Inorg. Nucl. Chem.* **12, 336.**
11. **D.F. Peppard, G.W. Mason and R.J. Sironen (1959),** *J. Inorg. Nucl. Chem.* **10, 117.**
12. **D.F.Peppard, G.W. Mason, W.J. Driscoll and R.J. Sironen (1958),** *J. Inorg. Nucl. Chem.* **7, 276.**
13. **J.R. Ferraro, G.W. Mason and D.F. Peppard (1961),** *J. Inorg. Nucl. Chem.* **22, 285.**
14. **D.F. Peppard, J.R. Ferraro and G.W. Mason (1958),** *J. Inorg. Nucl. Chem.* **7, 231.**
15. **J.R. Ferraro, D.F. Peppard and G.W. Mason (1965),** *J. Inorg. Nucl. Chem.* **27, 2055.**
16. **Y. Rao, Ramachandra and S. Acharya (1993),** *Hydrometallurgy* **32 129.**
17. **M.M Huff and E.O. Otu (2004), Solvent Extr.** *Ion Exch.* **22, 695.**
18. **G.S. Rao, G.W. Mason and D.F. Peppard (1966),** *J. Inorg. Nucl. Chem.* **28, 887.**
19. **E. Högfeldt, R. Chiarizia, P.R. Danesi and V.S Soldatov (1981),** *Chem. Scripta* **18, 13.**
20. **G.J. Lumetta, B.A. Moyer, P.A. Johnson and N.M. Wilson (1991), So/v.** *Extr. Ion Exch.* **9,155.**
21. **B.A. Moyer, C.F. Baes, Jr., G.N, Case, G.J. Lumetta, and N.M. Wilson (1993), Sep.** *Sci. Technol.* **28, 81.**
22. **R. Chiarizia, R.C. Gatrone and E.P. Horwitz (1995),** *Solvent Extr. Ion Exch. 1***3, 615.**
23. **Handbook of Chemistry and Physics, 77th Edition, pp.5-102 - 5-106, 1996-1997.**
24. **S. Kotrly and L. Sucha (1985), Handbook of Chemical Equilibria in Analytical Chemistry, Ellis Horwood Limited, Chichester,** *West Sussex,* **pp. 116-11.**
25. **E.O. Otu and A.D. Westland (1990),** *Solvent Extr. Ion Exch.* **8, 827.**
26. **P.R. Danesi, R. Chiarizia, M.A. Raieh and G. Scibona (1975),** *J. Inorg. Nucl. Chem.* **37, 1489.**
27. **M.A. Raieh, N. Zakareia and H.F. Aly (1979),** *J. Radioanal. Chem.* **52, 285.**
28. **Y. Marcus (1985), Ion Solvation, J. Wiley & Sons, New York, Chapter 5.**

The effects of diluent on the extraction behavior of uranium (VI) with benzyloctadecyldimethylammonium chloride (BODMAC) from chloride solution

Jin-xin Guo \ Si-xiu Sun [u] , ming-xia Li \ Zhi-lei Yin[1] , Hua Pang[1] , zi-lan Wang \ Zhao-li Meng[2]

School of Chemistry and Chemical Engineering, Shandong University, Jinan 250100, P.R. China

[2] School of Pharmacy, Shandong University, Jinan, 250012, P.R. China

The extraction mechanism of uranium (VI) from highly concentrated chloride solution by the quaternary salt benzyloctadimethylammonium chloride (BODMAC) in three diluents was investigated. The mechanism of extraction of uranium (VI) belongs to ion association. The composition of extracted species were $R_4N \cdot U0_2Cl_3$ and $(R_4N)2 \cdot U0_2Cl_4$in different diuents. The dependence of the extraction distribution ratios on the concentrations of aqueous hydrochloric acid, extractant, salting-out agents and the temperature was investigated. The experimental results show that the extraction capacity of BODMAC is not only dependent on the diluents, but also on the types of salting - out agents.

INTRODUCTION

The uranium recovery from seawater has attracted extensive attention from chemists because of its importance in relation to energy problems. Bittern of seawater is an important chemical resource that contains a lot of concentrated valuable metals such as NaCl, $MgCl_2$and $MgS0_4$. The concentration of uranium (VI) in the bittern is usually 500-600 times higher in comparison with that in the seawater. Therefore it is significant to study on the extraction of uranium (VI) from bittern resources.

Highly hydrophobic quaternary ammonium salts have long been regarded as excellent

' E-mail: ssx@sdu.edu.cn

extractants because of their high loading capacity at essentially all pH values and fast kinetics, which can also be used in the liquid emulsion membrane (LEM) technique and ion exchange process. We have previously investigated the influence of some factors on uranium (VI) extraction with benzyloctadecyldimethyl ammonium chloride (BODMAC, R_4NCl) in chloroform from chloride solution [1], As the effect of diluent plays an important role [2-6] in uranium (VI) extraction, the present work extends to the study of influence of the diluents on the distribution behavior of BODMAC.

EXPERIMENT

Reagents and apparatus

BODMAC (Dalian Chemical Factory) was recrystallized from a mixture of anhydrous ethanol and acetone. Uranium chloride solutions were prepared by dissolving uranyl chloride ($U0_2Cl_2 \cdot H_20$) (A.R.), sodium chloride (NaCl)(A.R.) and magnesium chloride ($MgCl_2$)(A.R.) with non-ionic water. All other reagents used were A.R. grade.

A self-made vibrator(temperature controlled with a precision: ±1K) and 752 type UV grating spectrophotometer (Shanghai Third Analysis Instrument factory) has been used.

Experimental methods

The solvent extraction experiments were carried out by shaking equal volumes of BODMAC dissolved in three diluents, and uranyl chloride solution with different contents of chloride solution in a stoppered tube at 298_+IK for 40 minutes. The extraction systems were then centrifuged to complete the separation of the phases. The uranium (VI) concentration in the aqueous phase was determined by Arsenazo III spectrophotometric method [7], The Uranium (VI) concentration in the organic phase was calculated by mass balance. The initial uranium (VI) concentration C°u in the aqueous phase was 4.75×10^{-5} mol/l.

RESULTS AND DISCUSSIONS

Influence of extractant concentration

The extraction of uranium (VI) from aqueous solution containing 1.5 mol/l magnesium chloride and 1.0 mol/l sodium chloride at pH3.84 with BODMAC in three diluents increases with extractant concentration (Fig. 1).

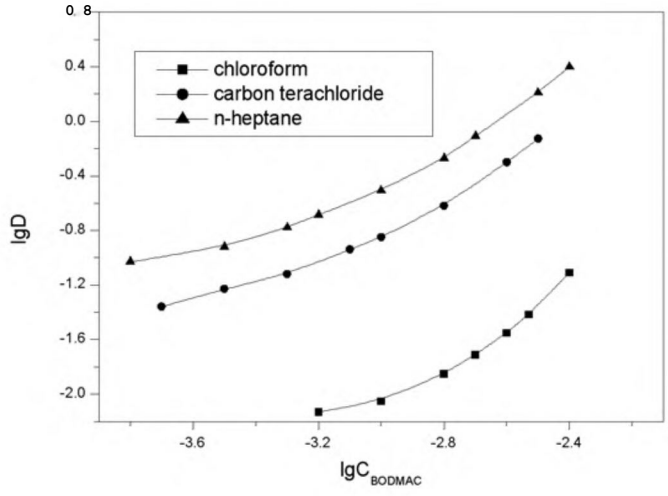


Figure. 1 Dependence of the distribution ratio D of U (VI) on the BO DM AC concentration

As seen in Fig. 1, the plots of lgD vs. lgC BODMAC give curves with slopes of about 1 and 2 in three diluents employed, which indicates that there are two extracted complexes in three diluents and can be expressed as R_4N •$U0_2Cl_3$and $(R_4N)_2$ *$U0_2Cl_4$. Therefore, the extraction reaction can be expressed as follows:

$$U0_2^{2+} + 2Cr + R_4NCl_{(o)} = R_4N \bullet U0_2Cl_{3(o)} \qquad Kex\text{-}, \qquad (1)$$

$$U0_2^{2+} + 2Cl' + 2R_4NCl_{(o)} = (R_4N)_2 \bullet U0_2Cl_{4(0)} \qquad Kex_2 \qquad (2)$$

And the distribution ratio D:

$$D = \{ Kexi\ [Cl\ 1^2[R_4NCl]\ (o) + Kex_2\ [Cl\ *]\ ^2[R_4NCl]^2\ _{(o)} > /\{ 1 + E\ 3\ i[Cl]^1\} \quad (3)$$

$$lg\ D = lg\{ Kex,\ [Cl]\ ^2[R_4NCl]\ _{(o)} + Kex_2\ [Cl]\ ^2[R_4NCl]^2\ _{(o)}\} - lg\{ 1 + EP\ ,[Cl]^1\} \quad (4)$$

where Kex is the equilibrium constant, the subscript (o) denotes organic phase, other substances in aqueous phase without subscripts; [ ] denotes the equilibrium concentrations; 0 i is the stability constant for uranium(VI) complex[8]. Since the uranium (VI) concentration is negligible compared with that of BODMAC, the equilibrium concentration of BODMAC is equal to the initial concentration. Therefore, the equilibrium constants were calculated by Eq. (4). The results presented in Table 1. show that the extraction efficiency of BODMAC for uranium (VI) in three diluents decreases in the order: n-heptane, carbon tetrachloride and chloroform. Here, the interaction between molecules of BODMAC and diluents should be considered. Chloroform is a strong polar solvent, thus there is strong interaction between molecules of BODMAC and chloroform compared with that of the other two solvents, which led to the low extraction efficiency. It is worth noticing that in the extraction process, when the concentration of BODMAC in three dilutes increased to a certain

value, W/O emulsion phenomena appeared respectively though the concentration of inorganic electrolytes in the aqueous phase is high. The high emulsion ability means that BODMAC could be use for liquid emulsion membrane (LEM) extraction of uranium(VI) from solutions containing certain amount inorganic electrolytes.

Influence of sodium chloride and magnesium chloride concentrations

The extraction of uranyl chloride solutions containing various concentrations of sodium chloride and magnesium chloride respectively with BODMAC (3.0 XIO'^{3} mol/l) in chloroform and BODMAC (2.0X10'^{3} mol/l) in carbon tetrachloride and n-heptane gave the results shown in the Figs.2 and 3. It can be seen that the distribution ratios increase slowly at low concentrations and then increase obviously at higher concentrations in n-heptane and carbon tetrachloride systems, but the increase of distribution ratio is not very obvious in chloroform system due to the strong solvation of chloroform. Sodium chloride and magnesium chloride here act as not only salting-out agents that increase the uranium (VI) activity by hydration, but also as homoions, shifting the extraction equilibrium to the right.

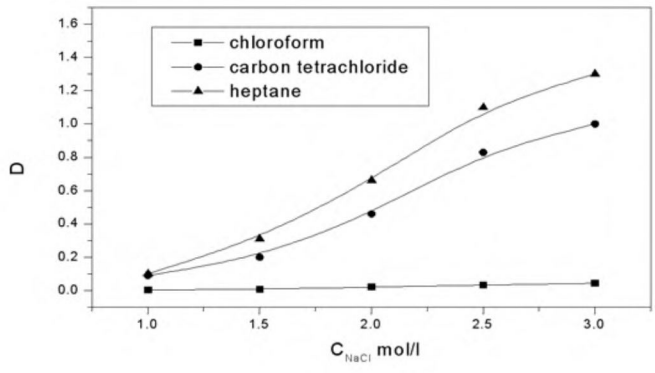


Figure2. Effect of sodium chloride concentration on the distribution ratio D

Influence of sulfate magnesium concentration

The results obtained are shown in Fig.4. In the solutions containing 1.5 mol/l magnesium chloride and 1.0 mol/l sodium chloride at pH3.84, the distribution ratio of BODMAC for uranium (VI) decreases with the increase of sulfate magnesium concentration. Since relatively low concentration of $S0_4^{2"}$ anions are sufficient for forming complex uranyl ions suitable for extraction. The decrease of distribution ratio arises from the formation of less readily extractable complexes. Therefore, the higher concentration of sulfate magnesium, the lower extraction efficiency of BODMAC for uranium (VI) from high concentrated chloride solution. It is known that the compounds formed by BODMAC and uranium (VI) sulfate complexes are more hydrophilic than that formed by BODMAC and uranium (VI) chloride complexes due to the strong hydration ability of $S0_4^{2'}$ anions. Hence they are more difficult to be extracted to non-polar carbon tetrachloride and n-heptane systems compared with polar chloroform system, especially for n-heptane system, the distribution ratio is much lower than that of the other two systems. Therefore the extraction efficiency of

BODMAC for uranium (VI) from chloride solution containing certain amounts of magnesium sulfate in three diluents increases in the order: n-heptane, carbon tetrachloride and chloroform.

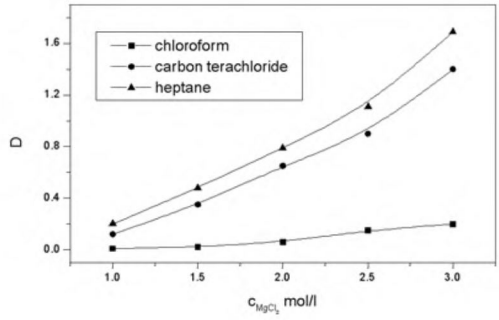


Figure3. Effect of magnesium chloride concentration on the distribution ratio D

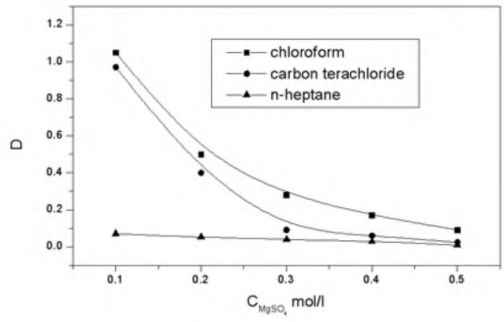


Fig.4 Effect of magnesium sulfate concentration on the distribution ratio D ; CBODMAC = 3.0 x 10-3 mol/l (in chloroform); CBODMAC = 2.0 x 10-3 mol/l (in carbon tetrachloride and n-heptane);

Influence of hydrochloric acid concentration

It is seen from Fig.5 that when uranium (VI) is extracted from hydrochloric acid solutions of different acidity into three diluents of BODMAC, the distribution ratios at first rise with acidity up to a maximum of 4 mol/l and then fall again. The tendency of the change in extraction distribution ratio is similar in three diluents. The increase in the distribution ratio is attributed to the salting-out effect of hydrochloric acid and the formation of a uranyl chloride hydrochloric acid complex at low acidity. While at higher acidity, the decrease in the distribution ratio is attributed to the formation of less readily extractable complexes and the interaction between hydrochloric acid and BODMAC.

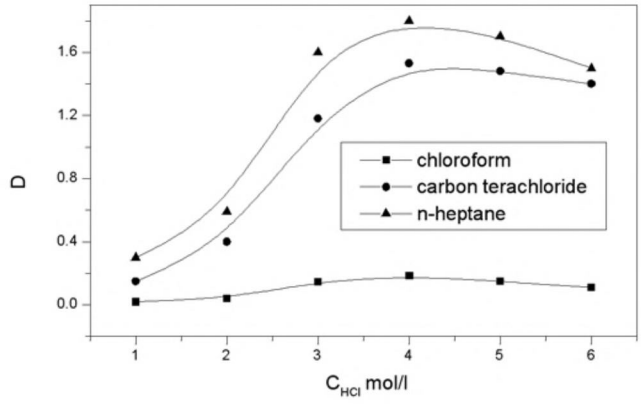


Figure5. Effect of hydochloride concentration on the distribution ratio D; $C_{BO}DMAC$ = 3.0 x 10'3 mol/l (in chloroform); $C_{B}ODMAC$ = 2.0 x 10~3 mol/l (in carbon tetrachloride and n-heptane)

Influence of the temperature

In this case organic solutions of 3.0x10'3 mol/l BODMAC in chloroform and 2.0 xlO'3 mol/l BODMAC in n-heptane and carbon tetrachloride were used; the aqueous phases contained 4.75x10'5mol/l uranium (Vl) in the presence of 1.5mol/l $MgCl_2$ and 1.0 mol/l NaCl at pH3.84. The results (Fig.6) show that the distribution ratio decreases with rising temperature in three diluent systems. This indicates that the extraction process is exothermic and low temperature is beneficial to the extraction process in all dilutents.

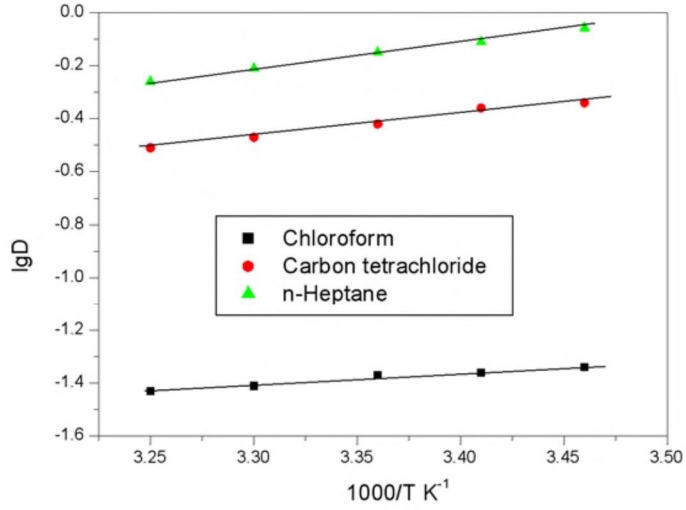


Figure6. Effect of temperature on the distribution ratio D; $C_{BO}DMAC$ = 3.0 x 10'3 mol/l (in chloroform); $C_{BO}DMAC$ = 2.0 X 10'3 mol/l (in carbon tetrachloride and n-heptane);

According to Van't Hoff equation:

d lgD / (d(1/T)= -AH°/2.303R

The enthalpy change for the reaction *(AH°)* **can be calculated. The value** *of A H°* **in three diluent systems are shown in tablel.**

Tablet Equilibrium constants at 298 ± 1K and extraction enthalpy of U (VI) with BODMAC in different diluents

Diluent	chloroform	carbon tetrachloride	n-heptane
lgKexf	-0.04	1.41	1.82
lgKex2	3.02	4.23	4.43
A H°, kJ/mol	-8.42	-15.32	-18.19

As the extraction system contains several reactions, the calculated *A ff* **is a complicated thermodynamic function to some degree, which may be also influenced by different interaction between diluent and extractant and between molecules of the extracted complex. The more negative** AH^0 **is, the easier the extraction reactions take place. As more energy is needed to destroy the strong interaction between molecules of BODMAC and chloroform, the** AH^0 **is smaller compared with that of the other two diluents. The other factors such as the charge of density distribution of the extracted complex should also be considered.**

CONCLUSIONS

The extraction efficiency of BODMAC for uranium (VI) from chloride solution in three diluents increases in the order: chloroform, carbon tetrachloride and n-heptane. In different diluents the extraction capacity of BODMAC is different, but the extracted complexes are the same and can be expressed as $R_4N \cdot U0_2Cl_3$ **and** $(R_4N)_2 \cdot U0_2Cl_4$ **.The distribution ratio increases with the increase of hydrochloride acid concentration and reaches the maximum, then decreases. The extraction of uranium (VI) increases with increase of sodium chloride and magnesium chloride concentration in three diluents. However, in the presence of magnesium sulfate in chloride solution, it can be seen that the order of extraction efficiency is not only opposite to that of the chloride solution in three diluents, but the distribution ratio decreases with the increase of the magnesium sulfate in the aqueous phase. The extraction process is exothermic and low temperature is beneficial to the extraction though the enthalpy change is much different in three diluents.**

REFERENCES

1. J. X. Guo, Y. Z. Yang, S. X. Sun et al (2004), *J. Radioanal. Nucl. Chem.* **261: 221-224.**

2. S. X.Sun, G. X. Sun, Y. Cui et al (1997), *Chim. Acta,* **64 (in Chinese)**

3. S.X. Sun, Y. Li, Y H. Yang, et al (1996), *Chim. Acta,* **1101 (in Chinese)**

4. I. Komasawa, T. Otake, Y. Ogawa (1984), *J. Chem. Eng. Japan,* **17: 410-412**

5. Z. Li, B. R. Bong, M. H. Wu (2001), *J. Radioanal. Nucl. Chem* **.250 :195-197**

6. J. X. Guo, Y. Cui, X. Y. Song, X. M. Li, X. Sun, W. L. Fan, G. X. Sun, S. X. Sun (2003), *J. Radioanal. Nucl. Chem.* **257: 317-321**

7. L. Y. Dong, Analytical Chemistry of Uranium, Nuclear Energy Publishing Company, Beijing, 1982, P. 174

8. A. н ,Moskevn(1984), *Coordinate Chemistry of Actinides,* **Nuclear Energy Press, Beijing, , Pl3, P36 (in Chinese)**

DEPENDENCE OF EXTRACTION EQUILIBRIUM OF MONOCARBOXYLIC ACID ON THE RELATIVE BASICITY OF EXTRACTANT (TRPO)

Xinchang SHAN, Wei QIN*, Youyuan DAI

State Key Laboratory of Chemical Engineering, Department of Chemical Engineering, Tsinghua University, Beijing 100084, China

The extraction method based on reversible chemical complexation is highly effective and selective for separating polar organic solutes from dilute solutions. In this work, TRPO-1-octanol and TRPO-kerosene were selected as the solvents, eleven kinds of carboxylic acids were used as the solutes, and the relative basicity of the extractant to the solute extracted ($pK_{a,BS}$) was measured at various TRPO concentrations. An equilibrium model representing the relationship among the apparent extractive equilibrium constant, *K*n, the nature of the solute extracted, pK_a, and the extractants basicity, pK_{aBS}, was proposed on the basis of the reactive extraction theory. The results shown that the pK_{aBS} increases a little with TRPO concentration for the diluent, 1-octanol, while it is not dependent on the TRPO concentration for kerosene as the diluent apparently. The properties of carboxylic acid extracted, hydrophobicity and pK_a, effect the pK_{aBS} obviously. The mathematic models proposed can be used to predict the extractive equilibrium of monocarboxylic acid extracted by TRPO well.

INTRODUCTION

Liquid—liquid extraction is an efficient, economical and environmentally friendly method for separation of acid. It is, therefore, applicable in recovery of acids from waste streams, facilitation processes through separation of acidic products or by products, recovery of acidic fermentation products, etc.[1'4]

King et al.[5] proposed that the equilibrium constant of a 1:1 complex decreases by about 1 logarithm unit for each unit increase in pK_a for the extraction equilibria of carboxylic acids (acetic, lactic, succinic, malonic, fumaric and maleic acids) with amines, but the results of the experimental data did not fit the above rule well. Hano et al.[6] investigated the extraction equilibria of organic acids (acetic, glycolic, propionic, lactic, pyruvic, butyric, succinic, fumaric, maleic, itaconic, tartaric, citric and isocitric) with trioctylphosphine oxide (TRPO) in hexane and concluded that the number of carboxyl groups and the extraction equilibrium were controlled by the hydrophobicity of the acid.

Eyal et al. [1] defined the amine apparent basicity (pK_{aB}) which is suggested to express the nature of extractant:

$$\overline{R_3NJW} \xleftrightarrow{K_{a,B}} \bar{I}p + H' \qquad {}_PK_{a\,B} = {}_PK_{a\,B}\pounds_d s_a \qquad (1)$$

where $pK_{a\,8}$' is the specific basicity which can be determined by half neutralization with HCl,

and the species in the organic phase are marked with an overbar. pK_{aB} depends on the amine concentration and diluent type.

Wei Qin et al.[7'9] studied the extraction equilibrium behaviours of mono-carboxylic acids by trioctylamine (TOA) in various diluents, 1-octanol, $CHCl_3$, MIBK, hexane and CCl_4, and the specific basicity of TOA with HCl solution was measured. It was found that the apparent reactive equilibrium constant (*K*n) shows the same tendency with the pK_{aB}\ and the most important factors effecting the extraction

equilibrium of the acids are the hydrophobicity parameter (log P), the electronic parameter (pK_a) and the extractant parameter (pK_{aB})'. A correlation equation with the constants log P, pK_a and $pK_{a\,B}$' is express as follows:

$$\log K_1 i = 1.3164\,(pK_{aB}'-pK_a) + \log(87.93P) \qquad r=0.9587 \qquad (2)$$

Eq. (2) can be used to predict the extraction equilibrium of organic acids with TOA.

The specific basicity (pK_{aB}') is the relative basicity of the mixture solvent to HCl, excluding the solute nature. Obviously, if the basicity of the mixture extractant is relative to the solute extracted, this relative basicity can present all of the nature of the solute extracted, diluent and extractant, as well as the solvation power.

The main objective of this research is to define a new basicity of the solvent, the relative basicity of the extractant to the solute extracted ($pK_{a\,BS}$), propose a new method used to measure the relative basicity, and obtain the $pK_{a\,BS}$ with eleven kinds of monocarboxylic acid. Also, the feasibility of mathematic models proposed based on the chemical reactive theory, to describe the extractive equilibrium behaviours with only two parameters, pK_a and pK_{aBS}, was investigated and verified.

MATERIALS AND METHODS

Chemicals.

All of the acids, formic, acetic, propionic, butyric, caproic, monochloroacetic, dichloroacetic, trichloroacetic, hydrochloric, glycolic, glyoxylic and lactic acids were analytical reagents. Characteristics of carboxylic acids are presented in Table 1 and Table 2. The extractant, TRPO, was kindly supplied by CYTEC Canada Incorporation free of charge and used without further purification. Hydrogenated kerosene from Petro China and 1-octanol (analytical reagent) were used as diluent.

Relative Basicity of TRPO Determination. The relative basicity of the extractant ($pK_{a\,BS}$), which is suaaested to exDress the nature of extractant, defined as follows:

$$\overline{S}\,\overline{H^+} \rightleftharpoons \overline{S} + \overline{H^+}$$

$$K_{a<B} = [\overline{S}][H^+]/[\overline{S}\,\overline{r}] \qquad (3)$$

Where S represents TRPO, the species in the organic phase are marked with an overbar, and all of the concentrations are expressed in molar terms. According to Eq. (3), pK_{aBS} is almost equal to the solution pH value if [5] = [5-// $^+$]. Thus, pK_{aBS} in various diluents and TRPO concentrations is determined if the extraction experimental conducts under the condition of [5] = [<S-//$^+$].

The solvents used were TRPO-diluent mixtures. All extraction experiments were conducted in 100 ml_ flasks at 25±0.5°C. An organic phase was prepared containing 0.5 mol/L TRPO in diluent and a 1:1 stoichiometric amount of monocarboxylic acid. A sample of 30~40g of the organic phase was mixed with a 0.3 mol-L"[1] NaOH solution. The phase volume ratio was chosen to reach an extracted acid to NaOH ratio of 2:1. The two phases were mixed for 1~2 h, separated two phases, and the pH of the aqueous phase was determined.

Analysis Methods.
The pH value of the aqueous phase was determined with a pH meter (Hanna pH 201 model) with deviation of ±0.02.

Mathematic Models of Extraction Equilibrium

The reactive extraction equilibrium for polar dilute solutions of organic solutes can be described by the mass action law in which the equilibrium behaviour is modelled by postulating the formation of various stoichiometric complexes of acid and TRPO. In this paper, the extraction equilibrium was described by a set of equilibrium involving the dissociation equilibrium of carboxylic acid in the water, and the association of TRPO with carboxylic acid. It is assumed that only 1:1 complex was formed and that the extraction reaction between TRPO and carboxylic acid took place at the organic-aqueous interface.
The reactive extraction equilibrium:

$$HA + \overline{S} \text{+-^} \overline{HA\text{-}S} \qquad (4)$$

In the case of this paper, $pK_{a\,BS}$ is the pH values in the aqueous phase at $\overline{S}$ « $\overline{HA}$ ■ $\overline{S}$, and the dissociated equilibrium of carboxylic acid is concern, then

$$K_{u} = \frac{[\overline{HA}]}{[H^{+}f]} = CK \qquad (5)$$

$$\log K_{u} = 2pK_{aBS} - pK_{a} + C' \qquad (6)$$

Where C is a constant less than 1, which reflect the dependence of solute extracted by the diluent on the complexes concentration in the organic phase at $[\overline{S}] = [\overline{HA \cdot S}] + [\overline{HA}]$. As most of the acid back-extracted in the aqueous phase was sodium acetate, the concentration of undissociated acid is very less, C^l. Eq. (6) becomes,

$$\log K_{n} = 2pK_{aBS} - pK_{a} \qquad (7)$$

RESULTS AND DISCUSSION

Effect of TRPO Concentration on the $pK_{a\,BS}$-

Figure 1~2 and Table 1 shown the relative basicity of extractant solvent at various TRPO concentration in the 1-octanol and kerosene. The varying of $pK_{a\,BS}$ with TRPO concentration depended on the diluent type, $pK_{a\,BS}$ increases a little with increasing TRPO concentration for the protic and polar diluents, 1-octanol, while pK_{aBS} is not dependent on the TRPO concentration for kerosene as the diluent apparently.

Tablet Model parameters for TRPOAe **rosene -** *carboxylic acid systems*

<PTRPO	pK_a BS	log/Ci^mol-L'1)10	P^a.BS	logKnOnolL1)10
	formic acid, pK_a= 3.75,logP= -0.538		acetic acid, pK_a = 4.75,logP= -0.313	
0.1	2.22	0.8248	2.66	0.6794
0.3	2.23	0.8248	2.66	0.6794
0.5	2.26	0.8248	2.69	0.6794
0.7	2.27	0.8248	2.70	0.6794
0.9	2.28	0.8248	2.70	0.6794
1	2.31	0.8248	2.73	0.6794
	propionic acid, $pK_{,3}$ = 4.87,logP= 0.29		butyric acid, pK_a = 4.81 ,logP= 0.802	
0.1	2.90	1.0864	3.12	1.5490
0.3	2.91	1.0864	3.14	1.5490
0.5	2.92	1.0864	3.15	1.5490
0.7	2.97	1.0864	3.16	1.5490
1	2.97	1.0864	3.18	1.5490
	caproic acid, pK_a = 4.85,logP= 1.99		chloroacetic acid, pK_a = 2.87, logP= 0.139	
0.1	3.17	1.6138	2.28	1.8124
0.3	3.20	1.6138	2.31	1.8124
0.5	3.22	1.6138	2.32	1.8124
0.7	3.25	1.6138	2.33	1.8124
0.9			2.36	1.8124
1	3.26	1.6138	2.36	1.8124
	dichloroacetic acid, pK_a=1.26, logP=0.705		trichloroacetic acid, 0.713	pK_a = 0.52,logP=
0.1	2.35	3.1139	2.36	4.0719
0.2			2.38	4.0719
0.3	2.37	3.1139	2.38	4.0719
0.5	2.38	3.1139	2.39	4.0719
0.7	2.40	3.1139	2.41	4.0719
0.9	2.40	3.1139	2.43	4.0719
1	2.41	3.1139	2.46	4.0719
	lactic acid, pK_a = 3.86,logP= -0.78			
0.1	1.84	0		
0.3	1.89	0		
0.5	1.90	0		
0.7	2.009	0		
1	2.04	0		

Table2. Model parameters for TRPO/1 -octanol—carboxylic acid systems

<PTRPO	*PKa* ,8S	LogKi-iCmolL'1)10	P^a BS	logK^mol-L'^10
	acetic acid, pK_a= 4.75,logP= -0.313		propionic acid, pK_a = 4.87,logP= 0.29	
0.1	2.09	-0.5332	2.33	-0.1212
0.3	2.45		2.63	
0.5	2.52		2.72	0.5962
1	2.73		2.97	0.9079
	glycolic acid, pK_a= 3.83, logP= -1.097		glyoxylic acid, pK_a = 3.34,logP= -0.413	
0.2	1.14	-1.5079	1.84	0.3696
0.3	1.97		1.88	
0.5	2.25		2.16	
1	2.52		2.33	

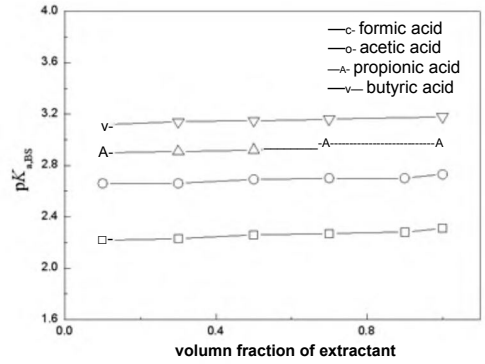


Figure 1. Effect of extractant volume fraction on $pK_{a\,B}$s in the TRPO/kerosene

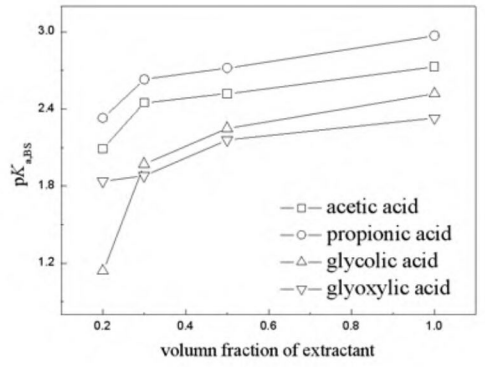


Figure 2. Effect of extractant volume fraction on $pK_{a\,B}$s in the TRPO/1-octanol

Effect of Acids on the $pK_{a,B}$s-

Generally, the nature of the extracted acid, its hydrophobicity and acidity, is one of the most important factors affecting the degree of extraction, and the degree of extraction is expected to increase with increasing acidity and hydrophobicity of the acid. Carboxylic acids used in this paper were categorized into two types to investigate the dependence of nature of the acid on the p/<$_{a\ BS}$: (1) organic acids with large difference in hydrophobicity and a similar pK_a values; (2) carboxylic acids with larger differences in their pK_a values.

As indicated in Figure 3, the relative basicity of TRPO for carboxylic acids with similar pK_a values fall in the order, caproic acid > butyric acid > propionic acid > acetic acid > formic acid. It is apparent that the longer-chain carboxylic acids are more hydrophobic and can be extracted better by TRPO, therefore, $pK_{a\,B}$s increases with increasing logPof the solute.

For the acids with larger differences in the pK_a, the stronger the acidity of an acid, the stronger the dissociation power between the acid and TRPO, so that the carboxylic acid with less pK_a can be better extracted into the organic phase. Similarly, the results obtained in this work (Figure 4) show the order being trichloroacetic acid > dichloroacetic acid > monochloroacetic acid > formic acid. pK_{aBS} increases with increasing acidity of the solute extracted. It is clear that the relative basicity of the extractant solvent depended on the nature of organic acids extracted, the pK_a and log *P.* Compared these two parameters of the solute extracted, pK_{aBS} is more sensitive to log *P* of the acid, which is same as the results obtained by Hano[161].

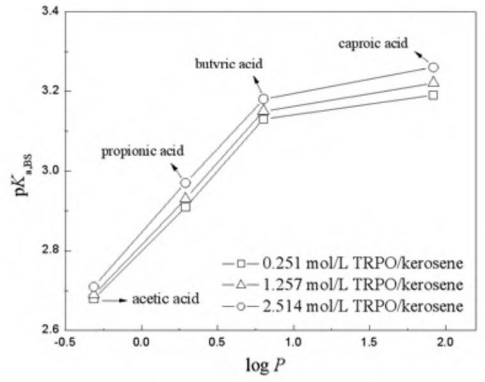


Figure 3. Effect of log P on the relative basicity in the TRPO/kerosene systems

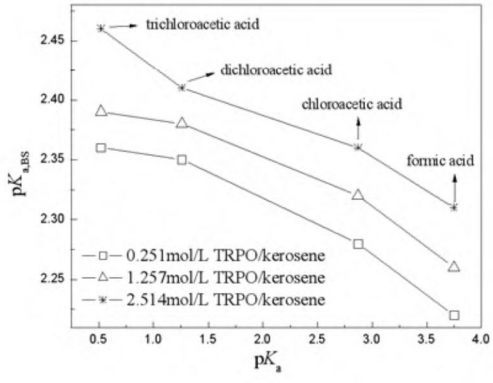


Figure 4. Effect of pK_a on the relative basicity in the TRPO/kerosene systems

Effect of Diluent on the pK_{aBS}.

In general, the dilute, especially the polar diluent, effects on the extraction equilibrium excluding the simple dilute power, As shown in Figure 5, the similar results was obtained in this work, and the relative basicity of TRPO in inert diluents, kerosene, is higher than that in polar diluents, 1-octanol. This is opposite of the result for TOA/diluent system. It maybe results from the decreasing of reactable TRPO concentration with the acid, since 1-octanol can H-bonded to TRPO. Therefore, the optimal mixture extractant solvent is TRPO - inert diluent.

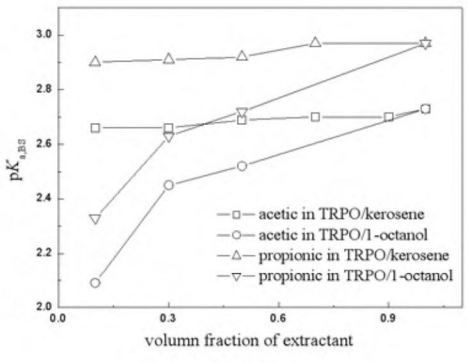


Figure 5. Comparison of pK_{aBS} of TRPO in 1-octanol to that in kerosene

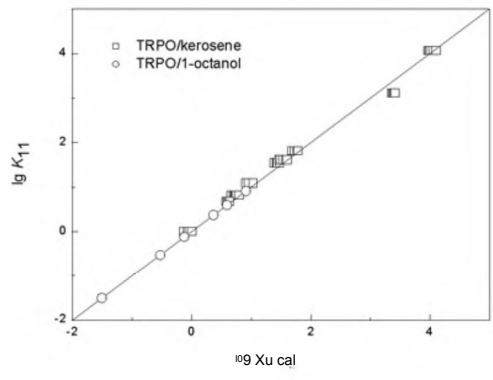


Figure 6. **$logK_{11ca}$, vs logKn**

Verifying the mathematic models.

The apparent extraction equilibrium constants K-n for eleven monocarboxylic acids with TRPO are listed in Table 1 and 2. Plot of logK-n vs $logK\text{-}n_{ca}$i based on the Eq. (7) proposed in this paper shown in Figure 6, and a higher correlation coefficient (r), 0.9947, and the less deviation (within ±5%) between the calculated logK-n values and the measured data were obtained. It proved that the calculated logKn values fit the measured data very well. Thus, Eq. (6) can be used to predict the extraction equilibrium of organic acids extracted with TRPO with more accuracy.

CONCLUSIONS

In the present work, the relative basicity of the extractant to the solute was measured at various TRPO concentrations. pK_{aBS} increases a little with increasing TRPO concentration for the diluents 1-octanol, while $pK_{a,BS}$ did not changed with TRPO concentration apparently. . The properties of carboxylic acid, hydrophobicity and pK_a, effect the $pK_{a\,BS}$ obviously.

The research results in this work proved that the extraction equilibrium of the mono-carboxylic acids extracted by TRPO can be predicted base on the two parameters, $pK_{aB}s$ and pK_a, with high accuracy.

ACKNOWLEDGMENTS

This work was supported by National Natural Science Foundation of China, Grant No. 29836130

REFERENCES

1. **Eyal. A. M.; Canari. R. pH Dependence of Carboxylic and Mineral Acid Extraction by Amine-Based Extractants: Effect of pK_a, Amine Basicity and Diluent Properties.** *Ind. Eng. Chem. Res.* **1995, 34, 1067-1075.**
2. **King C J.** *Separation Process Based on Reversible Chemical Complexation, Handbook of Separation Process Technology(Rowseau R W ed.).* **New York: John Wiley& Sons, 1987, 760-774**
3. **Zhang Jin, Dai Youyuan. The swing effects in extract ion processes based on chemical complexation.** *Modern Chemical Industry,* **1999, 19(3): 8-11.**
4. **Tamada J A, Kertes A S, King C J. Extraction of carboxylic acids with amine extractants. 1. equilibria and law of mass action modeling.** *Ind. Eng. Chem. Res.,* **1990, 29(7): 1319-1326**
5. **Tamada. J.A.; King, C. J. Extraction of Carboxylic Acids with Amine Extractants. 2. Chemical Interactions and Interpretation of Data.** *Ind. Eng. Chem. Res.* **1990.29.1327-1333.**
6. **Hano. T.; Matsumoto, M; Ohtake, T.; Sasaki, K.; Kawano, Y. Extraction Equilibria of Organic Acids with Tri-n-octylphosphineoxide. J.** *chem.. Eng. Jpn.* **1990, 23,734-738**
7. **Wei Qin; Zhengyu Li; Youyuan Dai. Extraction of Monocarboxylic Acids with Trioctylamine: Equilibria and Correlation of Apparent Reactive Equilibrium Constant.** *Ind. Eng. Chem. Res.* **2003, 42, 6196-6204.**
8. **LI Zhenyu, QIN Wei and DAI Youyuan. Extraction Equilibria Behavior of Monocarboxylic Acids by Trioctylamine (I): Extraction Equilibria.** *Journal of Chemical Industry and Engineering (China).* **2004, 1, 54—58.**
9. **LI Zhenyu, QIN Wei and DAI Youyuan. Extraction Equilibria Behavior of Monocarboxylic Acids by Trioctylamine (II): Apparent Extraction Equilibrium Constant and Correlation.** *Journal of Chemical Industry and Engineering (China).* **2004, 1, 59—64.**
10. **Yundong Wang, Yuxin Li, Yi Li, Jingyi Wang, Zhengyu Li, and Youuan Dai. Extraction Equilibria of Monocarboxylic Acids with Trialkylphosphine Oxide.** *J. Chem. Eng. Data.* **2001, 46, 831-837.**

EXTRACTION PROPERTIES OF PLATINUM GROUP METALS WITH DIAMIDE COMPOUNDS

Hirokazu Narita, Mikiya Tanaka and Kazuko Morisaku

National Institute of Advanced Industrial Science and Technology (AIST), Tsukuba, Japan

The extraction properties of the platinum group metals (PGMs) from a hydrochloric acid solution using the following five neutral diamide compounds in chloroform were investigated: bidentate /V,/V'-dimethyl-/V,/\/'-diphenyl-malonamide (MA); tridentate A/, A/'-dimethyl-A/, A/'-diphenyl-diglycolamide (DGA); tridentate A/,/V'-dimethyl-/V,/\/'-diphenyl-dipicolinamide (DPA); tridentate A/,A/'-dimethyl-A/,A/'-diphenyl-thiodiglycolamide (TDA); and tetradentate A/,A/'-dimethyl-A/,A/'-diphenyl-3,6-dioxaoctanediamid e (DOODA). The extractabilities for all the PGM ions using MA and DPA are insufficient. However, in the TDA system, the extraction of Pd(II) is almost 100% over a wide HCl concentration range. A good separation between Pd(II) and Pt(IV) is also obtained below 5 M HCl. Additionally, the extraction rate of Pd(II) is very high. In the DGA system, the high extractability of Pt(IV) is achieved at the higher HCl concentrations.

INTRODUCTION

In recent years, the extensive use of the platinum group metals (PGMs) has been in automotive industries for catalytic converters, in electronics and chemical industries and so on. Simultaneously, their wastes have increased. Therefore, the recovery of the PGMs is of commercial and environmental importance. The separation of PGMs by solvent extraction is one of the most popular methods in the field of PGM recovery. Since PGMs possess similar chemical properties, their mutual separation is very difficult. Furthermore, the slow extraction of PGM ions from aqueous chloride media has been one of the toughest problems for a long time. Hence, many organic extractants for PGMs have been synthesized and studied [1,2],

Diamide compounds have been attracting much attention as extractants for trivalent lanthanides (Ln(III)) and actinides (An(III)) in spent nuclear fuel treatment processes. Among them, bidentate malonamides have been widely studied at the CEA, France [3], However, their extractabilities are not as good as conventional neutral bidentate organophosphorus extractants like CMP, CMPO and DPDO. In contrast, tridentate diglycolamides [4-7] and dipicolinamides [8,9] showed high distribution ratios of Ln(III) and An(III). The magnitude of the Ln(III) extraction by O-donor diamide extractants is in the order of bidentate malonamide < tetradentate 3,6-dioxaoctanamide << tridentate diglycolamide [6], However, extraction studies on PGM with diamide compounds were still limited. Recently, we have carried out PGM extractions using /V,A/'-dimethyl-A/,A/'-dioctyl-thiodiglycolamide (MOTDA), which has a sulfur atom instead of the ether atom in the diglycolamides [10], MOTDA can immediately extract Pd(II) with a high selectivity. Therefore, the diamide-type compounds can be expected to be used for the different PGM extractions.

In order to elucidate the extraction properties of the PGMs with diamide extractants, a

comparison of the extractabilities obtained by some diamide extractants having different numbers and types of donor atoms can provide useful information. Consequently, this study carried out the solvent extraction of PGMs in hydrochloric acid solution using the following five diamide compounds: bidentate A/,A/'-dimethyl-/V,/\/'-diphenyl-malonamide (MA), tridentate /S/,A/'-dimethyl-A/,A/'-diphenyl-diglycolamide (DGA), tridentate A/,A/'-dimethyl-A/,A/'-diphenyl-dipicolinamide (DPA), tridentate *N,*A/'-dimethyl-A/,/V'-diphenyl-thiodiglycolamide (TDA) and tetradentate A/,A/'-dimethyl-/\/,A/'-diphenyl-3,6-dioxaoctanediamide (DOODA). On the basis of the obtained extractabilities, their extraction properties are discussed.

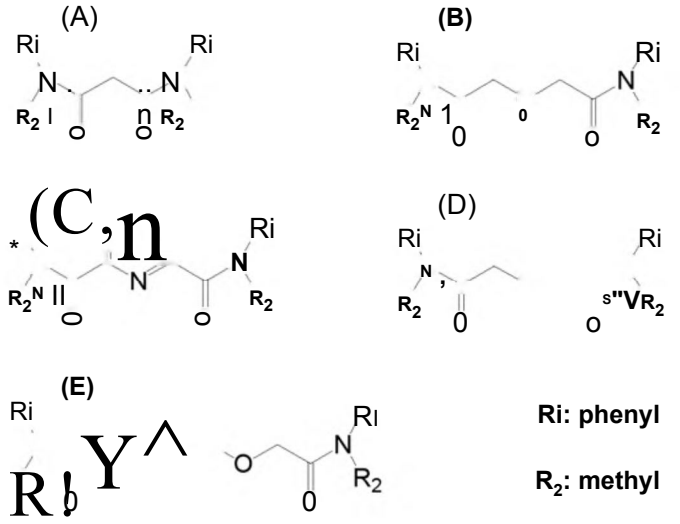


Figure 1. Structure of diamide compounds.
(A) MA, (B) DGA, (C) DPA, (D) TDA, (E) DOODA

EXPERIMENTAL

Reagents

All the diamide compounds were synthesized using a procedure described below. The stock solutions of metals were prepared by mixing atomic absorption standard solutions of ruthenium, rhodium, palladium, iridium and platinum (Aldrich). All the other chemicals used in this study were of reagent grade.

Extractant Syntheses

All the extractants were synthesized based on the procedure described in previous papers [11,12], as follows.

TDA and DOODA

Thiodiglycolic acid (or 3,6-dioxaoctanedioic acid) was converted to thiodiglycolic chloride (or 3,6-dioxaoctanedioic chloride) by refluxing a solution of thiodiglycolic acid dissolved in thionyl chloride with a small amount of /V,/V-dimethylformamide for 3 hours at 50°C. The resulting solution was dropwise added to a mixed solution of triethylamine and A/-methylaniline in chloroform, and then refluxed with stirring for 3 hours at 60°C. After removal of the chloroform under vacuum, the residue was successively washed with water, 1M HCl and a 5% aqueous sodium carbonate solution. The product was purified by recrystallization from a mixture of hexane and methyl acetate.

MA, DGA and DPA

The carboxylic chlorides (malonyl chloride, diglycolic chloride, 2,6-pyridinedicarboxy

dichloride) were commercially available (Aldrich). The reaction procedure with *N*-methylaniline and the subsequent purification were similar to that described above.

The purities of all the extractants were over 98% on the basis of element analysis, ^{1}H NMR and liquid chromatography.

Solvent Extraction

The extractant diluted by chloroform was pre-equilibrated with the same volume of HCl solution in the absence of the metal ions. One milliliter of the pre-equilibrated organic solution and the same volume of the mixed metal solution; i.e., HCl solution containing 50 pg/L of the metal ions (Ru, Rh, Pd, Ir, Pt), were vertically shaken in a 10-mL glass tube at the amplitude of 100 mm and a frequency of 200 spm, and then centrifuged. The concentrations of the metal ions were measured by ICP-AES (Horiba, ULTIMA2). The mass balance of the metals determined the concentrations in the organic phase before and after the extraction.

RESULTS AND DISCUSSION

Effect of HCl Concentration

Figure 2 shows the extraction percentages (E%s) of the PGM ions with the diamide compounds as a function of the HCl concentration. As for the diamide compounds having only O donor atoms; i.e., MA, DGA, and DOODA, the magnitude of the *E%* of Pt(IV) is in the order of MA < DOODA < DGA. This order is similar to that for the Ln(III) extraction properties [6], Since PGM ions belong to soft acids [13], it is readily expected that the MA hardly extracts all the PGM ions. In contrast, the E%s of PGM ions except for Rh(III) with the DGA increase with the HCl concentration and then that of Pt(IV) reaches over 98% above 5 M HCl. Taking into account that the DGA has only 'hard' O donor atoms, the formation of a complex with Pt(IV) would not be very stable, according to the HSAB theory [13], In the higher HCl region, therefore, protonated DGA could extract $PtCl_6^{2-}$ anions, which is the dominant species in this HCl region [14], by ion-pair formation. This estimation seems to apply to the extraction of Pd(II), which dominantly exists as $PdCl_4^{2-}$ above 1 M HCl solutions [15],

While the DPA possesses a pyridine N donor atom, which is softer than an O donor atom, the E%s of all the PGM ions are very low. This suggests that the pyridine N donor atom is not responsible for the coordination to the PGM ions and that the protonation of the DPA is much less than that of the DGA.

The extraction pattern of Pd(II) with the sulfur-containing diamide, TDA, is different from that with the other four extractants. The E% of Pd(II) is almost 100% in the wide HCl concentration range. Since S donor atoms have a stronger affinity for soft acids [13], it would appear that the thioether S directly takes part in the Pd(II) extraction. On the other hand, the Pt(IV) extraction is enhanced with an increase in the HCl concentration like the extraction with DGA, suggesting that the protonation of the TDA may also occur. Therefore, it is assumed that the extraction of Pd(II) is explained by intermediate mechanism between an ion-pair and a coordinative.

In terms of mutual separation, the TDA shows a good selectivity for Pd(II). The E% of the PGM ions except for Pd(II) from $\leq$5 M HCl solution is below 5%, while that of Pd(II) reaches almost 100%.

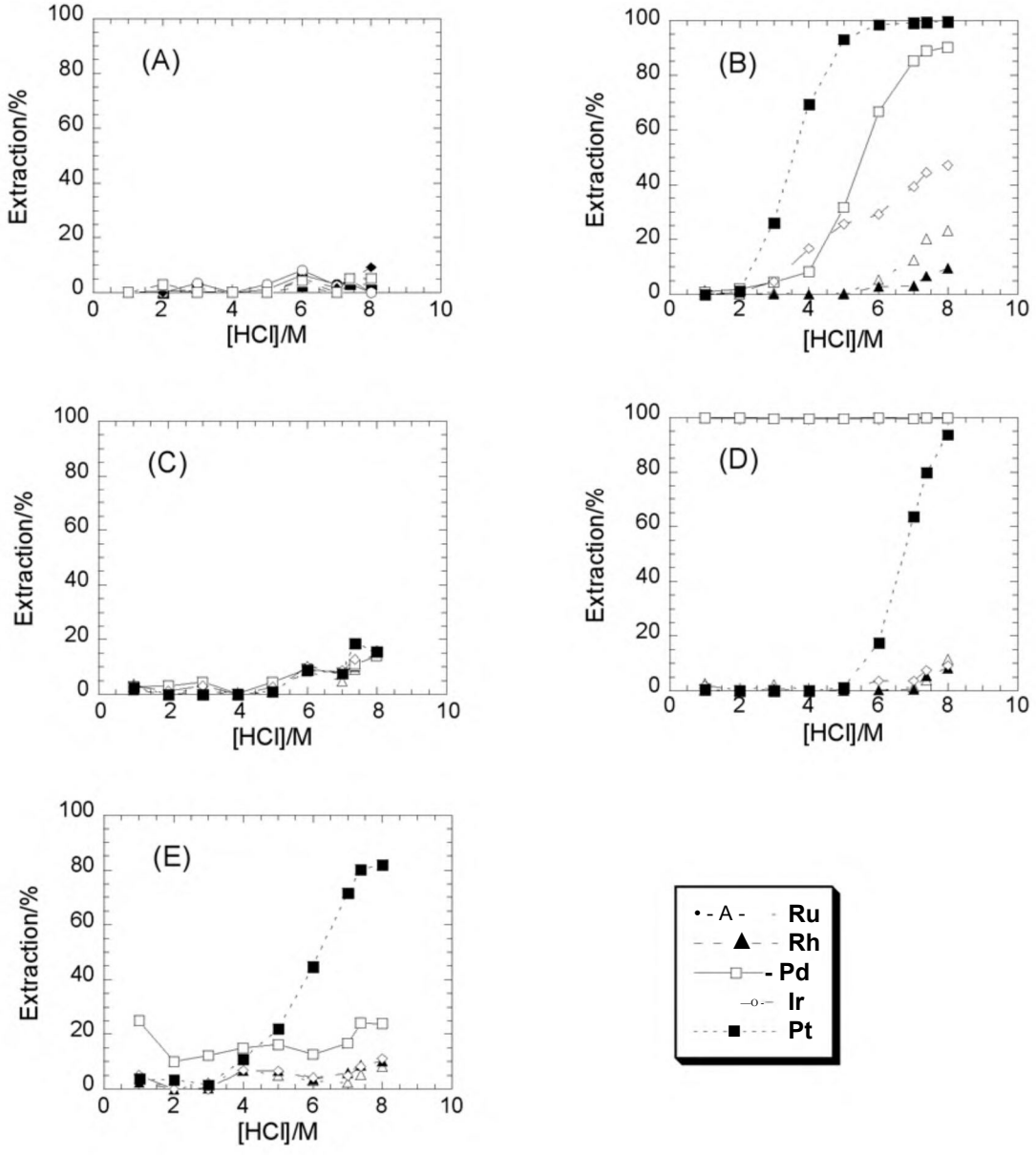


Figure 2. Extraction percentages of the PGM ions with (A) MA, (B) DGA, (C) DP A, (D) TDA, (E) DOODA. [Extractant]: 0.5 M in $CHCl_3$, Contact time: 120 min.

Extraction Rate and Selectivity in the TDA and DGA Systems

Since the TDA-Pd(II) and DGA-Pt(IV) systems show high extractabilities, the dependence of the E% on contact time was investigated (Fig. 3). In the 0.5 M TDA - 1 M HCl system, the E% of Pd(II) reached almost 100% in less than 5 min, while Pt(IV) is hardly extracted during all the contact times. Taking into account that the major problem of the selective extractions of Pd(II) has been their slow extraction, this rapid extraction of Pd(II) with a high selectivity is noteworthy. In the 0.5 M TDA - 6 M HCl system, Pd(II) is also rapidly extracted. In addition, the Pt(IV) extraction immediately attains equilibrium. So far, the Pd(II)/Pt(IV) mutual separation has been performed on the basis of the large difference in the extraction rate between Pd(II) and Pt(IV) from aqueous chloride solutions. Therefore, the mutual separation in the TDA system seems to undergo a different mechanism in conventional separation

systems. Similarly, the extraction rates of the PGMs in the 0.5 M DGA - 6 M HCl system are high.

It has been suggested that the extraction of PGM from HCl solutions in accordance with ion-pair formation is fast, since the protonated extractant quickly forms a chlorocomplex ion-pair which is immediately transferred to the organic phase [16,17], Accordingly, these results verify that the protonation of the DGA and TDA would occur.

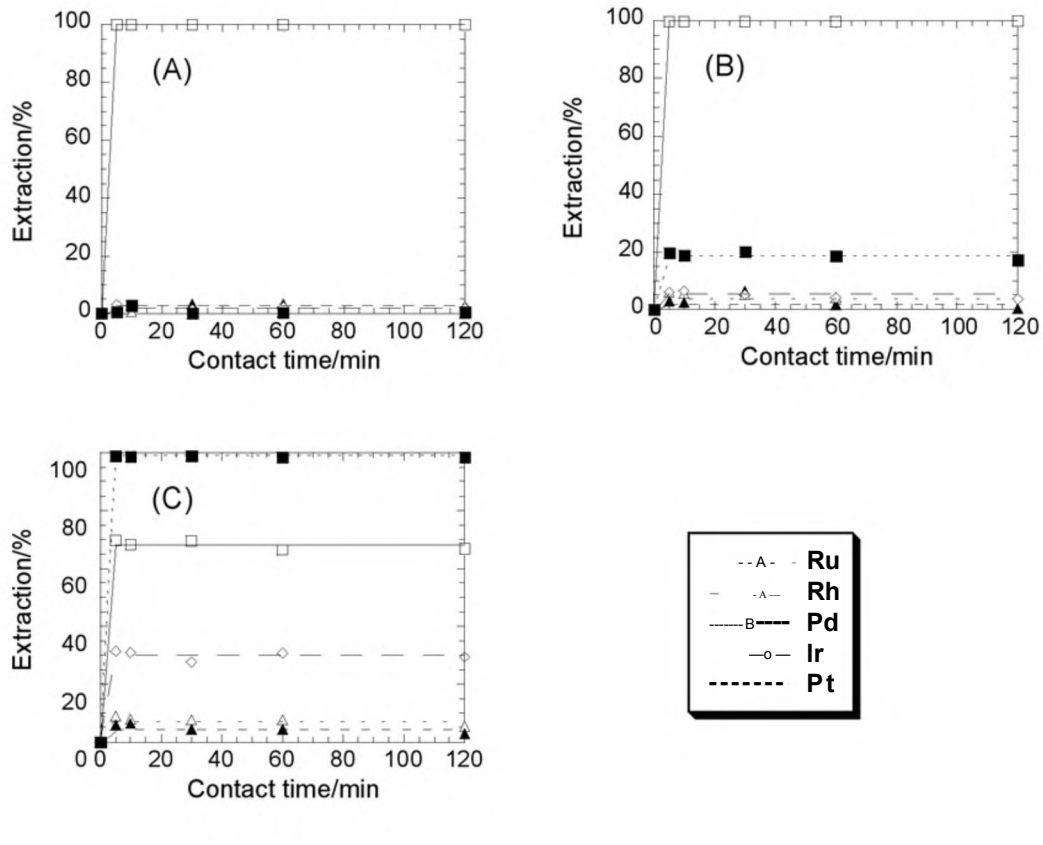


Figure 3. Extraction percentages of the PGM ions as a function of contact time. (A) TDA-1 M HCl, (B) TDA-6 M HCl, (C) DGA-6 M HCl, [Extractant]: 0.5 M in $CHCl_3$.

CONCLUSIONS

The five types of diamide compounds showed the different extraction properties of the PGM ions, which significantly depend on the number and kind of donor atoms. Both MA and DPA hardly extract all the PGM ions, suggesting that the pyridine N donor atom of the DPA does not participate in the coordination to the PGM ions. For the higher HCl concentrations, the E%s of Pt(IV) with DGA were over 98%. The Pd(II) extraction with TDA was almost 100% in the wide HCl concentration range. Therefore, the S donor atom of the TDA would take part in the coordination. This is consistent with the HSAB theory, in which S and Pd are soft. The extraction rates of the PGM ions with DGA and TDA were very high. These results indicate that an ion-pair mechanism could dominate in the DGA extraction system and an intermediate between an ion-pair and a coordinative mechanism in the TDA extraction system.

ACKNOWLEDGEMENTS

The authors wish to thank Dr. Tsuyoshi Yaita, Japan Atomic Energy Research Institute, for useful discussions and Mr. T. Abe, Chiba Institute of Technology, for experimental assistance. This study was supported by Industrial Technology Research Grant Program in '03 from New Energy and Industrial Technology Development Organization (NEDO) of Japan.

REFERENCES

1. **A.T. Yordanov and D.M. Roundhill (1998),** *Coord. Chem. Rev.,* **170, 93-124.**
2. **M. Cox (1992), Solvent Extraction and Hydrometallurgy: Principles and Practices of Solvent Extraction, J. Rydberg, C. Musikas and G.R. Choppin (eds.), Marcel Dekker, Inc., New York, pp. 357-412.**
3. **C. Madic, M. Lecomte, P. Baron and B. Boullis (2002), C.** *R. Physique,* **3, 797-811.**
4. **H. Narita, T. Yaita, K. Tamura and S. Tachimori (1998),** *Radiochim. Acta,* **81,223-226.**
5. **H. Narita, T. Yaita, K. Tamura and S. Tachimori (1999),** *J. Radioanai. Nucl. Chem,* **239, 381-384.**
6. **H. Narita, T. Yaita and S. Tachimori (2004),** *Solvent Extr. Ion Exch.,* **22, 135-145.**
7. **H. Narita, M. Tanaka, T. Yaita, K. Tamura and S. Tachimori (2004),** *Solv. Extr. Res. Dev., Jpn.,* **11, 53-62.**
8. **A. Shimada, T. Yaita, H. Narita, T. Yaita, S. Tachimori and K. Okuno (2004),** *Solvent Extr. Ion Exch.,* **22, 147-161.**
9. **A. Shimada, T. Yaita, H. Narita, T. Yaita, S. Tachimori, T. Kimura, K. Okuno and Y. Nakano (2004),** *Solv. Extr. Res. Dev., Jpn.,* **11, 1-10.**
10. **H. Narita, M. Tanaka, K. Morisaku and T. Abe (2004),** *Chem. Lett.,* **33, 1144-1145.**
11. **G. Thiollet and C. Musikas (1989),** *Solvent Extr. Ion Exch.,* **7, 813-827.**
12. **L. Yao, R.M. Wharf and G.R. Choppin (1995), Solvent Extraction of Eu(III) and Am(III) with thio and amide extractants: Separations of f Elements, K.L. Nash and G.R. Choppin (eds.), Plenum Press, New York, pp. 31-42.**
13. **R.G. Pearson (1963),** *J. Am. Chem. Soc.,* **22, 3533-3539.**
14. **Lars Gunnar Sillén (1971), Stability constants of metal-ion complexes, Supplement No 1, The Chemical Society, London.**
15. **G. Levitin and G. Schmuckler (2003),** *Reactive and Functional Polymers,* **54, 149-154.**
16. **M. Wisniewski (2000),** *J. Radioanai. Nucl. Chem,* **246, 693-696.**
17. **J.S. Preston and A. C. du Preez (2002),** *Solvent Extr. Ion Exch.,* **20, 359-374.**



A Preliminary Study of the Toluene/Water/Acetone/Phenol System

Alcina Mendes, Peter Curtis, Colin Tamsett and Mark Pursell

**Department of Chemical Engineering, Imperial College London,
London SW7 2AZ, United Kingdom**

A preliminary study has been conducted into solute partitioning and interfacial tension for the toluene/water system with the solutes acetone and phenol added to the aqueous phase. The concentration range studied was 0 - 1M for acetone and 0 - 0.2M for phenol.

The partition coefficient of each of the solutes was affected when both solutes were present in the aqueous and over the concentration range studied the partition coefficient for each solute was found to be a linear function of the other solute's concentration. The magnitude of the effect was found to be greater in the case of phenol i.e. phenol has a greater effect on the partitioning of acetone than acetone has on the partitioning of phenol.

The addition of either solute to the aqueous phase reduced the interfacial tension, with phenol giving a greater reduction; when both solutes were added to the aqueous phase the lowering effect on the interfacial tension was cumulative. An empirical correlation has been derived for interfacial tension in the quaternary toluene/water/acetone/phenol system.

INTRODUCTION

The optimisation of mass transfer processes has become very important in recent years and the need to conduct fundamental studies on multicomponent systems has increased. This is clearly shown in the amount of research done in the last few years in comparison to the last thirty. Multicomponent diffusion has been treated mathematically (e.g. [1][2]) but there has been very little experimental research on multicomponent physical mass transfer reported in the literature e.g.[3][4][5][6][7][8][9][10][11]). A lot more experimental work is needed for knowledge in this field to progress.

The preliminary work presented here aims to start filling this knowledge gap, by investigating both partition coefficient and interfacial tension for the quaternary Toluene/Water/Acetone/Phenol (TWAP) system. It is important to note though, the experiments carried out provide only a first step in understanding some of the physical properties of complex multicomponent systems.

PREVIOUS WORK

An investigation into the previous research relevant to this work has shown that the ternary system Toluene/Acetone/Water (TAW) has been the most researched. The work published by Misek [12] for the EFCE, gives correlations for predicting both interfacial tension and partition coefficients for a given system with a specified aqueous mass fraction of acetone.

Another ternary system that has been investigated before, but to a much lesser degree than TAW is the Toluene/Phenol/Water (TPW) system. Of the few papers found, the work of Dutta and Patil [13] is amongst the most relevant. Their work involved the addition of phase transfer catalysts to the toluene/water system to examine the effect on interfacial tension. Their aim was to investigate the effect of surfactants on the interfacial tension and hence mass transfer. In addition, the "uncontaminated" system of toluene/water with phenol as solute was also studied.

Brodkorb and Slater [10] studied phenol in extractors and attempted to relate the performance of a rotating extraction column to single drop mass transfer experiments. In real extractors, phenol appears to alter the interfacial tension of droplets, which alters droplet formation and flow regimes in the system. It seems to be hard to predict the extraction of phenol as surface activity and concentration gradients vary according to drop motion. As quoted in their conclusion "in order to achieve better simulation of pilot-plant column performance, more extensive investigation of interfacial tension effect with phenol is advocated".

Von Reden's work [6] constituted a step forward in the knowledge of the ternary and quaternary systems. He stated that despite advanced knowledge of the TAW system, there was no quaternary data of any sort relating to the TWAP system. However, the most comprehensive investigations were carried out by Brodkorb et al. [8] [11] into describing mass transfer in the TWAP system.

The review of literature has confirmed that very little experimental data has been collected on quaternary multicomponent systems, particularly on the TWAP system; in industry, the TWAP system is a common system, and is found in the production of both acetone and phenol by the Hook process, as well as in caprolactam production. Therefore, the TWAP system was selected to be investigated in the present work.

EXPERIMENTS

In this work experiments have been carried out to measure the partition coefficients of acetone and phenol in the toluene/water system, and the interfacial tension of the organic/aqueous interface in the presence of both solutes.

All results have been obtained after equilibration of the phases. The separating flask used for equilibration held 50ml of each phase and was shaken and then left for a period of time to reach equilibrium, typically 24 hours.

Partition Coefficients

The partition coefficient is defined here as the ratio of concentration of the solute in the organic phase to that of the aqueous phase under equilibrium conditions; the concentration of solutes present in the aqueous phase was measured using gas chromatography.

The chromatography solution contained 0.7ml of the aqueous phase and 20j.il of 1-butanol used as an internal standard. After calibration tests two conversion graphs were constructed for converting peak area ratios into solute concentration - one for acetone and one for phenol which were then used to determine the aqueous phase concentrations.

Interfacial Tension

The interfacial tension between the organic and aqueous phases was measured using a Kruss K12 Process Tensiometer using the du Noiiy ring method. A volume of 15 ml of each phase was used and the experiments were carried out at 25 C.

RESULTS AND DISCUSSION

Partition Coefficient

Figure 1 shows a plot of the measured acetone concentration in the aqueous phase against the calculated organic phase concentration for the range of solute concentrations studied. Figure 2 shows similar plots for the phenol system. In these figures the experimental points have been joined by lines so that the trends are shown more clearly.

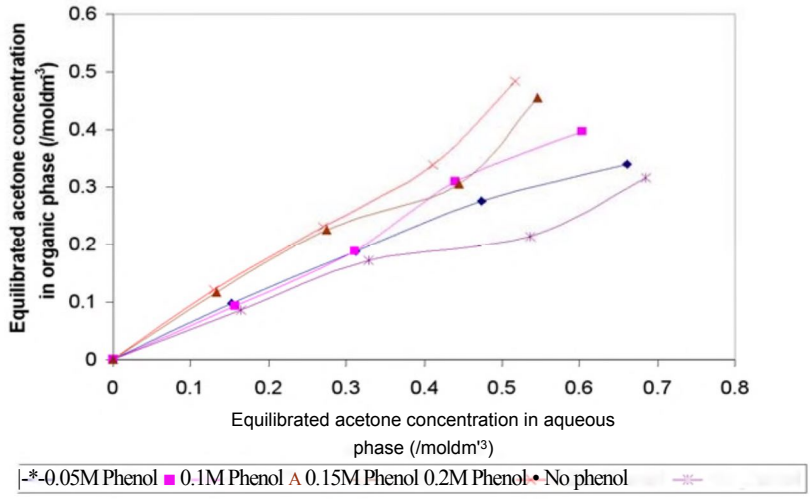


Figure 1 Phase concentrations of acetone with varying initial phenol concentrations

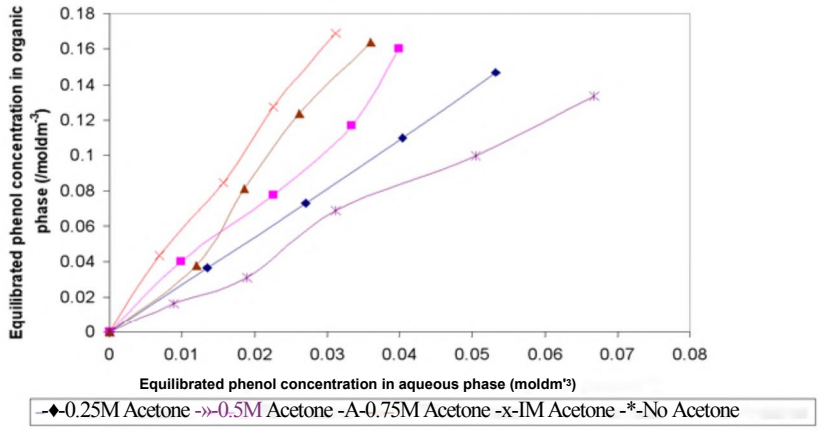


Figure 2 Phase concentrations of phenol with varying initial acetone concentrations

Both graphs suggest that a linear relationship exists between the equilibrium concentrations in both phases. Assuming such linearity exists, the gradient of each line will give an average value of partition coefficient. Therefore, it was decided to plot the average value of one solute partition coefficient against the average value of the equilibrated concentration of the other solute. These graphs are not shown here, for brevity, but the lines obtained have been

found to be represented by y = 11.75 x + 0.42 for the acetone partition coefficient and y = 5.77 x +1.99 for the phenol partition coefficient. These equations indicate that the presence of one solute induced further transfer of the other solute into the organic phase. Furthermore, the gradient of the line for the acetone partition is nearly twice that of the line for the phenol, suggesting that phenol has a greater effect on acetone partitioning than vice-versa.

It is also interesting to note, from those equations, how the partition coefficient for the TAW system is less than one and for TPW is greater than one. This implies that for the concentration ranges investigated here, acetone prefers to remain in the aqueous phase while phenol prefers the organic phase i.e. liquid-liquid extraction would be more effective at removing phenol than acetone from the aqueous phase.

Interfacial Tension

The interfacial tension measurements were carried out with the systems after equilibration and therefore the value of interfacial tension recorded corresponds to the value for the equilibrated concentration of solute.

In Figures 3 and 4 the average interfacial tension values are plotted against both acetone and phenol aqueous concentrations separately and each graph includes experimental points joined by lines (which serve as visual aids only) representing constant concentrations of phenol and acetone respectively. Some of the points may have higher errors associated with them but on average the experimental error has been estimated to be around 3%.

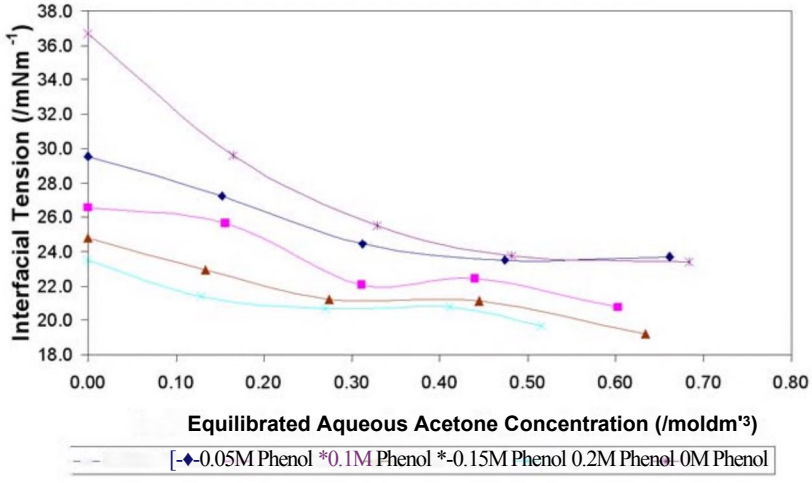


Figure 3 Variation of entire averaged interfacial tension with acetone concentration for various phenol concentrations

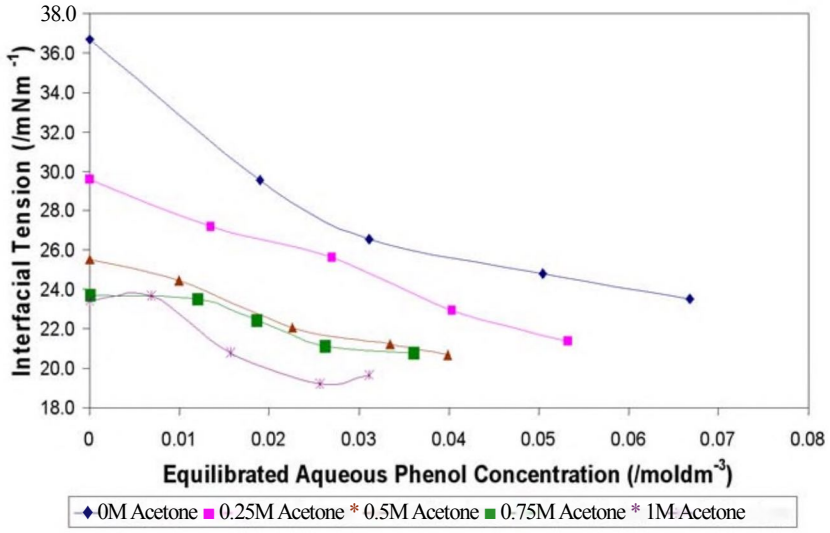


Figure 4 Variation of entire averaged interfacial tension with phenol concentration for various acetone concentrations

From the graphs the following conclusions may be drawn:

- **An increase in concentration of either solute causes the interfacial tension to reduce.**
- **An increase in concentration of both solutes causes the interfacial tension to reduce.**
- **The drop in interfacial tension per unit of solute added is more pronounced at bothlow phenol and low acetone concentrations.**

. For higher phenol concentrations and all acetone concentrations, the system appears to be approaching a constant interfacial tension value.

- **At high phenol concentrations, the effect of acetone on interfacial tension is less distinct.**
- **At very high solute concentrations, all the lines may converge to a single value.**
- **A comparison of the plots in Figures 3 and 4 shows that the presence of phenol at the toluene/water interface has a greater effect on the interfacial tension than acetone:**

Joint Effect of Phenol and Acetone

Using the trendline function in Excel, it was possible to formulate trendlines for all curves of equal acetone or phenol concentrations. Cubic trends were used as they gave a good compromise between good fit and simplicity. Thus, from each of the data series from Figures 4 and 5, correlations have been found for the interfacial tension (y) **of acetone and of phenol and are, respectively:**

$$r = \sum_{n=0}^{3} Y.C_{\gg} C_{ace}, a_q e_q^n$$ **Where**

	Co	C-i	C_2	C_3
TAW (no phenol)	36.7	-55.0	76.4	-35.5
0.05M Phenol	29.3	-16.3	12.1	-1.37
0.1M Phenol	26.2	-3.85	-25.5	33.3
0.15M Phenol	24.5	-16.2	29.1	-20.1
0.2M Phenol	23.4	-22.0	82.7	-97.6

and r = Z^{r}-c;- $_{phe,aq,eq}$ where:

	Co	Ci	C_2	C_3
TPW (no acetone)	36.7	-536	8040	-44700
0.25M Acetone	29.6	-200	1060	-1800
0.5M Acetone	25.5	137	15600	241000
0.75M Acetone	23.7	235	-24000	438000
1M Acetone	23.4	84.0	-16700	359000

Note that the above correlations are only valid for the range of concentrations studied.

Three - Dimensional Plot

The graphs in Figures 4 and 5 only display the effect of one solute whilst keeping the concentration of the other constant. To enable the simultaneous visualisation of the effects of both solutes on the interfacial tension a 3-D plot has been created using Excel which is shown in Figure 5. In this plot equilibrated aqueous acetone concentration are shown on the x-axis, initial aqueous concentration on the y-axis and interfacial tension on the z-axis.

A correlation to predict the formula of the above surface has also been attempted by carrying out a least squares fit in Maple and Mathematica. The objective formula is of the type:

$$\hat{\sigma} = \sum_{n=0}^{3}\sum_{m=0}^{3} C_{n.m} r^{*n}_{ace.aq.eq} C^{m}_{phe.aq.eq}$$

where the values generated for the constants are shown in Table 1.

Figure 5 must not be used for an in-depth quantitative study. However, it is useful qualitatively to see trends: an increase in the concentration of either solute decreases interfacial tension, and phenol has a far greater effect on the interfacial tension than acetone.

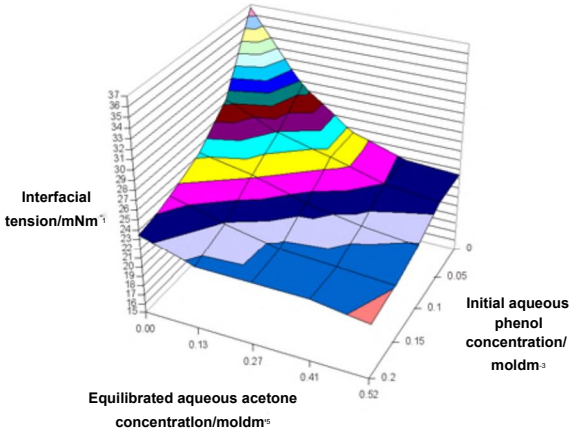


Figure 5 Three dimensional graph showing the correlation determined from experimental data

Co,o	36.7073
Co,i	-537.154
Co,£	8111.95
Co,3	-45562.
Cj.,0	-54.3312
Cl,l	2113.5
Ci ,z	-21923.5
Cl,*	-179325.
Cz,u	71.1554
Ct, i	650.214
C*,t	-228966.
C*,3	4.05642x10'
Cj,o	-29.4875
CJ,l	-3159.35
Cj ,t	234769.
C3,3	-2.2484x10⁵

Table 1 Values of the constants in the 3-D surface correlation

CONCLUSIONS

The preliminary experimental work presented here for the toluene/water system with acetone and phenol as added solutes has led to the following results for solute partitioning and the effect of the solutes on interfacial tension:

Partition Coefficient

- **For the range of concentrations studied, linear correlations have been obtained which are positive in gradient, thus showing that the presence of one solute in the aqueous phase increases the partitioning of the other solute into the organic phase; they also show that acetone prefers to remain in the aqueous phase while phenol prefers the organic phase i.e. liquid-liquid extraction would be more effective at removing phenol than acetone from the aqueous phase.**
- **Phenol has a greater effect on the partitioning of acetone than acetone has on the partitioning of phenol.**

Interfacial Tension

- **Addition of either or both solutes to the toluene/water system decreases the interfacial tension.**
- **Phenol had a greater effect than acetone on decreasing the interfacial tension.**
- **A preliminary correlation has been derived which allows the prediction of interfacial tension for any concentration of phenol and acetone in the concentration range studied.**

REFERENCES

1. **Wesselingh, J.A. and Krishna, R., 1990,** *Mass Transfer,* **Ellis Horwood.**
2. **Taylor, R. and Krishna, R., 1993,** *Multicomponent Mass Transfer,* **Wiley.**
3. **Maroudas N.G. and Sawistowski, H, 1964,** *Chem. Eng. Sci.,* **19, 919-931.**
4. **Zhang, S.H., Wang, Z. M. and Su, Y.F., 1990,** *Trans. Inst. Chem. Engrs,* **1968, Part A, 84-92.**
5. **von Reden, C., Slater, M.J. and Gorak, A., 1996,** *Proc. ISEC'96,* **Melbourne, 99-104.**
6. **von Reden, C., 1998,** *PhD Thesis,* **University of Dortmund, Germany.**
7. **Brodkorb, M. J., Gomis, V. and Slater, M. J., 1999, J.** *Chem. Eng.* **Data, 44, 591-596.**
8. **Chen, L-H and Lee, Y-L, 2000,** *AIChE J,* **46 (1), 160-167.**
9. **Lohner, H., Czisch, C., Lehman, P. and Bauckhage, K., 2001,** *Chem. Eng. Techn.,* **24 (11), 1157-1163.**
10. **Brodkorb, M. J. and Slater, M. J., 2001,***Trans IChemE,* **79 (Part A), 335-346.**
11. **Brodkorb, M. J., Bosse, D., Gorak, A., von Reden, C, Slater, M.J., 2003,** *Chem. Eng. & Proc.,* **42, 825-840.**
12. **Mišek, T., 1978,** *EFCE Recommended Systems for Liquid Extraction Studies.*
13. **Dutta N.N. and Patil, G.S, 1993,** *Can. J. of Chem. Eng,* **71, 802-804.**



NANOSCALE SELF-AEEMBLIES OF AMPHIPHILIC ACYLPYRAZOLONES FOR METAL ION RECOGNITION

Hengli Ma, Jun Yang, and Subra Muralidharan

Department of Chemistry and the Nanotechnology Research and Computation Center
Western Michigan University, Kalamazoo, MI 49008.
Phone: 269-387-3150
Email address: hma@unix.cc.wmich.edu; henglil_ma@hotmail.com

ABSTRACT

We have designed and synthesized a new and novel family of amphiphilic acylpyrazolones with various substituents in the 1,3, and 4 positions for the efficient separation of metal ions especially the trivalent lanthanide metal ions. These acylpyrazolones form nanoscale self-assemblies in the aqueous phase and on reverse phase silica chromatography support as inferred by transmission electron microscopy (TEM) and HPLC studies. Many of these amphiphilic ligands are capable of separating a mixture of light and heavy lanthanide ions in the pH range 2 - 3 . This separation is highly dependent on the self-assembling characteristics of these ligands. The variation of substituents in the 1,3, and 4 positions have a significant influence on the self-assembling properties and metal ion selectivities. A correlation between the separation selectivities and efficiencies and the self-assembling nature of these ligands have been made. Our studies for the first time demonstrate systematically the nature of nanoscale self-assemblies of amphiphilic ligands and the optimization of metal ions selectivities employing these systems. These studies demonstrate the importance of nanoscale self-assemblies of ligand systems for the recognition of closely related metal ions.

INTRODUCTION

Recognition of metal ions is important for a variety of applications such as recovery of metal ions and environmental remediation. Separation of lanthanide metal ions with high selectivity continues to be a challenge despite nearly sixty years of research dating back to the Manhattan Project. Self-assemblies at the nanoscale offer a new approach to this challenging problem, as properties at the nanoscale are often dramatically different from molecular and bulk material properties [1-3], One of the focus areas of research in group is he design, synthesis, and characterization of molecules that undergo spontaneous or stimulated self-assembly to yield nanostructures that have unique molecular recognition characteristics. We have previously demonstrated the efficacies of some acylpyrazolones for the separation of tervalent lanthanide metal ions by centrifugal partition chromatography and the role of the liquid-liquid interface in these separations [4,5], We have now synthesized amphiphilic acylpyrazolone and acylisoxazolone ligands for the recognition of lanthanide metal ions, characterized

their self-assemblies in the aqueous phase, and investigated their lanthanide metal ion recognition efficacies by employing them in the mobile phase of reverse phase HPLC. The acylpyrazolones and acylisoxazolones were chosen as the basic ligand structures for the recognition of lanthanides due to their low pK_a values (acylpyrazolone ~ 4 and acylisoxazolone = 1.5). The role of three important factors, namely (1) substituents on the acylpyrazolone ring, (2) nature and position of the lipophilic substituent, and (3) nature of the nanoscale self-assemblies in the aqueous phase and on the reverse phase silica support have been examined. The significant details of these studies are discussed in this paper.

EXPERIMENTAL APPROACH AND RESULTS

Synthesis of the acylpyrazolone ligands: The acylpyrazolone ligands with different substituents in the 1,3, and positions and different lipophilic groups in the 4 position were synthesized in excellent yields (80-95%) as indicated in Figures 1 and 2.

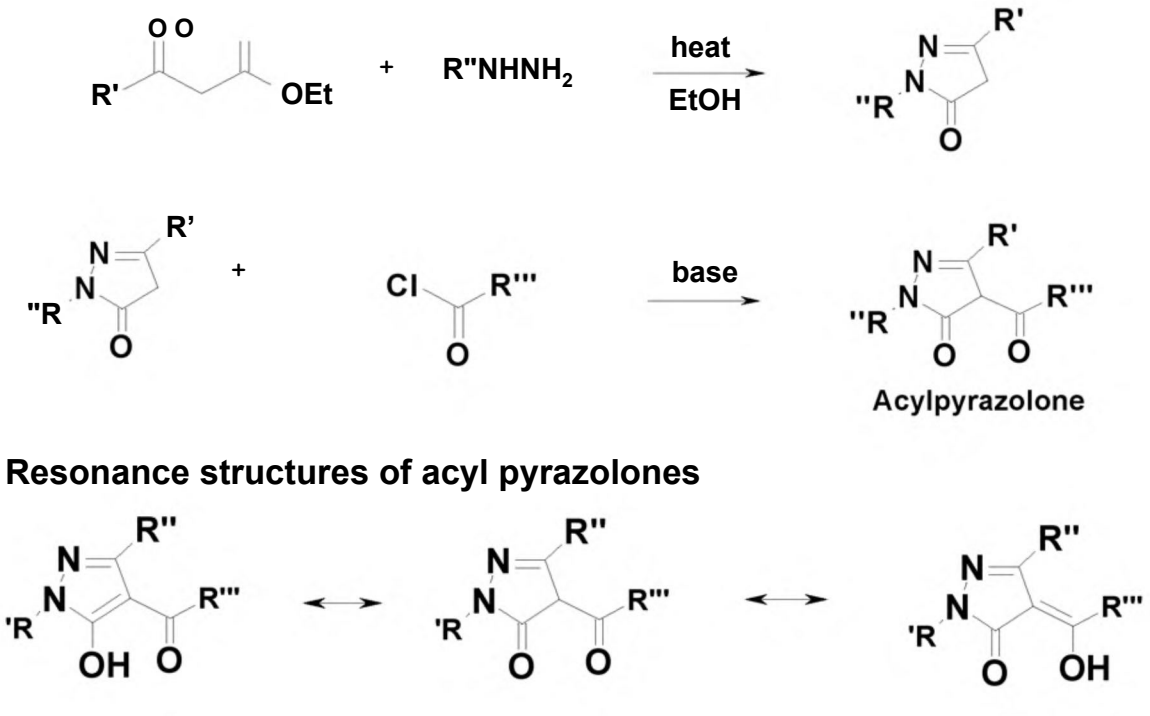


Figure 1. Synthetic scheme for acylpyrazolones

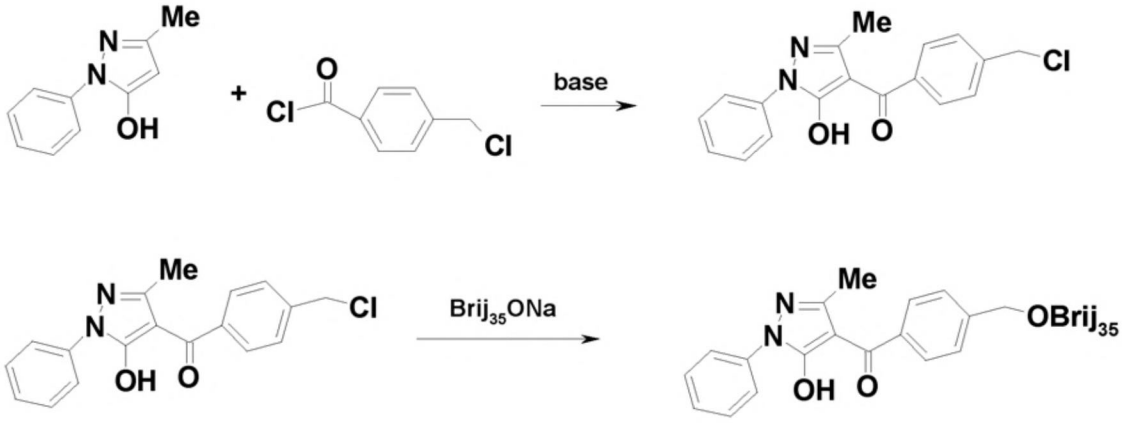


Figure 2. Synthetic scheme for amphiphilic acylpyrazolones

The separation of a mixture of light and heavy lanthanides is by 1-phenyl-3-methyl-4-benzoyl-5-pyrazolone with PEG 750 on the benzoyl ring (HPMBP750); see Figure 2) and 1-phenyl-3-methyl-5-valeryl-5-pyrazolone with PEG 750 (HPMVP750) is shown in Figure 3.

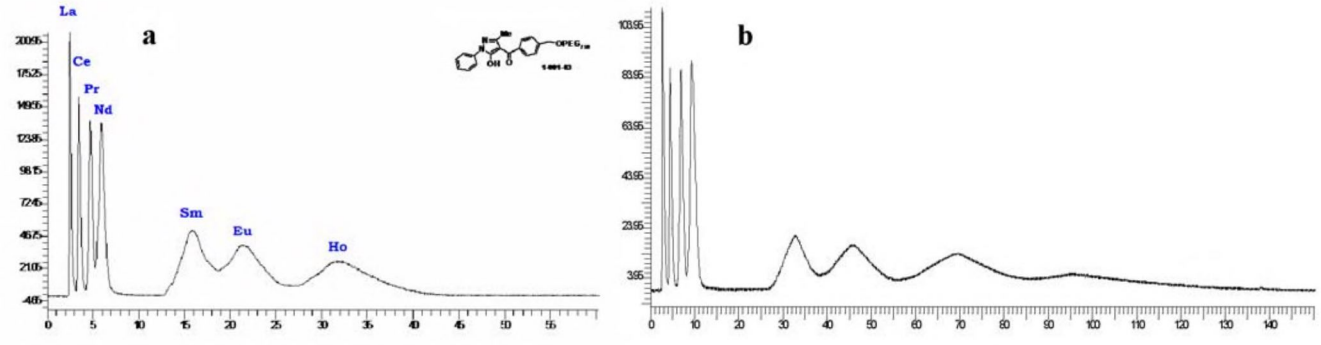


Figure 3. Separation of trivalent La, Ce, Pr, Nd, Sm, Eu, HO and Lu by (a) HPMBP750, ligand concentration = 5 x 10^{6} M, pH = 2.35 and (b) HPMVP750, ligand concentration = 5 x 10^{6} M, pH = 2.88 on **C$_{18}$** *reverse phase HPLC column*

The exoeriments were conducted bv addina the aooroDriate liaand to the mobile chase at the appropriate pH, equilibrating the reverse phase C_{18} column with the mobile phase, injecting 20 pL of the metal ion mixture and detecting the eluted metal ions by postcolumn derivatization with Arsenazo III at a wavelength of 590 nm. The HPMBP750 and HPMVP750 represent the best separations obtained to date among a family of pyrazolone ligands and various PEG (polyethylene glycol) groups studied. These two ligands in solution exhibit spherical, dendritic, linear assemblies including nanotubes which influence their separation efficacies. These structures could be discerned by transmission electron microscopy (TEM) imaging as displayed in Figure 4.

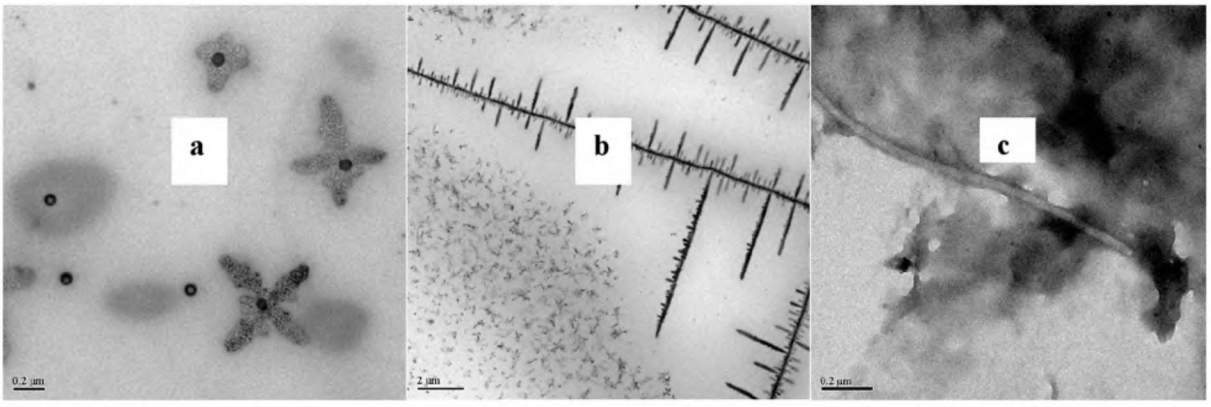


Figure 4. Self-assemblies of HPMBP750 and HPMVP750 in the aqueous phase exhibiting (a) spherical and dendritic, (b) linear, and (c) nanotube structures

This self-assembly in the aqueous phase influences the separation of the metal ions which depends on the equilibrium depicted in Figure 5. This indicates that the separation of the metal ion occurs by the competition for the metal ion by the ligands in solution and the ligands adsorbed on the Ci_8 stationary phase. It is proposed that the ligands due to their amphiphilic nature form a self-assembled monolayer on the C_{18} stationary phase. It is possible that more complex structures are present on the stationary phase and we are currently investigating these structures.

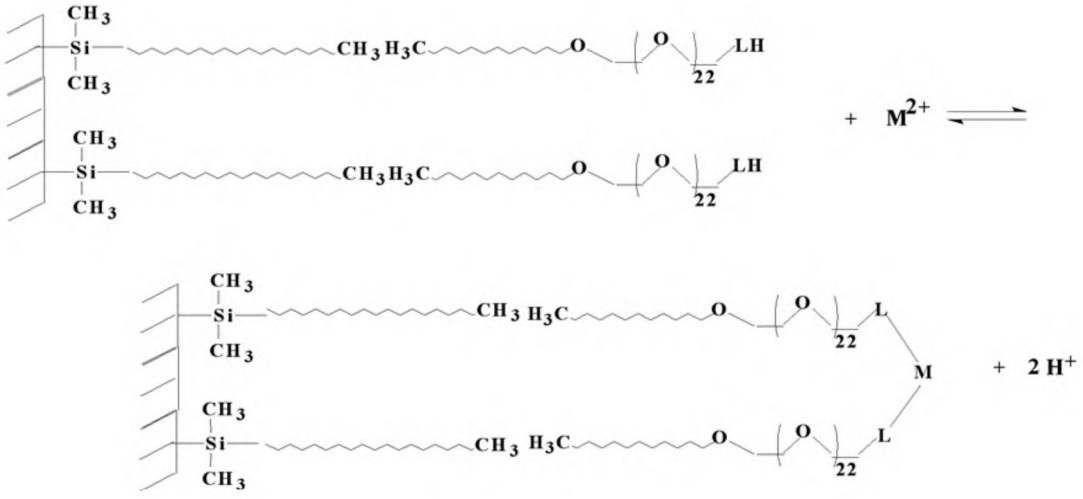


Figure 5. Proposed mechanism for the separation of lanthanide metal ions with amphiphilic acylpyrazolone ligands.

DISCUSSION AND CONCLUSIONS

The amphiphilic acylpyrazolone ligands mediate separation of tervalent lanthanide metal ions through a competitive mechanism depicted in Figure 5. These ligands self-assemble in the aqueous phase to form spherical, dendritic, linear, and nanotube structures. The interplay of the effect of the

substituents, the self-assemblies in solution and the competitive mechanism dictate the observed selectivities of these ligands. The ligand HPMBP750 only forms spherical and dendritic structures while the ligand HPMVP750 forms all the structures. We have observed that in the HPMBP ligands the presence of linear structures in solution adversely affects their selectivities. Similarly the substitution of the phenyl ring in the 4 position with alkyl group s also adversely affects the selectivities except in the case of HPMVP750 where the presence of linear structures and nanotubes enhances the selectivity to provide the best observed selectivity of the amphiphilic ligands.

REFERENCES

1. **"Recent Progress in Actinide Separation Chemistry", Z. Yoshia, T. Kimura and Y. Meguro, Editors, 1997,** *World Scientific,* **Singapore.**
2. **"American Chemical Society Symposium on Recent Advances in Metal Ion Separation and Preconcentration", M. L. Dietz, R. D. Rogers, and A. H. Bond, Editors,1999,** *ACS,* **Washington DC.**
3. **C. J. Sarzanini, J. Chromatogr. A, 1999, 850, 213.**
4. **G. Ma, H. Freiser, and S. Muralidharan, Anal. Chem., 1997, 69, 2827.**
5. **G. Ma, H. Freiser, and S. Muralidharan, Anal. Chem., 1997, 69, 2835.**

ACKNOWLEDGEMENT

This research was supported by the Office of Basic Energy Sciences of the U.S. Department of Energy.



Solid-liquid and liquid-liquid extraction for the pseudoternary system Hg^{2+}, Cl7H_20, TIOA (Tri-Iso-Octyl-Amine)/kerosene

C. P. Souza[1], M. B. D. Bezerra, E. M. B. D. Sousa

Universidade Federal do Rio Grande do Norte - UFRN
Departamento de Engenharia Quimica - DEQ/CT
Campus Universítario, Lagoa Nova CEP: 59072970 Natal, RN, Brazil.
Tel.: 055(84)215-3769 r 39 fax: 055(84) 215-3770
e-mail: carlson@ufrnet.br

ABSTRACT

The main purpose of this paper is to study phase diagrams of the systems which heavy metals and organic compounds are involved. The ternary system TI0A-H_20-$HgCl_2$ was studied using the Quasi-isothermic Thermometric Method and others like conductimetry and cloud point methods. This diagram is important for the extraction processes of pollutant agents. Quasi-isothermic Thermometric Method gets solubility data based on the heat measurements associated to transformations that occur in system at almost constant temperature. The global composition of the mixture is known and modified by the diluent addition. In accordance with the temperature behavior, one knows the exactly where it had the transition, this interval of time is transformed into solubility data, such data allows to construct an isotherm at 25°C.

Keywords: Phase diagram; Thermometry; Solid-Liquid Equilibrium, Liquid-Liquid Equilibrium.

INTRODUCTION

The study of phase diagram in electrolyte systems, especially the representation of salt solubilities, provides important information for scientific and industrial applications.

In the thermodynamic equilibria of polyphase systems, the appearance and disappearance of the phases are related with the changing of the composition of the mixture. These phenomena have been used previously by Chrétien (1929), Schrenemakers (1930), Campbell (1930), Babinets and Polishchuk (1981) to determine solid-liquid phase diagrams. Among the physical properties, the density has been used by Berthet et al (1991) and Souza (1992) and the conductivity have usually been exploited Bouchacourt (1976), El Hadek (1981).

When a solid electrolyte dissolves in water, a positive or negative heat effect occurs. It is caused by the destruction of the crystal lattice and the formation of hydrated ions. The degradation of the crystal lattice is an endothermic process because energy is required to breakdown the chemical bonds; whereas the hydration of the ions is exothermic. Depending on the type of lattice, radius and the charge of the ions (charge density), the resulting enthalpy

of solution can be endothermic or exothermic. Mercury Chloride is an exothermic salt, it exists in both hydrated and dehydrated forms, in this case, and one assumes that during the dissolution of the hydrated salt only the degradation of the crystal lattice occurs. Temperature behavior illustrate the mass transfer in Solid-liquid equilibrium, a curve gives informations where occurs any phase transition thought its maximum and minimum points, it means, how and where the global composition take changes.

EXPERIMENTAL

Materials

The salt mixtures were prepared with P. A. Grade (Aldrich and Merck) reagents, with the following purity grades in mass percent, i.e., $HgCl_2$ (purity 99%), TIOA (purity 99.99%), alcohol (purity 98%), kerosene (purity 99%). Binary and the ternary mixtures have been prepared using double distilled water. TIOA solution contains 1%TIOA, 4% alcohol and 95% kerosene, all percentage in volume. Alcohol, classified as octyl alcohol, was added to solution to crack and dissolve homogeneously any bubble of phase that came to appear on interface between the phases. Kerosene was added to TIOA solution as a diluent cause its affinity with TIOA and promotes the phase separation more easily cause TIOA in high concentration does not extract the salt selectively and create a very viscous and single phase.

Apparatus

A schematic diagram of the QTT apparatus (see Figure 1) for the measurement of salt solubilities is composed by: the cell is a glass tube (120 cm^3), which is placed in a jacketed glass reactor. The temperature control of the cell is provided by circulating water in the jacket with the aid of a thermostatic bath (HETO, ± 0.01 K). The titration of the solvent is performed by an automatic burette (METROHM 665) with capacity of 50 cm^3 and accuracy of 0.01 cm^3. The temperature in the cell is measured by a thermistor probe PT100 (Cole-Parmer, 100 W Platinum RTD probe with alpha coefficient of 0.00385 Q/(Q /K) and time constant of 15 seconds), which is connected an interface analogical-digital. The experiment is monitored and recorded with a specific computer program (AQDADOS Lynx - version 4.8).

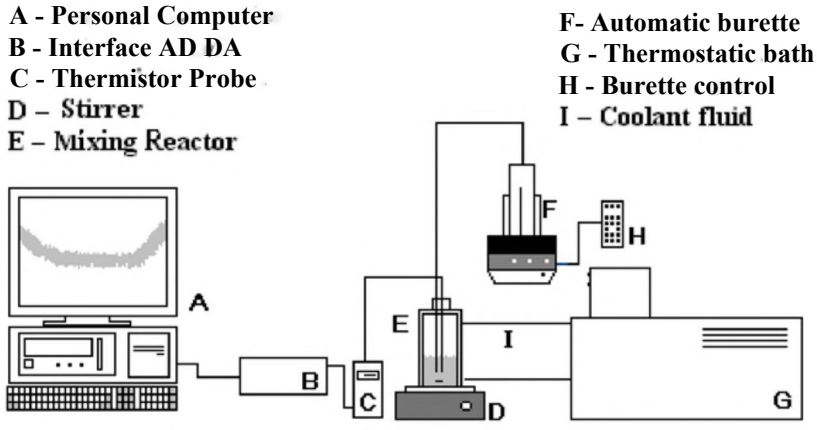


Figure 1. Experimental setup scheme for determination of solid-liquid equilibrium data using the Quasi-isothermic Thermometric Method.

The condutivimeter (DIGIMED model DM-31) has been used with a cell with a constant equal to 10, which means a measuring range from 20 to 200 mS/cm. The reproducibility of the

conductivity measurements of the aqueous salt solutions with respect to the composition determined via gravimetric measurements, is estimated to be an average deviation of 0.5%.

Procedures

The principle of the method is to measure the thermal effects associated with the dissolution and mixing processes, Salminen et al. (2000), Tavares et al. (1999). The global composition of each mixture is known and changed progressively by the continuous and regular addition of a prefixed volume of water and the temperature evolution depends on the dissolution and dilution enthalpies of the different phases.

In a typical experiment to determine data solubilities using QTT the following procedure is done. First, a mixture containing, e.g., one or two substance and water, or other solvent, is prepared gravimetrically with a composition conveniently chosen, i.e., in the region where at least one solid phase is present. The tube containing this mixture is then placed in the jacketed glass reactor, which is covered properly with the equipped lid, i.e., temperature probe and filling tube of the burette. The system is stirring and the temperature of the cell is controlled and adjusted via the thermostatic bath. When the thermal equilibrium is reached, the experiment may start through the water injection from the automatic burette at the specified addition rate. During the experiment, the temperature in the cell is monitored and recorded by the interface AD/DA and the software. Based on the retrieved data the phase boundaries and solubility limits can be determined. In practice, the boundary phase, or the solubility is determined by the intersection of the two segments.

In order to study a ternary system with two solutes, it is necessary first to measure the binary solubilities, determining the optimum addition rate of solvent, respectively. Based on the rate conditions of the two solutes obtained separately, the ternary mixture rate is easily found.
For each experiment, the curve of temperature versus volume of water is obtained and it allows the determination of the limits of solubility, by finding the transition between the dissolution and dilution phenomena that is characterized by the dissolution of the last crystal of the saturated solution.

RESULTS AND DISCUSSION

For results, it was selected the mains experiments, principally the ones that begins without any water cause it will be added to initial mixture.

All data are collected electronically. Aqdados lynx software works like a operational system allowing that many parameters be configured, parameters like data acquisition frequency is on the range of 0.5 to 1 point per second, this parameter depend on the intrinsical characteristics of each salt. Temperature interval is configured based on the thermal effects that came to appear too, normally it is on the range of 20 to 30°C. It's very important all thermal effect that come to change any variable of the system, then, a salt that has low or no thermal effect will give bad results for solubility data, but, if it occurs, one change the physical property, and from that moment, for example, the conductivity is monitored. Cases like this occurs with systems with a low salt concentration for any phase presented. The apparatus is the same used in the last method, its use is justified because in some cases heat effect is not measurable, it means, there's no thermal effect in the dissolution or dilution process. It may pointed out that the behavior of the two curves on conductivity is inverse after the complete dissolution, i.e., on the dilution process. Furthermore, for the binary mixtures, the dissolution part presents a constant value, since the point is invariant. By the other hand, for the ternary mixtures, it may be observed one degree of freedom on the dissolution process, by the inclination of the curve. But, still the difference between the inclinations indicates the solubility limit. The conductivity versus diluent amount plot indicates the dissolution and

dilution processes allowing the determination of the solubility limit, i.e., by the intersection of the experimental fitted lines.

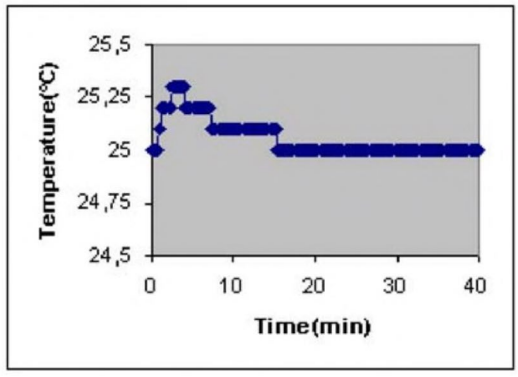


Figure 2. Study of solubility data for binary system TIOA/water at 25°C.

As it shows figure 2, the TIOA that is used to interact with the salt Mercury Chloride has low solubility in water for being diluted in kerosene, the technique used here it was the TTQ, even so it does not exist salt. The thermal effects of this system allowed the capitation of the peak of the curve that represents the maximum amount of water that dissolves the TIOA contained in the mixture.

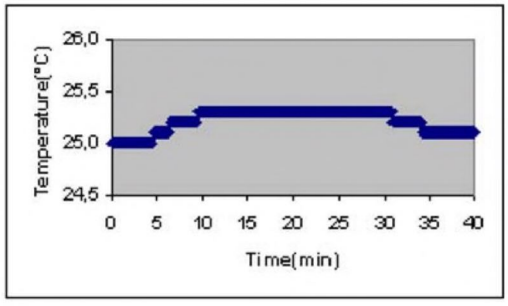


Figure 3. Study of the solubility of the salt $HgCl_2$ in water 25°C.

Figure 3 represents the representative curve of the dissolution of mercury chloride gotten for the TTQ. The solubility of the $HgCl_2$ is very low in water and initially the global mixture is warm before the beginning of the assay. To follow, the experiments with ternary mixtures with the most varied compositions are shown, the criterion of choice of the initial composition depends on the heat necessary to have the dissolution of the salt, or either, leaves with low heat requires strategies of choice, in case that contrary, does not perceive the discontinuity of the curve.

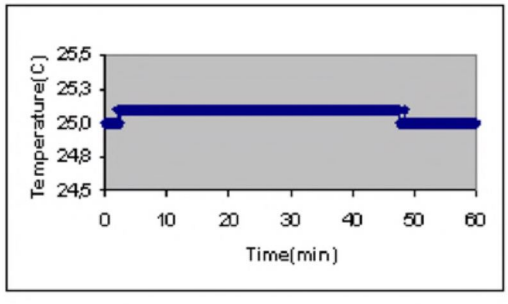


Figure 4. Study of the solubility of ternary mixture TIOA, $HgCl_2$ and H_20 25°C.

As figure 4, that it represents the solubility of an three-phase mixture, where the composition is equivalent 10% salt, 40% water, and 50% TIOA. The mixture initiates with three phases and with the addition of the water the solid phase adds giving origin to a liquid viscose, in this experiment the action of the alcohol was of great importance in view of the formation of bubbles in the interface. The minimal variation of the temperature it indicates that the thermal effects of the mixture are compensated by the different phases that appear and disappear.

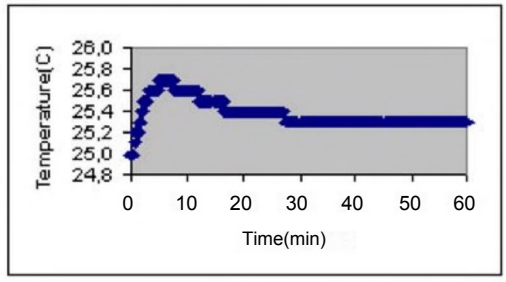


Figure 5. Study of the solubility of Mercury Chloride in TIOA with water addition, 25°C.

As figure 5, the solubility of the salt in TIOA with water addition is very low. An initial composition, 50% salt and 50% TIOA, or either, two phases, a solid and another liquid, to the end, we find two liquid in balance with a solid, fact this had a low interaction of the water with the TIOA. Other results had been gotten through the technique cloud point, that consists of evidencing the sprouting or disappearance of another phase through the addition of one of the components - except the salt. The experiment was made in pipes of assays, and is repeated of 2 to 3 times with the objective of if getting an average value, or, constant for the calculation of the new fractions that are converted into solubility. In some regions of the diagram of phases the pHmetry was applied, however its results are oscillatory, then its application in the too much regions of the diagram, as well as this, others also had been and are being studied.

This is the phase diagram for the ternary system Mercury Chloride - TIOA - H_20:

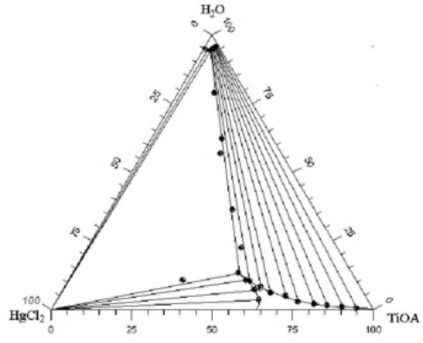


Figure 6. Diagram of phases for the $HgCl_2$ system + TIOA + H_20 at 25°C.

As figure 6, we see that the three-phase region predominates in area in the diagram. Some regions are limited by new composites that are formed during the dissolution process, and the origin of these is explained by the formation of complexes, what it brings difficulty to the data collecting, a time that a physical property is being monitored and any disturbance influences in the behavior of this with the time.

To follow the main data of the concluded diagram are presented:

Table 1. Main data of solubility for the system at 25°C.

%w $HgCl_2$	%w TIOA	Phases
5,02	0,0	HgCh + H_20
5,00	2,3	$HgCl_2$ + H_20
4,89	4,71	$HgCl_2$ + H_20
36,8	63,2	$HgCl_2$ + TIOA
34,7	60,2	$HgCl_2$ + TIOA
33,2	54,7	$HgCl_2$ + TIOA
35,8	48,6	$HgCl_2$ + TIOA
27,3	46,1	$HgCl_2$ + TIOA + H_20
18,0	25,3	$HgCl_2$ + TIOA + H_20
11,1	13,5	$HgCl_2$ + TIOA + H_20

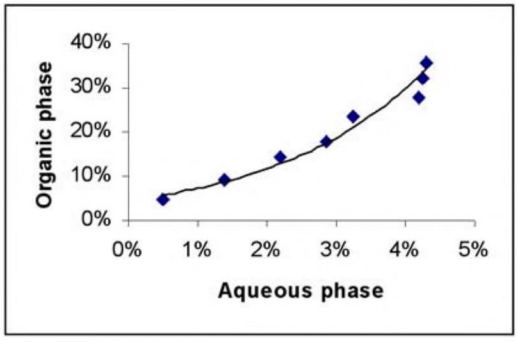


Figure 7. Curve of distribution of mass of the salt in the organic and watery phases.

As figure 7, that it represents the distribution of the salt in the two liquid phases, can be evidenced the affinity that was attributed to the organic phase, the data is in mass fraction. The curve supplies conditions the study of straight operation lines with the objective to extract the maximum possible metal load.

CONCLUSIONS

In accordance with the diagram, we have two curves of solubility for the salt, one with the watery liquid, and another one with the organic liquid. The region of two liquid phases constitutes the best region for operations of extraction of the salt. As the diagram, vide Figure 6, liquid phase TIOA obtains to extract greater ratio of the metal due its bigger affinity and chemical interaction, this region was rigorously analyzed with the objective to determine the concentration of the salt in each liquid layer. The analysis methods had revealed efficient, the TTQ that is the main tool and contributed strong for the determination of the diagram. The construction of the diagram will come to optimize the operations of extraction, that in if treating to you leave Mercury, assumes basic importance in view of the increasing and current industrial interest.

REFERENCES

1. **LINKE, W. F., SEIDELL, A.,** *Solubilities of inorganic and metal organic compounds.* **4. ed., Washington: American Chemical Society, 1965.**

2. **SILCOCK, H. L.,** *Solubilities of inorganic and organic compounds.* **Oxford: Pergamon Press Ltd., 1979.**

3. **NÝVLT, J.** *Solid-Liquid Phase Equilibria.* **New York: Elsevier, 1977.**

4. **BABINETS, D. M.; POLISHCHUK, A.G.** *Apparatus for Measuring the Solubility of Salts in a Mixed Solvent.* **Russian J. Phys. Chem., Russia: 55(2), 304-305, 1981.**

5. **CHIAVONE-FILHO, O.; RASMUSSEN, P.** *Solubilities of Salts in Mixer Solvents. Journal of Chemical and Engineering Data,* **New York: 38, 367-369, 1993.**

6. **BERTHET, J.; SAID, J.; COUNIOUX, J.J.** *Etude des equilibres solide-liquide par thermometrie quasi-isotherme. Journee des Equilibres Entre Phases (JEEP),* **17, 1991, Utrecht, Holanda, 3-4 abril, V. I, p. 195-197.**

7. **BOUCHACOURT, M.** *Contribution a L'etude du Systeme Quaternaire Reciproque* Na^+, Zn^{*2}, **Cr,** $S0_4^{2'}$, H_20. **114p. These, Universite Claude Bernard. Lyon. Franga, 1976.**

8. **EL HADEK, M.** *Contribution a L'etude des Equilibres Liquide-solide du Systeme Quaternaire Reciproque* Na^+, NH_4^+, $HC0_3'$, **Cr,** H_20. **123p. These, Universite Claude Bernard. Lyon. Franga, 1981.**

9. **SOUZA, C.P. Le** *systeme Quaternaire Reciproque Co**, Na*, Cf,* $S0_4''$, H_2O_t *Etude a 25 °C.* **117p. These, Universite Claude Bernard-Lyon, France, 1992.**



SYNERGISTIC EXTRACTION OF EUROPIUM(III) WITH 2-THENOYLTRIFLUOROACETONE AND A LEWIS BASE AND THE APPLICATION TO PREPARATION OF BINUCLEAR COMPLEXES

Yuko Hasegawa, Satoshi Kumaki, and Koichiro Tanaka

Department of Chemistry, Faculty of Science, Science University of Tokyo, Kagurazaka, Shinjuku-ku, Tokyo, 162-8601, Japan

In the extraction of lanthanoids(III) with 2-thenoyltrifluoroacetone (Htta) and a Schiff base complexed copper(II), the distribution ratio of europium(III) has been measured as a function of pH, Htta concentration and the concentration of the Lewis base based on Schiff bases, otherwise identical. As the Lewis base, Cu(saltn) (saltn: disalicylidene trimethylenediamine) was prepared by the reaction of Cu(salicylaldehyde) which was prepared by the reaction between copper(II) acetate and salicylaldehyde with trimethylenediamine. The extraction was synergistically enhanced, while the enhancement with H_2saltn which is not complexed with Cu" was much smaller than with Cu(saltn). It was found that Cu(saltn) dissociates into Cu^{2+} and H_2saltn, and Cu^{2+} was extracted with Htta at the same time in the extraction of Eu^{1}". However, the synergistic extraction with Htta and Cu(saltn) is effective, i.e., the complex between $Eu(tta)_3$ and Cu(saltn) is very stable like that between $Eu(tta)_3$ and trioctylphosphine oxide.

As a conclusion, the usage of synergistic extraction of lanthanoids(III) with Htta and a metal complex with Schiff bases can be a promising method to prepare binuclear complexes possessing new functions.

Keywords : Synergistic extraction, Schiff base, Cu(saltn), lanthanoids(III), stability constants, binuclear complexes

INTRODUCTION

Synergistic extraction of metal ions with p-diketones and Lewis bases has been studied over

50 years. Although the synergistic extraction equilibrium has been mostly focused to study on the extraction of one kind of ions, recently it has been reported that in the extraction of lanthanoids(III) using p-diketones and several metal chelates with p-diketones as Lewis bases, synergistic enhancement in the extraction of lanthanoids(III) was observed due to the formation of binuclear complexes as extracted species [1-3], Nowadays much attention has been paid to the synthesis of binuclear complexes involving especially d- and f- elements as new functional materials. On the basis of such back-ground, the equilibrium in the synergistic extraction of europium(III) with 2-thenoyltrifluoroacetone(Htta) and copper(II) complexes with Schiff bases was studied in the present paper.

EXPERIMENTAL

As a Lewis base being Schiff bases, Cu(saltn) (saltn: disalicylidene trimethylenediamine) was prepared according to the method in literature [4] ; Cu(salicylaldehyde) which was made from copper(II) acetate and salicylaldehyde was reacted with trimethylenediamine. The total ionic concentration was adjusted to 0.1 M (1M = 1 moldin'3) with $NaCl0_4$. Eight milliliters of aqueous solution containing 10'4 - 10'5 M Eu^m were shaken with the identical volume of $CHCl_3$ containing TTA and/or Cu(saltn). Separately, the extraction of Cu" in the presence of Eu"1 with Htta was measured. The concentration of copper(II) as well as lanthanoids(III) was measured ICP/AES (Hitachi P-4000). The pC_H (= -log[H^+]) at equilibrium was determined potentiometrically (Corning 445).

RESULTS AND DISCUSSION

Extraction of lanthanoids(III) with TTA and Cu(saltn)

When europium(III)(Eu^{MI}) is extracted with a p-diketone (HA) and a Lewis base (B), the distribution ratio, *D* (the concentration ratio of Eu1" between both phases) can be usually represented as,

$$D = \frac{[EuA_{3}]_0 + [EuA_3 \bullet B]_0 + [EuA \bullet 2B]_0 + \ldots}{[Eu^{3+}]} \qquad (1)$$

Introducing the formation constants $(J\bar{3}_n)$ of the complexes between EuA_3 and B into Eq. (1),

$$\beta_n = \frac{-[EuA_3 - nBjp}{[EuA_3]_0[B]_0^n} \qquad (2)$$

the following equation can be obtained,

$$D = Kex(1 + 1 \bar{p}_n [B]_0^n) [H^+]^{-3} [HA]_0^3 \quad (3)$$

where Kex is the extraction constant of tris(p-diketonato)europium(III), Kex = $[EuA_3]_0[H^+]^3[Eu^{3+}]^{-1}[HA]_0^{-3}$.

If Cu(saltn) is very stable in $CHCl_3$ and the solubility in water is very low, at a given concentration of Htta and Cu(saltn), log *D* should be proportional to $3pC_H$.

In order to confirm the validity of Eq. (3), the dependence of log *D* on pC_H and on $log[Htta]_0$ was examined. Figure 1 shows the plot of log D as a function of pC_H, when Eu^{111} was extracted into $CHCl_3$ containing 2.5x10"^{3}M of Cu(saltn) and Htta of 1.25x10"^{2}M (°), 2.5 xl 0'^{2}M (A), or 5.0x10‘^{2} M (•). The slope is +3 in a higher pC_H region, although the pC_H region seems to depend on the Htta concentration.

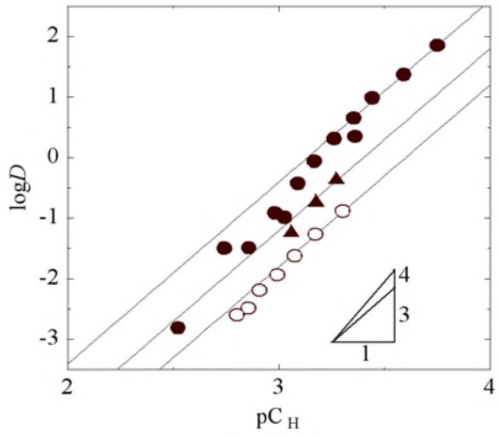


Figure 1. Distribution ratio of Eu^{1}" as a function of pC_H.
Aq. phase : 0.1 M $NaCl0_4$ containing 7.5x1 O'^{5}M Eu^{1}"
Org. phase : $CHCl_3$ containing 2.5x10'^{3}M Cu(saltn) and
Htta of 5.0x10 ^{2}M (•), 2.5x1 O'^{2}M(A) or 1.25xW^{2}M(o).

To examine the effect of Htta concentration on the distribution ratio of Eu^{1}" in the presence of Cu(saltn) in more detail, in Fig. 2, $logD - 3pC_H$ was plotted as a function of $log [Htta]_0$ in the presence of two different Cu(saltn) concentration and in a higher pC_H region in which the slope of the plot of logD vs. pC_H was +3. On using the higher concentration of Cu(saltn) (2.5x10'^{3}M), the slope showed +3 while in the lower concentration (2.5x10'^{4}M), the slope

gradually decreases along with increase of Htta concentration. These data may suggest different extraction equilibria under different situations. It may be due to the dissociation of Cu(saltn). To check the dissociation of Cu(saltn), Cu" concentration in the organic and the aqueous phases was measured when chloroform containing Cu(saltn) of 2.5x10'^{4}M and Htta of 1.25x10'^{2}M was shaken with 0.1 M $NaCl0_4$ at different pC_H. When the pC_H was lower than 3, the copper ion in aqueous phase increased. At pC_H 2.4, the concentration in aqueous phase reached 1.2x10'^{4}M, i.e., almost 50% of Cu" disappeared from the organic phase, although when Htta was 0.05M, the concentration was only 2.5x10'^{5}M. Copper(ll) concentration in aqueous phase will depend on TTA concentration as well as pC_H. The results suggest that copper ion released with proton from the saltn complex is extracted with Htta. Then the following equation will be valid:

$$[Cu^M],otai = [Cu(saltn)]i_nHiai = [Cu^{2+}] + [CuA_2]_0 + [Cu(saltn)]_0 \qquad (4).$$

When Cu^{2+} is extracted with Htta from 0.1M $NaCl0_4$ into $CHCl_3$, the extraction constant, K_{ex} (= $[CuA_2]o[H^+]^2[Cu^{2+}]'^1[HA]_0'^2$) was reported to be 10'^{125} [5], Using K_{ex} and the concentration of Cu" in aqueous phase, Eq. (4) can be rewritten as follows:

$$[Cu(saltn)]initiai = [Cu^{2+}](1 + K_{ex}\,[HA]_0{}^{-2}[H^+]^2) + [Cu(saltn)]_0 \quad (5)$$

Accordingly, the proportion of the concentration of Cu(saltn) at equilibrium to the total concentration of Cu(saltn) should be,

$[Cu(saltn)]_0/\,[Cu(saltn)]_{inrtia}$, = $([Cu(saltn)]_{initia}$, - $[Cu^{2+}](1 + K_{ex}[HA]_0{}^2[H^+]^{-2}))/\,[Cu(saltn)]_{initial}$.

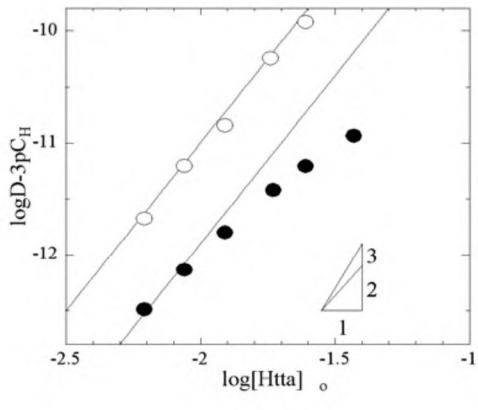


Figure 2 Distribution ratio of Eu"^{1} as a function of $[Htta]_0$

Experimental condition : $[Eu"']_T$ = 7.5x1 O'^{5}M

O pC_H 3.2 -3.7 $[Cu(saltn)]_T$ =2.5x10~^{3}M

• pC_H 3.5-3 6 $[Cu(saltn)]_T$ =2.5x10'^{4}M

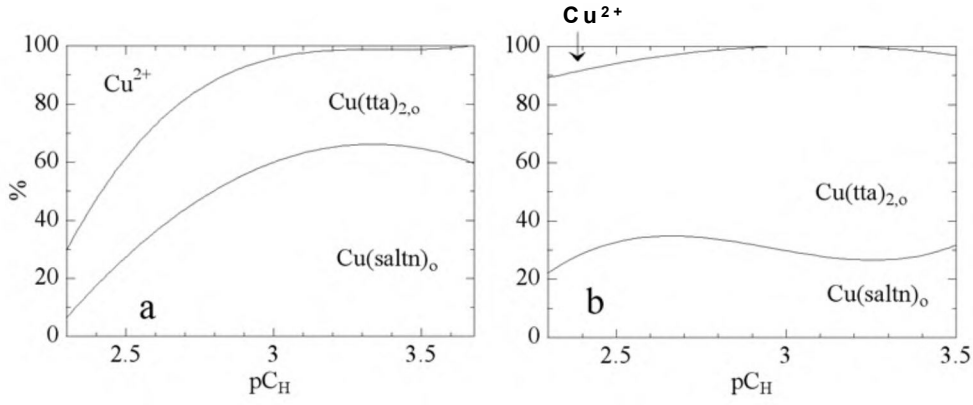


*Figure 3. The proportion of Cu" species when $CHCl_3$ containing Cu(saltn) of 2.5x1 O'⁴M and Htta **(a:** 1.25x10~²M **b** : 5.0x10'²M) was shaken with 0.1M $NaCl0_4$ at vahous pC_H.*

Figure 3 shows the proportion of Cu" species when $CHCl_3$ containing 2.5x10"⁴M Cu(saltn) and Htta of 1.25x10'²M (Fig. 3-a) and of 5.0x10'²M (Fig. 3-b) was shaken with 0.1M $NaCl0_4$ at various pC_H. It is clearly seen on the comparison of the two figures in Fig. 3 that the proportion of Cu" in aqueous phases is much smaller on the use of higher concentration of Htta, however, the proportion of $Cu(tta)_2$ is much larger than on use of the lower Htta concentration so that the proportion of Cu(saltn) is much smaller on use of the higher concentration of Htta. The higher Htta concentration leads formation of a larger amount of $Cu(tta)_2$. When Cu(saltn) dissociates into Cu^{2+} and H_2saltn and Cu^{2+} is extracted as $Cu(tta)_2$ in the presence of Eu"¹, $Cu(tta)_2$ as well as H_2saltn may coordinate to $Eu(tta)_3$, i.e., the extraction of Eu¹" may be synergistically improved with Htta and H_2saltn or Htta and $Cu(tta)_2$. Then the extraction of Cu" as well as Eu"¹ with Htta from aqueous solution containing Cu" and Eu¹", and further the extraction of Eu"'with H_2saltn were examined. In Fig. 4, • shows the enhancement of the distribution ratio of Eu"¹ with 0.05M Htta and H_2saltn itself as a function of H_2saltn concentration. The enhancement in the presence of H_2saltn was small, e.g., even in the presence of 1CT²M H_2saltn, the enhancement is much less than one decade, although the data are scattered. The data shown by ▲ in Fig. 4 gives the distribution ratio of Eu"¹ as a function of the concentration of Cu" extracted with Htta together with Eu¹" into $CHCl_3$. Any special enhancement of D of Eu¹" is not observed over all the range of $Cu(tta)_2$ concentration studied, although it was expected from the report that in the presence of coordinately saturated chelates such as tris(acetylacetonato)aluminum(lll), scandium(lll), chromium(lll), iron(lll), and cobalt(lll), the extraction of lanthanoids(lll) with Htta was remarkably enhanced [2], and $Cu(tta)_2$ seems to be saturated coordinately.

From the relation shown in Fig. 3, the concentration of Cu(saltn) at equilibrium was calculated. The enhancement of the extraction is also given as a function of the concentration of Cu(saltn) calculated in Fig. 4(o). The data were analyzed on the basis of Eq. (3) and the formation constants represented in Eq. (2) were determined to be 5.4 as log *P*\ and 9.8 as log#,-.

These formation constants are almost comparable or a little larger than those of the complexes between $Eu(tta)_3$ and TOPO (trioctylphosphine oxide) known as a typical strong Lewis base (log *P*\ = 5.4 and log # = 7.6 [6]). Also, the H_2saltn without Cu" does not seem to form stable complexes with $Eu(tta)_3$, as mentioned above.

The difference of the effect between Cu(saltn) and H_2saltn is not clearly explained up to now. The difference may be caused by the formation of intramolecular hydrogen bonding of H_2saltn and the differene of hard/soft property of metals; since the affinity of Cu" to N donor atoms is larger than to O atoms, Cu" may combine more strongly with N atoms so that the electrodensity of the oxygen atoms may increase in Cu(saltn) than that in H_2saltn. It may permit to form more stable complexes between $Eu(tta)_3$ and Cu(saltn) than between $Eu(tta)_3$ and H_2saltn.

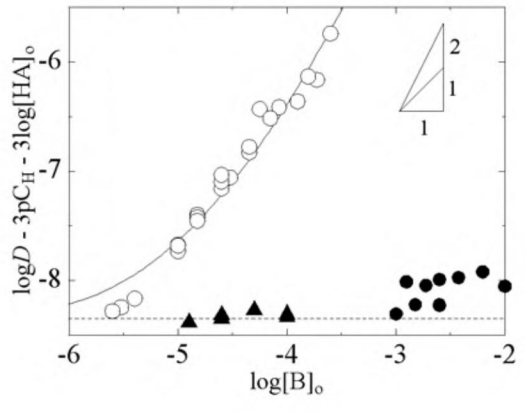


Figure 4. Distribution ratio of Eu^{111} as a function of a Lewis base

o B. Cu(saltn) Extraction at pC_H 3.2 -3.7 into $CHCl_3$ containing 1.25x10'2M Htta and Cu(saltn)

• B: H_2saltn Extraction at pC_H 3.2- 3.7 into $CHCl_3$ containing 5.0x1 O'2M Htta and H_2saltn

▲ B: $[Cu"]_0$ Extraction with 1.25x10'2M Htta in $CHCl_3$ from 0.1 M $NaCl0_4$ containing $[EL/"]_t$= 7.5x1 0'4M and $[Cu"]_T$ =(0.13 - 1.0)x10 4M at pC_H 4.3 - 4.6

CONCLUSION

The extraction of $Eu^{"1}$ was synergistically enhanced with Htta and Cu(saltn), although Cu(saltn) dissociated into Cu^{2+} and H_2saltn with depending on pC_H and the concentration of Htta. It was found that the dissociated Cu^{2+}as extracted with Htta, however, $Cu(tta)_2$ does not form stable complexes with $Eu(tta)_3$. Accordingly, to prepare the binuclear complexes between $Eu(tta)_3$ and Cu(saltn) effectively, $Eu^{"1}$ should be extracted at pC_H around 3 and with lower concentration of Htta (e g., 0.01 M).

REFERENCES

1. **H. Imura, N. Kameta, M. Osada, K. Ohashi, T. Kimura, and Z. Yoshida (1999),** *Solv. Extr. Ion Exch.,* **17, 585-596.**
2. **N. Kameta and H. Imura,** *Anal. Sci.* **(2001), 17, 957-962.**
3. **N. Kameta and H. Imura,** *Bull. Chem. Soc. Jpn.* **(2001), 74, 1641-1647.**
4. **"Jikken Kagaku Kohza" (How to prepare inorganic complexes and chelates), Ed. by Japan Chemical Society, p.306, Maruzen (1991)**
5. **T. Sekine and D. Dyrssen,** *J. Inorg. Nucl. Chem.* **(1964), 26, 1727-1742.**
6. **T. Sekine and D. Dyrssen,** *J. Inorg. Nucl. Chem.* **(1967), 29, 1475-1480.**

EXTRACTION OF Am(III), Th(IV), Np(V) AND U(VI) BY BIDENTATE AND TRIDENTATE DIAMIDES

Yuji Sasaki and Takaumi Kimura

Japan Atomic Energy Research Institute, Tokai-mura, Ibaraki-ken 319-1195, Japan

Many diamide-typed extractants were synthesized and tested for the extraction of actinides (III), (IV), (V) and (VI). The diglycolamide with two amidic oxygen and one ether oxygen, which shows the tridentate feature, have the high extractability of actinides. In order to increase the lipophilic property, the diglycolamides with the different length of the alkyl chains attached to N atoms were synthesized and examined for their extractability. It was found that W,/V,N',W'-tetraoctyl-diglycolamide and A/,W,/V',A/'-tetradecyl-diglycolamide have the high solubility in the aliphatic solvent of n-dodecane and show the high distribution ratio of actinides from nitric acid to n-dodecane. These are promising extractants for the process planning of the high level radioactive liquid waste

INTRODUCTION

The development of the novel extractants for the actinide (An) ions have been widely studied for the chemical treatment of the high level radioactive liquid waste (HLW). The diamide extractants can extract directly the metal ions from HLW of 3M $HN0_3$, because an ion-pair extraction using the neutral donor gives the high distribution ratio of metals under a high ionic concentration. One of the indispensable advantages of the diamide extractant is incinerability, after utilization, diamide can be gasificated by combustion and produces no radioactive solid waste.

Many diamide extractants, i.e., malonamides, succinamide, glutalamide and adipamide, have been studied for the application to the recovery of An for last two decades [1-5]. It is important to elucidate the effect on the structure of the diamide in order to obtain the best property for the extraction of An. However, few papers have discussed An extraction abilities of the diamides with the different structural backbones [3].

In the present investigation, the structure of the central frame of the diamides with and without one ether oxygen or sulfur has been systematically changed and its influence to the extractability toward An(III), (IV), (V) and (VI) were studied. Nine diamides having the different length of C, O and S atom chains between two carbonyl groups have been synthesized. The diamides used here: oxalamide ($(CONR_l,R_2)_2$, abbreviated as OXA); malonamide (CH_2-$(CONR_l,R_2)_2$, MA); succinamide ($(CH_2)_2$-$(CONR_,,R_2)_{2l}$ SCA); maleamide ($(CH)_2$-$(CONR_,,R_2)_{2l}$ MLA); glutalamide ((CHsMCONR^Rzk, GLA); diglycolamide (0-$(CH_2$-$CONRi,R_2)_2$, DGA); oxydipropionamide (0-$((CH_2)_2$-$CONR_,,R_2)_2$, ODPA); thiadiglycolamide (S-$(CH_2$-$CONR_{1l}R_2)_2$, TDGA); and thiadipropionamide (S-$((CH_2)_2$-$CONR_,,R_2)_2$, TDPA). The structures of the diamide compounds are illustrated in Fig. 1. After determination of the best extractant, we studied the application of its extractant to the process planning of HLW.

EXPERIMENTAL

Chemicals

The reagents used for the organic synthesis were commercially available. The standard solutions of lanthanides and the other non-radioactive metal ions for the atomic absorption

spectrometry (Wako Pure Chemical Industries, Ltd) were used. The radioactive tracers of "Tc, ^{233}U, ^{230}Th, ^{237}Np and ^{241} Am were obtained from Isotope Products Laboratories. All the other reagents were of an analytical grade.

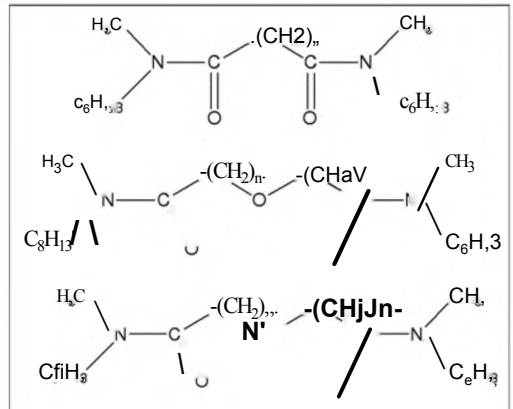


Figure 1 Structure of diamide extractants

n= 0; oxalamide (OXA), 1; malonamide (MA),
2; succinamide(SCA), 2; maleicamide (-CH=CH-) (MLA),
3; glutalamide (GLA)
n'= 1; diglyoolamide (DGA), 2; oxydipropionamide (ODPA)
n"= 1; thiadiglycolamide (TOGA), 2; thiadipropionamide (TDPA)

Organic Synthesis

OXA is synthesized from the oxalic chloride and the secondary amines [6]. The initial reagents are mixed slowly in a chloroform media with the triethylamine, under the freezing point of water and stirred overnight.
After the organic reaction, the product was washed with the distilled water, 1M HCl and 1M NaOH, and the materials obtained were purified by distillation and silica gel column chromatography. MA is synthesized from the malonic ester and the secondary amines [6].
The starting materials with hydrochloric acid are mixed and stirred at 200 °C for 1 hour. The product was dissolved in toluene and washed with the distilled water, 1M HCl and 1M NaOH, and purified by distillation and silica gel column chromatography. Other diamides, such as SCA, MLA, GLA, DGA, TDGA, ODPA, and TDPA, were synthesized and purified by the same method as the ref. [7], All diamides synthesized were identified by NMR (UNITY plus 400, varian) and GC-MS (TurboMass, Perkin Elmer Inc.) spectrometers.

Extraction Procedure

Three cm^3 of the organic solvent containing diamide concentration with 5x1 O'^{6} to 0.2 mol/dm^3 (= M in the following sentences) was shaken with an equal volume of 0.1 M $NaCl0_4$ with pH=3 or the nitric acid of the desired concentration. After centrifugation, 2 cm^3 of the pre-equilibrated organic phase was taken and mixed with 2 cm^3 of the aqueous phase of the same concentration as in pre-equilibration, spiked with 10'^{2} cm^3 of the radioactive tracer solution or the non-radioactive metal solution. The mixture was shaken mechanically for 2 hours at 25 ± 0.1 °C. After centrifugation and separation of the phases, duplicate 0.50 cm^3 aliquots were measured by NaI scintillation counter (COBRA 5003, Packard Instrument Company) for the gamma activities of^{241} Am, liquid scintillation counter (Tri-Carb 1600 TR, Packard Instrument Company) for the alpha activities of "Tc ^{230}Th, ^{233}U and ^{237}Np in 5 cm^3 of ULTIMA-FLO (Packard Instrument Company) cocktail. The preparation and counting of $^{237}Np(V)$ were followed that described in reference [8], The amounts of the non-radioactive metal ions in the sample solutions prepared from the aqueous and the organic phases were measured by ICP-AES (SPS 3100, Seiko Instruments Inc), ICP-MS (SPQ 9000, Seiko-EG&G).

RESULTS AND DISCUSSION

Extraction of Actinides by Different Diamides

The distribution ratio, D(Am), expressed by the ratio of Am(III) concentration in the organic phase against that in the aqueous phase, were shown in Fig. 2. The order of the ion-pair extractability of diamides for Am(III) is DGA » TDGA > MA, ODPA > MLA, TDPA > SCA >

GLA > OXA. D(Am) by DGA is much higher than any other diamides in this work. TDGA, an analogue to DGA but with an ether sulphur atom, exhibits the second highest D(Am). Assuming that S atom in TDGA doesn't coordinate with the metal, TDGA would form an eight membered ring with metal ion similarly to GLA. TDGA showed much higher extractability toward Am(III) than that of GLA. This result strongly suggests the tridentate coordination by TDGA with three donors of two amidic oxygen and one ether sulfur. Slopes for the log D(Am) vs. log[extractant] in Fig. 2 are: MA(2.72±0.05); SCA(3.0±0.2); MLA(2.5±0.4); DGA(2.73±0.09); TDGA(2.5±0.2); ODPA(0.5±0.05). Assuming that the activity coefficient of the respective diamide is almost constant in their concentration range used, the slope values obtained above are associated with the number of the diamide molecules in the extraction reactions.

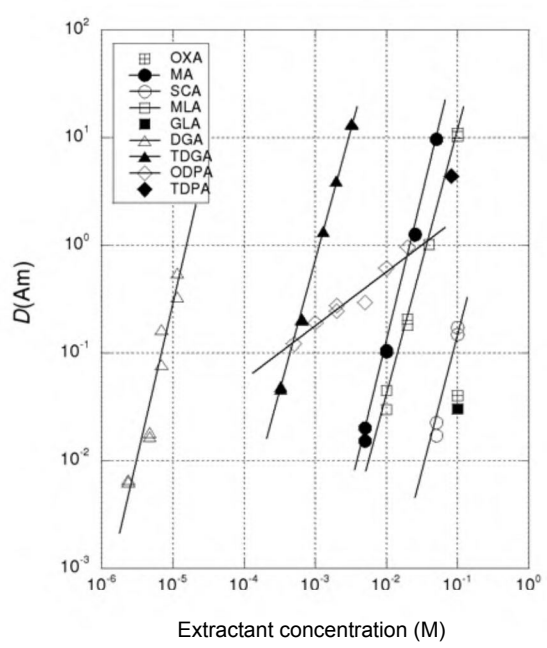


Figure 2 Extraction of Am(lll) by diamides

Organic diluent: nitrobenzene
Aqueous phase: 0.1 M $NaCl0_4$, pH 3.0

The distribution ratios of Th(IV), D(Th), by the various diamides were plotted as a function of diamide concentration. The experimental condition used is identical with that of Am(III) extraction. The order of the ion-pair extractability of diamides for Th(IV) is; DGA » TDGA > MA, ODPA > MLA > SCA, GLA > TDPA > OXA. DGA also exhibits the highest potential for Th(IV) extraction. The slopes of the plots in Fig. 3 were 1.5±0.2 for MA, 1.7±0.3 for SCA, 1.5±0.2 for MLA, 0.97±0.08 for DGA, 1.3±0.1 for TDGA, 0.56±0.12 for ODPA and 1.3 for TDPA. The numbers of the diamide molecules associated with the main extraction reactions are estimated to be one or two.

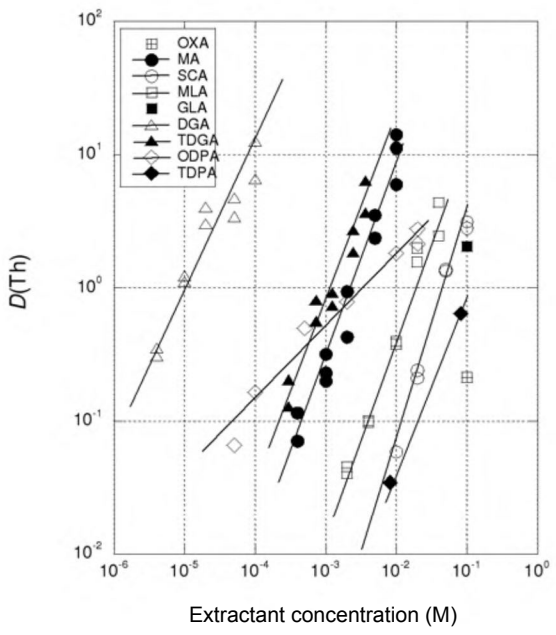


Figure 3 Extraction of Th(IV) by diamides

Organic diluent: nitrobenzene
Aqueous phase: 0.1M $NaCl0_4$, pH 3.0

In the previous study, a high D(Np) value has been obtained for the extraction of Np(V), ca. 10 by 0.06M DGA [8]. In the present study, D(Np) was measured using the extractants, OXA, MA, SCA, MLA, GLA, TDGA, ODPA and TDPA. The distribution ratios in all of the extraction systems, i.e., 0.03-0.1 M [extractant]/ nitrobenzene vs. pH=3 of 0.1 M $NaCl0_4$ were very low (lower than 0.02), thus Np(V) is poorly extracted by these extractants.

The distribution ratios of U(VI), D(U), by the various diamides are shown in Fig. 4. The order of the extractability for U(VI) is DGA » ODPA > MA, TDGA > SCA, MLA > GLA > TDPA > OXA. Both DGA and ODPA, introducing an ether O atom into the central carbon chain, gave higher D(U) than those by other diamides. For SCA and MLA, showing the seven

membered ring chelation by two carbonyl oxygens, the D(Am,Th) with MLA is higher than D(Am,Th)-SCA, whereas D(U) with SCA is a little higher than D(U)-MLA. As MLA has an ethylene bond in its backbone, MLA-metal complex is stabilized by the electronic conjugation, which may be more effective in Am and Th extractions. Whereas SCA has the free rotation of C-C bond in the backbone, which may reduce the strain in chelating to the equatorial coordination sites of U(VI). The slopes of the plots in Fig. 4 were calculated to be 1.7+0.2 for MA, 1.9±0.2 for SCA, 2.1+0.3 for MLA, 2.1±0.4 for GLA, 2.0+0.1 for DGA, 1.5±0.1 for TDGA, 1.0±0.1 for ODPA and 1.4±0.2 for TDPA, suggesting the number of the diamide molecules in the main extraction reactions to be one or two.

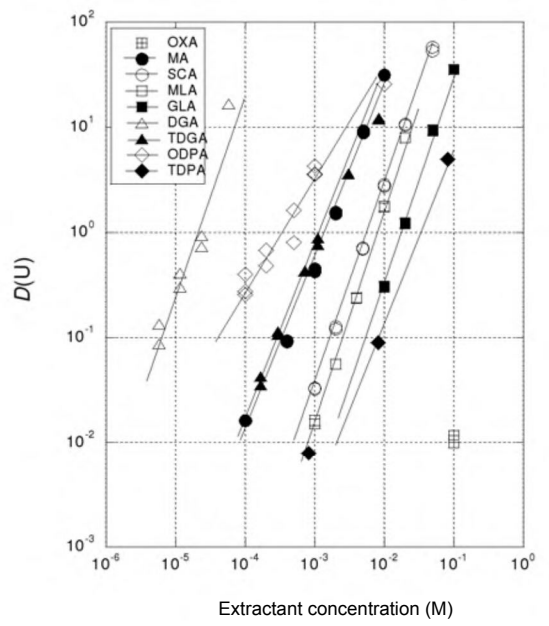


Figure 4 Extraction of U(VI) by diamides

Organic diluent: nitrobenzene
Aqueous phase: 0.1 M $NaCl0_4$, pH 3.0

Modification to DGA Compound with High Lipophilic Property

As an aliphatic diluent has been usually employed in the liquid-liquid extraction process involving HLW, the high solubility of the extractant in a solvent, n-dodecane, is required. In this work, DGA compounds, which shows the highest extractability of An, with the different length of the alkyl chain attached to amidic N atoms were synthesized. The existence of the long alkyl chain in an extractant may decrease the polarity of its metal complex and increase the solubility in the non-polar solvents. Six DGA compounds obtained were 0-($CH_2C0N(C_nH_2n_+i)2)2$ with n=3 (abbreviated as TPDGA), 4 (TBDGA), 5 (TADGA), 6 (THDGA), 8 (TODGA) and 10 (TDDGA). The solubility in water, *n*-dodecane and D(Am) using these samples were determined and summarized in Table 1. From this table, TPDGA, TBDGA, TADGA and THDGA are slightly soluble in n-dodecane, the solutions were not clear. The reason of the low solubility into such solvent is due to a high hydrophilicity of these organic compounds. The carbon/oxygen (C/O) atom ratios in the molecules of TPDGA, TBDGA, TADGA and THDGA are 5.3, 6.7, 8 and 9.3, respectively. As these values, lower than those of the representative extractants, i.e. 0(t>D(iB)CMPO; 12 and DMDBTDMA; 13.5, signify their poor lipophilicity, TPDGA, TBDGA, TADGA and THDGA are not applicable to $HN0_3$-n-dodecane extraction system.

The solubilities of six diglycolamides into water, in mM, are 57 for TPDGA, 2.3 for TBDGA, 0.27 for TADGA, 0.11 for THDGA, 0.042 for TODGA and 0.042 for TDDGA. These values also support the fact that diglycolamides with shorter alkyl chain attached to amidic N atoms exhibit higher

Table 1 Solubility of DGA' in water and n-dodecane, and D of Am(III)

	n	solubilily in water	dissolution in n-dodecane	D(Am)" chloroform	D(Am)" n-dodecane
TPDGA	3	57 (mM)	poor	0.41	-
TBDGA	4	2.3	poor	0.24	-
TADGA	5	0.25	poor	0.11	-
THDGA	6	0.11	soluble	0.089	40
TODGA	8	0.042	unlimited	0.071	30
TDDGA	10	0.042	unlimited	0.042	18

*: General structure of DGA; $0\text{-}(CH_2CON(C_nH_{2n+,})_2)_2$ (n= 3, 4, 5, 6, 8, 10)

**: Determined by using 0.1 M DGA/solvent and 1M $HN0_3$.

hydrophilic property. On the other hand, TODGA and TDDGA, which show the low solubility in water, can be dissolved in n-dodecane satisfactorily. Gasparini and Grossi suggested [9] that amide with more than 12-13 carbon atoms does not form a third phase. TODGA and TDDGA having 36 and 44 carbon atoms but with 3 oxygens (C/O ratio equal to 12 and 14.7) also indicated no third phase formation, even equilibrated with an aqueous solution of 6M $HN0_3$.

Distribution ratio of Am(III) in the system of an aqueous 1 M $HN0_3$ and an organic 0.1 M diglycolamide/ diluent are shown in Table 1, and it is clear that the D_M values gradually decreased from TPDGA(n=3) to TDDGA(n=10), showing that longer alkyl chain suppresses the extraction. There are few papers concerning the effect of the length of the alkyl chain in monoamide and diamide derivatives on distribution of An [5], the correlations, however, were not defined clearly.

Extraction of Actinides and Related Metal Ions in HLW Using TODGA

The extraction behavior of An ions and the related metal ions in HLW by TODGA were illustrated in Fig. 5. D(An) and D(M) were plotted against $HN0_3$ concentration. The extractability of An has in the order, in general, An(IV) > An(VI) > An(III) > An(V), by using TBP, TOPO and HTTA, however, the order of extractability of An by TODGA is An(IV) > An(III) > An(VI) > An(V). Most of the extractants employed in SF and HLLW are mono- or bi-dentate ligands. TODGA is the tridentate ligands, which may exhibits the different character from the previous results. For U(VI) and Np(V) showing the coordination sites with the equatorial surface of An, TODGA may work as the bidentate chelation rather than the tridentate one, which results in low *D* of U(VI) and Np(V) compared to those of An(III) and (IV). From this figure, it appears that *D* of all An ions by TODGA shows the exponential increase with $HN0_3$ concentration, which might be due to the extraction reaction accompanying $HN0_3$ in addition with the counter anion, $N0_3$ [10].

In Fig. 5, the extraction behavior of Np(IV) and Pu(III) by TODGA were shown. We obtained the similar results as the same oxidation state of other An and confirmed that at the reducing condition, An ions, Np(IV), Pu(III), (IV), Am(III) and Cm(III), can be extracted thoroughly by TODGA. We also studied the extraction behavior of Np(VI) and Pu(VI) by TODGA after oxidation by $HCl0_4$ fuming. Np(VI) and Pu(VI) were very unstable during the extraction by TODGA, and the satisfactory results of such An(VI) ions were hardly obtained up to now.

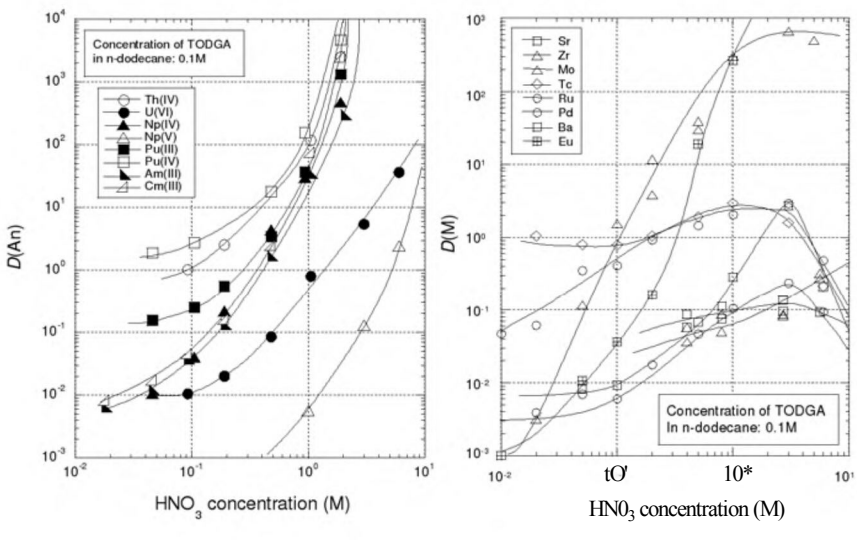


Figure 5 Extraction of An and related metal ions by TODGA

Organic phase: 0.1 M TODGA/ n-dodecane
Aqueous solution: $HN0_3$

The extraction behavior of the related metal ions in HLW was investigated, and the results are plotted in Fig. 5. *D* values for Zr(IV), Tc(VII), Pd(II), Ru(III), Sr(II) and Eu(III) are relatively high, however, the other FP, e.g., Te(IV), Cs(I), and Rh(III), are less extracted. From this figure, anionic Tc(VII), nitrocyl Ru complex, and Pd(II) ions have the high *D* values with less dependence of $HN0_3$ concentration.

CONCLUSIONS

The diamide extractant containing the different bridge between the amide groups in the molecule were investigated for the extraction of An with the various valence states. The highest distribution ratio for An(III), (IV) and (VI) was demonstrated by DGA compound. The molar ratio of An:ligands measured by the slope analysis was mainly 1:2 and 1:3 for Am(III), 1:1 and 1:2 for Th(IV) and U(VI).

Moreover, DGA compounds were studied concerning the solubility in the non-polar solvents in order to estimate the applicability to the process. It is clear that TODGA and TDDGA with the carbon/oxygen (C/O) atom ratios of 12 and 14.7 exhibited no third phase formation, even equilibrated with an aqueous solution of 6M $HN0_3$. Using TODGA, the extraction of An and non-radioactive metal ions from nitric acid to n-dodecane were investigated and it was obvious that An(III), An(IV), Ln(III) and Zr(IV) are highly extracted.

ACKNOWLEDGEMENTS

The authors acknowledge gratefully Professor Emeritus G.R. Choppin of Florida State University and Professor K. Oguma of Chiba University for the useful discussion and Drs. S Suzuki, Fl. Suzuki and Y. Kitatsuji and Ms. Y. Sugo for the experimental supports in the laboratory.

REFERENCES

1. **C. Madic, P. Blanc, N. Condamines, P. Baron, L. Berthon, C. Nicol, C. Pozo, M. Lecomte, M. Philippe, M. Masson, C. Flequet, M.J. Hudson (1994),** *CEA-CONF-12297.*
2. **X.-F. Tan, Y.-S. Wang, T.-Z. Tan, G.-F. Zhou, B.-R. Bao (1999),** *J. Radioanal. Nucl. Chem., Articles* **242, 123-126.**
3. **C. Shen, B. Bao, J. Zhu, Y. Wang, Z. Cao (1996),** *J. Radioanal. Nucl. Chem., Articles,* **212, 187-196.**
4. **M.C. Charbonne, C. Musikas (1998),** *Solv. Extr. Ion Exch.,* **6, 461-478.**
5. **L. Spjuth, J.O. Liljenzin, M. Skalberg, M.J. Hudson, G.Y.S. Chan, M.G.B. Drew, M. Feaviour, P.B. Iveson, C. Madic (1997),** *Radiochim. Acta,* **78, 39-46.**
6. **T.H. Siddall III, M.L. Good (1967),** *J. Inorg. Nucl. Chem., 29,* **149-158.**
7. **Y. Sasaki, G.R. Choppin (1996),** *Anal. Sci.,* **12, 225-230.**
8. **Y. Sasaki, G.R. Choppin (1998),** *Radiochim. Acta,* **80, 85-88.**
9. **G. M. Gasparini, G. Grossi (1986),** *Solv. Extr. Ion Exch.,* **4,1233-1271.**
10. **H.Suzuki, Y. Sasaki, Y. Sugo, A. Apichaibuol, T. Kimura (2004),** *Radiochim. Acta* **92, 463-466.**



SEPARATION PHASES WITH DEGRADATION PRODUCTS OF AMINE AND ALCOHOL

Bruno Courtaud - Philippe Morel

Procedure and Analysis Study Department
COGEMA/SEPA - B.P.N°71 - 87250 BESSINES/GARTEMPE (France)

Uranium plants generally use a solvent extraction process for the purification of uranium solutions.

Extraction is most commonly carried out with a solvent consisting of tertiary amine (~0.12 M), tridecanol (~10% vol.) and kerosene. The extraction process consists of contact with a sulphuric acid aqueous phase and regeneration with a carbonate aqueous phase. Problems can occur with the velocity of phase separation.

A phase disengagement rate test shows that the secondary and primary amine have no effect on the velocity.

Carboxylic acid as a degradation product of alcohol has no effect on the phase disengagement rate with the acid aqueous phase; however, it does have a very significant effect on the phase disengagement with carbonate phase. It is an interfacial effect of the carboxylate negatively charged with a stabilization of the mixture.

This study shows the results of tests on the effect of carboxylic acid and amine degradation products on the phase disengagement rate.

INTRODUCTION

Uraniferous mineral processing plants produce uranium by using various dissolution, separation, filtration and precipitation procedures and liquid-liquid extraction in particular. Liquid-liquid extraction is an important phase in uranium concentration and purification. Various types of solvent are used and the choice thereof depends on the type of dissolution of the mineral. Generally sulphuric dissolution will be followed by amine solvent extraction. These are relatively susceptible to oxidation and the presence of degradation products can be found in their composition which can adversely affect the uranium extraction process (1).

Problems are encountered in an uranium production plant, with very high losses of solvent and with the reduction of the capacity of the solvent with respect to uranium. A first study showed that clarification of the pregnant solution was one obvious cause of losses.

Another hypothetic cause could be problems of disengagement of phases due to degradation of the solvent.

The study presented in this document deals with the analytical characterization of degradation products and their effect on phase disengagement.

EXPERIMENTAL METHODS

Measurement of Surface and Interfacial Tension

In systems in which immiscible liquids are used, the interfacial tension between these liquids is paramount in order to estimate the stability of dispersions.This interfacial tension represents the work that must be brought to the system to create a surface or interface between the two immiscible phases : dw = - y dS. This work, which is necessary to increase the interface (dw), is proportional to the increase of this surface (dS). The proportionality factor is the interfacial tension (y). We can see immediately from this ratio that for the same quantity of work brought to the system, the smaller y it is, the greater the surface area created. This results in a constant volume through the formation of droplets of smaller diameters.

Other phenomena are involved (2). These are also related to interfacial tension and the size of the droplets dispersed and are sedimentation, skimming, and phase separation. This phase separation may take a shorter or longer time but it always exists; the dispersed systems are thermodynamically unstable (apart from microemulsions). The velocity with which this separation of phases occurs is described well by Stockes' Law :

$$V = \frac{2\ gr?d1 - d2)}{9n} \qquad (1)$$

In this law we find the size of droplets (q) squared, the viscosity of the continuous phase (h), the density of each phase (d^ d_2) and gravitational acceleration (g). The essential information that can be derived from this law is that the smaller the droplets are, the slower the velocity of phase separation (it should be noted that this approach does not take coalescence phenomena into account).

When the approach of interfacial tension is combined with sedimentation, it appears that the lower the interfacial tension between two immiscible liquids, the smaller the size of the particles and the longer the disengagement time.

The weighed drop method is relatively simple and can be used to measure the surface tension of aqueous liquid or solvent (phase-ambient air measurement) as well as the values of interfacial tension between two immiscible liquids (liquid 1-liquid 2). This method is described in detail in numerous works, in particular, the book by Paul Becher (3).

The simplified principle is as follows: A droplet is formed at the end of a capillary tube, whose diameter is known, using a micrometric syringe. When the weight of the drop is sufficient to create air-liquid surface tension at the junction of the capillary tube, it breaks away. The value of its mass is used to find the surface or interfacial tension using the TATE ratio :

$$Ap.v.g.= 27t.r.y.F \qquad (2)$$

Ap Difference of the density between the liquid and the air or other liquid,
v : Volume of the drop,
g : Gravitational acceleration,
r : Internal radius of the capillary tube,
y : Surface or interfacial tension.

F : Correction factor taking into account the volume of the drop and the radius of the capillary tube (charts used).

Measurement of Disengagement Velocities

Disengagement velocities are determined using a set-up that makes it possible, after subjecting both phases to controlled agitation, to measure the phase separation front(s) over time once agitation has stopped.

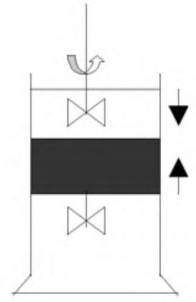


Figure 1. Measuring apparatus

The equipment comprises a ll graduated cylinder and a double helix agitator. The organic phase is put into the cylinder (200 cm^3). Agitation is maintained at 500 rpm. The aqueous phase is "carefully" poured into the cylinder (200 cm^3). Agitation is increased to 1,200 rpm for 3 minutes. When agitation is stopped, both ascending (rising curve) and descending (descending curve if visible) phase separation is recorded overtime.

Samples

As the industrial solvent is a mixture of amine III alcohol and diluent, the samples of this study are mainly commercial products of the plant : Amine III is trioctylamine (Alamine 336 from COGNIS), Alcohol is tridecanol (Exxal from Exxon) and Kerosene is the aliphatic diluent (Keroil from Total). Amine II is dioctylamine, Amine I is monooctylamine (laboratory reagents from Aldricht). Because the industrial solvent ("Plant" in table 2) shows amine II and amine I from the degradation process (not yet clarified) different compositions of solvent have been prepared as shown in table 2

Sample reference	Amine III	Amine II	Amine 1	Alcohol	Kerosene
AIM	0.18 M	0	0	12 % vol.	QS
AMI - AII	0.09 M	0.09 M	0	12 % vol.	QS
AMI - AII - AI	0.06 M	0.06 M	0.06 M	12 % vol.	QS
Plant	0.08 M	0.098 M	0.06 M	12 % vol.	QS

Table 1. Composition of the samples

RESULTS

Interfacial Tension

The interfacial tension measured by the weighed drop method (equation 2) on each compound of the solvent with acid and alcaline aqueous media are in table 2.

The interfacial tensions between a new solvent prepared in the laboratory, the plant solvent and sulphuric acid are almost identical, which must result in phase separation velocities of the same order of magnitude. On the other hand, the interfacial tensions with carbonated solutions are totally different, which shows a difference between these two solvents.

Table 2. Measured interfacial tension (mN.rn[1])

	H_2S0_4 20 g.T[1]	Na_2C0_3 100 g.l'[1]
Kerosene	48.1	14.7
Alamine 336	21.8	Very dirty alamine, drops cannot be seen forming
Tridecanol	21.8	15.9
New solvent	10.8	11.8
Plant solvent	12	No drop forms y very low

New solvent must separate easily upon regeneration whereas plant solvent is liable to form a stable suspension. While this behaviour is due to solvent degradation products, these are only tensio-active in an alkaline medium which leads one to think of ionizable products with a high pH such as carboxylic acids.

Phase Disengagement Velocities

Influence of amine degradation products

The effect of amine II and amines I from amine III degradation on phase separation velocities with acid solution is shown in the figure 2. It simulates the extraction and stripping steps in the plant.

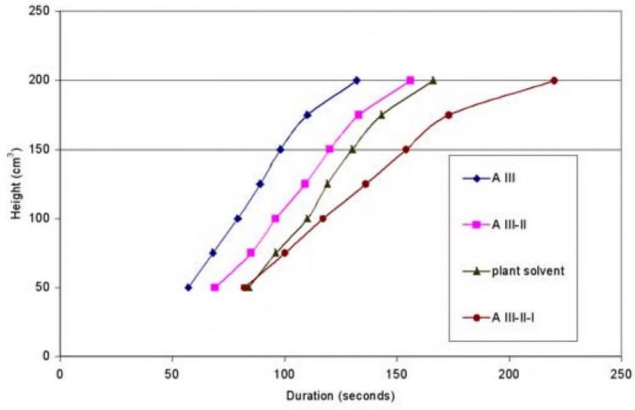


Figure 2. Phase separation velocities - solvent / H_2S0_4, 20 g/T[1]

The more the amine deteriorates, the longer, the phase separation between the solvent and sulphuric acid is. There is a good concordance between plant solvent and new solvent prepared in lab (AMI - AII). The effect on phase separation velocities with alkaline solution is shown in the figures 3 and 4. It simulates the regeneration step in the plant.
Plant solvent separates very poorly and remains cloudy at the end of measuring. The latter contains 50% amine II and the behaviour in relation to a carbonated solution is different from that of a synthetic solvent prepared with amine II. This behaviour is not attributable to the presence of amine II.

In order to illustrate the effect of amine III degradation products on the velocities of disengagement, we have "zoomed in" on the curves from Figure 3 which are in the new figure shown in figure 4.

The more deteriorated the amine, the faster the velocity of phase separation. A phases disengagement problem on the plant solvent is consequently not attributable to the presence of amine II.

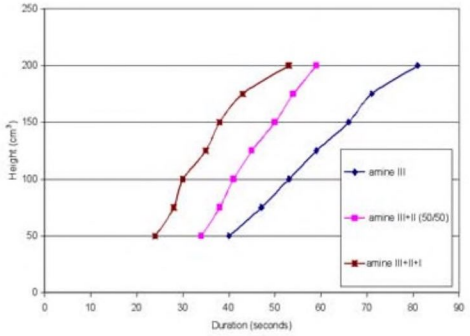


Figure 3. Phase separation velocities
Solvent/$C0_3Na_2$, IOOg/T[1]

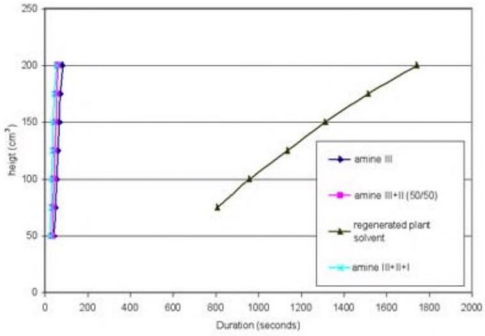


Figure 4. Solvent phase separation velocities
Solvent /$C0_3Na_2$, 100 g/l

Influence of alcohol degradation products

One of the degradation products of alcohol liable to be found in the solvent is decanoic acid. We introduced this product into a new solvent with a content of 0.1% by volume.

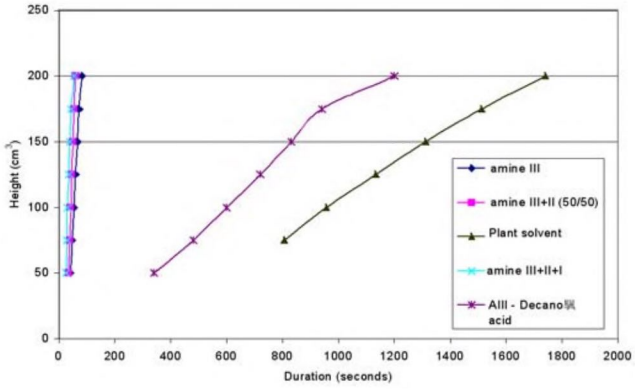


Figure 5. Solvent phase separation velocities with $C0_3Na_2$ in the presence of decanoic acid

The decanoic acid has a tensio-active role in an alkaline medium. This results in a stabilization of the oil-water dispersion. The separation of the phases is significantly slower. In light of these results, it becomes necessary to research similar degradation products using a vast analytical program.

ANALYTICAL CHARACTERIZATION

Sairmles

A study of the characterization of solvent degradation products has been carried out on the following samples : Amine III (Alamine 336), Tridecanol (Exxal), Kerosene (Keroil), New solvent prepared in the laboratory from each compound, and the plant solvent.

Results

Table 3. Analytical characterization

	Amine II (Total % amines)	Amides (Total % amines)	% Light alkanes / heavy alkanes
Alamine 336	**1.7**	**0.12**	-
Keroil	-	-	**2.6**
New solvent	**13.4**	**~ 0**	**22.4**
Plant solvent	**46**	**3.28**	**25.7**

The following interpretations can be made from the table 3 :

- **Commercial Alamine 336 contains amines II and amides.**
- **The signature of the different reagents of which it is composed (alamine 336, kerosene, alcohol) is found in the new solvent.**
- **The plant solvent contains a high proportion of secondary amines (~ 50 %), as well as a relatively high quantity of amides.**
- **The analysis of the alcohol, which is not shown in the table, is a complex mixture of iso and cyclo-alcohols in C n, Ci_2, C_{13} and C_{14}.**
- **The amines II / amides ratio is 14 for plant solvent and alamine 336. This suggests that the degradation of the solvent entails the formation of amides jointly with the formation of amines II.**
- **No trace of carboxylic acid was detected, but it does not mean that there is no carboxylic acid at all because traces in such mixtures are very difficult to determine.**
- **The amides were recently tested in phase disengagement velocities and had no effect in acid medium or alkaline medium.**

CONCLUSIONS

The analytical characterization, the measurement of the phase disengagement velocities and the interfacial tension values are consistent and allow us to make the following observations :

- **The degradation products of amine disrupt the phases in an acid medium but not in a carbonate medium.**

- **The behaviour of the plant solvent was well simulated by the addition of decanoic acid. It has a very significant effect on the phase disengagement with carbonate, which simulates the regeneration step in the solvent plant.**

Carboxilyc acid shows an interfacial effect and could stabilize the emulsion as a carboxylate in alkaline medium.

Further tests are planned with more precise identification of the amides and more thorough research of carboxylic acids.

BIBLIOGRAPHY

1. **C. Manson (1983), Handbook of Solvent Extraction,** *Tech. C10-MHI BAIRD*
2. **M.D. Bishop, Z.A. Gray, T.L. Young and M.G. Greene, Technical Developments Leading to Modern Solvent Extraction Diluents.** *SME*
3. **P. Becher, (1959), Emulsions - Theory and Practice,** *Reinhold*

TRANSPORT PHENOMENA DURING THE EXTRACTION OF METAL OXOANIONS BY ALIQUAT 336 AS STUDIED BY ANALYTICAL ULTRACENTRIFUGATION AND THE MODELLING WITH FDM

Nguyen T. K. Dzung and Rainer Ludwig

Freie Universitaet Berlin, Institute of Chemistry/Inorg. & Analyt. Chem., Fabeckstr. 34-36, 14195 Berlin, Germany

The transport of Mo(VI) and Cr(VI) oxoanions and their complexes in aqueous and in organic solutions respectively was investigated in terms of diffusion and extraction experiments. The apparent diffusion coefficients and the transport coefficients were determined as a function of metal concentration, phase composition and temperature. The mass transport was monitored as refractive index gradient using an analytical ultracentrifuge, allowing phase contact without stirring. A model based on finite elements was applied to model the transport and to calculate concentration and gradient profiles as a function of time and distance from the interface.

INTRODUCTION

Various techniques are applied to determine kinetic parameters of mass transport such as diffusion coefficient (D), transport rate across the interface (a), mass flux (J) and flux density (j) [1], The method of analytical ultracentrifugation combined with optical detection systems [2] was shown to complement other methods such as stirred cell, rotating disk and single drop methods, because the bulk phases are unstirred, the transport is one-dimensional and the interface is rigid [3-5]. This is achieved by the impact of the centrifugal force, which on the other hand is low enough to avoid sedimentation of species in the solutions.

We were interested in the diffusion and extraction of cationic as well as of anionic species such as TcO_4^-, ReO_4^-, $Cr_2O_7^{2-}$ under the influence of chemical reactions [6-8], The subject of this contribution is the diffusion of MoO_4^{2-} at neutral pH and its extraction by quaternary ammonium ions. Although data on the extraction equilibria were reported before [9-13], few kinetic data are available. The mass transport will be described by assuming hindrance at the interface, whereby one boundary condition is that the interface has infinite thickness [14,15]. The finite difference method [16] was applied to solve the corresponding transport equations [17], In the extraction of MoO_4^{2-} by Aliquat 336, we observed Marangoni convection [18] at the organic side of the interface at 298 K, similar to the case where $Cr_2O_7^{2-}$ was extracted. We discussed it in terms of rapid mass transport in the aqueous phase and across the interface, followed by slow diffusion in the organic phase. Therefore, we now varied the temperature and observed that at lower temperature (282 K) no turbulence occurs. The program with the implemented model then correctly describes the mass transport in bulk solutions and at the interface under this condition. The model also predicts under which conditions turbulence occurs.

EXPERIMENTAL

Equipment

An analytical ultracentrifuge Beckman model E with Schlieren optical system, videosystem and graphic tablet (Wacom) was used to study the mass transport [7]. The synthetic-boundary type double-sector centerpiece made of epoxy/carbon was sealed with sapphire windows and placed in the measurement cell. The solutions (aq./aq. or aq./org.) were filled into the corresponding sectors and the cell was placed in the rotor (type Ti-AN-H) inside the evacuated, thermostated (isothermal conditions) chamber. Acceleration to 5800 rpm (30000g) lead to the overlay as the solution from one sector floats through the capillary on the surface to the other sector. The surface at this speed is rigid thus avoiding stirring. The volumes of over- and underlaid phase are equal (120 pi). Figure 1 shows schematically the centerpiece with the sectors. The Schlieren-picture and the time were recorded continuously.

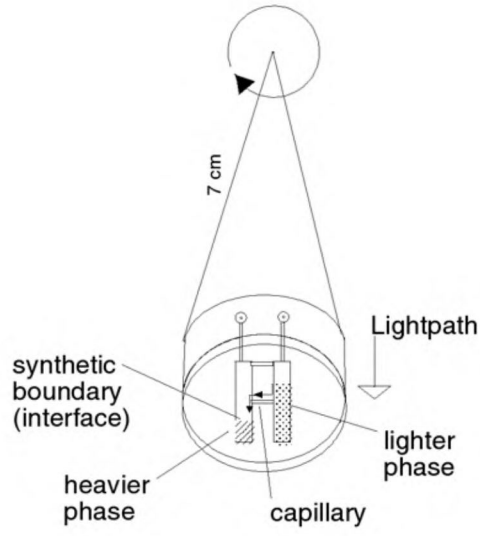


Figure 1. Schematic view of the centerpiece indicating the flow of the lighter phase during overlay

Solutions

Except for the metal ions or complexes under investigation, all other components were adjusted to equal concentrations with respect to both phases including pre-equilibration of the organic phase with aqueous, metal-free solutions in order to avoid interfering concentration gradients. The composition of the solutions is given in Table 1. Aqueous solutions were prepared by dissolving the corresponding salts in aqua dest. and the metal concentrations were confirmed by ICP-AES. $(NH_4)_6Mo_7024$ p a. was used to prepare Mo(VI) stock solutions. The concomitant diffusion of NH_4^+ can be neglected because of the small refractive increment of low-molecular weight ions. The organic phase for an extraction run containing xylene and Aliquat 336 was pre-equilibrated with with NH_4Cl solution. For an organic diffusion run, the metal-loaded organic phase was prepared by extracting Mo(VI) from the aqueous phase. The distribution ratio (log D = 2.98) was determined from the mass balance in the aq. phase before and after batch-wise extraction at 298 K at comparable concentrations by ICP-AES.

Table 1. Composition of the molybdate diffusion and extraction systems

Diffusion (aqueous)		Diffusion (organic)	
c of metal ion[a])	matrix	c of metal complex[3])	matrix
4.6 to 17 mM $Mo0_4^{2-}$	H_20	4.6 to 13 mM $(NR_4^+)_2Mo0_4^{2-}$	xylene, 10 v% Aliquat 336[b]), (equil. 27 mM NH_4Cl)
4.6 to 13 mM $Mo0_4^{2-}$	27 mM NH_4Cl T: 282 K, 298 K		
Extraction (282 K, 298 K)			
aqueous		**organic**	
c_{jnit} 0.0128 mM $Mo0_4$ 2- in 0.027 M NH_4Cl		xylene, 10 v% Aliquat 336 (equilibrated with 0.027 M N H_4Cl)	

[a]) the concentration c is that concentration where the solutions from both sectors meet (which is half of the initial one according to the error function, eqn. 2)

[b]) Aliquat 336° is a quaternary amine (R4 = tri(C_8.io-alkyl)methyl) used in solvent extraction

RESULTS AND DISCUSSION

DIFFUSION

The second law of transport (Eqn. 1) is applied, and the concentration of the diffusing compound is given by differentiating the error function (Eqn. 2). In the resulting Eqn. 3, the concentration gradient is substituted using the refractive increment and the height of the Schlieren peak. Integration gives Eqn. 4, which allows to determine the apparent diffusion coefficient *D* from the experimental data (peak area A, height H_{max}) and the optical amplification factors fL. The integration constant b doesn t influence the value of *D*. The values of cross diffusion coefficients cannot be determined this way but require an interference optical system instead.

$$\left.\frac{dc}{dt}\right|_x = D\left.\frac{\partial^2 c}{dx^2}\right|_t \quad (1)$$

$$c = \frac{c_0}{2}\left(1 - \frac{2}{\sqrt{\pi}}\int_0^f e^{-y^2}dy\right) \quad (2)$$

$$\left[\frac{c_0}{\left.\frac{dc}{dx}\right|_{x=0}}\right]^{-2} = An.\,Dt + b \quad (3)$$

$$A^2/H^2_{max} = 4n(f_1 \cdot f_2)^2 U^2 Dt + b \quad (4)$$

The diffusion coefficient for Mo(VI) as a function of its concentration in the aqueous phase is depicted in Figure 2. The metal concentration refers to that at the synthetic boundary (x=0), equal to half the initial one. In the presence of 0.027 M NH_4Cl, the diffusion coefficients are lower compared with pure water due to higher ionic strength and viscosity. The variation over the metal concentration range was discussed in terms of long-range interaction in the aqueous phase [6, 19]. At lower temperature, the value of *D* decreases due to the higher viscosity and stabilization of the water structure. In case of TcO_4^- however, the diffusion coefficient did not vary significantly between 298 and 323 K, probably due to the leveling effect of the 3M HNO_3 used as matrix in those experiments.

The range of D-values is comparable with that determined previously for Cr(VI) and Re(VII) and we conclude that Mo(VI) under the experimental conditions exists as MoO_4^{2-} ion.

The diffusion coefficients in the organic phase are also included in Figure 1. A decrease in temperature by 15 K had no significant influence on the value of *D* at low concentration of Mo(VI). At the highest concentration investigated here (13 mM with regard to MoO_4^{2-}), we observed Marangoni convection in the organic phase. We interpret it in terms of the high value of dc/dx which subsequently leads to the interaction with solvent molecules.

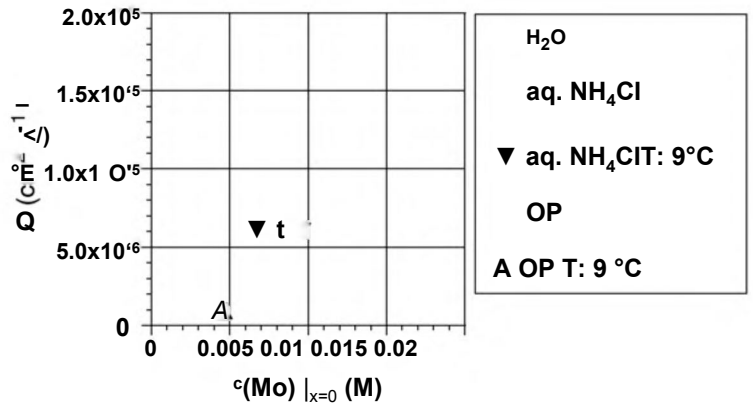
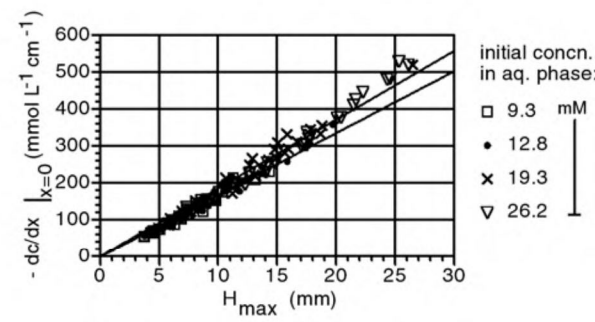


Figure 2. Apparent diffusion coefficients of Mo(VI) in aqueous (H_2O or 27 mM NH_4Cl) and organic (xylene, 10 V% Aliquat 336) phase at 298 and 282 K.

CONCENTRATION GRADIENTS

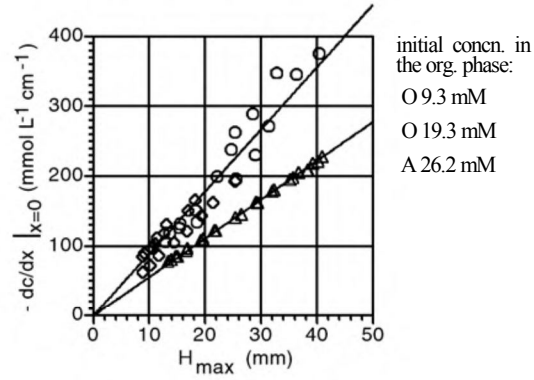
Based on the data from diffusion runs, a correlation between peak height and concentration gradient according to Eqn. 5 is plotted in Figures 3 and 4 for aqueous and organic phase respectively. It serves as a basis for the subsequent treatment of data from extraction runs. The concentration range where the corresponding correlation is valid is given in brackets. We concluded that in aqueous solution the speciation doesn t significantly change within the metal conceimaiiuM lanye, while in Lhe organic phase it changes at higher concentration.

$$\left(\frac{dc}{dx}\right)_{x=0} = -\frac{c_{init}}{\sqrt{2\pi D t}} = f(H_{max}) \qquad (5)$$



f(x) = 16.78676 * x (9 mM ≤ c ≤ 13 mM)

f(x) = 18.61836 * x (19 mM < c < 26 mM)



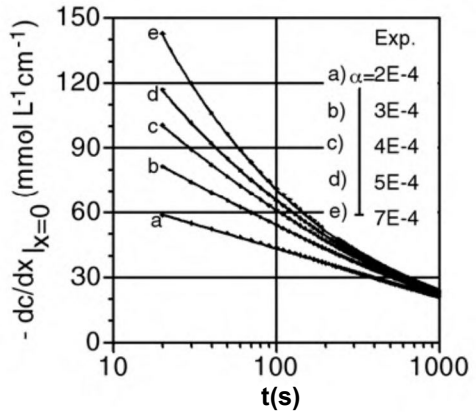
f(x) = 8.910043 * x (9 mM ≤ c ≤ 19 mM)

f(x) = 5.561021 * x (c = 26 mM)

Figures 3 (left) and 4 (right). Correlation between concentration gradient at the interface and peak height.

EXTRACTION

At 298 K we observed turbulence at the organic side up to 0.3 mm from the interface for several minutes after overlay. We considered that either the fast input of mass across the interface, followed by slow diffusion into the bulk organic phase, causing an high concentration gradient, or the heat of complex formation at the interface could be responsible for the turbulence. Therefore, we carried out the experiments at reduced temperature, where the diffusion in the aqueous phase is slowed down. At 282 K, the Marangoni convection is not observed. The concentration gradient at both sides of the interface with data from 5 experiments is shown in Figures 5 and 6.



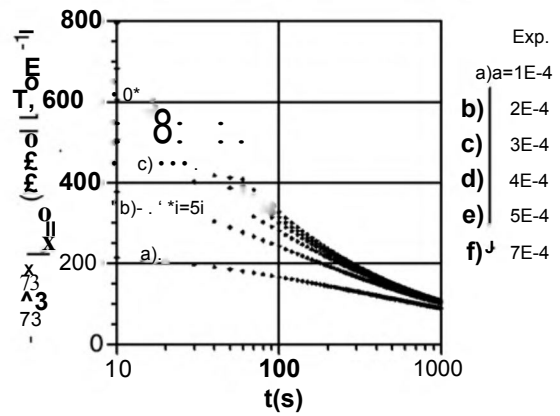


Figure 5 (left, aqueous phase) and 6 (right, organic phase). Finding the optimum transfer coefficient a for the extraction of Mo(VI) into 10 v% Aliquat 336 in xylene at 282 K (conditions see Table 1). Experimental data are shown from 5 different centrifuge runs. With a -=4 10~⁴ cm s'¹ the best fit at the early stage of extraction is found. Deviation at later time is interpreted as (i) optical distortion at peak height < 1mm, and (ii) overlapping chemical reaction kinetics.

The one-dimensional mass transport can be described by the model established by Drickamer[15]. Instead of the original solution by Laplace-transformation, we solved the transport equations (1), (6) and (7), the latter representing the transport across and the continuity at the interface, by the method of finite differences. The measurement cell is divided into 2x1000 finite elements (Figure 6) where the concentration gradient between neighboring elements is approximated by Eqn (8). The mass balance in the element (i+1) is calculated according Eqn. (9) where the mass flux J_A through the area A is given by Eqn. (10) and the time interval is defined by the stability critereon.

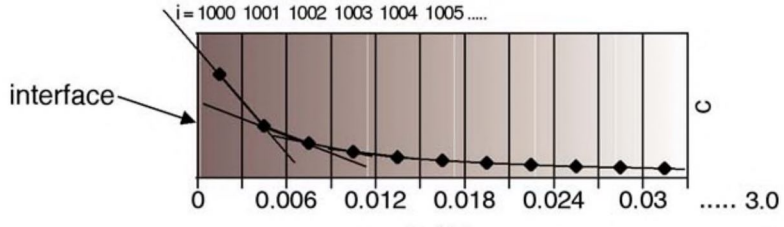


Figure 7. Scheme of FDM applied to the one-dimensional transport in the organic phase

$$\vec{J}^{(c}(x=-0,t)' {}^{c}(x=+0,\ t)] = a\ ({}^{c}(x=-0,f)' \quad \frac{1}{K_u}{}^{c}(x=+0,r)\} \tag{6}$$

$$-D_1 \frac{\partial c_e}{\partial x}_{x=-0,t} = -D_2 \frac{\partial c_e}{\partial x}_{x=+0,t} = \vec{J} \tag{7}$$

$$\frac{\partial c}{\partial x}_{G(i-i+l)} \approx \frac{(c(x_i) - C(*_{i+1}))}{\Delta x} \tag{8}$$

$$C_{i+l} = c_i - \frac{J_A}{\Delta X} \tag{9}$$

$$y_A(j->i+l) = \frac{J_{(i \cdot 1)}}{cL4} \sim D \cdot G_r \quad i\ (l —* i+1)^{v} A\ t \qquad \text{with } m < \frac{(\Delta x)^2}{\sim 2D \sim} \tag{10}$$

$$c_i \mathrel{+}= \frac{D\,((c_{i-1} - C_i) - (C_i - C_{i+1}))\,\Delta t}{\Delta x^2} \tag{11}$$

$$c_{999} \mathrel{+}= \frac{\alpha\,(c_{999} - \frac{1}{K_D} c_{1000})\,\Delta t}{\Delta x^2} \quad \text{and} \quad c_{999} \mathrel{-}= \frac{\alpha\,(c_{999} - \frac{1}{K_D} c_{1000})}{\Delta x} \tag{12a, b}$$

Out of the first element (the bottom of the cell), the mass is transported by diffusion. The next elements (i = 2...998) are characterized by input and output of mass by diffusion (Eqn. 11). The element at the aqueous side of the interface receives input by diffusion and release mass by phase transfer according to Eqn. (12a, b). At the organic side, the transport is described accordingly. The transfer coefficient a is varied until the calculation shows agreement with the experimental data. In case of the extraction of Mo(VI) (Figures 5 and 6), the calculation deviates significantly at longer time. We consider two reasons for this: (i) the resolution of the optical system is insufficient for peak heights < 1mm (concn. gradient < 30 mmol/(L·cm)), and (ii) any chemical reaction, which would cause a to change with time, is not yet included in the model at this stage.

We also modeled this and other extraction systems (Mo(VI), Cr(VI), U(VI)) at 298 K (instead of 282 K), where the experiment shows Marangoni convection, taking into account that the model at this stage doesn t include a term for turbulent flow. The model in these cases predicts a concentration maximum at the organic side of the interface on the time-axis; such a maximum is of course not observed experimentally because the steep concentration gradient leads to

turbulence. On the other hand, extraction systems without turbulence, such as Mo(VI) at 282 K and Tc(VII) are described correctly by the model. Thus, from the four parameters D-|, D_2, K_D and a the occurrence of turbulent flow can be predicted.

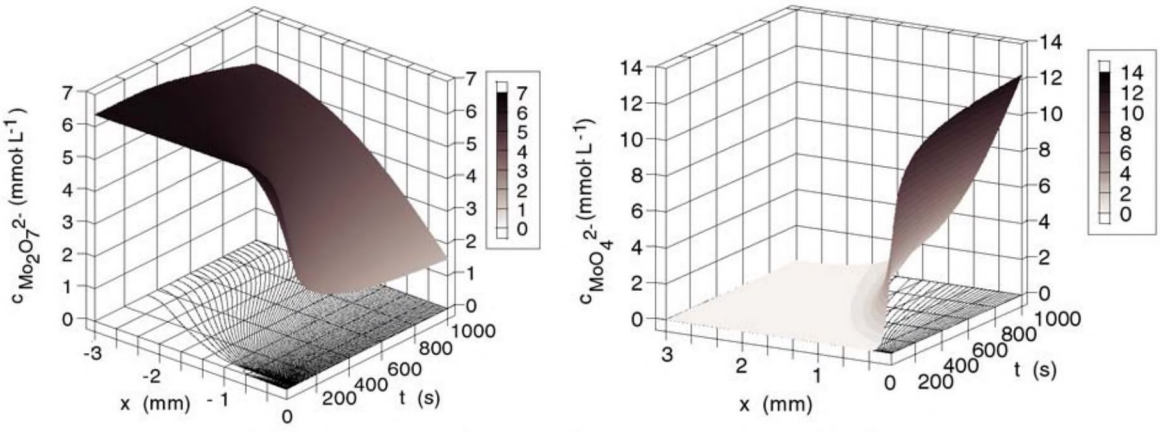


Figure 8 (left, aqueous phase) and 9 (right, organic phase). Concentration profiles calculated with optimum value of a = 4·10~4 cm s'1 for the extraction of Mo(V) at 282 K from 0.027 mM NH_4Cl into 10 v% Aliquat 336 in xylene (Table 1). In aq. phase the dominance of dimeric Mo(VI) **was** *evident. In org. phase monomeric Mo(VI)* **was** *evident, x is the distance from the interface.*

ACKNOWLEDGEMENTS

Part of this work was supported by DFG (SPP 1105). N.T.K.D. acknowledges the financial contribution by Natural Science Council, MOST.

REFERENCES

[1] J. Rydberg, M. Cox, C. Musikas and G. R. Choppin (Eds.) (2004), Solvent Extraction Principles and Practice; 2nd ed., Marcel Dekker: New York, Basel.

[2] P. H. Lloyd (1974), Optical methods in ultracentrifugation, electrophoresis, and diffusion with a guide to the interpretation of records, Clarendon, Oxford.

[3] H. Murso, B. Plewinsky, D. Leopold and G. Marx (1982), In Scientific Basis for Radioactive Waste Management V, W. Lutze (Ed.), Elsevier, New York, pp 491-496.

[4] V. Friehmelt, A. He, Z. Yang and G. Marx (1986), Inorg. Chim.Acta , 111 89-93.

[5] R. Gauglitz, M. Miertschink and G. Marx (1989), Coll. Polym. Sci., 267 (12), 1108-1112

[6] M. Nabeshima, R. Ludwig, T. K. D. Nguyen and G. Marx (2000), Solvent Extraction Research and Development, Japan, 7 85-92.

[7] R. Ludwig, T. K. D. Nguyen and M. Nabeshima (2001), Radiochim. Acta , 89, 169-177.

[8] T. K. D. Nguyen, H. Higuchi and R. Ludwig DECHEMA/GVC Fachausschussitzung Extraktion (2002), VDI, 2002, p 3.08.

[9] L. Karagiozov and K. Vasilev (1981), J. Inorg. Nucl. Chem., 43 (1), 199-200.

[10] M. B. MacInnis and T. K. Kim (1981) US 4278642

[11] L. Karagiozov and K. Vasilev (1984), Hydrometallurgy , 12 (1), 111-116.

[12] N. R. Das and P. Chattopadhyay (1989), Bull. Chem. Soc. Jpn. , 62 (10), 3278-3282.

[13] Y. Bal, G. Cote and D. Bauer (1992), Process Metallurgy 7A, pp. 919-924.

[14] E. J. Scott, L. H. Tung and H. G. Drickamer (1951), J. Chem. Phys., 19 (9), 1075-1078.

[15] L. H. Tung and H. G. Drickamer (1952), J. Chem. Phys., 20 (1), 10-12.

[16] J. D. Faires and R. L. Burdon (2000), Numerische Methoden, Spektrum, Heidelberg.

[17] R. Ludwig, T. K. D. Nguyen, H. Higuchi and J. Henniger (2004), Progr. Coll. Polym. Sci. , Vol. 127: Analytical Ultracentrifugation VII, Springer, Heidelberg, pp 89-97.

[18] D. Isvoranu and M. D. Staicovici, (2004), International Journal of Heat and Mass Transfer, 47 (17-18), 3769-3782.

[19] V. Friehmelt, A. He, Z. Yang and G. Marx (1987), Analyt. Chimica Acta , 201 135-144.



Drop Coalescence behavior for AOT reversed micellar systems

Yasuhiro Nishii, Takayuki Yano, Takumi Kinugasa,
Susumu Nii*, Katsuroku Takahashi*

Niihama National College of Technology, Niihama, Japan
'Nagoya University, Nagoya, Japan

Drop coalescence plays an important role for solvent extraction columns. Factors affecting the drop coalescence time, such as cations in the aqueous phase and surfactants in the organic phase, proteins, were studied for reversed micellar systems. Differences in coalescence time among cation species were observed, which was explained by the interaction between drop and bulk interfaces. The peak of coalescence time appeared at the middle range of cation concentration in KCI system. That is because proteins in the vicinity of interfaces sterically interfere the coalescence. For the cases of divalent cations, the peak-shift to high concentration was observed. It causes by the difference of protein extraction behavior between monovalent and divalent cations. Proteins in the divalent cation systems extract at higher salt concentration region than that in the monovalent one. The coalescence time increased with decreasing aerosol-OT concentration, which is caused by the Marangoni effect due to the interfacial tension gradient.

INTRODUCTION

The reversed micellar extraction has been paid much attention as a protein extraction method for two decades. However, few researches have been done in the area of the apparatus for reversed micellar extraction [1-3], The author [4] conducted the experiment of protein extraction using reversed micelles in a sieve-tray column. The results indicated that the characteristics of the dispersion upon the tray and the coalescence below the tray affected the stage efficiency and the mass transfer capacity coefficient. It was confirmed that the coalescence behavior below the tray is essential in the design of the sieve-tray column.

The drop coalescence with a planar interface proceeds in the following three steps [5], The first step is the approach of a drop to the planar interface, which is controlled by the hydrodynamics of the two liquid phases. The second is the drainage of the thin liquid film between the drop and the interface, which is controlled by the hydrodynamics within the thin film and the surface properties of the drop and the interface [6, 7], The last is the film rupture through surface instability, which is considered to be rapid in comparison to the other steps.

In the present study the effect of salt in the aqueous phase on drop coalescence in a reversed micellar system was investigated to reveal the influence of the surface properties. In addition the effect of the presence of proteins on the coalescence time was also examined in the apparatus simulating the situation in a sieve-tray column.

EXPERIMENTAL

Figure 1 shows the schematic diagram of the experimental setup. It was imitated the situation in a sieve-tray column. The coalescence module is made of a glass tube and a FEP tube, which allows to observe the droplets through the transparent part in the module. The organic droplets were formed through a capillary tube (i.d.=0.85 mm) after filling both the aqueous and the organic solutions into the module. Fifty coalescence movies of droplets were taken by a digital video camera and the representative coalescence time, t_c and the drop diameter, d_p were determined by analyzing the movies with PC.

An aqueous solution was prepared by dissolving a certain salt at a given concentration and lysozyme at 0.1kg/m^3 except for the protein-free experiments. The salt species used were NaCl, KCl, $BaCl_2$ and $CaCl_2$. An organic solution was prepared by dissolving aerosol-OT (bis (ethylhexyl) sodium sulfosuccinate, AOT) in isooctane at 50 mol/m^3 except for the experiments measuring the effect of AOT concentration. The two phases were not inter-saturated and used as they were. The anionic surfactant, AOT purchased from Nakalai Tesque, Inc. was used without further purification. Lysozyme was obtained from Sigma-Aldrich Co. and used without further purification. All the other chemicals were of analytical grade from Wako Pure Chemical Industries, Ltd. or Katayama Chemical.

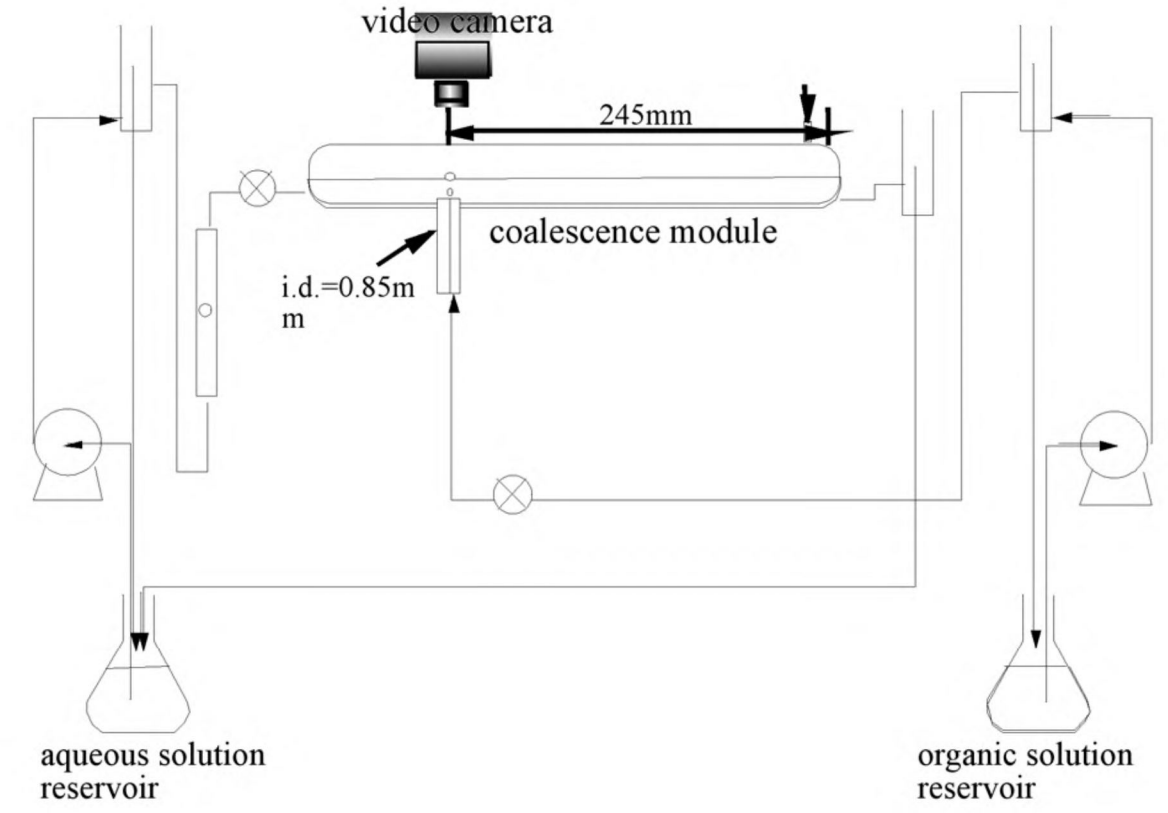


Figure 1 Experimental setup

The relations between the coalescence time and the salt concentration for the case in the absence of lysozyme are shown in Figure 2. For NaCl system, the coalescence time was longer than the other systems and the drop did not coalesce at 0.1 kmol/m³ of NaCl. This is due to the small interfacial tension of NaCl system, which leads the small droplets and the small buoyant force. This is the reason why the coalescence time is large. The decrease of the coalescence time with increasing NaCl concentration is caused by the increase in the electrostatic shield effect.

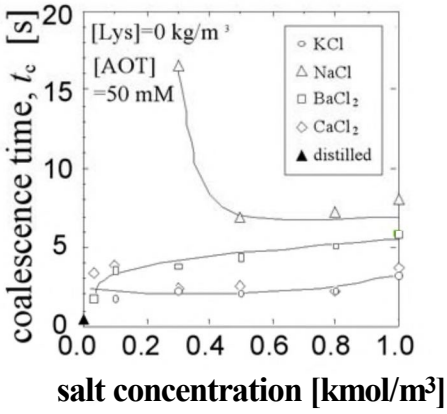


Figure 2 Coalescence time change in absence of lysozyme

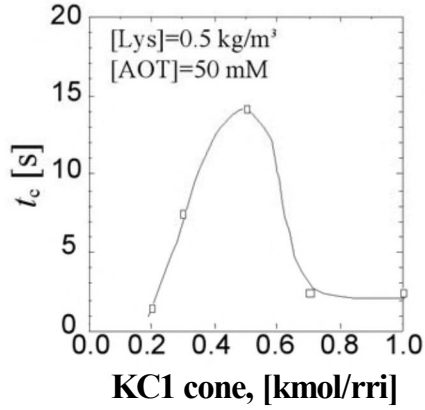


Figure 3 Effect of KCl cone, on coalescence time in the presence of lysozyme

Figure 3 shows the effect of KCl concentration on the coalescence time. With increasing KCl concentration, the coalescence time increased and reached the peak at the middle range of concentration, and then decreased at the high range. At the high range the repulsive force between drop interface and balk interface weakens by increasing of the electrostatic shield effect and the coalescence proceeds fast. At 0.5 kmol/m³ the existence of unextracted proteins in the vicinity of interface prohibits the coalescence sterically. At the low KCl concentration the turbulence of interface was caused by the frequent extraction of proteins and it enhances the coalescence.

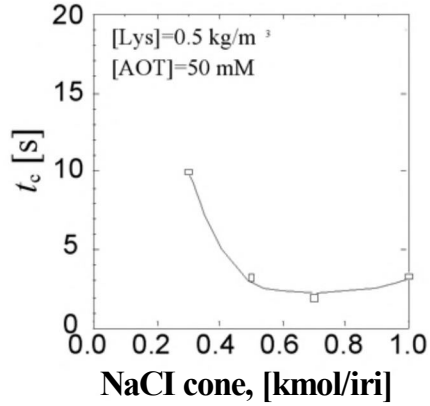
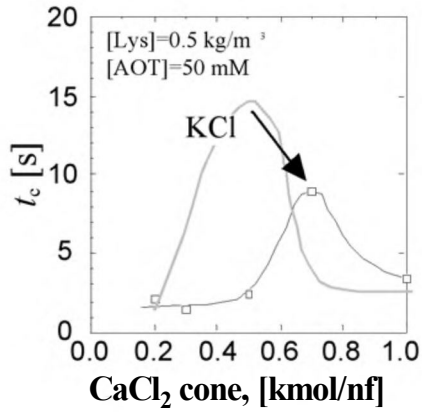


Figure 4 Effect of NaCI cone, on coalescence time in the presence of lysozyme

The results for NaCl system are shown in Figure 4. At the low NaCl concentration the interfacial tension lowers significantly, which causes the very small droplets. The diameters are sixth as large as that for the other systems. That decreases the buoyant force and

delays the coalescence time. Although the extraction of proteins is very frequent for NaCl system, it doesn't affect the coalescence.



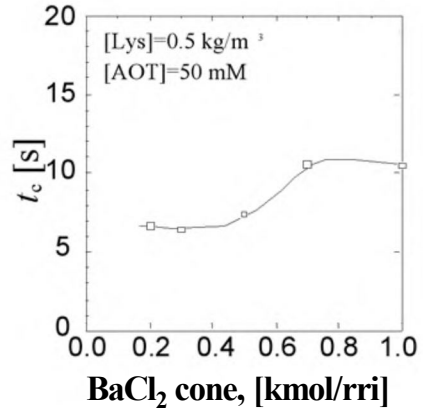


Figure 5 Effect of CaCI $_2$ cone, on coalescence time in the presence of lysozyme

Figure 6 Effect of Bad $_2$ cone, on coalescence time in the presence of lysozyme

The results for $CaCl_2$ system are shown in Figure 5. The peak shifted to the high salt concentration compared with KCl system. Here, we should quote the fact that for divalent cation systems the extraction rate of lysozyme does not lower at the high salt concentration compared with monovalent cation systems. This fact leads the electrostatic shield effect is small even at the high salt concentration for divalent cation systems. Therefore, the coalescence time was high even at the high salt concentration. On the other hand, even at the middle concentration the coalescence time is small due to the protein extraction.

The results for $BaCl_2$ system are shown in Figure 6. The peak-shift appeared as well as $CaCl_2$ system. The long coalescence time for all range of salt concentration is due to the large interfacial tension.

Figure 7 shows the effect of AOT concentration on the coalescence time for KCl system at the absence of proteins. The peak appeared at 0.05 mol/m³ in the AOT concentration range between 0.01 to 50 mol/m³.

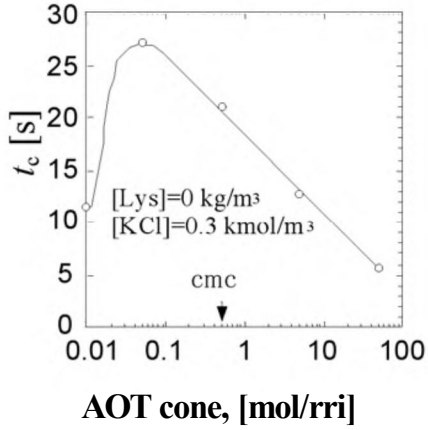


Figure 1 Effect of AOT cone, on coalescence time in the absence of lysozyme

In general, the coalescence includes the process of the liquid drainage between interfaces. During this process the drainage makes the AOT concentration gradient at the drop interface. This gradient leads Marangoni flow, which flattens a surfactant concentration gradient at

interface. Since Marangoni flow is against the drainage, the coalescence is suppressed. At the high AOT concentration Marangoni flow does not happen since AOT molecules in the organic phase are re-distributed onto the drop interface. As a result, the coalescence time becomes small. With decreasing AOT concentration the coalescence time became large. This is due to the delay of AOT distribution onto the interface because of its smaller concentration. At very small AOT concentration, since there are not enough AOT molecules at the drop interface to cause Marangoni effect, the coalescence proceeds rapidly.

Figure 8 shows the effect of AOT concentration on the coalescence time in the presence of lysozyme for KOI and $CaCl_2$ systems. The peak shifted to the higher AOT concentration compared with the case in the absence of lysozyme. Over the cmc (critical micelle concentration) for AOT system, the coalescence time decreased drastically. This indicates that the formation of reversed micelles makes the interfacial turbulence. The larger peak than protein-free system is due to the unextracted proteins at the interface, which interfere the deformation of the interface. At the smaller range of AOT concentration than cmc, the coalescence time decreased more steeply than protein-free system. The interaction between proteins and AOTs prohibits the Marangoni flow. This leads the small coalescence time. The difference between KOI and $CaCl_2$ systems in the range over cmc is due to the high protein extraction ability of $CaCl_2$ system compared with KOI system.

The results for NaCl and $BaCl_2$ systems are shown in Figure 9. For NaCl system, over all the range of AOT concentration the coalescence time was relatively small. At 0.3 kmol/m^3 NaCl, the interfacial tension is very small compared with the other systems. It means the interface is very spreadable and Marangoni effect becomes weak. For $BaCl_2$ system, over all the range of AOT concentration the interfacial tension is high, which causes the difficulty to move AOTs at the interface. For both salt systems Marangoni effect is weakened and the coalescence time becomes small.

CONCLUSION

The unique properties of drop coalescence behavior were investigated for each system. For the absence of lysozyme the coalescence time was totally small, but for NaCl system the coalescence occurred slowly due to the small droplet formation. For KCl system in the presence of lysozyme, the peak appeared because the extraction of lysozyme affected the interface. For $CaCl_2$ system, the peak shifted to the high salt concentration, which is caused by the difference of protein extraction behavior between monovalent and divalent cation systems. For the results for the effect of AOT concentration in the absence of lysozyme, the degree of Marangoni effect changed the coalescence behavior. For KCl and $CaCl_2$ systems in the presence of lysozyme the peak shifted to the high AOT concentration, which related to the formation of reversed micelles. Since interfacial tensions were very small or large for NaCl or $BaCl_2$ svstem Maranaoni flow did not haoDen easilv. the coalescence time held steady.

ACKNOWLEDGEMENTS

This research has been subsided with Grants-In-Aid for Scientific Research by Ministry of Education, Culture, Sports, Science & Technology, Japan (subject number:16760612).

REFERENCES

1. J. Tong and S. Furusaki, *J. Chem. Eng. Jpn.,* **28, 582-589 (1995)**
2. G. J. Lye, J. A. Asenjo and D. L. Pyle, *AlChE J.,* **42, 713-726 (1996)**

3. **Y. Nishii, S. Nii, K. Takahashi and H. Takeuchi,** *J. Chem. Eng. Jpn.,* **32, 211-216 (1999)**
4. **Y. Nishii, C. Hara, T. Kinugasa, S. Nii and K. Takahashi,** *Solv. Extr. Res. Dev., Jpn.,* **9, 111-119 (2002)**
5. **G. W. Stevens, H. R. C. Pratt and D. R. Tai,** *J. Colloid and Interface Sci.,* **136, 470-485 (1989)**
6. **S. R. Deshiikan and K. D. Papadopoulos,** *J. Colloid and Interface Sci.,* **174, 313-318 (1995)**
7. **C. Chen, J. Maa, Y. Yang and C. Chang,** *Surface Sci.,* **406, 167-177 (1998)**

THE INTENSIFICATION OF ACID STRIPPING UPON GENERATING WAVES AT INTERFACE

Kizim N. F., Golubina E.N.

Institute of Mendeleyev University of Chemical Technology, Novomoskovsk, Russian

ABSTRACT

During spontaneous surface convection arising in the course of extraction process the interface oscillations are observed. The spectrum of oscillations is wide enough; it involves average frequent oscillations of sound range. The external mechanical influences on the interface allow to provoke resonance and thus to affect the kinetics of stripping. The experimental installation and the methods of carrying out an experiment are described. It has been stated by experiments, that the magnitude of effect of intensification is determined by the form of a vibrating elements, by the construction of the experimental cell and by the phase height too. The resonant frequency is determined by the nature of contacting phases. The effect of intensification is caused by the reduction of magnitude diffusive resistance of mass transfer.

INTRODUCTION

It is known that liquid extraction is often accompanied by spontaneous surface convection caused by hydrodynamic instability of interface. Spontaneous surface convection, as the experiment shows, is revealed in many ways: wave movement of the surface, the rise and development of roll cells, interfacial turbulence. Sometimes disturbances of interface are so great that eruptions are observed. Oscillations with a frequency of 0.2 to 20 Hz were observed during extraction in [1], Later, the same authors [2 - 6] thoroughly studied the collisions and formation of waves and reflection wave at interface during the adsorption of surfactants, which take place the number of Marangoni is higher critical.

Since the spectrum of interfacial waves arising during spontaneous surface convection in extraction systems is wide enough and contains constituents in the average frequent area of sound ranqe, we made efforts to strenqthen them bv means of qeneratinq waves on interface. It is clear that during resonance the supply of additional energy to the dynamic interfacial layer is the most effective, and extraction speed increase could be expected.

The aim of the work was experimental confirmation the ability of intensification extraction (or stripping) upon generating waves on interface and to determine factors having an influence on the magnitude effect.

EXPERIMENTAL SECTION

Experiments were carried out on a setup composed of a low-frequency generator, a conductometer with ADC (analog-digital convector), a glass cell, and a vibrator (Figure 1). The vibrator is a high-frequency electrodynamic head (2-18 kHz) with a stainless steel rod (5-10"^{4} m in a

diameter and 4,3-1 O'² m long), one end of which was rigidly fixed at the center of the diffuser, and the other was connected to the vibrating element. The vibrating element had the following construction: a 0,5-10"²x1,1-10'²x0,3-10"² m rectangular fluoroplastic plate (vibrator 1); a fluoroplastic trihedral prism an isosceles triangle cross-section, a height of 0,5-1 O'² m, and a base of 1,1-10'²x0,3-10'² m (oriented so that the base or the vertex of the isosceles triangle faces in the interface; vibrations 2 and 3, respectively) and a glass sphere 0.3-10'² m in diameter (the vibrator 4). The signal of the conductometer was registered by means of the computer. At mass transfer of acid was observed by conductometer. After 30 seconds the magnitude of electroconductivity is registrated by computer.

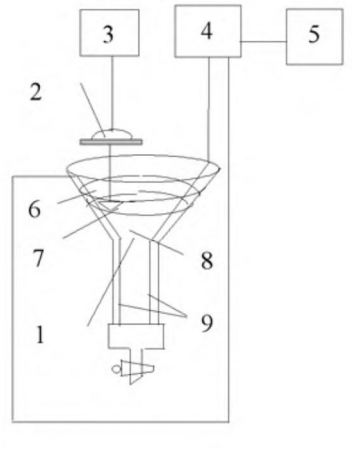


Figure **1** *The sketch of installation. 1 - a conical glass cell, 2 - a vibrator, 3 - a low-frequency generator, 4 - a conductometer, 5- a computer, 6- an extract, 1 - the vibrating element, 8 - an aqueous phase, 9 -an electrode.*

The glass cells were variously shaped (cylindrical, diameter 9,7-ICT² m, wall height 1,5-10'² m; conical, lower diameter 1,0-10'² m, upper diameter 5,6-10'² m, generatrix length 4,8-10'² m; and rectangular (5-10"²x 1,8-10'²x3,2-10'² m)).

The amplitude-frequency characteristics were measured for all vibrators; investigations were not performed in the natural frequency regions. The working frequency range was 4-11 kHz. The electrodynamic head was powered by a sinusoidal voltage from a low-frequency generator.

To estimation the influence of different factors on the process of mass transfer of nitric acid was estimated in terms of the mass transfer coefficient, which calculated to organic phase:

$$k - \frac{dC/dt}{\sim a \blacksquare (C—C^*)}$$

a - is specific surface; C, C* - is concentration of nitric acid in point of time and equilibrium, correspondingly. The primary experiment was shown, that limiting phase is organic.

RESULTS AND DISCUSSION

The motion of the vibrating element in contact with the interface produces identical motions of adjacent elements of the liquid. The disturbance is transferred to the neighboring elements of the liquid, and a wave propagates throughout the system. When the applied frequency approaches the natural vibration frequency of the system, the phenomenon of resonance is observed. The amplitude of induced vibrations at a frequency close to the natural vibration frequency may be many times greater than the amplitude of quasi-static vibrations of the system. Since, the speed varia-

tions in the phase with the external force, the resonant mode is the most suitable for the pumping of energy into the vibratory system, which represents, in this case, the dynamic interfacial layer. Input energy should intensify mass transfer in the transition layer. This effect will manifest itself as an increase in the effective mass transfer coefficient at the resonance frequency.

THE INFLUENCE OF FREQUENCY OF GENERATED WAVES ON THE EFFECTIVE MASS TRANSFER COEFFICIENT

Represented in Figure 2 dependence effective mass transfer coefficient as a function of the frequency shown existence of resonance frequency in which the effective mass transfer coefficient is a 5 times higher than for the process without external impact. In future the frequency of vibrations, which result in abrupt increase of the effective mass transfer coefficient (will be called resonant). Similar depends were receive a number of extraction systems, which is shown on Table 1.

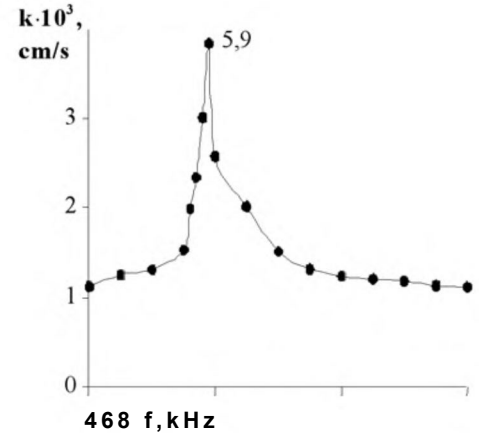


Figure 2. Effective mass transfer coefficient as a function of the frequency of the vibrational perturbation on the **stripping** *in toluene-$HN0_3$-H_20 system in conical cell with vibrator 2.*

THE INFLUENCE OF EXTRACTION SYSTEM COMPOSITION ON RESONANT FREQUENCY

Table 1. The influence of extraction system composition on resonant frequency

No	Solvent	k-10³, cm/s	f_r, kHz	k_r-10³, cm/s
1	Toluene	0,80	5,9	4,00
2	Benzene	1,19	5,8	3,40
3	Tetrachloromethane	0,07	6,6	0,33
4	Trichloromethane	0,76	5,6	3,30
5	1- Octanol	1,38	4,5	2,39
6	Hexahydrobenzene	0,20	7,4	0,97
7	Decane	0,15	7,8	0,59
8	Nonane	0,10	7,6	0,59
9	Heptane	0,63	7,4	2,81

Change of solvent send for resonant frequency. In Table 1 for every system studied during stripping of $HN0_3$ is resonant frequency (f) determined by experiments with an accuracy of ± 0,1 kHz, effective coefficient of mass transfer without generating waves by the vibrating element on the interface (k) and during generating waves at the resonant frequency (k_f) are presented. The organic phase is extracted from $HN0_3$in a solvent indicate of column 2 in the table. The receiving phase is water saturated indicated as a solvent.

The study of resonant frequency dependence on various factors (kinematical viscosities of contacting liquids, densities, the interfacial tension) allowed to detect the existence of close correction bond with the interfacial tension which became the basis of a new method of interfacial tension determination.

THE EFFECT OF THE GEOMETRY OF THE VIBRATING ELEMENT ON THE EFFECTIVE MASS TRANSFER COEFFICIENT

Typical time dependences of the effective mass transfer coefficient for the four vibrating elements (different in shape) are presented in Figure 3. The greatest intensification of the stripping process is observed for vibrator 3. In this case, the lateral faces of the vibrating element (located at an angle of 42° to the interface) generate the main longitudinal waves carrying an additional energy into the transition layer. It is known that tangential motion of the fluid occurs in the presence of the Marangoni effect. This motion is initiated by the local gradients in the interfacial tension that are caused by a nonuniform surface distribution of surface-active substances. In spite of the fact that, in our case, the tangential motion of the elements fluid is caused by interfacial waves can be considered as a controlled, artificial Marangoni effect. Waves directed to the bulk of the aqueous phase quickly decay, and their influence on mass transfer is unimportant.

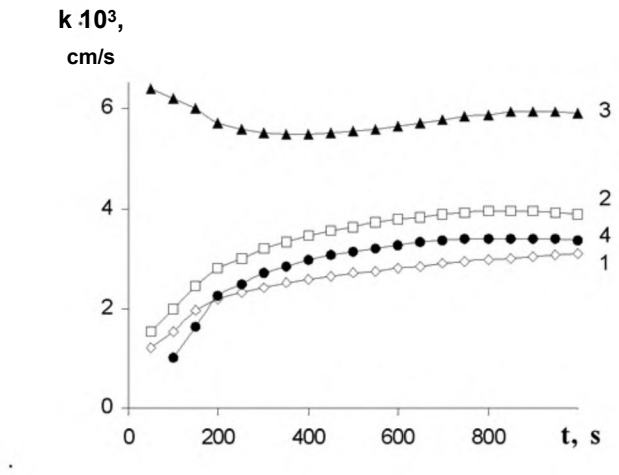


Figure 3. Dependence of the effective mass transfer coefficient on the duration **of stripping** *for vibrators nos. 1-4. The cone cell; the frequency of mechanical vibration 5.9 kHz.*

For vibrator 2, the intensity of interfacial longitudinal waves is lower, and the proportion of transverse waves is more significant, which decreases the intensification effect as compared to vibrator 3. Waves directed to the bulk of organic phase quickly decay producing no reflected waves.

For vibrator 4, the intensification of the stripping process is still smaller. The spherical vibrating element originally brought in contact with the surface of the aqueous phase executes small-amplitude vibrations and produces only weak transverse and longitudinal waves.

Vibrator 1 predominantly generates transverse waves and exerts the weakest intensifying effect on mass transfer. The transverse waves propagate from the two opposite sides at the base of the plate. In other words, we can consider that this vibrating element involves two spatially separated sources of waves.

The transverse waves propagate towards each other and reflects from the walls of the cell. The waves are identical in frequency and similar in amplitude. The result is the formation of standing waves that cannot intensify the process of mass transfer. The observed intensification is probably due to longitudinal waves originating from fluid elements flowing out (and flowing in) during the oscillatory motion of the base of the vibrating element. We believe that longitudinal waves influence the formation of standing waves: a longitudinal wave passing through the front of a transverse wave or through standing wave destroys the standing waves or affect the character of the transverse wave.

THE EFFECT OF THE CELL SHAPE ON THE EFFECTIVE MASS TRANSFER COEFFICIENT

The cell shape also affects the intensity of mass transfer process, but resonant frequency doesn't change.

The lowest oscillation intensity was observed in the rectangular cell (Figure 4), in which incident and reflected waves have the same frequency (the amplitude of the latter is slightly lower) and their phases differ by π radians. A collision of two waves with equal frequency gives rise to standing waves, which are known to be incapable of transferring energy.

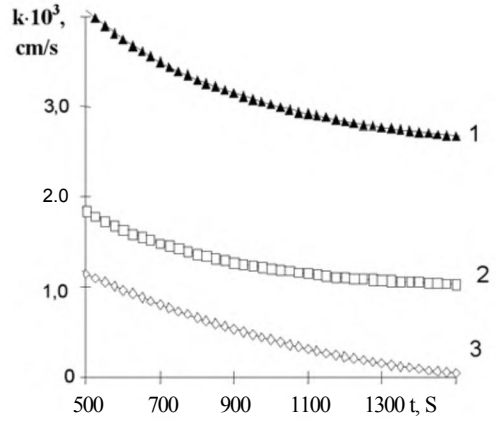


Figure 4. Dependence of the effective mass transfer coefficient on the **shape of stripping of** *the cell, 1- conical shape, 2 - cylindrical cell, 3* **-** *rectangular cell. Frequency of applied vibrations 5.9 kHz.*

The much higher mass transfer coefficient in the conical shape can be explained by dissipation of reflected waves in the bulk of the organic phase. Of course, the motion of liquid elements near the interface is complex, comprising both longitudinal and transverse components. However, a reflected wave is out of phase with the incident wave and its intensity is noticeably lower; as a result, their interaction insignificantly reduces the oscillation intensity.

The wall effect is minimum in a cylindrical cell; however, the mass transfer coefficient is intermediate for this cell design. The wave propagation distance is maximum and oscillation damping is more pronounced in this cell, which substantially reduces the intensity of a reflected wave. Additional formation of longitudinal waves in a cylindrical cell is unlikely.

THE INFLUENCE OF THE HEIGHT OF THE CONTACTING PHASE

The change of the height of contacting phases result in the change of wave-formation intensity and, therefore. It results in the change of effective mass transfer coefficient and negligible change of resonant frequency.

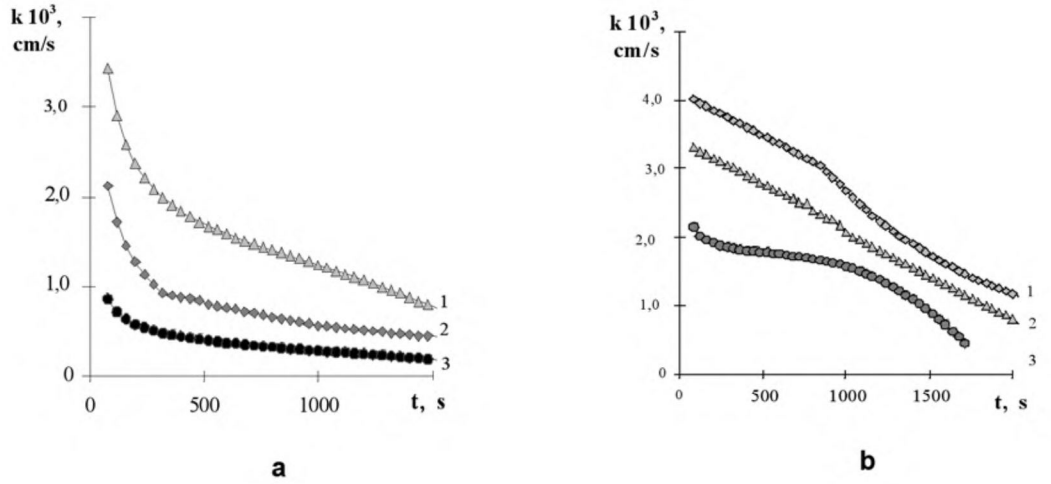


Figure 5. Dependence of effective mass transfer coefficient on duration of stripping at various height of the aqueous (a) and the organic phase (b): 1- 0.2; 2 - 0.4; 3 - 0.8 cm. The height of organic (a) and aqueous (b) phase is 0.2 cm. The cell is of cylindrical shape.

With an increase in the height of organic phase, the oscillation intensity decreases; this is associated with the higher pressure at the surface and, accordingly, the stronger oscillation damping (Figure 5).

CONCLUSIONS

The generating waves of resonant frequency is intensification stripping of acids since effective supply energy to the dynamic interfacial layer. The effective coefficient of mass transfer at resonant frequency is much higher than that characteristic for the process carried out without generating waves. It has been stated that the effect of intensification of stripping process is mainly due to the exciting longitudinal waves carrying the additional energy in the dynamic interfacial layer of the extraction system. The effect of intensification depends on frequency and amplitude generated on wave interface, on geometry of the cell, on the vibrating elements and its position in the cell too. In our opinion the effect of intensification is due to the increase of interface area, the change of hydrodynamic situation in the contacting phases (reduces the thickness of diffusion layer) and the dispersion according to the mechanism Rayleigh-Tailor.

REFERENCES

1. **H. Linde, E. Schwarz (1963)** *Z. Phys. Chem.* **B. 224, N° 5-6, 331-352.**
2. **H. Linde, M.G. Velarde (1997)** *J. Colloid Interface Sci.* **V. 188, Ne 1, 16-26.**
3. **A. Wierschem, M.G. Velarde, H. Linde (1999)** *J. Colloid Interface Sci.,* **V. 212, Ne 2, 365-383.**
4. **H. Linde, M.G. Velarde, W. Waldheim (2001)** *J. Colloid Interface Sci.,* **V. 236, Ne 4, 214-224.**
5. **A. Wierschem, H. Linde, M. G. Velarde (2001)** *Physical Review E ,* **V. 64, No 2, 601-604.**
6. **N. F. Kizim, E.N. Golubina, A. M. Chekmarev (2003)** *Doklady Russian Academy of Sci..* **T. 392, Ne 3, 362-364.**
7. **N. F. Kizim, E.N. Golubina (2004)** *Journal of Physical Chemistry (Russian)* **T. 78, Ne 3, 555-557.**

GELS, MICROEMULSIONS AND LIQUID CRYSTALS IN THE EXTRACTION SYSTEMS WITH DEHPA

Eugeny V. Yurtov, Natalia M. Murashova

Mendeleev University of Chemical Technology, Moscow, Russia; yurtov@muctr.edu.ru

The formation of gels, microemulsions and liquid crystals was investigated in extraction systems containing DEHPA and an alkaline metal ion (Na), a non-ferrous one (Ni) and a rare-earth (Tb). The dispersed structures were investigated both in the bulk at equilibrium and near the oil-water interface during mass-transfer.

INTRODUCTION

In extraction systems of alkali, nonferrous, and rare-earth metal compounds, a whole number of dispersion structures can be formed, such as micelles, microemulsions, liquid crystals, gels in aqueous and organic phases, amorphous and crystalline precipitates, and stable emulsions [1], Such structures can occur both in the bulk of an aqueous or organic phase and in the interfacial region. Structurization in extraction systems affects distribution and separation coefficients, extraction rates, and phase-separation rates. The knowledge of the formation mechanisms, existence regions, and properties of dispersion structures in extraction systems gives a means for influencing the structurization and, through this, for enhancing the extraction efficiency, improving the existent extraction systems, and for developing new ones.

Structurization in extraction systems can occur both through the association of amphiphilic molecules producing micelles, microemulsions, vesicles and liquid crystals, and through the formation of coordination polymers and solid particles, which give precipitates, hydrogels (gels in an aqueous phase), and organogels (gels in an organic phase). It is well known, for example, that hydrogels of coordination polymers can be formed in the extraction systems with zirconium. Microemulsions can arise in some extraction systems as third liquid (second organic or aqueous) phase [2],

In this work we demonstrate the formation of gels in the organic phase, microemulsions and liquid crystals in the systems containing DEHPA and Na, Ni and Tb both in the bulk at equilibrium and near the oil-water interface during the mass-transfer.

EXPERIMENTAL

Di(2-ethylhexyl)phosphoric acid from Merck (minimum 98%) was used, the other reagents - decane, NaOH, $Tb(N0_3)_3*5H_20$, $NiS0_4*7H_2O$ were pure grade. Twice distilled water was prepared by the standard procedure.

The samples for studying the phase equilibria were prepared by mixing the required

quantities of a DEHPA solution in decane with a weighed amount of NaOH and water. A phase diagram for the NaDEHP-decane-water system was obtained by increasing the water concentration while keeping the NaDEHP-to-decane ratio fixed. Evidence of microemulsion formation was the ultra low interfacial tension; the liquid crystalline phase was identified by polarizing microscopy.

Terbium hydroxide was precipitated by the reaction of $Tb(N0_3)_3$ with NaOH and carefully washed. To study the gelation, terbium hydroxide suspensions in water were mixed with the required amounts of DEHPA solution in decane. The mixtures were carefully shaken for 30 s and the samples were allowed to stand for 24 h at 20 °C. The organogel formation was visually identified as the absence of fluidity of more then 90 % of the organic phase volume.

Nickel di(2-ethylhexyl)phosphate ($Ni(DEHP)_2$) was prepared according to a procedure described in [3] consisting of an exchange reaction between potassium di(2-ethylhexyl)phosphate and nickel sulfate in aqueous solution. The region of liquid crystals existence was established by polarizing microscopy. The viscosity of the samples was measured with a Rheotest-2 rotation viscometer.

The zone of phase contact was inspected with a Axiostar optical microscope (Carl Zeiss) with a photo adapter for 1--30 min from the establishment of contact. The sample was prepared by placing droplets (0.02 ml each) of the aqueous and the organic phases one by one at a distance of 2.5--3 cm from one another on a microscope slide (25x75 mm) . The droplets were carefully covered with another microscope slide so that they spread between two slides and were brought into contact.

ORGANOGEL

The gelation of terbium di-(2-ethylhexyl)phosphates in the bulk organic phase was investigated. If basic (mono- or di-substituted) terbium di-(2-ethylhexyl)phosphates predominate in the system, gel formation takes place. We observed 100 % gelation at CDEHPA/CTb(OH)3<2.0, no gelation at CDEHPA/C-rb(OH)3>2.8; in the region of CDEHPA/Cjb(OH)3 value from 2.0 to 2.8 the probability of gelation diminished (fig. 1). The gelation in the boundary region (2.8≤C_DEHPA/CTb(OH)3≤2.0) is a stochastic process in which a different gelation result can be observed at the same C_DEHPA/CTb(oi-i)3 value.

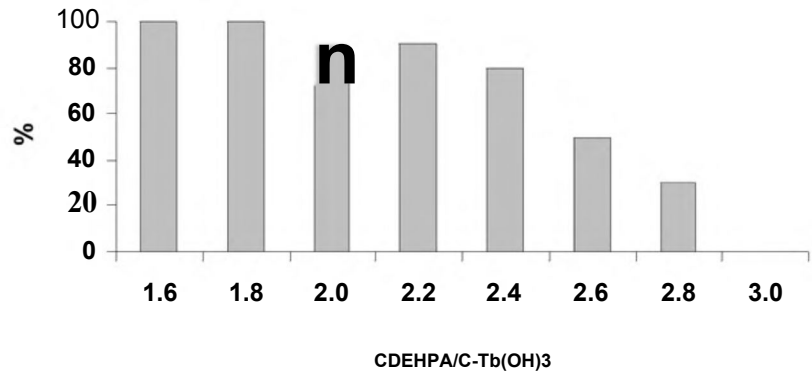


Figure 1. The probability (%) of the gelation of organic phase in the system $Tb(OH)_3$-DEHPA - decane - water. T=20 °C, C_{DEHPA}=0. 1M

The structure of the organogel consists of rod-like aggregates; their diameter is 100-200 nm (fig.2). The rod-like shape of the aggregates is in agreement with the shape of crystals of neutral rare-earth di-(2-ethylhexyl)phosphates [4],

The same organogel can arise near the oil - water interface at the contact of water solution of terbium nitrate and the solution of DEHPA in decane at non-equilibrium. During the mass-transfer in the system DEHPA solution in decane - water solution of $Tb(N0_3)_3$ the structured film was observed in the organic phase near the oil-water interface (fig.3). It is in good agreement with the peculiarities of extraction kinetics of lanthanides with DEHPA [5],

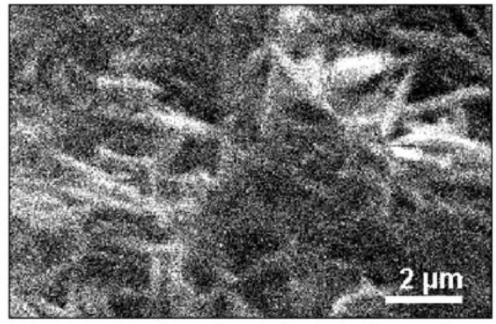


Figure 2. Electron microphotograph of the xerogel of **basic terbium di-(2-ethylhexyl)phosphate** *C_{DE}HPA/cTb<0H>3=1-5.*

The gelation near the interface was observed at concentrations of $Tb(N0_3)_3$ in water of more than 0.03 M. The probability of gelation near the interface, as well as of gelation in the bulk organic phase, depends on the DEHPA and terbium concentration. The fraction of gel-covered oil-water interface increases from 1 % to 90 % with the C_Tb growth from 0.03 to 1 M (atCoEHPA=1 M).

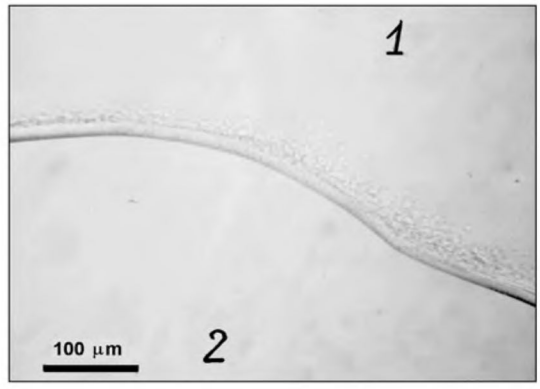


Figure 3. Interfacial region upon the contact of 0.3 M DEHPA solution in decane (1) with 0.3 M water solutions of $Tb(N0_3)_3$ (2). The time from the establishment contact is 18 min.

The kinetics of the gel formation near the interface in the system DEHPA solution in decane - water solution of $Tb(N0_3)_3$ was studied (fig.4). The dependence of thickness of the gel layer (h) on time (t) is well described by $h=k*t^{1/2}$, which is in accordance with the theory of diffusion kinetics.

MICROEMULSION AND LIQUID CRYSTALS

Reverse microemulsions of NaDEHP are well-known in the systems with different organic solvents [6], Besides microemulsions, NaDEHP can form liquid crystals. The regions of existence of reverse micelles and microemulsion (1) and liquid crystals (2) in the system NaDEHP - decane - water are shown in the figure 5. The following phase equilibria was found in this system (fig.5): NaDEHP and water solution in decane at equilibrium with

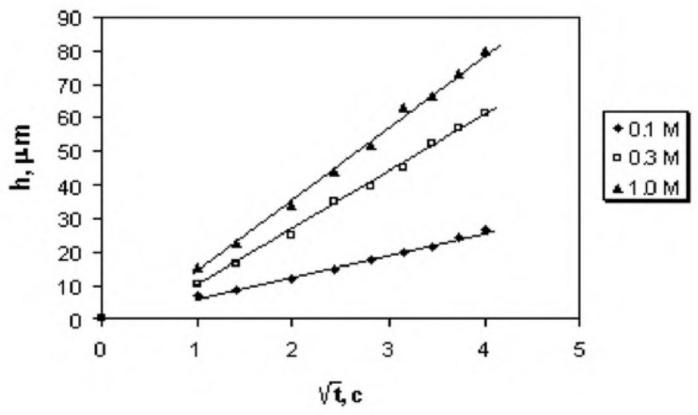


Figure 4. Kinetics of the gelation near the interface in the systems 1 M DEHPA solution in decane - 0.1, 0.3, 1.0 water solutions of **$Tb(N0_3)_3$.**

microemulsion (3); microemulsion at equilibrium with liquid crystals (4); NaDEHP and water solution in decane at equilibrium with microemulsion and liquid crystals (5); NaDEHP and water solution in decane at equilibrium with liquid crystals (6).

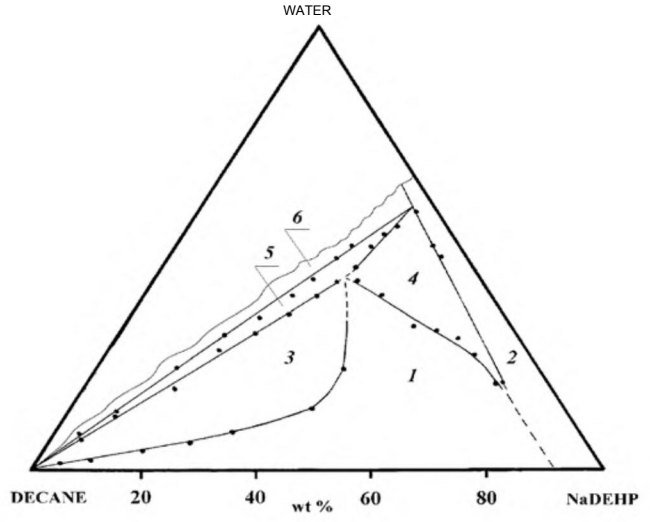


Figure 5. Phase diagram of the system NaDEHP - decane - water. T=20 C.

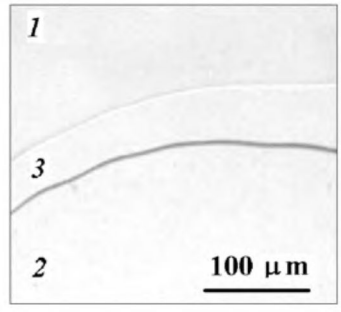


Figure 6. Interfacial region upon the contact of NaDEHP micelle solution in decane (1) with water (2). 3 - microemulsion phase. The time from the establishment contact is 3 min.

At non-equilibrium conditions, when sodium di-(2-ethylhexyl)phosphate solution in decane contacts with water a third liquid phase appears (fig.6). At equilibrium two liquid phases coexist in the investigated systems. The analysis of the phase diagram of the system NaDEHP - decane - water shows that the third liquid phase in the system is a microemulsion.

Di-(2-ethylhexyl)phosphates of the other metals can also form liquid crystals. Formation of liquid crystals lwas found in the systems nickel di-(2-ethylhexyl)phosphate - octanol [7] and nickel di-(2-ethylhexyl)phosphate - DEHPA - decane (fig.7). The region of the liquid crystalline phase existence in the system $Ni(DEHP)_2$ - DEHPA - decane is showned in figure 8. The viscosity of liquid crystals in the system $Ni(DEHP)_2$ - DEHPA - decane reaches the value of hundreds and thousands Pa*s. The sharp decrease in viscosity and the change in the flow curves corresponds to the transition from liquid crystals to solution.

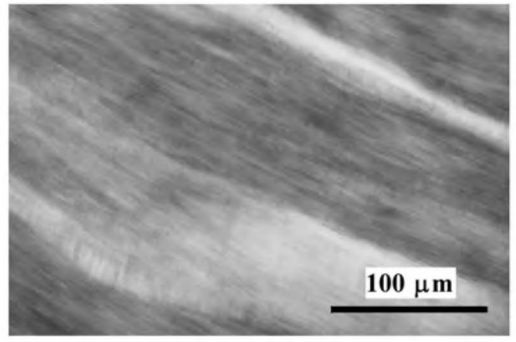


Figure **7.** *Liquid crystal of $Ni(DEHP)_2$ under polarizing microscope. The sample composition: $Ni(DEHP)_2$ - 80 wt %, DEHPA - 15 %, decane - 5 % .*

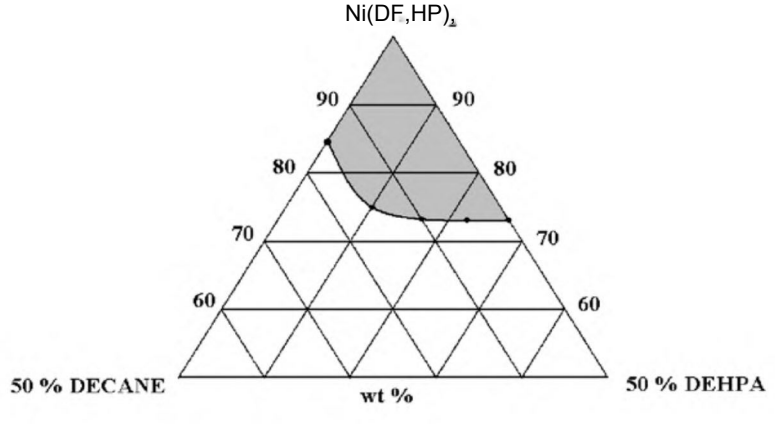


Figure 8. Liquid crystal region in the phase diagramme of the system $Ni(DEHP)_2$ - DEHPA - decane. T=20 °C.

Unlike the organogel in the system $Tb(OH)_3$ - DEHPA - decane - water and NaDEHP microemulsion, liquid crystals in the system $Ni(DEHP)_2$ - DEHPA - decane exist at rather high $Ni(DEHP)_2$ concentrations. Liquid crystal formation was not found near the oil-water interface during the contact of concentrated solutions of DEHPA in decane (≤2.5M) and $NiS0_4$ in water (<1,5M) at T=20 °C.

Liquid crystals were described in the systems La or Eu di-(2-ethylhexyl)phosphate - CCl_4 - octanol [8], The same structure can form near the oil-water interface during the extraction process. The interfacial film arising in the system $Tb(N0_3)_3$ - water - DEHPA - CCl_4 - octanol is presented in figure 9. The transparent and optically anisotropic area of the interfacial film is

considered to be liquid crystal.

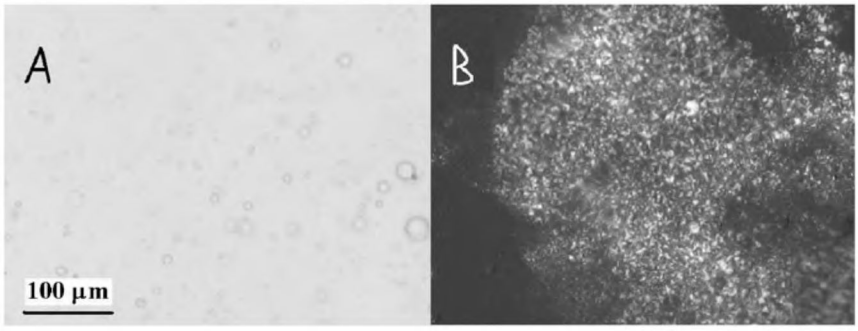


Figure 9. The liquid crystal, arising near the oil water interface 30 min after the contact of 1.0 M DEHPA solution in the mixture of CCl_4 (85 vol%) and octanol (15 vol %) with 0.3 M water solution of $Tb(N0_3)_3$. A - polaroids are not crossed, B - polaroids are crossed.

CONCLUSIONS

The formation of organogels, microemulsions and liquid crystals of DEHPA salts in the bulk phase and near the oil-water interface was investigated. Gel formation in the organic phase was observed in the system $Tb(OH)_3$ - DEHPA - decane - water at equilibrium and during the contact of the water solution of terbium nitrate with the solution of DEHPA in decane. Microemulsions occurred both at equilibrium in the system NaDEHP - decane - water and during the mass-transfer of NaDEHP from decane into water. A liquid crystalline phase exists in the system $Ni(DEHP)_2$ - DEHPA - decane. Liquid crystals were also found near the oil-water interface in the system $Tb(N0_3)_3$ - water - DEHPA - CCl_4 - octanol. The structures near the interface were similar to the ones observed in the bulk at equilibrium.

ACKNOWLEDGEMENTS

This work was supported by Russian Foundation for Basic Research (grant 04-03-32789), Russian Program "Integration" (project 1-0420) and Moscow Government (grant GB-28/03).

REFERENCES

1. **E.V. Yurtov, N.M. Murashova (2002)** *Proc. Int. Solvent Extraction Conf., ISEC 2002 (Ed. K.C. Sole, P.M. Cole, J.S. Preston and D.J. Robinson),* **Cape Town, South Africa, Vol.1, 197-202.**
2. **K. Osseo-Asare (2002)** *Proc. Int. Solvent Extraction Conf., ISEC 2002 (Ed. K. C. Sole, P.M. Cole, J.S. Preston and D.J. Robinson),* **Cape Town, South Africa, Vol.1, 118-124.**
3. **V. I. Golovanov, O.N. Vekshina, and I.V. Inyaev (1990)** *USSR Inventor's Certificate* **No. 1805129 (July 21).**
4. **T.Harada, M. Smutz and R.G. Bautista (1971)** *Proc. Int. Solvent Extraction Conf. ISEC'71,* **London, 1971, vol. 2, 950-956.**
5. **Z.-J. Yu, R.D. Neuman (1995)** *Langmuir,* **Vol. 11, No. 4, 1081-1086.**
6. **V.V. Tarasov, G.A. Yagodin, A.A. Pichugin (1984)** *Kinetics of Extraction of Inorganic Substances (Rus.)* **Moscow, VINITI Publisher, 171 pp.**
7. **E.V. Yurtov, N.M. Murashova (2003),** *Russian Journal of Inorganic Chemistry,* **Vol.48, No. 7, 1096-1101.**
8. **Yu. I. Trifonov, E.K. Legin and D.N. Suglobov (1990)** *Proc. Int. Solvent Extraction Conf. ISEC'90, Kyoto,* **Tokyo: Elsevier, 1992, 279-284.**

ADSORPTION BEHAVIOR AND ANALYSIS BY REFLECTION SPECTROMETRY OF PROTONATED LIPOPHILIC TETRAPHENYLPORPHYRIN DERIVATIVES AT A LIQUID-LIQUID INTERFACE

Nobuaki Ogawa, Yoshio Moriya and Shinichi Nakata

Faculty of Engineering and Resource Science, Akita University, Akita, Japan

Analysis by reflection spectrometry was performed to clarify the interfacial adsorption states of acid dications of tetraphenylporphyrin (TPP) and lipophilic TPP derivatives in a dodecane-aqueous sulfuric acid system, and to confirm the utility of partial reflection spectrometry. Interfacial adsorption was not observed for the porphyrins substituted at the 2,6 positions of meso-phenyl groups. A J-aggregate of protonated species was produced in the cases of TPP and tetra-p-torylporphyrin. The adsorption state changed from a monolayer form to a multilayer one with a change of reflection coefficient. From the value of saturated interfacial molecular density, the averaged tilt angle of the pyrrole ring plane was estimated to be 47-48° against the interface normal. Positive and negative bands were observed in the p-polarized partial internal reflection (p-PIR) spectra with the same band locations as well as in p-polarized external reflection (p-ER), but with reversed sign of p-ER spectra. These suggest that the interface selection rule of the p-PIR spectrometry has a reversal rule of the p-ER spectrometry, and the PIR method can also be used for the analysis of molecular orientation.

INTRODUCTION

The liquid-liquid interface has received a great deal of attention, because it provides a unique chemical reaction location in which molecular species are spontaneously trapped to generate organized molecules with an orientation that is not observed in a bulk solution. To understand the interfacial adsorption states, the development of some direct spectroscopic techniques is indispensable.

We have contributed to develop reflection spectrometry in connection with a direct measurement of the acid dication of meso-tetraphenylporphyrin (TPP) in an aggregate formed at the toluene/aqueous sulfuric acid interface [1-3]. It was found that external reflection (ER) spectrometry, where incident light was irradiated obliquely on the interface from the aqueous phase to the organic phase, could provide not only a single spectrum of interfacial adsorbate without interference of organic bulk phase, but also qualitative knowledge about the molecular orientation by observing positive/negative bands in the p-polarized ER (p-ER) spectrum.

The present work describes the interfacial adsorption-precipitation phenomena, which may happen in the cases of some available TPP derivatives in the dodecane-aqueous sulfuric acid system. The aim of this work is to confirm the feasibility of interfacial adsorption and to clarify the utility of partial reflection spectrometry, including ER and partial internal reflection (PIR).

EXPERIMENTAL

Reagents

TPP (Dojindo Laboratories) and its lipophilic derivatives (Tokyo Kasei Kogyo Co. Ltd .), including tetra-p-tolyl-, tetrakis-(2,4,6-trimethylphenyl)-, tetrakis-(2,6-dichlorophenyl)-, and tetrakis-(pentafluorophenyl)-porphines, were used as received; the free base of porphyrin (P) for those reagents are shown in Figure 1 along with their abbreviations. Stock solutions of those reagents were prepared by dissolving them in dodecane (Wako Pure Chem. Co. Ltd.).

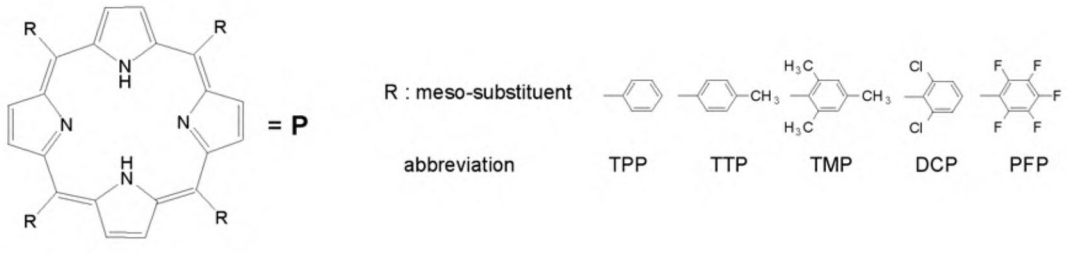


Figure 1. Structures and abbreviations of the free-base porphyrins used in this study

Apparatus and procedure

Two kinds of optical equipment were used for the present study: a prism-cell device and a variable-angle device. The optical arrangements for the two devices are schematically shown as (a) and (b), respectively, in Figure 2.

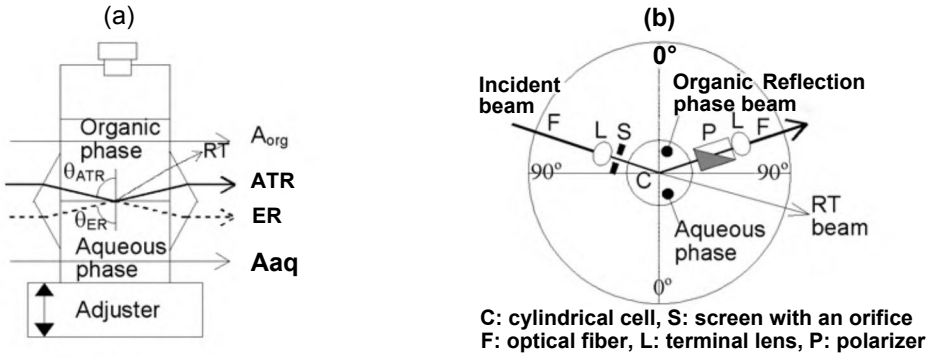


Figure 2. Schematic illustrations of (a) a prism-cell device and (b) a variable-angle device. RT is the refracted transmission.

The prism-cell device, comprising a quartz liquid-cell (light path length: 2 cm, cell width: 1 cm) and a pair of quartz prisms (30°-30°-120°), was designed for the quantitative analysis of interfacial molecular density. By changing the height of the device, the measurement mode can be switched for the transmission absorption spectra of the organic and aqueous phases (A_{org}, A_{aq}) and the reflection spectra at the liquid-liquid interface (ER, ATR), which are dragged down with the corresponding blank spectra. The refractive indices of the organic and aqueous media were experimentally determined with an Abbe refractometer (Erma Optical Works, Ltd.). Spectroscopic measurements were carried out on a double-beam UV-visible spectrometer (Perkin-Elmer, Model ,,40). Absorption spectra of dodecane solutions ($A_{SO}i_n$) for the free base of porphyrins were measured using an optical cell of 1cm light path length at first. In order to accelerate the interfacial adsorption reaction, a mixing-standing procedure was used. That is, a mixture of the same volume (3 cm^3) of aqueous and organic solutions was shaken in a

Teflon test tube at 250 strokes/min for 30 min, then it was centrifuged, transferred entirely into a prism-cell and left standing for 20 min before performing spectral measurements.

A variable-angle device was designed to allow measurements with transmission, ER, ATR and PIR geometries. Optical fibers with some focus lenses and a polarizer were assembled on a goniometer, and a cylindrical cell (capacity 8 cm^3 with 2-cm i. d. and 2.55 cm in length) was placed at the center. Spectroscopic measurements in this case were carried out on a CCD array spectrometer (Ocean Optics, Model USB2000). After preparing the mixture of dodecane-aqueous sulfuric acid solution, an aliquot (4 cm^3) of aqueous phase and the same volume of dodecane phase were introduced into the cylindrical cell for the blank measurements at several angles of incidence. Then a small volume of dodecane phase in the cell was replaced with a stock solution of porphyrins, and only the organic phase was mildly stirred with a Teflon needle to yield a homogenous organic solution. The spectral measurement of interfacial adsorbate was carried out after 1 day, since a period of time over 12h was required for the adsorption equilibration.

RESULTS AND DISCUSSION

Interfacial adsorption behavior of TPP derivatives

By using the prism-cell device, the interfacial adsorption of protonated porphyrin was examined for each of the lipophilic porphyrins shown in Figure 1. The four kinds of spectra, i.e. A_{org}, ATR, ER and A_{aq} were measured in the two-phase contact system made up of 4 M H_2S0_4 and a dodecane solution of free-base porphyrin (P) of total concentration $[P]_t$ = 0.2 pM.

In the cases of the three porphyrins TMP, DCP and PFP, we could not find any reflection bands corresponding to interfacial adsorbates. In fact, absorbance in the initial organic phase ($Asoi_n x2$) was not reduced by contact with the acidic aqueous phase. The feature common to the three porphyrins is to have substituents at the 2,6 positions of the meso-phenyl group.

It is known that N-protonation induces a structural change because the free-base porphyrin converts from a configuration in which the aryl moiety twists relative to the macrocycle plane to one in which it is nearly coplanar, thus promoting aggregation [4], The 2,6-position substituents could prevent a phenyl group from revolving around the C-phenyl axis, and also could prevent the H_2PX_{2J} from associating by a steric hindrance. This explanation is supported by the fact that the aggregate formation was not observed even in the case of tetrakis-(3,5-dimethoxyphenyl)-porphine [5],

It was only for TPP and TTP that the reflection spectra of protonated chemical species were clearly observed within the tested porphyrins. Both TPP and TTP have no 2,6-position substituents in the meso-phenyl group. This fact supports the above-mentioned consideration about the steric hindrance. Similar J-aggregate formations are also found for the other TPP derivatives having a substituent at the p-position of the meso-phenyl group, such as tetra-p-nitrophenylporphyrin, tetra-p-methoxyphenylporphyrin, and so on [5],

Interfacial adsorption-precipitation states of the protonated TPP and TTP

As for the TPP with a total concentration [TPP], of 0.14 pM in dodecane-4 M H_2S0_4 system, a Soret band at 416 nm of free base porphyrin (molar absorptivity, $s_{SO}|_n^{416}$ = 4.33x10^5 M^cm'^{1}) disappeared in the organic-phase spectrum to yield a protonated interfacial species, H_2TPPX_{2ii} (X: $HS0_4^-$), which subsequently changed to a J-aggregate, $(H_2TPPX_2)_{ai}$ at the interface and a monomeric ion, $H_2TPP^{2+}{}_{aq}$, in the aqueous phase. The absorbance of A_{aq}, ATR and ER spectra changed slightly with time. Five spectra related to TPP at 3h after are shown

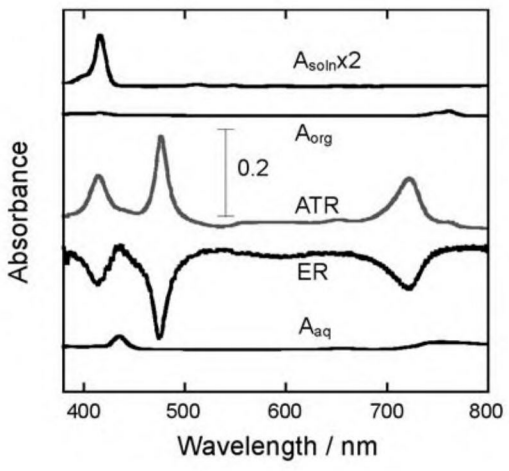


Figure 3. Five spectra of TPP in the dodecane-4 M FI_2SO_4 system with different optical geometries. The initial solution spectrum ($A_{so}i_n x2$) is shown for comparison. $[TPP]_t$ = 0.14 pM.

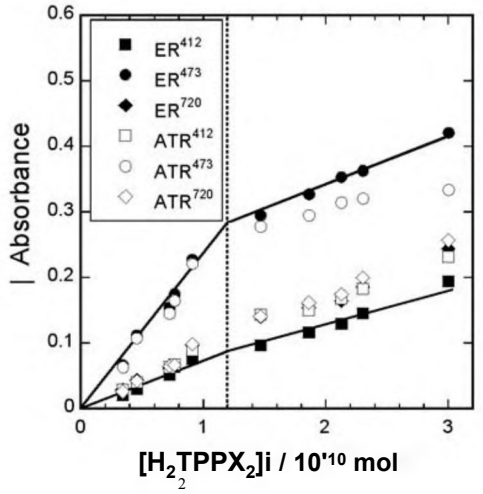


Figure 4. Relationships between the absorbance and the interfacial molecular density, **$[H_2TPPX_2]j$.** *Saturated interfacial density in a monolayer form is estimated to be 1.2x1 O'10 mol cm'2.*

in Figure 3. We could observe the ATR and ER spectra having main three bands at 720, 473 and 412 nm within the visible wavelength region. Sharp and intense absorption bands at 473 nm could arise from the dipole moment polarized along the long axis with the aid of an interporphyrin charge resonance in the excited states, whereas a broad absorption band at 412 nm could arise from the moment along the short axis [6],

The interfacial molecular density, $[H_2TPPX_2]i$ (mol cm'2) under our experimental conditions could be evaluated by using the values of $A_{SO}i_n^{416}$, A_{aq}^{435}, $e_{SO}i_n^{416}$ and the molar absorptivity of aqueous species e_{aq}^{435} which was estimated to be 3.81x10^5 M^crrf1.

In order to observe the absorbance change corresponding to the interfacial molecular density in a relatively short period of time, the spectroscopic measurements were performed using a dodecane solution of TPP within 0-0.24 pM after 25±5 min. The absorbance of ATR and ER in absolute quantity at 720, 473 and 412 nm were plotted against the value of $[H_2TPPX_2]i$ in Figure 4. An inflection point appeared in every plot at $[H_2TPPX_2]j$ = 1.2x1 O'10 mol cm'2. Reflection absorbance is proportional to the molecular density up to this value. It suggests that the molecular orientation is fixed by the aggregate formation. The linearity breaks beyond the value, and another linearity with a different slope appears. Such a phenomenon strongly suggests that the interfacial adsorption state changes from a monolayer form to a multilayer one (interfacial precipitation), which would result in a different reflection coefficient at a fixed angle of incidence. Therefore, the saturated interfacial molecular density (D_i^*) in the monolayer could correspond to the value, 1.2x1 O'10 mol cm'2.

By considering the molecular cross-section area (1.9 nm2) of the H_2TPP^{2+} species [7], the tilt angle of the pyrrole ring plane is roughly evaluated to be 47° from the interface normal, on an assumption that the projections of the planes onto the interface are not overlapped with those next to each other [8],

Five spectra related to TTP in the dodecane-5 M H_2S0_4 system are shown in Figure 5. Unlike the case of TPP, neither absorbance change with time nor aqueous species was observed. Therefore, the reflection spectra correspond only to interfacial species. The spectrum has four main bands at 695, 477, 466, and 400 nm together with some shoulder bands. Split bands at

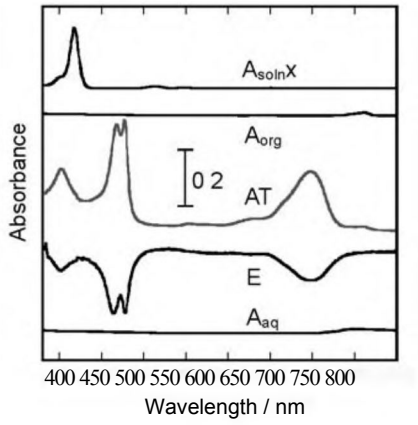


Figure 5. Five spectra of TTP in the dodecane-5 M H_2S0_4 system. [TTPh = 0.20 juM.

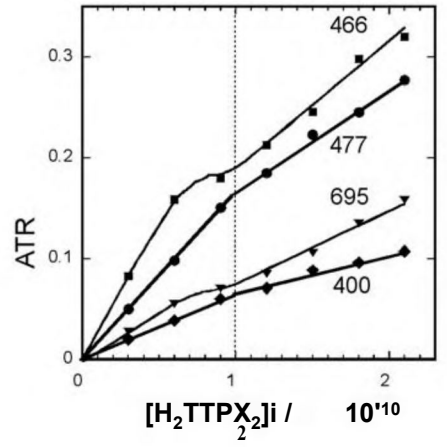


Figure 6. Relationships between the absorbance and the interfacial molecular density, **$[H_2TTPX_2]i$.**

477 and 466 nm, and a broad band at 400 nm with a shoulder at around 360 nm correspond to the 473 nm and 412 nm bands of $(H_2TPPX_2)_{,,,}i$ in the J-aggregate, respectively. This indicates the coexistence of two kinds of J-aggregates (Ji and J_2) with a polymorphous relation in the case of TTP.

The ATR absorbance for each of the four main bands was plotted against $[H_2TTPX_2]i$, as shown in Figure 6. The absorbance at 477 nm, which may belong to $J_r$aggregate, increased in proportion to $[H_2TTPX_2]i$, and slowly increased along another line with a different slope after passing an inflection point. The increasing trend of the 466 nm band, which may belong to the J_2-aggregate, changed along a loose curve near the inflection point. This suggests that the J_2-aggregate formation is depressed by the smooth .^-aggregate formation. The common inflection point at $[H_2TTPX_2]j$ = I.OxlO'10 mol cm'2 in Figure 6 must correspond to D_f*. By considering an estimated value of 2.2 nm2 of the molecular cross-section area of the FI_2TTP^{2+} species, the average value for the tilt angle of the pyrrole ring plane was roughly evaluated to be 48°, which is near to that of H_2TPP^{2+} species [9],

Utility of p-polarized partial reflection spectra

The p-ER spectrum is known to be useful for a semi-quantitative analysis of the molecular orientation at an air-solid [10], an air-liquid [11], or a liquid-liquid interface [2], The angle-dependent spectra of the present liquid-liquid system were measured by using a variable-anale device under the monolaver form condition.

Figure 7 shows the p-ER and p-PIR spectra of $(H_2TPPX_2)n,i$ at several angles of incidence. In the p-ER spectra, the two bands at 720 and 473 nm appeared positively, whereas the band at 412 nm negatively. The p-PIR spectra appeared with the same band locations, but with reversed sign, of p-ER spectra. Absorbance in absolute quantity increased with decreasing angle of incidence toward the Brewster's angle (0_B~45°). According to the interface selection rule of ER [12] with the angle of incidence bellow 0_B, the positive bands can be attributed to the chromophore having an electron- transition moment parallel to the interface; the negative band is attributed to the chromophore having an electron-transition moment perpendicular to the interface. Therefore, an interface selection rule for PIR spectrometry could be opposite to that for ER one [8], Anyway, the pyrrole ring plane in the aggregate must be oriented obliquely at the interface, when we take into account the

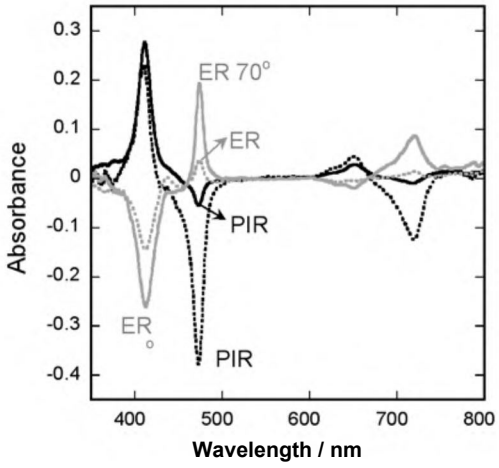


Figure 7. The p-polarized ER and PIR spectra for $(H_2TPPX_2)_{„J}$ at some angle of incidence.

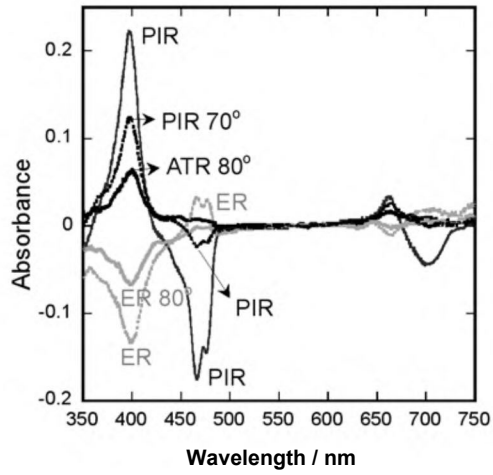


Figure 8. The p-polarized ER and PIR spectra for $(H_2TTPX_2)n.i$ at some angle of incidence.

band-assignments of J-aggregate as described above. The result is also consistent with the tilt angle evaluated from the value of D*.

The similar p-polarized spectra were observed for $(H_2TTPX_2)_{„,j}$ as shown in Figure 8. It is noteworthy that all bands in the ATR spectrum appear with positive absorbance and that both of the split bands at 477 and 466 nm appeared positively for ER and negatively for PIR. The orientation of the two J-aggregates would nearly the same [9], Thus an appreciable analytical usefulness of partial reflection spectrometry was demonstrated by the measurements conducted in the system protonated lipophilic tetraphenylporphyrin derivatives in dodecane-aqueous sulfuric acid.

ACKNOWLEDGEMENTS

This work was supported by a Grant-in-Aid for Scientific Research (No. 13650865) from the Ministry of Education, Culture, Sports, Science, and Technology, Japan.

REFERENCES

1. **Y. Moriya, N. Ogawa, T. Kumabe, and H. Watarai (1998),** *Chem. Lett.,* **221-222.**
2. **Y. Moriya, R. Amano, T. Sato, S. Nakata, and N. Ogawa (2000),** *Chem. Lett.,* **556-557.**
3. **N. Ogawa, Y. Moriya, and S. Nakata (2002), Proceedings of the International Solvent Extraction Conference (ISEC 2002, Johannesburg), 58-63.**
4. **D. L. Akins, H. Zhu, and C. Guo (1996),** *J. Phys. Chem.,* **100, 5420-5425.**
5. **S. Okada and H. Segawa (2003),** *J. Am. Chem. Soc.,* **125, 2792-2796.**
6. **O. Ohno, Y. Kaizu, and H. Kobayashi (1993),** *J. Chem. Phys.,* **99, 4128-4139.**
7. **H. Nagatani and H. Watarai (1998),** *Anal. Chem.,* **70, 2860-2865.**
8. **Y. Moriya, T. Hasegawa, K. Hayashi, M. Maruyama, S. Nakata, and N. Ogawa (2003),** *Anal. Bioanal. Chem.,* **376, 374-378.**
9. **Y. Moriya, S. Nakata, H. Morimoto, and N. Ogawa (2004),** *Anal. Sci.,* **in press.**
10. **T. Hasegawa, S. Tageda, A. Kawaguchi, and J. Umemura (1995),** *Langmuir,* **11, 1236-1243.**
11. **E. Okamura, T. Hasegawa, and J. Umemura (1995),** *Biophysical Journal,* **69, 1142-1147.**
12. **T. Hasegawa (1998),** *Bunseki,* **582-588 (in Japanese).**

EXTRACTION SYSTEM UNDER INFLUENCE OF AN ELECTRIC FIELD OF DIFFERENT FREQUENCY

Alexey Petrov, Mikhail Afonin and Eevgenij Komarov

Saint-Petersburg State Institute of Technology,

Saint-Petersburg, Moscovski pr. 26, Russia, asamou@tu.spb.ru

The influence of alternating electrical current (AC) with frequency range 20 - 20000 Hz upon the extraction system containing Belousov-Zhabotinsky (BZ) reaction components was investigated.

The metals separation was carried out in extraction set up consisting of two extractors coupled by liquid membrane (0.5 M TBP in kerosene or tetradecane). Two platinum electrodes were inserted to one extractor to induce the cyclic BZ reaction, which is governing the extraction-stripping process in this extractor. The audio generator was used to modulate electrical tension between the electrodes. The frequency range of external electrical field investigated is 20 - 20000 Hz.

After applying the electric field the concentration ratio of the pair Pr/Nd in the aqueous phase was oscillaing.

Reversible change of turbidity of emulsions of the investigated solutions is discovered at applying of AC with only frequency 23 Hz.

Introduction

Liquid-liquid extraction driven by oscillatory oxidation-reduction reaction in aqueous phase gives the opportunity to separate similar elements using multiple repetition of metals extraction/stripping [1],
It was found recently that the application of external electric field could stabilize the frequency and magnitude of red/ox potential of BZ reaction [2],

Oscillatory repeated effect of extraction/stripping in one extractor along with influence of an electric current of various frequencies may improve separation of similar element using multiplication of the small kinetic difference.

Under action of an external field created by the alternating current of various frequency the polarization occurs of molecules which increase the dipole moment proportionally intensity of a field that results in change of thermodynamic characteristics of chemical system.

Macroscopic constants ε, μ and σ - physical characteristics of substance: the dielectric constant, magnetic permeability and electro conductivity - essentially depend on frequency of electromagnetic fields [3], It is very promising to influence on these fundamental parameters in extraction system to possibly increase separation factors of similar elements.

Experimental

The metals separation was carried out in extraction set up consisting of one or two extractors. In the case of two-extractor set up the extractors were coupled by bulk liquid membrane (0.5 M TBP in kerosene or tetradecane). Two platinum electrodes were inserted to one extractor to induce the cyclic BZ reaction, which is governing the extraction-stripping process in this extractor. Separation of organic phase and aqueous phase was performed using centrifugal separator. The audio generator was used to apply AC between the electrodes. The frequency range of external electrical current was in the range 20 - 20000 Hz. Turbidimeter Kernco-966R measured the turbidity of the extraction emulsion. The metal's concentration in the aqueous and in the organic phase had been measured by three diode-array spectrophotometers every 6-15 seconds. All experimental data was registered on-line using LabView software. Full specification of the experimental set up is given elsewhere [4], The above mentioned experimental setup principal schema enhancement is shown on the fig 1. All reagents: TBP, tetradecane ($C_{14}H_{30}$), $HN0_3$, $NaN0_3$, malonic acid (HMal - $CH_2(COOH)_2$), $KBr0_3$, $Ce(N0_3)_3$, $Pr(N0_3)_3$, $Nd(NQ_3)_3$) were analytical grade.

Results and Discussion

The influence of alternating electrical current (AC) upon the extraction system containing BZ reaction components was investigated.

In aqueous phase of the extractors the solutions of equimolar Nd and Pr in 6 and 7 M $NaN0_3$ in presence of potassium bromate and malonic acid were used.

The new phenomenon was observed during the applying of the alternating electrical current to the emulsion (organic in aqueous phase, O: A=1:1). The turbidity of the emulsion is changing reversibly when electrical current is applied. When the AC is switch on the turbidity is increasing, when AC is not applied - the turbidity is decreasing as it shown on the fig 2. All other conditions except presence or absence of the electrical current are exactly the same. It is shown that there is at least one frequency of AC that can produce reversible changing of the emulsion turbidity. The influence of AC frequency in the range 20 - 20000 Hz on solutions of sodium nitrate is shown on the fig 3 and 4. It was found that the reversible change of turbidity occurs only at the frequency 23 Hz and if the aqueous solution contains the Belousov-Zhabotinsky reaction components or while the concentration of sodium nitrate in aqueous phase is equal to 0.1 M.

After applying the AC the oscillation of concentration ratio of the pair Pr/Nd in aqueous phase of extractor, which was disturbing by AC was observed (see fig. 5). The concentration ratios of the same pair in another aqueous phase and in organic phase were relatively constant. This observation requires further investigations.

Conclusions

1. Reversible change of turbidity of emulsions of the investigated solutions is revealed at applying of frequency in 23 Hz.

2. Applying of an alternating current of various frequencies allows shifting chemical equilibrium in the extraction system with bulk liquid membrane in oscillatory conditions. This approach may allow influencing on separation of chemically similar elements because of the influence of AC on the reaction kinetics constants in aqueous and organic phase, and on the boundary surface.

Acknowledgements

This work was supported by the U.S. Department of Energy, Office of BasicEnergy Sciences, under grant RC0-20000-SC14 administered by the CivilianResearch and Development Foundation.

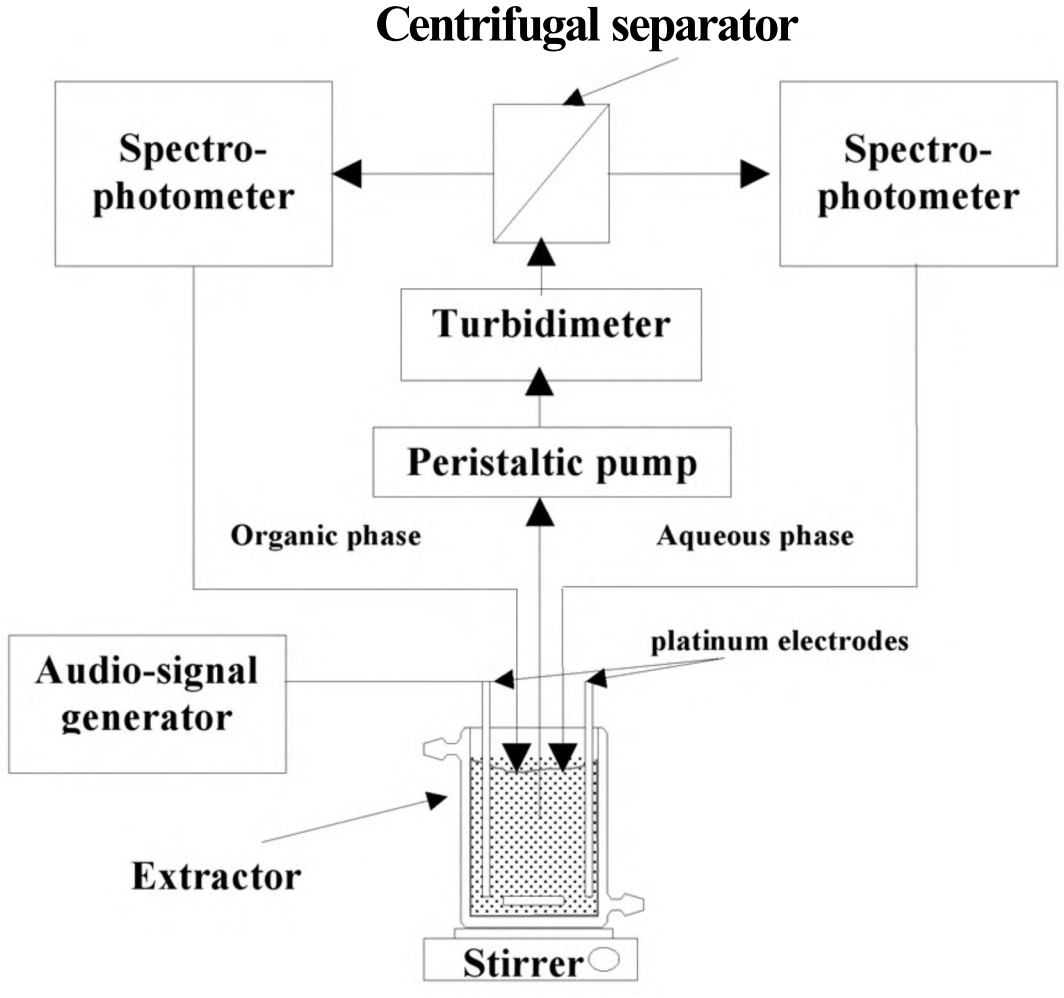


Figure 1. The schema of experimental setup.

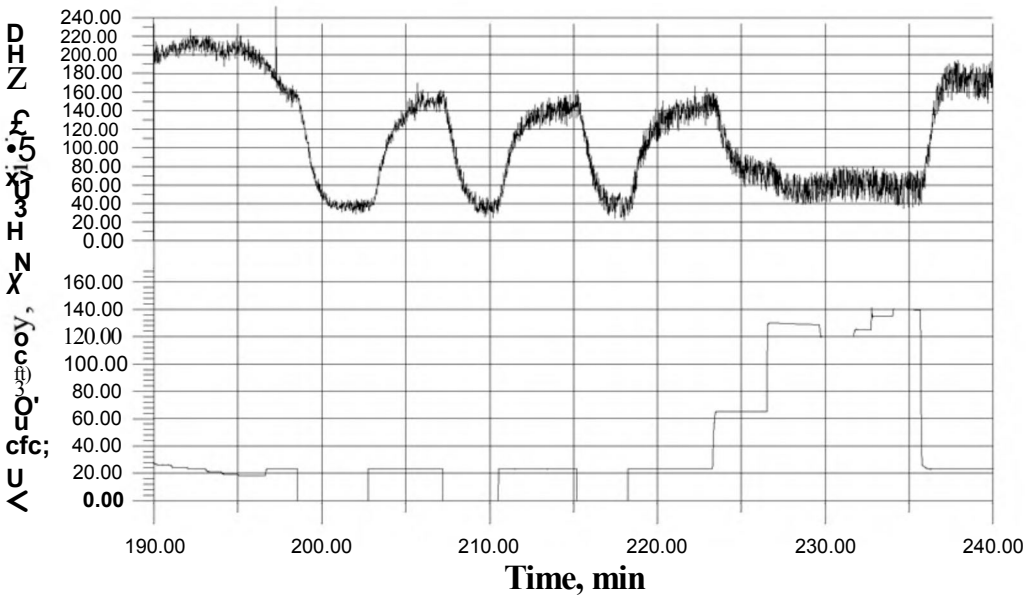


Figure 2. Temporal dependence of turbidity on external alternating current frequency.

Composition of the solution: Organic phase - 0.5M TBP on kerosene, aqueous phase - 7 M NaN03, 0.039 M $Nd(N0_3)_3$, 0.7 M $C_3H_40_4$, 0.7 M $KBr0_3$, 0.25 M $Ce(N0_3)_3$, Volume of organic phase= volume of aqueous phase = 150 ml. Full emulsifying took place in the extractor at rotation speed of the stirrer - 300 rpm. Flow rate to turbidimeter Kernco 966R - 66 ml/min. External AC ~ 3 V. T=25 C.

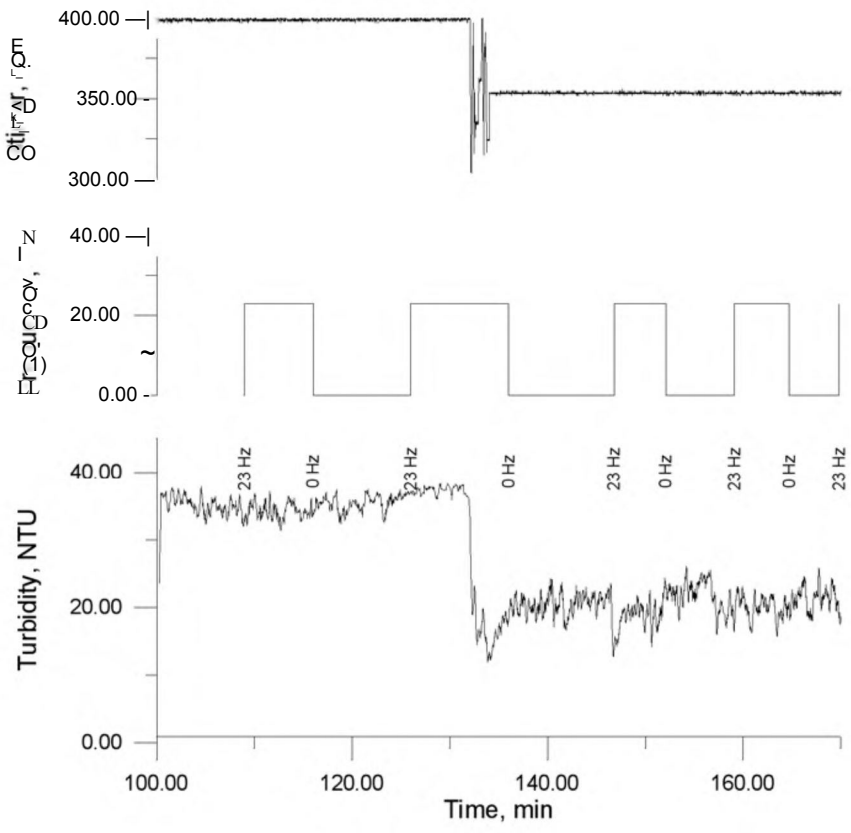


Figure 3. Temporal dependence of turbidity and frequency in batch experiment.

One extractor. Total volume of organic phase 150 ml - 0.5 M TBP in kerosene, aqueous phase 150 ml - 6 M $NaN0_3$„ T=25 C.

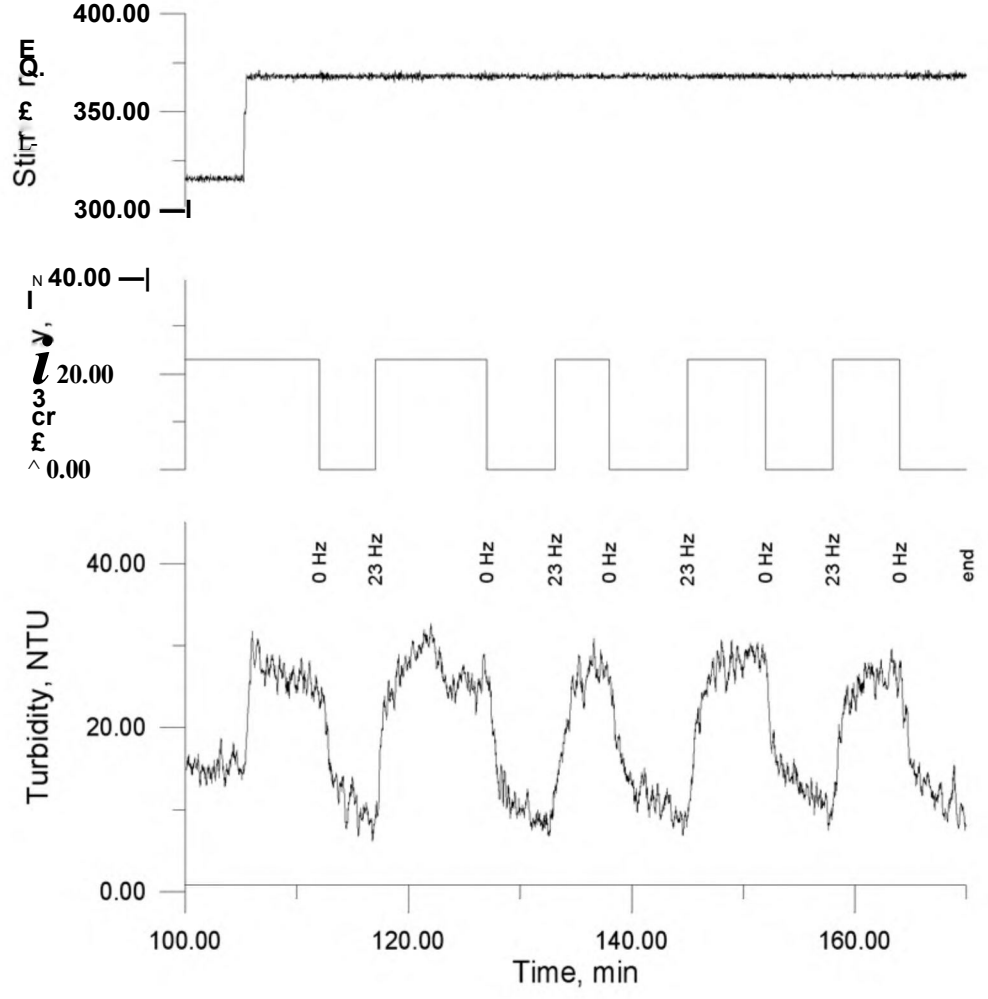


Figure 4. Temporal dependence of turbidity and frequency in batch experiment.

One extractor. Total volume of organic phase 150 ml - 0.5 M TBP in kerosene, aqueous phase 150 ml - 0.1 M $NaN0_3$. T=25 C.

Two extractors coupled by bulk liquid membrane (rate=3*22 ml/min). Total volume of organic phase 240 ml, aqueous phase 250 ml. Extractant - 0.5 M TBP in kerosene. Initial concentrations in the aqueous phases: 1st extractor - 6 M $NaN0_3$, 0.7 M $KBr0_3$, 0.7 M HMal, nitrate of Ce (0.25 M), Pr (0.1 M), Nd (0.1 M). T=25 C. 2nd extractor 0.1 M $HN0_3$ - strip solution.

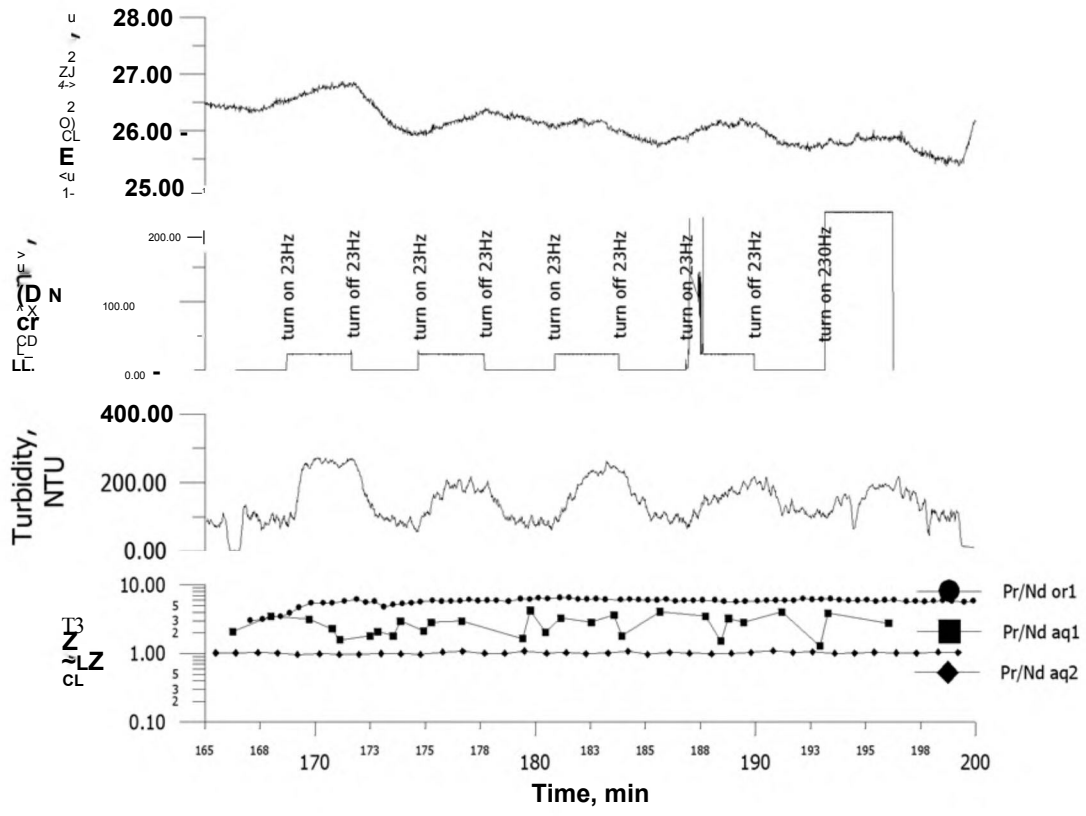


Figure 5. Temporal dependence of turbidity, frequency and concentration ratio of Pr/Nd pair in extractors in batch experiment.

References

1 Afonin M.A., Romanovski, V.V. Scherbakov V. A., Solvent Extraction and Ion Exchange, 16, 1215(1998)

2 Parmananda P. et all, J. Phys. Chem. B, 104, 11748 (2000)

3 K.O. Shifrin, Rasseynie sveta v mutnoy srede., GITTL, M,L, 1951,288 p. (In Russian)

4 M.A. Afonin, A.A. Kopyrin, A.I. Shvalbe, A.A. Baulin, A.S. Petrov, Chemical and electrochemical oscillatory extraction of F-elements—new procedure development., Journal of Alloys and Compounds 374 (2004) 426.



EFFECT OF THE SURFACTANT ON THE PRODUCTION AND STABILITY OF AQUEOUS DECONTAMINATION FOAMS

Mingmei Wang ", Zhidong Chang, Hailing Xi ", Yanjun Zuo ",
Wenjun Li and Huizhou Liu

Institute of Process Engineering, Chinese Academy of Sciences, Beijing, P. R. China
*** University of Science and Technology Beijing, Beijing, P. R. China**
****The Academy of Chemical Defence, The People's Liberation Army, Beijing, P. R. China**

The use of foam in applying decontamination solutions has proven to be an effective waste minimization technology. In order to get an aqueous foam decontamination solution with better foamability and foam stability, the effects of solution viscosity and surface tension of 1wt% surfactant aqueous solutions on the foamability and the foam stability were studied. The effect of a disinfector on the different surfactants and surfactant mixtures on the foam properties of decontamination solutions were also studied. By measuring the foam life-spans, anionic surfactant Sodium-dodecylsulphate (SDS), amphoteric surfactant BS-12 and a tertiary amine cationic surfactant were selected due to their better foamability and foam stability. These three different surfactants were then mixed and experimental results indicated that the mixture produced better foams when mixed with the decontamination solutions than the single surfactants.

INTRODUCTION

Decontamination is widely needed to deal with some paroxysmal incidents, such as preventing an epidemic from spreading rapidly and widely and decontaminating polluted water. Especially in the case of SARS and birds flu, to find an effective way of decontamination seems to be much more important than willful persecution.

Traditional aqueous decontamination solutions are mostly used nowadays with a disinfector concentration of about 10wt%. The decontamination solution is usually sprayed to objects and contaminated areas using a sprayer with high pressure. There are some shortcomings in this process. Firstly, large amount of decontamination solution is consumed, especially when the contaminated area is wide, resulting in large number of containers required to carry them. Secondly, when decontamination solutions are sprayed onto the vertical walls or other complex surfaces, most of the decontamination solution flows down to the ground rapidly due to gravity, resulting in much shorter contact time. This behaviour precludes the effective wetting of the surface and therefore an effective reaction with the poisonous substances.

In applying decontamination solutions, using a foam as a carrier has proven to be an effective waste minimization strategy. In order to develop new and better aqueous foam decontamination solutions to take the place of traditional aqueous solutions, we need to know the factors that influence foam stability and foamability. Foam stability refers to the foam lifetime, and foamability refers to how difficult the foam is generated and how much is

produced. Foam properties were studied by various researchers [1-5]. Foams evolve by three basic processes [6] encompassing: the gravitational drainage [7] from the films separating the foam bubbles, the coalescence of adjacent bubbles due to the rupture of inter-bubble lamellae and Ostwald ripening which is a coarsening process caused by inter-bubble gas transport. Our aim is to obtain surfactant formulas that can make more stable foam. In this study we measure foam stability in order to select the best surfactant system.

MATERIALS

Sodium-dodecylsulphate (SDS) and Span 60 were purchased from Beijing Chemical Reagent Company, China. Tertiary amine, 0-20 and BS-12 were purchased from Tianjin Surfactant Company, China. Brij 35, MES, lycine, CEMA, CAB-30, 3 - lycine, TML, 6501(1:2), 6501(1:1), Polyethylene glycol) distearate, Polyethylene glycol 150dimethyl ether, N-Lauryldiethan and No.1 were supplied by the Academy of Chemical Defence, PLA, China. They were all of industrial purity.

APPARATUS AND METHOD

Foam stability estimates

The foam stability was determined using a modified Bikerman method [8], Experiments were performed in a glass cylindrical column with a glass grit filter with 16-30pm porous size at the bottom. The column is 80cm high with inner diameter of 7.5cm. The schematic diagram of the experimental apparatus is shown in Figure 1.

Foam stability was studied by measuring the change of foam height in the column as a function of time. Compressed-air foaming is used in this experiment. The surfactant was weighed, mixed with deionised water to produce a 1wt% surfactant solution, and agitated with an electromagnetic agitator until well mixed. About 30ml of this solution was poured into the foam generator. The initial height of solution (about 0.7cm) was then recorded. The valve was opened and N_2 at high-pressure was introduced through the porous frit located at the bottom of the column into the solution with a flow rate of 30 ml/min. After 5 minutes, the injection of N_2 was stopped and the foam height h_0 was written down. Then the foam height h was recorded every 10 minutes. A h-t (height-time) curve was drawn with these data, and then the foam properties would be seen from the curve as a function of time.

Surface tension

A set of 1wt% aqueous solutions, each of about 30ml, was prepared with different surfactants. Their surface tension was measured with a ZL-2 Auto-Tensiometer (Zibo, China) three times per solution at room temperature (20±1”C). The mean value for each solution was then calculated, and adopted as the surface tension of the corresponding surfactant solution.

Solution viscosity

A set of 1wt% aqueous solutions, each of about 500ml, was prepared with the different surfactants. Their apparent viscosity was measured on the DV-E Viscometer (Brookfield company, USA) with 2# rotor at 20 ± 1 °C and lOOr/min. The mean average of three measurements was adopted as the viscosity of the corresponding surfactant solution.

RESULTS AND DISCUSSION

Compatibility between disinfector and surfactant solution

Every disinfector has its own properties, so the compatibility between the surfactant solution

and the disinfector has a very important effect on the effectiveness of the aqueous foam system applied to the decontamination solution. Therefore, the foamability of the surfactant solution with about 10wt% disinfector was explored. The compatibility results are shown in Table 1.

The surfactants that can be dissolved in water and their foamabilities were not affected by the disinfector can be selected from Table 1. From Tablel, it can be seen that CEMA, N-Lauryldiethan, Span 60, and Poly (ethylene glycol) distearate cannot satisfy our requirements

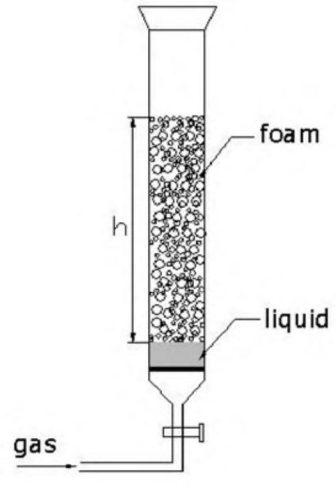


Figure 1. Compressed-air foam generator.

Table 1. Compatibilities between surfactant solutions and disinfector.

Surfactant	Compatibility	Surfactant	Compatibility
Brij 35	-	CAB-30	-
MES	-	0-20	-
lycine	-	BS-12	-
tertiary amine	-	SDS	-
CEMA	*	|3- lycine	-
Polyethylene glycol 150 dimethyl ether	–	N-Lauryldiethan	*
TML	+	6501(1:2)	-
Span 60	*	6501(1:1)	-
Polyethylene glycol) distearate	*	NO.1	+

+: incompatible (Disinfector decreases the foamability of surfactant solution seriously).

–: compatible (Disinfector nearly doesn't influence the foamability of surfactant solution) .

***: Surfactants that can't be dissolved in cool water at room temperature (20± 1 °C).**

because they can't be dissolved in cool water. TML and NO.1 react with our disinfector so strongly that when they are dissolved in deionised water containing the disinfector the mixed solution cannot generate a foam any more. The rest of the surfactants were selected to continue the study.

Surface tension

Surface tension is related to the number of surfactant molecules per unit area adsorbed at the air/water interface. The surface tension would decrease with increasing surface

concentration [9] until the surfactant concentration reaches the cmc (critical micelle concentration). The surface tensions of 1wt% aqueous surfactant solutions are shown in Table 2. From Table 2, it can be seen that the solutions of 6501(1:1) and 6501(1:2) have very low surface tensions. The surface tensions of SDS, tertiary amine, (3- lycine, CAB-30 and BS-12 aqueous solutions are a little higher. The ones of Brij 35 and 0-20 are highest among them.

But the surface tension is not the decisive factor that influences the foam properties. To generate foam, the surface film must be formed. Comparing the data with foam life-span curves as shown in Figure 2, we can see that lower surface tension does not necessarily lead to better foamability and foam stability. But the solutions of foams with excellent properties have lower surface tension than the rest.

Table 2. Surface tensions of 1wt% aqueous surfactant solutions (20±1 V).

Surfactant	Surface tension (mN/m)	Surfactant	Surface tension (mN/m)
Brij 35	44.0	CAB-30	36.8
tertiary amine	33.4	0-20	40.8
SDS	31.4	BS-12	37.5
6501(1:2)	29.7	6501(1:1)	29.3
|3- lycine	33.5	–	–

Solution viscosity

The viscosities of 1wt% aqueous surfactant solutions are shown in Table 3. High solution viscosity can prevent the liquid in the adjoining bubble films and Plateau Border from draining easily, thereby slowing down the film thinning velocity and enhancing the stability of the aqueous foams. From Table 3, it can be seen that the solutions of 6501(1:1) and 6501(1:2) have relatively high viscosities. The viscosities of 1wt% SDS, BS-12, tertiary amine and CAB-30 aqueous solutions are a little lower. Those of Brij 35,(3- lycine and 0-20 are the lowest among them.

Table 3. Solution viscosities of 1wt% aqueous surfactant solutions (20±1 V, 2# rotor, lOOr/min).

Surfactant	Viscosity (CP)	Surfactant	Viscosity (CP)
Brij 35	11.2	CAB-30	12.0
tertiary amine	12.0	0-20	11.6
SDS	12.4	BS-12	12.4
6501(1:2)	18.4	6501(1:1)	23.2
(3- lycine	11.6	–	–

Life-spans of foams

To obtain the foamability and foam stability data of the above surfactants respectively, the life-spans of their aqueous foams were measured and the results are shown in Figure 2.

From Figure 2, it can be seen that 1wt% aqueous solutions of BS-12, tertiary amine and SDS have better foamability and foam stability. These surfactant solutions also have both lower surface tension and higher viscosity as shown in Table 2 and Table 3, which fit very well with the theoretical analyses. The solution of a mixture of these surfactants may be a very good way to obtain a better foam system [10,11]. Therefore the foam properties of surfactant mixtures were studied. Experimental results are shown in Figure 3. We tried the weight ratio as that SDS : BS-12 : tertiary amine =1 : 40 : 40, and the foam properties of the mixture were

good enough for both our study and application. The concentration of disinfector in the mixture solution was 10wt% as commonly used in traditional aqueous solutions.

The surfactant counterion strongly influences the cmc (critical micelle concentration), micellar catalysis, micelle size, and emulsion size as observed by various researchers [12-14], It can be seen that both the foamability and foam stability of the mixture solution are better than those of pure surfactants in our study. In these three surfactants, SDS is an anionic surfactant, tertiary amine is a cationic surfactant, and BS-12 is an amphoteric surfactant. When these three surfactants are mixed in one solution, SDS and tertiary amine combine the end of BS-12 with opposite charge respectively. Therefore the length of molecule is longer, and the surface film is more stable. Comparing Figure 3 with Figure 2, it can be seen that the foam stability and foamability of the solution of mixed surfactants with different charge are better than those of pure surfactants. A similar behaviour of solutions of surfactant mixtures with respect to single surfactant solutions can be found in the literature [15,16],

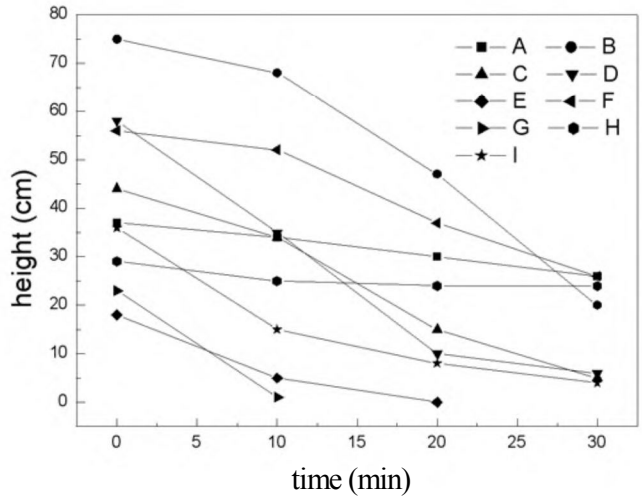


Figure 2. 1wt% surfactant solution foam height-time curve.
A: SDS, B: BS-12, C: 0-20, D: CAB-30, E: P-lycine, F: tertiary amine,G: 6501(1:2), H: 6501(1:1), I: Brij 35.

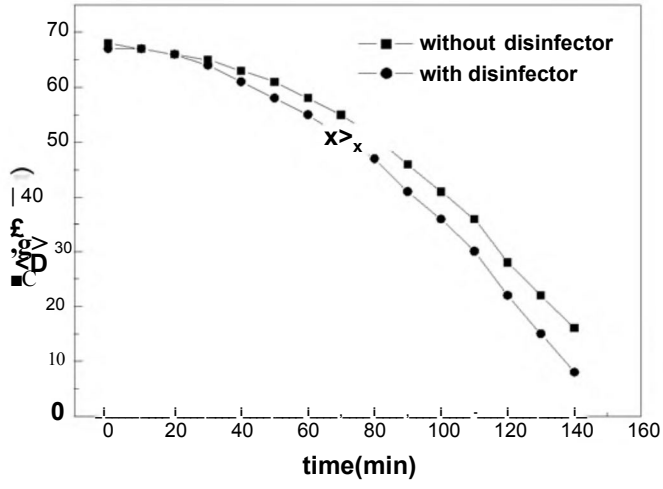


Figure 3. Foam properties of 1wt% surfactants mixture with and without disinfector.

In addition, we can also see from Figure 3 that the disinfector has such a little influence on the surfactant mixture solution as can be accepted by both our study and application.

CONCLUSION

Low surface tension and high viscosity of surfactant solutions are necessary conditions but not sufficient to obtain stable foams.

An effective foam system with better foam stability and high foamability was obtained through mixing different surfactants. This foam system can satisfy the application requirements. The mixture is composed of an anionic surfactant, a cationic surfactant and an amphoteric surfactant whose foam stability and foamability was much better than those of the three single surfactant systems.

The given disinfector has little influence on our foam system, and can be added into the surfactant mixture solution to conduct foam decontamination effectively.

ACKNOWLEDGMENTS

This work was supported by a grant from the Academy of Chemical Defence, the People's Liberation Army and the National Natural Science Foundation of China (No. 20406021, No. 20236050, No.20221603).

REFERENCES

1. **K. Theander and R. J. Pugh (2003),** *J. Colloid Interface* **Sc/'., 267, 9-17.**
2. **K. S. Lim, M. Barigou (2004),** *Ultrason. Sonochem.,* **in press.**
3. **P. S. Gautam and K. K. Mohanty (2004),** *J. Colloid Interface Sci.,* **273, 611-625.**
4. **M. Golding, A. Sein (2004),** *Food Hydrocolloids,* **18, 451-461.**
5. **D. Beneventi, B. Carre, A. Gandini (2001),** *Colloid Surf. A-Physicochem. Eng. Asp.,* **189, 65-73.**
6. **S. A. Magrabi, B. Z. Dlugogorski, G.J. Jameson (1999),** *Chem. Eng. Sci.,* **54, 4007-4022.**
7. **A. Bhakta and E. Ruckenstein (1997),** *J. Colloid Interface Sci.,* **191, 184-201.**
8. **J. J. Bikerman(1973), Foams, Springer-Verlag, New York.**
9. **J. P. Heller and M. S. Kuntamukkula (1987),** *Ind. Eng. Chem. Res.,* **26, 328-325.**
10. **M. J. Rosen (1978), Surfactants and Interfacial Phenomena, Wiley, New York.**
11. **M. J. Rosen (1989), Surfactants and Interfacial Phenomena, 2nd ed., Wiley, New York.**
12. **S. G. Oh, D. O. Shah (1993),** *J. Phys. Chem.,* **97, 284-286.**
13. **P. Mukerjee, Adv (1967).** *Colloid Interface Science,* **1, 24.**
14. **D. H. Kim, S. G. Oh, C. G. Cho (2001),** *Colloid Polym. Sci.,* **279, 39-45.**
15. **D. Langevin(2001),** *Adv. Colloid Interface Sci.,* **89-90, 467-484.**
16. **K. M. Askvik , S. A. Gundersen , J. Sjoblom , J. Merta , P. Stenius (1999),** *Colloid Surf. A-Physicochem. Eng. Asp.,* **159,89-101.**

THE SURFACE EXCESS ISOTHERM AND THE INTERFACIAL ACTIVITY OF CYANEX 302 IN DIFFERENT DILUENTS

Dongbei Wu and Deqian Li *

Key laboratory of Rare Earth Chemistry and Physics,
Changchun Institute of Applied Chemistry, Chinese Academy of Science,
Graduate school from Chinese Academy of Science
Changchun, 130022, PR China.

Different adsorption isotherms such as the Gibbs, Langumiar, Szyszkowski, Temkin, and Polynomiar of the third order are used to match the experimental interfacial tension and compare the interfacial activity of Cyanex 302 in various diluents. The results obtained suggest that using different isotherms, ambiguous conclusions can be drawn. However, the consistence of interfacial activity can be obtained for Langumiar isotherm, Gibbs isotherm and Temkin isotherm and there is an order as follows: Heptane > carbon tetrachloride > toluene > benzene > chloroform.

INTRODUCTION

Bis (2, 4, 4-trimethylpentyl) monothiphosphinic acid (Cyanex 302) has been used for years in separation of metal ions by liquid/liquid extraction^-2] .Taking into account the high amphipathic nature of Cyanex 302 one can deduce that extraction should precede at the interface or in close proximity to it, the interfacial activity of this extractant is obviously an important parameter to interpret kinetics data as in the case of metal extraction from acidic solutions with Cyanex 302. However, up to now, the interfacial activity of Cyanex 302 has not been described.

The objective of this work is (1) to treat with the interfacial tension isotherm using analytic concentration of Cyanex 302, (2) using different adsorption isotherm to compare interfacial activity of Cyanex 302 in various diluents.

EXPERIMENTAL

The extractant Cyanex 302 is supplied by Cyanamid Canada, Inc., and is used without further

purification. All other chemicals used are of analytical grade.

The interfacial tension was measured by the Du Nouy ring method with a Sigma-701 tensiometer. The highest concentration for extractant in different diluents is prepared by dissolving known weights of the extractant in the solvent. The remaining solutions are made from these by volume dilution.

Mutually presaturated phases are used. Equal volumes (15cm^3) of both phases are automatically shaken in equilibrium tubes at 287±1K for 20min and then left for 2h for full separation. Buffer solution acetic acid- sodium acetic is used to adjust the aqueous pH 4.57.

THE INTERFACE TENSION AND SURFACE EXCESS ISOTHERM

The surface excess isotherms are calculated according to the Gibbs isotherm, Langmuiar, Szyszkowski and Temkin isotherms and the Polynomial of the third order. Using the Gibbs isotherm (Eq. (1))

$$\Gamma = -\frac{C}{RT}\frac{dy}{dC} \qquad (1)$$

Where C denotes the analytic concentration of Cyanex 302, the term dy/dc is calculated by graphical or numerical differentiation of the relation y vs. C [5], The relations of y vs lnC are also considered, and the gradients of the linear parts of these curves are used to calculate the surface excess at the "saturated" interface (r_{sat}^{s}).

In the case of the Langmuiar isotherm, (Equ (2)), Szyszkowsli isotherm (Equ.(3)), Temkin isotherm (Eq.(4)), and the Polynomial of the third order (Eq.(5))

$$\frac{c}{n} = \frac{1}{ab} + \frac{c}{b} \qquad (2)$$

$$\gamma - \gamma^{\circ} = -Bln(C/A + 1) \qquad (3)$$

$$hgC^{*}K_T = j^{\wedge}(\gamma^{\circ} - rr \qquad (4)$$

$$y = a,(/nC f + a_2(/nC)^2 + a_3 lnC + a_4 \qquad (5)$$

where A, B, K_T, B_T, a_{1t} a_2, a_3, a_4, a ,and b are the appropriate constants and y°is the interfacial tension for C=0, these functions are first matched to the experimental data, and the appropriate constants are calculated using the least-squares method for Equ. (2), (4) and (5), and the non-linear fitting for the Eq.(3).

RESULTS AND DISCUSSION

The interfacial activity of extractant can be characterized by adsorption efficiency defined by (I) the minimum bulk concentration required to produce a saturated interface, C* (II) the extractant concentration required for a selected decrease of interfacial tension, C_2, and/or (III) the interfacial tension corresponding to a chosen concentration, y .

Adsorption effectiveness can be defined by the lowest interfacial tension possible to obtain in the considered extraction system or by the highest extractant interfacial concentration equal to the surface excess r_{max}.

Some adsorption parameters are given in Table 1. C_1 is estimated from the interception of two asymptotes to the interfacial tension, i e at a low concentration region (an asymptote parallel to the concentration axis) and at a region in which the interfacial tension isotherm has a linear character. Thus, C, determines the concentration at which a significant decrease at the interfacial tension is observed. C_2 denotes the compound concentration corresponding to the interfacial pressure of 10 N/m because the studied compounds do not exhibit such high efficiency of adsorption, y denotes the interfacial tension corresponding to the concentration of lxlO'³ mol L'VFrom Table. 1, we can know that the various solvents have an important influence on the interfacial activity of Cyanex 302 and there is an order as follows: heptane> carbon tetrachloride> toluene>benzene>chloroform.

Table. 1. Parameters characterizing interfacial activity as calculated by graphical methods

Solvents	Efficiency			Effectiveness	
	-logC-! (mol/L)	-logC_2 (mol/L)	Y (mN/m)	1- Slope / 1 max (molcm'²xl0¹⁰)	Ai (A^2)
CCl_4	2.94	2.36	30.39	1.54	107.9
C_6H_6	2.60	1.88	29.80	1.20	138.4
C_7H_{16}	2.59	1.49	29.04	1.19	139.6
C_7H_8	2.46	1.30	27.82	0.98	169.5
$CHCl_3$	2.38	0.99	26.24	0.97	171.2

Important differences are, however, observed between surface excess isotherms obtained by differentiating Equs. (2), (3), (4) and (5) and introducing the dy/dC term into the Gibbs isotherm, the following relations for the surface excess (Eqs.(6)-(9)) are then obtained:

$$j\text{-}Lan __ = \frac{C}{RT\,ah\,h\,ah}\left(\frac{1}{L^{\wedge}}\right)^{-2} \qquad (6)$$

$$r^{Sz}\ \frac{By^{0}\ C}{RT\ C + A} \qquad (7)$$

$$_{r}r__\frac{2(y°\text{-}y)^{as}}{2.303RT} \qquad (8)$$

$$\Gamma^{Pol} = -jjj;[3a_l(/nC)^2 + 2a_2\ lnC + a_3\ ] \quad (9)$$

which are used to calculate the surface excess.

The free energy of adsorption of Cyanex 302 is calculated from the A, Syszkowski adsorption coefficient according to equation (11).

$$AG = RT\ In\ A(kJ / mol) \quad (10)$$

Table 2. Values of the constants obtained by different isotherms

	Szyszkowski constants			Temkin constants		Langumiar constants		Polynomiar constants			
Solvents	A xIO^3	B xIO	AG xIO^3	K_T	Bjx 10^3	a xIO	b	ai ×10^5	a_2 xIO^3	a 3	a 4
CCl_4	0.48	0.85	-18.2	-4.58	2.11	12.0	16.7	0.5	-9.7	-3.91	9.94
C_6H_6	0.94	0.87	-16.6	-4.27	2.22	9.8	12.8	-0.83	-34.4	-4.77	7.56
C_7H_{16}	0.06	0.72	-23.2	-5.25	2.21	15.9	21.0	-1.96	-64.2	-7.68	0.21
C_7H_8	1.63	1.07	-15.3	-2.29	1.36	8.35	15.0	2.73	-82.5	-8.24	1.29
$CHCl_3$	2.73	1.03	-14.1	-3.95	2.21	7.3	11.4	1.79	-58.9	-6.24	5.32

Table 3. The surface excess at the saturated interface

Solvent	pslope xIO^{10} (mol/cm^2)	r^o xio^{10} (mol/cm^2)	r-Lan xIO^{10} (mol/cm^2)	r^T xio^{10} (mol/cm^2)	I-Sz xio^{10} (mol/cm^2)	j-Poly xio^{10} (mol/cm^2)
CCl_4	1.20	1.35	1.72	1.46	1.22	1.43
C_6H_6	0.98	1.28	1.28	1.26	1.06	1.40
C_7H_{16}	1.54	1.94	2.11	1.63	1.08	1.99
C_7Hs	1.19	1.67	1.44	1.36	1.36	1.83
$CHCl_3$	0.97	1.95	1.18	1.19	1.18	1.57

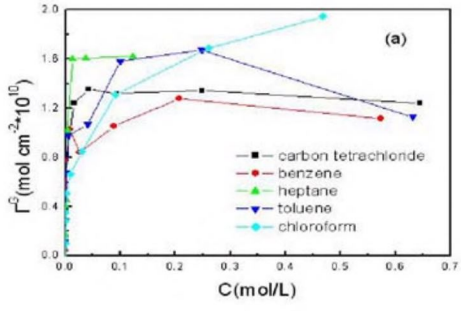


Figure 1. Gibbs isotherm

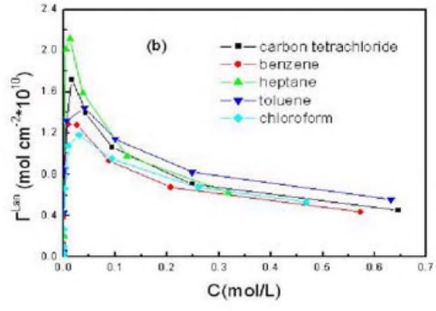


Figure 2. Langmuiar isotherm

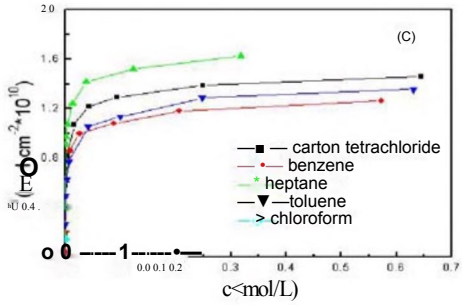


Figure 3. Temkin isotherm

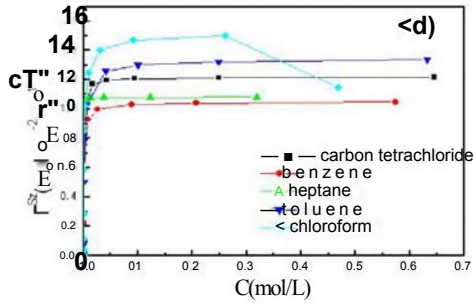


Figure 4. Szyszkowszki isotherm

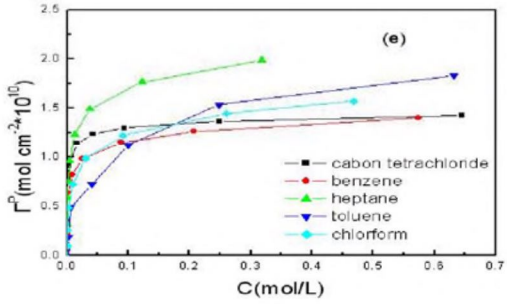


Figure 5. Surface excess calculated according to the Polynomiar isotherms for systems containing Cyanex 302 in different solvents

the values of the appropriate constants in different isotherms obtained for Equs.(4)-(7) are given in Table. 2. The Plots of C against T calculated by Gibbs isotherm, Langmuiar isotherm and Temkin isotherm are illustrated in Figs 1-5 and the values of r_{max} are given in Table.3.

From these Figs, and Tables, one can know that the values of r_{sat} slopes are all lower than the surface excess determined previously by the differentiation of the relation y vs C, ie, the values of 1"° The shape of the relations calculated according to the Temkin isotherm and Langmuiar isotherm are different. However, the surface excess isotherms calculated according to the Temkin isotherm shows characters similar to these calculated according to the Langmiar isotherm and Gibbs isotherm (here denotes the slope method). The influence of the considered parameters upon adsorption is qualitatively the same. The same orders of the surface excess change are observed, but the absolute values are somewhat different. The saturation of the interface is observed at higher concentrations in comparison to the Temkin isotherm, and in reality, the constant values of the surface excess are not obtained in the region of the concentrations investigated, because of this, the highest values of the surface excess were considered here as an estimation of the saturated interface. Cyanex 302 concentrations above which the interface is "saturated" were arbitrarily chosen as those above which, in the investigated region, the surface excess does not change more than 10% and the same choice to be used for the Polynomiar isotherm and Szyszkowski isotherm. Using the Langmuiar isotherm, in some cases the monotonic functions and in other ones functions having distinct maxima were obtained. Because of this, the highest values of the surface excess observed at the maximum or at the highest compound concentration were

considered as the estimation for the saturated interface (Table 3). In the cases of the Gibbs isotherm, the obtained surface excess isotherms always have maxima as is demonstrated in Fig. 1. In this case the values at the maximum were chosen as those characterizing the saturated interface. The same analysis has been reported by Jan Szymanowski[6],

As we compare the shape of the surface excess isotherms presented in Figsl-3, one must admit that each one is more or less different. Thus, although each one different adsorption isotherm can often be converted into another one and their matching to the experimental data seems good, then for an actual experimental case, different shapes of the surface excess isotherms obtained can also lead to ambiguous or even false results, because of this, conclusions must be drawn very cautiously.

The comparison of the interfacial activity for Cyanex 302 in different solvents

Form Table 1, by comparing the values of C_i calculated from different isotherm equations, the orders of interfacial activity are obtained. Almost the same order of increasing interfacial efficiency is observed for Gibbs isotherm (slope method), Langmiur isotherm and Temkin isotherm: heptane> carbon tetrachloride> toluene>benzene>chloroform, which is same to the results reported by Sun [7], However, it is not clear why the order is different using Gibbs isotherm, Szyszkowski isotherm and Polynomiar isotherm.

It was established that the greater the interaction of the extractant with the organic diluent, the less its interfacial activity. In this work, the less interfacial efficiency of aromatic hydrocarbon may be due to aromatic character try “o” interact with water molecules by their Tr-electrons and to obtain the position parallel to the interface[8].The stronger polar solvent chloroform does not exhibit as strong repulsion for the hydrophilic portion of the molecules as does the aliphatic hydrocarbon. Its greater solvating ability would also act to lower dimer stability which seemingly would result in greater interfacial activity, and the latter effect appears less important than the former.

CONCLUSIONS

In this paper, by using different adsorptions such as Gibbs, Langumiar, Szyszkowski, Temkin, and Polynomiar of the third order, interfacial activity of Cyanex 302 in various diluents have been investigated systemically. The results obtained are summarized as follows:

1. Using different isotherms, ambiguous conclusions can be drawn.
2. The various solvents have an important influence on the interfacial activity of Cyanex 302 and there is an order of interfacial efficiency as follows: heptane> carbon tetrachloride> toluene>benzene>chloroform.

ACKNOWLEDGEMENTS

This project was supported by the National Program entitled 'Basic Research of Rare Earths’

(G1998061301), National Natural Science Foundation of China (20371046) and National "863"project (2002AA647070).

REFERENCES

1. **K. C. Sole and J. Brent Hiskey (1995),** *Hydrometallurgy*, **37,129-147**
2. **A. Almela and M. P.Elizalde (1995),** *Hydrometallurgy,* **37, 47-57**
3. **B. K. Tait (1993),** *Hydrometallurgy,* **32 (3), 365-372**
4. **C. Sella and D. Bauter (1988),** *Solv. Extr. Ion. Exch.,* **6, 819-833**
5. **J. Szymanowski and K. Provhaska (1988),** *J. Colloid Interface Sci.* **123, 456-465**
6. **J Saymanowski and K Prochaska (1987),** *J.Chem.Tech. Biotechnol,* **40,177-193**
7. **Sun Guo Xin and Cui Yu (2000),** *Solv. Extr Ion Exch.,* **18 (3), 517-531**
8. **G. F. Vaandergrift and E.P.Horwits (1980),** *J. Inorg. Nucl. Chem ,* **42, 119-125**



INTERFACIAL BEHAVIOUR STUDIES OF DEHEHP AT NITRIC ACID SOLUTION - ORGANIC DILUENT INTERFACE

Junmei Zhao, Wei Li and Deqian Li*

Key Laboratory of Rare Earth Chemistry and Physics, Changchun Institute of Applied Chemistry, Graduate School of Chinese Academy of Sciences, Changchun 130022, P. R. China.

Interfacial properties of DEHEHP have been extensively investigated. The interfacial tension (y) of DEHEHP in heptane or other diluents against $HN0_3$ has been measured at certain temperature except the temperature experiments. The surface excess is calculated according to the different adsorption equations such as the Gibbs, Szyszkowski, Polynomial and Langmuir function. The adsorption parameters calculated are presented in comprehensive tables. Increasing the concentration of the extractant resulted in a decrease in the y value, which shows that DEHEHP has interfacial activity as surfactant. Type of organic diluent and temperature affect the interfacial activity of DEHEHP.

INTRODUCTION

DEHEHP, di(2-ethylhexyl) 2-ethylhexyl phosphonate, are well-established extractant in extracting Ce(IV) from acidic nitrate solutions in the previous work of our group [1], The mechanism and rate of extraction of cerium(IV) from nitric acid solutions by DEHEHP in heptane has shown the importance of the interfacial behaviour of an extractant.

Interfacial tension (y) is important parameters influencing phenomena such as wetting, adsorption, foaming, miscibility, etc. Sun et al. [2] studied the interfacial properties of acidic extractants HEH(EHP) and HDEHP. Tong et al. [3] systematically examined the interfacial properties of neutral extractant Cyanex923 in nitric acid medium.

The objective of this work was to study the interfacial activities of DEHEHP at a nitric acid - organic diluent interface in different conditions such as the type of diluents and temperature.

The results are connected with the cerium extraction kinetics by DEHEHP.

EXPERIMENTAL

Commercial DEHEHP was used after equilibrium with lmol/L $HN0_3$ for two times. Various concentrations of DEHEHP in heptane or other diluents were prepared. Distilled water was used in preparing the aqueous solutions.

Interfacial tension was measured as described previously using the Du Nuoy ring method as described previously [4], These measurements were performed on a Du Nouy surface tensiometer (sigma 701, Holand) and a platinum / iridium ring of 9.545mm diameter. And solution densities were also determined using the same instrument.

DATA TREATMENT

Different adsorption equations were used for processing the interfacial tension data and calculated the adsorption parameters. C_{min}, the minimum bulk concentration of the extractant necessary to saturate the interface, is determined from the graph of y vs. lnC. It can be assumed that $\log C_{min}$ is a measure of adsorption efficiency. In all the adsorption parameters, C_{min} is the most important parameter to determine the adsorption efficiency of extractant molecule in the surface. The following equations have been used:

Gibbs Isotherm [5]

$$\Gamma = -\frac{C}{RT}\frac{dy}{dC} \qquad (1)$$

where I~= surface excess concentration, mol/m^2; R= universal gas constant; T= absolute temperature; y= interfacial tension, mN/m and C= bulk concentration of extractant, mol/L. When y is in mN/m and R=8.314J/mol/K, f is in mmol/m^2.

Szyszkowski Isotherm [6]

$$r = ro[i - B_{sz}H\frac{C}{K_{sz}} + V] \qquad (2)$$

where Yi is the interfacial tension for a given extractant concentration C, Yo is the interfacial tension for the system without extractant (C=0) and A_{sz} (mol/L)and $B_{sz}$are the adsorption coefficients. The Szyszkowski coefficients A_Sz and B_Sz are calculated by the least square method matching Eq. (2) to the experimental data.

The two Szyszkowski adsorption constants, A_Sz and B_Sz, have physico-chemical meanings and can be used to determine maximum surface excess at saturation, r_{max}. minimum interfacial area occupied by a statistical molecule in the absorbed layer (Ai) and the free energy of adsorption, AG_ad, according to the following relations:

$$r_{,\infty} = \frac{\wedge szY_0}{RT} \quad (3)$$

$$A_{:\cdot} = \frac{18}{N_A \Gamma_\infty} \quad (4)$$

$$AG_{ad} = RT\backslash n(A_{sz}) \quad (5)$$

Where N = Avogardo's number and When T is in mol/m², *A,* is in nm².

By differentiating Eq.(2) and introducing the dy / dC term into the Gibbs isotherm, the following relation for the surface excess is then obtained:

$$r^{s:} = \frac{By_0 C}{' RT C + A^{\wedge}} \quad (6)$$

Langmuir Isotherm [7]

$$\frac{r_\infty - r * c}{1 + KC} \quad (7)$$

Rearranged the Eq.(3) and the following equations can be got:

$$c/r = \frac{1}{KV_{,\infty} r} + \frac{C}{-\infty}$$

where K is interfacial adsorption constant of surfactant. From the slope and intercept of the plot of *C/* r vs. C, K and can be calculated.

In addition, Eq. (3) also can be transformed as follows:

$$r = r_\infty \bullet \frac{C}{\frac{1}{K} + C} \quad (8)$$

Compared Eq. (6) and (8), there are:

$$\frac{r_- {}^{B}Y\pm}{\text{“ } RT} \qquad {}^{A}_\frac{1}{S\ Z} \sim K$$

Combined with Eq. (5), the relation between AG_{ad} and K is as follows:

$$AG_{Jad} = 2.303RT \log A_{SZ} = -2.303RT \log K$$

From above, it can be concluded that Szyszkowski isotherm is consistent both with the Gibbs and Langmuir isotherm.

Different values of the surface excess are obtained from different adsorption isotherms, but these results show a similar change tendency, which does not influence qualitative analysis for interfacial activity of extractant.

RESULTS AND DISCUSSION

It can be seen that as the concentration of the DEHEHP increases, the y values decrease which is due to amphiphilic property of extractant molecule. The interfacial property of each amphiphilic reagent is strongly affected by temperature and the type of organic diluent.

From experimental data, the adsorption parameters, regression coefficients as well as the correlation coefficients and the model errors derived from the adsorption equations are listed in tables. The interfacial activity of DEHEHP is clearly demonstrated by the values of C_{min}.

Effect of Type of Diluent and Temperature

The adsorption parameters, regression coefficients as well as the correlation coefficients and the model errors derived from the isotherms are listed in table 1 in various diluents at 298K in DEHEHP -1.0mol/LHNO_3 systems and at various temperature in the system of DEHEHP - heptane - I.Omol/L $HN0_3$.

The efficiency of adsorption changes with the type of diluents in the following order: aliphatic hydrocarbons > carbon tetrachloride > aromatic hydrocarbons > chloroform from the value of C_{min}. It also appears that DEHEHP behaves very differently in aliphatic and aromatic systems. In systems containing aromatic hydrocarbons the interactions between water and aromatic molecules become important. Generally, the surface excess at saturation at the aromatic / aqueous interface is low than aliphatic / water interface. The larger interfacial area of extractant in aromatic hydrocarbons may be explained by solvation of the extractant at the interface.

Temperature changes also show large effects on interfacial activity. Studies show that the higher the temperature of the system, the lower the extractant's interfacial activity. An increase in temperature results in an increase in the area per molecule, presumably due to increasing thermal motion and out-of-order property.

The Interfacial Activity and the Rate of Cerium(IV) Extraction

Generally, acidic extractants with a strong acidic and hydrophilic group exhibit a very high efficiency of adsorption ($\log C_{min} < -5$) [8], as an extractant, is usually regarded as the interfacial chemical reaction mechanism [9], But solvating reagents exhibit significantly lower efficiency of adsorption than acidic extractants. In this work, the adsorption parameters obtained for DEHEHP are of the same quantitative order as the values reported for solvating extractant. From the research of cerium(IV) extraction kinetics by DEHEHP in our group, we can concluded that the most probable reaction regime is in the aqueous homogeneous phase, which is inconsistent with the interfacial activity studied in this text. The rate of extraction is determined by many factors. So this is a complicated problem. Moreover, the outside conditions such as the type of diluent and temperature similarly affect extraction rate because they are also the influence factors for the interfacial activity of extractant.

Table 1. Interfacial adsorption parameters in various diluents at 298K in DEHEHP-1.0 and at various temperature in the system of DEHEHP - heptane - I.Omol/L

	Szyszkowski Function								
	v -C non-linear fitting				relative formulas			Gibbs Function r -C curve fitting	
	A sz (mol/L)	Error of A_Sz	Bsz	Error of B_Sz	r_{max} xio⁶ (mol/m²)	AG (KJ/mol)	Ai (nm²)	r^*_{max} xio⁶ (mol/m²)	$logC_m$ (mol/L
K	0.6E-04	0.2E-04	0.06367	0.00611	1.090	-23.84	1.524	1.088	-1.63!
K	2.00E-05	3.12E-06	0.05946	0.00083	1.040	-27.26	1.597	1.040	-1.311
K	2.10E-05	1.80E-06	0.06601	0.00913	1.009	-27.58	1.646	1.009	-1.32!
K	1.00E-05	5.78E-06	0.05957	0.00005	0.944	-29.96	1.759	0.944	-1.26-
	1.6E-04	0.6E-04	0.06549	0.00474	1.104	-21.44	1.505	1.098	-i.5o:
	9.4E-04	2.7E-04	0.05748	0.01432	0.8409	-17.09	1.975	0.8355	-0.83!
	10.9E-04	4.2E-04	0.06481	0.00781	0.9069	-16.73	1.832	0.901	-0.77!
	13.2E-04	2.7E-04	0.06644	0.00322	0.8845	-16.26	1.878	0.8774	-0.78!
	14.9E-04	7.2E-04	0.06483	0.00644	0.8451	-15.96	1.966	0.8389	-0.69:
	17.6E-04	9.3E-04	0.05628	0.00601	0.6345	-15.56	2.618	0.6296	-0.64'

CONCLUSION

The interfacial activity of DEHEHP varies significantly depending on diluent type and temperature. The efficiency of adsorption changes with the type of diluents in the following order: aliphatic hydrocarbons > carbon tetrachloride > aromatic hydrocarbons > chloroform. This is connected with the interactions among extractant, diluent and interfacial aqueous phase one another, or even some more complicated unknown factors. An increase in temperature results in an increase in the area per molecule, presumably due to increasing thermal motion and out-of-order property.

ACKNOWLEDGEMENTS

This project is supported by the National Program entitled 'Basic Research of Rare Earths' (G1998061301), National Natural Science Foundation of China (20371046) and National "863"project (2002AA647070).

REFERENCES

1. **J.M. Zhao, Sh.L. Meng and D.Q. Li (2004),** *Solv. Extr. Ion Exch.,* **22 (3), 429-447.**
2. **J. L. Shen, Zh. K. Xi and S. X. Sun et al (1984),** *Chinese J. of Applied Chem.,* **1 (4), 57-62.**
3. **H. Tong (2003), The Interfacial Properties of Cyanex923 and the Solvent Extraction Kinetics of RE(III), Master Thesis, Wuhan University of Technology, PR. China.**
4. **G. F. Vandergift and E.PHorwitz (1977),** *J. Inorg. Nucl. Chem.,* **39, 1425 -1432.**
5. **J.W. Gibbs (1928), The Collected Works of J. W. Gibbs. Longmans, Green, London, vol. I, 119.**
6. **B. Szyszkowski (1908), Z.** *Phys. Chem.* **64, 385.**
7. **I. Langmuir (1917),** *J. Am. Chem. Soc.* **39, 1848.**
8. **K. Prochaska (2002),** *Adv. Colloid Interf. Sci.,* **95, 51-72.**
9. **P. R. Danesi and R. Chiariza(1980),** *Criti. Rev. in Anal. Chem.,* **10,1-126.**

EXPERIMENTAL STUDY OF MARANGONI EFFECT ON MASS TRANSFER OF PENDENT SINGLE DROPS IN MIBK-ACETIC ACID-WATER SYSTEM

Ping Lu[1,2], Guangji Zhang[1] and Zai-Sha Mao[1]*

1 Institute of Process Engineering, CAS, Beijing 100080, China
2 Graduate School of the Chinese Academy of Sciences, Beijing 100049, China

The experimental study on the mass transfer characteristics of single drops was carried out in the MIBK-acetic acid-water system, in which acetic acid was the solute, MIBK the dispersed phase and water the continuous phase. A precision syringe pump was used to produce uniform pendant drops attached at the needle tip. A Schlieren optical system was used to observe the Marangoni effect and it was recorded by a camera. When the solute was transferred from the dispersed phase to the continuous phase, the interfacial roll cells were observed at low solute concentration and became more striking along with the increase of concentration. The eruption occurred at certain concentration, meanwhile the ordered interfacial convection at the interface became turbulent suddenly and the mass transfer rate was also enhanced. When drops size and the formation time of drops changed respectively, the degree of the interfacal instability changed as well in spite of the same concentration.

INTRODUCTION

Solvent extraction, which has been widely used in petrochemical, pharmaceutical, hydrometallurgical and environmental processes, is an important method for separation and purification. In solvent extraction process, mass transfer is promoted by the Marangoni convection under certain conditions. The "Marangoni effect" as a result of interfacial tension gradient can lead to the interfacial convection, and the mass transfer rate is hence enhanced. Many studies indicate that Marangoni convection can increase mass transfer rate even by a order of magnitude [1], In general, the interfacial convection will develop from ordered-flow (convective instability) into disordered-flow (eruption) along with the increase of concentration driving force. This paper addresses the effects of the initial disturbance at different concentration, the formation time of drops and the drop size on the mass transfer rates.

* Email address: zsmao@home.ipe.ac.cn. Tel.: (+86) 10 6255 4558.

Most of mass transferred during solvent extraction are between single drops (or drop swarm) and continuous phase, and the understanding of this process is the base for develop and optimize commercial extraction units. Many researchers [2-3] studied mass transfer of moving drops, but only the effect of flow condition on mass transfer coefficient was investigated. Agble [4] reported the Marangoni effect of contaminated systems. Because of the effect of movement of drops and contamination of the system may mask the influence of the Marangoni effect, the experiments on mass transfer of pendent drops are performed to get a straightforward view of the inherent Marangoni effect.

EXPERIMENTAL

Apparatus

The experimental apparatus mainly contains two subsystem. One is used to determine the mass transfer coefficient of pendent drops to reveal the effect of Marangoni convection, and the other is a Schlieren system capturing the visual phenomena of interfacial disturbance at drop surface.

Figure 1 shows a diagram of the experimental apparatus for the determination of mass transfer coefficient. The quartz glass box has the cross section of 100 mm by 80 mm, and the working height is 100 mm. There are two *</>20* mm holes at the box top and bottom respectively. Stainless steel needle is inserted into the column through the bottom hole and a funnel is fixed 30 mm above the needle tip through the top hole.

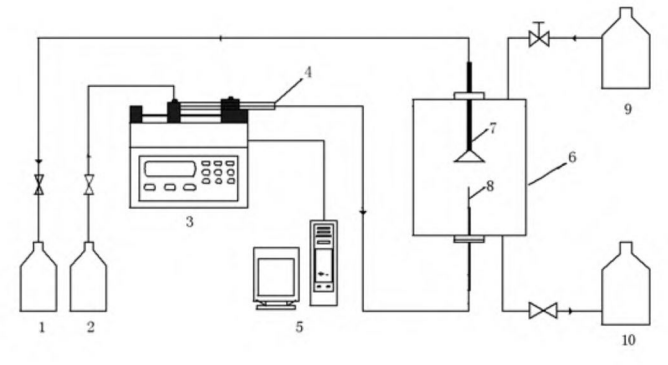


Figure 1. Diagram of Mass Transfer Apparatus
1,2.dispersed phase tank **3.precision syringe pump 4. gastight syringe**
5.computer 6.extraction box 7.funnel 8. needle 9, 10. continuous phase tank

A programmable precision syringe pump (Model 22, Harvard Apparatus) with a gastight syringe (Hamilton Gastight Syringe 81527# 5ml) is used to produce pendent drops. The syringe pump controlled by a PC computer not only guarantees the same formation time *t* and pending time *t'* of a single drop, but also allows changing *t* and *t'* according to the need of experiment. Three different gauges of medical needles were used to produce drops of different size. Teflon tubing is used as connector between needle and syringe.

Figure 2 shows a diagram of Schlieren system, which was manufactured by Jinzhou Optical

Apparatus Company. The Schlieren image of a homogenous test space is a black background only, due to the absence of light blocked out by the knife-edge. If there are any inhomogeneities in the test space, some light will be deflected and therefore no longer be focused on the knife-edge. This results in the formation of bright patches on the Schlieren image. A Schlieren image of a non-homogenous test space is therefore characterized by the presence of these light patches, and non-symmetric movements of these light patches indicate the presence of Marangoni convection [4],

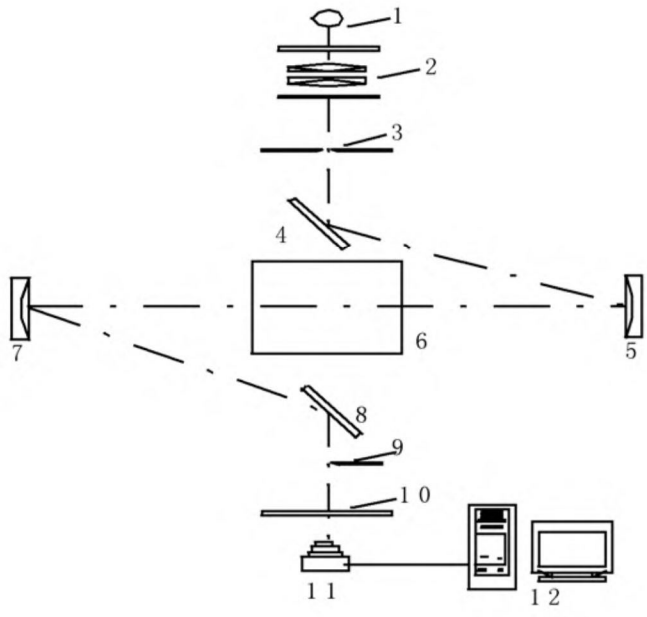


Figure 2 Diagram of Schiierent system
1.point source 2 convergent lenses 3.slit 4,8. fully reflecting mirror
5,7.concave fully reflecting mirror 6.ectraction column 9. knife-edge
10. screen 11. CCD 12.computer

Test System

The MIBK-acetic acid-water system recommended by European Federation of Chemical Engineers was chosen. The MIBK was the dispersed phase, distilled water the continuous phase and acetic aci (A.R., Beijing Chemical Reagent Co.) the solute that is transferred from the dispersed phase to the continuous phase. The physical properties of this system are shown in Table 1 [5],

Component	Temperature fC)	Density (kg/m^3)	Viscocity (mPa.s)	Surface tension (mN.rrf^1)	Refractive index	Purity (%)
Water	20	998.2	1.003	72.8	1.333	99.99
MIBK	20	800.2	0.582	23.9	1.396	99.81
Acetic acid	20	1049.3	1.229	27.5	1.371	99.9

Table 1 Physical properties of components in the test system

Procedure

The test box was filled with distilled water that was already saturated by MIBK. The box is gastight so that the volume of collected dispersed phase is equal to that of drops injected by the syringe pump. The interface of the two phases in the collecting funnel should be adjusted at appropriate place so that the contact area of the collected drops with the continuous phase is the smallest. The flow rate of the pump, the formation and pending times of drops are accurately controlled by the computer. The volume of drops was almost the maximum which can be pending at the needle tip. At the very moment of the next drop is going to be produced, the previous drop left the tip at this very weak trigger. The volume of drops V_6 can be calculated from Q designated to the pump and the formation time of drops. The mass transfer coefficient K_{oi} of pendent drops is calculated by

$$K_{od} = -\frac{d_p}{6(t_2' - t_1')} \ln(1-£)$$

$$E = \{y_2 - y_x) K y^* \sim y_x)$$

where y_x, y_2 is the drop average concentration at pendent times $l_{,,}$, t_2' respectively, and y*is the drop concentration is in equilibrium with the continuous phase. Because of the concentration of the continuous phase is zero, hereby* = 0.

During the mass transfer, after the drop was formed, the photograph of drop at different time was captured by the Schlieren system, until drop left the tip of needle.

Method of Analysis

The samples were analyzed, generally in triplicate, by titration with sodium hydroxide solution, using phenolphthalein as indicator. A sample of about 4 ml dispersed phase was analyzed three times.

RESULTS AND DISCUSSION

Mass Transfer Coefficients at Different Concentration

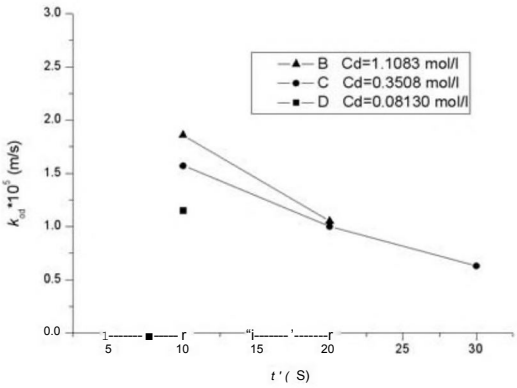
The mass transfer coefficients of drops with different concentration are shown in Figure 3. The concentration of experimental runs B, C and D is 1.1083, 0.3508, 0.08130 mol/L respectively. The average diameter of drops is d_p=3.14 mm. It is clear that the mass transfer coefficients of run B are the largest, followed by runs C and D. The mass transfer coefficients of runs B, C and D have significant difference because of the Marangoni effect. In the mass transfer process of D, no interfacial convection was observed but different degrees of interfacial disturbance were aroused in runs B and C. Larger driving force of B with larger concentration than C can create more large interfacial concentration gradient and interfacial tension gradient. More intensive interfacial disturbance at interface for run B can enhance mass transfer rate. So if concentration of solute is large enough, the Marangoni effect can enhance the convective instability at interface, which even develops to eruption at interface and creates larger influence on mass transfer rate.

Mass Transfer Coefficients with Different Formation Time

The mass transfer coefficients of drops with different formation time are shown in Figure 4. The formation time *t* of B and C is 2 s and 1 s respectively. The concentration of B and C is 0.3508 mol/L. From Figure 2, the mass transfer coefficients of B are larger than those of C. For moving drops, the faster formation rate can help create circulation in drops to enhance mass transfer rate. But here, for single pendant drops, the longer the formation time, the larger the mass transfer coefficient.

Photographs of Marangoni Convection at Drop Interface

The photographs of the Marangoni convection at the interface are shown in Figures 5 and 6 with different pendent time taken by the Schlieren system. The initial concentrations of drops in Figures 5 and 6 are 0.35 mol/L. It is clear that the interfacial convection weakens with mass transferred.



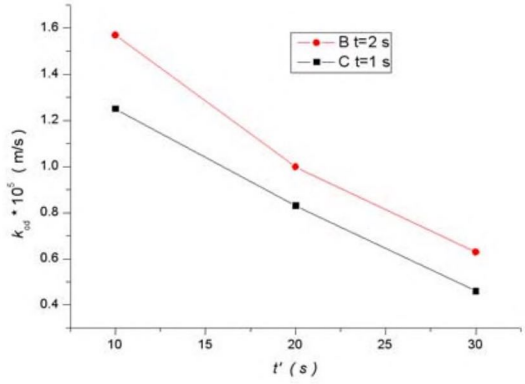


Figure 3 Mass transfer coefficients of drops with different concentration

Figure 4 Mass transfer coefficients with drops with different formation time



Figure 5 Photograph of Marangoni convection (t'=5s)

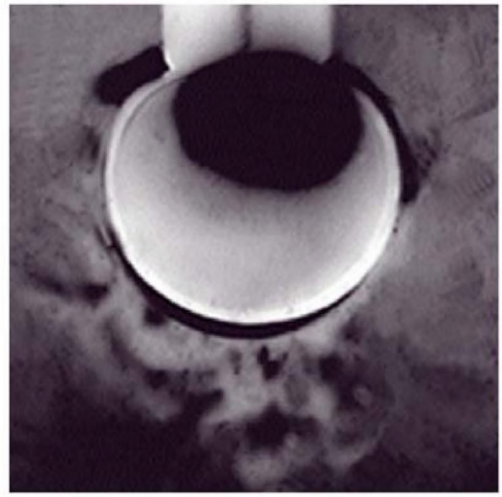


Figure 6 Photograph of Marangoni convection (t'=30s)

CONCLUSIONS

1. **For the MIBK-acetic acid-water system, when the solute is transferred from the dispersed phase into the continuous phase, larger solute concentration can create more intensive interfacial disturbance even eruption. The Marangoni effect enhances the mass transfer coefficients.**

2. **For pendant drops, when the system has no Marangoni effect, the formation time has no influence on mass transfer coefficient. But when the Marangoni effect happens in the mass transfer process, larger formation time can enhance mass transfer coefficient.**

3. **The Marangoni effect dies away gradually as mass is transferred. The larger the concentration of solute, the slower the speed of damp.**

ACKNOWLEDGEMENT

This work is supported by the National Nutural Science Foundation of China (Nos. 20490206, 20236050).

SYMBOLS

d_P	[m]	drop diameter
V**d**	[m^3]	drop volume
Q	[ml/min]	pump flow rate
E	[-]	extraction fraction
K_{o}**d**	[ms^1]	overall dispersed phase mass transfer coefficient
t	[s]	drop formation time
t'	[s]	drop pending time
y	[mol/l]	concentration of dispersed phase

REFERENCES

1. **M. Pertler, M. Haberl and W. Rommel, (1995),** *Chem. Eng. Process.,* **34(3), 269-277.**
2. **J. Temos, H.R.C. Pratt and G. W. Stevens, (1996),** *Chem. Eng. Sci,* **51 (1), 27-26.**
3. **M.J. Brodkorb, D. Bosse, C. von Reden, A. Gorak and M.J. Slater, (2002),** *Chem. Eng. Process.,* **1-16.**
4. **D. Agble, M.A. Mendes-Tatsis, (2000),** *Int. J. Heat Mass Transfer,* **43, 1025-1034.**
5. **T. Misek (ed), EPCE publication Series,** *Inst. Chem. Engrs.,* **Rugby, UK. 1978**



SPECTROSCOPIC DETECTION OF CHIRAL AGGREGATION AT LIQUID-LIQUID INTERFACES

Hitoshi Watarai, Sayaka Wada and Kazuhiko Fujiwara

Osaka University, Osaka, Japan; watarai@chem.sci.osaka-u.ac.jp

New spectroscopic methods to detect the optical activity of liquid-liquid interfaces have been develoDed: the first one is the centrifuaal liauid membrane fCLIVn method combined with a conventional CD spectropolarimetry and the second one is more interfacial specific second harmonic generation circular dichroism (SHG-CD) spectrometry. In the CLM-CD method, a cylindrical glass cell containing small amounts of organic and aqueous phases was rotated at about 7000 rpm in a sample chamber of a CD spectropolarimeter to generate an interface with a high specific interfacial area between the two-phase liquid membranes. The CD spectra of the J-aggregate of protonated 5,10,15,20-tetraphenylporphyrin formed at the toluene/sulfuric acid interface have been measured. As for the SHG-CD, a circularly polarized wavelength-variable fs -laser system was constructed to measure the interfacial SHG spectra of a flat liquid-liquid interface. The ion-associated aggregation of a water-soluble anionic porphyrin promoted with a cationic amphiphile at the heptane/water interface was observed by this technique and the observed SHG-CD spectra proved the generation of a characteristic optical activity accompanied by the formation of the interfacial aggregate of inherently achiral porphyrin molecules. These methods will pioneer a new field of interfacial chiral chemistry in the studies of solvent extraction mechanisms.

INTRODUCTION

Optical activity is a fundamental property, which provides valuable information on the structure of molecules and the conformation of their assemblies. Therefore, it is widely used in many fields including organic chemistry, coordination chemistry and biochemistry. However, it has been rarely applied in the field of surface and interfacial chemistry, in spite of great requirement of chiral measurement of such systems. The main problem might be in a very low amount of the interfacial compound and also in a difficulty to match such interfacial amount with conventional measurement methods. This situation clearly required some invention for proper combination of sample system and optical measurement system. We described here two new experimental methods to measure the optical activity of liquid-liquid interfaces, which are very useful for the studies of interfacial phenomena in solvent extraction systems.

The liquid-liquid interface is a specific reaction field, at which key reactions to determine the solvent extraction kinetics can proceed in most systems [1], Interfacial compounds behave usually with different manners from those in bulk phases. The liquid-liquid interface is also considered as a model of biomembrane. However, it is quite difficult to measure the optical activity of the interface, although the optical activity is the most important property of biomolecules and biomembranes. There have been no previous reports about the measurement of optical activity of the liquid-liquid interface.

In the present study, we propose a conventional and reliable method to measure the CD

spectra at liquid-liquid interface and further a more interfacial specific laser spectroscopic method of SHG-CD, which is the first application on the liquid-liquid interface.

The centrifugal liquid membrane (CLM) method, which provides the thin two-phase liquid membrane system in a rotating cell, has been used to measure *in situ* interfacial spectra such as UV/Vis [2], fluorescence [3] and Raman spectra [4], In the present study, we have applied the CLM method to measure the circular dichroism spectra at the liquid-liquid interface in combination with a conventional circular dichroism spectropolarimetry.
Another promising technique to measure the chirality at the interface will be the second harmonic generation-circular dichroism (SHG-CD) spectroscopy, as demonstrated by Hicks and co-workers [5,6], SHG is advantageous to other spectroscopic techniques in its inherent high interfacial selectivity due to the second order non-linear susceptibility and in its high sensitivity afforded by the resonance effect in an adsorbed dye molecule. Therefore, SHG spectroscopy can provide specific information on the electronic state and orientation of dye molecules, which is exhibited only at the interface.
SHG spectroscopy has been utilized to study solvation and aggregation of dye molecules at the electrochemical liquid-liquid interfaces. Recently, the non-linear optical activity of originally chiral molecules adsorbed at various interfaces has been observed by means of SHG-CD [7,8], However, the non-linear optical activity of the liquid-liquid interface adsorbed by an aggregate of achiral molecules has never been reported. The present study reports the non-linear chirality of J-aggregate formed from the achiral tetrakis(4-sulfonatephenyl)porphyrin diacid (H_4TPPS^{2-}) and cetyltrimethylammonium (CTA^+) surfactant at the heptane/water interface by the SHG-CD spectroscopy.

Porphyrin has been investigated extensively, because of its spectroscopically unique properties including a large molar absorptivity and biological activity. Optical activity of porphyrin derivatives has also been studied [9], Ohno et al. reported that a water-soluble achiral porphyrin, tetrakis(4-sulfonatophenyl)porphyrin (H_2TPPS^{4-}), showed optical activity, once it formed J-aggregate in an acidic aqueous solution or in a high ionic-strength solution, suggesting an exciton coupling of the extend dipoles in the porphyrin aggregate [10], Porphyrin aggregates in bulk solutions have been characterized by various spectroscopic techniques. However, no report has been known on the chirality of porphyrin aggregate at the liquid-liquid interface. In the present study, we used H_2TPP as a hydrophobic porphyrin and H_2TPPS^{4-} as a water-soluble porphyrin, both of which were expected to form J-aggregate at the interface in proper solution conditions.

CENTRIFUGAL LIQUID MEMBRANE/CIRCULAR DICHROISM SPECTROMETRY

Material

5,10,15,20-Tetraphenylporphyrin (Aldrich, H_2TPP) was dissolved in toluene at the concentration of 4.0×10^{-5} M and it was diluted to 1.0×10^{-5} M in the CLM experiment. Toluene (nakarai tesque, G.R.) was purified by distillation after the treatment with a mixture of fuming sulfuric acid and sulfuric acid. Sulfuric acid (nakarai tesque, G.R.) for the CD experiments was diluted to the concentration of 4 M. The aqueous solutions were prepared with water distilled and deionized through a Milli-Q system (Millipore, Milli-Q SP.TOC.).

CLM/CD measurement

CD spectra were measured by a CLM cell installed in a circular dichroism spectropolarimeter (JASCO, J-820) in the configuration shown in Figure 1. CLM cell, which has 3.3 cm height and 2.1 cm outer diameter with a sample inlet hole of 2 mm in diameter at the bottom was fixed horizontally in the sample chamber of the CD spectropolarimeter. A portion of 0.500 cm^3 of 4 M H_2S0_4 and 0.300 cm^3 toluene were put into the cylindrical cell thorough the sample inlet hole. Then, the cylindrical cell was rotated at about 7000 rpm by the high-speed motor (Nakanishi Inc., NK-260) fixed on XZ-stage, connected to a speed controller

(Nakanishi Inc., NE-22E). The toluene phase was spread as an inner liquid membrane and the aqueous phase as an outer liquid membrane by a centrifugal force. The shape and size of the cross section of the light beam of the spectropolarimeter was controlled by a round hole slit with the diameter of 9 mm, to adjust the light beam center to the center of the liquid membranes cell.

The sum of the CD spectra of the interface, the bulk organic phase and the bulk aqueous phase can be measured by this method. After the blank was measured, H_2TPP toluene solution (0.100 cm^3) was injected rapidly by a micro-syringe from the sample inlet hole to initiate the protonation of H_2TPP and the aggregation of H_4TPP^{2+}. Normal absorption spectra of the interface were also measured by the CLM cell with a photodiode array spectrophotometer (Agilent Technologies, Agilent 8453), by the same manner with the previous studies [11], All measurements were carried out at 298 ± 2 K.

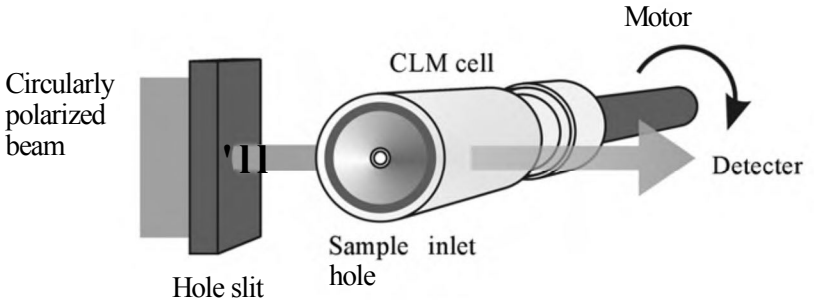


Figure 1. Centrifugal liquid membrane cell

CD spectra of interface

UV-vis absorption spectra of the J-aggregate of H_4TPP^{2+} adsorbed at the toluene/4 M H_2S0_4 interface and H_2TPP monomer in the bulk toluene solution are shown in Figure 2. H_2TPP monomer in toluene has the Soret band at 419 nm and Q band around 515 nm. Two red shifted bands of 473 nm and 720 nm in Fig. 2(a) were assigned to the J-aggregate of H_4TPP^{2+} formed at the interface. It took about 5 min for the completion of the formation of the J-aggregate after the addition of H_2TPP toluene solution. The interfacial adsorption equilibrium in the toluene-4 M H_2S0_4 system can be represented by,

$$H_2TPP_0 + 2H^{+}\text{^} H_4TPP^{2+}i \quad (1)$$

$$nH_4TPP^{2+}i \text{—>} (H_4TPP^{2+})_n, \quad (2)$$

where the subscript i shows the species adsorbed at the interface. The monomer of the protonated H_2TPP (H_4TPP^{2+}), whose absorption maximum is at 438.0 nm, was not clearly noted in Fig. 2(a), because most of it formed the aggregate by the reaction (2) under the present H_2TPP concentration.

In the case of H_4TPPS^{2-}, the exciton-coupled circular dichroism of the J-aggregate has been assigned to the helical alignment of the porphyrin in J-aggregate [10]. It can be thought that the CD spectrum of the J-aggregate of H_4TPP^{2+} observed in the present study has a similar helical alignment. Ohno et al. assigned the CD dispersions at 491 nm and 420 nm of the J-aggregate of H_4TPPS^{2-} to the transition dipoles of long axis of rod-shaped J-aggregate of H_4TPPS^{2-} and to the short axis perpendicularly to the long axis, respectively [10], Therefore, the CD band of H_4TPP^{2+} aggregate centered at 473 nm may be assigned to the linear oscillator transitions polarized in the long axis of the J-aggregate. The CD band centered at 412.5 nm shown in Fig. 2(a) may correspond to the electric transition of short axis of H_4TPP^{2+} in the J-aggregate. The CD signal at 412.5 nm of the H_4TPP^{2+} aggregate showed only positive one. Optically inactive H_2TPP monomer in toluene, having the Soret band at 419 nm, gives neither CD signals in the measurements using an ordinary quartz cell, nor CLM cell. Hence, it was confirmed that the free H_2TPP monomer in toluene had no CD band at 412.5 nm. We also observed the CD signal of the J-aggregate in the Q band region. In the wavelength region, the CD signal was broader and weaker than that for the Soret band.

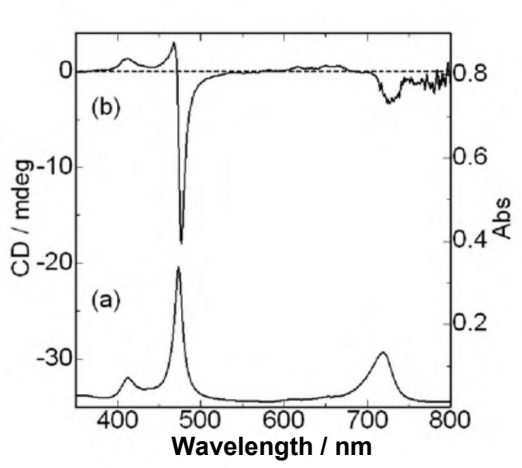


Figure 2. (a) Absorption spectrum and (b) CD spectrum of the J-aggregate of H4TPP²′ in the toluene/4 M sulfuric acid system measured by the CLM method. Initial H_2TPP concentration in toluene **was** *1.0 x 10⁵ M.*

Figure 2(b) shows the CD spectrum of the interfacial aggregate of H₄TPP². \J\le* **could observe the circular dichroism band similar to positive and negative Cotton effect centered at 473 nm, which corresponds to the absorption maximum wavelength of the J-aggregate. The CD signal in the J-band increased with time and reached its maximum value after about 5 minutes. The absorbance at 473 nm also showed a similar increase. These results indicated that the observed optical activity was assigned to the J-aggregate formed at the interface. The CD measurement has been made also for the non-aggregated system of 1.0 x 10'⁵ M H_2TPP toluene/water. As expected, it didn't show any signal in CD spectrum. Therefore, it was confirmed that the bulk H_2TPP monomer in toluene had no optical activity and only the optical activity of the interfacial J-aggregate was measured in the present study.**

SECOND HARMONIC GENERATION - CIRCULAR DICHROISM SPECTROMETRY

SHG experiments

The apparatus of SHG measurements included a Ti:sapphire laser (Spectra-physics Maitai; 80MHz, lOOfs, tuning range of 780-920nm) and a photon counter (Stanford research systems, SR400) . An angle of the linearly polarized fundamental beam was adjusted by an achromatic half waveplate and a circularly polarized fundamental beam was generated using an achromatic quarter waveplate (Newport, 10RP44-3). All SHG spectra were acquired in total internal reflection condition with the incident angle of 74.1°, and the beam spot of the fundamental beam at the interface was about 2.0 mm. For the SHG measurements, the heptane/water interface was formed in a rectangular optical quartz cell with a flat interfacial area of 2.0 x 1.0 cm², which was thermostated at 300 ± 0.5 K. UV/vis and ordinary CD spectra of bulk solutions were measured by jasco V-550 spectrophotometer and jasco J-710 circular dichroism spectropolarimeters, respectively.

Interfacial aggregation of TPPS

The aqueous phase contained initially 5.35 x 10'⁷ M TPPS and 3.36 x 10'⁶ M cetyltrimethylammonium bromide (CTAB) at pH 3.0 controlled by 10³ M hydrochloric acid. An interfacial SHG spectrum measured by an irradiation of p-polarized fundamental beam showed a maximum at 420 nm. UV/vis spectra of the aqueous solution including TPPS and CTAB gave an absorption maximum at 434 nm, assigned to H_4TPPS^2monomer, which was blue-shifted to 420nm as the CTAB concentration was increased. The absorption maximum

of 420 nm was assigned to the J-aggregate of $H_4TPPS_2^-$. Thus, the formation of J-aggregate of $H_4TPPS_2^-$ at the heptane/water interface was confirmed. Furthermore, it was concluded that the J-aggregation of H_4TPPS^{2-} was promoted preferentially at the interface by the ion-association adsorption with CTA^+ molecules.

SHG-CD of interfacial TPPS aggregate

We studied the SHG-CD of the interfacial aggregate by using a circularly polarized fundamental beam. s-Polarization detected SH spectra of the interface were measured, irradiated by left and right circularly polarized incident beams. The left circularly polarized SH intensity was larger than the right circularly polarized one around the resonant SH response maximum at 420nm. The difference between left- and right-circularly polarized SH spectra is represented as SHG-CD spectrum defined by,

$$I_{SHG\text{-}CD} = \frac{4[(I_m \chi_{[m]})\,\mathrm{Re}(\chi_{Re}\chi_{Re})\,\mathrm{Im}]}{|f|^2 + |g|^2 + |h|^2 - 2(f_{Re}g_{Re} + f_{Im}g_{Im})} \quad (3)$$

where subscripts lcp and rep are the left-circularly polarized and right-circularly polarized fundamental beams, respectively. The coefficients f, *g* and *h* are linear combinations of various electric-dipole and magnetic-dipole susceptibility components and the relative weights of these components depends on s- and p-polarized components of the second harmonic field [12,13], Subscripts Re and Im represent real and imaginary parts of each coefficient. Figure 3 shows the SHG-CD spectrum of the aggregate of H_4TPPS^{2-}observed by a circularly polarized fundamental beam, in which the intensity was zero at the absorption maximum of the monomer, 430 nm, and positive and negative peaks were observed at 420 nm and 438nm, respectively.

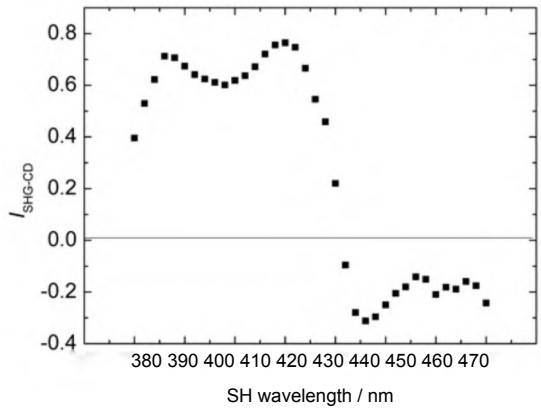


Figure 3. SHG-CD spectrum of adsorbed TPPS aggregate at the heptane/water interface. Aqueous phase ; 5.1 x 10^{-7} M TPPS, 1.15 x 10^{-6} M CTAB, 0.01 M HCl (pH 2.0)

There observed no CD spectrum by an ordinary CD spectrometer for the same aqueous solution used in SHG experiments. Although a SHG-CD spectrum is not directly comparable to an ordinary CD spectrum, it is found that the SHG-CD spectrum of the interfacial J-aggregate indicates two components with opposite signs, similar to the exciton-coupled circular dichroism of ordinary linear CD spectrum of J-aggregate in bulk solution.

When the SHG-CD measurements were repeated in the same conditions, we obtained the same spectra with that of Fig. 3 and the completely opposite signed SHG-CD spectra to that of Fig. 3 with even probability, having negative and positive peaks at 420 nm and 438 nm, respectively. This means that the liquid-liquid interface itself has no chiral selectivity in the

ion-associated aggregation of TPPS diacid with CTA cation.
The measurements of SHG-CD spectra were also carried out in the absence of CTAB in the acidic aqueous phase (pH 3.0) and in the presence of CTAB in the neutral condition (pH 8.0). Under neither condition, however, there observed significant SHG-CD signals.

CONCLUSIONS

It was demonstrated that the CD spectra of the interfacially adsorbed species were successfully measured by the use of CLM method with a conventional CD spectropolarimeter. The circular dichroism of the J-aggregate of H_4TPP^{2+} formed at the toluene/sulfuric acid could be observed directly. Its CD spectrum suggested a rod-like shape of H_4TPP^{2+} J-aggregate twisted to one direction. This method can be applied to any optical active species adsorbed at liquid/liquid interfaces, provided that it has a large molar absorptivity. Especially, it will become a promising tool for the study of biological processes including enzymatic reaction of protein at the liquid/liquid interface.

The SHG-CD spectrometry was demonstrated to be a more interfacial specific and more sensitive method to observe the optical activity of the liquid-liquid interface. The SHG-CD method found out the chirality of the ion-associated aggregate of TPPS diacid with CTA cation at the heptane/water interface. The analysis of SHG polarization spectra revealed the contribution of a magnetic dipole effect to the spectra, which could be assigned to the helical structure of the aggregate.

It is believed that CLM/CD and SHG-CD methods developed by our studies will become powerful techniques to explore the optical activity of interfacial species including self-assembled compounds, amino-acid, proteins and DNA adsorbed at the liquid-liquid interfaces of solvent extraction processes.

ACKNOWLEDGEMENTS

This work was supported by the Grant-in-Aid for Scientific Research (No. 16105002) from the Ministry of Education, Science, Sports and Culture, Japan.

REFERENCES

1. **H. Watarai, S. Tsukahara, H. Nagatani, A. Ohashi (2003),** *Bull. Chem. Soc. Jpn.,* **76, 1471.**
2. **H. Nagatani and H. Watarai (1998),** *Anal. Chem.,* **70, 2860.**
3. **H. Nagatani and H. Watarai (1999),** *Chem. Lett.,* **701.**
4. **A. Ohashi and H. Watarai (2002),** *Langmuir,* **18, 10292.**
5. **T. Petralli-Mallow, T. Wong, M.; J. D. Byers, H. I. Yee, J. M. Hicks (1993),** *J. Phys. Chem.* **97, 1383.**
6. **J. M. Hicks, T. Petralli-Mallow, J. D. Byers (1994),** *Faraday. Discuss.* **99, 341.**
7. **T. Verbiest, M.Kauranen, A. Persoons (1999),** *J. Mater. Chem.* **9, 2005.**
8. **M. J. Crawford, S. Haslam,; J. M. Probert, Y. A. Gruzdkov, J. G. Frey (1994),** *Chem. Phys. Lett.* **229, 260.**
9. **X. Huang, K. Nakanishi and N. Berova (2000),** *Chirality,* **12, 237.**
10. **O. Ohno, Y. Kaizu, and H. Kobayashi (1993),** *J. Chem. Phys.,* **99, 4128.**
11. **Y. Yulizarand H. Watarai (2003),** *Bull. Chem. Soc. Jpn.,* **76, 1379.**
12. **J. J. Maki, T, Verbiest, M. Kauranen, S. V.Elshocht, A. Persoons (1996),** *J. Chem. Phys.* **105, 767.**
13. **M. C. Schianne-Klein, F. Hache, A. Roy, C. Flyzanis, C. Payrastre (1998),** *J. Chem. Phys.* **108, 9436.**

LIQUID-LIQUID EXTRACTION OF COPPER IN A PULSED SIEVE PLATE COLUMN

Paulo F.M.M. Correia and Jorge M.R. de Carvalho*

Instituto Superior Técnico
CPQ - Chemical Processes Centre
Av. Rovisco Pais, 1049-001 Lisboa
PORTUGAL

This paper deals with drop size analysis under extraction and stripping conditions in a pulsed sieve-plate column under extraction and stripping conditions for Copper extraction by using purified Acorga M-5640 (5-t-nonylsalicylaldoxime) for Copper extraction. It was found that drop size depends much more on the direction of mass transfer than on the absolute values of the static interfacial tension. Under stripping conditions, the drop size was smaller than under extraction conditions for the same level of agitation.
To interpret our experimental results, dynamic interfacial tension studies were carried out. Under stripping conditions, it was found that fine droplets never coalesce with each other and the final drop size must be mainly determined by a break-up mechanism. Under extraction conditions it was found that drops with ages lower than 1 minute can easily coalesce during mass transfer. However, drops with ages higher than 1 minute hardly can coalesce.
All these phenomena were explained through dynamic interfacial studies.

INTRODUCTION

Solvent extraction of copper has become an important process and is used in several hydrometallurgical plants to recover copper from oxide ores and post-flotation tailings producing the least expensive copper in the world. Hydroxyoximes are well-established extractants for copper extraction, and they are used in several industrial installations [1-6], If an extractant can exhibit fast kinetics for copper extraction, column contactors can be used with economic advantages instead of mixer-settlers, due to solvent inventory, control systems, occupied space, etc. The presence of Marangoni effect can be very relevant to increase kinetics.

The interfacial tension exhibited between immiscible solvents and aqueous solutions plays an important part in determining the performance of liquid-liquid extraction equipment. The size of drops of one phase dispersed in the other is determined in part by the static and dynamic interfacial tension and direction of mass transfer; the interfacial area available for mass transfer is a function of drop size.

In some systems it has been observed that drops change in size on passage through contacting equipment because of the changes in solute concentration in the two phases. In

* **To whom correspondence should be addressed (Tel: +351-21-8417311; Fax: +351-21-8499242; E-mail address: jcarv@ist.utl.pt)**

extreme cases severe reductions in drop size will impose a low limit on allowable throughputs.

EXPERIMENTAL

Reagents: The commercial reagents Escaid 100 (ExxonMobil) was studied as delivered. The extractant used contains 93.5 wt. % of 5-t-nonylsalicylaldoxime after purification of Acorga M-5640. Copper sulphate used in the aqueous phase was reagent grade.

Apparatus: The equipment used was a pulsed sieve plate column of one inch diameter glass tubing (QVF in 1 ft sections). The plates were stainless steel, with 18 x 3mm diameter holes, giving 23 % free area. Plates were two inches apart. The total height of plates was 14 ft (4.27 m). The column volume in the section with plates was 2.17 l and the total column volume with sections was about 5 l. A schematic diagram is shown elsewhere [7],

DCL metering pumps were used with rotameters as checks on flow rates. Piping was stainless steel for organic and PVC in part initially for aqueous flows. Glass, steel and polypropylene storage vessels were used.

The organic inlet tube has a one-way valve was fitted to the end of the inlet pipe followed by a PTFE cap with two 5 mm holes. Very large drops were then always formed (5-10 mm) and flooding was avoided.

A single mixer-settler was used for continuous stripping of the loaded organic after collection from the column in a 20 l vessel.

A modified drop weight method [7-9] was used for all measurements of static and dynamic interfacial tension using an Agla micrometer syringe with an assembly to form the organic drops. The assembly consisted of a PTFE jet (wetted only by solvent) was surrounded by a glass sleeve (a piece of capillary tube) as shown in Fig. 1.

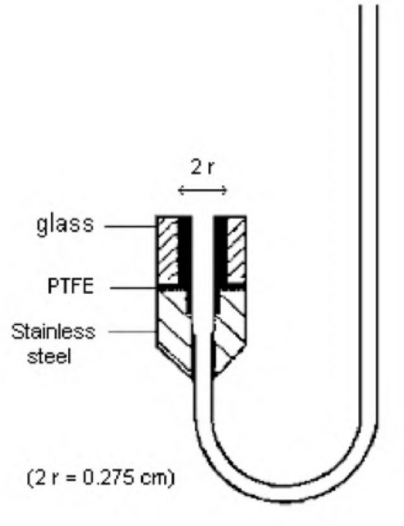


Fig. 1 - Sketch of modified syringe tip.

Araldite was used to glue the PTFE to the glass giving a precision circle at which drops form. The top surface of the capillary tube was well polished and made flat to guarantee that it was wetted easily by aqueous phase. The hole through the assembly was about 2mm diameter. It was important to have a very good seal between the stainless part and the bottom of the PTFE. This was achieved bv usina PTFE taoe between the parts. For the determination of interfacial tension it is necessary to know the outside diameter of the PTFE section. This diameter was determined by a travelling microscope in several directions and a mean value was used. Two assemblies were built with diameters of 0.316 and 0.044 cm, respectively.

A photographic technique for recording the dispersions inside the column was used. A Nikon F90X camera connected to a Nikon PB-6 bellows, to a 60 mm f/2.8D Micro Nikkor objective was used and to a Nikon Speedlight SB-26 flash connected to the camera through a Nikon SC-17 TTL cable was used to record the drop size distribution, at about 1 cm away from the

column wall in the several boxes, on Ilford FP4 film. The negatives were scanned through an Epson FilmScan 200 negative scanner. The digitised negatives were analysed by using KS-100 image analysis software (Kontron Elektronic GmbH).
Techniques: 5-t-nonylsalicylaldoxime was isolated from the Acorga M-5640 extractant from Cytec Industries. The purification of 5-t-nonylsalicylaldoxime was done in two stages following a procedure slightly adapted from the one developed by Preston and Whewell [10] until a purity of 93,5 wt. % of oxime was achieved.

The experimental program involved the measurement, at several heights along the column, of the drop size distribution and local hold-up for several flow rates and pulsing intensity. In this investigation only the organic phase was dispersed as droplets in the column. The column described above was used and it was assumed that the pulse unit produced a pulse waveform that is an approximate sine curve. Temperature, while not controlled, was nearly constant. All experiments were carried out at about 20°C.

It was decided to clean the column with a 2 % "Decon 90" solution and to rinse with distilled water. A solvent solution (214 g/l of 5-t-nonylsalicylaldoxime in Escaid 100) was loaded with several levels of copper. Acid strength was adjusted to give solvent product carrying about 14 g Cu/l. The interface was lowered into the column section and the amplitude was measured there with a ruler. The pulse frequency and amplitude quoted were obtained when the DCL pump was switched off (some interference was found with the pump operating). To interpret the behaviour of the solvent in the column it was decided to analyse interfacial tensions of the solvent used in the column with different levels of copper in both phases. The interfacial tension of the two batches of solvent against copper aqueous feed was measured for different levels of copper in both phases.

The dynamic and static interfacial tension were analysed with the method and apparatus referred, which consists in forming organic phase drops of several volumes, corresponding to different $_{y}$ values, having the same formation time (8 s) and wait for their release to record the time in order to plot a curve of the interfacial tension versus time. To calculate interfacial tensions an average volume of not less than 4 drops was used in conjunction with the correction of Harkins and Brown. The accuracy was better than 3.0 %. For all the measurements of interfacial tension made in this work the two phases were mutually equilibrated by shaking for 24 hours and left one day for complete phase separation.

For drop size measurements, the quality of the negatives obtained by the procedure above was good, except when large hold-ups and very loaded solvents occurred. For each distribution measurement at least 500 droplets were counted, obtained from three or more separate photographs for each box, giving a statistical accuracy better than 2%.

Analysis: Samples were analysed for Cu by atomic absorption spectrophotometry.

RESULTS AND DISCUSSION

Some interfacial tension studies were carried out between Acorga M-5640 as supplied in n-heptane with 15 vol. % and 40 vol. % and an aqueous feed containing 16 g/L Cu and 10 g/L H2S04. Batch experiments using a 5:1 (A:0) ratio were undergone and after equilibration of the system, interfacial tension was measured and data is presented in Figs. 2.a and 2.b.

The results obtained show that the value of the interfacial tension difference $_{(yo-yr)}$ **is 2.9 mN/m and 3.5 mN/m despite of in both cases the solvent is nearly fully loaded.**

These results according to [7,8] illustrate that the extractant Acorga M-5640 must be

contaminated with several hydrophilic species.

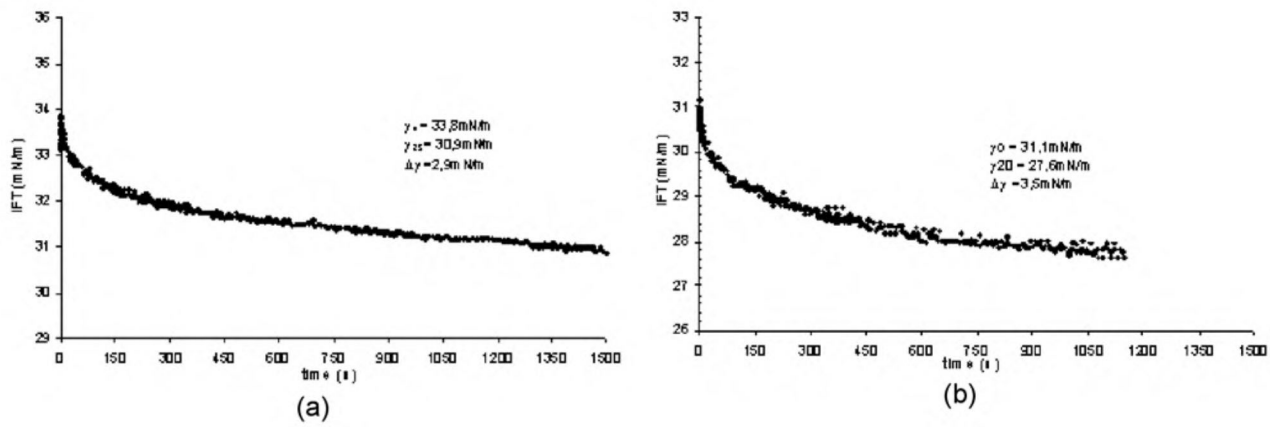


Fig. 2 - Interfacial tension curve determined for a drop of organic inside an aqueous phase resulting from an extraction 5:1 A:0 (v/v) between a copper solution ([Cu]=16g/l, [H2SO4]=10g/l, pH=1) and a solvent with: a) 15% (v/v) of Acorga M-5640 in n-heptane (0.27M); b) 40% (v/v) of Acorga M-5640 in n-heptane (0.71 M).

In these circumstances, the extractant was purified according to the method described in [10] and 3 systems under extraction conditions and 3 systems under stripping conditions were experimented covering a copper concentration range up to saturation. Dynamic interfacial tension for the systems described above when both phases are saturated and in equilibrium. Data is presented in Figs. 3 and 4.

It was decided to use the purified 5-t-nonylsalicylaldoxime in some column experiments. The data for mass transfer experiments are summarized in Table 1. The drop size is much more dependent on the direction of mass transfer than on the absolute values of the static interfacial tension. It was found that under stripping conditions the drop size was smaller than under extraction conditions for the same level of agitation, despite the density difference is of 0.280 comparing with an average value of 0.140 under extraction conditions.

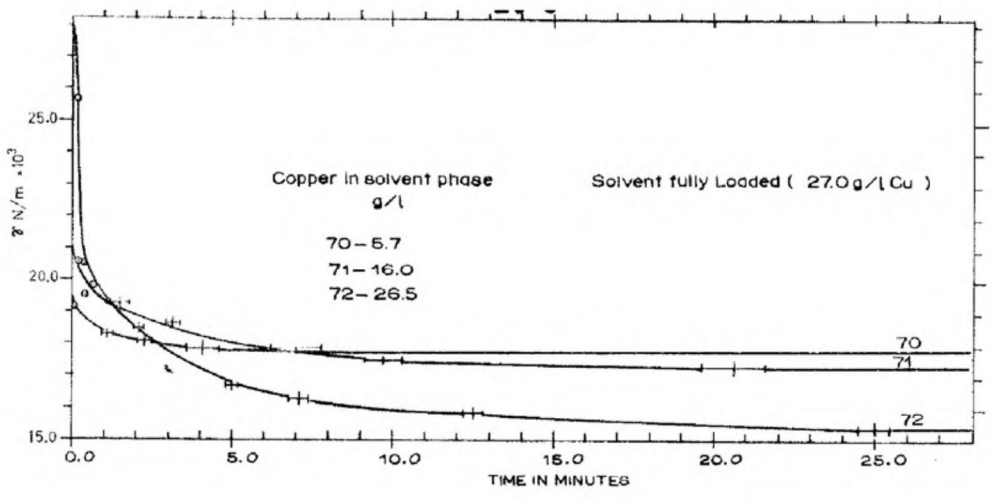


Fig. 3 - Behaviour of a solvent (214 g/l 5-t-nonylsalicylaldoxime in Escaid 100) under extraction conditions (Equilibrium conditions; Temperature 20 °C).

To interpret the results, we consider Fig. 4, where the dynamic interfacial tension for a solvent with three levels of copper under stripping conditions is presented. For drops with

ages less than 2 minutes, the interfacial tension of the system increases with the amount of copper in the solvent.

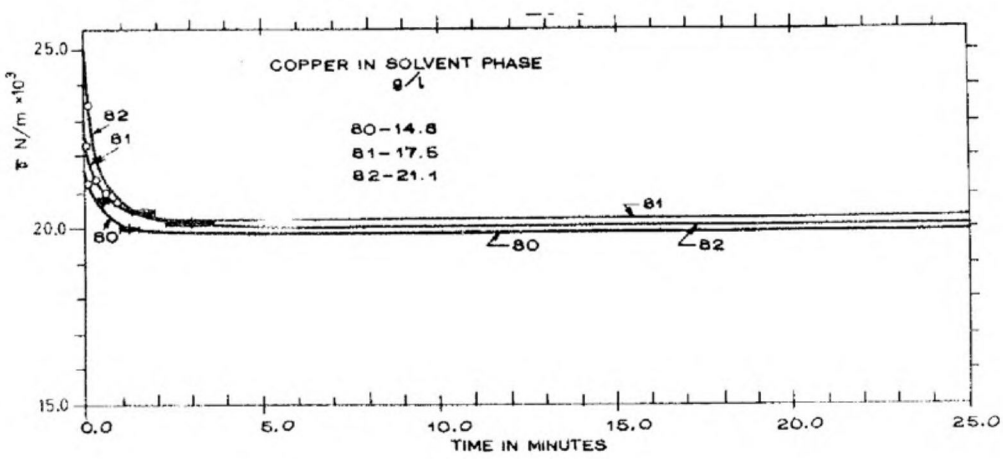


Fig. 4 - Behaviour of a solvent (214 g/i 5-t-nonylsalicylaldoxime in Escaid 100) under stripping conditions (Equilibrium conditions; Temperature 20 °C).

Table 1 - Operating Conditions and Experimental Data for Mass Transfer Experiments.

Exp. N°.	Flow rates		Agita-tion	Drop Size Data (distance from bottom section, cm)				Average Hold-up	Average Drop Size	External Concentrations			
	Aqueous F_c	Solvent F_d	AT	30.0	124	348	408	$\bar{h}$ (Range)	$\bar{dvs}$	Solv In	Solv Out	AQ. In	AQ. Out
	ml/min		cm/min	Sauter Mean Diameter, $d_{,,}$ mm				%	mm	CJ/I (Cu)			
Extraction Conditions. No axial mixing data													
53	81.7	82.1	124.2	3.85	3.40	-	2.4	7.6 (6.2-8.4)	3.10	3.5	12.6	17.3	8.0
63	74.5	132.6	243.9	1.39	1.67	-	1.42	16.0 (14.4-17.1)	1.50	3.2	12.1	16.3	0.6
69	81.0	82.0	124.2	3.42	-	-	3.80	7.6 (73-8.2)	3.52	13.4	18.4	17.2	12.0
70	81.0	82.0	216.0	1.47	1.37	1.65	-	12.0 (11.2-13.1)	1.60	12.2	22.0	17.3	7.2
66	202.5	88.9	216.0	1.70	1.43	1.57	1.29	13.0 (10.7-14.9)	1.64	3.6	20.0	17.0	9.9
57	84.0	84.6	216.0	1.80	1.76	1.34	1.78	11.8 (8.3-13.1)	1.53	2.4	16.5	17.5	3.4
105	79.5	83.5	134.8	2.07	1.71	1.35	1.75	10.0 (9.5-10.2)	1.60	12.1	18.5	16.6	9.7
90	81.9	83.6	216.8	-	1.57	1.14	1.21	12.2 (10.8-12.7)	1.40	12.5	21.5	17.3	8.1
106	83.6	84.3	135.0	1.69	2.03	2.08	1.89	8.5 (8.1-8.6)	1.92	3.3	13.8	16.8	6.1
107	208.0	85.5	135.0	1.68	2.32	1.78	2.22	9.2 (8.3-95)	2.10	2.3	15.2	16.9	11.4
108	80.0	126.0	135.0	3.39	2.62	2.62	1.91	11.0 (10.5-11.2)	2.70	11.8	17.0	17.0	9.0
Stri aping Conditions. No axial mixing data.													
81	82.2	83.9	189.0	1.31	1.40	1.20	1.15	12.4 (10.4-15.1)	1.20	20.7	16.0	20.9	25.6
91	80.3	85.0	119.2	2.53	2.29	2.10	2.80	7.0 (68-7.3)	2.40	23.8	20.8	20.7	23.9
100	202.6	89.0	133.5	0.87	1.16	0.87	1.10	13.5 (11.4-15.3)	1.05	24.0	17.3	19.4	22.5
101	78.6	124.8	135.0	3.99	1.93	1.69	1.81	17.8 (13.8-20.1)	2.40	24.1	18.6	19.5	28.0
102	81.0	82.0	133.5	1.46	1.31	0.97	0.91	12.1 (10.2-13.1)	1.10	24.4	18.5	20.2	26.4
103	79.2	86.0	96.1	1.83	1.77	1.67	1.66	7.8 (7.5-84)	1.70	24.6	21.6	20.0	23.3
104	80.5	82.5	136.5	1.39	1.02	1.08	**in**	12.0 (9.1-13.3)	1.10	25.0	19.0	20.1	26.2

For drops older than 2 minutes we find no variation of y with the copper level. Mass transfer out of the solvent drops produces between drops a zone of higher concentration and so of higher interfacial tension, which hinders coalescence between drops. It is difficult for the fines to coalesce and the final drop size must be mainly determined by a break-up mechanism. This explains why the largest drop size is not necessarily found in the experiments with the lowest hold-up values. In these circumstances the smallest drops have a strong contribution for the hold-up value and a very small one for the Sauter mean diameter.

To analyse the drop size behaviour under extraction conditions we consider in Fig. 3 three curves of dynamic interfacial tension for three different levels of copper in the solvent at equilibrium conditions. For drops with ages less than 1 minute, the interfacial tension increases with the level of copper in the solvent. In these circumstances, coalescence between solvent drops is improved. If drops coalesce in less than 1 minute, we may expect large drops and small hold-up during mass transfer.

For drops older than 1 minute, the interfacial tension decreases with increasing copper level in the solvent (as seen in Fig. 3). In these circumstances it is very hard for the drops to coalesce. This explains why drop size under extraction conditions is larger than under stripping conditions and the hold-ups much smaller. It is difficult for small drops (fines) to coalesce because generally they are older than 1 minute. The average residence time of organic phase in the column for the studies presented in Table 1 is in the range 1.8-3 min.

CONCLUSIONS

By analysing the dynamic interfacial tension for the system studied, we can explain why the Sauter mean diameter is smaller under stripping conditions than under extraction conditions for the same level of agitation.

The studies presented illustrate that the direction of mass transfer and the variation of interfacial tension with copper content are the relevant factors for the size of the drops.

Dynamic interfacial tension studies are important information for predicting the behaviour of a liquid-liquid extraction system.

AKNOWLEDGEMENTS

The authors would like to thank to Diogo Santos for his help in part of the experimental work. The financial support of FCT (Portuguese Funding Agency) is also acknowledged.

REFERENCES

1. **M. Bogacki (1999),** *Ind. Eng. Chem. Res.,* **38, 1611-1617.**
2. **M. Yamada, J.M. Perera, F. Grieser and G.W. Stevens (1998),** *Anal. Sci.,* **14, 225-229.**
3. **J. Szymanowski, K. Prochaska and K. Alejski (1990),** *Hydrometall.,* **25 (3), 329-348.**
4. **J. Szymanowski (1993), Hydroxyoximes and Copper Hydrometallurgy, CRC Press, Boca Raton.**
5. **K. Staszak, K. Prochaska (2004),** *J. Coll. Interf. Sci.,* **280, 184-191.**
6. **K. Prochaska (2002),** *Adv. Coll. Interf. Sci.,* **95, 51-72.**
7. **J.M.R. Carvalho (1982), PhD Thesis, University of Bradford, UK.**
8. **J.M.R. Carvalho, M.J. Slater (1983),** *Proc. ISEC'83,* **Denver, Colorado, USA, 297-298.**
9. **J.M.R. Carvalho, M.F. Pinto (1986),** *Proc. ISEC'86,* **Munchën, Germany, V. 5, 295-300.**
10. **J. S. Preston and R. J. Whewell (1977),** *J. Inorg. Nucl. Chem.,* **39(9), 1675-1678.**

EFFECT OF DL-HOMOCYSTEIC ACID ON THE W/O MICROEMULSION OF POTASSIUM 2-ETHYLHEXYL HYDROGEN 2-ETHYLHEXYLPHOSPHONATE/ n-HEPTANE SYSTEM

Yunlan Su, Limin Yang, Weihong Li, Shifu Weng, Jinguang Wu* and Guangxian Xu

The State Key Laboratory of Rare Earth Materials Chemistry and Applications, College of Chemistry and Molecular Engineering, Peking University, Beijing, 100871, China

The effect of DL-homocysteic acid (DL-2-amino-4-sulfono-butyric acid) on W/O microemulsion of potassium 2-ethylhexyl hydrogen 2-ethylhexylphosphonate / n-heptane has been found that the interaction between the amino acid molecules and the polar head groups of the surfactant through hydrogen-bond enhances the solubilization capacity in the aqueous cores.

INTRODUCTION

Liquid-liquid extraction has been considered as a potential technique for the separation of amino acids. The formation of reversed micelles or w/o microemulsions of the extractant is so closely associated with the separation process that the technique has been represented in terms of "extraction of amino acids or proteins by reversed micelles".[111] Significant interest has been focused on the aggregation behavior of extractants. Also, some biological active materials may be preserved in the aqueous core of the w/o microemulsion droplets instead of refrigeration. The aim of this work is to understand the behavior and the interaction between the biological compound, a peculiar amino acid (DL-homocysteric acid, abbreviated by DLH), and w/o microemulsion (1 mol/l potassium 2-ethylhexyl hydrogen 2-ethylhexylphosphonate (abbreviated by PC88A-K) /n-heptane. Their structures are shown in Figure 1.

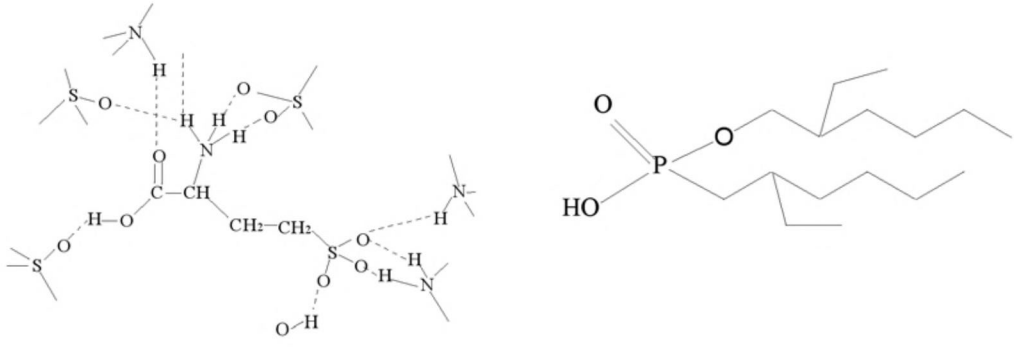


Figure 1 The structure of DLH with its H-bond network (left) and PC88A (right)

A special amino acid, DL-2-amino-4-sulfono-butyric acid (DLH) is an important free amino acid in central nervous system of human body,[2'31 with a characteristic chemical structure in its sulfonate group at the opposite end of the amino and carboxylate groups of the molecule. Contrary to the hydrophobic nature of amino acids, the DLH molecule is rather hydrophilic with high hydration affinity and solubility in water, because of the three polar groups on a tetratomic hydrocarbon chain. In its crystal lattice, one DLH molecule can form 10 H-bonds with its neighbors.[4)

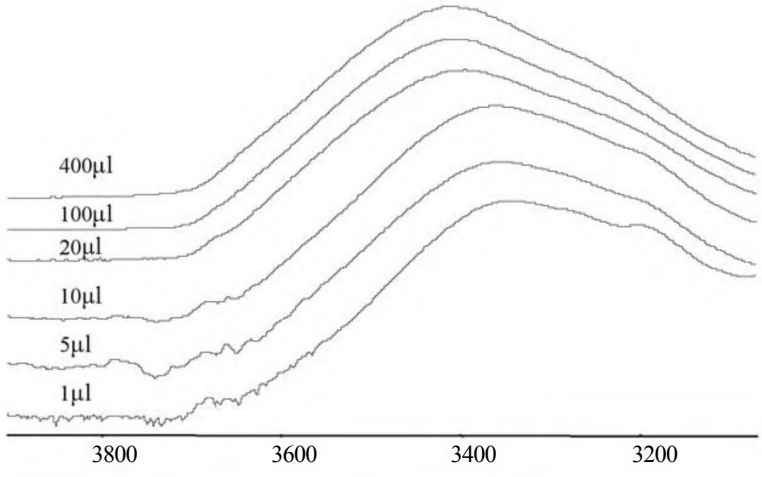
PROCESS DESCRIPTION

Various amounts of 0.1mol/l DLH aqueous solution or pure water were added to the different potassium metal saponified PC88A/n-heptane (shown in Table 1). The result indicated that the higher the saponification percentage, the dissolved amount of DLH or water increased. For example, when the saponification percentage was 88.90%, the amount of DLH per 0.5ml PC88A could reach 0.45ml (W_0=50, W_0 is the molar ratio of DLH to PC88A), while the amount of pure water is only 0.35ml (W_0=39, W_0, molar ratio of water to PC88A).

Table 1 The maximum amount of DLH solution or pure water added to the different potassium metal saponified PC88A/n-heptane

The saponification percentage of P507	The maximum amount of DLH per 0.5 ml PC88A (ml)	The maximum amount of H_20 per 0.5 ml PC88A (ml)
77%	0.15(W_0=17)	0.15(W_0=17)
80%	0.20(W_0=22)	0.20(W_0=22)
85%	0.32(W_0=36)	0.30(W_0=33)
88.9%	0.45(W_0=50)	0.35(W_0=39)

The FT-IR spectra of DLH were changed with the increase amount of DLH added to the 85% saponified PC88A-K (shown in Figure 2). The OH stretching vibration of water shifted to high wavenumber (3423 cm^{-1}) and was near to the absorption frequency of pure water (3417 cm^{1}). There was a break from 10(jl(Wo=1.1) to 20(jl(Wo=2.2): the band of vP=0 shifted from 1192 cm^{-1} ! to 1177 cm and the half band width became wider; the band of vP-O-C changed from two peaks 1061 and 1040 cm"[1] to one peak 1048 cm'[1]. In literature the P=0 stretching vibration of unhydrated sodium saponified PC88A was located at 1195 cm"[1] while vP=0 shifted to 1159 cm'[1] after the microemulsion was formed. [51The hydration of phosphate group resulted in the decrease of the intensity of P=0 bond and the shift to lower wavenumber in the FT-IR spectrum. When the amount of DLH increased to 20pl, the band of vP=0 was located at 1177 cm'[1], which indicated that the saponified PC88A-K/n-heptane solution was in the state of the reversed micelle. When the amount of DLH increased to 30pl, vP=0 shifted to 1166 cm"[1], which was in the intermediate state between the reversed micelle and the microemulsion and was near to 1159 cm'[1]. The microemulsion formed when $W_0$is over 10.



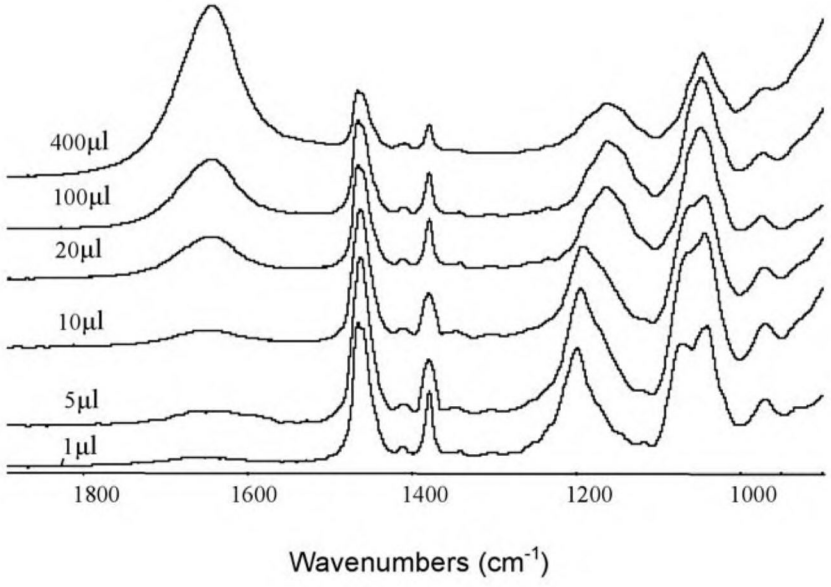


Fig. 2 The FT-IR spectra of different amount of 0.1 M DLH aqueous solution added to 0.5ml 85% saponified $PC_{88}A$-K/n-heptane solution (4000-900 cm'1) (Ipl, W_0= 0.11; 5pl, W_0=0.55; lOpl, W_0= 1.1; 20pl, W_0=2.2; lOOpl, W_0=11;400pl, W_0=44)

CONCLUSIONS

Not only the water molecule interacts with the surfactant but also DLH interacts with the surfactant in the PC88A-K/n-heptane solution. The NH_3^+group of DLH was easy to form the hydrogen bond with the P=0 group of PC88A which changed the original hydrogen bond structure to form stronger hydrogen bond and resulted in the shift of absorption band in IR spectrum. This was also the reason why the amount of DLH was higher than the amount of

water added to 85% and higher saponified PC88A solution. In summary, the result indicates that DLH exists in the water pool of microemulsion because of the interaction between DLH and PC88A-K/n-heptane/H_20 system.

ACKNOWLEDGEMENTS

This paper was supported by the State Key Project of Fundamental Research of China (G1998061311), and NSF of China (Grant No. 39730160-11 and 29671002, 50203001).

REFERENCES

1. **C. K. Wu, H. C. Kao, T. Chen, S. C. Li, T. C. King and K. H. Hsu (1980),** *International Conference Solvent Extraction,* **Liege, Belgium, Paper No. 80-23**
2. **S. Davanger, R. Torp andO. P. Ottersen,** *Neuroscience* **63 (1994) 123.**
3. **X. Zhang, Z. L.Yang, W. H. Li, H. Z. Jia and J. G. Wu,** *Spectroscopy and Spectral Analysis* **20(5) (2000) 638.**
4. **G.R. Clarke and E. G. Steward, J. Cryst.** *Mol. Struct.* **7 (1977) 41.**
5. **J. G. Wu, N. Shi, H. C. Gao, D. Chen, H. Guo, S. F. Weng and G. X. Xu (1983),** *Science in China* **(Series B), 12,1071.**
6. **Zhang X, Yang ZL, Li WH, Yang LM, Weng SF, Wu JG.** *SPECTROCHIMICA ACTA PART A-MOLECULAR AND BIOMOLECULAR SPECTROSCOPY* **60 (1-2): 235-240 JAN 2004.**

LIQUID-LIQUID EXTRACTION EQUILIBRIUM STUDIES OF PHENOLIC COMPOUNDS USING SEVERAL EXTRACTANTS

Celina M.L. Santos, Paulo F.M.M. Correia and Jorge M. R. de Carvalho

Instituto Superior Técnico
CPQ - Chemical Processes Centre
Av. Rovisco Pais, 1049-001 Lisboa, Portugal

In this work, several extractants were investigated for the removal of phenolic compounds typically present in olive mill wastewaters. Cyanex 923 and Aliquat 336 have been demonstrated to be very efficient for the liquid-liquid extraction of acidic phenolic compounds. However, while Cyanex 923 had the maximum extraction ability at acid pH values (loosing it for pH near 7), Aliquat 336 increased its extraction ability with the increase of pH and was much more effective for pH of about 7 indicating that phenolic anions were the main species extracted with this extractant. The use of 1-decanol as modifier in this system needs to be optimized since it reduces the extraction ability due to a complex formation with Aliquat 336. Aqueous alkaline and NaCl solutions proved to be useful for the Aliquat 336 stripping.

INTRODUCTION

From the processing of products of vegetable nature, large environmental impact wastewaters with phenolic compounds result. An example of this is the olive mill wastewater problem that occurs mainly in Mediterranean countries. Olives average world production is 7900 thousand ton. per year. About 90% of this production is used in olive oil production. The environmental danger of this activity is that only 20% of olives mass gives olive oil. The remaining 80% give rise to effluents either solid waste - the husks - (30%) or olive mill wastewater (50%) [1], To give an idea of this huge pollution problem, it is proved that processing 1 ton. of olives generates oxygen demand pollution equivalent to the one produced by 800 people. Several papers describe marked phytotoxic effects of these wastewaters [2-6], causing a very serious problem owing to their spreading on land suitable for agriculture. In fact, phenolic compounds are responsible for the antimicrobial and toxic effect for some species and their concentration in olive mill wastewater can be of up to 6gL^{-1} [7], Most of wastewater generated in these processes is discharged untreated into the water environment or sent to stabilization ponds where it remains for the rest of the year with subsequent bad and unpleasant odors and potential danger for the surrounding environment. Nevertheless, some phenolic compounds appear to have favorable health effects since they are valuable antioxidants and some have been shown to have a vasodilator action [8],

In this study, liquid-liquid extraction was used to recover some phenolic compounds usually present in olive mill wastewater.

The application of liquid-liquid extraction to effluents containing complex phenolic compounds has been limited. In the literature, an application from this process to the treatment of olive mill wastewaters by using conventional solvents, such as ethyl acetate, butyl acetate and diisopropyl ether is known [9], Pilot plant tests were even made and

interesting results were obtained with diisopropyl ether. However its partial miscibility in the aqueous phase was a severe limitation.

As an alternative to these conventional solvents, extractants with low solubility in the aqueous phase have been developed, such as tertiary amines, quaternary ammonium salts and trialkylphosphine oxides [11-17], The extractant reacts with simple phenols during the extraction stage, forming a complex soluble in the organic phase. Due to phenols' high boiling point (181.4°C for phenol [10]), chemical stripping by contacting the loaded organic phase with a concentrated aqueous solution of a strong base is more interesting economically than distillation.

Besides previous work of the same researchers [18-20], up to now, no work has been published considering the application of these extractants to the recovery of more complex phenols such as the ones present in olive mill wastewaters from aqueous solutions.

EXPERIMENTAL

Reagents

Phenolic compounds studied in this work (4-hydroxibenzoic acid, p-coumaric acid, caffeic acid and tyrosol) were supplied by Merck.

Organic phases were prepared by diluting the intended extractant in the isoparaffinic hydrocarbon solvent ShellSol T (paraffin content higher than 99 wt.%, Shell Chemicals Ltd.). Aromatic hydrocarbon solvent ShellSol A (aromatic fraction higher than 99.5 wt. %, Shell Chemicals Ltd.) was also tried out. The following extractants were tested in this study: Hostarex A327 (mixture of tri-n-octylamine and tri-n-decylamine, Clariant Chemical Co.), Cyanex 923 (a mixture of 4 trialkylphosphine oxides, Cytec Co.), Alamine 336 (tricaprylyl amine, Cognis Co.) and Aliquat 336 (water insoluble quaternary ammonium salt made by the methylation of mixed tri-octyl/decyl amine, Cognis Co.). 1-decanol (Riedel-de-Haën), tributylphosphate (TBP) (MERCK) were also used for preparing some organic phases. All chemicals were used as received. All organic phases were used after a preliminary washing with water.

For preparing the aqueous stripping solutions, sodium hydroxide (MERCK p.a.), HCl (MERCK p.a.) and NaCl (MERCK p.a.) were used.

Procedures

Liquid-liquid extraction equilibrium studies at several temperatures were performed by agitation of rigorous volumes of the aqueous and organic phases in an orbital agitator Aralab Agitorb 160E for at least six hours at 298 K, with temperature and agitation speed control, connected to a cooling unit Aralab Refri 320E. In the extraction step pH value was controlled by adding acid or base in the aqueous solution before extraction. After shaking, the phases were separated and samples from the aqueous phase were taken for analysis.

Analysis

Analysis of phenols in the aqueous phase samples was made ultraviolet spectrophometry in a Hitachi U2000 double beam ultraviolet/visible spectrophotometer.

pH measurement was performed by using a Metrohm 632 pH Meter with a Metrohm combined electrode.

RESULTS AND DISCUSSION

The aim of the research is to compare several extractants for the recovery of four phenolic

compounds usually present in olive mill wastewaters. The extraction ability was evaluated and compared for different extractants using the same molar concentration of the species (extractant and solute) and equal volumetric amount of aqueous and of organic phases.

Preliminary experiments showed that the aliphatic diluent ShellSol T did not solubilize Aliquat 336. This was confirmed elsewhere [21,22], Therefore, a mixture of the aliphatic diluent ShellSol T and the aromatic diluent ShellSol A was successfully tried. However, the use of an aromatic diluent has been questionable due to environmental concerns. Some authors tried to substitute the aromatic diluent by a modifier, namely an ester, a ketone or an alcohol [21], In this study, the 1-decanol was selected. However, as is shown in Fig. 1 for studies with 4-hydroxybenzoic acid, the presence of 1-decanol in Aliquat 336 organic phase hinders the extraction of 4-hydroxybenzoic acid. In Fig. 1, D_0 is the distribution coefficient for the extraction of 4-hydroxybenzoic acid with Aliquat 336 diluted in a mixture of ShellSol T and ShellSol A, *i.e.,* the organic phase without 1-decanol.

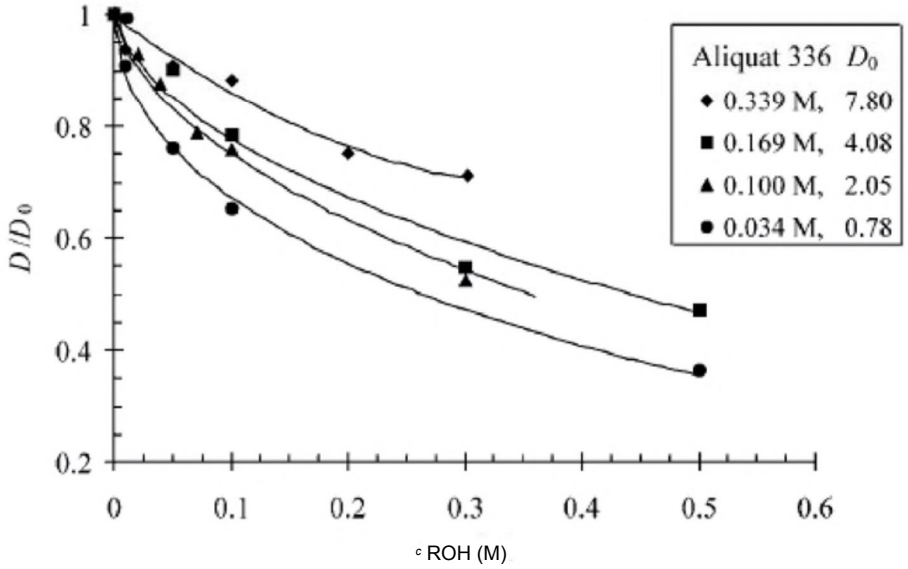


Figure 1. The influence of 1-decanol on the extraction of 4-hydroxybenzoic acid with Aliquat 336 (Initial aqueous phase: pH **= 7,** *2x1 O⁻³ M 4-hydroxybenzoic acid, 0.3 M KCI. Organic phase: Aliquat 336 diluted in 66.7 vol. % ShellSol T and 33.3 vol. % ShellSol A).*

The reduction of D/D_0 with the increase in the 1-decanol (ROH) concentration can be explained by the reduction of the concentration of free Aliquat 336 due to an interaction between Aliquat 336 and 1-decanol. The species QCI:ROH is supposed to be formed. Therefore the following equilibrium and equilibrium relationship can be written:

$$Q_{org} + ROH_0 \rightleftharpoons QCl{:}ROH_{org} \quad (1)$$

$$K_{QR} = \frac{C_{QCl:ROH}}{C_{QCl} \cdot C_{ROH}} \quad (2)$$

Assuming that QCI:ROH and ROH do not extract 4-hydroxybenzoic acid and after establishing the mass balances of Aliquat 336 and 1-decanol , the optimal K_{QR} was achieved by the least-squares method and was found to be (3.3±0.3)/M [18],

This deleterious effect of 1-decanol in the distribution coefficient was also noticed with the other extractants presented in this work, as shown in Table 1 for the case of Cyanex 923 as an example.

Table 1- Effect of 1-decanol addition in the distribution coefficients for phenolic compounds using Cyanex 923 (C_{in}niai = 0.036M) diluted in SST (Volumetric ratio $V_{aq}/V_{or}g$ = 1; T=298 K).

	4-Hidroxybenzoic acid (Cjnitiai = 3.2 mM)		p-Coumaric acid (Cjnitiāi — 3.1 mM)		Caffeic acid ($C_{in}jt_{ia}$ = 3.2 mM)		Tyrosol (Cjnitiāi - 3.3 mM)	
	pH	D	pH	*D*	pH	*D*	pH	D
Cyanex 923 in ShellSol T	4.65	14.6	4.22	27.9	4.31	14.5	4.84	0.3
Cyanex 923 in ShellSol T + 0.109 M 1-decanol	4.65	1.6	4.12	2.2	3.80	1.0	4.66	0.1

Extraction results

Four different extractants were used for phenolic compounds distribution experiments. Aliquat 336 and Cyanex 923 were found to be effective solvents (Table 2). Alamine 336 and Hostarex A327 (tertiary amines) and TBP only exhibited high extraction capability (for acidic phenolic compounds) at very low pH values.

Table 2. Distribution coefficients for phenolic compounds using Aliquat 336 and Cyanex 923 (Cinitial= 0.036M) diluted in SST. (Volumetric ratio $V_{aq}A/_0rg$ = 1, T= 298 K).

	4-Hidroxybenzoic acid (Cjnitiai= 3.2 mM)		p-Coumaric acid (Cjnitiāi 3.1 mM)		Caffeic acid (Cjnitiai = 3.2 mM)		Tyrosol (Cjnitiāi - 3.3 mM)	
	pH	D	pH	D	pH	*D*	pH	D
Aliquat 336 + 0.109 M 1-decanol	1.21	1.7	1.45	4.4	1.38	6.4	1.56	0.4
	2.75	2.9	2.80	7.3	2.74	7.7	3.74	0.3
	7.13	15.4	7.66	60.7	6.55	61.0	6.94	0.3
Cyanex 923	1.21	20.3	1.47	49.6	1.43	20.5	1.57	0.3
	4.65	14.6	4.22	27.9	4.31	14.5	4.84	0.3
	7.1	0.0	7.36	0.1	7.98	0.1	7.00	0.4
Hostarex A327	1.3	11.6	1.54	23.7	1.49	29.6	1.62	0.05
	3.93	0.17	3.7	0.24	3.87	0.3	6.36	0.0
	7.48	0.0	7.46	0.0	7.63	0.12	7.45	0.0
Alamine 336	1.29	13.1	1.53	22.5	1.47	24.2	1.6	0.1
	3.74	0.0	3.54	0.03	3.84	0.04	5.84	0.0
	7.13	0.0	5.26	0.0	7.05	0.02	6.84	0.0
TBP	1.23	9.7	1.52	0.29	1.51	0.05	1.75	0.0
	3.63	0.07	3.55	0.18	3.64	0.02	5.85	0.0
	7.7	0.0	7.7	0.0	7.53	0.01	7.30	0.0

From the data listed in this table, it can be seen that the equilibrium pH is an important factor for acidic phenolic compounds extraction with any of the extractants. Similar results were found for 4-hidroxybenzoic acid extraction with Aliquat 336 and a pH dependency of the acid extraction was observed at constant ionic strength [18], Only for tyrosol, the pH values (in the studied range) did not affect the distribution coefficient using any of the extractants. In fact, the value of pKat for tyrosol is about 10 and in the pH range studied tyrosol is non-dissociated. For the pH range studied, the tyrosol extraction mechanism was, therefore, the same.

When Cyanex 923 was used for acidic phenolic compounds extraction the efficiencies followed (in reverse order) the proportion of charged ions at the different pH values. Acidic phenolic compounds have their pKai around 4. For pH values under 4, these compounds

were in their non-dissociated form and Cyanex 923 extracted them by a hydrogen bond mechanism. However, above pH 4, the acidic phenolic compounds were, mainly, in their dissociated form and Cyanex 923 was unable to extract them.

For Aliquat 336, high pH values of aqueous solutions of acidic phenolic compounds were very promissing. In these pH values, acidic phenolic compounds were in their dissociated form and Aliquat 336 extracted the anionic form of the compounds by an anion exchange reaction mechanism, as shown by the following chemical equation [18]:

$$Q^+Cl^-_{org} + A^-_{aq} \leftrightarrow Q A^+_{org} + Cl^-_{aq} \quad (3)$$

However, Aliquat 336 had good results also for low pH values of aqueous solutions. This can be explained by an addition mechanism of non-dissociated form of phenolic compounds to the amine, as shown by the following chemical equation [18]:

$$Q^+Cl^-_{org} + HA_{aq} \leftrightarrow Cl^-(HA)_{org} \quad (4)$$

From the results above, we can conclude that Cyanex 923 is a powerful acidic phenolic compounds extractant at low pH values and Aliquat 336 is useful to extract any acidic phenolic compound in a considerable range of pH values.

Stripping results

Stripping experiments were done for Aliquat 336 extractant as this compound revealed the best extraction results. The stripping behavior of these extractants was investigated using different stripping solutions at various concentrations. The results are presented in Table 3.

Table 3. Stripping percentage of 4-hydroxybenzoic acid from Aliquat 336 10%v/v (diluted in ShellSol T and 0.109 M 1-decanol). (Volumetric ratio V_a/V_{org} = 1, T=298 K). 4-hydroxybenzoic acid **was** *extracted at pH* **= 7.**

Stripping agent	Concentration (M)	% Stripping
HCl	1	7
NaOH	0.5	30
	1.0	43
	2.0	49
NaCl	1.0	45
NaOH + NaCl	0.3M NaOH + 0.5M NaCl	100
	0.5M NaOH + 0.5M NaCl	100

As shown in the table, Aliquat 336 stripping required both alkaline and NaCl solution to obtain a recovery value of 100% for 4-hydroxybenzoic acid. Similar results have been obtained with p-coumaric acid stripping as presented elsewhere [19], According to the possible ion exchange reaction, a salt solution was necessary to make the extraction process reversible (as shown in Eqn. (5)) and the alkalinity stabilized the stripped anion in solution.

$$Q^+A^-_{org} + Cl^-_{aq} \leftrightarrow Q^+Cl^-_{org} + A^-_{aq} \quad (5)$$

For the other extractants, such as Cyanex 923, a strong base solution has been shown enough for stripping as presented elsewhere [20, 23],

CONCLUSIONS

The extraction performance of several phenolic compounds with various extractants was examined. The experimental data showed that Cyanex 923 and Aliquat 336 performed better than the other extractants studied. Cyanex 923 was suitable to remove phenolic compounds

from low pH aqueous solutions. Aliquat 336 could also extract phenolic compounds at low pH values but its efficiency is higher when phenolic compounds are present as anionic forms leading to an ion exchange mechanism. The use of 1-decanol as modifier, although useful for solubilizing Aliquat 336, it should be optimized due to a deleterious effect in the extraction caused by the formation of a complex between the extractant and 1-decanol.

Stripping experiments proved that for Aliquat 336 solvent phases, NaCl must be added to an alkaline solution in order to have high stripping levels.

ACKNOWLEDGEMENTS

The authors would like to thank Cognis Corporation, Clariant Chemical Co. and Cytec Co. by the reagent samples offered to this work. The financial support of FCT is also acknowledged.

REFERENCES

1. **J. Vives-Rego, C. Sala and O. Diaz (1995), Diario de Mallorca, June 1995.**
2. **M.L. Janerdel Valle (1980),** *Grasas Aceites,* **31, 273.**
3. **F. Zucconi and N.J. Bukovac (1969),** *Rivista dell/Ortoflorofrutticolt. Ital.,* **53, 443.**
4. **D. Potenz, E. Righetti, A. Bellettini, F. Girardi, P. Antonacci, L. A. Calloano and G. Pergolese (1985),** *Inquinamento,* **27 (4), 49.**
5. **A. Marisot (1979),** *L'Oliviers,* **19, 8.**
6. **L. Di Giovacchino, A. Mascolo and L. Seghetti (1988),** *Rivista Ital. Sost. Grasse,* **65, 481.**
7. **P. Garcia, A. Garrido, A. Chakman, J.P. Lemonier, R.P. Overend and E. Chornet (1989),** *Grasa Aceites Seville***, 40, 291.**
8. **L. Vasilets, V. Mokh and L. Plekhanova (1988),** *Eksperimental noi Biologii i Meditsiny***, 106, 554.**
9. **E. Fedeli and F. Camurati (1981), Semin. Internat. sur le valoriz. des prod, de l'olivier, Roucastin, Tunisie, pp. 111-113.**
10. *Perry's Chemical Engineers' Handbook,* **6th. Ed., R.H. Perry, D.W. Green and J.O. Maloney (eds), McGraw-Hill, New York, 1984.**
11. **G. Braun, W. Grünbein, M. Mayer and B. Wojtech (1986),** *ISEC'86 - Preprints,* **DECHEMA, München, Federal Republic of Germany; Vol. III, 885-891.**
12. **B. Wojtech, G. Braun and R. Steiner (1988),** *ISEC'88 - Conference papers,* **Moscow, USSR, 1988; Vol. III, 370-373.**
13. **H. Tetzlaff and S. Rittner (1992),** *Solvent Extraction 1990,* **T. Sekine (ed.), Elsevier Science Publishers, 1992, 479-484.**
14. **E.K. Watson, W.A. Rickelton, A.J. Robertson and T.J. Brown (1988),** *ISEC'88 - Conference papers,* **Moscow, USSR, 1988; Vol. III, 370-373.**
15. **A.M. Urtiaga and M.I. Ortiz (1997),** *Sep. Sci. Technol.,* **32(6), 1157-1162.**
16. **W. Cichy, S. Schlosser and J. Szymanowski (2001),** *Solvent Extr. Ion Exch.,* **19, 905-923.**
17. **W. Cichy and J. Szymanowski (2002),** *Environ. Sci. Technol.,* **36, 2088-2093.**
18. **C.M.L. Santos, M.R.C. Ismael, M.L.F. Gameiro and J.M.R. Carvalho (2005),** *Solv. Extr. Ion Exch.,* **in press.**
19. **J.R. Carvalho, C. Santos, R. Ismael, L. Ferreira (2002),** *Proc. Int. Solvent Extraction Conf.,* **Cape Town, South Africa.**
20. **C.M.L. Santos (2004), PhD Thesis, Instituto Superior Tecnico, Portugal.**
21. **H. Mizelli and H.-J. Bart (1994),** *Ind. Eng. Chem. Res.,* **33 (2), 329-335.**
22. **B. Galan, A.M. Urtiaga, A.I. Alonso, J. Irabien and M.I. Ortiz (1994),** *Ind. Eng. Chem. Res.,* **33 (7), 1765-1770.**
23. **P.F.M.M. Correia, L.M. Ferreira, J.M.R. Carvalho (2005),** *Proc. Int. Solvent Extraction Conf.,* **Beijing, China (in press).**



FT-IR INVESTIGATION OF MICROEMULSION FORMATION AND NEODYMIUM EXTRACTION OF NA-PC88A-HEPTANE SYSTEM

Wenxuan Yin[1,2], Yufeng Liu[1], Yuanfu Zhang[1] , Shifu Weng[1] , Jinguang Wu[r], Guangxian Xu[1]

1 College of Chemistry, Peking University, Beijing, 100871, China
2 College of Chemical Engineering, China University of Mining Technology and Engineering, Xuzhou, 221008, China

ABSTRACTS

In this study, the Naphthenic acid(NA)-PC88A-Heptane system is adopted in Neodymium extraction, the function of mixed extractants is instead of a co-extractant. 10M KOH aqueous solution was used to saponify a NA (0.5 mol-L'[1])- PC88A(0.5 mol-L'[1])- heptane solution, the obtained solution with transparent and clear appearance indicated w/o micelles and/or microemulsions formed. This solution was characterized using FT-IR spectroscopy, the intensity of P-O-H band at 979cm'[1] decreased and the peak position of P=0 at 1197cm'[1] shifted to 1159 cm"[1] as the saponification percentage increased from 5 to 75% suggesting that K^+ ions are interacting with the P-O-H and P=0 groups . In addition, the carboxyl groups of NA from 1704cm'[1] to 1689 cm'[1], v_s and v_{as} of COO' group at 1406 crrf'and 1558cm'[1] were observed suggesting that NA is also binding with K^+ ions in the microemulsion.

Extraction of neodymium was performed with 75% saponified microemulsion. The extracted organic phase was transparent with the special pink color of Nd^{3+}. FT-IR measurements show that the P=0 band shifts from 1157 to 1135cm'[1], the v_s of COO' group shifts from 1406cm'[1] to 1424 cm'[1], and v_{as} of COO' vibration is from 1558cm'[1] to 1551 cm'[1] as the loading percentage of Neodymium increases. The IR results demonstrate that Nd (III) is coordinated to P=0 and COO" groups simultaneously, and the supramolecules with self-assemble structure formed containing PC88A and NA, which are binding with Nd(III) in the extracted organic phase.

Key words: mixed extractant, microemulsion, FT-IR, saponify

* To whom correspondence should be addressed. Tel.01062757951 ,E-mail:wujq@pku.edu.cn
[1,2] Visiting scholar of Peking University from China University of Mining and Technology.

INTRODUCTION

Naphthenic acid (NA) and PC88A are important acidic extractants in rare earth production. The authors have previously shown that the saponification of extractants such as naphthenic acid, PC88A, etc., form a w/o microemulsion[11-21] and that the extraction of rare earth ions by a saponified extractant entails destruction of the w/o microemulsion and the formation of new aggregations. Microemulsion are very important in the process of the extraction of metal ions and bio-molecules, and extends to other fields[13'71]. In this study, the NA-PC88-heptane system was employed in the extraction of the neodymium (III) ion. The interaction of NA and PC88A as well as the co-extraction effect were studied. This study will provide some important information about the practical application of microemulsion to hydrometallurgy and bio-technique processing.

EXPERIMENTAL

1. Reagents

Naphthenic acid was bought from Shanghai Yung-Feng Chemical Works, treated with urea to remove the straight chain hydrocarbons and then redistilled to collect the fraction between 150°C and 210°C under a reduced pressure of 3-5 mmHg. The average molecular weight was determined to be 269. PC88A was bought from Beijing Chemical Works and it's purity after purification was determined to be 99.7%. Heptane and KOH is reagent of A.R. grade.

2. Instruments

(1) Centrifuging tube 5mL,2mL. Fixed quantity sample injector, Finnpipette Digital 5~40pL .
(2) BIO-RAD FTS-65AType FTIR Spectrometer with ATR accessory.

3. Sample preparation

(1) Mixing extractant: Naphthenic acid (lmol-L'[1] heptane solution) equal volume mixed with PC88A (lmol-L'[1] heptane solution).
(2) Saponifying Mixed extractant: 10M KOH aqueous solution was used to saponify mixed extractant, saponification percentage was from 5% to 75%. A series of systems with different saponification percentage were obtained.
(3) Extraction rare earth ion: Equivolume(lmL) (2) microemulsion extracted with different volume $NdCl_3$ aqueous solution. A series of organic phase containing different loading percentage of Nd(III) were prepared.
(4) Measuring FTIR spectra: BIO-RAD FTS-65AType FTIR Spectrometer with ATR accessory was used to measure the IR spectra of the above microemulsions and extracted organic phase containing Nd(III). Scan 16, resolution 4cm'[1], wave numbers range 650-4000cm'[1].

RESULTS AND DISCUSSIONS

1. IR Spectra of mixed extractant

IR Spectra of Naphthenic acid, PC88A and the mixed extractant of Naphthenic acid and PC88A are shown in Fig. 1. Obviously, the IR Spectrum of the mixed extractant was not a sum of the two components. In the IR Spectrum of the mixed extractant of Naphthenic acid-PC88A, the peak position of the $v_{C}OOH$ shifted from 1702 cm'[1] in Naphthenic acid to 1704 cm"[1]. Similar difference can be observed for the relative intensity of $v_{p\cdot 0}$.c (1034 cm'[1]) and Vp-o-H (979 cm'[1]). And the band shape of $v_{P}=_{0}$ (1197 cm"[1]) also changed in the mixed system. The 1288cm'[1] peak in IR spectrum of Naphthenic acid was disappeared in the mixed extractant of Naphthenic acid-PC88A. These results indicate that there is interaction between Naphthenic acid and PC88A.

2. IR Spectra of Saponified mixed extractant

Fig.2 is the IR spectra of the systems saponifying with 10 mol-L'[1] KOH (saponification from 5% to 75%). The peak position of P=0 shifted to lower wave numbers obviously. The peak intensity of $v_{p<J\cdot H}$ (979 cm'[1]) decreased gradually as the saponification percentage (5% to 75%) increased. The peak position of COOH(1704cm'[1]) shifted obviously until saponification percentage 45%. v_{s} and v_{as} of COO' group at 1406cm'[1] and 1558cm'[1] were observed when saponification percentage was more than 60%. The results indicated both NA and PC88A can bind with K^{+} ion in the the saponifing process.

The change of the relative Intensities of some correlated peaks compared with that of the peak at 1459cm"[1] was shown in Fig.3 and Fig.4. Several interesting observations follow. The stretching vibration of OH was observed when saponification percentage was up to 45% and its relative Intensity gradually increased as the saponification percentage increased. In addition, the relative Intensities of v_{s}(COO'), v_{as}(COO') gradually increased while that of v(COOH) weakened. Interestingly, the relative Intensities of v(P=0) and v(P-O-C) gradually increased before a saponification percentage of 70% but they weakened when the system was saponified higher than 70%.

3. IR Spectra of organic phases containing Nd(III)

IR Spectra of organic phases with different loading of Nd^{3+} are shown in Fig. 5. The contents of $H_{2}0$ in organic phases decreased as the loading of Nd^{3+} increased. This indicates the microemulsion is broken down in the organic phase and the aggregation changed. Additionally, the peak of v(P=0) at 1157 cm'[1] shifted to 1135 cm'[1], and v_{as}(COO') at 1558 cm'[1] shifted to 1551 cm"[1]. It revealed that both NA and PC88A are binding with Nd^{3+} ion. The peak position of v_{s}(COO") shifted from 1404 cm"[1] to 1424 cm'[1]. It indicated that the structure was complex when mixed extractants are binding with Nd ion.

Results suggested that, in the process of extracting Nd^{3+}, self-assembled supramolecular structure formed in the saponified mixed extractants. Both the PC88A and NA components binded with Nd(III) and interactions were observed between naphthenic acid and PC88A in

the extracted organic phase.

CONCLUSIONS

FT-IR investigation of the acidic extractants NA and PC88A, it indicated NA and PC88A are binding to K^+ ion in the saponified NA-PC88A-heptance microemulsion system with lOmol-L^{-1} KOH solution.

The effective extracts of Nd(III) was performed using the microemulsion of NA-PC88A mixed extractants. The result demonstrated that the interactions of Nd(III) with NA and Pc88A occurred simultaneity.

ACKNOWLEDGEMENTS

This work was supported by State Key Project of Basic Research (200CCA01900), Key Project of **National Natural Science Foundation of China (30371604 and 50203001) and Doctoral Project of Education Ministry of China.**

REFERENCES

1. WU Chin-Kwang, KAO Hung-cheng, CHEN Tien, et al. Proceed. *ISEC'80,* **Vol. 1, Paper No.80.**
2. WU Jin-guang, SHI Nai, GAO Hong-cheng, et al. *SCIENTIA SINICA(B)* **1983 (12): 1071**
3. K. Osseo-Asare. *SEPARATION SCIENCE AND TECHNOLOGY,* **1988, 23(12& 13), pp.1269-1284**
4. WENG Shi-fu, WU Jin-guang , Xu Guang-xian. *SPIE.* **Vol.553 1985** *Fourier and Computerized Infrared Spectroscopy* **(1985), 431**
5. WU Jin-guang, ZHOU Nai-fu, WANG Du-jin, et al. *SCIENCE IN CHINA(Ser\es* **B) 1998,41(1)**
6. ZHOU Nai-fu, LI Quan, WU Jing-uang, et al. *Langmuir* **2001,17,4505**
7. MAGang, WENG Shi-fu, WU Jin-guang, *Spectroscopy and Spectral Analysis,* **1999, 19 (2): 161**

Captions

Fig. 1 IR Spectra of NA, PC88A and NA+PC88A
Fig. 2 IR Spectra of NA-PC88A-Heptane Systems with different saponification percentage
Fig.3 Variations of the correlation peaks relative Intensities with different saponified percentage
Fig. 4 Variations of the relative Intensities of v_0H, v_S and v_{as} of COO" group with different saponified percentage
Fig. 5 IR Spectra of Organic Phases with Different Loading of Nd^{3+}

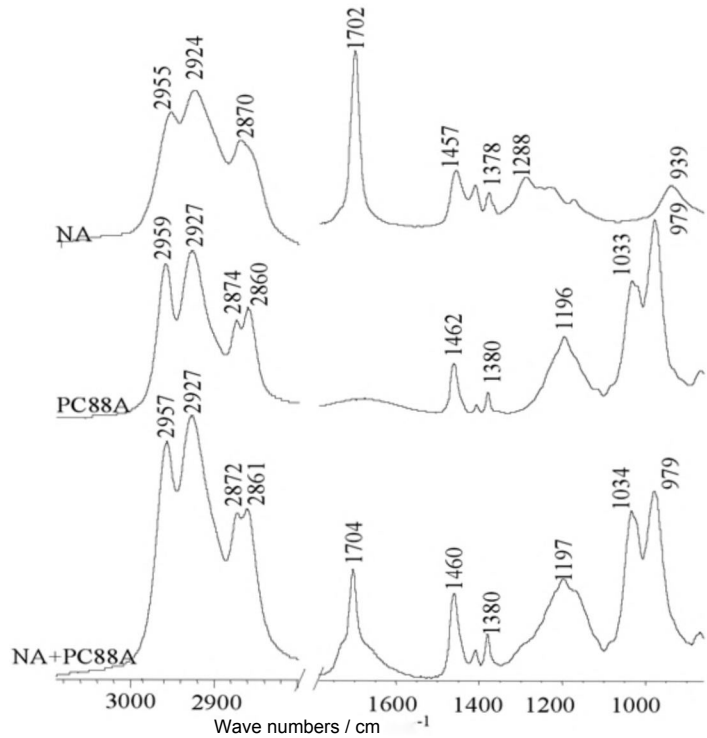


Fig. 1 IR Spectra of NA, PC88A and NA+PC88A

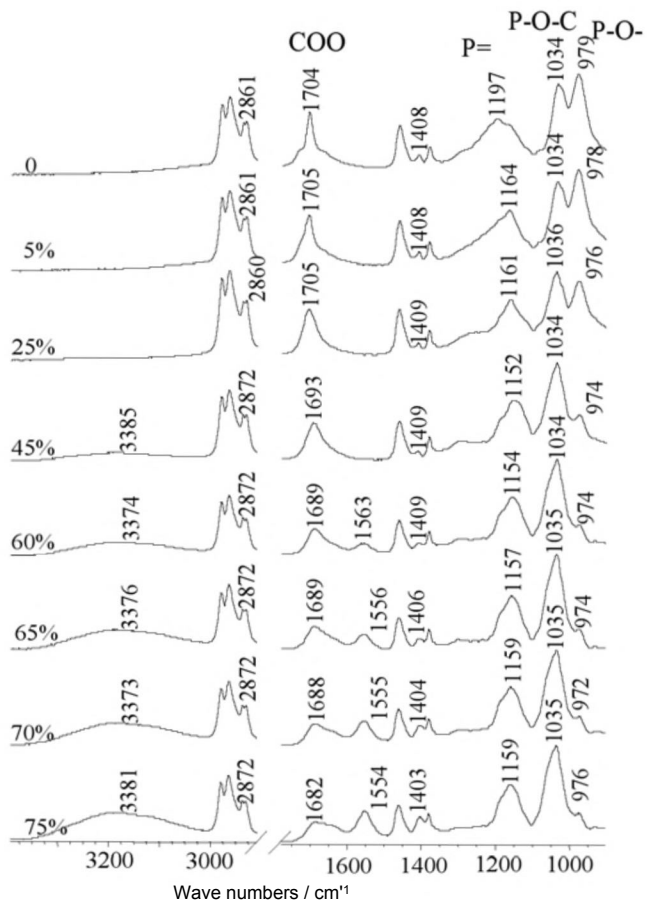


Fig.2 IR Spectra of NA-PC88A-Heptane Systems with different saponification

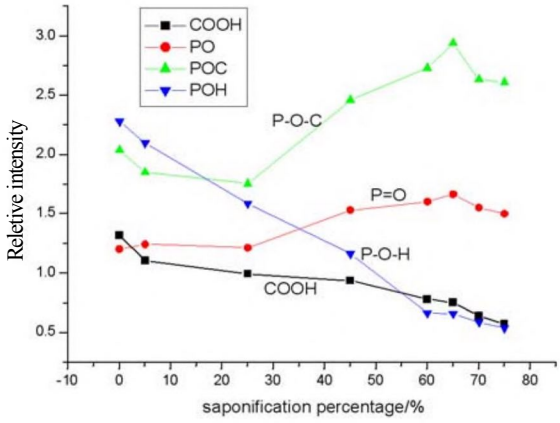


Fig. 3 Variations of the correlation peaks relative Intensities with different saponified percentage

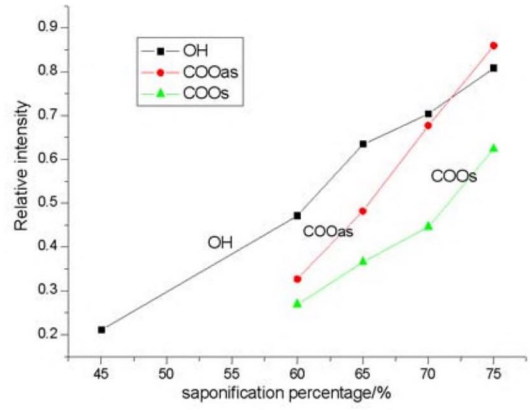


Fig. 4 Variations of the relative Intensities of v_0H, v_s and v_{as} of COO' group with different saponified percentage

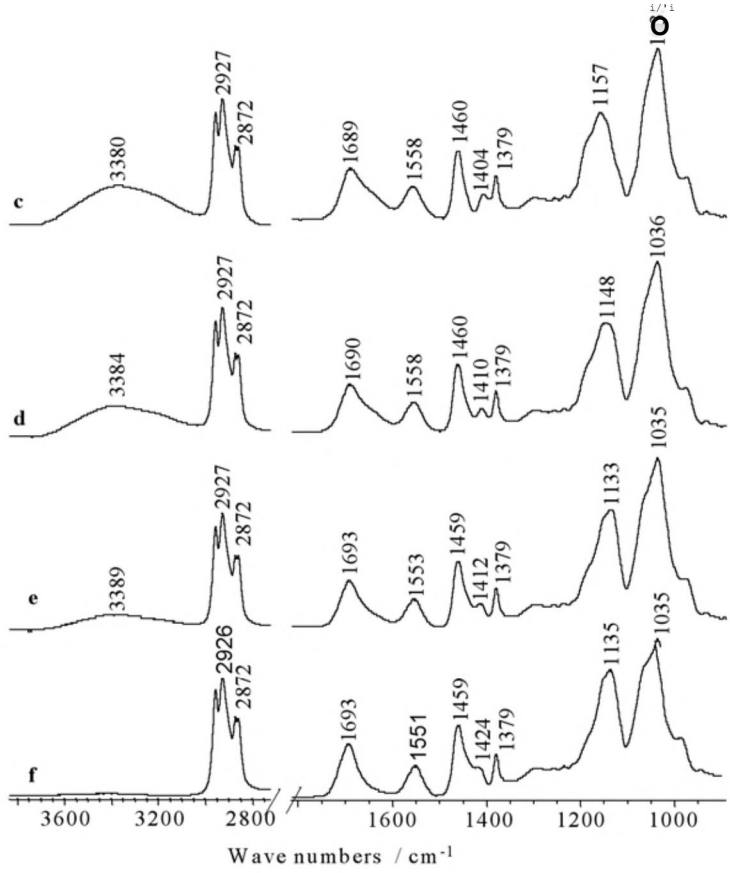


Fig. 5 IR Spectra of Organic Phases with Different Loading of Nd^{3+}

c: Loading 0%; d: Loading 21%;

e: Loading 42%; f: Loading 60%



EFFECT OF NON-EQUILIBRIUM METAL AGGREGATION ON PARAMETERS OF METAL EXTRACTION BY TBP

Oksana A. Sinegribova, Kuaw Thu Win, Lidia V.Troegubova, Olga V. Muraviova, Galina V. Pokrovskaya

D.Mendeleyev University of Chemical Technology of Russia,
Moscow, Russia

The main focus of the present work is the study of the influence of non-equilibrium aggregates in the extraction system on the parameters of metal extraction by TBP. It was shown that the presence of such associated species in the aqueous phase causes a dependence of the extraction isotherms on the conditions of the experiment (Vorg:Vaq). The formation of non-equilibrium aggregates in the organic phase leads to non-coincidence of the metal isotherms for extraction and back-extraction at the same acidity of the aqueous phase.

The presence of polynuclear stable metal compounds in the aqueous phase causes a metal imbalance in the extraction process across the flat interface due to stable polynuclear compounds concentrating at the interface. In this case the rate of mass transfer sharply decreases during the experiment. The formation of non-equilibrium structures in the organic phase leads to an increase in the rate of mass transfer. The appearance of stable structures in the organic phase affects the selectivity of the extraction process.

INTRODUCTION

The extraction process can be complicated by polymerization and formation of different aggregates in the aqueous phase. It is especially typical for the extraction of polyvalent metals, in particular zirconium. The ability of zirconium to hydrolysis, polymerize and its tendency to complexation defines the state of this metal in solution. The chemical behavior of hydrolyzed and non- hydrolyzed species of zirconium is different [1], Polynuclear zirconium compounds containing bridged oxygens are very stable and often reactionless.

Colloid formation is possible in the extraction process due to the tendency of organophosphorus extractants and their extracted compounds to aggregate into dispersed structures, typical of a surfactant, on account of their amphiphilic nature [2,3], Colloidal structures can consist of thermodynamically stable aggregates, like micelles, microemulsions, lyotropic liquid crystals, or of thermodynamically non-equilibrium aggregates, like vesicules [4],

This structurization in extraction systems can take place in the bulk phases and at the aqueous/organic interface. The formation of colloidal particles, their composition and type, the ion parameters of their interaction and the structure of the mesomorphic phases so formed can affect the kinetic and thermodynamic features of metal extraction. The high metal loading in the organic phase and the addition of co-surfactants (aliphatic alcohols) can

promote colloid formation [5],

In the present work the influence of non-equilibrium aggregates in the extraction system on some parameters (isotherms, rate of mass transfer and selectivity) of the extraction process has been investigated for the process of metal extraction by TBP solutions. Zirconium was mainly used as the extracted metal.

EXPERIMENTAL

The concentration of Zr was determined by complexometric titration with EDTA or by a gravimetric method. The Zr content in the interfacial condensed film was calculated from the material balance equation. The concentration of Hf in admixture with Zr was determined by mass-spectrometry.

The solutions containing non-extracted polynuclear compounds of zirconium were produced by heating for a long period of time. The amount of non-extractable zirconium was determined by complete removal of the extractable species by repeated contacts between the metal solution and fresh TBP solutions (70% TBP in octane). The percentage of non-extractable metal was -50 *% of* the initial Zr concentration in solution 1, ~20% in solution 2 and ~0% in solution 3.

For the extraction kinetics study the well known diffusion cell with mixing and the horizontal rotating cell [6] were used.

RESULTS AND DISCUSSION

Extraction isotherms for Zr by 70%TBP in n-octane, obtained by extraction from solutions 1-3 with the different initial concentration of metal in aqueous phase and V_0rg:V_{aq} = 1 : 1 are shown on Figure 1.

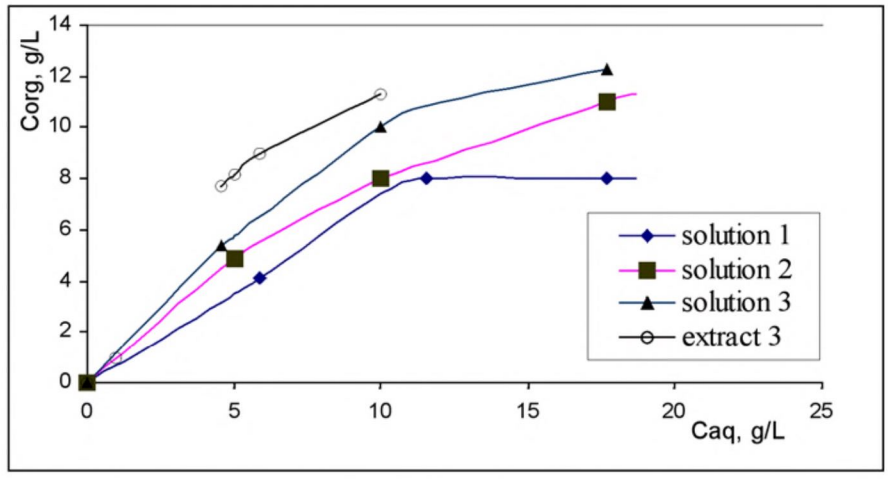


Figure 1. Extraction isotherms of Zr by TBP at different initial metal concentrations in the aqueous phase and V_0^:V_{aq} = 1 : 1 , [$HN0_3$] = 4 mole A.; 70% TBP in n-octane

The non-coincidence of the extraction isotherms occurs due to the presence of non-extractable species of zirconium. The presence in the aqueous phase of such polynuclear stable metal compounds, which are in a state of non-equilibrium with the extractable monomeric forms of metal, causes the dependence of the extraction isotherms on the ratio of the organic and aqueous phase volumes. The extraction isotherms obtained at constant

initial concentration of metal in the aqueous phase and the different organic and aqueous phase volume ratios (V_{org}:V_{aq}= 3:1, 2:1, 1:1,1:2, 1:3) are presented in Fig. 2.

Non-coincidence of the extraction isotherms for solutions with different amounts of stable polynuclear Zr compounds, that are not in equilibrium with extractable species, seems logical. The astonishing fact is the non-coincidence of the back-extraction isotherms (Figure 3).

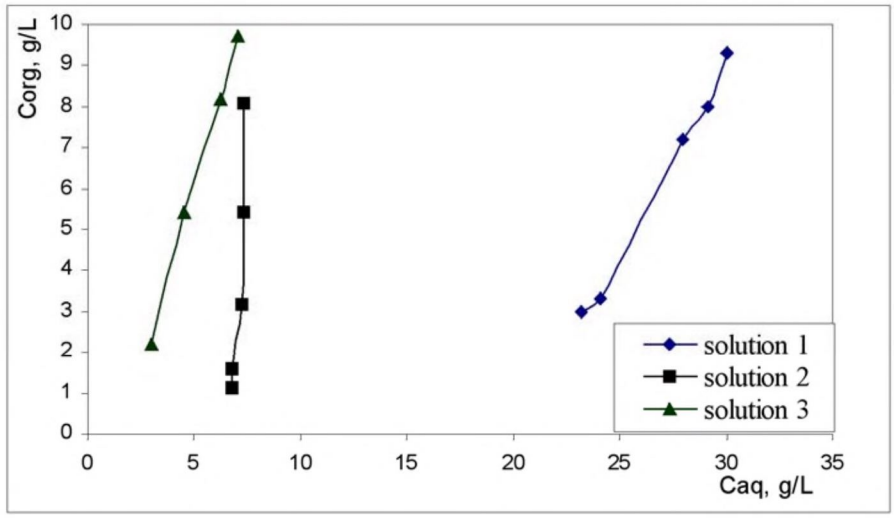


Figure 2. Zr extraction isotherms with TBP at constant initial concentration of metal in the aqueous phase and various V_0^:V_{aq}, [$HN0_3$] = 4 mole/L; 70% TBP in n- octane

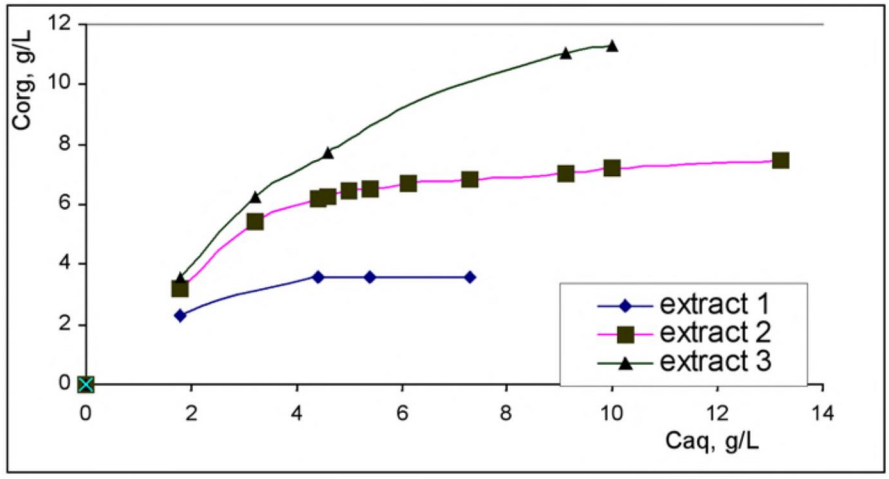


Figure 3. Back-extraction isotherms at V_0^:V_{aq} = 1 : 1 , [$HN0_3$] = 4 mole /L; 70% TBP in n-octane

If the extractable compound in all cases is the equilibrium species $Zr(N0_3)_4$.2TBP, the back-extraction isotherms should coincide at similar acidities of the aqueous phase for extracts 1-3. However the data in Figure 3 indicate differences in these curves. Moreover the extraction and back-extraction isotherms were not coincident even for solution 3 (without stable non-extractable Zr compounds) (Figure 1). A prolonged time of back-extraction didn't lead to any change in the back-extraction curves. The reason for non-coincidence of these isotherms may be either a different composition of extractable compounds or the formation of stable aggregates in the organic phase.

Inorganic polynuclear compounds present in the aqueous phase containing polyvalent metals (like Zr) are able to concentrate at the interface. This will cause metal imbalance when metal extraction takes place across the flat interface due to the concentration of stable polynuclear compounds at the interface (Table 1).

The concentration of stable polynuclear compounds at the interface leads to the appearance of spontaneous interfacial convection in the initial time of contact of phases, but later the interfacial film forms.

Table 1. Metal accumulation at the interface during Zr, Hf extraction by TBP from nitrate solution after 30 min experimental time, % from initial concentration

Metal	diffusial cell	horizontal rotating cell
Zr	13.8	17
Hf	26	28

$[Me]_{aq.init.}$= 0.075 mole/L, $[HN0_3]$ = 4 mole/L, [\ f5<t>]= 40% in toluene

If zirconium transfers across the flat interface (in the diffusion cell, the device with an unrenewable flat interface), the accumulation of metal at the interface and the formation of the interfacial film causes reduction and cessation of zirconium mass transfer (Figure 4). However, in the horizontal rotating cell, slowly rotating around its horizontal axis of symmetry, the interfacial field undergoes weak mechanical movements, which leads to perturbation of the interfacial layers which can destroy the formed interfacial film.

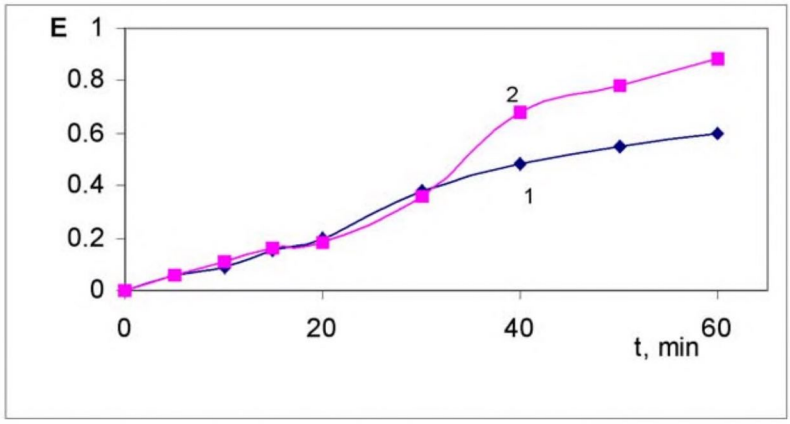


Figure 4. Kinetics of zirconium extraction by 40 %-TBP in toluene in the diffusion cell (1) and in the horizontal rotating cell (2)

A study of the kinetics of extraction, carried out in the horizontal rotating cell to prevent film formation at the interface, indicated that the mass transfer coefficient for the organic phase increases with increasing zirconium concentration in the organic phase (Table 2), probably due to the association in the organic phase.

Table 2. Mass transfer coefficients for extraction of Zr by 70% TBP in octane

N°	Initial metal concentration, g/L	mass transfer coefficients, sm/s
1	22	1,261 O'3
2	27	1,231 O'3
3	36	1,371 O'3
4	45	1,361 O'3
5	65	2,441 O'3

The separation of similar metal ions is performed less efficiently due to colloid formation in the extraction systems. The appearance of colloidal structures in the organic phase must influence the selectivity of the extraction process either as a result of complex aggregate formation (e.g. micelles or vesicules, containing two or more different metals) [7], or as a result of solubilization [8], which will lead to contamination of the target component.

A decrease in selectivity is observed for the separation of Zr and Hf (Table 3). The formation of colloidal structures took place due to octanol addition as co-surfactant [5], The separation coefficient dramatic decreases at low concentrations of Hf in Zr solutions When the concentration of Hf in solution is equal to the concentration of Zr, a decrease in the separation factor is also observed.

Table 3. Separation coefficients for the pair Zr and Hf on extraction with TBP

Medium	Se paration coefficients		
	Without octanol	U=0.025	U=0.05
From nitric medium Zr/Hf	6,32	2,14	-
From sulphate - thiocyanic medium Hf/Zr	14,06	3,82	2,05
From sulphate - thiocyanic medium Hf/Zr *	12,92	11,56	8,92

[Zr^{4}> 0. 1 mole/L, [Hf^{4+}]=0,01 mole/L (* - [Hf^{4+}]=0.1 mole/L), [NH_4CNS]= 2.0 mole/L. [H>4 N, [TBP]= 1.46 mole/L in toluene

When micellar aggregates appear in the organic phase it is reasonable to suppose that co-extraction of similar elements occurs due to the possible formation of complex micellar aggregates. Vesicule formation in the organic phase was observed in the system Ln - HCl - HDEHP - toluene on addition of a low concentration of butanol or octanol [5], At a certain concentration of alcohol the distribution coefficients of the lanthanides sharply decrease due to association of extractable compounds in the organic phase. Under these conditions the separation factors for lanthanide pairs in the mixture decrease although the separation factor calculated from the distribution of the individual lanthanides is higher for the system with added alcohol than for that without it. In spite of the different ability of lanthanides to aggregate in the organic phase they form combined vesicules when jointly present.Co-extraction of other metals into the organic phase may be caused by the solubilization of such other metals into the polar core of the colloidal aggregates formed by the macrocomponent. This fact is confirmed by the transfer of Fe in Zr extraction, though iron is almost non-extracted by TBP from $HN0_3$solutions.. The distribution coefficients of Fe at the presence of Zr are presented in Table 4.

Table 4. Distribution coefficients for Fe(III) in the presence of Zr in the extraction by 70% TBP in octane

N°	Initial concentration, g/L		Concentration in aqueous phase g/L		Concen tration in organii:phase g /L	
	Zr	Fe	Zr	Fe	Zr	Fe
1	6,4	0,4	3,2	0,4	3,2	0
2	36	0,56	20	0,43	16	0,13
3	45,8	0,36	29,2	0,21	16,6	0,15

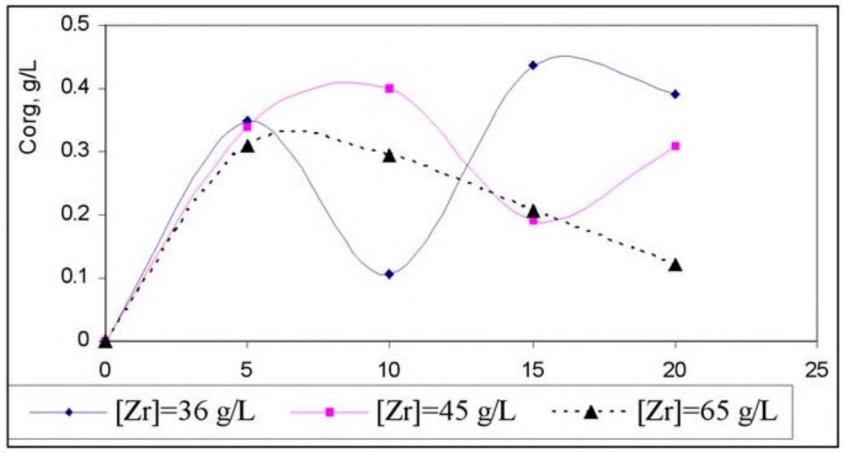


Figure 5. Behavior of Fe(III) overtime in the extraction of Zr by 70% TBP in octane

In the experiment with the rotating cell the change in the amount of Fe in the organic phase with time (Figure 5) indicates the possible structural transition of Zr associates, followed by a change in the amount of inner water, where iron dissolves.

CONCLUSIONS

The presence of non-equilibrium aggregates in the extraction system affects the parameters of the extraction process. The existance of stable polynuclear compounds of metal in the aqueous phase causes a dependence of the extraction isotherm on the ratio of the organic and aqueous phase volumes. For solutions with various amounts of stable polynuclear compounds, the isotherms of extraction and of back-extraction are different. The lack of coincidence of the metal isotherms for extraction and back-extraction at similar acidities of the aqueous phase for solutions without stable compounds in the aqueous phase indicates the formation of non-equilibrium species in the organic phase. The presence of polynuclear stable metal compounds in the aqueous phase will cause an imbalance in the metal extraction cross the flat interface due to the concentration of stable polynuclear compounds at the interface. The formation of non-equilibrium structures in the organic phase increases the rate of mass transfer in the organic phase.The appearance of colloidal structures in the organic phase influences the selectivity of the extraction process both as a result of complex aggregate formation (e.g. micelles or vesicules, containing two or more different metals), and by solubilization, thus leading to contamination of the target component.

REFERENCES

1. G.A.Yagodin, V.G.Kazak (1973), *Jorn. Neorg. Chem.,* 18, 107-110
2. K.Osseo-Asare K. (1991), *Advances in Colloid and Interface Scince.,*37,123-180.
3. K.Osseo-Asare K. (2002), *Proc. ofISEC'2002,* , Youth Africa, 1, 150-157.
4. E.Paatero, J.Sjoblom (1990), *Hydrometallurgy*, 1, 231-250.
5. O.A.Sinegribova, O.V.Muraviova, L.V.Troegubova, U.V.Bortnikova (2002), *"50 years of Russian Extraction"* (collected articles, Russ.), 58-63
6. V.V.Tarasov, O.A.Sinegribova, O.V.Sviridenkova (1999), *Proc. of ISEC'1999,* 2, 825-828.
7. S.Stoyanov (1993), *Proc. of ISEC'93,* York, UK, 2, 1720-1727
8. V.I.Bukin, A.M.Reznik, V.Ju.Makotinskii (1999), *Modern problems of chemistry and technology of extraction* (Collected articles, Russ.), 1, 90-112

DEVELOPMENT OF A MICRO SOLVENT EXTRACTION SYSTEM FOR THE SEPARATION OF RARE EARTH METALS

Syouhei Nishihama and Kazuharu Yoshizuka

Department of Chemical Processes and Environment, Faculty of Environmental Engineering, The University of Kitakyushu, Hibikino 1-1, Kitakyushu 808-0135, Japan

A micro solvent extraction svstem for the seoaration of rare earth metals has been investigated. The micro flow channel is fabricated on a poly(methyl methacrylate) (PMMA) plate, and solvent extraction progresses by feeding aqueous and organic solutions into the channel simultaneously. The extraction equilibrium is quickly achieved, without any mechanical mixing, when a narrow channel (100 pm width and 100 pm depth) is used. The solvent extraction results from the binary solutions (Pr/Nd and Pr/Sm) revealed that both rare earth metals are firstly extracted together, and then the lighter rare earth metal extracted in the organic solution alternatively exchange to heavier rare earth metal in the aqueous solution to achieve the extraction equilibrium. A high separation efficiency therefore can be obtained, when the flow rate of the aqueous and organic solutions are slow.

INTRODUCTION

Solvent extraction has been widely applied for the separation of metals in the industrial scale. This technique, however, has a disadvantage as it needs very large amounts of organic solvent in order to dissolve the extractant. Alternative separation techniques, such as ion exchange, have therefore been paid much attention from an environmental friendly point of view. Micro chip technology is presently one of the active issues in the analytical chemistry field [1], and pTAS (micro total analysis system) has been especially advocated. Since the pTAS includes pre-treatment of samples, reaction of samples with reagent, and sensitive detection, the micro chip used in pTAS is called lab-on-a-chip. Solvent extraction also has been applied to the micro chip for the pre-treatment of trace metal assays [2] and for the liquid membrane system for the separation of metal ions [3], The application of micro solvent extraction systems, however, for the purpose of industrial separation of metals has hardly been carried out.

In the present work, a micro solvent extraction system for practical operating conditions has been developed. The micro solvent extraction chip was fabricated on a PMMA plate, and the extraction properties of rare earth metals were firstly investigated. The separation of the rare earth metals (Pr/Nd and Pr/Sm) was then conducted on the micro extraction chip, to compare with the conventional extraction system.

EXPERIMENTAL

The commercial extractant 2-ethylhexyl phosphonic acid mono-2-ethylhexyl ester (EHPNA,

marketed as PC-88A by Daihachi Chemical Industry Co. Ltd.) was used as received. EHPNA was diluted in kerosene. All of the inorganic chemicals were supplied by Wako Pure Chemical Industries as analytical-grade reagents. The aqueous feed solutions were prepared by dissolving appropriate amounts of rare earth chlorides in deionized water. The pH was adjusted using a CH_3COOH-CH_3COONa buffer solution. Extraction equilibrium data for the conventional solvent extraction system were obtained by conventional procedures under an organic/aqueous (O/A) volume ratio = 1 at 298 K.

The micro solvent extraction chip was made on a 3 cm x 7 cm PMMA plate using a table type NC detailed processing machine (PMT Corporation Co. Ltd.). The micro flow channel was firstly designed with CAD software, and then the channel was dug with a square end mill. Figure 1 shows the layout of the channel. In the present study, two types of micro flow channel (width = 500 pm and depth = 200 pm; width = depth = 100 pm) were prepared. The channel was stuck to a PMMA plate cover in a constant temperature oven at 393 K. The organic and aqueous feed solutions were fed into the micro flow channel via two inlets with the same flow rate using programmable syringe pump (Harvard, PHD 2000-M). The mixture of the solutions was then collected at the outlet of the chip, and weighed organic samples were stripped with 3 mol/L HCI. The resulting aqueous samples were analyzed by using an inductively coupled plasma atomic emission spectrometer (Perkin Elmer, Optima 4300DV Cyclon). The aqueous pH was measured with a Horiba F-23 pH meter.

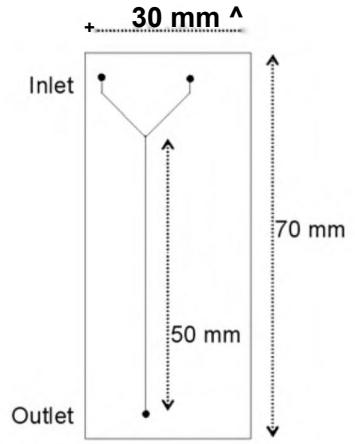


Figure 1. Micro solvent extraction chip fabricated in the present study.

RESULTS AND DISCUSSION

Extraction Equilibrium

The extraction equilibrium for the rare earth metals with EHPNA in kerosene, up to high loading ratios, were investigated in a previous paper [4], It is well known that aggregated species appear when the metals are extracted with acidic organophosphorus compounds. The maximum loading ratio ($[\overline{Ln}]/[\overline{(RH)_2}]_{feed}$) of the rare earth metals with EHPNA is 0.4, suggesting that the aggregated species contains the dimeric extractant and rare earth metal at a molar ratio of 5 : 2. The extraction equilibrium of the rare earth metals are therefore expressed as:

$$Ln^{3+} + 3\overline{(RH)}\text{^} \text{ <-> } \overline{LnRj(RH]}\text{^} + 3H'; K_{ex}\text{-i} \quad (1)$$

$$Ln^{3'} + \overline{LnR_3(RH)_3} + 2\overline{(RH)_2} \text{ <-» } \overline{(LnR_3}\overline{7_2(RH)_4} + 3H'; K_{ex2} \quad (2)$$

The extraction equilibria of Pr, Nd, and Sm were also investigated. The experimental distribution ratios of Sm are plotted, as a function of pH in Figure 2. The extraction

Table 1. Rare Earth Metals Extraction Equilibrium Constants.

	Pr	Nd	Sm
K_{ex1}	6.55 x io $^{3-}$	9.72 x 10'^{3}	1.17 x 10^{1-}
$K_{ex\cdot2}$	8.06 x IQ'^{4}	1.81 x IQ'^{3}	1.80 x 10'^{1}

equilibrium constants are determined by a nonlinear least squares method as summarized in Table 1. The distribution ratio of each rare earth metal is capable of prediction by using these constants, as reported in the previous work. The predicted distribution ratios are shown in Figure 2 by solid lines. The results obtained with single metal extraction can be extended to the extraction of Pr/Nd and Pr/Sm from binary solutions. The experimental distribution ratios are plotted in Figure 3, as a function of pH, together with the predicted results using the extraction equilibrium relations described above.

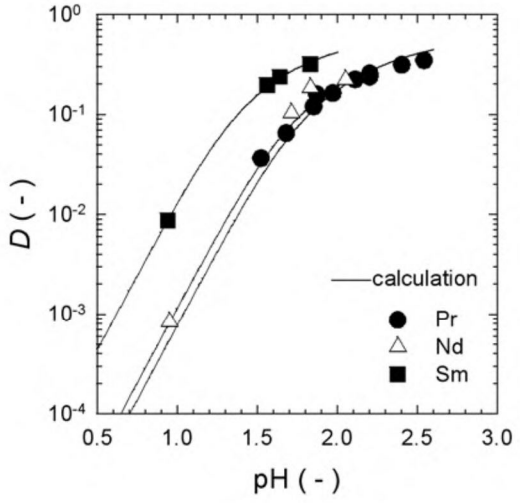


Figure 2. Effect of pH on distribution ratios for rare earth metals in single metal systems. $[\overline{(RH)_2}]_{fee(j}$ = 0.05 mol/L and $[Ln^{3*}]_{feed}$ = 0.05 mol/L

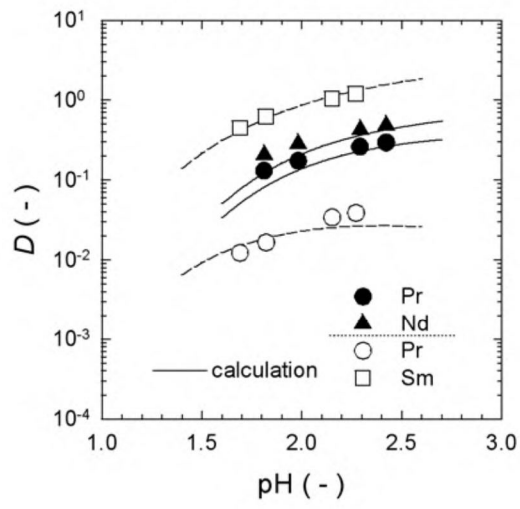


Figure 3. Effect of pH on distribution ratios for rare earth metals in a binary system. Closed keys show the Pr/Nd system, and open keys show the Pr/Sm system. $[\overline{(RH)_2}]_{leed}$ = 0.05 mol/L and [Ln^heed = 0.025 mol/L.

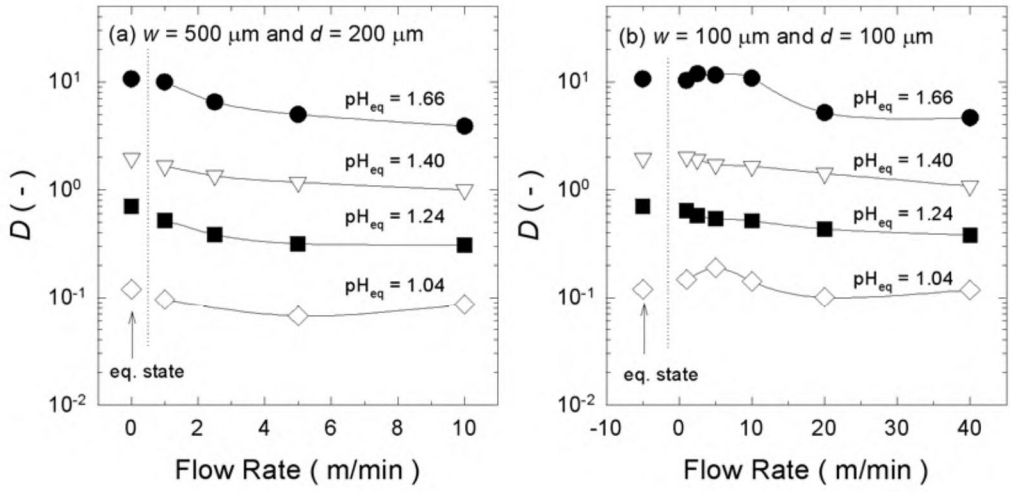


Figure 4. Effect of flow rate on the distribution ratio of Pr in a micro flow channel of (a) w = 500 pm and d = 200 pm and (b) w = 100 pm and d = 100 pm. $[\overline{(RH)_2}]_{leed}$ = 0.25 mol/L and [P^Jfeeo = 0.01 mol/L.

Characteristics of the Micro Solvent Extraction System

Figure 4 shows the effect of the linear velocity, which is defined as the ratio of flow rate

[m^3/min] to the cross sectional area of the flow channel [m^2], on the distribution ratio, together with the extraction equilibrium data obtained from the conventional extraction system. Extraction equilibrium is not quite achieved even with a very slow flow rate in the case of *w* = 500 pm and *d* = 200 urn, while it is easily achieved in the narrow micro flow channel. This suggests that the ratio of the interfacial area between the aqueous and organic phases to the volume of each phase dramatically increases when the narrow flow channel is used. The separation process of the metals with solvent extraction under equilibrium conditions can be easily carried out by using a very narrow flow channel just by feeding each phase into the micro solvent extraction chip. In addition, non-equilibrium separation may be expected by using a thicker flow channel.

Separation of Rare Earth Metals with the Micro Solvent Extraction Chip

The separation of rare earth metals (Pr/Nd and Pr/Sm) on the micro solvent extraction chip *(w = d* = 100 pm) was carried out. In these cases, the aqueous solution containing a higher concentration of each metal than that of the extractant was used from the view point of practical operation. Figure 5(a) shows the effect of linear velocity on the distribution ratios of each metal in the Pr/Nd binary system. At low pH (pH_{eq} = 1.81), the distribution ratios of Pr and Nd increase with decreasing linear velocity. At high pH (pH_{eq} = 2.42), the distribution of Pr decreases with decreasing velocity, while that of Nd increases. This suggests that the exchange reaction between Pr in the organic phase and Nd in the aqueous phase progresses to achieve the extraction equilibrium state. Such an exchange reaction between one metal extracted into the organic phase and another existing in the aqueous phase has been already reported in a column separation process [5], Figure 5(b) shows the results of micro solvent extraction in the Pr/Sm system. The exchange reaction was also observed in this system. Thus highly effective separation can be achieved at a low linear velocity. We successfully present the first protocol for the effective separation of rare earth metals on the micro solvent extraction chip.

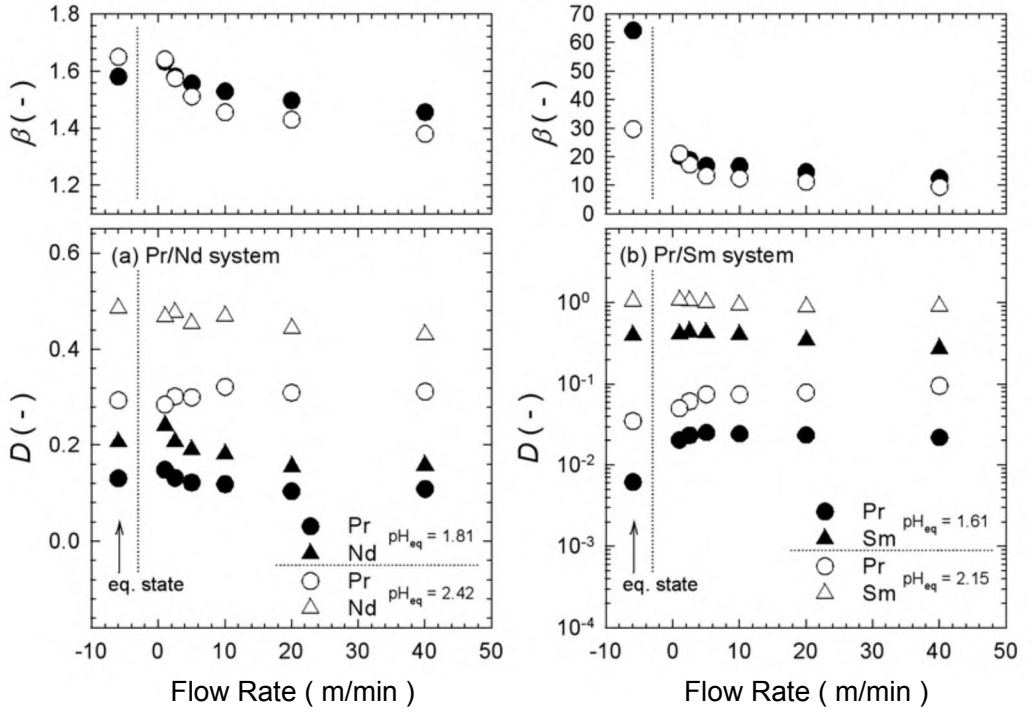


Figure 5. Effect of flow rate on the distribution ratio of (a) Pr and Nd and (b) Pr and Sm with EHPNA in the micro flow channel where w = 100 /.im and d = 100 /.im. $[\overline{(RH)_2}]_{leed}$ = 0.05 mol/L and $[Ln,^{3+}]_{feed}$ = 0.025 mol/L.

CONCLUSIONS

A separation system for rare earth metals in a micro solvent extraction system has been investigated, with the following results: (1) The micro solvent extraction system can be developed on a PMMA chip by mechanical fabrication, and extraction equilibrium can be achieved when the narrow micro flow channel was used. (2) The exchange reaction between the lighter rare earth metal in the organic phase and the heavier rare earth metal in the aqueous phase progresses along with a decrease in the flow rate, and effective separation can be achieved under the low linear velocity conditions.

ACKNOWLEDGEMENTS

The authors are grateful to Mr. Yasuyuki Tajiri for his experimental assistance and to the Ministry of Education, Culture, Sports, Science, and Technology for the financial support through a Grant-in Aid for Scientific Research (No.15760571).

REFERENCES

1. A. Manz and H. Becker (Eds.) (1999), *Microsystem Technology in Chemistry and Life Sciences,* Springer-Verlag, Berlin.
2. M. Tokeshi, T. Minagawa, K. Uchiyama, A. Hibara, K. Sato, H. Hisamoto, and T. Kitamori (2002), *Anal. Chem.,* 74, 1565-1571.
3. T. Maruyama, H. Matsushita, J. Uchida, F. Kubota, N. Kamiya, and M. Goto (2004), *Anal. Chem.,* 76, 4495-4500.
4. A. Hino, S. Nishihama, T. Hirai, and I. Komasawa (1997), *J. Chem. Eng.* Japan, 30, 1040-1046.
5. S. Nishihama, N. Sakaguchi, T. Hirai, and I. Komasawa (2002), *Hydrometallurgy,* 64, 35-42.



PURIFICATION OF COPPER LEACH SOLUTION IN THE NEW ENERGY-SAVING CUPROUS ELECTROWINNING SYSTEM

M. Shafiq Alam, Mikiya Tanaka, Kazuya Koyama and Jae-Chun Lee*

National Institute of Advanced Industrial Science and Technology (AIST), Tsukuba, Japan
* Korea Institute of Geoscience and Mineral Resources (KIGAM), Daejeon, Korea

A solvent extraction process has been developed to purify a copper leach solution within the framework of our energy-saving cuprous electrowinning system. In this process, nickel, cobalt and zinc were selectively removed from an ammoniacal alkaline solution containing a large amount of cuprous ion using an oxine-type chelating extractant (LIX 26). Equilibrium and kinetic studies were carried out under different conditions with or without synergistic agents. Almost complete removal of Co, Ni and Zn was achieved at pH 10 - 11. Copper was not extracted with LIX 26 from the ammoniacal alkaline solution where copper remained as a cuprous ammine complex. Under this experimental condition, LIX 26 extracts Co, Ni and Zn, present as cationic ammine complexes, via a cation exchange mechanism.

INTRODUCTION

In recent years, electronic waste has been rapidly increasing. Every year Japan produces about 30 million square-meters of printed circuit boards [1] and this figure will be much higher in the near future because of the tremendous use of electronics goods in the modern world. A large amount of copper is present in these metallic wastes, which are now mostly land-filled. To help protect the environment and metal resources, it is necessary to recover and recycle copper from the electronic waste in a sustainable way. Greenhouse gas emissions can also be significantly lowered by resource recovery, because it displaces the need for virgin resources and increases the economic output per unit of energy consumption. A literature survey revealed that an 85% energy savings could be realized through the recycling of copper [2],

Considering the environmental and economic advantages, at AIST, we are developing a new hydrometallurgical process to recycle copper from electronic scrap especially from waste printed circuit boards (PCB). In this process [3, 4], copper in the PCB is leached into an ammonia/ammonium-sulphate solution (pH = 10.5), where the Cu(II) ion acts as an oxidizing agent. In the leach liquor, copper exists as the Cu(I)-ammine complex. Besides copper, some other metals, such as, Co, Ni and Zn also report to the leach solution as impurities. To obtain a high purity metallic copper, these impurities must be removed from the leach liquor before feeding to the electrowinning circuit. In this study, a suitable method using solvent extraction has been developed for the selective removal of impurities from the electrolyte containing a large amount of cuprous ion.

EXPERIMENTAL

Procedure

All experiments were carried out with a synthetic aqueous solution that contained cobalt, nickel, and zinc as impurities in addition to a large amount of cuprous ion. To cover a wide range, the impurity concentrations in the synthetic solution were considered to be much higher than those found in the actual leach liquor. Impurities were removed by solvent extraction. All tests were carried out under a nitrogen atmosphere in a glove box to avoid the oxidation of Cu(I). Before using nitrogen gas from the laboratory pipeline, it was further purified in order to remove entrained oxygen using a pyrogallol solution, which is a mixture of 15 wt% pyrogallol (1,2,3-tri-hydroxy benzene) and 30 wt% potassium hydroxide.

Analytical

The metal concentration in the aqueous solution was measured by ICP-AES (Seiko, model: SPS-4000). The metal concentration in the organic phase was calculated by the mass balance from the aqueous metal concentrations before and after equilibrium. The concentration of Cu(I) was calculated from the difference between the total copper measured by ICP and Cu(II) measured using a UV/Vis. spectrometer.

Reagents

The synthetic solution was prepared by dissolving reagent grade metal salts in an ammonia-ammonium sulphate solution. The organic extractant was prepared by diluting LIX 26 in Shellsol D70, and 1-decanol was used as a modifier. Different types of organic extractants, namely VA 10, PC88A, D2EHPA, DNNSA, LIX 63, and LIX 841 were used as the synergic agents.

Extraction

Aqueous and organic solutions were mixed together and stirred at room temperature (25°C) under various experimental conditions. After phase separation, the aqueous feed and raffinates were analysed for the metal concentrations.

Scrubbing and Stripping

The loaded organic was scrubbed with de-ionized water and regenerated by stripping the metal ions using dilute sulphuric acid at room temperature (25°C).

RESULTS AND DISCUSSION

Solvent Extraction (SX)

The SX recovery of Co, Ni and Zn was carried out with LIX 26, which is an oxine-type extractant that contains 7-tetrapropylenyl-8-hydroxyquinoline (Figure 1).

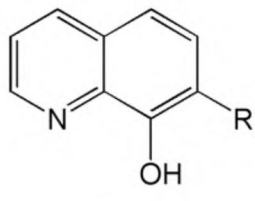


Figure 1 *Structure of LIX 26 (R: Tetrapropylenyl).*

Figure 2 shows the extraction of the metal ions from their individual solutions. The aqueous feed contained 1 g/l Co, 1 g/l Ni, 5 g/l Zn in [5M NH_3+ 1M $(NH_4)_2S0_4$] solution (pH = 10). The organic feed was LIX 26 (5 vol% for Co and Ni, 10 vol% forZn) in Shellsol D-70 in addition to 2-5 vol% 1-decanol as a modifier. Both the aqueous and organic feeds were stirred for over

2 hr at room temperature (25°C). As shown in Figure 2, almost complete extraction of Co, Ni and Zn was achieved at the different A/O ratios.

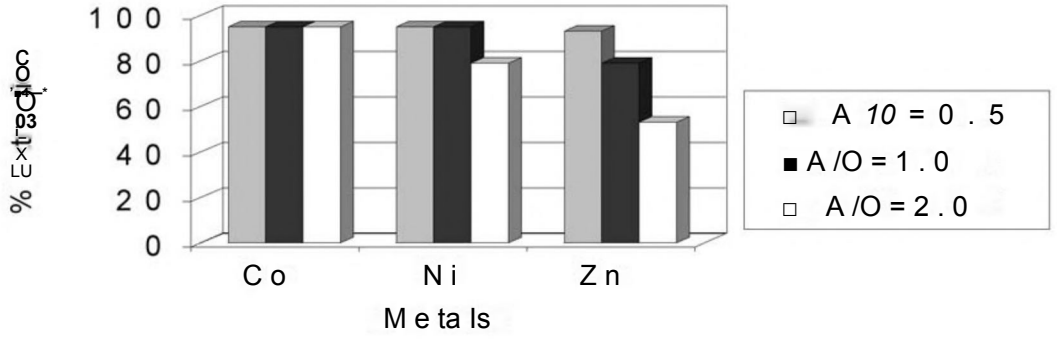


Figure 2. Metals extraction with LIX 26 from their individual solutions.

LIX 26 was further examined to determine its extraction behavior for Cu(I) from the ammoniacal alkaline solution. The test was conducted under a nitrogen atmosphere in a glove box to avoid oxidation of Cu(I). Table 1 shows that copper extraction from its single metal solution in which the copper extraction by LIX 26 is negligible. This is because, under these experimental conditions, almost all the copper existed as Cu(I). Though the extraction of Cu(II) by oxine is strong [5], this extractant does not extract Cu(I) from the ammoniacal alkaline solution as found in this study. However, Muir et al. observed some extraction ability by oxine (Kelex 100) for Cu(I) from chloride media [6],

*Table 1. Recovery of Copper with LIX 26**

Elements	Cu concentration in feed (g/l)	Cu concentration in raffinate (g/l)	Cu concentration in organic (g/l)	% Cu extraction
Cu (total)	31.1	30.3	0.8	2.6
Cu(II)	1.7 (Color = Light blue)	0.06 (Color = Clear)	-	-
Cu(I)	29.4 (95%)	30.25 (99.8%)	-	-

*Aq. feed = Cu(I) in [5M NH_3 + 1M ($NH_4)_2SO_4$], Org. feed = 15 vol% LIX 26 and 5 vol% 1-decanol in Shellsol D70, Time = 10 min, Temp.= 25°C, A/O ratio = 1.

Since LIX 26 works well for the removal of impurities from an ammoniacal alkaline solution and the copper loss by this extractant is negligible, it was used to remove impurities from the leach solution. The aqueous solution containing mixed metal ions was stirred at room temperature with a mixture of 15 vol% LIX 26 and 5 vol% 1-decanol in Shellsol D70. The contact time was 10 min and the A/O ratio = 1.

Table 2. Recovery of metals with LIX 26 from a mixed metals solution.

Metals	Metal concentration in feed (g/l)	Metal concentration in raffinate (g/l)	Metal concentration in organic (g/l)	% Metal extraction
Co	1.1	0.01	1.09	99
Ni	1.1	0.5	0.6	55
Zn	5	1.2	3.8	76
Cu (total)	17.3	15.2	2.1	12
Cu(II)	1.8 (10%)	0.2 (1%)	-	-
Cu(I)	15.5 (90%)	15 (99%)	-	-

As shown in Table 2, the percentages of metal extraction are similar to those found in the single metal systems though Ni extraction is lower and Cu extraction is slightly higher. The low Ni extraction is attributable to its slow kinetics as shown in Figure 3, where Ni was completely extracted only after a 30 min contact time. In this mixed metal system, some copper (12%) was extracted by LIX 26 due to the presence of 10% Cu(II) in the feed solution. The copper loss could be minimized by fully converting Cu(II) to Cu(I) with better instrumental control. The color of the aqueous feed containing the mixed metal ions was blue. However, after impurity removal, the aqueous raffinate became colorless, which proved that only Cu(I) remained in the purified leach solution. The presence of Cu(I) in the purified electrolyte also favors the electrowinning of copper with much less power consumption (284 kWh/tonne Cu as found in this process, whereas 2000 - 2500 kWh/tonne Cu is required in the conventional system [3]).

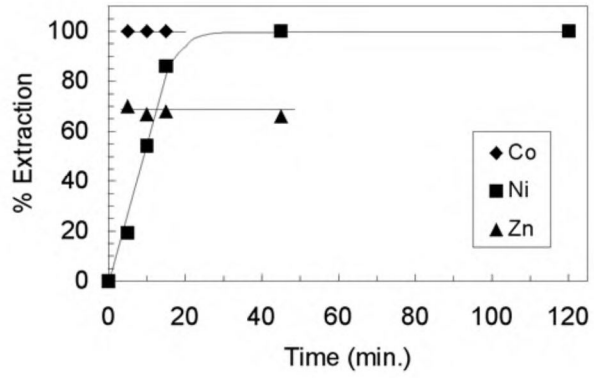


Figure 3. Kinetics of metals extraction.
Aq. feed = 1 g/l each of Co and Ni, and 5 g/l Zn in [5M NH_3 + 1M $(NH_4)_2S0_4$]. Org. feed = 15 vol% LIX 26 and 5 vol% 1-decanol in Shellsol D-70. Temp. = 25°C, A/O ratio = 1:1.

Table 3 shows the extraction of Co, Ni and Zn from an ammoniacal alkaline solution containing a large amount of cuprous ion. The aqueous feed contained 1 g/l each of Co and Ni, 5 g/l Zn and 35 g/l Cu in [5M NH_3+ 1M $(NH_4)_2S0_4$] solution. The organic feed was a mixture of LIX 26 and 5 vol% 1-decanol in addition to the different types of synergic agents in Shellsol D-70. Equal volumes of the aqueous and organic feeds were stirred for 15 min at room temperature (25°C). The shorter contact time (15 min) was chosen to examine the kinetic synergistic effects on Ni extraction. As shown in Table 3, Co, Ni and Zn were extracted to the same extent as before, while copper extraction is very low. Cobalt was completely extracted in all cases. Nickel extraction was greatly enhanced due to the kinetic synergistic effects of the acidic extractants like VA 10, PC88A, D2EHPA and DNNSA. Zinc extraction was increased by the addition of hydroxyoximes (LIX 63 or LIX 841), though in that case, Ni extraction was slightly suppressed, probably due to adduct formation.

Table 3. Synergic extraction of Co, Ni and Zn with LIX 26 from ammoniacal alkaline solution.

Organic extractants	% Co Extraction	% Ni Extraction	% Zn Extraction	% Cu Extraction
15% LIX 26	100	86	72	9.5
15% LIX 26 + 3% VA 10	100	100	68	7.5
15% LIX 26 + 3% PC88A	100	100	67	9
15% LIX 26 + 3% D2EHPA	100	100	68	8
15% LIX 26+ 3% DNNSA	100	100	68	11
15% LIX 26 + 3% LIX 63	100	47	77	10
15% LIX 26 + 3% LIX 841	100	79	76	11
15% LIX 26 + 3% LIX 841 + 3% VA 10	100	100	76	11

Equilibrium studies were carried out for the extraction of Co, Ni and Zn with LIX 26 using single metal systems. The feed contained 1.17 g/l Co, 0.94 g/l Ni and 5.12 g/l Zn in [5M NH_3 + 1M $(NH_4)_2S0_4$] solution at pH 10.0. The concentration of LIX 26 was 5 vol% for the Co and Ni extraction and 10 vol% for Zn extraction. The mixture of the aqueous and organic solutions was stirred for over 2 hr at room temperature. The A/O ratios were varied to cover a wide range of loading values. Saturation loadings of about 2.5 g/l Co, 2 g/l Ni and 7 g/l Zn were obtained under these experimental conditions. Figure 4 shows the McCabe-Thiele diagrams for Co and Ni extraction with 5 vol% LIX 26, and Zn extraction with 10 vol% LIX 26 from their individual solutions. These diagrams indicate that 2 stages of extraction for Co, and 3 stages for Ni and Zn would be sufficient to completely recover these metals from the starting concentrations of 1 g/l Co, 1 g/l Ni and 5 g/l Zn at an A/O ratio of 2 for Co and Ni, and 1 for Zn extraction.

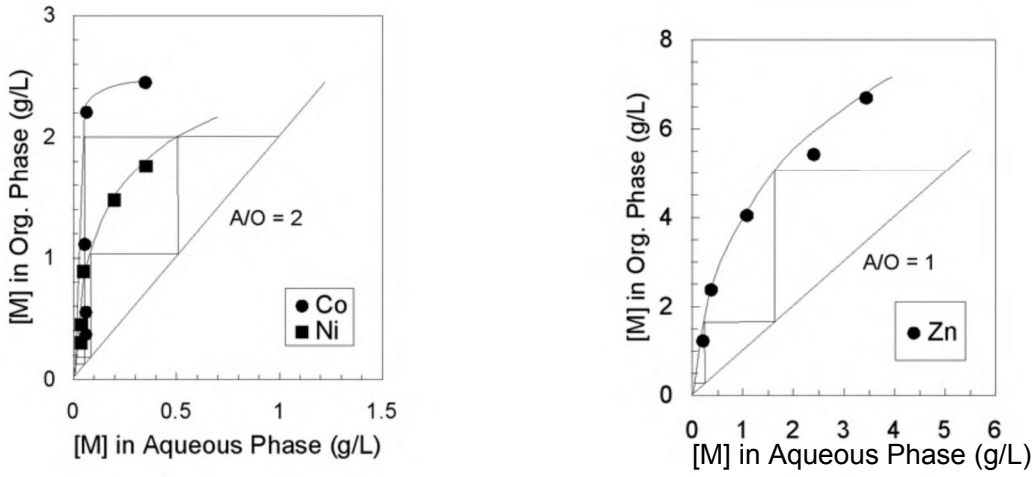


Figure 4. McCabe-Thiele diagrams for Co, Ni and Zn extraction.

Scrubbing and Stripping

The loaded organic was scrubbed with an equal volume of de-ionized water to remove any entrained ammonia. Metal loss during scrubbing is negligible as shown in Table 4. The scrubbed loaded organic was then regenerated by stripping the metals using 20 vol% sulphuric acid. An equal volume of organic and strip solution was contacted for 15 min at 25°C. Table 4 shows the results of the stripping tests, in which all the loaded metals were completely stripped in a single contact. Though Ni and Zn are easily stripped from the loaded oxine (LIX 26 / Kelex 100) with dilute acid [5, 7], the stripping of cobalt is rather difficult unless cobalt exists as cobaltous in the organic phase [8], Hubred et al. patented a process for cobalt stripping using dilute acid where Co(III) in the organic phase was reduced to Co(II) using metallic Cu and NH_3 [9], In the present process, since Co was stripped as Co(II) and the extraction/stripping tests were carried out in a glove box under a nitrogen atmosphere, there was no chance for the oxidation of Co(II) in the loaded organic. Hence Co was easily and completely stripped in this study.

Table 4. Stripping of metals from the loaded organic phase

Metals	Metal concentration (g/l)				% Metal stripping
	Aq. feed	Loaded organic	Scrubbed organic	Stripped organic	
Co	0.1	0.1	0.1	0	100
Ni	1	0.94	0.91	0	100
Zn	4.7	3.4	3.4	0	100
Cu	55	5.8	5.5	0	100

Extraction Mechanism

Under the experimental condition at pH 10.5, metals exist as cationic ammine complexes, such as $Co(NH_3)_6^{2+}$, $Ni(NH_3)_6^{2+}$, and $Zn(NH_3)_4^{2+}$. Since LIX 26 is a cation exchange chelating extractant, the metal (M) was extracted via a cation exchange mechanism as shown in Equation 1, where LIX 26 is denoted by R-HQ and the bar represents the organic phase.

$$M(NH_3)_m^{n+} + n\,\overline{R\text{-}HQ} = \overline{M(RQ)_n} + n\,\overline{NH_4^+} + (m\text{-}n)NH_3 \qquad (1)$$

CONCLUSIONS

A suitable method has been developed to remove impurities from a copper leach solution in the new energy-saving cuprous electrowinning process. In this method, Co, Ni and Zn were selectively removed from an ammoniacal alkaline solution (pH = 10 - 11) containing a large amount of copper by solvent extraction with LIX 26. Saturation loadings were about 2.5 g/l Co and 2 g/l Ni for 5 vol% LIX 26, and 7 g/l Zn for 10 vol% LIX 26. McCabe-Thiele diagrams suggested that 2 stages for Co, and 3 stages for Ni and Zn extraction is sufficient to completely remove all impurities under these experimental conditions. The extraction kinetics for Co and Zn are very fast (a couple of minutes), while complete Ni extraction was achieved after 25 min of contact. The nickel extraction rate was greatly enhanced due to the kinetic synergistic effects of the acidic extractants, whereas Zn extraction was increased by the addition of hydroxyoximes. The metals were extracted with LIX 26 via a cation exchange mechanism. The loaded organic was regenerated by stripping metals completely using dilute sulphuric acid. Copper loss in the purification stage is negligible, and, after purification of the leach solution, copper remained as monovalent copper in the electrolyte that favors the electrowinning of copper with much less power consumption, which made this process robust in terms of energy-savings.

ACKNOWLEDGEMENTS

Financial support from the Japan Society for the Promotion of Science (JSPS) is gratefully acknowledged. The authors thank Cognis for providing the LIX 26 used in this study.

REFERENCES

1. Japan Printed Circuit Association, Citation formats (in Japanese) for Internet sources *[Internet],* Available from: <http://www.jpcanet.or.jp>. *[Accessed 7 October 2004],*
2. M. Clapham (2004), *TMS - EPD Congress 2004*, North Carolina, USA, pp. 541-553.
3. K. Koyama, M. Tanaka and J. -C. Lee (2003), *Proc. Fifth Int. Conf. in Honor of Prof. Ian Ritchie.* TMS. Vancouver. Canada, pp. 1555-1563.
4. M. S. Alam, M. Tanaka, K. Koyama and J. -C. Lee (2004), *Proc. 43rd Annual Conf. of Metallurgists of CIM,* Hamilton, Canada, pp. 199-213.
5. G. M. Ritcey and B. H. Lucas (1975), *Hydrometallurgy*, 105-113.
6. D. M. Muir, M. D. Benari and J. S. Preston (1980), *Proc. Int. Solv. Extr. Conf.,* pp 80-77.
7. V. I. Lakshmanan, R. Sridhar and M. S. Alam (2002), *Canadian Pat.,* No. CA 2347552 (Nov. 14).
8. G. M. Ritcey and A. W. Ashbrook (1979), Solvent Extraction: Principles and Applications to Process Metallurgy, Part II, Elsevier, Amsterdam, pp. 343.
9. G. L. Hubred, R. N. Kust, D. L. Natwig and J. P. Pemsler (1975), *U. S. Pat.,* No. 4,083,915 (Nov. 20).

CYANIDE RECOVERY FROM ALKALINE SOLUTIONS BY SOLVENT EXTRACTION

Rodrigo C. Andrade and Afonso H. Martins

Universidade Federal de Minas Gerais
Departamento de Engenharia Metalurgica e de Materiais,
Rua Espirito Santo 35 sala 206-AG, Centro, Belo Horizonte (MG), CEP 30160-030, Brazil.
Phone:(5531)32381810 Telefax:(5531)32381815 E-mail: ahmartin@demet.ufmg.br

This technical note presents the preliminary experimental results at laboratory bench scale-up for the study involving the usage of commercial organic extractant CYANEX 921® (trioctylfosfine oxide) diluted in xylene for cyanide extraction from pure alkaline aqueous solution with a chemical composition similar to a typical cyanidation liquor of gold ore.

The experimental results for only one contact stage showed that an increase of the CYANEX 921® concentration in the organic phase improved the percent of cyanide extraction. Besides, the zinc presence in the feed aqueous phase also improved the cyanide extraction (38.48%) comparing the result for the experiment without zinc (35.50%). The highest values for percent of cyanide extraction were obtained at the initial pH of the aqueous phase equals to 9.0.

INTRODUCTION

Cyanide is used in the leaching for gold extraction from ores and it is an expensive hydrometallurgical reagent. Most of this cyanide for gold leaching is consumed by its oxidation to cyanide salts and due to the metal cyanocomplexes formation in the leach liquor. Cyanide recovery procedures assume an important role for mineral industrial plants for gold recovery under the economic point of view. Besides, cyanide is a highly toxic compound, which its emission to the environment is limited to 0.2 g/l by the legislation of several countries.

Several cyanide recovery techniques from industrial cyanidation liquors have been studied. Among these techniques some of them with potential of application can be mentioned, for instance, oxidation by using $S0_2$, natural degradation, AVR (acidification, volatilization, regeneration) process, chemical oxidation and biological treatment [1], However, little attention has been paid to the application of solvent extraction as an alternative process for cyanide recovery [2-7],

This work presents the experimental results for cyanide extraction from an alkaline synthetic aqueous solution with a cyanide concentration similar to a typical leach liquor for gold extraction by using CYANEX 921® (trioctylfosfine oxide) diluted in xylene.

EXPERIMENTAL PROCEDURE

Tests were performed by contacting an aqueous phase containing cyanide and an organic phase formed by CYANEX 921® diluted in xylene. These two phases were put into physical contact by different times and submitted to different experimental conditions taking into consideration some parameters, such as, cyanide concentration in the aqueous phase, CYANEX 921® concentration in the organic phase, initial pH of the aqueous phase and presence of zinc metal in the aqueous phase working in the system as a complex agent for free cyanide.

Tests were carried out at 25±1°C in Erlenmeyer glass flasks of 500 ml capacity were the organic and aqueous phases were kept under magnetic stirring for 30 minutes. After contact between organic and aqueous phases, they were fed to a glass separation funnel for decantation and to collect an aqueous phase sample for cyanide concentration determination by chemical analysis.

Synthetic aqueous solutions used in the experiments were prepared by dissolving 4.0 g of NaOH and 2.5 g of NaCN in 100 ml of distilled water. Some experiments used aqueous solutions having additions of 0.2 g of zinc metal (99% pure).

Different concentrations of CYANEX 921® (Cyanamid-USA) diluted in xylene were used to prepare the organic phases for each test. The maximum solubility of the extractant CYANEX 921® in xylene used in the experiments was 450 g/l.

The cyanide concentration in the samples of aqueous phases collected during the experiments was determined by titration using a $AgN0_3$ (0.0192N) solution and dimetylaminebenzolrodanine as indicator [8], Percent of cyanide extraction was determined by the difference between the initial cyanide concentration in the feed aqueous solution and the cyanide concentration in the aqueous phase after contacting with the organic phase.

RESULTS

Previous research work [8] has determined some solvent extraction parameters used in the experiments of this work, for instance, aqueous and organic phases ratio and organic phase volume used for contacting with the aqueous phase.

Table 1 shows the experimental results for percent of cyanide extraction for different times of contact between aqueous and organic phases kept under intense magnetic stirring. The experimental conditions used in the tests were 4.0 g of NaOH and 2.5 g of NaCN in 100 ml of aqueous phase, initial pH equals to 12.8, 3.0 g of CYANEX 921® diluted in 20 ml of xylene in the organic phase and 2 hours for separation of phases.

Table 1 - Experimental results for percent of cyanide extraction versus time of contact between phases

	time of contact between phases (minutes)		
	30	45	60
Initial concentration of CN (g/l)	13.97	13.96	13.96
Final concentration of CN (g/l)	12.78	12.87	12.97
Cyanide extraction (%)	8.49	7.86	7.12

The best result was obtained for 30 minutes of contact between phases showing 8.49% of cyanide extraction. Besides, for the experimental conditions adopted in this work, the longer times of contact the lower percent of cyanide extraction.

Table 2 presents the experimental results for the percent of cyanide extraction for increasing the concentration of organic extractant CYANEX 921® in the organic phase under the same experimental conditions used in the experiments which the results were shown in Table 1. The increase of organic extractant concentration from 3.0 g to 9.0 g of CYANEX 921® diluted in xylene in the organic phase raised the cyanide extraction from 8.57% to 36.38%. This expressive increase was related to a higher number of functional groups of the organic extractant available in the system for contacting more cyanide ions in the aqueous phase causing an increase in the cyanide extraction.

Table 2- Experimental results for the percent of cyanide extraction versus CYANEX 921® concentration in 20 ml of organic phase

	mass of CYANEX 921® in 20 ml of organic phase (g)		
	3.0	6.0	9.0
Initial concentration of CN (g/l)	13.96	13.97	13.99
Final concentration of CN (g/l)	12.77	9.86	8.90
Cyanide extraction (%)	8.57	29.44	36.38

The experimental results for percent of cyanide extraction in function of the initial pH of the aqueous phase are presented in Table 3. The experimental conditions used in the tests were 4.0 g of NaOH and 2.5 g of NaCN in 100 ml of aqueous phase, 9.0 g of CYANEX 921® diluted in xylene, 30 minutes of contacting time between phases and 2 hours of time for separation of aqueous and organic phases.

Table 3 - Experimental results for percent of cyanide extraction in function of the initial pH of the aqueous phase

	initial pH of the aqueous phase		
	12.88	10.00	9.00
Initial concentration of CN(g/l)	13.97	13.96	13.97
Final concentration of CN (g/l)	13.07	10.78	9.01
Cyanide extraction (%)	6.40	22.80	35.50

The results in Table 3 indicated that diminishing the value of the initial pH of the aqueous phase it favored the raise of percent of cyanide extraction. These results might be related to a higher hydration of the CN' ions in the aqueous solution caused by lowering the initial pH with additions of hydrochloric acid.

Table 4 showed the results obtained for some experiments performed with additions of 0.2 g of zinc metal (PA) in the aqueous phase and using the same experimental conditions depicted for the results shown in Table 3. The goal of the addition of zinc metal in the aqueous solution was to evaluate the contribution of the complexed CN to the total cyanide extraction by CYANEX 921®.

The presence of zinc in the aqueous phase enhanced the cyanide extraction for all three pH values tested comparing to the results showed in Table 3, especially, for pH=11.5. The highest value for cyanide extraction 38.48% was also obtained for the lowest pH studied

equals to 9.0, however, the positive influence of the zinc addition was much lower than for pH= 11.5.

Table 4 - Experimental results for percent of cyanide extraction in function of the initial pH of the aqueous phase having additions of 0.2 g of zinc metal to the aqueous feed solution

	initial pH of the aqueous phase with addition of 0.2 g of Zn		
	11.5	10.0	9.0
Initial concentration of CN (g/l)	13.96	13.97	13.97
Final concentration of CN (g/l)	11.58	11.11	8.59
Cyanide Extraction (%)	17.03	25.50	38.48

Due to the result obtained for just 0.2 g of zinc added to the aqueous phase, another experiment was carried out to evaluate the influence of the increase of the zinc concentration in the aqueous phase on the cyanide extraction. Table 5 showed the results obtained for the percent of cyanide extraction for different zinc metal concentration added to the aqueous phase. The experimental conditions were the same used in the experiments with addition of just 0.2 g of zinc metal but the initial pH of aqueous phase was maintained in 9.0.

Table 5 - Experimental results for percent of cyanide extraction versus concentration of zinc metal in the aqueous phase

	Zn [g/l]	
	2.0	3.0
Initial concentration of CN (g/l)	13.97	13.98
Final concentration of CN (g/l)	8.59	9.61
Cyanide Extraction (%)	38.48	31.24

The increase of zinc concentration initially added to the aqueous phase diminished the percent of cyanide extraction. It was expected that more zinc in solution would enhance the complexation of free cyanide in solution and more cyanide would be extracted by the organic extractant. However, this excess of zinc ions in solution was preferentially extracted by the CYANEX 921® leaving less chemical bonds of the extractant available for cyanide extraction from the solution.

CONCLUSIONS

The presence of zinc metal in the aqueous feed solution enhanced the cyanide extraction (38.48%) when compared to the experiment without zinc metal addition (35.50%) under the same experimental conditions. However, the more positive effect was detected for pH=11.5.

The highest values for the percent of cyanide extraction were obtained for the initial pH of the aqueous phase equals to 9.0.

The increase of the CYANEX 921® concentration in the organic phase also improved the percent of cyanide extraction passing from 8.57% for 3.0 g of CYANEX 921® diluted in 20 ml of xylene to 36.38% of cyanide extraction for 9.0 g of CYANEX 921®.

ACKNOWLEDGMENTS

The authors wish to thank Foundation for Supporting Scientific Research of the Minas Gerais State (FAPEMIG)/Brazil and Millennium Science Initiative Program- Water: a mineral approach (Brazilian Science Foundation-CNPq) for financial support this work.

REFERENCES

1. J.S. Scott. An overview of cyanide treatment methods for gold mill effluents. Proc. Cyanide and the Environment Conference, Ed. D. van Zyl, Tucson, Arizona, 2, 1984, 307-327.
2. F.J. Alguacil, C. Caravaca, A. Cobo, S. Martinez. The extraction of gold (I) from cyanide solutions by the phosphine oxide CYANEX 921. *Hydro metallurgy,* 35, 41-52, 1994.
3. F.J. Alguacil, C. Caravaca. Synergistic extraction of gold(I) cyanide with the primary amine Primene JMT and the phosphine oxide CYANEX 921. *Hydrometallurgy,* 42, 197-208, 1996.
4. C. Caravaca, F.J. Alguacil, A. Sastre. The use of primary amines in gold (I) extraction from cyanide solutions. *Hydrometallurgy,* 40, 263-275, 1996.
5. F.J. Alguacil, C. Caravaca, J. Mochon, A. Sastre. Solvent extraction of Au $(CN)'_2$ with mixtures of the amine Primene JMT and the phosphine oxide CYANEX 923. *Hydrometallurgy,* 44, 359-369, 1997.
6. M.I. Martin, F.J. Alguacil. Synergism in gold-cyanide extraction with Primene JMT-CYANEX 925 mixed extractant system. *Hydrometallurgy,* 49, 309-32, 1998.
7. J.H. Bright. A feasibility study for the extraction of cyanide from aqueous solution by solvent extraction with tri-n-octylphosphine oxide (TOPO). Progress Report number 83-17, American Cyanamid Company-USA, 4 pages, 1983.
8. R.C. Andrade. *Solvent Extraction Applied to the Cyanide Recovery.* Scientific Initiation Program/FAPEMIG/PROBIC, Final Report, February 2004, Belo Horizonte, Minas Gerais, Brazil, 13 pp. (in Portuguese).

NOVEL COMPUTATIONAL CHEMISTRY FOR MOLECULAR DESIGN OF RADIOACTIVE METAL COMPLEXES

Kazuharu Yoshizuka, Hans-Juergen Pietzsch*, Sepp Seifert*, and Holger Stephan*
The University of Kitakyushu, Kitakyushu, Japan
*Forschungszentrum Rossendorf, Dresden, Germany

We are now developing a novel molecular modelling of Re and Tc complexes combined with the molecular mechanics and the molecular dynamics for estimatina the oartition coefficient of these complexes between water and 1-octanol (LogP). The MM potential parameters developing with MOMEC program were fitted to all relevant X-ray crystal structures of $[TcO(DMSA)_2]^-$ and $[ReO(DMSA)_2]^-$ (DMSA: dimercaptosuccinic acid). The MM potential parameters were transferred to that in the MD program, MASPHYC. The MD simulations also indicate that a quantitative structure property relationship (QSPR) is obtained, which relates the internal energy difference between the Tc/Re-DMSA complexes in water phase and that in 1-octanol phase with experimental LogP value.

INTRODUCTION

Computing of the structures and properties of chemical compounds is gaining increasing importance as computational techniques become increasingly accurate, and as high-performance computing and molecular graphics become available at relatively low cost. Computational chemistry is now widely recognized as a powerful tool for the design of new molecules with specified properties, and for interpreting their stabilities, reactivities and other physical properties [1, 2], Molecular mechanics (MM) calculations are among the simplest and fastest techniques, and are therefore extremely useful when considering very large molecules (e.g. biomolecules) or a large number of structures (e.g. a whole set of isomers or conformers of complex molecules). Molecular dynamics (MD) simulations using empirical potential functions and parameters are being widely applied to elucidate the dynamic behavior and the thermodynamic properties of molecules in dense phases, such as aqueous and organic solutions.

By virtue of its ideal nuclear physical characteristics for routine nuclear medicine diagnostics and its ready availability, technetium-99m (^{99m}Tc) is still of outstanding interest in the development of novel radiopharmaceuticals. Its congener rhenium in form of the beta-emitting isotopes ^{186}Re and ^{188}Re is an attractive radioisotope for radiotherapy and radioimmuno-therapy. A variety

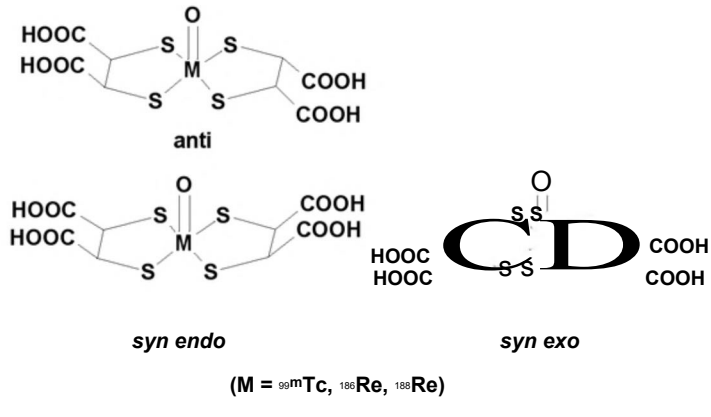
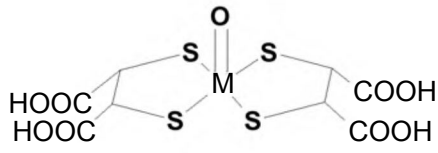


Figure 1 Tumorseeking Tc and Re-DMSA complexes as used in diagnostics and palliative radiotherapy

of ligands for complexation technetium and rhenium at oxidation states +5, +3, and +1 has been described in the literature. Among them dimercaptosuccinic acid (DMSA) is a well-known ligand that forms isomeric complexes with technetium(V) and rhenium(V). The tumourseeking agents $[MO(DMSA)_2]'$ has found clinical application for imaging (^{99m}Tc) and therapy (^{86}Re, ^{188}Re).

Since the lipophilicity of radiotracer complexes is well correlated to the biodistribution [3], it is eager to develop a novel estimation method of LogP for radiotracers. We are now developing such an estimation method of LogP of Re and Tc complexes combined with the molecular mechanics (MM) and the molecular dynamics (MD).

In this paper, we describe a novel molecular modelling of Re and Tc complexes combined with both the computational chemistry and quantitative structure-property relationship (QSPR), for estimating LogP of Re and Tc complexes with dimercaptosuccinic acid (DMSA) derivatives as model compounds. Figure 2 shows the chemical structure of the Tc/Re complexes used in this study, that is $[TcO(DMSA)_2]'$ and $[ReO(DMSA)_2]'$ (DMSA: dimercaptosuccinic acid).



(M = ^{99m}T c, ^{186}Re, ^{188}Re)

Figure 2 Tc and Re-DMSA complexes used in this study

CALCULATION METHOD

MM Calculations

The MM calculations were performed with the strain minimization program, "MOMEC97" [4, 5], Within the molecular mechanics frame work, the structure of a molecule is modified in order to minimize its total strain energy ($L/_{to}tai$) consisting of bond length deformation (E_b), valence angle deformation (E_0), torsion angle deformation *(E$)* and nonbonded interaction (E_{nb}), as expressed by Eq.(1).

$$Utotal = S(Eb + Eo + E_4, + Enb) \quad (1)$$

A harmonic M-L stretching potential is used for the metal-donor interaction. The angular geometry around the metal center is modeled by interligand nonbonded interactions, and torsional potentials, as well as nonbonded interactions involving the metal center are neglected [6],

Input coordinates were obtained from X-ray crystal structure data in the Cambridge Crystallographic Data Centre (CCDC) literatures [7, 8], The constant values of force field parameters were adjusted until an optimal agreement between calculated and observed structures was obtained throughout the entire range of available structures. The final differences between observed and computed bond distances are ≤0.02A, those for valence angles are ≤3°.

MD Simulations

The MD simulations were performed the MD program, "WinMASPHYC Pro" [9], The potential parameters for MD calculations were transferred from those of MM described above. The numbers of water and 1-octanol molecules are 267 and 25, respectively, in 1.61x1.61x6.05 nm boundary cell to realize the practical density (p = 0.914 g/cm^3). One molecule of metal-DMSA complex is set either into water phase or into 1-octanol phase. Calculation was performed by each 0.1 fs for 100 ps under the NTV ensemble at 298 K.

RESULTS AND DISCUSSION

MM Calculations

Figure 3 shows RMS overlays of the lowest energy structure of the Re-DMSA complex calculated by MOMEC97 and the crystal structure cited in [7, 8], Since both structures are in good agreement (RMS = 0.24A), we consider that this force field parameters are also adaptable for the calculation of similar complex structures.

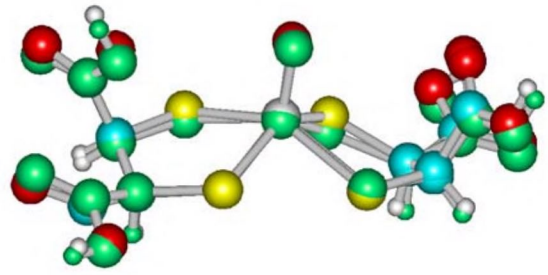


Figure 3 Overlay of computed MOMEC and X-ray structures of DMSA-Re complex.

MD Simulations

Figure 4 shows the MD snapshot of DMSA-Re complex in water-1-octanol binary system after 100 ps. The DMSA-Re complex is stabilized by solvation of DMSA moieties with surrounding 1-octanol molecules.

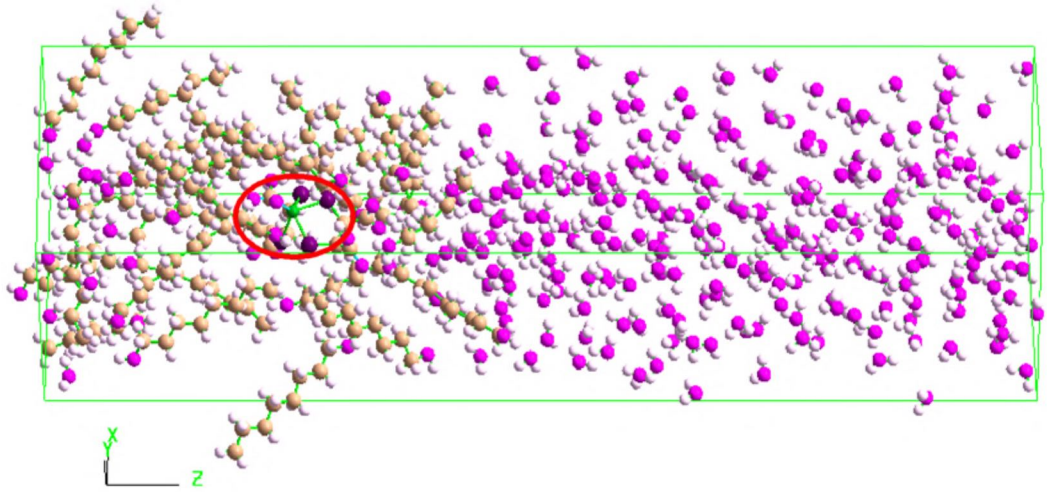


Figure 4 MD snapshot of DMSA-Re comolex m water — 1-octanol hmarv svstem• circle indicates the position of DMSA-Ri

Figure 5 shows the time course of internal energy of water-1-octanol binary system as shown in Fig. 4. After 50 ps, since whole internal energy of the boundary cell of the binary system is approached to a constant value, we consider that this internal energy is defined to be an equilibrium internal energy within the micro scale of interfacial area of binary system.

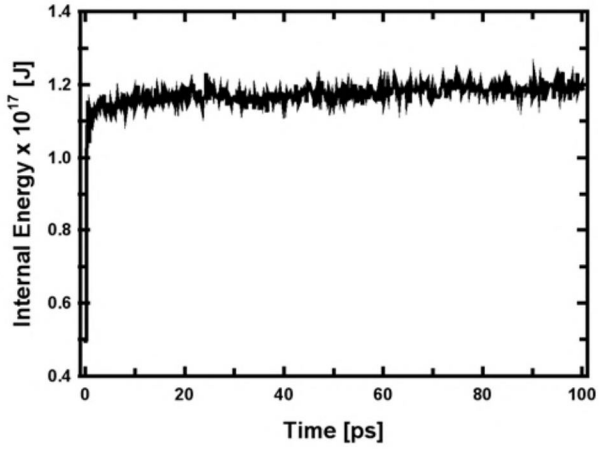


Figure 4 Time course of internal energy of DMSA-Re complexes in water-1-octanol binary system.

QSPR for estimating logP of DMSA-metal complexes

The relation between the internal energy difference of DMSA-metal complex contributing from DMSA-metal complex to the water-1-octanol binary system, A*U,* can be expressed by [10]:

$$A\,U = U_M - U_{soj} - U_{com} \qquad (2)$$

where *U,* (i = all, sol, com) are the relevant internal energies of all molecules in the binary system, solvent molecules in the system and DMSA-metal complex alone, respectively.
From these internal energy differences, the QSPR equation for estimating logP can be is obtained:

$$AA\,U = AL/\text{-}|.\text{octanol} - AL/_{W}\text{ater} - Cl\ \log P \qquad (3)$$

where a is the apparent QSPR constant of above relationship, and subscript "1-octanol" and "water" indicate the internal energy difference of DMSA-metal complex existing either in 1-octanol phase or water phase in the boundary cell.

Table 1 lists the energy difference *AAU* and the corresponding LogP values for the DMSA complexes of technetium and rhenium. *AAU* of the technetium complex with DMSA is smaller than the corresponding rhenium complex. This means that the technetium complex is more lipophilic than the rhenium analogue. That can be mainly explained on the basis of different *van der Waals* interaction of the complexes with surrounding 1-octanol molecules. Moreover, it is elucidated that *AAU* directly reflects the energy difference between non-bonded interaction of the complex and solvent. The experimentally determined LogP values corroborate the calculated results. Currently, we are attempting to obtain the apparent QSPR constant a between the calculated *AAU* and the experimental values of LogP for tumortropic ester derivatives of Tc(V)- and Re(V)-DMSA.

Table 1: The energy difference AAU and LogP values of $MO(DMSA)_2]$' (M = Tc, Re).

complex	*AAU* [kJ/mol]	Log P
$[TcO(DMSA)_2]$-	-45.96	-2.12±0.02*
$[ReO(DMSA)_2]$'	-6.02	-2.37±0.03**

*** [^{wm}TcO(DMSA)$_2$r , ** [^{188}ReO(DMSA)$_2$]'**

CONCLUSION

We propose a novel molecular modelling of Re and Tc complexes combined with the molecular mechanics and the molecular dynamics for estimating the lipophilicity of Tc- and Re-DMSA complexes. A molecular mechanics force field for DMSA-metal complexes is also developed by fitting to all relevant X-ray crystal structures of DMSA complexes. By the MD potential functions and parameters transferred from MM force field, the MD simulations were carried out to obtain the dynamic behaviour of Tc/Re-DMSA complexes in water and 1-octanol phases. The quantitative structure property relationship (QSPR) between the internal energy difference of Tc/Re-DMSA complexes in water-1-octanol binary system and the experimental logP value can be derived.

ACKNOWLEDGEMENTS

We gratefully acknowledge the financial support under a bilateral program between JSPS and DAAD for staying at Forschungszentrum Rossendorf. The present work is also supported by Grant-in-Aids for Scientific Research and for 21st Century COE Program from the Ministry of Education, Science, Sports and Culture of Japan.

REFERENCES

1. A. R. Leach (1999), “Molecular Modeling, Principles and Applications”, Longman.
2. K. Yoshizuka (2004), *Anal.Sci.,* 20, 761-765.
3. S. Seifert, R. Syhre, H. Spies, B. Johannsen (1997), *Appl. Radiat. Isot.,* 48, 1051-1057.
4. P. Comba, T. W. Hambley (1995), “Molecular Modeling of Inorganic Compounds”, VCH, Weinheim.
5. P. Comba, T. W. Hambley, N. Okon (1997), “MOMEC97, a molecular mechanics package for transition metal complexes”, University of Heidelberg, Germany.
6. P. Comba, K. Gloe, K. Inoue, T. Krüger, H. Stephan, K. Yoshizuka (1998), *Inorg. Chem.,* 37, 3310-3315.
7. J. Singh, A. K. Powell, S. E. M. Clarke, P. J. Blower (1991), *Chem. Commun.* 1115-1117.
8. P. Leibnitz, G. Reck, H.-J. Pietzsch, H. Spies (2001), *Report FZR-311,* Forschungs-zentrum Rossendorf, 46-47.
9. Fujitsu Co. Ltd. (2002), “WinMASPHYC 2.0 Pro.”.
10. K. Yoshizuka, K. Inoue, P. Comba (2000), *Kagaku Kogaku Ronbunshu*, 26, 517.

EXTRACTION OF GOLD (III) IONS FROM AQUEOUS SOLUTIONS USING EMULSION LIQUID MEMBRANE TECHNOQUE

Ali Kargari ; Tahereh Kaghazchi*; Mansooreh Soleimani

Department of Chemical Engineering- Amirkabir University of Technology
(Tehran Polytechnic) - Tehran 15875-4413 - Iran
Telefax: 0098-21-649-9066; E-mail: kaghazch@aut.ac.ir

Experimental results for the batch extraction of gold (III) ions using an emulsion liquid membrane with an internal alkaline aqueous sodium sulfite are presented. Experiments were performed using LK-80 as the biodegradable emulsifier for the first time in emulsion liquid membrane technology. The effects of various parameters, such as Au(lll) concentration in the aqueous phase, concentration of carrier in the membrane phase, concentration of sodium sulfite in the internal stripping phase, pH of the external aqueous phase and the speed of agitation on the extraction rate were studied. Results showed that nearly all of the Au(lll) ions in the aqueous phase were extracted in few minutes. By proper selection of the extraction conditions, almost all of the gold ions present in a concentrated feed solution were extracted within less than 25 minutes. A Taguchi analysis has been performed on the experimental results, which determined the effects and contribution of each of the parameter on the extraction efficiency and interaction between the parameters.

INTRODUCTION

Solvent extraction has been widely used in the recovery of metals from aqueous solutions [1], In these processes, metal ion containing solution contacts with a large amount of selective solvent. After extraction, this process is followed by stripping. Solvent extraction is very difficult for the separation of trace amounts of metal ions because of low driving force, and then a large amount of solvent is required. These make the extraction and stripping of desired species very expensive.

The idea to perform extraction in a three-phase system with emulsion liquid membranes (ELM's) is relatively new. The first papers on liquid membranes have appeared in 1968 bv N.N. Li [2,3], Separation techniques using ELM's have been noted as an attractive means of affecting a wide variety of separation of hydrocarbons [4], recovery and removal of organic acids and amines [5,6], waste water treatment [7-10], recovery and purification of metal ions [9-11] and biomedical applications such as artificial kidney [6],

Emulsion liquid membranes are typically made by, first dispersing the internal phase in an immiscible liquid and then dispersing this emulsion in a third phase (called the external phase). Normally, the internal and the external phases are miscible, but both are immiscible with the membrane phase separating them [12,13],

Gold can be recovered from different solutions by well-defined techniques such as cementation, carbon adsorption, solvent extraction, etc. In the case of conventional solvent extraction technique for the recovery of gold from hydrochloric acid solutions, several studies have been performed using various types of extractants such as basic extractants like amines, solvating extractants such as neutral organophosphorus compounds and other

extractants containing S as the donor atom. Few studies have been done on the separation of gold ions by liquid membranes [14-17], Most of them were done by using supported liquid membranes [14], The only study of gold extraction by emulsion liquid membrane was carried by N. Yan and co-workers [18],

In the present study, extraction of gold by emulsion liquid membrane was investigated. A novel emulsifier was used for preparation of desired emulsions, which is very stable to highly alkaline-reducing and acidic aqueous solutions. The emulsifier has a natural base and so is biodegradable. We named it LK-80. Chemically, it is a wax rather than a fat, being a complex mixture of esters and polyesters of 33 high-molecular-weight alcohols and 36 fatty acids. In this work, methyl iso-butyl ketone (MIBK) was used as carrier and liquid paraffin as membrane phase.

EXPERIMENTAL

Apparatus

All experiments were performed at constant temperature of 25±0.2 °C using a water bath equipped with a P- type controller and an agitator. Extraction experiments were carried out in a cylindrical glass container with 105mm diameter and 145mm height equipped with four round glass baffles with 8mm diameter. The stirrer for the extraction experiments was made of glass with 43mm diameter and had four pitched blades with 30° angle. Stirring driver was a laboratory mixer model RE-166 from Ika-Werk Germany with variable speed from 50-6000 rpm. The stirrer for the emulsion preparation was made from stainless steel and coated with LDPE to minimize contamination of emulsion. It had six pitch blades with 45° angle and 63mm diameter.

Sampling were done at predetermined time intervals by disposable sanitary syringes and centrifuged by a laboratory centrifuge in order to separate emulsion phase from external phase. To determine the concentration of gold ions in the external phase, an atomic absorption spectrophotometer of Unicam model 939 was used. pH measurements were carried out by Teb Azma pH meter.

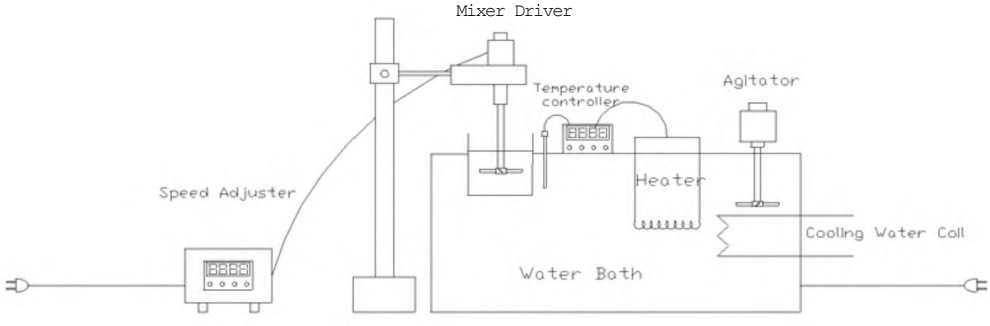


Figure 1- A scheme of experimental set up.

Reagents

Sodium hydroxide , sodium sulfite , iso-butyl methyl ketone, nitric acid and auric chloride were of reagent grade and purchased from Merck. Emulsifier LK-80 was purchased from local market. The HLB value for LK-80 was 4.5. Liquid paraffin with density of 0.82-0.84 gr/cm^3 at 20°C and viscosity of 25-26 cP at 40°C was supplied from Rose Polymer Co.

Stock gold chloride solution was prepared by dissolution of pure metallic gold with 99.99 assays in a mixture of hydrochloric acid and nitric acid with a defined volumetric ratio (aqua-regia). The solution that completely dried by evaporation was then dissolved in a mixture of

hydrochloric acid and distilled water with defined proportion. Distilled water was used throughout.

Procedure

All experiments were performed at 25±0.2°C. Emulsions were prepared by mixing the liquid paraffin and the emulsifier under moderate heating. Then, the internal phase was added to the mixture and mixed for 10 minutes at 6000rpm. Finally, the carrier was added to the emulsion and mixed for additional 2 minutes. The final volume of the emulsion was about 137 ml.

The external phases were prepared by diluting of the stock solution with distilled water to 500ml followed by pH adjustment. The external phases were placed into a water bath for 20 minutes and then the emulsion was added to the external phase with stirring. The external phase solution was periodically sampled at certain time intervals. The concentration of gold in the solution was determined after separation of the emulsion phase, by the atomic absorption spectrophotometer at 242.8 nm.

RESULT AND DISCUSSION

It is well established that an anion carrier can act as a selective carrier for chemical species in transportation processes [19]. In chloride solutions, gold exists as complex anion $AnClj$. MIBK molecule presents oxygen-unpaired electrons, so they tend to unite with protons (H^+) in acidic solution and then react with $AuCl_{\sim 4}$. The carrier MIBK extracts gold on the external surface of emulsion droplets according to the following reactions:

$$AuHCl_4\ AH_20 + H_20\text{-}AuCl; + 5H_20 + H^+ \quad (1)$$

$$[C_AH_9\text{-}(CH_3)C = 0 : H]^+ AuCl; \rightarrow [C\backslash H_9\text{-}(CH,)C = O\ .\ H]'\ AuCI; \quad (2)$$

The gold-MIBK complex transfers across the membrane phase and reacts with the internal phase at the outer surface of internal phase droplets according to the following reaction:

$$2Na_2SO_3 + (C_4//_9\text{-}C(CH_3) = O\ .\ H)^+\ AUCl_A + NaOH \rightarrow$$

$$NaAuSO, + Na_2SO_A + C_AH_9\text{-}(CH_3)C = O : +2HCl + 2Nad \quad (3)$$

According to the above reaction, Au^{3+} reduces to Au^+ in the alkaline sulfite solution. At the extraction condition, Au^+ ions are not able to form complex with MIBK and move back to the external solution [18],

Effect of external phase concentration

Effect of Au^{3+} concentration in the external phase, at speed of agitation of 510 rpm, has been shown in Figure 2. It is reasonable that by increasing the Au^{3+} concentration in the external phase, the time for extraction also increases. The fixed amount of carrier in the experiments causes nearly the same extraction rate. In other words the time for extraction increases by increasing the external phase concentration. This is true for all extraction processes.

Effect of the carrier concentration

Effect of the MIBK as the carrier in the membrane phase is shown in Figure 3. Increasing the amount of carrier has two effects. The viscosity of membrane phase, which limits the extraction rate, decreases by increasing the carrier concentration and hence the carrier acts as thinner for the membrane phase. At the same time, increasing the carrier concentration over a certain limit decreases the stability of the emulsion [20-24], On the other hand, increase in concentration of the carrier in the membrane phase increases the ability of the membrane phase for extraction. The best value of the carrier concentration was found to be about 2.92vol% based on emulsion phase in our experiments.

Effect of reagent concentration in the internal phase

Effect of the internal phase concentration on the extraction efficiency has been shown in Figure 4. Increase in the internal phase reagent concentration increases the ability of the internal phase for stripping the gold-MIBK complex at the external surface of the internal

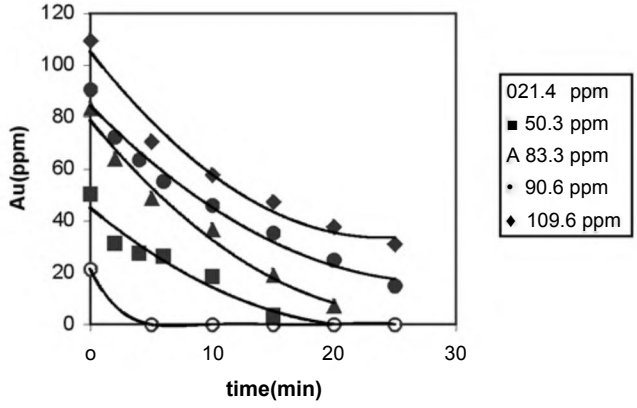


Figure 2- Effect of the external phase on the extraction efficiency.
C_i *= 0.4M* Na_2SO_y, 0.4*M NaOH;* C_c = 1.1 %; R_{ew} - 0.274; *pH* - 0; 510 *rpm.*

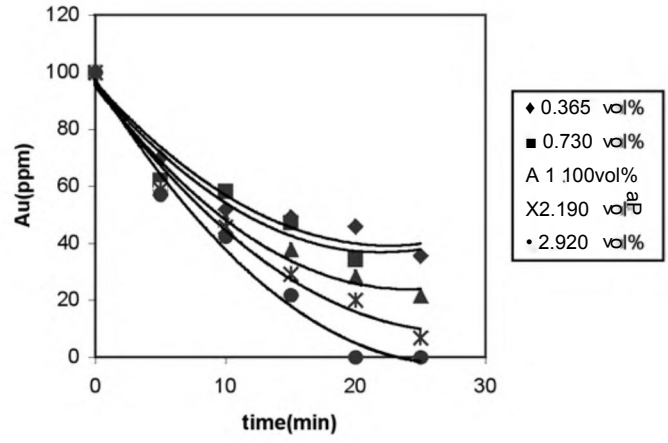


Figure 3- Effect of earner concentration on the extraction efficiency.
C, = 100 *ppm*; *C, = 0 AM* $Na_2SO_{,,}$ *0AM NaOH: R,,* = 0.274*: pH* = 0; 510 *rpm.*

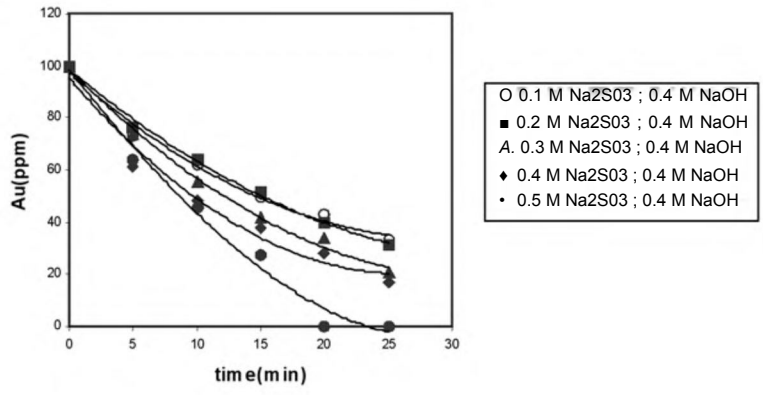


Figure 4- Effect of internal phase reagent concentration on the extraction efficiency.
C. = 100 *ppm*; C_c = 1.1%; $R_{e,,}$ = 0.274; *pH* = 0; 510 *rpm.*

droplets and reduces the concentration polarization at the surface; so increases the driving force for the extraction [12], The results showed that the best concentration for the internal phase regent was 0.5M for sodium sulfite. These experiments were performed at constant NaOH concentration of 0.4M and different concentrations of sodium sulfite.

Effect of the external phase pH

Effect of the pH at the external phase on the extraction efficiency has been shown in Figure 5. Any decrease in pH increases the extraction efficiency. This effect can be explained by the Eqn. (2).

The rate of the complex formation depends directly on the H^+ concentration in the external phase, so by reducing the pH value for the extraction phase, the extraction efficiency increases.

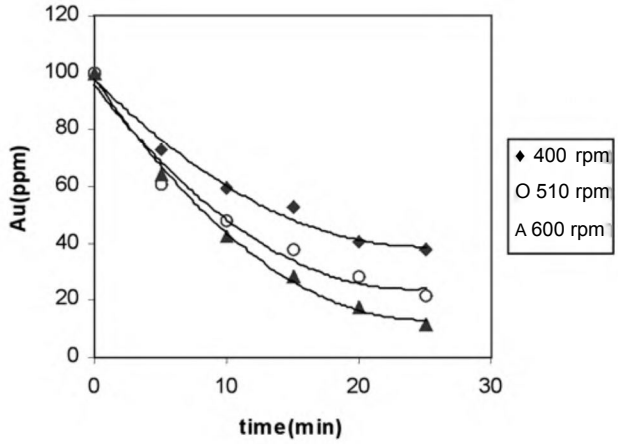


Figure 5- Effect of external phase pH on the extraction efficiency.
C_e = 100 *ppm*; C_i = 0.4M $Na_2SO_{\%}$, *0 AM NaOH*; C_c = 1.1%; R_{ew} = 0.274 ;510*rpm.*

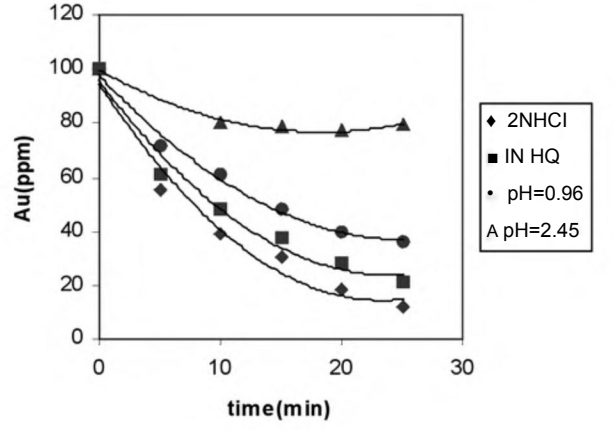


Figure 6- Effect of speed of agitation the extraction efficiency.
C' = 100*ppm*; $c,$ = *0AM* $Na_2SO,$, *0AM NaOH:*C_c = 1.1%; = 0.274 *:pH = 0.*

Effect of agitation speed

Effect of agitation speed on the extraction efficiency has been shown in Figure 6. By increasing agitation speed, the shear forces which act on the emulsion globules increases and this makes the globules smaller. As other authors have pointed out, the external surface area of globules rather than the internal phase droplet surface area control the extraction process with ELMs [3,12,13,25], so by increasing the speed of agitation the area for mass

transfer increases and the extraction efficiency increases. Increasing the speed of agitation above a critical value, not only does not increase the extraction efficiency considerably, but also affects the stability of the emulsion and increases the osmotic swelling of the membrane and makes the emulsion unstable [21].

CONCLUSION

A new efficient emulsifier has been introduced for the extraction of gold (III) ions from acidic aqueous media using MIBK as carrier and alkaline sodium sulfite solution as internal reagent. The extraction and stripping of Au^{3+} from acidic solutions by a W/O/W emulsion formed with LK-80 as emulsifier has been investigated. The extraction rate increases with the increase of the carrier concentration, internal phase concentration, agitation speed and decrease of the external phase pH according to the acidity of 2N HCl.

NOMENCLATURE

C_c Concentration of carrier in the emulsion phase, vol%.

C_e Concentration of gold (III) ions in the external phase, ppm.

C, Concentration of sodium sulfite in the internal phase, mol/lit.

R_n. The ratio of emulsion phase to the external phase, vol/vol.

REFERENCES

1. T. Zhang, B. Huang, W. Zhou, H. Gao, H. Wu, J. Wu, J. *Chem. Technol. Biotechnol.* 76(2001) 1107.
2. N.N. Li, *US-Patent* 3410794 (1968).
3. E.R. Elzinga, N.N. Li, *US-Patent* 3389078 (1968).
4. N.N. Li, AlChE J., 17(1971)459.
5. A.E. Eyal, E. Bressler, 41(1993) 287.
6. J.D. Way, R.D. Nobel, T.M. Flynn, E.D. Soan, *J. Membrane Sci.,* 12(1982) 239.
7. Y.H. Wan, X.D. Wang, X.J. Zhang, *J. Membrane Sci.,* 135(1997) 263.
8. W.S. Ho, T.A. Hatton, E.N. Lightfoot, N.N. Li, AlChE J., 28(1982) 662.
9. A. Bhowal, S. Datta, *J. Membrane Sci.,* 118(2001) 1.
10. A. Jabbari, M. Esmaeili, M. Shamsipur, 24(2001) 139.
11. R.H. Zhang, L. Xiao, *J. Membrane Sci.,* 51(1990) 249.
12. W.S.W. Ho, K.K. Sirkar, *Membrane Handbook, Chapman & Hall Inc.* N Y, 1992.
13. R. Rautenbach, O. Machhammer, *J. Membrane Sci.,* 36(1988) 425.
14. A. Sastre, A. Madi, J.L. Cortina, N. Miralles, *J. Membrane Sci.,* 139(1998) 57.
15. T. Zhang, B. Huang, W. Zhou, H. Gao, H. Wu, J. Wu, *J. Chem. Technol. Biotechnol.,* 76(2001) 1107.
16. J. Fu, S. Nakamura, K. Akiba, *Analytical Sci.,* 10(1994) 935.
17. T.L. Deng, M.X. Liao, M.H. Wang, Y.W. Chen, N. Belzile, *Minerals Eng., 14{*2001)263.
18. N. Yan, Y. Shi, Y. Su, *Water Treatment,* 5(1990) 190.
19. A.A. Ensafi, H. Eskandari, *Microchemical J.,* 69(2001) 45.
20. A.V. Mukkolath, P.T. Gaderkar, K. Tiwari, *Chemistry & Industry,* March (1990) 192.
21. J. Yan, R. Pal, J. *Membrane Sci.,* 190(2001) 79.
22. P. Walstra, *Chem. Eng. Sci.,* 48(1993) 333.
23. D. Clausse, I. Pezron, L. Komunjer, *Colloids and Surfaces A,* 152(1999)23.
24. M.F. Bobin, V. Michel, M.C. Martini, *Colloids and Surfaces A,* 152(1999) 53.
25. Shere, A.J., M. Cheung, *Chem. Engng. Comm.,* 48(1988) 143.

EMULSION IN URANIUM SOLVENT EXTRACTION PLANT - CASE STUDY

C. A. Morais*, J. S. Benedetto* and L. A. Gomiero**

*Comissão Nacional de Energia Nuclear (CNEN) - Centro de Desenvolvimento de Tecnologia Nuclear (CDTN) - Campus da UFMG - Pampulha
Cx. Postal 941 - 30123-970 - Belo Horizonte (MG) - Brazil.
cmorais@cdtn.br jsb@cdtn.br
**Indústrias Nucleares do Brasil S/A - INB - Unidade de Caetité - BA.
Fazenda Cachoeira s/n° - Zona Rural - Distrito de Maniaguí
Cx. Postal 7 - 46400-000 - Caetité (BA) - Brazil
gomiero@inb.gov.br

The only uranium concentrate production plant currently operating in Brazil is located in Caetité, BA. Because of the great water shortage in Caetité region, all water used for uranium processing is recirculated to the process. Water recirculation has caused continuous changes in the composition of pregnant liquor mainly in the sulfate and chloride concentrations. After some water recirculation cycles, a decrease in the uranium extraction efficiency was noted, which was followed by the formation of stable emulsion at uranium extraction stage. This study provides a detailed characterization of process flows and some types of treatment to reduce raffinate sulfate content and alkaline treatment of stripped solvent. It helped not only to identify the causes of emulsion formation at the solvent extraction stage but also the ways to prevent them.

INTRODUCTION

Indústrias Nucleares do Brasil S/A - INB is producing uranium concentrate since 1982. The first industrial plant for uranium concentrate production was installed in Caldas - MG. The process successfully used in that plant for 10 years is similar to that used in the Caetité-BA plant called Uranium Concentrate Plant - UCP. This process consists of sulfuric acid ore leaching, uranium separation and purification by solvent extraction using Alamine 336® as the extractant agent, uranium stripping by sodium chloride (NaCl) acid aqueous solution and precipitation of ammonium diuranate-ADU ((NH^^Oy) by ammonium hydroxide (NH_4OH) addition to the pregnant strip solution (PSS).

The main differences between Caldas and Caetité processes are: (i) use of crushed ore heap leaching technique instead of tank agitated ore milled pulp leaching; (ii) molybdenum stripping by sodium carbonate (Na_2C0_3) solution after uranium stripping by sodium chloride (NaCl) solution: as Caetité ore contains no molybdenum, the latter stage was removed from the process; (iii) process water recirculation: as Caldas plant did not face the water shortage problem, aqueous effluents were released to the environment after neutralization and monitoring.

In contrast, there is a serious water shortage in the Caetité region. This led INB to modify the UCP project to consume less water and make the whole process using recirculation of water. In this way, the aqueous effluent from the solvent extraction stage (raffinate) containing high sulfate content and part of filtrate from ADU precipitation ($NaCl/Na_2S0_4$ solution) are used to prepare the sulfuric acid solution used in ore leaching.

In the first year, the plant operated as expected. However, due to water recirculation cycles, the increased salinity of the pregnant leaching solution (PLS) started to affect adversely the uranium concentrate production, creating in addition a stable emulsion at the uranium solvent extraction stage.

IIMB/UCP PROCESS

In the ADU production process adopted by INB, the uranium present in the ore as $U0_3$ is leached by sulfuric acid solution, according to the reaction indicated by equation (1).

$$U0_3(_S) + 2\ H^+_{(aq)} + 3\ S0_4{}^{2'}{}_{(aq)} = [U0_2(S0_4)_3]^{4'}{}_{(aq)} + H_2O_{0)} \qquad (1)$$

Uranium present in PLS in form of trisulfate uranyl complex is separated from the other chemical species by solvent extraction technique using a tertiary long-chain amine (Alamine 336®), as extractant which is in the chloride form in this process. The extraction stage is represented by equation (2).

$$4\ R_3NHCl_{(org)} + [U0_2(S0_4)_3]^{4}\text{-}_{(aq)} = (R_3NH_4)_4U0_2(S0_4)_{3(org)} + 4\ Cr_{(aq)} \quad (2)$$

According to UCP project, 50% of the raffinate from uranium solvent extraction stage recirculate to ore leaching stage without any prior treatment. Uranium stripping is carried out by contacting the loaded organic phase with an aqueous NaCl solution (Equation 3).

$$(R_3NH_4)_4U0_2(S0_4)_{3(org)}+4NaCl = 4R_3NHCl<_{org)}+[U0_2(S0_4)_3]^{4}>4Na^+ \quad (3)$$

After the stripping stage, the stripped solvent recirculates to the extraction stage, while the uranium present in the PSS is precipitated as ADU by ammonium hydroxide addition, according to equation (4).

$$2\ [U0_2(S0_4)_3]^{4'}+6\ NH_4OH = (NH_4)_2U_20_{7(S)}+6\ S0_4{}^{2'}+4\ NH_4{}^+ +3\ H_20 \quad (4)$$

EXPERIMENTAL

Chemical characterization of samples was based on qualitative analysis by X-ray fluorescence and quantitative analysis by atomic absorption spectrophotometry, specific ion, flame photometry and gravimetry. Laboratory experiments for solvent regeneration, sulfate precipitation, and uranium extraction were carried out in mechanically agitated beakers, while suspended solid flocculation experiments were carried out in 1,000 mL graduated glass cylinder; all of them at the temperature of 25 ± 1°C.

Reagents and solutions

Organic solutions, PLS and raffinate were supplied by INB. PLS originates from uranium ore leaching stage, while raffinate is the depleted aqueous solution from uranium extraction. The solvent constitutes of Alamine 336® (0.15 mol/L) and tridecyl alcohol (3%), used as modifier, diluted in purified kerosene. Both Alamine 336® and tridecyl alcohol were supplied by Cognis do Brasil Ltda. Purified kerosene (Solbrax ECO 175/235) was supplied by Petrobrás Distribuidora S/A. Flocculants Poliox WSR 301® and F11® were supplied by Dow Chemical

Brasil S/A and GEBetz do Brasil Ltda., respectively. All other reagents were analytical grade and their respective solutions were prepared with distilled water.

RESULTS AND DISCUSSION

The problem of stable emulsion formation leading to cruds formation is common in solvent extraction operations in mining industries. This physical-chemical phenomenon may lead to an excessive solvent loss along the circuit, which adversely affects the operating costs. The major factors contributing to emulsion formation include: ore type, PLS composition, solvent composition, project and type of agitation [1,2,3,4],

With the objective of identifying the causes of stable emulsion formation in INB/UCP production process, a detailed chemical characterization of process flows was performed, namely: PLS from ore leaching; raffinate; loaded solvent; stripped solvent; ADU filtrate; process water; and suspended solid observed in PLS. The results from that characterization are shown in Table 1.

Table 1. Chemical characterization of process flows

Specie	PLS(1)	Raffinate	LO(2>	**so(3)**	Emulsion	Filtrate	Water	SS(4)
	(g/L)	**(g/L)**	**(g/L)**	**(g/L)**	(%)	**(g/L)**	**(g/L)**	(%)
u_3o_8	1,80	0,006	4,20	0,1	2,05	< 0,001	< 0,001	3,16
$S0_4^{2'}$	84,0	82,1	10,4	< 0,05	11,2	76,0	< 0,01	12,1
$Si0_2$	0,90	0,92	0,05	< 0,05	7,00	<0,02	< 0,02	23,0
Fe	6,40	6,40	0,007	< 0,005	0,59	< 0,001	< 0,001	6,24
Mg	2,82	2,80	0,61	0,26	0,50	0,10	<0,001	0,14
Ca	<0,001	<0,001	1,90	1,91	0,29	0,09	0,07	3,42
cr	3,79	4,00	2,34	5,40	1,50	15,3	0,26	0,32
Na	3,50	3,95	< 0,01	0,01	0,42	31,0	0,05	0,57
K	0,08	0,08	< 0,01	<0,01	0,11	0,03	0,02	0,58
Ti	-	.	-	-	< 0,1	-	-	6,6
P	-	.	-	-	< 0,1	.	.	3,35
Zr	.	.	.	.	.	.	.	0,41
SS(4)	0,09	.	.	.	.	.	.	.
pH	1,2	**1,2**	.	.	.	**8,0**	6,5	.

(1)PLS = Pregnant Leaching Solution; (2)LO = Loaded Organic; (3)SO = Stripped Organic; (4)SS= Suspended Solids

From Table 1, one can note a high silica and sulfate content in the emulsion. Table 1 also shows that PLS displays a significant quantity of suspended solids (90 mg/L), and high sulfate and chloride content, that interfere adversely in uranium extraction efficiency [5,6,7], It can also be noted the low uranium content in loaded solvent (4.20 g/L of U_30_8). A typical load of a 0.15 mol/L of Alamine 336® in solvent is around 7.5 g/L of U_30_8. According to Soldenhoff et al [5], 2.0 g/L of chloride in PLS is sufficient to affect the uranium extraction efficiency by Alamine 336®. The effect of sulfate concentration on uranium extraction by tertiary amines is mentioned by Merritt [7], According to Meritt, for a solution containing 0.1 mol/L sulfate, the distribution coefficient of uranium extraction is around 1,000, while for a solution containing 1.0 mol/L sulfate, it drops to values below 100.

Sulfate Removal

High sulfate content in PLS is due to recirculation of raffinate without prior treatment. With the purpose of reducing the sulfate and metals content in PLS, experiments of calcium sulfate and metallic hydroxides precipitation from the raffinate were carried out through lime addition. In such experiments, the final pH was varied from 5.5 to 9.5.

Final pH value in this case is not a predominant factor for the sulfate removal. Calcium sulfate precipitation is controlled primarily by the quantity of calcium added. In contrast, metallic hydroxide precipitation depends on final pH. At the final pH of 5.5, more than 50% of sulfate was removed. At that pH, there was also a significant reduction of iron and complete removal of silica, remaining 27 g/L $S0_4^{2'}$, 0.17 g/L Fe and 3.5 g/L Mg. Partial removal of magnesium was only noted at pH 7.0, when the presence of iron was completely dropped. To prevent a significant increase of magnesium content in PLS due to raffinate recycling, neutralization should reach a pH above 9. At the final pH of 9.5 the content of sulfate, calcium and magnesium in the filtrate were 3.0 g/L, 1.45 g/L and 0.03 g/L, respectively.

Removal of Suspended Solid Content

Suspended solid content reduction was investigated by flocculation technique. Prior to feeding the solvent extraction stage, PLS passes through a thickener and an anthracite coal filter. Suspended solids present in PLS were derivate from the complete emptying of one of the PLS storage pond in the plant. Once the pond was refilled, particulate solid material deposited on the pond bottom mixed to PLS and, because of its great thinness, it was not retained in the thickener or filter. Flocculation experiments were carried out using flocculants Poliox WSR 301®, from Dow Chemical, and F11® from GEBetz, both used at the concentration of 0,2% w/v. Best results were obtained with flocculant F11® at the dosage of 4 mg/L (2.0 L of solution/m^3 of PLS). According to IAEA [6], suspended solid levels around 30 - 50 mg/L are tolerable for emulsion formation. Under that treatment, it was possible to reach suspended solids levels lower than 20 mg/L. Reducing the solids present in PLS to such levels was sufficient to control emulsion formation at industrial scale, and allowed UCP to go back to normal operation, however, with a production output below the expected.

Chloride Removal

Part of the chloride present in aqueous phase originates from the solvent, which recirculates in the plant without prior Na_2C0_3 treatment (Equation 2). As removing the chloride ion from aqueous phase is complex and can represent high costs, a study was performed to remove chloride from the solvent by its prior treatment. The treatment of the stripped organic containing 5.4 g/L chloride were carried out with 1.0 mol/L Na_2C0_3solution at a stirring time of 5 minutes in the presence and absence of sodium hydroxide solution (10 mol/L NaOH) used to control the equilibrium pH. The addition of NaOH to control the equilibrium pH between 10 and 10.5 during the stripped organic regeneration or scrubbing by Na_2C0_3 is mentioned by Mackenzie [8], The volumetric ratios of organic and aqueous phases (O/A) where varied from 1 to 10. Evaluated parameters included the phase separation time and the chloride content remaining in solvent.

It was observed that more than 90% of chloride ions were removed at one single contact stage. The introduction of a second contact stage led to a hardly emulsion formation, with difficult separation. The equilibrium pH control by addition of NaOH solution does not benefit significantly the displacement of chloride ions from the organic phase. The results of these experiments are shown in Table 2.

After the investigation of stripped organic treatment, two uranium extraction isotherms from the leaching solution (PLS) were plotted, one for stripped solvent without Na_2C0_3 treatment (Fig. 1) and the other with the solvent submitted to treatment under the conditions of experiment 2 (O/A = 5) of Table 2 (Fig. 2). PLS was centrifuged for suspended solid removal. These extraction isotherm/McCabe-Thiele's diagrams showed in Figures 1 and 2, were

established according to the successive contaction technique for saturation of solvent and depletion of aqueous phase.

Table 2. Chloride removal from solvent as a function of O/A ratio and final pH

Experiment	O/A	Aqueous Phase			$Cl^-_{organic}$	Removal
		Solution	pH initial	pHfinal	(g/L)	(%)
1	1	N32CO3	10,8	10,1	0,20	96,3
2	5	N32CO3	10,8	8,5	0,45	91,7
3	7	N32C03	10,8	7,8	0,63	88,3
4	10	N32C03	10,8	6,9	0,67	87,6
5	1	Na_2C0_3/Na0H	10,8	11	0,15	97,2
6	5	Na_2C0_3/Na0H	10,8	11	0,40	92,6
7	7	Na_2C0_3/Na0H	10,8	11	0,54	90,0
8	10	Na_2C0_3/Na0H	10,8	11	0,57	89,4

Initial Cl' concentration in solvent = 5,4 g/L

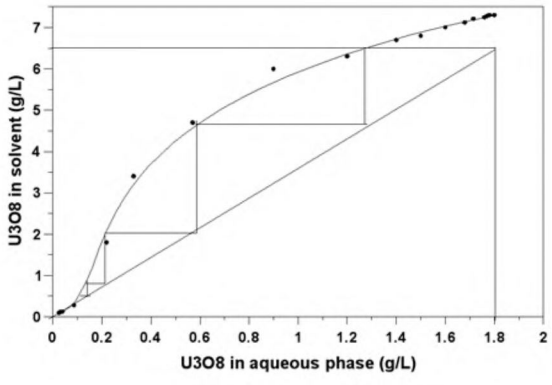


***Figure 1** - PLS uranium extraction isotherm with non treated stripped solvent*

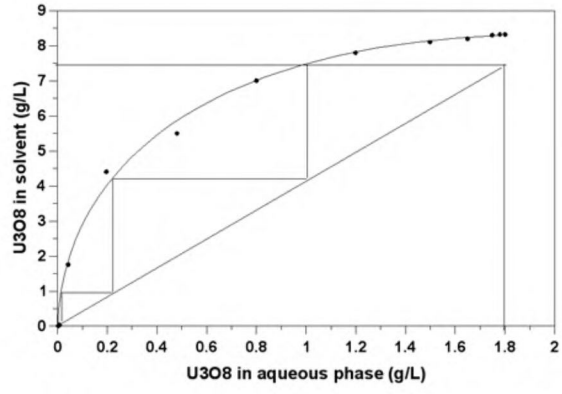


***Figure 2** - PLS uranium extraction isotherm with Na_2C0_3 treated stripped solvent*

Figures 1 and 2 shows the effect of Na_2C0_3 treatment of the stripped solvent on the uranium extraction efficiency. Maximum load obtained for non-treated stripped solvent was lower than 7.5 g/L U_30_8 (Fig. 1), while the load for the treated stripped solvent with Na_2C0_3 was approximately 8.5 g/L U_3O_s (Fig. 2). The theoretical stages number was determined by McCabe-Thiele's method [9], It is noted that, for Na_2C0_3 treated stripped solvent, 3 stages are sufficient to extract almost all uranium present in PLS. For non-treated stripped solvent, an inflexion can be observed for low uranium concentration at the equilibrium. This indicates the difficulty for complete uranium extraction, leading to a higher number of stages at the extraction phase. Solvent treatment with Na_2C0_3 alone does not prevent emulsion formation, but it increases the uranium extraction efficiency.

Another process flow that should be given attention is the filtrate from ADU precipitation. This flow presents high sulfate, sodium, and chloride content. Part of this flow (about 40%) recirculates to prepare NaCl stripping solution. The other part is mixed to the raffinate to compose a waste solution that can be used to prepare the ore leaching solution, or can be neutralized with milk of lime up to pH 9, where the chloride ions are not removed. After solids sedimentation in lined ponds, the aqueous phase of the neutralized waste solution is also recirculated to the ore leaching stage. Assuming the low rate of filtrate flow (0.96 m^3/h), as compared to that of raffinate (30 m^3/h), it is ideally expected that the excess of the NaCl

solution preparation, corresponding to approximately 0.58 m^3/h, shall not recirculate together with raffinate to the leaching stage to prevent the increment of sodium and chloride ions in PLS.

CONCLUSION

Stable emulsion formation at the solvent extraction plant in Caetité unit was mostly caused by suspended solids present in the pregnant leaching solution (PLS). The reduction in uranium extraction efficiency is due to the high PLS salinity, and especially to its high sulfate and chloride content. Raffinate treatment by lime was efficient at the final pH of 9.5, where practically the whole sulfate and metals content are removed.

Experiments of solvent treatment with Na_2C0_3 suggested that the equilibrium pH control by NaOH addition does not benefit significantly the displacement of chloride ions. When the volumetric ratio between the organic and aqueous phases (O/A) varied from 1 to 10, chloride removal dropped from 96.3% to 87.6%. For a uranium stripping process with NaCI solution, the treatment of the stripped solvent with Na_2C0_3 improves its efficiency in a new operation of uranium extraction. Maximum loads obtained were 8.5 g/L of $U_3O_s$and 7.3 g/L of U_3O_s, for treated and non-treated stripped solvent respectively. It could also be noted that the number of stages requested for full uranium depletion from PLS is much lower for treated solvent than for non-treated solvent.

Stripped solvent treatment with sodium carbonate associated with the reduced suspended solids content in PLS and the raffinate treatment with lime reduces the continuous changes in the composition of PLS that feeds the solvent uranium extraction phase. It prevents drops in uranium extraction output and the formation of stable emulsion at the organic/aqueous phase. Another important factor is the non-recirculation of the aqueous flow of ADU precipitation and the aqueous flow of the organic treatment to the process.

REFERENCES

1. G. M. Ritcey (1980), *Hydrometallurgy,* 5, 97-107.
2. G. M. Ritcey (1982), *Proc. XIV International Mineral Processing Congress,* Toronto, Canada, pp. VII-10.1-VII-10.18.
3. G. M. Ritcey and E.W. Wong (1988), *Proc. ISEC'88,* Moscow. Russia, pp. 116-119.
4. J. Menacho and Y. Zinvkovic (1994), Proc. *IV Meeting of the Southern Hemisphere on mineral technology,* Vol. Ill, Concepción, Chile, pp. 163-182.
5. K. Soldenhoff; D. Wilkins; M. Shamieh and R. Ring (2000), *Proc. International Symposium on the Process Metallurgy of Uranium,* Saskatoon, Canada, pp. 339-351.
6. IAEA- International Atomic Energy Agency (1993), *Technical Reports Senes n°.359*, Vienna, Austria, pp. 183-206
7. R. C. Merritt (1971), The Extractive Metallurgy of Uranium, Colorado School of Mines Research Institute, United States of America, pp 194-201
8. J. M. W. Mackenzie (1997), Uranium Solvent Extraction Using Tertiary Amines, *Proc. Uranium Ore to Yellow Cake Seminar,* Melbourne, Australia.
9. G.M. Ritcey and A. W. Ashbrook (1984), Solvent Extraction: Principles and Applications to Process Metallurgy, Part I, Elsevier, Amsterdam, pp. 40-86.

EQUILIBRIUM STUDY OF THE GADOLINIUM SOLVENT EXTRACTION FROM CONCENTRATED METAL SOLUTIONS USING D2EHPA AND HEH(EHP)

Carlos Antonio Morais* and Marcelo Borges Mansur**

* Comissão Nacional de Energia Nuclear (CNEN) - Centro de Desenvolvimento de Tecnologia Nuclear (CDTN) - Campus da UFMG - Pampulha
Caixa Postal 941 - 30123-970 - Belo Horizonte (MG) - Brazil.
E-mail: cmorais@cdtn.br
** Departamento de Engenharia Quimica - UFMG
Rua Espirito Santo, 35, 6° andar, 30160-030, Belo Horizonte, MG, Brazil
E-mail: mansur@deq.ufmg.br

The equilibrium extraction of gadolinium in very high metal and extractant concentrations thus reproducing the industrial process conditions has been investigated in this study. The gadolinium extraction was carried out using a phosphoric acid (D2EHPA) and a phosphonic acid (HEH(EHP) or Ionquest® 801) extractants. The concentration of gadolinium in the hydrochloric acid solution varied from 16 g/L to 40 g/L (0.104 mol/L to 0.255 mol/L) while the extractants from 0.5 mol/L to 1.5 mol/L. The acidity varied from 0.001 to 0.005 mol/L of H^+ ions. Data fitting including the statistical analysis of equilibrium parameters has been done using a statistical software and the stoichiometric expression suggested by Peppard and collaborators [1] was found adequate for both extractants. The equilibrium constant for the system Gd-D2EHPA was 1.9 ± 0.3 and for the system Gd-HEH(EHP) was 0.028 ± 0.003.

INTRODUCTION

Gadolinium is one of the rare earth elements that have a large application in the nuclear and medicine fields. It creates a strong contrasting effect in magnetic resonance imaging (MRI), and it has been used increasingly for this. Because of its high cross section, gadolinium is a good thermal neutrons absorber and it has been used in nuclear area and also in cancer therapy as neutron-capture. It can be used also as an alternative contrast agent for sialography in patients with iodine sensitive [2, 3, 4, 5],

Generally the separation of rare earth elements is carried out into groups of light rare earths (La, Ce, Pr, Nd), middle rare earths (Sm, Eu, Gd) and heavy rare earths (Tb, Dy, Ho, Er, Tm, Yb, Lu, Sc, Y) [6], In the group of middle rare earths, Eu is removed by reducing Eu^{3+} to Eu^{2+} followed by precipitation as $EuS0_4$ [7, 8, 9], The remaining Sm/Gd is then separated by solvent extraction process [10, 11],

The mechanism involved in the extraction of rare earths (RE) elements using cationic extractants such as D2EHPA and HEH(EHP) was firstly described by Peppard and collaborators in 1950s [1] and later confirmed by others authors [12] as:

$$RE^{3+}{}_{(aq)} + 3\ (HX)_{2\ (org)} = RE\ X_3(HX)_{3\ (org)} + 3\ H^+{}_{(aq)} \qquad (1)$$

In the last years, the formation of other complex species like $REX_3.2HX$ and REX_3 was also proposed by some researchers, mainly at very dilute organic and aqueous solutions [13], In this case, Sánchez [13] worked with neodymium using dilute nitrate aqueous medium (10^{-5} mol/L to 10^{-4} mol/L of Nd) and D2HEPA diluted in kerosene (10^{-5} to 0.03 mol/L). Sato [14] studying the dysprosium (III) extraction with D2EHPA in kerosene from hydrochloric acid solutions has suggested $DyCl_3.HX$ as the extracted specie when higher aqueous acidity are used (2.5 and 7.0 mol/L HCl).

Several studies involving rare earth extraction from hydrochloric acid media using phosphoric acid and derivatives were found in the literature. However, most of them were carried out at low metals and extractants concentrations. In this context, the goal of the present work is to study the equilibrium extraction of gadolinium using high metal and extractant concentrations thus reproducing the industrial process conditions. The extraction was carried out using a phosphoric acid (D2EHPA) and a phosphonic acid (HEH(EHP) - lonquest 801®) extractants. Data fitting including statistical analysis of equilibrium parameters has been done using statistical software in order to identify the extraction stoichiometry of gadolinium with both acidic extractants investigated.

EXPERIMENTAL

Reagents and Solutions

The gadolinium chloride solutions were prepared by dissolving a gadolinium carbonate in hydrochloric acid solution. The commercial gadolinium carbonate used in this study was supplied by INB (Indústrias Nucleares do Brasil S.A.) and its chemical composition is shown on Table 1. The extractants D2EHPA (di-2-ethylhexyl phosphoric acid, 97%wt purity) and HEH(EHP) (2-ethylhexyl phosphonic acid mono-2-ethylhexyl ester, 96.5 %wt purity) thus commercialized under the trade name of lonquest 801® were supplied by Albright & Wilson Americas Inc. The extractants were diluted in Exxsol® (purified kerosene) supplied by Exxon Quimica Ltda. All other reagents were of analytical grade and their solutions were prepared with distilled water.

Table 1: Chemical composition of the europium and gadolinium carbonate mixture

Species	Sm^{3+}	[illegible]	Gd^{3+}	Tb^{3+}	CO_3^{2-}	Cr	H_2O
Content (%wt.)	< 0.005	0.01	47.0	< 0.005	43.3	2.30	7.4

Extractions experiments

The experiments were carried out in beakers and liquids were mechanically agitated using a glass impeller for 10 minutes, at 25±1°C. The results of preliminary experiments indicate that 3 minutes are sufficient to achieve equilibrium. The liquid phases were then separated by means of a separation funnel. The experiments were carried out in 5 different concentrations of extractants (0.50, 0.75, 1.00, 1.22 and 1.50 mol/L). The gadolinium chloride solutions were prepared in the following concentrations and respective pH values: 0.255 mol/L (pH 5.0, 3.2, 2.2 and 1.1), 0.202 mol/L (pH 5.0), 0.154 mol/L (pH 5.0, 2.9, 1.8 and 1.0) and 0,104 mol/L (pH 5.2). The experiments were carried out in the aqueous to organic (A/O) volumetric ratio of 0.5, 1 and 2, without pH control. The concentration of Gd in the aqueous phase was determined by atomic emission spectrometer with inductively coupled plasma (ICP/AES). The pH of the aqueous solutions was measured precisely with a glass pH electrode attached to a Digimed pH-meter, model DM 20.

Extraction of Gd(III) with D2EHPA and Ionquest 801

The presence of europium in the gadolinium solutions was neglected in this study due its low concentration and the well-known similarity extraction distribution coefficient of Eu^{3+} and Gd^{3+} [14], The extraction behavior of gadolinium with D2EHPA and Ionquest 801 accordingly to the initial concentration of metal in the aqueous phase and the initial concentration of extractant in the organic phase is shown in Figures 1(a) and 1(b), respectively. Relatively higher percentages of Gd extraction were obtained with D2EHPA for similar operational conditions thus indicating that D2EHPA is more efficient for gadolinium extraction than Ionquest 801 for the operational conditions investigated. The superior extractions obtained with D2EHPA in comparison to Ionquest 801 has been mentioned by Morais and Ciminelli [6]; such result has been explained based on the "soft" and "hard" "acid/base" theory, and in the relatively higher hydrophilic nature of the phosphate group of D2EHPA as compared to the phosphonic group of Ionquest 801. An increase on the concentration of both extractants for a given initial concentration of metal in the aqueous phase resulted in an increase of the percentage of extraction of metal. In addition, a quite linear increase on the percentage of metal extracted has been found with the decrease of the initial concentration of metal in the aqueous phase for a given initial concentration of both extractant in the organic phase. Both effects were expected and are related to the relative initial quantities of metal and extractant in the liquid-liquid system.

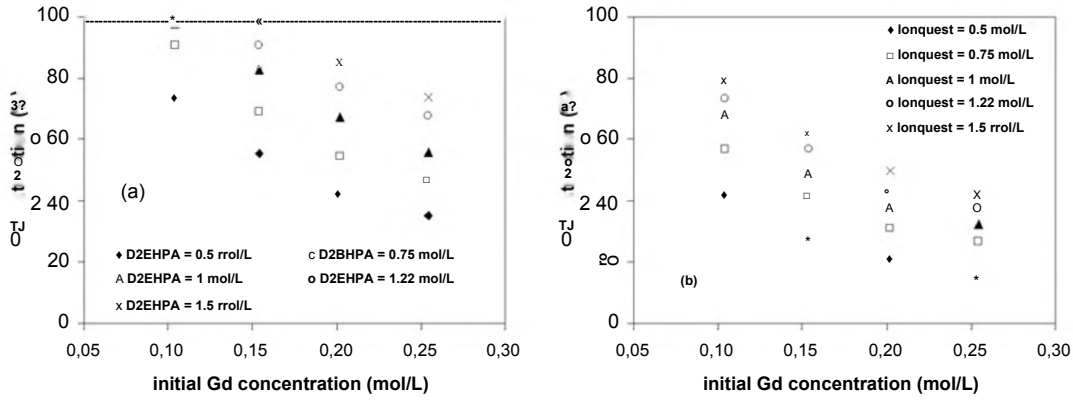


Figure 1. Influence of initial Gd concentration and initial concentration of extractant on the extraction of Gd(III) with (a) D2EHPA and (b) Ionquest 801 (A/O = 1, initial pH = 5, T = 25°C)

Experiments were carried out in this study with no pH control, i.e., no acid or base has been added to the liquid-liquid system in order to keep the pH at a specified value. Consequently low metal extractions are expected because extraction will end up when equilibrium pH is reached. Actually, the variation on initial and final (or equilibrium) pH has been measured. This methodology has shown to be easier to handle in laboratory scale because no error due to the addition of reagents to control the pH (variation of volumes, presence of other species that may interfere on the equilibrium, for example) has to be considered. Figures 2(a) and 2(b) shows the equilibrium pH for experiments presented in Figure 1. The same conclusions can be drawn by analyzing the equilibrium pH responses as well because higher extraction levels lead to lower equilibrium pH values.

Modeling of equilibrium and data fitting results

The equilibrium extraction of gadolinium(III) by cationic extractants as is the case of D2EHPA and Ionquest 801 can be described by the following general expression:

$$Gd^{3+} + n\,(HX)_2 \rightleftharpoons GdX_3(HX)_{2n}\text{-}3 + 3\,H^+ \qquad (2)$$

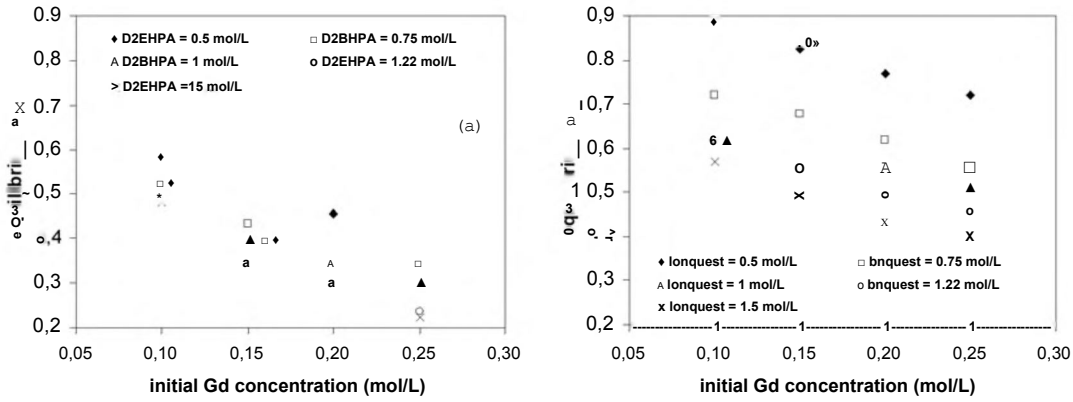


Figure 2. Influence of initial metal concentration and initial concentration of extractant on the equilibrium pH) with (a) D2EHPA and (b) lonquest 801 (A/O = 1, initial pH = 5, T = 25°C)

where "HX" is the molecule of the acidic extractant and "n" the unknown stoichiometric constant. It is well known that organophosphorous acids exist predominantly in the form of dimmer molecules when they are dissolved in aliphatic diluents of low polarity [15, 16], Substituting the mass balance of metal in the equilibrium expression of Eq. (2), the following equation is obtained in terms of equilibrium pH:

$$pH_E = -\log\left[\frac{K_E C_B^{n}}{(A/O)}\left(\frac{O_A}{O_O - O_A}\right)\right] \qquad (3)$$

where "pH_E" is the equilibrium pH, "C" is the molar concentration and "K_E" is the apparent equilibrium coefficient. Subscripts "A" and "B" represent metal and extractant species, respectively, while superscript "o" represents the initial condition. The mass balance of extractant is given by:

$$C_B = C_B^o - n(c^o_A - C_A)(A/O) \qquad (4)$$

Substituting Eq. (4) in Eq. (3) results in a non-linear equation depending of experimental measured variables C_A and pH_E with two parameters (n and K_E) to be determined by data fitting. In this study, the software Statistica has been used. The parameters n and K_E were estimated using the quasi-Newton optimization method and fitting results for D2EHPA (80 data) and lonquest 801 (60 data) are shown in Table 2. Figures 3(a) and (b) compares experimental and calculated concentrations of Gd(III) in the aqueous phase.

Fitting results revealed no correlation between parameters n and K_E (p-level = 0), so values shown in Table 2 may describe satisfactorily experimental data for the extraction of Gd(III) with extractants D2EHPA and lonquest 801 in the concentration operational conditions range investigated in this work. Substituting n = 3 in Eq. (2), one concludes the extraction of Gd(III) for both extractants considered in this study is described by Eq. (1), thus corroborating Peppard and others [1, 12].

Comparing with other works found in the literature, a relatively lower value of K_E has been obtained in this study [$\log(K_E) = 0.30$ for D2EHPA and $\log(K_E) = -1.55$ for lonquest 801], possibly due to the high concentration of Gd(III) used in the tests (no activity coefficient has been considered in the equilibrium model). Working with diluted solutions (10^{-4} mol/L of Gd and 0.002 mol/L of D2EHPA), Masuda and Zahir [17] have found $\log(K_E) = 2.7 \pm 0.03$. In this case, experiments were carried out at pH of 3.5 using succinic acid as buffer and perchlorate

Table 2: Fitting results for the extraction ofGd(lll) with D2EHPA and ionquest (T = 25°C)

	D2EHPA	Ionquest 801
n	3.0 ±0.1	2.9 ± 0.1
K_E	1.9 ±0.3	0.028 ± 0.003
R^2	0.82	0.96
p-level	0.00	0.00

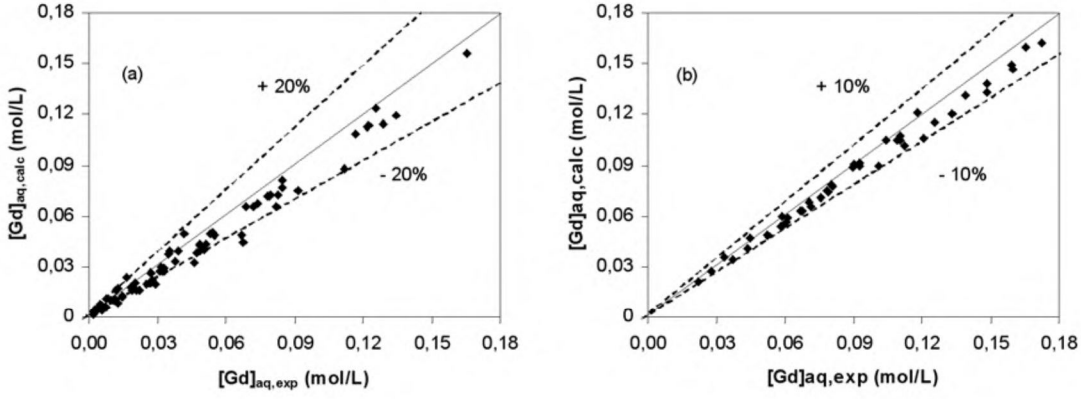


Figure 3. Experimental versus calculated concentration of gadolinium(lll) in the aqueous phase for (a) D2EHPA and (b) Ionquest 801 (T = 25°C)

sodium to control the ionic strength. On the other hand, Sánches and collaborators [18] has cited that log(KE) for the extraction of neodymium(lll) decreases as the concentration of extractant increases. In this case, log(K_E) varies from 1.13 to 0.38 as the concentration of D2EHPA changes from 0.04 to 0.6 mol/L for the system Nd/Cl/D2EHPA//i-heptane. In the present work, the concentration of both extractants varied from 0.5 to 1.5 mol/L. In addition, as the extraction distribution coefficient of lantanides increases from La to Lu with cationic extractants such as D2EHPA and Ionquest 801 [6, 14], the equilibrium constant for Gd is expected to be higher than that for Nd for the same system when these extractants are used.

CONCLUSIONS

Experimental results have shown that the extraction of gadolinium (III) with D2EHPA and Ionquest 801 dissolved in Exxsol is controlled by just one reaction at high metal and extractant concentrations. Data fitting has pointed out $GdX_3(HX)_3$ as the extracted species.

The apparent equilibrium coefficient (K_E) obtained for this system was much smaller than that one found in dilute metal and extractants conditions. It can be possibly related to the non incorporation of activity coefficients to the model. However, the model has reproduced satisfactorily the experimental data for the extraction of Gd(lll) with extractants D2EHPA and Ionquest 801 in the operational conditions range investigated in this work.

REFERENCES

1. D. F. Peppard, G. W. Mason, W. J. Driscoll and R. J. Sironen (1958), *Journal Inor. Nucl. Chem.,* 7, 276-285.
2. N. Fatin-Rouge, E. Toth, R. Meuli and J-C. G. Biinzli (2004), *Journal of Alloys and Compounds*, 374, 298-302.

3. T. Watanabe, H. Ichikawa and Y. Fukumori (2002), *European Journal of Pharmaceutics and Biopharmaceutics,* 54, 119-124.
4. M. D. Williams, A. B. Moody, C. A. Newlands and D. C. Howlett (2003), *Int. Journal Oral Maxillofac. Surg.,* 32, 561-562.
5. H. G. Riella, M. Durazzo, M. Hirata and R. A. Nogueira (1991), *Journal of Nuclear Materials,* 178, 204-211.
6. C. A. Morais and V. S. T. Ciminelli (2004), *Hydrometallurgy,* 73, 237-244.
7. C. A. Morais and V. S. T. Ciminelli (2002), *Separation Science and Technology,* 37 (14) 3305-3321.
8. C. A. Morais and V. S. T. Ciminelli (2001), *Hydrometallurgy,* 60, 247-253.
9. C. A. Morais and V. S. T. Ciminelli (1998), *Hydrometallurgy,* 49, 167-177.
10. J. S. Benedeto, V. S. T. Ciminelli and J. Duarte Neto (1993), *Minerals Engineering,* 6(6), 597-605.
11. P. Miranda Jr. and L. B. Zinner (1997), *Jornal of Alloys and Compounds,* 249, 116-118.
12. A. Geist, W. Nitsch and J-Il Kim (1999), *Chemical Engineering Science,* 54, 1903-1907.
13. J. M. Sanches, M. Hidalgo, M. Valiente and V. Salvado (2001), *Proc. ISEC'99,* v.2, Barcelona, Spain, pp. 1121-1125.
14. T. Sato (1989), *Hydrometallurgy,* 22, 121-140.
15. Z. Kolarik (1982), Pure & Appl. Chem., 54(12), 2593-2674.
16. M. B. Mansur, M. J. Slater and E. C. Biscaia Junior (2002), Hydrometallurgy, 63, 117-126.
17. Y. Masuda and H. Zahir(1995), *Talanta,* 1 (42) 93-100
18. J. M. Sánches, M. Hidalgo and V. Salvadó (1999), *Solvent extraction and Ion Exchange,* 17(3), 455-474.

COMPETITIVE LIQUID-LIQUID EXTRACTION OF NICKEL AND COBALT WITH D2EHPA

Jóse dos Prazeres Ferreira Filho, Adriane Salum and Marcelo Borges Mansur

Departamento de Engenharia Quimica, Universidade Federal de Minas Gerais
R. Espirito Santo, 35, 6° andar, Belo Horizonte, MG, Brazil, E-mail: mansur@deq.ufmg.br

The competitive extraction of Co and Ni present in aqueous solutions was studied for the reactive system $NiS0_4$/$CoS04$/D2EHPA/n-heptane, at room temperature. Tests were carried out with no pH control in order to allow metals to compete one another for D2EHPA while pH decreases until equilibration is reached. When both metals compete for D2EHPA, separation factors distinct from unity were found only at lower concentrations of D2EHPA in the organic phase (10 mol/m^3). At this operational condition, two distinct behaviours have been observed depending on the initial concentration of metals in the aqueous phase: Ni was preferentially extracted with respect to Co from diluted aqueous phase (5 mol/m^3) while Co was preferentially extracted over Ni from concentrated ones (50 mol/m^3). The high aggregation number of the CO-D2EHPA complexes in the organic phase which value decreases exponentially as the Co concentration in this phase increases and the low aggregation number of Ni-D2EHPA complexes that keeps its value independently of its concentration in the organic phase might explain such unexpected behaviour.

INTRODUCTION

Liquid-liquid extraction has shown to be a suitable technique for the recovery and separation of metals from diluted and concentrated medium thus resulting in products with high purity level at low environmental impact. Industrial liquors and effluents containing several metals in solution that compete one another for the extractant present in the organic phase are normally treated by liquid-liquid extraction. A successful separation by this technique thus depends on operational conditions that maximise the selective extraction of one or even a group of metals present in the aqueous phase. The competition of metals for a common extractant arises from different chemical reaction velocities which depends on several factors such as valence of cations, chemical content and composition of both liquids, pH of the aqueous phase, volumetric ratio, type of extractant, and so on [1],

In this work, the competitive extraction between Ni and Co has been investigated using the extractant D2EHPA (di-(2-ethylhexyl) phosphoric acid). These metals have been chosen for this study due to their chemical similarity. The Ni-Co separation is not very effective with D2EHPA thus resulting in low separation factors, i.e., $p_{Co/Ni}$ around 1.6 at pH 5-6 [1], Other extractants based on phosphonic and phosphinic acid groups give much better results for this separation. However, for this particular work, D2EHPA seems to be the more adequate choice. The use of more selective extractants and the control of operating conditions (keeping pH constant during extraction, for example) may favour one or other metal, thus imposing a given condition which inhibits the effect of their competition for the extractant.

Cobalt and nickel forms coloured complexes in the organic phase with D2EHPA. In the case of Co, the colour changes from pink (octahedral) to blue (tetrahedral) as the concentration of Co-D2EHPA complex increases. On the other hand, Ni octahedral coordinating structure does not change at varying concentrations of Ni-D2EHPA complex, so the colour of the organic phase remains green. It is known that D2EHPA molecules assume dimmer molecular structure in non-polar diluents such as aliphatic kerosenes, for example [2], The extraction chemistry of Ni and Co with D2EHPA is decisive for their separation. Some phenomena such as the “aduct” formation, polymerisation of organo-metallic complexes or aggregation are commonly mentioned by several authors to explain unexpected behaviours in metallic systems. Yu *et al.* [3] have studied the aggregation behaviour of divalent cations such as Co, Ni and Cu extracted with D2EHPA dissolved in n-heptane. The authors have carried out experimental measurements of vapour pressure osmometry, viscometry and dynamic scattered light. According to their study, Co-D2EHPA complexes tend to form very large macromolecular species mainly at low concentration of Co in the organic phase (aggregation number = 225 for 10 mol/m^3 CO-D2EHPA complex, for example). The size of these macromolecules reduces exponentially as the concentration of Co in the organic phase increases. Opposing effect has been found for Cu. In the case of Ni, the size of macromolecular species of Ni-D2EHPA complex is relatively small (aggregation number = 5) independently of the concentration of Ni in the organic phase. The authors have suggested that macromolecular species result from the association of quasi-monodimensional microstructures in the form of reversed micelles. It has been observed also that Ni-D2EHPA complex solvates around 10 times more water molecules than Co-D2EHPA complexes [3], Therefore, in practical applications, Co is preferentially separated over Ni by liquid-liquid extraction with organophosphorous acids due to the different coordinating structures of the Ni and Co complexes and their different polarities, i. e., Co forms tetrahedral structures with the extractant while Ni forms octahedral ones and the complex of Co is hydrophobic and Ni complex is hydrophilic [4], But aggregation may influence such behaviour at competitive operational conditions for D2EHPA.

EXPERIMENTAL

Reagents

D2EHPA (97%wt purity) was supplied by Albright & Wilson Americas Inc. and used without further purification. The following diluent and salts were analytical grade: n-heptane (VETEC, 99.5% purity), $NiS0_4.6H_20$ (VETEC, 99% purity) and $CoS0_4.7H_20$ (VETEC, 97% purity).

Equilibrium conditions and procedure

Experiments were carried out at normal temperature in a reactor made of glass provided with mechanical stirring. Both phases (total volume = 120 mL) were contacted for 15 minutes; this time was found adequate in preliminary analysis. No modifier agent has been added because Dhases seoaration was fast and clean solutions were obtained after 5 minutes. All experiments were carried out with no pH control in order to not interfere on the metals competition for D2EHPA. The pH at the beginning of runs was that exhibited by the aqueous solution after its preparation (respective salts dissolved in distilled water only); its average value was around 6.5 for all cases considered. During extraction, pH decreases as extraction proceeds until stabilises on the equilibrium pH value. The following variables were studied: initial concentration of all metals in the aqueous phase (5, 10 and 50 mol/m^3), initial D2EHPA concentration (10, 50 and 100 mol/m^3) and volumetric phase ratio A/O (0.5, 1 and 2). Two aqueous phase systems were investigated, a monocomponent (Ni or Co) and a bicomponent one (Ni and Co). In all cases, the total concentration of metals at the beginning of runs was kept at 5, 10 and 50 mol/m^3. The metal concentration in the aqueous phase was measured using atomic absorption spectrometry (CG AA 700 SBC) and mass balances were done for calculate the metal concentration in the organic phase. The pH of the aqueous solutions was measured with an on-line pH-meter (Micronal, model B 374).

RESULTS AND DISCUSSION

Monocomponent Systems (Ni or Co)

The influence of the initial concentration of D2EHPA on the percentage of Ni and Co at different A/O ratios is shown in Figure 1(a), for the initial metal concentration of 5 mol/m^3. It is observed that percentages of extraction of Ni or Co increase with higher initial concentrations of D2EHPA, independently of the A/O ratio. For a given initial concentration of D2EHPA, the percentage of extraction is higher for lower volumetric ratios. These results can be explained by the higher amount of free D2EHPA at higher initial D2EHPA concentrations and at lower A/O ratios. As expected, the percent extraction was quite low, not more than 22%, once tests were carried out with no pH control. The correspondent pH decaying curves are shown in Figure 1(b). They confirm the previous results presented. In this Figure, it can be seen that higher metal extraction percentages are associated to lower equilibrium pH. The percentages of metal extracted are low because once the equilibrium pH is reached, the extraction does not advance anymore, despite reagents still being available.

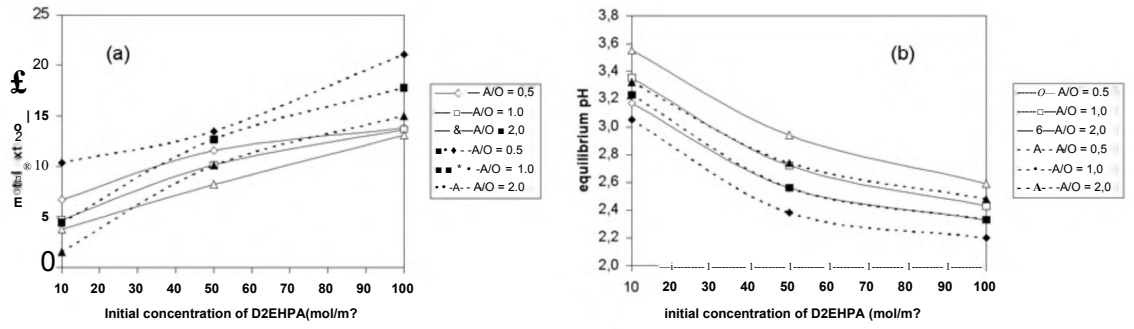


Figure 1. Influence of the initial D2EHPA concentration and A/O ratio on (1) Ni and Co extraction percentages and (2) equilibrium pH (Ni: —, Co: —, Initial metal cone, in the aqueous phase C_{Ni}° = 4,7 mol/m^3 and C_{Co}° = 5,7 mol/m^3).

The same behaviour has been observed for the two other initial metal(s) concentrations in the aqueous phase investigated. For the whole set of experiments whose starting pH of the aqueous solution was 6.5, the equilibrium pH was 3.3 ± 0.3, 2.7 ± 0.2 and 2.4 ± 0.2, for D2EHPA initial concentration of 10, 50 and 100 mol/m^3, respectively.

The equilibrium extraction of Ni and Co with D2EHPA obeys the following reaction [5]:

$$M^{2+} + n_M\overline{(HA)_2} \Leftrightarrow \overline{MA_{2nM}H_{2nM-2}} + 2H^+ \text{ with} \qquad K_M = \frac{C_{CM}C_H^2}{C_M C_B^{n_M}} \qquad 0)$$

where M represents metals Ni or Co, $(HA)_2$ the molecules of D2EHPA as dimmers, K_M is the apparent equilibrium coefficient, subscript B is the dimmer-D2EHPA, CM the metal-D2EHPA complex and H the hydrogen ions, and superscript o is the initial condition. Substituting mass balance equation of metal in Eq. (1) and rearranging, the following expression in terms of equilibrium pH can be drawn:

$$pH_E = -\log\left[\sqrt{\frac{K_M P^{n_M}_{M-B}\,(c^{\wedge}_{M}}{\frac{A}{O}\;\; I\text{-}C^{\circ}_{MM}\,J}}\right] \qquad \textbf{(2)}$$

Comparing experimental equilibrium pH and that estimated by Eq. (2), it can be observed

that ApH a Alog(C_B) for an increase of extractant concentration of 10 times, so n_M « 2 for Ni and Co. The effect of A/O ratio on the variation of pH is less significant, i.e., ApH a A log [(A/O)'^{05}] and for a change of A/O from 0.5 to 2, ApH is almost 0.3. The effect of the initial concentration of metal on the equilibrium pH variation is still lesser, i.e., ApH a log [C_M(C_M^0-C_M)'$Y^{/2}$ and for a change in CA° from 5 to 50, ApH is around 0.1. Hence, the influence in the metal extraction decreases in the following order: initial extractant concentration, A/O ratio and initial metal concentration in the aqueous phase.

Bicomponent System (Ni + Co)

Similar behaviour exhibited by the monocomponent systems for the operational variables investigated has been found for the bicomponent system, so the following discussion will be restricted to the metals competition. In Figure 2(a), 2(b) and 2(c), the separation factors p_{Co}/Ni values are plotted against the A/O ratios, for the total initial metal concentration of 5, 10 and 50 mol/m^3, using initial D2EHPA concentration of 10, 50 e 100 mol/m^3, respectively.

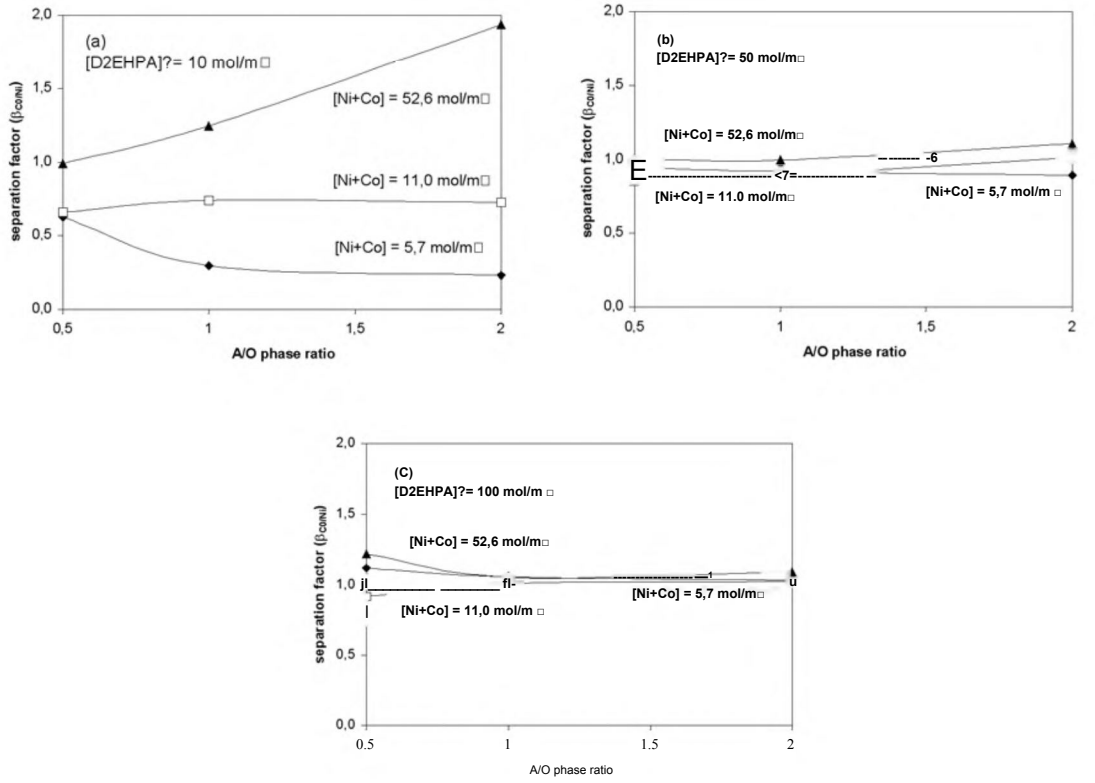


Figure 2. Co/Ni separation factors versus A/O volumetric phase ratios, for different initial metal concentration in the aqueous phase and initial D2EHPA concentration (C_B°) in the organic phase, (a) C_B° = 10 mol/m^3, (b) C_B° = 50 mol/m^3 and (c) C_B° = 100 mol/m^3.

Comparing Figures 2(a), 2(b) and 2(c), it is seen that metals separation occurs only at lower concentration level of initial D2EHPA concentration, Figure 2(a). In this case, a decrease of the separation factor Co/Ni with the increase of A/O ratio for the lowest initial metal concentration in the aqueous phase investigated (5.7 mol/m^3) and an increase of p_{Co}/Ni with the A/O ratio for the highest one (52.6 mol/m^3) has been obtained. In the first case, nickel was preferentially extracted and, in the last one, the extraction of cobalt was favoured. Maybe, the separation factor that benefits Ni in diluted systems can be derived from the different aggregation numbers of the macromolecular arranges exhibited by Ni and Co in D2EHPA/n-heptane systems [3], According to Yu *et al.* [3], Ni-D2EHPA complex has aggregation number of 5, independently of the Ni concentration in the organic phase. On

contrary, the aggregation number for Co varies from 8650 to 470 by extrapolating its behaviour, reducing exponentially as Co concentration in the organic phase varies from 0.09 to 4.37 mol/m^3. Probably, if organic-nickel complex has a smallest structure, its formation is easiest, compared to the organic-cobalt complex. For this reason, the Ni extraction can be favoured at lower concentrations of extractant and metal in the aqueous phase.

Equilibrium Data Fitting

Data fitting was carried out using the software Statistica® for Windows and Eq. (3) was used to fit data for the bicomponent system. It was obtained by rearranging Eq. (1) in the case of M = Ni and substituting the mass balance of extractant for the bicomponent system. In order to fit data from the monocomponent system, the last term of Eq. (3) has to be deleted.

$$2pH_E = \log\left[\left(\frac{\hat{}\,c^{\circ}\text{-}\,c\,'tV}{C_{\blacksquare' CNi\,J}}\right)\frac{aq}{\mathbf{V}_{\bullet rg}}\right] \text{-log(Kj-}$$

$$-n_{Ni}\,loo\left[C_{B}\,\mathbf{R}_{\blacksquare\,\blacksquare\,Ni}\,n_{Ni}\mathbf{Jc^{\circ}} - C_{M}\right)\frac{V_{aq}}{V_{org}} - \mathbf{n}_{,Co}\,\mathbf{Jc^{\circ}}_{Co} - \mathbf{oj}_{'Co}\ \frac{V_{aq}}{\mathbf{V}_{\bullet rg}}\right] \quad \textbf{(3)}$$

Apparent equilibrium coefficients $\mathbf{K_M}$ and stoichiometric constants n_M have been obtained by data fitting using experimental information from the aqueous phase only (metals and pH) and incorporating mass balance of extractant as well. The Quasi-Newton optimisation method was used and the objective function to be minimised was the absolute deviation between pH_E calculated and experimental. It has been found that stoichiometric constants for Ni and Co converge to n_M = 2 for the conditions investigated. Estimates of K_M are shown in Table 1, including 95% confidence level. Figures 3(a) and 3(b) compares calculated and experimental pH for the monocomponent and bicomponent systems, respectively. No correlation between estimated parameters has been detected (p-level = 0).

Table 1. Apparent equilibrium coefficient for the extraction of Ni and Co with D2EHPA.

	Monocomponent system		Bicomponent system	
	Ni	Co	Ni	Co
K	**(1.1 ± 0.3)** x **icr^4**	(2.4 ± 0.6) x 10‘^{4}	(2.7 ± 0.3) x 10‘^{4}	(2.3 ± 0.4) x 10‘^{4}
R"	0.813	0.809	0.964	0.929

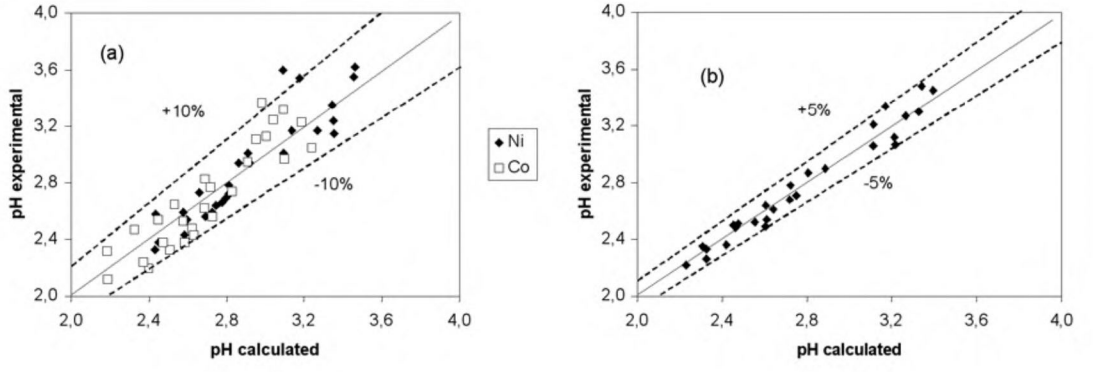


Figure 3. Calculated versus experimental equilibrium pH for (a) monocomponent system and (b) bicomponent system.

According to estimates of K_M shown in Table 1, both metals Ni and Co are extracted with

D2EHPA in a very similar way because KM values are quite close. For the monocomponent case, Kco is a bit higher than K_{Ni} thus indicating some preference of D2EHPA for Co as found in the literature [1, 2, 4, 5], However, K_M values are statistically the same for the bicomponent system. It seems that, for the operational conditions investigated in this study, the extraction of Ni is enhanced when both metals compete for D2EHPA at the liquid-liquid interface. The large aggregation number of Co at dilute concentrations of Co-D2EHPA complex in the organic phase may interfere in the Co extraction while Ni extraction proceeds with no interference until equilibrium pH is reached. This behaviour deserves further investigation.

CONCLUSIONS

The percentage extractions of Co and Ni were low, less than 22%, once there was no pH control during extraction. Considering the individual effects of the variables investigated in this study and according to the selected ranges, the concentration of D2EHPA in the organic phase exercised the prevailing effect, followed by the volumetric ratio A/O and, finally, the initial metal concentration in the aqueous phase. For the particular case of the bicomponent system, lower concentrations of D2EHPA affect the Co/Ni separation factor. Nickel extraction is favoured when it is associated to low metal concentration in the aqueous phase (10 mol/m^3). Otherwise, when the metal concentration is high (100 mol/m^3), Co is preferentially extracted. Probably, it happens due to the smallest aggregation number of Ni organic complex, independently of the Ni concentration in the organic phase that may turn it easier to be formed compared with Co organic complex. The aggregation number of Co organic complex reduces exponentially as the Co concentration in the organic phase increases.

The extraction of Ni and Co with D2EHPA for the operational conditions investigated in this study has been obtained by equilibrium data fitting as:

$$M^{2+} + 2(\overline{HA})_2 \circ \overline{MAJ\text{-}L} + 2H^{\wedge} \qquad (4)$$

and estimates of the apparent equilibrium coefficient have shown that $Kc_0 > K_N i$ for the monocomponent system and $Kc_0 * K_{Ni}$ for the bicomponent one. This behaviour is possibly associated to the formation of aggregates in the organic phase.

ACKNOWLEDGEMENTS

This work was developed with financial support for J. P. Ferreira Filho as scholarship holder for master degree by CAPES and CNPq (Brazilian Government Agencies).

REFERENCES

1. G. M. Ritcey and A. W. Ashbrook (1984), Solvent Extraction, Principles and Applications to Process Metallurgy, Part I, Elsevier, New York, USA.
2. Z. Kolarick (1982), Pure and Appl. Chem., 54(12), 2593-2674.
3. Z. -J. Yu, T. H. Ibrahim and R. D. Neuman (1998), *Solvent Extraction and Ion Exchange,* 16(6), 1437-1463.
4. P. R. Danesi, L. Reichley-Ynger, G. Mason, L. Kaplan, E. P. Horwitz and H. Diamond (1985), *Solvent Extraction and Ion Exchange,* 3, 435-451.
5. B. K. Tait (1993), Hydrometallurgy, 32, 365-372.



EXTRACTION TREATING OF CARBONATE SOLUTIONS OF TUNGSTEN-CONTAINING MINERAL LEACHING

S.I.Stepanov, V.G.Giganov, G.P.Giganov*, A.M.Chekmarev

D.Mendeleev University of Chemical Technology of Russia
*FSUE «GINZVETMET Institute^ Moscow, Russia.

Extraction of tungsten and molybdenum from carbonate solutions by MTAA salts has been studied according to polymerization mechanism. It was demonstrated that the fact of polymerization promote preferable extraction of W, its purification from non-polymeric impurities and rising of extractant capacity. It was staffed that effective re-extraction from organic phase can be fulfilled by depolymerization of W polyanions in presence of alkalis. Ammonium reextracts which were obtained in this process are near to ammonium reextracts obtained in extraction by amine salts from point of view of tungsten content and its quality. Variants of technological scheme for carbonate solution of W mineral concentrates leaching treating by the tungsten extraction directly from carbonate solution were discussed.

INTRODUCTION

Using sodium leaching of W and Mo-containing ore concentrates the carbonate solutions with high sodium carbonate and sodium tungstate content and low sodium molybdate content are obtained [1], Solvent extraction treating of such solutions is carried out after sodium carbonate neutralization by mineral acid, e.g. sulfuric or hydrochloric acid. Tertiary amines salts are used as extractants. Negative features of such method of carbonate solutions treating are irrevocable losses of sodium carbonate and acid and big amount of waste waters formation at the stage of neutralization.

The alternative scheme of the carbonate solutions treating is extraction of these metals directly from carbonate solution with using of quaternary ammonium salts (Q.A.S.) in particular methvltrialkvlammonium carbonate (MTAA) 121.

In the carbonate solutions with pH>8,5 W and Mo are present in the anion forms W042- and Mo042-, that is why extraction of W and Mo from such solutions with MTAA carbonate is usually related to an anion exchange reaction [3]:

$$(R4N)_2C03org. + WO^ag. = (R4N)_2W0_{4\ 0}rg. + CC^'aq. \quad (1)$$

W and Mo extraction regulations according to reaction (1) are studied sufficiently well in the works [2-4], With sodium carbonate concentration increasing in water solution the coefficient of metal distribution (DW(Mo)) is decreasing while effective extraction can not be already achieved at sodium carbonate concentration more than 100 g/l. Significant depressing influence on W and Mo extraction from carbonate solutions according to mechanism of anion exchange single-charged anions such as NQ3- and Cl- and especially HCQ3- produce.

These anions usually present in carbonate solutions as impurities. They are used for stripping of W and Mo from organic phase according to the reaction of anion exchange:

$$(R_4N)_2W0_{4\ org} + 2HC0_3'_{aq.} = 2R_4NHC0_3org. + W0_4^{2-}{}_{aq.} \quad (2)$$

Stripping of W and Mo by ammonium or sodium bicarbonate is connected with the high discharge of these salts and with difficult following reprocessing of reextracts. These and some other reasons restrain industrial using of W and Mo extraction from carbonate solution by MTAA carbonate.

EXPERIMENTAL

W concentrate, containing (%): W03 -30-35, Si < 10, P < 0,11, As - 0,2, F -1,0-1,5 was used in present work. Autoclave soda leaching was carried out in steel autoclaves 0,5 L by volume, under T = 225°C and pressure 25 atm. Soda equivalent was varied from 2 to 4. Technical soda without purification was used as sodium carbonate. The content of NaCI in soda was < 0,5%. The main extractant was methyltrialkylammonium carbonate, general formula [(C7H15-C9H19)3CH3N]2C03 which was prepared from industrial sample of MTAA methylsulphate. The content of O.A.S. was not less 96 % and amines not more 4% on recalculation to “wet” product. MTAA carbonate was prepared from MTAA methylsulfate by reprocessing: 9,0 M H2S04 - 3 contacts, 0:W=1:1, 5,0% NaOH up to pH =10-11 of final water phase and 5,0% Na2C03 - 3 contacts, O: W= 1:1.The fullness of the conversion was checked by the functional chemical analysis of R4N+, C032-. The diluent employed for the solvent extraction was kerosene with 5-15% - iso-octanol. Analyses of W and impurities in water solutions were made, using common analytical methods.

RESULTS AND DISCUSSION

W and Mo extraction according to polymerization mechanism.
W and Mo extraction according to the anion exchange takes place at pH > 8,5. Another mechanism of extraction can be suggested for explanation of extraction regularities which are observed in pH interval 7-8,5 in the case, if the MTAA bicarbonate is used as an extractant. In this case significant rising of distribution coefficient of W and Mo is observed, Table 1, in spite of the fact that single-charged anion HC03- is better extracted to organic phase according to anion-exchange mechanism, reaction (1), than double-charge anions W042- and Mo042-.

Table 1. Extraction of W and Mo by carbonate and bicarbonate of MTAA from 55 g/l Na_2C0_3 and 12 g/i $NaHC0_3$ solutions, correspondingly. 0:W=1:1.

25% $(R_4N)_2C0_3$ kerosene + 15% Iso-octanol						30% R_4NHCO_3 kerosene + 15% Iso-octanol		
Cw, aq.j g/i	Cw, org.. g/i	Dw	CMO, aq., g/i	CMO, org.. g/i	DMO	Cw, aq., g/i	Cw, org., g/i	Dw
11,0	22,2	2,02	1,06	2,40	2,27	59,4	21,5	0,36
23,7	26,8	1,13	2,40	3,36	1,40	63,6	17,3	0,27
50,0	27,8	0,56	5,18	4,03	0,78	53,3	27,6	0,52
63,4	28,5	0,45	7,10	4,22	0,59	33,8	47,1	1,39
-	-	-	-	-	-	24,6	56,3	2,28

Such behavior of W and Mo is connected with polymerization of oxyanions W042- and Mo042- in organic phase under bicarbonate group proton influence:

$$8R_4NHC0_3org. + 7W0_4^{2'}{}_{aq.} = (R_4N)_6W_70_{24\ org.} + (R4N)_2C0_3org. + 4H_zO + 7C0_3^{2''}{}_{aq.} \quad (3)$$

The reaction of extraction passing according to the reaction (3) was named by us as polymerization mechanism of extraction [5], Its realization is possible at using as an extractant MTAA mono-tungstate. In Table 2, the results of W extraction by tungstate of MTAA from carbonate solutions at conditions creation for oxytungstate anions polymerization in organic phase effective extraction of W in organic phase is observed.

Table 2. W extraction by 30% vol. MTAA tungstate in kerosene +15% vol. iso-octanol according to polymerization mechanism. 0:W=1:1.

pH	Cw aq IQ/I	Cw orq., Q/I	D w
8,7	79,1	51,5	0,65
8,3	48,4	83,5	1,73
8,0	28,3	103,7	3,66
7,5	18,4	113,6	6,18
7,3	10,1	122,6	12,1
7,0	4,6	125,0	27,2

The peculiarity of W extraction according to the polymerization mechanism is low speed of the process. In the Table 3 the results on W distribution to organic phase in connection with the time of the process are presented. The maximum of distribution is reached for 45 - 60 min. At the same time this defect of polymerization extraction is compensated by sufficiently full W withdrawing at one stage of extraction. For deep W withdrawing from such solutions according to anion exchange mechanism from 3 to 5 stages of extraction are required.

Table 3. Dependence of W distribution from the time of the extraction by 20% vol. MTAA carbonate in toluene according to polymerization mechanism. 0:W=1:4.
C_w initial = 42 g/l, C Na_2CQ_3 = 10 g/l.

Time, min	pH eq	Cw aq.,9/1	Cw orq., 9/1	Dw
2	9,5	33,0	36	1,09
5	8,3	26,5	62	2,34
10	7,8	14,5	110	7,59
20	7,5	12,5	118	9,44
45	7,5	11,8	121	10,3
60	7,4	11,5	122	10,6

W and Mo stripping from polymeric extracts.
On formation of W and Mo polyanions in organic phase stripping according to mechanism of anion exchange is complicated:

$$(R_4N)_6W_70_{24}\ org. + 6HC0_3'aq. = BF\text{^}NHCO,\ org. + W_70_{24}{}^{6}{}_{aq.}{}^{-} \quad (4)$$

For fulfilling of such stripping solutions of bicarbonate salts with high initial concentration and multistage process are needed. At the same time the stripping can be carried out with using of the depolymerization of W polyanions reaction which takes place in the presence of alkaline reagents:

$$(R_4N)_6W_70_{24org.} + 80H_{aq.} = 3(R_4N)_2W0_{4org.} + 4W0_4^{2'}{}_{aq.} + 4H_zO \quad (5)$$

In this case more then a half of all tungsten, which is in organic phase, passes to aqueous phase at one stage, Table 4. The rest of tungsten in the state of MTAA tungstate can be stripped additionally according to anion exchange reaction or without any treatment can be passed to the stage of polymerization extraction.

Table 4. W stpipping from MTAA polytungstate by alkaline reagents.
C_w org. initial = 110,3 g/l

N°	Stripping solution	O:W	C NH_4OH, M	Cw, aq.i Q|/l	Pw,%
1	1,75 M NH_4OH	1:1	0,98	69,9	63,3
2	2,0 M $(NH_4)_2C0_3$	1:1	-	86,4	78,3
3	2,35 M NH_4OH	3:1	0,52	169,1	51,1
4	2,5 M $(NH_4)2C0_3$	3:1	-	161,8	72,1
5	3,5 M NH_4OH	3:1	1,03	228,0	68,9
6	2,5 M $(NH_4)_2C0_3$ + 2,35 M NH_4OH	2:1	0,83	178,3	80,8

Technological scheme of W extraction from carbonate solutions.
Formerly the technological scheme of tungsten extraction from carbonate solutions of autoclave leaching of mineral raw materials (e.g. wolframite concentrates) was suggested [2] (Fig. 1). The scheme included W extraction with MTAA carbonate, scrubbing of the organic phase by water, stripping by carbonate - bicarbonate solutions of ammonium salts with following isolation from it ammonium para-tungstate (A.P.T.). The complication of the last stage consists of difficulties of the solutions treating, which contain 20-60 g/l W and 200 - 300 g/l (NH4)2C03 + NH4HC03. They must be evaporated or carbonate salts must be decomposed.

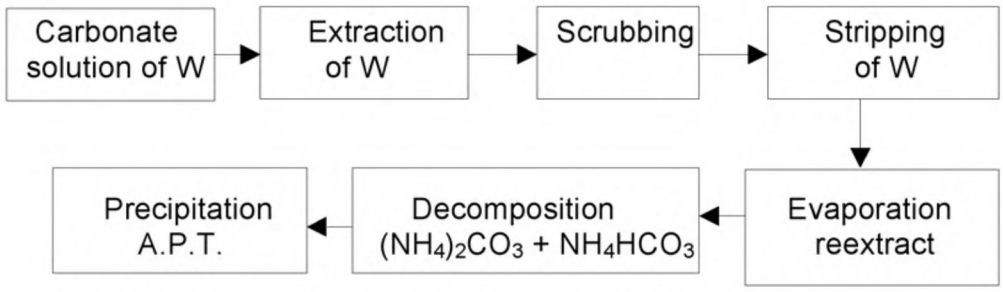


Figure 1. Principal flowsheet for the recovery of tungsten from carbonate leaching solution according to the anion exchange mechanism of extraction.

Former discussed regularities of the W and Mo polymerization extraction allow to propose principally other variant of technological scheme formation (Fig.2). At the first stage W extraction from sodium carbonate solutions is fulfilled. The extraction is carried out by MTAA carbonate according to anion exchange mechanism, reaction (1), with following stripping by concentrated solutions of ammonium bicarbonate, reaction (2). Obtained reextracts are sent to the second stage of extraction which is carried out by MTAA tungstate according to polymerization mechanism. Saturated by tungsten organic phase is washed by water for impurities removing and is re-extracted by ammonia solutions with high value of pH. Formed MTAA tungstate is recycled to the second stage of extraction without additional purification. Formed reextract with W concentration up to 100 g/l is reinforced by ammonia and send to repeated stripping of ammonium polytungstate till W concentration in the reextract reach 200-250 g/l. After that the reextract is took out for A.P.T. producing by evaporation of the solution and crystallization.

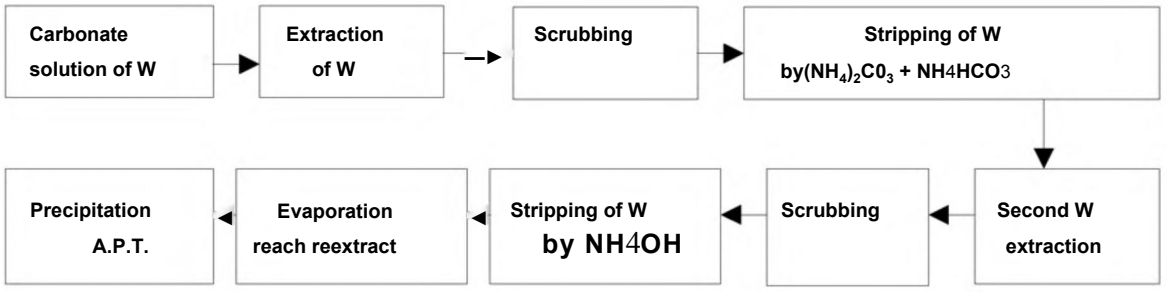


Figure 2. Principal flowsheet for the recovery of tungsten from carbonate leaching solution according to the polymerization mechanism of extraction.

Suggested variant of the technological scheme settles the problems of the treating of concentrate carbonate - bicarbonate solutions with comparatively low W content without evaporation or carbonate salts decomposition. At the same time the second extraction according to polymerization mechanism allows to carry out deep purification of W solutions from impurities. This raises the quality of the last product - A.P.T. It is necessary to point out that both: the stage of polymerization extraction and the stage of depolymerisation stripping are one stage processes.

For an enlarged laboratory testing technological solutions of autoclave sodium carbonate leaching of W concentrate of the next composition, g/l: W - 74, Na2C03 - 80, Si02 -1,5, As -0,1, F - 2,2, were used. As an extractant at the first stage of extraction it was used 25% vol. solution of MTAA carbonate in kerosene with 10% vol. of iso-octanol. Extraction was carried out at 0:W = 3:1 at the 3-stages of countercurrent division. Concentration in the organic phase was 22-24 g/l of W. The rest W concentration in the raffinate was 1,5-2 g/l. The organic phase saturated with W was scrubbed by water at 0:W = 5:1 at two stages of the division. Sodium concentration in the scrubbing water was 1,3 g/l after the first stage and 0,07 g/l after the second stage of scrubbing.

W stripping from the washing up organic phase was fulfilled by water solution containing 90 g/l NH4HC03 and 2 g/l W at 0:W = 1:1 at four stages of countercurrent division The reextract contained 22-24 g/l W and circulating organic phase - 1,2 - 1,8 g/l W. Sodium concentration in the reextract was not more than 3-4 mg/l, which guarantees obtaining of the high grade commercial A.P.T.

From joint reextracts containing 22-24 g/l of W and 50-60 g/l NH4HC03 the extraction of tungsten was fulfilled in the conditions at which polymerization mechanism took place by 10% vol. solution of MTAA tungstate in kerosene with 5% vol. of iso-octanol at 0:W = 1:1,5 at one stage of extraction. Obtained extract contained 33-35 g/l W The rest W concentration in the raffinate of the second extraction was 1,5-2,0 g/l W.

Stripping of MTAA polytungstate was carried out by 8% vol. water solution of ammonia at 0:W = 5:1 at one stage. At the first circle of stripping the solution with W concentration near 103 g/l was obtained. This reextract was made more concentrated up to concentration of NH3 excessive 8% vol. and it was used at the second cycle of polytungstate stripping. The solution with W concentration 205 g/l was obtained. The last reextract was evaporated up to 50% of its initial volume with successive cooling and A.P.T. crystallization. 155 g/l of A.P.T. crystals was obtained with corresponded to the industrial standards of impurities content.

CONCLUSION

The extraction of W and Mo according to polymerization mechanism was studied. It was shown that at polymerization of oxytungstate anions in organic phase in the presence of mineral acid proton the polytungstate of different composition (preferably W70246-) are formed. The extraction can be carried out with MTAA tungstate and it is accompanied by significant rising of extractant capacity and additional purification from the impurities.

Suggested technological scheme of carbonate solutions which were produced by leaching of mineral raw material and which include two stages of W extraction with successive obtaining of ammonia reextracts of W and precipitating from them the ammonium para - tungstate of high quality.

LITERATURA

1. G.P.Giganov, A.M. Tzericova, T.Sh. Agnokov, V.A.Penchalov, V.B.Levich. (1988), *Zvet. Met.,* 5, 67-71 (Russ. Edit.)
2. S.I.Stepanov, V.G.Giganov, G.P.Giganov, A.M.Chekmarev (1999), *Proc. ISEC'99,* SCI, 2, 1493-1497.
3. V.P.Zaitsev, I.M.Ivanov, N.K.Kalish, T.V.Us. (1992), *Proc. 2 Int. Conf. Hydromet.,* Changsha, 137-141.
4. V.G.Giganov, M.G.Bolotin, S.I.Stepanov. (1990), *Proc. MUCTR,* Moscow, 3-7. (Russ. Edit.)
5. S.I.Stepanov, A.M.Chekmarev. (2002), *Proc. Conf. 50 Years of Russian Solvent Extraction,* St.-Petersburg, 149-154. (Russ. Edit.)

RECOVERY OF NITRIC AND HYDROFLUORIC ACIDS FROM INDUSTRIAL WASTE

Jeaneth dos S. Benedetto, Carlos A. Morais and Percy A. Bocardo
Jsb@cdtn.br; cmorais@cdtn.br

Centro de Desenvolvimento da Tecnologia Nuclear - CDTN/CNEN
Belo Horizonte, Brazil

This paper presents a study of the recovery of nitric and hydrofluoric acids mixture present in industrial waste from stainless steel pickling processes. Acids are recovered by solvent extraction using tributylphosphate as extractant and a pure aqueous phase in the stripping step. Continuous experiments were carried out in a pulsed column circuit. In this work, it was investigated the effect of H_2S0_4addition on the nitric and fluorite acids recovery.

Hydrodynamic parameters were investigated in order to obtain the operating conditions of the pulsed column. Dispersed phase hold-up was determined by sampling the mixture from the middle of the column and mass transfer performance by measuring the inlet and outlet rate flow and analysing the Fluoride and nitrate content.

It was possible to obtain an aqueous solution of high purity containing nitric and hydrofluoric acids that may return to the steel pickling process after adjusting to the required concentration. In order to remove these acids it was necessary to add another acid of lower cost to the liquor as sulphuric acid. Consequently $N0_3'$ and F^- were freed to be extracted. The yield of the extraction of these acids was 91% for the nitric acid and 62% for the hydrofluoric acid.

INTRODUCTION

In general, neutralisation is carried out before the discharge of the pickling bath, resulting in the precipitation of the metals and anions present in the solution. The re-utilisation of acids represents large savings potential aiming at the reduction of the environmental impact, while keeping a favourable economic balance.

The technique of solvent extraction by its selectivity has been broadly applied to the recovery of elements and compounds present in aqueous solutions with a high degree of purity. Neutral organophosphorous compounds have the ability to extract acids and have therefore been proposed to be used in the nitric and fluoride acid recovery. One of the properties of these reagents which has been of particular interest is the ability to form complexes with mineral acids in ratios of acid to extractant of greater than unit. For example $TBP.xHN0_3$, where x = 1,2,3 or 4. The preferential extraction of acid for TBP in high acidity medium is due to the metal species in the aqueous phase became anionic [1],

If a large number of theoretical stages is required, agitated or pulsed columns offer an

economical solution. In a pulsed sieve plate extractor, the sieve plate is rigidly installed inside the column and the liquid content of the column is pulsed by an external pulsator flanged to the column bottom[2].
This paper presents a study of the recovery of a nitric and hydrofluoric acids mixture present in industrial waste from stainless steel pickling processes. Acids are recovered by solvent extraction using tributylphosphate as extractant and pure water in the stripping step. The continuous tests were carried out in a pulsed column circuit.

It is known that undissociated acids like $HN0_3$ and HF form adduct complexes with organic compounds containing oxygen donor atoms. Because the adducts formed are soluble in organic solvents, the acids can be removed from aqueous solutions by organic solvents. However, in the pickling bath most of the nitrate and fluorite is bound to the metals as nitrate and fluorite complexes. By adding H_2S0_4 to the pickling bath, $S0_4^{2-}$ replaces some of the $N0_3^-$ and F^-
leading to the formation of extractable species, $HN0_3$ and HF [3],

PROCESS DESCRIPTION

Materials

The aqueous phase used in this work is a waste liquor from stainless steel pickling processes. The composition of the waste is shown in table 1. Tributylphosphate-TBP diluted in isoparaffin was used as the extractant for the acids extraction and water was used as the stripping agent. Sulphuric acid was added to the feed liquor as conditioning solution.

Table 1. Chemical characterisation of the waste solution.

Species	Concentration
H^+	1.80 mol/L
NO_3^-	150 g/L
F^-	49.0 g/L
Fe^{3+}	37.8 g/L
Ni^{2+}	4.1 g/L
Cr^{3+}	6.1 g/L

Apparatus and Measurement Techniques

Acid extraction and stripping were tested in a pulsed column circuit as shown on figure 1. The height of the main section of the columns consisted of a 300 cm glass tube for the extraction stage and 200 cm for the stripping with internal diameter of 26mm enclosing a stack of perforated plates. The distance between the plates was 50 mm. The diameter of the holes in the plates was 3 mm and the hole area 23 % of the column area. The diameter of the top and bottom settlers of the column was 35mm. The aqueous and organic phases were fed in counter current flux through peristaltic pumps which allowed constant flows, which essential to maintain a stable operation. The pulse was generated by a diaphragm pump.

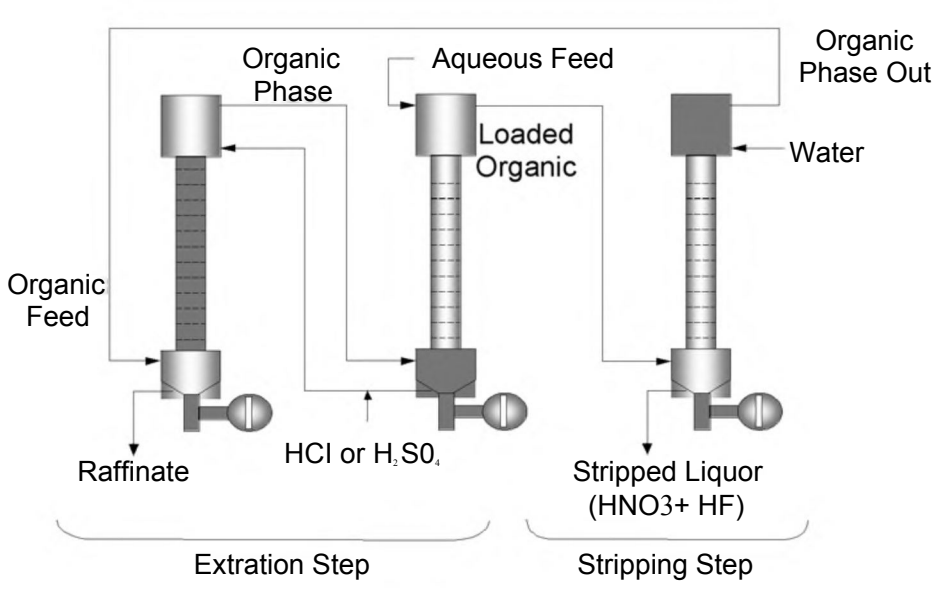
Hydrodynamic parameters were investigated to determine the operating conditions of the pulsed column. Dispersed phase hold-up was determined by sampling the mixture from the middle of the column.

Mass transfer performance was investigated by measuring the inlet and outlet rate flow and analysing the Fluoride and nitrate content. They were measured with a selective ion electrode and acidity was determined by potentiometric titration with sodium hydroxide.

RESULTS

Hydrodynamic of the Column

The extraction step operated with two pulsed columns. In the first one, where the aqueous phase was fed, it was carried out an aqueous continuous phase to improve the organic loading. The second column operated with an organic continuous phase in order to obtain maximum acids extraction. For the striping step, one column was installed with the same characteristics of the column 1 which was maintained the organic dispersed system.



Figurel. Diagrammatic arrangement of pulsed column.

The results for operating characteristics in emulsion regime indicated an amplitude of 8 mm and a frequency range of 25 - 30 cycles/minute. Holdup was previously determined under operating conditions of the column and maintained during the runs.

Nitric and hydrofluoric acids equilibrium data

By adding HCl or H_2S0_4, the metal complexes with nitrates and fluorides in the waste are converted into chlorides or sulphates, and $HN0_3$ and HF are set free. Next, nitric-hydrofluoric acids are extracted using TBP as extractant.

To obtain satisfactorily high distribution ratios for these acids, the TBP concentration in the organic phase was chosen to be 70% (by volume) in isoparaffin. Although higher TBP concentration produces better distribution ratios, the physical properties of the higher concentration are not recommended. In these conditions, two phase systems make handling them difficult under practical extraction conditions[4].

Figure 2 shows the distribution of acids between aqueous and organic phases after H_2S0_4 conditioning and without H_2S0_4 addition.

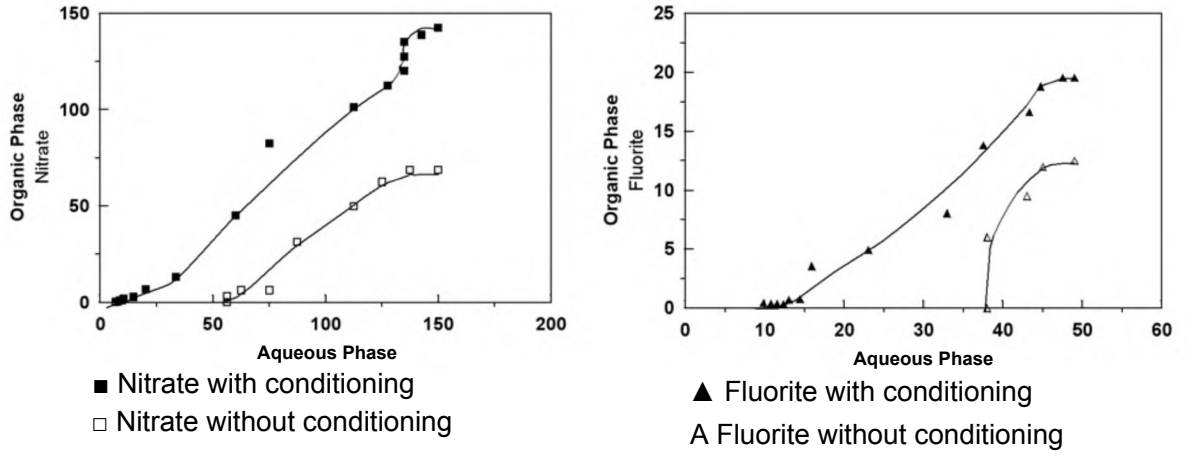


Figure 2. Acids extraction equilibrium data

Based on the Equilibrium data we can see that the H_2S0_4 conditioning was fundamental to obtain a high acids recovery. MacCabe-Thiele diagram indicates a high number of theoretical stages for extraction of the acids in a phase ratio A/O = 0.5, as shown by the operation line. The results have not shown a clear number of theoretical stages. In this case pulsed columns are recommended since they offer high separation efficiency and a simple design. Results of simulations indicated pulsed columns with 300cm of effective height for the extraction step, under the previous conditions investigated for this sample.

Continuous experiments

Operational conditions for experimental runs in a pulsed column are presented in table 2. These conditions were based on hydrodynamic studies of the column. The $HN0_3$ and HF in the aqueous phase were then contacted with a counter-currently flow of the organic solvent. The interface was kept at a constant level by automatic control. Steady-state operation was achieved after a throughput of 4-6 continuous phase volumes. Samples were collected for analysis from aqueous and organic extract.

Previous experiments were carried out to define the amount of sulphuric acid to be added in a feed solution based on a stoichiometric relation in terms of metals content in the liquor. The H_2S0_4 excess varied from 0 to 30%. The stoichiometric relation presented the same results of the tests done with excess of sulphuric acid.

The goal of this study was to investigate the point in the circuit extraction of sulphuric acid addition and its influence on the acids recovery since there was some parts of the acids that were not complexed with the metals. It was expected that these free species would be extracted before conditioning and would probably change the extraction coefficient. On the first test - HI, the point of conditioning with sulphuric acid was between the two columns and in test H2 it was before the feeding extraction step.

Table 2. Operational conditions for the runs

Run	Conditioning		Hold up		O/A	
	Acid	Local addition	Extraction	Stripping	Extraction	Stripping
HI	H_2SO_4	Between the two extraction columns	7.5	13.0	2	1
H2	H_2SO_4	Before the first column	8.0	13.0	2	1

Typical results from the extraction and stripping are shown in table 3. Test H2 presented better mass transfer than test HI on the extraction step. However the stripping showed the same performance in both experiments. The extraction of $HN0_3$ and HF reached 91% and 62% respectively, under operating conditions of the test H2 showed in the table 2. Practically all the extracted acids were stripped by water in both experiments.

CONCLUSIONS

- It was possible to obtain an aqueous solution of high purity containing nitric and hydrofluoric acids that may return to the steel pickling process after adjusting to the required concentration. In order to remove these acids it was necessary to add another acid of lower cost to the liquor - sulphuric acid. Consequently $N0_3$‘ and F^- were freed to be extracted. The yield of the extraction of these acids was 91% for the nitric acid and 62% for the hydrofluoric acid.
- The work carried out provided the necessary information to subsidise a study of economic pre-feasibility and market analysis.

Table 3. Continuous experiments results

Test	Flow	Medium flow rate (mL/min)	NO_3-		F^-	
			Concentration (g/L)	Distribution (%)	Concentration (g/L)	Distribution (%)
HI	Aqueous feed	7.7	150.0	100.0	49.0	100.0
	Final raffinate	7.4	20.0	87.2	22.0	56.9
	Loaded organic	17.0	59.2	12.8	12.6	43.1
	Stripping liquor	16.5	60.0	85.5	12.7	55.8
H2	Aqueous feed	7.9	150.0	100.0	49.0	100.0
	Final raffinate	7.4	14.0	**91.2**	20.0	**61.8**
	Loaded organic	17.0	63.6	8.8	14.1	38.2
	Stripping liquor	16.3	63.7	**89.4**	14.4	**60.6**

ACKNOWLEDGEMENTS

The authors thank the FINEP - CT MINERAL for financial support to this work.

REFERENCES

1. G. M. Ritcey and A.W. Ashbrook (1984), *Solvent Extraction: Principles and Applications to Process Metallurgy,* Part I, Elsevier, Amsterdam, pp. 146 - 153

2. J. C. Godfrey and M. J. Slater (1994), *Liquid-liquid Extraction Equipment,* John Wiley & Sons Ltd, Chichester, pp.277 - 305

3. J. Rydberg, , H. Reinhardt, B. Lunden and P. Haglund (1973, *Proc.International Symposium on Hydrometallurgy,* pp. 589 -611.

4. C. E. Da Silva, J. S. Benedetto and E. B. Tambourgi, 1999, *Proc. International Solvent Extraction,* Barcelona, Spain, pp.189 - 194.

GALLIUM EXTRACTION BY MICROEMULSIFIED SYSTEMS USING SAPONIFIED COCONUT OIL

T.N. Castro Dantas*, M. H. de Lucena Neto, A. A. Dantas Neto, M. C. P. A. Moura, and E. L. Barros Neto

*Universidade Federal do Rio Grande do Norte
Programa de Pós-Graduagão em Engenharia Quimica
Campus Universitário - 59.072-970 Natal/RN/Brazil
e-mail: tereza@eq.ufrn.br

In this research the extracting agent used was saponified coconut oil (SCO) applied in microemulsified systems. Gallium extraction process by microemulsions occurs in a Winsor II region. In this research the variation of the cosurfactant/surfactant ratio (C/S) was investigated (4 to 60) being accomplished with the purpose to use the smallest amount of surfactant. After chosen the C/S ratio, the study of the surfactant saturation was accomplished varying the metals concentration in the Bayer liqueur. After optimization of the extraction process, eighteen extraction rehearsals were made with its composition previously defined in the obtained pseudoternary phase diagram, organized according an experience matrix, in agreement with the Scheffé's Net. The aim of the Scheffé's Net is to faithfully translate the variations of the answers (extraction percentiles) as a function of the mixture constituents. Using the experimental results, made in duplicate, statistical software was employed to supply the mathematical models and the isoresponse curves, which allowed a better evaluation of the extraction behavior. In a second stage, the study of the reextraction process was made using different concentrations of hydrochloric acid (HCl) solutions with the purpose of obtaining the selectivity between gallium and aluminum.

INTRODUCTION

Bayer process is a way of making alumina extraction from bauxite. Essential steps in the Bayer process involve grinding the bauxite then dissolving or digesting the gibbsite in hot caustic soda solution. The insoluble bauxite residue, called red mud, is separated from the solution by allowing it to settle out leaving the liquor, rich in alumina. Gallium follows the aluminum in its bauxite ores, whose content is from 20 to 80 ppm. In the Bayer process about 70% of the gallium is leached from the bauxite and follows the aluminum into the caustic soda solution, the remaining 30% being disposed with the red mud [1-2].

Gallium is a scarce but not rare element. It is found most commonly in association with zinc, germanium, and aluminum. The toxicity of metallic gallium or gallium salts is very low. The application of gallium that has received the most attention is the production of semiconducting compounds and analog integrated circuits. The most important compounds of gallium are the ones made with antimony, arsenic or phosphorus. Nowadays gallium arsenide (GaAs) is undoubtedly the most used. This compound is used in the production of several electronic parts such as diodes and transistors. Other gallium arsenide applications

are the microwave generation and also in several sensors to measure temperature, light or magnetic field [2-4],

Solvent extraction is the facile method for metal ions removal. To extract gallium in a selective way, in relation to aluminum, the most used extracting agent is Kelex-100 [1; 5-6], The search of a new extracting system is the aim of this research, where microemulsions systems made using saponified coconut oil were developed. A microemulsion is defined as a system formed by the dispersion of microdroplets of two immiscible liquids, stabilized by an interfacial membrane formed by surfactant and cosurfactant. They are thermodynamically stable, homogeneous and optically isotropic solutions. The microemulsions can exist in equilibrium with other phases, aqueous or organic, forming four types of multiphase systems: Winsor I (WI), when the microemulsion phase is in equilibrium with an organic phase in excess; Winsor II (WII), when the microemulsion phase is in equilibrium with an aqueous phase in excess; Winsor III (Will), a three phase system, where the microemulsion is at the same time in equilibrium with an aqueous and with an organic phases; and Winsor IV (WIV), a monophase system, in macroscopic scale, constituted only by a microemulsified phase [7-**11**].

The knowledge of the characteristics of microemulsified systems, as well as of its properties, requests previous studies based on pseudo-ternary phase diagrams. These diagrams were made using a mixture of surfactant, cosurfactant, aqueous phase and oil phase.

The extraction region used in this research was a Winsor II region. To study the extraction process behavior experiments were accomplished according an experience matrix in agreement with the experimental planning methodology (Scheffé Net) that was used with the purpose to translate faithfully the variations of the answers (extraction percentiles) as a function of system composition [12], After the obtaining of the experimental results, statistical software was applied to supply the mathematical models and the isoresponse curves, allowing a better evaluation of the extraction behavior.

PROCESS DESCRIPTION

Chemicals

Chemicals used during experimental were analytical grade, except coconut oil (regional production) and kerosene (Petrobrás - chemical composition: paraffinic hydrocarbons - min. 70%, aromatic hydrocarbons - max.20%, and olefinic hydrocarbons - max.5%; density < 1; viscosity 2.7 cSt at 20 °C; distillation range 150 - 300 °C at 760 mmHg), and were used without previous purification. Water used in all experiments and solutions was distilled (Tecnal TE-078 distiller).

Synthetic Bayer liquor

The preparation of the synthetic Bayer liquor was based on the compositions obtained from spent Bayer liquor obtained from Alcan (Aluminio do Brasil Ltda.), presenting the following concentrations: 0.195 g.L^{-1} Ga, 35.5 g.L^{-1} Al, and 132 g.L^{-1} NaOH. Metals concentrations on the aqueous samples were analyzed by flame atomic absorption spectroscopy (FAAS) using an air/acetylene reducing flame with gallium or aluminum hollow cathode lamp.

Microemulsion region determination

Pseudoternary phase diagrams were constructed with the purpose to delineate the Winsor's regions. To determine the Winsor's regions, the oil phase was mixed with the surfactant /cosurfactant phase (pseudo-constituent pure) and the mixture was titrated with the Bayer liquor, observing the diverse phases formed and its transitions. The volume of Bayer liquor used for each transition was recorded. The pseudoternary phase diagrams were constructed by plotting the amounts of aqueous phase, oil phase, and surfactant/cosurfactant phase

used in the experiment (Figure 1). All systems were composed by Bayer liquor (aqueous phase); kerosene (oil phase); (SCO- surfactant) and isoamyl alcohol (cosurfactant).

Gallium extraction and reextraction processes

In the extraction process mixtures of surfactant, cosurfactant, oil phase and aqueous phase were made, whose composition of each experimental point was determined by an statistical planning methodology (Scheffé Net), inside the experimental domain area (WII region), as can be seen in Figure 1.

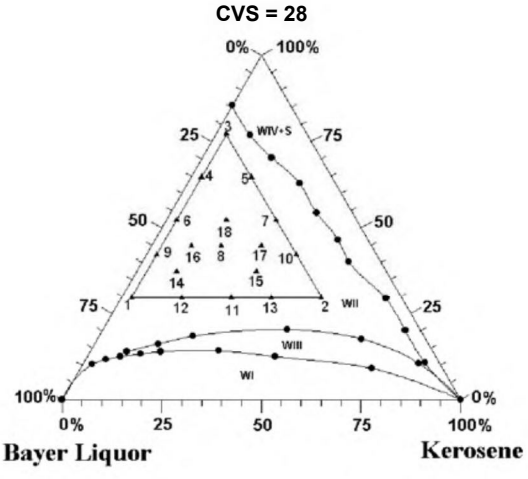


Figure 1. Pseudoternary phase diagram for the studied system showing the Scheffé Net and Winsor's regions.

The selected points to carry out the extraction study were organized according to an experience matrix [12-14] (Table 1). These points were chosen inside the water-rich region, making possible the evaluation, through mathematical models and isoresponse curves, of the extraction percentiles as a function of microemulsion system composition.

Each system was contacted, with mechanical stirring, during 30 min (time required to reach equilibrium). Afterwards, they were kept under rest to allow phases separation (microemulsion and aqueous phase). The aqueous phase was collected and gallium and aluminum concentrations could be evaluated. The metals extraction percentiles were calculated using the following equations:

$$M^{+n}_{ADDED} = V_{ss} \times C_{ss} \quad (1)$$

$$M^{+n}_{AQUEOUS\ PHASE} \equiv V_{AP} \times C_{AP} \quad (2)$$

$$\%E = \frac{M^{+n}_{ADDED} - M^{+n}_{AQUEOUS\ PHASE}}{M^{+n}_{ADDED}} * 100 \quad (3)$$

where: M^{+n}_{ADDED} is the total amount of metal added to the systems (g), $M^{+n}_{AQUEOUS\ PHASE}$ is the total amount of metal in the aqueous phase after extraction (g), V_{ss} is the used volume of synthetic solution, C_Ss is the metal concentration of the synthetic solution (Ga and Al - g.L^{-1}), C_Ap is the extracted phase concentration (Ga and Al - g.L^{-1}), V_Ap is the aqueous phase volume after phase extraction, and %£ is the metal (M^{+n}) extraction percentile.

In reextraction process hydrochloric acid was used. Its concentration was varied from 0.5 to 6 M. Acid solution was contacted with a gallium/aluminum-rich microemulsion phase (Winsor

IV) and shaken during thirty seconds, time required to promote acid and surfactant interaction, resulting in metal release from the microemulsion phase to a new aqueous phase formed. Figure 2 shows the extraction-reextraction flowsheet.

RESULTS AND DISCUSSION

Cosurfactant/surfactant ratio (C/S) influence in the extraction process

In this study was used point 1 composition showed in Table 1 (pH 6). C/S ratio was varied from 4 to 60 seeking to obtain Ga and Al extraction percentiles with the purpose to select the best ratio to be applied in the experimental planning.

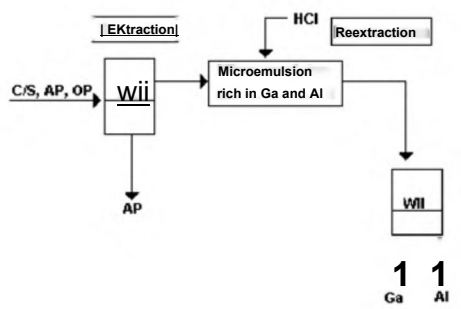


Figure 2. Gallium (Ga) and Aluminum (Al) extraction/reextraction flowsheet. (C/S - cosurfactant/surfactant ratio; AP - aqueous phase; OP - oil phase)

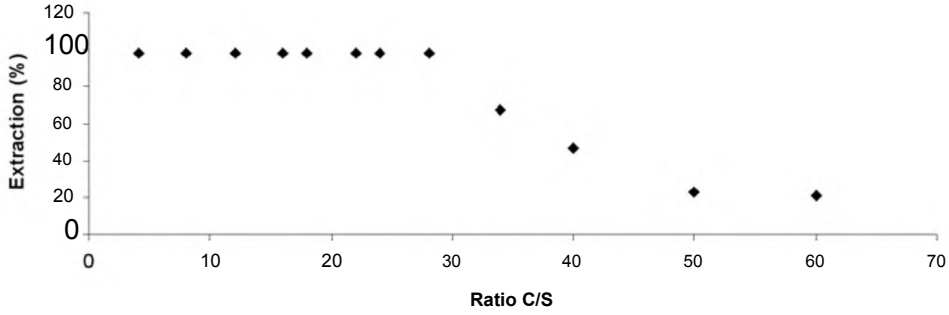


Figure 3. Cosurfactant/Surfactant (C/S) ratio influence in Ga extraction process. (T = 27 °C; pH = 6).

Figure 3 shows that Ga extraction percentile is very high until C/S ratio equal to 28, however after this value a decrease in the extraction percentile occurs, reaching very low values. This phenomenon can be explained by a reduction in surfactant amount present in the microemulsion phase, resulting in a decrease in the microemulsion load capacity, making difficult the electrostatic interactions between the co-ions of the surfactant and the ions in solution (Ga^{+3} and Al^{+3}). This study also showed that it is possible to extract these metals in low surfactant concentrations, that is, in high C/S ratios (4 to 28), which propitiate a low operational cost of Ga and Al extraction process by microemulsion.

Influence of Bayer liquor Ga and Al concentrations in the extraction process

This study was carried out with the purpose to obtain information about surfactant load capacity in removing the studied metals. It was accomplished using point 1 composition (Table 1). Ga and Al concentrations in the Bayer liquor were varied, 100 to 2000 ppm for Ga and 3000 to 6000 ppm for Al (pH 6 - C/S = 32 - T = 27 °C). The extraction percentiles for Gallium and Aluminum were obtained using equations 1 to 3.

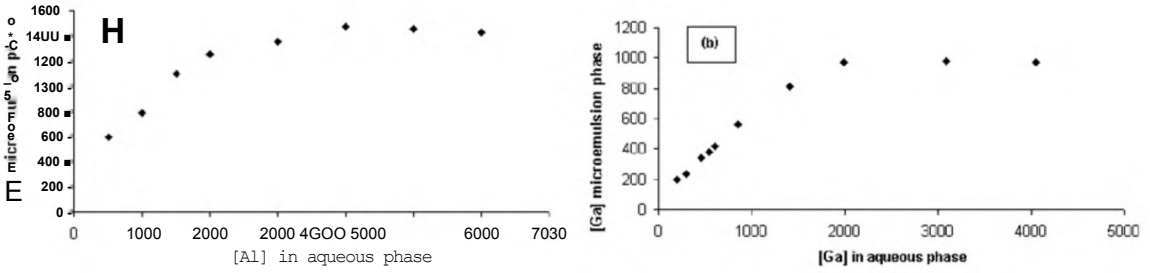


Figure 4. Al (a) and Ga (b) extraction by microemnulsion to evaluate surfactant saturation.

Figure 4 shows the obtained results, where can be observed that surfactant saturation in the microemulsion phase occurs in a concentration higher than 4000 ppm for aluminum (Figure 4 a) and higher than 2000 ppm for Gallium (Figure 4 b).

Extraction process optimization

The compositions of extraction points were chosen based on an experimental methodology - Scheffé Net [12-141. The simultaneous studv of several parameters, which affect a chemical process, generates answers whose optimization, through traditional procedures, is not able to represent the best experimental conditions without requiring a large number of experiments. Therefore, it is necessary to present an experimental planning methodology to obtain the development of the process, getting results that cover a large region of study, with a small number of experiments. The Scheffé Net model is based on the variation of the properties of pseudo-ternary mixtures as a function of its constituent concentrations. Figure 1 shows the pseudoternary diagram with the experimental points that form the Scheffé Net and its compositions are presented in Table 1, with its corresponding extraction percentiles (response).

Table 1. Point compositions and extraction percentiles for the studied system (T = 27 °C; pH = 14).

Points	Point Composition (mass fraction)			Extraction Percentiles (%E)	
	X_{AP}	Xop	Xc/s	Aluminum	Gallium
1	0.675	0.025	0.300	97.83	99.63
2	0.200	0.500	0.300	68.70	44.82
3	0.200	0.025	0.775	98.62	93.45
4	0.325	0.025	0.650	98.76	94.36
5	0.200	0.150	0.650	96.98	94.29
6	0.450	0.025	0.525	96.98	94.32
7	0.200	0.275	0.525	57.36	94.22
8	0.375	0.175	0.450	96.86	78.30
9	0.550	0.025	0.425	97.90	98.32
10	0.200	0.375	0.425	96.94	56.36
11	0.425	0.275	0.300	94.03	88.98
12	0.550	0.150	0.300	96.36	96.37
13	0.325	0.375	0.300	58.28	55.39
14	0.525	0.100	0.375	96.89	96.08
15	0.325	0.300	0.375	59.60	53.86
16	0.450	0.100	0.450	86.36	96.70
17	0.275	0.275	0.450	58.78	51.23
18	0.325	0.150	0.525	85.86	92.04

The statistical treatment of experimental results, using the software Statistica 5.0, provided the extraction percentile mathematical models. Equations (4) and (5) show the mathematical models obtained for aluminum and gallium, respectively:

$$\% E (Al) = 91.63 X_{AP} + 66.63 X_{OP} + 100.68 X_C/s \quad (4)$$

$$\%E (Ga) = 102.28 X_{AP} + 74.67 X_{OP} + 96.02 X_{c/S} \quad (5)$$

From Table 1 can be observed that the extraction percentiles were very satisfactory, reaching values (maximum) of 99.63% for gallium and 98.89% for aluminum. Figures 5a (aluminum) and 5b (gallium) shows the obtained isoresponse curves for the studied system, obtained through quadratic mathematical models (Eqs. 4 and 5).

From Figure 5a can be observed that the best results for aluminum extraction are obtained in the regions with higher water mass (Bayer liquor) and active material mass (C/S) fractions. Figure 5b shows that the best results for Ga extraction were achieved in the area with higher water mass (Bayer liquor) fractions and presenting between 35% - 40 % active material (C/S).

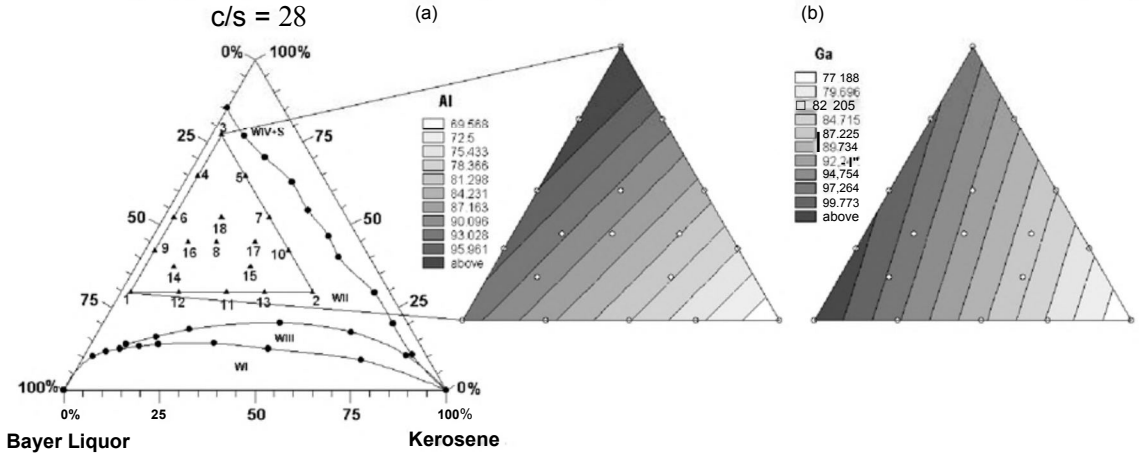


Figure 5. Isoresponse curves for aluminum (a) and Gallium (b) extraction percentiles. (C/S = 28; pH = 6; T = 27 °C)

Gallium and aluminum reextraction (stripping) process

Gallium and aluminum reextraction percentiles and selectivity were evaluated. Points 1 and 2 of extraction process were used (Table 1). Hydrochloric acid was used as a reextracting agent (HCl) in concentrations varying from 0.5M to 6M.

Acid concentration and metals reextraction percentiles were calculated through a mass balance. In Figure 6 can be observed gallium/aluminum selectivity in reextraction process as a function of hydrochloric acid concentration.

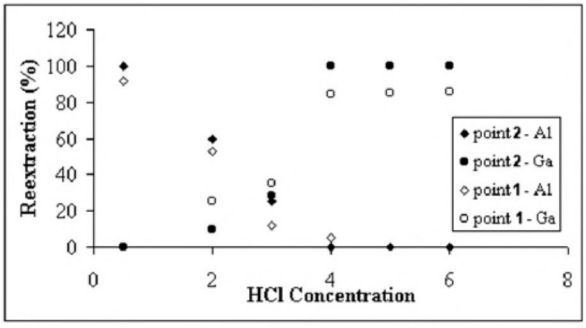


Figure 6. Gallium and aluminum reextraction percentiles (%) as a function of hydrochloric acid concentration.

CONCLUSIONS

The accomplishment of this research allowed to conclude that the surfactant synthesized from coconut oil, when applied in microemulsified systems, is an effective agent in the gallium and aluminum removal from a synthetic Bayer liquor, presenting results similar to the ones obtained using Kelex 100 [1; 6 ; 15].

The use of an experimental methodology (Scheffé Net) makes easy the evaluation of the extraction process behavior inside the interest region (Winsor II), allowing the optimization of the extraction system.

The metals reextraction (stripping) from microemulsion phase is possible and can be made in a selective way as hydrochloric acid concentration is varied. Preliminary studies showed that the microemulsion phase, after reextraction process, can be reused several times.

The surfactant can be recovered by aqueous solution neutralization, in the form of fatty acid. If the cost of this operation goes very high, the surfactant can be discarded in the solution, once it is 100 % biodegradable.

REFERENCES

1. T.N. de Castro Dantas, M.H. de Lucena Neto, and A.A. Dantas Neto, *Talanta,* 56 (2002), 1089-1097.
2. A.M.G. Figueiredo, W. Avristcher, E.A. Masini, S.C. Diniz, and A. Abrao, *Journal of Alloys and Compounds* **344** (2002), 36-39.
3. Gallium. In: http://nautilus.fis.uc.Pt/st2.5/scenes-e/elem/e03190.html (accessed in February 2003).
4. R.E. Kirk and D.F. Othmer, Kirk-Othmer Encyclopedia of Chemical Technology, 4th ed., Vol. 12, John Wiley and Sons, USA, 1994, 299-317.
5. J. Helgorsky and A. Leveque, *U.S. Patent* **4, 724,** 129, 1992.
6. G.V.K. Puvvada, K. Chandrasekhar, and P. Ramachandrarao, *Minerals Engineering,* **9** (10) (1996), 1049-1058.
7. K.A. Khan, N. Camillone, J.A. Yarmoff, and R.M Osgood Jr., *Surface Science,* **458** (2000), 53-62.
8. **H.** Watarai, *Journal of Chromatography A,* **780** (1997), 93-102.
9. B.K. Paul and S.P. Moulik, *Journal of Dispersion Science and Technology,* 18 (4) (1997), 301-367.
10. S.P. Moulik and B.K. Paul, *Advances in Colloid Interface Science,* 78 (1998), 99-195.
11. J. Klier, C.J. Tucker, T.H. Kalantar, and D.P. Green, *Advanced Materials,* **12** (23) (2000), 1751-1757.
12. G. Sado and M. C. Sado, Les Plans d'Experiences: De ['Experimentation a l Assurrance Qualité. ASNOR, 1991, pp. 125-145.
13. G.E.P. Box, W.G. Hunter, J.S. Hunter. *Statistics for Experiments - an introduction to design, data analysis and model building.* USA: John Wiley & Sons, Inc., 1978.
14. J.P. Forestier, E. Puech, and J. Tichadou, *International Journal of Cosmetic Science,* 7 (1985), 219-233.
15. G.V.K. Puvvada, *Hydrometallurgy* 52 (10)(1999), 9-19.



COPPER EXTRACTION BY MICROEMULSIFIED SYSTEMS

Tereza Neuma de Castro Dantas, Mônica Rodrigues de Oliveira,[1] Everlane Ferreira Moura,[2] Eduardo Lins de Barros Neto,[2] Afonso Avelino Dantas Neto

Universidade Federal do Rio Grande do Norte, ^epartamento de Quimica, [2]Departamento de Engenharia Quimica, Campus Universitário, 59072-970, Natal/RN, Brasil,

e-mail: tereza@quimica.ufrn.br: tereza@ea.ufrn.br

The use of microemulsified systems in heavy metal extraction, applying surfactants derived from vegetable oils, has presented good results, once these systems have characteristics that turn them more efficient when compared to the conventional solvent extraction systems. The extraction by microemulsion occurs in Winsor II equilibrium, where the microemulsion phase, that is immiscible with the aqueous phase, extracts the heavy metals that are present in the aqueous phase. Therefore, this research investigated the main parameters that have influence in the extraction process, such as: pH, copper concentration and distribution coefficient. The system used was composed by: surfactant - saponified coconut oil; cosurfactant - n-butanol; oil phase - kerosene; aqueous phase - aqueous solution of copper sulfate (0.02 mol.L^{1}, 2% NaCl). All experiments used a constant cosurfactant/surfactant ratio (C/S = 4) and temperature (27 ± 1 °C). The pH influence in the copper extraction process was verified, with the metal being completely extracted starting from pH 6 up to 10.The dependence of pH and heavy metal concentration in the aqueous phase after the extraction process is represented by the distribution coefficient (D), which is defined by the ratio of heavy metal concentration in the organic phase to the one in the aqueous phase. In this case the logarithm of D (log D) reached values approximately 3 in the pH interval from 6 to 10, for the microemulsion extraction. When compared with the results obtained using Cyanex 272 (bis(2,4,4-trimethylpenthyl phosphinic acid), a surfactant used commercially, was observed that the microemulsion process is more effective in copper removal from aqueous solutions. The extraction by microemulsion yielded extraction percentiles near to 99%. This research demonstrates the microemulsion efficiency, showing that it is possible to extract copper from aqueous phases with very low concentrations.

INTRODUCTION

Copper is a widespread anthropogenic pollutant of environment and the determination of this metal is an actual problem [1], It is a widely used industrial metal whose applications include electrical wiring, plumbing, air conditioning tubing and roofing. Additionally, copper, which is an essential nutrient to humans and other life forms, is biostatic/biocidal to certain organisms. However, copper(ll) is known to be one of the heavy metals most toxic to living organisms and it is one of the more widespread heavy metal contaminants of the environment. The potential sources of copper in industrial effluents include metal cleaning and plating baths, pulp, paper board mills, wood pulp production, fertilizer industry, etc. The conventional

methods of copper (II) removal from wastewaters include precipitation, ion exchange, electrolysis, adsorption on activated carbon, etc [2],

Studies have also been carried out in order to use liquid-liquid extraction for effluent treatment, including metallic cations extraction. The utilization of microemulsified systems in metallic cations extraction has been a good alternative, since they have some characteristics, which can make them profitable when compared to the conventional solvent extraction, mainly regarding to contamination by solvents and energy consumption [3-5], Some researchers reported that microemulsions are quite efficient in the recovery processes of metallic ions in laboratory scale. They developed and used a new technique applicable to the Brazilian reality [6-9],

Microemulsions are thermodynamically stable, macroscopically homogeneous and optically isotropic systems. They are formed by the dispersion of microdroplets of two immiscible liquids, generally oil and water, stabilized by an interfacial membrane formed by surfactant and cosurfactant. The microemulsions can exist in equilibrium with other phases, aqueous or organic, forming four types of multiphase systems: Winsor I (WI), when the microemulsion phase is in equilibrium with an organic phase in excess; Winsor II (WII), when the microemulsion phase is in equilibrium with an aqueous phase in excess; Winsor III (WIII), a three phase system, where the microemulsion is at the same time in equilibrium with an aqueous and with an organic phases; and Winsor IV (WIV), a monophase system, in macroscopic scale, constituted only by a microemulsified phase [10],

The extraction of metal ions in WII system is often very effective for the accelerated extraction and the improved extractability. The increase of the extraction rate is explained by an enormous rise of the microinterfacial surface area in the microemulsion phase and the participation of the microemulsion globules in the transport of metal ions from the aqueous phase to the organic phase [11],

Based on microemulsion properties, the purpose of the present research is to investigate copper removal from aqueous solutions by WII systems taking into consideration the main parameters that have influence in the extraction process, such as: pH, copper concentration, and distribution coefficient. The results that will be obtained in this research will be compared with the ones published by Sole and Hiskey [12], These authors used a solvent extraction process to remove copper (II) from an aqueous phase using as solvent phase Cyanex 272 diluted in xylene.

MATERIALS AND METHODS

CHEMICALS

The chemicals used in the exDeriments were analytical arade. exceDt coconut oil (reaional production — Rio Grande do Norte — Brazil) and kerosene (Petrobrás — chemical composition: paraffinic hydrocarbons—min 70%, aromatic hydrocarbons—max 20% and olefinic hydrocarbons—max 5%; density < 1; viscosity 2.7 cSt at 20° C; distillation range 150-300° C at 760mm Hg), and were used as supplied without further purification.

COPPER SYNTHETIC SOLUTION

Copper synthetic solutions (C*1.2 gL^1), with 2% NaCl, were prepared in distilled water using sulfate salt ($CuS0_4.5H_20$). Copper concentrations in aqueous samples were analyzed by flame atomic absorption spectroscopy (FAAS) using a VARIAN SpectrAA-10 PLUS in an air-acetylene flame.

MICROEMULSION (WINSOR II)

Winsor II system was composed by 25 wt% Cosurfactant/Surfactant ratio (C/S = 4; surfactant - saponified coconut oil (SCO) - molar mass 217.32 g.mol'[1]; cosurfactant - n-butanol - 99% P.A.); 60 wt% aqueous phase (copper synthetic solution - 1.2 gL'[1] with 2% NaCl); and 15 wt% oil phase (kerosene).

EXTRACTION EXPERIMENTS

The equilibrium distributions of copper in the Winsor II system as a function of pH were determined in all the studied systems. The systems were agitated during 10 min and after that maintained in rest until complete phases separation was obtained. When required, the pH was adjusted adding small amounts of NaOH or H_2S0_4. The aqueous phase in excess, poor in heavy metal, was separate withdrawing using a syringe and taken for analysis by FAAS. All experiments were carried out at room temperature (27 ± 1°C).

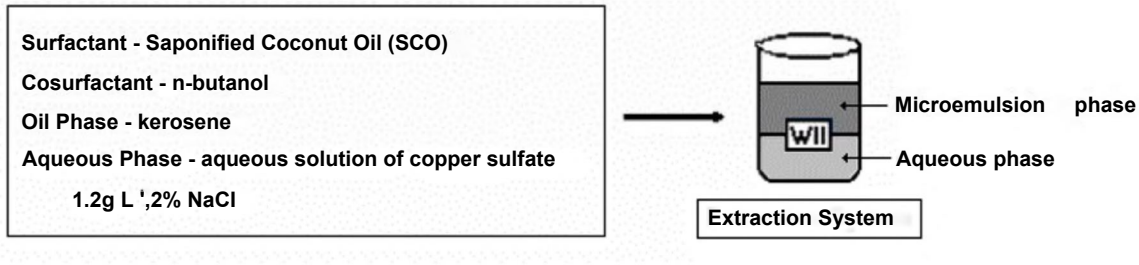


Figure 1. Winsor II extraction system.

RESULTS AND DISCUSSIONS

Extraction as a function of pH

Copper (II) was extracted in the pH range from 0.0 to 12.0. Figure 2, copper extraction as a function of pH value, illustrates a comparison between the data obtained in this work, using a Winsor II system, and the ones obtained by Sole and Hiskey [12], using a conventional solvent extraction process. As observed, aqueous solution pH value is an important controlling parameter in heavy metal extraction process.

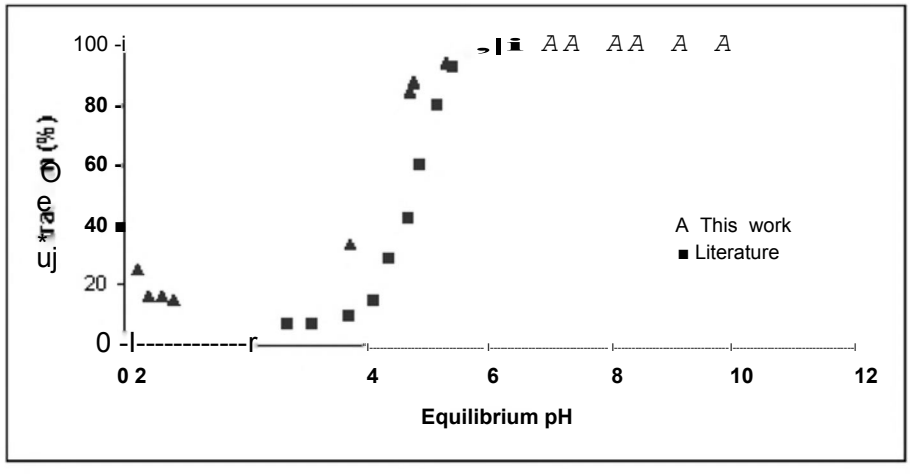


Figure 2. Comparison of the present work and the existing data for copper extraction as a function of pH value.

The high extraction percentiles obtained were observed due to a strong interaction among the surfactant molecule and the heavy metal cation, where the Cu^{+2} cation replace the surfactant ion Na^{+}. In the pH interval from 0 to 3, low metal extraction percentiles were obtained. This was observed due to a lack in surfactant-cation interaction caused by the high H^{+} concentration, resulting in a reversion of surfactant saponification reaction.

The pH dependence of copper extraction can be represented by the distribution coefficient (D), which is defined by the ratio of heavy metal concentration in the organic phase to the one in the aqueous phase (Figure 3).

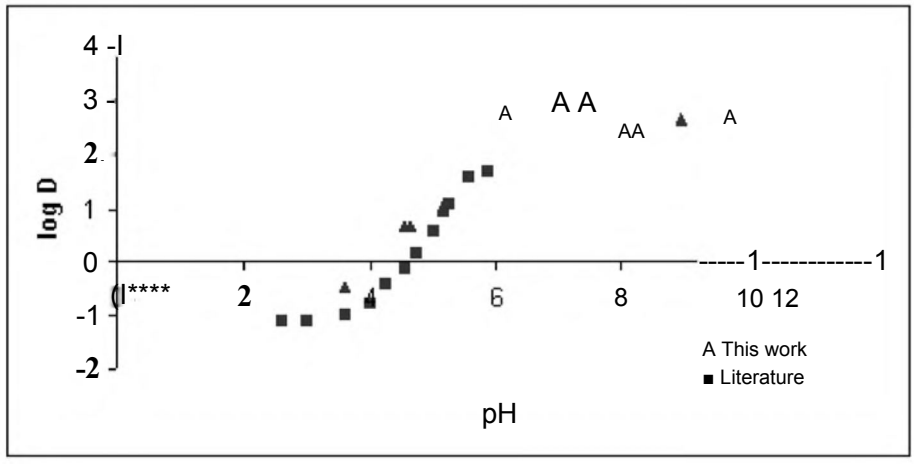


Figure 3. Comparison between the present work and the existing data [12] of the effect of surfactant concentration on the distribution coefficient D.

The basic interaction reaction between surfactant and Cu is:

$$Cu^{f} + 2Na(oC) \rightarrow C_{M^{+2}}(OC)_2 + 2Na^{*} \quad (1)$$

as Na^{+} ions not suffer hydrolyses, attention must be given to the anion hydrolyses (OC) that happens according to the following reaction:

$$(<0C) + H_2O \wedge H(OC) + OH^{-} \quad (2)$$

where the hydrolyses constant Kh is given by:

$$K = \frac{K_w _ \backslash H(OC)\}\backslash OH]}{" K_a (oc \sim i} \quad (3)$$

K_w = water ionization constant = $1.0 \times 10^{4-}$
K_a = acid ionization constant = $2.49 \times 10^{7-}$

As can be observed in Figures 2 and 3, the pH value has a direct influence in the extraction percentile, showing that the excess of H^{+} inhibits the process. According to this, Equations 1 and 2 can be associated, where the overlining represents the species present in the organic phase:

$$Cw^{+2} + 2HOC \rightarrow Cu^{*2}(oC \sim \backslash + 2H^{*} \quad (4)$$

$$K_A = \frac{\left[Cu^{+2}\left(OC^{-}\right)_2\right]\left[H^{+}\right]^2}{\left[Cu^{+2}\right]\left[HOC\right]^2} \quad (5)$$

$$\frac{\left[Cu^{+2}\left(OC^{-}\right)_2\right]}{\left[Cu^{+2}\right]} = D \quad (6)$$

knowing that pH = -log[// $^{+}$] and HOC **1** = A'$_{/i}$.[oC], then :

$$\log A- = \log/) - 2\,pH - pK_h \text{ -logjyC-J} \quad (7)$$

From the analyses of Figures 2 and 3 can be observed that SCO and Cyanex 272 [12] obey Eq.4, fact resulting due to dissociation of the anion from the used acid in the extraction process, which in the case of SCO have K_a =2.49x10-^{7}, value that is similar to the one of Cyanex 272 (K=2.5x10-^{7}) [12].

CONCLUSIONS

By comparing copper (II) extraction by SCO applied in microemulsified systems with Cyanex 272 diluted in xylene, one can observe a similar behavior. With decreasing pH value is observed a decrease in the extraction percentiles because both surfactants are derived from weak acids, where hydrolyses occurs only in a favorable pH interval. The surfactant used in this research was derived from a vegetable oil (coconut oil), presenting more pronounced distribution coefficients, fact that shows its potential in the extraction process by microemulsions.

This work was developed in laboratory scale seeking to apply this process to recover copper from industrial waste. The process will occur in two stages: extraction and reextraction. In the first one, the heavy metal ion present in the aqueous phase is extracted by the microemulsion phase. In a second step, the reextraction process occurs: the microemulsion phase, rich in metal, is acidified and the metal is recovered in a new aqueous phase, with higher concentration. Preliminary studies showed that the microemulsion phase can be used several times.

REFERENCES

1. Kulichenko S.A., Doroschuk V.O., Lelyushok S.O. *Talanta* 2003; 59:767-773.
2. Özer A., Özer D., Özer A.. *Process Biochemistry* 2004; 39: 2183-2191.
3. Dantas TNC, Dantas Neto AA, Moura MCPA. *Water Res* 2001;35(9):2219-24.
4. Dantas TNC, Dantas Neto AA, Moura MCPA, Barros Neto EL, Telemaco EP. *Langmuir* 2001;17:4256-60.
5. Dantas TNC, Lucena Neto MH, Dantas Neto AA. *Talanta* 2002;56:1089-97.
6. Leite R. H. L. (1994) *Chromium extraction from Tannery industries wastewater using microemulsion. Master of Science Thesis,* Rio Grande do Norte University - PPGEQ, Natal, Brazil (In Portuguese).

7. Ramos A. C., Dantas Neto A. A. and Castro Dantas T. N. (1997) *Application of an experimental methodology in the optimization of a tungsten concentration process by microemulsion.* Brazilian J. Chem. Eng. 14(02), 159-165.
8. Dantas T. N. C., Dantas Neto A. A. and Moura M. C. P. A. (1999) Use of impregnated natural clay with microemulsion in the treatment of effluents containing heavy metals. *Proceedings of International Conference of Urban Pollution Control Tecnology (ICUPCT), Hong Kong*, pp. S1_S6.
9. Forte K. R. (1998) Heavy metal extraction using microemulsion. Master of Science Thesis, Rio Grande do Norte University - PPGEQ, Natal, Brazil (In Portuguese).
10. Paul BK. Moulik SP. Microcmulsions: an overview. J Dispersion Sci Tcchnol 1997;18(4):301—67.
11. Watarai H. Microemulsions in separation science. *J Chromatogr A* 1997;780:93-102.
12. Sole, K. C., Hiskey J. B.. *Hydrometallurgy* 1995; 37: 129-147.

VALUE ADDITION IN THE PROCESSING OF COPPER BLEED SOLUTION BY SOLVENT EXTRACTION PROCESS

Vinay Kumar, B.D. Pandey, A. Agarwal,
D. Bagchi, S.Kumari and S.K. Sahu

Non-ferrous Process Group, MEF Division,
National Metallurgical Laboratory, Jamshedpur, India

Copper bleed solution generated during the electrorefining of anode copper has been used for the recovery of metals as value added products viz. metal powders following partial decopperisation, solvent extraction and electrowinning. In this process, a mixed crystal containing copper and nickel sulphates is produced from the partially decopperised bleed solution by crystallization. The mixed crystal is dissolved and iron is removed by precipitation. The copper is extracted from the purified solution using LIX84 diluted in kerosene leaving nickel in the aqueous raffinate. Bench scale simulation study for the separation of copper and nickel is further confirmed by extracting copper in a mixer settler unit. The purified solution has been used for producing copper and nickel powders by electrolysis.

INTRODUCTION

Copper bleed solution is generated during the purification of impure copper in the electro-refining plant. Due to recycling of the electrolyte the impurities viz. nickel, arsenic, iron, bismuth, antimony, chloride etc are enriched in the solution [1], When the concentration of the impurities increases above their upper limit of tolerance during recycling with time it becomes deleterious for the electro-refining. In order to control the purity of deposited cathode copper during refining, the solution is discarded as copper bleed stream (CBS). This discarded solution contains high concentration of copper and nickel. Various methods are employed to recover the valuable metals depending on the composition of the CBS. In conventional practice a portion of the electrolyte between the electrolytic cell and circulation tank is bled from the circulation tank to the liberator cell [1,2], The major operations followed are decopperisation, purification and crystallisation. In the decopperisation operation copper present in the electrolyte is deposited on the cathode up to a concentration level of 10 g/L of copper left in the solution. The decopperised solution containing other impurities is sent to the purification section, where the impurities co-deposit on the cathode with remaining copper. The purified solution is then crystallised to recover $NiS0_4$.xH20 and black acid thus generated is recycled to the circulation tank. The process is difficult to operate due to higher cost as reported by Shibata et al [3], Purification of crude nickel sulphate by precipitation method has recently been reported by Havlik et al (4) involving cumbersome procedure.

At SNCR (Sumitomo Nihama Copper Refinery), a process (5) has been developed for purifying the impurities like arsenic, antimony, bismuth and nickel which contaminate the electrolyte thus making it unsuitable for further processing. Shibasaki et al(6) reported a process for the treatment of copper bleed electrolyte at Naoshima Smelter and Refinery, Japan following decopperisation, neutralization and solvent extraction steps. A number of

processes have been developed by Japanese researchers(3) for the recovery of metals from bleed solution following SX and ion exchange and implemented in some plants. Other reports by different groups particularly Buttinelli et al(7) have also studied the treatment of CBS using SX techniques. SEC process (8) is based on SX - EW of Ni from the decopperised copper bleed stream at El Paso, USA. A process is also being developed at NML, India for the recovery of acid from the copper bleed solution followed by metal separation using SX(9).

The Sheritt process could be used for the separation of Cu and Ni from the solution. The process treated Cu & Ni from the metal amine sulphate solution obtained from the pressure leaching of sulphide concentrate and nickel matte at Sheritt Nickel Refinery at Fort Saskatchewan. The process of nickel powder preparation has mostly been adopted(IO) from the work of Schaufelberger(11). Hydrogen reduction of aqueous metal salts at elevated temperature and pressure in autoclave from the leach liquors of ores/concentrates has been reported for producing metal powders in batch(12) and continuous mode(13). Tagashi and Nagai(14) reported hydrogen reduction of copper from CBS at 190°C temperature and 20 atmosphere pressure. Major drawbacks of the process are the requirement of incomplete reduction of copper for producing acceptable grade of powder, and material of construction with high acid present in the solution. A new approach on selective hydrogen reduction of copper and nickel powder is being developed at NML to obtain value added products from such solutions. In the present studies, the value added products viz copper and nickel powder has been produced following partial dccopperisation, crystallisation, dissolution, solvent extraction and electrolysis steps.

EXPERIMENTAL

For the development of a process on bench scale, a synthetic solution with chemical composition similar to the copper bleed generated in copper refinery (ICC, Ghatsila, India), comprising of 38.42 g/L Cu, 19.37 g/L Ni., 0.757 g/L Fe. 0,2 g/L Bi and 171 g/L H_2S0_4 was taken. Subsequently, actual copper bleed solution generated in the smelter was used. The solulion was decopperised at current density of 100 A/m^2 followed by cryslallisation to get the mixed crystals. The crystal so obtained were washed with water, neutralised with NaOH to bring down the pH to 3.5-4.0, aerated for 2-4 h to precipitate iron as hydroxide and filtered. The filtrate so obtained was subjected to solvent extraction using LIX 84 to separate copper from nickel. The loaded copper was stripped with sulphuric acid and electrolysed to give pure metal powder. Nickel powder was produced from the raffinate by electrolyis.

Analyses of the samples for low concentration of metallic values were carried out by an Atomic Absorption spectrometer. Solutions containing high metals were analysed by conventional method. All the chemicals used for the chemical analysis were Analar grade reagents.

RESULTS AND DISCUSSION

To recover copper and nickel from CBS in the most usable form such as metal powders or salts, partial decopperisation, crystallization, solvent extraction and electrolysis has been followed.

Partial decopperisation and crystallization of copper bleed solution:
In order to recover the metallic values from the bleed solution, the solution was first decopperised by electrowinning at low current density (100 A/m^2) to bring copper concentration from 38.5 g/L to 17-18 g/L at room temperature. A good sheet deposit with a purity of 99.36 - 99.98% Cu was obtained in all the cases. The current efficiency and energy

consumption for the metal deposition were 96.86 - 98.33 % and 1.64 - 1.82 kWh/kg respectively. The quality of deposited copper so produced was least affected for commercial application.

After decopperisation, crystallisation was carried out in two stages to see the possibility of getting the mixed crystals. The solution obtained in partial decopperisation had 17.96 g/L Cu, 20.39 g/L Ni, 206 g/L sulphuric acid. In a two-stage crystallisation, the mixed crystals obtained in the first stage had a composition 21.716 % Cu, 2.295 % Ni indicating that copper crystallised before nickel and it can further be used for making powder or can be recycled for make up. The fractional crystallisation as obtained in stage-1 was mainly due to solubility factor of different metal sulphates. In second stage of crystallisation mixed metal sulphates with high nickel (15.6%) and low copper (8.09%) were obtained. The crystal obtained from the single stage crystallisation had chemical composition as: 12.13% Cu, 13.48% Ni, 0.539% Fe, 0.046% Bi and 15.03% sulphuric acid.

The crystal obtained in second stage was leached in water to give aqueous solution with the composition as 8.39 g/L Cu, 13.67 g/L Ni, 0.5 g/L Fe and 20 g/L sulphuric acid. The presence of iron is deleterious for solvent extraction because of its transfer to organic phase and then to electrolyte which on electrolysis decreases the cathode current efficiency leading to high energy consumption. Hence iron removal from the electrolyte is essential to save energy and increase the production rate. Thus, leach solution obtained as above containing 0.5 g/L Fe was neutralised with NaOH solution to increase the pH of solution from 1.12 to 4.4. After adjustment of pH, air was passed for a period of 6-8 h at 80°C to precipitate iron as ferric hydroxide thereby bringing down the iron content from 0.5 to 0.004 g/L. The iron free solution was subjected to solvent extraction.

Solvent extraction using LIX 84:
Initially, bench scale studies were carried out to optimise the process parameters for the separation of copper from nickel using LIX84. Aqueous solution generated by the dissolution of mixed crystal as mentioned above was shaken with 20% LIX84 at O/A ratio of 2/1 for 10 min at different equilibrium pH varying from 1-5 and the plot of percent extraction Vs equilibrium pH is shown in Figure 1. Thus, at an equilibrium pH of 2.5 copper extraction was 99.88% whereas nickel extraction was only 0.55%. Therefore, the equilibrium pH for further experiments was maintained around 2.5. A plot of copper distribution ratio (log D_{cu}) at different pH shows a straight line with a slope of 1.72 which indicates the release of $2H^+$ and extraction of copper as CuA_2 (HA: active organic hydroxyoxime species) in the organic phase. The loading capacity of 20% LIX84 determined by repeated contact method was found to be 7.94 g/L copper at O/A of 1 and equilibrium pH of 2.73. The loaded Cu was stripped with a solution containing 31.77 g/L Cu and 180 g/L H_2S0_4. Stripping was done at different 0:A ratio and at 0:A ratio of 4:1 the stripped solution was found to contain 57.18 g/L Cu, with low stripping efficiency of 80%. The stripping was maximum (96 %) at A/O ratio of 1.

The studies were also carried out to simulate counter current extraction of copper at A:0 ratio of 1:1 and 1:1.5. It was found that only 0.0004 g/L copper remained in the raffinate at A:0 ratio of 1:1.5, whereas 0.434 g/L Cu was left in the raffinate when A:0 ratio was maintained at 1:1. Based on this the stages were fixed in the mixer settler (volume: 0.6 L mixer and 0.86 L settler) units as: extraction: 4; scrubbing: 2; stripping: 2. Data on counter current extraction of copper in mixer settler unit with 25 % LIX84 in kerosene are shown in Figure 2. The composition of raffinate obtained in the mixer settler operation under different conditions is given in Table 1. A raffinate free of copper was obtained at O/A ratio of 1.6 and equilibrium pH of 2.68. The composition of raffinate, scrubbed solution and stripped solution showed the performance of the circuit (Figure 2). The stripped solution rich in copper was used for producing copper powder.

Table 1. Extraction of copper at different pH in the mixer-settler

Aqueous feed (g/L): 8.37 Cu, 13.69 Ni, 3.08 pH
Organic: 25% LIX 84 in kerosene, No. of stages in extraction: 4

pH of the raffinate	Aqueous feed flow rate (L/h)	O/A ratio	Copper in raffinate (g/L)
1.57	3.90	1.10	0.87
2.13	3.90	1.10	0.25
2.68	3.17	1.60	0.001

Electrolytic grade metal powder:
An attempt was made to produce copper powder at the current density in the range 600-1000 A/m^2 from the pregnant solution containing 37.75 g/L Cu and 166 g/L H_2S0_4. Thus, at different current densities copper powder of the purity varying from 99.50-99.98 % was produced. Decrease in time of electrolysis from 3.5 h to 2.0 h increased current efficiency from 98.36 to 99.70, but at 1000 A/m^2 the current efficiency dropped to 85 *%.* The purity of copper powder was found to be 99.93%. The raffinate produced in the counter-current mixer-settler operation was taken to recover nickel powder. The composition of the nickel electrolyte was adjusted to: 10 g/L Ni, 40 g/L $(NH_4)_2S0_4$, 10 g/L H_3B0_3, 0.2 g/L thiourea, pH 4.5. The solution was electrolysed at 65-70° C at the current density ranging from 4000-10,000 A/m^2 with current efficiency varying between 40-53 %. The energy consumption was 19.5kWh/kg of nickel powder at 5000 A/m^2 current density. The copper and nickel powders for P/M application can thus be produced.

CONCLUSIONS

The studies were carried out for the treatment of copper bleed electrolyte generated in the electrorefining of copper. Since this solution contains high concentrations of copper and nickel, various possibilities were worked out to augment the overall recovery of copper and nickel and produce value added products. Of the different process routes investigated, partial decopperisation, crystallisation, solvent extraction-electrowinning route was found suitable to produce copper and nickel powders of required purity.

ACKNOWLEDGEMENTS

Authors are thankful to the Director, NML, Jamshedpur for giving permission to publish the paper. Thanks are also due to Dept, of Mines, Govt, of India, New Delhi for sponsoring the project.

REFERENCES

1. A.K. Biswas and W.G. Davenport (1994), Extractive Metallurgy of Copper, Pergamon, U.K.
2. R. Shibayama, and T. Nagai, (1992), *Solvent Extraction* 1990, Part-B, T. Sekine (ed.), Elsevier, Netherlands, pp. 1193-1198.
3. T. Shibata, M. Hashiuchi and T. Kato (1987), The Electrorefining and Winning of Copper, J.E. Hoffman, R.G. Bautista, V.A. Ettel, V. Kudryk, and R.J. Wesel (eds.), AIME, Pennsylvania, pp. 99-116.
4. T. Havlik, M. Skrobian, R. Kammel, J. Curilla and D. Cmorejova (1996), *Hydromet.,* 41, 79-88.

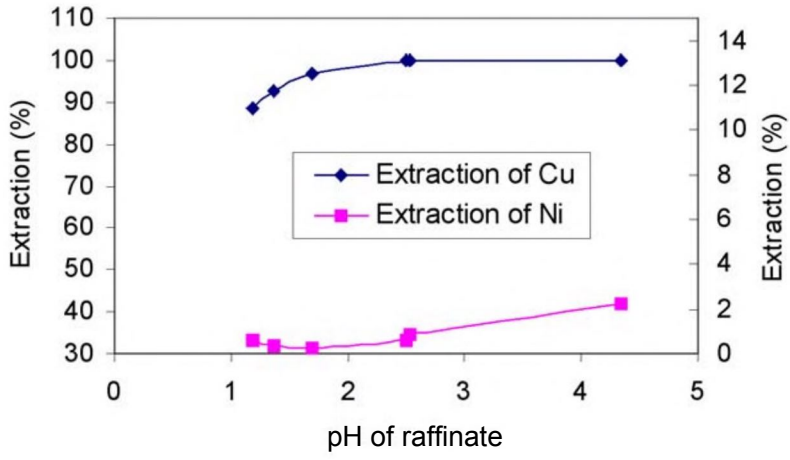


Figure 1. Extraction of metals with 20% LIX84 in kerosene [Organic = 20% LIX84 in kerosene, Aqueous feed (g/L) = 8.39 Cu, 13.67 Ni; A/0 = 1/2 for extraction; t = 10 min]

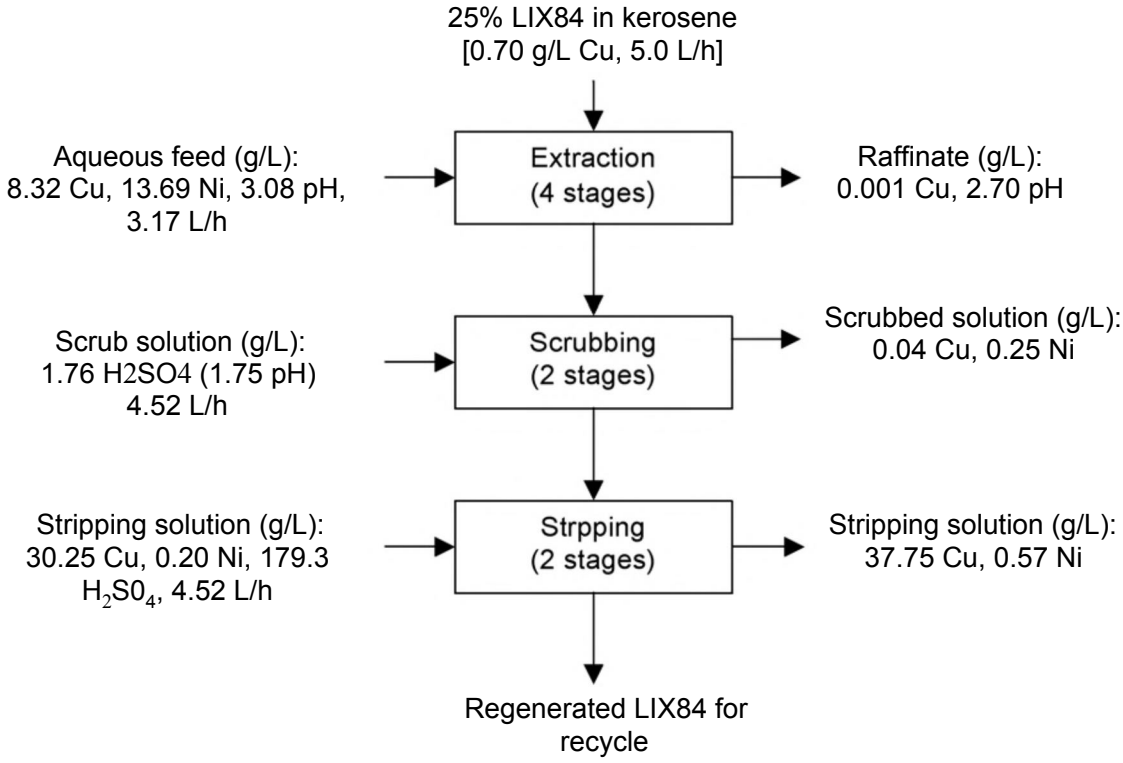


Figure 2. Extraction of copper in mixer settler unit from copper bleed solution

7. D. Buttinelli, C. Giavarini and A. Mercanti (1983), Proc. ISEC'83, Denver, USA, pp. 422-425.

8. G. M. Ritcey and A.W. Ashbrook (1979), *Solvent Extraction,* Principles and Applications to Process Metallurgy, Part II, Elsevier, Amsterdam.
9. A. Agarwal, B.D. Pandey, V. Kumar and Premchand (1996), Proc. Seminar Recovery of Valuable By-products from Intermediate Secondaries in Non-ferrous Industries, Ghatsila, India, pp. 36-43.
10. T. Saarinen, L.E. Lindfors and S. Fugleberg (1998), *Hydromet.,* 47, 309-324.
11. F.A. Schavfelberger (1956), *JOM,* 8, 695-704.
12. F.A. Forward and J. Halpern (1957), *Trans. Inst. Min. Met.,* 66, 191-218.
13. D.N. Neskora, R.L. Brown and C.M. Silepecvich (1974), U. S. Pat., No. 3,833,351 (Sept.).
14. R. Togashi and T. Nagai (1983), *Hydromet.,* 11, 149-163.

A CONTINUOUS SOLVENT EXTRACTION PROCESS FOR REFINING OF HYDROCHLORIC PICKLING BATHES CONTAINING CHROMIUM(iII) AND NICKEL(II)

D. Pareau \ N. Février[2], B. Vialatte[2], M. Stambouli[1]

^cole Centrale Paris/LGPM - Châtenay Malabry, France, 92295
[2]Ugine & Alz, Groupe Arcelor, Gueugnon, France

This work deals with the development of a process flowsheet for the recovery of highly toxic chromium(III) from hydrochloric acid aqueous solutions containing iron and nickel(II). These solutions typically correspond to pickling bathes of stainless steel which must be changed or treated before re-use. Hydrometallurgical processes based on solvent extraction technique represent promising alternatives on both economic and environmental aspects. An appropriate mixture of b/s(2-ethyl-hexyl) phosphoric acid, Aliquat 336 and octan-1-ol in dodecane was found to be quite efficient. Thus, the effect of different chemical parameters on chromium(III) extraction was investigated and analyzed through the slope method technique.
A whole flowsheet was proposed and tested on a lab scale mixer-settler pilot for the refining of the industrial pickling bathes including : (i) - a commonly known primary step of iron extraction with Tri-butyl phosphate TBP following the total oxidation of iron in its ferric form with H_20_2; (ii) - chromium(III) refining through extraction - scrubbing - stripping process. The three metallic chloride solutions then produced were pure enough to be easily valorised.

INTRODUCTION

Pickling bathes of stainless steel pieces have a limited life time, due to the accumulation of metals in them (mainly iron). They must then be changed periodically leading to the production of important volumes of effluents. So the Ugine stainless steel plant of Gueugon (France) produces several thousand cubic meters per year of such acid effluents, their treatment being a simple neutralisation and precipitation of metallic hydroxides. Along with the important base consumption, the resulting production of sludge is tremendous with all the related problems of energy costs (dessication) and final special storage.
The used bathes contain, along with a relatively high residual hydrochloric acid concentration (about 3 to 4 mol/L), iron (II) and (III), chromium (III), nickel (II) and traces of other metals. A special interest has been given in this work to the valorisation of chromium in these effluents.

Only a few studies on Cr(III) extraction in hydrochloric acid deal with industrial potential applications. The major papers indeed have analytical purposes, the extractants being for example acetylaceton [1] or thenoyltrifluoroaceton [2], Cationic liquid exchangers such as Cyanex 301 (bis(2,4,4-trimethylpentyl)dithiophosphinic acid) and DEHPA (bis(2-ethylhexyl) phosphoric acid) have been tested with a relatively poor success. Cyanex 301 [3] is not able to extract Cr(III) in a great range of HCI concentration (0 to 6 mol/L). DEHPA [4, 5, 6] is

effective only for pH > 3, the solution proposed to raise this difficulty is the use of DEHPA in the form of its ammonium salt. In all cases stripping of chromium seems to be slow and not quantitative.
The extraction of Cr(III) at low pH is then difficult; besides the selectivity of its extraction versus iron and nickel is not considered in the overviewed literature.

Experimental
Synthetic aqueous solutions were prepared with analytical grade chemicals (hydrochloric acid, chlorides of iron(II), iron(III), chromium (III), nickel (II)) from VWR. DEHPA, Aliquat 336, dodecan and octan-1-ol for preparation of organic solutions were supplied respectively by Avocado, Fisher and VWR.
All the experiments were made at room temperature. Chemical analyses (by atomic absorption spectrometry) were done on both aqueous and organic samples after extraction and stripping and mass balances verified.
Continuous counter-current extraction experiments were performed onto a lab scale mixer-settler pilot supplied by Robatel SA.

EXPERIMENTAL

Selection of the extracting system
The preliminary experiments were performed to measure the efficiency of different extracting systems versus pH. Equal volumes of an aqueous chromium solution (1 g/L) and organic phases were contacted till equilibrium (5 minutes) and the extraction yield of chromium p is calculated. DEHPA (denoted HA) and mixtures of DEHPA and Aliquat 336 (trioctyl-methyl ammonium chloride) (denoted R_4NCl) were tested. In this latter case addition of octanol-1 is necessary to prevent third phase formation. In these mixtures salification of DEHPA is achieved according to the equation : $\overline{HA} + \overline{R_4NCl} \rightarrow \overline{R_4NA} + HCl$, where the superscripts denote organic compounds. The experimental results are given in table 1, where the initial pH is given along with the equilibrium one.

Table 1 : Extraction yields of chromium (p) achieved with DEHPA and R_4NA for different experimental conditions

Extractant	Diluent	initial pH									
		3.8		2.9		2		1.3		0.6	
		P	pH_{eq}	P	pH_{eq}	P	pH_{eq}	P	pH_{eq}	P	PHeq
DEHPA 10% (v/v)	dodecan	36%	2	22%	1.9	13%	1.8	4%	1.2	3%	0.6
DEHPA 20% (v/v)	dodecan	46%	1.8	35%	1.7	23%	1.6	4%	1.2	4%	0.6
DEHPA 30% (v/v)	dodecan	58%	1.7	50%	1,6	35%	1.6	8%	1,25	5%	0.6
R_4NA 10% (v/v)+ DEHPA 15% fv/vl	octan-1-ol 15% (v/v) + dodecan	-	-	58%	2.3	45%	2.2	6%	1.3	-	-
R_4NA 30% (v/v)	octan-1-ol 10% (v/v) + dodecan	-	-	99%	7	92%	4.7	36%	3.3	-	-

The decrease in pH in the case of DEHPA is due to the cationic exchange of Cr(III) with protons. In the case of R_4NA, the variation of pH is mainly controlled by the acido-basic equilibrium: HA - R_4NA; for initial pH 1.3 and R_4NA 30% for example, the equilibrium pH is greater than the initial one, due to a partial re-acidification of R_4NA.
The conclusion of these preliminary tests is that a good extraction yield can be obtained, even for a low initial pH, when using R_4NA (salified DEHPA).
The selected system for further experiments is then R_4NA, octan-1-ol and dodecan.

Determination of the extraction mechanism

In the considered acid solutions (pH < 3), the presence of chromium (III) hydroxides can be neglected as well as chloride complexes. The major species is Cr^{3+}.
In all experiments DEHPA or R_4NA are diluted in a mixture of octan-1-ol and dodecan; the organic phase is polar enough to eliminate all DEHPA multimers; the monomer is the only species considered. Equal volumes of aqueous and organic solutions were contacted for a few minutes (2 to 4); in all cases equilibrium was found to be reached within this time.

• Extraction of chromium by DEHPA
The extraction mechanism of chromium (III) by DEHPA was confirmed by a few experiments, the slope method gave results in accordance with the following stoechiometry :

$$Cr^{3+} + 3\overline{HA} \leftrightarrow \overline{CrA_3} + 3H^+$$

• Salification of DEHPA by Aliquat 336
This reaction is represented by:

$$\overline{HA} + \overline{R_4NCl} \rightarrow \overline{R_4NA} + H^+ + cr \quad \text{with } K_2 = \frac{[\overline{R_4NA}][H^+][Cr]^-}{[\overline{HA}][\overline{R_4NCl}]}.$$

An organic solution containing R_4NA 30% (v/v) (0.384 mol/L) and octan-1-ol 10% (v/v) is contacted with hydrochloric acid solutions of different concentrations (0.01 to 1 mol/L). The volumes of both phases are equal and the agitation time is 4 minutes. The concentration of HA formed in the organic phase after contact is measured by titration.
The stoechiometry of the equation leads to: $[H^+] = [Cf]\ [HA] = [R_4NCl]$
A logarithmic relation can then be used for the treatment of the experimental results:

$$\log[\overline{HA}] = \frac{1}{2}\log K_2 + \frac{1}{2}\log[\overline{R_4NA}][H^+]^2).$$

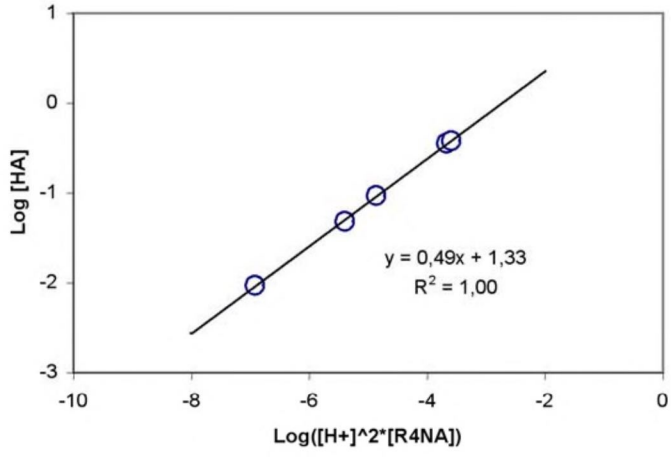


Figure 1: Validation of the extraction mechanism

As can be seen on figure 1, the model is well validated. K_2 is equal to $(2.2 \pm 0.6)\ 10^{-3}$.

Extraction of chromium by R_4NA
In order to determine the stoechiometry of the extracted metallic complex, the following equation is written:

$$Cr^{3+} + (3 + x)\overline{R_4NA} + 3Cl^- \leftrightarrow \overline{CrA_3(R_4NA)_x} + 3\overline{R_4NCl}$$

where x must be estimated thanks to the experimental results.

The equilibrium constant K_3 will also be calculated: $K_3 = \frac{[\overline{CrA_3(R_4NA)_x}][\overline{R_4NCl}]^3}{[Cr^{3+}]\,[\overline{R_4NA}]^{(3+x)}\,[Cl^-]^3}$

This representation assumes the formation of a complex containing both extractant molecules.

$$\log\left(D\left(\frac{[H^+]^3}{[HA]^3}\right)\right) = x \log[\overline{R_4NA}] + \log K_3 + 3\log K_2$$

By plotting $Y = \log\left(D\left(\frac{[H^+]^3}{[HA]^3}\right)\right)$ versus $\log[\overline{R_4NA}]$, a straight line must be obtained,

whose slope is x.

Several experiments were made by contacting equal volumes of solutions of chromium (1 to 10 g/L) of pH 1-2, and an organic solution containing 10% v/v octan-1-ol, 30% v/v R_4NA and dodecan The contacting time is 2 minutes.
The results are gathered in table 2 :

Table 2 : Determination of extracted chromium complex with R_4NA according to the slope method

$-\log\left(D\left(\frac{[H^+]^3}{[HA]^3}\right)\right)$	7,47	7,50	7,49	7,47	7,48	7,50	7,47	7,48
- Log[R_4NA]	0,51	0,52	0,53	0,54	0,55	0,57	0,58	0,59

Y being constant, x is equal to zero. The complexes extracted by R_4NA and HA are then the same. $K_3 = 3 \pm 0.5$.

Stripping of chromium

To strip chromium, hydrochloric acid solutions of various concentrations (1 to 12 mol/L) were tested on an organic solution containing 2 g/L Cr(III). The extraction rate increases with acid concentration (figure 3). Lower concentrations (< 4 mol/L) were however preferred because of a degradation of the organic phase for concentrated acid solutions.

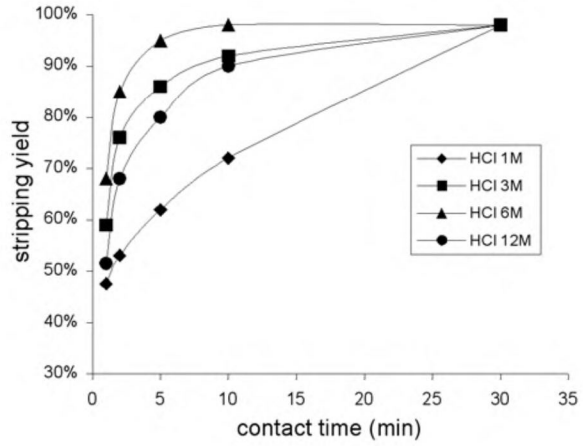


Figure 2: Stripping of chromium by HCl

Behaviour of iron (II), iron (III) and nickel (II)

As seen on figure 3, iron (III) is much better extracted than chromium. Iron (II) is not extracted at all.

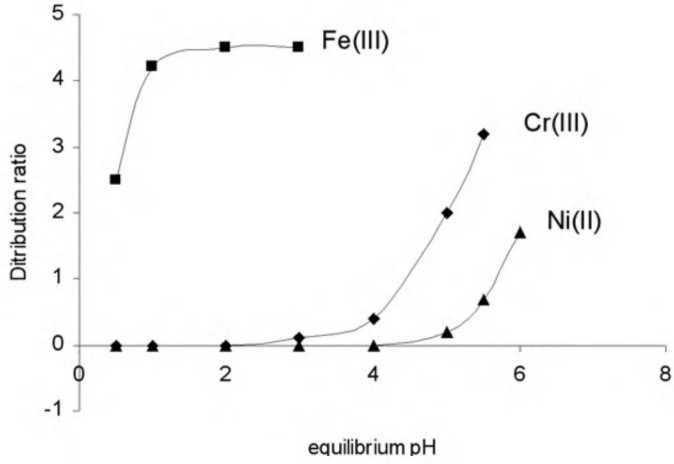


Figure 3: extraction of metals versus pH

Proposed flowsheet

The different steps of the proposed flowsheet were tested in conventional mixer-settler units operating in a counter current configuration. Tests were conducted with synthetic solutions to assess the technical feasibility of the proposed process. A preliminary step of iron (II) oxidation is proposed, followed by the extraction of iron(III) by TBP diluted in MIBK (Figure 4).

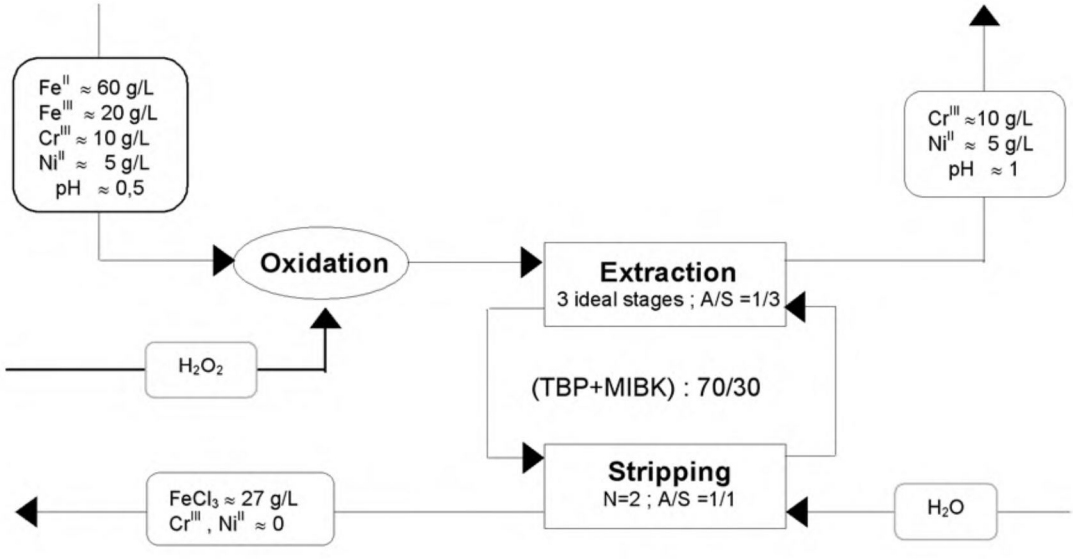


Figure 4 : Extraction of iron after its oxidation

The iron-free solution is then refined by solvent extraction based on the original mixture of extractants (DEHPA-Aliquat 336-Octanol) diluted in dodecan. The pure nickel raffinate could be then concentrated and valorised. Higher purification of the chromium liquor may be achieved through an extra scrubbing stage (Figure 5).

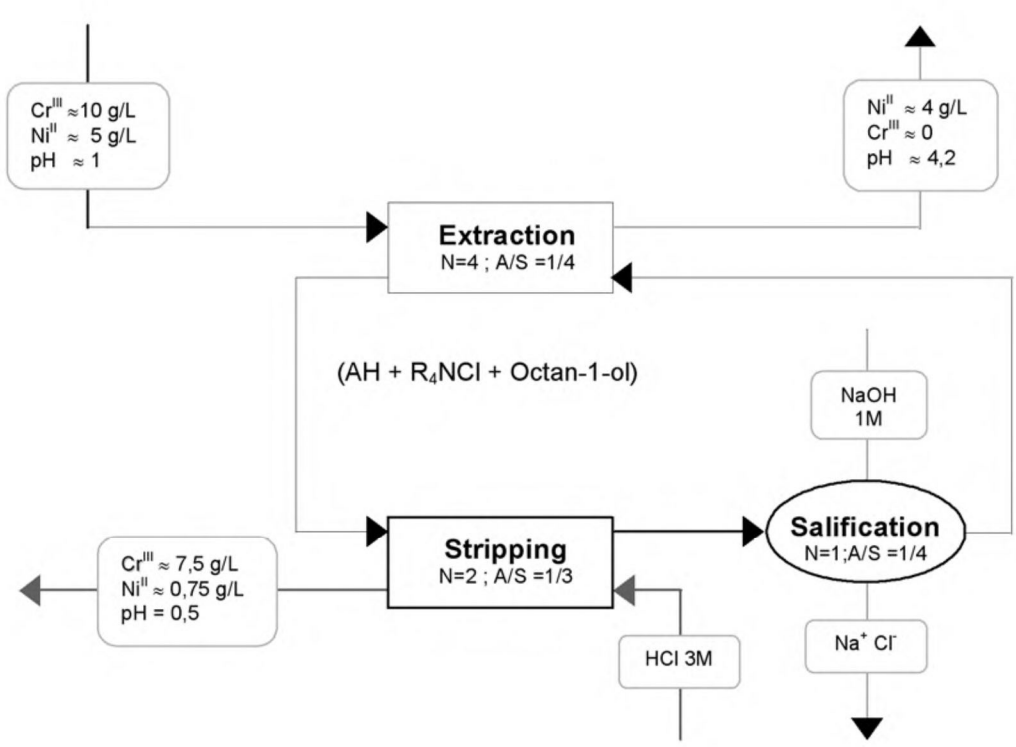


Figure 5 : Separation Nickel/Chromium from the iron-free raffinate stream

CONCLUSION

Technical feasibility of the proposed solvent extraction processes for chromium(III) removal and nickel(II) purification from hydrochloric pickling bathes of stainless steel have been successfully demonstrated.
Subsequent Cr(III)/Ni(II) separation was achieved. While the pure nickel liquor could be directly valorized, the Cr: Ni ratio was upgraded from 2 to 10 in the raffinate stream, and may be improved through an extra scrubbing stage.

REFERENCES

1. Mac KAVENEY J.P., FREISER H., *Anal. Chem.,* 30, 1965-1968, 1958
2. MAJUMDAR S.K.. DE A.K.. *Anal Chem..* 32. 1337-1339. 1960.
3. PANESAR K.S., SINGH O.V., TANDON S.N., *Talanta*, 41, 1341-1344, 1994.
4. PRESTON J.S., *Hydrometallurgy*, 10, 187-204, 1983.
5. PANDEY B.D., COTE G„ BAUER D„ *Hydrometallurgy*, 40, 343-357, 1996.
6. LEVEUGLE D., *Etude de la faisabilité d'un couplage entre l'extraction liquide - liquide et /'électrolyse pour la récupération électrochimique de métaux issus d'effluents du traitement de surface*, PhD Dissertation, Paris, 1998.

EXTRACTION AND SEPARATION OF PALLADIUM, PLATINUM AND RHODIUM WITH DIALKYL SULFOXIDE FROM CHLORIDE MEDIA—A FACILE RECOVERY OF NOBLE METALS FROM SPENT CATALYSTS

LI Yao-wei, GU Guo-bang, ZHU Ping, LIU Hai-yang

Department of Applied Chemistry, South China University of Technology,
Guangzhou, P.R. China

Liquid-liquid extraction and separation of palladium, platinum and rhodium with a dialkyl sulfoxide (MSO) from hydrochloric acid media have been investigated. The extraction of Pd(II) was essentially complete in 1-6 mol/l HCI media with 0.9 mol/l MSO in kerosene, while the extraction of Rh(III) was less than 5% at the same conditions. In the case of Pt(IV), more than 98% of Pt(IV) was extracted in 5.0-6.0 mol/l HCI media with 0.9 mol/l MSO in kerosene. The quantitative stripping of Pt(IV) and Pd(II) was achieved successfully with 0.1 mol/l HCI and 2.0 mol/l ammonia solution respectively. The separation of Pd(II), Pt(IV) and Rh(III) from spent catalysts leaching solution could be accomplished by controlling extraction and stripping conditions.

INTRODUCTION

The platinum group metals (especially, palladium, platinum and rhodium) are very important in industry. They are extensively used in catalysis, electronic devices and space materials etc. The high prices and increasing demands of these metals have stimulated investigations of their separation, concentration and purification by solvent extraction techniques from spent catalysts [1-3]. These metals occur in spent catalysts associated with the major base metal copper, iron and nickel. Both technical and commercial considerations demand the individual platinum group metals are separated not only from other metals but also from each other to high purity with high percentage of recovery. It's well known that separation and purification of these metals are difficult, because of their similar chemical behavior in chloride media [4], It is challenging to develop efficient recovery process for these metals. Here, we report a synthesized dialkyl sulfoxide (MSO) which can extract palladium(II) and platinum(IV) with excellent selectivity over rhodium(III), iron(III) and copper(II) from hydrochloric acid media. This dialkyl sulfoxide was also successfully used in the separation of palladium(II), platinum(IV) and rhodium(III) from spent catalysts leaching solution.

EXTRACTION REAGENTS AND PROCEDURES

The synthesized dialkyl sulfoxide (R_1SOR_2, R_1,R_2: C_5~C_7) is pale yellow and sticky liquid. Its main characters are shown as follows: the content of sulfur in MSO, 10.27%; density at 28“C, 0.899 g/cm'^{3}; viscosity at 28°C, 25 mPa-s. IR (cm'^{1}) 2960, 2929, 2873, 2860, 1462.1380, 1032. MS (M+l)/z: 275.2. Organic phases were prepared by dissolving the required amount of MSO in kerosene.

The stock solutions of Pd(II), Pt(IV) and Rh(III) were prepared by dissolving $RhCl_3$, H_2PtCl_6 and $PdCl_2$ in hydrochloric acid respectively and standardized by known methods [5], The work solutions (100mg/l metal, usually in 1-6 mol/l HCl) were prepared from the respective stock solutions by further dilution with double distilled water and addition of the requisite amount of 12 mol/l hydrochloric acid. All other chemicals used were of analytical reagent grade.

Experiments were carried out by shaking aqueous phase containing 100 mg/l of Pd(II)/Pt(IV)/Rh(III) ion with equal volume of organic phases containing 0.9 mol/l MSO in kerosene for 10 min in a mechanical shaker at a controlled temperature of 25±1°C. After equilibrium was reached, the two phases were allowed to separate and the metal concentration for each metal ion in the aqueous phase was determined by atomic absorption spectrophotometer. The equilibrium metal concentration in the organic phase was determined by mass balance of the metal before and after extraction.

RESULTS AND DISCUSSION

In order to facilitate the separation of these metals, the extraction of each metal ion was studied separately under the influence of hydrochloric acid concentration, extractant concentration and stripping agents.

Effect of hydrochloric acid concentration

The dependence of the extraction of palladium^ II), platinum(IV) and rhodium(lll) on HCl concentration was shown in Figure 1. The extraction of Pd(II) was essentially complete in 1.0-6.0 mol/l HCI media, and the extraction of rhodium(IU) was less than 5% at the same conditions. The extraction of platinum(IV) was low when the acidity was less than 2 mol/l HCI, and increased with increasing of HCI concentration. More than 98% of Pt(IV) was extracted at a higher acidity of 5.0-6.0 mol/l HCI.

Effect of extractant concentration

Extraction of platinum metals was carried out at various concentration of MSO in kerosene. The effect of extractant concentration on the extraction of platinum metals was shown in Table 1. MSO concentration for extraction of Pt(IV) and Pd(II) was optimized in 4.0 mol/l HCI media. For Pd(II), extractant concentration required for a quantitative extraction was 0.9 mol/l. In the case of Pt(IV), quantitative extraction took place at a higher extractant concentrationl .2 mol/l. However, the extraction of Rh(III) was not more than 10% even MSO concentration reached

1.5 mol/l at this acidity.

Table 1. Effect of extractant concentration on the extraction of platinum metals

MSO concentration (mol/l)	Percentage extraction (%)		
	Pd(II)	Pt(IV)	Rh(III)
1.50	99.60	99.40	6.91
1.20	99.60	99.40	4.36
0.90	99.60	96.88	2.11
0.45	96.43	90.36	1.34
0.30	88.71	83.15	0
0.15	75.20	64.17	0

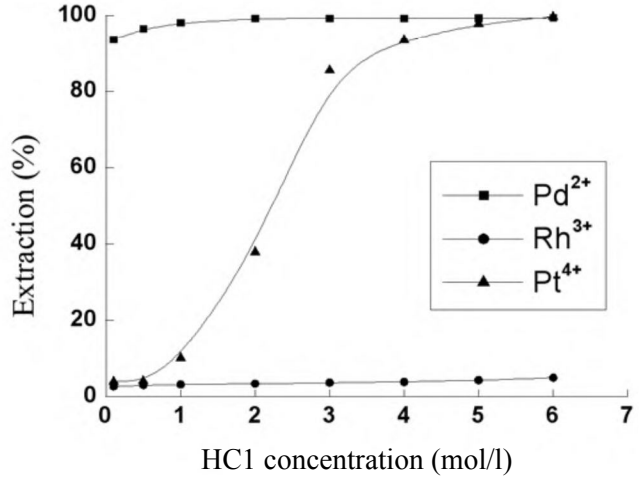


Figure 1. Dependence of the extraction of platinum metals on HCI concentration. (Organic phase: 0.9 mol/l MSO; Aqueous phase: 100 mg/l each platinum metal in 4 mol/l HCI solution)

Effect of stripping agents

Hydrochloric acid and ammonia solution are conventional stripping agents for platinum(IV) and palladium(II). The metal-loaded organic phase containing Pt(IV) was stripped successfully with 0.1 mol/l HCI. However, the higher concentration of HCI was unfavorable for the stripping of Pt(IV). In the case of Pd(ll), 2.0 mol/l ammonia solution was effective for the quantitative stripping.

SEPARATION OF PALLADIUM(II) PLATINUM(IV) AND RHODIUM(III)

The separation of Pd(ll), Pt(IV) and Rh(III) from their mixtures was carried out by taking advantage of their different extraction and stripping conditions towards MSO. The spent catalysts leaching solution consist of chloride complexes of Pd, Pt and Rh accompanied with large excess of Cu and lower amount of Fe. The solution was prepared in 4.0 mol/l HCI and the composition is given in Table 2. The flowsheet proposed for the treatment of this solution

is shown in Figure 2. The separation process includes three-stage co-extraction of palladium(II) and platinum(IV), two-stage scrubbing, two-stage stripping of platinum(IV), three-stage stripping of palladium(II) and one-stage regeneration of MSO.

Table 2. Composition of the spent catalysts leaching solution

Element	Pd	Pt	Rh	Cu	Fe
Concentration (mg/l)	6778	3273	453	21420	37.6

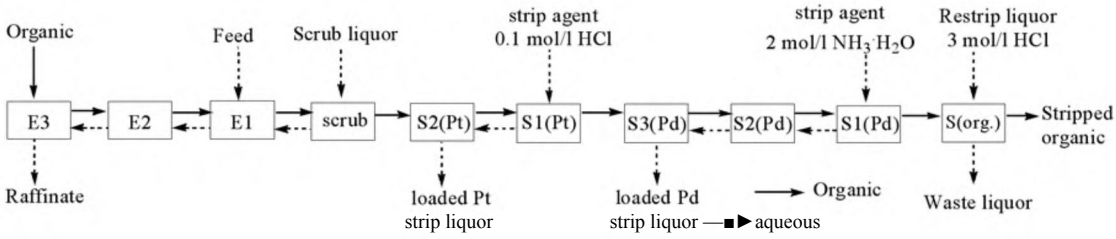


Figure 2. Flowsheet for the separation of palladium(If), platinum(IV) and rhodium(III) from spent catalysts leaching solution

Extraction

In order to carry out the separation of these metals, the leaching solution was equilibrated for 10 min with 0.9 mol/l MSO, using an volume phase ratio (0:A=1) of unity, when Pd(II) and Pt(IV) were quantitatively extracted along with co-extraction of Fe(III) (90.62%), Rh(III) and large excess of Cu were remained in the aqueous phase. Typical extraction efficiencies of the various elements in the leaching solution are listed in Table 3.

Table 3. Extraction efficiencies of various elements in the leaching solution

Element	Pd	Pt	Rh	Cu	Fe
Organic loading (mg/l)	6773.3	3234.7	~0	<0.1	34.07
Extraction (%)	99.93	98.83	~0	~0	90.62

Scrubbing

The organic phase loading Pt(IV), Pd(II) and Fe(III) was scrubbed with a scrub liquor at an volume phase ratio (0:A) of 2 and the impurities was scrubbed. In the case of Pd(II) and Pt(IV), the scrubbing efficiency was only 1.0% and 2.7% respectively. Most Fe(III) was still remained in organic phase and two-stage scrubbing efficiency of Fe(III) was only 10.84%.

Stripping

The organic phase loading Pt(IV), Pd(II) and Fe(III) was first stripped with 0.1 mol/l HCl, two-stage stripping percentage of Pt(IV) reached 100%. At the same time, the Fe(III) was also completely stripped. Pt(IV) was separated from Fe(III) by forming precipitate $(NH_4)_2PtCl_6$.

Then Pd(II) was stripped with 2.0 mol/l ammonia solution, three-stage stripping percentage was 99.2%.

CONCLUSIONS

The synthesized dialkyl sulfoxide has excellent selectivity to palladium(II) and platinum(lV) over rhodium(III), iron(III) and copper(II). Palladium^ II) and platinum(IV) were quantitatively co-extracted with 0.9 mol/l MSO in short period of equilibrations. However, rhodium(lll) was not extracted basically. Taking advantage of their different stripping conditions towards MSO, palladium^ II) was quantitatively separated from platinum(lV). Thus, the described method is simple, selective for the recovery and separation of palladium^ II), platinum(IV) and rhodium(lll) from spent catalysts leaching solution.

REFERENCES

1. C. Nowottny, W. Halwachs, K. Schugerl (1997), *Sep. Purif. Technol.,* 12,135-144
2. J.S. Preston, A.C. du Preez (1993), *Solvent Extraction in the Process Industries,* vol. 3, Elsevier, Oxford, pp. 1295-1302
3. A. A. Mahaske, P. M. Dhadke (2001), *Hydrometallurgy,* 61,143-150
4. E. Benguerel, G. P. Demopoulos, G. B. Harris (1996), *Hydrometallurgy,* 40,135-152
5. A. I. Vogel (1961), A Text Book of Quantitative Inorganic Analysis, 3rd edn., London, pp.513

STUDY ON EXTRACTIVE LEACHING OF SPHALERITE CONCENTRATE

Peng Peng', Xie Huiqin*, Lu Lizhu ***

* Institute of Process Engineering , Chinese Academy of Sciences, Beijing, China
** Engineering Command Institute of Chemical Defence, Beijing, China

The leaching process of sphalerite concentrate in H_2S0_4-$HN0_3$ and tetrachloroethylene extracting of sulfur was investigated. Variables investigated included: Leaching temperature, leaching time, liquid/solid ratio, and tetrachloroethylene concentration. The SEM images of sphalerite concentrate and residues were performed by the using of JEM-6700F Field Emission Scanning Electron Microscope. The relationship between the number of recycling and extraction ratio of zinc was studied. The results indicated that 99.6% of zinc was obtained after three hours of leaching at 85°C,0.1 MPa 0_2, with 20g sphalerite concentrate in 200ml leaching solution containing 2.0 mol/L H_2S0_4 and 0.2 mol/L $HN0_3$, in the presence of 10ml C_2Cl_4. The leaching time of zinc was 50% shorter than the leaching without C_2Cl_4. The recycled C_2Cl_4 exerted little influence on extraction ratio of zinc. The extractive effect was distinct.

INTRODUCTION

With more stringent policy on environmental protection and diminishing mineral resources, pyrometallurgy has in many respects been giving way to hydrometallurgical processes especially for low-grade and complicated sulfide ores. In hydrometallurgy, sulfur in the ore is converted to elemental sulfur, which remains in the solid residue, rather than sulfur dioxide in the gaseous effluent to pollute the atmosphere. However, the sulfur formed during leaching usually covers the ore particles, thus preventing effective contacting of the ore particles with the leaching solution, to reduce the leaching rate of the metal being extracted[1-6], To enhance leaching, increasing the intensity of stirring, controlling the temperature of leaching or addina catalvticaaents has been resorted to 17-151. but the results are bv no means ideal. In this paper, the leaching of sphalerite concentrate in H_2S0_4-$HN0_3$ was coupled to the extraction of the sulfur layer on the ore particles by adding tetrachloroethylene.

EXPERIMENTAL

Experimental materials

In present experiment, sphalerite concentrate having the chemical composition shown in Table 1 was first dried and then ground in a ball mill to below 74 P m. Sulphuric acid, nitric acid and tetrachloroethylene were all analytical grade.

*** Corresponding author. Tel.:+86-10-86200817.**
E-mail address: pengpeng@home.ipe.ac.cn

Table 1. Composition of sphalerite concentrate

Element	Concentration (Wt%l)	Element	Concentration (Wt%l
Zn	50	Cd	0.45
Fe	7	Ca	0.02
Pb	3	As	2.05
Cu	0.8	Ni	0.01
Mg	0.35	Mn	0.14
S	31	Co	< 0.001
$Si0_2$	2.65	Ag	500g/t
ALO,	0.62	Au	2.12g/t

Experimental methods

Experiments were carried out in a 500ml titanium lining autoclave with mechanical stirring, temperature controlling and gas injection. A weighed amount of sphalerite concentrate was leached in 200ml solution of 2.0mol/l H_2S0_4, 0.2mol/l $HN0_3$, and C_2Cl_4 varying from zero to 30ml at a temperature range of 45 to 85°C,under an oxygen pressure of O.IMPa, for time range from 0.5 to 6h. Sampling analyses were conducted during certain reaction time. The zinc content was analyzed by the EDTA titration method.

The principle of extractive leaching

The reactions involved in extractive leaching processes can be described by the following stoichimetric relationships:

$$2ZnS + O_z + 2H_2S0_4 \xrightarrow{\text{I-NO,}} 2ZnS0_4 + 2S° + 2H_zO \quad (1)$$

$$\tau S° + C_2Cl_4 = \tau s° \bullet C_2Cl_4 \quad (2)$$

$$S° \bullet C_2Cl, <,,, \xrightarrow{\text{strip-extraction by changing the temperature}} S\cdot(CA \quad (3)$$

The elemental sulfur formed in reaction (1) was extracted by tetrachloroethylene in time as shown in reaction (2), thus reducing the resistance of sulfur layer on the ore particles to leaching process. Tetrachloroethylene was chosen as the organic solvent for sulfur because of its high solubility for sulfur and its stability in the leaching pulp thus facilitating recycling as shown in reaction (3).

RESULTS AND DISCUSSION

Effect of leaching temperature on zinc extraction

Experiments were carried out with 20g sphalerite concentrate in 200ml solution containing 2.0mol/L H_2S0_4 and 0.2mol/L $HN0_3$ at O.IMPa 0_2 and temperature varying from 45°C to 85 °C and leaching time being 2h. The relationship between the leaching temperature and extraction ratio of zinc is shown in Table 2. The extraction ratio of zinc increased proportionally with the increase in the leaching temperature. The results indicated that the enhancement of leaching temperature accelerated not only the rate of leaching solution diffusing to the surface of ore particles but also the leaching reaction.

Table 2. Effect of leaching temperature on zinc extraction

Tcmpcralurc/°C	45	55	65	75	85
Extraction ratio of zinc/%	45.6	56.9	65.1	74.2	86.1

Effect of leaching time on zinc extraction

Table 3 shows the relationship between the leaching time and extraction ratio of zinc. The extraction ratio of zinc increased as the leaching time increased. After the sphalerite concentrate was leached 2h, the leaching rate of zinc increased slowly. It increased from 86.1% to 99.2% as the leaching time increased from 2h to 6h. The elemental sulfur layer formed in the surface of ore particles became thicker and thicker as the leaching process ran. Thus the resistance of the leaching solution diffusing to the surface of ore particles increased, leading to the result that the rate of leaching in later stage was more slow than the rate of leaching in earlier stage.

Table 3. Effect of leaching time on zinc extraction

Leaching time/h	0.5	1	1.5	2	3	4	6
Extraction ratio of zinc/%	51.0	70.1	82.0	86.1	92.3	96.7	99.2

Effect of liquid/solid ratio on zinc extraction

The relationship between the liquid/solid ratio and extraction ratio of zinc is shown in Table 4. The results indicated that the liquid/solid ratio exerted an obvious influence on zinc extraction. Increasing the liquid/solid ratio increased the zinc extraction. But when the ratio was greater than 10, the zinc extraction increased less. But the system loading increased evidently, the energy consumption went up, the productivity came down. The appropriate liquid/solid ratio was 10:1.

Table 4. Effect of liquid/solid ratio on zinc extraction

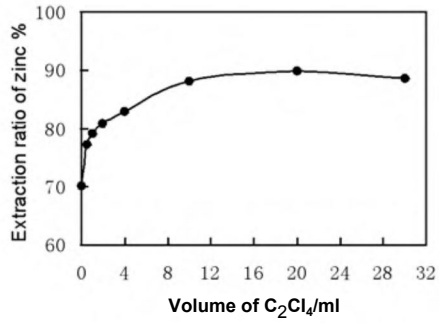
Liquid/Solid	1:1	5:1	10:1	15:1	20:1
Extraction ratio of zinc/%	45.1	70.4	86.1	90.5	91.7

Effect of tetrachloroethylene on zinc extraction

Figure 1 shows the relationship between the adding volume of C_2Cl_4 and extraction ratio of zinc. The zinc extraction increased as the adding volume of C_2Cl_4 increased. It indicated that C_2Cl_4 extracted and separated the elemental sulfur layer covering the ore particles and the new surface of ore particles exposed, which increased the contact chance of the ore particle surface and leaching solution, thus accelerated the leaching reaction. The leaching rate of zinc was enhanced evidently when the volume of C_2Cl_4 in 200ml leaching solution increased from 0 to 10ml, as the volume of C_2Cl_4 increased from 10ml to 20ml, the zinc extraction increased slowly. It increased from 88.1% to 89.91%. While the volume of C_2Cl_4 was more than 20ml, the extraction ratio of zinc began to reduce because the viscosity of C_2Cl_4 was large, which increased the resistance of the leaching solution diffusing to the surface of ore particles and reduced the leaching reaction.

The extractive leaching of sphalerite concentrate

Extractive leaching experiments were investigated at 85 °C, 0.1 MPa 0_2, in 200ml solution of 2.0mol/L H_2SO_4 and 0.2mol/L HNO_3, in the presence of 10ml C_2C1_4, the ratio of liquid and solid being 10:1. Figure 2 shows the comparison of leaching effect on sphalerite concentrate with or without C_2Cl_4. From Fig.2, the extraction ratio of zinc increased evidently after adding $_{10}$ml C_2C1_4. The leaching fraction of zinc amounted to $_{88.2}$% after one hour of leaching. However, under the same condition without C_2Cl_4, the extraction ratio of zinc was only 70.1%. After three hours of leaching under the extractive conditions, the extraction ratio of zinc reached 99.6%. But the leaching rate of zinc was 99.2% after six hours of leaching without C_2C1_4. As a result, the extractive leaching time of zinc was 50% shorter than the common leaching. The extractive effect was distinct.



Figurel. Effect of C_2Cl_4 addition volume on zinc extraction

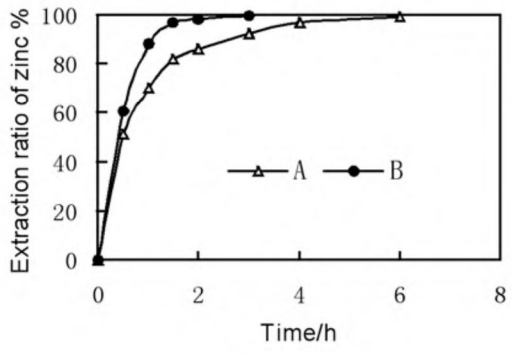
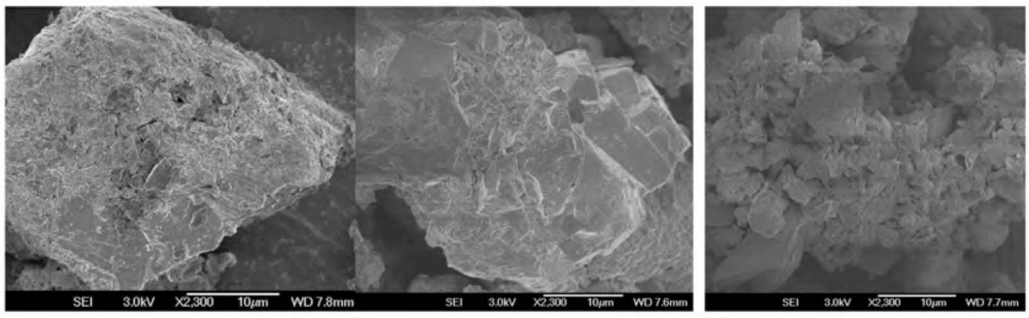


Figure 2. Comparisons of leaching effect on sphalerite concentrate with or without C_2Cl_4
A —without C_2Cl_4 B —with C_2Cl_4

Morphology of sphalerite concentrate surface

In order to analyze the effect of C_2Cl_4 during the leaching of sphalerite concentrate, The SEM images of sphalerite concentrate and residues were performed by the using of JEM-6700F Field Emission Scanning Electron Microscope. The results shown in Fig.3 indicated that a sulfur layer was formed on sphalerite concentrate particles during the leaching without C_2Cl_4 (shown in II) and the sulfur layer was dissolved and removed from ore particles surface obviously by adding C_2Cl_4(shown in III). The disappearance of the sulfur layer reduced the leaching resistance and accelerated the leaching rate notably.



I -Before leaching ***//-Residue leached without*** $C_2C/_4$ ***111-Residue leached with C_2Cl_4***

Figure 3. SEM images of sphalerite concentrate surface

Recycling and loss of C_2Cl_4

The organic phase containing sulfur was obtained by separating the organic and aqueous phase from the leaching solution while hot. High quality sulfur and the recycled C_2Cl_4 were recovered by cooling the organic phase. The recovery rate of sulfur was 86.4%. Table 5 shows the relationship between the number of recycling and extraction ratio of zinc. The results indicated that the recycled C_2Cl_4 exerted little influence on extraction ratio of zinc.

Table 5. Effect of the recycled C_2Cl_4 on zinc extraction

The number of cycle /n	0	1	2	3	4	5
Extraction ratio of z.inc/%	99.3	99.0	99.1	98.7	99.0	98.2

During the leaching reaction, C_2Cl_4 adhered to the surface of ore particles while it extracted and separated sulfur layer on ore particles. The stirring of leaching solution might separate the greater part of C_2Cl_4 from ore particles, but there was still a little C_2Cl_4 on the surface of ore particles which resulted in the loss of 15% C_2Cl_4. The loss percentage of C_2Cl_4 has been reduced to 5% by adding a small amount of surfactant sodium lignosulphonate which reduced surface tension of leaching solution and altered the hydrophilicity of ore particles, resulting in well-dispersion of ore particles in the leaching solution.

CONCLUSIONS

The extraction ratio of zinc was considerably enhanced while coupling the leaching of sphalerite concentrate to the tetrachloroethylene extracting of elemental sulfur formed during extraction, resulting in the zinc extraction up to 99.6% after three hours of leaching. The leaching time was 50% shorter than the common leaching. The optimum parameters to leach sphalerite were: a leaching temperature of 85°C; a liquid/solid ratio of 10:1; a leaching time of three hours; an oxygen pressure of 0.1 MPa and a C_2Cl_4-to-leaching solution ratio of 1:20.

ACKNOWLEDGEMENTS

The authors thank Prof. Mooson Kwauk for his review and improvement of the manuscript. The authors are grateful to the National Natural Science Foundation of China (No.20276074) for financial support.

REFERENCES

1. Warren G W, Henein H and Jin zuomei(1984), *Metallurgical transactions B,* 15B: 5-12.
2. Majima H. (1989) ,Can. *Metall. Quar.,* 24(4):283-291.
3. Dutrizac J E., Macdonald R J I. (1978), *Metallurgical transactions B,* 9B :543-551.
4. Dutrizac J E. (1990) , *Hydrometallurgy,* 23:153-176.
5. Dutrizac J E, Chen T T.(1990), *Metallurgical transactions B*, 21:935-993.
6. Lin H K , Rao P D , Li S.(1991*),Preprint-society of mining engineers ofAIME* , 91-114.
7. Venkataswamy Y, Khangaonkar P R.(1981), *Hydrometallurgy,* 7(1 -2):1 -5.
8. Neou-Singouna P, Fourlaris G.(1990) ,*Hydrometallurgy,* 23:203-220.
9. Bobeck G E, Su H. (1985),*Metallurgical transactions B,* 16B :413-424.

10. Crundwell F K.(1987), *Hydrometallurgy,* 19:227-242.
11. Dutrizac J E.(1989), *Can. Metall. Quar.,* 28(4):337-344.
12. Balaz P, Ebert I. (1991),*Hydrometallurgy,* 27(2):141-150.
13. Lochmann J, Pedlik M.(1995), *Hydrometallurgy,* 37:89-96
14. Maurice D, Hawk J A.(1998) , *Hydrometallurgy,* 49(1-2):103-123.
15. Maurice D, Hawk J A.(1999), *Hydrometallurgy,* 51(3):371-377.



SEPARATION OF Cr(III) AND Fe(III) FROM A TANNERY FILTRATE USING CYANEX 272

Akash Deep and J.M.R de Carvalho*

Centre of Chemical Processes, Department of Chemical Engineering,
Instituto Superior Tecnico,
Lisboa, Portugal

The present paper describes the extraction of Fe(III) from sulphate medium using a solution of Cyanex 272 in Escaid 110. Studies have revealed that the extraction of Fe(III) is selective over Cr(III) and Zn(II). The transfer of Fe(III) to the organic phase increases with the increasing pH suggesting the involvement of a cation exchange mechanism. The stripping of Fe(III) is achieved using 50 gpl H_2S0_4. Employing a two stage extraction and one stage stripping steps it has been possible to almost completely recover Fe(III) from a tannery filtrate leaving pure Cr(III) in the raffinate.

INTRODUCTION

The waste from tannery industry is often loaded with objectionable concentrations of Cr(III) and Fe(III) along with some other metals. The traditional precipitation methods do not necessarily offer the separate recoveries of Cr(III) and Fe(III). Solvent extraction has been pointed out as a potential alternative to recover pure metals from industrial wastes. Amongst the several extractants available for the metal extraction the organophosphorus extractants are regarded as most promising. Recently Flett [1] has reviewed the role of various organophosphorus extractants in different areas of hydrometallurgy. In the present project our idea was to separate Cr(III) and Fe(III) by performing the selective solvent extraction of Fe(III).

In the case of Fe(III) extractants like DEHPA [2] and versatic acid [3] the problem has been encountered during stripping of the extracted Fe(III), which requires a highly concentrated HCI medium or other difficult stripping conditions. To overcome this problem some researchers have proposed the use of synergistic mixtures of extractants [4-6], Cyanex 272 has been developed as a useful extractant for some metal ions including Co(II) and Ni(II). Some reports [7, 8] hints towards its ability to extract Fe(III) from sulphate and nitrate medium. However, a detailed study is required to test its viability for the separation and stripping of Fe(III).

We planned to test the utility of Cyanex 272 for the extraction of Fe(III) from sulphate medium and apply the method for the separation of Cr(III) and Fe(III) from a filtrate of tannery waste. This filtrate was obtained in a previous study [9] by sulphuric acid leaching (pH 0.46) of a tannery mixed sludge produced at waste water treatment plant, Alcanena (Portugal). Most of the metals were leached in the filtrate leaving the sludge safe for dumping or to be used in ceramics production and agriculture soil.

EXPERIMENTAL

In some preliminary tests the problem of crud formation was observed with a direct use of the filtrate in Cyanex 272 SX circuit. Consequently the filtrate was agitated with activated carbon (GR, Merck) to ensure the removal of any organic impurity. Some general experiments indicated the requirement of around 5 g of activated carbon for the treatment of 1 L of the filtrate so as to prevent any crud formation.
Cyanex 272 was received from Cytec Canada. Escaid 110 (Exxon) was used to prepare the dilute solution of Cyanex 272. All other chemicals were AR grade materials from MERCK. The stock solutions of the metal ions were prepared by dissolving their suitable salts in de-ionized water containing a minimum amount of sulphuric acid. Keeping in mind the level and ratio of concentrations of Fe(III), Cr(III) and Zn(II) in the tannery filtrate the working solutions of 500 ppm Fe(III), 500 ppm Cr(III) and 10 ppm Zn(II) were obtained by diluting the stock solutions.

For the solvent extraction experiments aqueous and organic phases (A / O = 1) were contacted for forty-five minutes on a wrist action shaker at room temperature (20 ± 2° C). Wherever necessary the pH of the aqueous phase was adjusted by adding suitable amount of NaOH or H_2S0_4. After the separation of the two phases the concentration of metals in the aqueous phase was determined by AAS (AAnalyst 200, Perkin Elmer). The stripping steps were carried out using a solution of 50 gpl sulphuric acid as stripping agent. The A / O ratio was kept to 1.

RESULTS AND DISCUSSIONS

Effect of Concentration of Cyanex 272 on the Extraction of 500 ppm Fe(III) / Cr(III) and 10 ppm Zn(II) from the Tannery Filtrate
The results at an equilibrium pH 1.8 are shown in Figure 1. 5% Cyanex 272 is required to extract around 90% of Fe(III) content. Cr(III) and Zn(II) are not extracted in any concentration of Cyanex 272. This study points out toward the selectivity of Cyanex 272 for the extraction of Fe(III) in the presence of Cr(III) and Zn(II).

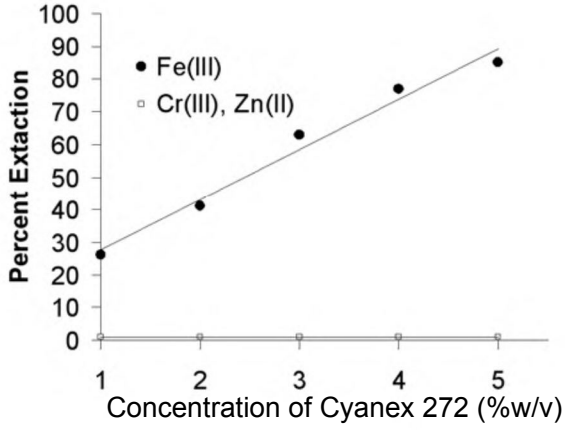


Figure 1. Effect of Cyanex 272 Concentration on the extraction of metal ions from tannery filtrate

Effect of Equilibrium pH on the Extraction of 500 ppm Fe(III) / Cr(III) and 10 ppm Zn(II) with Cyanex 272

Figure 2 depicts the effect of equilibrium pH on the extraction of metal ions from synthetic solutions at different sulphuric acid concentrations and tannery filtrate with 5% Cyanex 272. Following a cation exchange mechanism the extraction of Fe(III) increases with the increasing pH.

Under the investigated conditions Cr(III) is not extracted in Cyanex 272. Zn(II) is also unextractable barring a few fraction at a low sulphuric acid (5 gpl) concentration. The curves for Fe(III) extraction suggest that with the increasing sulphur substitution in the aqueous phase the transfer of the metal ion to the organic phase decreases. To further test the fact we investigated the effect of $S0_4$" ions (Na_2S0_4) addition on the extraction of Fe(III) from a solution containing 5 gpl sulphuric acid. The equilibrium pH was kept to 1.8. The results supporting the above observation are shown in Figure 3.

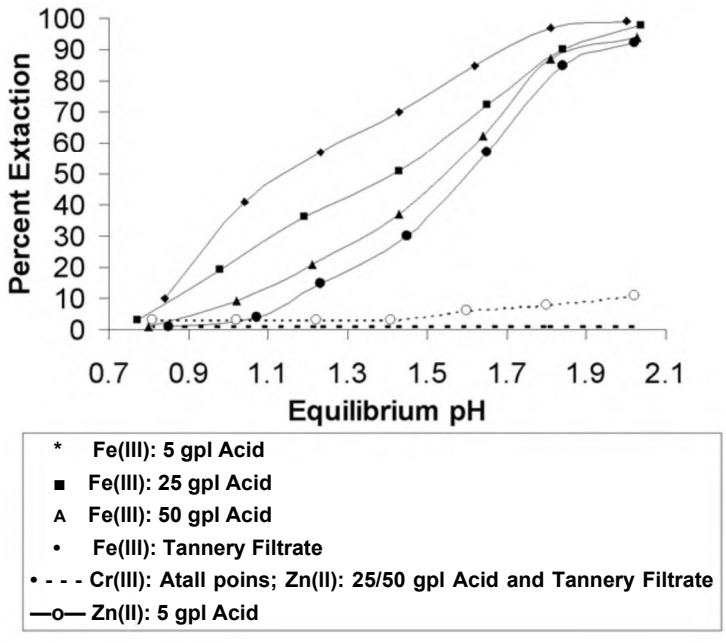


Figure 2. Effect of equilibrium pH on the extraction of metal ions

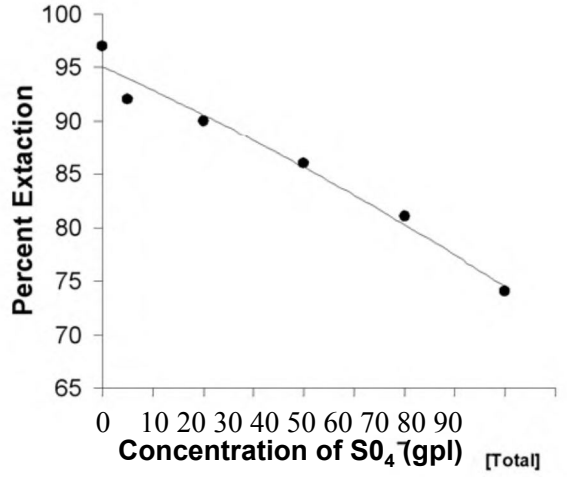


Figure 3. Effect of $S0_4$" ions on the extraction of Fe(III)

Fe(III) Extraction Kinetics and Isotherm
The extraction of Fe(lll) with 5% Cyanex 272 at an equilibrium pH 1.8 was recorded for different time intervals. Under the present experimental conditions a contact time of minimum of forty minutes is required to achieve the equilibrium.

A McCabe-Thiele extraction isotherm for Fe(lll) using 5% Cyanex 272 is shown in Figure 4. Apparently, almost complete removal of Fe(lll) from the tannery filtrate (Fe = 300 ppm) is possible in two theoretical stages at an equilibrium pH of 1.8.

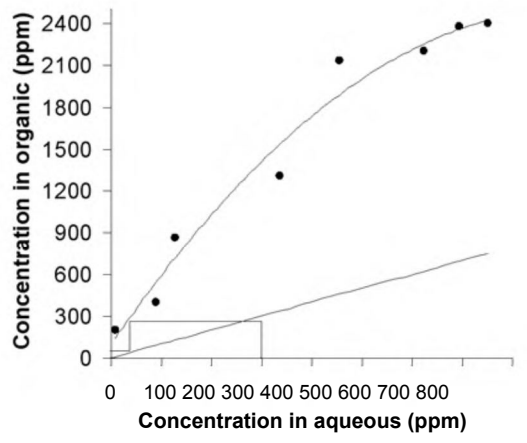


Figure 4. Extraction isotherm of Fe(lll)

Stripping Kinetics and Isotherm
The studies have reveled that a minimum of 20 minutes contacts of the organic phase with 50 gpl sulphuric acid is required to ensure more than 99% stripping of Fe(lll).
The stripping isotherm (Figure 5) indicates that 300 ppm Fe(lll) can be completely stripped in one theoretical stage.

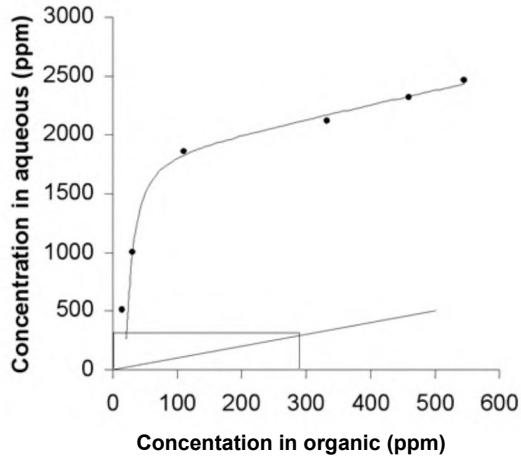


Figure 5. Stripping Isotherm of Fe(lll)

Application of SX Steps to Tannery Filtrate
A two stage countercurrent extraction (final pH = 1.8) and one stage stripping steps were employed to the tannery filtrate. The results for five such runs are given in Table 1. The

introduction of SX has resulted almost complete removal of iron from the tannery filtrate. The stripping of iron gives a reasonably pure solution.

Table 1. Separation of iron from tannery filtrate

Concentration of metals in tannery filtrate (ppm)			Counter-current Run No.	Concentration of metals in raffinate (ppm)			Concentration of metals in aqueous phase after stripping (ppm)		
Fe	Cr	Zn		Fe	Cr	Zn	Fe	Cr	Zn
295	395	7.00	1	6.11	394	6.98	288	n.d	n.d
			2	5.22	394	6.99	287	n.d	n.d
			3	4.59	394	6.99	286	n.d	n.d
			4	4.16	394	6.99	287	n.d	n.d
			5	4.96	394	6.99	288	n.d	n.d

CONCLUSIONS

The present work demonstrates the utility of Cyanex 272 for the extraction of Fe(III) from a tannery filtrate. The desired level of removal of iron from the tannery filtrate can be simulated by considering the extraction stages. The remaining solution of Cr(III) and the stripped solution of Fe(III) are pure enough to reuse. Zinc is not removed from Cr(III) solution, however, a pure Cr(III) hydroxide can be formed avoiding the precipitation of Zn(II).

It is possible to use a less concentrated solution of sulphuric acid to strip the loaded iron from the organic phase. This offers an important advantage over other extractants like DEHPA and PC-88A, which require a higher concentration of the acid for their regeneration.

ACKNOWLEDGEMENTS

The authors are thankful to Cytec Canada for providing Cyanex 272. Financial support by FCT is gratefully acknowledged.

REFERENCES

1. D.S. Flett (2005), *Journal of Orga no metallic Chemistry,* In Press.
2. G.P. Demopoulos and D.L. Gefvert (1986), *Hvdrometalluroy*, 12, 299-315.
3. M.I. Stefanakis and A.J. Monhemius (1987), *Hydrometallurgy,* 19, 187-198.
4. J. Chen, Y. Shuqiu, L. Huizhou, M. Xiquan and W. Zhichun (1992), *Hydrometallurgy,* 30, 401-416.
5. M.R.C. Ismael and J.M.R. Carvalho (1996), *Proceedings of the International Solvent Extraction Conference (ISEC'96),* 1, 599-604.
6. M.R.C. Ismael and J.M.R. Carvalho (1999), *Proceedings of the International Solvent Extraction Conference (ISEC'99),* 2, 915-919.
7. K.C. Sole and J.B. Hiskey (1992), *Hydrometallurgy,* 30(1-3), 345-365.
8. N. Miralles, A.M. Sastre, E. Figuerola and M. Martinez (1992), *Hydrometallurgy,* 31(1-2), 1-12.
9. E.I. El-Shafey, P.F.M. Correia and J.M.R. de Carvalho (2005), *submitted to Separation Science and Technology.*



A CONTINUOUS DIAMEX PROCESS IN A HOLLOW FIBRE MODULE MICRO-PLANT

Andreas Geist, Michael Weigl, Klaus Gompper

Forschungszentrum Karlsruhe, Institut für Nukleare Entsorgung
P.O. Box 3640, 76021 Karlsruhe, Germany
geist@ine.fzk.de

A liquid-liquid extraction micro-plant working in the mL/h flow rate range and consuming small feed phase volumes is introduced. Miniature hollow fibre modules are used as phase contactors. A successful DIAMEX process was performed, co-extracting americium and lanthanides from a simulated PUREX raffinate. Americium and lanthanides were transferred to the product solution. Co-extraction of other fission products contained in the feed solution was suppressed by scrubbing and by addition of aqueous masking agents.

INTRODUCTION

The radiotoxicity of spent nuclear fuel is governed by its content of plutonium and the minor actinides (neptunium, americium, curium) for several 10^5 years. The Partitioning and Transmutation strategy [1] aims at minimising the long-term radiotoxicity by separating these elements (partitioning) and fissioning them to short-lived and eventually stable nuclides (transmutation). The radiotoxicity of the remaining nuclear waste to be finally disposed of would decay to the level of natural uranium within less than 1,000 years.

The following partitioning strategy, based on liquid-liquid extraction, is investigated in Europe [1]: Plutonium and neptunium are separated in a modified PUREX process. Next, the DIAMEX (diamide extraction) process co-extracts trivalent actinides (americium, curium) and lanthanides directly from the PUREX raffinate (HAR). Finally, trivalent actinides are separated from the lanthanides by a SANEX (selective actinide(III) extraction) process.

Usually, such processes are performed using centrifugal contactors or pulsed columns. Alternatively, we use hollow fibre modules (HFM) as liquid-liquid phase contactors [2, 3], A HFM consists of a bundle of thin hollow fibre membranes potted into a shell tube. Aqueous and organic phases are macroscopically separated by the membrane material, and mass transfer takes place via the membrane pores. The interface is immobilised inside the membrane pores due to preferential wetting by one of the phases and a higher static pressure in the other phase. This results in operation free of typical hydrodynamic problems such as flooding, entrainment and back-mixing [4],

After having performed several successful DIAMEX and SANEX extraction tests in single miniature HFM [5], we decided to couple several HFM to run a complete DIAMEX process, with extraction, scrubbing, and stripping sections.

Several DIAMEX tests have already been performed in centrifugal contactors at other European laboratories [e.g., 6, 7, 8], using alkylated malonamides [9] as extractant. N,N'-dimethyl-N,N'-dioctyl-2-(2-hexyloxy-ethyl)malonamide (DMDOHEMA, Figure 1) in kerosene is the most capable DIAMEX extractant so far. DMDOHEMA extracts by solvation trivalent actinide and lanthanide nitrates and nitric acid. Unfortunately, zirconium, molybdenum, and palladium are co-extracted, interfering with a subsequent SANEX process. This can be suppressed by adding oxalic acid and N-(2-hydroxyethyl)-ethylenediamine-N,N',N'-triacetic acid (HEDTA) as masking agents.

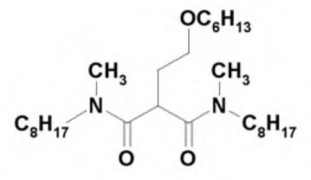


Figure 1. DMDOHEMA.

The main requirements for a DIAMEX process are high extraction efficiency regarding trivalent actinides (< 0.1 % in the raffinate), and low content of non-lanthanide fission products in the product solution. The final goal of a DIAMEX-SANEX process is a product containing "only" trivalent actinides. Thus, the efficiency of lanthanides co-extraction in the DIAMEX prcess is not crucial as they are separated from the trivalent actinides in the SANEX process.

EXPERIMENTAL

Flow-sheet

The flow-sheet is similar to the one developed in France for centrifugal contactor tests [8], Four HFM were coupled according to Figure 2. An acid scrubbing HFM was implemented to remove co-extracted nitric acid and oxalic acid from the organic phase. Optimum flow rates were found using (1) computer code calculations similar to the ones described in [3], (2) results from DIAMEX single-HFM extraction and stripping experiments [10],

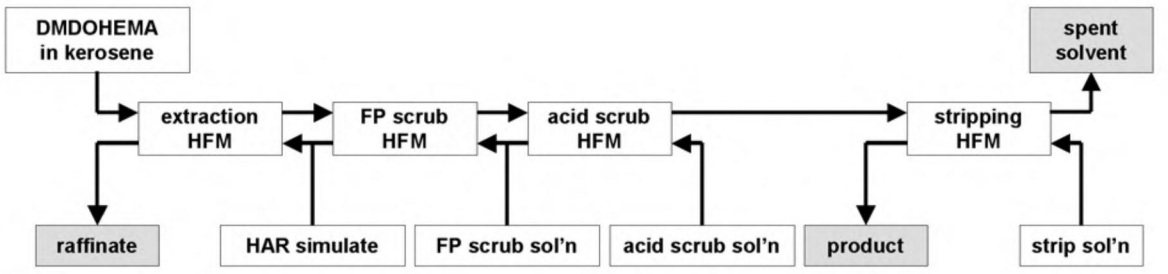


Figure 2. Setup for the 4-HFM DIAMEX process.

HFM Setup and Procedure

Miniature HFM were built by potting Celgard® X-30 hollow fibres (polypropylene, I.D. 0.24 mm, O.D. 0.30 mm, porosity 40 %, pore size 20 nm) into glass shell tubes with an internal diameter of 4 mm. The HFM consisted of 90 hollow fibres each with an active length of 0.20 m (extraction, fission product scrub and strip HFMs) or 0.10 m (acid scrub HFM). In the extraction module, aqueous phase flowed in the lumen of the hollow fibres. In the other three modules, organic phase flowed in the lumen of the hollow fibres [3], Aqueous phases were delivered by tube pumps, organic phase was delivered by a syringe pump. Flow rates were: Feed, Q_{feed} = 0.8 mL/h. Fission product scrubbing solution, $Q_{S}ci$ = 0.4 mL/h. Acid scrubbing solution, $Q_{S}c_2$ = 0.4 mL/h. Stripping solution, Q_{RX} = 0.8 mL/h. Organic phase, Q_{org} = 0.7 mL.

Exact flow rates (which are important to calculate mass balances) were determined by weighing feed vessels and effluent samples, which were collected for a known time interval.

Aqueous samples (feed, raffinate, product) were analysed by ICP-MS. Aliquots of organic samples were dissolved in a solution of (10 g/L Triton X-100 in 2 % $HN0_3$ suprapure) and analysed by ICP-MS. Americium in all samples was detected by gamma counting.

Reagents and Feed Solutions

Feed phase was a simulated inactive PUREX raffinate which was spiked with Am-241. Oxalic acid and HEDTA were added. The composition is given in Table 1. Fission product scrub solution was 0.2 M oxalic acid + 0.02 M HEDTA in 3 M $HN0_3$. Acid scrub solution was 1 M $HN0_3$. Stripping solution was 0.1 M $HN0_3$. Organic phase was 0.75 M DMDOHEMA (*Panchim,* France) in TPH (a kerosene-type diluent from *Prochrom,* France). DMDOHEMA was previously purified over Alumina B.

Table 1. Aqueous feed composition for the DIAMEX test (concentrations in mg/L unless stated otherwise).

Rb	Sr	Y	Zr	Mo	Ru	Rh	Pd
20	31	19	121	211	113	41	191
Ag	Cd	Sn	Sb	Te	Cs	Ba	La
7.7	16	2.4	8.8	47	373	161	102
Ce	Pr	Nd	Sm	Eu	Gd	Tb	Dy
185	83	292	83	15	29	3.1	6.4
U	Am-241	HNO_3	oxalic acid	HEDTA			
1810	20 MBq/L	3.7 M	0.2 M	0.02 M			

RESULTS

The test ran for 27.5 hours. Throughout this time, all effluent phases (raffinate, product and spent organic phase) were perfectly clear and without any entrainment. Relative transient effluent concentrations, $c_{out.rel}$ = (c_{ou}/c_{fe}ed) • *(Qou/Qreed),* over operating time, *t,* are shown in Figure 3 (raffinate), Figure 4 (product), and Figure 5 (spent organic phase).

Despite a slight increasing trend of some metals' concentrations in the spent organic phase (Figure 5), the test has practically reached steady state. Mass balances determined from the last sampling are between 89 % and 112 % (americium, 90 %).

Taking a look at Figure 3, less than 0.1 % of americium is found in the raffinate, meeting the required performance of a DIAMEX process. The lanthanides are extracted according to their atomic number, with the lighter lanthanides being better-extracted. Lanthanum behaves similar to neodymium. Yttrium is only slightly extracted. The other fission products go practically quantitatively to the raffinate, and hence are not shown in Figure 3. No uranium is found in the raffinate.

The product composition (Figure 4) reveals that the unwanted co-extraction of zirconium and palladium is effectively suppressed by the addition of oxalic acid and HEDTA, to approx. 0.01 % and 0.02 %, respectively. Molybdenum co-extraction is approx. 0.25 %. The effectivity of the scrubbing sections is expressed by the low contents of other fission products, being 0.1 % or well below, with the exception of ruthenium (1 %) and silver (0.25 %). Some 10 % of yttrium go to the product. Behaving similar to the lanthanides, it can be separated in a SANEX process. As uranium is extremly well-extracted by DMDOHEMA, only 30 % are found in the product, due to incomplete stripping under the experimental conditions selected.

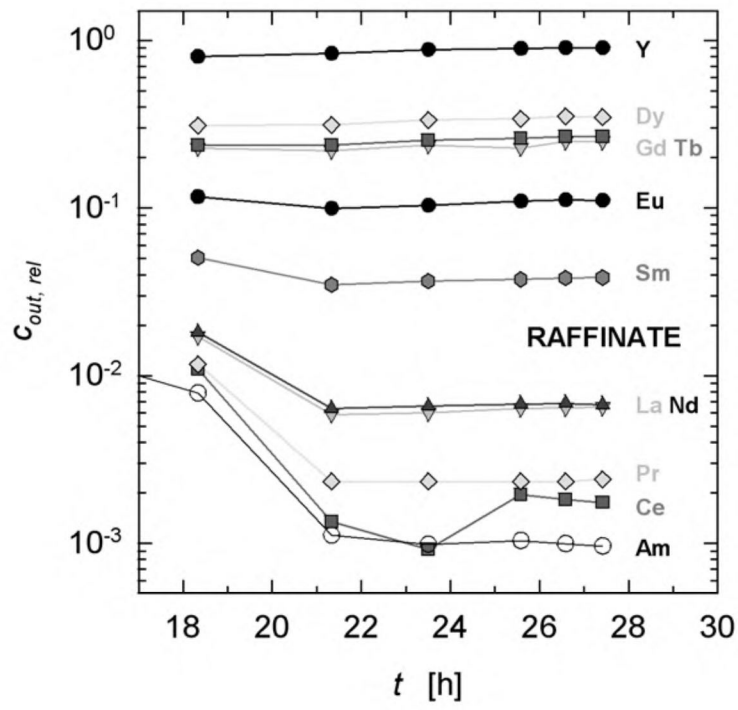


Figure 3. Relative transient raffinate concentrations (non-lanthanide FP omitted for clarity).

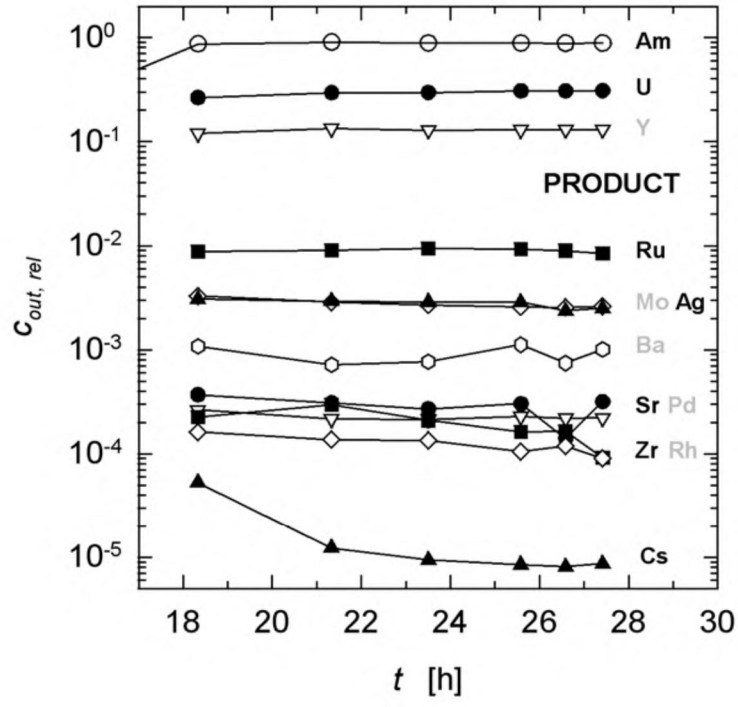


Figure 4. Relative transient product concentrations (lanthanide FP omitted for clarity).

Stripping performance is shown in Figure 5. 1.6 % of americium and 1.5-2.2 % of the lanthanides remain in the organic phase (other lanthanides fall in between Ce and Dy and hence are not shown). Furthermore, approx. 9 % of ruthenium and 1 % of palladium remain in the organic phase. This is a sign for accumulation in the organic phase. Approx. 70 % of uranium stays in the spent organic phase. All other metals are below 0.1 %, and hence not shown.

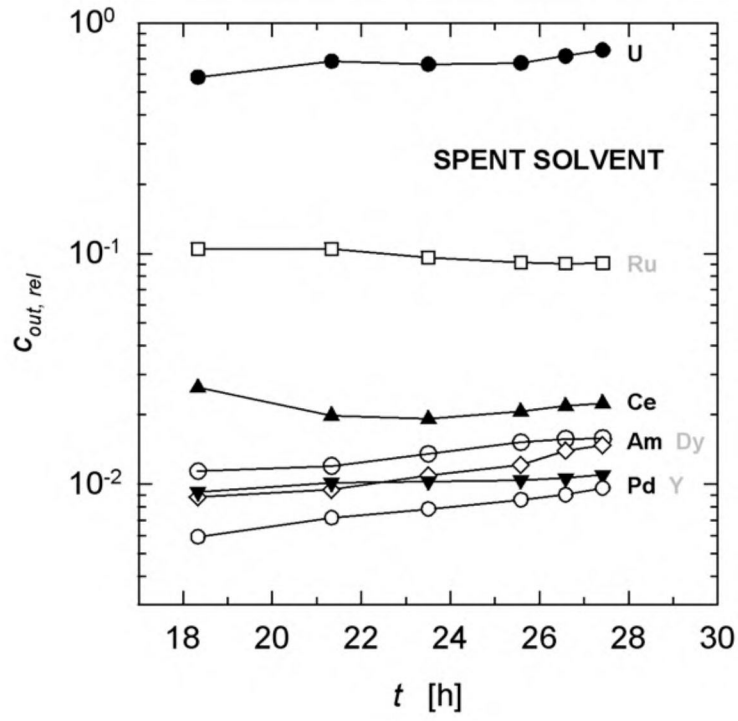


Figure 5. Relative transient concentrations of some metals in spent organic phase.

These results are in good agreement with those from a centrifugal contactor DIAMEX test using real highly active PUREX raffinate [8], The major difference is that somewhat better extraction and stripping efficiencies were achieved in [8], However, slightly reducing the flow rates in the HFM micro-plant should yield similar results.

CONCLUSIONS

A successful DIAMEX process was performed in the HFM micro-plant. The aim of the test, i.e., to have less than 0.1 % of americium in the raffinate and to generate a very pure actinide(lll)-lanthanide product, was achieved. The product should be suitable for direct use as a SAN EX feed.

To achieve americium and lanthanides stripping efficiency of 99.9 %, the organic phase flow rate must be reduced to approx. 0.5 mL/h, according to mass transfer calculations. In a full process, ruthenium would have to be removed from the organic phase in a solvent regeneration section. Furthermore, care has to be taken of uranium, to quantitatively direct it to one effluent.

Actinide partitioning is in line with ISEC 2005's theme, „SX for sustainable development": Liquid-liquid extraction is applied to optimise radioactive waste management, contributing to the sustainability of electric power generation by nuclear fission [11],

ACKNOWLEDGEMENT

The authors are grateful for the financial support from the Commission of the European Community (project EUROPART, contract FI6W-CT-2003-508854).

REFERENCES

1. *Actinide and Fission Product Partitioning and Transmutation, Status and Assessment Report,* OECD Nuclear Energy Agency, Paris (1999).
2. A. Geist, M. Weigl, U. Müllich and K. Gompper (2002), *Proc. Int. Solvent Extr. Conf. (ISEC 2002),* March 18-21, 2002, Cape Town, South Africa, pp. 693-698.
3. A. Geist, M. Weigl and K. Gompper (2002), Sep. *Sci. Techno!.,* 37 (15), 3369-3390.
4. G.W. Stevens and H.R.C. Pratt (2000), *Solvent Extr. Ion Exch.,* 18 (6), 1051-1078.
5 A. Geist, M. Weigl and K. Gompper (2005), *Radiochim. Acta* (in press).
6. C. Madic, M.J. Hudson, J.O. Liljenzin, J.P. Glatz, R. Nannicini, A. Facchini, Z. Kolarik and R. Odoj (2000), *New Partitioning Techniques for Minor Actinides.* EUR 19149 EN, European Commission, Luxembourg.
7. R. Malmbeck, O. Courson, G. Pagliosa, K. Romer, B. Satmark, J.-P. Glatz and P. Baron (2000), *Radiochim. Acta,* 88, 865-871.
8. D. Serrano-Purroy, B. Christiansen, R. Malmbeck, J.-P. Glatz and P. Baron (2003), *Proc. Int. Conf. GLOBAL 2003,* November 16-20, 2003, New Orleans, U.S.A., p. 1920-1925.
9. C. Musikas and H. Hubert (1987), *Solvent Extr. Ion Exch.,* 5 (5), 877-893.
10. A. Geist, M. Weigl and K. Gompper (2003), *Proc. Int. Workshop on P&T and ADS Development,* October 6-8, 2003, SCK-CEN, Mol, Belgium (Proceedings on CD).
11. *Nuclear Energy in a Sustainable Development Perspective,* OECD Nuclear Energy Agency, Paris (2000).



ALTERNATE EXTRACTANT FOR REPROCESSING OF SPENT POWER REACTOR FUELS: COMPUTER SIMULATION OF DI-SUBSTITUTED AMIDE BASED FLOWSHEET WITH NONREDUCTIVE TOTAL PARTITIONING BY INDIGENOUS COMPUTER CODE *SIMPUREXAE*

Shekhar Kumar*, Rajnish Kumar and Sudhir B. Koganti

Reprocessing R&D Division, Reprocessing Group
Indira Gandhi Centre for Atomic Research, Kalpakkam 603102, India
'Corresponding Author: shekhar@igcar.ernet.in

Reported French experimental run of aqueous reprocessing of 1% Pu Feed (~250 g/L U+2.5 g/L Pu) with 1 M DOHA solvent in mixers-settlers was simulated with indigenous computer code *SIMPUREXAE* and simulated results for given end points were compared with the reported values. Considering the lack of adequate distribution and physical property data, a good agreement between reported experimental values and simulated results was observed. A satisfactory non-reductive partition between uranium and plutonium was observed from simulated as well as reported experimental results.

INTRODUCTION

Although TBP has now more than fifty years of official association to solvent extraction from the time of publication of classical paper ofWarf [1] in 1949 and is being prompted as solvent in modern variants of PUREX process like Superpurex [2], Advancedpurex [3], UREX [4] etc., it has two main drawbacks- lack of complete incinerability and notably high solubility in aqueous salt solutions. The first drawback results in complicated handing in the waste management operations. The second drawback necessitates use of a diluent wash contactor before the dilute aqueous solution could be concentrated by means of evaporation, otherwise, TBP, dissolved in aqueous solutions, may react violently with the nitrates and nitric acid, if heated beyond initiation temperature [5-8], Thus, the alternate solvent must posses these two qualities- ability for complete incineration and possible lowest aqueous solubility in addition to the requirements of high stability to chemical and radiolytic attack, favourable transport properties, and moderate distribution coefficients to enable ease of extraction as well as stripping. Its degradation products should not interfere in the solvent extraction operation and should be easily separable.

Pursuit of alternate extractant for PUREX process led to several options - modifications in the TBP molecule itself (by selectively changing its constituent alkane groups) as well as several other classes of compounds. However for PUREX active feed compositions, many of the proposed replacements could not be successful. It is worthy to note that amides were proposed as alternate solvents as early as 1960 [9,10], There was no proper followup, and feasibility of amides as an alternate to TBP was re-established only in late 1980 [11-14],

Detailed studies indicated that amides have radiation damage similar or slightly higher than TBP [11,12], The main advantage with the amides is facilitation of complete incineration of waste solvent. In the case of TBP, incineration is not complete as phosphate constituent of TBP can not be burned and it is converted to polymeric phosphate species. During hydrocarbon pyrolysis experiments, using a tri-ethyl phosphite precursor and steam at 1000 K (it resulted in *in-situ* formation of phosphate), Kumar [15] reported formation of stable phosphate polymers a part of which could be leached by aqueous condensate. Therefore pyrolysis of TBP containing waste solvent is not desirable.

Another major impact of amides as an alternate solvent is the ability to selectively extract the desired actinide. By suitably tailoring the constituent chain, it is possible to focus on extraction of U(VI)-Pu(IV). Tachimori and coworkers [16-17] discovered the amazing nature of TODGA in extracting almost all the actinides of primary and secondary importance in fuel reprocessing. Another main feature of amide based reprocessing flowsheet, for power reactor fuels, is the simplified process for separation of uranium and plutonium. Unlike usual TBP based process, there is no need to reduce Pu(IV) to Pu(lll) for partitioning. By properly selecting solvent, it is feasible to facilitate partition just by changing the strip acidity. Pu(IV) can be selectively stripped (quantitatively ~100%) from a loaded solvent stream containing U(VI) and Pu(IV) by a moderately dilute acid strip, whereas U(VI) is stripped by a conventional 0.01 N acid strip. The simplicity in the process is reflected in lower amount of active waste generation, avoiding extraneous addition of energetic chemicals like hydrazine, simplified plant design and lower capital and operating costs.

The constraints of 21st century call for following four objectives. These are: highest possible recovery of designated actinides and fission products in a readily suitable form for recycle to reactor and contemporary transmutation systems, in addition to lowest possible release to the environment as well as effective cost-cutting derived from simple plant design and simpler technology implementation. It appears quite feasible that use of amides as solvent and centrifugal contactor based plant will certainly help in delivering the desirables provided process safety features are proved at plant scale trials.

In this study, reported amide (DOHA) based extraction run for 250 g/L U+2.5 g/L Pu (1% Pu) feed has been computer simulated with indigenous computer code *SIMPUREXAE.* Reported end results and simulated values are compared in this study.

SIMPUREXAE is a recently developed code at RR&DD, RpG, IGCAR for evaluation of PUREX and THOREX flowsheets based on new and emerging extractants. Exhaustive details of *SIMPUREXAE* or its constituent models have not been published.

DISCUSSION

Distribution equilibria

Regarding PUREX distribution equilibria in DOHA containing systems, limited information is available for the U(VI), Pu(IV) and nitric acid solutes[14]. The solvates with U(VI), Pu(IV) and nitric acid are assumed as $U0_2(N0_3)_2.2A$, $Pu(N0_3)_4.2A$ and $HN0_3.A$ respectively, where A is the amide molecule (DOHA).

Assumptions used for the simulation

Since there is no information about the organic densities in the DOHA based system, authors have tried to take the equivalent TBP system for the organic densities. For DOHA based solvent (C5Hi-|-CON(C_8H-i7)$_2$ or $C_{22}H_{45}ON$, MW=339, p ~0.863 kg/L from the literature data[11]) the equivalent percentage of TBP solvent can be calculated as follows:

$$100\%\text{DOHA} = 1000 * \frac{A_{\text{DOHA}}}{MW_{\text{DOHA}}} \text{ mol/L} = 2.545 \text{ mol/L} \quad (1)$$

Thus, for 1.0 M DOHA equivalent, the corresponding TBP concentration is 1.434 M (~39.29% v/v). The corresponding density of unloaded and dry 1M DOHA solvent will be about 0.792 kg/L against 0.835 kg/L for unloaded and dry 39% TBP solvent. If density equivalent alone is considered then equivalent TBP percentage is about 20% only. In these calculations, diluent is assumed as n-dodecane. In addition, applicability of a linear mixing rule is assumed. For the purpose of computer simulation, organic densities were assumed to be similar to that in 30% TBP system as apparent partial molal volumes for DOHA/n-dodecane system were not available. This assumption will introduce some error as amount of water extracted by TBP and DOHA will not be same at different solute concentrations in the organic phase. In addition, 100% stage efficiency for all the solvent extraction stages was assumed and no non-ideal effects like entrainment or solubility related other-phase carry-over were considered. It is to be noted that Musikas and Germain [14] had stated that partition battery operated at lower efficiency where as in computer simulation 100% efficiency has been assumed.

Simulation of the 1% Pu feed flowsheet

The schematic of the reported run [14] is shown in Fig. 1. The computer simulation was done by running SIMPUREXAE with amide dataset (DOHA subset) on a contemporary PC in Lahey FORTRAN-77 compiler. Fig.2 shows simulated stage profiles for U(VI) and Pu(IV) in the entire cascade. The simulated results have been compared with the reported end concentrations in the Table 1. Considering the sparse data for DOHA solvent and the constraints explained above, the agreement is quite good.

Probable problems with amides as an extractant

Use of amide as a solvent in nuclear fuel reprocessing is not absolutely free of problem. As mentioned above, the radiolytic degradation of the amides in presence of nitric acid is of the same order or slightly higher than TBP. Radiolytic degradation products of amides are generally soluble in water. Thermal stability of dissolved amide is a problem in presence of nitric acid at elevated temperatures. For solvent management by distillation route, it is required to strip the extracted acid completely. In addition, like TBP system, prior to the raffinate concentration by evaporation, removal of dissolved traces of amides is essential.

Table 1. *Comparison of simulated results and reported end concentrations.*

Parameter		Reported value g/L	Simulated Value** g/L
Loaded Organic HAP	U	81.7	79.0960
	Pu	0.805	0.7782
Raffinate waste HAW	U	0.0269*	$<10^{8}$
	Pu	0.0024*	<10®
Stripped Pu product HBXP*	U	0.5009*	0.0311
	Pu	1.2739*	1.3269
Stripped U product HOP	U	89.6476*	87.0975
	Pu	0.0378*	<10®

*Based on the given loss/recovery data.

** Assumed 100% stage efficiency and no non-ideal effects.

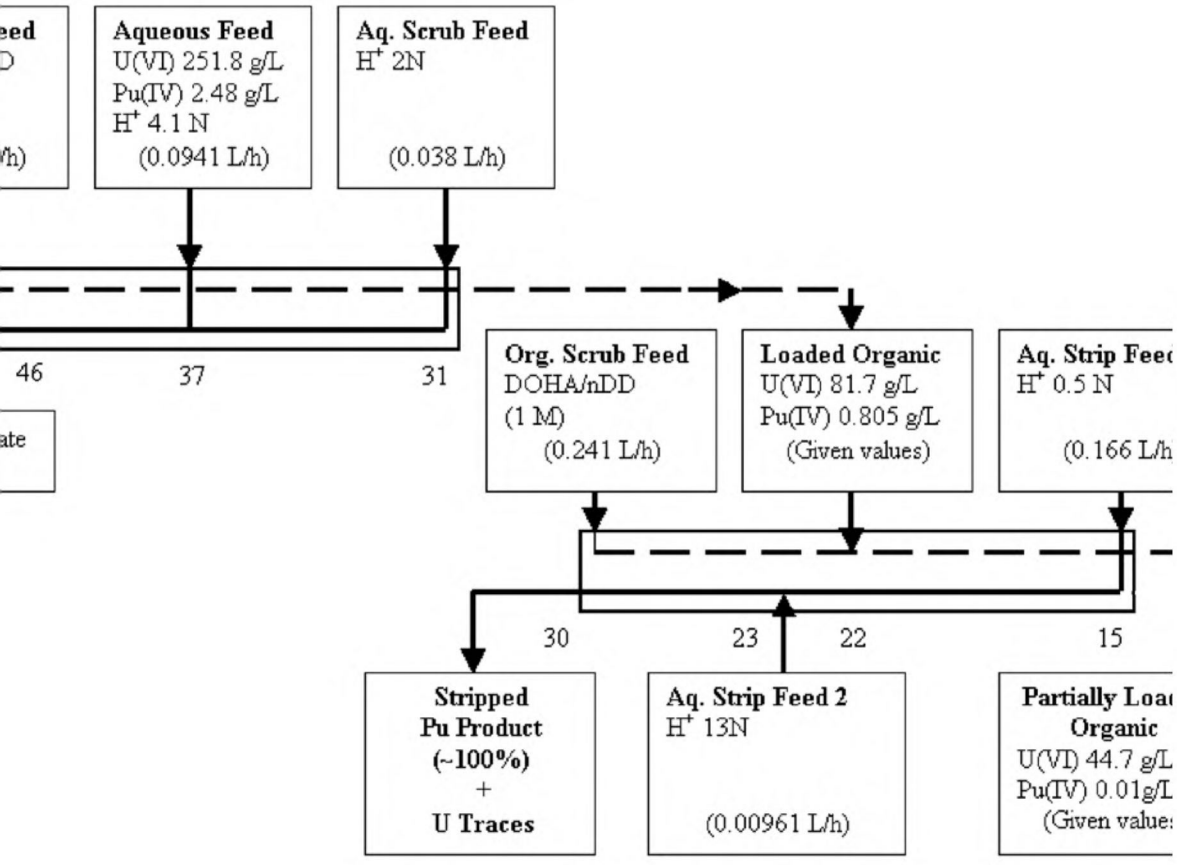


Figure 1. Schematic of experimental run (reported by Musikas and Germain, 1988), based < solvent and 1% Pu HAF compositions. For predicted product concentrations, pleast

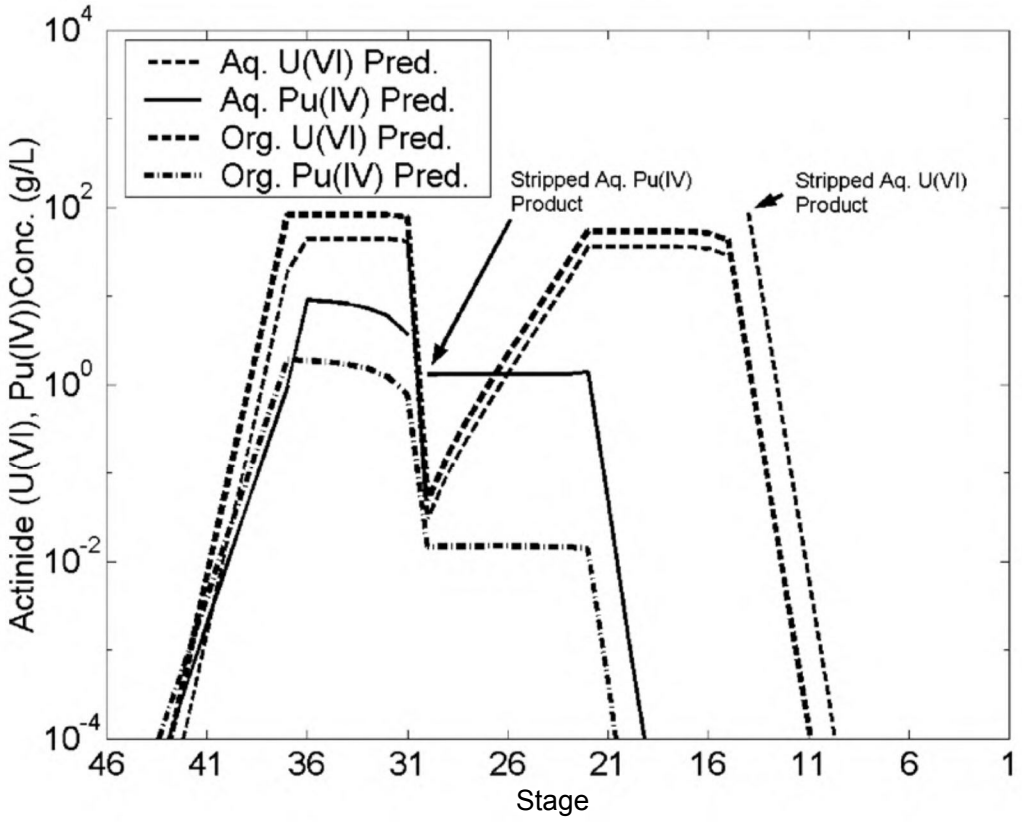


Figure 2. Predicted stage profiles (Simulated by SIMPUREXAE, VI.02, 2003) for U(VI) and Pu(IV) for the schematic shown in Fig. 1

CONCLUSIONS

Reported French experimental run of 1% Pu Feed (~250 g/L U+2.5 g/L Pu) with 1 M DOHA solvent in mixer-settlers was simulated with indigenous computer code *SIMPUREXAE* and simulated results of the product streams were compared with the reported values. Considering the lack of adequate distribution and physical property data, a good agreement between reported experimental values and simulated results was observed. A satisfactory non-reductive partition between uranium and plutonium was observed from simulated as well as reported experimental results. A significant simplification in the process flowsheet and plant design is feasible provided use of amide as an alternate solvent is proved at plant scale and necessary safety issues related to waste management are dealt with.

REFERENCES

1. J. C. Warf (1949), *J. Am. Chem. Soc.,* 71, 3257.
2. B. Ya. Zilberman, S. Yu. Fedorov, E. N. Mishin, L. V. Sytnik, O. V. Shimdt, D. N. Kukharev, N. D. Goletsky, R. G. Glekov, Yu. V. Palenik, and S. Yu. Sukhareva (2002) *Technical Report JAERI-Conf 2002-004*, Japan Atomic Energy Research Institute,

Ibaraki-ken Japan, pp 189-196.

3. R. J. Taylor (2000) *[Internet] Available from:* <http://www.bnes.org.uk/Reprocessing.pdf>.[Accessed 31 July 2003],
4. Advanced Accelerator Applications (AAA) *Quarterly Report for Oct-Dec 2001 (LA-UR-02-0724),* 31st Jan. 2002, Document No. *AAA-PDO-GEN-02-0005* (2002).
5. R. M. Wagner (1953) *Technical Report HA-27492,* Hanford Atomic Products Company, USA.
6. M. L. Hyder (1994) *Technical Report WSRC-TR-94-059,* Westinghouse Savannah River Company, Aiken, South Carolina.
7. M. L. Hyder (1995) *Technical Report WSRC-RP-95-259,* Westinghouse Savannah River Company, Aiken, South Carolina.
8. M. L. Hyder.(1996). *Nuclear Technol.,* 116, 327-333.
9. T. H. Siddall III. (1960) *J. Phys. Chem.* 64, 1863-1866.
10. T. H. Siddall III. (1961) *Technical Report DP-541*. El. Du Pont Nemours & Co. USA.
11. G. M. Gaspirani, and G. Grossi (1980), Application of N,N-Dialkyl Aliphatic Amides in the Separation of Some Actinides. *Sep. Sci. Technol.* 15(4), 825-844
12. G. M. Gaspirani, and G. Grossi. (1986). *Solv. Extr. Ion Exch.*. 4(6), 1233-1271.
13. C. Musikas and H. Hubert. (1983). *Proc. International Solvent Extraction Conference 1983 (ISEC'83).* date . Denver, 449.
14. C. Musikas and M. Germain. (1988). *Proc. International Solvent Extraction Conference 1988 (ISEC'88),* July 18-24, 1988, Moscow, USSR, Vol.IV, 124-128.
15. S. Kumar. (1999). *I&EC Research,* 38 (4), 1364-1368.
16. S. Tachimori. (2001) *Technical Report JAERI-Research 2001-048,* Japan Atomic Energy Research Institute, Ibaraki-ken Japan.
17. S. Tachimori, Y. Sasaki, Y. Morita, and S. Suzuki. (2003) Development of Amide-Based ARTIST Process. *[Internet]available from:* *<http://www.nea.fr/html/pt/docs/iem/jeju02/session2/SessionII-17.pdf>, [Accessed 28nd January 2004],*



FBR MOX FUEL REPROCESSING: II. COMPUTER SIMULATION OF MILLI EXPERIMENTS (REPROCESSING OF 70%$U0_2$+30%$Pu0_2$ DOUNREAY AND KNK FUELS) BY INDIGENOUS COMPUTER CODE *SIMPSEX*

Shekhar Kumar* and Sudhir B. Koganti

Reprocessing R&D Division, Reprocessing Group
Indira Gandhi Centre for Atomic Research, Kalpakkam 603102, India
'Corresponding Author: shekhar@igcar.ernet.in

German researchers had reported reprocessing of highly irradiated Dounreay and KNK-II fuels (Pu/(U+Pu) ratio=0.30) in MILLI pilot plant by a 30% TBP based flowsheet. They conducted extraction (with a mixed feed of Pu/(U+Pu) ratio -0.10) and U(IV) based partitioning. In this study, externally generated U(IV) based partitioning runs were computer simulated using the indigenously developed computer code SIMPSEX and simulated stage profiles were compared with the reported stage profiles. A good agreement was observed. These FBR flowsheets serve as benchmark for computer simulation of active reprocessing campaigns.

INTRODUCTION

German researchers had designed a shielded small experimental facility MILLI for alpha-active experiments on reprocessing of LWR and FBR fuels [1], The MILLI facility had a tentative capacity of 1 kg/day. It housed several mixer-settlers to conduct experiments in the various cycle configurations. Ochsenfeld et al. [2] reported a small-scale three-cycle reprocessing operation to reprocess highly irradiated Dounreay Fast Reactor MOX fuel with Pu/(U+Pu) ratio of 0.15 and burnup up to 61 GWd/t. The ^{235}U enrichment was 60% initially. Later Ochsenfeld et al. [3] reported dissolution of following MOX fuels with Pu/(U+Pu) ratio=0.30 - Rapsodie BM-15 (BU~ 93,000 MWD/t), Rapsodie AU-22 (BU~ 95,000 MWD/t), DFR 455 1A59/1A61/8A5/MILLI (BU~ 40,000-54,000 MWD/t). Linear heat ratings were between 355-480 W/cm. These fuels were fabricated via mechanical mixing of MOX route. During dissolution, these MOX fuel dissolved in boiling $HN0_3$ solution of concentration 10 mol/L and a residue of typically <5% (w/w) was left undissolved. Ochsenfeld *et al. [3]* had reported reprocessing of highly irradiated Dounreay fuel (Pu/(U+Pu) ratio=0.30) in MILLI pilot plant by a 30% TBP based flowsheet. They conducted 1st cycle extraction (with a mixed feed of Pu/(U+Pu) ratio ~ 0.10) and U(IV) based partitioning (externally generated U(IV) based run as well as electrochemically *in-situ* generated U(IV) based run). Later Bleyl *et al [4,5]* reported reprocessing of irradiated KNK-II fuel (Pu/(U+Pu) ratio=0.30) in MILLI pilot plant by a 30% TBP based flowsheet. They reported extraction (with a mixed feed of Pu/(U+Pu) ratio ~ 0.10) and U(IV) based partitioning.

SIMPSEX (SIMulation Program for Solvent Extraction) is an indigenous computer code for simulation of Pu-rich FBR fuel reprocessing flowsheet, which was developed by authors. Its benchmarking with various published flowsheets was recently discussed by authors [6,7],

DISCUSSION

In the present study, following four case studies are discussed-

I. HA extraction flowsheet for DFR (Pu/(U+Pu) ratio =0.3) fuel.
II. HBX partitioning flowsheet for DFR (Pu/(U+Pu) ratio =0.3) fuel.
III. HA extraction flowsheet for KNK-II (Pu/(U+Pu) ratio =0.3) fuel.
IV. HBX partitioning flowsheet for KNK-II (Pu/(U+Pu) ratio =0.3) fuel.

Case studies related to partitioning (II and IV) are based on external generation of U(IV) - the plutonium reductant.

Case Study I: 30%TBP Based Extraction Flowsheet for 10%Pu Feed Composition (HAF: U+Pu = 226/L, **Pu =20.8 g/L and O/A ~ 2.5)**

This run was reported by Ochsenfeld *et al.[3].* The feed for the extraction run was prepared by mixing several fuels of different Pu/(U+Pu) ratios and burn up to have a post-dissolution Pu/(U+Pu) ratio of 9.2% as shown in Fig. 1. The corresponding flowsheet is shown in Fig.2. For this case study, SIMPSEX simulations were performed. The reported experimental values and SIMPSEX values have been compared in Fig. 3 for U(VI), Fig.4 for Pu(IV) profiles and Fig.5 for nitric acid profiles. The agreement between reported experimental results and SIMPSEX simulated values was satisfactory. For simulation, stage efficiency of 100% is assumed whereas in the actual experimental run it was estimated to be 80-85%.

Case Study II: 30%TBP and Externally Generated U(IV) Based Partitioning flowsheet for 11%Pu Feed Composition (1BF: U+Pu = 88.5 g/L, Pu =9.5 g/L)

This run was reported by Ochsenfeld *et al [3],* The corresponding flowsheet is shown in Fig.6. For this benchmark, SIMPSEX simulations were performed. The reported experimental values and SIMPSEX values have been compared in Fig. 7 for U(VI), Pu(IV) and nitric acid profiles. Following is observed from the comparison-

- Predicted uranium (aqueous and organic) profiles in Fig.7 are in excellent agreement with reported experimental results in the stages 1-8 (macro level uranium concentration). In stages 9-16 (trace level uranium concentration), the code predicts uranium concentrations several order less than the reported values.
- Predicted aqueous plutonium profile in Fig.7 is in excellent agreement with reported experimental results in the stages 9-16 (macro level plutonium concentration). In stages 1-8 (trace level plutonium concentration), the code predicts plutonium concentrations less than the reported values.
- Predicted organic plutonium profile from the code is less than the reported values. The plausible reason is presence of Tc in the system, which causes destruction of holding reactant hydrazine. At present code does not account for this reaction and related parasitic reactions. As a consequence to parasitic reactions, significant re-oxidation of Pu(lll) to Pu(IV) is observed. Formed Pu(IV) is extracted by the organic phase.
- Overall balance for uranium and plutonium is quite satisfactory.
- DFy was reported in the range of 100-350. Thus for acceptable separation of plutonium product from uranium, an additional step would be required.

On considering the limitation of simulation and available information, the agreement between reported experimental results and SIMPSEX simulated values was satisfactory.

Case Study III: 30%TBP Based Extraction Flowsheet for 11%Pu Feed Composition (HAF: U+Pu = 250/L, Pu =27.5 g/L, Activity 27 Ci/L and O/A = 3)

This run was reported by Bleyl *et al.[4,5].* The feed was prepared by dissolving irradiated KNK-ll/1 inner-core zone element fuel (Pu/(U+Pu) ratio=30%) with a tentative burn up of 11.7 GWd/t (cooled for 25 months). The HAF activity level was stated to be 27 Ci/L. The corresponding flowsheet is shown in Fig. 8. The reported experimental values and SIMPSEX simulated values have been compared in Fig.9 for Pu(IV) profiles. The agreement between reported experimental results and SIMPSEX simulated values was excellent.

Case ***Study IV: 30%TBP and Externally Generated U(IV) Based Partitioning flowsheet for 11%Pu Feed Composition (1BF: U+Pu = 88.5 g/L, Pu =9.5 g/L***

This run was reported by Bleyl *et al.[4,5].* This run was similar to one reported earlier in the case study II. The corresponding flowsheet is shown in Fig.10. For this benchmark, SIMPSEX simulations were performed. The reported experimental values and SIMPSEX values have been compared in Fig.11 for U(VI), Pu(IV) and in Fig.12 for aqueous nitric acid and hydrazine profiles. Following is observed from the comparison-

- Predicted uranium (aqueous and organic) profiles in Fig.11 are in excellent agreement with reported experimental results in the stages 1-9 (macro level uranium concentration). In stages 10-16 (trace level uranium concentration), the code predicts uranium concentrations several order less than the reported values.
- Predicted aqueous plutonium profile in Fig. 11 is in excellent agreement with reported experimental results in the stages 9-16 (macro level plutonium concentration). In stages 1-8 (trace level plutonium concentration), the code predicts plutonium concentrations less than the reported values.
- Predicted organic plutonium profile from the code is less than the reported values. The plausible reason is presence of Tc in the system, which causes destruction of holding reactant hydrazine. At present code does not account for this reaction and related parasitic reactions. As a consequence to parasitic reactions, significant re-oxidation of Pu(lll) to Pu(IV) is observed. Formed Pu(IV) is extracted by the organic phase. This hypothesis is confirmed by experimentally observed depletion of hydrazine as shown in Fig.12. The available hydrazine concentration drops to ~0.03 M from 0.2 M at the feed stage. Thus in macro Pu bearing stages, there is no effective hydrazine presence and it results in observed organic Pu concentration (it must be Pu(IV)) as high as 10 g/L at stage 13 indicating severity of oxidation.
- Overall balance for uranium and plutonium is quite satisfactory.
- DFy was reported as 650. Thus for acceptable separation of plutonium product from uranium, an additional step would be required.

CONCLUSIONS

German researchers had reported reprocessing of highly irradiated Dounreay and KNK-II fuels (Pu/(U+Pu) ratio=0.30) in MILLI pilot plant by a 30% TBP based flowsheet. They conducted extraction (with a mixed feed of Pu/(U+Pu) ratio ~ 0.10) and U(IV) based partitioning. In this study, four case studies related to the extraction and externally generated U(IV) based partitioning runs were computer simulated using the indigenously developed computer code SIMPSEX and simulated stage profiles were compared with the reported stage profiles. A good agreement was observed. The successful simulation of partitioning experiments indicates viability of externally generated U(IV) based partitioning for FBR fuel reprocessing flowsheets.

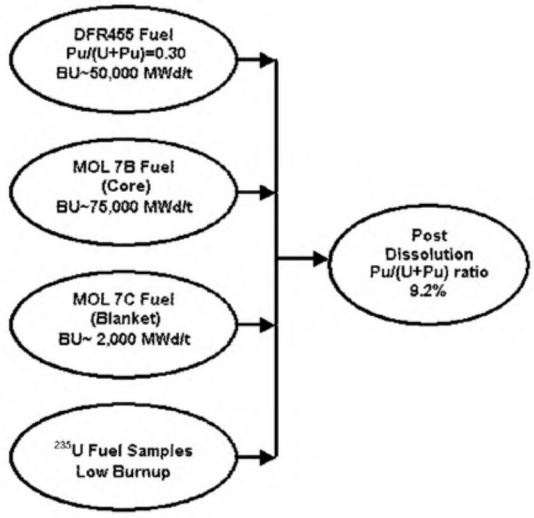


Figure 1. Schematic of Feed preparation for MILLI active experiments of Ochsenfeld et al.[3J.

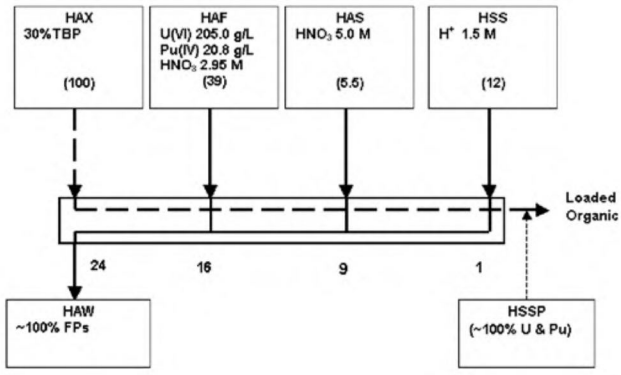


Figure 2. Schematic of active flowsheet run conducted in MILLI[3],

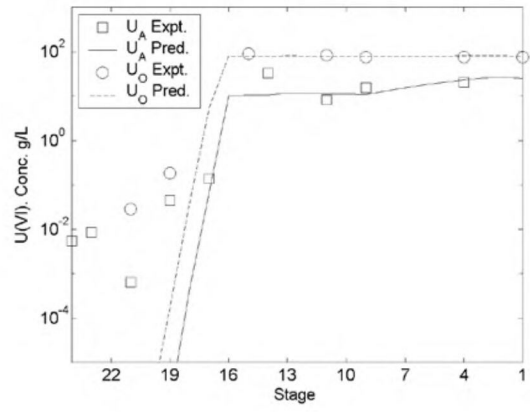


Figure 3. Uranium(VI)stage profiles for the schematic shown in Fig. 2.

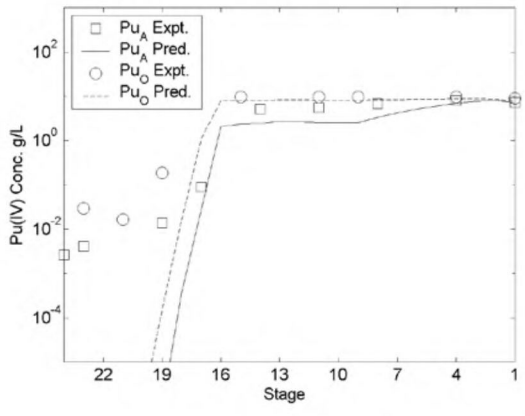


Figure 4. Plutonium stage profiles for the schematic shown in Fig. 2.

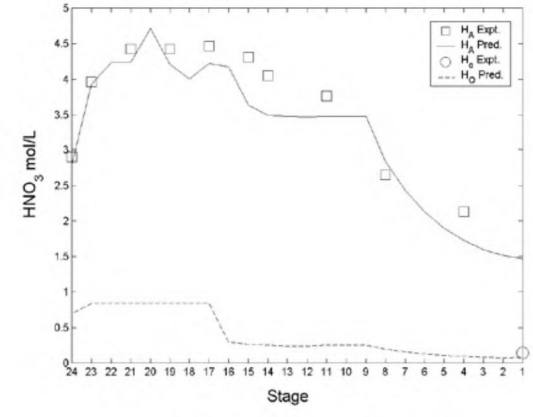


Figure 5. Nitric acid stage profiles for the schematic shown in Fig.2.

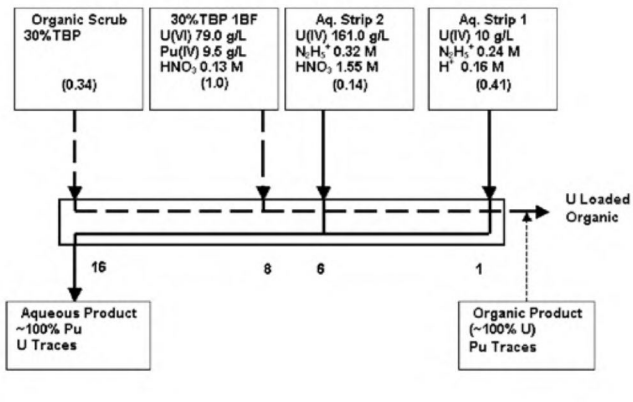


Figure 6. Schematic of active partitioning flowsheet run with externally generated U(IV), conducted in MILLI [3].

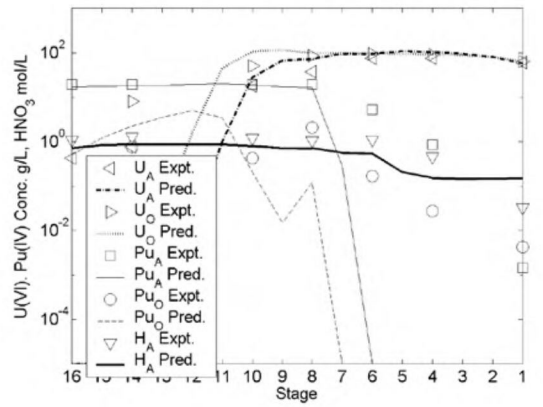


Figure 7. SIMPSEX predicted results for the schematic shown in Fig. 6.

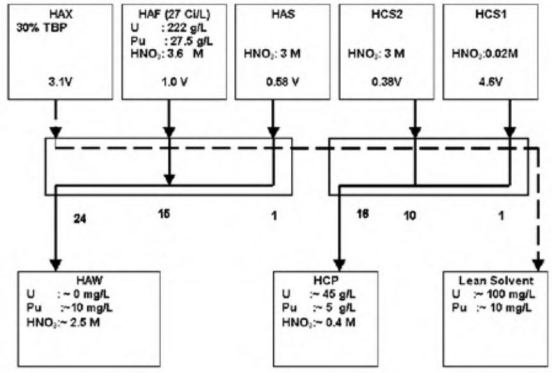


Figure 8. Schematic of KNK-II fuel reprocessing in MILLI [4,5],

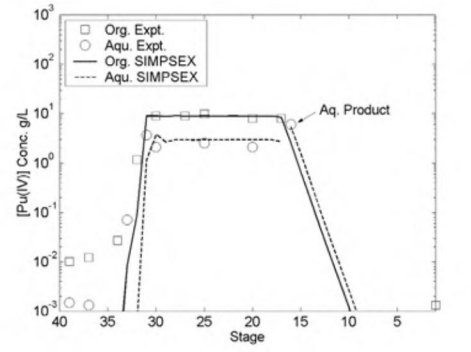


Figure 9. Comparison of reported expt. and SIMPSEX predicted results for the schematic shown in Fig. 8 for Pu(IV).

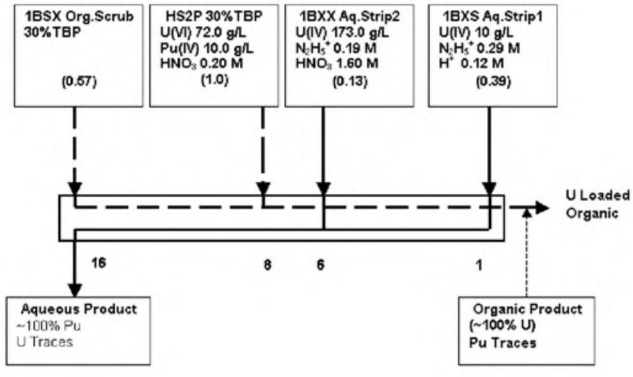


Figure 10. Schematic of active partitioning flowsheet run with externally generated U(IV), conducted in MILLI [4,5].

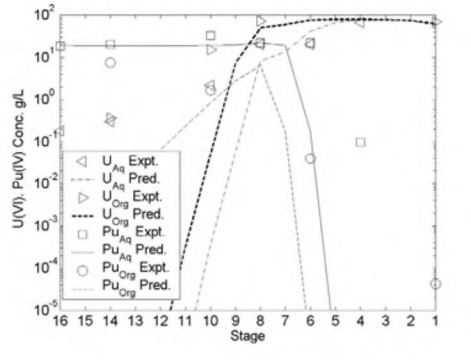


Figure 11. Comparison of reported expt. and SIMPSEX predicted results for the schematic shown in Fig. 10 for uranium and plutonium.

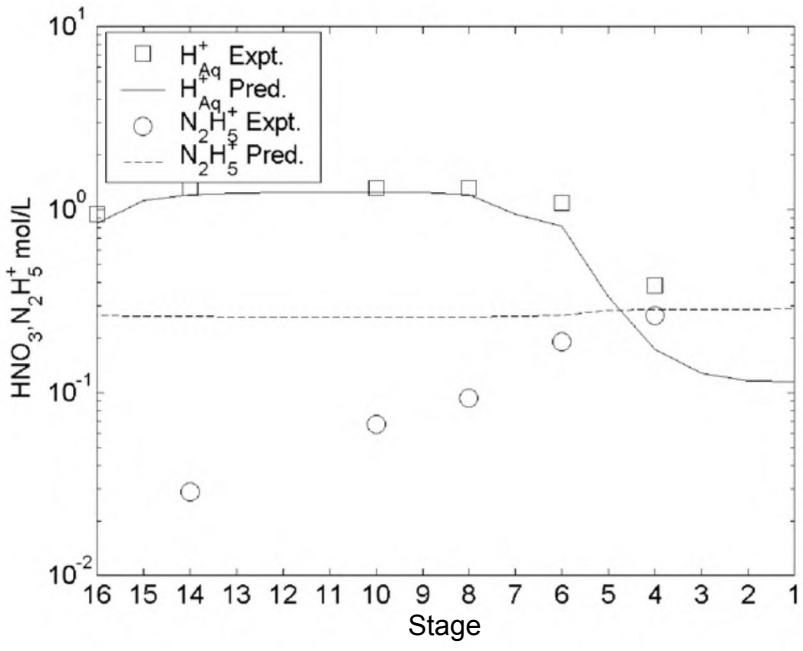


Figure 12. Comparison of reported experimental and SIMPSEX predicted results for the schematic shown in Fig. 10 for nitric acid and hydrazine.

REFERENCES

1. W. Ochsenfeld, F. Baumgartner, U. Bauder, H. J. Bleyl, D. Ertel and G. Koch (1977a), *Proc. International Solvent Extraction Conference 1977 (ISEC-77),* Vol.2, 605.
2. W. Ochsenfeld, F. Baumgartner, U. Bauder, H. J. Bleyl, D. Ertel, G. Koch, and E. Warnecke (1977b) (in German), *Technical Report KFK-2396.* Gesellschaft Fur Kernforschung M.B.H., Karlsruhe.
3. W. Ochsenfeld, H. J. Bleyl, D. Ertel, F. Heil, and G. Petrich (1979), *Proc. Symposium on Fast Reactor Fuel Reprocessing.* Dounreay, 15-18 may 1979, Society of Chemical Industry, London, 1980, 77-91.
4. H. J. Bleyl, K. H. Ebert, D. Ertel, and W. Ochsenfeld (1983), *Proc. International Solvent Extraction Conference (ISEC-83),* Denver USA, August 26-September 2, 1983, 327-328.
5. H. J. Bleyl, W. Ochsenfeld, H. Schmieder, H. O. Haug, D. Ertel, and L. Stieglitz (1984), ANS Int. Tropical Meeting, 26-29 August, 1984, Jackson, Wyoming, USA, Vol.2,2.462-2.469.
6. S. Kumar and S. B. Koganti (2002), *Technical Report IGC-234,* IGCAR,Kalpakkam.
7. S. Kumar and S. B. Koganti (2003), *Technical Report IGC-251*, IGCAR,Kalpakkam.
8. S. Kumar and S. B. Koganti (2004), *Technical Report IGC-257,* IGCAR,Kalpakkam.
9. S. Kumar and S. B. Koganti(2003), *Indian Nuclear Society Annual Conference 2003 (INSAC-2003) on CD,* IGCAR, Kalpakkam, December 17-19, 2003.

EXTENDED SALT EFFECT MODEL *(ESE* MODEL) FOR Th(IV) THIRD PHASE FORMATION IN 1-30%TBP BASED NUCLEAR SOLVENT EXTRACTION SYSTEMS

Shekhar Kumar* and Sudhir B. Koganti

Reprocessing R&D Division, Reprocessing Group
Indira Gandhi Centre for Atomic Research, Kalpakkam 603102, India
Corresponding Author. E-mail: shekhar@igcar.ernet.in

In LLE with mixed organic solvents (or solvent-diluent mixture), due to limited solubility of the extracted solute in one of the solvents (or diluent), the organic phase may split into heavy organic phase ("third Phase") and a "lean phase". Third phase formation is a common phenomenon in the commercial solvent extraction. Third phase formation is dependent on solvent (diluent) and prevailing operational temperature. However due to operational safety reasons, its formation must be prevented in the nuclear solvent extraction. In the present study, authors propose an extended Setschenow model forTh(IV) third phase formation in 1-30%TBP solvent.

INTRODUCTION

The quest for sustainable energy alternatives has made the thorium fuelled nuclear cycle option revitalized. For efficient closing of the fuel cycle, reprocessing of Th based fuels is required. Unfortunately in the conventional THOREX process and its variants (TBP diluted with an aliphatic diluent) the limiting organic concentration of Th(IV) is quite low. Therefore it is important to have an exclusive model for Th(IV) third phase formation in TBP based solvent extraction systems. Integration of the developed model with the solvent extraction codes will make the analysis of process upsets and other problems easier and user-friendly. The third phase formation was discussed in the literature at length and for a comprehensive review, reader is referred to Rao and Kolarik [1], Since third phase arises due to limited solubility of the solvate in the diluent, it is obvious that a solubility model can describe the phenomenon.

The Solubility Model as a Third phase Model

The classical solubility correlation of Setschenow [2] is listed as -

$$\log\left(\frac{S^0}{S}\right) = k_s C_s \qquad (1)$$

Where S° and S are the aqueous solubilities of non-electrolyte in the absence of the salt and in the presence of the salt. k_s is the salting coefficient, now named after Setschenow. C_s is the concentration of the salt. The relationship, shown in Eq. 1, is valid for low salt

concentrations. At higher concentrations, usually a power series in concentration is used. Eq.1 has been related to the theory of salt-effect by Long and McDevit [3] and Gordon [4],

Gordon [4] mentioned that the activity coefficient (y) of a non-electrolyte S, in the presence of an 1:1 electrolyte E (On dissociation, it will yield one univalent cation and one univalent anion) could be represented as-

$$l\text{»}Js = Z\text{^},< + Z\,Z \underset{i=0}{\overset{\infty}{}} \underset{/=0}{\overset{\infty}{}} b_{ij} m_S^i m_E^j \qquad (2)$$

Where *K,* are the Setschenow coefficients; b_n is interaction parameter and m_E and m_s are molal concentrations of electrolyte E and non-electrolyte S respectively. Gordon [4] also mentioned that the effect of presence of other non-electrolytes on the activity coefficient of the non-electrolyte could be correlated in form of a power series. The use of the molal scale of concentration is not very convenient; therefore the conventional form of the Setschenow equation is expressed in terms of molar concentrations. Thus Eq. 2 is rewritten as -

$$logy_s = -Z\,k,C_E^{\,i} + \underset{i=0}{\overset{oO}{}} \underset{7=0}{\overset{oO}{}} ZZ\,w \qquad (3)$$

Where y_s is the activity coefficient of the non-electrolyte S on the molar scale and C_E and C_s are molar concentrations of electrolyte E and non-electrolyte S respectively. As per theoretical considerations, left-hand side of Eq.3 should be taken as /og(y/y°).

On substitution of Eq.3 in Eq.1 with addition of non-linear terms for aqueous salt-effects and limiting of interactions only to second order terms and with *N* electrolytes (extracted or not extracted by organic solvent), The following form of extended Setschenow equation-

$$\log\left(\frac{y}{y^{\circ}}\right) = \log\left(\frac{S}{S^{\circ}}\right) = \sum_{k=1}^{N} Z\,k_y c_l + \left(K + Z\,a_{insolvent}\right) + \sum_{t=i}^{N} ZZ\,hf^{ct} \qquad (4)$$

Where a_0 and 3jS are empirical coefficients. C_{SO}ivent is the molar concentration of extractant (TBP) in the organic solvent. C_k is the molar concentration of k_{th} electrolyte. If a particular electrolytic solute is not extracted into the organic phase, its associated interaction parameter should be set to zero. The Eq.4 is termed as Extended-Salt-Effect Model (ESE-Model). The ESE-model is a general model with universal application to solubility problems. A simpler form was used earlier for third phase formation [5],The model was used to explain aqueous solubility of organic (representative case: Aqueous solubility of TBP in salt solutions and variable diluent content [6]), organic solubility of water (Representative case: organic solubility of water in TBP solutions with variable diluent content in presence of nitric acid [7]), aqueous solubility of gases (representative case: aqueous solubility of Krypton in salt solutions [8]) and extreme cases of third phase formation in nuclear solvent extraction systems (representative cases: Third phase formation in U(IV), Pu(IV), Th(IV) and U(VI) extraction systems [9]).

Application to Th(IV) Third Phase data

Fig. 1 shows an interpolated 3-D surface plot for boundary Th(IV) distribution coefficients in 1-30%TBP solvent. Related data was generated at Chemical Group, IGCAR [10]. The data could be modeled successfully with the ESE-model with good accuracy. Mean and standard deviations for Eq.4 were 0.03% and 2.59% for 41 experimental points of Suresh *et al.[10].* Since for the developed model, standard deviation is 2.59%, 90% of the predicted LOC may be taken as MCE (Most Conservative Estimate) as a boundary organic concentration of Th(IV) safely. Fig.2 shows an interpolated 3-D surface plot of the predicted data for Th(IV)

third phase formation in 1-30%TBP system. Fig.3 shows a parity plot between experimental and predicted LOC values. Where as Fig.4 shows a normal 2D plot of labelled comparison between reported and simulated LOC values. The coefficients of model are listed in Tablel.

The model is expected to be useful in analysis of low TBP (2-5%) based *interim-23* type flowsheets, used for U-233 separation from irradiated thorium.

Temperature dependency of LOC

Limiting organic concentration (LOC) is a strong function of temperature. In general, S° and S will increase with temperature. Limiting value of S will be the theoretical extraction limit of solvent (based on molar concentration of extractant) at a critical temperature (T_c). The extended Setschenow model was modified to take care of temperature dependence of standard solubility and the Setschenow coefficients. The coefficients of Eq. 4 are proposed to have a temperature dependency as follows-

$$\ln\left(\frac{S^{o}(t)}{S}\right) = k_1(1 + CL_2)C_k + (1\ 4\text{-}\ P/)C \quad (5)$$

Where $S°(t)$ could be ideally defined as

$$S°(t) = S°_{Q}\exp\left(-\frac{b_1}{\delta}\right) \quad (6)$$

And

$$5 = T_c\text{-}t \text{ and } b > 0 \text{ for } t < T_c$$
$$and \quad U)$$
$$b = 0 \text{ for } t > T_c$$

These parameters can be evaluated provided related data is available.

CONCLUSIONS

An extended salt-effect model is proposed for Th(IV) third phase formation in 1-30% TBP system. The model was extended for temperature dependency of the third phase LOC. A good comparison between reported experimental and predicted values was observed.

REFERENCES

1. P. R. V. Rao and Z. Kolarik (1996), *Solvent Extr. Ion Exch.,* 14, 955.
2. A. Z. Setschenow (1889), Uber die Konstitution der Salzlosungen auf Grund ihres Verhaltens Kohlensaure. Z. *Physik. Chem.* 4, 117.
3. F. A. Long and W. F. McDevit (1952), Activity Coefficients of Nonelectrolyte Solutes in Aqueous Salt Solutions. *Chem. Rev.* 51, 119.
4. J. E. Gordon (1975), The Organic Chemistry of Electrolyte Solutions, John Wiley & Sons, New York.
5. S. Kumar and S. B. Koganti (1998), *Solvent Extr. Ion Exch.,* 16, 829.
6. S. Kumar and S. B. Koganti (2000), *Nuclear Technol.,* 129, 279-283.

7. S. Kumar and S. B. Koganti (2003), *Technical Report IGC-247,* IGCAR, Kalpakkam.
8. S. Kumar and S. B. Koganti, Unpublished Work.
9. S. Kumar and S. B. Koganti, Unpublished Work.
10. A. Suresh, N. Ojha, C. V. S. B. Rao, T. G. Srinivasan. and P. R. V. Rao (2002), *Proc. International Solvent Extraction Symposium (ISSE-2002),* Bhubaneshwar, 26-27 Sept 2002, 424- 430.

Table 1. Coefficients of Eq.4 for Third Phase Formation Limit in 1-30% Th/TBP Systems.

Coefficient	Parameter-	Value
a_0	-	**2.6105x10°**
a*	[TBP]	**6.6266x1 O'²**
a_2	TTBP1²	**-1.9561x10‘³**
&3	[TBP]³	**-1.4909x10'⁴**
ki i	[Haq]	**5.0963x10'¹**
k_12	[Haq]²	**-3.3820x1 O'²**
ki3	[Haq]³	**5.9197x10⁻⁴**
k2i	$[Th_{aq}]$	**9.2106X10¹**
k22	$[Th_{aq}]^2$	**-1.0780x10°**
k23	$[Th_{aq}]^3$	**2.5327x10¹**
bm	[TBP] $[H_{aq}]$	**-8.8101x10"²**
bi2i	$[TBP]^2$ $[H_{aq}]$	**2.4387x10‘³**
bii2	[TBP] $[H_{aq}]^2$	**4.7559x10⁻³**
bi22	$[TBP]^2$ $[H_{aq}]^2$	**-9.6218x10'⁵**
b2ii	[TBP] $[Th_{aq}]$	**-6.9237x1 O’¹**
b221	$[TBP]^2$ $[Th_{aq}]$	**2.7742x1 O'²**
b212	[TBP] $[Th_{aq}]^2$	**3.7270x10'¹**
b222	$[TBP]^2$ $[Th_{aq}]^2$	**-1,7167x10"²**

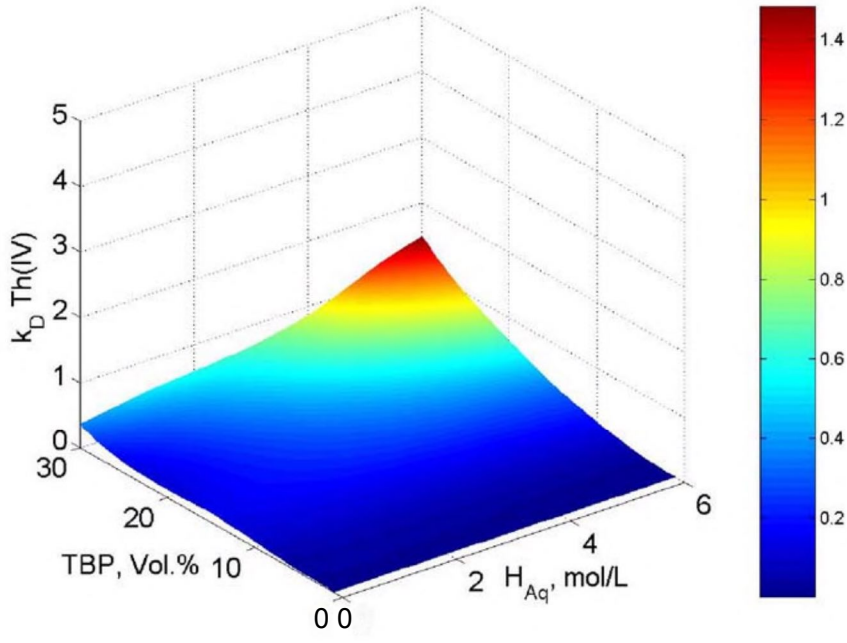


Figure 1. Boundary-line distribution coefficients of Th(IV) in 1-30% TBP Solvent.

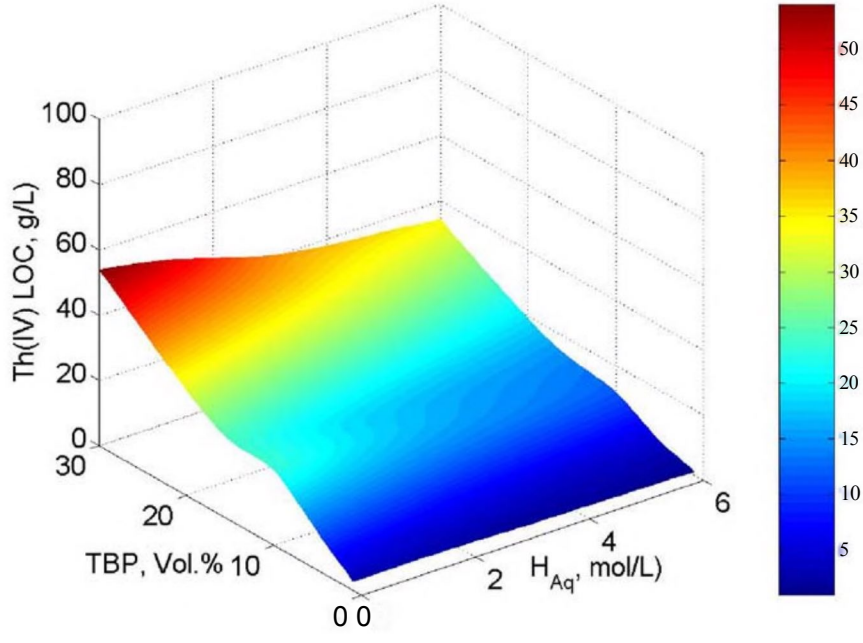


Figure 2. Variation of limiting organic concentration (LOC) for Th(IV) third phase formation in 1-30% TBP Solvent.

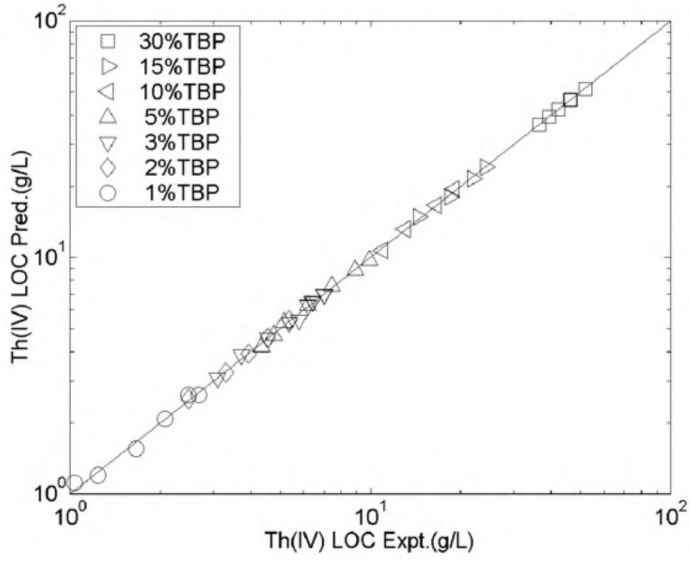


Figure 3. Parity plot for comparison of the Extended Salt-Effect model results and experimental results for Th(IV) third phase formation in 1-30%TBP/Dodecane solvent at 303 K.

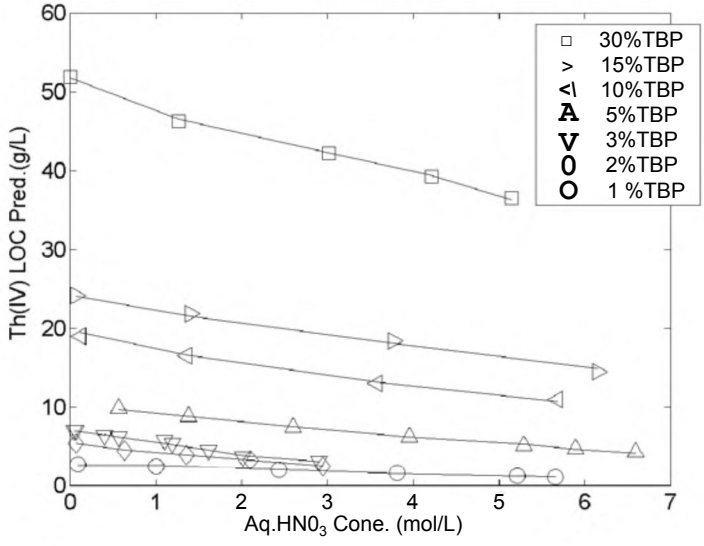


Figure 4. Detailed comparison of the Extended Salt-Effect model results and experimental results for Th(IV) third phase formation in 1-30%TBP/Dodecane solvent at 303 K.



COMPUTER SIMULATION OF REDUCTIVE BACK-EXTRACTION OF MACRO LEVEL PLUTONIUM IN CENTRIFUGAL EXTRACTORS

Shekhar Kumar* and Sudhir B. Koganti

Reprocessing R&D Division, Reprocessing Group
Indira Gandhi Centre for Atomic Research, Kalpakkam 603102, India
'Corresponding Author: shekhar@igcar.ernet.in

Centrifugal extractors are characterised by small stage-residence time. However few experimental results are available for back-extraction of macro Pu in centrifugal extractors. Two such reported experimental runs (HEDL and CEA experiments on reductive stripping of plutonium at macro level) in centrifugal extractors were simulated using an indigenous code SIMPSEX. In this study, computer simulation results will be compared and discussed.

INTRODUCTION

For concentration of dilute streams (e.g., diluted co-stripped actinide bearing streams), evaporation is a favoured choice. However in the case of FBR reprocessing flowsheets, where appreciable amount of plutonium is present, evaporation is not preferred as it results in increased Pu loss due to formation of Pu(IV) polymer, caused by falling of the condensate drops into the Pu bearing solution. PUREX solvent (30% TBP) does not extract Pu(IV) polymer species and in the next solvent extraction cycle, this Pu(IV) polymer will follow the raffinate stream. This problem necessitated a different technology for concentration of dilute Pu streams during solvent extraction in Pu-rich FBR flowsheets.

A remarkable turnaround in the PUREX process based reprocessing technology was caused by the publication of the classic paper by Orth et al.[1], in which, they reported successful implementation of HAS (Hydroxylamine Sulphate) based partitioning. Due to adverse implications of sulphate in the reprocessing streams, SRP operations switched over to HAN [1] (Hydroxylamine Nitrate). Another turnaround in the PUREX process based reprocessing technology was caused by the publication of the classic paper by Patigny et al.[2], in which, they reported concentration by means of reductive solvent extraction. Dilute Pu solutions (2 g/L Pu and 8 g/L) were extracted by 30% TBP at fractional O/A and then stripped by a strip feed containing 0.2-0.3 M HAN, 0.1 M hydrazine and 0.1 M $HN0_3$, resulting in a concentrated product solution (10 g/L and 32 g/L Pu respectively). In the same conference, Boudry and Miquel [3] described a three-cycle flowsheet for processing 75%U+25%Pu (initial ^{235}U enrichment ~ 60-90%) based Rapsodie fuel with 80 GWd/t burnup, developed at Cyrano Cells and used later at AT-1 plant. In the flowsheet, reported by them, HA cycle operated at O/A of unity where as next two co-decontamination cycles operated at an O/A of 0.5. Therefore diluted feeds to 1A and 2A cycles (U+Pu concentrations of ~34g/L and ~31 g/L respectively) were extracted with 30% TBP to give approximately U+Pu concentrations of 68 g/L and 62 g/L in the respective loaded organic products. In this way, the need for intercycle evaporators and paraphernalia like diluent wash columns at every cycle to remove traces of TBP from stripped mixed aqueous product was completely eliminated. This was a

remarkable achievement.

The current economic reasons push the conventional reprocessing domain towards new horizon. The currently hot technologies like ADVANCEDPUREX [4] and UREX [5] are likely to use compact solvent extraction contactors like annular centrifugal contactors for the new plants and improved disk and doughnut columns in the existing plants as retrofits.

HAN is not extracted by PUREX solvent (30% TBP). Therefore its reducing action towards Pu(IV) is limited to the aqueous phase only. Thus before HAN acts, Pu(IV) must be driven to aqueous phase by controlled acidity and salting. For the same reason, HAN cannot strip Pu from Pu solvate/complexes formed by HDBP and derivatives. Additionally a raised temperature (~ 40° C) and carefully manipulated aqueous acidity are prudent requirement for successful operation.

Baron et al.[7] reported use of centrifugal extractors during reductive plutonium stripping demonstration runs. This was a remarkable achievement in the PUREX process technology as traditionally reductive stripping (or partitioning) was performed either in pulse column or mixer-settlers. Even in the contemporary plant like THORP plant, partitioning is done in a pulse column and following Plutonium cycle also utilizes pulse columns. Mixer settlers are used only in the uranium cycle. Since current emphasis is to reduce active plant hold-up and shielded cell volume, centrifugal extractors are to be/being used in next generation processes like Advanced PUREX and UREX. In this context, results obtained by Baron et al.[7] are important in the respect of feasibility of an entire reprocessing plant based on centrifugal contactors with little plant hold up and several-fold reduction in the shielded cell volume and height.

Recently reported CEA experiments on reductive stripping of plutonium at macro level (feed organic concentration of 33g/L Pu, aqueous product concentration of 47 g/L Pu) in centrifugal extractors were simulated using an indigenous code SIMPSEX. In this study, simulation results of one of the experimental runs with HAN as main reductant and U(IV) as Pu barrier reductant will be compared and discussed.

DISCUSSION

Case I: 30%TBP Based Reductive Partitioning of Pu(IV) at Macro Pu Concentrations in Centrifugal Extractors (Loaded Organic Feed Pu ~ 8.2g/L).
Richardson and Swanson [6] reported this run. In this experimental run, plutonium was reduced with hydrazine stabilized HAN in miniature centrifugal extractors. The main purpose of the study was to ascertain operability under varied conditions. Two sets of experiments were reported. Few of them contained $Fe(N0_3)_3$ and no HAN. Experimental stage profiles were not reported. The schematic is shown in the Fiq.1. As Pu mass balance was excellent (100%) in Run#1, the results of the same are used for comparison. The SIMPSEX simulated end results are compared with the reported experimental end results in Table 1. An excellent agreement is observed.

Case II: 28%TBP Based (30%TBP assumed) Reductive Stripping of Pu(IV) at Macro Pu Concentrations in Centrifugal Extractors (Loaded Organic Feed Pu ~ 33g/L).
Baron et a l. [7] presented results of several experiments of plutonium stripping from loaded organic using HAN as well as U(IV) as the main reductant in the alpha-active facilities of ATALANTE. Their runs had a U(IV) based four- stage Pu barrier, constructed of centrifugal extractors. The centrifugal extractors used by them were of design different from the classical ANL design. Whereas ANL design had a fixed outer cylindrical bowl with feed and collection system and rotating inner bowl, CEA design is based on a cylindrical bowl rotating around a fixed central bowl with feed and collection system. Centrifugal extractor of CEA design had a

mixer chamber volume of 1 ml. and settler chamber volume of 7 ml_. Mixer chamber volume of Pu barrier stages was 3 ml_.

Baron et al.[7] noticed severe Pu reoxidation during the initial runs. They also anticipated that Murphree stage efficiency was about 85% only. Normally single stage centrifugal extractors exhibit typical stage efficiency of about 100%. When they are clubbed to form a cascade, often due to entrainment and other-non-ideal effects, the efficiency drastically comes down to typical 80%-90%.

Authors have taken the reference flowsheet shown in the Fig.7 of Baron et al.[7], a schematic of which is shown in the Fig.2 of this paper. Reported flowsheet test conditions were: no uranium scrubbing, O/A ratio of 1.4, 54°C temperature and an average residence time in the settler of 1.7s. Since SIMPSEX thermodynamic model was limited to 30% TBP, authors assumed 30% TBP as solvent. This assumption has introduced a small error in the simulated results, as listed TBP concentration was 28.2%. In addition, authors assumed 100% stage efficiency for the solvent extraction run.

The Pu product concentration was obtained from the simulation as 46.52 g/L against reported experimental concentration of 46.7 g/L. The simulated aqueous and organic profiles for Pu are compared with reported experimental stage profiles in Fig. 3. The simulated profiles are in excellent agreement with the reported profiles for 7-12 stages or aqueous phase and 8-12 stages for the organic phase. Simulated results predicted extremely low Pu loss in the lean organic stream, whereas in the actual experiment it was 0.5 mg/L. The reasons attributed are assumptions of 100% stage efficiency for calculations (actual estimated stage efficiency of 85%), 30% TBP (28.2%TBP in the experiment) and likely a small aqueous entrainment in the organic phase.

Densities of solutions: Contributions from reductants and Pu(III)
The reductants and holding reductants, not extracted by PUREX solvent, contribute to the density of aqueous phase sub-system only. In contrast, U(IV), the extracting reductant contributes to density of aqueous as well as organic streams equally. At present, the physical property module of SIMPSEX does not account for partial molal volume contributions for U(IV), HAN, ferrous sulphamate or hydrazine nitrate. Thus there is a small error in the predicted densities and volumes during partitioning conditions. Similarly, the presence of macro level of Pu(lll) in the aqueous phase has its' own effect. At present, due to non-availability of data, it is assumed that partial molal volume of Pu(lll) is identical to that of Pu(IV). This assumption works fine in the organic phase due to ultra low distribution coefficients of Pu(lll) in the PUREX partitioning system. However in the macro presence of Pu(lll) (~30-45 g/L) in the aqueous phase, this assumption may not be valid. Work is initiated to generate the required data for this task.

CONCLUSIONS

Two reported experimental runs of HEDL and CEA (experiments on reductive stripping of plutonium at macro level) in centrifugal extractors were simulated using an indigenous code SIMPSEX. The first case study pertained to HAN based reductive strip in centrifugal extractors for which reported end concentrations were compared with the SIMPSEX simulated values. In the second study a U(IV) based Pu barrier concept was also used in addition to HAN based partitioning. For the second case, reported Pu profiles were compared to the SIMPSEX simulated values. The agreement was good in the macro Pu bearing stages.

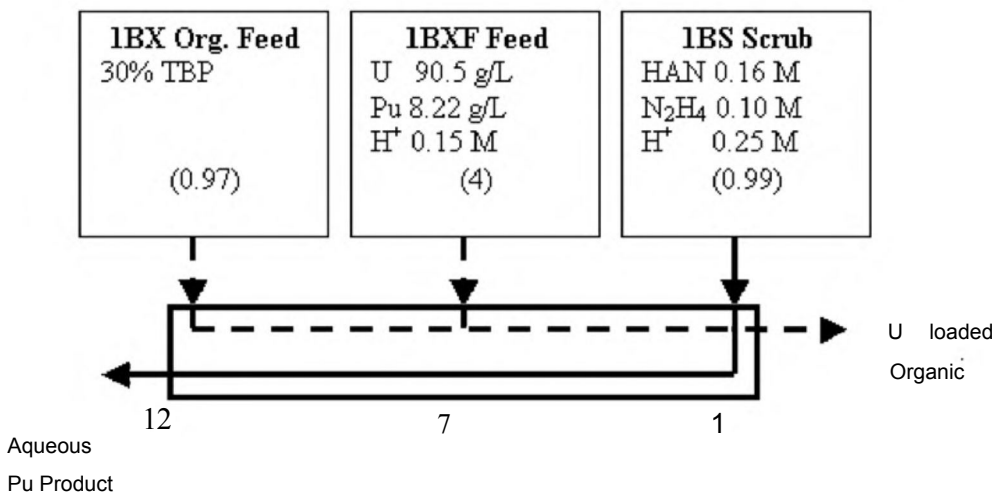


Figure 1. Schematic of HAN based run in centrifugal extractor, reported by Richardson and Swanson[7],

Table 1. HEDL Experiment[7] on HAN based Partitioning

HBXF Feed Concentration: ~ U 90.5 g/L, Pu 8.22 g/L, H* 0.15 mol/L

Run i.d.#1

Parameter	Reported Expt. Value	SIMPSEX Pred. Value	Remarks
U (organic product)	*64.26	72.80	g/L
Pu (organic product)	-	1.0 x 10®	g/L
H^+ (organic product)	0.054	0.016	mol/L
U (Aqueous product)	1.8 x 10'3	1.4 x 10^3	g/L
Pu (Aqueous product)	33.46	33.21	g/L
H^+ (Aqueous product)	0.78	0.775	mol/L

'Material balance on constant volume gives 72.83 g/L as $U(VI)_{org}$ concentration. Simulated values were corrected for change in volume.

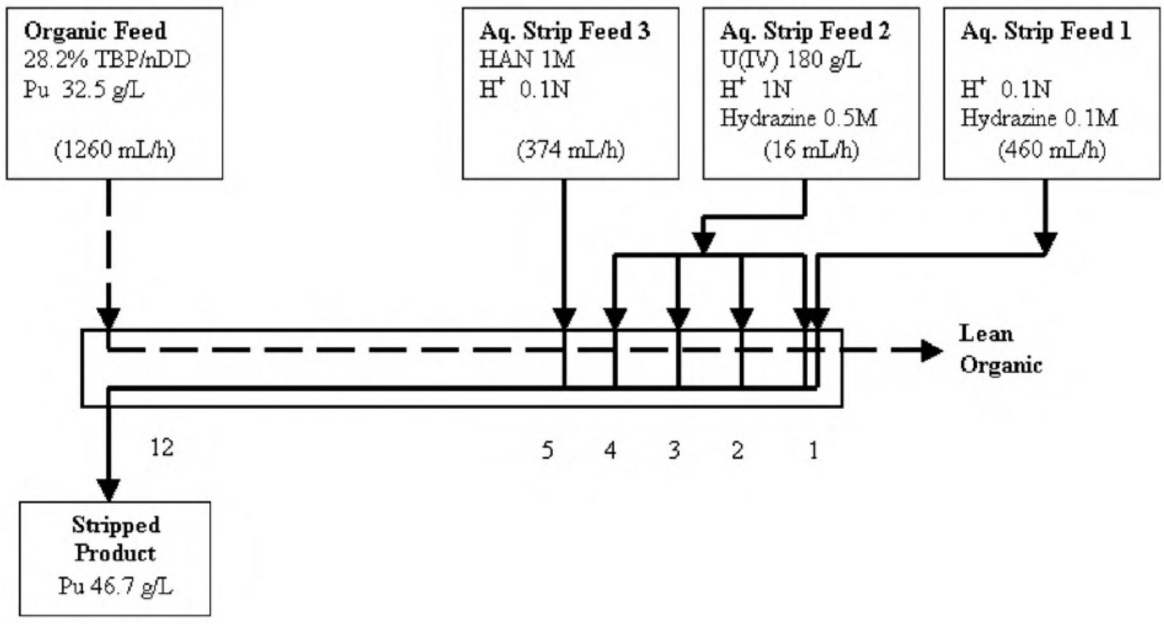


Figure 2. Schematic of experimental run, reported by Baron et al. (2000).

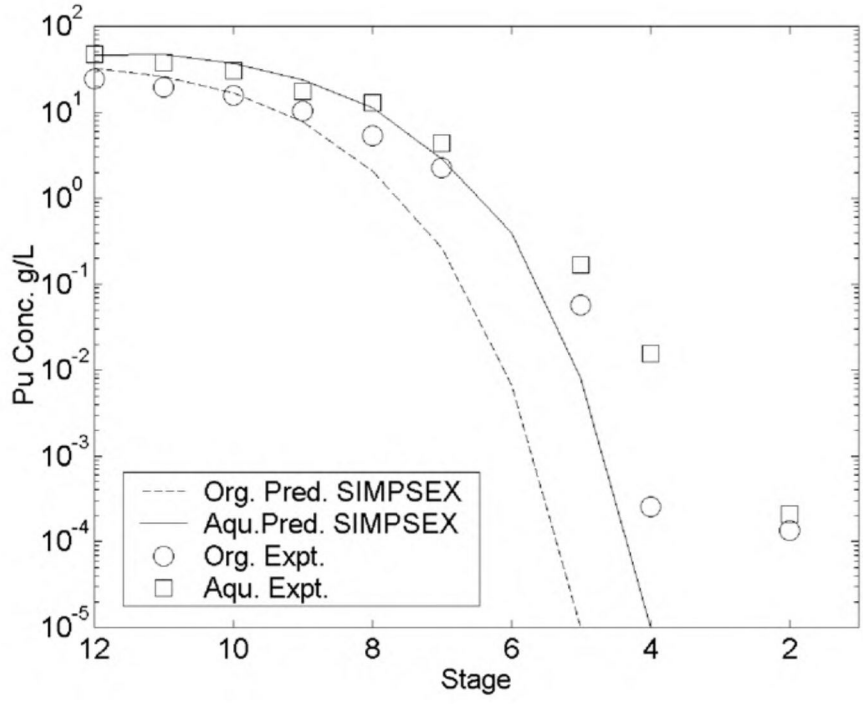


Figure 3. Comparison of SIMPSEX (30% TBP assumed) predicted stage profiles and reported values by Baron et al. (2000) for the schematic shown in Fig. 1.

REFERENCES

1. D. A. Orth, J. M. McKibben, and W. C. Scotten. (1971). *Proceedings International Solvent Extraction Conference (ISEC-71),* 1971, Vol.1, 514.

2. P. Patigny, J. Regnier, P. Miquel, and D. Taillard. (1974). *Proceedings International Solvent Extraction Conference (ISEC-74),* 1974, Vol.3, 2019.

3. J. C. Boudry, and P. Miquel. (1974). *Proceedings International Solvent Extraction Conference (ISEC-71),* 1974, Vol.2, 1551.

4. R. J. Taylor. (2000) Contemporary Trends in Nuclear Fuel reprocessing. *[Internet] Available form*< http://www.bnes.org.uk/Reprocessing.pdf>. [Accessed 31 July 2003],

5. Advanced Accelerator Applications (AAA). (2002) *Quarterly Report for Oct-Dec 2001 (LA-UR-02-0724),* 31st Jan. 2002, Document No. AAA-PDO-GEN-02-0005.

6. G. L. Richardson and J. L. Swanson. (1975). *Technical Report HEDL-TME-7531*, Hanford Engineering Development Laboratory.

7. P. Baron, B. Dinh, and B. Mauborgne. (2000). *Proceeding ATLANTE-2000.* 01.4.1-01.4.8.

8. S. Kumar and S. B. Koganti. (2002). *Technical Report IGC-234,* IGCAR, Kalpakkam.



STUDIES ON THE EXTRACTION OF ACTINIDES AND THE FISSION PRODUCTS BY DIAMIDE DERIVATIVES

Jing Chen* Xinghai Wang ShuweiWang

Institute of Nuclear Energy Technology, Tsinghua University, P.O.Box 1021, Beijing 102201, China
*Email: jingxia@tsinghua.edu.cn

Three diamide derivatives, N,N,N',N'-tetra-butyl-3-oxa-pentanediamide (TBOPDA), N,N,N',N'-tetra-hexyl-3-oxa-pentanediamide (THOPDA), and N,N,N',N'-tetra-(2-ethylhexyl) -3-oxa-pentanediamide (TEHOPDA), have been synthesized by a four-step reaction. The extraction of actinides and the fission products by the above products from the nitrate media has been studied. The results show that this kind of extractants have a strong affinity to tri- and tetra-valent actinides, Eu(III), Y(III), and Zr(IV), an intermediate affinity to Tc(VII), and Mo(VI), and a weak affinity to Np(V), U(VI), Ni(II), Fe(III), Cr(III), Ru(II), Sr(II) and Ba(II). The increase in the substituted alkyl length lowers the extraction ability to actinides and the nitric acid enhances the extraction mainly because of the salting-out effect.
Key words: extraction, actinides, fission products, diamide

INTRODUCTION

The safe treatment and disposal of the radioactive waste, specially high level waste(HLW), from nuclear power plant is crucial to the sustainable development of nuclear energy. Partitioning the long-life nuclides such as minor actinides from HLW and transmutating them is an advanced method to reduce the long-term risk of HLW. Some partitioning processes, such as TRUEX process/[11] DIMAEX process,[121] and TRPO process,[131] were developed to separate minor actinides from HLW.

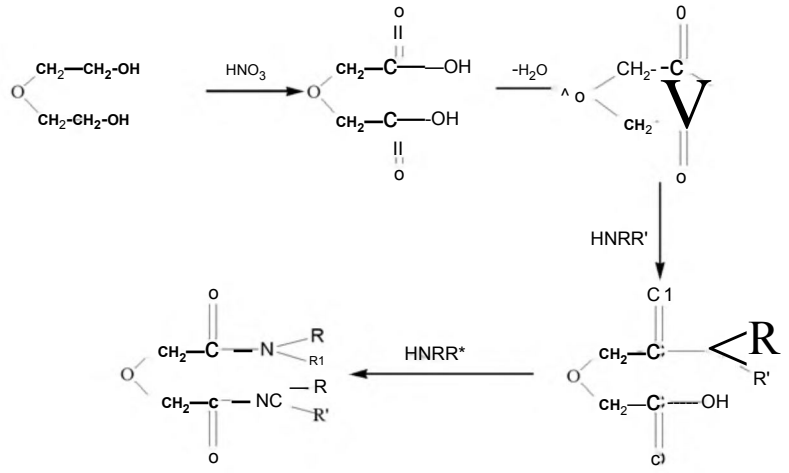
Some diamides derivatives, oxapentanediamides, were developed to separate actinides from HLW recently.[4,51] They are completely incinerable without secondary solid waste because they consist of only C, H, O and N elements. The remarkable advantage implies its great potential in the partitioning of HLW. Some research work was done to develop this kind of extractants in this work.

EXPERIMENTAL

Reagents

Three oxapentanediamides have been synthesized by the following four-step reaction in our laboratory.[161] The products are N,N,N',N'-tetra-butyl-3-oxa- pentanediamide (TBOPDA), N,N,N',N'-tetra-hexyl-3-oxa-pentanediamide (THOPDA) and N,N,N',N'-tetra-(2-ethylhexyl) -3-oxa- pentanediamide (TEHOPDA), respectively. Their purities were determined to be >95% by GC-MS. The n-octanol was used as the diluent.

The radionuclides ^{241}Am, ^{239}Pu, ^{237}Np, ^{233}U were obtained from the Institute of Atomic Energy, Beijing, and $^{152'154}$Eu was produced by neutron irradiation at the swimming pool reactor of INET. All radionuclides were radionuclide pure. "Tc was obtained from Amersham, the Netherlands. All other reagents used were of analytical grade.



Analytical Method

The activity of ^{241}Am and $^{152'154}$Eu was measured by y-counting in a NaI(Tl) well-type gamma counter (EKCO N700) in different energy ranges. The activities of ^{239}Pu, ^{237}Np, ^{233}U and ^{99}Tc were determined by the liquid scintillation counter (Packard Tri-Carb 2200CA). The content of other metallic elements was determined by the ICP-AES (Thermo Jarrell Ash). The nitric acid concentration of equilibrated aqueous phase was titrated by NaOH solution.

Procedures

Equal volumes of the organic and aqueous phases were equilibrated in glass stoppered test tubes with magnetic stirrer in a thermostatic water bath for 60 minutes. After centrifugation and phase separation, the nitric acid concentration of equilibrated aqueous phase was measured and each phase was sampled and analyzed . The distribution ratios (D_M) of metallic ion M^{n+} were calculated as organic phase content / aqueous phase content. All extraction experiments were carried out at 25±0.2°C.

RESULTS AND DISCUSSION

Figure. 1,2 and 3 show the extraction of Am(lll), Cm(lll), Pu(IV), Np(IV), Np(V) and U(VI) by three oxapentanediamides, respectively. The results in Figure 1 and 2 indicate that oxapentanediamides have a strong affinity to Am(lll), Cm(lll), and Pu(IV), an intermediate affinity to Np(IV), and a weak affinity to U(VI) and Np(V). In the system of TEHOPDA, the extraction of Np(IV) was enhanced to close to Pu(IV), especially at >3M $HN0_3$. The nitric acid enhanced the extraction of Np(V) to some extent. However, its distribution ratios are less than 1.0 even at 4M nitric acid. The three extractants show no obvious difference in the extraction affinity to Np(V).

The above results imply that this kind of extractants prefer to extract low valent actinides to high valent ones.

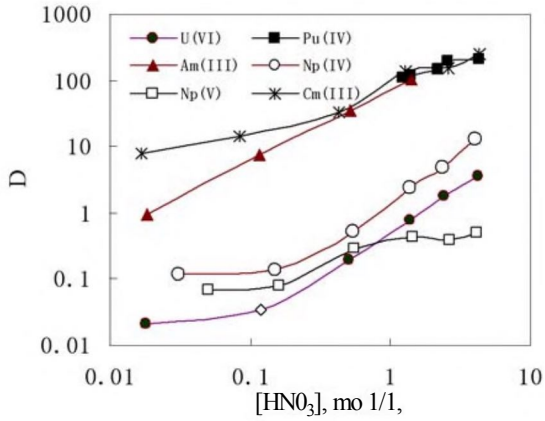


Figure 1. The extraction of different actinides ions by 0.1 M TBOPDA - n-octanol

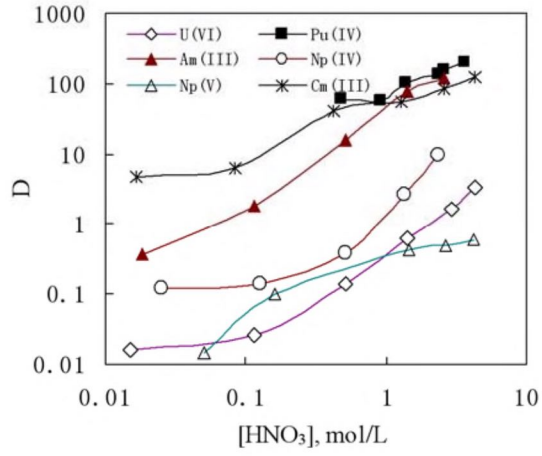


Figure 2. The extraction of different actinides ions by 0.1 M TFiOPDA - n-octanol

The constituent elements of spent nuclear fuel are complicated. Some representative fission products were selected in the present work. Figure 4,5,6 show that the extraction of the fission products Tc(VII), Zr(IV), Y(III), Eu(III), Ba(II), Sr(II), Mo(VI), Ni(II), Fe(III), Cr(III), and Ru(II) by three diamide derivatives. According to the extraction performance, they can be divided into three groups: (1) strong extraction: Eu(III), Y(III) and Zr(IV); (2) intermediate extraction: Tc(VII) and Mo(VI); (3) weak extraction: Sr(II), Ba(II), Ni(II), Fe(III), Cr(III), and Ru(II).

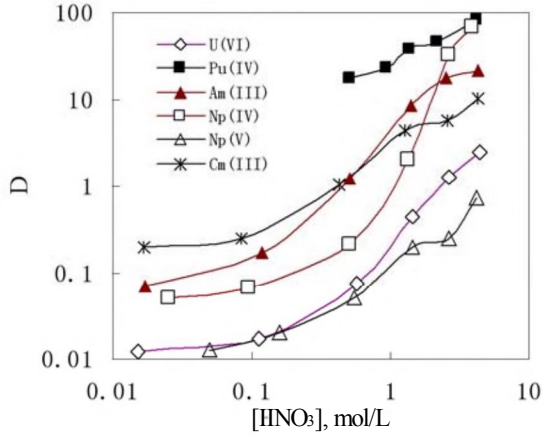


Figure 3. The extraction of different actinides ions by 0.1 M TEHOPDA - n-octanol

The extraction of Eu(III), Y(III) and Zr(IV) increased with the concentration of nitric acid. The effect of nitric acid on the extraction of Tc(VII) is complicated. The distribution ratio of Tc(VII) decreased when the nitric acid concentration is lower than 0.3mol/L, increased when the nitric acid concentration is over 0.3mol/L, and then decreased when the nitric acid concentration is over 2mol/L. The positive effect and the competition of nitric acid probably resulted in the above phenomenon because Tc(VII) was extracted in the form of $HTc0_4$and the nitric acid was co-extracted by the extractant and solvent n-octanol. The nitric acid caused no remarkable effects on the other ions.

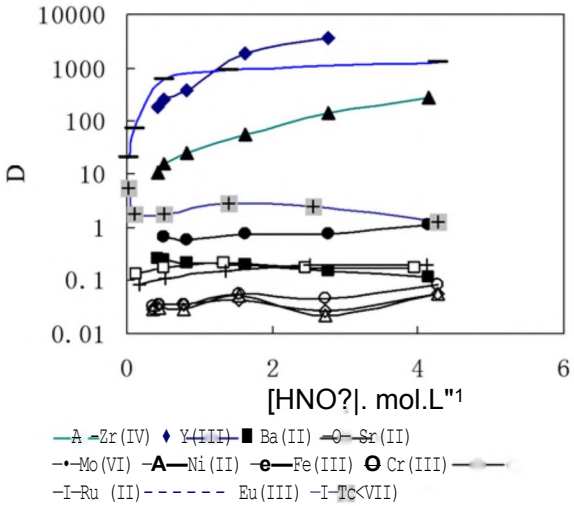


Figure 4. The extraction of different metallic ions by 0.1M TBOPDA - n-octanol

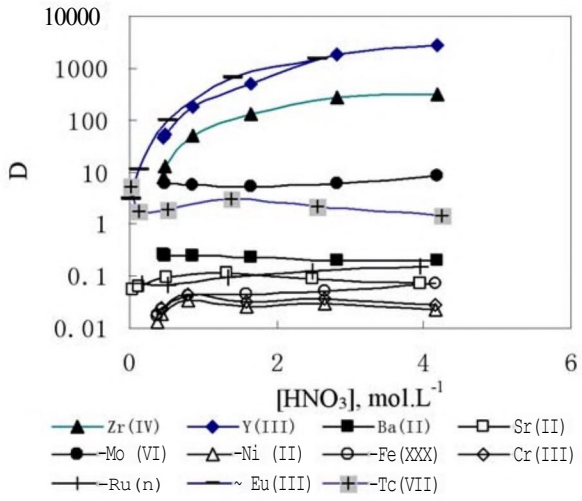


Figure 5. The extraction of different metallic ions by 0.1M THOPDA - n-octanol

In order to study the effects of substituted alkyl on the extraction of actinides, the results were rearranged in Figure 7, 8 and 9. It can be concluded that the general order of the extraction ability is TBOPDA >THOPDA > TEHOPDA. The length increase of substituted alkyl lowered the extraction ability due to the effect of spacial obstacle in the extraction complex.

A positive effect of nitric acid on the three actinide ions was observed. The extraction of Am(lll) sharply increased while increasing the nitric acid concentration of aqueous phase, and then maintained a constant at a higher nitric acid. The distribution ratios of U increase sharply when the nitric acid concentration is over 0.1 M (see Figure 9).

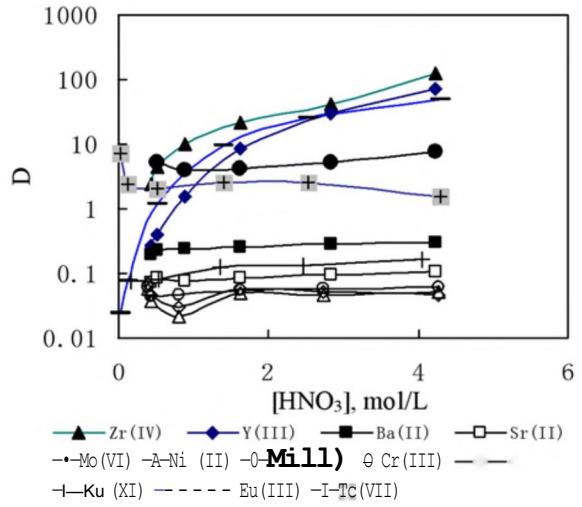


Figure 6. The extraction of different metallic ions by 0.1M TEFIOPDA - n-octanol

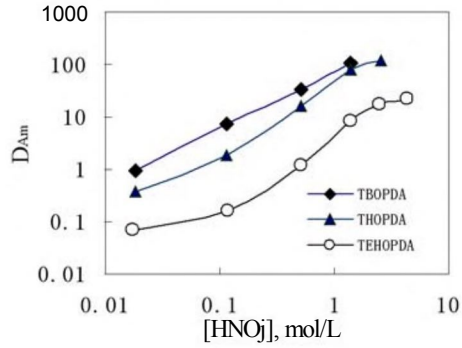


Figure 7. The extraction ofAm(lll) by three products with a concentration of 0.1M

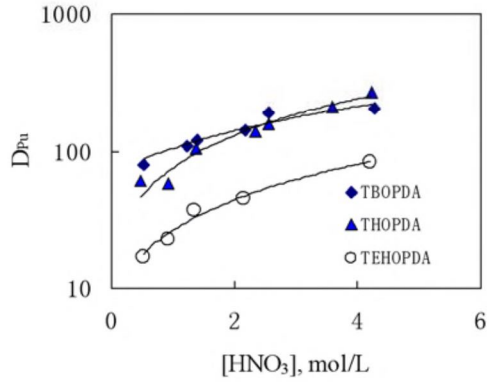


Figure8. The extraction of Pu(IV) by three products with a concentration of 0.1 M

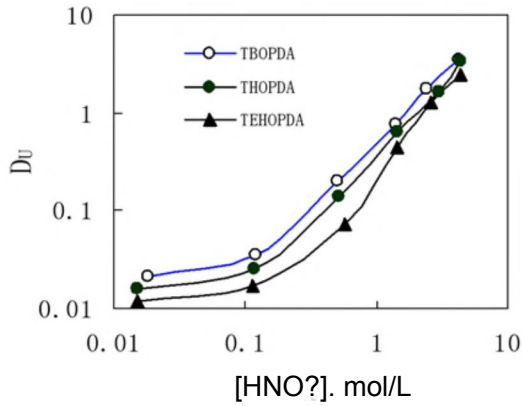


Figure 9. The extraction of U(VI) by three products with a concentration of 0.1 M

CONCLUSIONS

The extraction of actinides and the fission products by TBOPDA, THOPDA, and TEHOPDA from the nitrate media has been studied in the present work. This kind of extractants have a strong affinity to tri- and tetra- valent actinides, Eu(lll), Y(lll) and Zr(IV), an intermediate affinity to Tc(VII) and Mo(VI), and a weak affinity to Np(V), U(VI), Ni(ll), Fe(lll), Cr(lll), Ru(ll),

Sr(II) and Ba(II). The nitric acid enhanced the extraction mainly because of the salting-out effect. With respect to actinides, the increase in the substituted alkyl length lowered the extraction ability due to the effect of spacial obstacle in the extraction complex. The strong affinity to trivalent and tetravalent actinides suggests that oxapentane- diamides have great potential in the separation of minor actinides from high level waste.

ACKNOWLEDGMENTS

The present research work was supported by Natural Science Foundation of China (20106009).

REFERENCES

1 E.P. Horwitz, W.W. Schulz (1991). Edited by Cecille L, Casarci M and Pietrelli L New Separation Chemistry Techniques for Radioactive Waste and Other Specific Application . London UK: *Elsevier.* pp21.

2 C. Cuillerdier, C. Musikas, P. Hoel, et al. (1991), Sep. *Sci. Technol.,* 26, 1229-1244.

3 Y.J. Zhu, C.L. Song(1992). Edited by Morss LR and Fuger J. Transuranium Element Symposium 1990. Washington D.C: American Chemical Society. pp318.

4 Y. Sasaki, Y. Sugo, S. Suzuki and S. Tachimori (2001), *Solv. Extr. Ion Exch.,* 19(1), 91-103.

5 Y. Morita.Y. Sasaki, S. Tachimori (2001). *Global 2001,* Paris-France, 9-13, Sept. 2001.

6 P. Zhang, J. Chen, C.Y. Li, G.X. Tian (2003), *Chemical* Journal on Internet, 5(7),52-55..



SIMULTANEOUS EXTRACTION/RECOVERY OF CESIUM AND STRONTIUM FROM ACIDIC SOLUTIONS

Catherine L. Riddle, Jack D. Law, Terry A. Todd, John D. Baker, Christopher A. McGrath, David H. Meikrantz, Bruce J. Mincher, and Dean R. Peterman

Idaho National Engineering and Environmental Laboratory, Idaho Falls, Idaho, USA

A synergistic extraction solvent for the simultaneous extraction and recovery of cesium and strontium from acidic solutions has been investigated. The novel extraction solvent consists of 4,4' ,(5')-Di-(t-butyldicyclo-hexano)-18-crown-6 (DtBuCH18C6), Calix[4]arene-bis-(tert-octylbenzo-crown-6) (BOBCalixC6), and 1-(2,2,3,3-tetrafluoropropoxy)-3-(4-sec-butylphenoxy)-2-propanol (Cs-7SB modifier) in a branched aliphatic kerosene (Isopar® L). Extraction synergy for strontium was observed when the DtBuCH18C6 was combined with the BOBCalixC6 cesium extractant and Cs-7SB modifier or if the Cs-7SB modifier was substituted into the Strontium Extraction process (SREX) solvent in place of TBP. The novel solvent extracted both cesium and strontium simultaneously from 1M nitric acid solutions with distribution ratios of 7.7 and 8.8 for cesium and strontium, respectively, at ambient temperature. Cesium and strontium were also simultaneously stripped from the solvent using 0.01M nitric acid solutions.

This new extraction solvent shows promise for the treatment of radioactive wastes to remove highly radioactive fission products from the bulk waste matrix, or to treat dissolved spent nuclear fuel to reduce short-term heat load in a geologic repository. Distribution ratios for cesium and strontium from nitric acid solutions and in a dissolved spent fuel simulant were measured, and a preliminary process flowsheet was developed.

INTRODUCTION

The United States Department of Energy's Advanced Fuel Cycle Initiative (AFCI) is developing proliferation-resistant spent nuclear fuel treatment and transmutation technologies to optimize the nuclear fuel cycle in the United States (1). One of the primary goals of the program is to develop technologies to reduce the cost of geologic disposal of spent nuclear fuel. Near-term benefits include potential enhanced repository performance due to the reduction of volume (and mass) as well as reduction of the thermal load from the waste or fuel. Longer-term benefits include destruction of plutonium and minor actinides, resulting in reduced radiotoxicity in the repository. These goals culminate in eventual transition to a sustainable Generation IV nuclear energy system.

The enabling technologies for reducing the volume (and mass) of the spent fuel, as well as heat generating isotopes and management of minor actinides, are chemical separation processes. These processes include both aqueous-based processes and electrochemical-based processes; however, the current focus of the AFCI program for processing legacy light water reactor fuel is on aqueous-based technologies. Spent light water fuel is approximately

95% uranium (by mass); therefore, initial separation of the uranium from the spent nuclear fuel greatly reduces the size and complexity of subsequent processes. The AFCI program has successfully developed and demonstrated the Uranium Extraction (UREX) solvent extraction process, which effectively removes uranium and technetium (in separate streams) from spent nuclear fuel dissolved in nitric acid.

Separation of the primary short-term heat generators, cesium and strontium, can be achieved simultaneously utilizing solvent extraction technologies. Simultaneous separation of cesium and strontium reduce overall process complexity and allow for a single product form to be produced for decay storage. Two technologies are under development for the concurrent separation of cesium and strontium from the raffinate resulting from the UREX or co-extraction process. The first process utilizes chlorinated cobalt dicarbollide (CCD) and polyethylene glycol (PEG) in a phenyltrifluoromethyl sulfone diluent (2). The CCD/PEG process is most efficient when the feed is < 1M nitric acid; therefore, it can be used directly on the UREX process raffinate. This process has been demonstrated in countercurrent flowsheet tests using both simulated and actual UREX raffinates. Both tests demonstrated removal efficiencies for cesium and strontium of ~99% or greater, which is sufficient to reduce short term heat load to the repository.

The second technology for the separation of cesium and strontium is based on a combined solvent containing two extractants - 4,4 ' ,(5 ')-Di-(t-butyldicyclo-hexano)-18-crown-6 (DtBuCH18C6) and Calix[4]arene-bis-(tert-octylbenzo-crown-6) (BOBCalixC6) combined with a phase modifier- 1-(2,2,3,3-tetrafluoropropoxy)-3-(4-sec-butylphenoxy)-2-propanol (Cs-7SB) in a branched aliphatic hydrocarbon diluent (Isopar® L) (3). This solvent composition was based on the Strontium Extraction (SREX) process developed at Argonne National Laboratory and the Caustic Side Solvent Extraction (CSSX) process developed at Oak Ridge National Laboratory (for alkaline waste)(4,5). Nitric acid dependency, variation of DtBuCH18C6 concentration, variation of Cs-7SB concentration, temperature effects on extraction, and preliminary flowsheet development were studied. Results of these studies are the primary focus of this paper.

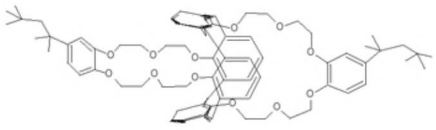
EXPERIMENTAL

All diluents were reagent grade and were used as received. Deionized water was used to prepare all aqueous acid solutions. The nitric acid was reagent grade from Aldrich Chemical Co. (Milwaukee, WI). Isopar® L isoparaffinic diluent was obtained from Exxon Chemical Company (Houston, TX). The ^{85}Sr and ^{137}Cs radiotracers used for spiking the simulants were obtained as $^{85}SrCl2$ in 1 M HCl and $^{137}CsCl$ in 1 M HCl from Isotope Products (Burbank, CA). The DtBuCH18C6 crown ether was purchased from Eichrom Industries, Inc. (Darien, IL). The BOBCalixC6 calixarene crown ether and Cs-7SB modifier, obtained from Oak Ridge National Laboratory, were originally received from IBC Advanced Technologies, Inc. (American Fork, UT1 and Boulder Scientific Comoanv (Mead. COT resoectivelv. and were used as received. Figure 1 shows the structures of the individual components.

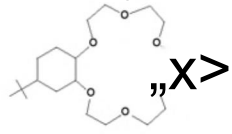
All test samples in this research were shaken by hand for 1 minute, centrifuged for 1 minute, the organic and aqueous fractions were separated, and the two phases analyzed. The organic and aqueous aliquots were y-ray counted using an HPGe detector. The 661 keV line of ^{137}Cs and the 514 keV line of ^{85}Sr were used to measure these elements. Nitric acid dependency tests were run for ^{137}Cs as above and extracted with CSSX solvent.

The solvents used in this testing consisted of 0.045 M to 0.358 M DtBuCH18C6, 0.007 M BOBCalixC6, and 0.01 to 0.80 M Cs-7SB modifier in an Isopar® L diluent. The extractant was prepared by adding neat DtBuCH18C6, BOBCalixC6, and Cs-7SB modifier to a mixing vessel. Approximately 10% of the required final Isopar® L volume is added to lower the viscosity and the mixture was left to stir overnight. The remainder of the Isopar® L was then

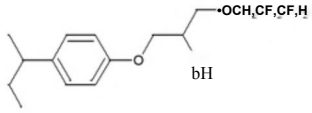
added the next morning. Ambient temperature throughout the experiments was 23°C ± 3°C .



BOBCalixC6



DtBuCHI 8C6



Cs-7SB modifier

Figure 1. Molecular structures of the cesium and strontium extractants and modifier.

RESULTS AND DISCUSSION

Nitric acid dependency for Cs and Sr distribution coefficients were measured using a solvent consisting of 0.15 M DtBuCH18C6, 0.007 M BOBCalixC6, and 0.75 M Cs-7SB modifier in an Isopar® L diluent. The composition chosen was based on the typical concentration of the DtBuCHI8C6 in the SREX (0.15 M) and the typical concentration of the modifier (0.75 M) and BOBCalixC6 (0.007) in the CSSX process. Nitric acid dependency is shown in Figure 2. Distribution coefficients for Cs and Sr increase with increasing nitric acid concentration, and are approximately 7 at 1.0 M $HN0_3$.

Development of an optimum mixture for the extractants has been initiated. Testing was performed using 1.0 M $HN0_3$, which is the approximate concentration expected in the raffinate from the UREX process. A plot of the cesium and strontium distribution coefficients from 1 M $HN0_3$, as a function of the DtBuCH18C6 concentration with 0.007 M BOBCalixC6, 0.750 M Cs-7SB modifier, 0.003 M trioctylamine and Isopar L®, is shown in Figure 3. As the DtBuCHI8C6 concentration is increased, the Sr distribution coefficients increase and the Cs distribution coefficients decrease. The Cs and Sr distribution coefficients are approximately equal (6.0) at a concentration of 0.1 M DtBuCH18C6. At the SREX DtBuCH18C6 concentration of 0.15 M, the Sr distribution coefficient is approximately 7.5 and the Cs distribution coefficient is approximately 4.2. A DtBuCH18C6 concentration of 0.10 M to 0.15 M appears to be an optimal range; however, it is likely that future work will involve increasing the calixarene concentration to prevent loading with Cs. This increase will likely result in a slight decrease in Sr distribution coefficients. If this is the case, the higher DtBuCH18C6 concentration (0.15 M) will be necessary.

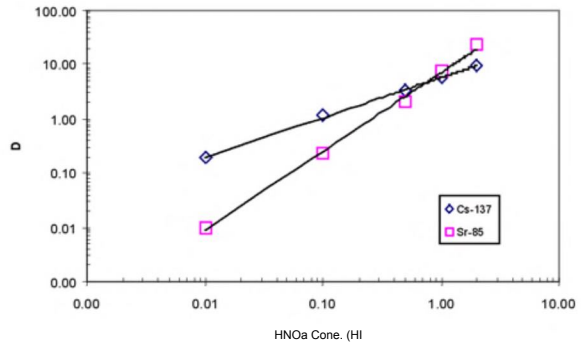


Figure 2. D_{Sf} and D_{Cs} versus nitric acid concentration for new mixed solvent (DtBuCHI 8C6, BOBCalixC6, Cs-7SB modifier in Isopai® L).

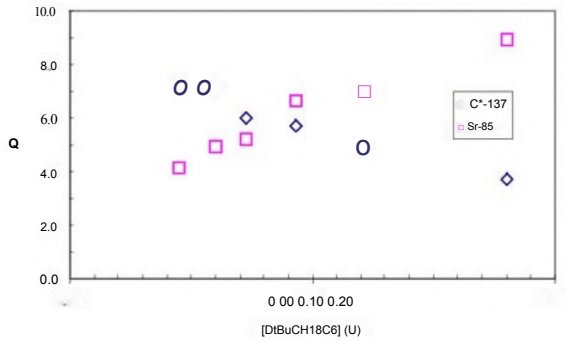


Figure 3. D_{Cs} and D_{Sr} in 1 M $HN0_3$ as a function of DtBuCH18C6 concentration in new mixed solvent (0.007 M BOBCalixC6, 0.75 M Cs-7SB modifier and 0.003 M TOA in Isopai® L).

The Cs-7SB modifier alone in Isopar® L exhibited no extraction of Cs and Sr from 1 M nitric acid solutions. However, when its concentration was varied in the mixed solvent the results shown in Figure 4 were measured. Distribution coefficients increased dramatically with increasing modifier concentration. At modifier concentrations greater than 0.8 M, increased viscosity of the solvent is likely to become problematic. Therefore, a modifier concentration of 0.75 M, which is used in the CSSX process, appears to be optimal for this process.

These tests indicate that the Cs-7SB modifier is responsible for the increased Sr distribution in this new solvent. It was also determined that the forward distribution of Sr from 1 M $HN0_3$ solutions can be improved from 0.7 (at ambient temperature using the SREX solvent) to between 5 and 7 by using a mixture of the SREX solvent with Cs-7SB instead of tri-butyl phosphate (TBP). This is a significant improvement over the SREX extractant for processes when only selective Sr removal from acidic solutions is desired. The positive effect of fluorinated modifiers is well documented for the extraction of cesium using crown ethers or calixarenes, but these modifiers have not been reported being applied to the SREX process for enhancing strontium extraction instead of using TBP.

As ambient temperature varied during testing, it was noted that Sr distribution coefficients increased with decreasing temperature. This was of interest since it is noted in the literature that BOBCalixC6 forward distributions are similarly temperature dependent. Since the data indicated an increase in D_{Sr} with increasing temperature, temperature dependence tests with the new combined solvent were conducted and are shown in Figure 5. With the mixed solvent at 10°C, the distribution coefficients for Sr and Cs were, 16 and 20, respectively.

Testing with Simulated Feed

The new solvent is being developed for the separation of Cs and Sr from spent LWR fuel. Laboratory batch contacts with simulated dissolved spent LWR fuel, the composition of which is shown in Table 1, has been performed. The extraction distribution coefficients for Cs and Sr from feed simulant, as a function of temperature, are shown in Figure 6.

Distribution coefficients for Cs are significantly lower from the simulated feed than from 1.0 M $HN0_3$. This is a result of partial solvent loading of the 0.007 M BOBCalixC6 with Cs in the feed simulant (0.004 M). The distribution coefficients are reasonably high; however, an increase in the Cs distribution is desirable. In order to increase the Cs distribution coefficients, it will be necessary to increase the BOBCalixC6 concentration. Research is underway to evaluate the effect of increased BOBCalixC6 concentration of Cs and Sr distribution coefficients, but is not addressed in this paper.

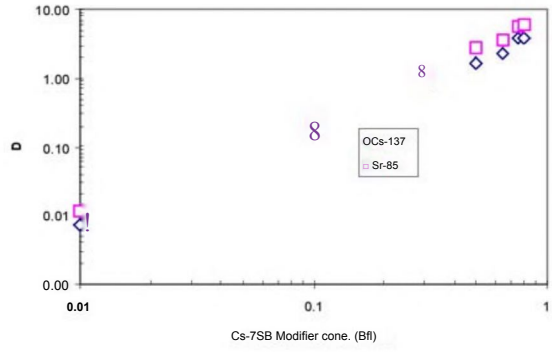


Figure 4. D_s, and D_{Cs} versus Cs-7SB concentration in 0.15 M DtBuCH18C6, 0.007 M BOBCalixC6 and IsopaF[9] L.

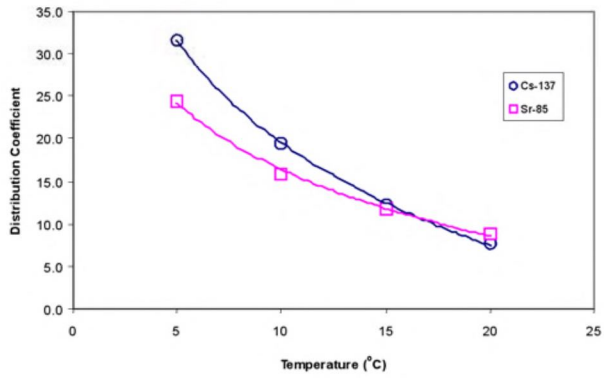


Figure 5. D_{Cs} and D_{Sr} from 1 M $FiNQ_3$ into new mixed solvent at various temperatures.

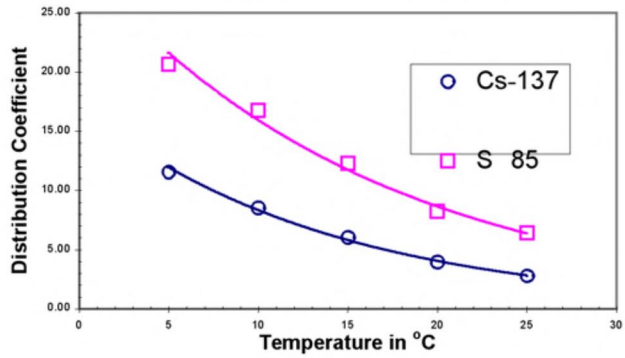


Figure 6. Distribution coefficients of Cs and Sr, as a function of temperature, from simulant using 0.15 M DtBuCH18C6, 0.007 M BOBCalixC6, 0.750 M Cs-7SB modifier and IsoparL[9]

Table 1. Feed Simulant Composition.

Component	Concentration (M)	Component	Concentration (M)
HNO_3	1.0	Ce	4.3E-03
Sr	2.0E-03	Nd	7.2E-03
Cs	4. IE-03	Sm	5.0E-03
Zr	1.07E-02	Gd	2.6E-04
Ba	3.7E-03	Eu	1.4E-04
La	2.2E-03	Y	1.4E-03

Flowsheet Studies

The distribution coefficients of Cs and Sr from simulated feed at 15 °C (Figure 6) were used

in conjunction with experimentally obtained strip distribution coefficients to model a preliminary flowsheet for the treatment of spent fuel. Strip distribution coefficients of 0.45 for Cs and 0.04 for Sr were obtained for the new solvent and a 0.01 M $HN0_3$ strip solution. The goal in development of the flowsheet was to obtain 99% separation of Cs and Sr. The resulting preliminary flowsheet is presented in Figure 7.

With 6 extraction, 4 scrub, and 10 strip stages, >99% of the Cs and Sr are separated from the spent LWR fuel. Additionally, the Cs and Sr are efficiently stripped from the solvent. This preliminary flowsheet will be modified as additional experimental data are obtained.

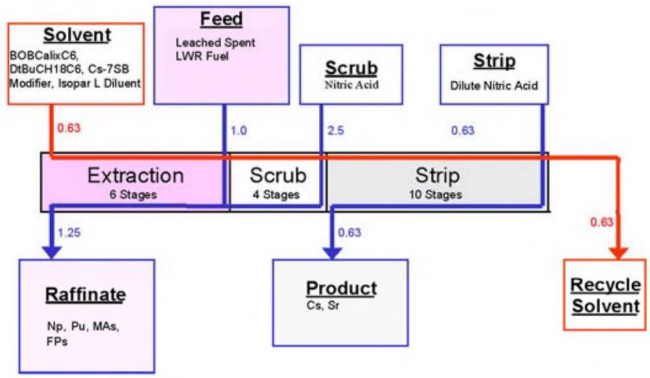


Figure 7. Preliminary flowsheet for the treatment of spent LWR fuel

CONCLUSIONS

A novel solvent consisting of DtBuCH18C6, BOBCalixC6, and a Cs-7SB modifier in an Isopar® L diluent has been demonstrated to be effective for the simultaneous extraction of Cs and Sr from acidic solution. This new extraction solvent shows promise for the treatment of radioactive wastes to remove highly radioactive fission products from the bulk waste matrix, or to treat dissolved spent nuclear fuel to reduce short-term heat load in a geologic repository. A preliminary flowsheet, consisting of 6 extraction, 4 scrub, and 10 strip stages, has been developed which should separate >99% of the Cs and Sr from spent LWR fuel. Flowrates for the flowsheet are shown relative to a feed flowrate of unity.

ACKNOWLEDGEMENTS

The authors wish to thank Drs. B. A. Moyer, L. H. Delmau and P.V. Bonnesen at Oak Ridge National Laboratory for the calixarene crown ether, the modifier and helpful discussions. This research was sponsored by the U. S. Department of Energy, Office of Nuclear Energy, Science and Technology under DOE Idaho Operations Office contract DE-AC07-99ID13727.

REFERENCES

1. J. Laidler, J. Bresee (2004), *proc. ATALANTE 2004,* Nimes, France.
2. J. Law, R. Herbst, D. Peterman, R. Tillotson, T. Todd (2004), *Nucl. Technol.,* 147, 284-290.
3. C. Riddle, J. Baker, J. Law, C. McGrath, D. Meikrantz, B. Mincher, D. Peterman, T. Todd (2004), *Solv. Extr. Ion Exch.,* in press.
4. P. Bonnesen, L. Delmau, B. Moyer, R. Leonard (2000), *Solv. Extr. Ion Exch.,* 18,1079.
5. E. P. Horwitz, et. al. (1985), *Solv. Extr. Ion Exch.,* 3, 75.



The Use of Regenerable Stripping Reagents for Treatment of Radioactive Wastes or Spent Nuclear Fuel

Terry A. Todd[1], Jack D. Law[1], R. S. Herbst[1], V. A. Babain[2], I. V. Smirnov[2], V. N. Romanovskiy[2], and V. M. Esimantovskiy[2]

^daho National Engineering and Environmental Laboratory, Idaho Falls, Idaho, USA
[2]V. G. Khlopin Radium Institute, St. Petersburg, Russia

Solvent extraction technologies for the treatment of radioactive waste or spent nuclear fuel have been developed to reduce the quantity of highly radioactive material that must be disposed in geologic repositories. Separation of transuranic (TRU) elements, and highly radioactive fission products, such as cesium and strontium, allow for the bulk mass of the spent fuel or waste to be handled and disposed of more economically. In a solvent extraction process tailored to separated TRU elements or fission products, these elements are typically extracted from the bulk aqueous solutions and subsequently stripped from the solvent for concentration, recovery or final immobilization.

Amine carbonate solutions have been studied for metal stripping for various organic solvents. These solutions make it possible to regenerate and reuse the majority of the stripping reagent and significantly reduce the organic and/or salt content of the strip product. This simplifies downstream processing and minimizes final product volume. Methylamine carbonate, with small amounts of complexant added, has been demonstrated for stripping of cesium, strontium, actinides and lanthanides from the Universal Extraction (UNEX) process solvent. This novel strip reagent has also been demonstrated in countercurrent flowsheet tests, using centrifugal contactors, where the strip product was collected, regenerated, and reused in the process. This reagent is also effective for stripping metals from other solvents, such as the Transuranium Extraction (TRUEX) and PUREX process solvents.

INTRODUCTION

Solvent extraction technologies offer many advantages in the treatment of highly-radioactive wastes or spent nuclear fuel, due to their high selectivity and separation efficiency. One of the benefits of using solvent extraction technologies is the concentration of highly-radioactive products relative to the original volume of radioactive wastes or dissolved spent nuclear fuel. The economics of waste treatment or spent fuel processing is highly dependent on the volume reduction of highly-radioactive product streams. To date, nearly all solvent extraction processes rely on a once-through strip reagent, to remove the extracted products from the organic solvent. This strip reagent is often subsequently concentrated via evaporation or other means. A strip reagent that could be regenerated and recycled, significantly reducing the amount of reagent in the final strip product stream could offer significant economic benefit.

A regenerable methylamine carbonate (MAC) strip solution has been developed, as a collaborative effort between the Khlopin Radium Institute (KRI) and the Idaho National Engineering and Environmental Laboratory (INEEL), for the stripping of actinides,

lanthanides, Cs, and Sr from cobalt dicarbollide based solvent extraction processes [1], This new class of strip reagent was developed to replace the baseline strip reagent used in the Universal Solvent Extraction (UNEX) process, namely guanidine carbonate, which contributes large amounts of organic material to the strip product concentration/solidification unit operations [2], Methodology and experimental results of developing this strip reagent and a distillation method for regeneration of the resulting strip solution are summarized. Additionally, counter-current flowsheet tests of the Universal Solvent Extraction (UNEX) process at the INEEL as well as KRI have been performed using this regenerable strip solution. Finally, a study of the radiation stability of the methyl amine carbonate strip reagent was completed.

EXPERIMENTAL

Development of amine carbonates as regenerable strip regents

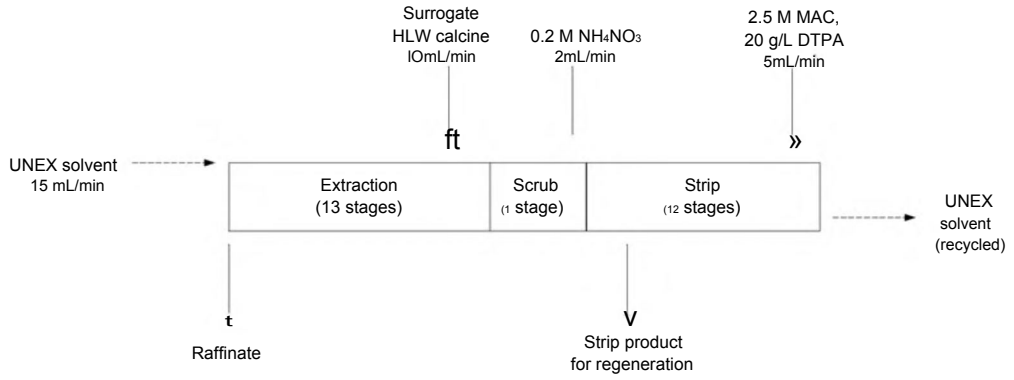
Various amine carbonates were evaluated as stripping reagents for Cs with the UNEX solvent by measuring the distribution coefficient of Cs. Once methylamine carbonate was chosen as the preferred amine carbonate, additional batch contacts were performed to optimize the concentration of MAC in the strip reagent. The optimal complexant (diethylenetriamine pentaacetic acid (DTPA) or nitrilotriacetic acid (NTA)) concentration in the strip reagent for Sr removal was also determined. At the optimal MAC and DTPA concentrations, distribution coefficients were measured for Cs, Sr, Am, Eu, U, Pu(IV), and Np. Distribution coefficients were determined radiometrically using trace amounts of radioactive isotopes of ^{137}Cs, ^{85}Sr, ^{241}Am, ^{152}Eu, ^{239}Pu, and ^{237}Np. Radiometric measurements were performed in duplicate and typical errors were ±15%. Uranium was determined by luminescence. All batch contacts were performed at an organic-to-aqueous phase ratio (O/A) of 1.0. Finally, the distillation of MAC, MAC/DTPA, and MAC/nitrilotriacetic acid (NTA) was studied.

Carbonates of organic amines were obtained by passing $C0_2$ through aqueous amine solutions until saturation. It is anticipated the species formed in these aqueous systems would be an equilibrium mixture of amine-carbonate ion pairs, either amine carbonates (i.e., $(RNH_3)2^+/C0_3^2$) or amine bicarbonates (i.e., $RNH_3^+/HC0_3$) and perhaps even carbamates ($R_2NC0_2^-$). For example, in similar ammonium carbonate systems, it has been established that a complex equilibrium exists between carbon dioxide, ammonia, ammonium, carbonate, bicarbonate, and carbamate species [3], Finally, the aqueous amine carbonate solutions were heated at 60°C to drive the salient reactions to equilibrium. Carbonate concentrations were determined both volumetrically and by mass.

Flowsheet testing with regenerable strip reagents

Flowsheet testing of the universal extraction (UNEX) process was performed in centrifugal contactors at both the INEEL and KRI using simulated dissolved INEEL high-level waste calcine feed. The target solvent composition was 0.08 *M* chlorinated cobalt dicarbollide (CCD), 0.5 vol.% polyethylene glycol-400 (PEG-400), and 0.02 *M* diphenyl-A/,A/-di-r?-butylcarbamoylmethylphosphine oxide (Ph_2Bu_2CMPO) in the diluent phenyltrifluoromethyl sulfone ($C_6H_5S0_2CF_{3l}$ designated as FS-13). The solvent was continually recycled during the testing. Approximately 1,000 mL of solvent were prepared at the INEEL for the flowsheet testing, resulting in the solvent being recycled through the system approximately 9 times.

The flowsheet tested at the INEEL, as shown in Figure 1, consisted of thirteen stages of extraction at an O/A of 1.25, one stage of scrub (0.2 *M* NH_4N0_3) at an O/A of 7.5, and twelve stages of strip (2.5 *M* MAC and 20 g/L DTPA) at an O/A of 3.0. Two flowsheet tests were performed. The strip product from the first flowsheet test was regenerated by distillation and used as the strip reagent feed for the second test. The methodology for the second test was the same as for the first flowsheet test.



The flowsheet tested at the KRI, consisted of thirteen stages of extraction at an O/A of 1.2, two stages of a scrub containing 4 *M* $HN0_3$ at an O/A of 6.7, one stage of an additional scrub (0.1 *M* $NaN0_3$) at an O/A of 11.6, and eight stages of strip (2.5 *M* MAC and 10 g/L NTA) at an O/A of 1.2.

Fiaure 1. INEEL UNEX Flowsheet Test with Methvlamine Carbonate Strip Reaoent

Radiation stability of methylamine carbonate strip reagent

Irradiation of the MAC strip reagent was conducted by a Co-60 source at a dose rate of 1.2 Gy/s (W/L) and at 23 °C. Integral dose to the strip reagent was 2.4 MGy (667 W-h/L). This high irradiation dose was due to the low radiation-decomposition yields of the solution components under investigation. In the course of irradiation, samples were taken for analysis.

Distribution coefficients were determined radio-metrically using the radioactive isotopes of ^{137}Cs, ^{85}Sr, and ^{241}Am. Uranium was determined by luminescence. Carbonates of organic amines were obtained by passing $C0_2$ through aqueous amine solutions until saturation. The solution was then heated to 60°C to convert all hydrocarbonates to carbonates. Concentrations of carbonates were determined by volume and weight methods.

Methods of potentiometric titration in different media by using a semi-automatic device with hydrogen and calomel electrodes were tested for quantitative analysis of aqueous MAC solutions. More reliable and reproducible results were obtained by titration of MAC solutions in a 3:1 mixture of acetone-ethyl alcohol. In this case, the non-dissociated MAC is titrated as one clearly pronounced potential jump characterizing methylamine neutralization. The sensitivity of this method is 10^2 *M* for MAC and reproducibility is within ±5%.

RESULTS AND DISCUSSION

A comparison study was conducted on stripping of cesium, which is the most difficult of the extracted elements to recover from the UNEX solvent, by ammonium carbonate solutions with mixtures of different amine carbonates. The amines tested and the corresponding Cs distribution coefficient data are given in Table 1.

The data indicate the addition of the basic amine carbonate solutions improves cesium stripping considerably. This effect is most pronounced in the case of pyrrolidine and piperidine. At least three amines (methylamine, dimethylamine and pyrrolidine) are rather efficiently regenerated from strip product by distillation. To provide the full regeneration of pyrrolidine, it is necessary to remove nearly all of the water from the strip product, and this is a complicated and hazardous process. Therefore, two compounds are candidates for using as regenerable strip agents: methylamine carbonate and dimethylamine carbonate. The obvious advantage of dimethylamine is the higher efficiency of cesium stripping: at the same molar concentrations of strip reagent, the cesium distribution coefficient is lower by a factor of 4-5. However, drawbacks exist for of dimethylamine, notably; 1) dimethylamine is much

more difficult to wash from the organic phase than is methylamine, and 2) dimethylamine can form stable and toxic N-nitrosamines. Hence, methylamine carbonate (MAC) was chosen as the regenerable strip reagent for further study with the UNEX-process.

Table 1. Cs stripping from UNEX solvent: 0.08 M CCD + 1% PEG-400 + 0.035 M Ph_2Bu_2CMPO in FS-13. Strip solution: 1M $(NH_4)_2$ $C0_3$ + 0.3 M base.

	Base	Formula	D_{Cs}
1	none		1.8
2	Piperidine	$(CH_2)_5NH$	0.05
3	Piperazine	$HN(CH_2CH_2)_2NH$	1.3
4	Pyridine	C_5H_5N	0.17
5	Pyrrolidine	$(CH_2)_4NH$	0.09
6	Morpholine	$0(CH_2CH_2)_2NH$	0.5
7	Methylamine	CH_3NH_2	0.8
8	Dimethylamine	$(CH_3)_2NH$	0.16
9	Guanidine	$(NH_2)_2C=NH$	0.47

Cesium stripping from the UNEX solvent was studied as a function of MAC concentration in the strip solution using a constant concentration of 10 g/L DTPA. Data indicate the optimal concentration of MAC is 1.5 - 2.0 *M* and additional increases of MAC concentration does not lead to a marked improvement in stripping.

The dependence of distribution coefficients for cesium, strontium and europium on DTPA concentration in the MAC-based stripping solution is shown in Table 2. The purpose of adding DTPA (or other complexants) is to strip multi-valence metals and avoid precipitation in carbonate media. This is apparent from the data in Table 2, as DTPA concentration has a negligible effect on the Cs distribution coefficient. The data for Sr and Eu indicate the optimal concentration of DTPA is ~20 g/L; additional increases of DTPA concentration does not lead to a marked improvement in stripping. It should be noted that other complexants, for example nitrilotriacetic acid (NTA) or oxyethylidenediphosphinic acid (OEDPA), could be used in place of DTPA. Also, the concentration of complexant (DTPA, NTA, etc.) is dependent on the total concentration of rare earth elements and Sr in the feed; the complexant concentration must be sufficient to complex the extracted multi-valent metals and prevent precipitation.

Table 2. Dependence of Cs, Sr and Eu distribution coefficients on DTPA concentration in the strip solution. Solvent: 0.08 M CCD, 0.03 M Ph_2Bu_2CMPO, 0.055 vol. % PEG-400 in FS-13. MAC concentration = 3 M.

		Distribution coefficients			
		Stripping DTPA concentration, g/L			
Element	Extraction	10	15	20	30
Cs	11.7	0.164	0.160	0.163	0.160
Sr	1.33	0.013	0.015	0.009	0.013
Eu	8.94	0.008	0.007	0.002	0.001

Data on stripping of different radionuclides from the UNEX-solvent (0.08 *M* CCD, 0.02 *M* Ph_2Bu_2CMPO, 0.5 vol % PEG-400 in FS-13) indicate that 1.5 *M* MAC + 10 g/l DTPA solution efficiently strips the radionuclides from the UNEX solvent.

Distillation of the strip solutions was investigated to determine the effect of the complexant contained in the strip solutions on the composition of the distillate. This was done as follows: 200 ml of strip solution were distilled and 30 ml fractions were taken as a function of time. In each fraction, the content of methylamine carbonate was determined by methylamine titration up to a pH of 2.5. Solutions of strip product having the following compositions were studied: a)

2.5 *M* MAC; b) 2.5 *M* MAC + 20 g/L DTPA; c) 2.5 *M* MAC + 10 g/L NTA. The data obtained are shown in Figure 2.

The distillation of methylamine carbonate differs considerably from the distillation of pure methylamine solutions. On distilling pure methylamine solution (5-6 M), the methylamine content in the first distillation fractions (10-20% vol.) is equal to 12 *M.* When MAC is distilled, the methylamine concentration in the resulting MAC solution is lower. Figure 2 indicates that for all the MAC solutions the concentration of methylamine in the first fractions does not exceed 8.1 *M* (calculated from actual 4.05 *M* MAC concentration). The presence of a complexant in solution affects the composition of the fractions: the MAC concentrations in the first fractions were somewhat lower than for the MAC solution without complexants. The main conclusion drawn from the data is that in order to provide practically complete regeneration of methylamine carbonate, about 75% of the solution volume should be distilled.

The resultant strip product containing the radionuclides can be evaporated with 93-95% MAC recovery. The distillate is a methylamine carbonate solution that can be regenerated and re-used in the strip process. Analysis of the distillate by $BaC0_3$ precipitation (for $C0_3^{2'}$ analysis) and potentiometric titration with standard HCI (to determine the methyl amine concentration) indicated the ratio of CH_3NH_2:$C0_3{}^{'2}$ was 2:1 in the regenerated strip solution.

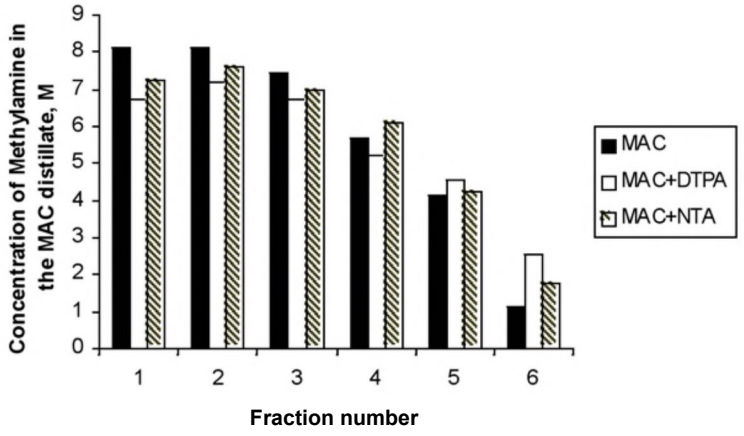


Figure 2. Methylamine concentration (as calculated from MAC concentration) in each successive 30mL distillate fraction from a 200 mL batch.

Results of flowsheet tests performed at the INEEL in centrifugal contactors showed excellent separation efficiencies of 99.92%, >99.998%, and >99.5% for Cs, Sr and Ce, respectively. During flowsheet testing, the UNEX solvent was recycled a total of nine times with no buildup of metals observed or decrease in removal efficiencies. Stripping results with freshly prepared and recycled strip reagent (methylamine carbonate/DTPA) were well within experimental error of each other, indicating that the recycled strip reagent is equally effective at stripping radionuclides from the UNEX solvent.

Centrifugal contactor flowsheet test results obtained at KRI also showed excellent separation efficiencies of 99.74%, 99.92%, and 99.96%, for Cs, Sr and Eu. During flowsheet testing, the UNEX solvent was recycled a total of twelve times with no build-up of metals observed or decrease in removal efficiencies. Stripping results of all metals with methylamine carbonate/NTA were nearly quantitative.

Based on the MAC decomposition rate in the presence of NTA and the calculated cycle dose (~ 0.29 kGy), the amount of MAC decomposed in a cycle would be no more than 0.125% of

the initial concentration. The amount of decomposed NTA based on an initial concentration of 0.044 *M* is approximately 0.33 %.

The data on concentration behavior of NTA as a function of irradiation dose in different solutions are presented in Table 3. Table 3 also includes data on MAC radiation decomposition as an illustrative example.

Table 3. Changes of MAC and NTA concentrations as a function of irradiation dose of solutions under investigation

MAC + NTA solution			Solution of MAC+NTA + salts		
Dose, MGy (W-h/L)	Concentrations		Dose, MGy (W-h/L))	Concentrations	
	MAC *m*	NTA, M		MAC *m*	NTA, M
0	2.21	8.40	0	2.19	8.30
0.49 (136)	2.18	3.60	0.50 (137)	2.17	3.60
1.08 (300)	2.15	1.46	1.08 (300)	2.15	1.45
1.69 (470)	2.11	1.09	1.69 (470)	2.10	1.07
2.45 (681)	2.08	0.78	2.45 (681)	2.08	0.80

The efficacy of stripping as a function of radiation dose was evaluated. No degradation of stripping efficiency was observed for Sr and Eu, even after exposure to doses in excess of 5 MGy. Cesium stripping improved with radiation exposure by a factor of two at 1 MGy dose over fresh strip reagent, and as much as a factor of 4 at a dose of 5.1 MGy.

CONCLUSIONS

A new class of regenerable strip reagents has been developed for the stripping of actinides, lanthanides, Cs, and Sr from cobalt dicarbollide based solvent extraction processes. Methyl amine carbonate, in combination with DTPA or NTA has been demonstrated as an effective strip solution in laboratory and countercurrent flowsheet tests using centrifugal contactors. The new regenerable strip reagent has been shown to be radiologically stable to doses in excess of 2 MGy.

ACKNOWLEDGEMENTS

The US Department of Energy Assistant Secretary supported this work for Environmental Management under DOE Idaho Operations Office contract DE-AC07-99ID13727. The US Department of Energy Office of Science and Technology's Efficient Separations and Processing Crosscutting Program also supported this work under the auspices of the Joint Coordinating Committee for Environmental Management (JCCEM), and the Tanks Focus Area.

REFERENCES

1. Romanovskiy V.N., Babain V.A., Smirnov I.V., Todd T.A., Herbst R.S., Law J.D. “Regenerable Stripping Reagents for HLW Reprocessing,” *Proceedings of Int. Conf. GLOBAL’03*- New Orleans, USA, Nov. 2003, p. 2239-2242.
2. Herbst, R. S., et al., Sep. *Sci. and Techn.,* 2003, 38(12&13), 2685-2708.
3. Wen N., Brooker M.H. “Ammonium Carbonate, Ammonium Bicarbonate, and Ammonium Carbamate Equilibria: A Raman Study,” *J. Phys. Chem.* 1995, Vol. 99, 359-368.

SOLVENT EXTRACTION OF URANIUM(VI) AND EUROPIUM(III) FROM NITRATE MEDIA BY PICOINAMIDE

Bao Bo-Rong Cheng Qian Cao Wei-Guo Xiang Qun Zhao Yujia

Department of Chemistry, Shanghai University, Shanghai 200436, China

Abstract: The extraction of U(VI) and Eu(lll) from nitric acid solution was studied with picolinamide in ethylene dichloride. The distribution ratios of U(VI) and Eu(lll) as a function of aqueous $HN0_3$ concentration , extractant concentration on organic phase and temperature as well as the salting-out agent concentration had been measured. The results showed that picolinamide had higher extractability for U(VI) than for Eu(lll). the composition of extracted species, equilibrium constants and enthalpies of extraction reaction have been also calculated.

Keywords: picolinamide , U(VI) , Eu(lll), solvent extraction

CLC numbers :0 615.11

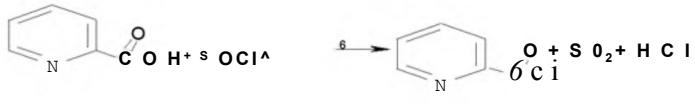
Introduction

The separation of actinide/lanthanide from effluents generated during the nuclear fuel reprocessing cycle has been extensively studied in recent years for improving the management of radioactive wastes [11,4]. It was demonstrated that the ligand with soft donor atom (pyridinic nitrogen for example) had higher affinity for the An(lll) than the Ln(lll) [p]. Furthermore, owing to their complete inflammability, and non-harmful radiolytic and hydrolytic degradation products, so picolinamide was a promising extractant. In this paper, we synthesized the extractant and studied systematically the extraction of U(VI) and Eu(lll) by picolinamide. The result showed that the distribution ratio of U(VI) was bigger than the distribution of ratio Eu(lll). The extraction mechanisms of U(VI) and Eu(lll) by picolinamide and thermodynamic parameters were also presented. [2]

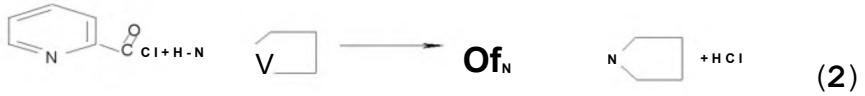
2 Experimental

2.1 Materials

Picolinamide has not been seen in literature, It was synthesized and purified at our laboratory, the synthetic route could be expressed as follows:



(1)



(2)

Its composition and structure were confirmed by IR> ^NMR and GS-MS .The result showed that the purity of the product was high enough (over 98%) for use in extraction experiments.

2.2 procedures

Distribution equilibrium was determined by contacting equal volumes of organic and aqueous phases in stopped tubes and shaking for about 30 min which was found to be sufficient for equilibrium to be reached. Experiments were carried out at 25°C except for temperature experiments. The uranium (VI) and europium(lll) contents in aqueous phase were determined by using Arsenazo-lll spctro photometric method[151] and those in organic phase were obtained by subtracting the aqueous concentration of U(VI) and Eu(lll) from the initial aqueous concentration. The distribution ratio(D) was calculated by D=concentration at organic phase/concentration at aqueous phase.

3 Results and discussion

3.1 Effect of acidity of aqueous phase on the distribution ratio

Under the conditions of 0.5mol/L picolinamide in 1,2-ethyldene dichloride and 5.0 x10"^{4}mol/L of U(VI) or 1.0x10'^{3}mol/L of Eu(lll) in aqueous phase, picolinamide has almost no extractability for U(VI) and Eu(lll) under high acidity, so we select pH=2.04 in aqueous phase in our later experiment in order to prevent the hydrolyze of metals.

3.2 Effect of the extractant concentration on the distribution ratio

The effect of the concentration of picolinamide on the distribution ratio of U(VI) and Eu(lll) show Fig 1 and Fig2. Fig 1 and Fig2 show that in the case of PH=2.04 and Cuo2^{2+}=5.0x10'^{4}mol/L or CEu(lll)=1.0x10'^{3}mol/L , the plot lgD Vs lgC$(L)_{(0}$ are straight lines with slopes0.85 and 0.88for U(VI) and Eu(lll) respectively. These values indicate that the compositions of extracted species are $U0_2(N0_3)_2L$·and $Eu(N0_3)_3L$.

Extraction reaction might be presented as follows:

$U0_2^{2+}(a)+2N0_{3(a)}^{-}+L_{(o)}=U0_2(N0_3)_2L_{(0)}$

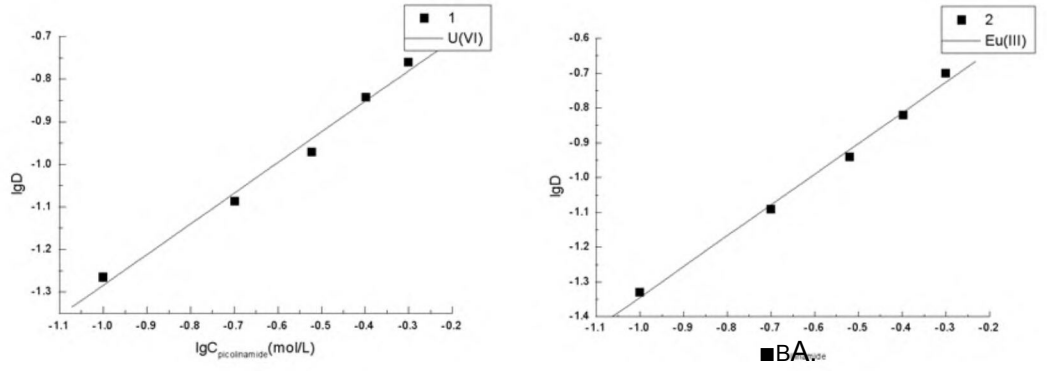
$Eu^{3+}(a)+3N0_3\ (_a)+L(0)=Eu(N0_3)_3L(0)$

Where subscript “o” refers to the species presented in organic phase and “a” refered to those in aqueous phase above reaction, the equilibrium constant Kex repectively was

$Kex_1=[U0_2(N0_3)_2\text{-}L]_{(0)}/[U0_2^{2+}]_{(a)}[N0_3'_{(a)}]^2[L]$ <„>

$Kex_2=[Eu(N0_3)3L]_{(0)}/[Eu^{3+}]_{(a)}[N0_3f[L]_{(0)}$

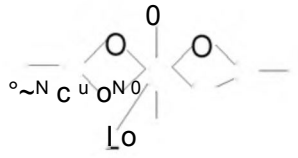
From the equation, we can get the value of Kex-i for U(VI) and Kex_2 for Eu(lll) in ethylene dichloride Kex-i= 1 .Semol^dm'^{3} , Kex_2=1.24mor^{3}dm'^{3}



FigI *Effect of picolinamide concentration in ethylene dichloride on distribution ratio of U(VI) $C_{(}uo22+)^{=}5^{x}$ 10'^{4}mol/L ,pH=2.04 ,T=298K , $V_{(0)}$:$V_{(W)}$=1:1, t=30min*

Fig2 *Effect of picolinamide concentration in ethylene dichlohde on distribution ratio of Eu(lll) C(Eu(iii))$^{=}$1 *10'^{3}mol/L ,pH=2.04 ,T=298K, $V_{(0)}$:$V_{(W]}$-1:1 , t=30min, $C_{Li}N03^{=}$4mol/L*

The IR spectra shows a shift of the pyridinic ring stretching vibration from 996.31cm'^{1} to 1011.66cm'^{1} and a shift of the carbonyl stretching vibration from 1628.56cm'^{1} to 1594.78cm'^{1}.These features imply the formation of a bidentate complex, the metal-picolinamide bonds arise through the oxygen of the carbonyl group and the nitrogen of the pyridinic ring. The appearance of bands at 1033.96cm'\ 1276.85cm'^ and 1479.07cm"^{1} in the spectra is attributed to the N-O stretching vibration and to the asymmetric stretching vibration of trans-coordinated nitrate groups , respectively, An additional band described as the U-O stretching vibration of the uranyl ion is noted at 928.37cm"$^{1(7,8)}$. Thus, these suggested structure of picolinamide/metal nitrate complex is depicted in the following scheme:



where “L” refers to picolinamide

3.3 Effect of temperature on the extraction distribution ratio

The effect of temperature in the extraction distribution ratio is shown in fig3 which indicates that D decrease with the increase in temperature for the extraction reactions of U(VI) and Eu(lll) . This means that the extraction reactions of U(VI) and Eu(lll) are exothermic.

From the slope of the graph, the enthalpies of extraction reaction could be evaluated with e q(1)

[[(lg D)/[(1/T)]p=-ArHm°/RT (1)

The heat of reaction for the extraction of U(VI) and Eu(lll) by picolinamide was estimated to be: AH°($U0_2^{2+}$)=-6.1KJ/mol

A/-/°Eu^{3+}=-7.81 KJ/mol

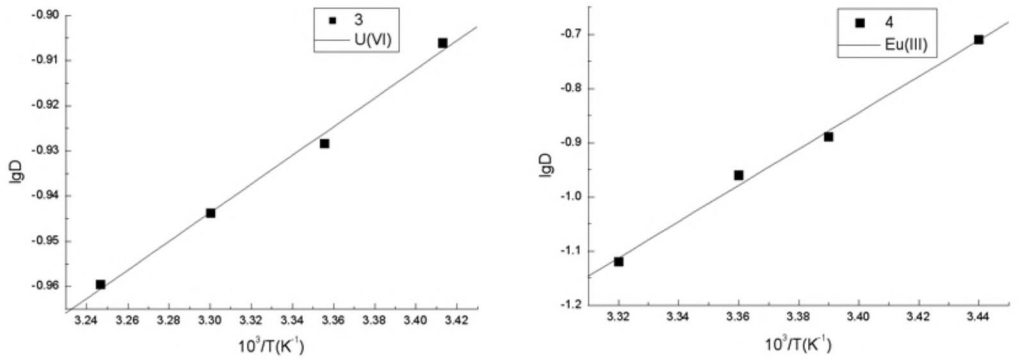


Fig3 *Dependence of distribution ratio of U(VI) on temperature*
*[U02²⁺]=5.0*1 O'⁴ mol/L'¹ , PH=2.04,$V_{(O)}$:$V_{(W)}$=1:1, t=30min,Cpicolinamide=0.4 mol/L'¹*
Fig4 *Effect of temperature on distribution ratio of Eu(lll)*
*C(Eu<iii)r1 *1 O'³mol/L ,pH=2.04 ,C(picolinamide)=0.3 mol/L'¹ ,V(o>:V(wr1:1, t=30min*
C_{UNO3} ~ 4 mol/L

3.4 Effect of salting-out agent concentration on distribution ratio of U(VI) and Eu(III)

In order to examine the variation of Du and DEu as a function of salting-out agent concentration, the extractability of U(VI) and Eu(lll) from 1 to 5 mol/L salting-out agent into 0.4mol/L picolinamide in ethylene dichloride was observed(Fig5). The experimental results show that Du and DEu increases with the increase of salting-out agent concentration. However, increase in distribution ratio for U(VI) is obvious with the increase of concentration of salting-out agent and the increase for Eu(lll) is not obvious. In addition, the tablel shows that a good separation factor $SF_{U/Eu}$ equal 14.36 was obtained for the whole $LiN0_3$ concentration range.

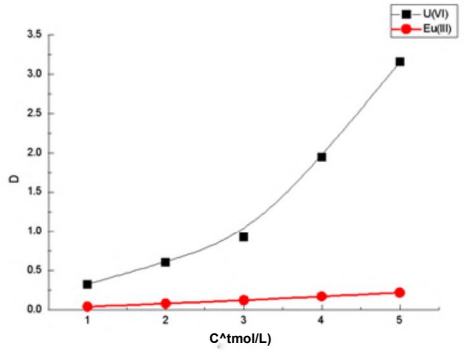


Fig5 *Extraction of U(VI) and Eu(lll) nitrate by 0.5mol/L picolinamide in ethyldene dichloride at room temperature. The aqueous phase contained HNO_3(0.01 mol/L) and $LiN0_3$.*

Tablel Variation of parti on coefficient with concentration of LiN03 in aqueous solution for the extraction of U(VI) and Eu(lll)

CLiN03(mol/L)	1	2	3	4	5
Du	0.33	0.61	0.93	1.95	3.16
DEu	0.041	0.08	0.12	0.17	0.22
pu/Eu	8.05	7.63	7.75	11.47	14.36

Conclusion

From the data, we can conclude that picolinamide has a better ability for the extraction of U(VI) than for the extraction of Eu(lll), the reason is that picolinamide with soft donor atom (pyridinic nitrogen) has higher affinity for An than for Ln. The addition of saluting-out agent can improve the separation of An and Ln. The extraction reactions for U(VI) and Eu(lll) are exotheromic, and compositions of extracted species are $U0_2^{2+}(N0_3)_2L\cdot$ and $Eu(N0_3)_3L.\cdot$

References

1 Nigand L, Condamines N, Cofdeer P.Y, et al. *Separation Science and Technology,* 1995, 30(7-9): 2075

2 Berthon L, Cordier P.Y, Bonvour F, et al. [A].ln:ISEC, MELBOURNE AUSTRALLA. AUSTRALLA, 1996.1339

3 Yu Shao-Ning, Ma Li, Bao Bo-Rong. *Radio analytical and Nuclear Chemistry.* 1999,240: 219-221

4 Yu Shao-Ning, Ma Li, Bao Bo-Rong. *Nuclear Science and TechniquesA998.9{2):'\'\8-'\20*

5 Xiang Qun, Bao Bo-Rong, Qian Qun, et al. *Nuclear Science and Techniques,*2003,14(3): 168

6 Sun Guo-Xin, Han Jing-Tian, Bao Bo-Rong. *Nuclear Science and Techniques,* 1998, 9:115

7 Han Jing-Tian, Shao Hua, Zhu Jian-kang, et al. Journal of *Radioanalytical and Nuclear Chemistry,* 1999,241 (3):679-681

8 Sun Guo-Xin, Bao Bo-Rong. et al. Journal of *Radioanalytical and Nuclear Chemistry,* 1997,218(1):101-102



MINI-PLANT TESTING OF URANIUM SOLVENT EXTRACTION PROCESS FOR ACID LEACH LIQUORS CONTAINING CHLORIDE

Karin Soldenhoff, Deborah Wilkins, Marleine Shamieh and Adrian Manis

Australian Nuclear Science & Technology Organisation, Sydney, Australia

Solvent extraction, using tertiary amine type reagents, is a well established technology used for the purification of uranium from sulphuric acid leach liquors. The presence of chloride ions is detrimental to this process, suppressing uranium extraction. This issue is of particular importance for uranium recovery from sites that contain chloride in the ground water and/or process water. In this work, we present results of a continuous mini-plant trial to test the performance of a mixed di-2-ethylhexyl phosphoric acid (DEHPA) and a tertiary amine (Alamine 336) solvent, for uranium extraction from sulphuric acid leach liquors containing 8 g L^{-1} chloride. We also introduce a novel concept of coupling nanofiltration and solvent extraction technologies in order to recycle acid to the strip circuit and reduce the overall acid consumption required for stripping.

INTRODUCTION

Solvent extraction is a well established technology used for the purification of uranium from sulphuric acid leach liquors. Tertiary amine type reagents are widely used for this purpose, with options for stripping including chloride [1], ammonium sulphate/ammonia [2] and sulphuric acid stripping [3], The presence of chloride ions is detrimental to uranium extraction, since chloride competes with uranyl sulphate anions for the amine [4], The sources of chloride in the feed to solvent extraction include the use of chlorate as an oxidizing agent during leaching and the salinity content in the ground water/process water. These sources of chloride can be exacerbated by the recycle of solvent extraction raffinate as process water.

The salinity content of the ground water is an issue pertinent to certain parts of Australia. In the case of the Honeymoon project in South Australia, the leach liquors contained such high chloride that the conventional solvent extraction process was not deemed to be appropriate. It was reported that a mixed solvent system containing di-2-ethylhexyl phosphoric acid (DEHPA) and a tertiary amine was tested in a trial plant, but few details have been published [5]

In our previous work, we reported on the selectivity for uranium of solvent systems containing mixtures of DEHPA and primary, secondary or tertiary amines [4], In this work we present results of a continuous mini-plant trial, to test the performance of a mixed DEHPA/ tertiary amine solvent, using strong acid stripping. We also introduce a novel concept of coupling nanofiltration and solvent extraction technologies in order to recycle acid to the strip circuit and reduce the overall acid consumption required for stripping.

EXPERIMENTAL

Batch Tests

Loading curves were obtained by contacting aqueous and solvent solutions at varying phase ratios at controlled pH. Extractants used were di-2-ethylhexyl phosphoric acid (DEHPA), supplied by Albright & Wilson and Alamine 336, a straight chained C_8C_{10} tertiary amine mixture, supplied by Henkel. Diluents used were Shellsol 2046 and Shellsol D70, supplied by Shell. Isodecanol was supplied by Exxon. Aqueous solution consisted of plant sulphuric acid leach liquor obtained from an operating uranium mine and doped with NaCl as required. Aqueous uranium concentrations were determined by ICP or ICP-MS. Solvent samples were stripped with Na_2C0_3 and the aqueous solution analysed for uranium by ICP. Chloride analyses were carried out with an ion-selective electrode.

Mini-Plant Equipment

The solvent extraction mini pilot-plant consisted of a series of mixer-settlers arranged as a 4-stage extraction, 4-stage scrub, 6-stage strip and a single stage wash circuit. The mixers in the extraction circuit were 0.5 L in volume with 0.017 m^2 settler area. All the other mixer-settlers were 0.15 L mixers with 0.006 m^2 settler area. The feed flowrate to the mini-plant was 9 L h'^1. The mini-plant was operated for 47 hours. The mixer-settlers were operated with organic recycle in the extraction circuit, and with aqueous recycle in the other circuits.

The recovery of sulphuric acid by nanofiltration was tested continuously on a flat-sheet (137 cm^2 membrane area), cross-flow apparatus. The membrane used was a DK nanofiltration membrane, supplied by Osmonics. The apparatus was operated at 4 MPa, with concentrate recycle and cross-flow velocity between 0.2-0.3 m s'^1. The feed flowrate was 0.28 L h'^1.

RESULTS AND DISCUSSION

Process Description

The circuit configuration used for testing an alternative process for uranium extraction is shown in Figure 1. Plant sulphuric acid leach liquor was obtained from an operating uranium mine and was used as feed for the mini-plant. The acidity of the feed was adjusted to pH 1.2 by addition of concentrated sulphuric acid, and the liquor was doped with NaCl to a concentration of 8 g/L Cl. The feed composition is given in Table 1. The solvent consisted of a mixture of DEHPA and Alamine 336 with Shellsol 2046 as a diluent. Uranium was selectively extracted into the solvent in the extraction circuit. A dilute acid scrub (0.1 M H_2S0_4) was used to remove co-extracted chloride and ferric ion from the loaded solvent. The uranium was stripped from the solvent with 5.6 M H_2S0_4. The strip solvent was washed with water to remove sulphuric acid, and the solvent was then recycled to the extraction circuit. Loaded strip solution produced during the mini-plant trial was used as feed to the nanofiltration to aenerate two streams: a oermeate stream containina mainlv subhuric acid for recycle to the solvent extraction strip circuit, and a concentrate stream containing most of the uranium for uranium precipitation.

Extraction and Scrub Circuit Performance

Extraction of uranium with a tertiary amine is suppressed by the presence of chloride in the feed liquor, when the chloride concentration is above 2 g L'^1 Cl. By way of comparison, uranium leach liquor was contacted with a conventional solvent containing 5 vol% Alamine 336, which is commonly used in uranium solvent extraction plants. Results of batch tests showed that a maximum of 6.3 g L'^1 uranium loading is achievable, for a feed solution containing 1 g L'^1 U and no chloride (Figure 2). Results for a similar feed, doped with 8 g L'^1 Cl, show that the maximum uranium loading decreased by 42% to 3.7 g $L"^1$ U. The reduced uranium loading capacity of the solvent limits the operating range ratio of aqueous to organic flowrate, thus effectively reducing plant throughput. Therefore, the presence of chloride can

have a significant negative impact on the uranium solvent extraction process using a tertiary amine type solvent.

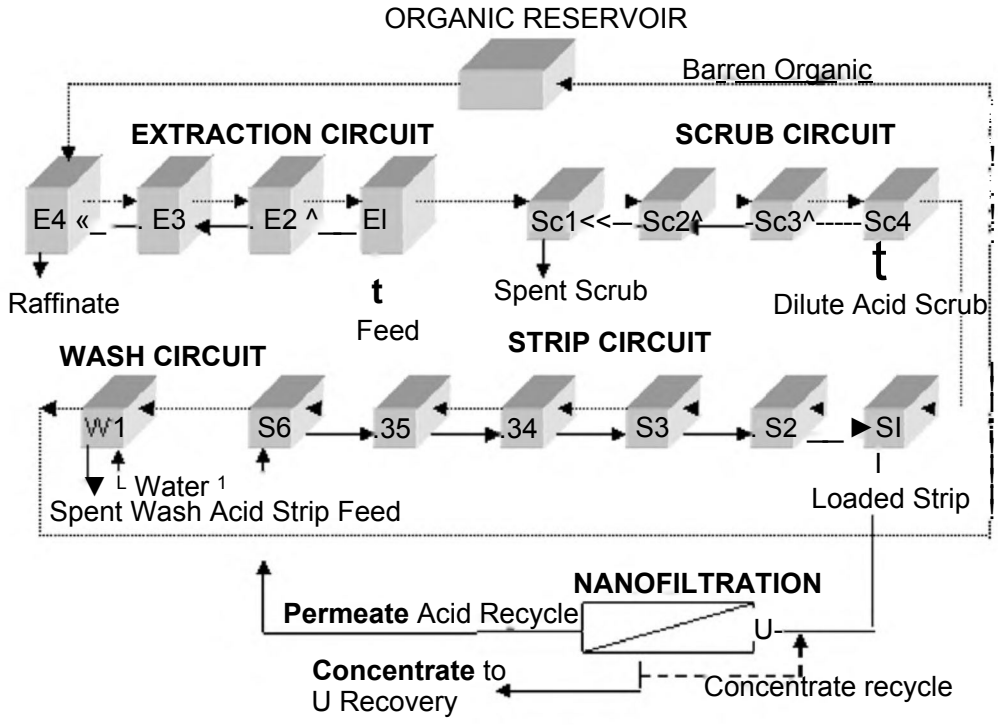


Figure 1. Flowsheet for an alternative uranium extraction process using a mixed solvent

ANSTO has been working on a modified uranium solvent extraction process, to target uranium extraction from sulphuric acid leach liquors containing chloride, using a solvent mixture of DEHPA and Alamine 336. Batch loading tests using the mixed solvent show that uranium extraction is not affected by the presence of chloride, unlike the Alamine 336 conventional solvent. For a feed liquor containing 8 g L^{-1} Cl, high uranium loadings can be achieved (see Figure 2).

The performance of the mixed solvent was further tested in continuous-counter current tests, carried out in a mini-plant, mixer-settler circuit. One of the main concerns with using an alternative solvent for uranium extraction is its performance with respect to selectivity for uranium over ferric ion. Operating conditions for the continuous mini-plant trials were therefore optimised to maximise rejection of ferric ion to the raffinate and spent scrub streams.

Mini-plant data for the extraction and scrub circuit is presented in Table 1. The feed liquor contained approximately 1 g L^{-1} U and 1.2 g L^{-1} Fe as ferric. The feed was doped with 8 g L^{-1} Cl. Under optimised conditions for rejection of ferric ion, >98% uranium extraction was achieved in four stages of extraction, with pH control at 1.2. The data is Table 1 show that very high selectivity for U over Fe was obtained during extraction. This was further enhanced by Fe rejection to the spent scrub, with only 0.17% of the total Fe present in the feed reporting to the scrubbed organic. Chloride was only partially extracted, but was effectively scrubbed. The scrub solution used was dilute sulphuric acid (0.1 M H_2SO_4).

The degree of rejection of Fe obtained in these tests is comparable to operations using conventional tertiary amines as the sole extracting reagent, so this testwork achieved one of

its main objectives, namely, to demonstrate in continuous counter-current tests, that high selectivity of uranium with respect to ferric ion is achievable with a mixed DEHPA/amine solvent.

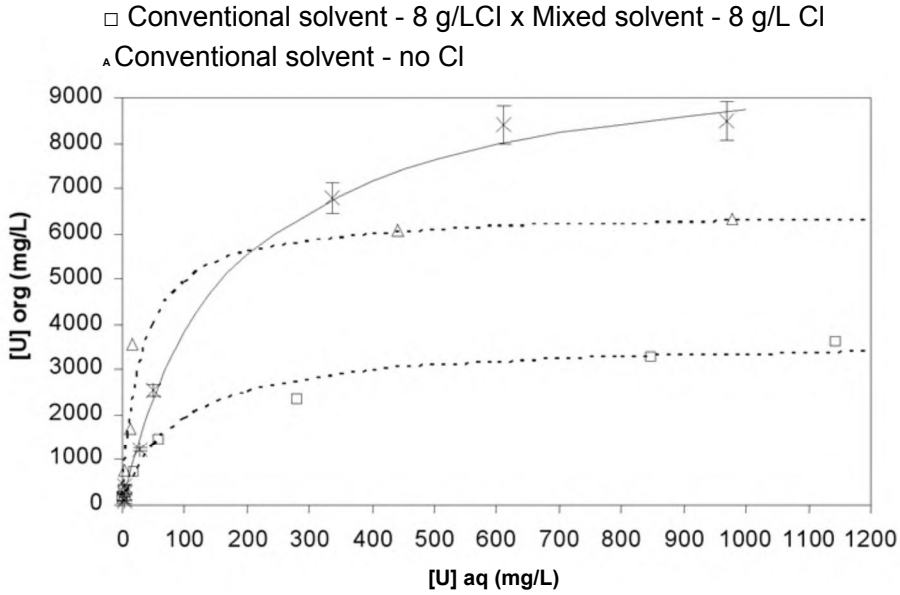


Figure 2. Equilibrium batch loading data comparing Uranium extraction from solutions containing 8 g L'[1] *chloride.*
Conventional Alamine solvent = 5 vol% Alamine 336, 2 vo/% isodecanol in Shellsol D70, pH = 1.5
Mixed solvent contains Alamine 336 and DEHPA in Shellsol 2046, pH = 1.2
Error bars represent ±5% error

Table 1. Mini-pilot plant data for uranium extraction with mixed DEHPA/Alamine 336 solvent
Extraction circuit A/Q=6.6, pH=1.2, Scrub circuit O/A =3.1

Element	Feed mg/L	Loaded Organic mg/L	Extraction Efficiency %	Spent Scrub mg/L	Scrub Efficiency %
U	975	6390	98.6	193	0.97
Fe	1170	34	0.44	64	61
Cl	8040	716	1.4	1377	62

Strip and Wash Circuit
There are a number of alternative options available for stripping uranium from a mixed DEHPA/Alamine 336 solvent, including alkaline and acid stripping. Stripping with ammonium sulphate/ammonia, is common practice in uranium solvent extraction plants, but it is not applicable to the mixed DEHPA/Alamine 336 solvent, as uranium is not stripped. However, ammonium carbonate or sodium carbonate stripping can be effective in stripping uranium, but if any ferric ion is co-extracted into the solvent, it will precipitate in the strip circuit.

In this work we opted to test acid stripping with in a six stage strip circuit, using 5.6 M H_2S0_4. Uranium concentrations in each stage of the strip circuit are shown in Figure 3. Under these conditions, in excess of 90% uranium stripping was obtained, with stripped solvent forwarded

to the wash stage containing 0.6 g L'[1] U. The loaded strip liquor contained 25 g L^{-1} U and 4.6 M H_2S0_4.

The stripped solvent was subject to a single stage water wash, to remove sulphuric acid from the solvent, prior to recycling of solvent to the extraction circuit. The wash stage was operated at a O/A flowrate ratio of 5.75 and the spent wash contained 0.32 M H_2S0_4. This stream was a clean acid stream which could be re-used in the scrub circuit. The wash circuit recovered approximately 25% of the acid lost from the aqueous strip liquor.

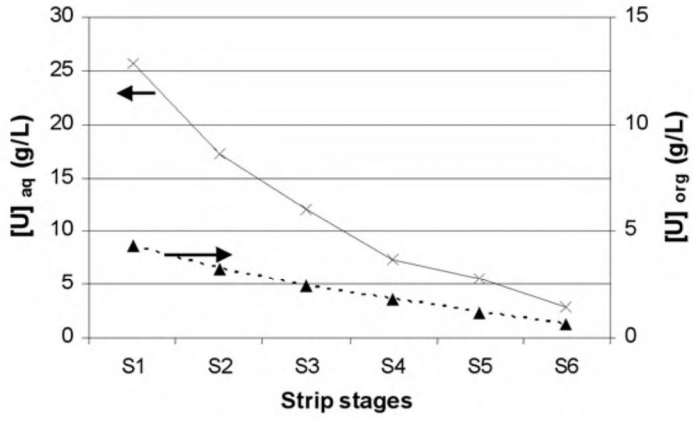


Figure 3. Uranium concentration profile in the mini-plant strip circuit

Nanofiltration for acid recycle from loaded uranium strip liquor

The acid concentration required for stripping the mixed solvent was found to be higher than that required for acid stripping of uranium from a tertiary amine solvent. It is reported that the Rabbit Lake operation in Canada, using the conventional amine solvent has five stages of strong acid stripping (4.5 M H_2S0_4). The loaded strip liquor then undergoes neutralisation and gypsum filtration, prior to uranium recovery by hydrogen peroxide precipitation [3], In comparison, the mixed solvent DEHPA/Alamine 336 required 5.6 M sulphuric acid for effective stripping.

In order to improve the economics of the mixed solvent uranium extraction process we tested a novel concept of coupling the strip circuit with a nanofiltration step. Nanofiltration membranes have pore sizes which fall between ultrafiltration and reverse osmosis membranes, and reject solutes based both on size and charge. Nanofiltration membranes are characterised by high rejection of divalent and higher charged cations, but tend to have lower rejections of monovalent cations and their counter ions.

The recovery of sulphuric acid from uranium loaded strip solutions was tested continuously on a flat-sheet cross-flow rig. The solutions used as feed for the nanofiltration were produced during operation of the mini-plant solvent extraction operation for uranium recovery. However, these two process units (ie. solvent extraction and nanofiltration) were not operated in an integrated, continuous mode.

An example of the potential of the nanofiltration technique for acid recovery is presented in Table 2. In this particular test, 97% local rejection of uranium was achieved with no rejection of sulphuric acid after 13 hours of continuous operation. These results illustrate how the uranium and the sulphuric acid fed to the nanofiltration unit were separated into two streams so that 72% of the sulphuric acid and 7.4 % of the uranium reported to the permeate solution, and 93% of the uranium reported to the concentrate solution. The permeate, after adjustment of acidity, could be recycled to the strip circuit. The concentrate, containing only 28% of the acid present in the loaded strip, could proceed to neutralisation and precipitation

for uranium recovery. Decreasing the molar ratio of H_2S0_4:U in the solution prior to uranium recovery can represent a significant saving in acid consumption. One drawback of nanofiltration technology applied in this context, is that the current membranes available have limited chemical resistance when exposed to high acid concentrations, and therefore, membrane lifetime is a current limitation of this technology.

Table 2. Flat-sheet cross-flow nanofiltration operated at 4 MPa
Permeate flux = 13 l_/m²/h, Flat-sheet Osmonics DK Membrane, 0.3 m s'¹ cross flow velocity

	Flowrate L/h	U g/L	Acid M	Molar Ratio H_2S0_4:U
Feed	0.28	11.3	4.00	84
Concentrate	0.08	39.3	4.17*	25
Permeate	0.20	1.2	4.06	832

* by mass balance

CONCLUSIONS

This work has demonstrated the potential of uranium extraction and purification from sulphuric acid leach liquors containing 8 g L'¹ chloride using a mixed DEHPA/Alamine 336 solvent. It was shown that whilst uranium extraction is significantly suppressed with a conventional tertiary amine solvent, the mixed solvent performed well in a continuous mixer-settler mini-plant.

The coupling of nanofiltration with an acid strip in a solvent extraction circuit potentially allows for acid recycle via the nanofiltration permeate. Negligible sulphuric acid rejection and high uranium local rejection (97%) were obtained in a test carried out on uranium loaded strip liquors using a cross-flow nanofiltration rig.

ACKNOWLEDGMENTS

This work is published with the permission of the Australian Nuclear Science and Technology Organisation (ANSTO).

REFERENCES

1. H.A. Schnell, E. Doel and E. Corpu (2000). *Uranium 2000 International Symposium on the Process Metallurgy of Uranium,* Saskatoon, Canada, pp. 131-147
2. Uranium Extraction Technology, (1993). *IAEA Technical Report Series* No.359, pp157-233
3. W. Milde (1989). *CIM Bulletin,* December 1989, pp 69-75
4. K. Soldenhoff, D. Wilkins, M. Shamieh and R. Ring (2000). *Uranium 2000 International Symposium on the Process Metallurgy of Uranium,* Saskatoon, Canada, pp. 339-351
5. T. Hunter (2002). *The AusIMM Bulletin,* September/October 2002, pp 12-20.



PHENOL EXTRACTION BY CLOUD POINT: SYSTEMS WATER/RENEX/PHENOL

A. A. Dantas. Neto, K. S. M. G. Sousa, E. L. Barros. Neto, T. N. C. Dantas, M. C. P. A Moura

Departamento de Engenharia Quimica - Universidade Federal do Rio Grande do Norte/UFRN, Campus Universitario, S/N - CEP 59.072-970 - Natal - RN - Brazil.

e-mail: Eduardo@ea.ufrn.br. karlasilvana@ea.ufrn.br

The objective of this work is to study the effect of parameters such as salinity and phenol concentration in the cloud curve of nonionic surfactants seeking its application in the extraction process of organic solutes. Phenol was chosen as model to represent pollutants that are present in wastewaters from petrochemical industry and NaCl as salt. Knowing the recognized importance of surfactants in different liquid-liquid extraction processes due to its high efficiency and extracting properties, they can be used, more precisely the nonionic ones, in substitution to organic solvents. In this research phase diagrams water/surfactants/phenol were obtained seeking to evaluate cloud temperature in several surfactant concentrations.

INTRODUCTION

The use of a new separation technique based on micelle mediated extraction procedures is the Cloud Point Extraction. The method is based on the phase separation properties of aqueous nonionic surfactant solutions upon increase of the solution to a certain temperature above which the solution becomes cloudy (hazy).These dynamic micellar entities, having a non-polar core, possess the capacity to interact with non-polar species by hydrophobic interactions. During the cloud point precipitation process, these micellar vesicles aggregate into a surfactant-rich phase, and any bound non-polar species concentrate in the surfactant-rich phase. Although considerable research has been presented hitherto aiming at the determination of non-polar organic compounds and metallic species, after proper derivatization [1], no attempt has been made towards the preconcentration of anionic species.

Nonionic surfactants find applications in several industrial fields. Its versatility and applications are enormous. Some applications are connected with adsorption abilities of surfactants having an amphiphilic character. Other applications exploit the abilities of surfactants to form micelles. However, surfactants are often used in such concentrations that both adsorption and micellization phenomena are exploited.

Extraction is a well-known technique used to recover and separate various substances including undesirable organic pollutants. The use of hydrocarbons as diluents is the main drawback of extraction. New ecologically friendly techniques are expected to be developed in the 21st century. Some new separation techniques were proposed and are extensively studied [2-11], Nonionic surfactants or polyoxyethylene dissolved in aqueous solutions can be separated as a surfactant-rich phase by the breaking of the hydrogen bonds between

oxygen atoms of polyoxyethylene chains and water molecules. That breaking can be achieved by an increase in temperature or by addition of appropriate electrolytes [7], The former is used to separate the surfactant phase above its cloud point. The separated surfactant-rich phase is less hydrophilic than the micellar aqueous phase. As a result, various organic substances can be transferred to the surfactant phase and significantly enriched as the volume of the surfactant phase is one order lower than the volume of the aqueous phase [8-10],

The extraction process by cloud point is influenced by parameters such as: salinity; phenol initial concentration; surfactant concentration; and difference between process temperature and temperature in which the solution becomes cloudy. As a consequence, the study of these parameters is necessary to evaluate the extraction process and its viability.

MATERIALS AND METHODS

Chemicals

The surfactant used in this research was Renex 95 (polyoxyethene) and it was kindly supplied by Oxiteno Ltd. The used reagents were phenol and NaCl (Merck). Distilled water was used in all experiments. The solvents used in liquid-chromatography were acetonitrile and methyl alcohol of high purity (Merck).

Obtaining of cloud curves

The cloud curves were obtained using Renex 95 in water solutions. After, phenol and NaCl were added to evaluate its effect. The extraction process was accomplished at temperatures above to the cloud temperature and the obtained phases were analyzed in a high performance liquid chromatography system.

Extraction Process

The cloud point of a solution containing nonionic surfactants in aqueous solutions can recover from an initial aqueous phase any solute that is soluble in the coacervate phase. These solutions when heated to a temperature above to its cloud point separate in two phases in equilibrium: the diluted phase (low surfactant concentration and solute) and the coacervate phase (high surfactant concentration and solute), as can be seen in Figure 1.

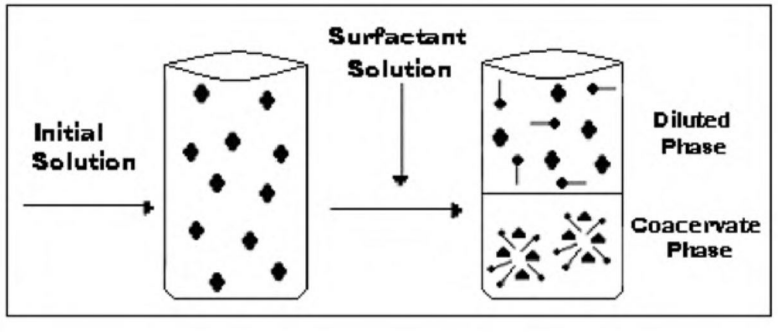


Figura 1: Schematic representation of the extraction system by coacervate.

RESULTS AND DISCUSSIONS

Cloud curves

The effects of addictives on the cloud temperature of the used nonionic surfactants were studied. Through the obtained diagrams (Figures 2 to 4) can be verified that the addition of eletrolytes and organic compounds alters the cloud temperature.

In Figure 2 can be observed that an increase in NaCl concentration reduces significantly the cloud temperature of nonionic surfactant solutions. This occurs because NaCl is totally solubilized in the aqueous phase, resulting in a reduction in the interactions between the hydrophilic portion of the surfactant and the water.

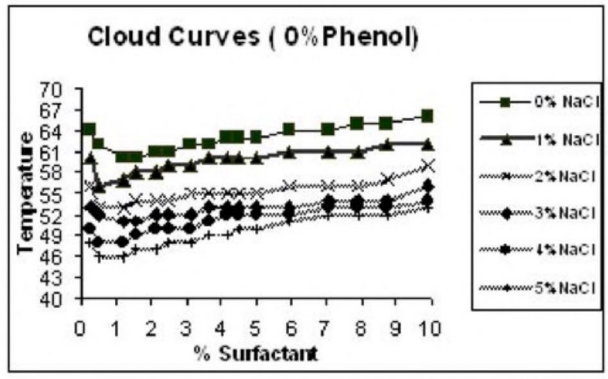


Figure 2: *Phase diagram showing salinity influence in the cloud point.*

Figures 3 and 4 show that the addition of phenol to nonionic surfactant systems also reduces the surfactant cloud temperature and the solubilitization of this compound by the surfactants affects in a direct way its solubility in water. This occurs due to the fact that phenol (a polar compound) to be positioned between the surfactant molecules that are in the micelles, as a result the surfactant-water interactions are reduced and the cloud point also decreases. Still analyzing the effect of phenol, one can observe that its addition cause a change in the form of the cloud curves, being more pronounced when the surfactant concentration is decreased, what differs of NaCl influence. This happens due to phenol saturation in micelles at low surfactant concentrations, that is, with increasing surfactant concentration the phenol-surfactant ratio decreases and the effect in the reduction of the cloud temperature is decreased.

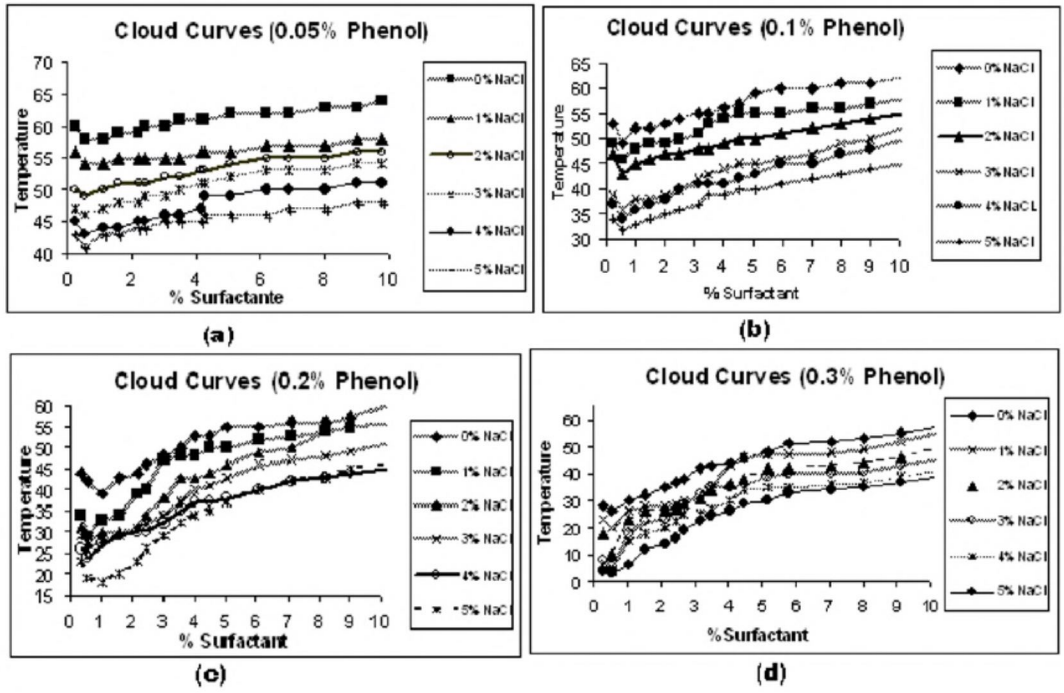


Figure 3:*. Phase diagrams showing salinity and phenol presence influence, (a) 0.05% phenol (b) 0.1% phenol (c) 0.2% phenol (d) 0.3% Phenol.*

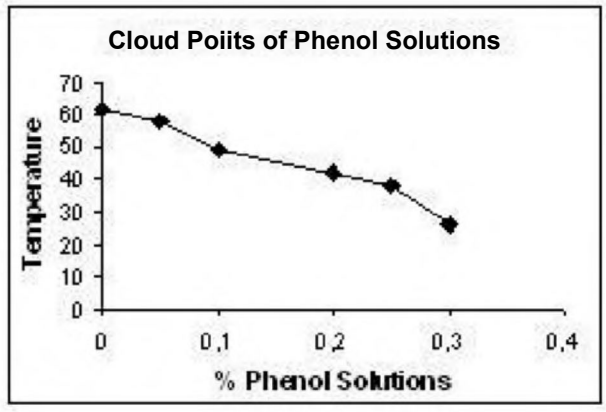


Figure 4: Cloud curve using phenol solutions.

CONCLUSIONS

From the obtained diagrams one can conclude that an increase in NaCl concentration in the systems containing nonionic surfactant causes a significant reduction in the cloud temperature due to the reduction of surfactant solubility in water. Phenol addition to nonionic surfactant systems also reduces the surfactant cloud temperature and the solubilization of phenol by surfactant affects directly surfactant solubility in water. Comparing the two addictives used one can observe that the reduction phenomenon in the cloud temperature always happen, but in each case it is made in a different way, where in the case of NaCl the solubilization occurs in the aqueous medium while with phenol the solubilzation occurs in micellar formations.

ACKNOWLEDGEMENTS

The authors are grateful for the financial support given by CNPq and also acknowledge OXITENO for providing surfactant samples.

REFERENCES

I. Giokas DL, Antelo J, Paleologos EK, Arce F, Karayannis Ml. Copper fractionation with dissolved organic matter in natural waters and wastewater - a mixed micelle mediated methodology (cloud point extraction) employing flame atomic absorption spectrometry. *J Environ Monit* 2002a;4:505

2 Scamehorn, J. F., *in* “Surfactant-Based Separation Processes: Surfactant Science Series” (J. H. Harwell. Ed.). Vol. 33. Dekker. New York. 1989.

3. Fillipi, B. R., Scamehorn, J. F., Christian, S. D., and Taylor,R.W., *J. Membr. Sci.* 145, 27 (1998).

4. Son, S. G., Hebrant, M., Tecilla, P., Scrimin, P., and Tondre, C. J., *Phys. Chem.* 96, 11072 (1992).

5. Tondre, C., Son, S. G., Hebrant, M., Scrimin, P., and Tecilla, P., *Langmuir* 9, 950 (1993).

6. Adamczak, H., Materna, K., Urbanski, R., and Szymanowski, J., *J. Colloid Interface Sci.* 218, 359 (1999).

7. Rogers, R. D., Zhang, J., and Bauer, C. B., *J. Alloys Compd.* 249, 41 (1997).

8. Hinze, W. L., and Pramauro, E., *Crit. Rev. Anal. Chem.* 24, 133 (1993).

9. Materna, K., Milosz, I., Miesiac, I., Cote, G., and Szymanowski, J. *Environ Sci. Technol.* 35, 2341 (2001).

10. Akita, S., and Takeuchi, H., Sep. *Sci. Technol.* 30, 833 (1995).

II. Akita, S., Rovira, M., Sastre, A. M., and Takeuchi, H., Sep. *Sci. Technol.* 33, 2159 (1998).

COMPLEXATION BEHAVIOR OF OLEFIN ISOMERS IN REACTIVE SOLVENTS

Bart Wentink, Norbert J.M. Kuipers, André B. de Haan, Japie Scholtz*, Harko Mulder *

University of Twente, Enschede, The Netherlands
*Sasol Technology, Sasolburg, South Africa

Recovery of (a-) olefin isomers is an important and most energy-intensive separation practiced in industry due to relative volatilities close to unity. These separations can be facilitated by application of reactive solvents based on transition metal-ligand complexes, which selectively and reversibly form 7t-complexes with these olefins. These metal-complexing ligands can be derived from those already developed and commercially applied in hydrometallurgy.

The feasibility of this concept is evaluated by analysis of the complexation behaviour of various synthesized silver-ligand complexes for different C6-olefin isomers (branched, cyclic and internal mono-olefins, di-olefins) as a function of their relative amounts and temperature. The effect of ligand structure is also investigated by varying the type of functional group and the size of the organic tail. The performance of these reactive solvents depends on the capability of the ligand to stabilize the silver in solution, while still retaining the silver ability to 7t-complex with the olefin.

Various types of ligands, like LIX26, LIX54, LIX79, TOPO, the Cyanexes 272, 301, 302, 471X and 15-crown-5 were screened and observed either to form no silver complexes or non-reactive complexes towards ethylene and therefore also with C6-olefins showing less complexing capabilities. However, both phosphoric acids and sulphonic acids like D2EHPA and DNNSA are suitable ligands for both ethylene and the C6-olefins due to their intermediate bonding strength with the silver ion. Different complex stoichiometries were identified for the various C6 isomers and characterised as primary, secondary and tertiary complexes, depending on the concentration of olefin relative to silver. Selectivity is obtained because the complexation constants depend on the olefin structure as a result of differences in the entropy of complexation. The enthalpy of complexation is the same for all tested mono-olefins. The selectivity can be further increased (> 1.3) by reducing the tail size as is observed for MEHPA (mono ethyl hexyl phosphoric acid), DBPA (di butyl phosphoric acid) and DBSA (dodecyl benzyl sulphonic acid).

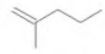
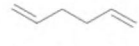
INTRODUCTION

Higher (> C_6) a-olefins are used in the polymer industries as co-monomers (mainly 1-hexene and 1-octene) in the production of HDPE or LLDPE, and also in the oxo-process to produce linear alcohols used in plasticizers. One possible production route is the recovery from Fischer-Tropsch streams. However, in this process many olefin isomers are co-produced

with a relative volatility close to unity with respect to the desired a-olefin. The separation of a-olefins from these streams is therefore a difficult operation, which is further complicated by the wide component spectrum of such streams. Table 1 presents a simplified composition of the C6-cut from such a Fischer-Tropsch process showing various structural isomers and their unfavourable relative volatility relative to 1-hexene.

Various synthesized metal-ligand complexes will be evaluated for reversibly forming complexes with ethylene, using the latter as a good indicator for the complexation ability of C6- olefins. If so, these complexes and promising derivatives of varying tail length and functional group are evaluated in a VLE-setup for sufficient selectivity and capacity to recover 1-hexene by Reactive Extractive Distillation (RED) from the isomer mixture in Table 1.

Table 1. Simplified component spectrum of C6-cut from Fischer-Tropsch stream and their relative volatility (RV) with respect to 1-hexene at 300 K.

Olefin type	Composi-tion (wt%)	Model component	Symbol	Structure	RV
a-olefin	58.6	1-hexene	1H		1.00
branched olefin	22.9	2-methyl-1-pentene	2M1P		1.06
internal olefin	2.2	2-hexene (cis/trans)	C2H,T2H		0.81,0.84
cyclic olefin	1.7	1-methylcyclopentene	1MCP		0.63
diolefin	0.032	1,5-hexadiene	15HD		1.20
paraffin	14.6	n-hexane	NH		0.82

POTENTIAL REACTIVE SOLVENTS

The selected reaction to be applied for the separation of olefin isomers is n-complexation where a rc-bond is formed when a transition metal ion reversibly bonds with an olefin, *n*-Complexation has the advantage that the selectivity is embedded within the olefin structure as the side-groups around the double bond result in steric hindrance. This means that the highest complexation constant, at equal carbon number and degree of unsaturation, should be found for the a-olefin and that it decreases with increasing substituent size around the double bond.

This reactive concept can be incorporated in Extractive Distillation by enriching a conventional extraction solvent with metal ions capable of forming ^-complexes. Practically these metals are restricted to either copper(I) or silver(I) because they form reversible complexes whereas the metals itself are relative inexpensive. Other transition metals like Pt(II), Pd(II) form more stable complexes that are too difficult to decomplex and are very expensive.

To apply a metal ion with sufficient loading capacity in a distillation process it should be dissolved in a liquid showing a high solubility for the olefin. Though silver nitrate (3 M) dissolved in ethylene glycol shows a high vapour-liquid selectivity of 1.8 (at 300 K) for 1H over 2M1P, its capacity is far too low for practical application. Therefore, a (dissolved) Cu(I) or Ag(I)-ligand complex is suggested. This concept is schematically represented in Figure 1.

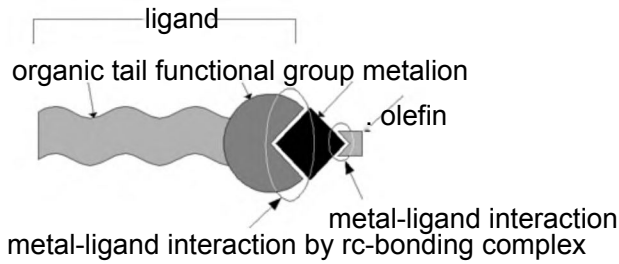
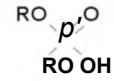
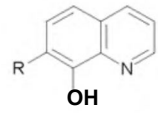
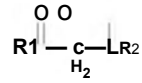
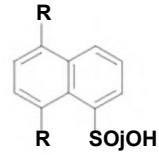
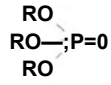
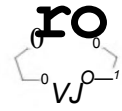
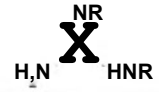


Figure 1. Schematic representation of a metal-ligand-olefin complex

Table 2. Overview selected silver-ligands (EM = extraction mechanism, A = acidic, IP = ion-pair, S = solvating, n.r. = not reported)

acronym	trivial name	formula	structural formula	organic tail (R, R,, R_2)	EM
D2EHPA	di(2-ethylhexyl) phosphoric acid	C16H36O4P		$CH_3[CH2]3CH(CH_2CH3)CH2$-	A
LIX26	(?) hydroxyl quinoline			unknown	A
LIX 54	P-diketone	Ci6$H_{22}0_2$		 $CH_3[CH_2]_6$—	A
DNNSA	di(nonyl)naphtha-lene sulphonic acid	C_28H440_3S		$CH_3[CH_2]_8$-	A
Cyanex 272	di(2,4,4-trimethyl pentyl) phosphinic acid	$C,_6H_{36}O_2P$		$CH_3C(CH3)2CH_2CH(CH_3)CH_2$—	A
Cyanex 301	di(2,4,4-tri methyl-pentyl) dithiophos-phinic acid	$C_{16}H_{36}PS_2$		$CH_3C(CH_3)_2CH_2CH(CH_3)CH_2$ —	A
Cyanex 302	di (2,4,4-tri methyl-pentyl) monothio-phosphinic acid	C16H360Ps		$CH_3C(CH_3)2CH_2CH(CH_3)CH_2$ —	A
TBPO	tri (butyl) phospho-ric oxide	$C_{12}H_{27}O_4P$		$CH_3(CH_2)_3$-	S
Cyanex 471X	tri (isobutyl) phos-phine sulphide	$CI_2H_{27}PS$		$(CH_3)_2CHCH_2$—	S
Cyanex 921	tri (n-octyl) phos-phine oxide (TOPO)	C_24H_5IOP		$CH_3[CH_2]_7$-	s
15C5	15-crown-5	$C,_0H_2O0_5$		-	s
LIX 79	N,N'-bis (2-ethyl hexyl) guanidine	$C_{17}H_{37}N_3$		$CH_3[CH_2]_3CH(CH_2CH3)CH2$-	IP

Potential ligands can be derived from those developed and applied in hydrometallurgy. Table 2 shows such ligands including various (modified) functional groups to be evaluated experimentally as reactive silver-complexes (silver gives more stable complexes as copper). They should show sufficient capability of the ligand to stabilize the silver in solution, while still retaining their ability to 7t-complex with the olefin. Ligand screening is performed by measurement of the ethylene solubility in the synthesised (reactive) metal-ligand containing solvents as indication of the reactivity of C6-olefins. The most favourable reactive solvents are consecutively evaluated for reactive vapour-liquid equilibria and the maximum achievable selectivity using a mixture of different C6-olefin isomers (branched, cyclic and internal mono-olefms, di-olefins) as a function of metal-complex-to-olefin ratio and temperature (pressure).

EXPERIMENTAL

Synthesis of metal-ligand complexes

Various metal-ligand complexes are synthesised at room temperature by liquid-liquid extraction of silver(I) from aqueous silver nitrate solutions. A stirrer magnet is put in a glass vessel of sufficient volume filled with an aqueous silver nitrate solution. The stirrer is started after which the organic solution, containing the extractant in an appropriate diluent, is added slowly. The metal content in the organic phase is measured directly with Atomic Absorption Spectroscopy (AAS). Solutions of Ag-D2EHPA in 1-methylnaphthalene (1MN) and n-methylpyrrolidone (NMP) were made indirectly by dissolving D2EHPA in n-hexane and, after extraction of silver, evaporation of n-hexane by flushing nitrogen followed by dilution in an appropriate solvent. Ligands like D2EHPA and di-nonyl naphthalene sulphonic acid (DNNSA) require the addition of NaOH (1 M solution) to enhance the extraction of silver to form a stable metal-ligand complex. More details are given in [1],

Reactive absorption of ethylene by metal-ligand complexes

The ethylene solubility in the synthesised liquids is measured at equilibrium with an Intelligent Gravimetric Analyser (IGA, model 003) from Hiden Analytical enabling the use of micro-volumes of reactive solvent, see [1] for details of set-up characterisation and experimental procedure.

Complexation behavior of olefin isomers in reactive solvents

Vapour-liquid equilibrium experiments are performed in a Fischer Technology VLE 602D apparatus equipped with a Fischer-system M101 control unit, an Edwards IEC34-1 vacuum pump and a Julabo F32 MW water bath for temperature control. Concentrations are determined by GC- analysis, see [1] for more details.

RESULTS AND DISCUSSION

Synthesis and screening of metal-ligand complexes for improved ethylene solubility

Two extractants, LIX 26 (a hydroxyquinoline) and LIX 54 (a diketone) do not easily extract silver but its extraction can be enhanced by adding NaOH. Nevertheless, the resulting metal-ligand complex is unstable because silver precipitates from the solution.

The thio-phosphoric acids Cyanex 301 and 302 show opposite behaviour by not requiring NaOH and easily extracting silver from the solution. The sulphur bonds directly with silver making the metal-ligand such stable that the silver-ion is not longer able to complex with C_2H_4: it has lost its ability to form rc-complexes. Due to an increase in solvent polarity the (physical) solubility even decreases upon addition of these ligands and even more for its silver-complexes (Figure 2).

Two other ligands, di(2-ethylhexyl)phosphoric acid (D2EHPA) and di-nonyl naphthalene sulphonic acid (DNNSA) also require the addition of NaOH to extract silver but in smaller

amounts as LIX 26 and 54, resulting in a stable metal-ligand complex [2], With both ligands the presence of silver almost triples the C_2H_4-solubility compared to the solvent without silver yielding a curved absorption isotherm which is characteristic for reactive sorption (Figure 3) [1]. The silver-D2EHPA complex is observed to complex a single C_2H_4-molecule whereas silver-DNNSA complexes two C_2H_4-molecules. This is explained by the stoichiometry between metal and ligand, DNNSA-silver form 1:1 complexes, while D2EHPA forms a 1:2 complex (metalligand). The presence of two ligands on one silver restricts its accessibility for C_2H_4 [1],

The remaining extractants were discarded for further investigation due to different reasons, like “polymerisation” in the organic phase (Cyanex 471X, Cyanex 272), insufficient extraction of silver (TBPO, LIX 79), no C_2H_4-complexation ability (TOPO), or reverse extraction of ligand towards aqueous phase (15-crown-5).

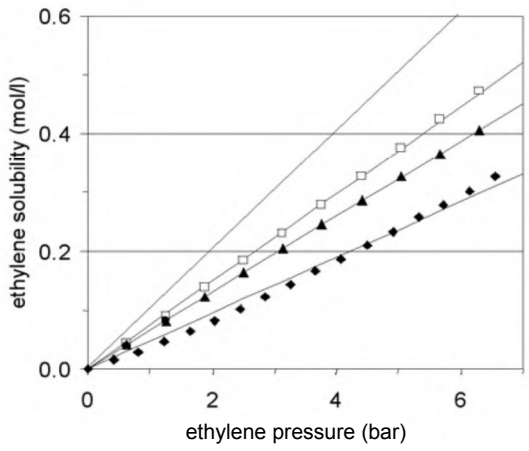


Figure 2. C_2H_4 solubility in solution of Cyanex 301 or 302 in dodecane (dod) with(out) Ag at 298 K. (D) 1 M C301/dod, (A) 1 M Ag/1 M C301/dod, (A) 1.8 M Ag/2 M C302/dod, (-) Pure dod.

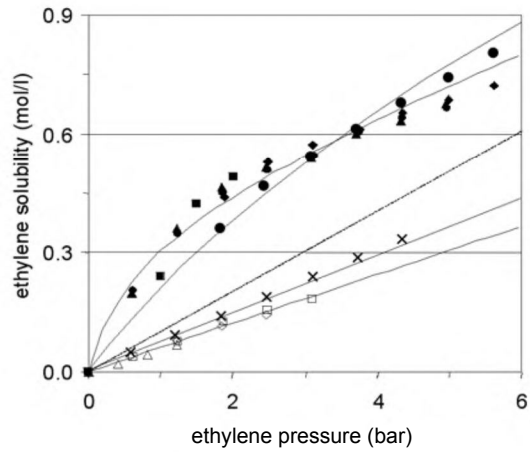


Figure 3. C_2H_4solubilityin D2EFIPA or DNNSA in dodecane with(out) Ag at 298 K. (•) 0.8 M Ag/2 M D2EHPA/dod,(x) 0.8 M2 M D2EHPA /dod, (■,♦,▲) *1 M Ag/1 M DNNSA/dod,* (□,0, A) *1 M DNNSA/dod, (—) pure dod.*

Complexation behaviour of C6-olefin isomers in various developed silver-ligand complexes

Silver-ligand complex performance for mixture of 1-hexene, 2-methyl-1-pentene, n-hexane

Vapour-liquid equilibrium experiments are performed to evaluate the suitability of the successfully developed silver-ligand complexes for application as reactive solvent (amount S) for a test C6-feed mixture (amount F) containing 50 wt% 1H, 25 wt% 2M1P and 25 wt% NH. Additionally, the effect of varying organic tail structure is investigated by selecting three phosphoric acid ligands: D2EHPA, di (butyl) phosphoric acid (DBPA) and mono (2-ethylhexyl) phosphoric acid (MEHPA) and two sulphonic acid ligands: DNNSA and dodecyl benzene sulphonic acid (DBSA), see Figure 4. The selectivity S_y = D/Dj with D, the distribution coefficient of i, i.e. the ratio of its vapour fraction and (reactive) solvent fraction (physical and complexed).

For S/F = 1 the selectivity for 2-methyl-1-pentene is higher as for n-hexane, except for Ag-DBSA. The selectivity of n-hexane without silver is below unity (0.82), while for 2-methyl-1-pentene it is already approximately unity such that the reaction did not overcome this difference yet. Ag-DBSA contains much more silver and is thus more polar thereby increasing the n-hexane selectivity significantly. The silver content of DBSA is the highest of all synthesised complexes so a high selectivity is expected and found but the high viscosity of this solvent restricted its use to S/F =1. The highest overall selectivity for both 2M1P and

NH over 1H was obtained for Ag-DBPA (S/F = 3, 20 wt% Ag), although closely followed by D2EHPA and DNNSA. However, its specific selectivity expressed per mol silver or kg solvent is relatively low (Figure 6).

Figure 4. Investigated ligands in vapour-liquid experiments with corresponding R-group

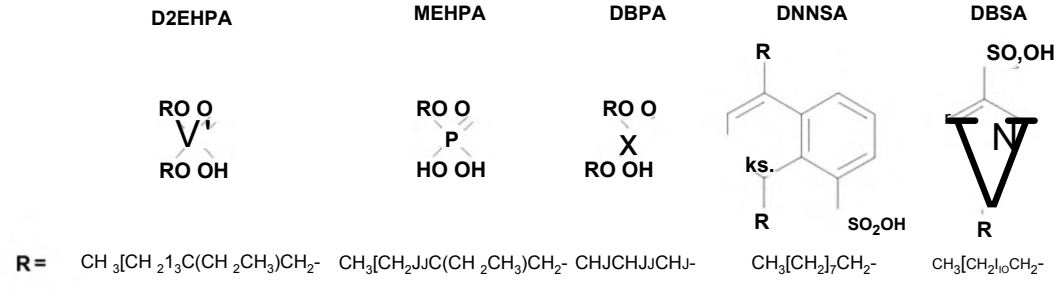


Figure 5 compares the maximum selectivities of n-hexane and 2-methyl-1-pentene relative to 1H and the boiling points of the metal-ligand complexes.

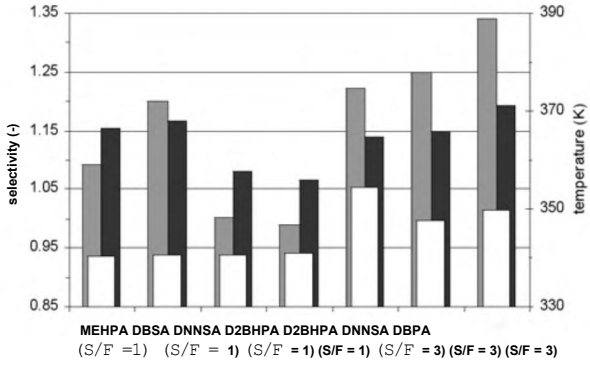


Figure 5. Obtained maximum selectivities S relative to 1H for various silver-ligand comple-xes and boiling points at 1.0 bar, (W) S2M1P/1H, (J S/vw/fH, (CJ boiling temperature (K).

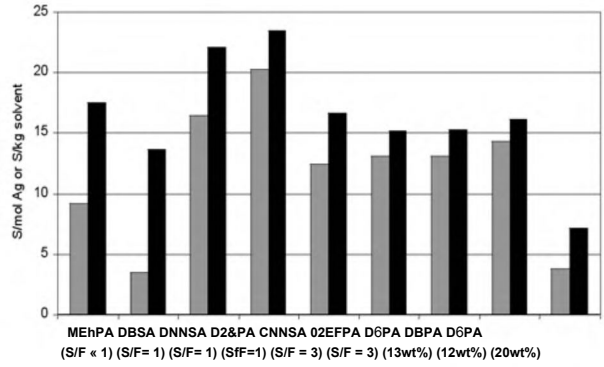


Figure 6. Selectivity of 2M1P relative to 1H per mol of silver or per kg of solvent. (M) selectivi-ty per mol silver, (M) selectivity per kg solvent.

Ag-DBPA complex performance for simplified Fischer-Tropsch mixture

Next, the distribution coefficients and selectivities for the simplified Fischer-Tropsch C_6-cut mixture of Table 1 are determined for Ag-DBPA (20 wt% Ag). The results are reported in Figure 7 and 8, respectively. The selectivity for 1-hexene increases from 15HD < 1MCP < T2H < 2M1P which is the same ranking as determined for the reactive solvent silver nitrate in ethylene glycol. This ranking in the obtained overall selectivities and overall distribution ratios can be explained quantitatively according to the boiling point of the olefin isomer or paraffin mixture and the complexation constants K_r of silver with the olefins. These are determined in LLE-experiments for a single olefin in n-hexane using silver nitrate in ethylene glycol. Assuming 1:1 complexation at 300 K this constant K_{r1} decreases from 15HD > 1H > C2H > 2M1P > 1MCP T2H with values of 63 ± 4, 6.5 ± 0.5, 4.64 ± 0.06, 3.43 ± 0.04, 2.68 ± 0.05, and 1.23 ± 0.03, respectively. The heat of complexation for all mono-olefins is -15.5 ± 0.7 kJ.mor[1] such that differences in complexation constants are the results of variation in the entropy. In addition it is should be concluded from the experiments with $AgN0_3$/ethylene glycol that all olefins but 15 HD and 1H form primary (1:1) complexes only. However, 15HD is also able to create tertiary complexes (metakolefine = 2:1) because of its two double bounds, whereas 1H is found to form primary and secondary complexes (metakolefine = 1:2) [1],

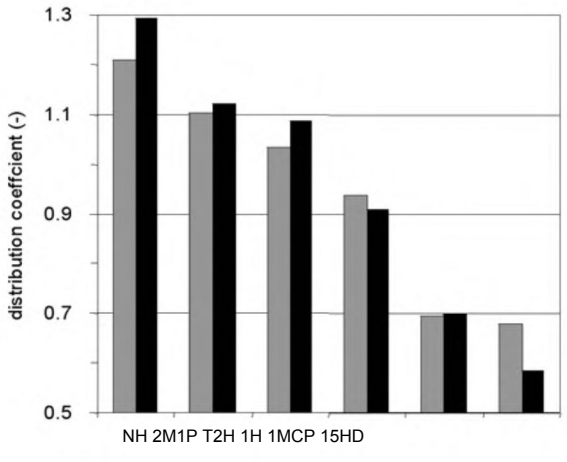


Figure 7.Distribution coefficient of NH, 2M1P, 1MCP, T2H and 15HD in 20 wt% Ag-DBPA at S/F = 3 at 1 bar (M), and 0.5 bar (U)).

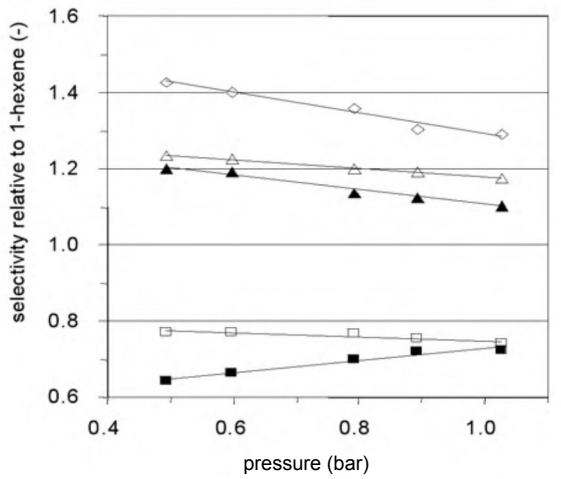


Figure 8. Selectivity S relative to 1H of NH, 2M1P, 1MCP, T2H and 15HD in 20 wt% Ag-DBPA at S/F = 3. (M) SISHD/IH, (O)SIMCPZIH, (A) S_2M1P/1H, (N ST2H/1H> (O) SNH/IH

CONCLUSIONS

It has been demonstrated that the presence of silver as a silver-ligand complex, increases the vapour-liquid selectivity between different olefins and between olefins and paraffins. These silver-ligand complexes employed in Reactive Extractive Distillation have the potential to become a promising alternative for the separation of a-olefins from Fischer-Tropsch streams. Selectivities increase for higher silver concentrations, to be realized by using smaller ligands, a higher S/F-ratio and lower temperatures (larger differences in complexation constants).

REFERENCES

1. A.E. Wentink, Functionalised solvents for olefin isomer purification by reactive extractive distillation, PhD thesis, University of Twente, Enschede, The Netherlands (2004).
2. Wentink, A.E., Krooshof, P.W.T., Kuipers, N.J.M., Haan, A.B. de, and Mulder, H. (2002). Novel application perspectives for metal extractants: Olefin separations. In Sole, K.C., Cole, P.M., Preston, J.S. & Robinson, D.J. (Ed.), *Proceedings of the International Solvent Extraction Conference, ISEC 2002.* (pp. 1301-1306). South Africa.

REACTIVE EXTRACTION OF ALCOHOLS FROM APOLAR HYDROCARBONS WITH AQUEOUS SOLUTIONS

Boris Kuzmanović[a], Norbert J.M. Kuipers[b], André B. de Haan[b], and Gerard Kwant[c]

[a]Akzo Nobel Chemical Research, Arnhem, The Netherlands
[b] University of Twente, Enschede, The Netherlands
[C]DSM Research, Geleen, The Netherlands

The use of aqueous solutions is evaluated as sustainable reactive extraction solvents for the recovery of monohydroxyl alcohols (benzyl alcohol, 1-hexanol, cyclohexanol) present in few-percent concentrations in apolar hydrocarbons (toluene, n-hexane, cyclohexane) by considering two approaches. An aqueous solution containing a reactive extractant, like borate salts, borate complexes, a monosalt of dicarboxylic acid, hydroxypropyl-cyclodextrins and silver nitrate, shows limited potential to be used. Besides moderate distribution ratios of the alcohol, these extractants are also found to increase the solubility of the apolar organic solvent in the aqueous phase and thereby cause a decrease in selectivity toward the alcohol. Another approach, in which the alcohol is chemically modified prior to the extraction into an easy-extractable form, in this case a monoester/carboxylic acid, shows much more potential. An environmentally benign solvent, like an aqueous solution of sodium hydrogen carbonate, can provide a distribution ratio of benzyl alcohol up to 200, leaving the solubility of the organic solvent in the aqueous solution unchanged relative to pure water and therefore increasing the selectivity with two orders of magnitude. The modification of aromatic, cyclo-aliphatic and linear aliphatic alcohols can be performed efficiently in the apolar organic solvent without need for a catalyst. The recovery of the modified alcohol can be performed by back-extraction in combination with a spontaneous hydrolysis which rate can be controlled by temperature. Hence, an efficient and selective recovery of alcohols can be achieved by reactive extraction with green salt solutions by prior reversible modification of the alcohol.

INTRODUCTION

Oxygenates like carboxylic acids, aldehydes/ketons and alcohols are often present in less than 10 wt% concentrations in apolar organic solvents from which they are industrially recovered by a highly energy-consuming distillation in which the bulk organic solvent has to be evaporated. A dramatic reduction in operational costs may be achieved by reactive extraction of these oxygenates with aqueous salt solutions. Here water is the green solvent which is practically immiscible with the apolar organic solvent and not contaminating the system. Its poor capacity can be significantly increased by the introduction of an environmentally and toxicologically benign salt if it could selectively and reversibly react with the oxygenate modifying it into a charged compound. This way, aldehydes and ketons, can be extracted by aqueous solutions of hydrogen sulphite or a hydrazine salt and back-recovered by a simple temperature shift [1], Carboxylic acids can be favorably extracted with an aqueous solution of sodium hydrogen carbonate whereas its back-recovery can be realized by carbon dioxide under pressure by new phase (liquid or solid) formation or by back-extraction due to a pH-shift. Due to structural similarities of water and alcohols, it can

be expected that potential extractants which can react with the hydroxyl group of the alcohol, will also interact with water, and therefore will not significantly increase the distribution ratio of the alcohol. Therefore another option, in which the alcohol is first modified into a monoester and subsequently exposed to reactive extraction, is also evaluated in this paper. Benzyl alcohol in toluene is used as representative organic alcohol/solvent mixture. The most promising reactive compounds are also evaluated for extraction of cyclohexanol from cyclohexane and 1-hexanol from n-hexane.

SELECTION OF REACTIVE EXTRACTANTS

Potential extractants for unmodified alcohols

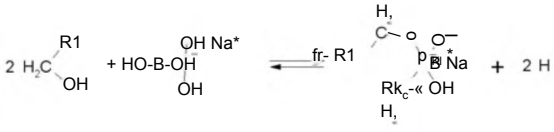
There is hardly any known application of reactive extraction in the recovery of alcohols, either from the organic or from the aqueous phase. Potential suitable reversible chemical interactions for reactive extraction of alcohols are presented in Table 1. To assure no solubility in the organic phase, the essential criterion for selecting suitable reactions is that both the reactive solute and the reaction product are charged or at least highly water-soluble species.

Potential extractants for modified alcohols

Various criteria determine the suitability of a modification reaction such as 1) a product that can be easily (and selectively) extracted into the aqueous phase, 2) a modification reaction which has to be attainable in the apolar organic solvent and must be reversible in order to regenerate the alcohol after extraction, 3) a modifying agent that should not contaminate nor have any undesirable effect on the other products in the organic phase, and 4) this agent should be easily regenerated after separation to be reused. Scheme 1 shows a potential promising procedure.

Table 1. Potential reversible reactions for reactive extraction of unmodified alcohol.

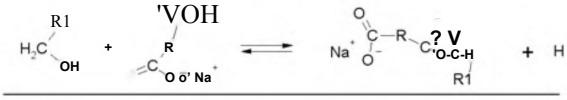
Reaction with borates



Complexation with borate-diol complexes

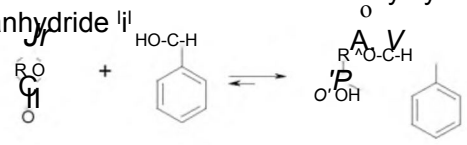


Esterification with monosalts of dicarboxylic acids



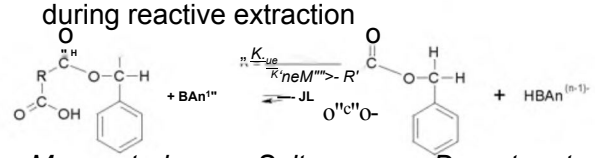
Scheme 1. Potential three steps procedure for reactive extraction of modified (benzyl) alcohol.

a) Monoesterification alcohol by cyclic anhydride



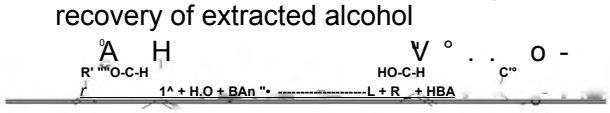
Cyclic Monoester/carboxylic acid (ME) *anhydride* *Benzyl alcohol*

b) Dissociation of monoester by basic salt during reactive extraction

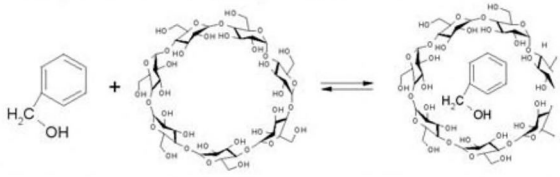


Monoesterl Salt Deprotonated Protonated carboxylic acid anion monoester (ME) salt anion

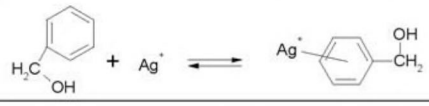
c) Hydrolysis of deprotonated alcohol monoester in aqueous salt solution during the recovery of extracted alcohol

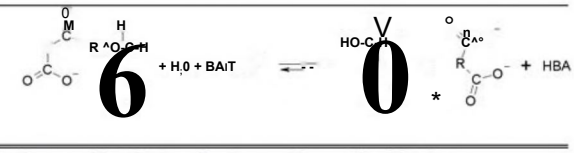


Complexation with cyclodextrins

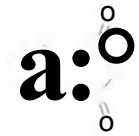


Complexation with transition metal ions

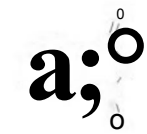




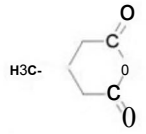
Scheme 2. Selected cyclic anhydrides.



Phthalic anhydride (PA)



Hexahydrophtalic anhydride (HPA)



3-methylglutaric anhydride (MGA)

The procedure shown in Scheme 1 satisfies all above criteria: partial and reversible esterification of a cyclic anhydride, so called monoesterification (Scheme la), would rapidly convert an alcohol into a monoester which is in the same time a carboxylic acid that can be easily extracted into aqueous alkaline solutions producing a charged and highly water-soluble carboxylate (Scheme 1b). Once extracted into the aqueous phase, the (de)protonated monoester, starts to hydrolyse spontaneously by which the alcohol is regenerated (Scheme 1c).

Three cyclic anhydrides are chosen for experimental evaluation of the monoesterification of benzyl alcohol in toluene: phthalic (PA), hexahydrophthalic(HPA) and 3-methylglutaric anhydride (MGA), see scheme 2. A suitable extraction salt was selected based on the dissociation constant of the monoester, which is taken as equal to the second dissociation constant of the adequate dicarboxylic acid. Due to the selection of hydrogen carbonate (BAn^{n}‘ is $HC0_3$‘ in Scheme 1b) just a mildly basic solution (pH « 9) could be operated with, yielding carbonic acid (H_2C0_3) as the dissociation product which can be removed from the aqueous phase as carbon dioxide.

EXPERIMENTAL

Reactive extraction of unmodified alcohol

For the reactive extraction of the unmodified alcohol, equilibrium measurements were performed in a set of jacketed glass at a phase volume ratio of 1. Experimental details and analysis methods are presented elsewhere [1], The overall distribution ratio of the alcohol (D_{AIc}) was calculated by dividing the total concentration of alcohol in the aqueous phase by its concentration in the organic phase, at equilibrium, whereas the selectivity toward alcohol (3AIC is calculated as ratio of equilibrium distribution ratios of alcohol and apolar organic solvent (AOS):

$$^{D}AIC = \frac{c^{a}_{AIc} + r \cdot c^{a}_{CEAlc}}{c^{O}_{Ale}} \qquad \textbf{(D} \qquad \textbf{P/A/c} = \frac{^{D}AIC}{^{D}AOS} \qquad (2)$$

where subscript *Ale* represents alcohol and *CEAlc* the chemically extracted alcohol, *r* is the number of alcohol molecules per molecule of chemically extracted product *(r* = 1 in all reactions with exception of the reaction with borate where *r*= 2).

Reactive extraction of modified alcohol

Monoesterification reaction
The monoesterification reaction was analysed on our automated workstation [2], The concentrations of reactants and product are measured as a function of reaction time from which the alcohol conversion is calculated by £$_A$ic = 1 - $c_A|_C/c^\circ_A|_C$. The reaction is performed in vials, in which the organic mixture containing the anhydride and the apolar organic solvent was introduced. The vial is agitated and heated to the required temperature (in the range of 60 - 150 °C). The reaction was initiated by introducing the alcohol in the vial. At predefined times a sample was taken and transferred into another vial that contained a derivatization agent (producing an inert silyl product) to stop the esterification reaction. The derivatized product was analysed by gas chromatography after which the monoester concentration could be determined.

Dissociation extraction
The dissociation extraction experiments were performed on the same automated workstation as the monoesterification experiments. The extraction is done in vials in which both phases with a phase volume ratio of 1, at the desired extraction temperature, are introduced. The organic phase was a solution of monoester in the apolar organic solvent, representing the modified alcohol solution, whereas the aqueous phase contained sodium hydrogen carbonate at different concentrations. At predefined times a sample of the upper organic layer was taken and transferred into another vial that contained the derivatization agent. The derivatized sample was analysed by gas chromatography. The overall distribution ratio of benzyl alcohol D_{BAfc} is:

$$ {}^{D}BAIC = \frac{c^{a}_{ME} + c^{a}_{ME} \quad + c, \overset{a}{BAIc}}{\mathcal{E}^{\circ}_{ME} + c^{\circ}_{ME} + {}^{c}BAIc} \qquad (3) $$

and is not considered at equilibrium, but monitored as a function of time. Subscript *ME* represents protonated monoester, *ME* is deprotonated monoester, and *BAIc* is benzyl alcohol. Superscript o denotes organic and a aqueous phase.

RESULTS AND DISCUSSION

Reactive extraction of unmodified alcohol
The measured overall equilibrium distribution ratios of benzyl alcohol for all evaluated reactive extractants are reported in Figure 1 (for an initial mass fraction of benzyl alcohol in toluene of 1.5 wt%, phase volume ratio = 1). Only hydroxypropyl (HP)-cyclodextrins (CD) (of various average molar substitutions AMS) and silver nitrate show a distribution ratio of about one order of magnitude higher than the physical distribution ratio. The enhancement achieved by the other evaluated extractants is insufficient and therefore will not be discussed. A silver nitrate solution shows a lower selectivity toward benzvl alcohol relative to Dure water (Figure 2), suggesting that the silver ion interacts more with toluene than with benzyl alcohol. However, as the selectivity is still rather high, an aqueous solution of silver nitrate can be used for the recovery of benzyl alcohol.
All three cyclodextrins cause an increase of the distribution ratio of benzyl alcohol with maximum values between 1.3 and 2.7, what makes them the most attractive among the evaluated extractants. p-CDs show a higher distribution ratio than the a, whereas the p-CD with the lower AMS performs somewhat better. With a distribution ratio of around 3 and a selectivity toward the alcohol of at least 100 (Figure 2), aqueous solutions of HP-CD show also sufficient potential to be used for the recovery of benzyl alcohol.

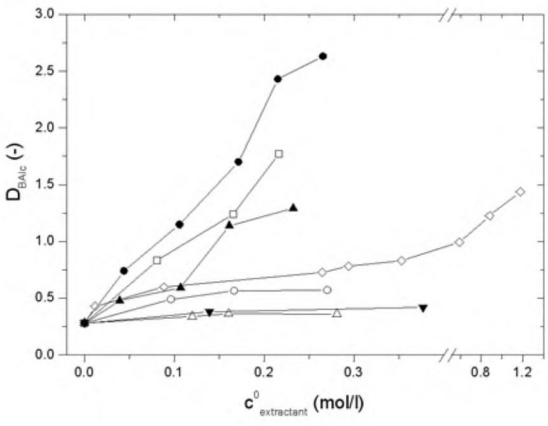


Figure 1. Overall equilibrium distribution ratio of benzyl alcohol between aqueous solution and toluene as function of initial extractant concentration at 25 °C: 0. *silver nitrate;* □, *HP-p-CD (AMS = 1.0);* •, *HP-p-CD (AMS = 0.6);A, HP-cc-CD (AMS = 0.6); o, sodium bo-rate;* ***A,*** ***1,****2-propanediol-borate complex;* ▼, *monosodium maleate.*

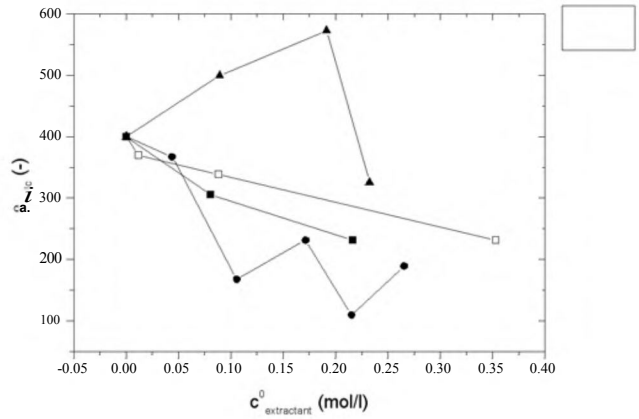


Figure 2. Selectivity of aqueous silver nitrate and cyclodextrin solutions toward benzyl alcohol relative to toluene as a function of the initial extractant concentration in the aqueous phase at 25 °C: □, *silver nitrate; a, HP-p-CD (AMS = 1.0);* *, *HP-p-CD (AMS = 0.6); A, HP-oc-CD (AMS = 0.6).*

Reactive extraction of modified alcohol

Monoesterification reaction

The alcohol conversion in the non-catalysed monoesterification is shown in Figure 3 as a function of time at various temperatures for benzyl alcohol with various anhydrides and in Figure 4 for cyclohexanol and 1-hexanol with 3-methyl glutaric anhydride (MGA).

A conversion higher than 90% can be achieved using HPA. This conversion is realised in approximately 100 min at 150 °C, what can be considered as relatively fast compared with a typical residence time in an oxidation reactor of 240 to 1800 min. Since HPA has a good solubility in apolar solvents, the conversion and the reaction rate can be even higher by using a higher excess of anhydride or higher temperature. Regarding the temperature effect, this reversible reaction seems to be exothermic.

Both, the equilibrium conversion and the rate of reaction of benzyl alcohol with PA, are lower than in the reaction with HPA. This is due to the low concentration of PA which is maximal and at its solubility limit.

The highest equilibrium conversion of benzyl alcohol is achieved with MGA. At 150 °C, the alcohol conversion into the monoester is almost 100%, whereas at the lower temperatures the equilibrium is not reached within the monitored time, but the equilibrium conversion can be expected to be at least as that at 150 °C considering the exothermic nature of the monoesterification reactions observed for the other two anhydrides. This suggests that the excess of anhydride does not need to be as high as six to obtain a high conversion of benzyl alcohol. On the other hand, the reaction rate in this case seems to be much more sensitive to the temperature than with either HPA or PA.

At the same temperature, the reaction rate decreases in the order 1-hexanol > benzyl alcohol > cyclohexanol. The rate sensitivity on temperature, i.e. the activation energy, seems to be similar for benzyl alcohol and cyclohexanol, whereas it is lower for 1-hexanol. On the other hand, the lowest equilibrium conversion at 150 °C is found for 1-hexanol. It is only around

50%, compared with 90% for cyclohexanol and close to 100% for benzyl alcohol.

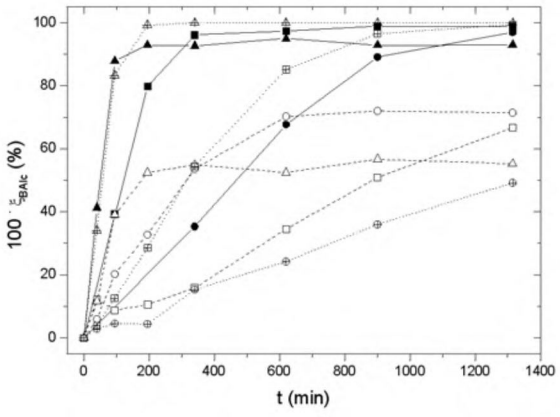


Figure 3. Conversion of benzyl alcohol (Z_{BAlc}) as a *function of time and temperature in the reaction with HP A (-●-, 60 °C; -■-, 100 °C; -* A*, 150 °C), PA (-a-, 100 °C;* -o-*, 125 °C; -A-, 150 °C), and MG A (-&-, 60 °C; -* **s-,** *100 °C; -*a*-, 150 °C) in toluene. A six-times-molar-excess of HP A and PA is used. (PA concentration = solubility at each T.* "& *= 0.8 wt%).*

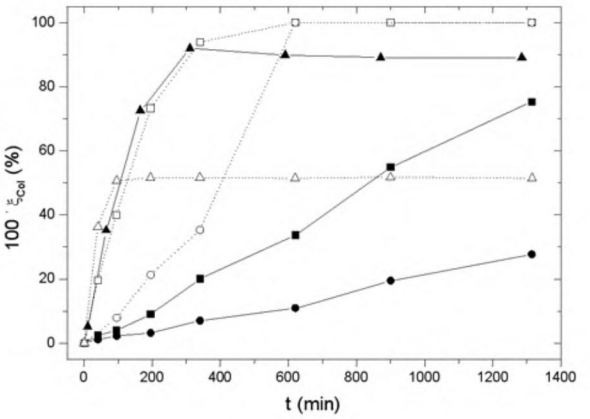


Figure 4. Conversion of cyclohexanol (solid symbols) and 1-hexanol (open symbols) as a function of time and temperature in the reaction with MG A in toluene: -●-, -o- *60 °C; -■-, D-100 °C; -* A *-A-, 150 °C.* $w^{o,0}_{Alc}$ *= 0.8 wt%. (with six-times-molar-excess of MG A).*

Dissociation extraction

Figure 5 shows the concentration profiles of benzyl alcohol and monobenzyl phthalate in the organic phase, and the calculated distribution ratio, for extraction with an aqueous solution containing an excess of sodium hydrogen carbonate. The distribution ratio rises from zero toward a maximum, after which it decreases toward the asymptote determined by the physical distribution ratio of the alcohol (around 0.3 for benzyl alcohol at this temperature). However, the value of the reached maximum differs from case to case. Figure 5 also shows that an aqueous sodium hydrogen carbonate solution can be used for the extraction of monobenzyl phthalate. A distribution ratio of around 200 is reached when $NaHC0_3$ is used in excess for which the pH is almost constant around 9. This is a three orders of magnitude increase of the distribution ratio relative to the physical distribution ratio of benzyl alcohol in pure water. This pH appears to be sufficient to enable a complete extraction of the monoester. Hence, it can be concluded that the sodium hydrogen carbonate obviously has the desired characteristics for a good extractant, it enables complete dissociation of the monoester, but does not cause a very fast hydrolysis.

Regeneration of alcohol by a temperature shift

Figure 6 shows a nearly ten times faster hydrolysis rate of benzyl alcohol due to a temperature increase from 50 and at 70 °C. On the other hand, the monoester concentration profile at 70 °C is roughly the same as that at the lower temperature, showing no noticeable influence of temperature on the extractability of the monoester. In conclusion, the alcohol regeneration can indeed be controlled by adjusting the temperature of the extract.

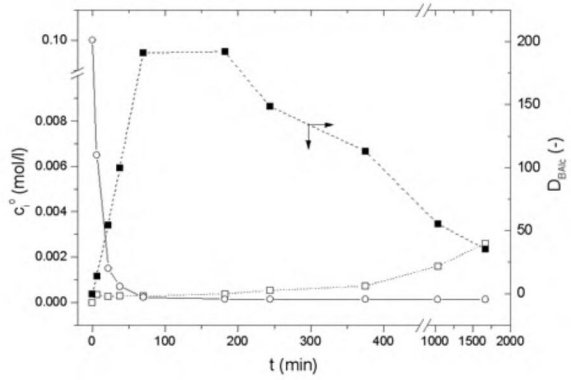


Figure 5. Concentration of components in the toluene-rich-phase ($c_i°$) [open symbols] and overall distribution ratio of benzyl alcohol (D_{BAlc}) [solid symbol] as a function of time for extraction of the modified alcohol at 50 °C into a 1 M $NaHC0_3$ aqueous solution: -□-, benzyl alcohol; -o-, monobenzyl phthalate.

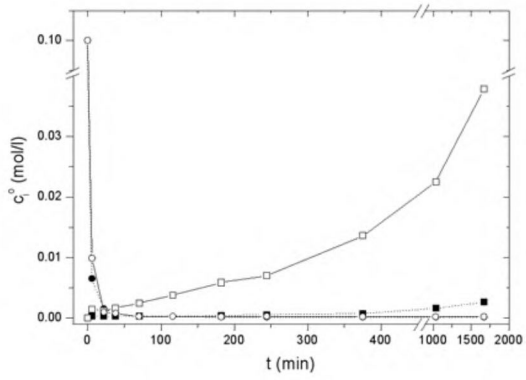


Figure 6. Concentration of components in the organic phase ($c_i°$) as a function of time for extraction of modified alcohol into a 1 M $NaHC0_3$ aqueous solution at 50 °C [solid symbols] and 70 °C [open symbols]: -□- and -■-, benzyl alcohol; -o- and -●-, monobenzyl phthalate.

ACKNOWLEDGEMENTS

We thank for the financial support of DSM, NWO-CW (Netherlands Organisation for Scientific Research - Chemical Science) and NOVEM (Netherlands Agency for Energy and Environment).

REFERENCES

1. B. Kuzmanović, N.J.M. Kuipers, A.B. de Haan, G. Kwant, *Reactive extraction of carbonyl compounds from apolar hydrocarbon using aqueous salt solutions, Ind. Eng. Chem. Res.* 42(13), 2885-2896 (2003).
2. B. Kuzmanović, M.L. van Delden, N.J.M. Kuipers, A.B. de Haan, *Fully automated workstation for liquid-liquid equilibrium measurements, J. Chem. Eng. Data* (2003) 48(5), 1237-1244.
3. B. Kuzmanović, Reactive extraction of oxygenates with aqueous salt solutions, PhD thesis, University of Twente, Enschede, *The Netherlands* (2003).



A NEW DEPETROLEUM ACIDS PROCESS USING THE MEMBRANE DISPERSION EXTRACTION

LUO LAI-Long[1],LUO GUANG-Sheng[2], NIU CHUN-Ge[1], ZHENG ZHI\XU JIAN-Hong[2], Ma Zhong-Ting[1]

Karamay petrochemical company, PetroChina China[1]
The State Key Lab of Chemical Engineering, Department of Chemical Engineering, Tsinghua University, Beijin,China[2]

A bench -scale (throughput <30l/h) experiment for extracting petroleum acids from Karamay heavy oil in china has been carried out using a membrane dispersion technology. Firstly a model system of naphthenic acid in paraffin was used as the working system to investigate the extraction performance. The influence of the operation conditions such as the composition of the aqueous solution, temperature, phase ratio and two-phase flow rate on the extraction process was studied. Two parameters of the extraction efficiency and the phase separation rate were applied to evaluate the new technology. The experimental results showed that the membrane dispersion extraction technology can fortify the mass transfer efficiency and avoid the emulsion of the mixed phase effectively. For the system of Karamay heavy oil, the extraction efficiency of petroleum acids could reach as high as 95%, and the phase separation process could be completely finished in fifteen minutes.

Key words: Petroleum acids, membrane dispersion, extraction

EXTRACTION OF SACCHARIDES WITH PHENYL BORONATE SALT OF QUATERNARY AMMONIUM

Michiaki Matsumoto, Kentaro Ueba and Kazuo Kondo

Department of Chemical Engineering and Materials Science, Doshisha University
Kyotanabe, Kyoto, 610-0321 Japan

We performed the extraction of saccharides with ion-pair extractant, phenylboronate anion and quaternary ammonium cation. Glucose and xylose were extracted efficiently using the organic phase containing the ion-pair extractant in a high pH region. However, the extractabilities of arabinose, fructose, ribose, galactose, mannose, and fucose were significantly lower than that of glucose. To clarify the selectivity, the quantitative structure property relationship (QSPR) of extractability of sugars with phenylboronate and quaternary ammonium salt was studied using molecular modelling with semi-empirical molecular orbital calculations considering solvent effects (SMO-COSMO method). The QSPR allows the quantitative prediction of extraction equilibrium relation in organic solvents with molecular modelling using the SMO-COSMO method.

INTRODUCTION

The efficient utilization of renewable, natural raw materials has become important because of the shortage of energy and chemicals derived from fossil fuels. However, the use of cheap, natural sources of polysaccharides in the processing yields an aqueous mixture of various simple saccharides, the separation of which is a difficult and costly task [1], The crystallization of pure sugars from an aqueous solution is known to be a poorly reproducible technique. Solvent extraction as an alternative technique has therefore gained interest. Because most saccharides are insoluble in organic solutions, a suitable extractant must be added. Lipophilic boronic acids, which are capable of forming reversible covalent complexes with diol groups in sugars, are the best known extractants for the extraction of saccharides [2], In an aqueous solution, the trigonal boronates are unstable, and the stable anionic tetrahedral boronate ester is formed in the high pH region. Therefore, in order to extract sugar to the organic solution, lipophilic counter cation is necessary.

The use of a mixture of phenylboronic acid and trioctylmetylammonium chloride for the separation of saccharides by solvent extraction and liquid membrane has been reported. In these papers, the extraction behaviour in the system has been not quantitatively but qualitatively investigated. Furthermore, the quantitative structure property relationship (QSPR) of extractability of sugars with phenylboronate and trioctylmetylammonium chloride was studied using molecular modelling with semi-empirical molecular orbital calculations considering solvent effects (SMO-COSMO method).

EXPERIMENTAL

Sugar extraction with trioctylmethylammonium chloride and phenylboronate

Phenylboronate and TOMAC were used as extractants without further purification. An

organic solution was prepared by dissolving phenylboronic acid and TOMAC in n-hexane/1-octanol (85:15, v/v), whose composition gave the highest extractability in our preliminary report [3], Aqueous solutions were prepared by dissolving sugar of G.R. grade in deionized water. The pH of the aqueous solutions was adjusted by adding phosphate buffer. Aqueous and organic solutions of equal volume (10 cm^3) were mixed in a vial tube and shaken at 303K to attain extraction equilibrium. Initial sugar and extractant concentrations were 10 mM and 100 mM, respectively. After the two phases were separated, the concentrations of sugar except for glucose in the aqueous solution were determined by HPLC. HPLC analysis was performed with a Sugar Column SH1011 column (Showa Denko, Japan) using a 5 mM sulfuric acid solution as the mobile phase and an RI detector (Shimadzu, Japan, RID10A). The glucose concentration was determined by UV-vis spectrum (Shimadzu UV2500-PC) at 550 nm using a colorimetric enzyme assay. The pH of the aqueous solution before and after equilibration was determined using a Horiba F-12 pH meter.
The formation enthalpies of the most stable structure of the complex in the organic phase were calculated by SMO-COSMO method [4],

RESULTS AND DISCUSSION

Sugar extraction with trioctylmethylammonium chloride and phenylboronate

The effect of pH on the distribution ratio of sugars, D, in the presence of phenylboronate and TOMAC were examined. Distribution ratios rose with increasing pH, suggesting that tetrahedral boronate anion complex is formed as an extracted species. The extractabilities of glucose and xylose are higher than the other sugars. Similar results have been obtained for the extraction of sugars from the solution derived from the acid hydrolysis of sugar cane bagasse [5],

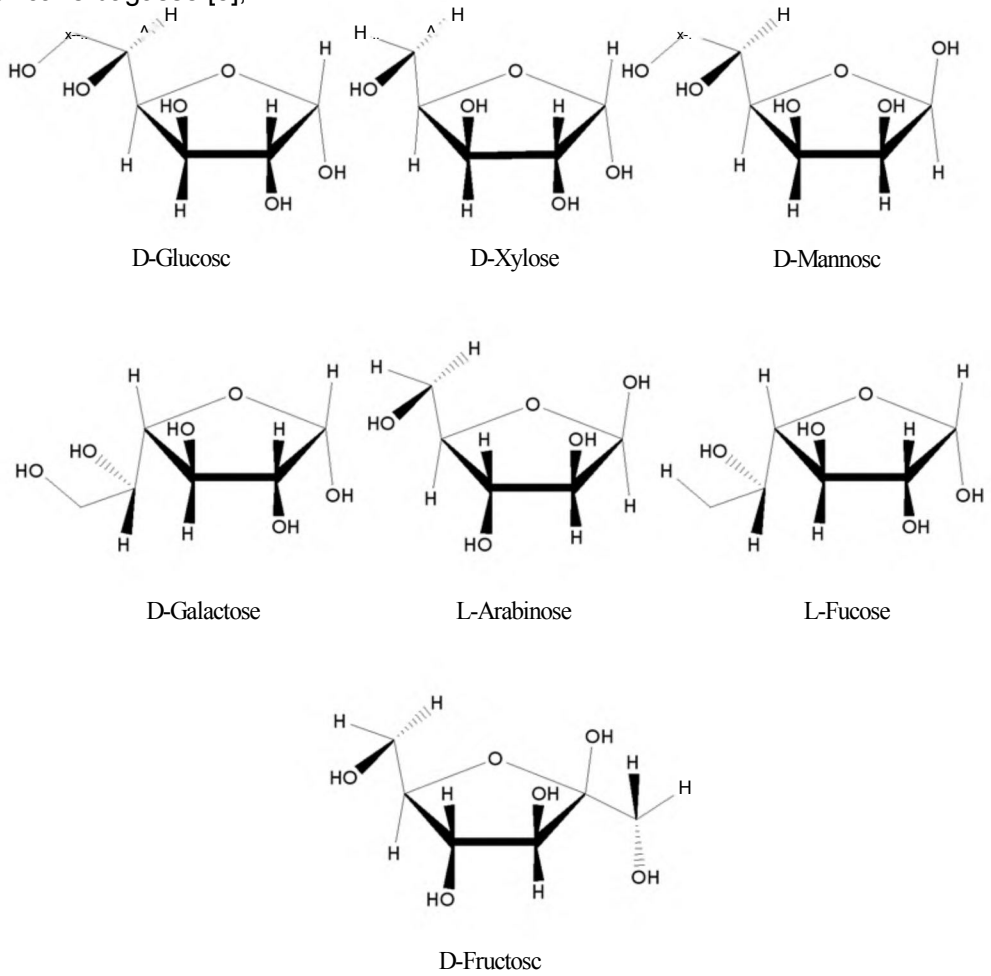


Figure 1. Structures of saccharides in their furanose form.

Based on the preliminary report, the following extraction reactions are presented:

$$BOH^{-}_{aq} + TCl_{org} + S_{aq} \leftrightarrow T^{+}BS_{org} + Cl^{-}_{aq} + 2H_2O \qquad :K_{ex} \qquad (1)$$

Distribution ratio D is defined as

$$D = \frac{[TBS]_0}{[S]_{org}} \qquad (2)$$

Considering that extractant concentrations were larger than the sugar concentration, we can assume that the TOMAC concentration at equilibrium is equal to its initial concentration and that the chloride concentration is constant during the extraction as a first approximation. Therefore, Eq. (2) is converted to Eq. (3).

$$D = \frac{K_{ex} K_a K_{PBA} [PBA]_{0,org} [TC1]_{0,org} [H^+]^{-1}}{1 + K_{PBA} K_a [H]^{-1}} \qquad (3)$$

where K_{PBA} and K_a are the distribution equilibrium constant and acid dissociation constant of phenylboronate, respectively. In a previous paper [6], we found the values of K_{PBA} (= 11.2) and K_a (= 1.05×10^{-9} mol/dm^3). $K_n = K_{f1}/[Cl^-]$ and subscripts 0, org, and aq denote the initial state, and the organic and aqueous phases, respectively. We determined the values of K_{f1}' for each sugar using a nonlinear least squares method as listed in Table 1. As seen in Table 1, the extraction equilibrium constants of glucose and xylose, which belong to group 3, are higher than the other sugars, contrary to our expectations based on the stability constants [7], The obtained extraction constants for group 2 sugars are almost the same. Except for mannose, the extractability of sugars increased in order from group 3 > group 2 > group 1.

These results suggest that phenylboronate bound to the 1,3-trans-diol group of sugar has less ability to form an ion-pair. It has been reported that the complex of fructose with borate, which is formed by using 1,3-trans-diol, leads to very compact ions for intraionic hydrogen bonding [8], This may reduce ion-pair formation.

The low K_f' values of mannnose, which belong to group 3 as well as glucose and xylose, are probably caused by steric hindrance. In contrast to glucose and xylose, the diol and $C_2H_4O_2$ groups of mannose are on the same plane as the five-membered ring.

Tablel Stabilty constants, Ks, between sugars and phenylboronate in aqueous solution and apparent extraction equilibrium constants, K_f'

group	sugar	K_{s1}[dm^{3}l/mol]	K_{S2}[(dm^{3}l/mol)^2]	K_{f1}[dm^{6}mol^{-2}]
1	fructose	2140	3.18×10^5	196
2	arabinose	145	1.91×10^4	352
	fucose	31.2	1.83×10^4	412
	galactose	88.8	1.17×10^4	438
3	mannnose	52.3	4.57×10^3	346
	glucose	34.9	4.39×10^3	2800
	xylose	19.2	3.31×10^3	1090

To clarify the selectivity, the quantitative structure property relationship (QSPR) of extractability of sugars with phenylboronate and quaternary ammonium salt was examined

using molecular modelling with semi-empirical molecular orbital calculations considering solvent effects (SMO-COSMO method). The plots of QSPR are shown in Fig. 2. Since plots of the QSPR gave good linear relationships, the trend of stability of complex formation between phenylboronate and sugars in water are predictable based on the plots. In the presence of organic solvent including phenylboronate and quaternary ammonium salt, the QSPR of the complex formation with sugars in the organic solvent also gave good linear relationship.

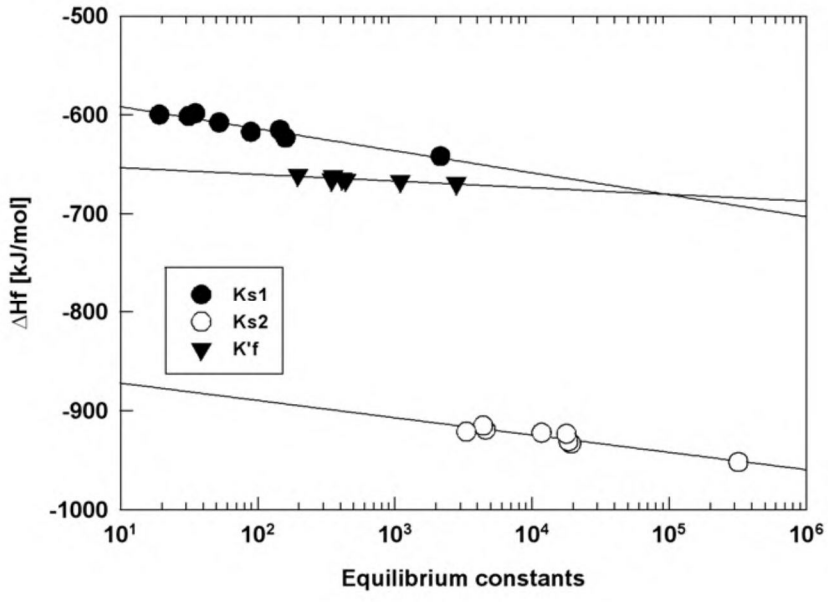


Figure 2. QSPR plot of extraction of sugars with phenyl boronic acid and TO MAC

CONCLUSION

Solvent extraction of sugar with an ion-pair of boronate anion and quaternary ammonium cation was carried out. Extraction reactions were formulated and extraction equilibrium constants were obtained based on the experimental results. Extraction equilibrium constants of glucose and xylose were greater than those of arabinose, fructose, galactose, mannose, and fucose. The QSPR allows the quantitative prediction of extraction equilibrium relation in organic solvents with molecular modelling using the SMO-COSMO method. Thus, with aid of the computational chemistry, it is possible to predict quantitatively the complex extraction behavior of sugars with phenylboronate and quaternary ammonium salt.

REFERENCES

1. J.-F. Verchère (2002), *Macromol. Symp.,* 188, 105-116.
2. B.D. Smith and S.J. Gardiner (1999), *Advances in Supramolecular Chemistry,* 5, 157-**202**.
3. M.Matsumoto, T. Tanaka and K. Kondo (2003), *J. Ion Exch.,* 14, Supplement, 341-344.
4. K. Yoshizuka, M. Matsumoto and K. Kondo, submitted to Kagaku Kogaku Ronbunshu.
5. G.J. Griffin and L. Shu (2004) *,J. Chem. Technol. Biotechnol.,* 79, 505-511.
6. M.Matsumoto and T. Ishizaki (2003), *Solv. Extr. Res. Dev., Japan,* 10, 29-35.
7. M.Matsumoto, K. Ueba and K. Kondo (2005), *Separ. Purif. Technol. In press.*
8. J. M Conner (1970), *J. Inorg. Nucl. Chem.,* 32, 3545-3548.

EXTRACTION OF a -CHYMOTRYPSIN BY REVERSE MICELLES: EFFECT OF pH ON WHOLE EXTRACTION

Liu Junguo [1,2]> Shen Rui \ Xing Jianmin \ Liu-Huizhou[1]*

laboratory of Separation Science and Engineering, Institute of Process Engineering, Chinese Academy of Sciences, Beijing, China, 100080
department of Bioscience and Bioengineering, Hebei University of Science and Technology, Shijiazhuang, Hebei Province, China, 050018

The effect of pH in the initial aqueous phase on the whole extraction process was investigated using a -chymotrypsin as a model protein. When pH rose from 5 to 7, transfer efficiency of forward extraction decreased steadily while that of backward extraction decreased sharply. The conformational change of chymotrypsin at different pH resulted in the change of interaction between chymotrypsin and AOT or solvent molecule: hydrophobic interaction enhanced when pH rose from 5 to 8. This contributed to the surprising effect of pH on the whole extraction process.

INTRODUCTION

Reverse micelles are self-organized aggregates of amphiphilic molecules in apolar media with nanometer-sized waterpools in their polar cores. Such a hydrophilic field hydrophobic surroundings has been attempted for use in the separation and purification of protein. And this technology has been widely noticed for its energy-saving feature and the possibility of sequential operations [1,2],

Many investigations have been carried out on the extraction equilibrium of various kinds of proteins in reversed micellar solution. Most research work regards the process as two separate steps: the forward extraction and the backward extraction. And the effect of forward

conditions on the forward extraction process as well as effect of backward conditions on the backward process is mostly investigated [3,4], Nevertheless, those forward extraction conditions benefit mostly for forward process often do not favorable for backward extraction, especially for enzyme activity recovery, and vice versa. Literature on the effect of operation factors on the whole extraction process is quite scarce.

The pH in the initial aqueous phase is generally considered to affect the net charge of protein, the electrostatic interaction between protein and ionic surfactants, and the percentage of transfer. As to AOT reverse micelles, the higher the ApH (pH -pi) is, the easier the forward extraction is; the more difficult the backward is [5], It is well known that pH affects the conformation of protein, but the following effect on the extraction behavior was little mentioned in the literature.

Several papers provide reports on the a -chymotrypsin extraction by AOT reverse micelles[6-8], Marcozzi et.al. tooku -chymotrypsin as a model protein and studied effect of the pH and ion species on the forward extraction process. [8], In this paper, the effect of pH (3~7) in the initial aqueous phase on the whole extraction process is first investigated and reported. Surprisingly we found that the pH in the initial aqueous phase has a strong effect on the backward extraction and tried to give explanation.

MATERIALS AND METHODS

Enzyme and chemicals

Bovine pancreatic a -chymotrypsin (MW=25K, pl=8.5) was purchased from Bioreagent Branch, Shanghai Chemical Reagent company. AOT was obtained from Sigma and used without further purification. All other reagents were purchased from Beijing Chemical Reagent Company.

Forward and backward extraction

Both forward and backward extraction is carried out with a volumetric phase ration of 5:5 in tightly stoppered 50ml glass flasks.

In the forward extraction, 50mM AOT/isooctane was used as the organic phase system, and 1.0 mg/ml a -chymotrypsin in 20mM pH=3.0~7.0 acetate or TRIS-HCI buffer at the given salt species and concentration was used as aqueous phase system. The two phases were mixed on an orbital shaker with a speed of 240 rpm for 2min in a water bath of 20°C o The mixtures were centrifuged at 4000rpm for 5min to reach a clear separation of two phases. Blank experiments were performed simultaneously with the aqueous phase containing no protein.

The separated micellar phase containing the solubilized protein after the forward transfer was added to an equivalent volume of aqueous solution (1M KCI pH=7.5 50mM phosphate buffer) to conduct backward extraction process. The back transfer was finished in an orbital shaker at a speed of 240rpm for 5min at 35°Co Then the mixtures were centrifuged at 4000rpm for

5min to reach a clear separation of two phases.

Protein assay

The protein concentration in organic and initial aqueous phase was measured by the absorbance at 280nm read from a Perkin-Elmer spectrophotometer. Sometimes the separated micellar phase containing the solubilized protein is turbid and the A_{280}nm become less reliable, a -chymotrypsin has negligible absorption at 350nm. Thus the absorbance of standard samples with known a -chymotrypsin concentration was measured at these two wavelength and the value obtained at 350nm was subtracted from the value at 280nm for calibration of analytical method. And samples of turbid organic phase were treated in the same way. The protein concentration in the aqueous phase after backward transfer was determined by Bradford assay method [9],

Enzymatic assay

a -chymotrypsin activity was measured by the hydrolysis of casein[10].The incubation mixture contained 5ml of 0.6% casein solution in 25mM pH=7.5 phosphate buffer and 1ml enzyme solution with suitable dilution. The incubation was carried out at *37°C* for 15 min and was stopped by adding 2ml of 0.4% trichloroacetic acid. The absorbency at 280nm of the supernatant obtained after centrifugation was determined. An activity unit was defined as the amount of enzyme that gave an increase in absorbency at 280nm equivalent to lug of tyrosine per minute at 37°C.

Definition

percentage of forward extraction: $FEx(\%)=\frac{V_{adorg}\cdot C_{ad\ or*}}{C_{ini.aqu.'\ ini.aqu}}\times 100\%$

percentage of backward extraction: $BE(\%)=\frac{V_{be\ aqua}\cdot C_{be\ c\text{“}<ua}}{C_{lad.org.\ lad.org}}\times 100\%$

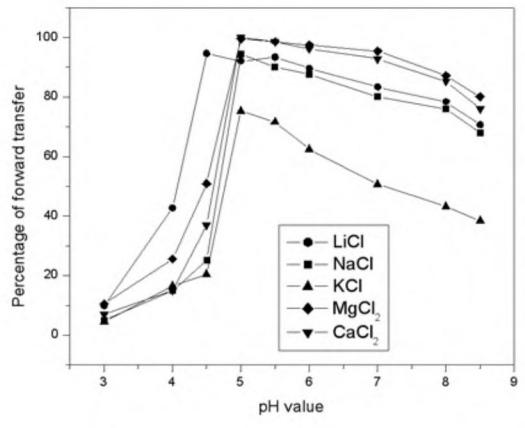
In the equations above, V means volume, C means concentration, lad org means laden organic phase, ini. aqu means initial aqueous phase, and be. aqu means back extraction aqueous phase.

RESULTS AND DISSCUSSION

Fig.la and Fig. 1b showed the effect of pH in forward extraction on the whole extraction process. Commonly, regardless of the salt in the aqueous phase, the FEx was very low between pH=3~4, highest at pH=5, and decreased steadily as the pH rose from 5 to 7. The FEx went up in an order of K^+ Na^+ $Li^+$$Ca^{2+}$ Mg^{2+}. These results were similar to the conclusion of other reports [11] and will not be discussed in this paper.

When pH rose from 5 to 7, FEx decreased steadily while the percentage of backward extraction decreased sharply as shown in Fig 1 regardless of the ion species in the initial

aqueous phase. This kind of phenomenon is never reported, and cannot be totally contributed to the electrostatic interaction between protein and surfactants.



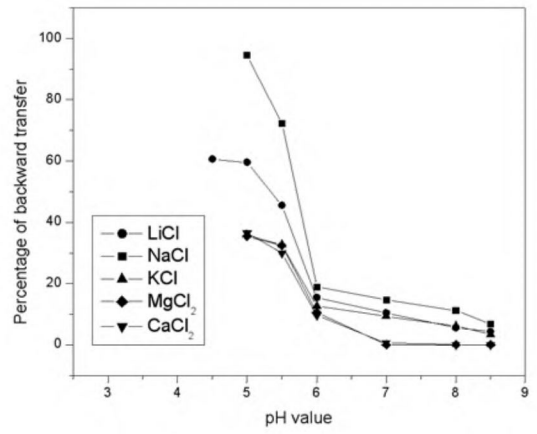


Fig. la *Fig. 1b*

Fig 1 Effect of pH in forward extraction on the whole extraction process. Fig. la, forward transfer; Fig. 1b, backward extraction. Conditions in forward extraction: Img/ml a chymotrypsin and IM.LiCI; 0.1 M NaCI, 0.1M KCI, Conditions in backward extraction^M KCI pH7.5 50mM phosphate buffer

The conditions adopted in the backward extraction were 1M KCI in pH7.5 20mM phosphate buffer. The high ionic strength and high pH in the stripping aqueous phase was aimed at reducing the electrostatic interaction between a -chymotrypsin and AOT. This strategy was effective at pH=5, and the BE was the highest. As to 0.1 M NaCI, the BE is so high as 94.5%. But as pH rose up, the fact that BEx decreased sharply no matter what kind of salt is used in the initial aqueous phase meant that other interaction affected backward extraction.

The effect of pH on the properties and structures of a chymotrypsin have been discussed exhaustively elsewhere[12,13]. In summary, there is strong evidence for the following: chymotrypsin contains a bingding pocket that interacts with aromatic specific substrates and inhibitors. The integrity of this binding pocket is destroyed in acid and alkaline form of chymotrypsin. There is an salt bridge between lle-16 and Asp-194 in the active form of chymotrypsin. And this is destroyed on the protonation of Asp194 in acid environment, which causes a conformational change. 85% percent of chymotrypsin is in active conformation at pH=7, while only 60% percent of chymotrypsin is in active conformation at pH=5[13], This conformational difference could be associated with the difference of extraction behavior in this paper.

Hydrophobic interaction was once reported to be the mechanism of chymotrypsin extracted to AOT/isooctane soution at very low concentration of AOT in the absence of reverse micelles[8]. Hydrophobic interaction between chymotrypsin and AOT or the solvent molecule could also be used to explain the abnormal phenomenon above.

Then we could make an assumption that increase of pH from 5 to 7 caused the conformational change, further led to the increase of hydrophobic area on the surface of chymotrypsin molecule. And the hydrophobic interaction between a chymotrypsin and AOT or isooctane enhanced. During the backward extraction, high ionic strength brought the increase of hydrophobic interaction above. This is probably the reason for the sharp decrease of BE(%).

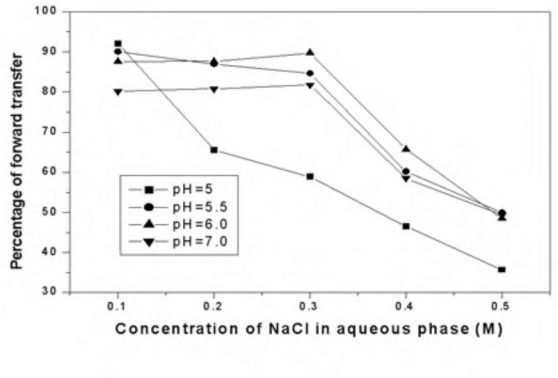


Fig.2. Effect of NaC! concentration and pH in the aqueous phase on the percentage of forward transfer. Condition in forward extraction: Img/ml a chymotrypsin. Condition in backward extractions M KCI pH7.5 50mM phosphate buffer

To confirm the presumption above, the effect of NaCI concentration and pH in the aqueous phase on the percentage of forward extraction was observed and the results were shown in Fig. 2. At pH=5, FEx(%) diminishes quickly when the concentration of NaCI rises up from 0.1M to 0.5M. But at pH=5.5~7, FEx(%) is stable when the concentration of NaCI is between 0.1M and 0.3M, while FEx(%) diminishes when the concentration of NaCI is higher than 0.3M. When concentration of NaCI is 0.5M, the FEx at pH=5 is lower than that at pH=5.5~7.

According to the analysis of Fig 1, electrostatic interaction is the main force of extraction at pH=5, and this was demonstrated by the data at pH=5 in Fig2. Fig2 shows that at pH=5.5~7 FEx(%) is stable when the concentration of NaCI is between 0.1M and 0.3M, and this is regarded as the integration effect of electrostatic and hydrophobic interaction. As the concentration of NaCI rose up, the eletrostatic interaction went down while the hydrophobic one went up, and the former one results in the reduction of FEx while the latter one brings the increase. Furthermore, the integration effect is the steadiness of FEx between 0.1M and 0.3M. This gave an evidence to the presumption that the hydrophobic interaction at pH=5.5~7 is much more stronger than at pH=5.

FEx diminished when the concentration of NaCI was higher than 0.3M regardless of the pH value, and this probably meant that electrostatic interaction became predominant, hydrophobic interaction reached a limit at 0.3M and didn't increase any more when the concentration of NaCI is higher than 0.3M. But the fact that the FEx at pH=5 was lower than that at pH=5.5~7 at 0.5M NaCI demonstrated that hyhrophobic interaction still affected the

extraction process. Behavior difference of forward tranfer at different pH also implied the change of interaction between chymotrypsin and AOT or isooctane molecule.

CONCLUSIONS

The pH in the initial aqueous phase had a strong effect not only on the forward extraction, but also on backward extraction. When pH rose from 5 to 7, FEx decreased steadily while the percentage of backward extraction decreased sharply. The conformational change of a chymotrypsin at different pH resulted in the change of interaction between a chymotrypsin and AOT or solvent molecule: hydrophobic interaction enhanced when pH rose from 5 to 7. This contributed to the effect of pH on backward extraction.

On one hand, pH in the initial pH affects the net charge of protein and electrostatic interaction between protein and surfactant. On the other hand, pH affects the conformation of protein, hydrophobic interaction between protein and surfactant or the solvent molecule and the extraction behavior, which is discussed in detail in this paper.

ACKNOWLEDGEMENTS

The authors acknowledge the financial support from National Natural Science Foundation of China (No.20221603).

REFERENCES

1. S. H. Krishna, N. D.Srinivas, K. S. M. S. Raghavarao, N. G.Karanth (2002), *Adv. Biochem. Eng. Biotechnol.,* 75, 124-183
2. N.W.Fadnavis, B.Satyavathi, & A.A.Deshpande (1997), *Biotechnol. Prog.,* **13,** 503-505.
3. D.Liu, J.Ma, H.Cheng, & Z.Zhao(1998), *Colloid Surface A:* 143, 59-68.
4. T.Kinugasa, A. Kondo, E.Mouri, S. Ichikawa, S.Nakagawa, Y.Nishii , K.Watanabe , & H.Takeuchi, (2003) *Separ. Purif. Technol.,* 31, 251-259.
5. B.A.Andrews, D.L.Pyle, J.A.Asenjo (1994), *Biotechno. Bioeng.,* 43,1052-1058
6. B.D. Kelley, D.I.C.Wang, & T.A. Hatton (1993), *Biotechnol. Bioeng.,* 42, 1199-1208.
7. G. Marcozzi, N.Correa, P.L.Luisi, & M. Caselli (1991), *Biotechnol. Bioeng.,* 38, 1239-1246.
8. V.M. Paradkar, & J.S.Dordick (1994) , *Biotechnol. Bioeng,* 43, 529-540.
9. M. M. Bradford. *Anal. Biochem.* (1976), 72:248~254
10. M.L.Ansen, *J.Gen. Physiol.^939),* 22, 8-79
11. T.Kinugasa, A.Kondo, E.Mouri, S.Ichikawa, S.Nakagawa, Y.Nishii, K.Watanabe, & H.Takeuchi (2003) , *Separ. Purif. Technol.,* **31,** 251-259.
12. L. Heremans, K. Heremans. (1989), *Biochim. Biophys. Acta.,* 999,192~197
13. A.R.Fersht, Y. Requena (1971) *J. Mol. Biol.,* 60, 279-290

PURIFICATION AND CONCENTRATION OF NATTOKINASE BY REVERSE MICELLES EXTRACTION FROM FERMENTATION BROTH

Jun-Guo Liu [1,2], Jian-Min Xing \ Rui Shen \ Cheng-Li Yang \ Hui-Zhou Liu[1]**

[1] Laboratory of Separation Science and Engineering, Institute of Process Engineering, Chinese Academy of Sciences, Beijing, 100080, China
[2] Department of Bioscience and Bioengineering, Hebei University of Science and Technology, Shijiazhuang, Hebei Province, 050018, China

Nattokinase is a novel fibrinolytic enzyme that is considered to be a promising agent for thrombosis therapy. Previous work demonstrated that nattokinase could be transferred from fermentation broth into AOT/isooctane reversed micelles and back without significant loss of activity. In this study, the purification and concentration of nattokinase with reverse micellar extraction was further investigated. Factors, including temperature and phase ratio used for the forward and backward extraction were examined for their effects on the extraction process. The optimal temperature for forward and backward extraction were 25 °C and 35 °C respectively. No concentration but dilution was found for forward extraction. While nattokinase could be enriched in the stripping phase 8 times the nattokinase concentration in reverse micelles phase during backward extraction.

INTRODUCTION

Reverse micellar extraction is one such potential and a promising liquid-liquid extraction, which has received immense attention for isolation and purification of proteins recently. Reverse micelle extraction has been extensively studied using model systems. However, There are only a few reports on the extraction studies of proteins from real systems of fermentation broth. Reverse mciellar systems have been used to isolate proteins from fermentation broth as follows: alkaline protease, a amylase inulinase, xylanase, extracellular acid phosphatse. However, the presence of nutrients, amino acids, cell debris and other contaminating proteins makes product recovery from whole fermentation broth a challenge.

So there is a need for extensive investigation of the extraction behavior of proteins present in these real systems [1],

Nattokinase, a novel fibrinolytic enzyme was primarily isolated from a traditional fermented food “Natto” in Japan by Sumi et al. [2], It is considered to be a promising agent for thrombosis therapy [3-5], The conventional purification of nattokinase is time-consuming and complicated, and it requires more than two days for it needed a ten-step process [6], In this paper, purification and concentration of nattokinase by AOT/isooctane reverse micelles system from fermentation broth was further investigated. Factors, including temperature and phase ratio used for the forward and backward extraction were studied.

MATERIALS AND METHODS

Nattokinase production

Bacillus natto NLSSE was cultivated in a seed medium containing:10 g l'[1] glucose, 10 g l"[1] yeast extract, 1 g l'[1] K2HPO4.3H2O and 0.5 g l'[1] $MgS0_4.7H_20$, for 12 hr at 37°C in an orbital shaker to obtain seed culture with a $OD_{6}oonm$ value of 7~8. Fermentation was started with a 5%(v/v) inoculum in a production medium consisting of: 8.28 g r’soy peptone, 0.64 g l'[1] calcium chloride, and 0.74 g l'[1] yeast extract, 20 g l'[1] maltose , 2 g l"[1] $K_2HP0_4.3H_20$ and 1 g l"[1] $MgS0_4.7H_20$ at 37°C. After 48 hr of fermentation, cells were removed by centrifugation, and the supernatant were frozen and stored at *-25°C* for further use in reverse micellar extraction within 9 days. The typical total protein and nattokinase activity were 0.7mg/ml and 1300u/ml, respectively.

Liquid-liquid extraction

AOT (sodium di [2-ethylhexyl] sulfosuccinate) was obtained from Sigma. All other reagents were of analytical grade and purchased from Beijing Chemical Reagent Company.

The purification and concentration of nattokinase by reverse micelles extraction consisted of two steps:(1) Forward extraction: 50mM AOT/isooctane and Fermentation broth, which was thawed, warmed to room temperature, and adjusted to pH 6.5 were mixed with given phase volume ratio in tightly stopped 100 ml conical flasks on an orbital shaker with a speed of 240 rpm for 8min. The mixtures were centrifuged at 4000rpm for 5min to reach a clear separation of two phases. (2) Backward Extraction: The micellar phase, containing the solubilized protein obtained after forward transfer was added to a stripping aqueous phase (20mM phosphate buffer, 0.2M KCI and 15% (v/v) isopropanol). The back transfer was finished in an orbital shaker at a speed of 240rpm for lOmin. Then the mixtures were centrifuged at 4000rpm for 5min to reach a distinct phase boundary. The total protein concentration and nattokinase activity in the fermentation broth and stripping solution was determined.

Protein determination

The protein concentration in supernatant of fermentation broth and stripping solution were measured by Bradford method [7] using bovine serum albumin as the standard protein.

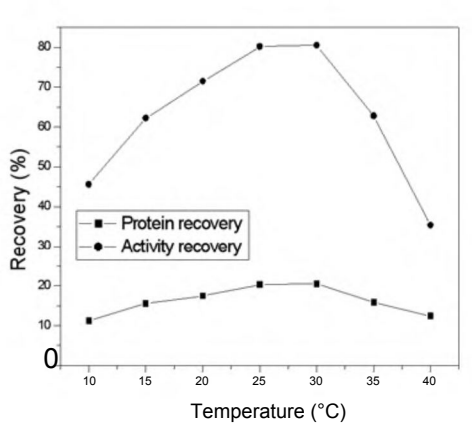
Assay of nattokinase activity [8]

Fibrinolytic activity of nattokinase was measured by the hydrolysis of fibrin. The incubation mixture contained 2.5ml of 12g/l fibrin solution (pH7.8), 6.5ml of 0.1M Tris-HCI buffer (containing 10mM $CaCI_{2l}$ pH7.8), and 1ml enzyme solution with suitable dilution. The incubation was carried out at *37°C* for 15 min and was stopped by adding 5ml of 0.11 M trichloroacetic acid containing 0.22M sodium acetate and 0.33M acetic acid. The absorbency at 275nm of the supernatant obtained after centrifugation was determined. A fibrinolytic unit was defined as the amount of enzyme that gave an increase in absorbency at 275nm equivalent to lug of tyrosine per minute at 37°C.

RESULTS AND DISCUSSION

Effect of temperature during forward extraction

The effects of temperature during forward extraction on nattokinase activity recovery, protein recovery and purification factor were shown in Fig. 1. The tendencies of both protein and nattokinase activity got to platforms as the temperature was between 25°C and 30°C. As the temperature raised from 10°C to 25°C, the protein and nattokinase activity recovery rose synchronously. This could be contributed to the increase of mass transfer coefficient caused by increase of temperature [9,10], But as the temperature was over 30°C, the protein and nattokinase activity recovery went down. AOT/isooctane microemulsion system is temperature sensitive, and a phase separation would be induced by a increase of temperature, for example, from 18°C to 34°C[11], This provided an explanation for the decrease of protein and nattokinase recovery. The purification factor kept stable for temperature < 35 “C and decreased greatly for temperature > 35 °C. This would be discussed together with the effect of temperature during backward extraction in 3.2.



Figl. Effect of temperature during forward extraction on nattokinase activity recovery (M), protein recovery(A), Backward extraction: 35 °C

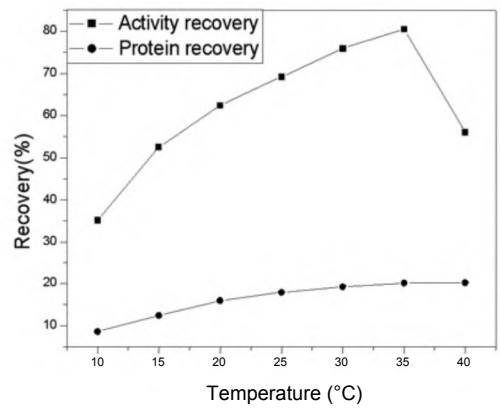


Fig2. Effect of temperature during backward extraction on nattokinase activity recovery (M), protein recovery(A), Forward extraction: 25 °C

Effect of temperature during backward extraction

Fig.2. displayed the results of nattokinase activity recovery, protein recovery and purification factor as a function of the temperature of backward extraction. Nattokinase activity recovery increased greatly for temperature < 35“C and decreased sharply after temperature > 35 °C. While protein recovery increased and got to a platform after temperature > 35°C. The purification factor showed no significant change for for temperature < 35“C and decreased after temperature > 35°C.

The results in Fig.2 indicated that higher temperatures resulted in higher protein and nattokinase Kommareddi found that increasing temperature would result in faster tumbling of the reversed micelles and increased lateral diffusion of the surfactant molecules due to increased thermal energy[9]. The results in Fig.2 implied that the same effect of temperature on the structure of reverse micelles occurred during extraction of nattokinase. That was to say, the migration time for nattokinase transfer through oil-water interface will be decreased because of the disruption of reverse micelles at higher temperatures, further this contributed to the higher protein and nattokinase activity recovery at higher temperatures.

At temperatures higher than 35°C, nattokinase activity recovery decreased greatly with little decrease of protein recovery. The same effect of temperature during forward extraction was observed in Fig. 1. These implied that some loss of nattokinase activity during extraction. Nattokinase was demonstrated to be relatively labile between 30-40°C[12], so the loss of acitivity could be contributed to the inactivity at higher temperatures.

Effect of volume ratio of organic to aqueous phase during forward extraction

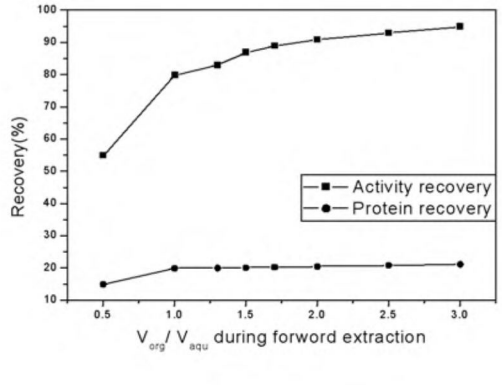


Fig3.. Effect of phase-volume ratio (V_0rg/V_aq) during forward extraction on nattokinase activity recovery(B), protein recovery(A),

The effect of volume ratio of organic to aqueous phase during forward extraction was shown in Fig.3. Nattokinase activity recovery and protein recovery increased with the phase-ratio increasing when the aqueous phase was fixed. The maximal nattokinase activity recovery was about 95% at the phase volume ratio of 3. Increasing the reverse micellar phase volume would have an increase in the number of reverse micelles and thereby the amount of

nattokinase extracted would increased. Nattokinase showed no concentration but dilution in the reverse micellar phase during forward extraction.

Effect of volume ratio of organic to aqueous phase during backward extraction

The time dependence of nattokinase activity recovery and protein recovery at a series of phase volume ratios were shown in Fig.4. The results showed that nattokinase could be concentrated 2 times during backward extraction with little decrease of activity recovery. When phase volume ratio was higher than 2, the maximal nattokinase activity recovery decreased greatly, accompanied by the slow decrease of protein recovery.

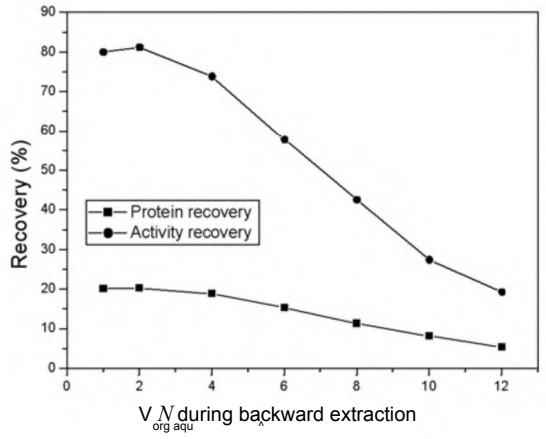


Fig4. Effect of phase-volume ratio ($V_{org}A/_{aq}$) during backward extraction on nattokinase activity recovery(O), protein recovery(M).

Nishiki investigated the enrichment of lysozyme during forward and backward transfer of reverse micellar extraction [13,14], It was found that lysozyme can be enriched in the reversed micellar phase (50mM AOT/isooctane) up to 14 times (Img/ml protein in initial aqueous phaseduring) during forward transfer and lysozyme could be enriched 23 times during backward trasfer (Img/ml lysozyme in reversed micellar phase). Nattokinase could be concentrated only 2 times during backward extraction with some 80% recovery of nattokinase activity. The enrichment of lysozyme during backward extraction was carried out by the use of model system of lysozyme, no concerning of activity recovery after extraction. Usually it takes long time for back extraction to reach equilibrium because of its slowness and little interfacial area at high volume ratio of organic to aqueous phase. This might the reason for the concentration difference between lysozyme and nattokinase.

CONCLUSIONS

Reverse micellar extraction was applied to the purification and concentration of nattokinase from fermentation broth. Factors, including temperature and phase volume ratio used for the

forward and backward extraction were investigated on the extraction process. The optimal temperature for forward and backward extraction are 25 °*C* and 35 °C respectively. Nattokinase became more thermosensitive during reverse micellar extraction than in aqueous solution. No concentration but a little dilution was found for forward extraction. While nattokinase could be enriched in the stripping phase 2 times the nattokinase concentration in reverse micelles phase during backward extraction. Less interfacial area and the inactivation at longer contact time restrained the concentration times of backward extraction.

ACKNOWLEDGEMENTS

The authors acknowledge the financial support from the National Natural Science Foundation of China (No.20221603).

REFERENCES

1. S. H. Krishan, N.D. Srinivas, K.S.M.S. Raghavarao, N.G. Karanth (2002), Adv. *Biochem. Eng. Biotechnol.,* 75, 124-183
2. H. Sumi, H. Hamado, H. Tsushima, H. Mihara, H. Murica (1987), *Experientia,* 43, 1110-1111
3. M. Fujita, K. Hong, Y. Ito, R. Fuji, K. Kariya, S Nishimuro (1995), *Biol. Pharm. Bull.,* 18, 1387-1391
4. H. Sumi, H. Hamada, K. Nakanishi, H. Hiratani (1990), *Acta. Haemotol.,* 84, 139-143.
5. M. Fujita, K. Hong, Y. Ito, S. Misawa, N. Takeuchi, K. Kariya, S. Nishimuro (1995), *Biol. Pharm. Bull.,* 18, 1194-1196
6. M. Fujita, K. Nomura, K. Hong, Y. Ito, A Asada, S Nishimuro (1993), *Biochem. Bioph. Res. Co.,* 197, 1340-47
7. M.M. Bradford (1976), *Anal. Biochem.,* 72, 248-254
8. M.L. Ansen(1939), *J. Gen. Physiol.,* 22, 78-79
9. N. S. Kommareddi, V. T. John, Y. Y. Waguespack, G. L. McPherson (1993), *J. Phys. Chem.,* 97, 5752-5761.
10. M. Dekker (1990), Enzyme recovery using reversed micelles, Ph D. thesis, Agricultural university of Wageningen, The Netherlands,
11. Larsson KM, Adlercreutz P, Mattiasson B. (1990) *Biotechnol. Bioeng.,* 36, 135-141
12. C. Chang, M. Fan, F. Kuo, and H. Sung (2000), *J. Agri. Food Chem.,* 48, 3210-3216
13. T. Nishiki, I. Sato, T. Kataoka, D. Kato (1993), *Biotechnol. Bioeng.,* 42, 596-600
14. T. Nishiki, A. Muto, T. Kataoka, D. Kato(1995), *Chem. Eng. J.,* 59, 297-301



APPLICATION OF DISSOLUTION EQUILIBRIUM IN AVERMECTINS PURIFICATION

Zhi Xie[1,2] Zhidong Chang[1] Xinghua Sun[1] Ji Liu[1] Huizhou Liu[1] and Wenjun Li[2]

1. Laboratory of Separation Science and Engineering, State Key Laboratory of Biochemical Engineering, Institute of Process Engineering, Chinese Academy of Sciences, P.O. Box 353, Beijing, 100080, PR. China
2. Department of Chemistry, Applied Science School, University of Science and Technology Beijing, Beijing, 100083

Avermectins are efficient green insecticides and miticides. There are eight components with similar structure in avermectins ferment broth, which make their purifications very difficult. The dissolution equilibrium is a dynamic equilibrium process, in which transfer of molecules of impurities from solution to solid phase is more difficult than that from solid phase to solution at the solid-liquid interface. Therefore, avermectins maybe can be purified using dissolution equilibrium. In the work, effects of equilibrium time, stirring speed, equilibrium temperature and crystal size on the efficiency of purification were studied. Results showed that the efficiency of purification increased with increase of equilibrium time, stirring speed, equilibrium temperature, and decrease of crystal size. The purification efficiency of different organic solvents was also studied. Results showed that methanol, n-butanol and acetone are the best solvents.

INTRODUCTION

Avermectins, produced by Streptomyes avenmilities, have a polyketide derived macrolide skeleton linked to a disaccharide composed of two a-linked i-oleandrose units. Avermectins are efficient insecticides and miticides. They are often used to control pests, such as nematodes, helminthes, of veterinary animals and crops [1,2], Avermectins have wide spectrum of activity, high potency, favorable safety margin, and unique mechanism of action. Most of the recent evidence suggests that avermectins can inhibit pharvnqeal pumping (and hence feeding), motility and fecundity in susceptible nematodes by opening chloride ion channels in cell membranes of peripheral nerve tissues of the parasite [3, 4], Because of the ability of the mammalian blood-brain barrier to efficiently partition these drugs out of the central nervous system, these compounds in mammals are safe [5-7], So they are green insecticides and miticides.

In the fermentation process of avermectins there are usually eight components with familiar structure, among which avermectin B_{1a} (AVM B_{1a}) is the most active compound [8], The presence of different components with similar structure makes the purification of avermectins very difficult. In order to get high-purity avermectins, conventional crystallization has to be

repeated again and again. It is necessary to develop a purification method with high efficiency.

In this paper, a new purification method, the dissolution equilibrium, was presented. The dissolution equilibrium is a dynamic equilibrium process. In dissolution equilibrium process, the transfer of molecules of impurities from solution into solid phase is more difficult than that from solid phase to solution in the solid-liquid interface. The purification efficiency of different factor was also studied in order to acquire the best operation conditions.

EXPERIMENTAL

Chemicals

Methanol, enthanol, 2-propanol isopropyl alcohol, n-butanol, n-amyl alcohol, acetone, ethyl acetate, tetrachloride and chloroform, are all of analytical grade, supplied by Concord Technology Company (Tianjin, China).

The crude avermectins crystals were supplied by North China Pharmaceutical Group Aino Company. The standard avermectin Bi_a was obtained by recrystallization. Working solutions of avermectin B_{1a} were prepared in methanol. All solutions were passed through a 0.45pm nylon filter before injection into the LC system.

Experimental

The experimental apparatus using for dissolution equilibrium was showed in Figure 1.

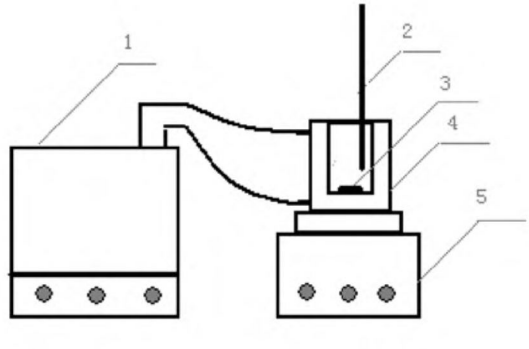


Figure 1. Experimental apparatus.
1-thermo-regulated water bath; 2-thermometer,- 3- magneton;
4-glass reactor,- 5-magnetic stirrer

Take 50ml solvent in the glass reactor and maintain solvent temperature by water bath. Avermectins crystals as two times as its theoretical solubility were mixed with the solvent, at the same time the mixture start to be stirred. 1ml solution was sampled at different time to centrifugalize. Then take clear solution or crystals to analyze using LC.

The liquid chromatographic system (HP1100 Agilent Technologies, USA) was equipped with a diode array detector and a stainless steel analytical column (ZORBAX SB-C18, 5pm particle size, 4.6mm * 250 mm). The mobile phase used was water 10% in methanol (v/v), isocratic at a flow-rate of 1.0 ml/min. Separations were carried out at 35°C and 10 pi was injected into the LC system [9],

RESULTS AND DISCUSSION

Effect of equilibrium time

The effect of equilibrium time on purification efficiency was studied when the stirring speed was 240r/min and the mean crystal size was 60pm at 25°C. Methanol, ethanol and n-butanol were selected to be used as solvents to study the effect of equilibrium time. Figure 2 showed the variation of the purity of AVM B_{1a} in solution with equilibrium time. The efficiency of purification increases with increase of equilibrium time. The purifying process reached equilibrium state in 3.0 hours with methanol as solvent. The result with ethanol as solvent was the same. But with n-butanol as solvent, the equilibrium state was fulfilled in 5.0 hours. The mass transfer is slow in the solid-liquid interface with n-butanol as solvent since it is very sticky. So it spent longer time with n-butanol as solvent to obtain the best efficiency of purification than those with methanol and ethanol as solvents.

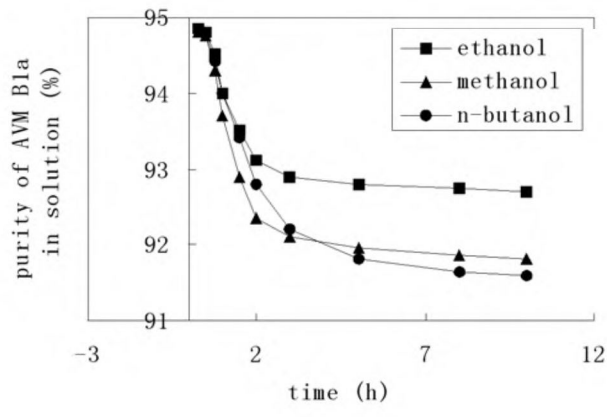


Figure 2. Effect of equilibrium time on efficiency of purification.

Effect of stirring speed

The effect of stirring speed on purification efficiency was studied when the solvent was n-butanol and the mean crystal size was 60pm at 25°C. As shown in Figure 3, the quicker stirring speed is, the shorter time it is to obtain the best efficiency of purification and the better purification efficiency is. The reason may be explained as that relative movement between the crystal and the solution become more and more quickly with increase of stirring speed. Therefore, the transfer of molecules at the solid-liquid interface will be enhanced. And the more impurity in crystal will be transferred into the solution because the mixture of solid and liquid will became more uniform with increase of stirring speed resulting in better efficiency of purification.

Effect of equilibrium temperature

The effect of equilibrium temperature on purification efficiency was studied when the solvent was n-butanol, the mean crystal size was 60pm and the stirring speed was 240r/min. As shown in Figure 4, the efficiency of purification increased and the time obtaining the best efficiency decreased with increase of equilibrium temperature. The reason may be that the transfer speed of molecules in the solid-liquid interface will increase with the increase of equilibrium temperature because it enhances the molecular movement. Therefore, it spends much shorter time to obtain the best efficiency of purification and the efficiency will be better.

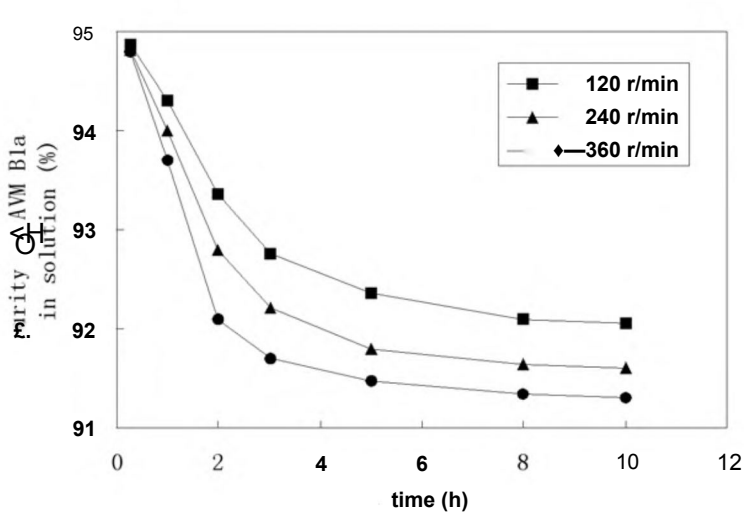


Figure 3. Effect of stirring speed on efficiency of purification.

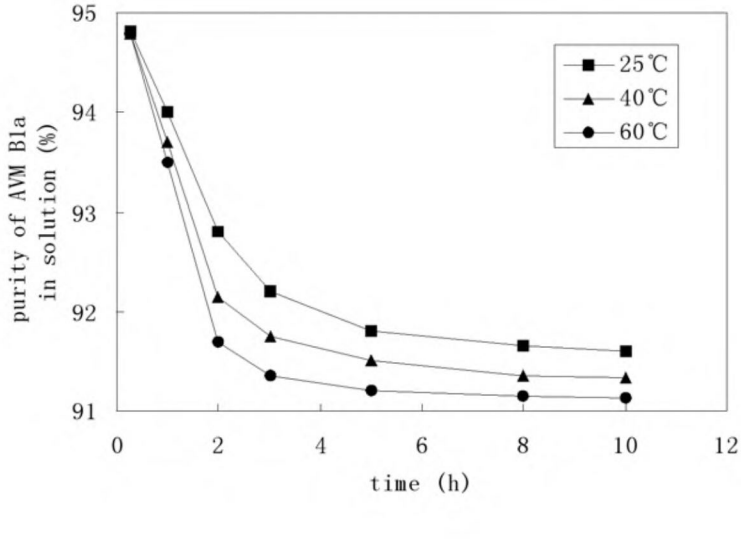


Figure 4. Effect of equilibrium temperature on the efficiency of purification.

Effect of crystal size

The effect of crystal size on purification efficiency was studied when n-butanol was used as solvent and the stirring speed was 240r/min at 25°C. As shown in Figure 5, smaller the crystal size is, better efficiency of purification is. The reason may be that the surface of crystal is larger under the small crystal size. The purification process of dissolution equilibrium mainly happened at the interface of solid-liquid. So with increasing the interface the efficiency of purification increases.

Effect of solvent

The effect of different solvents on purification efficiency was studied when the mean crystal size was 30pm and the stirring speed was 360r/min at 25°C. The histogram of the purity of AVM Bi_a in crystals versus solvent in Figure 6 shows. As shown in Figure 6, the best efficiency of purification will be obtained when methanol, n-butanol and acetone are used for solvent.

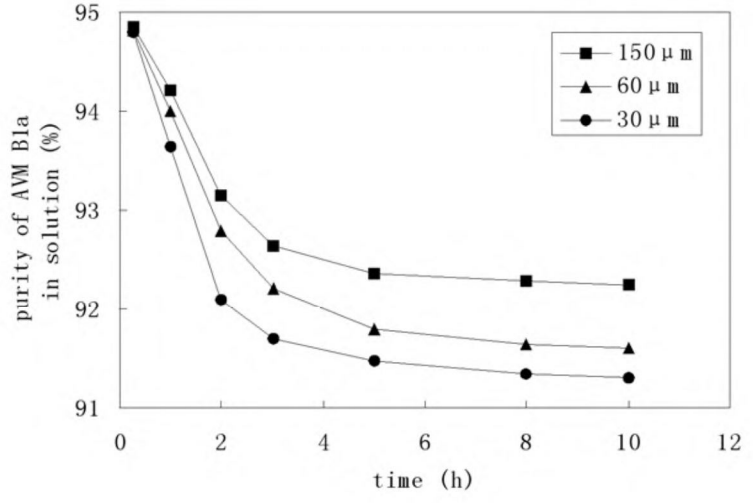


Figure 5. Effect of crystal size on the efficiency of purification.

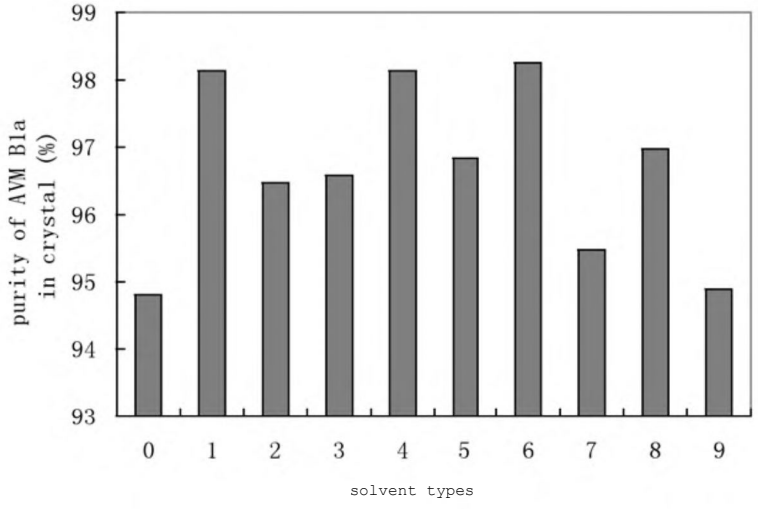


Figure 6. Effect of solvent on the efficiency of purification.
O-avermectins crystals, 1-methanol, 2-enthanol, 3-2-propanol isopropyl alcohol, 4-n-butanol, 5-n-amyl alcohol, 6-acetone, 7-ethyl acetate, 8-tetrachloride, 9-chloroform

CONCLUSIONS

The dissolution equilibrium as a new purification method was studied. Experimental results proved that the dissolution equilibrium was a good method for purifying avermectins. The results showed that the efficiency of purification increases with increasing equilibrium time, smaller crystal size, higher stirring speed and equilibrium temperature. The purification efficiency of different solvents was also studied. The results showed that methanol, n-butanol and acetone are the best solvents for purification of avermectins in dissolution equilibrium.

ACKNOWLEDGEMENTS

This work was supported by the National Science Foundation of China (No. 20406021, No. 20236050, No.20221603).

REFERENCES

1. W. L. Shoop, H. Mrozikand M. H. Fisher (1995), *Vet. Parasitol.,* 59, 139~156.
2. M. H. Fisher(1990), *Royal Society of Chemistry: Cambridge,* pp. 52-68.
3. J. M. Schaeffer and H. W. Haines(1989), *Biochem. Pharmacol.,* 38, 2339-2349.
4. Q. A. Mckellarand H. A. Benchaoui(1996), *J. Vet. Pharm. Therap.,* 19, 331 ~351.
5. A. H. Schinkel, J. J. Smitt, O. van Tellingen and J. H. Benijnen(1994), *Cell,* 77, 491-502.
6. A. H. Schinkel, E. Wagenaar, C. A. Mol and L. van Deemter(1996), *J. Clin. Invest.,* 9, 2517—2524.
7. J. M. Rose, S. L. Peckham, J. L. Seism and K. L. Audus(1998), *Neurochem. Res.,* 23, 203-209.
8. R. W. Burg, B. M. Miller, E. E. Baker and J. Birnbaum(1979), *Antimicrob. Agents Chemother.,* 15, 361-367.
9. J. S. Li and S. Q. Zhang(1996), *J AOAC Int.,* 79,1300.

PROTEIN ADSORPTION ON CIBACRON BLUE F3GA-ATTACHED MAGNETIC POLY (METHYLMETHACRYLATE) MICROSPHERES

Z. Y. Ma, Y. P. Guan and H. Z. Liu

Laboratory of Separation Science and Engineering, State Key Laboratory of Biochemical Engineering, Institute of Process Engineering, Chinese Academy of Sciences, Graduate School of the Chinese Academy of Sciences

Micron-sized magnetic poly (methylmethacrylate) (PMMA) microspheres were prepared by a modified suspension polymerization method in the presence of oleic acid-coated magnetic Fe_30_4 nanoparticles. After chemical modification with ethylene glycol to produce hydroxyl groups, an affinity dye ligand, Cibacron Blue F3GA, was covalently attached onto magnetic PMMA microspheres for bovine serum albumin (BSA) adsorption from aqueous solution. The results showed that the Cibacron Blue F3GA-attached magnetic PMMA microspheres had high adsorption capacity of BSA and BSA could be easily desorbed by using 1 M NaSCN solution. Dye ligand-attached magnetic PMMA microspheres, which have the advantage of low cost, high adsorption capacity and high magnetic content, have extensive potential application in large scale protein affinity separation or purification.

INTRODUCTION

Magnetic support based separation has been widely used in the various fields of biotechnology and biomedicine, such as enzyme immobilization, cell sorting, protein purification, drug delivery and hyperthermia [1-5], The principle of this method is to utilize maanetic oarticles to bind the taraet molecules via liaands. thereby tormina a comolex that can be separated from the bulk solution by a magnetic field gradient. Compared to conventional separation, the advantages of magnetic separation are attributed to its speed, accuracy, and simplicity. In particular, the separation process can be performed directly in crude samples containing suspended solid materials without any pretreatment. Most of the magnetic supports used in the separation involved the porous structure. The limitation of the porous supports is that they are prone to fouling with biological foulants. In contrast, nonporous supports are less prone to fouling and have improved binding and desorption kinetics, and allow greater accessibility of macromolecules to the immobilized ligands than porous adsorbents, thus permitting shorter contact time with the feedstock.

The affinity ligands immobilized on the supports can be divided into bioligands and pseudoligands, such as dyes and transition metal ions. The bioligands are extremely specific in most cases. However, they are expensive due to high cost of production and extensive purification steps. In addition, it is difficult to retain their original biological activity when they are immobilized on the matrix. Compared with the bioligands, dye ligands have many advantages. They are commercially available, inexpensive, stable, easily to be coupled to the supports with functional groups, especially hydroxyl groups, and have large capacities for protein adsorption [6], Dye ligands can bind most types of proteins, such as albumin, dehydrogenase and lysozyme.

Magnetic supports are mostly prepared with polymers since they have a variety of surface functional groups that can be tailed for specific applications. Many approaches have been employed to prepare magnetic polymer microspheres including coating the magnetic particles with synthetic or natural polymers, suspension polymerization, emulsion polymerization, and dispersion polymerization etc. [7-9], Copolymerization with functional monomer is always used to introduce the functional groups on the magnetic microspheres. However, most of the functional groups are buried in the supports with only a small part left on the surface for ligand binding.

In this paper, an affinity dye ligand, Cibacron Blue F3GA (CB) was attached on the magnetic poly (methylmethacrylate) (PMMA) microspheres for protein adsorption. The magnetic PMMA particles were prepared by a modified suspension polymerization in the presence of oleic acid-coated magnetite nanoparticles. Then they were chemically modified with ethylene glycol to produce functional hydroxyl groups (-OH). CB was covalently attached to them and their adsorption capability for a model protein, bovine serum albumin (BSA), was tested in a batch system.

EXPERIMENTAL

Materials

All chemicals used were purchased from Beijing Chemical Reagents Company unless otherwise stated. Methyl methacrylate (MMA) and divinylbenzene (DVB, crosslinker) were distilled under vacuum. Benzoyl peroxide (BPO) was used as an initiator. Poly (vinyl alcohol) (PVA-1788) was used as a stabilizer. BSA and CB were purchased from Sigma. Analytical-graded, ferric chloride hexahydrate ($FeCl_3$-$6H_20$), ferrous chloride tetrahydrate ($FeCl_2.4H_20$), ammonium hydroxide (25 wt %), oleic acid and ethylene glycol were used as received.

Methods

Synthesis of oleic acid-coated magnetic Fe_30_4 nanoparticles

The synthesis of oleic acid-coated magnetic Fe_30_4 nanoparticles was followed by a co-precipitation method [10]. 23.5 g of $FeCl_3$-$6H_20$ and 8.6 g of $FeCl_2$-$4H_20$ were dissolved in 800 mL deionized water under nitrogen at 80 °C. 25 mL NH_3- H_20 were added and 20 mL oleic acid were added afterwards. After several minutes, the magnetic precipitate was isolated from

the solvent by magnetic decantation and washed with deionized water several times to remove the excess oleic acid.

Preparation of Magnetic PMMA microspheres

Magnetic PMMA microspheres were prepared by a modified suspension polymerization. 25 g of the magnetic Fe_30_4 precipitates and 3 g of BPO were dissolved in a mixture of 95 ml_ MMA and 5 ml. DVB to form the organic phase. The mixture was transferred into a 2-liter beaker containing 800 ml_ H_20 with 30 g dissolved PVA. The beaker was equipped with four vertical stainless steel baffleplates, a nitrogen inlet and a 4-paddle mechanical stirrer. With agitation at 1000 rpm, the temperature was increased evenly from 45 "C to 60 °C within 1h, and then the temperature was maintained at 60 °C for 2 h while finally the temperature was increased to 70 °C and kept for 2 h. The reaction mixture was cooled to room temperature and the resulting magnetic microspheres were separated by a magnet and thoroughly washed with deionized water.

Surface modification and CB attachment on magnetic PMMA microspheres

The functional hydroxyl groups were introduced to magnetic PMMA microspheres via the surface modification with ethylene glycol. 2.0 g of magnetic PMMA microspheres was mixed with 100 ml_ of ethylene glycol and the temperature increased to 100 °C to remove water. Then 0.5 g sodium methylate was added, and the mixture temperature was kept at 100 °C for 24 h with mild stirring. The resulting microspheres were washed thoroughly with deionized water and methanol to remove the unreacted ethylene glycol. The procedure resulted in the plenty of hydroxyl groups on the magnetic PMMA microspheres.

The modified magnetic PMMA microspheres were suspended in 60 mL CB aqueous solution (6.0 mg/mL). The mixture was mixed with 3 g of sodium chloride and 4 g of NaOH. The reaction mixture was shaken at 80 °C for 4 h. After incubation, the magnetic microspheres were separated and washed with water extensively until all of the physically adsorbed CB was removed.

BSA adsorption

BSA was used as a model protein to test the adsorption characteristics of the CB-attached magnetic PMMA microspheres. Typically, 5 mg of microspheres was mixed with 5.0 mL of BSA solution of different concentrations. The adsorption experiments were conducted in 20 mM phosphate buffered saline (PBS, pH 5.0) at 25 °C for 2 h in a shaking incubator. The aqueous phase ionic strength was adjusted with NaCI. At the end of adsorption, the microspheres were magnetically separated, and the supernatant was analyzed for protein concentration with a UV/Vis spectrophotometer at 280 nm. The adsorbed quantity of protein was calculated by mass balance.

Characterization of magnetic PMMA microspheres

The moroholoav and size of the maanetic PMMA microsDheres was observed bv scannina electron microscopy (SEM, JEOL, JSM-6700F, Tokyo, Japan). The magnetization curves of the dried microspheres were recorded with a vibrating sample magnetometer (VSM) (model-155, Digital Measurement System, Inc.). Diffuse reflectance infrared Fourier transform spectra (DRIFTS) of both the unmodified and modified magnetic microspheres were obtained with a FTIR spectrophotometer (FTIR, Bruker, Vector 22).

RESULTS AND DISCUSSION

Preparation of Magnetic PMMA microspheres

Magnetic PMMA microspheres were prepared by a modified suspension polymerization method. Figure 1 shows the SEM photograph of the magnetic microspheres. It can be seen from the picture that the microspheres are spherical in shape and the average size is about 4 pm.

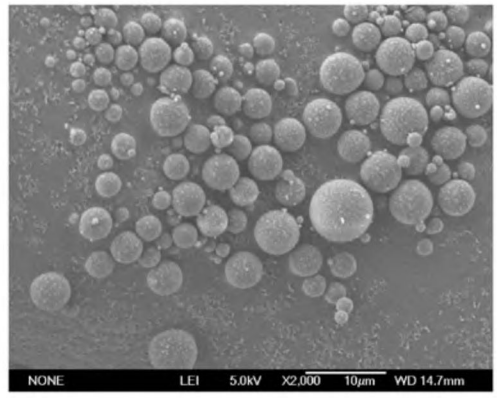


Figure 1. SEM photograph of magnetic PMMA microspheres

The magnetic properties of magnetic PMMA microspheres were recorded by VSM at room temperature (Figure 2). The characteristic superparamagnetic behavior is indicated by zero coercivity and zero remanence on the magnetization curve. The superparamagnetic property of magnetic microspheres is critical for their application in bioseparation, which prevents magnetic microspheres from aggregation and enables them to redisperse rapidly when the magnetic field is removed. The saturation magnetization of magnetic microspheres was found to be 11.5 emu/g. With such high saturation magnetization, they could be easily and fast separated from a suspension. This is very favorable to the magnetic separation of proteins on a large scale.

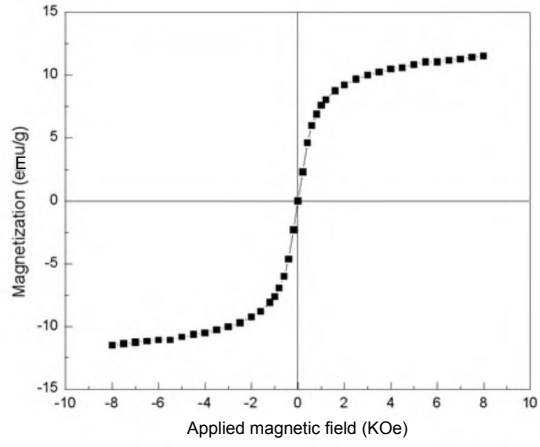
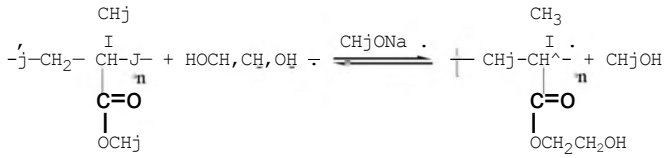


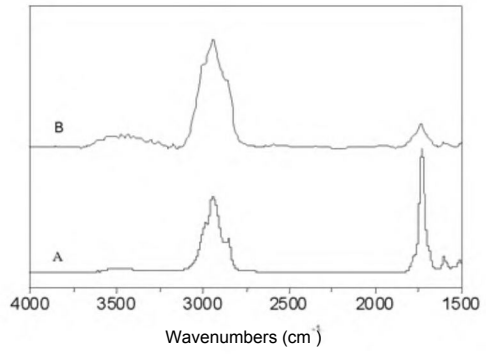
Figure 2. Magnetization curve of magnetic PMMA microspheres at room temperature

Surface modification and CB attachment

The surface modification of magnetic PMMA microspheres was carried out on the basis of the transesterification reaction with ethylene glycol in the presence of sodium methylate as the catalyst. The -OCH3 groups on the polymer surface were replaced with ethylene glycol as shown in the following reaction equation:



This change in the polymer surface structure was proven by the comparison of DRIFTS spectra of magnetic PMMA microspheres before (A) and after (B) transesterification as shown in Figure 3. The strong peak at 1732 cm'¹ indicates the presence of carboxylic ether due to



the C=0 stretching vibration on both the modified and unmodified PMMA microspheres. After transesterification, the relative intensity ratio of *\2s00-3000l\1732* increased owing to plenty of ethylene glycol coupling to the surface of the polymer microspheres. Meanwhile, the characteristic vibration bands of hydroxyl groups appear at 3400 cm'¹ in the modified PMMA microspheres.

Figure 3. DRIFTS spectra of unmodified (A) and modified magnetic PMMA microspheres

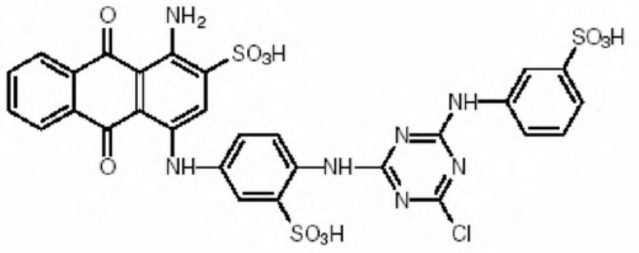


Figure 4. Chemical molecular structure of Cibacron Blue F3GA dyes.

After modification, CB as an affinity ligand was covalently attached on the hydroxylated magnetic PMMA microspheres via the reaction between the chloride groups of the reactive dyes and the hydroxyl groups of the microspheres. The chemical structure of CB molecule is shown in Figure 4.

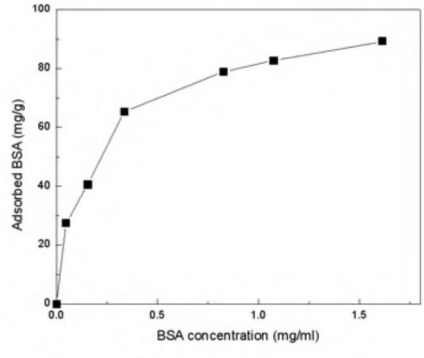


Figure 5. Adsorption isotherm of BSA on CB-attached magnetic PMMA microspheres

BSA adsorption

To investigate the affinity adsorption property of the CB-attached magnetic microspheres, BSA was selected as a model protein. Figure 5 shows the adsorption isotherm of BSA on CB-attached magnetic PMMA microspheres.

The adsorption was carried out in the 20 mM PBS of pH 5.0, because low aqueous phase ionic strength is favorable for protein adsorption and the maximum adsorption of protein is usually obtained when the pH is the isoelectric point of BSA (pl=4.7)[11], With increase of the protein concentration, the adsorption amount of protein increased and reached equilibrium. The adsorption capacity of BSA was 89.2 mg/g. The adsorbed BSA could be easily eluted with 1 M NaSCN. When the NaSCN was used, the electrostatic interaction between the positively charged groups of albumin and the negatively charged CB decreased. This forced the desorption of albumin. This allows repeated use of the CB-attached magnetic affinity adsorbents.

CONCLUSIONS

Magnetic support based separation has many advantages compared with the conventional separation methods. In this study, magnetic PMMA microspheres were prepared by a modified suspension polymerization with the average size of 4 pm. The magnetic microspheres had a superparamagnetic property and high saturation magnetization (11.5 emu/g). After modification with ethylene glycol to produce hydroxyl groups on the microspheres, CB as an affinity ligand was attached and the microspheres were used for the affinity adsorption of a model protein. The adsorption results showed that the microspheres had a high adsorption capacity (89.2 mg/g) for BSA. With the advantage of easy preparation, low cost, high magnetic content and high adsorption capacity, these magnetic microspheres have extensive potential for affinity separation of protein on a large scale.

ACKNOWLEDGEMENTS

This work was financially supported by the National High Technology Research and Development Program of China (No.2002AA302211), the National Natural Science Foundation of China (No. 20206032).

REFERENCES

1. R.F.H. Dekker (1989), *Appl. Biochem. Biotechnol.,* 22, 289.
2. M. Šafarik and I. Šafariková (1999), *J. Chromatogr. B,* 722, 33.
3. S. M. O'Brien. O. R.T. Thomas and P. Dunnill (1996V *J. Biotechnol.* 50. 13.
4. S. Gomez-Lopera, R. Plaza and A. Delgado (2001), *J.Colloid Interface Sci.* 240, 40.
5. S.K.Jones, P. Moroz and B. N. Gray (2002), *Eur. Cells Mater.* 3, 74.
6. H. Yavuz, E. Duru, O. Gene and A. Denizli (2003), *Colloid. Surf. A,* 223, 185.
7. Y. Lee, J. Rho and B. Jung (2003), *J. Appl. Polym. Sci.* 89, 2058.
8. N. Yanase, H. Noguchi, H. Asakura andT. Suzuta (1993), *J. Appl. Polym. Sci.* 50,765
9. D. HorAk (2001), *J. Polym. Sci. Part A Polym. Chem.,* 39, 3707.
10. Y.P. Guan, H.Z. Liu, Z.T. An, J.J. Ke, J.Y. Chen (1998), CN Pat. 98124516.1.
11. R. K. Scopes (1986), *J. Chromatogr,* 376, 131.

EXTRACTION OF PHENYLETHANOID GLYCOSIDES FROM *CISTANCHE DESERTICOLA* CULTURED CELLS BY MIXED ENZYMES AND ULTRASONICATION PRETREATMENT

Min Gao[1,2], Daqing Sun[3]and Chunzhao Liu[1,2*]

1 State Key Laboratory of Biochemical Engineering, Institute of Process Engineering, Chinese Academy of Sciences, Beijing, P.R. China

2 Graduate school of the Chinese Academy of Sciences, Beijing, P. R. China

3 Valley Research inc., South Bend Indiana, IN 46628, USA

'Correspondence to: Chunzhao Liu, Professor,

Tel/Fax: 010-82622280; E-mail: czliu@home.ipe.ac.cn

Phenylethanoid glycosides (PeGs) were extracted from *Cistanche deserticola* cultured cells in this study using enzyme treatment, ultrasound assisted extraction, and a combination of the two methods. In the enzyme treatment process, the maximal percentage extraction reached 2.1% after 4h, which was 1.5-fold higher than that in room temperature solvent extraction after 24 h. In the ultrasound-assisted extraction, the maximal percentage extraction was 1.5% after 20 min. In the combined extraction process, the amount of PeGs extracted was 2.1% after ultrasonic irradiation for 10 min followed by enzyme treatment for 2 h. The extraction efficiency of PeGs from C. *deserticola* cultured cells was improved greatly in the combined extraction process because of reduced extraction time.

INTRODUCTION

Cistanche deserticola is a traditional medicine in China, which contains many useful secondary metabolites, such as glycosides, flavonoids, alkaloids, amylose and naphtha [1-3], Phenylethanoid glycosides (PeGs), as the main bioactive components of this elite medicinal

species, have many activities like improving sexual function, scavenging free oxygen radicals and anti-decrepitude [4],

Extraction is the first essential step for the recovery and purification of bioactive compounds of medicinal plants. The functional basis of traditional extraction methods like solvent extraction, heat reflux extraction and Soxhlet extraction is mainly related to the choice of solvents and heat or mixing to increase the solubility or mass transfer rate of useful components [5-6], These methods are easy to perform but have the shortcomings of low yield and efficiency.

Enzyme assisted extraction is a new method, which has been investigated recently. Enzymes can help to enhance the extraction process by hydrolyzing the cellulous wrapping of the effective components. At the same time, it is environmental friendly and can be used safely without adverse health effects [7,8]. The main component of plant cell wall is cellulose, which is a polymer composed of anhydroglucose monomer units [9], The distinctive structural characteristics of anhydroglucose makes it resistant to attacks from both organic solvents and acid molecules [10,11], Enzymes can calmly hydrolyze the cellulose around the bioactive component, and improve the mass transfer process and the distribution coefficient. Treatment involving some form of physical disruption is often employed to improve the efficiency of enzyme treatment [12]. It is well known that ultrasound waves can destroy the cell wall of plants and permit intracellular metabolites to be released. A great number of studies have been performed on the application of ultrasound in the extraction of active components in medicinal plants [13,14],

In the present study, a carbohydrase and hydrolase mixture was used to extract PeGs from C. *deserticola* cultured cells. The optimization of enzyme treatment with ultrasound pretreatment was further carried out.

MATERIALS AND METHODS

Plant materials

The calli of C. *deserticola* were incubated on Murashiage and Skoog medium supplemented with 30 g/L sucrose and 5 g/L agar for PeGs production. The medium pH was adjusted to 5.8 with 1 M NaOH before autoclaving. The cultivation was carried out in 250 mL flasks containing 50 mL of the medium. After 25 days, the calli were collected and dried at 65 ”C in an oven until a constant weight was obtained.

Extraction methods

The dried cells of *C. deserticola* were ground using a pestle and mortar, and then passed through a stainless steel sieve with pore size of 0.45 mm before extraction.

Solvent extraction was performed in a 5 ml_ test tube, and 10 mg dried cells were put into the test tube. 4 ml_ methanol and 1 mL of a pH 3.8 buffer solution were added, after immerging the material for 24 h, the upper solution was collected for detection.

The enzymes were commercial *Crystalzyme* PML-MX (Valley Research Inc., USA) and were prepared with a pH 3.8 buffer solution for the later tests. Enzyme treatment was as follows: the dried cells of *C. deserticola* (10 mg) were transferred into a 5 mL test tube, after which 1 mL enzyme solution was added. The solution was placed in a water bath at 50 °C for 0.5-6 h, after which the test tube was taken out and 4 mL methanol was added. After 1 h, the extraction solution was collected for detection.

Ultrasound assisted extraction was carried out using an ultrasonic bath of 26 kHz and 250 W. 10 mg dried cells were put into a 5 mL test tube, after which 1 mL buffer solution and 4 mL methanol were added. After treatment with ultrasound for a given duration, the solvent was collected for detection.

For the combined process, the dried cells of *C. deserticola* (10 mg) were put into a 5 mL test tube, after which 0.5 mL buffer solution was added. The solution was put into the ultrasonic bath and treated with ultrasound for a given period of time. After ultrasonic irradiation, the 0.5 mL enzyme solution was added and the resulting mixture was kept at 50 °C in a water bath for a given time. Then 4 mL methanol was added and extraction continued 1 h, after which the upper solvent was collected for detection.

Analytical method

The extraction solution from the dried cells with methanol was concentrated, the residue dissolved in distilled water and then passed through a macroreticular resin column (AB-8, chemical product of Nankai University, Tianjing, China). The methanol eluate was collected and the total PeGs content was determined at 333 nm by using echinacoside as standard. The percentage extraction of PeGs can be estimated by: the yield of total PeGs/mass of C. *deserticola* X 100%.

RESULTS AND DISCUSSION

Enzyme treatment extraction

The main component of the enzyme mixtures used was cellulose enzyme, which has the ability to hydrolyze cellulose to water-soluble content [16], With the increase of enzyme concentration, the percentage extraction of PeGs was increased (Fig. 1). The amount of PeGs extracted nearly reached the maximum of 1.6% at an optimal enzyme concentration of 2.4 mg/mL for the given amount of plant material.

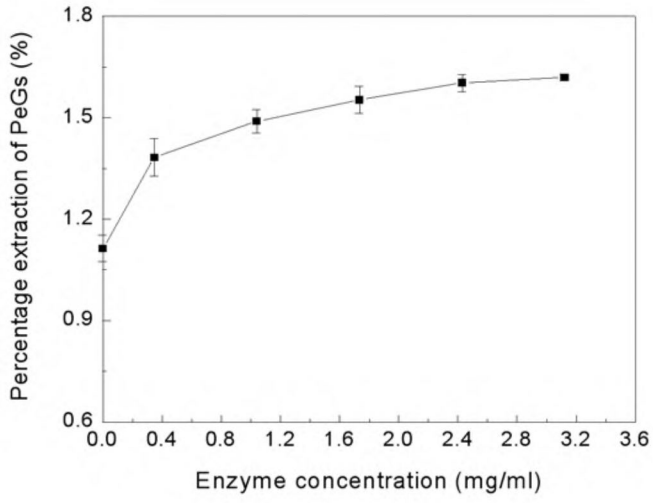


Fig. 1. Effect of enzyme concentration on the percentage of PeGs extracted.

The percentage of PeGs extracted increased rapidly with enzyme treatment time during the initial hours (Fig. 2). The percentage extraction reached 2.1% after 4 h enzyme treatment and stayed constant afterwards.

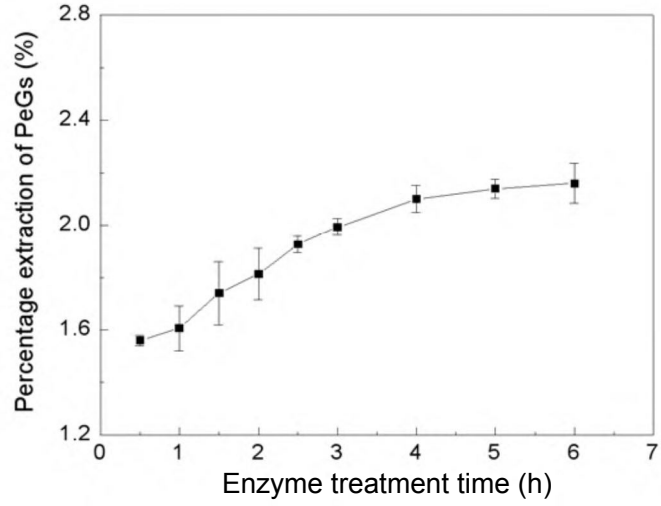


Fig. 2. Effect of enzyme treatment time on the percentage of PeGs extracted.
(The concentration of enzyme was *2.4 mg/mL)*

Ultrasound-assisted extraction

Ultrasonic waves can destroy the cell membrane and wall of microorganisms or plants, and permit intracellular phytochemicals to be released. After 20 min ultrasonic irradiation the percentage extracted reached the maximal amount of 1.4% (Fig. 3).

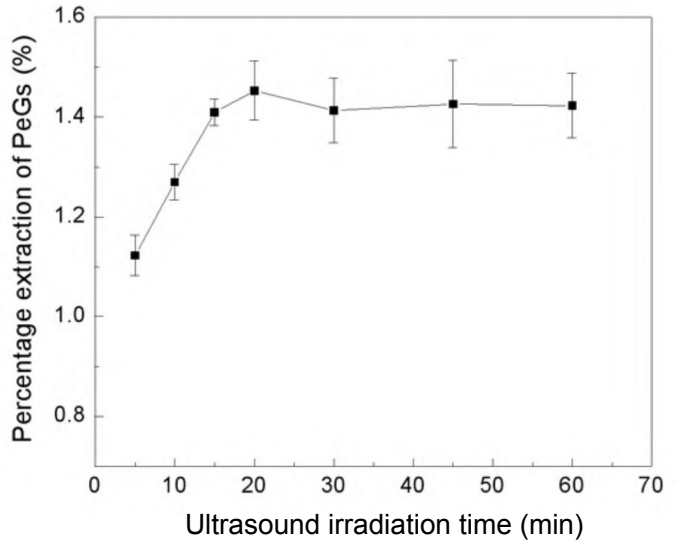


Fig. 3. Effect of ultrasound time on the percentage of PeGs extracted.

Enzyme treatment extraction with ultrasound pretreatment

With the aim of further improving the hydrolysis rate, the ultrasound irradiation as a pretreatment process was combined with the enzyme extraction. The combined method was more efficient than the single treatment with ultrasound-assisted extraction or enzyme treatment, and the result is shown in Fig. 4. The maximal percentage of PeGs extracted was 2.1% and this was obtained by enzyme treatment for 2 h combined with an ultrasound pretreatment for 10 min. With an increase in the ultrasound pretreatment time from 5 min to 10 min, the percentage of PeGs extracted was increased remarkably. The surface of the plant material became rough by the acoustic cavitation of ultrasound irradiation and therefore the surface area of the material was increased. The roughness of the surface furthermore promoted the adsorption of enzyme molecules on the surface of the cellulose fiber and increased the reaction rate. The plant cell particles stuck together under ultrasound irradiation for an increase in the pretreatment time from 10 min to 15 min and therefore the percentage extracted was not increased further.

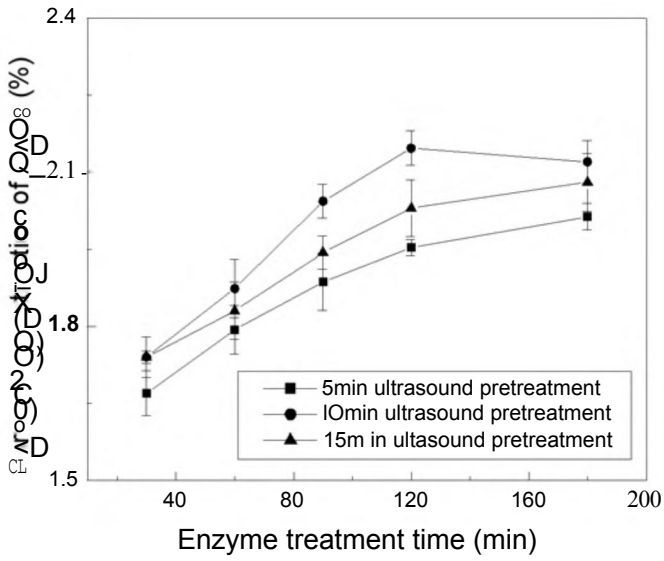


Fig. 4. Effect of enzyme treatment time on the percentage of PeGs extracted after different times of ultrasound pretreatment. (The concentration of enzyme was 2.4 mg/mL)

CONCLUSIONS

In this work, enzyme treatment, ultrasound extraction and the combined extraction of the two methods were investigated for the recovery of PeGs from C. *deserticola* cultured cells. Enzyme-assisted extraction is a mild process, which improved the percentage of extraction remarkably compared to conventional solvent extraction, but had a relative long extraction time. The percentage extraction of PeGs extracted in ultrasound-assisted extraction quickly reached the maximum amount. However, the percentage of extraction only reached the same extent of conventional solvent extraction due to the low intensity of ultrasound irradiation and collection effect of the solid particles in the solvent. In the combined method with ultrasound pretreatment followed by enzyme treatment, the percentage of PeGs extracted reached a value equal to enzyme treatment extraction, but in less time.

REFERENCE

1. L. W. Lin, T. H. Ming, H. T. Fan, W. H. Wang and C. Wu (2002), *J. Ethnopharmacology,* 83, 177-182.
2. M. C. Lu (1998). *J. Ethnopharmacology,* 59, 161-165.
3. J. Ouyang, X. D. Wang, B. Zhao and Y. C. Wang (2003), *Plant Sci.,* 165, 657- 661.
4. Z. Hromadkov and A. Ebringerov (2003), *Ultrasonics Sonochem.,* 10, 127 - 133.

5. T. Takeda, M. Inomata, H. Matsuoka, M. Hikuma and S Furusaki (2003), *Biochem. Eng. J.,* **15,** 205-210.
6. E. E. Stashenko, B. E. Jaramillo and J. R. Martýnez (2004), *J. Chrom. A,* **1025,** 105-113.
7. Z. L. Li, S. Wang, N. A. Lee, R. D. Allan and I. R. Kennedy (2004), Ana/. *Chimica Acta,* 503,171-177.
8. L. C. Vázquez, M.S. Pérez-Coello and M.D. Cabezudo (2002), *Anal. Chimica Acta.* 458, 39-44.
9. C. Osorio, C. Duque and F. B. Viera (2003), *Food Chem.,* **81,** 333 - 340.
10. S. Al-Zuhair, M. Hasan and K.B. Ramachandran (2003), *Process Biochem.,* **38,** 1155-1163.
11. B. Lignot, V. Lahogue and P. Bourseau (2003), *J. Biotech.,* **103,** 281-284.
12. H. Méndez, F. Alava, I. Lavilla and C. Bendicho (2002), *Anal. Chimica Acta,* **452,** 217-222.
13. M. Vinatoru (2001), *Ultrasonics Sonochem.,* 8, 303 - 313.
14. J. Ouyang, X. D. Wang, B. Zhao and Y. C. Wang (2003), *Plant Sci.,* **165,** 657-661.
15. B.S. Chu, S.Y. Quek and B.S. Baharin (2003), *Food Chem.,* 80, 295 - 302.

Key words: Phenylethanoid glycosides, enzyme treatment, hydrolyse, ultrasonic-assisted, ultrasound pretreatment, extraction

Presenter bibliography:

Min Gao, 1978-, Ph. D. student of the State Key Laboratory of Biochemical Engineering, Institute of Process Engineering, Chinese Academy of Sciences.

EQUILIBRIUM OF LACTIC ACID EXTRACTION WITH DI-OCTYL AMINE

Gao Min-tian*, Makoto Hirata*, Hiroshi Seki*, Michiteru Koide*, Eiichi Toorisaka*, Hirokazu Takanashi, Tadashi Hano***

'Department of Applied Chemistry, Oita University, Oita 870-1192, Japan
"Department of Bioengineering, Kagoshima University, Kagoshima 890-0065, Japan

In this study, the extraction behavior of lactic acid with di-n-octylamine, DOA, in butyl acetate was investigated to determine the extraction mechanism. It was obvious from the obtained results that distribution ratio depended on the formation and dissociation of the complex of dissociated lactic acid and protonated DOA. It was considered that physical extraction by butyl acetate and reactive extractions by DOA occurred simultaneously in the DOA/butyl acetate system. At low pH, physical extraction was dominant due to undissociation of lactic acid. At pH above the p*Ka* of lactic acid, reactive extraction was dominant due to the formation of the complex of dissociated lactic acid and protonated DOA. The mechanism prediction was found to be in good agreement with the experimental results.

INTRODUCTION

Lactic acid is a typical organic acid applied in food, chemical and pharmaceutical fields. Recently, there is a growing demand for L-lactic acid because it can be utilized as a raw material for biodegradable plastics. Now, production of L-lactic acid is realized with fermentation processes. Recovery of lactic acid from fermentation broth is an important step for the production of lactic acid. The conventional processes of recovery of lactic acid are based on precipitation, which are not only complicated and but unfriendly to the environment due to the production of large quantity of effluents and the formation of calcium sulfate.

The application of solvent extraction instead of precipitation results in lower production costs since intermediate isolation of a solid phase and its repeated dissolution are thereby eliminated [1], Many studies have been done on *in situ* extractive fermentation since the production of organic acid can be enhanced by extracting produced acid during fermentation. It was reported that amines had much higher distribution ratio for extraction of carboxylic acids than conventional extractants [2], Unfortunately, they are not suitable for *in situ* extractive fermentation due to their toxicity to microbes. With regard to toxicity to microbes, the extractants of less extractive capacity have to be chosen. Also, there is a question on diluents. In order to promote extraction, extractants are usually dissolved in an organic diluent. The choice of diluent is, therefore, very important for the processes of extraction. In consideration of toxicity to microbes, non-polar diluents are often adopted. Extractants are, indeed, of high capacities when dissolved in polar diluents [3], which are not suitable for *in situ* extraction due to toxicity. On account of those limitations of *in situ* extraction, the extractions in this study were performed as a downstream purification step instead with a view to easily solving the problem of pH and the toxicities of extractants and diluents. Extractions with tertiary amines have been investigated a lot. Nevertheless, there have, up to now, been only

few studies on extraction with DOA, a kind of secondary amine. It was reported that the secondary amine, DOA had more extractive efficiency than the tertiary amine, TOA in our previous study [4,5], However, the mechanism of extraction with DOA was still unclear. In this study, the effects of concentration of DOA, concentration of lactic acid in aqueous phase and equilibrium pH were investigated to clarify the mechanism of extraction with DOA. One of the polar diluents, butyl acetate was chosen for gaining high extraction capacity.

MATERIALS AND METHODS

Di-n-octylamine (DOA) of GR grade was used as an extractant without further purification. Organic solutions were prepared by dissolving DOA in butyl acetate and model solutions of lactic acid were prepared by dissolving lactic acid in distilled water to the concentration of 0.5 and 1.0 kmol/m^3. After pH was adjusted to 8 by the addition of aqueous ammonium solution, model solutions were refluxed for 12 h with a rotary evaporator to get lactic acid polymers hydrolyzed. And then, pH of the hydrolyzed solution was adjusted to appropriate values of pH before extraction. Aqueous and organic solutions of the same volume (10 ml) were mixed in a flask at constant temperature (25 °C) to attain equilibrium. After a complete separation of phases, samples were withdrawn from the aqueous solution, the concentrations of lactic acid were measured by HPLC system with a C-18 column (Finepak SIL C18-5, Japan Spectroscopic Co. Ltd.) and the acid concentrations in the organic phase were calculated by mass balance.

RESULTS AND DISCUSSION

Effects of DOA Concentration, Lactic Acid Concentration and Equilibrium pH on Extraction

To clarify the extraction behavior in DOA/butyl acetate system, the effects of DOA concentration, lactic acid concentration and equilibrium pH were investigated on distribution

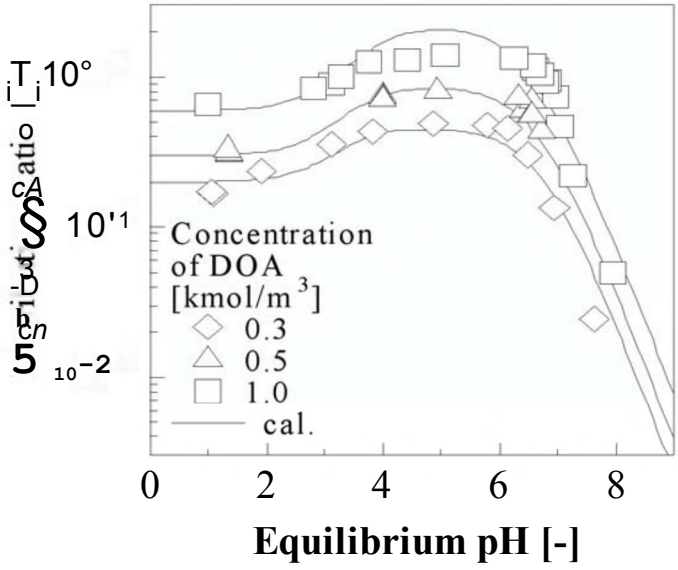


Fig. 1 Effects of DOA concentration and equilibrium pH on distribution ratio at 0.5 kmol/m^3 of initial lactic acid concentration in aqueous phase

ratio, D, which was given as the lactic acid concentration in the organic phase divided by the lactic acid concentration in the aqueous phase at equilibrium in this study,

$$D = [L]_{org,t} / [L]_{aq,t} \quad (1)$$

where the concentration of lactic acid included the concentrations of dissociated lactic acid,

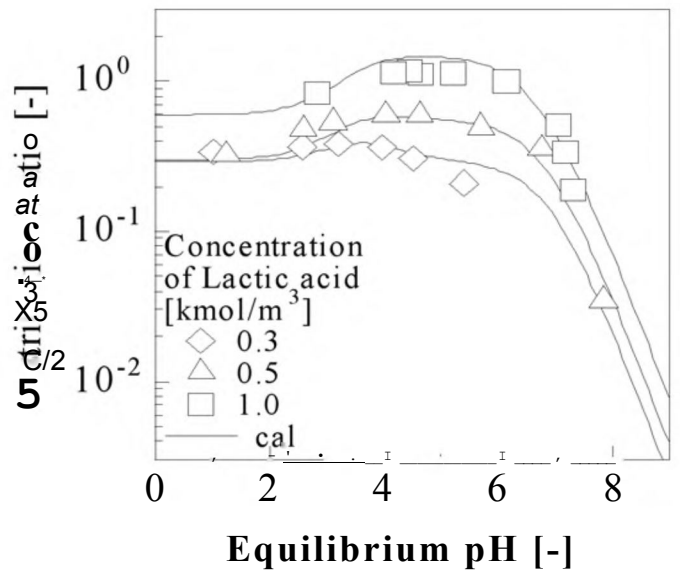


Fig.2 Effects of DO A concentration and equilibrium pH on distribution ratio at 1.0 kmol/m³ of initial lactic acid concentration in aqueous phase

undissociated lactic acid and complexed lactic acid, the subscripts t, org and aq denoted the total concentration, organic phase and aqueous phase, respectively.

As shown in Figs. 1 and 2, distribution ratio increased with an increase of DOA concentration for both initial concentrations of lactic acid in aqueous phase. The concentration of DOA was, however, of little effect on extraction as pH came to neutral region. The range of optimal pH was at 4-6.5 with the exception of the condition at 1.0 kmol/m³ of lactic acid in aqueous phase and 0.3 kmol/m³ of DOA in organic phase, at which the optimal pH was a bit lower. It was possibly because that the effect of diluent on extraction appeared remarkably due to the shortage of DOA for the high concentration of lactic acid in aqueous phase.

It was known that amines made organic acid extracted by the formation of the complex of protonic amine and dissociated organic acid. The amine group was protonated firstly in the interface between aqueous and organic phases, and then, formed a complex with a dissociated lactic acid which was in anionic form. DOA should not, therefore, be effective in extracting lactic acid at pH below the pKa of lactic acid due to the little dissociated lactic acid. Figure 1 shows, however, that the presence of DOA gave high extraction efficiency and extraction ratio increased with increasing concentration of DOA even at low pH region. To clarify the behavior of extraction at low pH, the effect of the concentration of DOA in organic phase on distribution ratio was investigated at pH 1. It was obvious from Fig. 3 that extraction of lactic acid took place even at pH 1. The distribution ratios were close to the distribution coefficient 0.0323 obtained in the system of pure butyl acetate at low concentrations of DOA whereas increased proportionally with increasing concentration of DOA at high concentration of DOA. Since DOA was not capable for extracting undissociated lactic acid and there was no effect of lactic acid concentration in aqueous phase on extraction, it could be considered that lactic acid was extracted by physical extraction at low pH and the physical extraction was enhanced by the increased polarity of butyl acetate by DOA.

Mechanism in DOA/Butyl Acetate System on Extraction of Lactic Acid

To explain the extraction mechanism, the following assumption was proposed. According to the results mentioned above, it was considered that physical extraction by butyl acetate and

reactive extraction by DOA occurred simultaneously in the DOA/butyl acetate system. Figure 4 shows the equilibrium of lactic acid extraction in this extraction system. At low pH, physical extraction was dominant. The behavior of physical extraction was expressed by partition

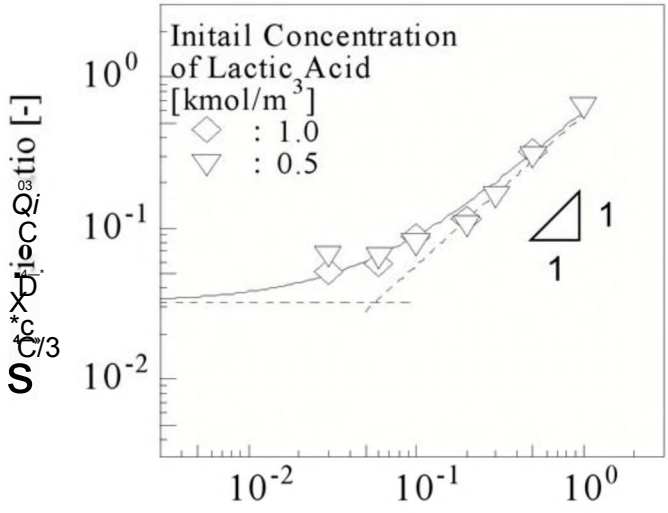


Fig. 3 Effect of DOA concentration on distribution ratio at pH 1

coefficient, P.

$$P = [HL]_{org}/[HL]_{aq} \quad (2)$$

where [HL] was concentration of undissociated lactic acid.

When pH was higher than the pKa of lactic acid, reactive extraction became dominant.

$$HL \text{ «-> } H^+ + L^-,\ K_{aL} = [H^+][L^-]/[HL]_{aq} \quad (3)$$
$$EH^+ \text{<-> } E + H^+,\ K_{aE} = [E][H^+]/[EH^+] \quad (4)$$
$$EH^+ + L'' \text{<-> } EHL,\ Kf = [EHL]/([EH^+][L']) \quad (5)$$

where [L'] was concentration of dissociated lactic acid, [E] was concentration of free DOA, [EH^+] was concentration of protonated DOA, [EHL] was concentration of complex of protonated DOA and dissociated lactic acid, K_{aL}, K_{aE} and K_r were dissociation constant of lactic acid, dissociation constant of protonated DOA and formation constant of complex of protonated DOA and dissociated lactic acid, respectively.

As $Vorg/V_{aq}$ =1 was adjusted during the equilibrium measurements, the concentration of lactic acid in organic phase, C_L or$_g$, and the concentration in aqueous phase, C_{Laq}, could be expressed by the following equations:

$$C_{L}.org = [HL]_{org} + [EHL] \quad (6)$$
$$C_{L}.aq = [HL]_{aq} + [L^-] \quad (7)$$

Initial concentration of DOA, $C_{E.i}$ could be calculated by

$$C_{E}.i = [EHL] + [EH^+] + [E] \quad (8)$$

then, with regard to Eqs. 1, 6 and 7, distribution ratio, D could be calculated by

$$D=([HL]_{org}+[EHL])/([HL]_{aq}+[L']) \quad \textbf{(9)}$$

From Eqs.2, 3 and 9, distribution ratio, D would be

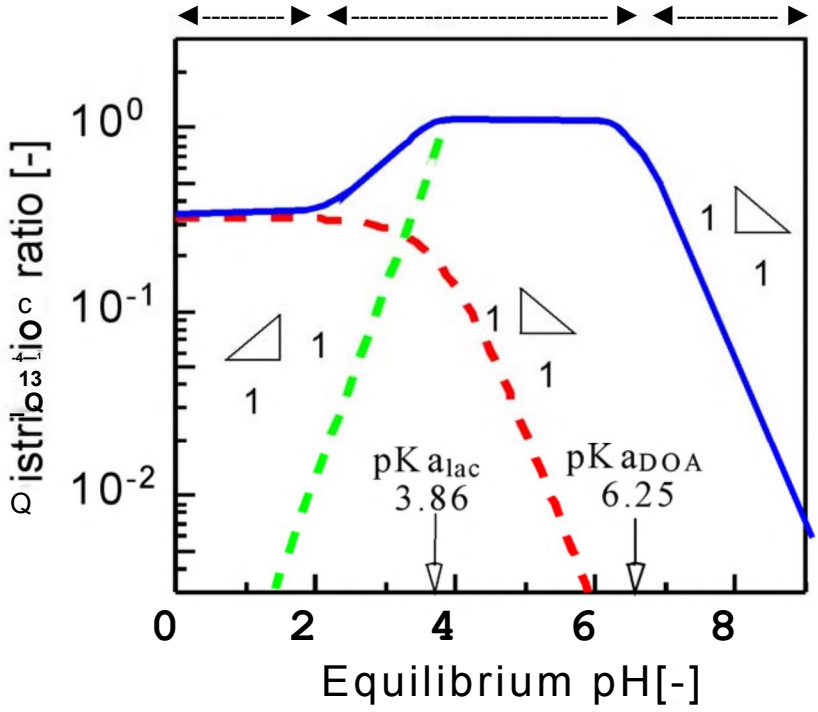


Fig.4 Assumption of equilibrium of lactic acid extraction in DOA/butyl acetate system

$$D=([EHL]/[HL]_{aq} + P)/(1+ K_{aL}/[H^+]) \quad (10)$$

At low pH, [EHL] could be considered to be negligible due to little dissociated lactic acid. Suppose just physical extraction takes place at low pH, distribution ration, D would be

$$D= P/(1+ K_{aL}/[H^+]) \quad (11)$$

The extraction mechanism supposed can be explained well by Equations 10 and 11. At low pH, the values of *D* are almost the same as P because $[H^+] \gg K_{aL}$, indicates that physical extraction is dominant. The physical extraction is, however, affected by the DOA concentration. When pH is within the range between the pKa of lactic acid and the pKa of protonated DOA, reactive extraction is dominant by the formation of the complex of dissociated lactic acid and protonated DOA. The highest distribution ratio was obtained at that region because of increasing [EHL], On the contrary, it is clear from Equation 10 that distribution ratio should decrease significantly at neutral region because [EHL] decreases significantly with an increase of pH at the region. From Figs. 1 and 2, we could recognize that the presentation with the proposed mechanism was in quite conformity with the result of experiments. Besides, based on the mechanism, the prediction of distribution ratio, D was done. When equations 4 and 5 are rearranged to

$$[E]=K_{aE}[EH^+]/[H^+] \quad (12)$$

$$[EH^+]=[EHL]/(K\text{^}LD \quad (13)$$

by Eq. 8, [EHL] can be expressed by

$$[EHL] = C_{Ei}\{1+(1+ K_{aE}[H^+])/(/qL])\} \quad (14)$$

Then, as per Equations 2 and 6, $C_{L,org}$ can be calculated by

$$C_L.org=P[LH]_{aq}+C_E,\{1 + (1 + K_{aE}[H^+])/(K^L-])\} \quad (15)$$

Since $C_{i}\sim C_{org}\hat{}C_{a}$,

$$C_L,q=C_u- P[LH]_{aq}- C_{E\,i}\{1+(1+ K_{aE}[H^+])/(K^L])\} \quad (16)$$

According Eqs. 2,3, 6 and 7, C_u can be represented as

$$C_{LJ} = [EHL]+[L]\{1+(1+P)[H^+]/K_{aL} \} \quad (17)$$

Putting Eq. 14 into 17,

$$Cu = C_E./(1+l/[L-])+m[L] \quad (18)$$

where $l = (1+K_{aE} /[H^+])/(K,[L])$, $m = (1+P)[H^+]/K_{aL}$.

Making $m[L-]2+c_{EJ}-[LH]_{aq}+lm)[L>l[L]_{aq}= 0$; $q = (C_{Ei}-[LH]_{aq}+lm)$, $l[LH]_{aq} = r$, [L] can be calculated by

$$[L] = \{-q+(q^2+4mr)^{1/2}\}/2m \quad (19)$$

Known [L], $[LH]_{aq}$ could be achieved by Eq. 3. Partition coefficient P, complex formation constant K_f, dissociation constant K_{aE} were obtained by curve fitting to experimental data. Therefore, putting Eqs. 15 and 16 into 1, values of *D* could be calculated. As shown in Figs 1 and 2, the experimental data were in good agreement with the calculated lines. It indicated that complicated behavior of the extraction equilibrium was well explained by the proposed mechanism.

CONCLUSIONS

To clarify the mechanism of DOA/butyl acetate system, the effects of DOA concentration, lactic acid concentration and equilibrium pH were investigated. Taken into account the influence of pH, the mechanism was supposed that physical extraction by butyl acetate and reactive extractions by DOA occurred simultaneously in the system. At low pH, physical extraction was dominant. Within the range from the pKa of lactic acid to the pKa of protonated DOA, reactive extraction was dominant by the formation of the complex of dissociated lactic acid and protonated DOA. The highest distribution ratio was obtained at the region because of increasing [EHL], On the contrary, distribution ratio decreased significantly with an increase of pH in neutral region. It indicated that the dissociation of protonated DOA in neutral region reduced the formation of complex of protonated DOA and dissociated lactic acid. The calculated results were in good agreement with experimental data.

REFERENCES

1. R. Wennersten, (1983) *J. Chem. Tech. Biotechnol.* 33B, 85-94
2. K. L. Wasewar, A. Bert M. Heesink, G. *F. Versteeg and V. G. Pangarkar* (2002), *J. Biotechno\.,* 97, 59-68
3. P. von Frieling and K. Schügerl, (1999), *Pro. Biochem.,* 34, 685-696
4. T. Hano, M. Matsumoto, S. Uenoyama, T. Ohtake, Y. Kawano and S. Miura (1993), *Biosep.* 3, 321-326.
5. T. Hano, M. Matsumoto, M. Hirata. and S. Miura, /SEC, 1996; 1447-1452



Release Mechanism of an Anticancer Drug from W/O/W Emulsions

Eiichi Toorisaka*, Noriho Kamiya, Masahiro Goto**, Makoto Hirata* and Tadashi Hano***

'Department of Applied Chemistry, Oita University, Oita 870-1192, Japan
"Department of Applied Chemistry, Graduate School of Enaineerinq, Kyushu University, Fukuoka 812-8581, Japan

The leakage mechanism from multiple water-in-oil-in-water emulsions was investigated for the anticancer drug, Irinotecan. The molecular structure of surfactants used for the preparation of the emulsions affected the leakage rate. A sugar-long alkyl chain ester was effective in suppressing the drug release from the emulsions, because this surfactant reduces the mobility of the inner aqueous droplets in emulsions. However, a surfactant with a flexible alkyl chain extensively dispersed the aqueous droplets and the emulsion rapidly released the drug. The leakage of drugs was deduced to be caused by the thin lamella membrane formed between the internal and external aqueous phases.

INTRODUCTION

A Water-in-Oil-in-Water (W/O/W) emulsion is a colloidal particle dispersion of water droplets into the oil phase of an Oil-in-Water (O/W) emulsion. Since the internal aqueous phase in W/O/W emulsions is separated from the external aqueous phase by an oil phase, they are the focus of interest as microcarriers of drugs [1], However, it is known that water soluble drugs leak from the internal to the external aqueous phase. Two possible mechanisms have been proposed for permeation of water-soluble materials: (1) pass through a thin lamella layer of surfactants that partially forms in the oil layer due to the fluctuation of its thickness [2,3]; and (2) diffusion across the oil layer by being incorporated in reverse micelles [4,5],

In this study, the effect of the molecular structure of surfactants forming emulsions on drug leakage is investigated. Since Irinotecan, used as the model drug, is an anticancer drug that has critical side effects, the development of a sustained-release capsule is widely anticipated.

EXPERIMENTAL

The molecular structures of surfactants used in this study are shown in Fig. 1. Sucrose erucic ester (ER-290), Sucrose oleic ester (0-170), Sucrose lauric ester (L-195), Polyglycerin steric ester (SWA-10D) and Polyglycerin erucic ester (ER-10D) were supplied by Mitubishi

Chemical Foods Co. (Japan). Tetraglycerin ricinolic ester (TGCR) was purchased from Sakamoto Yakuhin Kogyo Co. (Japan). D-glucose was obtained from Wako Pure Chemical Co. (Japan).

W/O/W emulsions were prepared by the two-step emulsification process. A 3 ml aqueous solution (glycin buffer, pH 3.0) containing 50 mg/ml Irinotecan and 154 mM NaCl was emulsified in a 6 ml soybean oil containing 5 wt% of lipophilic surfactant using a homogenizer at 26,000 rpm for 2 minutes to produce the primary emulsion. The primary emulsion was reemulsified in the same manner in 45 ml of the same aqueous phase containing 0.5 wt% hydrophilic surfactant SWA-10D and 154 mM NaCl at 15,000 rpm for 2 minutes.

The W/O/W emulsions prepared were stirred at 25 °C and an aliquot was withdrawn at the time indicated and filtered by centrifugal filtration. The concentration of Irinotecan in the filtrate was detected using fluorescence (ex.365 nm; em. 436 nm).

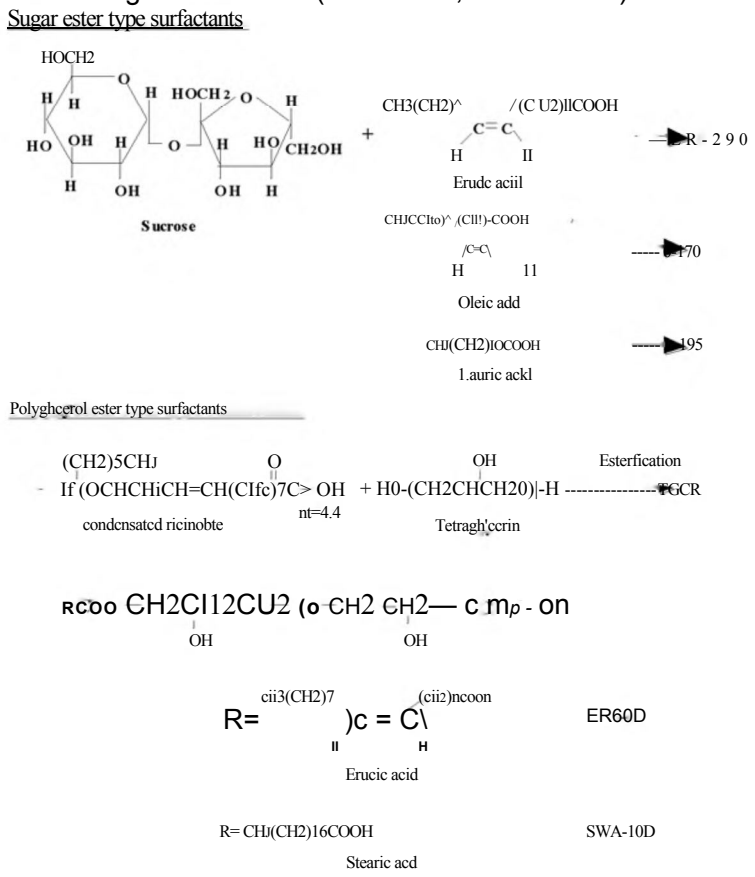


Fig. 1 Molecular structure of surfactants used in this study

RESULTS AND DISCUSSION

Effect of lipophilic surfactants on the release of Irinotecan

The effect of lipophilic surfactants on the release of Irinotecan is shown in Fig. 2. SWA-10D was employed as the hydrophilic surfactant forming the outer interface of the W/O/W emulsions. TGCR forms stable W/O emulsions. However, Fig. 2 shows that W/O/W emulsions prepared with TGCR rapidly release Irinotecan. On the other hand, the release rate from a W/O/W emulsion prepared with sugar ester surfactants was low. Also, it was found that the longer the alkyl chain of a sugar surfactant, the lower the release rate. The stability of the emulsion was confirmed by encapsulating Hemoglobin of high molecular weight. This shows that the release of Irinotecan does not result from the collapse of the

emulsion. Therefore, the formation of W/O/W emulsions was observed by an optical microscope. As shown in Fig. 3, the inner water droplets of a W/O/W emulsion prepared by TGCR were extensively dispersed in the oil droplets, while droplets prepared with ER-290 or ER-60D aggregated. Other sugar ester surfactants showed the same results as ER-290. It is predicted that the dispersibility of inner water droplets depends on the alkyl chain structure. The alkyl chain of TGCR is far longer than the other surfactants and has high flexibility. It can be seen that this structure raises the dispersibility of inner water droplets. These results suggest that the release of Irinotecan to the external aqueous phase is caused by the lamella membrane formed between the internal and external aqueous phases. That is, a surfactant with a flexible alkyl chain extensively disperses aqueous droplets, and the emulsion rapidly releases the drug through the lamella membrane.

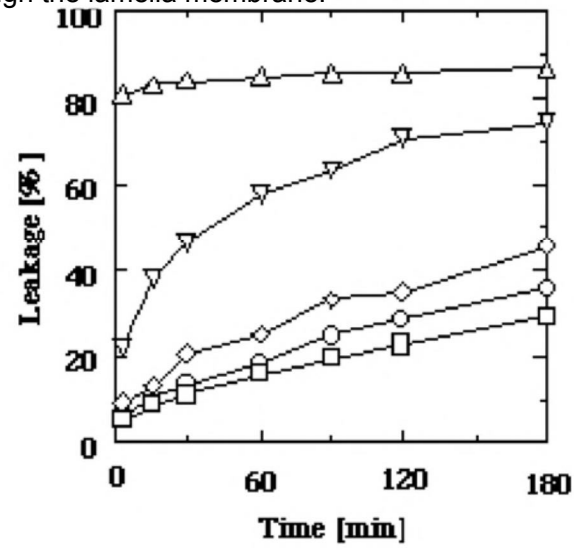


Fig. 2 Effect of lipophilic surfactants on the release of Irinotecan;
(□) ER-290, Q) ER-60D, £>)0-170, V) L-195,0) TGCR

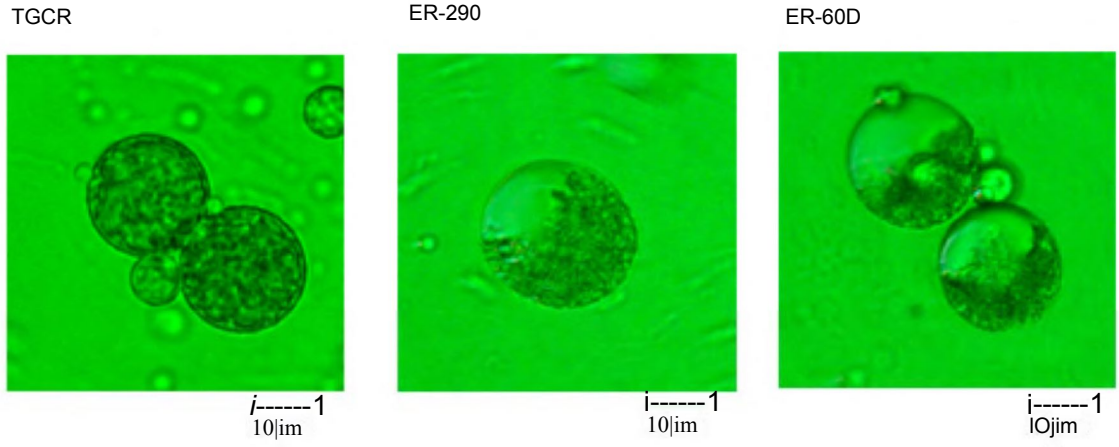


Fig. 3 Photomicrographs of W/OA/V emulsions prepared with three different lipophilic surfactants

Leakage of Irinotecan through the lamella membrane

W/O/W emulsions were prepared with 5 wt% ER-290 and TGCR concentrations varying from (0 to 2.5) wt% TGCR in order to investigate the relationship between dispersibility of inner water droplets and the release rate of Irinotecan. Figure 4 shows the release behaviour from

the respective W/O/W emulsions. The emulsions prepared with 5 wt% ER-290 and 1 wt% TGCR released the drug faster than the emulsion prepared with 5 wt% ER-290 alone. As the concentration of TGCR increased further, the release rate of the drug increased as well.

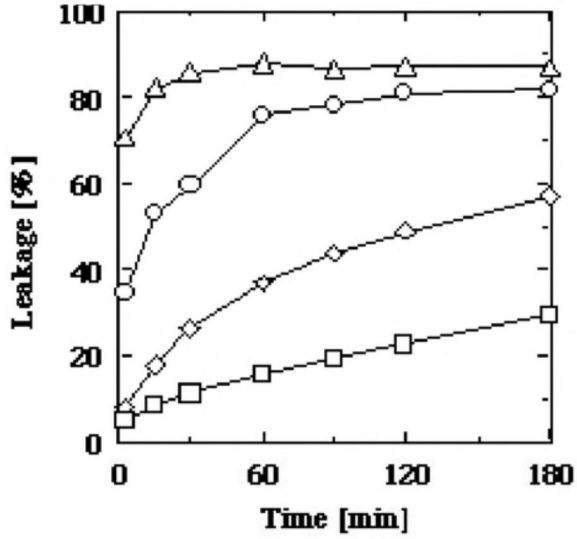


Fig. 4 Effect of TGCR concentration added to the oil phase of W/O/W emulsions: (!T15wt% ER-290, (<>1wt% TGCR and 5wt% ER-290, Q) 2wt% TGCR and 5wt% ER-290, (/) 2.5wt% TGCR and 5wt% ER-290,

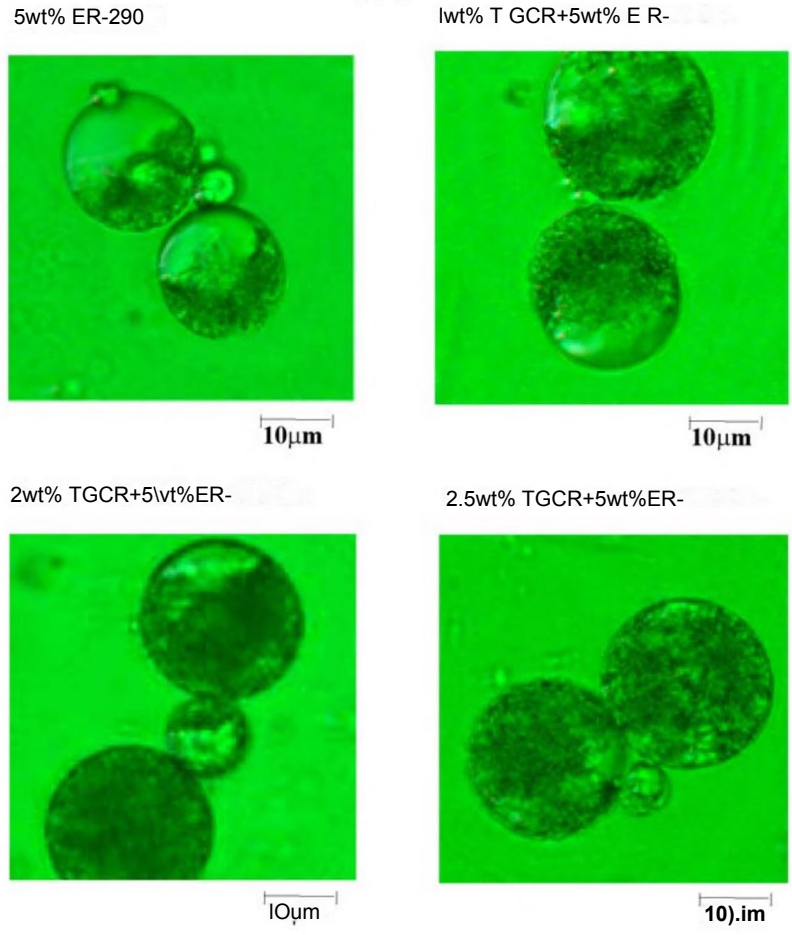


Fig. 5 Photomicrographs of W/O/W emulsions containing a different TGCR content

From this result, it can be concluded that TGCR accelerates the release of Irinotecan from the internal aqueous phase. The photomicrographs of these emulsions are shown in Fig. 5. The water droplets in the W/O emulsion containing ER-290 alone aggregated. However, when TGCR was added to the system the water droplets in the W/O emulsion dispersed. The higher the concentration of TGCR in the emulsions was, the better the dispersibility of water droplets. These results show that the dispersibility of W/O water droplets is closely related to the release of Irinotecan, and that the drug transport is carried out through the lamella membrane.

CONCLUSIONS

It was demonstrated that the leakage of Irinotecan from W/O/W emulsions is caused by the thin lamella membrane formed between the internal and external aqueous phases. The alkyl chain length of surfactants and the dispersibility of W/O water droplets affected the transport of the drug. This study showed that for inhibition of drug leakage from emulsions, a surfactant having a long alkyl chain and suppressing the dispersion of water droplets should be selected.

REFERENCES

1. H. Okochi and M. Nakano (2000), *Adv. Drug Deliv. Rev.,* 45, 5-26
2. Y. Kita, S. Matsumoto and D. Yonezawa (1978), *Nippon Kagakukaish\,* 1, 11-14
3. L. Wen and K.D. Papadopoulous (2000), *Colloid and Surfaces A : Physicochem. Eng. Aspects,* 174, 159-167
4. P. Colinart, S. Delepine, G. Trouve and H. Renon (1984), *J. Membrane Science,* 20, 167-187
5. K. Larson, B. Raghuraman and J. Wiencek (1994), *Ind. Eng. Chem. Res.,* 33, 1612-1619



SOLVENT EXTRACTION OF NUCLEOTIDES BY A LONG-CHAIN QUATERNARY AMMONIUM SALT

Fukiko Kubota[1], Hisashi Yamada[1], Masahiro Goto[1] and Shintaro Furusaki[2]

[1]Department of Applied Chemistry, Graduate School of Engineering,
Kyushu University, Fukuoka 812-8581, Japan
[2]department of Applied Life Science, Sojo University, Kumamoto 860-0082, Japan

Liquid-liquid extraction of adenosine nucleotides was performed by using a long-chain quaternary ammonium salt as extractant. The addition of a small amount of alcohol facilitated the solubilization of long-chain quaternary ammonium salts into hydrophobic organic solvents such as hexane and isooctane. Therefore, a solvent extraction system for nucleotides was obtained, where the use of chlorinated organic solvents was avoided. In the forward extraction, the pH value in the feed aqueous solution was the key factor to achieve quantitative extraction. Adenosine mono-nucleotide (AMP) can be separated from di- and tri-nucleotides (ADP and ATP) by adjusting the salt concentration. However, adenosine that has no phosphoric group was not extracted at all. Based on the results, the main driving force for the extraction was found to be electrostatic interaction between the phosphoric part of nucleotides and the cationic part of the extractant. In the stripping, salt species and its concentration were crucial parameters for the effective recovery of nucleotides from the organic phase. Under the optimum conditions, 96% nucleotides were recovered to a fresh aqueous solution.

INTRODUCTION

Nucleotides, which are the primary units of DNA and RNA, play an important role in biology such as signal processing, energy transduction and gene replication [1], Recently, much attention has been denoted to the application of nucleotides and their analogous compounds in the biochemical, medical, pharmaceutical fields. Nucleotides are usually produced by fermentation or enzymatic degradation methods, where the efficient isolation of each nucleotide from the product mixture is a great challenge. A number of studies concerning the separation of nucleic base related compounds have been carried out, however many of them are on high-performance liquid chromatography and capillary electrophoresis [2-6],

Liquid-liquid extraction is well known as one of the most effective separation techniques on an industrial scale. In this method, the extraction ability and selectivity of an extractant employed greatly affect the process efficiency. To date, several reagents, which selectively recognize nucleotides, have been reported, however, toxic organic solvents such as dichloromethane and chloroform were used to overcome the poor solubility of such newly synthesized reagents [7-11],

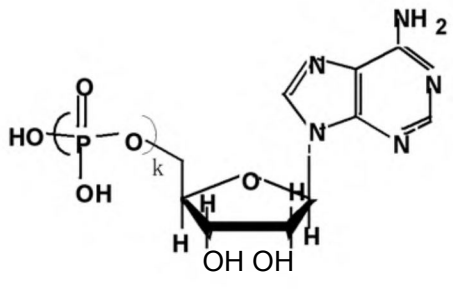
The aim of this work is to construct a chlorinated solvent-free extraction system for the practical application of liquid-liquid extraction for the separation of nucleotides. In the present study, commonly used reagents, long-chain quaternary ammonium salts, were chosen as the extractants. The extraction behavior of three nucleotides, adenosine mono-, di- and tri-phosphates (AMP, ADP and ATP) along with adenosine to the non-toxic aliphatic organic

solvent was examined. The recovery of nucleotides was also performed and the applicability of the system to the separation of nucleotides was discussed.

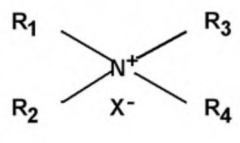
EXPERIMENTAL

Reagents

Analytical grade adenosine, the sodium salts of adenosine 5'-monophosphate and adenosine 5'-diphosphate, and disodium salts of adenosine 5'-triphosphate (Sigma Chemical Co., St. Louis, MO USA) were used as the nucleic acid related compounds. Quaternary ammonium bromide or chloride salts which have long chain alkyl groups of 8~18 carbons (abbreviated as nC_mQAB or nC_mQAC) were purchased from Tokyo Kasei Kogyo Co., Ltd., Japan. These quaternary ammonium salts were employed as the extractants without further purification. The molecular structures and abbreviations of adenosine, adenosine nucleotides and quaternary ammonium salts used as extractants are shown in Fig 1. Isooctane, hexane, dodecane and chloroform of analytical reagent grade were used as the organic solvent. All the organic and inorganic reagents were of analytical reagent grade.



nucleoside k=0, Adenosine
nucleotides
k=1, Adenosine 5'-monophosphate (AMP)
k=2, Adenosine 5-diphosphate (ADP)
k=3, Adenosine 5'-triphosphate (ATP)



Quartenary ammonium salt
X=Cl nC_mQAC
Br nC_mQAB

n: number of long chain alkyl groups in a molecule (n=1-4)
m: carbon number in a long chain alkyl group (m =8-18)

Fig. 1 Molecular structures and abbreviations of nucleotides and extractants

Procedure

Extraction equilibrium studies were performed by the conventional method. For the forward extraction, an aqueous solution was prepared by dissolving adenosine, sodium salts of AMP, ADP or ATP in a 10 mol/m^3 Tris solution, and pH was adjusted with 10 mol/m^3 Tris and 10 mol/m^3 HCl solutions. The chloride ion concentration was adjusted with sodium chloride. The organic solution was prepared by dissolving a quaternary ammonium salt in an organic solvent, where a small amount of 1-octanol was added to solubilize the ammonium salt. The organic solution containing AMP used for the stripping was prepared by the extraction of AMP to isooctane with the extratant, followed by separation from the feed aqueous phase. The aqueous solutions containing the salts such as NaCl, $MgCl_2$, KCl, KBr or KI was used as the stripping solution.

Equal volumes (5 cm^3) of the aqueous and the organic solutions were transferred in a sealed test tube and gently shaken at 303K for 24 hours to attain equilibrium. In the stripping, both phases were shaken by the mechanical shaker for 1 hour. The concentration of adenosine, AMP, ADP and ATP in the aqueous phase was measured by a UV/VIS spectrometer (JASCO V- 570, Japan) at 260 nm.

RESULTS AND DISCUSSION

Extraction ability of quaternary ammonium salts

The extraction ability of nine different quaternary ammonium salts for AMP was evaluated as shown in Tablel. The amount of 1-octanol added to the isooctane phase to solubilize the extractants is also listed along with the degree of extraction of AMP. Quaternary ammonium salts having one and four long alkyl chains, $1C_{18}QAB$ and $4C_{10}QAB$, showed the low degree of extraction. It was considered that ICisQAB distributes to the aqueous phase because the aqueous phase after contacting with the organic phase became turbid. No distribution of $4C_{10}QAB$ to the aqueous phase seemed to occur, however four long alkyl substituents of this compound may inhibit the interaction with AMP. The ammonium salts having two or three long alkyl chain substituents in a molecule exhibited relatively high extraction ability for AMP as shown in Table 1. There was no transfer of AMP to organic phase without ammonium salt. Subsequent experiments were mainly performed by using distearyl dimethylammonium chloride, $2C_{18}QAC$ (Ri, R2=CH_3, R_3, R4 =$C_{18}H_{37}$ in the structure shown in Fig. 1) as the extractant.

Table 1 Extraction ability of quaternary ammonium salts for AMP and amount of 1-octanol required for solubilizing extractants

Quaternary ammonium salts	1- Octanol (v/v %)	Degree of extraction (%)
1 $C_{18}QAB$	20.0	51.7
2C10QAB	3.5	87.5
$2C_{12}QAB$	3.5	92.2
$2C_{14}QAB$	3.5	90.2
$2C_{16}QAB$	3.5	89.5
$20_{18}QAB$	5.0	91.0
$2C_{18}QAC$	5.0	90.9
$3C_8QAC$	0.0	90.5
40IQQAB	3.5	1.0

[nC_mQAX]=10 mol/m[AMP]=0.05 mol/m pH=9 isooctane

Effect of organic solvents on the extraction ability of $2C_{18}QAC$

The effect of the organic solvent on the extraction ability of $2C_{18}QAC$ for AMP was examined. Table 2 shows the degree of extraction of AMP to four different organic solvents, along with the amount of 1-octanol added to each organic phase to solubilize $2C_{18}QAC$ completely. Using three kinds of aliphatic solvents such as isooctane, hexane and dodecane resulted in high extraction efficiencies, whereas AMP was scarcely extracted to chloroform solution. AMP is supposed to be extracted as the neutral species formed by the interaction of its phosphoric anions with the ammonium cations of $2C_{18}QAC$, as will be described later. In the polar solvent such as chloroform, the ion-pairs of this complex seem to be unstable. The amount of 1-octanol to be added increased with the increase in the carbon number of solvents. Isooctane was used as the solvent hereafter because isooctane required smaller amount of 1-octanol than dodecane as shown in Table 2 and is less volatile than hexane.

Table 2 Effect of solvent on extraction efficiency

Solvents	1- Octanol (v/v%)	Degree of extraction (%)
Hexane	3.5	91.3
Isooctane	5.0	90.4
Dodecane	10.0	90.4
Chloroform	0.0	5.1

[$2C_{18}QAC$]=10 mol/m^3, [AMP]=0.05 mol/m^3 pH=9

Extraction mechanism of AMP by $2C_{18}QAC$

AMP (abbreviated as H_2A) has two phosphoric protons in a molecule as shown in Fig. 1 and the second proton dissociates in the aqueous phase as follows:

$$HA' = A^{2'} + H^{+} \qquad : K_{a2} \qquad (1)$$

where K_{a2} is the dissociation constant of the second proton. The value of pK_{a2} was reported to be 6.8 [12], therefore, AMP exists mainly as di-anion species $A^{2'}$at high pH (pH = 9) in this experimental condition.

Assuming that AMP is extracted to the organic solution as 1:2 neutral species with $2C_{18}QAC$ (abbreviated as QCI), the extraction equilibrium is expressed as follows:

$$A^{2'}{}_{aq} + 2\text{-}QCI_{org} = A\,Q_2, org + 2\text{-}Cl'_{aq} : K_{ex} \qquad (2)$$

The equilibrium constant, K_{ex} is defined as follows:

$$Kex=[AQ_2][Clf / [QCI]^2[A^{2'}] \qquad (3)$$

By rewriting Eq. (3) with the distribution ratio D of AMP ($=[AQ_2] / [A^{2'}]$), the following equation is obtained.

$$logD = logKex + 2\text{-}log ([QCI] / [Cl']) \qquad (4)$$

The relationship between D and the concentration ratio of $2C_{18}QAC$ in the organic phase against chloride ion in the aqueous phase at pH 9 is shown in Fig. 2. The slope of this linear correlation is nearly equal to 2, that is, the experimental result is well explained by Eq. (4).

The values of K_{ex} determined from the data in Fig. 2 and Eq. (4) is $1.2x10'^{2}$[-]. The solid line in Fig. 2 is the calculated results by using this value.

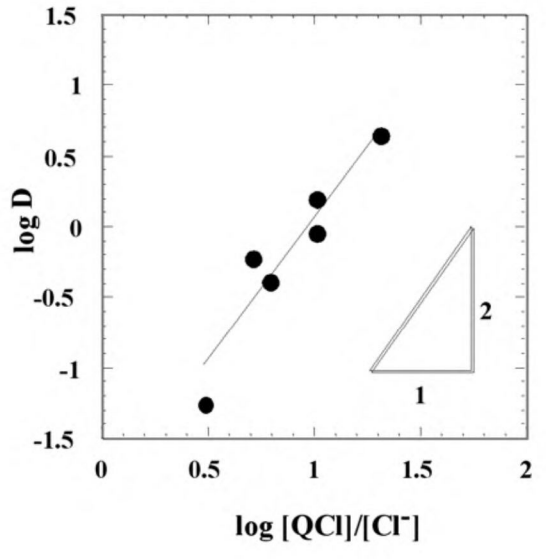


Fig. 2 logD vs log [QCl]/[Cr]

[AMP] = 0.05 mol/m^3

[NaCl] = 0.1 mol/m^3 pH=9

Stripping of AMP by various salts

AMP in the organic phase is expected to strip to the aqueous solution of high chloride ion concentration based on the reverse reaction of Eq. (2). Table 3 shows the effect of salts on the stripping efficiency of AMP extracted by $2C_{18}QAC$ or $3C_8QAC$, where the pH in the aqueous phase is 9. The salts such as NaCl, $MgCl_2$, KCl and KBr

provided high stripping efficiency, although the organic solution containing $2C_{18}$QAC is apt to emulsify when mixed with the aqueous solution with a high salt concentration. The stripping degree of AMP by these salts was about 40% in the case of $3C_8$QAC despite the excellent phase separation that was attained. Figure 3 shows the stripping behavior of AMP for the systems with the extractant-ion combination of $2Ci_8$QAC-NaCl and $3C_8$QAC-KCl. When $2C_{18}$QAC was used as an extractant, the stripping efficiency was increased with increasing salt concentration and quantitative stripping was achieved at a NaCl concentration of 50 mol/m^3 or more. In the latter case, the stripping was not promoted by further addition of KCl at concentration higher than 50 mol/m^3. Based on the results shown in Table 3 and Fig. 3, together with the high solubility of $3C_8$QAC in isooctane as shown in Table 1, it is considered that the complex of AMP with $3C_8$QAC exists in a more stable form, because of its higher hydrophobicity, than the AMP complex with $2C_{18}$QAC. It was also proved that $2Ci_8$QAC is excellent as the extractant for AMP.

Table3 Effect of salts in aqueous phase on stripping efficiency

Extractants	Salts	Stripping degree (%)
2CisQAC	NaCl	98.6
	KCl	94.2
	$MgCl_2$	89.2
	KBr	86.3
	KI	35.8
$3C_8$QAC	NaCl	44.2
	KCl	46.4
	$MgCl_2$	40.6
	KBr	42.3
	KI	15.1

Organic phase: Isooctane loaded AMP (0.05 mol/m^3) with 10 mol/m^3 extractant
Stripping Phase: [Salt] =100 mol/m^3, pH=9

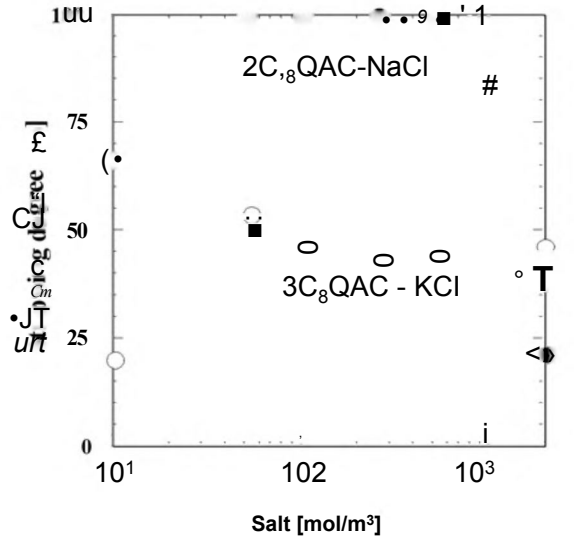


Fig. 3 Effect of salt concentration on stripping efficiency (pH=9)

Separation of adenosine and its nucleotides

Figure 4 shows the extraction behavior of adenosine and three related nucleotides, AMP, ADP and ATP, by $2C_{18}$QAC as a function of NaCl concentration in the aqueous phase at pH = 9. It was clarified that the extraction of AMP was controlled by the salt concentration in the aqueous phase according to the extraction equilibrium expressed by Eq. (2). Therefore, the degree of extraction of AMP, ADP and ATP, which are mono, di and tri phosphates, respectively, decreased with increasing NaCl concentration. The extraction ability of $2C_{18}$QAC increased in the following order in proportion to the number of phosphoric groups in the molecule: AMP < ADP < ATP.

Adenosine without phosphoric group to interact with the amino cation of $2Ci_8$QAC was not extracted even under the chloride ion free condition. Therefore, adenosine can be easily removed from the mixture of nucleotides.

The results shown in Fig.4 suggest that the separation among adenosine, AMP, ADP and ATP is possible by controlling the salt concentration in the aqueous phase.

CONCLUSION

The extraction and the stripping behavior of adenosine 5'-monophosphate, AMP, was systematically examined by using various quaternary ammonium salts, which could be solubilized in aliphatic solvents such as isooctane, hexane and dodecane by adding a small amount of 1-octanol. It was found that the ammonium salts having two or three long alkyl chains in the molecular structure (2C and 3C) exhibited relatively high extraction ability to AMP, however, with respect to the stripping performance, 2C is superior to 3C as extractant. The extraction mechanism of AMP by $2C_{18}$QAC was investigated and it was found that the predominant factor for the extraction of nucleotides was the electrostatic interaction between the phosphoric anions and the amino cation of $2Ci_8$QAC. Adenosine, without a phosphoric group in the structure, can easily be removed from the mixture and further separation and recovery of adenosine nucleotides is possible by controlling the operational conditions such as salts concentration and pH in the aqueous phase or extractant concentration in the organic phase.

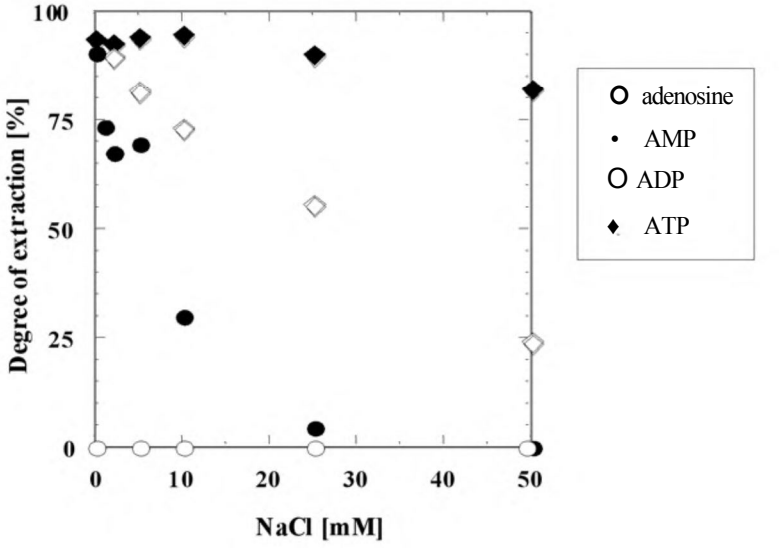


Fig. 4 Effect of salt concentration in feed aqueous solution on extraction efficiency of adenosine and its nucleotides.

[nucleotide] = 0.05 mol/m^3 [$2C_{18}$QAC]= 10 mol/m^3
pH=9

REFERENCES

1. V. Krai and J.L. Sessler (1995), *Tetrahedron*, 51, 539
2. R. Tuyttern, F. Lemiere, W. V. Dongen, H. Siegers, R. P. Newton and E. L. Esmans, (2004), *J. Chromatography B,* 809, 189
3. H. J. Fu, X. D. Hung, W. H. Jin and H. F. Zou (2003), *Curr. Opinion Biotecnol.,* 14, 96
4. Q. Deng, I. German, D. Buchanan, R. T. Kennedy (2001), *Anal. Chem.,* 73, 5415
5. Y. Esaka, S. Inagaki, M. Goto and M.Sako (2001), *Electrophoresis,* 22, 104
6. C. Fu, L. Song and Y. Fang (1999), *Analytica Chimica Acta,* 399, 259
7. Y. G. Jung, W. S. Yeo, S. B. Lee and J. I. Hong (1997), *Chem. Commun.,* 1061
8. J. A. Riggs, K. A. Hossler, B. D. Smith, M. J. Karpa, G. Griffin and P. J. Duggan (1996), *Tetrahedron letters,* 37, 6303
9. T. Li and F.Diederich (1992), *J. Org. Chem.,* 57, 6449
10. H. Furuta, M. J. Cyr and J. L. Sessler, (1991) *J. Am. Chem. Soc.,* 113, 6677
11. I. Tabushi, Y. Kobuke and J. Imuta, (1980), *J. Am. Chem. Soc.,* 102, 1774
12. M. Blackburn and M.J.Gait (1996) *Nucleic Acids in Chemistry and Biology,* Oxford

SOLVENT EXTRACTION OF TRIVALENT RARE EARTHS WITH NOVEL CALIX[4]ARENE PHOSPHONATE DERIVATIVE

Keisuke Ohto, Takashi Matsufuji, Akiyo Tada, Tatsuya Oshima and Katsutoshi Inoue

Saga University, Saga, Japan

Phosphonate derivatives of calix[4]arene in cone conformation have been molecular-designed and synthesized as novel type of the extractant fortrivalent rare earth metal (La, Pr, Nd, Sm, Eu, Gd, Ho, (Y), Er) ions. Each extractant has been synthesized four steps including cyclization, di-phosphonation at distal position, further di-phosphonation at the rest phenols, and hydrolysis with base. Effect of pH on distribution ratio has been investigated. It has been found that they extract rare earth ions by simple ion-exchange mechanism. The half pH value, pH-i/2, from the result of pH dependency shows that the extraction ability is higher and selectivity is less or comparable to the conventional extractants. It is attributed to multiplier effects of structure and functional group for heavier rare earths. The crossed type of calix[4]arene derivative with carboxylic and phosphonic acids has been also synthesized for rare earths recognition. Each same functional group in the extractant locates at distal position. Although this extractant also shows higher extraction ability compared with the commercial extractant, the selectivity for rare earth metal ions becomes poor for heavier rare earths. It is attributed to offset effect of phosphonic acid for heavy rare earths and carboxylic acid for middle and light rare earths.

INTRODUCTION

Calixarenes, macrocyclic oligomers, providing three-dimensional coordination site and controlled cavities have been still attractive and interesting compounds [1,2]. For such property, many researches on metal recognition have been investigated and reported [3], The authors have been also attracted to the ion recognition by calixarenes and have investigated their recognition property. In the previous work, p-t-octylcalix[4]arene tetracarboxylic acid was synthesized to investigate mutual separation of trivalent rare earth metals [4], In the system without alkali metals, the selectivity was observed at Pr to Sm, light to middle rare earth metals. The selectivity is quite similar to stability of acetic acid with rare earth metals. In next work, calix[4]arene with phosphonic acid at upper rim was prepared to investigate mutual separation of trivalent rare earth metals [5], because acidic phosphorus type of the extractants are the most effective among the extractants, such as 2-ethylhexyl 2-ethylhexylphosphonic acid (commercial name PC-88A, Daihachi Chemical Company) and di-2-ethylhexyllphosphoric acid (commercial name DP-8R, Daihachi Chemical company). Actually, calix[4]arene phosphonic acid derivative at upper rim showed much higher separation efficiency than the carboxylic acid derivative. The selectivity, however, is less than the corresponding monomeric derivative. It was concluded to be attributed to the offset by the high ring-size recognition ability at the upper rim of calix[4]arene to light rare earths and the high affinity of the phosphonate groups for heavy rare earths.

In the present work, we have synthesized calix[4]arene derivatives containing phosphonate groups at lower rim to investigate extraction behavior for rare earth metals (La, Pr, Nd, Sm, Eu, Gd, Ho, (Y), Er) for extraction ability and mutual separation efficiency.

EXPERIMENTAL

Reagents

Tetraphosphonic acid type and crossed phosphonic acid - carboxylic acids type of the extractants, compounds 1 and 2 shown in Figure 1 were used in the present work, together with compounds 3 and 4 for comparison.

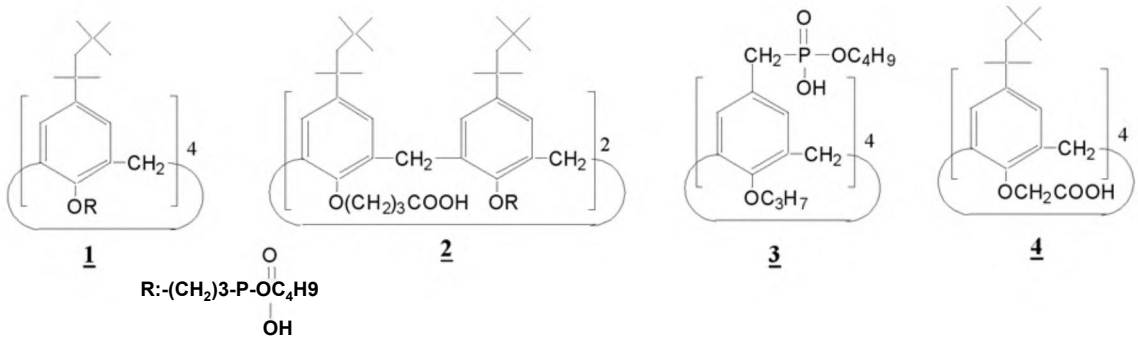


Figure 1. Chemical structures of the extractants.

The compound 1 has been prepared by the following processes; cyclization, diphosphonation at distal position, the further diphosphonation at the rest phenol oxygens, and final hydrolysis with base. The synthetic scheme of the compound 1 is shown in Figure 2. The compound 2 has been prepared by the following processes; cyclization, diphosphonation at distal position, esterification at the rest phenol oxygens, and final hydrolysis with base. The synthetic scheme of the compound 2 is shown in Figure 3. These extractants were identified by ^-NMR, IR spectra, thin layer chromatography, and elemental analysis. Tetraphosphonic acid at upper rim type of the extractant, compound 3 and tetracarboxylic acid type of the extractant, compound 4 were prepared in the previous work [5, 4], The present extractants, compounds 1 - 4 , are in cone conformation.

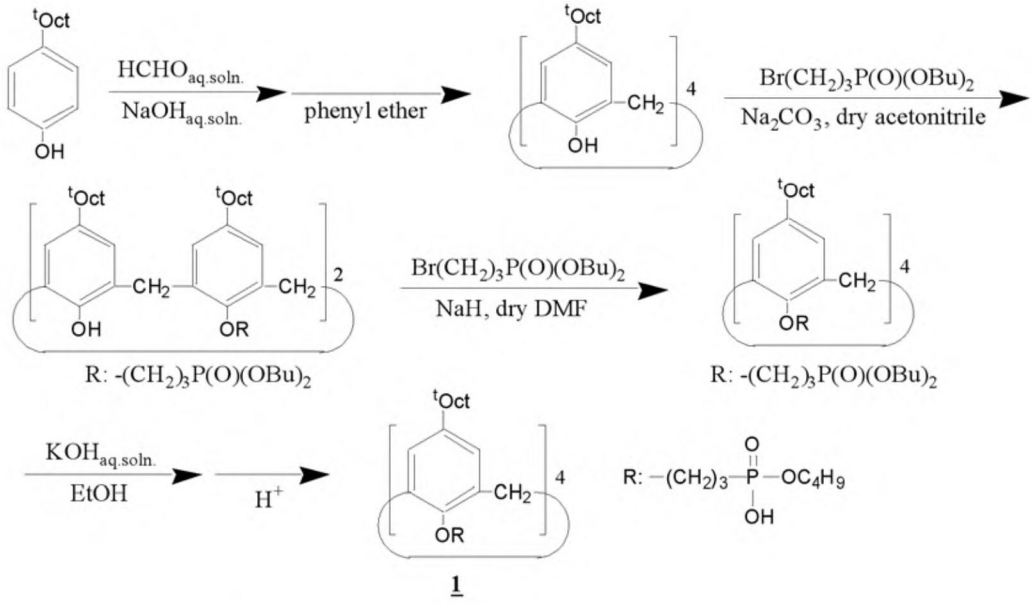


Figure 2. Synthetic scheme of Compound 1.

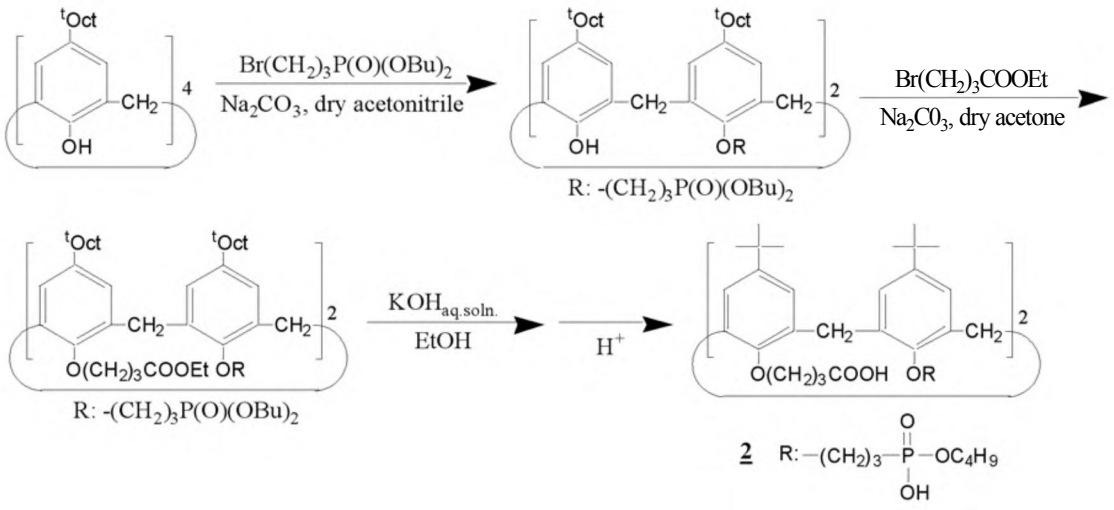


Figure 3. Synthetic scheme of Compound 2.

Distribution study of rare earth metals

An organic solution was prepared by diluting each extractant into an analytical grade of chloroform to desired concentrations. The following three kinds of aqueous solutions, each of which contained three kinds of rare earth ions, were prepared by dissolving the analytical grade of rare earth chloride (Some of them were prepared by dissolving rare earth oxide into hydrochloric acid.) into 0.1, 1.0, or 3.0 mol dm^3 diluting hydrochloric acid to desired concentrations: the first one contained La, Pr, and Nd, the second Sm, Eu, and Gd, the last Ho, Er, and Y. For Compound 2, 0.1 mol dm^{-3} diluting hydrochloric acid and 0.1 mol dm $^{3-}$ HEPESaqueosu solutions were used as aqueous media. The pH of aqueous solutions were adjusted by arbitrarily mixing the above three hydrochlroric acid stock solutions (HCI-HEPES). Equal volumes (3 cm^3) of both phases were mixed and vigorously shaken at 303K for more than 8 h. After phase separation, the metal concentrations in the aqueous solutions were measured by ICP-AES (Shimadzu ICPS-7500), respectively. The extracted metal ion concentrations were calculated from the differences of the metal concentrations in the aqueous phase between before and after the equilibration. The concentrations of proton were calculated from the mixing ratio of hydrochloric acid solutions. Then, the activities of proton were estimated by using activity coefficiency values.

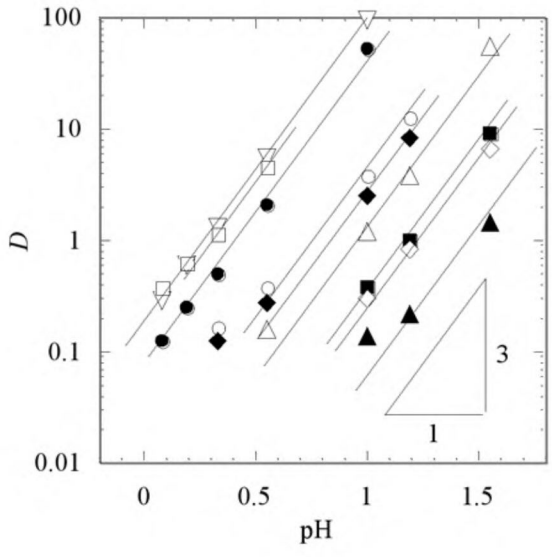


*Figure 5. Effect of proton activity on distribution ratio of trivalent rare earths with Compound 1. [Rare earth metal] = 0.1 mmol dm ~3 each, light rare earths A : La, o ; Pr, • : Nd, middle rare earths A : Sm, * : Eu, ° : Gd, heavy rare earths ° : Ho. * : Y, v Er. [Extractant] = 5 mmol dm ~3, 0.1 mol dm ~3 HCl - l mol dm ~3 HCl 3 mol dm ~3 HCl.*

RESULTS AND DISCUSSION

Effect of pH on distribution ratio of rare earth metals with Compound 2 is shown in Figure 4. All points in Figure 4 lie on straight lines

with slopes of 3, which is equivalent to the charge of rare earth metals. The extraction reaction is expected as eq.(1).

$RE^{3+} + H_4L$^ RE*HL + $3H^+$ (1).

Where RE and H_4L represent rare earth metals and tetrameric phophonic acid compound 2. Here, although the ion-exchangeable groups with trivalent rare earth metals are not clear, they would be two phosphonic acids and a carboxylic acid from strong affinity between rare earth metals and phosphonic acid. The extraction selectivity is as follows; Er > Y > Ho > Gd > Eu > Sm > Nd > Pr > La. Heavy rare earth metals are preferentially extracted to light ones. The tendency of the selectivity to rare earth metals is similar to those of conventional acidic phosphorus extractants, although it seems just poor. For acidic phosphorus extractants, yttrium is placed between holmium and erbium [6],

Effect of pH on distribution ratio of rare earth metals with Compound 1 is shown in Figure 5. All points in Figure 5 also lie on straight lines with slopes of 3. The extraction reaction is also expected as eq.(1). The extraction selectivity is also Er > Y > Ho > Gd > Eu > Sm > Nd > Pr > La, and the separation efficiency seems higher than that of compound 2.

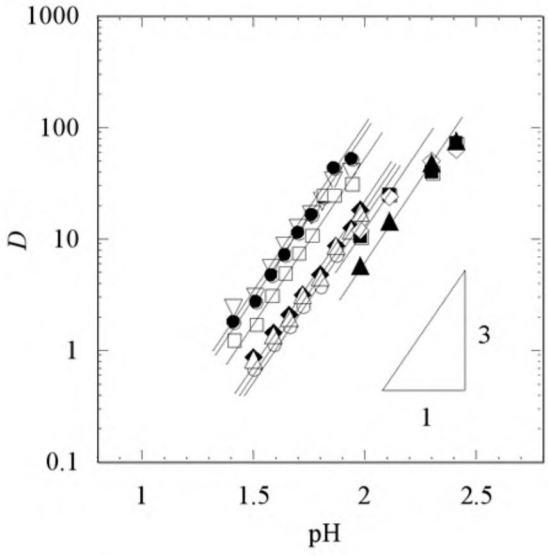


*Figure 4. Effect of pH on distribution ratio of trivalent rare earths with Compound 2. [Rare earth metal] = 0.1 mmol dm ~3, light rare earths A : La, o ; Pr, · : Nd, middle rare earths A : Sm, * : Eu, ° : Gd, heavy rare earths a : Ho, • : Y, v ; Er. [Extractant] - 4.28 mmol dm ~3, 0.1 mol dm ~3 HCI - 1 mol dm HCl - 3 mol dm ~3 HCl.*

The relation between half pH value, $pH_{1/2}$ and sequence of rare earth metals for Compounds 1 and 2 is shown in Figure 6, together with the plots of tetraphosphonic acid derivative at upper rim, Compound 3, tetracarboxylic acid, Compound 4, and commercial phosphonic acid extractant, PC-88A. (Data of PC-88A are estimated from the extraction equilibrium constant obtained in the previous study by Kolarik *et at.)* Y-axis is inverted, since half pH value, $pH_{1/2}$ of the the extractant with high extraction ability is lower. Although the concentrations of Compound 2 and PC-88A were different, the extraction ability of four extractants can be almost compared from Figure 6. That is, the plots of the extractant with higher extraction ability are higher than those of weaker extractants. Obviously, the extraction ability of two present extractants are higher than the others. Although the corresponding monomeric extractants of Compounds 1 and 2 have not been prepared yet, from the result of monomeric derivative of Compound 3 in the previous work [5] and pK_a value of common organophosphonic acid, the extraction ability of two extractants is extremely high. It must be attributed to highly preorganized structure for rare earth metals by size-fitting and cone conformation.

For separation efficiency, as described in the results of pH dependency, the extraction selectivity is as follows; Er > Y > Ho > Gd > Eu > Sm > Nd > Pr > La. Tetrad effect for both extractants is also observed. Since plots of the extractants with higher separation efficiency are broad, Compounds 1, 3 and PC-88A would be good extractants. Compound 2 is

phosphonic acid - carboxylic acid crossed type extractant. Carboxylic acid shows selectivity to middle rare earths, but poor to rare earth metals. On the other hand, phosphonic acid shows high heavy rare earth selectivity. Therefore, the selectivity of Compound 2 is offset by mixing of carboxylic acid with the middle rare earth selectivity and phosphonic acid with the heavy rare earth selectivity. Consequently, Compound 2 shows just poor separation efficiency. Compound 1 shows high separation efficiency due to the multiplier effects of structure (coordination site size) and functional group for heavy rare earths. The extraction ability of Compound 1, however, is so strong that it drastically achieves mutual separate of rare earth metals like commercial extractant, PC-88A. If coordination site size is controlled to exclude larger light rare earths, the extractant with the best separation efficiency to rare earths would be developed.

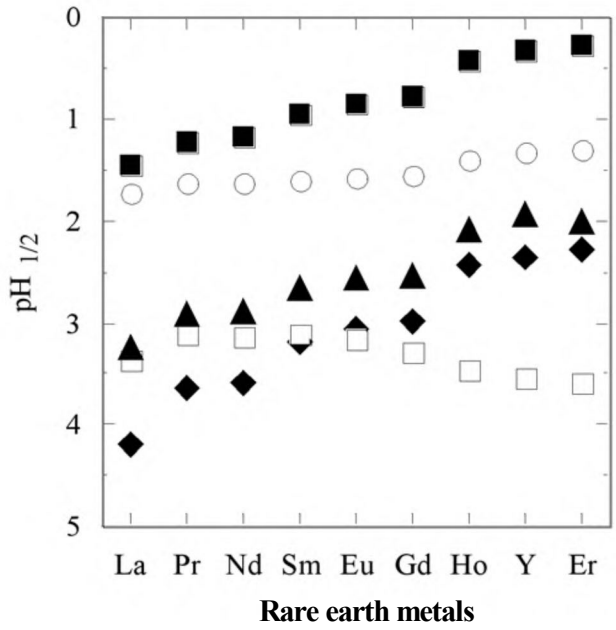


*Figure 6. Relation between half pH values, pH 1/2 and sequence of trivalent rare earth metals. ᵐ : Compound **1(5 mM), ° :** Compound 2 (4.28mM), ᴬ : Compound 3 (5mM), ᵃ : Compound **4** (5mM), ° : Compound **5** (estimatedas 15mM, naitrate media).*

CONCLUSIONS

Phosphonate derivatives of calix[4]arene in cone conformation have been molecular-designed and synthesized as novel type of the extractant for trivalent rare earth metals. The extraction ability of calix[4]arene tetraphosphonic acid at lower rim is higher and selectivity is less or comparable to the conventional extractants. It is attributed to multiplier effects of structure and functional group for heavier rare earths. The crossed type of calix[4]arene derivative with carboxylic and phosphonic acids has been also synthesized for rare earths recognition. Although this extractant also shows higher extraction ability compared with the commercial extractant, the selectivity for rare earth metal ions becomes poor for heavier rare earths. It is attributed to offset effect of phosphonic acid for heavy rare earths and carboxylic acid for middle and light rare earths. Further molecular design for exclusion of light rare earth metals with weaker affinity to tetraphosphonic acid type of calix[4]arene at lower rim is necessary.

REFERENCES

1. C.D.Gutsche (1998), "Calixarenes Revisited," Royal Society of Chemistry: Cambridge.
2. Z.Asfari, V.Boehmer, J.M.Harrowfield, J.Vicens (2001), "Calixarenes 2001", Kluwer Academic Publishers, Netherlands.
3. e.g. (a)R.Ludwig (1995), *JAERI-Review,* 95-022, 1-55. (b)D.M.Roundhill (1995), *Progr.Inorg. Chem.,* 43, 533-592. (c)F.A.Neu (1994), *Chem.Soc.Rev.,* 23, 235-241.

4. K.Ohto, M.Yano, K.Inoue, T.Yamamoto, M.Goto, F.Nakashio, S.Shinkai, and T.Nagasaki (1995), *Anal.Sci.,* 11, 893-902.
5. K.Ohto, H.Ota, and K.Inoue (1997), *Solv.Extr.Res.Dev., Jpn.,* 4, 167-182.
6. D.F.Peppard, G.W.Mason, and S.Lewey, (1960), *J.Inorg.Nucl.Chem.,* 31, 2271-2284.
7. Z.Kolarik and H.Pankova, (1966), *J.Inorg.Nucl.Chem.,* 28, 2325-2333.

PHOSPHORYLATED BACTERIAL CELLULOSE FOR ADSORPTION OF METAL IONS

Tatsuya Oshima*, Kanya Kondo, Keisuke Ohto, and Katsutoshi Inoue

Department of Applied Chemistry, Saga University, Japan
'Department of Applied Chemistry, University of Miyazaki, Japan

Bacterial cellulose is extracellular cellulose synthesized bv some bacteria. Since thickness of the microfiberous structure of bacterial cellulose is much smaller than that of plant cellulose, bacterial cellulose shows various advantageous properties and is expected as an advanced material.

In the present paper, phosphorylated bacterial cellulose is prepared as an adsorbent for metal ions. Scanning electron microscopy image of the phosphorylated BC indicated that the final product exists as an aggregated ribbon structure. Batchwise adsorption test of Fe(lll), Cu(ll), Mn(ll), Zn(ll), and Co(ll) on phosphorylated bacterial cellulose were examined. Quantitative adsorption of the metal ions was achieved under acidic condition. The results suggest potential of phosphorylated BC as a brand-new adsorbent for metal ions.

INTRODUCTION

Some bacteria represented by *Acetobacter xylinum* synthesize extracellular cellulose called bacterial cellulose (abbreviated as BC) [1], The primary structure of BC is similar to that of higher plant cellulose; cellulose is an unbranched polymer of p-1,4-linked glucopyranose residues. However, fibrous structure of BC is different from plant cellulose. BC is composed of microfibrils, which have a ribbon-like structure, and the thickness (O.lx 10^{6} m) is two orders of magnitude smaller than that of plant cellulose (10 x $10^{'6}$ m). In addition, the microfibrils retain a fine network structure. Because of the characteristic macrostructure, BC shows various advantageous properties, such as high tensile strength, elasticity, large surface area, *etc.*

Due to the unique characteristic, BC draws attention as a novel industrial material in recent years. BC-containing paper shows improved chemical adhesion and tensile strength. On the basis of the satisfactory elasticity, BC sheet is used as sensitive diaphragm for stereo headphones. In medical sector, BC is utilized as a material of artificial skin for therapy. In Asia, BC prepared from coconut milk or coconut water is tasted as a dessert food called 'nata de coco'. Evans and coworkers have recently developed metal-incorporated BC membrane as a thermostable electrode membrane [2],

Authors focused on BC as a starting material of a new adsorbent for metal ions. Natural polysaccharides are attractive for preparing adsorbents from the viewpoint of environmental compliancy [3], Various adsorbents are able to be prepared from polysaccharides. Authors have been developed various chitosan derivatives by introducing oxine, glycine, iminodiacetic acid (IDA), ethylenediamine-A/,A/,/V',/\/-tetraacetic acid (EDTA) or

diethylenetriamine-A/,/V,/V',/Ỿ"/V"-pentaacetic acid (DTPA) [4-7], Adsorption of metal ions on the chemically modified chitosans has comprehensively studied. Moreover, chitosan derivatives bearing A/-(2-pyridylmethyl) group, /\/-(2-thienylmethyl) group, and *N-[* 3-(methylthio)propyl] group exhibit high adsorption capacities for Pd(ll) compared to that of original chitosan [8], Thus chemical modification of natural polysaccharides provides good adsorbents for collection or separation of metal ions.

In the present paper, phosphorylated BC (abbreviated as PBC) was prepared as a brand-new adsorbent for metal ions. It has been reported that various metal cations are adsorbed on phosphorylated cellulose [9], Moreover, iron(lll)-loaded phosphorylated cellulose functions as an adsorbent for oxo anions [9, 10], The material is observed under electron microscopy to ensure the microfiberus structure. Adsorption behaviour of some transition metal ions on PBC was investigated.

EXPERIMENTAL

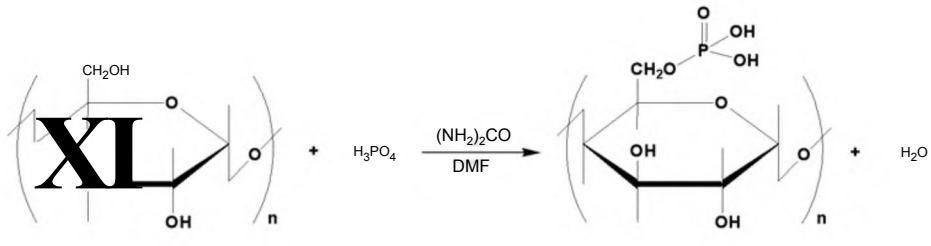
Preparation of phosphorylated bacterial cellulose

BC was kindly supplied from a food company. lOOg of wet cake containing 5 wt% of BC, which was stored under basic condition, was repeatedly washed with distilled water until the filtrate became neutral. After the filtration and lyophilization, about 5g of dry BC was obtained. The product was grounded and sieved to less than 200pm.

2.0g of BC powder was soaked in 100cm^3 of dimethyl formamide (DMF) along with 40g of urea. After the mixture was stilled for 1 hour, 20g of phosphoric acid was added. The mixture was stilled at 130°C for 4 hours. After cooling, the mixture was filtered and washed with a mixture of distilled water and 1-propanol, 0.1 mol/dm^3 dilute hydrochloric acid, and finally distilled water. The product was lyophilized and grounded. After sieving to less than 200 pm, 1.3g of PBC was obtained as white powder.

PBC was observed with a scanning electron microscope (TOPCON SM-300). Degree of phosphorylation of BC was determined as follows: 40mg of PBC was soaked in 1.5 mol/dm^3 surfuric acid and the mixture was stilled at 90°C for 24 hours to eliminate the phosphoric acid group. After cooling, the mixture was filtered and diluted with distilled water. Concentration of phosphoric acid in the solution was analyzed with an ICP/AES spectrometer (Shimadzu ICPS-5000), in order to determine degree of substitution by phosphoric acid group in BC.

Scheme. Synthetic route of phosporylated bacterial cellulose (PBC)



Adsorption test

Adsorption experiments were carried out in batchwise method. Two aqueous solutions were separately prepared by dissolving 0.1 mmol/dm^3 of a metal ion (Cu^{2+}, Mn^{2+}, Zn^{2+}, Co^{2+}, Fe^{3+}, or La^{3+}) into either 100 mmol/dm^3 hydrochloric acid or 2-[4-(2-hydroxyethyl)-1-piperazinyl]ethanesulfonic acid (HEPES) buffer solution. The pH in the aqueous solution was adjusted by mixing the above two aqueous solutions. 15 cm^3 portion of the aqueous solution and 20 mg of dried adsorbent PBC were mixed in a stoppered Erlenmeyer flask and vigorously shaken in a thermostated shaker at 303K. After 20 hours the adsorption reached

the equilibrium state and the mixture was filtrated to obtain the filtrate. The concentrations of the corresponding metal ion in the aqueous solution were determined by an atomic absorption spectrophotometer (Shimadzu AA-6650). From the metal concentrations before and after the adsorption (C_0 and C_e/mmol dm'3), percentage of the adsorption and the amount of the metal adsorption (q) were calculated according to the following equations;

$$\%\text{Adsorption} = \frac{C_0 - C_e}{Co} \times 100\ [\%]$$

$$q = \frac{C_0 - C_e}{W} \times F\ [\text{mmol/g}]$$

Where, W is the dry mass of adsorbent in grams and V is volume of solution in dm'3, respectively.

Elution test

Adsorption of Cu(ll) on lOmg of PBC was examined in the similar manner shown in the above section. After shaking at 303K for 12 hours, the mixture was filtered and the residue containing Cu(ll)-adsorbed PBC was washed with 100 cm3 of distilled water. The residue was mixed with 40 cm3 of aqueous solution and shaken at 303K for 12 hours. After filtration of the mixture, concentration of Cu(ll) in the eluate was analyzed. On the basis of the mass-action law, percentage of elution was calculated.

RESULTS AND DISCUSSION

Characteristic of the Material

As shown in Figure 1, the thickness of BC is much smaller than those of other fibers [11], In order to utilize the specific structure for various applications, microfibrous structure of BC should be maintained during the phosphorylation procedure. Drying process seemed to decide fibrous structure of the product PBC. As the results of preliminary experiments, it was found that lyophilization is more efficient drying method compared to drying in an oven. Degree of phosphorylation in the product PBC was 11.2% against monomer glucose unit of BC.

SEMs image of the product PBC is shown in Figure 2. Microfibrous ribbon structure is apparently observed on the surface of PBC powder. Width of the ribbon on PBC surface is around 0.1 pm. Namely, microfibrous structure of BC has maintained through the phosphorylation procedure.

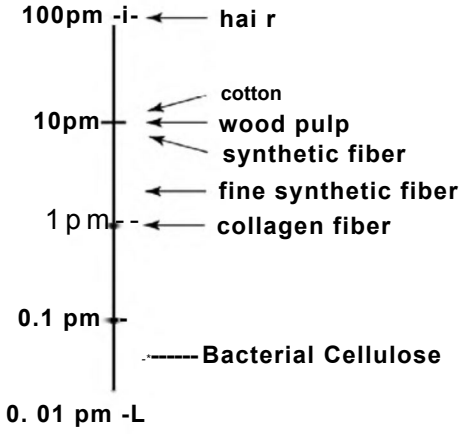


Figure 1. Thicknesses of various fibers[11].*

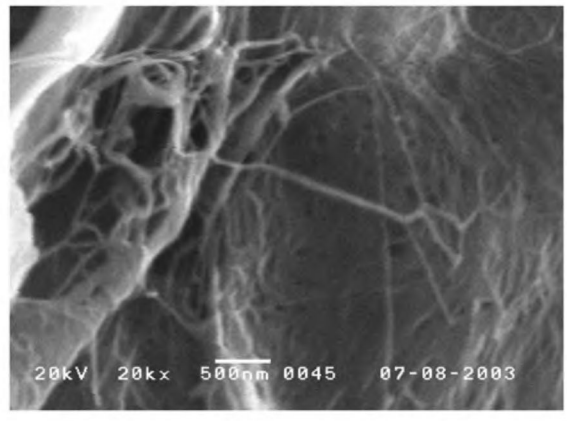


Figure 2. Scanning electron micrograph of PBC at 20,000x magnification.

Adsorption Behaviour of Metal Cations on Phosphorylated Bacterial Cellulose

Figure 3 shows adsorption behaviour of Cu(II) ion on BC and PBC as a function of pH. Adsorption of Cu(II) on PBC increases with increasing the aqueous pH value. At more than pH 4, Cu(II) is quantitatively adsorbed on PBC. On the other hand, the starting material BC does not adsorb Cu(II). Namely, phosphoric acid groups introduced in PBC functions for adsorption of Cu(II) ion.

Adsorption profiles of Fe(III), Cu(II), Mn(II), Zn(II), and Co(II) on PBC as a function of pH are shown in Figure 4. Fe(III) ion, which has a strong affinity with a phosphoric acid group, is quantitatively adsorbed on PBC under acidic condition. Divalent transition metal cations Cu(II), Mn(II), Zn(II), and Co(II) show similar adsorption behaviours: % adsorption values increases with increasing the aqueous pH value and reaches over 90% at more than pH 4.5.

As shown in the figure, selectivity for metal adsorption on PBC at around pH 3 is deduced as the following orders:

Fe(III) > Cu(II) > Mn(II) > Zn(II), Co(II)

The selectivity is originated from the characteristic of phosphoric acid group.

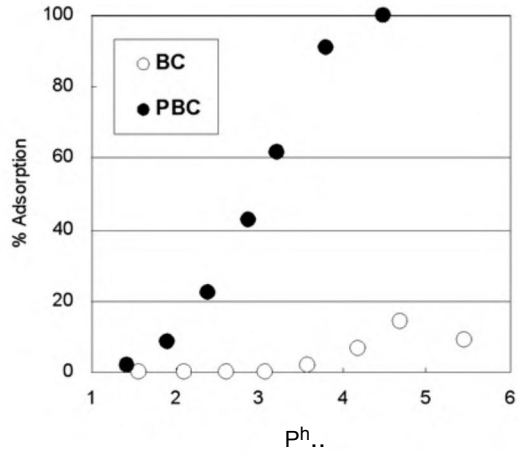


Figure 3. Adsorption profiles of Cu(II) ion on BC and PBC: adsorbent;20mg, Volume;15cm³, [Metal]i_{ni}=0.1mmol/dm³.

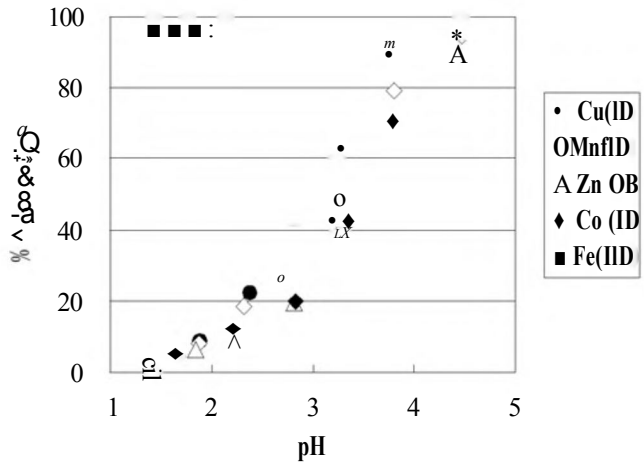


Figure 4. Adsorption profiles ofFe(III), Cu(II), Mn(II), Zn(II), and Co(II) on PBC: adsorbent;20mg, Volume;15cm³, [Metal]$_{in}$r0.1mmol/dm³.

Adsorption Isotherm

Adsorption isotherm of Cu(II) on PBC at varying equilibrium concentration is shown in Figure 5. The amount of adsorption increases with increasing the metal concentration and approaches to a constant value around 0.36 mmol/g.

The equilibrium experimental data were correlated with Langmuir isotherm model in order to determine the maximum adsorption capacity of Cu(II) on PBC *(q_{max})*. The Langmuir model assumes monolayer adsorption as shown in the following a mathematical expression:

$$\frac{C_L}{q} = \frac{C_L}{q_{max}} + \frac{1}{q_{max} K}$$

Figure 6 shows the Langmuir plot of the data shown in Figure 5. The points lie on a straight line and the q_{max} value was calculated as 0.37 mmol/g. The result suggests that adsorption of Cu(II) proceeds according to monolayer adsorption by complexation between Cu(II) and PBC. The maximum adsorption capacity of PBC in this study is smaller than those of various commercial chelating resins, due to the small rate of phosphorylation (11.2%). A systematic study to explore an optimal condition for phosphorylation of BC is now under the way.

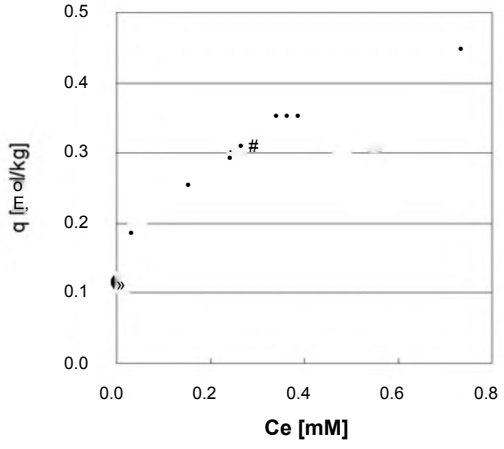


Figure 5. Adsorption isotherm of Cu(II) ion on PBC: 303K, pH4.3, adsorbent;10mg, Volume; 15cm³.

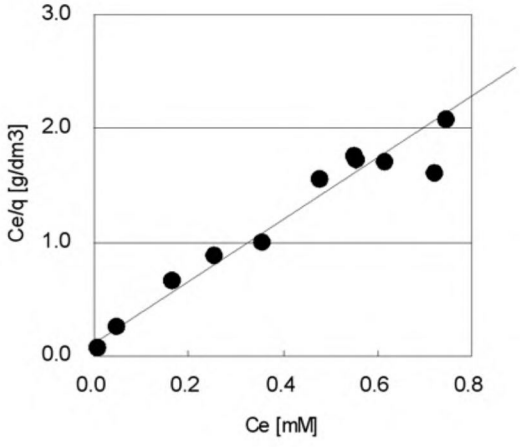


Figure 6. Langmuir plot for adsorption of Cu(II) ion on PBC

Elution of adsorbed metal ions

Percentages of elution for adsorbed Cu(II) on PBC with aqueous solutions varying pH is summarized in Table 1. As shown in the table, the elution is dependent on the aqueous pH and the adsorbed Cu(II) ion was quantitatively recovered in the acidic eluate solution. Therefore, PBC functions as a separation material for metal cations through adsorption and elution processes.

Table 1. Elution of Cu(II) ion adsorbed on PBC.

pHeq	Elution [%]
1.27	96
2.19	94
3.20	87
4.19	79

CONCLUSIONS

Phosphorylated bacterial cellulose exhibits adsorption behaviour for various transition metal ions. The microfibrous structure of the modified bacterial cellulose is retained during the phosphorylation procedure. On the other hand, further study is necessary to increase the degree of phosphorylation on BC.

Phosphorylated bacterial cellulose would appear different physical properties compared to that of conventional phosphorylated cellulose. The next study on phosphorylated bacterial cellulose should be focused on the application as an adsorbent for metal ions.

ACKNOWLEDGEMENTS

We are grateful for the Grand-in-Aid for Young Scientists (B, No. 15760561) from Ministry of Education, Science, Sports and Culture of Japan. The present research is partially supported by the REIMEI Research Resources of Japan Atomic Energy Research Institute. T. O. acknowledges financial support by the Foundation for Earth Environment, Japan.

REFERENCES

1. E. J. Vandamme, S. De Baets, and A. Steinbuchel (2003), *Biopolymers: Polysaccharides I: Polysaccharides from Prokaryotes,* WILEY-VCH, 37 pp.
2. B. R. Evans, H. M. O'Neill, V. P. Malyvanh, I. Lee, and J. Woodward (2003), *Biosens. Bioelectron.,* 18, 917-923
3. K. Inoue, Y. Baba, and K. Yoshizuka (1993), *Bull. Chem. Soc. Jpn.,* 66, 2915-2921
4. K. Inoue, H. Hirakawa, Y. Ishikawa, T. Yamaguchi, J. Nagata, K. Ohto, and K. Yoshizuka (1996), *Sep. Sci. Techno!.,* 31, 2273- 2280
5. K. Inoue, T. Yamaguchi, M. Iwasaki, K. Ohto, and K. Yoshizuka (1995), *Sep. Sci. Techno!.,* 30, 2477-2483
6. K. Inoue, K. Ohto, K. Yoshizuka, T. Yamaguchi, and T. Tanaka (1997), *Bull. Chem. Soc. Jpn.,* 70, 2443-2447
7. K. Inoue, K. Yoshizuka, and K. Ohto (1999), *Anal. Chim. Acta.,* 388, 209-218
8. Y. Baba, Y. Kawano, and K. Ohto (1996), *Bull. Chem. Soc. Jpn.,* 69, 1255-1260
9. K. Inoue, K. N. Ghimire, Y. Zhu, M. Yano, K. Makino, and T. Miyajima (2002), *Geosystem Eng.,* 5, 31-37
10. K. N. Ghimire, K. Inoue, K. Makino, and T. Miyajima (2002), *Designed Monomers Polym.,* 5, 401-414
11. F. Yoshinaga, N. Tonouchi, and K. Watanabe (1997), *Kagaku to Seibutu,* 35, 772-779

STUDY ON THE PREPARATION OF NANO-MATERIALS WITH EXTRACTANT AND EXTRACTION SYSTEMS

Xun Fu*, Zhengshui Hu, Guohua Gu, Debao Wang, Haitao Zhu, Xiaodong Zhou
Qingdao University of Science and Technology, Qingdao 266042, P.R.China

Based on the interfacial properties of extractants and the resultant interfacial phenomena of extraction systems, several nano-materials have been successfully prepared. Results already published and developed recently are summarized and reviewed in this paper.

INTRODUCTION

Acidic extractant (saponified), extractant containing nitrogen (salted), and neutral extractant are analogues of anionic, cationic and non-ionic surfactants respectively. The phase behavior of an extraction system is controlled by the amphiphilic properties of the extractant and extracted species [1], When a nano-material is prepared from an extraction system, the extractant behaves as both a phase transfer and modifying agent. These properties have been exploited for the preparation of $Ti0_2$ nano-particles, $Zr0_2$ materials with high surface area or mesoporous structures, sheet-like CdS nano-crystal, CdS hollow sphere with different diameters, and organic fluids with high concentrations of nano-particles of Ag, Ag_2S, PbS, Bi_2S_3, etc. Their applications have also been considered. $Ti0_2$ is applied as a photo catalyst, and paraffin containing silver nano-particles is used as an antiwear agent. Results previously published and recently developed are summarized and reviewed in this paper.

EXTRACTANT SYSTEMS USED AS A TEMPLATE TO PREPARE NANO-MATERIALS WITH SPECIAL STRUCTURE.

Preparation of metal oxides with high surface area or with mesoporous structure via third-phase formation with organophosphorous extractants

In TBP-Kerosene (40%, 60%, v/v)/ H_2S0_4-$TiOS0_4$ extraction system, a third phase appeared in the range of C_{H2}so4 (bottom) = 6.3~10.2 mol/L. This third phase with high loading Ti(IV) was used to prepare ultrafine $Ti0_2$ powders by hydrolysis. The amorphous precipitate changed to anatase crystals after calcination at 600°C, and to rutile crystals at 1200°C. The anatase powders had a narrow size distribution of 20 nm, but the high temperature calcination made the particles agglomerate (Figure-1) [2],

The $Ti0_2$ thus obtained featured high photocatalytic activity. A decolorization ratio of 98% was obtained when methylene blue above the $Ti0_2$ was illuminated for 25 min, and the COD removal efficiency was about 70% [3],

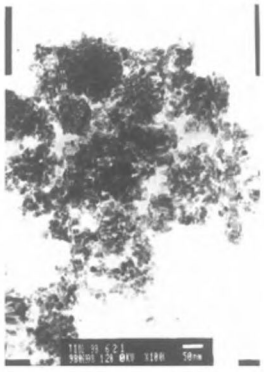


Figure-1 TEM of $Ti0_2$ powder

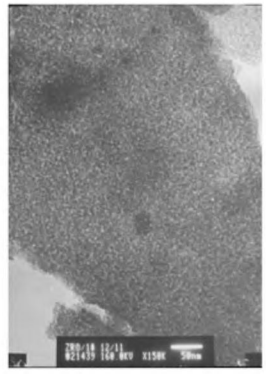
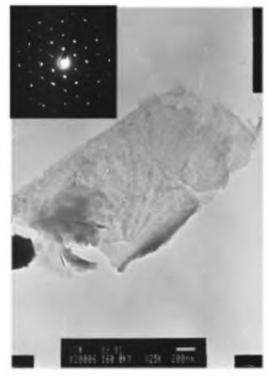


Figure-2 TEM of $Zr0_2$ powder



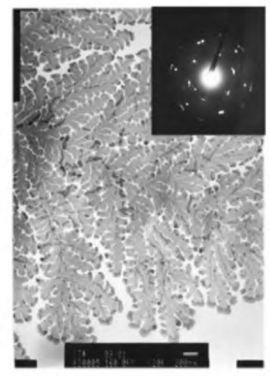


Figure-3 TEM of the CdS with sheet-like and leaf-like morphologies

A crude solution containing Ti(IV), Fe(II) and H_2S0_4 supplied by a plant was extracted with TBP-Kerosene solution. The third phase loaded with Ti(IV) was hydrolyzed to produce $Ti0_2$ powder with a narrow size distribution of 20 nm. The content of iron in the product was less than 90 ppm with only one stage of extraction and hydrolysis [4], The advantage of this method for preparing ultrafine $Ti0_2$ powder is that the processing solution has a higher metal content than with other methods used before in colloidal chemistry. Furthermore, the process is simple, requiring only one stage of extraction for effective separation of Ti/Fe and one precipitation step. This suggests that the method could be applied for the commercial manufacture of nano-$Ti0_2$ powder.

The third phase formed in TRPO-kerosene (30%, v/v)/ HCI (8.0 mol/L) -$ZrOCl_2$ (0.1 mol/L) extraction system was used as a Zr (IV) source to prepare $Zr0_2$ [5], The third phase was separated and reacted with aqua ammonia (1:1, v/v) at a low temperature (-10°C) to produce a precipitate that was then washied, dried and calcined. A mesoporous $Zr0_2$ powder with surface area of 163 m^2/g and d-value of 6.3 nm was prepared. The powder is composed of cubic and tetragonal crystals (Figure-2).

The microstructure of the third phase is related to the initial composition of the extraction system. An excess of solvent, extractant and polar additive (long-chain alcohol) solubilized in the middle phase can change, or even destroy the bi-continuous structure that form in a w/o microemulsion. So the products obtained could be nano-particles, nano-particles mixed with mesoporous, or mesoporous material with surface area ranging from 100 to180 m^2/g and pore size ranging from 2.5 to 3.5 nm [6],

Preparation of metal oxide with high surface area via Colloidal Liquid Alphorn products with organophosphorous extractants.

The extraction and phase behavior of the TOPO (orTRPO) and TBP-Kerosene/H_2S0_4-Ti (IV) systems were compared. The phase behavior in both systems were found to be similar, but

the extraction percentage of Ti (IV) for $R_3P=0$ in the two-phase region was much higher than that for $(R0)_3P=0$.

Colloidal Liquid Alphorns (CLA)were prepared by the predispersed method using the organic phase loaded Ti(IV) as the inner phase. When Ti (IV) in the oil core of the CLA was hydrolyzed at the boundary of the inner phase by adding 1:3 ammonia solutions, porous spherical $Ti0_2$ particles were obtained. The amorphous $Ti0_2$ changed to anatase crystal after calcinations at 550°C. A crude solution containing Ti(IV), Fe(II) and H_2S0_4 supplied by a plant was extracted using TOPO-Kerosene solution. The loaded organic solution was used to prepare a stable CLA as the inner phase. Linder favorable hydrolysis conditions, a porous spherical $Ti0_2$ of about 50~100 nm could be obtained. The content of iron in the product was less than 100 ppm [7],

A CLA was also prepared using the organic phase loaded Zr (IV) obtained from the extraction system of TRPO-Kerosene/HCI-$ZrOCI_2$ as the inner phase. The effects of Zr (IV) concentration in the extracted organic solution, ammonia concentration and hydrolysis temperature on the properties and structure of produced $Zr0_2$ were studied by N_2 isothermal adsorption, XRD and TEM [8], The results showed that the surface area of zirconium powder decreased with decrease of Zr (IV) and ammonia concentration Tetragonal zirconium powder with surface area of 231.4 m^2/g was obtained when Zr (IV) was hydrolyzed at room temperature.

Preparation of sheet-like nanocrystals via a liquid crystal template formed with an organophosphinic extrcatant.

A liquid crystal sample composed of Cyanex 302 (4.300 g), C_6H_{14} (0.500 g) and NaOH aqueous solution (5.63 mol/L, 1.544 g) was prepared. $Cd(N0_3)_2$ (1.50 mol/L 0.20 ml), was then precipitated with H_2S. The system was equilibrated at 25°C for two weeks. The TEM images of the CdS obtained (Figure-3) showed that sheet-like and leaf-like nano-crystals were prepared [9], The liquid crystal was formed with the acidic and sodium salt of the extractant in a suitable ratio range. The coordination between extractant and metal ion causes the neutralization fraction to be changed, so that the amount of Cd^{2+} added should be appropriate to avoid the liquid crystal structure being damaged. The other point is that the well-controlled sheet-like CdS nano-crystal prefers a thinner water layer, i.e., the concentration of NaOH solution used in preparing the liquid crystal should be high.

HIGHLY LOADED ORGANIC FLUIDS PREPARED BY DISPERSION OF NANO-PARTICLES IN AN ORGANIC SOLVENT

The preparation of metal colloidal dispersions in a non-polar solvent is known to be a complex problem. Two main methods have been reported for this purpose. The first one was named as “two-stage scheme" where the first stage was to synthesize nano-particles of metal, metal sulfide or oxide in the medium of water or polar solvents, and the second stage was to redisperse the nano materials into non-polar solvents. This method was reported to be used in the preparation of nano-fluids applied in the field of antiwear and heat-conduction. For

example, Xue Qunji et al (in the Key Lab of Tribology in Lanzhou, China) prepared several metal sulfide, such as Ag_2S [10], PbS [11], MoS_2[12], ZnS [13] and etc, in mixed solvent of alcohol-water with a modifier PyDDP (Pyridin salt of dioctadecyldithio phosphoric acid) or thiol. These sulfides when dispersed into liquid paraffin showed good antiwear properties.

The second method was called “two-phase synthesis”, where metal ions were transferred first from aqueous to organic solution followed by reduction or precipitation reactions in the presence or absence of a stabilizing agent such as thiol, surfactant, or copolymer. Vorobyova et al [14] reported the preparation of silver colloids dispersion in decane by transferring AgI_2' with a quaternary ammonium salt into organic solution and followed by reduction with $NaBH_4$ in the absence of the stabilizer. They considered that the phase transfer agent was absorbed onto the surface of the particles, thereby promoting the stabilization.

Unfortunately, papers concerned with the loading amounts of the nano-particles, or the in-situ concentration of metal colloids in the organic fluids, were only at relatively low concentration (the order of 1 g/Land below) [15], For example, the reference [14] mentioned above reported that the silver particles content in the colloidal dispersion was only 0.16 g/L.

Recently the “two-phase synthesis” method has been used in our lab to prepare metal or metal sulfide alkane fluids with Cyanex 302 or Cyanex 301 extractant systems, with particular attention paid to (1) the functions of extractants in the extraction of metal and the modification for the nano-particles loaded in the organic fluids, and (2) maximizing the amounts of the nano-particles loaded in the organic fluids.

Preparation of silver nano-particles fluid using Cyanex 302

The loading content of silver particles in kerosene is normally about 0.54 g/L. If a small amount of copolymer $(PEO)_{20}(PPO)_7o(PEO)_2o$ is added before the reduction of the Cyanex 302 -Ag (I) complex in the organic phase, the loading concentration of silver particles in kerosene could be greatly increased to 0.1 mol/L (10.8 g/L) at room temperature [16]. Based on TEM, IR and UV analysis, it was inferred that the silver nano-particles modified by Cyaned 302 could be solubilized more easily in reversed colloids formed with copolymer.

The tribological coefficient of a liquid paraffin containing 0.1% silver particles was measured, and the results indicated that the friction coefficient and wear scar diameter decreased 47% and 25%, compared with the pure paraffin oil, respectively, under the condition of 300 N, 30 min and 1450 r/min [17],

Cyanex 301 containing two sulfur atoms showed a much better modifying function for silver nano-particles. The loading concentration of silver particles in gasoline was higher than 0.1 mol/L without any additive agent. The prepared nano-fluids could be stored longer than several months and no precipitate appeared. All particles were in the sizes less than 20 nm, and the IR, UV analysis indicated that the bond force still existed between Cyanex 301 and Ag (0) particles [18],

Preparation of metal sulphide nano-particle fluids using Cyanex 301 and 302

Cyanex 301 or 302-gasoline/Pb^{2+}, Ag^{+} or Bi^{3+} extraction systems were used to prepare nano-fluids containing particles of PbS, Ag_2S, or Bi_2S_3. The loading concentrations in the fluids were compared with those obtained using the "two-stage method" where, PbS, Ag_2S, and Bi_2S_3 modified by Cyanex 301 or 302 instead of PyDDP were first synthesized from the medium of water plus alcohol [10-13] and the particles then redispersed into organic solvents.

Characterization of the particles with TEM, IR, UV, XRD and TG, showed them to be well modified by the extractants, but the loading concentration were different. The loading concentration in the same fluid prepared by "two-phase synthesis" were all higher than those prepared by "two-stage method" (Table 1):

Table 1. Loading amounts of different nano-fluids

System	Cyanex 302-Bi^{3+} Bi_2S_3 in gasoline	Cyanex 301-Pb^{2+} PbS in gasoline	Cyanex 301-Ag^{+} Ag_2S in gasoline
two-phase synthesis	19.27	10.7	25.2
two-stage method	9.96	5.0	7.44
References	[19]	[20]	[21]

It is concluded that the nano-particles produced using the extraction system are better modified than those obtained from the medium of water or polar solvent.

PREPARATION OF NANO-MATERIALS WITH OTHER METHODS

Preparation of CdS hollow spheres

The sodium salt of HDEHP can be used as an emulsifier to prepare a poly-(styrene-acrylic acid (PSA) balland using the ball as template to prepare CdS hollow spheres

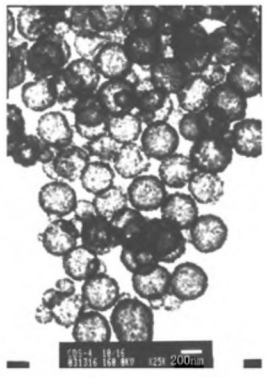


Figure-4 TEM of PSA latex coated CdS hollow spheres



Figure-5 TEM of CdS nanowires



Figure-6 TEM of Bi_2S_3 nanorods

CdS hollow spherical particles with sizes in the range of 150~400 nm were prepared using a core/shell fabrication method with PSA latex particles as template (Figure-4). The sodium salt of the extractant HDEHP was found to be a good emulsifier in producing well-distributed PSA particles. The diameters of the polymer core decreased with increasing amount of emulsifier.

The diameters of CdS hollow spherical particles could thereby be controlled using the emulsifier concentration (Table 2).

Table 2. Effect of the amount of NaDEHP on the PSA particles and the CdS hollow spheres

No.	emulsifier	emulsifier content/wt%	core diameter/nm	hollow sphere diameter/nm
1	NaDEHP	1.56	300	350-400
2	NaDEHP	2.60	200	250-300
3	NaDEHP	3.54	120	150-200

Preparation of CdS and Bi_2S_3 by extraction-solvothermal method

CdS nanowires and Bi_2S_3 nanorods have been successfully synthesized through decomposing the complex Cyanex 301-Cd^{2+} (Bi^{3+}) in gasoline by the extraction solvothermal method (see Figures-5 and 6 respectively). Cyanex 301 acted as both the extractant and the sulfur source of sulfides

REFERENCES

1. X. Fu, Z. Hu, D. Wang, H. Liu, http://www. *Chemistry mag*.org//cji/2000/23018re. htm
2. Z. Hu, X. Hu, W. Cui, D. Wang, X. Fu, (1999), *Colloids and Surfaces, A,* 155:383-393
3. Y. Bai, D. Kong, Z. Hu, X. Fu, and Q. Ye, (2002), *J. ofChem. Eng. of Chinese Universities* (in Chinese),16 (5): 530-535.
4. X. Fu, J. Shi, G. Gu, M. Wang, W. Cui, Hu Z., (2003), *Separation Science and Technology,* 38 (9): 2071-2080
5. L. Yu, G. Gu, J. Yang, **H.** Zhu, L. Chen, L. Feng, X. Fu, (2003), *J. of Colloid and Interface Sci.,* 265:101-105
6. X. Fu, L. Yu, Y. Lin, H. Zhu, H. Wang, X. Zhou, (2004), *Solvent Extr. Ion Exch., 22* (5): 885-895
7. J„ Shi, G. Gu, X. Fu, M. Wang, Z. Hu, (2001), *Colloids and Surfaces, A,* 194:207-212
8. X. Fu, H. Zhu, Y. Lin, L. Lin, Z. Hu, *Rare Metal Materials and Engineering* (in Chinese), To be published in 2005.
9. X. Fu, L. Chen, J. Wang, et al, (2004), *Colloids and Surfaces, A,* 233:189-192.
10. J. Zhou, X. Tao, Z. Zhang, W. Liu, Q. Xue, (1999), *Chem. Researches* (in Chinese) 4:1-5
11. S. Chen, W. Liu, L. Yu, (1998), *Wear,* 218:153-158.
12. Z. Zhang, Q. Xue, J. Zhang, (1997), *Wear,* 209: 8-12.
13. S. Chen, W. Liu, (2000), *Chemical J. Chinese Universitv.* (in Chinese) 3:472-474.
14. S.A. Vorobyova, A.I. Lesnikovich, (1999), *Colloids and Surfaces, A.* 152: 375-379.
15. M. Antonietti, E. Wang, L. Bronstein, M. Sereegina, (1995), *Adv. Mater.,* **7**: 1000-1005.
16. X. Fu, W. Yu, Y. Lin, D. Wang, H. Shi, *J. Disp. of Sci. and Tech.* To be published in 2005
17. W. Yu, X. Fu, (2004), *Tribology (in* Chinese), 5:425-428.
18. H. Shi, X. Fu, X. Zhou, Z. Hu, *J. Disp. of Sci. and Tech.* To be published in 2005.
19. S. Zhang, H. Shi, X. Fu, Z. Hu, *Rare metal materials and Engineering* (in Chinese), To be published in 2005
20. H. Shi, S. Zhang, Y. Lin, X. Fu, Z. Hu, *Rare metal materials and Engineering* (in Chinese), To be published in 2005
21. H. Shi, X. Fu, Z. Hu, Submitted to Solvent Extr. Ion Exch.

PREPARATION AND CHARACTERATION OF ORGANIC FLUIDS CONTAINING Bi_2S_3 NANO-PARTICLES

Zhang Shaoling, Shi Huaqiang, Fu Xun*, Hu Zhengshui

Qingdao University of Science and Technology, Qingdao 266042, P.R.China

Stable fluids containing Bi_2S_3 nano-particles in gasoline have been prepared by the solvent extraction method. Bismuth nitrate is extracted into the non-polar solvent by thio-substituted phosphinic acid extractant Cyanex302, then Bi(III) in the organic phase is reacted with H_2S. Bi_2S_3 nano-particles modified by Cyanex 302 are obtained. The products are characterized by IR, XRD and TEM. The highest nano-particle loading obtained in gasoline is 19.27 g/L.

INTRODUCTION

In 1995 Choi [1], at the American Argome National Laboratory, developed a concept of nanofluids, which was engineered by suspending ultrafine metallic or nonmetallic particles of nanometer dimensions in fluids such as water, engine oil, and ethylene glycol. Much attention has been focused on nanoparticles in recent years, owing to their superior of heat conduction and antiwear properties [2,3], The preparation of metal colloidal dispersion in a non-polar solvent is known to be a complex problem. Two main methods have been reported for this purpose. The first one named “two-stage scheme” in which the first stage is to synthesize nano-particles of metal, metal sulfide or oxide in the medium of water or polar solvents, and then the second stage is to redisperse the nano materials into non-polar solvents. For example, Xue Qunji et al (in the Key Lab of Tribology in Lanzhou, China) prepared several metal sulfides, such as Ag_2S [4], PbS [5], MoS_2 [6], ZnS [7] and etc, in the mixed solvent system of alcohol-water with a modifier PyDDP (Pyridin salt of dioctadecyldithio phosphoric acid) or thiol. The sulfides were then dispersed into liquid paraffin and showed good antiwear properties.

The second method was called “two-phase synthesis”, where the metal ions were first transferred from aqueous to organic solution followed by reduction or precipitation reactions in the presence or absence of a stabilizing agent such as thiol surfactant or copolymer. Brust

et al [8] prepared 1-3 nm gold particles using two-phase (water-toluene) reduction of $AuCl_4'$ by sodium borohydride in the presence of an alkanethiol. Vorobyova et al [9] reported that silver colloids dispersion in decane was prepared by transferring AgI_2' using a quaternary ammonium salt into an organic solution and followed by reduction with $NaBH_4$ in the absence of the stabilizer. They considered that the phase transfer agent was absorbed onto the surface of the particles, promoting the stabilization.

Few papers were concerned with the loading amounts of the nano-particles, or the in-situ concentration of metal colloids [10] in the organic fluids, and the dispersion was only at relatively low concentration (the order of 1 g/L and below). For example, the reference [9] mentioned above reported that the silver particles content in the colloidal dispersion obtained was only 0.16 g/L. The authors prepared kerosene fluid containing Ag nano-particles by the extraction-reduction method, and the loading concentration was about 0.5 g/L [11], When a little PEO-PPO-PEO was added prior to the reduction of the Cyanex 302-Ag(I) complex with KBH_4, a loading concentration of 10 g/L was achieved [12].

This paper described the preparation of stable organic fluids containing Bi_2S_3 nanoparticles by the two methods. The loading concentrations of Bi_2S_3 nano-particles in organic solvents (gasoline, benzene) were quantitatively analyzed and compared.

EXPEREMENTAL

Cyanex 302 was kindly supplied by Cytec Co. of Canada. A monoacid content of 84.47% was obtained by titration [13], Hydrogenated gasoline was the product of QiLu Petrolium Company in China. H_2S gas was obtained by the reaction of solid FeS with 6 mol/L HCI. The other reagents used such as bismuth nitrate, sodium sulfide, nitric acid, and benzene were all A.R. grade and used without further purification. Distilled water was used.

Extraction behavior of Bi^{3+} with Cyanex 302 and preparation of the organic fluids containing Bi_2S_3 nano-particles by “two-phase synthesis”, or “extraction synthesis” method

Equal volumes of Cyanex 302-n-heptane and aqueous $Bi(N0_3)_3$ solutions with different acidities were mixed with vigorous shaking . After equilibration (2h) and phase separation, a measured volume of aqueous solution was removed, and adjusted to pH=1.0-1.5. Using xylene orange as indicator, Bi^{3+} was analyzed by titration against standard EDTA solution. The relation of extraction percentage with the initial aqueous acidity was thus obtained.

The nanofluid of Bi_2S_3 in gasoline was prepared by direct reaction of Bi(III) in the extracted organic phase with H_2S gas with stirring at room temperature for longer than 18h. During the reaction the color of the organic phase changed from yellow to reddish brown and then to black. After centrifugation at 3000 r/min for 30 min, a small quantity of sediment was found. The fluids containing Bi_2S_3 nano-particles were obtained after separating out the precipitate. The solvent was then evaporated from a measured volume of the fluid and the resultant black

sediment was washed several times with acetone and alcohol respectively and then dried in a vacuum at 70°C for 8 h, These Bi_2S_3 nano-particles were used for characterization.

Preparation of Bi_2S_3 nano-particles by the "two-stage method" in alcohol-water medium [5]

A measured volume of Na_2S aqueous solution and an excess of $Bi(N0_3)$3aqueous solution (0.5 mol/l $HN0_3$ was added to prevent hydrolyzing) were added into the mixture of alcohol-water in the presence of Cyanex 302 and an equimolar quantity of NaOH, while stirring at 55 °C in a water bath for 3h. The precipitate was washed several times with acetone and alcohol and dried in a vacuum at 60 °C for 8h. A black powder of the Bi_2S_3 nano-particles modified by Cyanex 302 was thus obtained.

Characterization of Bi_2S_3 nano-particles

The particle size and morphology of Bi_2S_3 nano-particles were determined using a JEM-2000EX model transmission electron microscopy (TEM, JEOL Co.) The surface modification of products was analyzed using a 51 OP IR spectrometer (Nicolet Co., US). The X-ray powder diffraction (XRD) pattern was recorded using a D/max-rBX X-ray diffractometer.

Analysis of the loading concentration of Bi_2S_3 nano-particles in organic fluids

The loading concentration of Bi_2S_3 in organic fluid prepared by the "extraction synthesis" method was determined as follows: A measured volume of the organic fluid (for example 2.00 ml) was taken to first evaporate the solvent gasoline in a hot water bath. The sediment was washed with a larger volume of acetone (for example 18 ml). The quantity of Bi_2S_3 obtained was analyzed using EDTA titration after digestion of the Bi_2S_3 in $HN0_3$. The washing step was used to separate the solid nano Bi_2S_3 from the unprecipitated Bi(III)-Cyanex 302 complex in the gasoline fluid (if any) and the free extractant (uncoated on the nanoparticles) for its recovery. Comparing the titration data with the initial amount of Bi(III) in the extracted organic phase, a 4% difference was found. The 4% could include the amount of unprecipitated Bi(III) partly by H_2S gas in the period 18h and the amount of Bi_2S_3 dispersed in acetone. The reported data in this paper was the value obtained by titration analysis.

The loading concentration of Bi_2S_3 in organic fluid prepared by the "two-step method" was determined as follows: The black Bi_2S_3 particles were redispersed ultrasonically into organic solvents for 10 min, and centrifuged at 3000 r/min for 30 min. After evaporating the solvent from a definite volume of the fluid, the Bi_2S_3 obtained was analyzed by EDTA titration after first dissolving the Bi_2S_3 in $HN0_3$.

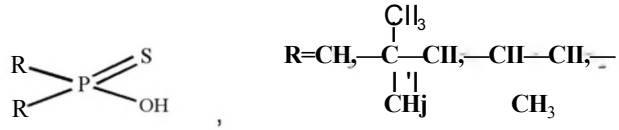
RESULTS AND DISCUSSION

Extraction behavior of Bi^{3+} by the extractant Cyanex 302

Figurel shows the relationship between extraction percentage and initial aqueous acidity for the equal volumes of 0.2 mol/l Cyanex 302-n-heptane solution and 0.1 mol/l $Bi(N0_3)_3$ aqueous solution extraction system. It indicates that the extraction percentage decreases

gradually with increasing initial aqueous acidity and then sharply in the range of 1.0-2.0 mol/1.

Cyanex 302 is a monoacid thiophosphinic extractant (HA). The major component is bis(2,4,4tri-methylpentyl) monothiophosphinic acid (HDTMPTP):



Cyanex 302 (HA) reacted with metal ions by the exchange of ions. Further experiments were performed using an aqueous acidity of 0.5 mol/l in order to make the best use of the extractant, and for Bi^{3+} to not be hydrolyzed.

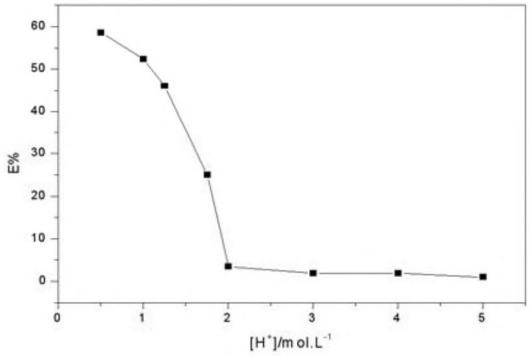


Figure 1. The relationship between the extraction % and acidity of the aqueous phase

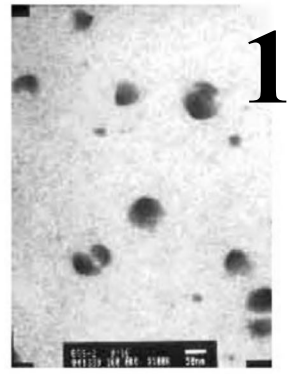


Figure 2. TEM image of the Bi_2S_3 nano-particles

Characterization of Bi_2S_3 modified with Cyanex 302

Figure 2 shows the TEM image of Bi_2S_3 nano-particles modified with Cyanex 302 by the extraction-synthesis method. It indicates that the size of the Bi_2S_3 particles is only several nanometers and the particles dispersed well in the organic solvent. It is speculated that the extractant molecules are adsorbed onto the surface of the particles to form organic modification layers, promoting the stabilization.

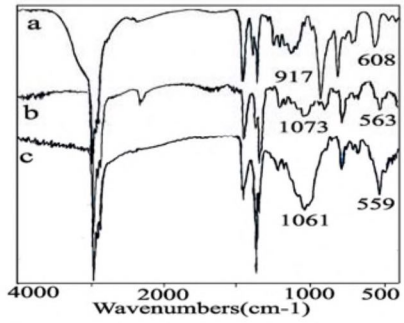


Figure 3. The IR spectra of Cyanex 302(a), the complex of Cyanex 302- Bi^{3+} (b) and Bi_2S_3 nano-particles modified by Cyanex 302 (c)

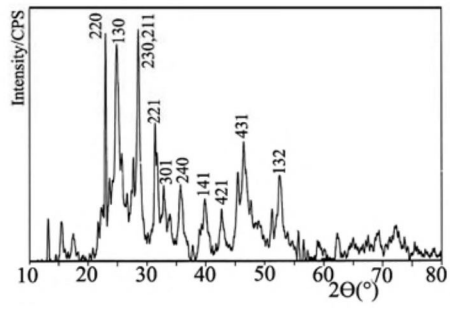
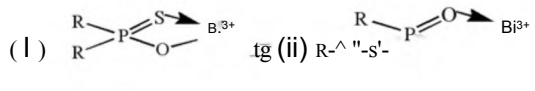


Figure 4. The XRD of Bi_2S_3 nano-particles modified by Cyanex 302

Figure.3 shows the IR spectra of the extractant Cyanex 302(a), Cyanex 302-Bi^{3+} complex(b) and Bi_2S_3 nano-particles modified by Cyanex 302(c).

Handley [14] reported that (di-n-butyl)-thiophosphoric acid exhibited two structural tautomerisms, and about 90% was found to exist in the thiono form in the solvent.The IR spectrum of Cyanex 302 (Fig.3-a) shows that the absorption peak of P=S is at 608 cm"[1] and the absorption peak of P-O(-H) is at 917cm'[1].This result is consistent with Handley [14],

The Cyanex 302-Bi (III) complex may have two forms:



In its IR spectra (Fig.3-b), the absorption peak of P=S- (M) appears at 559 cm'[1], indicating that there is a strong coordination force of P=S— Bi^{3+}. When Bi^{3+} is precipitated as Bi_2S_3, the IR spectra (Fig.3-c) shows that the characteristic peaks of the major group in the extractant including alkyl group all existed. This means that the extractant coated onto the surfaces of Bi_2S_3 nano-particles could not be washed off with the alcohol or acetone. Comparing with the complex, only the wave number decreases slightly from 563 to 559 cm'[1]. It is confirmed that there is also a strong chemical force of P=S —Bi_2S_3 particles.

Figure.4 shows the XRD of Bi_2S_3 nano-particles modified with Cyanex 302. The major peaks in the pattern can be indexed to orthorhombic Bi_2S_3, which is close to the reported data (JCPDS 17-320).

The analysis of loading concentration of Bi_2S_3 nanoparticles in non-polar solvents

The loading concentrations of Bi_2S_3 nano-particles prepared by the extraction-synthesis method in gasoline and benzene were 19.27 g/L and 4.61 g/L, respectively, (Table 1). 19.26 g/L is a larger value than that reported in references, indicating that Cyanex 302 is a very good modifier for Bi_2S_3 nano-particles. Bi_2S_3 nano-particles prepared by the two-stage method were redispersed in gasoline, and the loading concentration found to be 9.96 g/L. Comparing the two values, much better modification occurred in the extraction-synthesis method.

Table 1. The loading concentration of Bi_2S_3 nanoparticles modified by Cyanex 302 in organic fluids

Solvent	gasoline (g/L)	benzene (g/L)
Extraction system	19.27	4.61
Alcohol-water method	9.96	5.26

With the alcohol-water method, the amount of Cyanex 302 added has as important influence on the surface modification. The more extractant added, the larger the loading concentration in the organic solvent, (Table 2).

Table 2. The largest amount of dispersion in gasoline at different ratio of extractants to sulfur sources

The ratio of extractants to sulfur sources	1: 2	1: 1	1:0.9	1: 0.5
The loading amount in gasoline (g/L)	1.26	1.70	2.06	9.96

CONCLUSIONS

Organic fluids containing Bi_2S_3 nano-particles modified by Cyanex 302 were successfully prepared by extraction-synthesis methods and the nano-particles obtained were characterized by TEM, IR, and XRD methods. Loading concentration in gasoline as high as 19.27 g/L was obtained. Modification in the extraction-synthesis method is much better than in the “two-stage method”.

REFERENCE

1 Choi U S. (1995), *ASMEFED,* 231, 99-105.
2 Xie H. Xi T, Wang J. (2003), *Acta Physica Sinica,* 52(6), 1444-1449.
3 Wo Hengzhou, Hu Kunhong, Hu Xianguo (2004), *Tribology,* (in Chinese), 24(1), 33-37.
4 Zhou J., Tao X., Zhang Z., Liu W., Xue Q. (1999), *Chem. Reaearches* (in Chinese). 4,1
5 Chen S„ Liu W., Yu L. (1998), *Wear,* 218,153
6 Zhang Z., Zhang J., Xue Q. (1994), *J. Phys. Chem.,* 98, 12973
7 Chen S., Liu W., (2000), *Chem. J. Chinese University,* (in Chinese), 3,472
8 Brust M, Fink J, Schiffrin D J (1995), *J Chem Soc, Chem.Comm.,* 8,1655-1656.
9 Vorobyova S A, Lesnikovich A I, Sobal N S (1999), *Colloids and Surfaces, A,* 152, 375-379.
10 Antonietti M., Wang E., Bronstein L., Sereegina M. (1995), *Adv. Mater.,* **7** (12), 1000-1005
11 Yu W„ Fu X. (2004), *Tribology,* (in Chinese), 24(5), 425-428.
12 Fu X., Yu W., et al, to be published in *J.of Desp.Sci. Tech.,*2005.
13 Fu X., Xiong Y. et al (2002), *Solv. Extr. Ion Exch.,* 20(3), 331-344.
14 Handley T H. (1963), *Anal. Chem.,* 35, 991-995.

PREPARATION OF CdS HOLLOW SPHERES USING POLY-(STYRENE-ACRYLIC ACID) LATEX PARTICLES AS TEMPLATE

Xun Fu*, Lin Lin, Debao Wang, Zhengshui Hu, Caixia Song

Qingdao University of Science and Technology, Qingdao 266042, P. R. China

CdS hollow spherical particles with different sizes have been prepared using a core/shell fabrication method with poly-(styrene-acrylic acid) (PSA) latex particles as template. The sodium salt of the extractant P204 (di-(2-ethylhexyl) phosphoric acid) was used firstly as the emulsifier in the template synthesis. The diameters of the polymer core decreased from 300nm to 120nm on average with increase of the amount of emulsifier from 1.56% to 3.54%. As a result the diameters of the hollow spheres ranged from 150 nm to 400 nm. The products were characterized by TEM, IR and XRD.

INTRODUCTION

During the past decade, hollow spherical nano-crystals have been extensively studied. These are synthesized using different templates to fabricate the core/shell structures including liquid crystals [1], liquid droplets [2,3], micelles [4], polymer particles [5-10], or even inorganic compound nano-particles [11,12], After removing the core particles from the core/shell structure, hollow spheres are obtained. Polystyrene latex particles have been widely used as a template to prepare hollow spheres of magnetic [6], ceramic [5,7,10,11], metallic [13], and composite materials [10,14],

A template of poly-(styrene-acrylic acid) (PSA) has been successfully used in preparing CdS hollow spherical crystals, and uniform CdS hollow spheres with large diameters of 800 and 850 nm on average and wall thickness about 40-100 nm obtained [15], This paper describes the use of the sodium salt of extractant P204 (trade mark in China, di-(2-ethylhexyl) phosphoric acid is higher than 95%) as the emulsifier to prepare the PSA latex of different sizes, and to synthesize CdS hollow spheres with a controlled diameter in the range of 150-350 nm by templating against the as-prepared PSA latex particles.

EXPERIMENTAL

The extractant P204 was purified using the middle phase microemulsion method [16], and P204-Na salt was prepared by the method reported previously [17], The other chemicals used were all analytical grade.

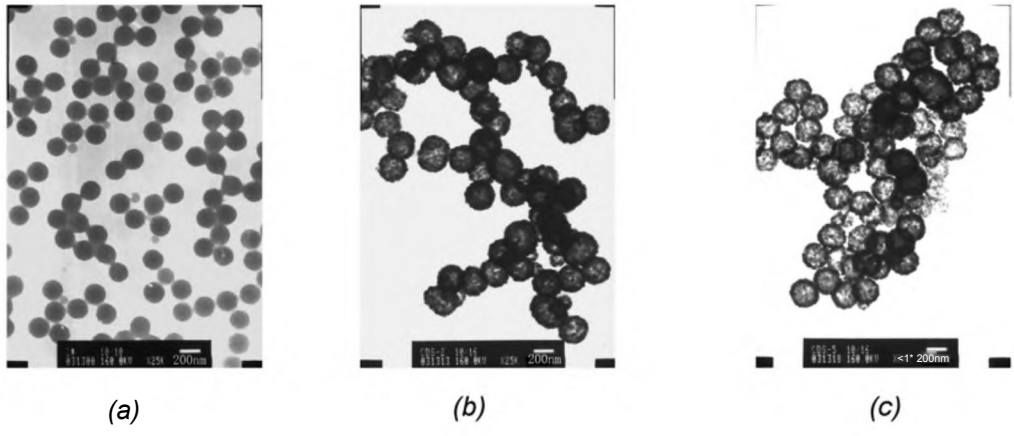
In the preparation of the poly-(styrene-acrylic acid) latex particles used as core materials (templates), reference [18] was consulted and some necessary changes were made, in particular the P204-Na salt was used as an emulsifier. The preparation and characterization of PSA/CdS core/shell composite structure and the CdS hollow spheres were based on the method reported in [15], The products were characterized by transmission electron microscopy (Model JEOL-2000EX electro microscope), XRD (Model RINT200X, X-ray diffraction meter) and FT-IR (51 OP FT-IR spectrometer) respectively.

RESULTS AND DISCUSSION

The emulsion polymerization reaction of monomers including styrene, acrylic acid, butyl acrylate and butyl methacrylate in the presence of 2.6% emulsifier P204-Na salt ($Wp_{20}4$-Na/Wtotai monomers) was initiated with $(NH_4)_2S_20_8$ at 85'C for 8h. The latex was then neutralized with aqueous ammonia to pH=7-8. The PSA particle latex was obtained after filtrating the gel, marked as No.2 in Table 1. It's TEM image is shown in Figurela.

The PSA/CdS core/shell composite structure was prepared by aging the colloid solution containing PSA latex, $CdCI_2$, thiourea, urea and poly-vinilpyrrolidone (PVP) at 85"C for 18h. The TEM image is shown in Figurelb.

The CdS hollow spheres were obtained after dissolving the core particles with toluene and drying in a vacuum. The TEM image is shown in Figurelc.



Figurel. Typical TEM images of PSA latex (a), coated particles (b) and CdS hollow spheres (c) for Sample No. 2 in Table 1.

TEM images indicate that, firstly, the PSA particles with average diameter of about 200nm are well distributed in aqueous solution in the presence of dispersing reagent PVP (Figurela),

and the emulsifier is satisfactory for this polymerization system. Secondly, the template core particles are well coated with smooth CdS shells (Figurelb). Thirdly, the strong contrast between dark edge and pale center is evidence of the hollow nature of the CdS hollow spheres produced (Figurelc). All the hollow spheres had diameters in the range of 250-300nm and wall thickness of 30-50nm.

The X-ray diffraction (XRD) patterns of coated particles and CdS hollow spheres are shown in Figure2. Both the CdS particles coated on PSA and the hollow shells obtained by dissolving PSA in organic solvent exhibit the pattern of hexagonal wurtzite structure CdS bulk crystals (JCPDS cards No.41-1049). No obvious impurity peaks are observed for CdS hollow spheres. The estimated cell parameters (a=0.413nm, c=0.674nm) are comparable with the reported values. The broadening of these diffraction peaks indicates that the nanometer-sized CdS particles could be constructed with much smaller CdS particles.

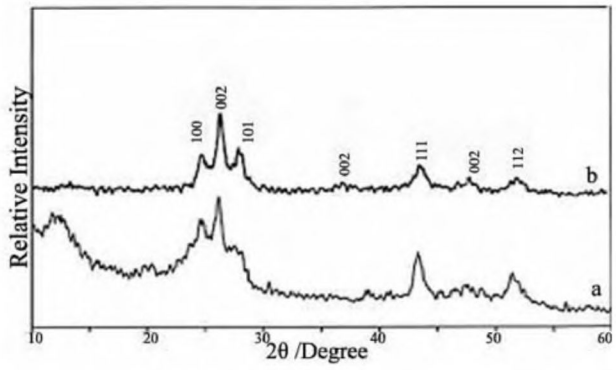


Figure 2. XRD patterns of (a) coated particles, (b) CdS hollow spheres

The FT-IR spectra for the PSA latex, coated particles and CdS hollow shells reveal that PSA latex particles can be successfully removed from the core/shell structures to form CdS hollow spheres.

Table 1. Effect of the amounts of P204-Na on the PSA particles and the CdS hollow spheres

No.	Emulsifier	Emulsifier content (wt%)	Particle diameter (nm)	Hollow sphere Diameter (nm)
1	P204-Na	1.56	300	350-400
2	P204-Na	2.60	200	250-300
3	P204-Na	3.54	120	150-200

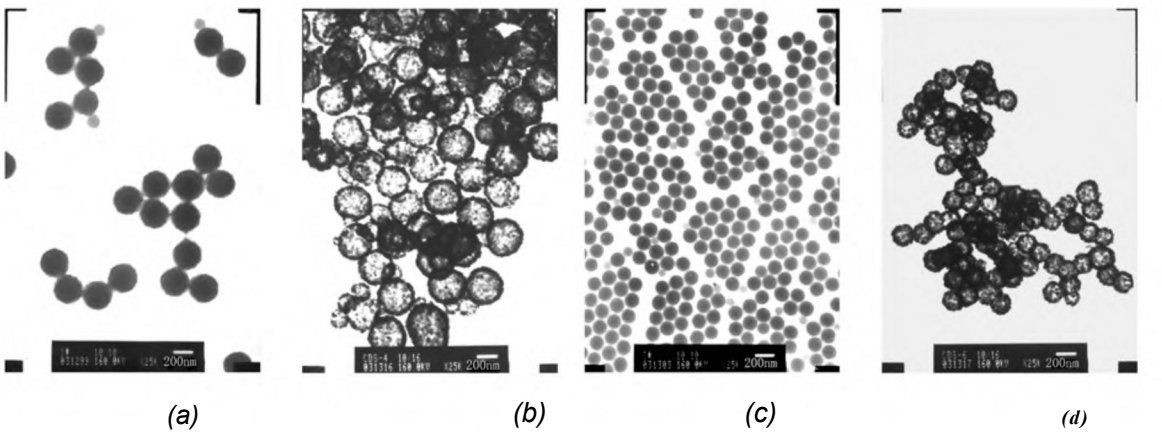


Figure 3. Typical TEM of PSA latex and CdS hollow spheres for sample No. 1 and 3 in Table 1. (a) PSA latex of No. 1 (b) CdS hollow spheres of No. 1 (c) PSA latex of No. 3 (d) CdS hollow spheres of No. 3

Keeping all the experiment conditions as above, except the quantity of the emulsifier P204-Na salt, well-distributed PSA particles with different diameters were obtained. The diameters of the polymer core decreased with increasing quantities of emulsifier. The TEM images of the PSA cores and the corresponding CdS hollow spheres are shown in Figure3 for the sample 1 and 3 respectively. These show that all the PSA particles are well distributed and the CdS shells are smooth and stable. The diameters of PSA particles decrease from 300 nm to 120 nm when the quantities of P204-Na salt increase from 1.56% to 3.54% and the corresponding diameters of the CdS hollow spheres range from 400nm to 150 nm. The size of the CdS hollow spheres can be controlled by the quantity of emulsifier used.

It was demonstrated that negatively charged sulfate stabilized polystyrene latex can be covered with a smooth inorganic layer by the hydrolysis of metal ion [4,5,6], Previous work [15] applied this methodology to sulfide using poly-(styrene-acrylic acid) latex as core particles whith -COO' groups covering on the surface to adsorb the metal ions. In this work the PSA latex particles, containing negatively charged phosphate provided by the extractant, were used as the template to prepare CdS. To the best of the author's knowledge, this is the first use of the extractant sodium salt as an emulsifier in emulsion polymerization.

The organic phosphorous extractants have been used in metal extraction and hydrometallurgy for many years. P204, an organo-phosphoric acid (HA), has a strong affinity to metal ions and a good separation function for a mixed system. The reaction of extractant with metal ion is easier when HA is changed to the form of the NaA salt, because the ion exchange between M^{n+} and $Na^{+}$is much easier than that for M^{n+} with H^{+}. From the point of view of colloidal chemistry, the sodium salts of organo-phosphoric (phosphonic, phosphinic) extractants are much like typical anionic surfactants. Their surface properties, including the FT-IR, NMR spectra [19], conductivity [20], thermodynamic functions [17, 21] and structure parameters [21] of the formed microemulsions, as well as the pseudo triangle phase diagrams of extractant - NaOH aqueous solution - hexane systems [22], have been studied extensively. It is speculated that P204-Na salt can be used successfully as an emulsifier for polymerization reactions.

The P204-Na stabilized PSA latex should have a stronger ability to attract metal ions. More important, they can selectively extract metal ions from aqueous solution. This might allow a hollow sphere to be made from a crude solution containing several metal ions, or a hollow sphere that is composed of composite materials. The selectivity of the extractant to metal ions will be the subject of further studies.

CONCLUSIONS

CdS hollow spherical particles of different sizes in the range of 150-400nm were prepared using core/shell fabrication method with poly-(styrene-acrylic acid) (PSA) latex particles as template. The sodium salt of extractant P204 (di-(2-ethylhexyl) phosphoric acid) was found to be a good emulsifier in producing well-distributed PSA particles. The diameters of the polymer core decreased with increasing quantitiy of the emulsifier, allowing the diameters ofCdS hollow spherical particles to be controlled by the emulsifier concentration. A furtherstudyon the selectivity of extractant in this system is required.

REFERENCES

1. P. V. Braun, S.I. Stupp, (1999), *Mater. Res. Bull.* 34:136.
2. J. Huang, Y. Xie, B. Li, Y. Liu, Y. Qian, (2000), S. Zhang, *Adv Mater.* 12:808.
3. X. Jiang, Y. Xie, J. Lu, L. Zhu, W. He, X. Liu, Can. (2002), *J. Chem.* 80:263.
4. H. Huang, E. E. Remsen, T. Kowalewski, K. L. Wooley, (1999), *J. Am. Chem. Soc.* 121:3805.
5. N. Kawahashi, E. Matijevic, (1991), *J. Colloid Interface Sci.* 143: 103.
6. H. Shiho, N. Kawahashi, (2000), *J. Colloid Interface Sci.* 226; 91.
7. S. Eiden, G. Maret, (2002), *J. Colloid Interface Sci.* 250: 281.
8. M. C. Neves, T. Trindade, A. M. B. Timmons, J. D. Pedrosa de Jesus, (2001), *Mater Res. Bull.* 36:1099.
9. H. Tamai, T. Ikeya, F. Nishiyama, K. Iida, S. Nojima, (2000), J. *Mater. Sci.* 35: 4945.
10. F. Caruso, R. A. Caruso, H. Möhwald, (1998), *Science* 282: 1111.
11. D. Wang, F. Caruso, (2002) , *Mater. Chem.* 14: 1909, and references therein.
12. D. J. Norris, Y. A. Vlasov, (2001), *Adv. Mater.* 13:371.
13. N. Kawahashi, H. Shiho, (2000), *J. Mater. Chem.* 10: 2294.
14. H. Bamnolker, B. Nitzan, S. Gura, S. Margel, (1997) , *J. Mater. Sci. Lett.* 16:1412.
15. C. Song, G. Gu, Y. Lin, H. Wang, Y. Guo, X. Fu, Z. Hu, (2003), *Mater. Res. Bull.* 38:917.
16. Z. Hu, Y. Pan, W. Ma, X. Fu, (1995), *Solvent Extr. Ion Exch.* 13: 965.
17. X. Fu, H. Xin, Z. Hu, Z. Liu, (1993) . *Acta Chimica Scmia* (in Chinese), 51:1151.
18. Y. Guo, G. Gu, X. Fu, Y. Jiao, Z. Hu, (2003), *Polymer Mater. Sci. & Eng.* (in Chinese), 19: 40.
19. X. Fu, Y. Pan, H. Xing, Z. Hu, H. Yu, (1995), Acta. *Chim. Sinica* (in Chinese), 53:178.
20. X. Fu, Y. Pan, Z. Hu, Z. Ma, (1996), *Colloids Surf. A* 110: 55.
21. X. Fu, Y. Xiong, Q. Wei, S. Xue, S. Zhang, Z. Hu, (2002), *Colloids Surf. A* 211: 249.
22. X. Fu, Y. Xiong, S. Xue, S. Zhang, Z. Hu, (2002), *Solvent Extr. Ion. Exch.* 20: 331.



PREPARATION OF CdS NANOWIRES AND Bi_2S_3 NANORODS BY AN EXTRACTION-SOLVOTHERMAL METHOD

Shi Huaqiang, Fu XurT, Wang Debao, Zhou Xiaodong, Hu Zhengshui

Qingdao University of Science and Technology, Qingdao 266042, P.R.China

CdS nanowires and Bi_2S_3 nanorods have been successfully synthesized through the decomposing of the complex Cd(II)-Cyanex 301 and Bi(III)-Cyanex 301 in gasoline by the extraction solvothermal method. The samples are characterized using XRD, UV, TEM and SEM methods respectively. The effect of the reaction temperature on the product's morphology is discussed.

INTRODUCTION

The preparation and characterization of semiconductor nanowires have received considerable attention in recent years because of their electronic, optical, chemical properties [1] and their potential application in constructing nanoscale electronic and optoelectronic devices [2], Many methods have been developed to prepare semiconductor nanowires, such as the template [3,4], microemusion [5], laserablation [6], single precursor thermolysis [7], solvothermal synthesis [8], and vapour-phase transport method [9], etc.

CdS is an important semiconductor with a wide band-gap of 2.4 eV at room temperature. Several methods have been used for the chemical synthesis of one-dimensional CdS nano-crystals. Routkevitch [10] fabricated CdS nanowire arrays by electrochemical deposition into porous anodic aluminum oxide (AAO) template (a hard template). Li et al. [11] synthesized CdS nanowires in hexagonal liquid crystals formed by surfactant C16.18EO7 (a soft template). Chen [5] reported the synthesis of CdS nanorods in microemulsion of CTAB. Li [8] reported the synthesis of CdS nanowires with a solvothermal method. Yan [12] successfully synthesized CdS nanowires using an organic precursor $Cd_2(S_2NEt_2)_4$ in ethylenediamine. We [13] successfully synthesized CdS nanowires with typical length more than 8 M m and width of 30 nm on average in microemulsion system of SDBS through Cd^{2+} reaction with CS_2 and ethylendediamine.

Bi_2S_3 is also an important semiconductor with a band-gap of 1.3 eV. Many methods relating to the preparation of Bi_2S_3 were found [14-17], but most reports were concerned with preparation of Bi_2S_3 nanofilms and nanoparticles, although nanorods crystals have been reported.

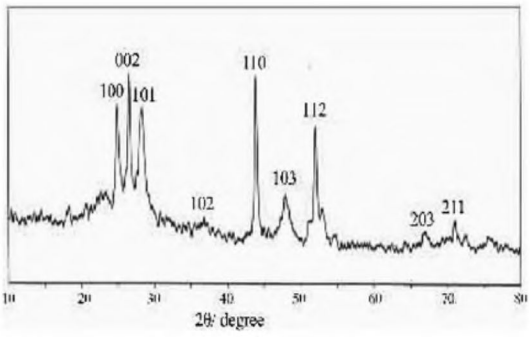
The work reported in this paper gives a new route to synthesize the CdS nanowires and Bi_2S_3 nanorods by the extraction solvothermal method. Cd^{2+} or Bi^{3+} is first extracted into organic solvent gasoline, and the organic phase containing the complex Cd(II)-Cyanex 301 or Bi(III)-Cyanex 301 then heated in an autoclave.

EXPERMENTAL

Cyanex 301 was kindly supplied by Cytec Co. of Canada, and used without further purification. Other reagents used in this work were of analytical purity. In a typical process, 50 ml 0.12mol/L $Cd(N0_3)_2$ aqueous solution and 50 ml 0.10 mol/L Cyanex 301 gasoline solution were added into a flask, shaken for several minutes and equilibrated. After phase separation, 38.00 ml organic phase containing the Cyanex 301-Cd^{2+} complex was transferred into a 50ml Teflon-lined stainless autoclave, then the autoclave was sealed and maintained at 130 ~ 170'C for 24 hrs. When the reaction was complete, the autoclave was cooled to room temperature. The CdS products were filtered off and washed with absolute ethanol and distilled water several times, dried in a vacuum at 70 "C for 8 hrs, and collected for further characterization. The Bi_2S_3 crystals were produced in ethanol and a mixture of ethanol-water when the Cyanex 301-Bi^{3+} complex was reacted in these solvents after evaporating the gasoline. The CdS and Bi_2S_3 products were characterized by X-ray powder diffraction, using a Rigaku (Japan) D/max r-B X-ray diffractometer with Cu Ka radiation (X =0.1514178nm). The transmission electron microscopy (TEM) images and electron diffraction (ED) patterns of the samples were recorded using a JEOL 2000EX microscopy with an accelerating voltage of 100 Kv. The scanning electron microscopy images were taken on a JSM-6700F field emission scanning electron microscopy. The CdS and Bi_2S_3 crystals were also measured by UV (756CRT UV-vis Spectrophotometer, Shanghai precision and scientific instrument Co. LTD, China).

RESULTS AND DISCUSSION

The XRD pattern of the as-prepared CdS sample is shown in Figure 1. The main diffraction peaks can be indexed to the pattern of hexagonal CdS crystal (JCPDS Cards, No. 41-1049) corresponding to its plane of (100), (002), (101), (102), (110), (103), (112), (203) and (211). The XRD patterns of Bi_2S_3crystal in Figure 2 obtained in gasoline (a) and in ethanol-water (b) indicated that the samples were both orthorthomic crystalline (JCPDS Cards, No. 17-320).



Figurel. XRD pattern of CdS nanowires

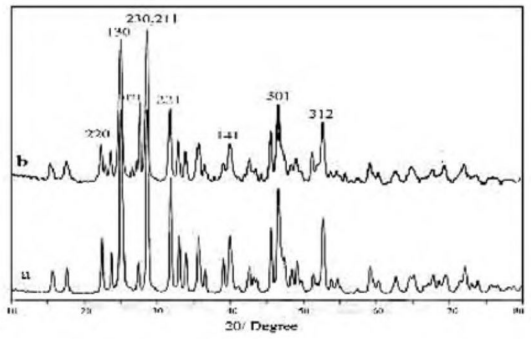


Figure 2 XRD pattern of Bi_2S_3 nanorods (a: in gasoline, b: in ethanol-water)

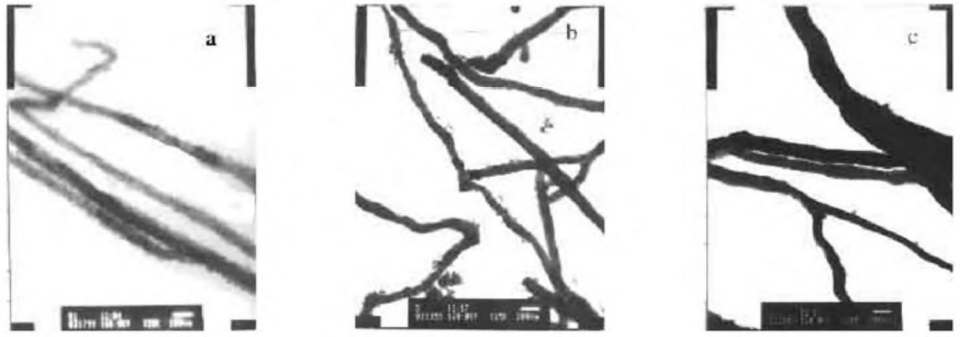
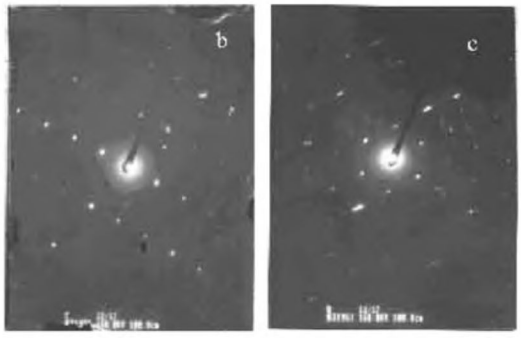


Figure 3 TEM images of CdS nanowires at (a)130 C, (b)150 V and (c)170 "C

Figure 3 shows typical TEM images of CdS nanowirs obtained at 130"C(a), 150“C(b) and 170"C(c), respectively. It can be seen than the width of the nanowires increase with the increase in reaction temperature The width of the nanowirs were about 70-100 (a) nm, 150-200 (b) nm and 200 nm or more (c), respectively. Figure 4 are the related electron differaction (ED) patterns of the CdS nanowires (b) and (c), and indicate that the nanowires are composed of hexagonal CdS crystals. Figure 5 shows the SEM image of CdS nanowirs (b), and these are composed mainly of CdS nanowires.



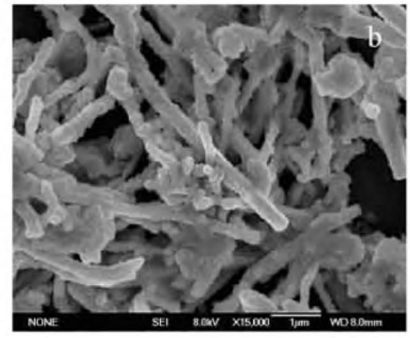


Figure 4 ED patterns of CdS nanowires (b) and (c) Figure 5 SEM images of CdS nanowires (b)

The morphology of the Bi_2S_3 samples obtained from different solvents were also examined

by TEM. Figure 6 shows the typical TEM images of the Bi_2S_3 nanorods, obtained at 150'C in gasoline (a), in ethanol-water (b) and in ethanol (c), respectively.

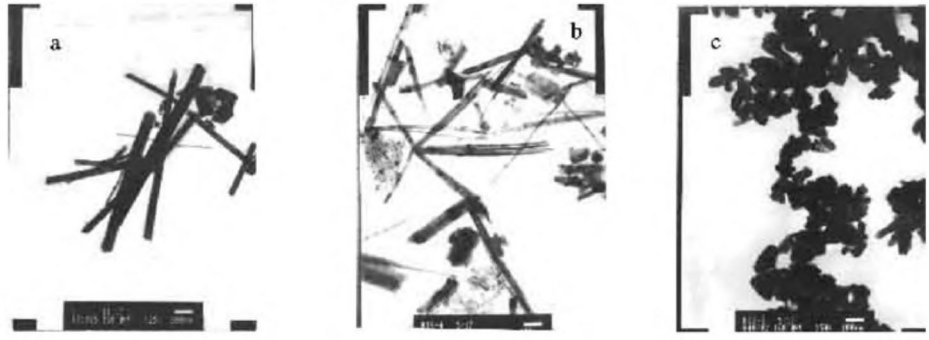


Figure 6 TEM of Bi_2S_3 nanorods prepared in gasoline (a), ethanol-water (b) and ethanol (c) at150 V

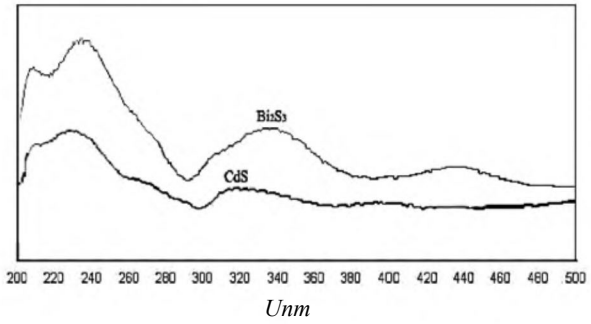


Figure 7 UV patterns of CdS nanowires and Bi2S3 nanorods in ethanol

To examine the quantum-confined effect of the samples, UV-vis absorption spectra of the CdS nanowires and Bi_2S_3 nanorods dispersed in ethanol were recorded (Figure7). The maximum at about 320 nm (CdS) and 340 nm (Bi_2S_3) are assigned to the optical transition of the first excitation state. The obvious blue shift of the absorption peaks may be attributed to the small dimension of the CdS relative to that of bulk CdS, 515 nm [18], The absorption peaks of obtained Bi_2S_3 shift obviously to 340 nm, which bulk Bi_2S_3 absorption peaks in 956 nm [19],

It is well known that both cadmium and bismuth have an affinity for sulfur, and Cyanex 301 (di- (2, 4, 4- trimethylpentyl) dithiophosphinic acid) could extract Cd^{2+} and Bi^{3+}efficiently to form the complex:



The structure, much like an anionic surfactant, will cause the extracted species assembled to some degree in the solvent. When the temperature and pressure are increased, the extracted species will decompose and the tiny crystal of CdS and Bi_2S_3 will form gradually. In this process, Cyanex 301 acts both as the extractant of metal ions and the sulfur source of the sulfides. One dimension growth of CdS and Bi_2S_3 might be related to the effects of the

solvent and the aggregation structure of the extracted species. A detailed study of the mechanism of this method is underway.

CONCLUSION

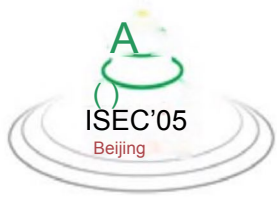
CdS nanowires and Bi_2S_3 nanorods prepared through the decomposing of the complex Cd(II)-Cyanex 301 and Bi(III)-Cyanex 301 by the extraction solvothermal method. In whole procedure, Cyanex301 could be used as both the extractant and the sulfur source. This method can be expanded to the preparation of other sulfide nanocrystals.

ACKNOWLEDGEMENTS

The authors thank Cytec Canada Inc. for its kindly supplying the extractant of Cyanex 301.

REFERENCES

1. D.Yu, Z. Bai, (1998), *Appl. Phys. Lett.,* 72:3458
2. G. A.Ozin, (1992), *Adv. Mater.,* 4:612
3. Y. C. Choi, W. S. Kim, Y. S. Park, S. M. Les, D. J. Bae, Y. H. Lee, G. S.Park, W. B. Choi, N. S. Lee, (2000), *Adv. Mater.,* 12:746
4. D. Xu, Y. Xu, D. Chen, (2000), *Adv. Mater.,* 12:520.
5. C. C. Chen, C. Y. Chao, Z. H. Lang, (2000) , *Chem. Mater.,* 129:1516
6. C. H. Liang, G. M. Weng, Y. Lei, F. Phillipp, L. D. Zhang, (2001) , *Adv. Mater.,* 13:1330
7. P. S. Nair, J. N. Radhakrishman, (2002) , *Chem. Commun.,* 564
8. Y. Li, H. Liao, Y. Ding, Y. Qian, L. Yang, G. Zhou, (1998), *Chem. Mater.,* 10:2301-2303
9. Y. Wu, P. Yang, (2000), *Chem. Mater.,* 12:605
10. D. Routkevitch, T. Bigioni, M. Moskovits, J. M. Xu, (1996), *J. Phys. Chem.* 100:14037
11. Y. Li, J. Wan, Z. Gu, G. Guo, L. Gui, Y. Tang, (2000), *Mater. Sci. Eng. A,* 286:106
12. P. Yan, Y. Xie. Y. Qian, X. Liu, (1999), *Chem. Commun.,* 1293-1294
13. X. Fu, D. Wang, J. Wang, H. Shi, C. Song, (2004), *Mater. Res. Bull.,* 39:1869-1874
14. C. Moterio, T. Trindate, (1989), *J. Crystal Growth,* 94: 9677
15. X. H. Liao, H. Wang, J. J. Zhu, H. Y. Chen, (2001), *Mater. Res. Bull.,* 36:2339
16. S. H. Yu, L. Shu, J. Yang, Z. H. Han, Y. T. Qian, (1999), *J. Mater. Res.,* 14: 4157
17. D. B. Wang, M. W. Shao, D. B. Yu, Y. T. Qian, (2002), *J. Crystal Growth,* 243:331
18. Y. M. Gao, P. Wu, J. Baolio, K. M. Dwight, A. Word, (1989), *Mater. Res. Bull.,* 24:1215
19. B. B. Nayak, H. N. Acharya, G. B. Mitra, B. K. Mathur,(1983), *Thin Solid Films,* 105:17



PREPARATION OF ORGANIC FLUIDS CONTAINING Ag_2S NANO-PARTICLES WITH THE EXTRACTANT CYANEX 301

Shi Huaqiang, Fu Xun*, Zhou Xiaodong, Hu Zhengshui

(Qingdao University of Science and Technology, Qingdao 266042, P.R.China)

Stable organic fluid containing Ag_2S nano-particles modified by Cyanex 301 (di- (2, 4, 4-trimethylpentyl) dithiophosphinic acid) has been prepared directly in alkane by solvent extraction-synthesis method. Ag^+ is extracted into alkane by Cyanex 301, then the Ag^+-Cyanex 301 complex obtained is reacted with H_2S to obtain the organic fluids containing Ag_2S nano-particles. The organic fluids are so stable that the nano-particles do not precipitate at room temperature for more than three months when the content of Ag_2S nano-particles is 42 g/ L. The particles are characterized by XRD, TEM, IR, UV-vis and TG-DSC respectively, showing that Ag_2S nano-particles are well modified by the extractant Cyanex 301.

The Ag_2S nano-particles obtained can be dispersed well in organic solvent again and the obtained new fluids are also very stable. Comparing with the two-step synthesis in solvent mixture of ethanol-water, the loading concentrations of Ag_2S nano-particles prepared by solvent extraction-synthesis are much higher than that prepared by ethanol-water method in the same solvent, and both of them decrease with the increase of the solvent polarity.

INTRODUCTION

Nano-sized particles have received considerable attention in recent years because of their different physical and chemical properties from bulk materials [1], and the synthesis of organic-inorganic composite materials has received much attention [2], For example, nano-particles of MoS_2 [3], PbS [4], Ag_2S [5] and ZnS [6] modified by DDP were synthesized successfully in a polar-solvent, such as alcohol-water, and could be dispersed into an organic solvent such as paraffin, benzene, toluene and chloroform because of the DDP coated on their surface. However, the preparation of particles dispersed directly in non-polar solvents is known to be a complex problem. Brust [7] et al. prepared and characterized gold particles of 1-3 nm using two-phase (water-toluene) reduction of $AuCl_4'$ by sodium borohydride in the presence of alkanethiol. The Au nano-particles, modified by alkanethiol, obtained did not show signs of precipitation or aggregation over several weeks. So et al. [8] prepared the alkanethiol derived silver particles in the same way.

The method of solvent extraction-reduction has been proposed for the preparation of the metal nano-particles. Song et al [9] prepared stable metallic Cu particles modified with extractant HDEHP (Bis(ethylhexyl) phosphoric acid) in organic phase by solvent extraction-reduction method. They considered that extractant was absorbed onto the surface of the particles because of their high activity, promoting the particle's stabilization. However, most procedures described so far to yield stable metal dispersions in non-polar solvents have not concerned the "loading concentration" of the nano-particles in the organic fluids, or loading concentration was only at relatively low values and not suitable for large-scale manufacture.

Cyanex 301 is one of the extractants that has been extensively investigated in solvent extraction. It is able to extract a large number of metals over a wide acidity range and its anion has a high surface activity. The authors prepared Ag particles modified with extractant Cyanex 302 [10] (di- (2, 4, 4- trimethylpentyl) monothiophosphinic acid) and Cyanex 301 [11] (di- (2, 4, 4- trimethylpentyl) dithiophosphinic acid) in alkane by solvent extraction-reduction method. The corresponding loading concentrations of silver particles were 0.5 and 10 g/L respectively.

In this paper, the preparation of stable fluids containing Ag_2S nano-particles in alkane using the extraction-synthesis method is described. Silver nitrate is extracted in non-polar solvent by Cyanex 301, and the Ag (I) complex is then reacted with gaseous H_2S. The results show that, with Cyanex 301 as both a phase transfer agent and a modify agent, the loading concentration of Ag_2S nano-particles in alkane can be enhanced up to about 42 g/ L.

EXPERIMENTAL

Reagents

Cyanex 301 was kindly supplied by Cytec Co. of Canada, and used without further purification. Hydrogenated gasoline was supplied by QiLu Petrolium Co. in China. Other reagents used in this work, such as heptane, benzene were all of analytical purity. H_2S was obtained by the reaction of solid FeS with HCI solution. Water was double distilled.

Preparation of organic nano-fluids containing Ag_2S nano-particles

Extraction-synthesis method (a): $AgN0_3$ aqueous solution (with measured concentration) was extracted firstly into organic phase by extractant Cyanex 301 at Vo/Va = 1. The distribution ratio was obtained from previous work [11], After phase separation, the complex Cyanex 301-Ag^+ in the organic phase was reacted directly with gaseous H_2S with vigorous stirring for 24 hrs. Upon the addition of H_2S, the color of the organic phase turned gradually from yellow to brown, dark or deep dark corresponding to the loading concentration of Ag_2S in it. The stabilities of the organic fluids containing Ag_2S nano-particles were evaluated by a vigorous centrifugation at 3000 r/min for 30 min. The organic nano-fluids were considered to be stable if no precipitate appeared at the bottom. The solid Ag_2S nano-particle samples were washed with acetone and ethanol alternatively after the solvent in the prepared organic fluid was

evaporated. The product was then dried in a vacuum at about 70°C for 8 hrs.

Ethanol-water method (b): The preparation of Ag_2S modified with Cyanex 301 according to [5] was as follows: 60 ml solvent mixture of ethanol-water ($V_{ethanol}$: V water =1:1) was put into a reaction flask, the mixture heated to 55°C with stirring, then the extractant Cyanex 301, Na_2S solution and $AgN0_3$ were added into the flask in turn. After 2 hrs continuous reaction, the dark precipitate obtained was collected by filtering and washed with acetone and ethanol respectively, then dried in a vacuum at about 70“C for 8 hrs.

Characterization of Ag_2S particles

The morphologies and the sizes of the dispersed particles were observed with TEM (JEM-2000EX Electro-Microscope, Jeol Co., Japan). The interaction between Ag_2S and extractant Cyanex 301 was confirmed by XRD (D/max-r B X-ray diffraction meter, Rigaku, Japan), IR (510P Fourier transform infrared spectrophotometer, Nicolet, USA) and UV (756CRT UV-vis Spectrophotometer, Shanghai precision and scientific instrument Co. LTD, China). The product of Cyanex 301 modified Ag_2S nano-particles were also determined by the measurement of TG-DSC (STA-449 thermal analyzer, Netzsch, Germany).

RESULTS AND DISCUSSION

Extraction of Ag^+ from $HN0_3$ Medium by Cyanex 301

Previous experiments [11] for extraction of $Ag^+$by Cyanex 301 from $HN0_3$ solution showed that the extent of extraction reached above 99% when the original acid concentration in the aqueous phase was lower than 5.0 mol/ L. Thus, it is confirmed that all the Ag^+ in the aqueous solution is efficiently transferred into the organic phase in the subsequent experiments where the initial aqueous solution is prepared just by dissolving $AgN0_3$ in water.

Characterization of Prepared Ag_2S Particles

Figure-1 shows the TEM image of Ag_2S in nano-fluid. The diameter of Ag_2S nano-particles



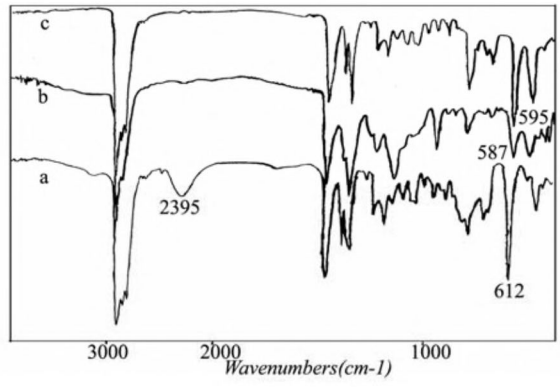


*Figure-1. TEM of Ag_2S nano-particle Figure-2 FT-IR spectra of Cyanex 301 (a), Cyanex 301-Ag*complex (b),Ag_2S particles modified by Cyanex 301 (c)*

was about 10 nm. The particles are well dispersed in non-polar solvents; there is no obvious aggregation.

Figure-2 shows IR spectra of extractant Cyanex 301 (line a), Cyanex 301-Ag^+ complex (line b) and the prepared solid Ag_2S nano-particle sample (line c) respectively. The typical peaks in (a) exist also in (c), indicating that Cyanex 301 absorbed onto the surface of Ag_2S nano-particles could not be washed off totally. The adsorption P=S peak of Cyanex 301 at 612 cm'1 in (a) shifted to 587 cm'1 in (b), then to 595 cm'1 in (c) after Ag^+ was reacted with H_2S, showing that there was a strong coordination effect between the P=S bond of Cyanex 301 and Ag_2S particles. The S-H stretching peak of Cyanex 301 at 2395 cm'1 in (a) disappeared in (b) because of the Cyanex 301-Ag^+ complex formation and it become lower due to the modifying effect in (c). The stabilizing function is expected to be similar to that of thiol ligands [7],

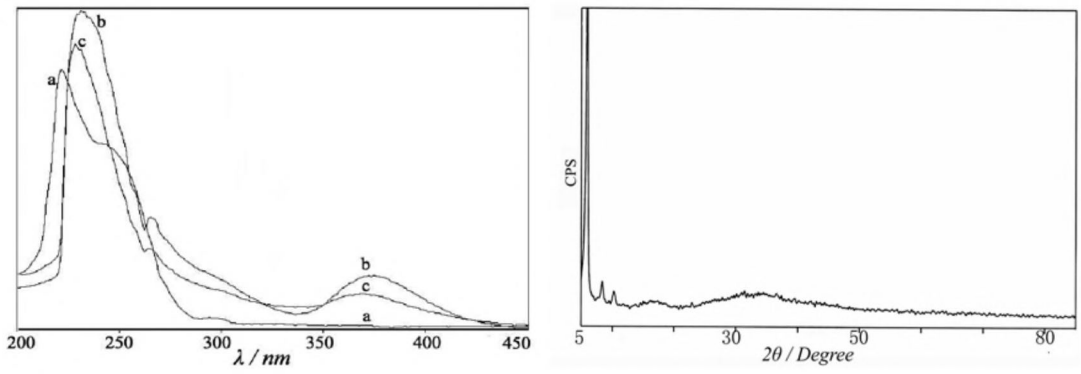


Figure-3 UV-vis absorption spectra of Figure-4 XRD pattern ofAg_2S particles
(a) Cyanex301, (b) Cyanex 301- Ag,*
(c) Ag_2S particles in heptane

Figure-3 shows the UV-vis absorption spectra of the Cyanex 301, Cyanex 301-Ag^+ complex and Ag_2S nano-particles in n-heptane, respectively. The absorption band at about 220nm in (a) should be attributed to the bond of P=S in extractant. After Cyanex 301-Ag^+ complex formed, the peak shifted to 240nm in (b) because that the electrovalent bond of Ag^+-S' in the complex

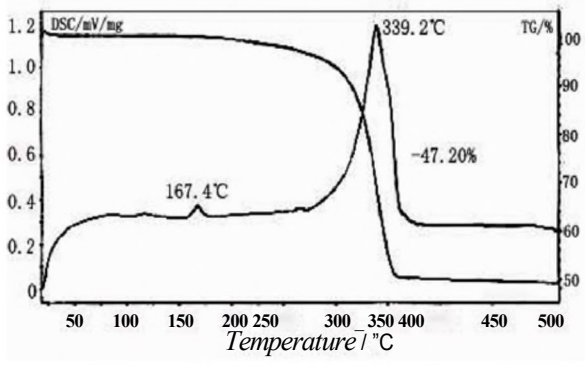


Figure-5TG and DSC curve of Ag-Cyanex 301 nano-particles

enhanced the flow ability of JI -electrons, resulting in a decrease of molecular orbital energy,

so showing an obvious “red shift”. After the complex Cyanex 301-Ag^+ was reacted with H_2S, the peaks moved to 235nm in (c) (between 220 nm and 240 nm) indicating that the bond force existed between Cyanex 301 and Ag_2S particles still, but the bond energy is little lower than that in Cyanex 301-Ag^+. It is identical with the conclusion obtained from IR analysis. However, the peak at about 370nm in (b) exists also in (c), indicating that the complex Cyanex 301-Ag^+ did not react completely. It is consistent with the previous conclusion.

Figure-4 shows the XRD pattern of the prepared solid Ag_2S nano-particle sample. It can be seen that the Ag_2S particles obtained had an amorphous structure, but the sharp peak at about 2 0=7 was considered to be due to the strong coordination effect between extractant Cyanex 301 and Ag_2S nano- particles.

Figure-5 shows the TG and DSC curves of solid sample of Ag_2S nano-particles prepared and there is a main peak at about 339.2°C. The weight loss was about 47.2%, corresponding to the decomposition of Cyanex 301 coated onto the Ag_2S nano-particles. It is confirmed that Cyanex 301 cannot be washed off completely by acetone and ethanol. Extractant Cyanex 301 is absorbed strictly onto the surface of Ag_2S by a chemical force. This is consistent with the IR, UV analysis.

Loading Concentrations of Ag_2S in Organic Solvents

The organic fluids containing Ag_2S nano-particles were prepared directly by the solvent extraction-synthesis at room temperature. There was no obvious precipitate after centrifugation at 3000 r/min for 30 min or keeping in the laboratory for more than 3 months at room temperature. The loading concentrations of Ag_2S particles in prepared organic fluids were measured as follows: A measured volume of the organic fluid (for example, 2.00 ml) was taken to evaporate it’s solvent gasoline, and then a larger volume of acetone (for example, 18.00 ml) was added. It was found that most of Ag_2S was precipitated on the bottom. The Ag_2S was carefully collected, dissolved with concentrated $HN0_3$, and analyzed using KSCN titration. A large value of 0.17 mol/ L was obtained. That is to say, the amount of Ag_2S loaded in the most concentrated organic fluids prepared was 42 g/L. This experimental step is important so that, firstly, the free extractant unbonded with Ag_2S and the Cyanex 301-Ag (I) complex unreacted with H_2S could be recovered, and these could be used again in the subsequent preparing procedure. Secondly, the loading amount Ag_2S nano-particles modified by Cyanex 301 in acetone was the lowest compared with that in the other organic solvent, so the loss of product was low.

If the collected Ag_2S was washed with acetone and alcohol several times, dried in a vacuum at about 70°C (such as the sample prepared for its characterization), and then redispersed into gasoline with the help of supersonic, the loading concentration of Ag_2S in the new fluids was again measured using KSCN titration. The loading concentration obtained decreased to 0.102 mol/L (25.3 g/L). When the Ag_2S nano-particles were redispersed into different organic solvents, the loading concentration decreased gradually with the increase of the solvent polarity, the lowest was found to be in acetone (Table 1).

When the Ag_2S nano-particles prepared by the ethanol-water method were dispersed into organic solvents to make organic fluids, the loading concentrations in them were much lower than that obtained from the extraction-synthesis method in the same solvent; and decreased gradually in the same order with respect to solvent.

Tablel the highest loading concentrations ofAg particles in different solvents

Solvent	gasoline	benzene	toluene	xylene	chloroform	acetone
Dipole moment (D)	0	0	0.375	0.620	1.780	2.880
$[Ag_2S]^{[a1]}$/ mol/L	0.102	0.090	0.088	0.080	0.039	0.006
$[Ag_2S]^{[bl]}$/ mol/L	0.030	0.028	0.023	0.015	0.013	0.005

[a] Extraction-synthesis method, [b] Ethanol-water method

From the data listed in Tablel, it was inferred that:

1. The organic fluids containing Ag_2S nano-particles prepared directly in gasoline by solvent extraction-synthesis method has a very large loading content of 42g/ L. This may be caused by a strong dispersion force between the modified Ag_2S particles and the free extractant Cyanex 301 released by after the formation of Ag_2S. When the free extractant of Cyanex 301 in the fluids was recovered by acetone (and ethanol), the particles are redispersed only in gasoline, the dispersion force become be much weaker.

2. The loading concentration of Ag_2S prepared by extraction method is much higher than that prepared by alcohol-water method in each organic solvent. This is because that the modification function in the first method is much better.

3. The loading concentration of Ag_2S decreased with the increase of the solvent polarity. This might be implied that the R group in Cyanex 301 has a higher affinity with non-polar solvent.

CONCLUSION

The organic fluids containing high concentration Ag_2S nano-particles coated with Cyanex 301 were directly prepared in non-polar solvent. Cyanex 301 acted as both phase transferring reagent and a particle modifying reagent during the whole procedure. A concentration of Ag_2S nano-particles in gasoline of 42 g/L was obtained. The modifying layer keeps particles from aggregating and away from air. This method provided a good industrial method for directly preparing high concentration nano-particles in non-polar solvents.

ACKNOWLEDGE

The authors thank Cytec Canada Inc. for its kindly supplying the extractant of Cyanex 301.

REFERENCE

1. A. Henglein, (1989), *Chem. Rev.,* 89:1961
2. K. T. Shea, D. A. Loy, (1992), *J. Am. Chem. Soc.,* 114:6700
3. Z. Zhang, Q. Xue, J. Zhang, (1997), *Wear*, 209: 8
4. S. Chen, W. Liu, L. Yu, (1998), *Wear,* 218: 153
5. J. Zhou, X, Tao, Z. Zhang, W. Liu, Q. Xue, (1999), *Chemical Researches,* 4:1
6. S. Chen, W. Liu, (2000), *Chemical J. Chinese University,* 21: 472
7. M. Brust,, M. Walker, D. Betheli, J (1994), *Chem. Soc., Chem, Common,* 801
8. Y. S.So,; K. Kwan , (1998), *Langmuir.* 14:226
9. X. Song, S. Sun, W. Zhang, (2004), *Journal of Colloid and Interface Science,* 273: 463
10. W. Yu, X. Fu, (2004), *Tribology* (in Chinese), 5:425-428.
11. H. Shi, X. Fu, X. Zhou, Z. Hu, (2005), *J. Disp. of Sci. and Tech.,* To be published.

AFFINITY SEPARATION OF PROTEIN BY UNIFORM MAGNETIC POLYMER MICROSPHERES CARRYING DYE-LIGAND

Chengli Yang*', Yueping Guan*, Jianmin Xing*, Junguo Liu*, Huizhou Liu***

'Laboratory of Separation Science and Engineering, State Key Laboratory of Biochemical Engineering, Institute of Process Engineering, Chinese Academy of Sciences, P.O. Box 353, Beijing 100080, China
''Graduate School of the Chinese Academy of Sciences, Beijing, China

A novel affinity carrier to obtain high protein adsorption capacity using Cibacron Blue F3GA as a dye-ligand was proposed. Magnetic poly(styrene-divinylbenzene-glycidylmethacrylate) microspheres with uniform size of 11 pm in diameter were synthesized by spraying suspension polymerization. Epoxy groups on the surface of magnetic microspheres were converted to amino groups by reacting with ethylene diamine for their attachment to affinity ligands. Then, dye-ligand, Cibacron Blue F3GA was covalently attached onto the aminated magnetic microspheres for affinity adsorption of bovine serum albumin. The results showed that the maximum bovine serum albumin adsorption capacity was about 81 mg/g at pH 5.0.

INTRODUCTION

The introduction of magnetic carriers in the 1970s can certainly be regarded as one of the highlights in the area of biosciences. Since then, they have occupied a wide variety of applications, especially for cell isolation, enzyme immobilization, protein separation and purification, immunoassay, and guided site-specific drugs delivery [1-5], A wide variety of functional molecules such as enzymes, coenzymes, antibodies, amino acids, proteins and nucleic acid may be used as ligands in the design of novel affinity carriers [6-10], But they are expensive due to high cost of production. Dye ligands have been considered as one of the important ligands for specific affinity separation because of its high selectivity and efficiency. Meanwhile, dye ligands are commercially available, inexpensive, and can easily be immobilized, especially on carriers bearing aminate groups.

In the present work, Uniform magnetic polymer microspheres with epoxy groups were synthesized by spraying suspension polymerization. Epoxy groups on the surface of magnetic microspheres were converted to aminate groups by reacting with ethylene diamine for their attachment to affinity ligands. Dye ligand, Cibacron Blue F3GA was covalently attached onto the aminated magnetic microspheres for affinity separation of bovine serum albumin (BSA). The influence of pH, ionic strength as well as the initial protein concentration on BSA adsorption has been investigated. Meanwhile, the BSA adsorption capacity as a function of time was also investigated.

EXPERIMENTAL

Materials

Styren (St), glycidyl methacrylate (GMA) and divinylbenzene (DVB) were reagent grade, distilled under reduced pressure to remove inhibitors, and stored in a refrigerator prior to use. Ethanol and ethylene diamine were analytical grade and were used without any further purification. Polyvinyl alcohol (PVA-217, degree of polymerization 1700, degree of hydrolysis 88%) was used as a stabilizer. Benzoyl peroxide (BPO), reagent grade, was used as an initiator for polymerization. Fe_30_4 magnetic nanoparticles were prepared by the method of coprecipitation [11], Water was purified by distillation followed by deionization using ion exchange resins. Bovine serum albumin (BSA) and Cibacron Blue F3GA were obtained from Sigma. Other chemicals were reagent grade and used as received.

Preparation of magnetic poly(St-DVB-GMA) microspheres

The magnetic poly(St-DVB-GMA) microspheres were prepared by spraying suspension polymerization. The schematic diagram of spraying suspension polymerization process was shown in a previous paper [11], The aqueous phase where 15 g PVA dissolved in 800 ml deionized water was stored in polymerization reactor. 15 g Fe_30_4 magnetic nanoparticles were dissolved in a mixture of 45 ml St, 25 ml GMA, 5 ml DVB and 3 g BPO, and were used as an oil phase. After the pressure of the oil phase storage tank was controlled at 0.2 MPa, The oil phase was sprayed through the spraying nozzle into the aqueous phase to form uniform droplets, which were polymerized at 80 °C in 1 h with gentle stirring. The resulting magnetic microspheres were separated by a permanent magnet and washed several times with deionized water and ethanol.

Modification of magnetic microspheres

Modification of the magnetic poly(St-DVB-GMA) microspheres with ethylene diamine was carried out by the ring-opening reaction of epoxide groups on magnetic microspheres. Briefly, 1.0 g of dry magnetic microspheres was mixed with a tenfold excess of ethylene diamine at pH 8.5 under very gently stirring, and the mixture was kept at 80 °C for 8 h. The aminated magnetic microspheres were washed thoroughly with ethanol, water.

Cibacron Blue F3GA attachment to magnetic microspheres

The aminated magnetic microspheres (1.0 g) were mechanically stirred in a reactor in 100 ml aqueous solution containing 300 mg Cibacron Blue F3GA for 30 min at 60 °C. This was followed by the addition of 7.0 g NaCl in order to stimulate the deposition of the dye on the surface of magnetic microspheres. After 30 min, 1.0 g NaOH was added to accelerate the reaction between dye and magnetic microspheres at 80 °C for 4 h. After incubation, the Cibacron Blue F3GA immobilized magnetic microspheres were washed with distilled water and ethanol several times until all the physically adsorbed Cibacron Blue F3GA molecules were removed. The samples were then stored at 4 ”C with phosphate buffered saline.

Protein affinity separation from aqueous solutions

The BSA affinity separation experiments were carried out batchwise in the media at different pH values. The effects of medium pH, ionic strength and the initial BSA concentration on the adsorption capacity of dye-ligand immobilized magnetic microspheres were investigated. The dye-ligand immobilized magnetic microspheres were dispersed in phosphate buffered saline with identical concentrations of 5 g/L. Different BSA concentrations were added into 10 ml solutions of magnetic microspheres respectively. The mixtures were incubated at 25 ”C for 1 h. At the end of adsorption, the solid phase was magnetically separated and the supernatant was analyzed for residual protein concentration. Adsorption capacity of BSA was calculated by mass balance.

In a typical kinetic experiment, capped glass tubes each containing 0.04 g magnetic microspheres and 6.0 ml of BSA solution with a definite concentration were shaken end-to-end in a shaking incubator at 25 °C. The tubes were taken out successively for supernatant protein concentration measurement. By this procedure, the decrease of BSA

concentration with time was determined. In addition, 1.0 *M* NaCl solution was employed as a dissociation agent to test the desorption characteristics of BSA.

Analysis and measurement

The diameter and surface features of magnetic poly(St-DVB-GMA) microspheres were investigated by scanning electron microscope (SEM, JSM-6700F, JEOL. Japan). The concentrations of BSA were determined from the absorbance at 280 nm by using a UV-640 spectrophotometer (Beckman, Fullerton, CA, USA).

RESULTS AND DISCUSSION

Properties of magnetic poly(St-DVB-GMA) microspheres

Figure 1 shows the SEM micrograph of the overall appearance of magnetic poly(St-DVB-GMA) microspheres prepared by spraying suspension polymerization. Obviously, Figure 1 shows that the magnetic microspheres are satisfactorily uniform with average diameter of around 11 pm and smooth surface. Compared with the conventional suspension polymerization, the spraying suspension polymerization process can make the droplets disperse uniformly by spraying dispersion instead of conventional mechanical stirring. Therefore, the magnetic microspheres are uniform in size as shown in Figure 1.

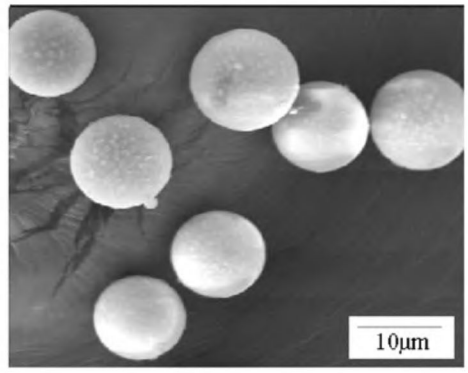


Figure 1. SEM micrograph of magnetic poly(St-DVB-GMA) microspheres

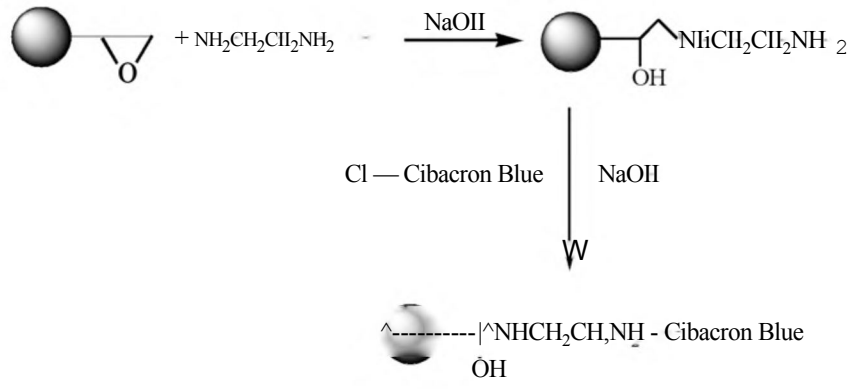


Figure 2. Formation of dye-ligand immobilized magnetic poly(St-DVB-GMA) microspheres

Cibacron Blue F3GA was used as the dye-ligand for specific binding of BSA molecules. It was found that the possible active sites to react with proteins are $S0_3H$, NH_2 and NH [12], In the present work, the functional epoxy groups containing magnetic poly(St-DVB-GMA) microspheres were modified with ethylene diamine. Cibacron Blue F3GA is covalently attached on aminated magnetic microspheres, via the reaction between the chloride groups of

the reactive dyes and the aminate groups of modified magnetic microspheres as shown in Figure 2.

Protein affinity separation from aqueous solutions

Effect of pH

The influence of different factors on the adsorption capacity of BSA onto the dye-ligand immobilized magnetic poly(St-DVB-GMA) microspheres was studied. Figure 3 shows the change of BSA affinity adsorption at equilibrium against the pH with the initial BSA concentration of 2.0 mg/ml. The pH value was varied from 3.5 to 8. The maximum adsorption of BSA was observed at pH 5.0, which is the isoelectric point of BSA. With the change of pH above and below the isoelectric point, the BSA adsorption capacity decreased. The decrease in the BSA adsorption capacity can be attributed to electrostatic repulsion effects between the identically charged groups. At pH different from the isoelectric point, the protein molecules are charged and repel from each other. In addition, the neutral dye-ligand immobilized magnetic microsphere surface acquires a positive or negative charge, which prevents the further protein adsorption.

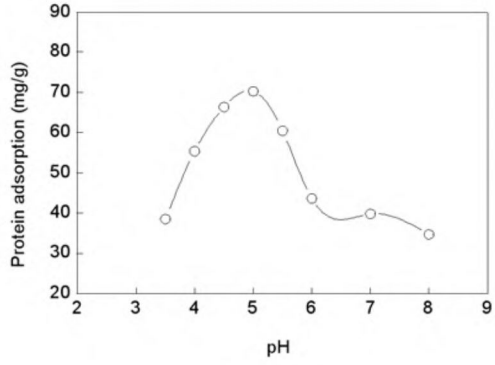


Figure 3. Effect of medium pH on protein adsorption: initial protein concentration, 2.0 mg/ml; time, 1 h.

Effect of ionic strength

Figure 4 shows the effects of ionic strength on BSA adsorption capacity. It was found that the presence of NaCl did not affect the BSA adsorption obviously in 0.05 *M* NaCl solution at pH 5.0. However, the amount of BSA adsorption substantially decreases with the increase of the

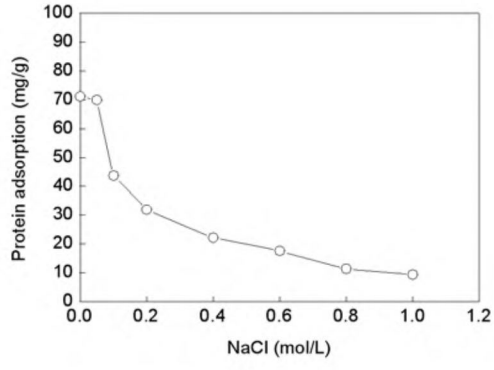


Figure 4. Effect of ionic strength on protein adsorption: initial protein concentration, 2.0 mg/ml; pH 5.0; time, 1 h.

salt concentration from 0.1 to 1.0 *M.* The decrease is owing to the repulsive electrostatic interactions between the dye-ligand immobilized magnetic microspheres and protein molecules. As the salt concentration increases in the medium, this can cause coordination of

the deprotonated sulfonic acid groups of the dye with sodium ions of the NaCI solution [13], resulting in low protein adsorption. Based on this principle, the protein will be desorbed from the dye-ligand immobilized magnetic microspheres by adding high salt concentration solution.

Effect of initial BSA concentration

Figure 5 shows the change of the amount of BSA adsorption with different initial BSA concentrations at pH 5.0. As can be seen from Figure 5, with increasing BSA concentration in solution, the BSA adsorption capacity per unit mass of magnetic microspheres increases until about 2.5 mg/ml, then reaches a plateau value. It was found that only small amounts of BSA were detached from the magnetic microspheres and hence most of the BSA molecules were affinity adsorbed onto the dye-ligand immobilized magnetic microspheres. The maximum adsorption capacity was found to be about 81 mg/g at an initial BSA concentration over 2.5 mg/ml, which is higher than the similar works [14], It can be explained that the aminated magnetic poly(St-DVB-GMA) microspheres have an appropriate space arms, which were suitable for coupling with the Cibacron Blue F3GA molecules. Consequently, much more active groups on the Cibacron Blue F3GA such as $S0_3H$, NH_2 and NH were suitable for selective interaction with the BSA molecules.

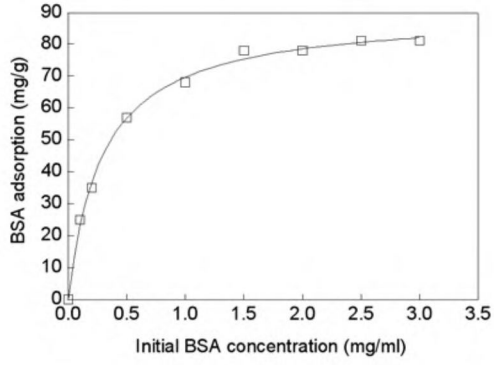


Figure 5. Effect of initial BSA concentration on protein adsorption: pH 5.0; time, 1 h.

BSA adsorption capacity as a function of time

The adsorption and desorption of protein on the dye-ligand immobilized magnetic microspheres were carried out in the medium of pH 5. Figure 6 shows the BSA adsorption

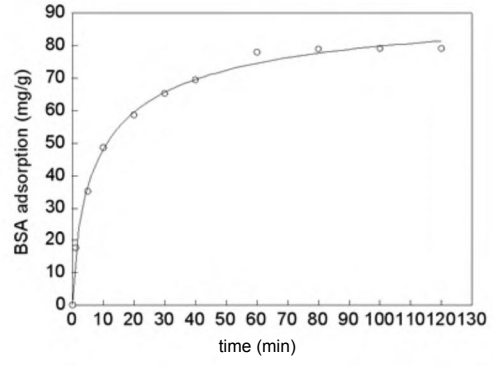


Figure 6. BSA adsorption capacity as a function of time: initial protein concentration, 2.0 mg/ml; pH 5.0.

capacity as a function of time on the dye-ligand immobilized magnetic microspheres. The adsorption equilibrium of BSA was obtained quickly in about 50 min because the adsorption between BSA and magnetic microsphere was carried out on the surface of microspheres. BSA desorption was also carried out in high salt concentration solution. About 90% BSA was desorbed from the magnetic microspheres by adding 1.0 *M* NaCI solution in about 40 min.

The results verified that the adsorption and desorption between BSA and magnetic microspheres were reversible processes, which showed fast adsorption and desorption kinetic characteristics.

CONCLUSION

The uniform magnetic poly(St-DVB-GMA) microspheres were synthesized by spraying suspension polymerization. The dye-ligand, Cibacron Blue F3GA was covalently attached onto the aminated magnetic microspheres for affinity adsorption of BSA. The results show that the maximum BSA adsorption capacity is about 81 mg/g at pH 5.0, and the adsorption and desorption between BSA and magnetic microspheres are reversible processes, which showed fast adsorption and desorption kinetic characteristics.

ACKNOWLEDGEMENTS

This work was financially supported by the National High Technology Research and Development Program of China (No.2002AA302211) and the National Natural Science Foundation of China (No.20206032).

REFERENCES

1. P. Kronick, R. W. Gilpin (1986), *J. Biochem. Biophy. Methods,* 12, 73 — 80.
2. X. H. Li, Z. H. Sun (1995) J. Appl. Polym. Sci., 58: 1991-1997.
3. T. Abudiab, R. R. Beitle (1998) *J. Chromatogr. A,* 795: 211—217.
4. L. Josephson (1987), *U.S. Pat.,* No. 4,672,040 (Sep. 6).
5. P K. Cupta, C. T. Hung (1989) *Life Sci.,* 44: 175-186.
6. S. Fisichella, G. Alberghina, M. E. Amato, D. Lafiandra (2000) *J. Cereal Sci.*28,77-85.
7. F. J. Wolman, M. Grasselli, E. E. Smolko, O. Cascone (2000) *Biotechnol. Lett.*22, 1407-1411.
8. A. Denizli, E. Piskin (1995) *J. Chromatogr. B,* 666, 215-222.
9. A. Denizli, A. Y. Rad, E. Piskin (1995) *J. Chromatogr. B,* 668, 13-19.
10. A. Denizli, E. Piskin (1995) *J. Chromatogr. B,* 670, 157-161.
11. C. L. Yang, Y. P. Guan, J. M. Xing, J. G. Liu, Z. T. An, H. Z. Liu (2004) *Science in China, Ser. B Chemistry,* 47, 349-354.
12. S. Zhang, Y. Sun (2001) *Biotechnol. Bioeng.* 75, 710-717.
13. L. Uzun, M. Odabasi, Y. Arica, A. Denizli (2004) *Separ. Sci. Techno!.,* 39, 2401-2418.
14. H. Yavuz, E. Duru, O. Gene, A. Denizli (2003) *Colloids and Surfaces A,* 223, 185-193.

THE DEVELOPMENT OF THE EXTRACTION AAS METHOD FOR TRANSITION METAL IONS BY USE OF EASILY SOLIDIFYING SOLVENT

Kaoru Fujinaga, Masao Sato, Yasushi Seike and Minoru Okumura

Department of Material Science, Faculty of Science and Engineering,
Shimane University, 1060 Nishikawatsu, Matsue 690-8504 Japan

The proposed method for the atomic adsorption spectrophotometric(AAS) determination of transition metals comprises three unique techniques, namely, utilization of easily-solidifying solvent, phase separation by cooling centrifugation, and *in situ* extractant formation method. In concrete terms, diphenylether was found out to be suitable for the easily-solidifying solvents, and organic phase was solidified by the cooling centrifugation at -5°C and 3000 rpm for 30min after shaking, and pyrrolidinedithiocarbamic acid forming system was utilized instead of ordinary ammonium pyrrolidinedithiocarbamate reagent extraction system. When 1 ml of mixed solvent was used to extract metals in the 50 ml aqueous solution, linear relationship between absorbance of organic phase and metal ion concentration was obtained in the concentration range of 0.2 to 0.75 ppb for Co^{2+}, 0.15 to 0.75 ppb for Cu^{2+} and Ni^{2+} with the correlation coefficients of 0.999, 0.981, and 0.991, respectively.

INTRODUCTION

The solvent extraction is venerable and sophisticated separation method, but if pressed, phase separation is tedious procedure to perform. If it is possible to solidify the organic phase, phases can be simply separated by decanting aqueous phase. Based on this idea, one of the authors proposed the utilization of easily-solidifying solvent as an extracting solvent. An easily-solidifying solvent possesses a melting point lying in the vicinity of room temperature, and becomes a solid by centrifugation cooling below its melting point after equilibration with aqueous phase. After phase separation by decanting an aqueous phase, an organic phase would reliquefy by leaving it for a while under the room temperature. This simplification in the phase separation brings about another advantage, the concentration. That is to say, it is possible to enlarge the volume ratio of aqueous phase to organic one greater than that used in the usual extraction methods.

The authors had already reported the application of easily-solidifying solvent to the metal extraction[1,2] and extraction photometry for ammonia[3]. In the previous studies, p-xylene and 1,2,4-trichlorobenzene were used, and showed fairly good extractability for the extracting species. However, p-xylene(m.p. : 13.263°C) solidified above the aqueous layer since its specific gravity is smaller than the unity(£/$_4^{20}$: 0.861), and therefore, it is not always simple to separate phases. 1,2,4-Trichlorobenzene(m.p. : 17-18°C, </^{26}: 1.446) was ideal as

easily-solidifying solvent in all respects but was hesitated to use because of halogenated solvent. Then, diphenylether(Ci_2Hi_0O, m.p. : 27-28°C, $r/_4^{20}$: 1.075) was mainly used in this study, and a special cap for extraction vial made by poly(tetrafluoroethylene), which has a hole with a volume of 1 cm^3, was newly devised in order to collect diphenylether thoroughly.

It has been reported in the previous papers that metal ions can be extracted into the organic phase without adding any chelate extractants by the present *in situ* extractant formation method. That is, a mixture of isoamylalcohol, pyridine, and carbon disulfide (CS_2) formed isoamylxanthic acid[4,5], one of diethylamine, CS_2, and chloroform($CHCl_3$) produced diethyldithiocarbamic acid[6,7], one of pyrrolidine(C_4H_8NH), CS_2, and p-xylene yielded pyrrolidinedithiocarbamic acid(PDC)[1,2], and one of salicylaldehyde and $CHCl_3$ formed salicylaldoxime[8], respectively. Since ammonium pyrrolidinedithiocarbamate(APDC) is commonly used for the extraction AAS to determining metals, PDC-forming system which consists of C_4H_8NH, CS_2, and $C_{12}H_{10}O$ was adopted in this study.

The present study was undertaken to confirm that these techniques can be applied to the extraction AAS determination of transition metals.

EXPERIMENTAL

Reagents and apparatus A Hitachi CF7D cooling centrifuge was used for phase separation, and a Hitachi model Z-5000 atomic absorption spectrophotometer was used to measure the metal concentration with a graphite furnace atomizer, and a Nihonbunko V-560 double-beam spectrophotometer was used to obtain absorption spectra with 1.0 cm pathlength quartz cells. The metal solutions were stored in polyethylene bottles and were mixed in a volumetric flask so that the concentration of each metal was 0.2 mM, prior to use. The other reagents were of analytical grade.

Extraction procedure Extraction AAS procedure is shown in Fig. 1. A 50ml portion of the metal ion solution, which was masked and buffered with 0.033 M diammonium hydrogen citrate and 0.017 M citric acid and was maintained ionic strength of 1.0 M with potassium nitrate, was equilibrated with a 1 ml of the PDC-forming solvent having a composition of 2.0:2.0:96(v/v%) for CS_2:C_4H_8NH: CI_2HI_0O in a 50 ml extraction vial equipped with a special cap by shaking vigorously for 1 h(Procedure A). The extraction vial was set in a rotor of a cooling centrifuge up side down, and centrifuge was carried out at -5°C at 3000 rpm for 30 min(Procedure B). The extraction vial was taken out and was placed in the stand in a normal position. At this time, diphenylether layer was all collected and held solidified in a hole of the cap. The cap was removed and was allowed to stand until diphenylether would reliquefy(Procedure C). The metal ion concentration in the diphenylether was determined by graphite furnace atomic absorption spectrophotometry.

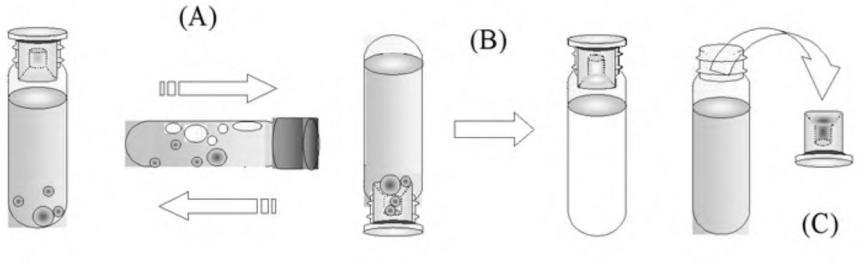


Fig. 1 Diagram of the manipulation of an extraction vial.

RESULTS AND DISCUSSION

Selection of easily-solidifying solvent The extraction mechanism of PDC-forming system was reported as shown in Fig. 2 and the relation between metal extraction and the concentration of CS_2 and C_4H_8NH was studied in detail in the previous study[1]. It was revealed that the extractability of metal ions in the PDC-forming system is governed by the concentration of formed PDC which depends on the concentrations of CS_2 and C_4H_8NH.

Then, diphenylether, diphenylmethane(Ci_3Hi_2, m.p. : 26-27°C, *df*\ **1.006** **),** 1,2,4-trichlorobenzene, and p-xylene were arbitrarily selected as a possible

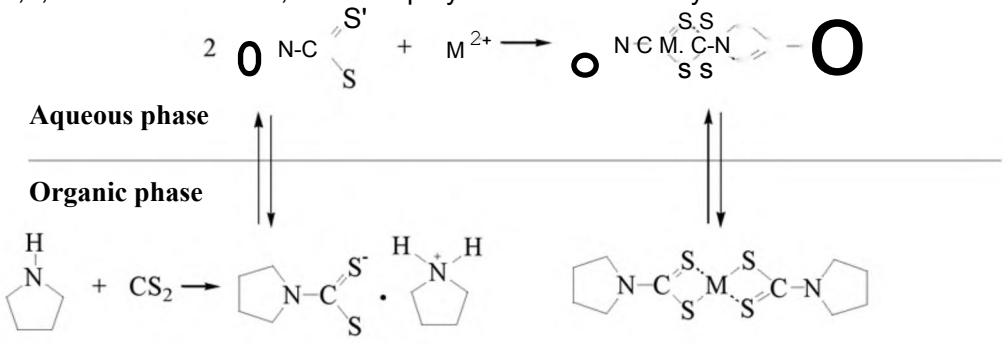
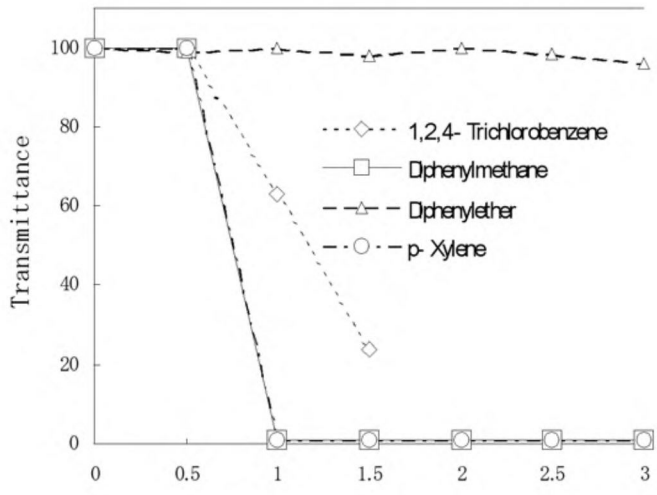


Fig.2 Extraction mechanism of *in-situ* extractant formation method.



Gbncentrdicn of CS2 and C4FBNH vd.%

Fig. 3 Solubility of solvent.

Table 1 E_T values for some solvents

Solvent	Amax(nm)	Ex value
Benzene	831 (833.5)	34.4 (34.3)
Acetone	689 (677.5)	41.5 (42.2)
Tctrahydrofuran	758 (764.4)	37.7 (37.4)
1,2,4-Trichlorobenzene	789.5	36.2
p-Xylcne	856.4	33.4
Diphenylether	804.0	35.6

easily-solidifying solvent and were examined with their solubility for CS_2 and C_4H_8NH. Figure 3 clearly demonstrates that diphenyl- ether dissolved the largest amounts of CS_2 and C_4H_8NH among the examined solvents and, therefore, was used as an easily-solidifying solvent in this study. Incidentally, the decrease of the transmittance shown in the other solvents was caused by the precipitation of pyrrolidinium pyrrolidinedithio-carbamate formed by the reaction between CS_2 and C_4H_8NH(Fig. 2). Next, polarity of solvent also governs metal extraction so much that polarity of diphenylether was evaluated by the E_T value[9], E_T value

$$E_T = \frac{28590 Kcal\ mol^{-1}\ nm}{\lambda_{max}\ nm}$$

can be calculated by the following equation, where A_{max} is absorption maximum of the solvent containing Reichard's dye. As can be seen from Table 1, the E_T values obtained with benzene, acetone, and

tetrahydrofuran coincided fairly well with those reported, and the E_T value implies that the polarity of diphenylether is intermediate between that of benzene and tetrahydrofuran. This result seems to be reasonable judging from molecular structure of these 3 solvents.

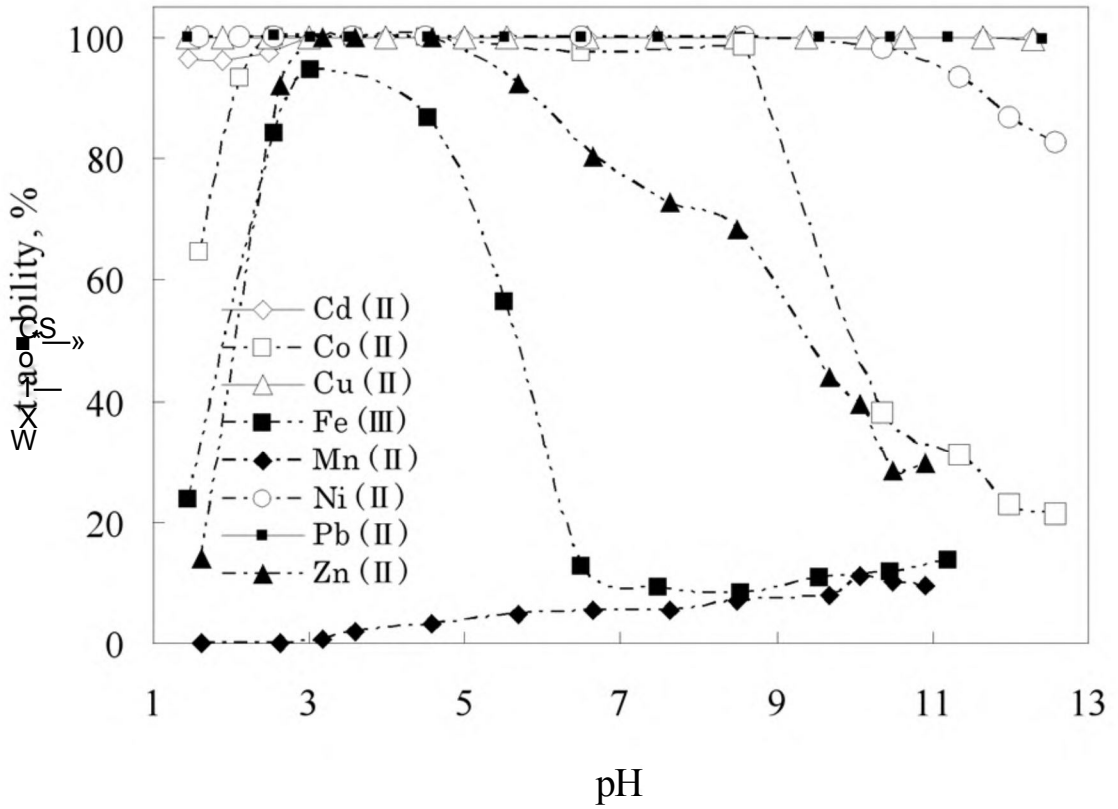


Fig.4 The relationship between pH and metal extraction.

Effect of pH on the extraction The previous paper reported that the order of extractability was Zn<Co<Ni<Cd in the PDC-forming p-xylene system and Zn was the most sensitive to the amount of the formed PDC. Figure 4 shows that the width of pH range for 100% extraction in the PDC-forming diphenylether system becomes wider in the similar order to the previous system, and it can be said that the effect on the metal extraction caused by changing the solvent matrix from p-xylene to diphenylether was not significant. It is considered that Cd, Cu, and Ni could be applicable to the extraction AAS method judging from the result shown in Fig. 4.

Determination of metal ions First, in order to atomize metals in the graphite furnace successfully, the optimal drying temperature was examined. Since boiling point of diphenylether is 259°C, drying temperature was set at 290°C. The optimal values was 290°C with 1.5'C·s"[1] ramp to avoid sputtering(Table 2). Ilnder this atomizing conditions, fairly good

Table 2 Furnace heating program

Step	Temperature(°C)	Ramp^C-s'[1])	Hold(s)
Dry	290	1.5	0
Calcination	600	15.5	0
Atomization	2400[a] 2700[b]	0	5
Cleaning	2500[a] 2800[b]	0	4

linear relationship between absorbance of organic phase and metal ion concentration was obtained in the concentration range of 0.2 to 0.75 ppb for Co^{2+}, 0.15 to 0.75 ppb for Cu^{2+} and Ni^{2+} with the correlation coefficients of 0.999, 0.981, and 0.991, respectively. Table 3 summarizes the results obtained for spring water and river water sampled in Matsue city, as well as the value determined by GFAAS without extraction. Cu^{2+} and Ni^{2+} were aptly determined by the present extraction AAS method, while all three metals in the samples could not be detected if sample water was subjected to GFAAS method directly.

Table 3 Results for environmental water sample

Sample	Co²H'/ngml'1		o。⁸⁺'/ngml'1		NT/ngml'1	
	GFAAS	Present method	GFAAS	Present method	GFAAS	Present method
Menashi spring	< 2.5	< 0.20	< 5.0	1.01	< 2.5	0.80
Hii River	<2.5	< 0.20	< 5.0	0.45	< 2.5	0.36

In conclusion, the present method is simple and convenient compared to the usual extraction since the organic phase was solidified by the cooling centrifugation and phases can be separated by the decantation, and is applicable to the determination of Co^{2+}, Cu^{2+}, and Ni^{2+} at sub-ppb level.

REFERENCES

1. K. Fujinaga, M. Fukai, Y. Seike, and M. Okumura, *Anal Sci.,* 15, 333-337 (1999).
2. K. Fujinaga, Y. Seike, and M. Okumura, 2001, *Proc. ISEC'99,* Volume 1, edited by M. Cox, et. al., Society of Chemical Industry, pp341-345.
3. K. Fujinaga, F. Kawanishi, Y. Seike, and M. Okumura, *Mem. Fac. Sci. Eng. Shimane Univ.,* 36, 1-7 (2003).
4. K. Fujinaga, *Anal Sci.,* 7, Supplement 29 (1991).
5. K. Fujinaga, *Anal. Chem. Acta,* 264, 71-77 (1992).
6. K. Fujinaga, Y. Seike, and M. Okumura, 1996, *Proc. ISEC'96,* edited by D. C. Shallcross, et al., The University of Melbourne, pp. 93-98.
7. K. Fujinaga, Y. Seike, and M. Okumura, *Anal. Sci.,* 13, 225-230 (1997).
8. K. Fujinaga, Y. Sakaguchi, T. Tsuruhara, Y. Seike, and M. Okumura, *Solvent Extr. Res. Dev., Jpn.,* 8, 144-158 (2001).
9. K. Dimroth, C. Reichard, T. Siepmann, and F. Bohlmann, *Am. Chem.,* 661, 1 (1963).

SOLVENT EXTRACTION OF CHROMIUM(VI) WITH QUATERNARY AMMONIUM IONS

J. Noro, H. Kokusen*, and Y .Komatsu*

NISSAN ARC, LTD., Japan
* Kanazawa Institute of Technology, Japan

The solvent extraction of chromiumfVH in 0.1 mol dm'^{3} sodium nitrate solutions with tetrabutylammonium ions (tba^+) into 1-octanol was studied. From the dependence of extraction on the concentration of hydrogen ion, tba^+, and chromium(VI), it was concluded that chromium(VI) was extracted in the form tba^+HCr0_4\ The first and second acid dissociation constants for chromic acid and the extraction constant for the ion-pairs were determined. Although there was not much difference in the extraction of tba^+ with co-existing $N0_3$' in the aqueous phase into 1-octanol and into chloroform, the extraction of $HCr0_4$' with tba^+ into 1-octanol was much improved compared with chloroform.

INTRODUCTION

The solvent extraction of chromium(VI) in the form of H_2Cr0_4 with 4-methyl-2-pentanone (MIBK),[1-4] tributyl phosphate (TBP),[5,6] and trioctylphosphine oxide (TOPO)[7,8] has been studied. The extraction of chromium(VI) in the form of $HCr0_4^-$ with tetrabutylammonium ions (tba^+)[9] into chloroform was also studied. It was reported in ref.9 that the extraction of chromium(VI) with tba^+ into chloroform was not effective. In the present work, the solvent extraction of chromium(VI) with tba^+ into 1-octanol was studied in order to find a more effective solvent extraction method for chromium(VI).

EXPERIMENTAL

All of the reagents and experimental procedures were similar to those in the previous study[9] except that 1-octanol was used as the solvent. All the solvent extraction experiments ware carried out at 298 K. The concentration of tba* in the aqueous phase at equilibrium was measured by the same method as described in Ref.10.

RESULTS AND DISCUSSION

In the present paper, chemical species in the organic phase are denoted by the subscript "org" and those in the aqueous phase are shown without any subscript. The volume of the two liquid phases is the same. The data are treated in the same manner as described in ref.9 on the basis of the following equations.

The equilibrium constants can be written as follows

$$H_2Cr0_4 \rightleftharpoons H^+ + HCrCV\ ;\ K_{a1} = [H^+]\,[HCrCV] / [H_2Cr0_4]. \quad (1)$$

$$HCr0_4' \text{ «=►} H^+ + Cr0_4'^{2'}\ ;\ K_{a2} = [H^+]\,[Cr0_4^{2}] / [HCr0_4]. \quad (2)$$

$$tba^+ + HCr0_4' \text{ *=* } tba^+HCr0_{4(org)}^-\ ;\ Ke_{XI} = [tba^+HCrO_4']_{0rg} / [tba^+]\,[HCr0_4]. \quad (3)$$

$$2tba^+ + Cr0_4^{2'} \text{ «=►} (tba^+)_2Cr0_4^{2'}{}_{(org)}\ ;\ Ke_{x2} = [(tba^+)_2CrCV]_0rg / [tba^+]^2\,[Cr0_4^{2}]. \quad (4)$$

$$2tba^+HCr0_{4(org)}^- \text{ «=* } (tba^+)_2Cr_2O_7^{2'}{}_{(0r}n) + H_20$$
$$;\ Kdin, = [(tba^+)_2Cr_2O_7^{2'}]_{0rg} / [tba^+HCrO_4^-]_{0rg}^2. \quad (5)$$

The distribution ratio of chromium(VI) extracted with tba^+ can be written as:

$$D = ([tba^+HCrO_4]_{0rg} + [(tba^+)_2CrO_4^{2}]_{0rg} + 2[(tba^+)_2Cr_20_7^{2}]_{org})$$
$$/ ([H_2Cr0_4] + [HCrCV] + [Cr0_4^{2}]) \quad (6)$$

$$= (Kexi[tba^+] + Ke_{x2}Ka_2[tba^+]^2 / [H^+] + 2K_{dim}K_{ex1}[tba^+]^2[HCr0_4])$$
$$/ ([H^+] / K_{a1} + 1 + Kg_2 / [H^+]). \quad (7)$$

When the extracted ion-pairs undergo dissociation, the extraction equilibrium of tba^+ with the anion of the background salt, $N0_3\backslash$ can be written as:

$$tba^+ + N0_3- \text{ <=* } tba^+\ N0_{3\ (org)}^-\ ;\ Ke_{xAB} = [tba^+\ N0_3]_0rg / [tba^+][N0_3] \quad (8)$$

$$tba^+NQ_3(_{0rg}) \text{ } M \text{ * } tba^+_{(org)} + NO_{3(0rg)}^-$$
$$;\ Kciss = [tba^+]_{org}\,[N0_3']_{org} / [tba^+\ N0_3^-]_{org} \quad (9)$$

The chemical form of tba^+ in the organic phase should be $tba^+N0_3'_{(0}rg)$ or $tba^+_{(org)}$. Since $N0_3'$ could not be extracted except with tba^+, the concentrations of $tba^+_{(org)}$ and $N0_3'_{(org)}$ should be identical. Thus the distribution ratio of $tba\backslash$ D_{tba} $=[tba^+]_{orgt}$otai / $[tba^+]_{aq}$'total can be written as:

$$D_{tba} = ([tba^+N0_3^-]_{org} + [tba^+]_{org}) / [tba^+]$$
$$= Ke_{xAB}\,[N0_3^-] + (KUeKq.ss\,[N0_3^-])^{05} / [tba^+]^{05} \quad (10)$$

The extraction of tba^+ with $N0_3$‘ from aqueous 0.1 mol dm'^{3} sodium nitrate solution into 1-octanol is given in Fig. 1. Literature data on the extraction of this ion-pair into chloroform[11] are also given in Fig. 1.

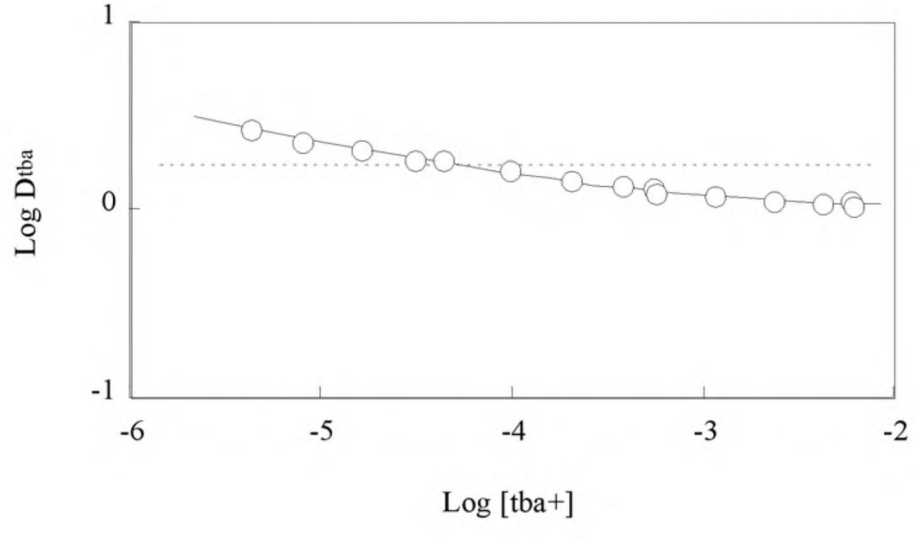


Figure 1. Distribution ratio of tba as a function of tba* concentration in the aqueous phase. The aqueous phase is 0.1 mol dm³ sodium nitrate solutions.*
The solid line is calculated by Eq. 8 using the values given in Table 1. The dotted line is the plots when solvent is chloroform taken from ref. 11.

As can be seen from Fig.1, more than 50% of tba^+ in the initial aqueous phase is transferred as the ion-pair, tba^+N0_3', into 1-octanol. It can also be seen from Fig.1 that the degree of extraction of the tba^+ ion-pair differs little between these two solvents. The decrease in the extraction of tba^+ into 1-octanol with increasing tba^+ concentration is explained in terms of a partial dissociation of the ion-pair in 1-octanol, while the lack of dependence of the distribution ratio on the tba^+ concentration when the solvent is chloroform should indicate negligible dissociation of the ion-pair. From these data, the extraction constant, KexAB in Eq.8, and the dissociation constant, K_{dlss} in Eq.9, of the ion-pair are calculated on the basis of Eq.10. The values obtained are listed in Table 1. The solid line in Fig.1 was calculated by introducing the values of $Ke_{XA}B$ and K_{dlss} in Table 1 into Eq.10.

Figure 2 gives the distribution ratio of chromium(VI) as a function of the hydrogen-ion concentration when the initial concentration of tba^+ is $2.5x10'^3$ mol dm^{-3} and that of chromium(VI) is 10^4 mol dm'^3.

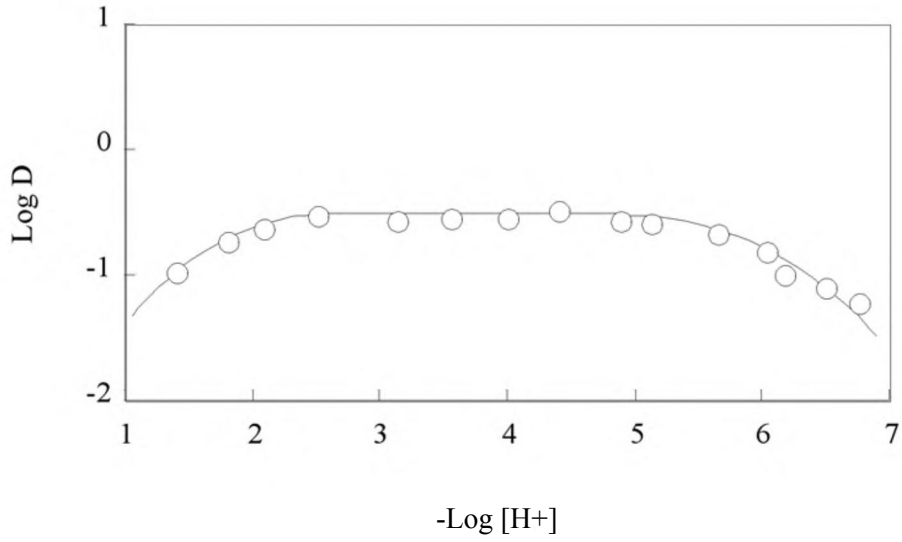


Figure 2. Distribution ratio of chromium(VI) as a function of the hydrogen-ion concentration. The solid line is calculated by Eq. 7 using the values given in Table 1

As can be seen from Fig.2, the extraction is nearly independent of -log[H^+] except when it is lower than 2 and higher than 5. Thus chromium(VI) should be present in the $HCr0_4^-$ form in the aqueous phase in this -log[H^+] range. The acid dissociation constants were calculated from these data on the basis of Eq.7 by a successive-approximation approach using a least-square computer program. The values of K_ai and K_{a2} obtained are listed in Table 1.

Table 1 Summary of equilibrium constants

	Log K_{a1}	**Log Ka_2**	**Log Kexi**	LOQ Kdi_{SS}	**Log** KexAB	**Log K<j,,m**
1-octanol	-1.3	-6.1	-2.4	-4.4	1.0	
chloroform	-0.8[11]	-	1.0[1']	-	1.32)	4.7[11]

1) taken from ref.9 2)taken from ref.11

Figure 3 gives the extraction curves of chromium(VI) with tba when -log[FT] is 3.0 and about* ***6***.

As can be seen from Fig.3, the distribution ratio when -log[H^+] is 3.0 is proportional to the tba^+ concentration. It is also found that the distribution ratio is not much affected by the change in -log[H^+] in this range as can be seen from Fig.2. On the other hand, when -log[H^+] is about 6, the slope of the plot gradually increases and this slope reaches an asymptote with a slope of +2. However, this is only an apparent effect. The extraction from the aqueous solutions when -log[H^+] is around 6 is much affected by the concentration as can also be seen from Fig.2. In this -log[H^+] range, the formation of H_2Cr0_4 in the aqueous phase should be negligible. Furthermore, the dimerization in the organic phase could be negligible as is described later. Thus the data

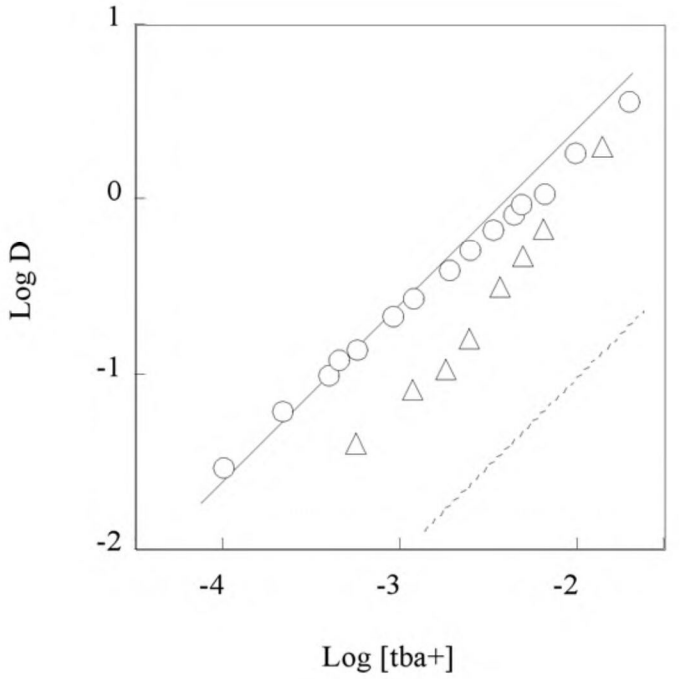


Figure 3. Distribution ratio of chromium(VI) as a function of the tba concentration at equilibrium. The hydrogen-ion concentration is 10-3.0 (O) and about 10-6 (A) mol dm³. The solid line is calculated by Eq. 7 using the values given in Table 1. The dotted line is the plot when solvent is chloroform taken from ref. 9*

when -log[H^+] is in this range, are normalized to the change in the hydrogen-ion concentration on the basis of the following equation which is derived from Eq.7.

DM + Ka_2 / rH⁺l) / rtba⁺l = Kexi + $Ke_{x2}K_{a2}$rtba⁺l / TH⁺1. M It

When X = [tba^+] / [H^+], Y = D(1 + K_{a2} / [H^+]) / [tba^+], K-, = K_{ex}i, and K_2 = $K_{ex2}K_{a2}$ (K-, and K_2 are the constant), Eq.11 can be written as Y = K-, + K_2X. Figure 4 gives the plot of log X vs. log Y. If the reaction in Eq.4, that is, the extraction of the $(tba^+)_2Cr0_4^{2'}$ species is taking place, the slope of this plot should reach an asymptote with a slope of +1. However, as can be seen from Fig.4, the slope of the plot is 0. From this, it can be concluded that the data, when -log[H^+] is about 6 where nearly half of the chromium(VI) is in the $Cr0_4^{2‘}$ form are well explained by the extraction of the $tba^+HCr0_4^-$ species only.

The effect of initial chromium(VI) concentration on the extraction is examined when -log[H^+] is 3.0 and about 6. When the pH is higher than 3, the formation of H_2Cr0_4 in the aqueous phase is negligible and the extraction of $(tba^+)_2Cr0_4^{2'}$ is also negligible as was already described. The data are normalized to the change in the hydrogen-ion concentration on the

basis of the following equation which is derived from Eq.7.

$$D(1+K_{a2} / [H^+]) = Kex\text{-}i[tba^+] + 2K,™ «e_{XI} [tba^+]^2[HCr0_4]. \quad (12)$$

Since the initial tba^+ concentration is identical under these experimental conditions, the values of $Ke_{XI}[tba^+]$ and $2Kd_{im}$ Ke_Xi $[tba^+]^2$ are constant. When P = $[HCr0_4]$, Q = $D(1+K_a2 / [H^+])$, K_3 = $Ke_{XI}[tba^+]$, and K_4 = $2K_{dim}$ Ke_{XI} $[tba^+]^2$, Eq.12 can be written as Q = K_3 + fQP. Figure 5 gives the plot of log P vs. log Q. As can be seen from Fig.5, the slope of the plot is 0. This indicates that the reaction in Eq.5, that is, the formation of dinuclear species in the organic phase should be negligible.

From these data, the extraction constant of hydrochromate ions with tba^+, Ke_{XI} in Eq.3, is calculated on the basis of Eq.7 as is listed in Table 1. The solid lines in Figs.2 and 3 are calculated by introducing the values of Ka-,, K_{a2}, and Ke_Xi in Table 1 into Eq.7. Each of the lines fits well with the experimental data.

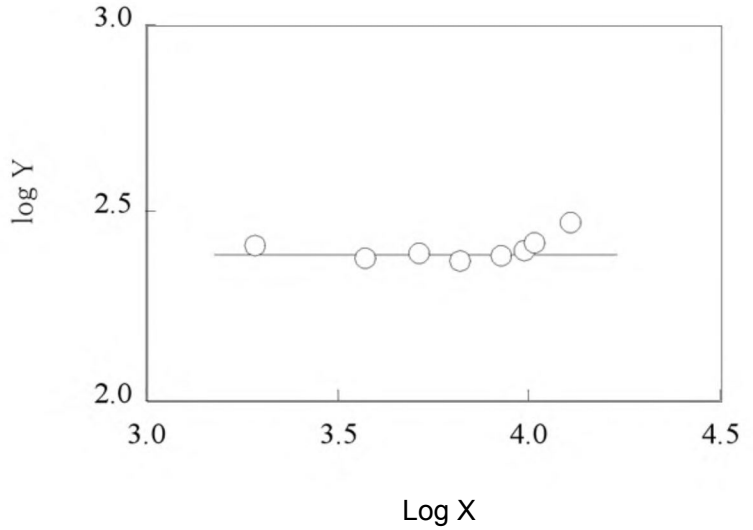


Figure 4. Reration between the log X vs. log Y when -log [FT] is about 6 (cf.Eq.11). Where X= [tba]/[FT] and Y= D(1 + K_{a2} /[FT]) / [tba*].*

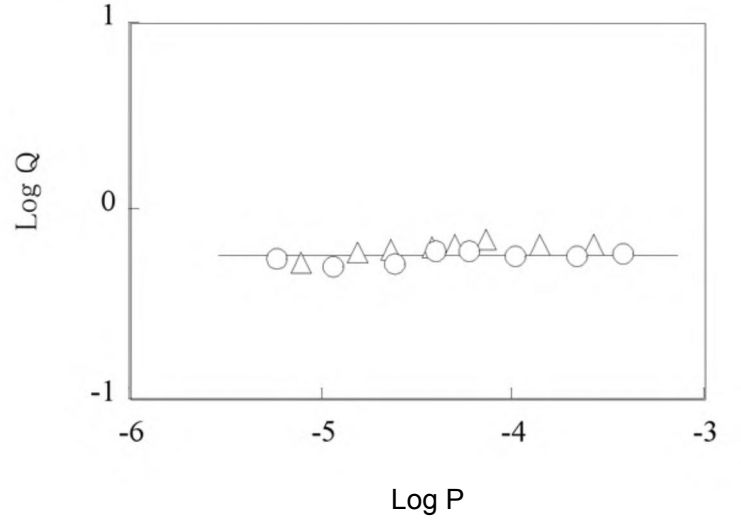


Figure 5. eration between the log P vs. log Q when -log [FT] is 3.0 (O) and about 6 (A) (cf.Eq. 12). Where P = [HCrQ$_4$] and Q = D(1+K_{a2}/[FT]).

It is noted that although the distribution ratio of chromium(VI) in aqueous 0.1 mol dm^{-3} sodium nitrate solutions with tba^+ at the same concentration into 1-octanol is about one order of magnitude higher than into chloroform as is seen from Fig.3, the extraction of tba^+ with nitrate anions is not very much different for 1-octanol and chloroform as is seen from Fig. 1. This should indicate that the hydrochromate ion in the extracted ion-pair species should be solvated with 1-octanol molecules. Furthermore, the present results show a much smaller tendency for dimerization in the polar solvent. Although dimerization of the extracted ion-pairs, $tba^+HCrO_4^-$, was recognized in chloroform when the chromium(VI) concentration in the organic phase was 10^{-6} mol dm^{-3}, negligible dimerization of the extracted species in 1-octanol when the concentration was not higher than $5*10^{-4}$ mol dm^{-3} was found. It was reported that the dimerization of $HCrO_4^-$ in aqueous solution was negligible when the concentration was less than 10^{-3} mol dm^{-3}.[8] This observation and the present results show a much smaller tendency for dimerization in polar solvents.

REFERENCES

1. H. A. Bryan and J. A. Dean (1957), *Anal. Chem.,* 29, 1289.
2. P.D. Blundy (1958), *Analyst* 83, 555.
3. S. A. Katz, W. M. McNabb, and J. F. Hazel (1961), *Anal. Chim. Acta.,* 25 193.
4. G. B. Marshall and T. S. West (1970), *Analyst,* 95, 343.
5. K. H. Arend and H. Specher, Z. Anorg (1964), *Allg. Chem.,* 333, 18.
6. A. A. Yadav and S. M. Khopkar (1670), *Indian J. Chem.,* 8, 290.
7. C. K. Mann andJ. C. White (1958), *Anal. Chem.,* 30, 989.
8. M. Niitsu and T. Sekine(1976) , *J. Inorg. Nucl. Chem.,* 38, 1057.
9. M. Yamada and T. Sekine (1996), So/v. *Extr. Res. Dev. Jpn.,* 3, 99.
10. J. Noro and T. Skine (1992), *Bull. Chem. Soc. Jpn.,* 65, 1910.
11. J. Noro and T. Skine (1993), *Bull. Chem. Soc. Jpn.,* 66, 450.

Separation of Alkaline Earth Metal Ions by the Multistage Solvent Extraction Method

S. Oshima[1'], H. Kokusen[21], T. Tanemoto[21], J. Noro[3'], S. Tsurubou[4'], M. Sekita[5'], H. Yamada[5'] and Y .Komatsu[2']

[1)]: Fukui National College of Technology, Fukui, Japan
[2>]: Kanazawa Institute of Technology, Ishikawa, Japan
[3>]: NISSAN ARC, LTD., Kanagawa, Japan
[4)]: Asahi Universitv. Gifu. JaDan
[5)]: National Institute for Materials Science, Ibaraki, Japan

The multistage solvent extraction mothod (CPC: centrifugal partition chromatograph method) was applied to separation of alkaline earth metal ions on the basis of the results obtained from normal solvent extraction method. In the system of two alkaline earth metal ions (Ba^{2+}-Mg^{2+}, Ba^{2+}-Ca^{2+} and Ba^{2+}-Sr^{2+}), the metal ions in the aqueous mobile phase were first extracted to the organic stationary phase containing thenoyltrifluoroacetone (TTA) as an extractant and tri-n-octhylphosphine oxide (TOPO) as an adductance when the pH of the aqueous phase was set to 5.5. Only Ba^{2+} has been back-extracted from stationary phase to mobile phase by adjusting pH value of aqueous solution, although the other metal ion has been kept in the stationary phase. In this process, the reaction was efficiently done by CPC method. Furthermore, the other metal ion could be recovered by changing the pH of the mobile phase to 1.0. As the results, Ba^{2+} could be separated from the other alkaline earth metal ions (Mg^{2+}, Ca^{2+} and Sr^{2*}).

INTRODUCTION

As a problem of nuclear pollution, there are existence and accumulation of long-lived nuclide. For example, ^{90}Sr having half-life of 27.7 year emits 13-rays, and if 13-rays goes into human body, it will be accumulated at a frame etc. Therefore, ^{90}Sr is one of most dangerous radioactive nuclide.

In order to separation selectively an only aimed metal ion, it has been studied by various methods such as solvent extraction and ion exchange. The separability can be enhanced by using various extractant, but it need long time for separation.

Centrifugal Partition Chromatography (CPC) has been developed in order to separation of natural organic compounds [1], In CPC method, it is expected to enhance the separability by multistage solvent extraction. The CPC method has been applied in separation of organic compounds [2], alkaline earth metal ions [3], transition metal ions [4] and lanthanoids and actinoids [5],

In this study, we focused our attention on separation of ^{90}Sr from other radioactive nuclide in radioactive waste from the viewpoint of decrease of the volume. Therefore, we attempted separation among alkaline earth metal ions, Mg^{2+}, Ca^{2+}, Sr^{24} and Ba^{2+}. In this time, we

reported separation of Ba^{2+} from the other alkaline earth metal ions by solvent extraction and CPC method.

EXPERIMENTAL

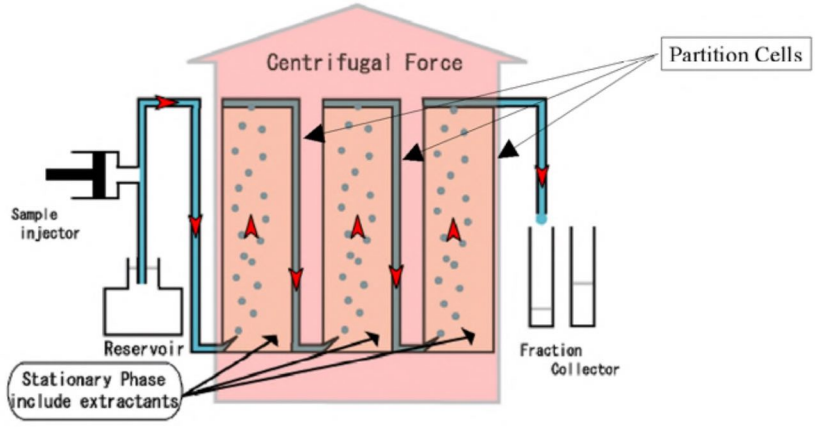
All chemicals were reagent grade materials and distilled deionized water was used throughout.

Normal solvent extraction method

The extraction of metal ions was studied as follows. In centrifuge tube, an aliquot of cyclohexane containing 0.1 mol dm'3 of TTA and TOPO, respectively, and equal volume of an aqueous phase containing 1 x 10'4 mol dm"3 of metal ion (Mg^{2+}, Ca^{2+}, Sr^{2*} or Ba^{2+}) and 0.02 mol dm'3 of the buffer (chloroacetic acid or acetic acid) were shaken with 300 strokes min'1 at 25 ± 1 °C for 24 hours. After the two phases were separated by centrifugation, the pH and the metal concentration in the aqueous phase were determined by pH meter equipped with a combined glass electrode and ICP-OES, respectively. The metal concentration in the organic phase was determined after back-extraction into 0.1 mol dm'3 nitric acid.

Murtistage solvent extraction method using CPC device

The outline figure in rotor of CPC device (Senshu Scientific co., ltd.) is shown in Fig. I.By applying centrifugal force within the CPC device, very small drops of mobile aqueous phase were moved into the stationary organic phase containing TTA and TOPO. In that process, the metal ion formed complex with TTA-TOPO and extracted into the stationary phase. The condition of CPC device is as follows: (i) in the packing stationary phase, the flow rate of organic solvent is 25 cm^3 min'1 and the rotor speed is 200 r.p.m. (ii) in flowing mobile phase and making the steady state of device, the flow rate of mobile phase is 5.0 cm^3 min'1 and the rotor speed is 600 r.p.m. (iii) in sampling, the flow rate of mobile phase is 1.0 cm^3 min'1 and the rotor speed is 600 r.p.m. The solutions of two metal ions (Mg^{2+}-Ba^{2+}, Ca^{2+}-Ba^{2+} and Sr^-Ba^{2*}) were prepared by dissolving magnesium chloride, calcium chloride, strontium chloride and barium chloride, respectively, and made them 1 x 10'4 mol dm'3. The stationary phase containing 0.1 mol dm'3 of TTA and TOPO, respectively, was prepared by dissolving TTA and TOPO into cyclohexane. The mobile aqueous phase is prepared by 0.2 mol dm'3 of 2-(A/-morpholino)ethanesulfonic adic (MES) and controlled to pH 5.5 by 0.1 mol dm'3 sodium hydroxide. The elution of barium ion from stationary phase was made by acidity mobile phase adjusted pH value by nitric acid to 3.4, 3.5 and 3.7 in Ba^{2+}-Mg^{2+}, Ca^{2+}-Ba^{2+} and Sr^-Ba^{2*} systems, respectively. The recovery of the other metal ion was made by changing the pH of mobile phase to 1.0. Every 5 min, the 5 cm^3 fraction of effluent was collected in sampling tube and the concentration of metal ion in the fraction was determined by ICP-OES. From the results, the recovery rate (%) was calculated.



RESULTS AND DISCUSSION

Normal solvent extraction of alkaline earth metal ions

Alkaline earth metal ions form the addition complex with TTA and TOPO and the metal complex can be extracted into organic phase as follows.

$$M^{2+} + 2HA_{(0)} + 2TOPO(_0) \leq\!\!=\!\!» MA_2(TOPO)_2(O) + 2H^+$$

Where HA means TTA and subscript 'o' denotes the organic phase. In this case, distribution ratio of M^{2*} (D) is described as follows:

$$D = \frac{[MA_2(TOPO)_{2(o)}1}{[M^{2+}]}$$

Therefore, we attempted to separate Ba^{2+} from the other alkaline earth metal ions in the normal solvent extraction system using TTA as an extractant and TOPO as an adductance. The logarithmic distribution ratios (log *D)* of Mg^{2+}, Ca^{2+}, Sr^{2+} and Ba^{2*} into cyclohexane were plotted as a function of the aqueous phase pH in Fig. 2. Further, the pH values of the 50 percent extraction ($pH_{1/2}$) of each metal ion were determined from Fig. 2 and shown in Table 1. From the results, the order of the extraction selectivity was determined as $Mg^{2+} > Ca^{2+} > Sr^{2*} > Ba^{2+}$ in this system, which suggested that metal ion having smaller ion radius showed higher selectivity. It was found the difference of the distribution coefficients for the alkaline metal ions; however, it was different to separate them by the normal solvent extraction system due that the different metal ions could be extracted to an organic phase. To overcome this difficulty, we have focused our attention on this difference between the distribution coefficients of the alkaline earth metal ions.

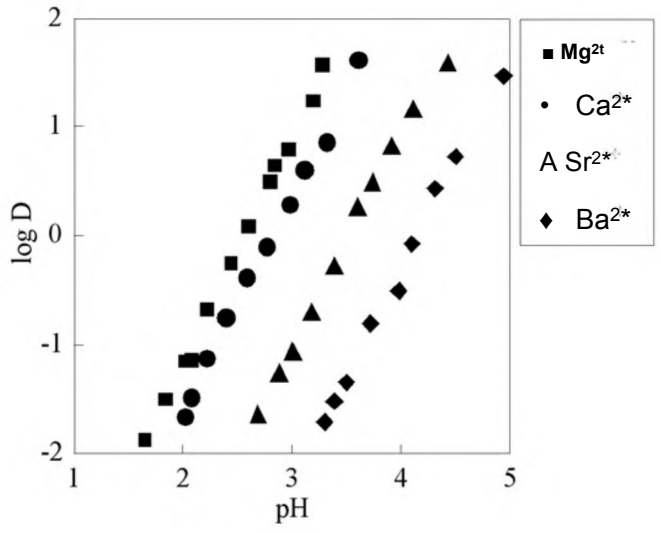


Fig. 2. Plots of log D of Mg^{2*}, Ca^{2+}, Sr^{2*} and Ba^{2*} into cyclohexane with TTA and TOPO in normal solvent extraction system.

Table 1. the $pH_{1/2}$ values of each metal ion.

	Mg^{2*}	Ca^{2*}	Sr^{2*}	Ba^{2*}
$pHi/_2$	2.6	2.8	3.4	4.1

Multistage solvent extraction method using CPC device

In this method, TTA and TOPO were filled in organic (cyclohexane) phase for the stationary phase, and then aqueous solution containing two metal ions (Mg^{2+}-Ba^{2+}, Ca^{2+}-Ba^{2+} and Sr^-Ba^{2*}) for mobile phase at pH 5.5 was flowed into the CPC device. In this process, the both metal ions in the mobile phase were moved into stationary (organic) phase by forming a metal addition complex with TTA and TOPO. Subsequently, by adjusting pH of mobile phase to 3.4 3.5 and 3.7 in Mg^{2*}-Ba^{2*}, Ca^{2+}-Ba^{2+} and Sr^{2+}-Ba^{2+} systems, only Ba^{2+} in the stationary phase was back-extracted into mobile phase. In contrast, the other metal ion (Mg^{2+}, Ca^{2+} or Sr^{2*}) has been kept into the stationary phase. The other metal ion could be recovered by changing pH of the mobile phase to 1.0. The recovery rate (%) was calculated as follow:

$$\text{Recovery rate (\%)} = \frac{\text{the amount of metal ion in the 5 cm}^3\text{ fraction}}{\text{the total amount of metal ion injected in CPC device}}$$

The measured amounts of metal ions versus the volume of effluent from the CPC device in Mg^{2+}-Ba^{2+}, Ca^{2+}-Ba^{2+} and Sr^{2+}-Ba^{2+} systems are shown in Fig. 3-5. As can be seen from Fig. 3-5, Ba^{2+} could be separated from the other metal ions (Mg^{2+}, Ca^{2+} and Sr^{2*}) in all systems.

From these results, it was found that this method using CPC made efficiently the reaction and may provide an automatic ion separation technique. In addition, the results of solvent extraction presented on Fig. 2 suggest the mutual separation between all investigated alkaline earth metal ions (Mg^{2+}, Ca^{2*}, Sr^{2*} and Ba^{2*}) by using CPC method and step elution.

REFFERENCES

[1] J. Cazes (2001), *Encyclopedia of Chromatography,* Marcel Dekker, New York.

[2] K. Ingkaninan, A. Hazekamo, A. C. Hoek, S. Balconi and R. Verpoorte (2000), *J. Liq. Chromatogra. Related Tech.,* 23, 2195-2208.

[3] T. Wang and Y. Nagaosa (2003), *J. Liq. Chromatogra. Related Tech.,* 26, 629-640.

[4] T. Wang and Y. Kanaosa (2003), *Anal. Lett.,* 36, 441-450.

[5] H. Hoshi, S. Nakamura and K. Akiba (1999), *J. Liq. Chromatogra. Related Tech.,* 22, 1319-1330.

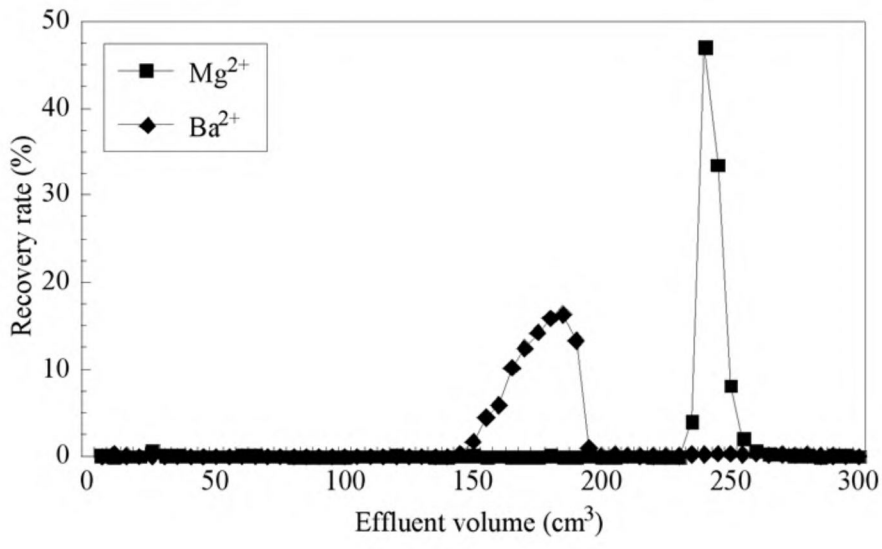


Fig. 3. The measured recovery rate (%) of Mg^{2*} and Ba^{2*} versus the effluent volume (cm^3).

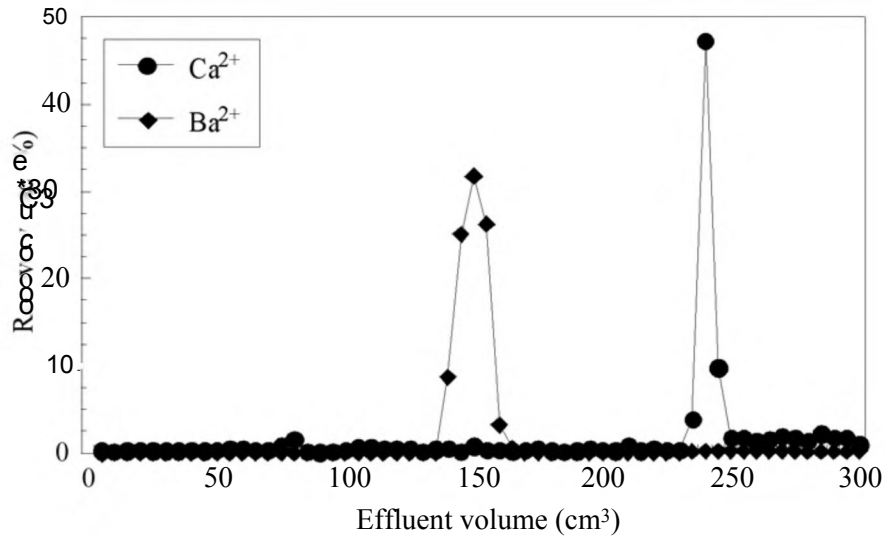


Fig. 4. The measured recovery rate (%) of Ca^{2+} and Ba^{2+} versus the effluent volume (cm^3).

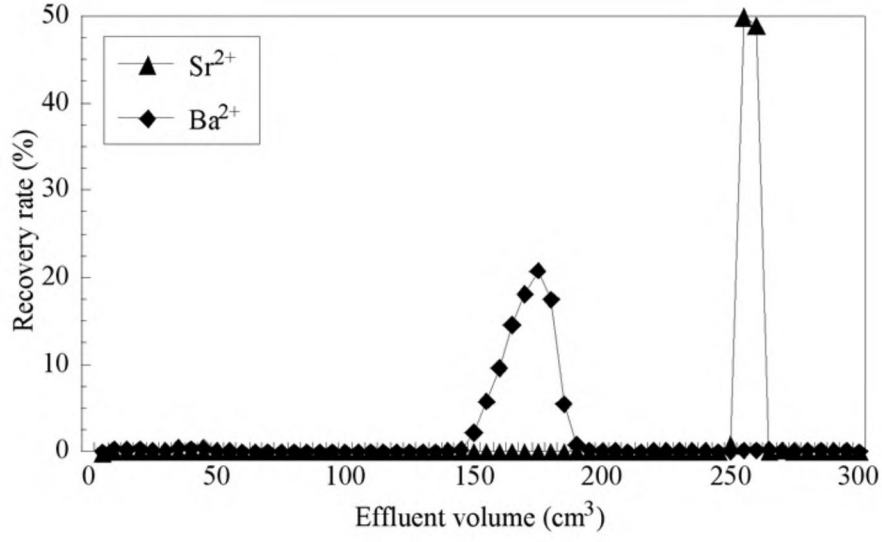


Fig. 5. The measured recovery rate (%) of Sr^{2*} and $E3a^{2+}$ versus the effluent volume (cm^3).



SEPARATION OF COBALT(II) AND NICKEL(II) BY ION-ASSOCIATIO N EXTRACTION WITH CROWN ETHERS FROM POTASSIUM THIOCYANATE MEDIA

Takaharu Honjo*, Cristina T. Camagong and Chisato Kariya

*Kanazawa University, Graduate School of Natural Science & Technology, Kakuma-machi, Kan azawa,
Ishikawa, 920-1192, JAPAN

A new method for the separation of cobalt(ll) and nickel(ll) with 0.01 M crown ether in nitrobe nzene has been established by means of ion-association extraction from KSCN in HCI medi a and back-extrac- tion combined with atomic absorption spectrometry (AAS). When the mixtur es of cobalt(ll) and nickel (II) were extracted with 0.01 M dicyclohexyl-18-crown-6 (DC18C6) for 5 min at 1 M HCI in the pres-ence of 0.05 M KSCN, only cobalt(ll) was extracted quantita tively, whereas nickel(ll) was remained in the aqueous phase. After the phases were separate d by centrifugation at 2, 000 rmp for 5 min, the organ-ic phase was shaken with 1 M $HN0_3$ f or 5 min in order to back-extract cobalt(ll), followed by centrifu-gation at 2, 000 rpm for 5 min. Metl ions were determined by AAS at 240.7 nm for cobalt(ll) and at 232.0nm for nickel(ll), re spectively. In the process, cobalt(ll) in nitrobenzene was found to form stableion-pair complex as $[K(DC18C6)_2]^+ \cdot [Co(SCN)_3]'$ by means of slope analysis. Interference studies of thepresent method revealed a high tolerance (1, 000 times) for most foreign ions investigated except for zinc(ll) and copper(ll) (100 times), and iron(lll) (150 times) among 7 cations and 2 anions. Th e Dro-Dosed method is aoDlicable to the Quantitative seoaration of cobaltflh from nickelfll) (1-1. 000 times) and the analysis of cobalt(ll) traces (1.34 ppm) in $Ni(NQ_3)_2$ reagent.

INTRODUCTION

In general, chemical behaviors of cobalt(H) and nickel(EI) are quite similar, and their analytical mu-tual separations are often difficult. The synergistic extraction separation of cobalt(IT) and n ickel(II) with thenoyltrifluoroacetone (TTA) and crown ethers was found inefficient because of t heir similar ex-traction behaviors [1, 2],

In preliminary experiments, the highest $ApH_{1/2}$ (the difference of the pH of the half extraction) of cobalt(II) and nickel(II) with 0.1 M TTA and 0.01 M crown ether in o-dichlorobenzene was 0.37 when using dicyclohexyl-24-crown-8 (DC24C8) among several crown ethers (0.07 for DC 18C6, 0.14 forB12C4, 0.19 for 12C4, 0.24 for 15C5 and DB18C6, 0.33 for 18C6 and DB24C 8), which is still consid-ered insufficient for the aimed separation.

It is reported that cobalt(II) can be extracted as thiocyanate ion-pair complex with crown ether s (18C6, DB18C6, and DC18C6) in 1,2-dichloroethane and/or nitrobenzene at pH 0-7, and d etermined by absorptiometry at623 nm [3-5].ln preliminary experiments, it was found that cobalt (II) can be highly extracted at pH2.4 as thiocyanate ion-pair complex with dicyclohexyl-18-crow n-6 (DC18C6) among several crown ethers (18C6, DB18C6, DC18C6, and DB24C6) in 1,2-dic hloroethane (100%, ppt.), o-dichlorobenzene (100%), nitrobenzene (100%), benzene (92%), cycl ohexane (92%), toluene (89%), chloroform(76%), and 1-octanol (18%), re-spectively.

On the basis of these facts, a new method for the separation of cobalt(II) and nickel(II) with 0.01 M DC18C6 in nitrobenzene has been established by using ion-association extraction fro m 0.05 M KSCN in 1 M HCI media and back-extraction with 1 M HN03 solution.

EXPERIMENTAL

Apparatus

A Hitachi Atomic Absorption Spectrophotometer equipped with a Zeeman Background Correcto r, model Z-1600 for Flame-AAS (FAAS), a Taiyo Recipro Shaker, model SR-II, a Tomy Seiko Swing TypeCentrifuge, model CD-50R and LC-100, and a Hitachi-Horiba pH meter, model F-12, were used.

Materials

Dicyclohexyl-18-crown-6 (DC18C6) was purchased from Kanto Chemicals Ltd., Japan,, and nitr o-Benzene (reagent grade) from Katayama Chemicals Ltd, Japan. All other chemicals (guarant eed grade)were used without further purification. The organic solvents were handled with care in a fume hood for
safety consideration.

Solvent extraction

Equal volume (5 ml) of an aqueous solution of 0.05 M KSCN in 1 M HCI containing 10 ppm cobalt(II)and 10 ppm nickel(H), and a nitrobenzene solution of 0.01 M DC18C6 were introdu ced into a 30-ml stoppered centrifuge tube. The mixtures were shaken vigorously for 5 min at room temperature. The twophases were centrifuged at 2, 000 rpm for at least 5 min to comp lete the phase separation. For back-extraction, 4 ml of the organic phase was pipetted into an

other centrifuge tube.

Back-extraction

To back-extract cobalt(II) contained in the organic phase (4ml), an equal volume of 1 M HNO 3 solutionwas added into a 30-ml stoppered centrifuge tube, and the mixture was shaken vigo rously for 5 min. Theconcentration of cobalt(D) back-extracted into the aqueous phase was de termined by FAAS at 240.7 nm.

RESULTS AND DISCUSSION

Solvent extraction

When the effect of increasing the amount of DC18C6 was investigated, the results showed th at com-plete extraction (> 95%) of cobalt(II) becomes possible for 0.006-0.05 M DC18C6 in n itrobenzene. For the concentration of 0.0005 M-0.006 M DC18C6, the extraction efficiency of c obalt(ll) decreased sig-nificantly, and 0.01 M DC18C6 in nitrobenzene was used for the subs equent experiment. The extract-ability of cobalt(II) and nickel(II) as a function of an aqueous phase acidity is shown in Figure 1.

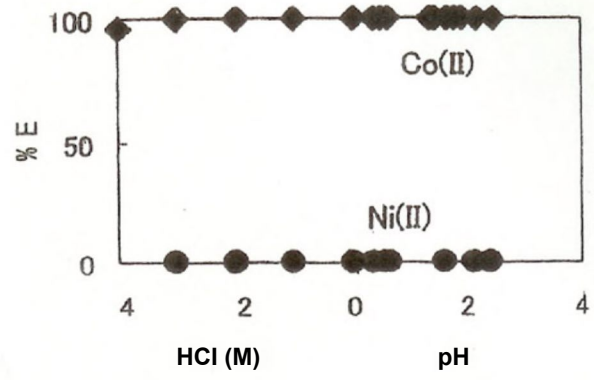


Figure 1. Extraction curve ofCo(U) and Ni(II) with DCI8C6 from KSC.N media in nitrobenzene.

Back-extraction

When the effect of increasing the amount of $HN0_3$ was investigated, the results showed that t he com-plete back-extraction of cobalt(II) becomes possible for 0.8-2.0 M $HN0_3$ solution. For the concentrationof 0.1 M-0.8 M $HN0_3$, the extraction efficiency of cobalt(II) decreased signific antly, and 1 M $HN0_3$ was used for the subsequent experiment.

Effect of shaking time

The optimum shaking time for both forward and backward extraction of cobalt(II) was ascertai ned by measuring the recovery of cobalt(II) after 30 sec-10 min shaking periods. It was foun d that the use of a short time (5 min) shaking for both procedures is sufficient to ensure the

quantitative recovery of cobalt(II). These facts indicate that the extraction equilibrium in the io n-association mechanism of cobalt(II)is rapidly achieved.

Composition of extracted species

The slope analysis method was used to determine the stoichiometry of the extracted species on the ex-traction of cobalt(II) with DC18C6 in nitrobenzene from 0.05 M KSCN in 1 M HCl solution. Except for the concentration of the crown ether in the organic phase, all other conditi ons were held constant. The variation in the distribution ratio, logD, of cobalt(II) with the incre asing concentration of log[DC18C6]o in the organic phase results in a straight line with a slop e of 2. Thus the extracted ion-association product is ascertained as [(DC18C6)2 • K]+[Co(SCN) 3]- •

Effect of foreign ions

The effect of different foreign ions on the extraction of cobalt(II) using the proposed method u nder optimum conditions was then investigated. Interference studies were conducted by adding different amounts of foreign ions to 1 ppm cobalt(II) solution before extraction, and the corre sponding tolerance limit was identified. Recovery data (> 95%) show that a high tolerance (1, 000 times) for most foreign ions investigated except for zinc(ll) and copper(ll) (100 times), and iron(lll) (150 times) among cations such as Li(I), Na(I), K(I), Mg(II), Ca(D), Sr(n), Ba (II), Mn(II), Ni(II), Cd(II), and Pb(II), and anions such as N03- and S042-. These facts c learly indicate the excellent tolerance of the proposed method.

Separation of cobalt(II) and nickel(II)

Separation of cobalt(II) and nickel(II) from their mixtures was made possible by exploiting the differ-ences in their extractability at different aqueous phase acidity. When a sample solution o f pH 3-4 M HClsolution in the presence of 0.05 M KSCN was shaken with 0.01 M DC18C6 i n nitrobenzene, the extrac-tion of cobalt(II) proceeded rapidly and quantitatively, while nickel **(II)** remained in the aqueous phase,as given in Table 1. The proposed method is applicable t o the quantitative separation of cobalt(II) from nickel(II) (1-1,000 times).

Table 1. Selective extraction separation of Co(II) from Ni(II)

Metal added, ppm		Recovery, %	
Co	Ni	Co	Ni
1.0	1	100	0.0
1.0	10	100	0.0
1.0	100	98.4	0.0
1.0	1,000	96.7	0.0

The amount of cobalt in $Ni(N0_3)_2$ of guaranteed grade reagent dissolved in water was found t

o be 1.34 ppm by means of the proposed method.

CONCLUSIONS

A new method for the separation of cobalt(II) and nickel(II) with 0.01 M DC18C6 in nitrobenze ne has been established by means of ion-association extraction from 0.05 M KSCN in 1 M H Cl media and back-extraction with 1.0 M HN03. The optimum conditions involved only a few steps and short equilibrium time within 5 min. In the process, cobalt(II) was found to form sta ble neutral ion-association complex, [(DC18C6)2 • K]+[Co(SCN)3]- in nitrobenzene. Interference studies show that the excellent tolerance (1, 000 times) of the proposed method for most forei gn ions investigated except for zinc(II) and copper(II) (100 times) and iron(III) (150 times), re spectively.

REFERENCES

1. T. Honjo (1997), Bunseki (Review), 1997, 127-136.
2. Cristina T. Camagong, K.Z. Hossain and T. Honjo (2001), *Solv. Extra. Res. Develop*., Japa n, 8, 63-73.
3. M. Yoshio, M. Ugamura, H. Noguchi and M. Nagamatsu (1978), *Anal. Letters*., A11(4), 28 1-286.
4. S. Xu, M. Chen, Z. Den. and G. Pang (1998), *J. Sichuan Univ.* (Natural Science Edition), 35, 137-140.
5. M. Chen, J. Zhou, and S. Xu (1999), *J. Sichuan Univ.* (Natural Science Edition), 36, 605-6 08.

SEPARATION OF YTTRIUM(III) AND STRONTIUM(II) BY SYNERGISTC EXTRACTION WITH THENOYLTRIFLUOROACETONE AND CROWN ETHERS

Takaharu Honjo*, Tomokazu Tsuchiya, Tomoaki Kondo and Kaji Zakir Hossain

'Kanazawa University, Graduate School of Natural Science & Technology, Kakuma-machi, Kan azawa,
Ishikawa, 920-1192, JAPAN

A new method for the separation of yttrium(III) and strontium(II) with 0.1 M thenoyltrifluoroacetone (TTA) and 0.01 M crown ether in benzene has been established by means of synergistic extraction and back-extraction combined with inductively coupled plasma atomic emission spectrometry (ICP-AES). When the mixtures of yttrium(III) and strontium(II) were extracted with 0.1 M TTA and 0.01 M dibenzo-18-crown-6 (DB18C6) for 5 min at pH 4.0 (acetate buffer solutions), only yttrium(III) was extracted quantitatively, whereas strontium(II) was remained in the aqueous phase. After the phases were separated by centrifugation at 2, 000 rmp for 5 min, strontium(II) was extracted quantitatively with 0.1 M TTA and 0.01 M dicyclohexyl-18-crown-6 (DC18C6) in place of 0.01 M DB18C6 for 5 min at pH 5 (ace-tate buffer solutions) again. Then, the two phases were each shaken with 0.1 M HCl for 5 min in order to back-extract yttrium(III) and strontium(II), and were centrifuged at 2, 000 rpm for 5 min; both metalions were determined by ICP-AES at 371.029 nm for yttrium(III) and at 407.8 nm for strontium(II), respectively. In the process, yttrium(III) and strontium(II) TTA chelates in benzene were found to form stable adducts as YfTTA13DB18C6 with DB18C6 and Sr(TTA)2DC18C6 with DC18C6 by means of slope analysis. Interference studies of the present method revealed a high tolerance (500-1, 000 times) for most foreign ions investigated except for iron(III) (10 times, ppt.) among 18 cations and 3 anions in yttrium(III) and for aluminium(III) (50 times, ppt.) among 8 cations and 5 anions in strontium(II), respectively.The proposed method is applicable to the quantitative separation of yttrium(III) from strontium(II) (1-1, 000 times).

INTRODUCTION

“Y is produced from its parent ^Sr according to the decay process (G= 0.5 MeV, $t_{1/2}$ = 28.9 y). Analysis of ^Sr and in environmental samples is complicated because of their pure G emitters, and their quantitation must be preceded by chemical separation. Radioisotope “V has also been recognized as nuclear medicine for tumor therapy studies.

High-purity and carrier-free “V can be separated from ^Sr by solvent extraction with 0.01 M i onizable crown ethers in chloroform at pH 6.5 [1],

In a previous work, a new method for the separation of lanthanum(III) and barium(II) as their thenoyltrifluoroacetone (TTA) complexes with dibenzo-18-crown-6 (DB18C6) in o-dichlorobenze ne has been established [2, 3], and this method was applicable to the selective extraction of ^La from ^{140}Ba parent. Now, the present authors report a new method for the mutual separati on of Y(III) and Sr(II) with TTA involving DB18C6 , followed by using DC18C6 in benzene b y synergistic extraction and back- extraction by 0.1 M HCI solution.

EXPERIMENTAL

Apparatus

A Shimadzu Sequential Type Plasma Emission Spectrometer ICP-1000 III(Kyoto, Japan), a Tai yo Recip-ro Shaker, model SR-II, a Tomy Seiko Low Speed Centrifuge, model LC-100, and a Hitachi-HoribapH meter, model F-12, were used.

Materials

TTA (reagent grade) was purchased from Dojindo Chemicals Ltd., Japan. Dibenzo-18-crown-6 (DB18C6) and dicyclohexyl-18-crown-6 (DC18C6) obtained from MERCK-Schuchardt, Germany, were used without further purification. The organic solvents were handled with care in a fume hood for safety consideration.

Solvent extraction

An aliquot (10 ml) of a sample solution containing each of yttrium(III) (1 ppm) and strontium(II) (0.5 ppm), and buffer solution (0.05 M ammonium acetate buffer) was taken into a 30 ml glass-stoppered centrifuge tube. The solution was then adjusted to the desired pH value by the addition of 0.05 M HCI and/or 0.05 M NH3 solution. A 10 ml of the benzene solution containing 0.1 M TTA and 0.01 M crown ether was added to the centrifuge tube, and the mixtures were shaken on a shaking machine for 5 min. The two phases were separated by centrifugation at 2, 000 rpm for 5 min, and then the organic phase was taken by pipetting into another centrifuge tube for back-extraction. The equilibrium pH of the aqueous phase

was determined again after the extraction.

Back-extraction

The organic phase (7 ml) containing each of the extracted yttrium(III) and strontium(II) was shaken with 7 ml of 0.1 M HC1 solution for 5 min in order to back-extract yttrium(III) and strontium(II).The amount of metals stripped from the organic phase was determined by ICP-AES at 371.029 nm for yttrium (III) and at 407.8 nm for strontium (II), respectively.

RESULTS AND DISCUSSION

Synergistic extraction

The extraction of yttrium(III) was quantitative (> 95%) using a combination of TTA and DB18C6 in benzene. The extraction curves of yttrium(III) and strontium(II) with a combination of TTA and DB18C6 in benzene are shifted to a more acidic region (synergistic extraction) than in the case of TTA alone, are shown in Figure 1. Strontium(II) was hardly extracted with TTA alone at various pH values. The difference in the extraction efficiency as a function of pH for yttrium(III) and strontium(II) clearly shows that a nearly quantitative separation of these metal ions is possible at pH 4.0. In preliminary experiments, it was found that the pH1/2 (the pH of the half extraction) of strontium(II) with 0.1 M TTA involving 0.01 M crown ether in benzene increases in the order of DC18C6 (3.4) < 18C6 (4.8) < 15C5 (5.9) < DB24C8 (6.0) < DB18C6 (6.2) < 12C4 (6.6), respectively. Then, DC18C6 having lower extraction pH region was used for the subsequent experiment of strontium(II).

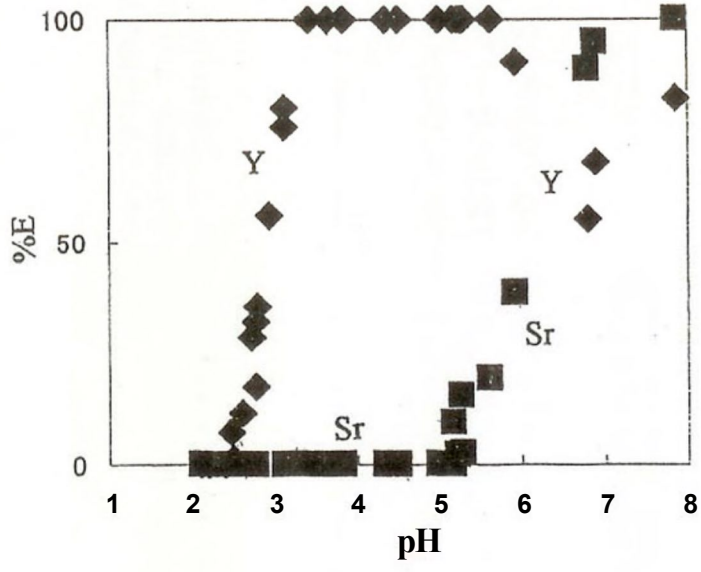


Figure 1. Extraction curve ofY(HI) cmd Sr(JJ) with TTA with or without DB18C6 in benzene.

Effect of shaking time

The optimum shaking time required to reach the extraction equilibrium was ascertained by measuring the recovery of yttrium(III) and strontium(II) for various shaking time (0-10 min) at pH 2.9 and pH 4.0 for yttrium(III), and at pH 5 for strontium(II). It was found that the extraction equilibrium is attained rapidly within 1 min. The stripping of each of yttrium(III) and strontium(II) from the organic phase by 0.1 M HCI was also fast and completed within 1 min. Then, a 5 min shaking was adopted as shaking time for the complete extraction and back-extraction of yttrium(III) and strontium(II), respectively.

Composition of extracted species

The composition of extracted species in organic phase was ascertained by plotting logD vs. pH (slope = 2.9), logD vs log[TTA]o (slope = 2.8), and logD vs. log[DB18C6]o (slope = 0.9) at fixed pH 2.9 for yttrium(III) and by plotting logD vs. pH (slope = 2), logD vs. log[TTA]o (slope = 2), and logD vs. log[DC18C6]o (slope = 1) at fixed pH 4.0 for strontium(II) by slope ratio method. It was found that yttrium(III) and strontium(II) TTA chelates in benzene form stable adducts with crown ethers as Y(TTA)3(DB18C6) and Sr(TTA)2(DC18C6), respectively.

Effect of foreign ions

The effect of foreign ions on the extraction of yttrium(III) using the proposed method under the optimum conditions was then investigated. Interference studies were conducted by adding different amounts of foreignions to 1 ppm yttrium(III) solution before extraction, and the corresponding tolerance limit was identified. Recovery data (> 95%) show that a high tolerance (> 500 times) for most foreign ions investigated except for Fe(lll) (10 times, ppt.) among cations such as Na(I), K(I), Mg(II), Ca(II), Ba(II), Mn(II), Co(II), Ni(II), Cu(II), Zn(II), Cd(II), Pb(II), Al(III) (ppt.), Sc(III), La(III), Ce(III), and Yb(III) and anions such as Cl- , N03-, and S042- in yttrium(lll) and for Al(lll) (50 times, ppt.) among cations such as Na(I), K(I), Mg(II), Ca(II), Ba(II), and Fe(III) (ppt.), and anions such as Cl-, N03-, C032-, HP042-, and S042- in strontium(ll), respectively. These results clearly indicate the excellent tolerance of the proposed method.

Separation of yttrium(III) and strontium(II)

Separation of yttrium(III) and strontium(II) from their mixtures was made possible by exploiting the differences in their extractability at different aqueous phase acidity. The separation of yttrium(III) and strontium(II) by synergistic extraction with TTA and DB18C6 in benzene is given in Table 1.

When a sample solution adjusted to pH 4.0 was shaken with 0.1 M TTA and 0.01 M DB18C 6, the extraction of yttrium(III) proceeded rapidly and quantitatively, while strontium(II) remaine d in the aqueousphase. After the phases were separated, the aqueous phase containing stront ium(II) was again adjusted to pH 5 and shaken with 0.1 M TTA and 0.01 M DC18C6 in ben zene. The extraction of strontium(II) also proceeded rapidly and quantitatively. Then, the two

Table 1. Selective extraction separation of Y(III) from Sr(H)

Metal added, ppm		Recovery, %	
Y	Sr	Y	Sr
1.0	1	100.6	0.00
1.0	10	100.0	0. 00
1.0	100	100. 1	0.01
1.0	1,000	100.2	0. 03

phases were respectively shaken with 0.1 M HCI in order to back-extract these metals from the organic phases. The proposed method is applicable to the quantitative separation of yttrium(lll) from strontium(II) (1-1000 times).

CONCLUSIONS

A new method for the separation of yttrium(lll) and strontium(II) with TTA involving DB18C6, followed by using DC18C6 in benzene has been established by means of synergistic extraction and back-extraction by HCI solution. The optimum conditions involved only a few steps and short equilibrium times within 5 min. In the process, yttrium(III) and strontium(II) TTA chelates in benzene were found to form stable adducts as Y(TTA)3(DB18C6) and Sr(TTA)2(DC18C6), respectively. Interference studies of the present method revealed a high tolerance (> 500 times.) for most foreign ions investigated except for iron(III) (10 times, ppt.) in yttrium(III) and for aluminum(III) (50 times, ppt.) in strontium(II), respectively.

REFERENCES

1. D. J. Wood, S. Elshani, H. S. Du, N. R. Natale and C. M. Wai (1993), *Anal. Chem.,* 65, 1350-1354.
2. T. Honjo (1997), *Bunseki (Review),* 1997, 127-136.
3. T. Tsuchiya and T. Honjo (2000), *Bunseki Kagaku.,* 49, 895-899.

EQUILIBRIUM AND MASS SPECTROMETRIC STUDIES ON THE ION-PAIR EXTRACTION OF ANTIMONY(III) AND ANTIMONY(V) WITH PYROGALLOL AND TETRAPHENYLARSONIUM CHLORIDE

Hisanori IMURA, Natsuki INAZUMI, Akira OHASHI, Kousaburo OHASHI

Department of Environmental Sciences, Faculty of Science,
Ibaraki University, Mito, 310-8512 Japan

A novel extraction system with pyrogallol (H_3PG) and tetraphenylarsonium (TPA^+) in 1,2-dichloroethane has been studied for Sb(III) and Sb(V). Sb(III) was quantitatively extracted from the aqueous phase containing 0.20 M H_3PG at pH 3-4 into the organic phase of 0.0010 M TPACI. The extraction and the back-extraction equilibrium were readily attained within 1 min. The equilibrium analysis indicated the formation of an ion-pair complex, $TPA^+Sb(HPG)_2$\ which was supported by electrospray ionization mass spectrometry (ESI-MS). On the other hand, Sb(V) was quantitatively extracted from 2-8 M sulfuric acid solutions containing 0.20 M H_3PG to the organic phase of 0.0010 M TPACI, but the extraction was much slower than that of Sb(III). Additionally, the back-extraction behavior of Sb(V) was quite different from that of Sb(III). Sb(V) extracted from 4.0 M sulfuric acid was not stripped with 2.0 M sulfuric acid, while completely stripped with 2.0 M perchloric acid. The equilibrium and ESI-MS study revealed the extraction of TPA^+-$Sb(HPG)_3$' and $TPA^+Sb(HPG)_2(OH)_2$\ Sb(V) can be quantitatively separated from Sb(III) in 4-6 M sulfuric acid.

INTRODUCTION

Antimony occurs in both the trivalent and pentavalent states as the stable oxidation states in the environment. Extraction and separation of Sb(III) and Sb(V) have been investigated in various systems based on the formation of chelates or ion association complexes. Especially, the extraction of Sb(III) has been thoroughly studied using chelating extractants such as A/-benzoyl-/V-phenylhydroxylamine [1-3], diethylammonium diethyldithiocarbamate [4], ammonium pyrroridinedithiocarbamate [5, 6], potassium ethylxanthate [7], and 0,0'-Diethyl dithiophosphate [8], Besides chelates, simple halides such as $SbBr_3$ [9] and SbI_3 [10] are selectively extracted into nonpolar solvents.

On the other hand, little is known about the extraction of Sb(V), which is only based on the formation of $SbCl_6$' in hydrochloric acid. Sb(V) was extracted as an ion-pair of $SbCl_6$' with cationic dyes such as rhodamine B [11] and thiazolyl blue [12] from 3-8 M (1 M = 1 mol dm'^3) hydrochloric acid or with oxonium solvated with isopropyl ether from 6.5-8.5 M hydrochloric acid [13], However, the reduction of Sb(V) during the extraction has to be prevented with appropriate oxidising agents.

In the present paper, the extraction of both Sb(III) and Sb(V) were studied in detail with pyrogallol (H_3PG) and tetraphenylarsonium chloride (TPACI) into 1,2-dichloroethane. The equilibrium analysis was performed to clarify the composition of the extracted species of Sb(III) and Sb(V). Furthermore, electrospray ionization mass spectrometry (ESI-MS) was

applied to the extracts of Sb(III) and Sb(V) to get the direct evidence of the composition of the Sb(III)- and Sb(V)-pyrogallol complexes.

EXPERIMENTAL

Reagents and Apparatus

A stock solution of Sb(III) was prepared by dissolving high-purity metal (Mitsuwa, 5N+% purity) with concentrated sulfuric acid and diluting with water to be a 3 M sulfuric acid solution. A stock solution of Sb(V) was prepared by dissolving the high-purity metal with aqua regia, evaporating to dryness after addition of sulfuric acid, and redissolving with 3 M sulfuric acid solution. Redox titration with potassium bromate was used to ascertain that the Sb(III) content in the Sb(V) solution was negligible small (< 1%). H_3PG (Kanto, 99.0% purity) was used as obtained. TPACl hydrate (ACROS, 99% purity) was dried over P_4Oi_0 in a desiccator in vacuo. 1,2-Dichloroethane (Kanto, 99.5% purity) was used as obtained.

An ICP atomic emission spectrophotometer (ICP-AES, Nippon Jahrel Ash, ICAP-575) was used for the determination of Sb(III) and Sb(V) in aqueous solutions at 217.581 nm. An ESI-MS (Waters, Platform LCZ) at negative ion mode was used for the measurement of molecular mass of anionic Sb(III) and Sb(V) complexes extracted. The organic phase was diluted with acetonitrile to be (1.0-2.5) x 10^{-5} M Sb(III) or (2.5-5.0) x $10'^{5}$ M Sb(V) in the test sample.

Procedure

An organic phase of 1 x 10^{4}-3.0 x $10'^{3}$ M TPACl was shaken with an aqueous phase containing 2.0 x $10'^{5}$-2.0 x $10'^{1}$ M H_3PG and 5.0 x $10'^{5}$-1.0 x $10'^{4}$ M Sb(III) or 2.0 x $10'^{5}$-2.0 x $10'^{4}$ M Sb(V) in 1 x $10'^{4}$-8 M sulfuric acid for 1min-6 h. After centrifugation, an aliquot of the aqueous phase was taken out, and the Sb(III) or Sb(V) concentration was determined with ICP-AES. The Sb(III) or Sb(V) concentration in the organic phase was determined in the same manner after the stripping of Sb(III) or Sb(V) with 2 M perchloric acid. The percent extraction (%E) and the distribution ratio (D) of Sb(III) or Sb(V) were calculated from the concentrations in both phases. All the procedures were done in a thermostated room at 25°C.

In the back extraction, the organic phase prepared above was shaken with 2.0-8.0 M sulfuric acid or 0.10-2.0 M perchloric acid at varying intervals. The percent back-extraction ($\%E_b$) and the *D* were determined in the same manner as mentioned above.

RESULTS AND DISCUSSION

Extraction of Sb(III)

The extraction of Sb(III) with 0.20 M H_3PG and 0.0010 M TPACl was carried out by equilibrating the two phases for 30 min. The *%E* was independent of the shaking time during 1-240 min. The extraction curve of Sb(III) is shown in Fig. 1 together with the back-extraction curve with sulfuric acid. Sb(III) is quantitatively extracted above pH 2 and quantitatively back-extracted with 2-8 M sulfuric acid as expected. Thus the extraction equilibrium was readily attained under the given conditions.

To understand the extraction equilibrium of Sb(III) the following analysis was considered. Since Sb(III) occurs as $Sb(OH)_2^+$ or $Sb(OH)_3$ in acidic aqueous solutions [14],

$$Sb(OH)_2^+ + mH_3PG + nTPA^+ = n(TPA^+)\text{-}Sb(HPG)_m^{n-}{}_{org} + 2H_20 + 2(m\text{-}1)H^+, \quad (1)$$

where the subscript, org, stands for the organic phase. The extraction constant is defined by

$$K_{ex} = \frac{\mathbf{KTPA^+J\text{-}}\ Sb(HPG)/Xg[H^+]^{2(\wedge}}{[Sb(OH);][H_3PG]"\ \mathbf{[TPA^+r}} \quad (2)$$

When the distribution ratio of Sb(III) is written by

$$D = \frac{[/?(TPA^*)\text{-}Sb(HPG)_m"\tilde{}]_{org}}{[Sb(OH)^+_2]}, \quad (3)$$

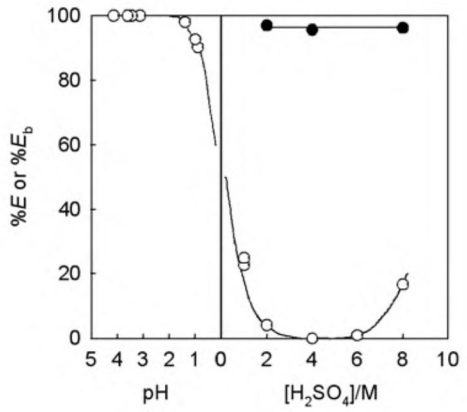


Figure 1. Extraction ofSb(lll) with 0.20 M H_3PG and 0.0010 M TPACI. Shaking time=30 min. t, *Forward extraction;* n, *back extraction.*

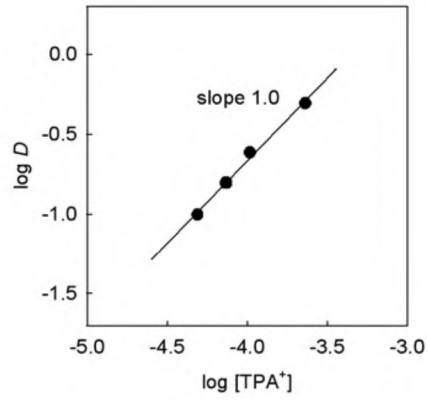


Figure 2. Distribution ratio of Sb(lll) as a functionof the TP A concentration in the aqueous phase. 0.20 M H_3PG, 1.0 M H_2S0_4, shaking time = 60 min.*

the following equation is obtained from Eqs. (2) and (3),

$$\log D = m\log [H_3PG] + n\log [TPA^+] - 2(m-1)\log [H^+] + \log K_{ex} \quad (4)$$

Figure 2 shows the plot of log *D* vs. log [TPA^+], where the TPA^+ concentration in the aqueous phase was calculated by subtracting the organic concentration of TPA^+ determined by UV spectrophotometry from the total concentration. A straight line with a slope of unity is obtained, indicating the formation of a 1:1 ion pair between TPA^+ and an anionic Sb(III)-pyrogallol complex. The same result was also obtained by molar ratio method for the determination of composition of the ion pair under the following conditions; the Sb(III) concentration ranged from 1.8 x 10'6 to 6.1 x 10'5 M against a constant concentration of 1.0 x 10'5 M TPACI in the presence of 0.20 M H_3PG at pH 2.9-3.1.

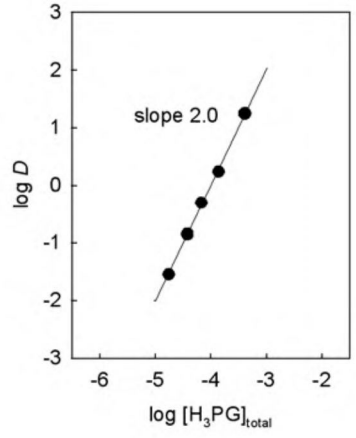


Figure 3. Distribution ratio ofSb(lll) as a function of the total concentration ofH/>G at pH 3.0. 0.0010 M TPACI, 0.0013 M HSO;, 0.017 M SO.²'.

In order to determine the composition of the anionic Sb(III)-pyrogallol complex, the plot of log *D* vs. log [H_3PG] based on the Eq.(4) is shown in Fig. 3, where the total concentration of H_3PG was used instead of the aqueous concentration because of its distribution constant as low as 10-177. The plot gives a straight line with a slope of 2.0 and indicates the formation of a 1:2 complexes of Sb(III) with H_3PG. Considering the structure of H_3PG, the complexation should occur at the adjacent two hydoxy oxygen atoms of H_3PG, so that the anionic Sb(III) complex, $Sb(HPG)_2$\ is formed as was expected in Eq. (1). These results are supported by the study of ESI-MS for the Sb(III) extract as described later.

Extraction of Sb(V)

The extraction of Sb(V) with 0.20 M H_3PG and 0.0010 M TPACI was carried out by shaking the two phases for 30-300 min. Figure 4 shows the extraction curves of Sb(V) at the different shaking times. Sb(V) was quantitatively extracted by shaking for 30 min from 4-8 M sulfuric acid and for 240 min from 2-8 M sulfuric acid. On the other hand, Sb(V) extracted was not stripped with 4-8 M sulfuric acid. Thus, the extraction behavior of Sb(V) was quite different from that of Sb(lll).

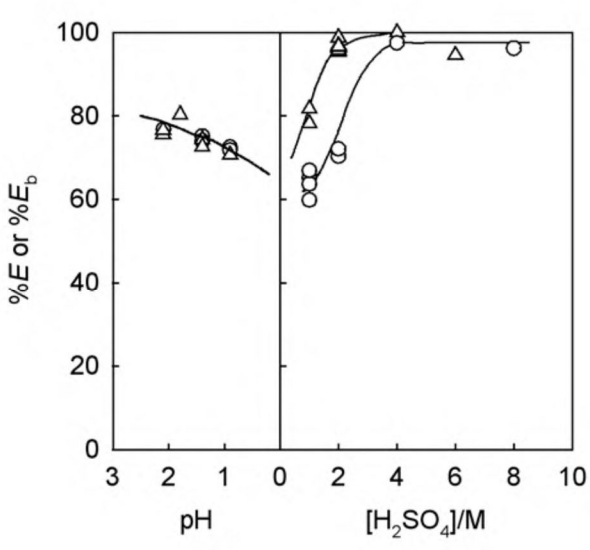


Figure 4. Extraction of Sb(V) with 0.20 M H_3PG and 0.0010 M TPACI.
(i., ***shaking time = 30 min; shaking time = 240 min.***

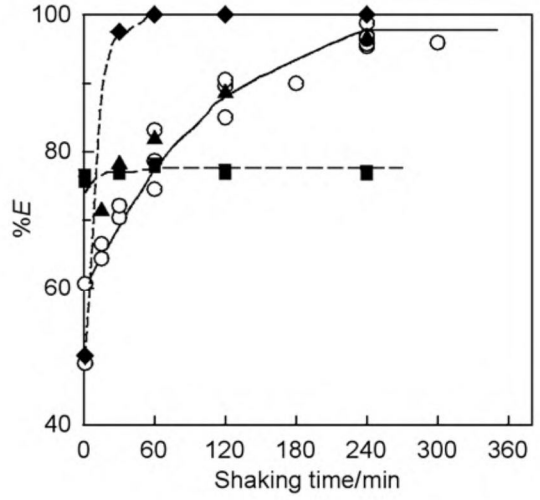


Figure 5. Effect of the shaking time on the extraction of Sb(V) with 0.20 M H_3PG and 0.0010 M TPACI.
W, ***0.10 M H_2S0_4;*** y, ***2.0 M H_2S0_4;***
н, 4.0 M H_2S0_4; £ successive extraction at 2.0 M H_2S0_4.

Figure 5 shows the effect of the shaking time on the extraction of Sb(V) with 0.20 M H_3PG and 0.0010 M TPACI at different sulfuric acid concentrations. The extraction rate is evidently dependent on the acidity of the aqueous phase. In the case of 0.1 M sulfuric acid, the extraction rate is so high that the equilibrium seems to be attained within 1 min although the extractability is lowest after the equilibration. In 2.0 and 4.0 M sulfuric acid, the rate is much lower than that at 0.1 M sulfuric acid. Such differences in the extraction rate were associated with the composition of Sb(V)-pyrogallol complexes to be extracted.

The back extraction behavior of Sb(V) which was extracted with 0.20 M H_3PG and 0.0010 M TPA^+ at various acidities and shaking times was studied using 2.0 M sulfuric acid without H_3PG. $\%E_b$ was confirmed to be constant at the shaking time of more than 15 min. As shown in Table 1, $\%E_b$ highly

Table 1. Back extraction behavior ofSb(V) with 2.0 MH_2SO_4.

Forward extraction*			%£„[b]
Acidity	Shaking time/min	%E	
pH 2.1	1	77	56
	30	77	55
	60	78	52
	120	77	53
	240	77	53
1.0 M H_2S0_4	1	59	44
	30	62	36
	60	64	31
	120	71	22
	240	79	14
2 .0 M H_2S0_4	1	61	23
	30	72	13
	60	79	8
	120	90	4
	240	97	0.3
4.0 M H_2S0_4	1	50	2
	30	97	0
	60	100	0
	120	100	0
	240	100	0

"Conditions: 0.20 M H_3PG, 0.0010 M TPACI.
"Shaking time = 15 min.

depends on the forward extraction conditions such as the acid concentration and the shaking time. The extraction rate at pH 2.1 is so high that the extraction equilibrium attained within 1 min, and only about 55% portion of the extract is readily back-extracted with 2.0 M sulfuric acid. This means that there is a Sb(V) species which is not stripped with 2.0 M sulfuric acid. On the other hand, in 1.0-4.0 M sulfuric acid the extraction rate is low as was shown in Fig. 5, and the longer the shaking time in the forward extraction, the lower the $\%E_b$ in the back extraction with 2.0 M sulfuric acid. Especially, Sb(V) extracted from 4 M sulfuric acid is not stripped at all. Therefore, these results strongly suggest the existence of the two kinds of the Sb(V) species extracted into the organic phase; one is rapidly extractable but unstable to the 2 M sulfuric acid, another is slowly extractable but quite stable.

To clarify the composition of the ion pair between TPA^+ and Sb(V)-pyrogallol complexes, the back extraction with perchloric acid was studied since the perchlorate ion has a strong tendency to form the ion pair with TPA^+ and should compete with anionic Sb(V)-pyrogallol complexes. Figure 6 shows the effect of the perchloric acid concentration and the shaking time on the back extraction of Sb(V), which was prepared by the prolonged equilibration until 240 min from 2 M sulfuric acid, and hence it is stable to 2 M sulfuric acid. $\%E_b$ at varying acidities keeps almost constant during first 30 s, and then gradually increases with increase in the shaking time. This behavior can be ascribed to the rapid back extraction of the anionic Sb(V) complex caused by the anion exchange with perchlorate ion toward TPA^+ in the organic phase, and followed by the slow decomposition of the Sb(V)-pyrogallol complex in 2 M perchloric acid solution.

The rapid equilibrium of the back extraction with perchlorate was considered as the following ion exchange mechanism,

$$n(TPA^+)\text{-}Sb(HPG)^{*n'}{}_0rg + r?ClO_4{}' = Sb(HPG)^{\wedge} + r_7TPAClO_4.org \quad (5)$$

$$K_{ex,b} = \frac{[Sb(HPG)''_k][TPAClO_4];\ {}^{n}{}_{org}}{[n\ (TPA^+) \bullet Sb(HPG)£']_{org}[ClO_4^-]^n}. \quad (6)$$

When the distribution ratio of Sb(V) is written by

$$D = \frac{[n\ (TPA^{\pm}) \bullet Sb(HPG)\%\sim]_{org}}{[Sb(HPG)''_k]}, \quad (7)$$

the following equation is obtained from Eqs. (6) and (7),

$$\log D = -n\log [ClO_4'] + n\log [TPAClO4]_{0rg} - \log K_{ex\cdot b}, \quad (8)$$

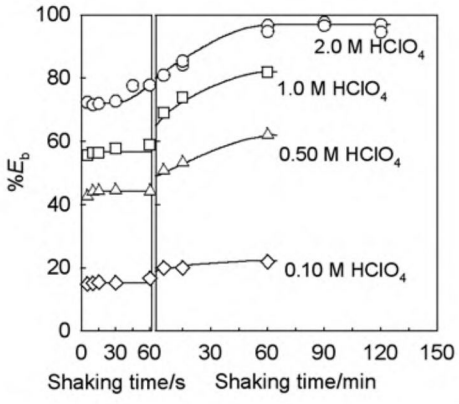


Figure 6. Effect of the shaking time on the back extraction of Sb(V) with 0.10-2.0 M $HCl0_4$. Forward extraction conditions: 0.20 M HjPG, 0.0010 M TPACI, 2.0 M H_2S0_4, shaking time = 240 min.

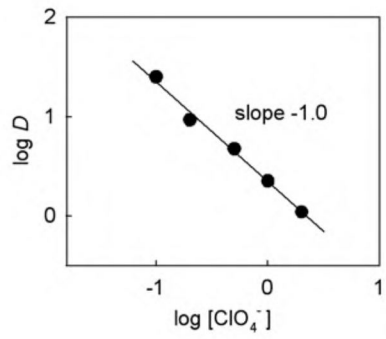


Figure 7. Distribution ratio of Sb(V) as a function of the $Cl0_4^-$ concentration in the aqueous phase at pH 1.3 and I = 2.0 M (Na, H)($S0_4$, $HS0_4$, CIOJ. Forward extraction conditions: 0.20 M H_3PG, 0.0010 M TPACI, 2.0 M H_2S0_4, shaking time= 240 min.

where the concentration of TPACIO4 in the organic phase is approximately constant because a large excess of $Cl0_4^-$ was used and should be extracted to form the ion pair with a constant but lower concentration of TPA^+. Figure 7 shows the plot of log D vs. log [$Cl0_4$] at a constant ionic strength. A straight line with a slope of unity is obtained, indicating the formation of a 1:1 ion pair between TPA^+ and a Sb(V)-pyrogallol complex.

ESI-MS study for Sb(III) and Sb(V) extracts

To **Obtain** a direct experimental evidences for the anionic Sb(lll,V)-pyrogallol complexes described above, the ESI-MS technique was applied to the respective extracts. The results are summarized in Table 2. Since Sb has two isotopes, ^{121}Sb and ^{123}Sb, of which the % abundance is 57.36 and 42.64 respectively, the mass spectrum of the complex is expected to give two m/z in a 57 : 43 ratio. Table 2 shows that the ratio of the inten-sity for each m/z is consistent with the theoretical value within the resolution of the spectrometer or measurement errors.

Table 2. Identification of Sb(lll)- and Sb(V)-pyrogallol complexes by ESI-MS.

Sample	Found	m/z[a] observed		Relative intensity[11]		Ratio of intensity
		^{121}Sb	^{123}Sb	$^{12.}Sb$	^{123}Sb	$^{12.}Sb$ / ^{123}Sb
A	$Sb(HPG)_2$‘	368.6-369.2	370.6-371.2	20000	16000	55/45
B	$Sb(HPG)_2(OH)_2$‘	402.3-403.2	404.3-405.1	470	420	53/47
	$Sb(HPG)_3$-	492.4-493.2	494.2-4952	18000	18000	50/50
C	$Sb(HPG)_2(OH)_2$'	402.7-403.2	404.4-405.3	27000	23000	54/46
	$Sb(HPG)_3$-	492.1-493.0	494.1-495.1	2000	1800	52/48

A, Sb(lll) extracted with 0.20 M H_3PG and 0.0010 M TPA* from 0.10 M H_2S0_4 by shaking for 15 min;
B, Sb(V) extracted with 0.20 M H_3PG and 0.0010 M TPA* from 2.0 M H_2S0_4 by shaking for 4 h;
C, Sb(V) extracted with 0.20 M H_3PG and 0.0010 M TPA* from 1.0 M H_2S0_4 by shaking for 1 min.
“Mass to charge ratio; "total intensity.

In the mass spectrum of Sb(lll) (the sample A in Table 2), there was only a couple of m/z corresponding to the molecular weights of 368.94 and 370.94, which demonstrate the formation of $^{121}Sb(HPG)_2$' and $^{123}Sb(HPG)_2$' respectively. The same was true for the extract of Sb(lll) at pH 3.0 and completely agreed with the result obtained in Fig. 3. On the other hand, the mass spectra of Sb(V) significantly depended on the extraction conditions. The sample B was prepared by shaking 2.0 M sulfuric acid solution of Sb(V) with the organic phase for 4 h, and consequently Sb(V) extracted is stable toward 2 M sulfuric acid. This sample gives the strong peaks corresponding to the molecular weight of 492.95 and 494.95

for $^{121}Sb(HPG)_3$' and $^{123}Sb(HPG)_3$‘ respectively as well as much weaker ones, the molecular weight of 402.94 and 404.94 for $^{121}Sb(HPG)_2(OH)_2$‘ and $^{123}Sb(HPG)_2(OH)_2$' respectively. The sample C was prepared by shaking 1.0 M sulfuric acid solution of Sb(V) with the organic phase for 1 min. Hence, the extract must contain the Sb(V) species unstable to 2 M sulfuric acid. The mass spectrum indicates the strong peaks corresponding to $^{121}Sb(HPG)_2(OH)_2$' and $^{123}Sb(HPG)_2(OH)_2$‘ and the weaker ones, $^{121}Sb(HPG)_3$‘ and $^{123}Sb(HPG)_3$'. Therefore, it can be concluded that the stable Sb(V) complex was $Sb(HPG)_3$‘ but the unstable one, $Sb(HPG)_2(OH)_2$\

CONCLUSIONS

Sb(lll) and Sb(V) could be quantitatively extracted with H_3PG and TPACI from acidic aqueous solutions and mutually separated. The ESI-MS combined with the equilibrium analysis was successfully applied to the determination of the extracted species, i.e., ion-pair complexes, TPA^+-$Sb(HPG)_2$' for Sb(lll) and TPA^+-$Sb(HPG)_3$‘ and TPA^+-$Sb(HPG)_2(OH)_2$‘ for Sb(V).

REFERENCES

1. S. Garbos, E. Bulska, A. Hulanicki, Z. Fijalek and K. Soltyk (2000), *Spectrochim. Acta,* B55, 795.
2. S. Han-wen, S. Xian-quan and N. Zhen-ming (1982), *Talanta,* 29, 589.
3. S. J. Lyle and A. D. Shendrikar (1966), *Anal. Chim. Acta,* 36, 286.
4. T. Honjo and H. Imura (1988), *Fresenius Z. Anal. Chem.,* 330, 711.
5. S. Garbos, M. Rzepecka, E. Bulska and A. Hulanicki (1999), *Spectrochim. Acta,* B54, 873.
6. K. Subramanian and J. C.Meranger (1981), *Anal. Chim. Acta,* 124, 131.
7. E. M. Donaldson and E. Mark (1982), *Talanta,* 29, 663.
8. K. Hayashi, Y. Sasaki, S. Tagashira, Y. Soma and S. Kato (1986), *Anal. Sci., 2,* 347.
9. A. P. Grimanis and I. Hadzistelios (1968), *Anal. Chim. Acta,* 41, 15.
10. A. R. Byrne and D. Gorenc (1972), *Anal. Chim. Acta,* 59, 81.
11. R. E. V. Aman, F. D. Hollibaugh and J. H. Kanzelmeyer (1959), *Anal. Chem.,* 31, 1783.
12. A. V. Alexandrov, S. Kostova and J. Hala (1982), *Talanta,* 29, 795.
13. F. C. Edwards and A. F. Voigh (1949), *Anal. Chem.,* 21, 1204.
14. C. F. Baes, Jr. and R. E. Mesmer (1976), *“The hydrolysis of cations",* John Wiley & Sons, New York, 370 pp.

EXTRACTION AND ELECTROLYSIS RECOVERY OF GOLD FROM ALKALINE CYANIDE SOLUTIONS

Weijin Zhou[1], Weihong Li[1], Jiaxun Tao[1], Yong Zhou[2], Jun Yang[1], Hongcheng Gao[1], Jing Chen[2], Nai Shi[1], Jinguang Wu[1]*, Guangxian Xu[1]

[1]State Key Laboratory of Rare Earth Materials Chemistry and Applications, College of Chemistry and Molecular Engineering, Peking University, Beijing 100871, P. R. China
[2]Kunming Institute of Precious Metals, Kunming 650221, P. R. China

ABSTRACT

The extraction of gold from alkaline cyanide and cetyltrimethylammonium bromide (CTMAB) solution by TBP-heptane solution using ^{198}Au radiotracer was investigated. This extractive system exhibits high loading capacities at a wide range of gold concentration from 0.005 to 50mmol/L. However, traditional stripping procedure is not quite effective. In this study a method of direct electrolysis recovery of gold from loaded organic phase was performed.Then the aqueous electrolyte solution was added into organic phase, and an emulsion system is formed by stirring, and an adherent sheet of gold with high quality was obtained on the surface of cathode directly. Mixing of NaOH and KSCN of suitable concentration in aqueous is an excellent electrolyte solution, which can improve the efficiency of current flow and the recovery rate of gold. Adding a small quantity reducer of Na_2SO_3int0 the electrolyte aqueous solution the recovery rate and purity of gold can be further improved. The electrolysis method is even better when the concentration of gold is higher than 0.1 g/L in loaded organic phase.

Keywords: electrolysis recovery, gold, extraction, CTMAB

INTRODUCTION

Solvent extraction of gold(I) from aurocyanide solutions using amines has been studied by metallurgists for many years[1-21]. Quaternary amires are regarded as excellent extractants because of their high loading capacity at the range of available pH values, good selectivity for gold. Our group have performed a series studies on Au(I) 1998[13-71]. Various quaternary ammonium salt systems were used to carry out the thorough research on the mechanism and behaviour of extracting gold from alkaline cyanide solution, showing that these systems are effective, and good performence on gold extraction. However quaternary ammonium salts such as CTMAB are binding strongly to $Au(CN)_2'$ in the organic phase, it is very difficult to strip gold from loaded organic phases. Although some research [14] about stripping of

* To whom the correspondence should be addressed Fax: 86-10-62751708, E-mail: wuig@pku.edu.cn

gold from loaded organic phases has been reported, no satisfactory stripping system has been obtained yet, thus the application of solvent extraction in industry is greatly limited.

Miller, et. al.[8,91 used pure alkyl phosphorus esters to extract gold and electrolyse it from organic phase to recover the gold at higher temperatures. In this paper, we studied the extraction of gold from $Au(CN)_2$‘ and CTMAB aqueous solution by an organic phase TBP/C_7HI_6. A method of direct electrolysis recovery of gold from extracting loaded organic phase was investigated.

EXPERIMENTAL

Material

cetyltrimethylammonium bromide (CTMAB), Beijing Xi Zhong Chemistry Factory; tributyl phosphate (TBP) , n-heptane, KSCN, NH_4SCN, NaOH were of A.R. grade; $KAU(CN)_2$ was prepared and its purity is > 99%.

Instrument:

F-H408 and ET-603 **y** scintillation counter, Beijing Nuclear Instrument Factory; ZD-2 vibrator, Jiangsu Instrument Factory; DDS-II conductometer, Shanghai Analysis Instrument Factory. Electrolysis equipment: WYK302 DC power, C-72-mA DC ammeter, DT-830 digital voltmeter, magnetic mixer, 75 UV-spectrophotometer, Z8000 atomic absorption spectrophotometer.

Analysis method:

Gold concentrations of both aqueous and organic phases were determined by the radioactive isotopic trace method, ICP or atomic absorption method. ^{198}Au was used as the tracer. After the separation of the aqueous and organic phases, equal volumes of each phase were taken fory radiometric measurement. The distribution coefficient of gold was calculated with $KAu(CN)_2$ tracer solution as standard sample.

Extraction experiment:

30%(v/v) TBP in n-heptane was used to the organic phase: The aqueous phase contained CTAB and $KAu(CN)_2$, in which the concentration of $KAu(CN)_2$ was from 0.005mmol/L to O.IOmol/L, to keep molar ratio of CTAB/Au as 1.1/1.0, and pH~10.5; After the extraction of equal volumes of aqueous and organic phase for 10 min., the extracting mixtures were centrifuged to obtain two clear phases and the gold concentrations of both two phases were determined.

Electrolysis experiment:

Electrolysis systems were composed of loaded organic phase noted as o containing Au(I) and aqueous electrolyte solutions (w) with a phase ratio of w/o=1/1. The electrolysis was conducted at room temperature by taking platinum slice 0.5x0.5cm (single side) as anode and stainless steel slice 1x2cm as cathode.

RESULTS AND DISCUSSION

Effect of gold concentration on extraction

The dependence between extraction rate of gold and concentration of gold from aqueous phase was shown in Figure 1. It indicated that when the concentration of gold in aqueous phase is higher than 0.5mmol/L, gold was almost completely extracted into organic phase, so this system exhibits high capability for gold

extraction. Also, when the concentration of gold is< 0.5mmol/L, the extraction rate reduces sharply with the decrease of gold content.

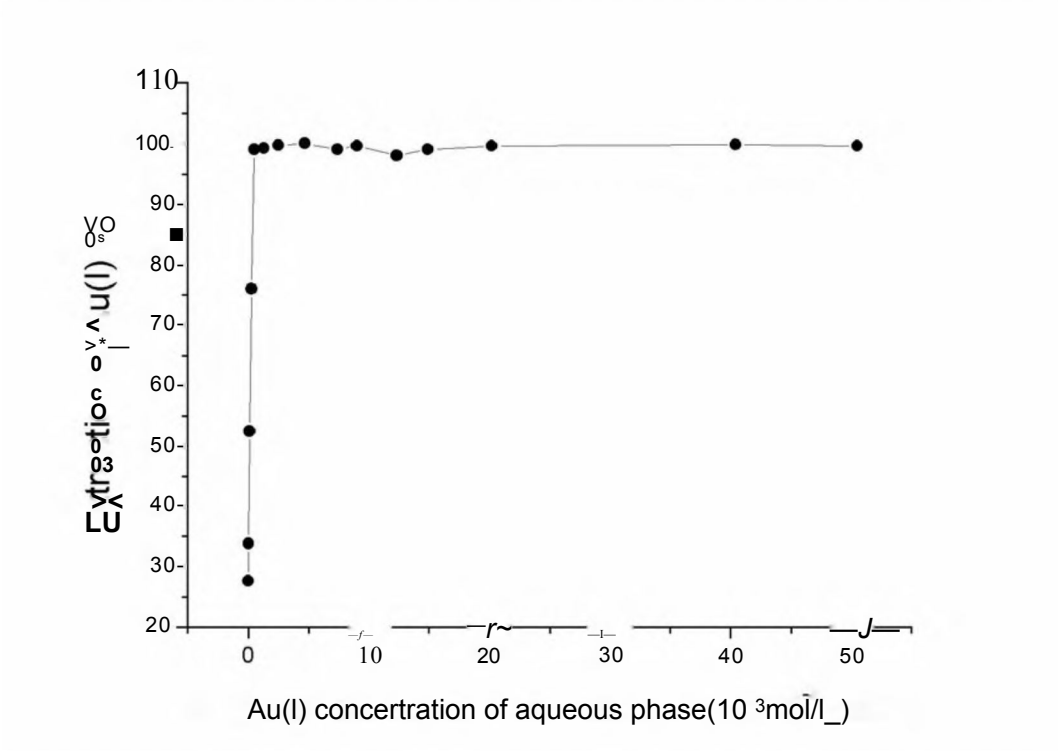


Fig. 1 Effect of Au concentration (molar ratio of CTMAB /Au =1.1/1.0) on the extraction of Au using TBP(30%)-heptane

Effect of NH_4SCN concentration on stripping gold

Various inorganic and organic compounds as stripping solutions, that none of them appeared to be feasible. We also have tried to use different concentration of aqueous NH_4SCN solution on stripping gold. It shows that the back extraction rate of gold increases with the rise of the NH_4SCN concentration. But when it reaches or exceeds 6 mol/L, stripping rate can only be ~65%, but it is impossible for repetition use. So we have to find a new way for stripping Au from organic phase directly.

Electrolyze recovery of aold from loadina oraanic phases

Firstly the influence of the gold concentration in the loaded organic phase on the conductivity of organic phase was investigated. Figure 2 shows that when the gold concentration in the loaded organic phase varies from 1 to 8 g/L, its conductivity rises slightly with the increase of gold content. But the total conductivity is quite low, only in pScm'1, so it is difficult for electrolysis recovery of Au directly. In order to improve its conductivity, we added an aqueous solution of inorganic electrolyte into loaded organic phase using the ratio of volume 1:1, with stirring. When 0.5mol/L KSCN solution was added, the conductivity of the system increased a few orders of magnitude and reached TxIO^Scm'1. A mixed solution contained 1.0 mol/L NaOH and 0.2mol/L KSCN and the conductivity reached to round lO^Scm'1. The increase of electrolyte concentration is helpful in improving the conductivity and the high

conductivity may ensure to perform easily the electrolysis recovery of gold from loaded organic phase.

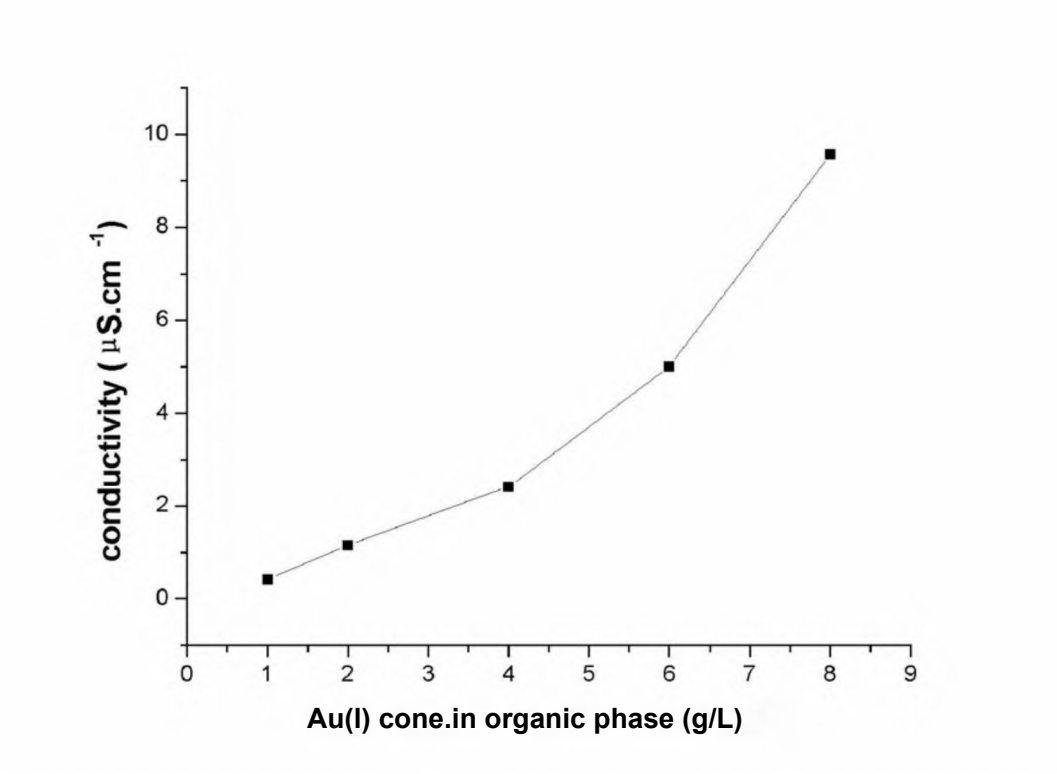


Fig.2 Effect of Au(I) concentration on the conductivity in the organic phase

Principle of electrolysis recovery gold

Our research had indicated that gold was extracted by TBP as an ion pair, $CTMA^+Au(CN)_2^-$, which solvated by strong Lewis-base alkyl phosphorus esters (as TBP)and molecule H_20, according to the following reaction and our loaded organic phase with gold was prepared in this way.

$Cl_6H33(CH_3)3N^+_{(W)}+Au(CN)_2^-_{(W)}+ 4TBP(O) + 4H_20 = [Ci6H_33(CH_3)3N]^+ [Au(CN)_2]' \bullet 4TBP\text{-}4H_20_{(0)}$

Electrolysis reaction:

Cathode: $Au(CN)_2^- + e^- \rightarrow Au + 2CN^-$ $cp^0 = -0.60V$

$H_20 + e^- \rightarrow 1/2\ H_2 + OH^-$ $<p^0 = -0.829V$

Anode: $4\ OH^- - 4e \rightarrow 2\ H_20 + 0_2$ $<p^0 = 0.401V$

So the theoretical standard potential would be ^I.OV.

Electrolysis principle:

When an electrolytic aqueous solution with certain stripping capabilities contacts sufficiently with the loaded gold organic phase, the stripping part of $Au(CN)_2'$ from organic phase can enter into aqueous phases, then the electrolysis will occurred. With the occurrence of electrolysis, the concentration of $Au(CN)_2'$ in aqueous solution decreases, the equilibrium between the two-phases moved.

Cathode polarization curve

In order to find the best conditions of electrolysis, the components of the aqueous phase was exchanged and their cathode polarization curves of electrolysis were recorded as shown in Figure 3, in which the saturated calomel electrode was used as reference and electrode current was obtained when the cell voltage increases from 0 to several voltage (V). The curve 1 was obtained using a loaded organic phase of 0.01 g/L gold concentration and 1.5mol/L KSCN aqueous solution under room temperature. It shows that the platform of polarization potential appears within -(1.1-1.35) V. The obtained gold foil through electrolysis is of high quality, and has metallic lustre. Once the cathode polarization potential is low -1.35V, the current increases steeply, and the H^+ ion will reduce to H_2 at the cathode. When the mixture of Imol/L KOH and O.lmol/L KSCN was used as electrolyte aqueous solution, the result was shown in curve 2. Thus using system a current below 10mA within the wide range of polarization potential, it is very helpful for improving the current efficiency and recovery rate of gold. IN addition the effect of electrolytic time on the recovered Au was listed in Table 1.

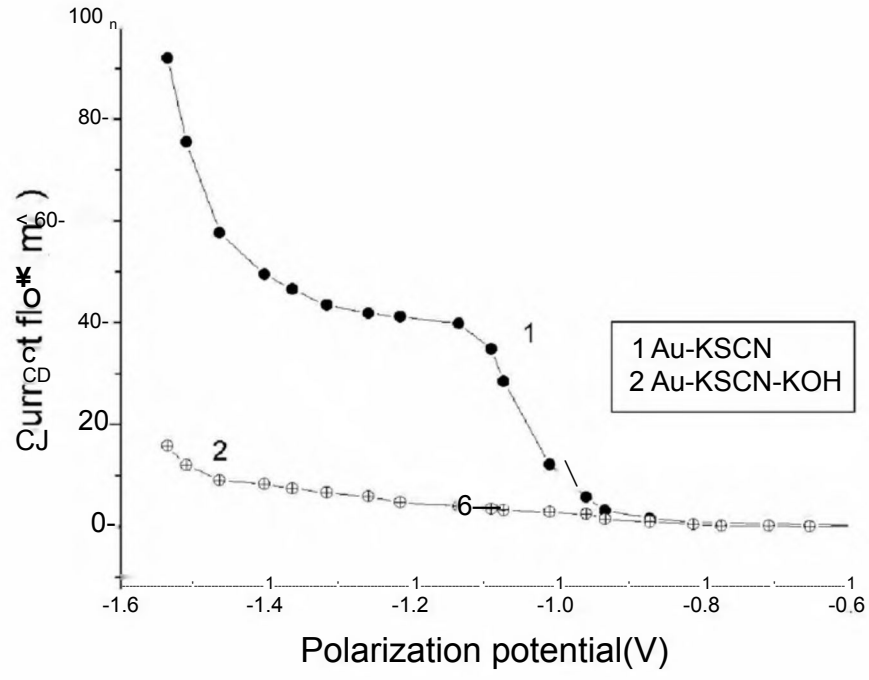


Fig. 3 Cathode polarization curves of auocyanide in organic phase mixed with aquerous solution

Table 1 Effect of electrolyte time on the recovery of Au (I) in the organic phase

Time (min)	5	10	15	20	25	30	35
Recovery Au(I) %	63.5	89.5	96.6	96.0	97.0	96.5	100

CONCLUSION

1. When the TBP/ n-heptane is the extractant, adjusting the molar ratio of cationic surfactant of CTMAB to Au can improve the extraction rate for very low concentration of Au (even to 0.005 mmol/L (Ippm)). This method is especially suitable for direct extraction of cyanide leaching solution from lean gold ore.
2. A method of electrolysis recovery of gold directly from loaded organic phase, is proposed. This method overcomes the difficulties of stripping and obtained adherent sheet of gold with high quality in cathode by direct electrolysis.
3. For low concentration of gold, higher cell voltages should be applied to deposit gold completely. When the concentration of gold >0.1 g/L in loaded organic phase the electrolysis method is much more effective.

ACKNOWLEDGEMENTS

This work was supported by the Collaboration Project of Yunnan Province and Peking University, Key Project (30371604 and 50203001) of National Natural Science Foundation of China.

REFERENCES

[1] Mooiman, M. B., Miller, J. D., 1983. The solvent extraction of gold from aurocyanide solutions. Proceedings of the International Solvent Extraction Conference. New York, pp. 530-531

[2] Miller, J. D., Mooiman, M. B., 1984-85. A Review of new developments in amine solvent extraction systems for hydrometallurgy. Separation Science and Technology 19, 895-909

[3] Ma, G., Yan, W.F., Hu, T.D., Chen, J., Yan, C.H., Gao, H.C., Wu, J.G., Xu, G.X., 1999. FTIR and EXAFS investigations of microstructures of gold solvent extraction: hydrogen bonding between modifier and $Au(CN)_2'$. Physical Chemistry Chemical Physics 1(22), 5215-5221

[4] Ma, G„ Yan, W.F., Chen, J„ Zhou, W.J., Wu, J.G., Xu, G.X., 2000. Stripping of gold from quaternary amine extraction systems. Solvent Extraction and Ion Exchange, 18(6), 1179-1187

[5] Jiang J.Z., Zhou, W.J., Gao, H.C, Wu, J.G., Xu, G.X., Chen, J., 2002. Gold stripping from loaded organic phase in quaternary amine system by inorganic salts; Acta Scientiarum Naturalium Universitatis Pekinensis 38(4), 453-458

[6] Zhang, T.X., Huang, B.G., Zhou, W.J., Gao, H.C., Chen, J., Wu, H.S., Wu, J.G., 2001. Extraction and recovery of gold from $KAu(CN)_2$ using cetyltrimethylammonium bromide microemulsions. Journal of Chemical Technology and Biotechnology (online) 76, 1107-1111

[7] Jiang, J.Z., Wang, X.Y., Zhou, W.J., Gao, H.C., Wu, J.G., 2002. Extraction of gold from alkaline cyanide solution by the tetradecyldimethylbenzylammonium chloride/tri-n-butyl phosphate/n-heptans system based on amicroemulsion mechanism. Physical Chemistry Chemical Physics 4, 4489-4494

[8] Miller, J. D., Wan, R.Y., Mooiman, M. B., Sibrell, P.L., 1987. Separation Science and Technology 22(3), 487-502

[9] Wan, R.Y., Miller, J. D., 1986. Solvent extraction and electrodeposition of gold from cyanide solutions. Journal of Metals, 35-40

SOLVENT EXTRACTION OF MAGNESIUM AND CALCIUM FROM AQUEOUS SOLUTIONS BY LONG-CHAIN ALKYL QUATERNARY AMMONIUM CARBOXYLATE

Taichi Sato,*' Masahiro Yamamoto* and Shigeru Murakami***

* Faculty of Engineering, Shizuoka University, Hamamastu, Japan
** Metallurgical Engineering Department, Queen's University, Kingston, Canada

The extraction of aqueous solutions containing magnesium and calcium chlorides by long-chain alkyl quaternary ammoniuim carboxylates, prepared by combination of trioctylmethylammonium chloride ($R_3R'NC1$) and carboxylic (caprylic, capric and lauric) acids (R"COOH) in benzene, has been investigated under different conditions. The organic phases were examined by infrared spectral measurement. As the results, it is found that the extraction efficiency is in the order Ca > Mg, and that the extraction process is expressed as $M^{2+}(aq) + 2Cl'(aq) + 2R_3R'NR"COO(org) \Longrightarrow M(R"COO)_2(org) + 2R_3R'NC1(org)$ in which M = Mg and Ca.

INTRODUCTION

The extraction of metals from acid solutions by high molecular weight amines has been reported by a number of investigators, but there are few observations on the extraction of metals from aqueous solution in the vicinity of neutral range. Although carboxylic acids are a possible group of reagents to extract the metals in the vicinity of neutral range [1], their extraction efficiencies depend remarkably on the pH of the aqueous phase. On the other hand, it is known that quaternary ammonium compounds are effective extractants for the extraction of metals forming the oxo-anions from alkaline solutions [2 - 4], Accordingly the mixed ionic solvent system consisting long-chain alkyl quaternary ammonium carboxylates is considered of effective for such extraction. We have previously studied on the extraction of bivalent transition metals from aqueous solutions by alkyl quaternary ammonium carboxylates [5], Therefore the present study extends the work to the extraction of magnesium and calcium in the similar extraction system.

[For Correspondence] : 3-14-1, Daita, Setagaya-ku, Tokyo, 155-0033, Japan.

EXPERIMENTAL

Reagents

The alkyl quaternary ammonium carboxylates were prepared by mixing calculated amounts (equal volumes of solutions in 0.5 mol dm'3 each) of trioctylmethylammonium chloride

(TOMAC, $R_3R'NCl$, Koei Chem. Ind. Co., Ltd.) and carboxylic acids (caprylic, capric and lauric acids, R"COOH), and treated with an excess amount of sodium hydroxide, and then washed throughly with distilled water to remove sodium and chloride ions. The resulting materials ($R_3R'NR"COO\text{-}5H_20$) were diluted with benzene. The aqueous solutions of metals were prepared by dissolving magnesium and calcium chlorides ($MgCl_2 \blacksquare 6H_20$ and $CaC1_2\text{-}6H_20$) in water and its pH value was adjusted by adding perchloric acid. The used reagents were of analytical grade.

Extraction and analytical procedures

The procedure for obtaining distribution coefficient (E® , the ratio of the equilibrium concentration of metal in the organic phase to that in the aqueous phase) was as follows: equal volumes (15 cm3 each) of the organic and aqueous phases were shaken for 10 min, and then the metal in the organic phase was stripped with 1 mol dm'3 hydrochloric acid. All experiments were carried out at 20°C except the examination on temperature-dependence of distribution coefficient. The concentrations of magnesium and calcium were determined by EDTA titration using BT (Eriochrome Black T) as an indicator. The chloride concentration and water content of the organic phase determined by the uses of Volhard's method and Karl-Fischer's titration, respectively.

Infrared spectral measurement

The infrared spectra of the organic extracts were determined on JASCO models IRA-1 (4000 - 650 cm'1) and IR-F (700 - 200 cm'1) using a capillary film between thallium halides or polyethylene films.

RESULTS AND DISCUSSION

Extraction isotherms

In the previous paper [5], it has been reported that the extraction of bivalent transition metals such as manganese, cobalt, nickel and copper from aqueous chloride solutions by long-chain alkvl auaternarv ammonium carboxvlates is exDressed bv the followina eauation: as an example for the extraction of nickel

$$Ni^{2+}(a) + 2Cl'(a) + 3R_3R'NR"COO(o) \rightleftharpoons (R_3R'N)_{n\cdot 2}[(R"COO)_3](o)+2R_3R'NCl(o) \quad (1)$$

where (a) and (o) are aqueous and organic phases, respectively.

Accordingly if we assume that the extraction of bivalent magnesium and calcium from aqueous solutions by quaternary compounds proceeds in the reaction similar to Eq. (1)

$$M^{2+}(a) + 2Cl'(a) + nR_3R'NR''COO(o) \rightleftharpoons (R_3R'N)_{n\cdot 2}M(R"COO)_n(o) +2R_3R'NCl(o) \quad (2)$$

in which M = Mg and Ca, this leads to the relation

$$K = [(R_3R'N)_{n\cdot 2}M(R''COO)_n]_{org}[R_3R'NCl]_{org}^2/[Mg^{2+}]_{org}[Cr]_{aq}^2[R_3R'NR''COO]_{(3)}$$

where K is the equilibrium constant. As it is supposed that the following relationship is derived :

$$K = [M]_{org}^3/[M]_{aq}^3[R_3R'NR''COO]_{org}^n = £°_a^3/[R_3R'NR''COO]_{org}^n. \quad (4)$$

Thus Eq. (3) should be satisfied by

$$\log E_a® = n/3 \log [R_3R'NR''COO]_{org} + 1/3 \log K. \quad (5)$$

In the extraction of magnesium(ll) and calcium(ll) from aqueous solutions containing their chlorides at 1 g dm'3, respectively, with trioctylmethylammonium laurate, the log-log plots of $£a^0$ vs. the quaternary compound concentration, $[R_3R'R''COO]_{org}$, give straight lines with the slope of approximately 0.65, suggesting a two-thirds power dependence of the distribution coefficient on the solvent concentration (Fig. 1). Additionally it is seen from Fig. 1 that the extraction efficiency is in the order Ca >Mg. Hence it is considered that the expression put n = 2 into Eq. (2) will be given for the extraction of bivalent magnesium and calcium:

$$M^{2+}(a) + 2C1'(a) + 2R_3R'NR''COO(o) \rightleftharpoons M(R''COO)_2(o) + 2R_3R'NCl(o). \quad (6)$$

In the extraction of magnesium(ll) and calcium(ll) from lithium chloride aqueous solutions containing magnesium and calcium chlorides at 1 g dm'3, respectively, with 0.02 mol dm'3 alkylammonium carboxylate, the distribution coefficients at first rose with increasing the lithium chloride concentration, and passed through the maxima at ~1 mol dm'3 $[Cl']_{aq}$ and then failed at higher lithium chloride concentration (Fig. 2). The rise in the distribution coefficients is due to the formation of carboxylate complexes with metals arising from the dissociation of extractant:

$$R_3R'NR''COO(o) + C1'(a) \rightleftharpoons R_3R'NCl(o) + R''COO'(o). \quad (7)$$

At above 1 mol dm'3 $[Cl]_{aq}$, the fall in the distribution coefficients arises from the decrease of the available carboxylate ion concentration to form the metal complex by the combination of R"COO" and Li^+ with increasing the lithium ion concentration. Accordingly it is considered that the extraction of magnesium and calcium should be carried out at below 1 mol dm'3 $[Cl]_{aq}$.

Infrared spectra

The infrared spectra of the organic extracts from the extraction of aqueous solutions containing metal chlorides by trioctylmethylammonium carboxylates were compared with those of the extractants. In the infrared spectrum of carboxylic acid, the C-O stretching bands appear at 1710 and 1400 -1200 cm"1 [6]. The quaternary compounds show the similar bands at 1560 and 1380 cm'1, indicating that the extractant exists in the organic phase as a

carboxylate. As for the infrared spectra of the organic magnesium extracts, the C-O

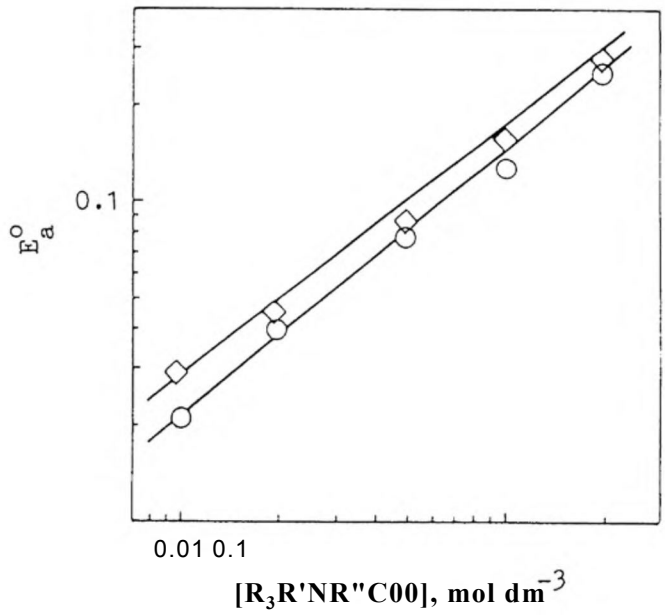


Figure 1. Log-log plots of E% vs. $[R_3R'R"COO]_{Inn}$ for the extraction from aqueous solutions containing magnesium and calcium chlorides at 1g dm'³, respectively, by alkylammonium carboxylate (o and 0 *represent magnesium and calcium, respectively).*

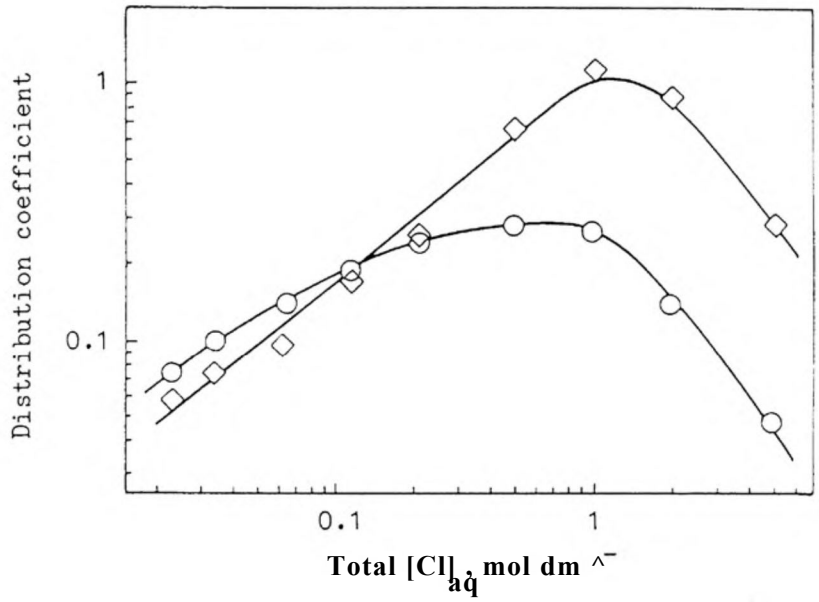


Figure 2. Extraction of magnesium(ll) and calcium(ll) from lithium chloride aqueous solutions containing magnesium and calcium chlorides at 1 g dm'³, respectively, by 0.02 mol dm'³ alkylammonium carboxylate (o and 0 *represent magnesium and calcium, respectively)*

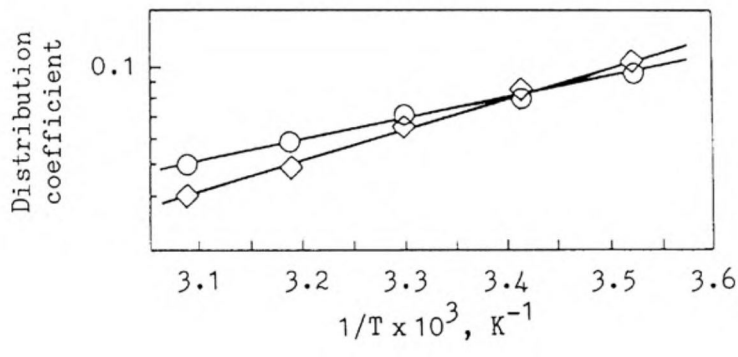


Figure 3. Temperature-dependence of distribution coefficient for the extraction of magnesium and calcium chlorides at 1 g dm'³, respectively, by 0.02 mol dm³ alkylammonium (o and 0 represent magnesium and calcium, respectively).

stretching modes appear at the same frequencies as those of the quaternary compound. However, since the carboxylate group is coordinated to magnesium ion as a bidentate ligand [7,8], the relative intensity relation between the absorption bands at 1465 and 1380 cm'1 becomes converse in comparison with that for the quaternary compound. In addition, the absorption due to the Mg-CI vibration is not observed in far-infrared region, suggesting that the chloride ion in the organic phase is coordinated to magnesium ion. Similar infrared results are also observed for the extraction of calcium.

Effect of carboxylic acid

In the extraction of aqueous solutions containing magnesium and calcium chlorides at 1 g dm"3, respectively, by quaternary ammonium compounds with caprylic, capric and lauric acids, the plots of D_a^0 vs. free [$R_3R'NR"COO$] gave a straight line with the slope of nearly for respective carboxylates. Therefore the effect of the different kinds of carboxylic acid on the extraction efficiency is not remarkable, although their efficiencies increase in the order of caprylic, capric and lauric acids. Thus the extraction mechanism of magnesium and calcium by quaternary compounds is supposed to be almost the same for each carboxylate.

Temperature effect

The extraction of aqueous solutions containing magnesium and calcium chlorides at 1 g dm'3, respectively, with 0.02 mol dm'3 trioctylmethylammonium laurate at the temperature 283 -323 K gives the results that the distribution coefficients decrease with rising the temperature (Fig. 3). The values of heat of reaction (change in enthalpy, -AH) in Eq. (6) are estimated to be 36.8 and 55.2 kJ mol'1 for the extraction of magnesium(ll) and calcium(ll), respectively. The values of the heat of reaction are in the order Ca > Mg, corresponding to the extraction efficiency.

CONCLUSION

The long-chain alkyl quaternary ammonium carboxylates extract magnesium(ll) and calcium(ll) from aqueous solutions containing chloride ion according to equilibrium equation

$$M^{2+}(a) + 2C1'(a) + 2R_3R'R''COO(o) \;\rightleftharpoons\; M(R''COO)_2(o) + 2R_3R'NCl(o),$$

although the extraction efficiency by $R_3R'NR''COO$ is in the order Ca > Mg. In this system, however, it is expected that the extraction is carried out at below 1 mol dm'^3 $[Cl]_{aq}$ at room temperature.

REFERENCES

1. e.g., F. Miller (1974), *Talanta*, 21, 685.
2. T. Sato, T. Nakamura and Y. Takeuchi (1984), *Solvent Extr. Ion Exch.,* 2, 1033- 1045.
3. T. Sato (1995), *J. Min. Met. Inst. Jpn.,* 111,119.
4. T. Sato (1995), ibid., lll, 781.
5. T. Sato (1982), *Bull. Chem. Soc. Jpn.,* 55, 90.
6. L. J . Bellamy (1958), The Infra-red Spectra of Complex Molecules, John Wiley, New York, 161pp.
7. K. Nakamoto (1978), *Infrared and Raman Spectra of Inorganic and Coordination Compounds,* 3rd ed., Wiley-lnterscience, New York, 230pp.
8. S. D. Robinson and M. F. Uttley (1973), *J. Chem. Soc.,* 1912.

Keywords: Solvent extraction, Magnesium, Calcium, Long-chain Alkyl quaternary Ammonium carboxylate

THE EXTRACTION OF URANIUM(VI) AND THORIUM(IV) FROM HYDROCHLORIC ACID SOLUTIONS BY DIHEXYL SULPHOXIDE

Taichi Sato,*** Keiichi Sato,* Katsuhiko Adachi* and Izumi Ishikawa*

* Faculty of Engineering, Shizuoka University, Hamamatsu, Japan
** Metallurgical Engineering Department, Queen's University, Kingston, Canada

The extraction of uranium(VI) and thorium(IV) from hydrochloric acid solutions by dihexyl sulphoxide (DHSO, R_2SO) in benzene has been investigated under different conditions. The organic extracts were examined by infrared spectrophotometry. As the results, it is found that the distribution coefficients rise with increasing the chloride ion concentration of aqueous solutions, and then the extraction efficiency of DHSO for uranium(VI) is higher than that for thorium(IV). The extraction of uranium(VI) and thorium(IV) from hydrochloric acid solutions by DHSO is expressed by the following equilibrium equations :

$U0_2Cl_2(aq) + 2R_2SO(org) \rightleftharpoons U0_2Cl_2\text{-}2R_2SO(org)$ and

$ThCU(aq) + 3R_2SO(org) \rightleftharpoons ThCl_4\text{-}3R_2SO(org)$.

In addition these extraction systems were compared with the extraction of uranium(VI) and thorium(IV) from hydrochloric acid solutions by TBP and TOPO.

INTRODUCTION

As the presence of sulphur atom facilitates the combination of the extractants with the class b metal ions, sulphur-containing compounds have been used as the solvent extractants for precious metals. Particularly it has been found that dialkyl-sulphides, and -sulphoxides are the effective extractants for silver and mercury. The present author has therefore investigated the extraction of mercury(ll) by dihexyl-sulphide (DHS, R_2S) and -sulphoxide (DHSO, R_2SO) [1], and of zinc(ll) and cadmium(ll) by DHSO [2], Consequently it has been seen that although the extractability of metal by DHSO is generally more effective than that by DHS, those extractants combine with metals by the solvating reaction due to the ion association similar to the neutral organo-phosphorus compounds such as tributyl phosphate (TBP) and trioctyl phosphine oxide (TOTO). TBP and TOPO are however used in various industrial fields, especially in the progress of nuclear fuel for conspicuous extractability of uranium and in the processing of radio-active products from nuclear reactors. Thus the present study extends the work to obtain further information on the extraction of uranium(VI) and thorium(IV) from hydrochloric acid solutions by DHSO in comparison with TBP and TOPO [3-5],

[For Correspondence]: 3-14-1, Daita, Setagaya-ku, Tokyo, 155-0033, Japan

F>

EXPERIMENTAL

Reagents

The DHSO was synthesized by means of oxidation from DHS (Daihachi Chem. Ind. Co., Ltd.) : 1) 35cm^3 each of acetic acid and acetic anhydride and 20 cm^3 of aqueous solution of hydrogen peroxide in 30% were added to 50cm^3 of DHS dropwise for 1 h., the mixture was cooled with ice and then stripped for 3 h at 0°C.; 2) After end of the reaction was confirmed by TLC, DHSO extracted into chloroform was washed at first with water and then with 10 % sodium carbonate, and finally with water again.; 3) White crystal obtained from the removal of chloroform by evaporator was refined by recrystallization method. The DHSO was dissolved in benzene.

The uranyl chloride hydrate ($U0_2C1_2$-$2H_20$, Yokozawa Chem. Co., Ltd.) was of high purity and was used without further purification. Thorium chloride solutions were obtained by precipitating thorium hydroxide from thorium nitrate ($Th(N0_3)_4$-$4H_20$, Koso Chem. Co., Ltd.) solution with aqueous ammonia, washing thoroughly with ammonium nitrate solution and distilled water and dissolving in hydrochloric acid solutions of selected concentrations. In general the concentration of the metal salts was 0.01 mol dm"^{3}. All chemicals were of analytical reagent grade.

Extraction and analytical procedures

Equal volumes (15 cm^3 each) of organic and aqueous phases were placed in 50 cm^3 stoppered conical flask and shaken for 10 min at *20°C,* except the experiment on temperature effect. Preliminary experiments showed that equilibrium was complete in 10 min for both metals. The mixture was quickly separated by centrifuge, and then both phases were assayed to determine the distribution coefficient (E® , the ratio of the equilibrium concentration of metal in the organic phase to that in the aqueous phase). Uranium and thorium in the organic phases were stripped with 6 mol dm'^{3} hydrochloric acid and 10 % sodium carbonate solutions, respectively. The concentrations of metals in aqueous solutions were determined by EDTA with xylenol orange (XO) as indicator.

Infrared spectral measurement

The infrared (IR) spectra of the organic extracts were determined on JASCO models IRA-1 (4000-650 cm'^{1}) and IR-F (700-200 cm"^{1}) using a capillary film between thallium halide plates or polyethylene films.

RESULTS AND DISCUSSION

Extraction isotherms

The extraction of uranium(VI) from hydrochloric acid solutions by DHSO was carried out by varying the aqueous acidity. The distribution coefficient of uranium(VI) rose with increasing the initial concentration of hydrochloric acid as shown in Fig. 1. When hydrochloric acid in the aqueous phase was replaced by lithium chloride, the extraction behaviour of uranium(IV) resembled that from hydrochloric acid solutions alone (Fig. 1). Besides the extraction of thorium(IV) from hydrochloric acid solutions by DHSO indicated the distribution behaviour similar to the extraction of uranium(VI) : the distribution coefficient rose with increasing the acidity as given in Fig. 2, although its extraction efficiency is lower than that of uranium(VI).

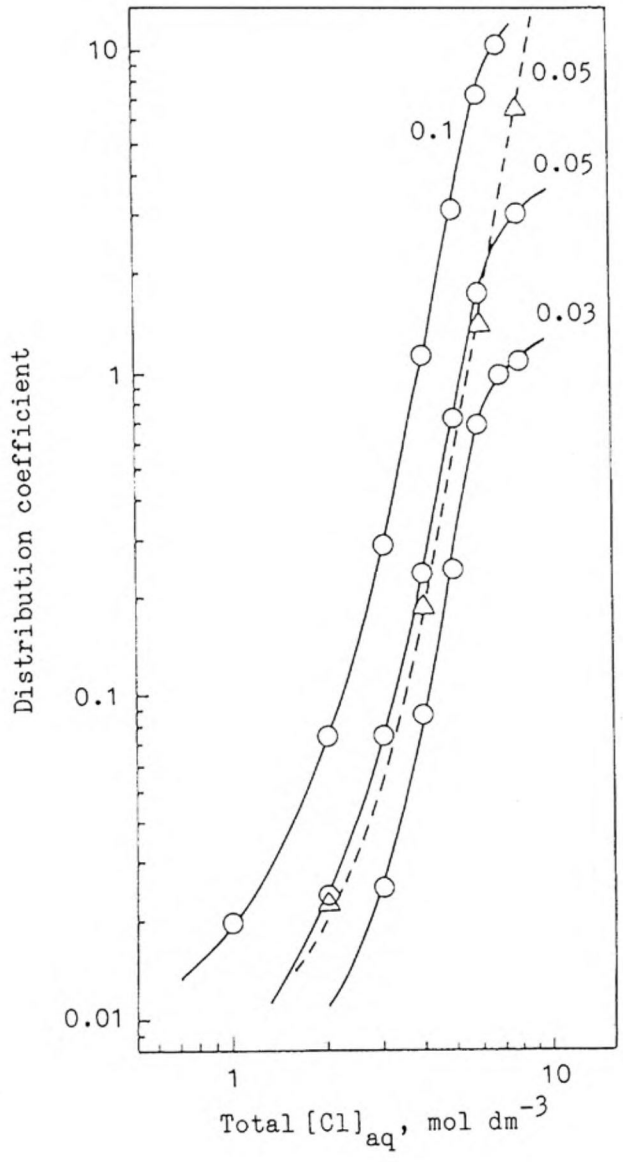


Figure 1. Extraction of uranium(VI) from hydrochloric acid solutions by DHSO in benzene (numerals on curves are DHSO concns., mol dm³; continuous and broken lines represent the extraction from HCl soln., and mixed 0.1 mol dm'³ HCl + LiCl solns., respectively).

The log-log plots of E® vs. $[R_2SO]_{eq}$ = [F^SO]^ - **n[M]org**, where M = U or Th, at $[Cl]_{jn}$jt $_{aq}$ gave the straight lines with the following slopes : for uranium(VI) as n = 2, 1.8, 2.2 and.1.8 at 2, 4 and 6 mol dm'³ HCl, respectively, and 1.8, 2.2 and 1.8 at 0.1 mol dm"³ HCl + LiCl (of 2, 4 and 6 mol dm^{-3}), respectively; for thorium(IV) as n = 3, 2.7, 2.8 and 2.6 at 5, 6 and 7 mol dm'³, HCl, respectively, and 2.8, 2.9 and 2.9 at 0.1 mol dm'³ + LiCl (of 6, 7 and 8 mol dm'³) , respectively. These results show that the dependences of distribution coefficients on the DHSO concentration are in second- and third- powers for the extraction of uranium(VI) and thorium(IV), respectively.

In the extraction of uranium(VI) and thorium(IV) from hydrochloric acid solutions by DHSO, the

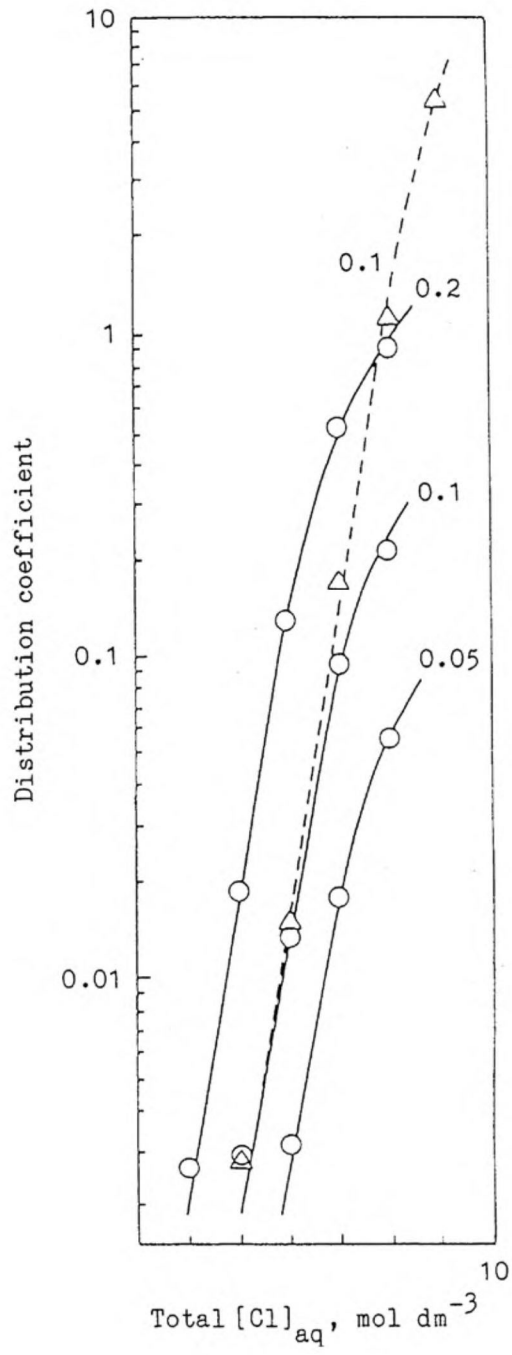


Figure 2. Extraction of thorium(IV) from hydrochloric acid solutions by DHSO in benzene (numerals on curves are DHSO concns., mol dm'³; continuous and broken lines represent the extraction from HCI solns. and mixed 0.1 mol dm³ HCI+LiCI sol ns., respectively).

continuous variation of $[M]_{org}$ plotted as a function of mole fraction $[M]_{init}aq + [R_2SO]_{init}$) at a fixed total concentration of $[M]_{init\ aq} + [R_2SO]_{init} = 0.1$ and 0.2 mol dm'³ for uranium(VI) and thorium(IV), respectively, gave the following maxima : for uranium(VI), 0.33 at 5 mol dm'³ HCl or 0.1 mol dm'³ HCI + 4.4 mol dm'³ LiCI; for thorium(IV), 0.25 at 6 mol dm'³ HCI. This exhibits

that the combinations of DHSO with uranium(VI) and thorium(IV) are in the molar ratios of 2 : 1 and 3 : 1 , respectively. Accordingly it is seen that the following stoichiometric species will be formed in the extraction of uranium(VI) and thorium(IV) : for uranium(VI), UO2 CI2·2 R2 SO ; for thorium(IV), $ThCl_4$-$3R_2SO$.

Hence the equilibrium equations are inferred for the extraction of uranium(VI) and thorium(IV) from hydrochloric acid solutions by DHSO : for uranium(VI)

$$U0_2Cl_2(a) + 2R_2SO(o) \rightleftharpoons U0_2Cl_2\text{-}2R_2SO(o) , \qquad (1)$$

and for thorium(IV) :

$$ThCU(a) + 3R_2SO(o) ;== ThCl_4\text{-}3R_2SO(o) \qquad (2)$$

in which (a) and (0) represent the aqueous and organic phases, respectively.

Infrared spectra

The organic phases obtained from the extraction of uranyl chloride solutions at 5, 20 and 50 g dm'3 and of thorium chloride solutions at 5, 10 and 20 g dm'3 containing 0.1 mol dm'3HC1 + 6.9 mol dm'3 LiCI with 0.2 mol dm'3 DHSO in benzene were examined by IR spectroscopy.

The IR Spectra of the organic extracts for uranium(VI) and thorium(IV) exhibit the absorption due to the S=0 stretching vibration at 960 and 985 cm'1, respectively, shifted from the band which appears at 1050 cm"1 in a free DHSO. This suggests that DHSO coordinates to metals through the oxygen atom. In addition the uranium(VI) extracts show the absorption at 930 cm'1 assigned to the asymmetric stretching frequency of the uranyl group [3-5] , and the intensity of its absorption progresses with increasing the uranium concentration of the organic phase. Simultaneously the intensity of the absorption due to the OH stretching band at 3400 cm'1 for DHSO decreases with increasing the concentration of uranium or thorium in the organic phase. This fact is supported by the water content of the organic phase. Consequently the IR results confirm that the uranium and thorium extracted into DHSO solution are bonded to sulphur through oxygen atom [6], and that the uranyl and thorium chloro complexes possess the stoichiometric formulas $U02Cl_2$-$2R_2S0$ and $ThCl_4$-$3R_2SO$, corresponding to $U0_2Cl_2$-2TBP, $U0_2Cl_2$-2T0P0, $ThCl_4$-3TBP and $ThCl_4$-3TOPO [3-5],

Temperature effect

The extraction of uranium(VI) and thorium(IV) from hydrochloric acid solutions by DHSO (U(VI) from 6 mol dm-3 HCI with 0.05 mol dm-3 DHSO; Th(IV) from 7 mol dm-3 HCI with 0.2 mol dm-3 DHSO) at the temperature 283 -323 K gave the results that the distribution coefficients decrease with rising temperature due to the exothermic reaction. (The values of heat of reaction (change in enthalpy, - AH) in Eqs. (1) and (2) were estimated as 22.5 and 22.4 kJ for the extraction of U(VI) and Th(IV), respectively).

CONCLUSION

The extraction of uranium(VI) and thorium(IV) from hydrochloric acid solutions by DHSO is expressed by Eqs. (1) and (2).

$U0_2Cl_2(a) + 2R_2SO(o)$ ^ $U0_2Cl_2$-$2R_2SO(o)$ and $ThCl_4(a) + 3R_2SO(o)$ ^ $ThCl_4$-$3R_2SO(o)$. In addition, although the extraction behaviours for uranium(VI) and thorium(IV) by DHSO, TBP and TOPO resemble each other, their extraction efficiencies of U >Th are in the order TOPO > DHSO >TBP.

REFERENCES

1. T. Sato, I. Ishikawa and K. Sato (1998), *J. Min. Meter. Process. Inst. Jpn.,* 114, 33-39.
2. T. Sato, I. Ishikawa and K. Sato (2000), ibid., 116, 44 - 48.
3. T. Sato (1966), *J. Appl. Chem.* , 36, 53 - 57.
4. T. Sato and T. Nishida (1976), *J. Inorg. Nucl. Chem.,* 36, 2087 - 2089
5. T. Sato and M. Yamatake (1969), *J. Inorg. Nucl. Chem.,* 31, 3633 - 3642
6. P. Biscarini and L. Fusina (1972), *J. Chem. Soc., Dalton,* 1003.

Keywords: Solvent extraction, Uranium(VI), Thorium(IV), Hydrochloric acid, Dihexyl sulphoxide

THE MICROEMULSION SOLUTION AS A NEW SOLVENT SYSTEM FOR COUNTERCURRENT CHROMATOGRAPHY

Yanmei Yu, Duolin Du and Jian Chen*

State Key Laboratory of Chemical Engineering, Department of Chemical Engineering, Tsinghua University, Beijing 100084, PR China

First proposed by Ito in late 1960's, countercurrent chromatography (CCC) based on the liquid-liquid extraction with hundreds or thousands of separation stages has been used as an analytical and production chromatography in fields of environmental protection, natural product separation, biochemistry, pharmacy and material science. Aqueous - organic two-phase solutions, such as chloroform - methanol - water, hexane - ethyl acetate - methanol - water, are used as the solvent systems in CCC. In this work, a microemulsion solution with surfactants such as AOT is proposed as the solvent system in CCC. This kind of CCC can be called microemulsion CCC or MCCC. Experiments were carried out with the solvent system of isooctane - AOT - water - NaCl. Operation conditions such as concentration, flow rate of the fluent phase, column rotation rate and retained volume of the stationary phase were optimized for the separation of isomers catechol and hydroquinone. The result shows that two isomers can be separated successfully in a microemulsion countercurrent chromatography.

INTRODUCTION

Countercurrent chromatography (CCC), first proposed by Ito in late 1960's, can be used as an analytical and production chromatography based on the liquid-liquid extraction with hundreds or thousands of stages. Solutes are separated for their different distribution coefficients in two liquid phases, which flow in countercurrent directions in tubes. One liquid phase is used as the stationary phase and another phase as the fluent phase. CCC has been widely used in fields of environmental protection, natural product separation, biochemistry, pharmacy and material science [1,2].

Usual liquid solutions like chloroform - methanol - water, hexane - ethyl acetate - methanol - water, are used as the solvent systems in CCC. In this work, a microemulsion solution with surfactants, such as AOT, is used. The advantage of the solvent system [3,4] is that there are

microemulsion cells of water in the organic phase and strangely water-soluble solutes can be distributed and separated in liquid-liquid equilibrium with microemulsion in the aqueous phase. This kind of CCC can be called microemulsion CCC or MCCC.

The isomers catechol and hydroquinone are strongly dissolved in water and less dissolved in organic phase, so the microemulsion particles of water in the organic phase can improve their solubility. Experiments for the separation of isomers catechol and hydroquinone were carried out in CCC with the solvent system of isooctane - AOT - water - NaCl. The possibility of their separation and operation conditions of CCC are discussed.

EXPERIMENTAL SECTION

High speed CCC apparatus

The high-speed CCC apparatus used for the present study is a coil planet centrifuge named as GS10A2 that was fabricated by Beijing New Technology Application Institute. The apparatus has a pair of column holders symmetrically to the rotating central axis. The coiled column was mounted on the gear-side holder, which undergoes a planetary motion. The synchronous planetary motion of the holders produces countercurrent movement of two phases through the coiled column. The coiled column was made of a poly-(tetrafluoroethylene) tubing with the diameter of 1.6 mm and total capacity of 220 ml. The rotation rate can be controlled in the range of 100 - 1000 rpm. The CCC apparatus also includes a fluent phase input pump (Type NS-1007), which can produce a fluid with flowing rate of 100 to 500 ml/hour. The separation was monitored by a UV detector (Type 8823A) at 280 nm and chromatograms were recorded.

Materials

The usual microemulsion solution of isooctane - AOT - water - NaCl was selected as the solvent system for the separation of isomers catechol and hydroquinone. All chemical agents were of analytical grade (99%) and used without further purification. Aerosol OT (AOT), isooctane, NaCl, catechol and hydroquinone were obtained from Beijing Chemical Agents Company and Beijing Xudong Chemical Company.

Experimental procedure

First two phases in liquid-liquid equilibrium were prepared at room temperature. The organic phase with microemulsion particles was used as the stationary phase in CCC, and the aqueous phase as the fluent phase. The solubility of water in the organic phase was measured using the CA05 Moisture meter from Mitsuibishi. In order to improve the phase split rate after the mixing of two phases, NaCl was added to increase the density of the aqueous phase, thus enlarge the difference between densities of two phases.

After the two phases were separated, the organic phase of a given volume was input into the CCC column through the input pump. Then the aqueous phase was input into the column with a given rate and the baseline was monitored for several hours. After the baseline was straight, a aqueous sample of 5 ml for the mixture of catechol and hydroquinone was input as a sample

and the separation result was monitored with the UV detector and recorded graphically.

RESULTS AND DISCUSSION

Composition of solvent system with microemulsion

For best separation results using CCC, the solvent system is one of most important effects. The usual standards for a solvent system are density difference, less viscous fluid and phase split rates.

As widely known, liquid-liquid equilibrium systems with a microemulsion solution are such ones that need long time for phase split. In this work, the widely used microemulsion system of isooctane - AOT - water was selected for an example. With the concentration of AOT less than 10 mass % [5], the system can be split into two phase, one is aqueous and another is the organic phase. But densities of two phases are close and the phase split is difficult to happen. Table 1 shows the phase-split results for the system with different composition after strong mixing with a magnetic stir. All systems with AOT cannot have a successful phase split after ten minutes. And further in the operation of CCC with the high-speed rotation of the column, it will be completely more difficult to achieve phase split in CCC column.

Table 1. Phase split result for the system isooctane - AOT - water

Mass ratio	Phase split and transparency after 10 minutes	Phase split and transparency after 12 hours	Water content in the organic phase (mass %)
100: 0: 100	Yes, good	Yes, good	0.016%
100: 1.5: 100	Yes, bad	Yes, almost good	0.95%
100: 3: 100	Yes, bad	Yes, almost good	2.10%
100: 6: 100	Yes, bad	Yes, almost good	7.2%
100: 12: 100	No	No	15.2%
100: 16: 100	No	Yes, good	17.4%
100: 25: 100	No	Yes, good	20.9%

Table 2. The effect of the addition of NaC! in isooctane - AOT - water solution (100:3:100)

NaCI	Phase split time and transparency of two phases
0.2 g	8min, bad
0.4 g	3min, bad
0.8 g	Imin, bad
12 g	30 sec, good
2.0 g	5 sec, good
4.0 g	1 sec, good

For rapid phase split in CCC column, the density of two phases should be increased. In this work, an inorganic salt NaCI was added to the system. Most of added NaCI should be solved

in the aqueous phase and the density of the aqueous phase will be larger than that without NaCl. The addition of NaCl in the isooctane - AOT - water system will improve the phase split rate. Table 2 lists the time needed to achieve the phase split with different amount of NaCl added in the isooctane - AOT - water system. The time needed for the phase split can be as small as 1 sec, which is necessary for its usage in CCC.

Water content in the organic phase will have important effect on the solubility of isomers catechol and hydroquinone, and will also affect the separation result. As shown in Table 1, the higher the AOT concentration, the higher the water content in the organic phase. The separation result should be better with more water content in the organic phase, but the phase split rate becomes worse. So AOT content should have an optimized value.

Based on above results, the system of isooctane - AOT - water - NaCl with mass ratios as 100:3:100:4 or 100:6:100:4 was used as the solvent system in CCC for the separation of isomers catechol and hydroquinone.

CCC conditions and separation results

First the effect of column rotating speed on retained stationary phase was examined. Figure 1-3 show the baselines with the column rotating speed of 200, 500, 800rpm, while the flow rate of the fluent phase is 0.5ml/min and the solvent system is of the mass ratios as isooctane: AOT: water: NaCl = 100:3:100:4. The results show that the high rotating speed of the countercurrent chromatographic column will destroy the baselines of microemulsion CCC. The valid speed should be less than 500 rpm for the system in this work.

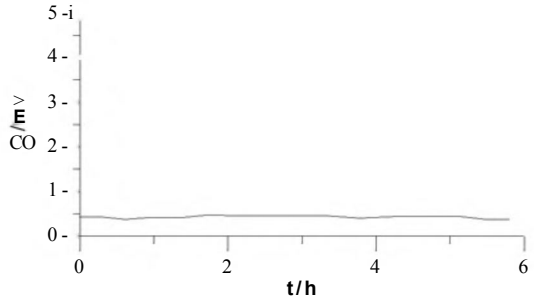


Figure 1. The CCC baseline with conditions of 200 rpm, 0.5ml/min, 100:3:100:4, and 110 ml.

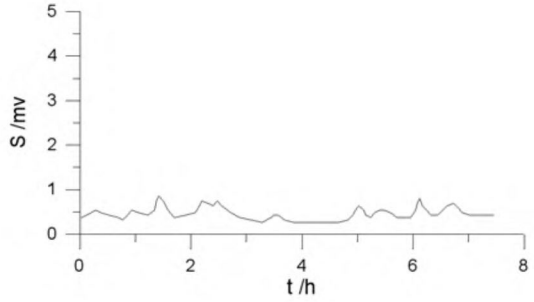


Figure 2. The CCC baseline with conditions of 500 rpm, 0.5ml/min, 100:3:100:4, and 110 ml.

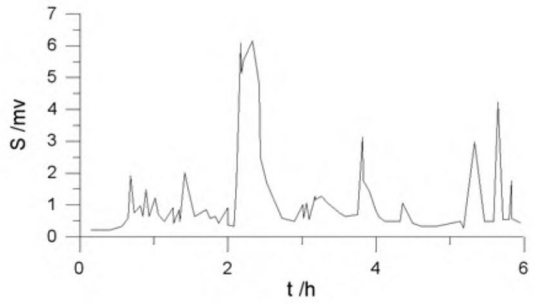


Figure 3. The CCC baseline with conditions of 800 rpm, 0.5ml/min, 100:3:100:4, and 110 ml.

Then the effect of the AOT concentration on the separation of isomers was tested. Figure 4 and 5 show the results with isooctane: AOT: water: NaCl = 100:3:100:4 (water content in the organic phase is 0.92%), with flow rate of the fluent phase as 0.5 ml/min and column rotating speed of 400 and 500 rpm, respectively. The results show that the isomers have not been separated satisfactorily. The reason should be that there is no enough water content in the organic phase.

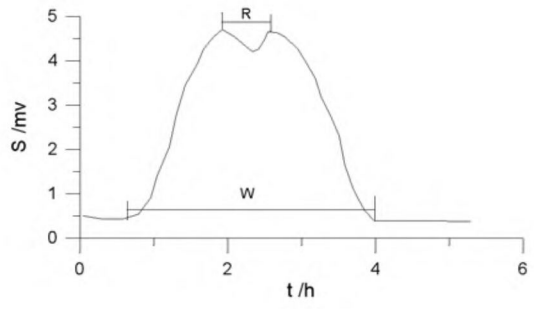


Figure 4. The CCC result with conditions of 400 rpm, 0.5ml/min, 100:3:100:4, and 110 ml.

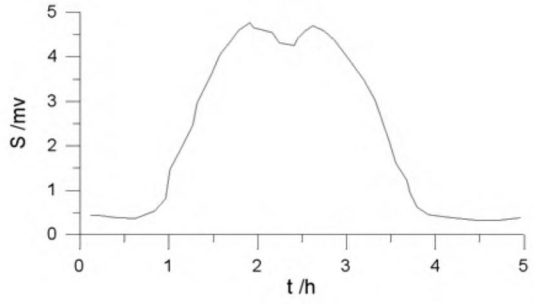


Figure 5. The CCC result with conditions of 500 rpm, 0.5ml/min, 100:3:100:4, and 110 ml.

In order to improve the separation result, the water content is increased with the increase the AOT content in the system. Figure 6 and 7 show the results with isooctane: AOT: water: NaCl = 100:6:1200:4(water content in the organic phase is 2.2%), with the same flow rate and column rotating speeds. The separation factor of isomers is distinguished improved.

The results in Figure 6 and 7 also show that the separation factor is improved with the 500

rpm than that with 400 rpm, but the base line is worse and not acceptable. For actual operation, the rotating speed should be selected to keep the acceptable baseline.

The effect of flow rate of fluent phase on the separation factor was examined also though measurements. Figure 6 and 8 show the results for 400 rpm, isooctane - AOT - water - NaCl = 100:6:100:4, but with different flow rate of fluent phase as 0.4 ml/min and 0.5 ml/min. The slow flow rate of the fluent phase can improve the separation factor as expected.

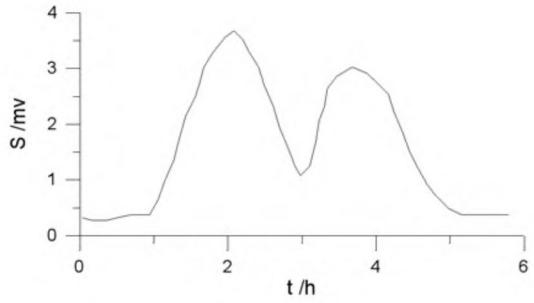


Figure 6. The CCC result with conditions of 400 rpm, 0.5ml/min, and 100:6:100:4, and 110 ml.

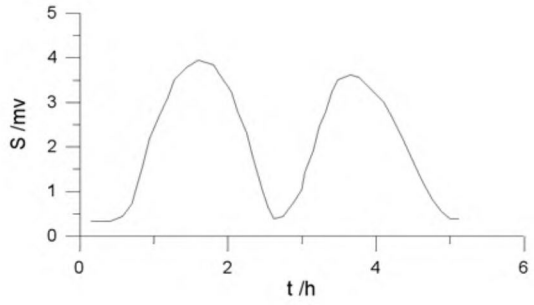


Figure 7. The CCC result with conditions of 500 rpm, 0.5ml/min, and 100:6:100:4, and 110 ml.

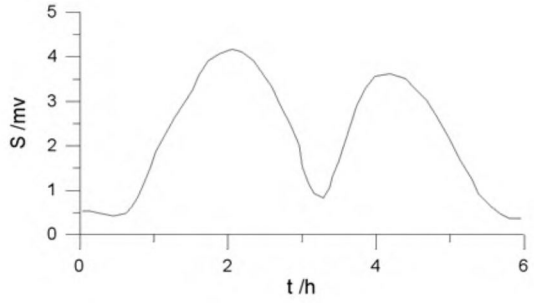


Figure 8. The CCC result with conditions of 400 rpm, 0.4ml/min, and 100:6:100:4, and 110 ml.

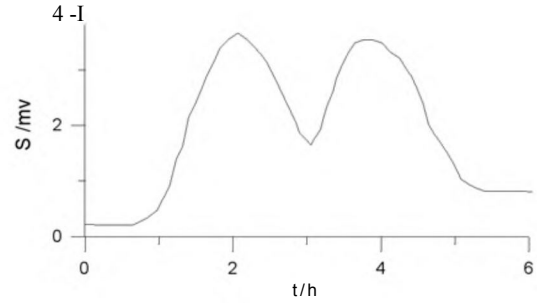


Figure 9. The CCC result with conditions of 400 rpm, 0.5ml/min, 100:6:100:4 and 80 ml.

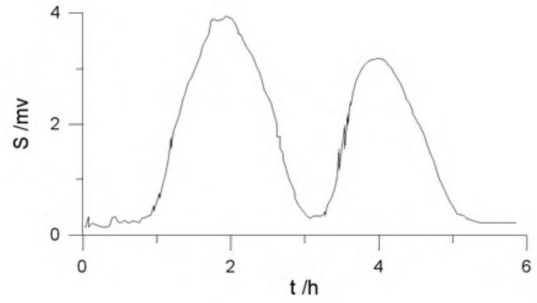


Figure 10. The CCC result with conditions of 400 rpm, 0.5ml/min, 100:6:100:4, and 110 ml.

Table 3. The effect of different operation conditions on the separation factor

Mass ratio	V (ml)	F (ml/min)	S (rpm)	Ms (g)	W (cm)	R (cm)	R_s
100:3:100:4	110	0.5	400	0.025	3.2	0.7	0.44
100:3:100:4	110	0.5	500	0.025	3.1	1.0	0.65
100:6:100:4	110	0.5	400	0.025	4.0	1.7	0.85
100:6:100:4	110	0.5	500	0.025	4.2	2.3	1.10
100:6:100:4	110	0.4	400	0.025	4.9	2.2	0.90
100:6:100:4	80	0.5	400	0.025	4.5	1.7	0.75
100:6:100:4	110	0.5	400	0.0125	4.5	2.1	0.93

Mass ratio: isooctane: AOT: water: NaCl; V: retained volume of stationary phase; F: Flow rate of fluent phase; S: column rotating speed; Ms: input mass of catechol or hydroquinone in 5ml aqueous sample; W: Baseline width; R: distance between chromatography peaks of catechol or hydroquinone; Rs: separation factor = R/W.

The effect of retained volume of the stationary phase on the separation factor was checked. Figure 9 show the results with retained volume of the stationary phase of 80 ml with the condition of 400 rpm, 0.5ml/min, AOT: water: NaCl = 100:6:100:4. Compared with the result in Figure 6 for the result with 110 ml retained volume, the separation factor became worse. Although the result shows that the separation factor can be improved with the increase of retained volume of the stationary phase as usual, the baseline became better as shown in Figure 9 with less retained volume of the stationary phase.

All the results in Table 3 show that the separation of compounds in CCC with a microemulsion solution as the solvent system is possible. The operation conditions as composition of the solvent system, column rotating speed, flow rate of the fluent phase and retained volume of the stationary phase can affect the separation factor.

CONCLUSIONS

Experiments were carried out for the separation of isomers catechol and hydroquinone in CCC with the microemulsion solvent system of isooctane - AOT - water -NaCI. Operation conditions such as concentration of the surfactant, flow rate of the fluent phase, rotational rate are examined for the separation. The result shows that microemulsion countercurrent chromatography can be used to analysis and separate organic compounds successfully.

REFERENCES

1. N.B. Mandava and Y. Ito (eds.) (1988), Countercurrent Chromatography (Chromatography Science Series, vol. 44), Dekker, New York.
2. W.D. Conway (1990), Countercurrent Chromatography: Apparatus, Theory and Applications, VCH, Weinheim.
3. A. Berthod and M. De Carvalho (1992), *Anal. Chem.,* 64, 2267-2272.
4. H. Watarai (1997), *J. Chromatogr.* A, 780, 93-102.
5. B. Tamamushi and N. Watanabe (1980), *Colloid & Polymer Sci.,* 258, 174-178.

THE EXTRACTION OF TIN(IV) FROM HYDROCHLORIC ACID SOLUTIONS BY NEUTRAL ORGANIC-PHOSPHORUS COMPOUNDS

Taichi Sato* Hitoshi Yasumura* and Keiichi Sato***

* Faculty of Engineering, Shizuoka University, Hamamatsu, Japan
** Metallurgical Engineering Department, Queen's University Kingston, Canada

The extraction of tin(IV) from hydrochloric acid solutions by TBP and TOPO in benzene has been investigated under various conditions. The organic extracts were examined by infrared spectrophotometry. As the results, it is found that although the extraction efficiency for the tin(IV) is in the order TOPO > TBP, the following equilibrium equations are proposed for the extraction by TBP and TOPO : for TBP, $SnC1_4$(aq) +2TBP(org) $\rightleftharpoons$ $SnCl_4$-2TBP(org); for TOPO, $SnC1_4$(aq) + 2TOPO(org) $\rightleftharpoons$ $SnC1_4$-2TOPO(org). Further it is seen that the both extracted species are in an octahedral structure by the tin with the coordination of eight. In addition the obtained results are compared with the extraction of tin(IV) from hydrochloric acid solutions by high-molecular weight amines.

INTRODUCTION

Tin is mostly used for the surface plating of steel pig iron, copper and so on owing to its strong anticorrosive properties. However, since the manufacture and recover of tin depend on mainly electrolytic refinding methods, the introduction of a chemical process such as solvent extraction technology will rise problems in the refinding of tin. On the other hand, as tin is an amphoteric element and forms a number of compounds, studies on the solvent extraction of tin are of interest from a chemical viewpoint. In the previous papers [1,2], the extraction of tin(IV) from hydrochloric acid solutions has been investigated by using di-(2-ethylhexyl)phosphoric acid (DEHPA) and high-molecular weight amines (trioctylamine (TOA) and trioctylmethylammonium chloride (TOMAC). Therefore the present paper

[For Correspondence]: 3-14-1, Daita, Setagaya-ku, Tokyo, 155-0033, Japan

extends the work to the extraction of tin(IV) from hydrochloric acid solutions by tributylphosphate (TBP) and trioctylphosphlne oxide (TOPO).

EXPERIMENTAL

Reagents

The TBP (Daihachi Cbem. Ind. Co., Ltd.) was purified by usual method [3] . The TOPO (Koei Chem. Ind. Co., Ltd.) of high purity was used without further purification. TBP and TOPO were diluted and dissolved with benzene, respectively. The aqueous solutions of metal were prepared by dissolving stannic chloride ($SnCl_4xH_20$) in concentrated hydrochloric acid and diluted with deionized water to a required concentration. The concentration of the metal salt was 2g dm^{-3} except for the loading test. Other chemicals were analytical reagent grade.

Extraction and analytical procedures

Equal volumes (15 cm^3 each) of the aqueous and organic phases were shaken for 10 min in 50cm^3 stoppered conical flask at 20°C, except for the experiment on temperature effect. Preliminary experiments showed that the equilibrations achieved in 10 min. The mixture was separated by centrifuge, and then both phases were assayed to determine the distribution coefficient ($E_a°$, the ratio of the equilibrium concentration of metal in the organic phase to that in the aqueous phase) . Tin in the organic phase was stripped with 0.5 mol dm'^3 hydrochloric acid. The concentration of tin in the aqueous solution was determined by EDTA titration using xylenol orange (XO) as an indicator. The chloride concentration and water content in the organic phase were determined by Volhard's method and Karl Fisher's titration method, respectively.

Infrared spectrophotometry

Infrared (IR) spectra of the organic extracts were determined on JASCO models IRA — 1 (4000 —650cm'^1) and IR —F (700 —200cm'^1) using a capillary film between thallium halide plates or polyethylene films.

RESULTS AND DISCUSSION

Extraction isotherms by TBP

The extraction of tin(IV) from hydrochloric acid solutions by TBP gave the results shown in Fig. 1. With increasing aqueous acidity, the distribution coefficient rises steeply. When

hydrochloric acid in the aqueous phase is partly replaced by lithium chloride, the extraction behaviour of tin(IV) resembles that from hydrochloric acid solutions only. It is thus deduced that for the extraction of tin(IV) from hydrochloric acid solutions by TBP, the controlling factor is the total chloride ion concentration.

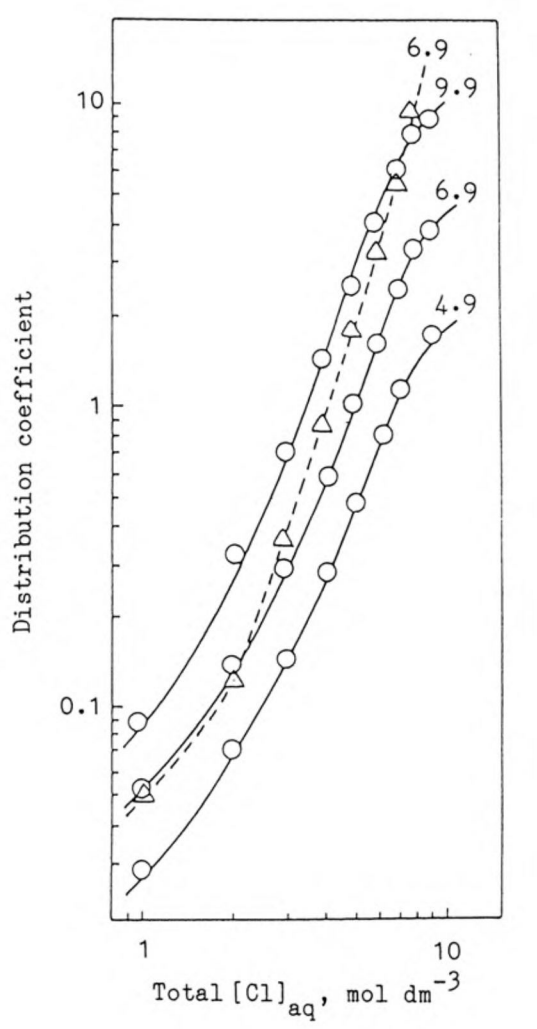


Figure 1. Extraction oftin(tV) from hydrochloric acid solutions by TBP In benzene (numerals on curves are TBP concns., %(v/v); continuous and broken lines represent the extraction from HCI solns. and mixed 0.2 mol dm'3 HCI + LiCI sol ns., respectively).

In the extraction of tin(IV) from hydrochloric acid solutions by TBP, the log-log plots of $E_a°$ vs. $[TBP]i_ni_t$ gave the straight lines with the slope of ~2, suggesting the second-power dependency on TBP concentration. Besides the continuous variation of $[Sn]_{org}$ as a function of the mole fraction $[Sn]_{in}jt_{aq}/([Sn]jnit_{aq} + [TBP]_{jnit})$ at a fixed total concentration $[Sn]_{ini}iaq^{+}$ [TBP] (nit = 0.7 mol dm'3 gave result that a maximum in $[Sn]_{org}$ appeared at the mole fraction of

~0.33 in the extraction of Sn(IV) from 0.2 mol dm'3 hydrochloric acid solution. Therefore the obtained result indicates the formation of the stoichiometric composition $SnCl_4$ 2TBP.

Hence the extraction of tin(IV) from hydrochloric acid solutions by TBP is expressed by the following equilibrium equation :

$$SnC1_4(a)+2TBP(o) === SnCl_4\text{-}2TBP(o) \quad (1)$$

in which (a) and (o) represent aqueous and organic phases, respectively.

Infrared spectra for TBP extraction system

The organic extracts of tin(IV) from hydrochloric acid solutions with 9.9% (v/v) TBP in benzene at 20°C were examined by IR spectrophotometry. With increasing metal concentration in the organic phase, the OH stretching band at 3480 cm'1 and the OH bending band at 1640cm"1 due to the compound TBP· H_20 [3] decreased in intensity and then almost disappeared, indicating that the extracted complex had no water molecule. Simultaneously the P —O stretching bands for the $TBPH_20$ at 1260cm'1 shifted to lower frequency at 1235cm'1 [4].

Further the organic extracts exhibited the Sn-CI stretching bands at 342, 330 and 320(shoulder) cm'1. In addition to the changes in those absorptions, any significant changes in the [P-O]-0 stretching vibration were observed with increasing the concentration of tin(IV) in the organic phase: the peak at 1020 cm"1 (actually a triplet 1055, 1020 and 990 cm'1) was noticed in the TBP spectrum showed a slight shift tol030cm'1; the two peaks at 1055 and 990cm"1 which appeared with an intensity slightly less than that of the peak at 1020cm"1 appeared as very shallow shoulders, but the intensity of the former peak increased and that of the latter peak decreased. It was thus assumed that the change in the [P-0]-C stretching vibration resulted from the interaction between the oxygen atom of this linkage and the extracted stannic chloride. The IR results confirm that the tin extracted into TBP solution is bonded to the phosphoryl oxygen atom.

Extraction isotherms by TOPO

The extraction of tin(IV) from hydrochloric acid solutions by TOPO gave the results indicated in Fig. 2. With increasing aqueous acidity, the distribution coefficient is almost the same and then falls gradually at above about 7 mołdin'3. The log-log plots of E_a° vs. $[TOPO]_{ini}$t gave the straight lines with the slope of ~2, suggesting the second-power dependency on TOPO concentration. Besides the continuous variation ot $[Sn]_{org}$ as a function of the mole fraction $[TOPO]i_{n4}/([Sn]jnKaq+[TOPO]init)$ at a fixed total concentration $[Sn]_{in}jt_aq^+$ [TOPO]jnit = O.OImol dm"3 showed the result that a maximum in $[Sn]_{org}$ appeared at the mole fraction of -0.67 in the

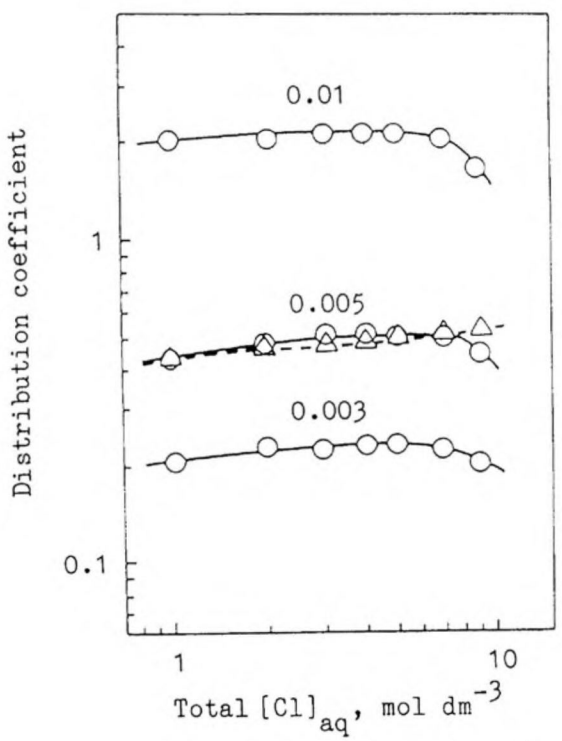


Figure 2. Extraction of tin(IV) from hydrochloric acid solutions by TOPO in benzene (numerals on curves are TOPO concns., mol dm'3; continuous and broken lines represent the extraction from HCl solns., and mixed 0.2 mol dm'3 HCl + LiCl solns., respectively).

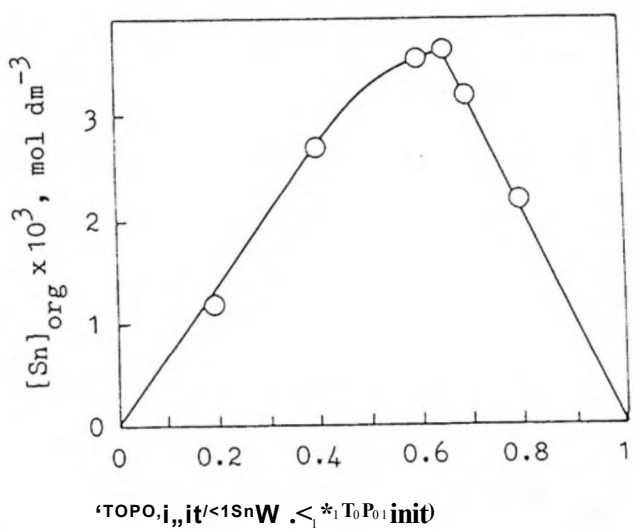


Figure 3. Continuous variation of $[Sn]_{ol}g$ plotted as a function of mole fraction $[rOPO]_{init}/([Sn]i_n i_{taq} + [TOPO]_{init})$ at a fixed total concentration of [Snjintaq + [TOPO]i_{nn} = 0.01 mol dm'3 for the extraction of Sn(IV) from 2 mol dm3 HCl by TOPO.

extraction of tin(IV) from hydrochloric acid solution at 2 mol dm^3 (Fig. 3). Further the stoichiometry of the extracted species was examined by a loading test of metal in the organic phase. In the extraction of tin(IV) from aqueous solutions containing 5 mol dm'3 HCI or 0.2 mol dm'3 HCI + 4.8 mol dm'3 LiCI, the molar ratio [Sn]/[CI]/[TOPO] approached to 1:4:2 with increasing the metal concentration in the organic phase. Therefore it is seen that the extracted species have no coordinated water molecule. Accordingly these results suggest the formation of the compound $SnCl_4$-2TOPO. Hence the extraction of tin(IV) from hydrochloric acid solutions by TOPO is expressed by the following equilibrium equation :

$$SnCl_4(a) + 2TOPO(o) \rightleftharpoons SnCl_4\text{-}2TOPO(o). \quad (2)$$

Infrared spectra for TOPO extraction system

The organic extracts of tin(IV) from hydrochloric acid solutions with 0.005 mol dm'3 TOPO in benzene at 20°C were examined by IR spectrophotometry. With increasing metal concentration in the organic phase, the P-O stretching band for the compound HCl· T0P0 ·$H_2$0 [5] at 1150 cm'1 shifted to the lower frequency at 1065 cm'1. In addition the organic extracts exhibited the Sn-CI stretching bands at 330, 320 and 300 cm'1. Consequently the IR spectra indicate the formation of the chloride coordinated metal ion species, supported by the $[CI]_{org}$ determined.

Temperature Effect

The extraction of tin(IV) from hydrochloric acid solutions by TBP and TOPO at the temperature 283 ~323 K gave the results that the distribution coefficients decreased with rising temperature due to the exothermic reaction.

CONCLUSION

The extraction of tin(IV) from hydrochloric acid solutions by TBP and TOPO is expressed by Eqs. (1) and (2). From the obtained results it is deduced that the complexes, $SnCl_4$-2TBP and $SnCl_4$-2TOPO, are in the octahedral structure of trance type.

REFERENCES

1. T. Sato and S.Kikuchi, (1988), *Hydrometallurgy,* 20, 97 — 108.
2. T. Sato, K. Sato, and Y. Noguchi (1999), *Solvent Extr. Res. Dev., Jpn.,* 6, 33-40.
3. T. Sato, K. Sato, Y. Noguchi and I. Ishikawa (1997), *Solvent Extr. Res. Dev., Jpn.,* 4, 35-50.
4. T. Sato (1965), *J. Appl. Chem.,* 15, 489- 495.
5. T. Sato, H. Watanabe and H. Yamatake, (1976), *J. Appl. Chem. Biotechnol.,* 26, 697-704.

Keywords: Solvent extraction, Tin(IV), Hydrochloric acid, TBP, TOPO

STUDY OF DYNAMIC SIMULATION AND ITS INFLUENCE ON THE CONTROL OF AN AGITATED LIQUID-LIQUID KÜHNI EXTRACTION COLUMN

M.L.A.C.N. Gomes*, M.M.L. Guimarães*, J. Stichlmair and J.J.C. Cruz-Pinto*****

*Dep. Eng. Quimica, IPP / Instituto Superior de Engenharia, Porto, Portugal
**Lehrstuhl für Fluidverfahrenstechnik, Technical University of Munich, Germany
***CICECO / Dep. Quimica, Universidade de Aveiro, Aveiro, Portugal.

Experimental data obtained in a pilot-scale Kühni liquid-liquid extraction column and simulated data generated by means of a drop population balance model and algorithm were used to describe and compute the local drop size distributions and dispersed phase hold-up profiles. After step variations in the agitation intensity, some particular aspects in the evolution of the hold-up profiles show either overshooting or undershooting behaviour, together with lag effects. In addition, after drastic variation in the agitation intensity, the system may fall in metastable situations. This experimental behaviour requires physical interpretation and has so far defied accurate modelling.

The results obtained and presented in this paper can be summarized as follows: (i) simulated using a drop population balance model exhibit reasonable agreement with experimental data, after the required fit of model parameters; (ii) in experimental runs, hold-up overshoots were observed in response to input disturbances, as an important characteristic of the dynamic behaviour of the extraction column; this effect is also predicted by the model and algorithm used.

INTRODUCTION

Environmental and safety regulations, growing demands on product quality, as well as increasingly competitive markets call for continuous improvement of chemical processes in minimal time at minimal cost. The modern trends toward greater process integration, tighter design margins and decreased product variability require systematic evaluation of dynamic operability to seek designs that maximize economic return while satisfying the operability requirements.

Industrial liquid-liquid extraction processes are usually run under steady-state conditions and without intended variation of the operating conditions. Operation under transient conditions seldom occurs, but is unavoidably introduced both by (a) random variation of uncontrolled external factors that are either too difficult or too expensive to keep within narrow bounds, and (b) deliberate corrective action undertaken by the operator or by automatic control systems in order to compensate for the effects of changing external factors.

In recent years, many authors have spent considerable efforts in modelling mechanically agitated devices for liquid-liquid contact and in attempting the experimental validation of their

models. Such models [1-3] have often been claimed able to describe within reasonable accuracy the results of their authors' experiments, even if most of them adopted significant simplifications - such as ignoring coalescence and/or contemplating the steady-state alone, in order to make calculations feasible in reasonable time.

In this work, simulation data were obtained by application of an algorithm (previously developed for a stirred vessel [4] and further adapted by Regueiras[5] to model an agitated column as a cascade of stirred vessels) for stagewise solving the population balance equations under dynamic conditions, designed to obtain the drop size distribution and local dispersed phase hold-up profiles along the column. The proposed model and parameter optimisation algorithm combine the drop interaction model developed by Coulaloglou and Tavlarides [6] as solved in [4], with its well-known four interaction parameters for breakage and coalescence and an original phase interstage transport model [5] with three additional transport parameters. The optimisation algorithm selected was Levenberg-Marquardt's. The objective function is defined as a weighed sum of the squared deviations between calculated and experimental values of the overall and local dispersed phase hold-ups and of the local cumulative, number-based, drop size distributions. Its application yielded encouraging agreement with experimental results (both static and dynamic) obtained in a pilot plant Kühni column [7, 8],

These experimental results suggest that particular evolutions of operating conditions, mainly step increases in the agitation intensity, may lead to the fall of the system into metastable states. Under these conditions, consequences may be serious from the point of view of feedback control: in the absence of a predictive master controller, pure (blind) feedback control may become counterproductive by throwing the system into metastable states from which it will either come out in serviceable time only at the cost of severe oscillations, or not at all.

The objective of this paper is to report these important new features of extraction column dynamics using the above-mentioned algorithm to clarify the experimental results. Since hydrodynamics alone was contemplated, all experiments were conducted in the absence of mass transfer, with mutually equilibrated, solute-free, continuous and dispersed phases.

EXPERIMENTAL WORK

The experimental work was carried out by Gomes [7] in a Kuhni pilot plant column (150 mm inside diameter, active height of 2520 mm, divided into 36 stirred compartments with 25% free area baffle plates, at Munich University). The test system was the standard equilibrated high interfacial tension toluene (dispersed phase) - water (continuous phase) system Experiments at room temperature, under both steady-state and dynamic conditions, were oerformed under normal and extreme aaitation intensity and disDersed and continuous chase flow rates. Details of the data contained in [7] may be obtained from the authors and other similar data are available from [9],

The extraction column is equipped with measurement devices that allow the investigation of the hydrodynamic conditions along the column. A photoelectric technique, initially developed by Pilhofer (cf. [10]), was used to measure the axial drop size distribution profiles. The drop slug length in a capillary was determined with two pairs of photoelectric cells on a calibrated capillary. This instrumentation was installed in the 2nd, 5th, 11th, 21st and 35th compartments of the column. Unfortunately, the experimental set-up does not provide for the acquisition of the feed drop size distribution (which was simulated as Gaussian with optimized average and standard deviation), nor even of the drop size distribution at the first column stage.

Local hold-ups were monitored at the 4th, 10th, 16th and 22nd compartments, using a non-invasive ultrasonic technique described by Yi and Tavlarides [11], As a check, the overall column hold-up was also measured using the pressure difference between the top and bottom of the active part of the column. All these data, as well as the intensity of agitation and the flow rates of the dispersed and continuous phases, were recorded on-line using a personal computer. Experimental results were obtained as data files created by *Hydromess,* a computer program developed at the University of Clausthal [10] and implemented at the University of Munich's pilot-scale Kühni column. From a collection of 1000-drop size measurements, this program computes number, volume and surface area drop size distributions and mean diameters. Drop size distributions were obtained under steady-state conditions only.

Different runs have been performed under the same operating conditions but under non-controlled environmental conditions (namely, temperature). Although this could be expected to be an important source of variation of the size and hold-up measured data, no significant difference was observed between measurements in two experimental campaigns at different times of the year.

Several experiments were planned and performed, under both steady-state and controlled transient conditions. For the latter, stepwise variations of 10 and 30% were imposed on the agitation rates. Two different standard operation conditions, corresponding to usual levels of flow-rates (F) and agitation rates, were tested: F_D = 160 L.h'1; F_c = 125 L.h'1; rpm = 140 and F_D = 120 L.h'1; F_c = 94 L.h'1; rpm = 170.

RESULTS AND DISCUSSION

Experimental results were studied from the point of view of the effects of positive and negative steps in the agitation intensity on the dispersed phase hold-up.

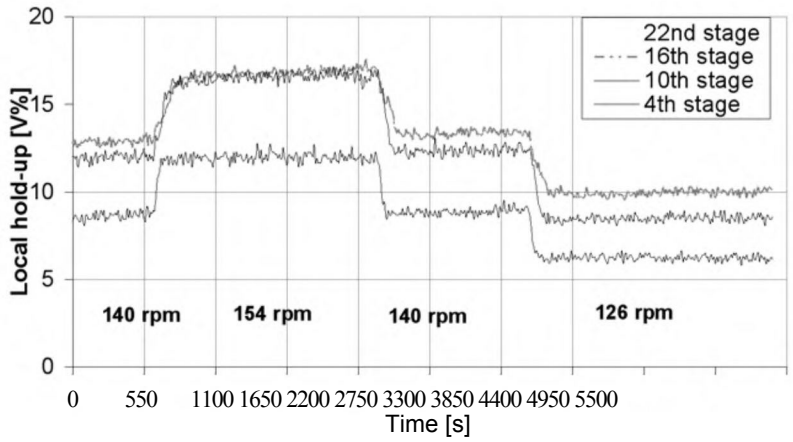


Figure 1. Experimental dispersed phase hold-up profiles before and after positive and negative (±10%) step variations in agitation rate, for operating conditions F_D = 160 L.h'1, F_c= 125 Lh'1.

Figure 1 shows that, after a step increase in agitation speed from a normal value (140 rpm) to an unusual high value for this type of equipment (154 rpm), the return to the normal value does neither follow the same path nor leads the system rapidly back to the original steady-state. In fact, the small drop population that originates at high agitation intensity (with the resulting high hold-up and residence time) does not re-coalesce easily, and thus does not promptly rebuild the original hold-up profile. The near superposition of the curves for the 16th

and 22nd stages after the transition from 140 to 126 rpm (unusually low agitation rate) may be interpreted as an effect of the increase in the coalescence / breakage frequency ratio. When the rotor speed is reduced, massive coalescence occurs, mainly at the upper stages where the drop population used to be made up of smaller sized droplets; concurrently, the larger drops thus formed, which have higher ascending velocities, climb swiftly, and do not suffer significant breakage at these lower agitation levels, thus decreasing the hold-up in the upper stages. The difficulty of the dispersion to return to the state corresponding to the previous agitation level leads to the possible conclusion that some particular evolutions of operating conditions may give rise to the fall of the system into metastable situations.

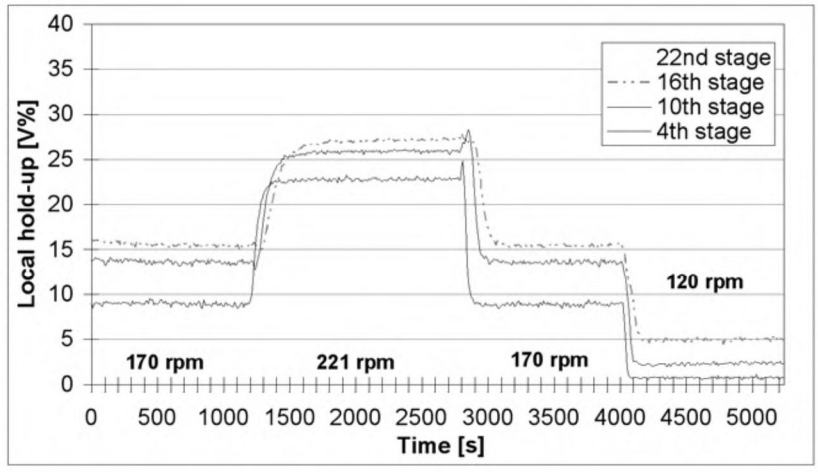


Figure 2. Experimental dispersed phase hold-up profiles before and after positive and negative (±30%) step variations in agitation rate, for operating conditions F_D = 120 L.h^{-1}, F_c = 94 L.h^{-1}.

Figure 2 shows the experimental dispersed phase hold-up profile for step variations in the agitation speed under lower flow rates. The superposition of the curves for the 16th and 22nd stages after the 170 to 120 rpm disturbance is also verified. However, after the negative step (221 to 170 rpm), the system does not exhibit the metastable behaviour observed in the previous situation (higher flows and smaller agitation rate variations). This fact may now be justified by the longer residence times of the drops in the column cells.

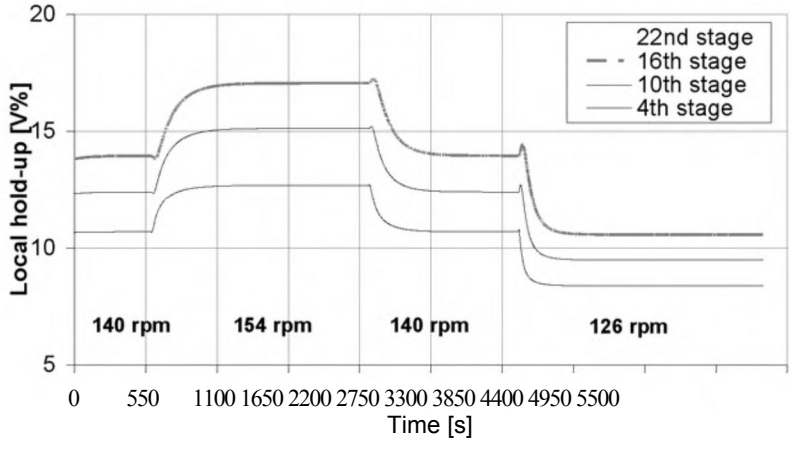


Figure 3. Simulated dispersed phase hold-up profiles for (±10%) step variations in agitation rate, for operating conditions F_D = 160 L.h^{-1}, F_c = 125 L.h^{-1}.

Simulated hold-up profiles are presented in Figures 3 to 4. Figure 3 shows the evolution in time of the local dispersed phase hold-up for step variations in agitation rates similar to the

first experiment discussed above. The transient behaviour predicted by the model incorporates the same overshooting and undershooting effects that were observed in the experimental runs and the ascending and descending paths are different, this phenomenon being particularly noticeable at the upper stages. However, the metastable effect observed in the experimental runs (Figure 1) is not noticeable in the simulated runs, which also show slower transitions than the experimental ones.

An additional simulation (for three equally spaced stages along the column height) was carrout (0-100- 182- 100 rpm), without exact equivalence in the experimental programme, but involving the most drastic possible changes in the agitation rate, for which we had corresponding steady-state data. The results are presented in Figure 4

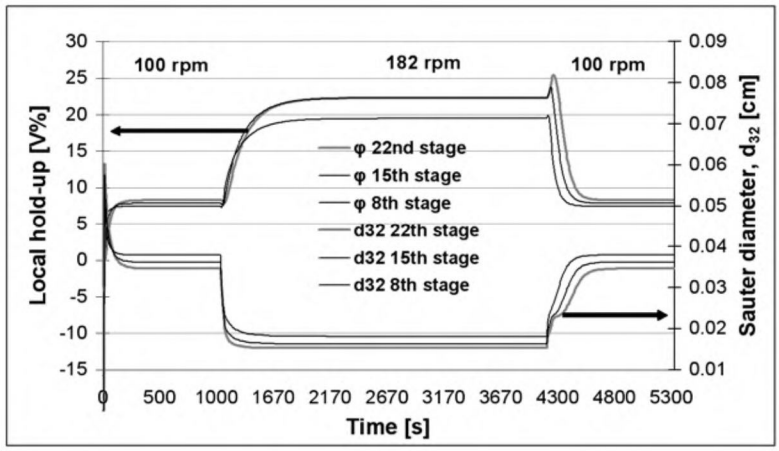


Figure 4. Simulated dispersed phase hold-up and average (d_{32}) drop size profiles for step variations in agitation rate (0-100-182-100 rpm), for operating conditions F_D= 160 L.h'¹, F_c = 125 L.h'¹.

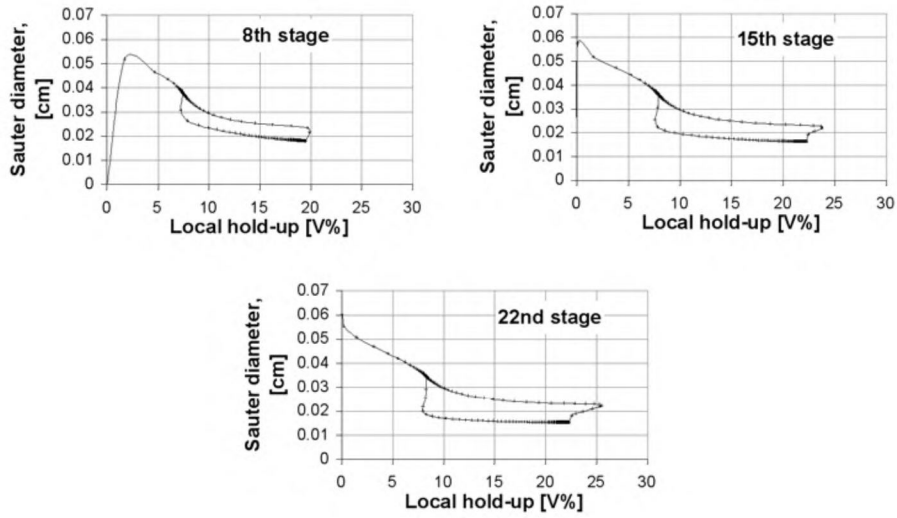


Figure 5. Plots showing a lag of hold-up and Sauter diameter in response to up and down steps in agitation rate for the simulation run of Figure 4.

As may be observed, the increase in the hold-up values, after a step increase in agitation rates goes along with a correspondent decrease in the Sauter-mean diameter. The experimental results obtained [7] have shown that the value of d_32 at each stage decreases with increasing agitation intensity and, for constant agitation intensity, it decreases along column height, while the hold-up increases consistently with both agitation intensity and

height along the column. This was to be expected since - the Kühni column being a strongly agitated device - drop breakage should dominate over coalescence.
Figure 5 shows, for the simulation described in Figure 4, the different ascending and descending paths as well as the (experimentally not always observed) return to the former state. This particular kind of representation, in mean diameter *vs.* hold-up coordinates with time as a hidden parameter, makes the phenomenon more apparent and clearly shows the peculiar relationship between the two variables during the disturbances.

CONCLUSIONS

Experiments performed in a pilot plant Kühni liquid-liquid extraction column illuminate a few particular aspects in the column response to step changes in agitation intensity.

The model and algorithms developed describe the Kühni column as a cascade of agitated vessels where drop interaction (breakage and coalescence) occurs and correctly predict the over and undershoot effects. The existence of a lag effect is thus demonstrated and explained.

However, the algorithm does not provide evidence for the experimentally demonstrated metastable states, at high flows and small agitation rate disturbances.

ACKNOWLEDGEMENTS

This work was carried out under the gratefully acknowledged financial supports of the IPP-Fundo de Apoio à Investigagão and the staff of Lehrstuhl für Fluidverfahrenstechnik.

REFERENCES

1. J.J.C. Cruz-Pinto (1979), *Experimental and Theoretical Modelling Studies of the Hydrodynamic and Mass Transfer Processes in Countercurrent-Flow Liquid-Liquid Extraction Columns*, Ph.D Thesis, The Victoria University of Manchester, UK.
2. C.Tsouris, V.l. Kirou, L. L. Tavlarides (1994), *AlChE. J.,* **40,** 407-418.
3. A. Gerstlauer, A. Mitrovic, E.D. Gilles, G. Zamponi and J. Stichlmair (1996), *In Value Adding Through Solvent Extraction,* University of Melbourne, pp. 1091-1096.
4. L.M. Ribeiro, P.F.R. Regueiras, M.M.L. Guimarães, Madureira C.M.N. and J.J.C. Cruz-Pinto (1997), *Comput. Chem. Engng.,* 21, N1 5, 543-558.
5. P.F.R. Regueiras, L.M. Ribeiro, M.M.L. Guimarães and J.J.C. Cruz-Pinto (1996), *In Value Adding Through Solvent Extraction,* University of Melbourne, pp. 1031-1036.
6. C.A. Coulaloalou and L.L. Tavlarides f 19771. *Chem. Ena. Sci..* **32.** 1289-1297.
7. M.L.A.C.N. Gomes (1999), Comportamento Hidrodinâmico de Colunas Agitadas de Extracgão Liquido-Liquido, Ph.D Thesis, Universidade do Minho, Portugal.
8. Luisa N. Gomes, Margarida L. Guimarães, José C. Lopes, Carlos N. Madureira, Johann Stichlmair and José J. Cruz-Pinto (2004), *Ind.Eng.Chem. Res.,* **43,** 1061-1070.
9. G. Zamponi (1996), Das dynamische Verhalten einer gerührten Solventeextraktionskollonne, Ph.DThesis, Technische Universität München, Germany.
10. B. Genenger, B. Lohrengel, M. Lorenz, A. Vogelpohl (1991), Hydromess-Mepsystem zur Bestimmung der Blasen - und Tropfengröpe in Mehrphasenströmungen.TU Clausthal, Germany.
11. J. Yi and L.L. Tavlarides (1990), *Ind. Eng. Chem. Res.,* 29, 475-482.



Computerized Simulation of Extraction Process using the laboratory simulation approach

Gideon Harel, Baruch Grinbaum*, Amiad Alexandron**

Consultant, Habonim 12 St. ,Kiriat Tivon 36031, Israel.
* - TAMI(IMI) Institute for R&D, POB 10140, Haifa Bay 26111, Israel.
** - Haifa Chemicals, POB 10809, Haifa Bay 26120, Israel.

The technique for lab simulation of counter-current multiple stage solvent extraction processes, using rows of separating funnels, is widely and successfully used in the laboratory for the development of new processes. It has been repeatedly proved that the simulated results are very close to the continuous process, provided that adequate number of rows of funnels is used.

This brought us to the idea to use this approach for computerized simulation. As in the computer there is no limit to the number of rows that may be implemented, the accuracy of such a simulation should be similar to this of a rigorous model.
The proposed approach has several advantages: 1) it converges fast 2) it works with non-linear equilibrium function. 3) it may be easily programmed on a PC without knowledge of programming languages.

The liquid-liquid equilibrium equations, in the form of **Y=f(T,X),** are similar to those used in any standard simulation program. The equations may be non-linear and there is no limitation on the number of stages or species to be extracted.
Comparison of the results obtained by this approach with results obtained by using rigorous models, as reported in the literature, proves that the model is accurate. The Excel program is rather short and the run of the most complex case took less than one minute.

INTRODUCTION

The technique for simulation of counter-current multiple stage solvent extraction processes at the lab using rows of separating funnels, as described by Treybal [1], is widely and successfully used in the laboratory for the development of new processes. And since its development 35 years ago no better method for laboratory simulation of countercurrent extraction processes has been developed. It has been repeatedly proved that the simulated results are very close to the continuous process, provided that adequate number of rows of funnels is used.

This brought us to the idea to use this approach for computerized simulation. As in the computer there is no limit to the number of rows that may be implemented, the accuracy of such a simulation should be similar to this of a rigorous model.

This approach is totally different from standard simulation methods. While the other methods try to solve a mathematical model of the countercurrent plant, our approach simulates the laboratory experiments in cross-current flow. Yet, just as the laboratory results of this method are reliable, so is its numerical application.

THE ALGORITHM

Lets assume a four stage counter-current extraction battery, as described in Fig. 1:

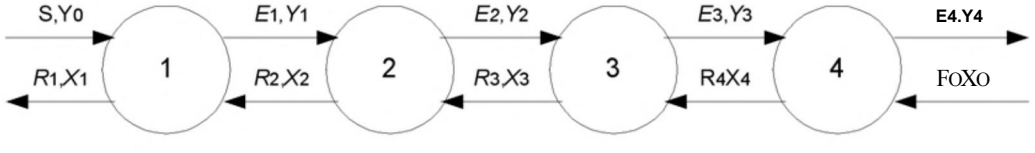


Figure 1: Counter Current SX battery with 4 stages

The simulation of this battery by repeated cross-current calculations is shown schematically in Fig. 2:

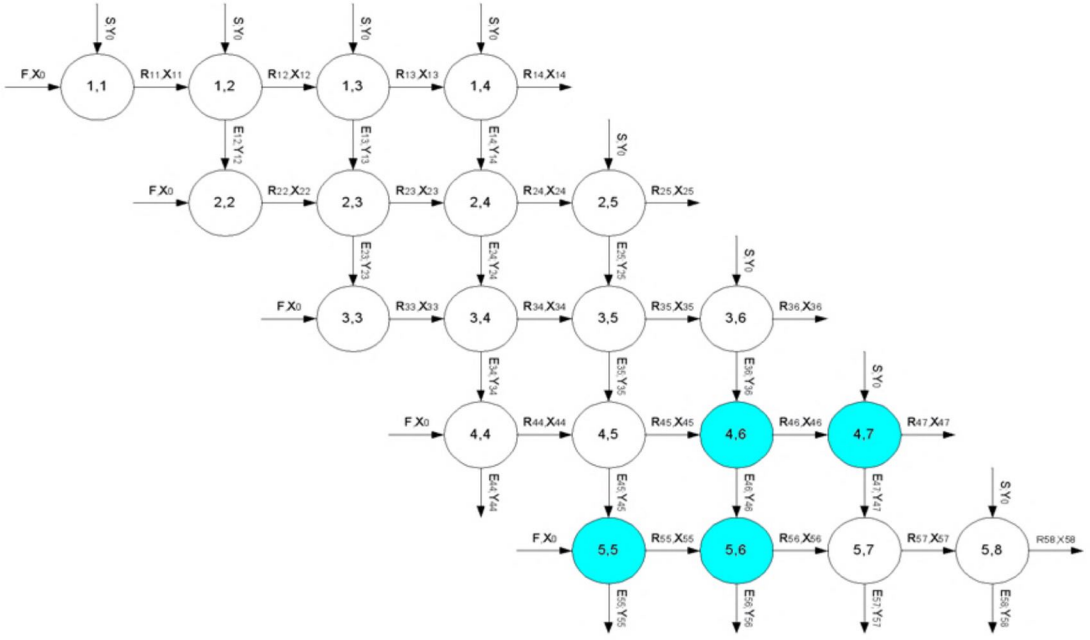


Figure 2: Multiple row cross-current scheme for 4 stages

Each of the circles represents an equilibrium stage. Starting at top left stage **(1,1),** an aqueous feed, **F,** with a composition $\mathbf{X_0}$, is contacted with an organic feed, **S,** having composition $\mathbf{Y_0}$. The extract from this stage $\mathbf{Ei_{t1}}$, is withdrawn, while its raffinate, $\mathbf{R_{1t1}}$ is fed to the next stage **(1,2).** The extract leaving stage **(1.2),** $\mathbf{EI_{,2}}$, is fed to stage **(2,2)** where it is contacted with the feed **F** and so on.

The extract streams move downwards. The raffinate streams move along the rows from left to right. The phase ratio, **S/F,** and the composition of the feed streams Y_0 and $X_{0,}$ for the multiple row cross-current scheme and for the counter-current are the same.

The calculations are carried out stage by stage, starting from the top row and moving from left to right, until the last stage, then going down to the next row and restarting at the first stage and so forth.

The extract and raffinate compositions **Yy** and **Xy** respectively, approach asymptotically the counter-current stages compositions as the row number / increases.

The number of rows M should be larger than the number of the counter-current stages, **N.** The convergence rate depends on the extraction factor *K* = **DS/F ,** where **D** is the distribution coefficient.

The method may be extended to a multiple component case. Vector **Xy** is replaced by the matrix $\mathbf{Xy_{,z}}$ where the subscript **z** stands for component.

Mass Balance for Stage i,j

(1) **Ry-lXy.i + EMJYMJ - Ry Xy + Ey Yy =0**

Yy is calculated by using the distribution coefficient relationship **Dy**

(2) **Dy** = f(**Xy) Yy = Xy Dy**

Mass balance for the solvent free solute in both phases:

(3) RiJ■i (1 - Xy-i) = Rij (1 - **Xy)**

(4) E_{M}Ud- Yi-ij) **= Ey(1** - Yy)

(5) Ry-i Xjj.i + f =M j Yj-ij - Rij Xy + Ey Dy Xy - 0

Xi.i is obtained by solving equations (2) to (5) for Xy

(6) Rij **= F** for j = i-1

(7) **Ey** = S for i = 0; j = 1 „..N
i = 1.. .M-1 ; j = N+i

The raffinate and extract streams flows and compositions of the lasts rows approach asymptotically the raffinate and extract streams flows and compositions of the equivalent counter-current battery.

so that

(8) **Rk -** $R_{S,T}$ k odd S **=** M - (k - 1 *)/2* T **=** M **+** (k-1)/2

k even S **=** M - k/2 +1 T = M + k/2

(9) E_k **=** $E_{s,T}$ k odd S **=** M - (k - 1)/2 T **=** M **+** (k-1)/2

k even S **=** M - k/2 +1 T **=** M **+** k/2

THE COMPUTATION METHOD

Implementation of the algorithm by a commercial spreadsheet like Microsoft Excel is straightforward. The spreadsheet configuration is similar to the pattern shown in

Fig Ia. The rows and columns depicted in Fig. 1 become rows and columns at the spread sheet, forming a block having the same pattern. At least five coherent blocks are required . Every block has the same number of rows and columns.

I	Aqueous composition for every stage	
II	Organic composition for every stage	equation (2)
III	Rafinatte flow for every stage.	equation (3)
IV	Extract flow for every stage	equation (4)
V	Mass balance for every stage	equation (5)

Block I cells have values, start with any values say 0.0 . Blocks II to IV cells contain mathematic expression using the values of the corresponding cells of the previous blocks. Block V cells contain equations that are solved cell by cell (stage by stage) starting from the top row from left to right by the function GOAL SEEK for equal to zero by changing correspondingly the values of cell of block I.

Actually there is no iterative computation the stage by stage calculation are straight forward and the GOAL SEEK function for every cell converges very fast, less than a fraction of second.

All the flow rates and compositions of the counter-current battery stages are obtained from the cells rows and columns as expressed by equations (8) and (9).

RESULTS

Simulation of recovery of Sulfuric acid by TEHA (tri-ethylhexylamine) with octanol as a modifier was studied by (2).

The equilibrium isotherm of H_2S0_4 between the aqueous and organic phase is highly non-linear, as expressed by the following equation:

(10) $$Y = A + \frac{B}{\left(1 + \left(\frac{X}{C}\right)^{D}\right)}$$

Y = $[H_2S0_4]org$; x = $[H_2S0_4]_{aq}$ mol/kg

Table 1: Profile computed by cross-current method (12 rows) for extraction of H_2S0_4[2]

Stage	Aqueous phase		Organic Phase	
	ton/h	H2S04%	ton/h	H2S04%
1	105.1	12.03	175.7	9.54
2	99.6	7.14	170.8	6.95
3	97.1	4.71	165.2	3.82
4	96.1	3.73	162.8	2.37
5	95.6	3.29	161.8	1.77
6	95.4	3.08	161.4	1.51
7	95.3	2.97	161.2	1.39
8	95.3	2.91	161.1	1.32

The results of the cross-current simulation are shown in Table 1 for extraction and in Table 2 for stripping. Each battery has 8 counter-current stages.

Operating Conditions: Feed 110 ton/h of 16% H_2S0_4 ; Solvent 161 ton/h of 1.29 % H_2S0_4; Extraction temperature 35°C.

Table 2: Profile computed by cross-current method (12 rows) for stripping of H_2S0_4 [2]

Stage	Aqueous phase		Organic Phase	
	ton/h	H2S04%	ton/h	H2S04%
1	104.2	4.06	156.5	1.65
2	106.7	6.32	160.7	4.21
3	108.3	7.67	163.2	5.69
4	109.4	8.58	164.7	6.54
5	110.3	9.34	165.7	7.15
6	111.2	10.05	166.6	7.62
7	112.2	10.88	167.5	8.10
8	113.7	12.08	168.5	8.65

Operating Conditions: Feed 100 ton/h water; Extract 174 ton/h 9.47 % H_2S0_4 Stripping temperature 60°C.

The results for both extraction and stripping are almost equal to those obtained by Gottlibsen [2], As both programs used the same equilibrium correlation, it proves that the reliability of both algorithms is similar

The rate of convergence, as a function of number of rows, is shown in Fig. 3:

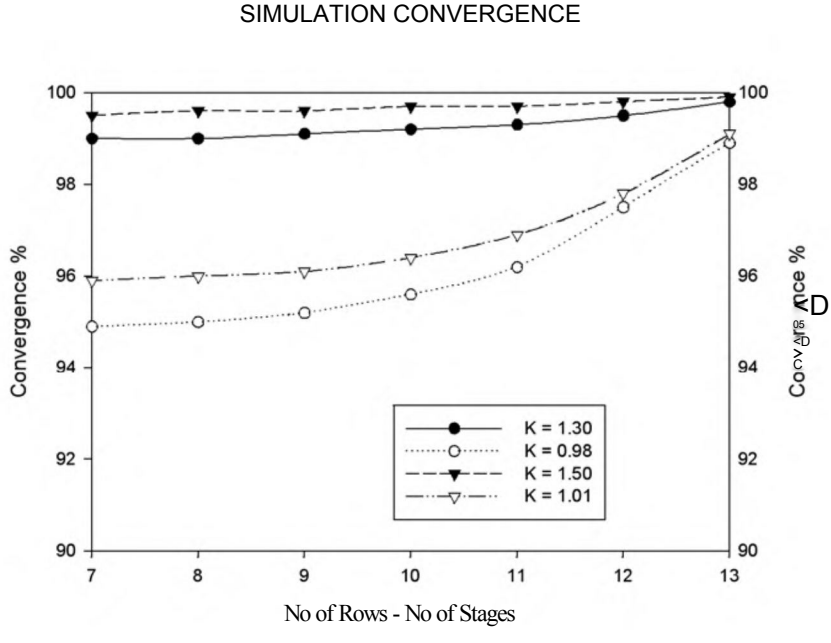


Figure 3: Simulation convergence

CONCLUSIONS

The results of the cross-current simulation are very similar to those of the rigorous counter-current one, and prove that the method may be used for simulation of SX processes. The programming, using Excel only, is quite easy, and the algorithm may be applied to any PC or laptop.

References

1> R.E. Treybal, Liquid Extraction 2nd Edition McGraw-Hill, 1971, Chapter 9.

2^ K.Gottliebsen, B. Grinbaum, Dehon Chen, and G. W. Stevens, *Hydrometallurgy* 56 (2000) 293 - 307.

Nomeclature

Djj distribution coefficient
Ej Extract from stage i for the counter-current battery., kg/h
Ejj Extract from stage i row j for the multiple row-cross-current, kg/h.
F Aqueous feed, kg/h
K Extraction factor - distribution **D S/F**
M Number of cross-currentrows.
N Number of counter currentstages.
Ri Raffinate from stage i for the counter-current battery., kg/h
Rij Raffinate from stage i , row j - for multiple row cross-current, kg/h
S Solvent feed kg/h
T Temperature C.
Xjj Solute in Raffinate concentration kg solute / kg Raffinate.
Yjj Solute in Extract concentration kg solute/ kg Extract.



Computerized Simulation of Extraction Process using the laboratory simulation approach

Gideon Harel, Baruch Grinbaum*, Amiad Alexandron**

Consultant, Habonim 12 St. ,Kiriat Tivon 36031, Israel.
* - TAMI(IMI) Institute for R&D, POB 10140, Haifa Bay 26111, Israel.
** - Haifa Chemicals, POB 10809, Haifa Bay 26120, Israel.

The technique for lab simulation of counter-current multiple stage solvent extraction processes, using rows of separating funnels, is widely and successfully used in the laboratory for the development of new processes. It has been repeatedly proved that the simulated results are very close to the continuous process, provided that adequate number of rows of funnels is used.

This brought us to the idea to use this approach for computerized simulation. As in the computer there is no limit to the number of rows that may be implemented, the accuracy of such a simulation should be similar to this of a rigorous model.
The proposed approach has several advantages: 1) it converges fast 2) it works with non-linear equilibrium function. 3) it may be easily programmed on a PC without knowledge of programming languages.

The liquid-liquid equilibrium equations, in the form of **Y=f(T,X),** are similar to those used in any standard simulation program. The equations may be non-linear and there is no limitation on the number of stages or species to be extracted.
Comparison of the results obtained by this approach with results obtained by using rigorous models, as reported in the literature, proves that the model is accurate. The Excel program is rather short and the run of the most complex case took less than one minute.

INTRODUCTION

The technique for simulation of counter-current multiple stage solvent extraction processes at the lab using rows of separating funnels, as described by Treybal [1], is widely and successfully used in the laboratory for the development of new processes. And since its development 35 years ago no better method for laboratory simulation of countercurrent extraction processes has been developed. It has been repeatedly proved that the simulated results are very close to the continuous process, provided that adequate number of rows of funnels is used.

This brought us to the idea to use this approach for computerized simulation. As in the computer there is no limit to the number of rows that may be implemented, the accuracy of such a simulation should be similar to this of a rigorous model.

This approach is totally different from standard simulation methods. While the other methods try to solve a mathematical model of the countercurrent plant, our approach simulates the laboratory experiments in cross-current flow. Yet, just as the laboratory results of this method are reliable, so is its numerical application.

THE ALGORITHM

Lets assume a four stage counter-current extraction battery, as described in Fig. 1:

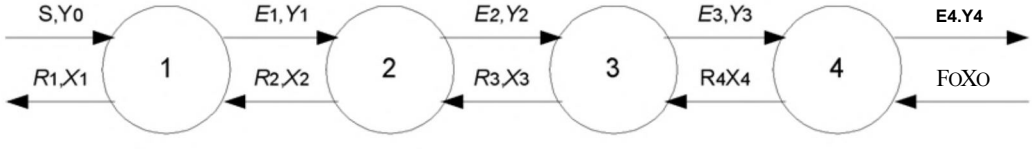


Figure 1: Counter Current SX battery with 4 stages

The simulation of this battery by repeated cross-current calculations is shown schematically in Fig. 2:

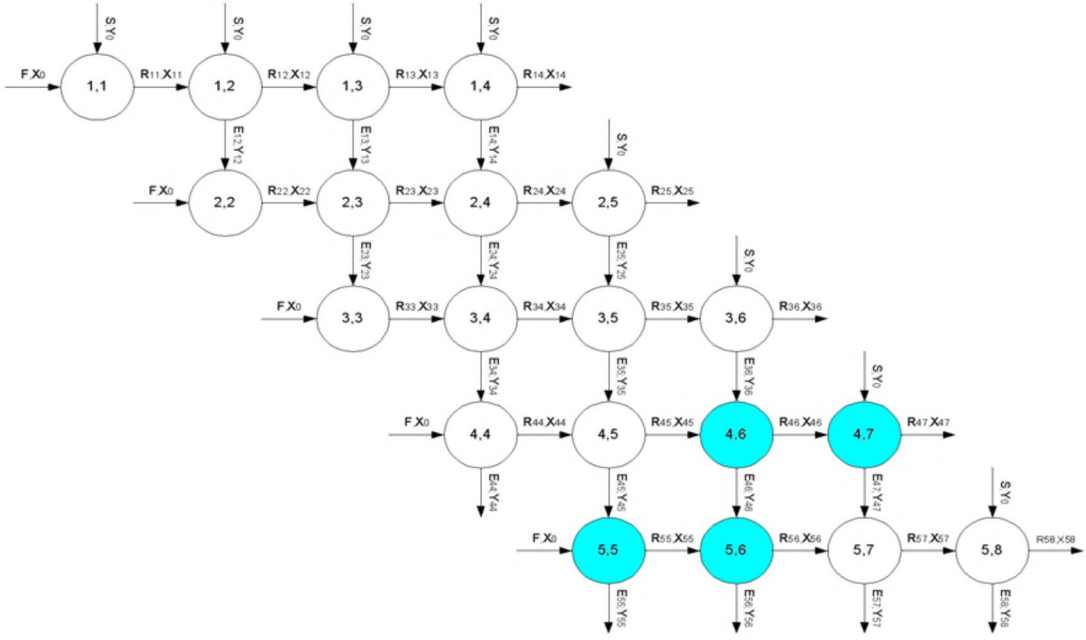


Figure 2: Multiple row cross-current scheme for 4 stages

Each of the circles represents an equilibrium stage. Starting at top left stage **(1,1),** an aqueous feed, **F,** with a composition $\mathbf{X_0}$, is contacted with an organic feed, **S,** having composition $\mathbf{Y_0}$. The extract from this stage $\mathbf{Ei_{t1}}$, is withdrawn, while its raffinate, $\mathbf{R_{1t1}}$ is fed to the next stage **(1,2).** The extract leaving stage **(1.2),** $\mathbf{EI_{,2}}$, is fed to stage **(2,2)** where it is contacted with the feed **F** and so on.

The extract streams move downwards. The raffinate streams move along the rows from left to right. The phase ratio, **S/F,** and the composition of the feed streams Y_0 and $X_{0,}$ for the multiple row cross-current scheme and for the counter-current are the same.

The calculations are carried out stage by stage, starting from the top row and moving from left to right, until the last stage, then going down to the next row and restarting at the first stage and so forth.

The extract and raffinate compositions **Yy** and **Xy** respectively, approach asymptotically the counter-current stages compositions as the row number / increases.

The number of rows M should be larger than the number of the counter-current stages, **N.** The convergence rate depends on the extraction factor *K* = **DS/F ,** where **D** is the distribution coefficient.

The method may be extended to a multiple component case. Vector **Xy** is replaced by the matrix $Xy_{,z}$ where the subscript **z** stands for component.

Mass Balance for Stage i,j

(1) **Ry-lXy.i + EMJYMJ - Ry Xy + Ey Yy =0**

Yy is calculated by using the distribution coefficient relationship **Dy**

(2) **Dy** = f(**Xy) Yy = Xy Dy**

Mass balance for the solvent free solute in both phases:

(3) RiJ■i (1 - Xy-i) = Rij (1 - **Xy)**

(4) E_{M}Ud- Yi-ij) **= Ey(1** - Yy)

(5) Ry-i Xjj.i + f =M j Yj-ij- Rij Xy + Ey Dy Xy -0

Xi.i is obtained by solving equations (2) to (5) for Xy

(6) Rij **= F** for j = i-1

(7) **Ey** = S for i = 0; j = 1 „..N
i = 1...M-1 ; j = N+i

The raffinate and extract streams flows and compositions of the lasts rows approach asymptotically the raffinate and extract streams flows and compositions of the equivalent counter-current battery.

so that

(8) **Rk -** $R_{S,T}$ k odd S **=** M - (k - 1 *)/2* T **=** M **+** (k-1)/2

k even S **=** M - k/2 +1 T = M + k/2

(9) E_k **=** $E_{s,T}$ k odd S **=** M - (k - 1)/2 T **=** M **+** (k-1)/2

k even S **=** M - k/2 +1 T **=** M **+** k/2

THE COMPUTATION METHOD

Implementation of the algorithm by a commercial spreadsheet like Microsoft Excel is straightforward. The spreadsheet configuration is similar to the pattern shown in

Fig Ia. The rows and columns depicted in Fig. 1 become rows and columns at the spread sheet, forming a block having the same pattern. At least five coherent blocks are required . Every block has the same number of rows and columns.

I	Aqueous composition for every stage	
II	Organic composition for every stage	equation (2)
III	Rafinatte flow for every stage.	equation (3)
IV	Extract flow for every stage	equation (4)
V	Mass balance for every stage	equation (5)

Block I cells have values, start with any values say 0.0 . Blocks II to IV cells contain mathematic expression using the values of the corresponding cells of the previous blocks. Block V cells contain equations that are solved cell by cell (stage by stage) starting from the top row from left to right by the function GOAL SEEK for equal to zero by changing correspondingly the values of cell of block I.

Actually there is no iterative computation the stage by stage calculation are straight forward and the GOAL SEEK function for every cell converges very fast, less than a fraction of second.

All the flow rates and compositions of the counter-current battery stages are obtained from the cells rows and columns as expressed by equations (8) and (9).

RESULTS

Simulation of recovery of Sulfuric acid by TEHA (tri-ethylhexylamine) with octanol as a modifier was studied by (2).

The equilibrium isotherm of H_2S0_4 between the aqueous and organic phase is highly non-linear, as expressed by the following equation:

(10) $$Y = A + \frac{B}{\left(1 + \left(\frac{X}{C}\right)^{D}\right)}$$

Y = $[H_2S0_4]org$; x = $[H_2S0_4]_{aq}$ mol/kg

Table 1: Profile computed by cross-current method (12 rows) for extraction of H_2S0_4[2]

Stage	Aqueous phase		Organic Phase	
	ton/h	H2S04%	ton/h	H2S04%
1	105.1	12.03	175.7	9.54
2	99.6	7.14	170.8	6.95
3	97.1	4.71	165.2	3.82
4	96.1	3.73	162.8	2.37
5	95.6	3.29	161.8	1.77
6	95.4	3.08	161.4	1.51
7	95.3	2.97	161.2	1.39
8	95.3	2.91	161.1	1.32

The results of the cross-current simulation are shown in Table 1 for extraction and in Table 2 for stripping. Each battery has 8 counter-current stages.

Operating Conditions: Feed 110 ton/h of 16% H_2S0_4 ; Solvent 161 ton/h of 1.29 % H_2S0_4; Extraction temperature 35°C.

Table 2: Profile computed by cross-current method (12 rows) for stripping of H_2S0_4 [2]

Stage	Aqueous phase		Organic Phase	
	ton/h	H2S04%	ton/h	H2S04%
1	104.2	4.06	156.5	1.65
2	106.7	6.32	160.7	4.21
3	108.3	7.67	163.2	5.69
4	109.4	8.58	164.7	6.54
5	110.3	9.34	165.7	7.15
6	111.2	10.05	166.6	7.62
7	112.2	10.88	167.5	8.10
8	113.7	12.08	168.5	8.65

Operating Conditions: Feed 100 ton/h water; Extract 174 ton/h 9.47 % H_2S0_4 Stripping temperature 60°C.

The results for both extraction and stripping are almost equal to those obtained by Gottlibsen [2], As both programs used the same equilibrium correlation, it proves that the reliability of both algorithms is similar

The rate of convergence, as a function of number of rows, is shown in Fig. 3:

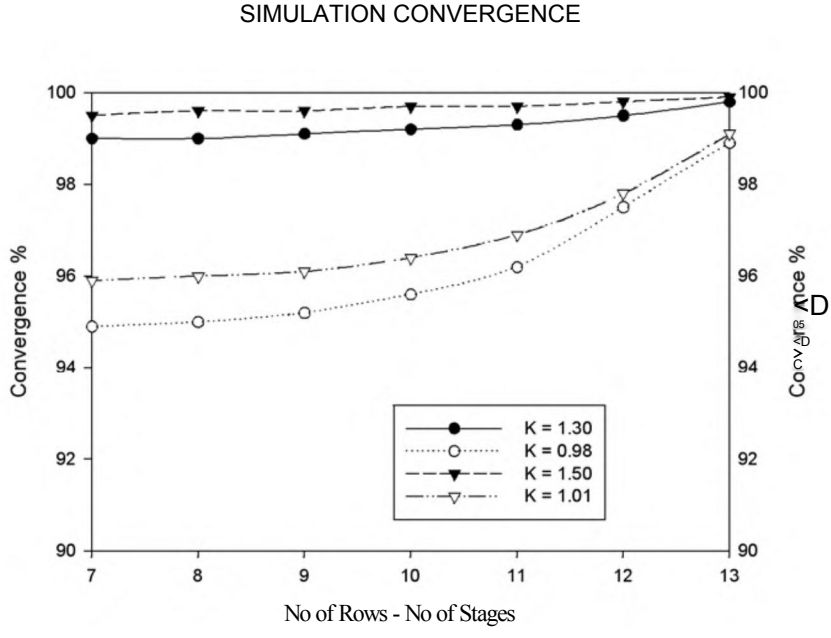


Figure 3: Simulation convergence

CONCLUSIONS

The results of the cross-current simulation are very similar to those of the rigorous counter-current one, and prove that the method may be used for simulation of SX processes. The programming, using Excel only, is quite easy, and the algorithm may be applied to any PC or laptop.

References

1> R.E. Treybal, Liquid Extraction 2nd Edition McGraw-Hill, 1971, Chapter 9.

2^ K.Gottliebsen, B. Grinbaum, Dehon Chen, and G. W. Stevens, *Hydrometallurgy* 56 (2000) 293 - 307.

Nomeclature

Djj distribution coefficient
Ej Extract from stage i for the counter-current battery., kg/h
Ejj Extract from stage i row j for the multiple row-cross-current, kg/h.
F Aqueous feed, kg/h
K Extraction factor - distribution **D S/F**
M Number of cross-currentrows.
N Number of counter currentstages.
Ri Raffinate from stage i for the counter-current battery., kg/h
Rij Raffinate from stage i , row j - for multiple row cross-current, kg/h
S Solvent feed kg/h
T Temperature C.
Xjj Solute in Raffinate concentration kg solute / kg Raffinate.
Yjj Solute in Extract concentration kg solute/ kg Extract.



FROM SINGLE DROPLET TO COLUMN DESIGN - A REVIEW

Hans-Jörg Bart

Institute of Thermal Process Engineering
TU Kaiserslautern, D-67653 Kaiserslautern, Germany
http://www.uni-kl.de/LS-Bart/

The state of the art to design counter-current extraction columns is based on the performance of pilot plant experiments. The modelling is then either with the equilibrium or dispersion model, whereas in the latter the dispersion coefficient accounts for all hydrodynamic non-idealities. A new approach uses single droplet experiments to obtain the basic laws and functions governing droplet breakage, coalescence, relative velocity and axial dispersion when using droplet populance balance models (DPBM).

INTRODUCTION

Liquid-liquid extraction (LLEC) columns are highly efficient and are widely used in petroleum, pharmaceutical and chemical industry [1, 2] due to in their high throughputs and low costs in respect to number of stages, solvent inventory, etc. [3, 4], The calculation of the height of a column with the equilibrium stage model needs HETP values from pilot columns which are then scaled empirically to industrial ones [4, 5], The dispersion model is a non-equilibrium model and accounts for mass transfer kinetics and back-mixing, considering the deviations from ideal column plug flow. In the scaling procedure the different axial dispersion of differently sized columns will be considered according to semi-empirical laws [6], The simulation of LLEC based on DPBM provides a useful means to stimulate the transient and steady state behavior of such an important unit operation. The complex dispersed phase interactions, like coalescence, break-up, droplet rise and back-mixing, are the basic phenomena which have to be taken into account in the DPBM [7-9], In a trilateral operation of TU Munich, RWTH Aachen and TU Kaiserslautern efforts were made to implement DPBM with pulsed and stirred columns. For the latter a Windows based program will be presented.

MODEL

The polydisperse nature of the turbulent droplet swarm in agitated liquid-liquid contacting equipment makes its mathematical modelling and the solution methodologies a rather delicate process. This polydispersion could be modelled as a population of droplets distributed with some internal properties (e.g. size, solute concentration) at a specific column height using DPBM as a mathematical tool [9-11]:

$$\frac{^5\text{'W,(V/)}}{8t} = -\frac{^5\text{KW}</.\text{C}\ (\text{V'})|}{8z} + \frac{d}{dz}\left[D, \frac{^5\text{«rf.c,(V')}}{dz} \right] - \text{£}\underset{<=i}{\overset{2\,d\,[\dot{C}\,n\,\hat{}\,(u/)j\ O'''}{\hat{o}Qi\ A}} + \text{-7-}\ ^{n\,'!}\ (d,c_y,t)8(z\text{-}z_y) + r\{\backslash(/\} \quad (1)$$

The vector $y/ = [d\ c\ z\ t\backslash$ in Eq. (1) represents the droplet internal coordinates (d,c_y), the external coordinate (column height, z) and the time (t). The nonstationary term follows a transport term (droplet rising velocity, u_y) and the velocity vector along the internal coordinates is given by $\text{£} = \backslash d\ c_y]$. One the right hand side the axial dispersion (D_y) is followed by the feed flow (Q_y^{in}) over the cross-sectional area (A_c) at the location (z_y) with an inlet number density (n_y^{in}) and is treated as a point source in space. The last source term (^{y/}) is more complex and is discussed by Attarakih et al. [12, 13] in detail. It consists of a breakage and coalescence source term. In both terms the gain (birth) and loss (death) of droplets in respect to a certain droplet class is considered. Here the breakage source term is characterized by the breakage frequency $r\backslash d,<f>_y$) and the daughter droplet distribution $p_{„}(d,d)$ and the coalescence source term is described by the coalescence rate $G)(d,d',<f>_y)$, which will be discussed below in detail.

The transport equations describing hydrodynamics and the solute concentration (c_x) in the continuous phase takes the mass transfer from the continuous to the dispersed phase into account. The equation is coupled to the solute balance in the continuous phase through the convective and the source terms of Eq. (1) and could be written as

$$\frac{WO}{8t} = \frac{\partial}{p^{U\hat{}}} \left(\frac{W,)}{dz} \right) + \frac{Q'''}{A_c} \text{¥*-}S(z\text{-}_{z}.\text{v}) \quad (2)$$

$$\frac{\hat{c}(W,cJ}{Pit} = \frac{d}{\partial z}\left(»Ac_x + D_x\text{-}2£d\text{-} \right) + \frac{Q^{in}c^{W}}{\sim 1r^{JLS(Z}\ \sim Zy)} \sim \text{Jo"}\mathbf{r}\ \mathbf{c'}\ \text{V}\hat{}\text{K;;}\ iv)8ddc_y \quad (3)$$

Here the first and the second term on the left side of Eqs. (2) and (3) is to be interpreted analogous to the respective terms in Eq. (1). The last term appearing in Eq. (3) describes the mass transfer of the solute. To solve the full DPBM is still expensive from a compulational point of view since the balance models are normally integral partial differential equations (IPDE). An efficient approach in the numerical solution of these equations is to project the infinite system (with respect to droplet volume or diameter) of IPDEs given by Eq. (1) onto a finite system of partial differential equations (PDE) using the generalized fixed pivot technique. The idea in this technique is to divide the internal droplet coordinate (volume) into contiguous finite subdomains covering the range of this internal coordinate. In each subdomain, the total volume concentration is obtained by integrating the volume concentration distribution with respect to volume (diameter) over the boundaries of this subdomain. This local volume concentration is then concentrated at a single point in this subdomain called the fixed-pivot, X/, and is given by

$$<P,(zj) = \text{P}^{*1'2}v(v)n(v,z,t)dv = \text{v(x,)A}\hat{}_{(}(\text{z,r}),\ i = l,2...M_x \quad (4)$$

This replaces the IPDE given by Eq. (1) by M_x finite number of PDEs that are non-linearly coupled through the convective and the source terms. These PDEs are then discretized based on upwind and central differencing schemes and the numerics are treated in detail by Attarakih et al. [9-13], In addition, the source term takes into account the conservation of any integral properties, such as the total droplet number and volume.

SAMPLE PROBLEM

The user input in the LLECMOD (Liquid-Liquid Extraction Column Module) is shown in Fig. 1 and for the chosen RDC geometry in Fig. 2. Once all the input is echoed the user is asked to choose the droplet phase-space solver. When the final simulation time is exceeded or the steady state tolerance is achieved the LLECMOD presents the results in graphical form showing the most important data for the simulation such as the hold-up, Sauter diameter and droplet size distribution as well as a summary of the simulation results displayed in a separate window. The graphics library used to generate the output is an improved and modified version of the SIGRAPH library provided with the Compaq visual FORTRAN version 6.6. LLECMOD in its current version comprises the geometries of the KÜHNI and RDC column and serves the following hydrodynamic aspects. The relative rising or slip velocity is taken from literature [14] with droplet class dependent parameters used according to Garthe [15], The axial dispersion coefficient of the continuous phase was taken according to Sommeregger et al. [16] and the dispersed phase droplet class dependent ones after a correlation from Modes [17]. Generally it can be said that dispersion coefficients approach to similar values in either phase and become independent from the classes at high specific throughputs and power input [18], which simplifies calculations.

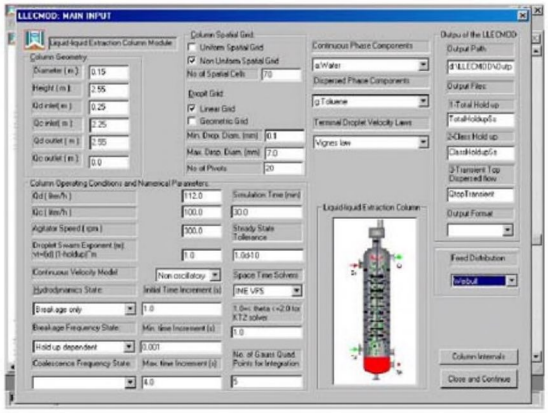


Fig. 1: The main input dialog of the LLECMOD showing the input of a sample problem.

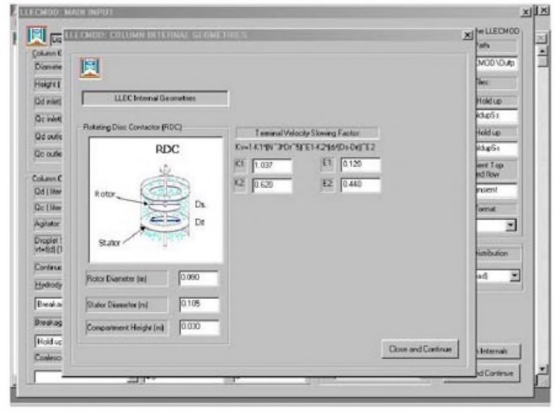


Fig. 2: The LLECMOD input dialogue for internal RDC column geomethes.

For the droplet breakage probability correlations have be developed which take into account column geometry (rotor speed and diameter) and physical properties (viscosity, density, interfacial tension) of the systems used [19], They can be selected or modified within the LLECMOD.

In a stirred extraction column the coalescence process is always accompanied by breakage and cannot be estimated independently. Moreover, the coalescence probability of droplets strongly depends on droplet size, hold-up and system properties (e .g. pH-value, ionic strength, zeta potential) and also on mass transfer direction. If the mass transfer is from the dispersed to the continuous phase, the interdroplet film is accelerated and coalescence promoted. In the opposite direction coalescence is hindered and may be neglected in a first guess, which makes calculations easier [20], However, minor impurities (e.g. surfactants) may drastically changes that behavior and measurements in small lab-scale devices [21] will give coalescence parameters, which only depend on the chemical system used and not on operating conditions or column geometry. Currently in LLECMOD the model of Coulaloglou and Tavlarides [22] is implemented, where the coalescence frequency is a product of collision rate *h(d,df,<p)* and coalescence efficiency *A(d,d*’**,</>):**

a (d,d',</>) = h(d,d\c/)-A(d,d\</>) (5)

with one adjustable parameter in rate and efficiency, respectively.

The mass transfer correlations and equilibria can also be selected or user specific data may be used. For the dispersed phase the model of Handlos and Baron [23] and for the continuous phase the model of Kumar and Hartland [24] is recommended. For high accuracy simulations it is better to use experimental data from small lab-scale devices as discussed elsewhere [7, 8, 21] instead of the breakage and mass transfer correlations. With this the effect of impurities and by-products in industrial applications is better reflected.

Fig. 3 shows the experimentally obtained hold-up profile in the RDC technical column in comparison to the simulated profiles for a phase ratio of one and a rotor speed of 350 1/min.

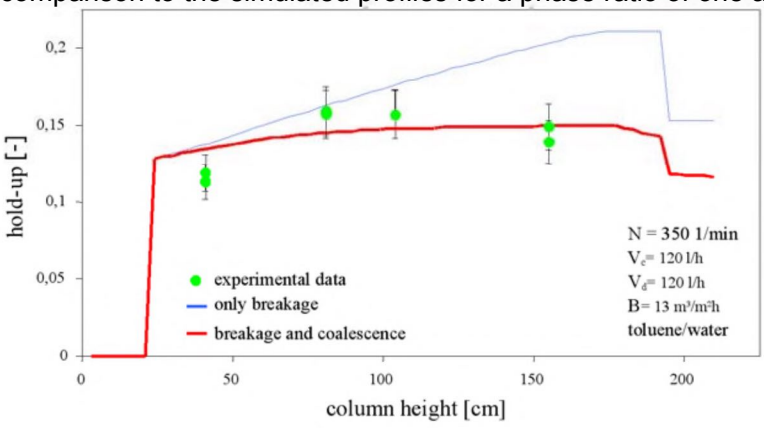


Fig. 3: Comparison of experimental and simulated hold-up profiles taking into account breakage and coalescence.

Since the model accounts for all the hydrodynamic aspects (back-mixing, convection, coalescence and break-up), a qood reproduction of the experimental data can be observed. Neglecting the droplet coalescence, the droplet size distribution in the column tends to the small size range, which yields a higher hold-up due to an increased droplet residence time in the compartments. Besides the calculation of the hold-up, the calculation of the droplet size distribution along the column height is decisive for mass transfer and hydrodynamics.

Fig. 4 shows the simulated mean Sauter diameters d_32 in comparison to the experimental ones according to data with [15, 25] and without mass transfer [20], The mean relative error between simulated and experimental values averages about 15%.

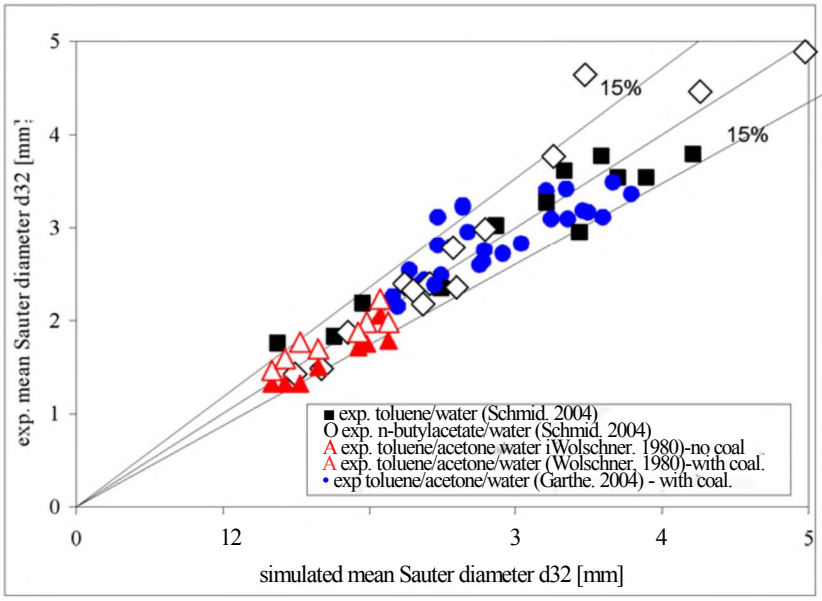


Fig. 4: Comparison of experimental and simulated mean Sauter diameters d_{32}.

For the validation of the column performance under mass transfer conditions the measured concentration profiles of different authors were compared with simulated ones. For this prediction the coalescence parameters for the different column geometries were estimated in a lab-scale unit in our laboratory [19, 20] and otherwise only the correlations from LLECMOD were used As can be

seen in Fig. 5, the concentration profiles in extraction columns at different operating conditions can be predicted within a good accuracy (mean relative error about 20 %).

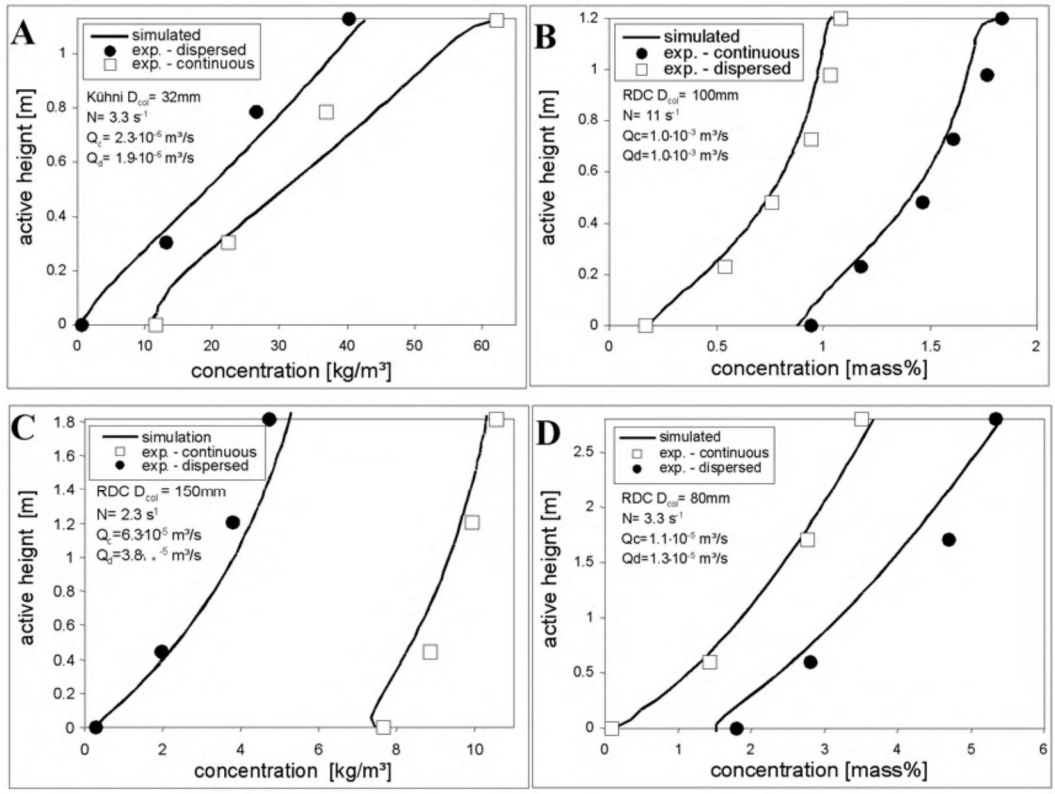


Fig. 5: Acetone concentration profiles for different column types and geometries; toluene/acetone/water (A - Kolb [26], B - Wolschner [25], C - Brodkorb [27], 25° C, D-Garthe [15]).

CONCLUSIONS

The Windows-based program LLECMOD successfully describes hydrodynamics and mass transfer of liquid-liquid extraction columns using the generalized fixed pivot technique to solve the DPBM equations. The user-friendly input dialoge and the user functions input module make the program very general and simple to use. Stable simulation results on a 1.7 MHz PC for hydrodynamics simulations are obtained in less than 2 minutes and for the bivariate case, including mass transfer, in less than 10 minutes. The mean Sauter diameter, hold-up and concentration profiles could be well predicted, which promotes the use of DPBM models for further applications in industrial scale.

ACKNOWLEDGEMENTS

The authors wish to thank the AiF (Arbeitsgemeinschaft industrieller Forschungsvereinigungen ,,Otto von Guericke" e.V.), the BMWA (Bundesministerium für Wirtschaft und Arbeit) and the DFG (Deutsche Forschungsgemeinschaft) for financial support.

REFERENCES

1. Brandt, H.W., Reissinger, K.-H., and Schröter, J. (1978), *Chem. Ing. Techn.,* 50, 345-354.
2. Lo, T.C., Baird, M.H.I., and Hanson, C., eds. (1983), *Handbook of Solvent Extraction.* J. Wiley & Sons, New York.
3. Godfrey, J.C. and Slater, M.J., eds. (1994), *Liquid-Liquid Extraction Equipment.* J. Wiley & Sons, Chichester.
4. Robins, L.A. and Cusack, R.W. (1997), *Perry's Chemical Engineers' Handbook:* Liquid-Liquid Extraction Operations and Equipment, R.H. Perry and D.W. Green (eds.), McGraw Hill: New York. p. 15/1-15/47.
5. Thornton, J.D., ed. (1992), *Science and Practice of Liquid-Liquid Extraction.* **Vol.** 1-2. Oxford University Press, Oxford.
6. Pilhofer, T. (1988), *Chem. Eng. Techn.,* 11, 259 - 263.
7. Bart, H.J. (2001), Reactive Extraction: Springer, Berlin.
8. Bart, H.-J. and Stevens, G. (2004), *Reactive Solvent Extraction-.* Ion Exchange and Solvent Extraction, **Vol. 17,** M. Kertes and A.K. Sengupta (eds.), Marcel Dekker: New York. p. 37-82.
9. Kronberger, T., Ortner, A., Zulehner, W. und Bart, *H.-J. (1995) Comput. Chem. Engng.,* 19, 5639-5644.
10. Attarakih, M., Bart, H.J., and Faqir, N.M. (2003), *Chem. Eng. Sci.,* 12 (58), 1251-1269.
11. Attarakih, M., Bart, H.J., and Faqir, N.M. (2005 accepted), Chem. Eng. Sci.
12. Attarakih, M.M., Bart, H.-J., and Faqir, N.M. (2004), *Chem. Eng. Sci.,* 59, 2567-2592.
13. Attarakih, M.M., Bart, H.-J., and Faqir, N.M. (2004), *Chem. Eng. Sci.,* 59, 2547-2565.
14. Bailes, P.J., Gledhill, J., Godfrey, J.C., and Slater, M.J. (1986), *Chem. Eng. Res. Des.,* **64,** 43-55.
15. Garte, D., *Personal Communication.* 2004, Technische Universität München.
16. Sommeregger, E., Wolschner, B., and Marr, R. (1980), *Chem. Ing. Techn.,* 52, 277.
17. Modes, G., *Grundsätzliche Studie zur Populationsdynamik einer Extraktionskolonne auf Basis von Einzeltropfenuntersuchungen.* 2000: Shaker Verlag, Aachen.
18. Gourdon, C., Casamatta, G., and Muratet, G. (1994), *Liquid-liquid extraction equipment.* Population balance based modelling of solvent extraction columns, J.C. Godfrey and M.J. Slater (eds.), John Wiley & Sons: New York. p. 137-226.
19. Schmidt, S.A., Simon, M., Attarakih, M.M., Lagar Garcia, L., and Bart, H.-J. (2005, accepted), *Chem. Eng. Sci.*
20. Schmidt, S.A., *Simulation gerührter Extraktionskolonnen auf der Basis von Einzeltropfenuntersuchungen.* PhD Thesis, 2004, TU Kaiserslautern, submitted.
21. Simon, M., Schmidt, S.A., and Bart, H.-J. (2003), *Chem. Eng. Technol.,* 26, 745-750.
22. Coulaloglou, C.A. and Tavlarides, L.L. (1977), *Chem. Eng. Sci.,* 32 (1289-1297).
23. Handlos, A.E. and Baron, T. (1957), *AIChEJ,* 3, 127-136.
24. Kumar. A. and Hartland. S. *(*1999V *Trans. Inst. Chem. Ena..* 77. 372-384.
25. Wolschner, B.H., *Konzentrationsprofile in Drehscheibenextraktoren.* PhD Thesis, 1980, Technische Universität Graz.
26. Kolb, P., *Hydrodynamik und Stoffaustausch an einem gerührten Miniplantextraktor Bauart Kühni.* PhD. Thesis, 2004, TU Kaiserslautern.
27. Brodkorb, M., *Multikomponent and Contamination Effects in Liquid-Liquid Extraction.* PhD Thesis, 1999, University of Bradford.

Numerical simulation of mass transfer coupled with motion of a drop by the level set method

Jianfeng Wang[123], Chao Yang[1], Zai-Sha Mao[1]*

1 Institute of Process Engineering, Chinese Academy of Science, Beijing 100080, China
2 Graduate School of the Chinese Academy of Science, Beijing 100049, China
3 Zhengzhou University, Zhengzhou 450052, China

The interphase mss transfer of single drops is formulated and numerically simulated in a moving reference coordinate system by solving the flow and mass transfer equations coupled with a level set equation for capturing the interface. Numerical simulation demonstrates the evolution of mass transfer rate and average drop concentration. The present study provides necessary basis for further work on three-dimensional numerical simulation.

INTRODUCTION

Mass transfer of a solute to or from a buoyancy driven drop is of fundamental importance in liquid-liquid extraction and reaction. Many numerical investigations have been performed, however, a moving drop undergoing mass transfer with a finite degree of deformation was scarcely reported. Petera and Weatherley [1] simulated mass transfer from a falling drop by a modified Lagrange-Galerkin finite element method. Davidson & Rudman [2] developed a volume-of-fluid (VOF) method for the mass transfer controlled by the dispersed phase.

The main difficulty in numerical simulation is that the motion of a deformed drop with simultaneous mass transfer must be solved with the unknown shape of free surface [1], In recent years several different methods for solving multiphase flow have been developed, e.g., marker and cell (MAC) method [3], volume-of-fluid method [4], front tracking method [5], boundary integral method [6], etc. Since Osher and Sethian [7] introduced the level set method for modelling fronts, this method has been applied in many fields with the particular advantages in easy and accurate capture of interface. The method is stable, surface geometric parameters such as curvature become easy to be calculated and three-dimensional problems become easy to be implemented.

In our study the drop interface evolution is modelled by the level set method, in which the interface is represented by the embedded set of the zero level of a scalar function defined in the whole computational domain. Numerical simulation of a single drop in a liquid-liquid extraction system is performed in an axisymmetric cylindrical reference frame. The motion of a drop with a finite degree of deformation is coupled with simultaneous mass transfer.

Formulation

* *Email address:* zsmao@home.ipe.ac.cn, Tel: -86-10-62554558. 62573446

In this study, we consider the axisymmetric flow of a liquid drop moving under gravity through an immiscible liquid with the following assumptions: (1) the two fluids are viscous, Newtonian and incompressible, (2) the flow is isothermal, (3) the interface tension is taken as constant and there is no interfacial resistance to mass transfer, (4) mass transfer is assumed to have no effect on the physical properties of the system.

Governing Equations

The equations of laminar flow and mass transfer in dimensionless form are written as

$$\frac{du}{dx} + \frac{1}{r}\frac{d}{dy}(rv) = 0 \tag{1}$$

$$\frac{\partial}{\partial r}(pu) + \frac{\partial}{\partial x}\left(pun - \frac{p}{Re}\frac{du}{dx}\right) + \frac{1}{r}\frac{d}{dy}\left(rpvu - r\frac{p}{Re}\frac{du}{dy}\right) = -\frac{\partial p}{\partial x}\frac{1}{Fr} + \frac{1}{We}PZ_x$$
$$\frac{1}{We}\kappa(\phi)\delta_\varepsilon(\phi)\frac{\partial \phi}{\partial x} + \frac{1}{Re}\frac{\partial}{\partial x}\left(\mu\frac{\partial u}{\partial x}\right) + \frac{1}{Re}\frac{1}{r}\frac{\partial}{\partial y}\left(r\mu\frac{\partial v}{\partial x}\right) \tag{2}$$

$$\frac{\partial}{\partial t}(pv) + \frac{\partial}{\partial x}\left(pvu - \frac{p}{Re}\frac{dv}{dx}\right) + \frac{1}{r}\frac{d}{dy}\left(rpvv - r\frac{p}{Re}\frac{dv}{dy}\right) = -\frac{\partial p}{\partial y}\frac{1}{Fr} + \frac{1}{We}PZ_y$$
$$-\frac{1}{We}\kappa(\phi)\delta_\varepsilon(\phi)\frac{\partial \phi}{\partial y} + \frac{1}{Re}\frac{\partial}{\partial x}\left(\mu\frac{\partial u}{\partial y}\right) + \frac{1}{Re}\frac{1}{r}\frac{\partial}{\partial y}\left(r\mu\frac{\partial v}{\partial y}\right) - \frac{2}{Re}\frac{\mu}{r^2} \tag{3}$$

$$\frac{d\phi}{dt} + u\frac{d\phi}{dx} + v\frac{d\phi}{dy} = \frac{1}{Pe}\left(\frac{d^2\phi}{dx^2} + \frac{1}{r}\frac{d}{dy}\left(r\frac{d\phi}{dy}\right)\right) \tag{4}$$

$$\frac{dC}{dt} + u\frac{dC}{dx} + v\frac{dC}{dy} = \frac{1}{Pe}\left(\frac{d^2C}{dx^2} + \frac{1}{r}\frac{d}{dy}\left(r\frac{dC}{dy}\right)\right) \tag{5}$$

$$P = P_2 + (P_1 - P_2)H_\varepsilon(\phi) \tag{6}$$

$$\rho(\phi) = \rho_2 + (\rho_1 - \rho_2)H_\varepsilon(\phi) \tag{7}$$

where ϕ is the level set function, $\kappa(\phi)$ is the curvature of free surface:

$$\kappa(\phi) = \nabla \cdot \mathbf{n} = \nabla \cdot \left(\frac{\nabla\phi}{|\nabla\phi|}\right) \tag{8}$$

where n is the unit vector normal to the interface pointing towards the continuous phase, $\delta_\varepsilon(\phi)$ is the regularized delta function defined as

$$\delta_\varepsilon(\phi) = \begin{cases} \frac{1}{2\varepsilon}\left(1 + \cos\left(\frac{\pi\phi}{\varepsilon}\right)\right) & \text{if } |\phi| \le \varepsilon \\ 0 & \text{otherwise} \end{cases} \tag{9}$$

where $\varepsilon = 0(h)$ prescribes the finite "thickness" of the interface, we take $\varepsilon = 1.5h$ generally, and h is equal to the dimensionless uniform mesh size near the interface. $H_\varepsilon(\phi)$ is the regularized Heaviside function expressed as

$$\text{«M=-}\quad \begin{cases} \text{fo} & \text{if}\ \phi < £ \\ \frac{1}{2}\left(1+\frac{\phi}{£}+\sin\left(\pi\phi/£\right)\right)/k & \text{if}\ |\phi| \le s \\ 1 & \text{if}\ \phi > £ \end{cases} \tag{10}$$

The subscripts 1 and 2 denote the continuous phase and drop, respectively. The level set function </> and concentration of solute are advanced with the local velocity.

The dimensionless parameters in the above equations are the Reynolds, Froude, Weber and Peclet numbers, respectively

$$Re = \frac{p_J\, 2RU}{P\backslash} \blacksquare K = \frac{U^2}{2\,Rg},\ We = \frac{2\,Rp_xU^2}{\sigma},\ Pe = \frac{RU}{A} \tag{ii}$$

where $\rho_1, \mu_1,$ and D_x are the density, viscosity, and diffusivity of continuous phase; R is the initial radius of spherical drop and the characteristic velocity is defined as $U - J2Rg$.

Reinitialization of *tj>* as a distance function

Generally, *<J)* will no longer be a distance function (i.e., |V^| * 1) after some iterations, even if eq. (4) moves the interface *(<J>* = 0) at the correct velocity. Maintaining ^ as a distance function is essential for providing the interface with an invariant width. This problem can be solved by adopting a reinitialization method proposed by Sussman et al. [8] to keep the solution accurate and maintain mass conservation of the drop by solving the following problem to steady state:

$$\frac{\partial \phi}{\partial \tau} = \operatorname{sgn}(\phi_0)(1 - |\nabla \phi|) \tag{12}$$

$$^(*.0) = \#_0(*) \tag{13}$$

where r is the virtual time for reinitialization, $^_u(x)$ is the level set function at any computational instant, and $\operatorname{sgn}(^_0)$ is the sign function needed for enforcing V^ = I. Eq. (12) has the property that *<f>* remains unchanged at the interface, therefore, the zero level set of *(/>$_0$* and *tj)* is the same. Away from the interface *<j>* will converge to $|\nabla\phi| = 1$, therefore, i.e., the actual distance.

Equations of mass transfer

Rewriting equations of mass transfer

Special care must be taken for resolving the discontinuity in the equation for concentration of solute at *<j)*- 0, as the distribution coefficient of a solute *(m*) is not equal to unity. Eq. (5) is rewritten as the following two transport equations in each phase:

$$\frac{0C,}{dt} + \mathbf{u} \bullet \nabla C, = \frac{1}{Ye}\left(\frac{d}{\partial x}\left(D_1 \frac{\partial C}{\partial x}\right)\right) H\text{----}\frac{1}{r}\frac{d}{dy}\left(rD\frac{dC_x}{dy}\right) \tag{14}$$

$$\frac{ac.}{dt} + \mathbf{u} \cdot \nabla C_2 = \frac{1}{Ye}\left(\frac{d}{\partial x}\left(A_D \frac{dC_2''}{dx}\right)\right) + \text{-}\frac{1}{r}\frac{d}{cfy}\left(rD\frac{cC_7^{N\backslash''\backslash}}{dy\ J)}\right) \tag{15}$$

together with two interfacial conditions:

$$D_1 \frac{\partial C_1}{\partial n} = D_2 \frac{dC_2}{\partial n} \quad \text{(flux continuity at the interface)} \tag{16}$$

$$C_2 = mC_x \text{ (interfacial dissolution equilibrium)} \tag{17}$$

To keep the concentration continuous at the interface for the case of m^*, we make transformations as follows [9]:

$$\hat{C}_1 = C_1 \sqrt{m}, \quad \hat{C}_2 = C_2 / \sqrt{m} \tag{18}$$

and Eq. (17) is turned into

$$\hat{C}_1 = \hat{C}_2 \tag{19}$$

Thus, the concentration becomes continuous in the computational domain. Similarly, the boundary condition (16) becomes

$$\frac{D_1}{\sqrt{m}} \frac{\partial \hat{C}_1}{dn} = \sqrt{m} D_2 \frac{\partial \hat{C}_2}{dn} \tag{20}$$

Eqs. (14) and (15) are rewritten as

$$\frac{\partial \hat{C}_1}{\partial(\sqrt{m}t)} + \frac{1}{\sqrt{m}} u \cdot \nabla \hat{C}_1 = \frac{1}{Pe} \left[\frac{\partial}{\partial x} \left(\frac{f_A}{\sqrt{m}} \frac{dC}{dx} \right) + \frac{1}{r} \frac{\partial}{\partial y} \left(r \frac{A}{\sqrt{m}} \frac{\partial C}{\partial y} \right) \right] \tag{21}$$

$$\frac{\partial \hat{C}_2}{\partial(t/\sqrt{m})} + \sqrt{m} u \cdot \nabla \hat{C}_2 = \frac{1}{Pe} \left(\frac{\partial}{\partial x} \left(f_{sn} \frac{\partial C}{\partial x} \right) + \frac{1}{r} \frac{\partial}{\partial y} \left(r \frac{\partial C}{\partial y} \right) \right) \tag{22}$$

through different definition of $\hat{f}, \hat{D}$ and u by the Heaviside function $H_\varepsilon(\phi)$:

$$\hat{f}(\phi) = \begin{cases} f & \text{if } \phi < 0 \\ \sqrt{m} & \text{if } \phi \geq 0 \end{cases} \tag{23}$$

$$\hat{D}(\phi) = \sqrt{m} + \left(\frac{1}{\sqrt{m}} - \sqrt{m} \right) H_\varepsilon(\phi) \tag{24}$$

$$\hat{u} = \sqrt{m} u + \left(\frac{1}{\sqrt{m}} - \sqrt{m} \right) u H_\varepsilon(\phi) \tag{25}$$

Eqs. (21) and (22) can be rewritten as one common equation over the whole domain

$$\frac{\partial \hat{C}}{\partial \hat{t}} + \hat{u} \cdot \nabla \hat{C} = \frac{1}{Pe} \left[\frac{\partial}{\partial x} \left(\hat{D} \frac{\partial C}{\partial x} \right) + \frac{1}{r} \frac{\partial}{\partial y} \left(r \hat{D} \frac{\partial C}{\partial y} \right) \right] \tag{26}$$

By our numerical experience, the transformation has no adverse effect on the numerical solutions of interphase mass transfer.

Mass transfer coefficient

The overall mass transfer coefficient k_{od} may be expressed as

$$k_{od} = -\frac{V_d}{S}\frac{1}{t_{out}-t_{in}}\ln\frac{C_2^*-C_{2,out}}{C_2^*-C_{2,in}} \tag{27}$$

where $\bar{C}_2$ is the average concentration of the drop at any time, V_d and S are the volume and surface area of the drop. The corresponding Sherwood number is

$$Sh_{od} = \frac{d}{D_1}k_{od} \tag{28}$$

Computational scheme

Numerical solution method

Yang & Mao [9] simulated mass transfer after the steady state of flow was reached by the level set method, in which the mass transfer equation was decoupled from the flow field. No simulation of unsteady mass transfer by the level set method was reported. Moreover, the governing equations are solved in the reference coordinate system fixed with the drop in this work. The advected acceleration of the drop must be formulated in the governing equations in the moving reference coordinate system. Eq. (2) is now rewritten as

$$\frac{d}{dt}M + \frac{8}{dx}\left(\frac{f}{\mathrm{Re\,Sc}}\frac{\partial u}{\partial n}\right) + \frac{1}{r\,dy}\left(rpvn - r\frac{H}{\mathrm{Re}}\frac{dn}{dy}\right) = -\frac{dp}{dx}\frac{1}{hr} + P\pounds,\sim P,\ a$$
$$+\frac{1}{We}\kappa(\phi)\delta_\varepsilon(\phi)\frac{\partial\phi}{dx} + \frac{1}{Redx}\left\{\frac{1}{dx_y}\left(\mu\frac{\partial u}{\partial x}\right) + \frac{1}{\mathrm{Re}}\frac{1}{r\,dy}\left(r/u\frac{\partial v}{\partial x}\right)\right. \tag{29}$$

where a is the convected acceleration of the drop and $p_r = p_2/p_1$, a is calculated by

$$a = \frac{u_{n+1}-u_n}{At} \tag{30}$$

where u_n^ is the axial velocity of the drop at t_{n+1}, u_n is the velocity at t_n, and At is the time step.

The governing equations are discretized according to the control volume formulation with the power-law scheme as described by Patankar [10], To ensure the difference accuracy, we use a fifth-order WENO method [11] for the approximation of the convective terms of the mass transfer and ^ equations, a third-order TVD Runge-Kutta [12] scheme is adopted for time discretization of the WENO scheme.

Numerical procedure

The algorithm is summarized as

Step 1. Initialize the flow field *(u*, v and *p),* physical parameters *(p, p*, cr, *D* and C in each phase) and *tj)* as signed normal distance to the interface.

Step 2. Solve eqs. (3), (29) and (4) for one time step.

Step 3. Solve the concentration field.

Step 4. Construct a new distance function by solving eqs. (12) with (13) to steady state, and the steady state solution is denoted as $\langle f \rangle^{n+}$'.

Step 5. Advancing one time step. The zero level set of $\langle f \rangle^{n+}$ gives the new interface position. Renewing physical properties, repeat steps 2, 3 and 4.

Special attention is taken to see that in the moving reference fixed on the drop, the boundary conditions must be corrected at every time step to assure the average velocity of the drop u^,. satisfy the following two conditions:

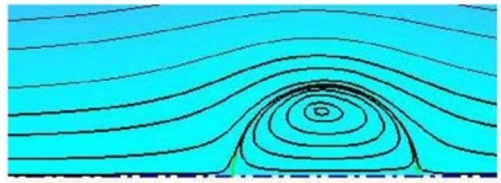
$$|U_{aver}| = 0, \qquad u_{aver} = -\frac{1}{\Omega_2}\int_{\Omega_2} \mathbf{u}\, d\Omega \tag{31}$$

Q_2 denotes the area of the drop at the current instant. To satisfy the conditions is the most difficult part in the present numerical work. The relaxation factors need to be adjusted for different physical parameters to meet the correct boundary condition.

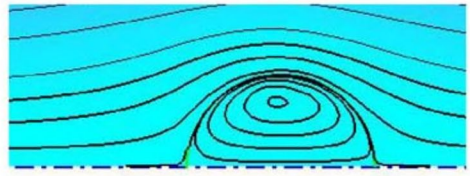
Results and discussions

We consider a buoyancy-driven drop surrounded by an incompressible Newtonian fluid bounded in a wide cylindrical column (Q = {(-T^O < x < 40/?,0 < y < 157?}) to validate the numerical algorithm for interphase mass transfer. The free-slip boundary condition is adopted at the column wall. A 182x 76 spatial grid was applied in all the numerical solution of fluid flow and mass transfer to ensure spatial accuracy and computational efficiency.

Figure 1 depicts the steam function contours at different time and Figure 2 shows development of concentration profiles for mass transfer resistance both in the external and internal domains of a single drop. Figure 3 shows the evolution of average drop concentration and overall mass transfer Sherwood number.

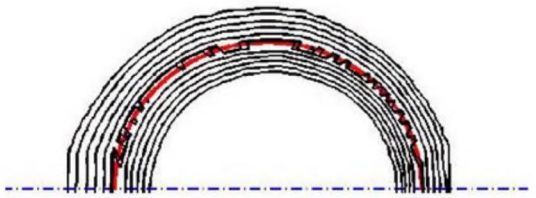


(a) t = 6.6 (Re = 2.\0, We = 0.0\,Pe = \ 045)

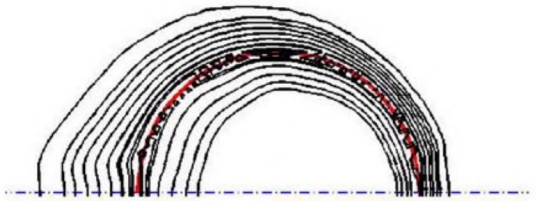


(b) t = 30.6 (Re = 2.74 We = 0.02; *Pe =* 1370)

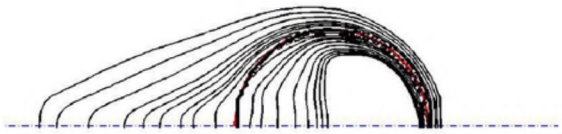
Fig. 1. Steam function contours at different time (r = 2 x 10^{-4} m, p_2 p_j =1.1, /z_2 ///, = 2, <j = 0.001 N/m)



(a) t -5.4 (Re -1.96, *We* = 0.01, *We* = 980*)*

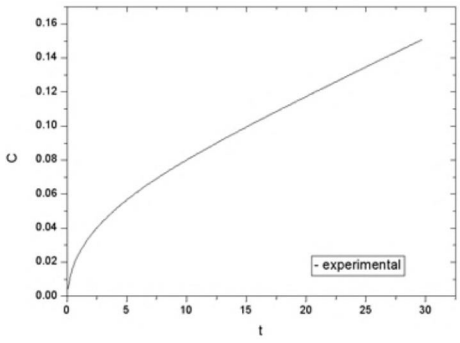


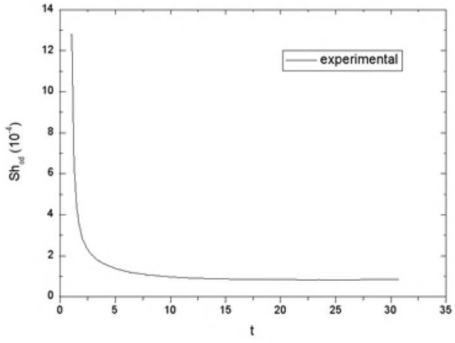
(b) t = \\.*9 (Re* = 2.39, 0V = 0.01, 7V = 1195j



(c) t = 29.4 (Re = 2.73, We = 0.02, TV = 1365;

F/ġr.2. *Concentration contours at different time.*





(a) Average drop concentration *(b) Overall mass transfer coefficient*

Fig. 3. Experimental concentrations and average Sh_{od} number *as a function of mass transfer time (d* **=0.2** *mm,* I), = **2x ur⁹** *m²/s,* D_2 = **4xio** $^{9}m^2/s$, *m* = **2.0, C,°** = 1 *mol/l,* C_2° **= 0** *mol/l; solute transfer direction: from continuous phase to drop , other conditions the same as in Fig. 1)*

It is obvious that the distortion of the concentration contours develops gradually to form a series of closed contours along with the increase of mass transfer time. As the Reynolds, Weber and Peclet numbers increase, the concentration contour lines are swept to the downstream direction and the concentration profiles distort more severely, suggesting that convective mass transfer does play an important role. The convection at the drop nose promotes the transport of solute to the drop, making the contour lines compressed spatially.

The concentration fields are similar to the results by a decoupled algorithm for mass transfer and flow [9]

As shown in Fig. 3, the experimental drop average concentrations and average Sherwood number for mass transfer direction from the continuous phase to the drop are also similar to the results in [9],

Conclusions

A level set method for numerical simulation mass transfer from or to an unsteady falling drop in an immiscible liquid in the laminar flow regime is developed. The mass transfer equations coupled from with two phase fluid flow equations are solved numerically in a moving reference coordinate fixed on the drop for the case with resistance in both drop and continuous phase and distribution coefficient differing from unity. The results are in agreement with the related reference qualitatively. The present study provides necessary basis for further work on three-dimensional numerical analysis of the Marangoni effect induced by surface tension gradient.

Acknowledgements

This work is supported by the National Natural Science Foundation of China (Nos. 20490206, 20236050)

Notation

C dimensionless concentration of solute

C^* dimensionless concentration in equilibrium with other phase

$\hat{C}$ dimensionless transformation form of concentration

$\overline{C}$ dimensionless average concentration of solute

d diameter of drop, m

D molecular diffusivity, m^2/s

$\hat{D}$ transformation form molecular diffusivity of solute, m^2/s

g acceleration vector of gravity m/s^2

p dimensionless pressure

r dimensionless radial coordinate

S surface area of drop, m^2

/ dimensionless time

$\mathbf{u}$ dimensionless velocity vector

$\hat{\mathbf{u}}$ dimensionless transformation form of velocity vector

u dimensionless axial velocity

U characteristic velocity, m/s

v dimensionless radial velocity component

x dimensionless axial coordinate

y dimensionless radial coordinate

Greek letters

p dimensionless viscosity

p dimensionless density

p_r relative density $p_z\, jp_x^{'}$

<x surface tension, N/m
τ virtual time

Subscripts

in first measurement location
od overall
out second measurement location
0 initial time

References

1. J. Petera and L. R.Weatherley (2001), *Chem. Eng. Sci,* 56, 4929-4947
2. M. R. Davidson and M. Rudman (2002), *Numer. Heat Transfer B,* **41,** 291-308.
3. F.H. Harlow and J.E. Welch. (1965), *Phys. Fluids,* 8, 2182-2189
4. C.W. Hirt and B.D. Nichols (1981), *J. Comput. Phys,* 39, 201-255
5. O.S. Unverdi and G.Tryggvason (1992), *J. Comput. Phys,* **100,** 25-37
6. G.R. Baker and D.W. Moore. (1989), *Phys. Fluids A,* 1 , 1451-1459
7. S Osher and J Sethian.(1988), *J. Comput. Phys,* 79, 12-49
8. M.Sussman, P.Smereka and S.Osher (1994), *J. Comput. Phys,* **114,** 146-159
9. C.Yang and Z.-S.Mao (2005), *Chem. Eng. Sci,* **60** (in press)
10. S. V. Patankar (1980), *Numer. Heat Transfer and Fluid Flow.* Washington Hemisphere
11. S. Chen, B. Merriman, S. Osher and P. *J.* Smereka (1997), *Comput. Phys,* **135,** 8-29
12. R. Fedkiw, T. Aslam, B. Merriman and S.Osher (1999), *J. Comput. Phys,* **152,** 457 - 492

PREDICTION OF DISTRIBUTION COEFFICIENT OF CAPROLACTAM AND METHYL CAPROLACTAM BY UNIFAC MODEL

X.C. Gong, Y.C. Lu, G.S. Luo*

State Key Lab of Chemical Engineering, Department of Chemical Engineering, Tsinghua University, Beijing 100084, China

The extraction of toluene and mixed toluene/benzene solvent for caprolactam had been carried out. Based on the experimental results, new interaction parameters had been calibrated by defining new UNIFAC groups. Using UNIFAC model, the distribution coefficients of caprolactam and methyl caprolactam in toluene, benzene or mixed toluene/benzene solvent can be predicted. The predicted results indicated it is possible to separate methyl caprolactam from crude caprolactam only using the extractants mentioned above.

INTRODUCTION

Caprolactam, one of important industrial chemicals, is mainly used to manufacture nylon 6 and resins. Nylon 6 is widely used in textile trade, and resins are extensively used in carrying trade and food industry. Because caprolactam polymers have many good merits, the demand and price of caprolactam continue rising these years.

There are several different production processes of caprolactam[11], such as DSM/HPO method, BASF-NO reduction method and SNIA toluene method. The technological processes of these methods are complex, working operation and equipments used are excessive, and the byproducts and waste are in large amounts. Purification process is mandatory step to achieve high quality caprolactam. At most occasions, extracting caprolactam from crude product and the following water stripping are the core of purification process. In industry, benzene and toluene are the most commonly used extractant. There are some publications relating to caprolactam extraction processes. G. H. van Bochove[2,3,41] et al. measured the equilibrium of caprolactam using heptanol, benzene and heptanone as extractants, especially under the conditions when aqueous phase containing salt. They used the modified extended electrolyte NRTL to model the equilibrium of caprolactam. M. L. van Delden[15,61] et al. investigated liquid-liquid equilibrium of the quaternary system water + caprolactam + ammonia sulphate + benzene or toluene. They used NRTL to model the equilibrium phase composition data. But few results are related with the phase equilibrium and selectivity of solvents. The most likely reason is the system is very complicated. Although some thermodynamic models can predict the distribution of caprolactam well, they are not suitable for the derivatives of caprolactam yet.

* Corresponding author. E-mail: gsluo@tsinghua.edu.cn

In the paper, the extraction characteristics of benzene and toluene for caprolactam have been investigated, and their distribution coefficients are predicted with UNIFAC method. With the new evaluated parameter constants the distribution coefficients of methyl caprolactam are predicted, and the selectivity of benzene and toluene will be discussed.

EXPERIMENTAL

Experimental

Liquid-liquid equilibrium experiments of different working systems under different temperatures were carried out in a triangular flask with temperature control. After agitated for 24 hours, the equilibrium state could be reached and the caprolactam concentrations in the organic phases were measured with gas chromatogram. Provided water and extractants are insoluble to each other. Then calculate the concentration in aqueous phase using mass conservation.

RESULTS AND DISCUSSION

The extraction system containing ammonia sulfate and the back-extraction system without the salt were simulated, and their distribution coefficients were compared. Table 1 shows the results for the ternary system water + toluene + caprolactam at 25, 35 and 45°C. Table 2 shows the results for the quaternary system water + toluene + caprolactam + ammonia sulfate at 25, 35 and 45°C. Ammonia sulfate content in the aqueous phase is wt. 4 %. In table 3, the Benzene and toluene were mixed at volume ratio 1:1 at 25°C.The equilibrium curve at 25, 35 and 45°C had been measured. Table 4 shows the results for 1:1 mixed benzene/toluene solvent and aqueous phase containing wt. 4% ammonia sulfate at 25, 35 and 45°C.

Table 1. Caprolactam distribution in toluene phase and aqueous phase

T=25°C		T=35°C		T=45°C	
Co(wt.%)	Cw(wt.%)	Co(wt.%)	Cw(wt.%)	Co(wt.%)	Cw(wt.%)
0.0053	0.0712	0.0077	0.0696	0.0083	0.0693
0.0143	0.139	0.0169	0.137	0.0193	0.135
0.0220	0.210	0.0286	0.206	0.0333	0.204
0.0340	0.278	0.0380	0.276	0.0483	0.271
0.0467	0.344	0.0520	0.341	0.0613	0.337
0.0565	0.401	0.0652	0.396	0.0755	0.392

Table 2. Caprolactam disthbution in toluene phase and aqueous phase containing salt

T=25°C		T=35°C		T=45°C	
Co(wt.%)	Cw(wt.%)	Co(wt.%)	Cw(wt.%)	Co(wt.%)	Cw(wt.%)
0.0082	0.0682	0.0111	0.0661	0.0143	0.0641
0.0214	0.130	0.0286	0.125	0.0374	0.119
0.0425	0.191	0.0489	0.186	0.0548	0.182
0.0611	0.251	0.0659	0.248	0.0676	0.246
0.0752	0.303	0.0806	0.300	0.0952	0.290
0.0974	0.369	0.1050	0.364	0.1195	0.354
0.1340	0.444	0.1527	0.433	0.1807	0.415

Table 3. Caprolactam distribution in benzene/toluene phase and aqueous phase

T=25°C		T=35°C		T=45°C	
Co (wt.%)	Cw(wt.%)	Co(wt.%)	Cw(wt.%)	Co(wt.%)	Cw(wt.%)
0.0071	0.0601	0.0085	0.0592	0.0101	0.0583
0.0132	0.0985	0.0160	0.0966	0.0195	0.0944
0.0203	0.131	0.0277	0.126	0.0289	0.125
0.0325	0.184	0.0418	0.177	0.0478	0.173
0.0455	0.257	0.0595	0.249	0.0678	0.244
0.0509	0.277	0.0655	0.267	0.0704	0.264

Table 4. Caprolactam distribution in benzene/toluene phase and aqueous phase containing salt

T=25°C		T=35°C		T=45°C	
Co(wt.%)	Cw(wt.%)	Co(wt.%)	Cw(wt.%)	Co(wt.%)	Cw(wt.%)
0.0071	0.0446	0.0096	0.0432	0.0124	0.0419
0.0235	0.0943	0.0241	0.0940	0.0315	0.0900
0.0554	0.184	0.0515	0.186	0.0711	0.177
0.113	0.243	0.0983	0.252	0.119	0.241
0.181	0.330	0.176	0.333	0.216	0.311
0.241	0.442	0.245	0.439	0.289	0.405

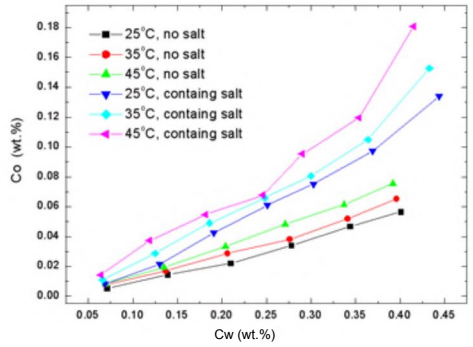


Figure 1. Distribution curve of caprolactam with toluene as extractant

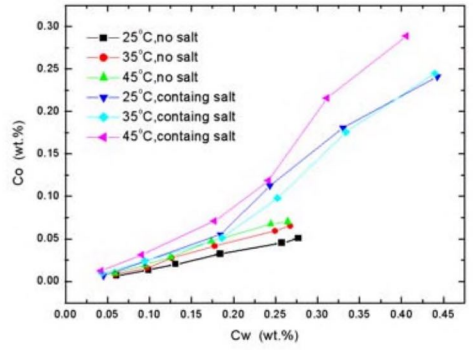


Figure 2. Distribution curve of caprolactam with benzene/toluene as extractant

For the two working systems, the distribution coefficients of caprolactam are increased with the temperature increasing. For the system containing ammonia sulfate, the distribution coefficients of caprolactam in toluene or benzene/toluene phase are higher than those without salt.

MODELING

In order to predict the distributions of the derivatives of caprolactam, not only just for caprolactam, we used UNIFAC model to predict the equilibrium, because it is a very effective model for the system containing similar derivatives. With the above experimental data, we defined the groups as listed in table 5. The binary interaction parameter constants for the system were evaluated, and the results are listed in table 5. With the evaluated parameter constants, we predict the distribution curves of caprolactam with benzene and toluene as extractant respectively. The comparison of the prediction with the experimental data is plotted in figures 4 and 5, which show a well agreement.

Table 5. Interaction parameters of UNIFAC groups

Group 1	Group 2	ai2	a2i
CH2	caprolactam	5.36	159
ACH	caprolactam	43.3	-37.5
ACCH2	caprolactam	-74	17.5
H2O	caprolactam	5.14	-124.8

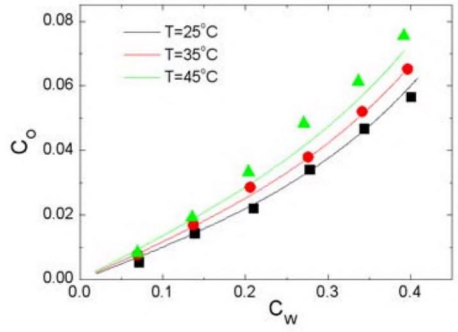


Figure 4. Toluene as extractant

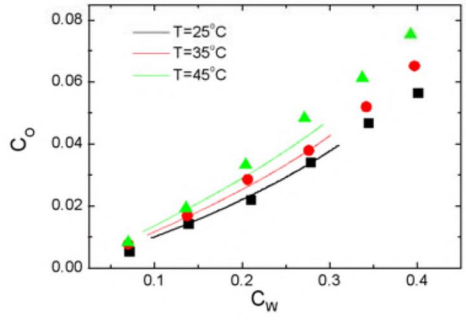


Figure 5. Benzene as extractant

PREDICTION

With the new interaction parameters, the distribution of methyl caprolactam had been predicted. Figure 6 shows the calculated data when using toluene as the extractant. The distribution coefficient of methyl caprolactam and caprolactam at low concentration is about 1.68 and 0.17 respectively. Figure 7 shows the calculated data when using benzene as the extractant. The distribution coefficient of methyl caprolactam and caprolactam at low concentration is about 1.52 and 0.16 respectively. When mixed benzene/toluene solvent volume ratio is 1:1, the predict results are shown in Figure 8. Benzene and toluene were mixed at 25°C. The distribution coefficient of methyl caprolactam and caprolactam at low concentration is about 1.62 and 0.17 respectively.

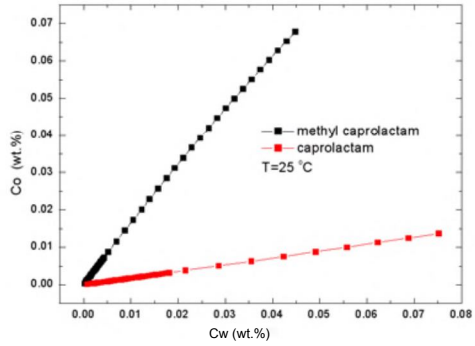


Figure 6. Toluene as extractant

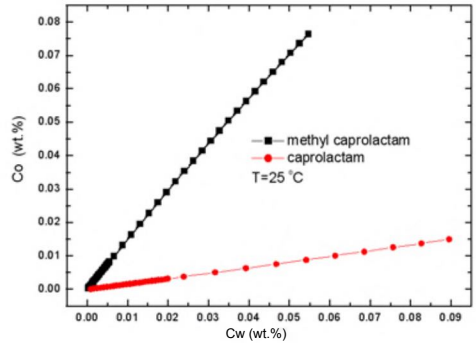


Figure 1. Benzene as extractant

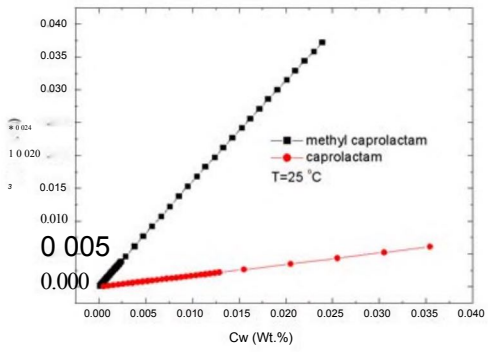


Figure 8. Mixed toiuene/benzene as extractant

At low concentration, the distribution coefficient of methyl caprolactam is much higher than caprolactam. Benzene and toluene are preferred to extract methyl caprolactam than caprolactam. So it is possible to separate the byproduct methyl caprolactam from crude caprolactam using benzene or toluene as the extractant.

CONCLUSION

In this paper, extraction of caprolactam using toluene and mixed toiuene/benzene as extractants had been carried out. The distribution coefficients increase with the increasing of temperature. When the aqueous phase contains ammonia sulfate, the distribution coefficients enlarge too. Based on the experiments data, new interaction parameters were calibrated by UNIFAC model, with which the distribution coefficient of caprolactam or methyl caprolactam can be predicted. The calculated data indicates it is possible to separate methyl caprolactam from crude caprolactam by extraction with toluene, benzene or mixed toiuene/benzene as solvent.

ACKNOWLEDGEMENTS

We acknowledge the support of the National Natural Science Foundation of China (20490200) on this work.

REFERENCES

1. A. Romero, A. Santos and R Yustos (2004), *Ind. Eng. Chem. Res.,* **43,** 1557-1560.
2. G. H. van Bochove, G. J. R Krooshof and Th. W. de Loos (2002), *Fluid Phase Equilibria,* 194-197, 1029-1044
3. G. H. van Bochove, G. J. R Krooshof and Th. W. de Loos (2000), *Fluid Phase Equilibria,* 171, 45-58
4. M. Wijtkamp, G. H. van Bochove, Th. W. de Loos and S.H. Niemann (1999), *Fluid Phase Equilibha,* 158-160, 939-947
5. B. Kuzmanovic, M. L. van Delden, N. J. M. Kuipers and A. B. de Haan (2003), *J. Chem. Eng. Data***, 48,** 1237-1244
6. M. L. van Delden, N. J. M. Kuipers and A. B. de Haan (2004), *J. Chem. Eng. Data,* **49,** 1760-1770



DESIGN OF ROTATING DISC CONTACTORS - NUMERICAL SIMULATION OF RESIDENCE TIME DISTRIBUTION

Tobias Haderer, Rolf Marr, *Stefan Martens and ''Matthäus Siebenhofer

Department of Chemical Engineering and Environmental Technology,
University of Technology Graz, Graz, Austria
'Fluent Deutschland GmbH, Darmstadt, Germany
" VTU-Engineering GmbH, Grambach/Graz, Austria

In this project Computational Fluid Dynamics has been investigated for its accuracy in generating axial dispersion coefficients for the continuous phase in stirred liquid-liquid extraction columns (e. g. Rotating Disc Contactors RDC with 100 mm diameter). As known from literature axial dispersion coefficients determined from single phase flow experiments can be used to estimate two phase flow conditions. By consideration of this fact, only continuous phase flow simulation is mandatory for estimation of reliable data for axial dispersion coefficients. The choice of the turbulence models has a significant effect on the simulation results too. To prove simulation and CFD model reliability, simulation results were compared with experimentally obtained data, recorded from several investigations with the test system Toluene/Water and correlations known from literature.

INTRODUCTION

Information on hydrodynamic parameter such as axial dispersion, hold-up and characteristic velocity is indispensable for the scale-up and design of extraction columns. Many of these design activities must be carried out in laboratories, and plant optimization and determination of chemical and engineering design parameters still need expensive experiments. For reasons of time saving and cost cutting it is desirable to carry out plant and process design with a minimum of scale up steps. Pilot plant tests are expected selectively to confirm design data. Although several correlations have been published for the parameters mentioned above further improvement is necessary because results predicted from CFD simulation strongly depend on the applied correlation and may vary widely.

The objective of this research work has been to derive design parameters for RDC design with Computational Fluid Dynamics (CFD) and to compare simulation results with experimentally obtained data. The accuracy of current turbulence models and iteration algorithms was investigated and compared with experimental data of Laser Doppler Anemometry (LDA) measurement and CFD calculations carried out previously [1], In addition first experiments were executed to determine Residence-Time-Distributions (RTD) in action-related dependence of operating conditions [2],It is possible to obtain results of acceptable quality from computation by applying appropriate assumptions such as periodic boundary conditions (translational and rotational) and two-dimensional geometries. The crucial

question is, how many and which assumptions need to be made to achieve results that still represent the flow pattern with sufficient accuracy.

Investigations were carried out with an RDC contactor of 100 mm diameter. The construction schema is shown in Figure 1 ($D_{Ro}t_Or$=60 mm; $D_S$iaior=70 mm; $D_S$hafi=35 mm; H_{Co}mp=36 mm) [3],

RDC 100 mm

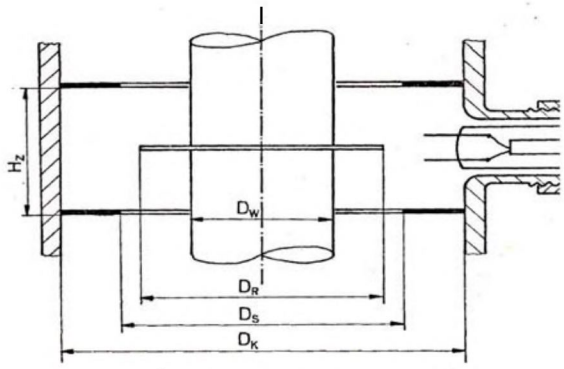


Figure 1. Construction schema of the compartment geometry of the investigated RDC ***[D_{Rotor}=60 mm; $D_S$tator=70 mm; $D_S$han=35 mm; H_{CO}mp=36 mm]***

DEVELOPMENT OF THE SIMULATION STRATEGY

In previous research activities [1] the influence of the commonly used turbulence models on the results of the calculated flow pattern in RDC extraction columns was discussed. In the present project the realizable k-e-model and the Reynolds Stress Model were ascertained as models for use. In the continuative work a scale-up parameter (axial dispersion coefficient **E_{ax},c)** should be computed with the aid of Computational Fluid Dynamics (CFD). For the determination of this parameter the calculation of the residence time distribution (RTD) has to be realized. To compute the RTD of the continuous phase (water) with CFD, a two-phase-flow model (Euler-Lagrange) is needed.

The Euler-Lagrange model provides modeling of spherical particles, bubbles or droplets which are dispersed in the continuous phase. The fluid phase (water) is treated as continuum by solving the time-averaged Navier-Stokes equations, while the dispersed phase is solved by tracking a large number of particles through the previous calculated flow field. Particle tracking is realized by computation of the force balance on each particle moving through the continuum. The particles generated for simulation of RTD must have the same physical properties like the continuous phase and they must have a very small diameter of 1*1 O'^{06} m, to ensure that they will strictly follow the flow field [2, 4],

Determination of the Residence Time Distribution

To compute the Residence Time Distribution (RTD) of the continuous phase with the Euler-Lagrange two-phase flow approach, injection locations for the particles have to be created. In this work seven injection locations were generated at which droplets with identical physical properties to those of the continuous phase (water) and a droplet diameter of 1 -10$_{-06}$ m were released. The injection locations were placed in a plane at the height of a stator-ring with increasing distance of neighboring particles from the stator ring to the shaft. The boundary

conditions for the calculation of the particle trajectory at the column shell and the internal equipment were set to reflect and to escape through the inlet plane and the outlet plane, enabling the particles to leave the observation space. The dispersion of particles due to turbulence in the fluid phase was predicted with the stochastic tracking model.

The transition time was recorded by passing a counting line which was created at the height of a stator ring too. The investigated domain for the RTD is a multiple of the height of one compartment.

The transition time was recorded in a "*.dpm-file" which allows the display of a residence time curve. The run of the curve was fitted the RTD-solution of Levenspiel [5] for the open-open systems dispersion model with the fit parameters Pe-number, the mean residence time rand the scaling factor A_0. The results generated through CFD simulation were compared with experimental data and empirically determined correlations (Bauer [6]; Kumar and Hartland [7]) to finally establish a simulation set-up with satisfying accordance of the simulated and the real flow field.

RESULTS

In first simulation runs, the flow field of four compartments was calculated for different operating conditions without disperse phase flow by varying the flow rate of the continuous phase from 56.3 l/h to 160 l/h and the rate of rotation from 0 rpm to 900 rpm. The flow pattern was calculated considering turbulence with the realizable *k-s* model [1], The Residence Time Distribution (RTD) of the continuous phase was estimated for two compartments in the center. The first and the last compartment were reserved for inlet and outlet. Figure 2 shows the comparison of the calculated RTD data with data records from experiments executed in the RDC extractor of 100 mm diameter.

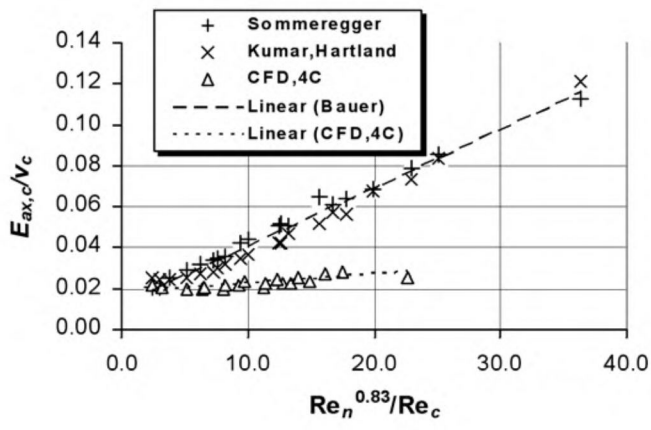


Figure 2. Comparison of experimental data for E_{axc}/v_c with empirical correlations and CFD data [2]

The generated results clearly show that at low rate of rotation and high continuous phase throughput only simulation results match experiments with acceptable accordance. The simulated mean velocity deviated from experimental data tremendously. The simulated mean velocity data were larger than the experimentally obtained values. As a consequence the data-points of the CFD,4C-line in Figure 2 do not match the data from experiments. The discrepancy between CFD simulation and experiments at higher rate of rotation is significant.

Nevertheless it was demonstrated that CFD is able to achieve acceptable results for low rate of rotation and moderate to high throughput of the continuous phase.

Strategy of improvement of CFD-results focused on extension of the simulation area (number of compartments), and application of different turbulence models.

Influence of the Number of Compartments

The RTD simulation in this case was carried out for 16 compartments. Simulation was performed for a representative mean operation state. The volumetric throughput of the continuous phase was set to 160 l/h ana the rate of rotation was set to 900 rpm.

In this simulation runs the disperse/phase boundary condition reflect at the inlet was compared with escape boundary conditions. The flow field of 16 compartments was calculated and the residence time /distribution of 4, 6, 8 and 10 compartments was determined. The DPM calculations were always carried out for the compartments in the center of the geometry which resulteg in run times of approximately five days. The results are shown in Figure 3.

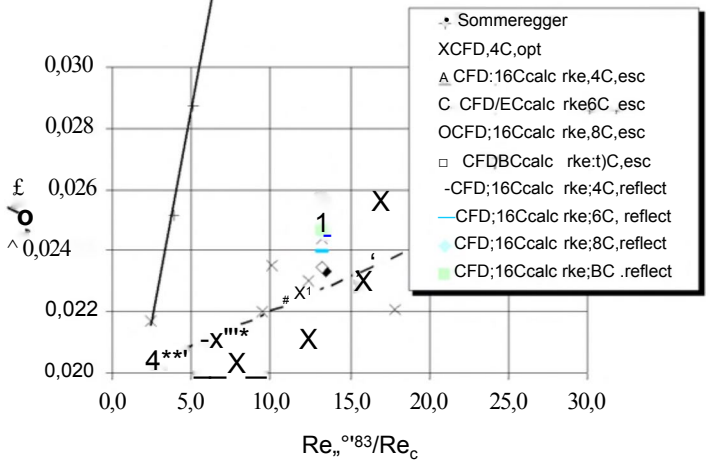


Figure 3. Comparison of axial dispersion coefficients (operating conditions: 160 l/h; 900 rpm; turbulence model: realizable k-s model)

As demonstrated with the series of “16 compartments” (CFD;16Ccalc) simulations in Figure 3 the expected improvement of the simulated dispersion coefficient through enlarging the simulation area was definitely not observed. As a consequence RTD is not influenced by the number of the compartments used for the DPM calculations. The 16 compartments simulations result in comparable axial dispersion coefficients to the 4 compartments simulation. No dependency of the calculated results on the employed inlet boundary conditions (reflect or escape) for the disperse phase can be ascertained.

The Reynolds Stress Model (RSM)

Based on poor accordance of CFD calculation with experiments, the DPM research was retried using the Reynolds Stress model (RSM). Simulation of flow pattern with RSM differs significantly from simulation with the realizable *k-s* model [1], Comparison of the models shows, that at high rate of rotation the RS Model produces a much stronger effect of the energy input on the flow pattern in radial direction Therefore the RTD investigations were

performed again with implementation of the Reynolds Stress Model. To retain a better survey the calculations were executed at same operating conditions (RSM; 160 l/h; 900 rpm; 16 compartments and 56 l/h; 900 rpm; 16 and 32 Compartments) as applied in the simulations with the realizable k-£ model. The inlet boundary condition for the disperse phase was set on “trap”, which stops the trajectory calculation for lost particles. With this boundary condition the number of particles is identified which quits simulation area at the inlet. In this case the simulated flow fields are not equal and a comparison of the velocities is nonsensical. The DPM iteration was carried out for 6 compartments. The result is displayed in 8. In these simulations the mean velocity of simulations was in good agreement with experiments and no unification procedure was necessary.

In an additional step worst case simulation conditions (56.3 l/h throughput and 900 rpm) were investigated with the same simulation parameter settings as listed above. 2 and 6 compartments files were created and the RTD was determined in a simulation geometry of 16 compartments. The residence time curves are shown in Figure 4.

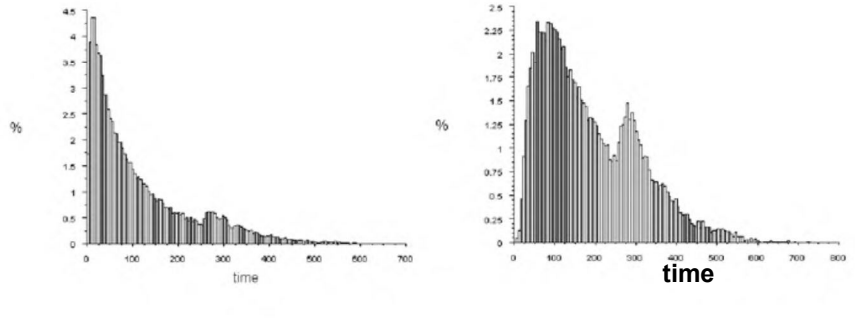


Figure 4. Histogram of the 2 and 6 Compartments RTD calculation (56.3 l/h; 900 rpm; RSM)

In Figure 4 the residence curves show surprising result. A second (at 250-300 seconds) and even a third peak (circa 500 seconds) are displayed. The peaks are much more distinct in the 6 compartments simulation and do not permit further computations. An explanation could be the loss of particles. As already mentioned above the trapped boundary condition is implemented to count particles which are leaving the computation area at the inlet. In the 2 compartments simulation 204 particles and in the 6 compartments simulation 594 particles were captured at the inlet face. At least the same number of particles is missed in the parameter determination (axial dispersion coefficient and mean residence time). The 2 compartments simulation results were used for computing the axial dispersion coefficient. In addition the computation area was enlarged again (simulation area of 32 compartments) to reduce the effect of particle loss. With the 32 compartments file RTD calculations for 4 compartments were executed (CFD,32calc). The results of these calculations are shown in Figure 5.

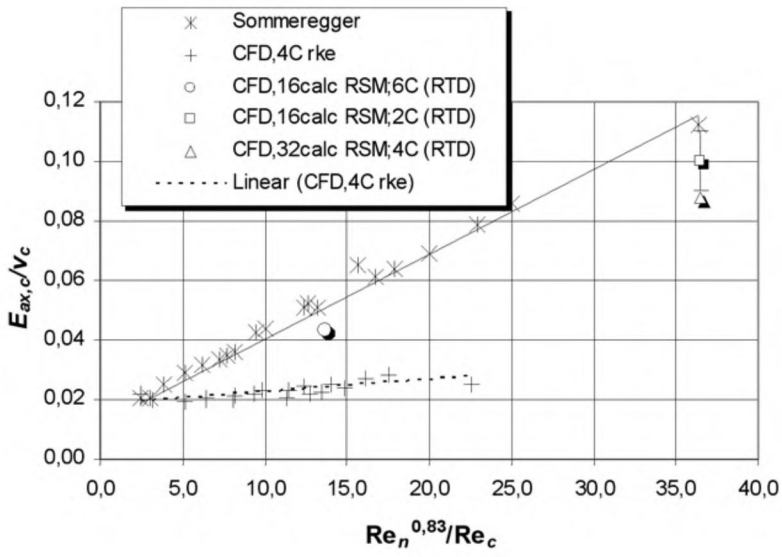


Figure 5. Axial dispersion coefficients determined with different CFD settings

SUMMARY

Target of investigations was to establish simulation of axial dispersion coefficients for the continuous phase in RDC extraction columns. After optimization of the parameter settings the computed data are in sufficient accordance with experimental data and empirical correlations. It was shown that the selection of the turbulence model is of predominating influence. As displayed in the results the RS-model proved best in modeling the rotating disc contactor extraction column. The influence of the computation area on RTD was worked out too. The results of RSM simulations lead to the conclusion that RTD investigation must be executed in large simulation geometries. It has to be ensured that particle leaving the computation area against the main flow direction can be kept at minimum. Application of trapping boundary conditions is therefore recommended.

eferences

1 Haderer, T.; Huber, Ch.; Marr, R.; Martens, S.: Numeric flow simulation of a RDC extraction column; *Proceeding of 15th International Congress of Chemical and Process Engineering, CHISA 2002,* (CD-ROM 1295.pdf); *Praha, CZE,* 25.-29.8.2002

2 Haderer, T.; Marr, R.; Martens, S.; Siebenhofer, M.: Apparatus Design in *Liquid-Liquid Extraction*; CFD Supported Modelling of Residence Time and Residence Time Distribution, *Proceedings of AIChE Annual Meeting 2003,* San Francisco, CA, Nov 16-**21,** 2003; *OMNIPRESS* American Institute of Chemical Engineers, New York, NY, 2003; 314c.pdf, 2003

3 Sommeregger, E. Hydrodynamik in Drehscheibenextraktoren; PhD Thesis; Institut für Thermische Verfahrenstechnik und Umwelttechnik, TU Graz, 1980

4 Kolb, P.; Bart, H.-J.; Fischer, L.: Entwicklung einer Miniplant-Extraktionskolonne; Chemie Ingenieur Technik, **74,** 3, 243-247, 2002

5 Levenspiel, O.: Chemical Reaction Engineering, John Wiley & Sons, New York, 1962

6 Bauer, R.: Die Längsvermischung beider Phasen in einer gerührten Extraktionskolonne, Dissertation ETH Zürich, 1976

7 Kumar, A.; Hartland, S.: Prediction of Axial Mixing Coefficients in Rotating Disc and Asymmetric Disc Extraction Columns; *Can. J. Chem. Eng.]* 77-89; 1992



A CFD STUDY OF THE MOVEMENT AND DEFORMATION OF LIQUID DROPS

A. R. Uribe-Ramirez and J. Alejandri-Alvarez

Facultad de Quimica, Universidad de Guanajuato, Col. Noria Alta s/n, C.P.36050
Guanajuato, Gto., México, e-mail: agustin@quijote.ugto.mx

A CFD Study of the movement and deformation of toluene drops dispersed in a water continuous phase by using the Volume of Fluid Method is presented. Several equivalent drop diameters, between 0.6 and 5 cm, were used. It was found that the drop shapes were within the ellipsoidal and the spherical-cap regimes, which agrees very closely with experimental reported results. The Eötvös and Morton numbers were calculated and the rising velocities were within the observed limits for drops with these characteristics.

INTRODUCTION

Drops and bubbles are fluid particles that occur in many natural phenomena, as well as in a wide variety of industrial unit operations (e.g. liquid extraction, drying, fermentation, etc.). The shape of fluid particles affects their rising velocity and, therefore, their residence time in the system under study. Moreover, heat and mass transfer between fluid particles and the surrounding media (continuous phase) is greatly influenced by the interfacial area, which is determined by the volume and the shape of the fluid particle. The particle will deform only when it is under the influence of non-uniform or non-symmetrical forces, such as those due to the movement or to the pressure or temperature variation that may overcome the stabilizing influence of the interfacial tension.

The movement of fluid particles is a well known phenomenon and so it is the mass and heat transfer from/to them. However, the relations that explain these phenomena are mostly empirical, which are determined from a large amount of experimental data [1, 3, 4, 6], Nevertheless, a more formal treatment from a fundamental study of the complex laws that govern those processes is not equally developed due to several reasons. The main one is the difficulty to predict the behavior of drops and bubbles, since the forces that take effect over these moving particles vary in such a way that are not easily understood, influencing their shape, velocity and drag. The complex relationship between pressure, buoyancy, surface tension, inertia and viscous forces cause fluid particles to deform in a way that their characterization is difficult, except when the continuous-phase Reynolds number is very low (spherical regime). Besides, the surface-active contaminants at the interface between the phases influence the drops hydrodynamics and shape [5],

According to their shape, fluid particles are divided into three main regimes [1]: a) Spherical, when surface tension forces and/or viscous forces are much more important than inertial forces, b) Ellipsoidal if the bubbles or drops are oblate with a convex interface around the

entire surface. Ellipsoidal drops and bubbles suffer from periodic dilatations and random oscillatory movement that make their characterization particularly difficult, c) Spherical cap when bubbles and drops are very large and they tend to adopt flat or concave bases and lack completely fore and aft symmetry. These particles may seem to be segments from spheres or low eccentricity ellipsoids.

METHODOLOGY

For a fluid particle that moves freely in a continuous media, its shape is strongly influenced by the forces in the continuous phase. In order for the particle to have a stable shape, normal and shear stresses have to be balanced at the interface. If the surface viscosities are ignored, the normal and tangential stresses for a fluid particle are written as:

$$0^{*}r\,\tau : nn - (p + \tau : nn) = \langle j\left(\frac{1}{R_1} + \frac{1}{R_{\cdot U}}\right) \qquad \bar{T}\cdot t - x\,t = V_s cr \quad (1)$$

where R, and R_2 are the radii of curvature, p is the total pressure equal to the summation of the static pressure p_s and the dynamic pressure p_d, the symbol A indicates dispersed phase properties, x is the viscous stress, **n** is the surface normal vector, *t* is the surface tangential vector and V_s is the gradient along the surface.

In the special case of spherical fluid particles, whose movement is mainly produced by gravity, it is convenient to scale dynamic pressure in the continuous and the dispersed phase with the quantities $2pgR$ and $2\hat{p}gR$, respectively, and the velocities with *U,* which represents the drop rising velocity. The normal stress condition in Eq. (1) in dimensionless form becomes:

$$Eo\left[\frac{\dot{P}^{f}}{Ap}\left(\text{次}^{*} - 2\frac{\hat{F}r}{\hat{R}e}\frac{d\hat{u}_r^{*}}{dr^{*}}\right) - \frac{\pounds}{Ap}\left(\text{L}_{r_d}^{*} - 2\frac{Fr}{Re}\frac{\partial u_r^{*}}{dr^{*}},\right)\right] = \frac{2R}{\sigma}(p_s - p_s) + 4 \qquad (2)$$

The Eötvös number (Eo) is a measure of the importance of gravity force with respect to surface tension force, whereas the Froude number (Fr) is a measure of the importance of the inertial force with respect to the gravity force. This dimensionless equation shows that for fluid particles that rise or fall due to gravity, the important number to consider is the Eötvös. Another dimensionless number commonly considered in these cases that exclusively characterizes the physical properties is the Morton number (M). These dimensionless numbers are defined as:

$$Eo = \frac{gEpd;^{2}}{\sigma} \qquad M = \frac{gP^{4}Ap}{P^{2}a'} \qquad \text{Re} = \frac{pd.U}{\mu} \qquad Fr = \frac{U}{gd.}$$

where g is the gravity constant, p is the continuous phase density, Ap is the density difference between the continuous and the dispersed phase, cris the interfacial tension, U is the drop rising velocity, d_e is the equivalent diameter and p is the continuous phase viscosity. Dispersed phase viscosity has not an appreciable influence over the drop deformation.

For drops and bubbles that rise or fall freely in a continuous media it is possible to represent the shape regimes in a generalized plot as a function of Eo, M, and Re, such as that reported by Clift el al.[1].

There are several methods to simulate multiphase flow by CFD. The one used in this work is known as the Volume of Fluid Method (VOF), which is included in the FLUENT computer

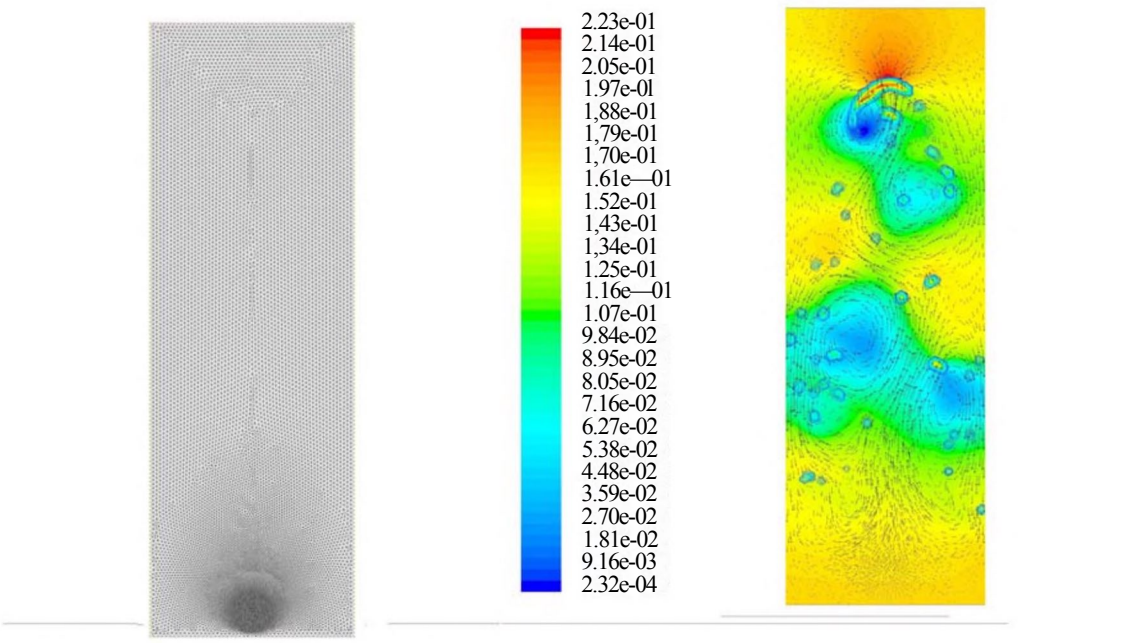
code [2], based on the assumption that two immiscible fluid phases do not penetrate each other. For each additional phase added to the model, a new variable is introduced: the volume fraction in the computational cell. For each phase *q*, a_q is the volume fraction in the cell, and can have three different values: $a_q = 0$ if the cell is empty, $a_q = 1$ if the cell is full, $0 < a_q < 1$ if the cell has an interface between the fluid *q* and one or more fluids. In order to calculate the volume fraction, the continuity equation for the volume fraction in each phase has to be solved, along with the Navier-Stokes equation and the mass balance at the interface. The volume fraction conservation equation is:

$$\frac{\partial a_q}{\partial t} + v \cdot \nabla a_q = \frac{S_{a_q}}{\rho_q} \qquad (3)$$

RESULTS AND DISCUSSION

For the simulation of the drop movement through a continuous, immiscible liquid phase, toluene drops in a continuous water phase were used, mainly because of the low solubility of toluene in water and vice versa. The physical properties for the two phases are:

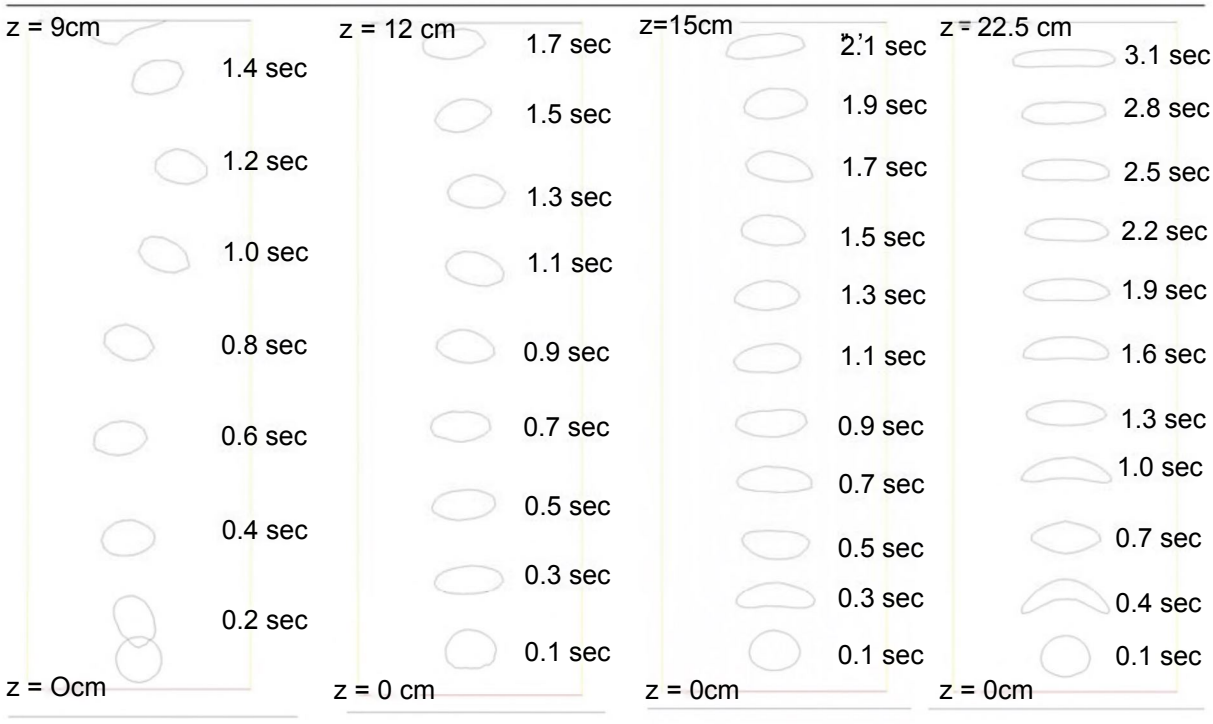
$P,o,_{,m}$ = 866 %; ρ_{water} = 998.2 %; Mlohim = 0.000586-^- ; = 0.001003^-; a = 0.024 N



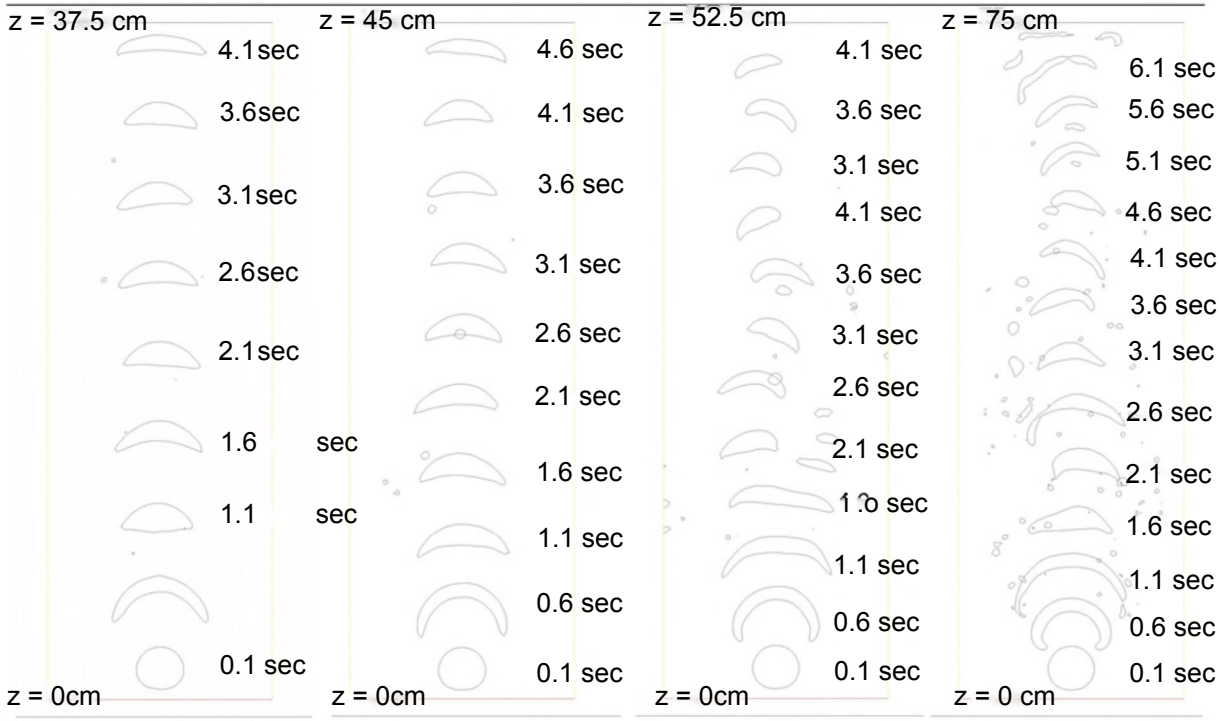
Grid (Time=5.5000e+00) Velocity Vectors Colored By Velocity Magnitude (mixture) (m/s)
FLUENT 6.1 (2d, segregated, vof, lam, unsteady) FLUENT 6.1 (2d, segregated, vof, lam, unsteady) (Time=5.5000e+00)

Figure 1. Typical computational mesh used in the simulations. *Figure 2. Pressure and volume profiles and velocity vectors in a typical simulation.*

Using values, the Morton number is $M = 9.525 \times 10^{-ii}$; i.e., log these (M) = -10.021. For the unsteady-state simulations, the time step size used was 0.005 s. In Figs (1) and (2) the computational domain and a typical mesh used, as well as the pressure, volume and velocity profiles in a typical run are shown.



a) Diameter = 0.6 cm b) Diameter = 0.8 cm c) Diameter - 1.0 cm d) Diameter = 1.5 cm



e) Diameter = 2.5 cm f) Diameter = 3 cm g) Diameter = 3.5 cm h) Diameter = 5 cm

Figure 3. Volume contours showing the drop shapes for different equivalent diameters at different times

In Fig. (3) the results of the simulations carried out in drops with equivalent diameters of 0.6, 0.8, 1.0, 1.5, 2.5, 3.0, 3.5 and 5.0 cm are shown. In this Figure, several sequences of drops showing the drop shape and the path they follow as they rise through the continuous phase, as well as the time they take to rise to a certain height, are presented. In Table (1) the results from these simulations are given. According to the values reported by Clift et al. [1], the drops with diameters of 0.6, 0.8, 1.0 and 1.5 cm are within the ellipsoidal regime, which can be clearly observed in Figs. (3a-3d), whereas for a 2.5 cm diameter, the drop is very close to the limit between the ellipsoidal and the spherical cap regime, observed in Fig, (3e), and therefore it shows a combination of both behaviors.

Table 1. Simulation Results.

Equivalent Diameter	Computational Domain		Eötvös	Reynolds	Rising Velocity	Regime
d_e (m)	Width (m)	Height (m)	Eo	Re	U (m/s)	
0.006	0.03	0.09	1.945	760	0.1273	Ellipsoidal
0.008	0.04	0.12	3.457	940	0.1181	Ellipsoidal
0.010	0.05	0.15	5.402	1080	0.1085	Ellipsoidal
0.015	0.075	0.225	12.154	1800	0.1206	Ellipsoidal
0.025	0.125	0.375	33.761	3400	0.1366	Ellipsoidal/Spherical Cap
0.030	0.15	0.45	48.616	4200	0.1407	Spherical Cap
0.035	0.175	0.525	66.172	5800	0.1665	Spherical Cap
0.050	0.25	0.75	135.046	9100	0.1829	Spherical Cap

The drops with diameters of 3.0, 3.5 and 5 cm are in the spherical cap regime, although they are very unstable because of the large size of these drops. It can be observed that these drops break at short distances after their release, which result in smaller drops that fall in a different regime (spherical or ellipsoidal), changing completely their behavior. Therefore, the formation of the spherical cap is not so obvious. However, the results are very close to the experimental observations shown by Clift et al.

CONCLUSIONS

In this work, the movement and deformation of toluene drops dispersed in a continuous water phase, by using the CFD techniques in the computer code FLUENT v6.1, were simulated. The results obtained coincide very closely with the experimental results published elsewhere [1, 3, 4], These results are very promising, and it can therefore be stated that the simulation of different multiphase problems such as heat and mass transfer and chemical reactions in drops and bubbles can be studied with a good chance of getting the right results, which can be applied to the study of several unit operations such as distillation, extraction, gas absorption, chemical reactors, etc.

ACKNOWLEDGEMENTS

This work was carried out in the Chemical Engineering Department at the University of Guanajuato.

REFERENCES

1. R. Clift, J.R. Grace and M.E. Weber, (1978), *Bubbles, Drops and Particles, Academic Press Inc., USA.*

2. Fluent, Inc. (2003). *FLUENT 6.1 User's Guide.*

3. J.R. Grace and T. Wairegi (1992), Shapes of Fluid Particles. In: Transport Processes in Bubbles, Drops and Particles R.P. Chhabra and D. De Kee, (eds.), Pp. 133-145. Hemisphere, New York.

4. J.R. Grace and T. Wairegi (1986), Properties and Characteristics of Drops and Bubbles. In: *Encyclopedia of Fluid Mechanics,* N.P. Cheremisinoff, (ed.), **Vol. 3,** Cap. 3, Pp. 43-57. Gulf Publishing, Houston, TX.

5. S.S. Sadhal, P.S. Ayyaswamy and J.N. Cheng (1997), Transport Phenomena with Drops and Bubbles, Springer-Verlag New York, Inc.

6. S. Winnikow and B.T. Chao (1966), *Phys. Fluids,* 9, 1, 50-61.

CRUD FORMATION AND ITS CONTROL IN SOLVENT EXTRACTION

WANG Chengyan

Beijing General Research Institute of Mining & Metallurgy, Beijing 100044, China

All commercial solvent extraction plants suffer from crud, which mainly caused by solids. The crud can influence phase continuity, emulsion stability, aqueous solution and air distribution. The problems of crud formation, its control and disposition have been discussed from organic phase, aqueous phase, solid particles and air in this paper.

INTRODUCTION

As an important section of hydrometallurgy, solvent extraction is paid attention for the properties of less pollution, less energy loss, lower cost, and higher efficiency. However, all commercial solvent extraction (SX) plants, inevitable, suffer from stable multi-phase emulsions, which mainly caused by solid particles. We generally call those stable multi-phase emulsions as crud, or gunk. The crud is made of organic, aqueous, air, and solid phases, and is often found to distribute itself randomly throughout the separating phases, and sometimes floating on top of the organic, causing floating crud, or “fish eyes”. It can influence phase continuity, emulsion stability, and air distribution during SX. In extreme cases, it can cause phase inversion, which the operating can’t run smoothly. It not only increases the loss of organic with entrainment, but also increases the cost. The effecting elements on the crud formation is complex, however, up to now, the mechanism of this is not clearly understood. In this paper, based on the practices of the author in recently years, the reasons of crud formation and its control during SE are discussed preliminarily.

REASONS OF CRUD FORMATION

Mineralogy studies indicate that the solid particles, which form stable multi-phase emulsions, are typically less than 1 micron in size and average 0.16-0.37 micron. Major elements present are Si, Al, and Fe, and crystalline mineral species found include alpha-quartz, micas, clays,

jarosites and gypsum. Chemical composition of the crud, which was obtained from a copper SX plant in China, is shown in Tab. 1.

Tab. 1 Chemical composition of crud

	Si02	Al_2O_3	Fe_20_3	CaO	MgO	$Mn0_2$	S	C	Cu	As
1	48.52	13.43	6.87	0.94	2.09	0.20	0.30	15.89	0.008	0.035
2	35.58	18.26	7.88	1.42	1.85	0.43	0.22	10.53	0.015	0.023

Usually, the crud is made of organic, aqueous, and solid phases. Sometimes, it floats on the surface of the organic with air, causing floating crud, or “fish eyes”. So, the questions of crud formation can be considered from four aspects: organic phase, aqueous phase, air and solid particles.

Effect of organic phase

The organic phase during SX is made of extractant and diluent (usually is kerosene). The quality of them has a great effect on crud formation. For example the extractantes of P204 and P507, made of China, which were used to separate nickel and cobalt, usually contain a little lower carbon-carbon chain hydrocarbon compounds because of the backward equipments of fractional distillation during their synthesis. The lower carbon-carbon chain hydrocarbon compound will tend to induce the crud formation and lengthen the mixed phase separation during SX. In extreme cases, the operating will total loss of control.

Because the sulfonated kerosene is expensive, most of the SX plants in China use civil kerosene being the diluent. The civil kerosene is impure, and often contains unsaturated hydrocarbons in it. These impurities and unsaturated hydrocarbons also have a great effect on the crud formation and the mixed phase separation.

Effect of aqueous phase

The soluble organic acids and organic substances in the pregnant leach solution are the main reasons for the aqueous phases to urge the crud formation. Information from operating SX plants shows that these soluble organic acids and organic substances are introduced by three main methods: (1) Dead animals and vegetables. For example, during the heap leaching of low grade copper mineral, an amount of soluble humic acid in mineral will go into the organic phase with pregnant leach solution; (2) Soluble composition of the corrosion preventive coating. Economic considered, some SX plants usually use pitch as the anticorrosion material to preserve the storage cells or ponds, the soluble organic acids and organic substances in pitch, inevitable also, will dissolve in solution. (3) Organic substances carried by minerals (such as the used catalyst and waste electroplate solution etc.) themselves. During SX, these soluble organic acids and organic substances will combine with extractant to form organosol, and results in the crud formation at last. In addition, the aqueous pH value also has a great effect on the crud formation.

Effcet of solid particles

As the key factor of crud formation during SX, solid particles can be introduced via five main ways: (1) Suspension in pregnant leach solution; (2) Dusts from environment; (3) Precipitates as aqueous pH value increases; (4) Solid impurities in industrial chemicals; (5) Solid particles from recovery organic phase. Moreover, during the copper L-SX-EW, the powdery dropper from anode is another way of solid particles introduced.

The ways of solid particles introduced are different with the technologies. When using P204 and P507 extractantes to separate Co from Ni, suspension in pregnant leach solution maybe is the main way of solid particles introduced. When using heap leaching, dusts from environment will be the main way. In order to reducing the organic loss, major plants recovery organic from buffer cells and return them to the circuit, solid particles in the recovered organic, inevitable, will be introduced. In the smelter acid being added as make-up, somehow these solid impurities were finding their way from the acid into the organic phase in the strip settler.

Solid particles, which exhibit both hydrophilic and hydrophobic tendencies, are particularly likely to give problems. High specific gravity particles are not believed to cause much of a problem, as they tend to settle fairly quickly to the bottom of the settler unit where they accumulate and removed at intervals. However, the smaller particles, especially the precipitates as aqueous pH value increases can be a major problem and is often associated with the presence of soluble silica, or with calcium in the feed leading to precipitation of gypsum. In the rainy season, considerable amounts of clays and other solids would be washed into the pregnant leach solution storage ponds. In extreme cases, it would cause phase inversion, a phenomenon known in the industry as a “gunk run”.

During the electro-winning of copper, the powdery droppers from anode are particularly to give attention. These droppers are mainly made of $Pb0_2$ that have high oxidation. If they are carried by the strip solution into the strip stage, the extractant will be oxidized, and lose the capacity of extraction, a phenomenon known in the industry as an “extractant poisoning”. In extreme cases, the operating will total loss of control.

Effect of air

The effect of air on the crud is shown in the adsorption between solid particle and gas. If a solid particle carried in the pregnant leach solution is only partly water-wetted, the hydrophobic portion of its surface will most probably have a tin layer of air adsorbed on it. If sufficient air is trapped and coalesced within the interfacial layer it can result in the local average specific gravity falling below that of the upper organic layer. Thus the air/mineral/organic/water crud complex can rise through the organic layer to the surface, causing floating crud, or “fish eyes".

Other sources of air occlusion in composite crud particles are caused by excessive vortex of mixers, by allowing the mixed phase to exit too vigorously from the mixer unit into the settler unit, by lack of attention to solution levels in overflow weirs, and by carried air of pipes.

CRUD CONTROL

As is seen from above that the crud formation is connected tightly with organic phase, aqueous phase, solid particles, and air. So, the ways to minimize the crud also should focus on the four aspects.

Organic phase control

Practices from operating SX plants show that using high concentration HCI to wash the organic phase beforehand can take off its major impurities, such as lower carbon-carbon chain hydrocarbon, unsaturated hydrocarbons etc. For example again the extractantes of P204 and P507, if using 6M0I/L HCI to wash them beforehand, not only the phase separation time is short largely, but also the crud is less.

Aqueous phase control

Removing trees, shrubs, and other vegetation from the immediate areas surrounding storage ponds can help to eliminate the bacterial growth, and lower the soluble organic acids and organic substances. If possible, using the pyrometallurgy beforehand to treat those solid wastes, which contain organic substances such as the used catalyst, can largely eliminate organosol formation. In addition, using neutralization precipitation, and washing with water to treat the waste electroplate solution beforehand also can help to eliminate organosol formation.

Solid particles control

Roofing settler and buffer cells can largely eliminate ingress of dust. Also, ingress of clay, which carried by rain, can be largely eliminated by retaining wall around the storage ponds. In addition, adding a little vegetable glue (a kind of flocforming agent and surfactant) in the pregnant leach solution storage ponds can have great help to eliminate the suspension in pregnant leach solution. The vegetable glue can ensure complete wetting of the solid particle surfaces, including the hydrophobic regions, and can adsorb strongly onto the hydrophobic surfaces to displace any adsorbed air. At the same time, those solid particles, such as $Si0_{2l}$ $AI(OH)_3$, and $Fe(OH)_3$ etc. will be adsorbed together by the vegetable glue and being a big particles to settle quickly to the bottom of the storage ponds.

As is mentioned above, during the electro-winning of copper, the droppers from anode are particularly to give attention. If the anode is made of Pb-Ca-Sn or Pb-Ca-Sn-Sr, the droppers are usually being a thin piece to settle to the bottom of the electrolytic cell, where they accumulate and can't be carried by the strip solution, are no longer capable of causing much of a problem. If the anode is made of pure lead or Pb-Sb, the droppers are usually being powdery and can be carried into the strip stage with the electrolytic solution, where they would react with extractant. Up to now, the "extractant poisoning" had taken place, at least, at two copper plants in China by lack of attention to anode materials.

Another problem about the copper L-SX-EW plants is the reclaim of organic phase in electrolytic cells. Major SX plants in China, economic considered, reuse the recovered

organic phase. However, this is very unsuitable. During the copper electro-winning, 0_2, which has high oxidation, will be produced on anode. So, most of the extractant in electrolytic cells has been oxidized and hydrolytic degradation, and has lost the capacity of extraction. If return them to the circuit, they are no use beside trouble only.

Air control

Extraction tank, as the key equipment of SX, its design is very important for air control, especially the design of the mixer's rotational speed and its diameter. When the mixer's diameter is determined, the slower the rotational speed, the smaller the suction power; and the flow of solution can't get to the project. On the contrary, if with excessive rotational speed, it not only causes excessive vortex, but also sucks an amount of air from pipe into mixer unit. It is very disadvantage for the mixed phase separation. In addition, paying attention to solution levels in overflow weirs, and keeping the mixed phase to flow gently from the mixer unit into the settler unit is very important also.

The pipes connected with the extraction tank, should be as short as possible, if possible, don't use U type bend. It can help to lower the solution resistance and eliminate air carried.

Conditions of SX

Practices from operating SX plants show that with the organic phase as the continuous, or external phase can compact the crud into the aqueous phase, where they can be resisted by the hurdles in settler, and removed at intervals. Whereas under aqueous continuous conditions, the crud tends to become less well compacted, distributed throughout the organic phase, and is less easily removed from the system.

CRUD DISPOSAL

Typical crud handling methods in SE plants in foreign involve removing crud by suction from the interface, allowing primary separation by gravity in storage tanks, returning the supernatant organic to the circuit, and centrifuging the remainder to recover additional organic. In China, because major SX plants is small, and moreover the centrifuge is expensive, economic considered, most of them use natural separation by gravity method to disposal the crud. However, in recently years, some of them have begun to use bentonite to treat the crud. Studies indicate that if solid particles are hydrophilic, and preferential wetting by the aqueous phase will tend to accelerate the separation of mixed phase, whereas if solid particles are preferential wetted by the organic phase will tend to stabilize the mixed phase. At this condition, the separation of mixed phase will become very difficult. So, using bentonite to treat the crud is based on its hydrophilic property, expansibility, adherence, thixotropy, and adsorption property to impel the crud demulsification. The solid particles, such as $Si0_2$, $Al(OH)_3$, $Fe(OH)_3$, and others colloid particles in crud, are adsorbed by bentonite to precipitate with bentonite together, and then the organic is reclaim.

Another method to disposal the crud is using steam to raise the temperature of the crud to

about 45°C to impel the crud demulsification. Suitable temperature in here must be attention. Excessive temperature can give harm to the extractant and bring about the hydrolytic degradation of the extractant.

CONCLUSION

The crud during SX is made of organic, aqueous, solid phases and air. Its formation is connected tightly with organic phase, aqueous phase, solid particles, and air, and with many effecting elements. The mechanism of this is not clearly understood. The crud can influence phase continuity, emulsion stability, aqueous solution and air distribution. In extreme cases, the operating will total loss of control. Solid particles are the key factor of crud formation, and suspension in pregnant leach solution is the main way of solid particles introduced. So, to eliminate the suspension in pregnant leach solution as being as possibly is very important for the crud control. A well designed of extraction equipments and well-run conditions all can help to the crud control.

REFERENCES

1. WANG Chengyan, *MINING AND METALLURGY (in Chinese),* Vol.10, No.1,68-71.
2. Tom Burniston, et al. E & MJ, 1992, 1, 32-35.

HYDRAULIC AND MASS TRANSFER CHARACTERISTICS FOR CAPROLACTAM EXTRACTION WITH TOLUENE IN THE BATEMAN PULSED COLUMN

M. L. van Delden, G. S. Vos, N. J. M. Kuipers, A. B. de Haan

University ofTwente, Enschede, The Netherlands

Caprolactam is industrially recovered from an aqueous feed containing ammonium sulphate by extraction with an organic solvent (toluene) followed by back-extraction with water. In this paper the characteristics for this extraction in the Bateman Pulsed Column were evaluated. Pilot plant experiments were performed to determine the hydraulic and mass transfer characteristics as a function of the operating parameters. The experimental conditions covered the industrial operating range with respect to concentrations, temperature and phase continuity. The obtained hydraulic data could be related and described well via empirical correlations using physical properties, energy input and phase flows.

INTRODUCTION

Caprolactam, the monomer of Nylon-6, is recovered from the neutralized Beckmann rearrangement mixture, which consists of two liquid phases. The aqueous crude caprolactam top phase, containing 65-70 mass % caprolactam and 1 mass % ammonium sulfate, is in equilibrium with a nearly saturated aqueous ammonium sulfate solution. After separation of both phases caprolactam is recovered from the crude caprolactam phase by extraction with an organic solvent (toluene). After this so-called forward extraction (FE) caprolactam is back-extracted (BE) from the organic solvent with water [1], For both processes columns like the Rotating Disk Contactor (RDC) and Pulsed Packed Column (PPC) are applied [1],

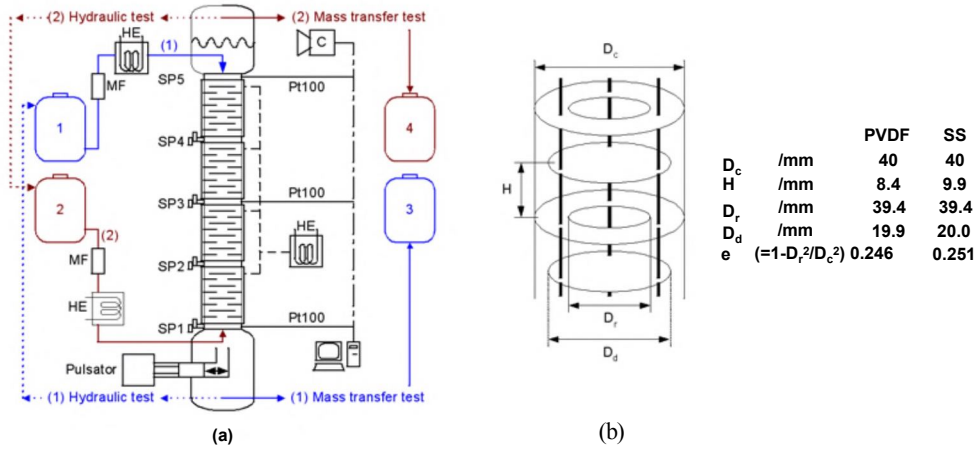
In this paper the characteristics of the Bateman Pulsed Column (BPC), a pulsed disc and doughnut column, was investigated for application in the caprolactam extraction process. The motivation is that its construction is simpler and cheaper compared to the RDC whereas the BPC is less susceptible to fouling than a PPC. The BPC is already applied in metal extraction and its characteristics are known for these type of applications [2,3], Furthermore fundamental research is performed on hydraulic and mass transfer characteristics by means of numerical simulations [4,5], However, for the extraction of organics that possess different physical properties than (reactive) metal extraction systems, information is limited [6],

In the extraction process, hydraulics, being hold-up, drop size and operational window, and mass transfer determine the column capacity [7], The present study investigated the hydraulic and mass transfer characteristics of the BPC for both the forward and back-extraction of caprolactam as function of operating parameters, being flow rates and pulsation intensity. The conditions covered the industrial operating range with respect to caprolactam and ammonium sulfate concentrations, flow ratio, temperature and phase continuity.

EXPERIMENTS

Experimental set-up

The BPC pilot set-up is schematically shown in Figure 1(a). The column consisted of four jacketed glass segments of each 1.04 m length. Settlers of 42 cm height and 80 mm internal diameter enclosed the column. The internals consisted of alternating disc and doughnut baffles as presented in Figure 1(b). The internals were made of SS or PVDF material to prevent wetting in case the aqueous (1) or organic (2) phase was continuous, respectively. In the bottom settler a piston type pulsator was placed. Each phase was pumped from its storage vessel (1,2) via a mass flow controller (MF) and heat exchanger (HE) to the column, where they were introduced via a single glass tube. The temperature in the column was monitored via three PtIOO temperature sensors (PtIOO) in the top, middle and bottom. With the interface level located in the top of the column (BE) continuous observation was possible via a camera (C). When the interface level was located at the bottom of the column (FE) it was visually observed. The level was controlled via a manually operated valve in the aqueous outgoing stream. The top stream left the column via an overflow.



		PVDF	SS
D_c	/mm	40	40
H	/mm	8.4	9.9
D_r	/mm	39.4	39.4
D_d	/mm	19.9	20.0
e	(=1-D_r^2/D_c^2)	0.246	0.251

Figure 1. Schematic presentation of the BPC (BE operation) (a) and BPC internals (b).

Experimental procedure

The physical properties used, being densities (p), viscosities (p) and interfacial tension (^), are presented in Table 1, dependent on the concentration and the temperature (T).

Table 1. Physical properties in the forward and back-extraction of caprolactam

	T °C	*WcPL.* aa -	W/is.aa -	*WcPL.ora* -	Phase [c]	10'³p_c kgrrT³	10³/?$_c$ kg-m'^s'¹	10'³p_d kg·m'³	10³p_d kgm'¹s'¹	10 ³-*y* N-m'¹
FE	40	**0.000**	**0.000**	**0.000**	org	0.848	0.47	0.991	0.67	34.7
		0.475		0.119		0.870	0.60	1.027	3.03	1.60
		0.114	0.031	0.023		0.852	0.49	1.018	0.95	10.8
		0.337		0.083		0.863	0.55	1.035	1.99	3.65
BE	20	**0.000**	-	**0.000**	aq	0.998	1.02	0.868	0.59	35.8
		0.468		0.090		1.039	5.69	0.884	0.72	1.92
	40	0.087	-	0.012		0.998	0.84	0.850	0.48	14.4
		0.461		0.114		1.026	2.89	0.869	0.59	1.84

The physical properties were correlated [8], where the interfacial tension relation was extrapolated for $w_{cPL,org}$ > 0.05. The operational parameters in the forward and back-extraction, being flux (= sum of the phase velocities: V_d+V_c), flow ratio ($R = V_d/V_c$) and

pulsation intensity (= product of pulsation stroke and frequency: S_p7), varied from flux/mh'1 = 12-30, Sp f/m s'1 = 15-35 x 10'3 and *R* = 0.2-1.0 and 1.0-3.0, respectively.

All hydraulic experiments were performed at equilibrium concentrations. The system was first equilibrated, followed by creating a steady state condition by maintaining a constant interface level. Drop sizes were determined by comparing drops on digital photos of the column contents with the known size of the column internals as reference. Operating regimes were determined from the digital images, where a zone without drops and a dispersed phase layer on the internals were characteristic for mixer-settler operation. A uniformly filled column was taken as dispersion regime characteristic [7], Visual observation of the emulsion regime was, however, not possible. Hold-ups were measured by sampling the column contents via four ball valves (SP1-SP4), which were placed in the flenses connecting the segments. The obtained volumes were left to settle after which the volumes of both phases were measured. By gradually increasing the pulsation stroke at steady state operation and meanwhile observing column behaviour the operational window was determined. Concentration profiles were measured via sample ports, consisting of two separate tubes with 3 mm internal diameter. One was wetted by the organic phase and faced downwards. The other was wetted by the aqueous phase and faced up. The phases were thus sampled separately. The samples were analysed by gas and ion chromatography for the caprolactam and ammonium sulfate concentrations, respectively. Sample ports were placed in each flense (SP1-SP5) and at the column feed side three additional sample ports were placed in the glass segment.

HYDRAULIC DATA CORRELATION

In the operation of pulsed extraction columns various operating regimes can be distinguished [7] and comparable characteristics have been reported for a pulsed disc and doughnut column [6], These regimes are described as mixer-settler (MS), dispersion (D) and emulsion (E) regime [7], The first is limited by flooding due to a too low amount of energy applied. The other regimes are limited by flooding due to a too small relative velocity between the phases, phase inversion or the maximal allowable entrainment level [7], Within the operational window that depends on physical properties, mass transfer and flow ratio, the hold-up and drop diameter in relation to the operational parameters characterize column performance.

Following Kumar and Hartland [9] the drop size (d_{32}) was correlated with a relation derived for pulsed sieve-plate columns (PSPC), which is valid in all operating regions, makes use of geometrical shapes that can be translated to the BPC and covers a wide range of conditions.

$$d\$2 \sim C \left[H \left(\frac{1}{\rho_* \cdot g} \right)^{n_2} \left(\frac{\eta_d \cdot g}{\gamma_* \cdot \rho_*} \right)^{n_3} \left(\frac{Y}{\gamma_*} \right)^{n_4} \left[C_2 + \exp \left(\frac{-W^*}{e \cdot (\gamma_* \cdot g)^{0.25}} \right)^{0.25} \right] \right] \left(\frac{\gamma}{\Delta\rho \cdot g} \right) \qquad (1)$$

where *p-* and *y-* are reference values of water at 20 °C (p*/kg· m'3 = 998.2, ^/N·m'1 = 0.0728). The physical properties were assumed to be described well with the original parameters [9] and furthermore the characteristic dimensions of the internals used change hardly. Therefore C_2 = 0.16, *rii* = 0.30, n_2 = 0.18, n_3 = 0.14 and n_A = 0.06 [9], The internals were, however, shaped differently compared to a PSPC and as a result the energy input is also different. Therefore parameters Ci and C_3 were expected to differ from the values for a PSPC. These were fitted by minimization of the absolute value of the relative error (AARE). All 69 data-points could be represented with an AARE of 13.8 % when Ci = 2.68 and C_3 = 2.41.

The transition from the mixer-settler to the dispersion regime and the onset for the emulsion regime are correlated and predicted by Equation 2 following Kumar and Hartland [7],

$$f_p \cdot S_{I\,MS\,ID} = k, \{f\,Ap^{\circ s} \cdot e / \eta_d^{0.75}\}^{0.33} \quad (2a)$$

$$f\text{-}S_{J\,P\backslash DIE} = 0.5\text{-}?/\sqrt{0.96\text{-}e^2 / p_c} \quad (2b)$$

A minimum and maximum value for /c_3 were obtained from the conditions at the last observation of the mixer-settler regime and the first observation of the dispersion regime, respectively. It was found that 8.03-10"^{3} < k_3 < 9.16 10'^{3} and 1.45-10'^{2} < k_3 < 1.73-10'^{2} for BE and FE operation, respectively, compared to the original value of k_3 = 9.69 10'^{3} [7],

Following Kumar and Hartland [10] hold-up (x) data were correlated via a unified equation x = n <P ^{1}f'-r The groups are defined by Equation 3. The correlation is valid in the dispersion and emulsion regime. Data measured in the mixer-settler regime were excluded, where Equation 2a with the fitted values for k_3 was used to determine the critical pulsation intensity.

$$\mathbf{n} = C_n \left[\frac{\varepsilon}{g} \cdot \left(\frac{f\,'Pc}{z\text{-}r)} \right)^{025} \right]^{n_1} \quad \text{with } s = \frac{2'*2\wedge\sim e2)}{3\text{-}H\,0.36\text{-}e^{2p}} (/S_p)^3$$

$$cD = r_d \left[\frac{Pc}{U\text{-}rJ} \right]^{0.25"\,n_z} \cdot \exp\left[\ll_3 v_c \blacksquare \left(\frac{Pc}{U\text{-}rJ} \right)^{0.25"} \right] \quad (3)$$

$$vF = C_4 \cdot \left(\frac{\backslash p\wedge}{\rho_c} \right) \cdot \left(\frac{Vd}{n_w} \right)^{n_5} \quad \text{and } r = C_r \cdot e^{e\%} \cdot \left[H \blacksquare \left(\frac{Pc'\,8}{\{ r\,J} \right)^{0.5} \right]^{n_7}$$

Equation 3 was modified by replacing the dummy //$_w$ with >;$_c$. C® was taken unity and n_6 = 0, which was the value used for all pulsed columns [10], It was assumed that the influence of the physical properties and flows was correlated well with the original parameters n_2 = 0.87, n_3 = 3.34, n_4 = -0.58 and n_7 = -0.39. The parameters C_n, C_r, r?i and n_5 could differ, because of the influence of different internals, different energy input and modified viscosity. These were fitted by minimization of the AARE. All 349 data-points could be represented with an AARE of 11.3 % for C_n = 1.73, C_r = 0.78, ^ = 0.38, n_5 = -0.09 and n_7 = -0.24.

In the operational window flooding limits the operation at low pulsation and the necessity of a minimum amount of pulsation intensity was observed, but not quantitatively determined. For high pulsation intensities flooding (F) was observed as the limiting process for the forward extraction and phase inversion (PI) for the back-extraction. At the flooding point a critical hold-up value is reached. Via the slip velocity concept this criterion can be related to the velocities of both phases. Kumar and Hartland [11] use this approach in combination with the correlation of two drag coefficients dependent on the slip velocity and drop size. This correlation was also applied here. However, near the operational boundary the behaviour of a system changes, especially with respect to drop coalescence [7], which results in the validity of Equation 1 being questionable. The increased coalescence was approximated by fitting C_1 and C_2 in Equation 1 by minimization of the AARE in the flooding data. With C-\ = 4.95 and C_2 = 0.06 the AARE in the flooding data from the hydraulic tests was 16.4 %. In the back-extraction process phase inversion was observed as the limiting process for the operational region. Yeo *et al.* presented for batch systems a criterion for the critical hold-up at phase inversion based on the systems interfacial energy [12], as presented in Equation 4.

$$x_{org,PI} \blacksquare {}^d32.a_q \backslash_{org[c]} = {}^d22.org \backslash_{aq[c]}' \qquad (1 \text{“} x_{org.Pl}) \quad (4)$$

Via Equation 3 the critical hold-up was related to the flow rates. This hold-up calculated with Equation 4 does not agree with the hold-up calculated using Equation 3, which is probably

caused by a change in behaviour of the system near the operational boundary. Different drop coalescence behaviour was accounted for in Equation 3 by fitting parameters influencing the interfacial tension and energy input. Minimization of the AARE in the phase inversion data resulted in C_n = 0.00, C_r = 6.05, n_1 = 0.38 and n_7 = -0.21 with an AARE 16.2 %.

EXPERIMENTAL AND FIT RESULTS

Using the derived equations for the flooding and phase inversion limitations, Equation 4, and the transition of the operational regimes, Equation 2a and b, an operational diagram can be constructed for the hydraulic tests for a system, like the BE system where $w_{CPL.aq}$ = 0.192, R = 3.0 and 77°C = 40 (Figure 2). Within this operational diagram the hold-up and Sauter mean diameter can be described for each operational point (characterized by the flux and pulsation intensity) using Equation 1 and 3 (Figure 3).

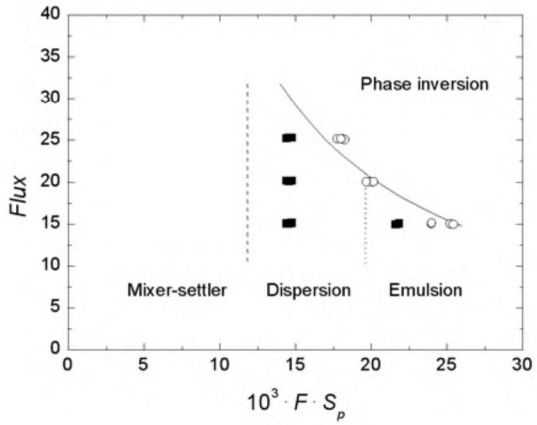


Figure 2. Operational diagram for $w_{cpL.aq}$ = 0.192 in BE with R = 3.0: M, column operation; **O,** *phase inversion data; —,phase inversion fit; - MS to D transition fit; ■■■, D to E transition fit.*

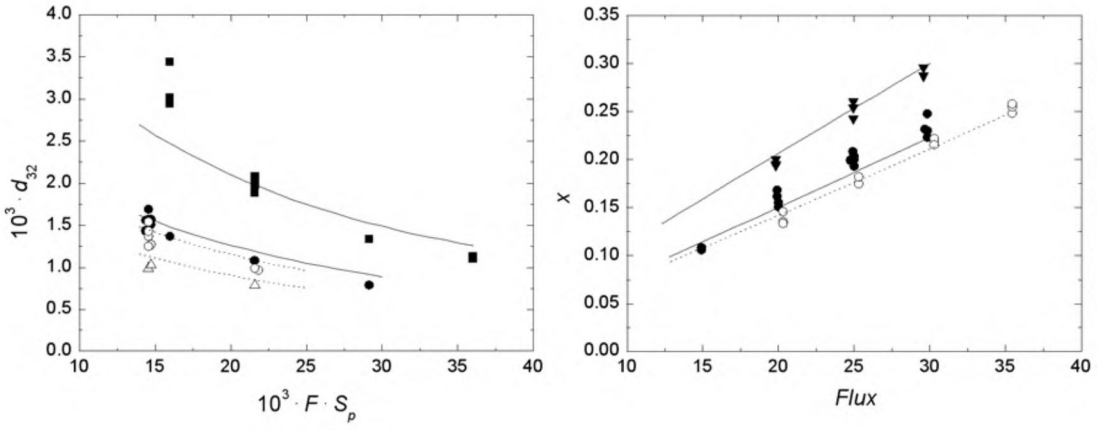


Figure 3. Experimental and fitted values for d_{32} and x in the BE process at 20 °C and R = 1.0, unless stated otherwise: **■,** *$w_{cpL.aq}$ - 0.0;* **•,** *$w_{cpL.aq}$ = 0.091;* **▼,** *$w_{cpL.aq}$ = 0.091 and R = 3.0;* **O,** *$w_{cPL.aq}$ = 0.087 at 40 °C;* **A,** *$w_{cpL.aq}$ = 0.192 at 40 °C; and:* **—,** *BE fit; BE fit at 40 °C.*

An operational point was selected for both processes in the dispersion regime at about 80 % of the maximum flux (Table 2). Concentration profiles were determined at this point.

Table 2. Selected operational points for the FE and BE extraction process of caprolactam

Process	Feed	Phase [c]	**WCPL, feed**	S_p//mS ^{1}	*TI°C*	*Fluxl* mh'^{1}	*R*
FE	aq	org	0.50	0.016	40	20	0.18
BE	org	aq	0.14	0.016	20	20	2.9

The influence of flux, pulsation intensity, temperature and ammonium sulfate concentration (for FE) on the mass transfer profile was investigated relative to the operational point. The caprolactam concentration profile over the column length is shown in Figure 4 for FE and BE.

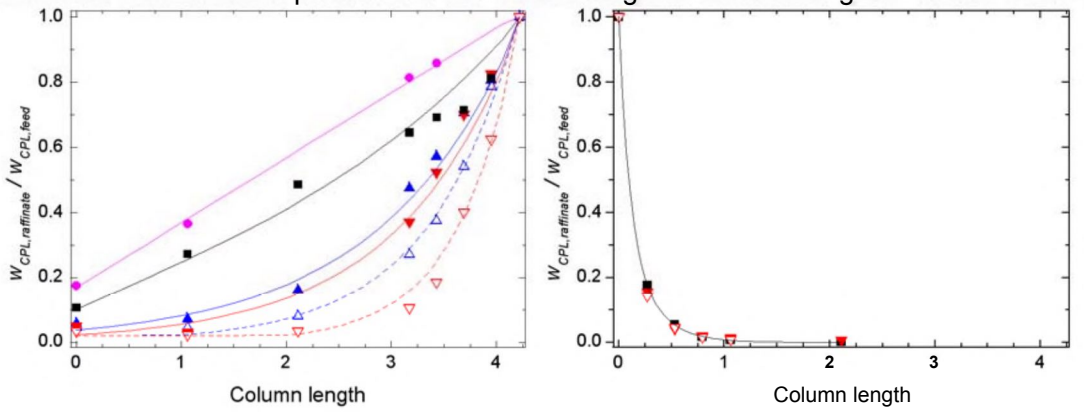


Figure 4. Experimental concentration profiles in the FE (left) and BE (right) process for: M, the operation point; •, flux/m/h = 26 (FE); A, $w_{AS,reed}$ = 0.01 (FE); A, $w_{AS,reed}$ = 0.01 and Spf/ms'^{1} = 22x 10 ^{3} (FE); T, AT/°C = +20; V, AT/°C = +20 and Spf/ms^{1} = 22 x 10 ^{3}.

The influence of flux can be attributed to an increase in the ratio of flow and mass transfer, although the hold-up was increased as expected from the hydraulic tests. The different influences on physical properties and distribution ratio affected both the hold-up and drop size. The influence of pulsation intensity is directly related to a decrease in the drop size and therefore an increase in mass transfer. However, for solute transfer to the continuous phase increased drop sizes were obtained compared to the hydraulic situation.

CONCLUSION

The BPC was applied in the forward and back-extraction of caprolactam. The BPC showed qualitatively comparable operational characteristics to a PSPC. Hold-up and Sauter drop diameter values and mass transfer profiles were measured within the operational window and respectively correlated using existing theory and explained using hydraulic tests results.

LITERATURE

1. A. J. F. Simons and N. F. Haasen. Extraction of Caprolactam; from T. C. Lo, M. H. I. Baird and C. Hanson (1983), **Handbook of Solvent Extraction,** Wiley, New York, pp. 557-566.
2. E. M. Buchalter, R. Kleinberger and B. Grinbaum (1998), *Proc. of Extraction Metallurgy Africa '98,* Johannesburg, South Africa, pp. 185-199.
3. A. B. Jahya,.G. W. Stevens and H. R. C. Pratt (2000), *Proc. of MINPREX 2000,* Melbourne, Australia, pp. 281-284.
4. G. Angelov, C. Gourdon and A. Line (1998), *Chem. Eng. J.,* **71,** 1-9.
5. S. D. Al Khani, C. Gourdon and G. Casamatta, *Ind. Eng. Chem. Res.,* 27, 1988, 329-333.

6. A. B. Jahya, G. W. Stevens and H. R. C. Pratt (2001), *Proc. of Chemeca'99,* Newcastle, Australia.
7. J. C. Godfrey and M. J. Slater (1994), *Liquid-Liquid Extraction Equipment,* John Wiley & Sons, Inc., New York.
8. M. L. van Delden, N. J. M. Kuipers and A. B. de Haan (2004), *J. Chem. Eng. Data,* web ed.
9. A. Kumar and S. Hartland (1986), *Chem. Eng. Comm.,* **44,** 163-182.
10. A. Kumar and S. Hartland (1995), *Ind. Eng. Chem. Res.,* **34,** 3925-3940.
11. A. Kumar and S. Hartland (1988), *Ind. Eng. Chem. Res.,* 27, 1988, 131-138.
12. L. Y. Yeo, O. K. Matar, E. S. Perez de Ortiz and G. F. Hewitt (2002), *Chem. Eng. Sci.,* **57,** 1069-1072.

NON-INVASIVE DISPERSED PHASE HOLD-UP MEASUREMENTS IN LIQUID-LIQUID DISPERSIONS: PROPAGATION DELAY TIME - HOLD-UP - TEMPERATURE CORRELATIONS

Ribeiro, M.M.M. (*), Gongalves, C. Regueiras, P. F. (**), Guimaraes M.M.L. (*), Cruz Pinto, J.J.C. (***)

* Dep. Engenharia Quimica, Instituto Superior de Engenharia do Porto, Porto, Portugal.
** Faculdade de Engenharia, Universidade do Porto, Porto, Portugal
*** CICECO/Dep. Quimica, Universidade de Aveiro, Aveiro, Portugal

ABSTRACT

In this work, the use of the ultrasonic technique was shown to enable precise measurements of the dispersed phase hold-up in liquid-liquid dispersions. Correlations of travel-time *vs.* temperature for hold ups from 5% to 40% were established, and a general correlation was also obtained for travel-time *vs.* temperature and hold-up, which may be used as a calibration equation.

Keywords: liquid-liquid dispersions, dispersed phase hold-up, ultrasound

INTRODUCTION

The use of the ultrasonic technique allows the evaluation of the dispersed phase hold-up in liquid-liquid systems by measuring the sound propagation velocity in dispersions and emulsions. This technique uses the difference between the sound velocities in the organic and aqueous phases to evaluate the dispersed phase fraction (hold-up). The experimental results yield the dependence of the sound velocity on the hold-up, by comparing the travel time through the dispersion with that through the pure phases.

Among the pioneering studies in this field, the one by Havlicek and Sovova's [1] should be particularly mentioned, because the technique was tested with four different physical systems typically used in liquid-liquid extraction processes. Their experiments showed the dependence of the ultrasound velocity on the hold-up and its independence on the size of the droplets forming the dispersion. The experiments contemplated the temperature-dependence of the ultrasound velocity in single-phase liquids.

The ultrasonic technique developed by Bonnet and Tavlarides [2] allowed the measurement of dispersed phase hold-up by a non-invasive method. Their technique estimated the hold-up exclusively from the ultrasonic waves' time-delays across the dispersion and across each one of the pure phases, thus obtaining estimate errors in the neighbourhood of 27%.

Later, Jongheop Yi and Tavlarides [3] proposed a modification of this model, in which the effects of spherical and polydispersed drops on the path length of ultrasound wave

transmission are considered, together with the physical properties of both phases. Their experimental results showed that the true hold-up could be predicted with a relative error of up to 7.7%, although their experiments were performed with moderate to high hold-up values.

Tsouris and Tavlarides [4] applied the latter technique (using the ultrasound travel-time through the liquid dispersion to estimate the volume fraction) to low dispersed phase fractions and for long path lengths. They obtained good results for volume fractions higher than 5% when using a linear model that considers sound reflection and refraction at the drop - continuous phase interface. However, for volume fractions lower than 5% an empirical model was applied.

Recently, Gon?alves *et al* [5] have clearly demonstrated the applicability of a feasible non-invasive technique to the accurate measurement of the hold-up, even for low hold-up values. In the present work, this technique was used in transmission mode and different types of time-travel estimates were tested, in order to circumvent the difficulties associated with multi-echo signals, which are particularly serious at high hold-ups. Then, the preferred travel-time estimate (t_2s) was correlated with temperature.

EXPERIMENTAL SETUP AND MEASUREMENT TECHNIQUE

The liquid-liquid system used for our experiments consists of toluene as the dispersed phase, and distilled water as the continuous phase. The phases were previously equilibrated by mutual contact in the same mixing apparatus depicted in Figure 1 together with the whole of the equipment.

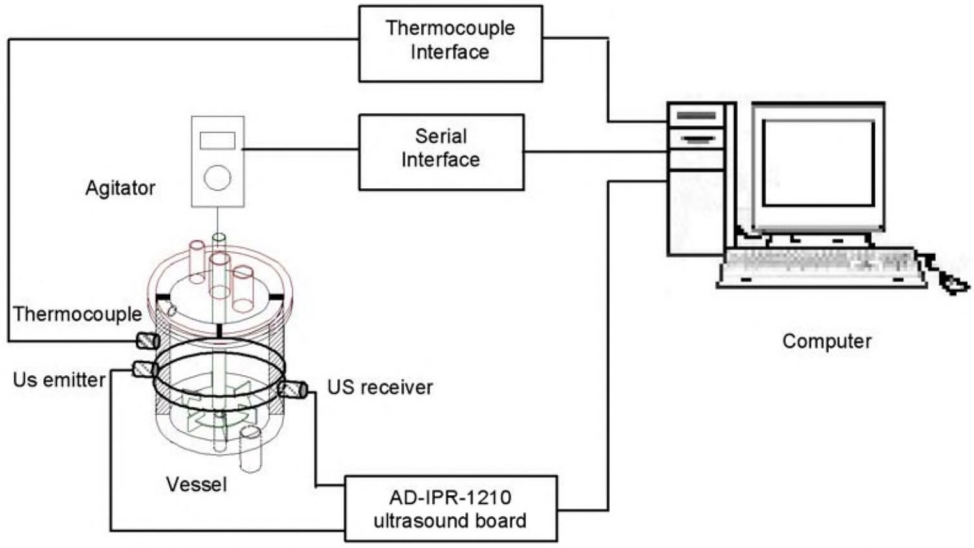


Figure 1 - Schematics of the mixer vessel and data acquisition equipment.

A glass vessel (20 cm diameter by 20 cm height) with a flat bottom and four baffles was used. A standard Rushton turbine of 0.1 m diameter (1/2 of vessel diameter) placed at 1/3 of the height from the bottom of the vessel provided the agitation (as used in Ribeiro *et al* [6]).

Ultrasound transducers with a 1 MHz central frequency were used, mounted outside the vessel in a diametrically opposite (transmission) configuration. Two contact thermocouple probes were placed on the outside surface of the vessel to measure the temperature in a continuous and non-invasive way.

A computer program was used to control and collect data from the ultrasound board, the stirrer and the pair of thermocouples. With this program, we were able to control the ultrasound board by (1) setting the energy and duration of the electric pulse to be applied to the emitter transducer, (2) setting the start time, rate and duration of the received signal sampling, and (3) setting a broad time interval to visualize the received signal.
Based on preliminary work designed and performed to minimize the noise signal for a large range of hold-ups, the electric pulse parameters were fixed at the following values (1) Voltage - 300 V, (2) High-pass filter - 0.5 MHz, (3) Low-pass filter - 2.5 MHz, (4) Energy - 820 pF.

The program also implements automatic gain control of the input amplifier, as well as the capability to execute, without operator intervention, a series of measurements if the number and the time interval between them is previously defined. The travel time of the ultrasound pulse is then calculated, based on the signal received by means of a pre-defined narrower time window. Using this program, we can also set the stirrer speed and read the actual values of agitation speed and torque, as well as the temperature measured by one to eight thermocouples. All data collected can be saved on a file, for off-line processing.

PROCEDURE

Due to the signal dispersion, a plausible travel time can be calculated in different ways. The objective is to choose the travel-time definition that fits better the entire working range of hold-up values. In this work the following travel-time definitions were tested:

(1) $t_C E$: energy centre, resulting from signal integration along 20 ps,
(2) $t_2 5\%$: 25% of the maximum amplitude of the signal envelope,
(3) $t_{33\%}$: 33% of the maximum amplitude of the signal envelope,
(4) t5o%: 50% of the maximum amplitude of the signal envelope.

The experiments were performed and the different travel-times and fluid temperatures were recorded. The fluid temperature was measured at several time intervals with a glass thermometer immersed just before each series of measurements. The temperatures given by the contact probes (T_0 and T-i) were recorded automatically by the acquisition software for future correlation of the external surface temperature with the fluid temperature.

This routine was repeated for different vessel contents (saturated single phases, and dispersions with 10%, 20%, 30%, and 40% hold-up fractions).

RESULTS

Figure 2 shows the relation between the various travel-times and temperature for water saturated with toluene and for toluene saturated with water. As may be seen in the two upper figures, an inverse variation of travel time with temperature is obtained, while for toluene a direct proportionality is found. The great differences that result between the travel-time values for the energy centre and the signals for 25, 30 and 50% of the maximum amplitude of the signal envelope is easily justified by the long right queue exhibited by the signal.

For each type and level of vessel contents (saturated single phases, and dispersions with 10%, 20%, 30%, and 40% hold-up fractions), the correlations of the different travel times *vs.* temperature were studied, and the standard deviations between the experimental and correlated values are shown in Table 1.

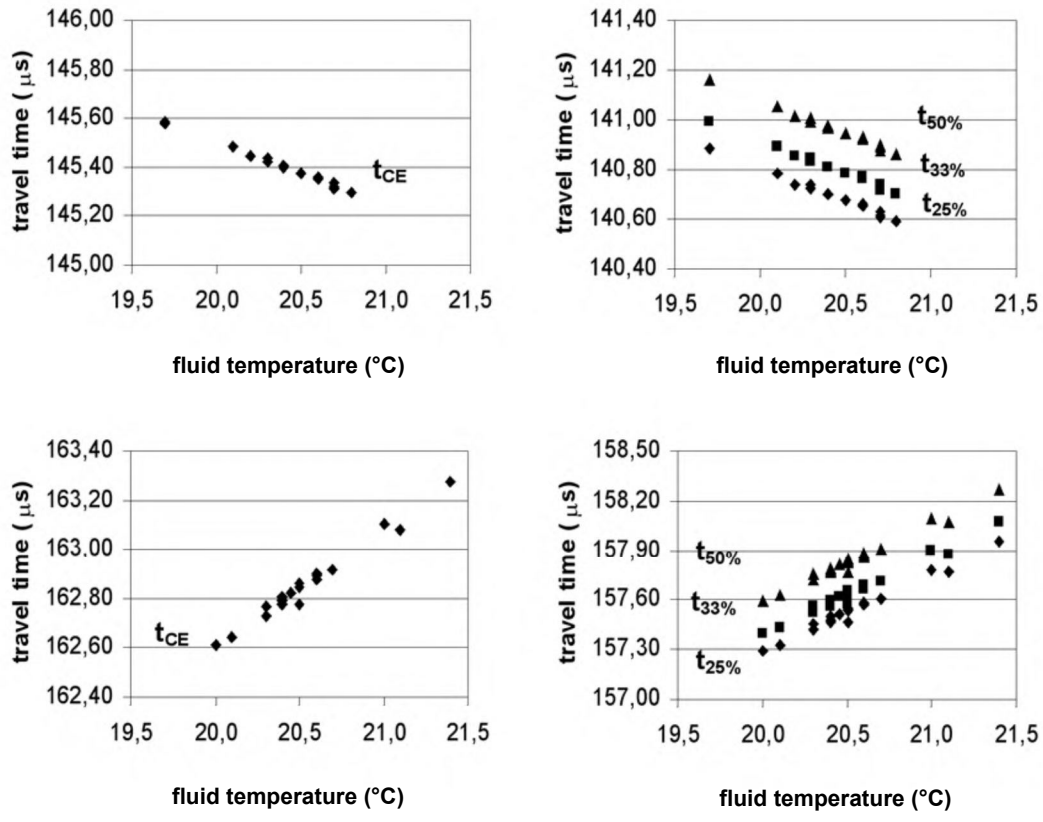


Figure 2 - Variation of the different travel-times with temperature for water saturated with toluene (top) and for toluene saturated with water (bottom).

Table 1 - Standard deviation of the differences between experimental and correlated values

		tcE	t25%	t33%	t50%
Saturated Water		0,0033	0,0047	0,0054	0,0041
Hold-up	10%	0,0158	0,0114	0,0133	0,0123
	20%	0,0090	0,0067	0,0050	0,0056
	30%	0,0114	0,0095	0,0132	0,0174
	40%	0,0254	0,0045	0,0096	0,0048
Saturated Toluene		0,0134	0,0126	0,0128	0,0127

As may be seen in this table although the standard deviations for t_2s%, t33% and t_{50}% are very similar, the correlation of t_{25}% is the one that better fits the experimental data for the whole range of vessel hold-ups (least standard deviation). It seems adequate to point out that the largest standard deviation occurs for tcE at 40% of dispersed phase hold-up. The travel time based on the energy centre fits quite well for low hold-ups (up to 10%); however, for higher hold-ups, the received ultrasonic signal is strongly spread on time and, consequently, t_CE is affected by this fact. Calculating the travel-time based on the wave front, namely at t_2s%, is thus more independent of this signal spreading.

Therefore, Figure 3 shows the correlations and experimental data of travel time $t_2$5o$_{//(}$,with the temperature for the different vessel hold-up and the corresponding equations are given in Table 2.

Table 2 - Correlations for time travel as a function of temperature

		Correlation
Saturated Water		*25°/ =' 0,2641a? +146,09
Hold-up	10%	*25% =-°-1516^ +145,81
	20%	'25% =-°.°412^ +145,6
	30%	'25% =0'0372^ +145,85
	40%	'25% = °'1328 ® +145,71
Saturated Toluene		'25% = 0,472515 +147 84

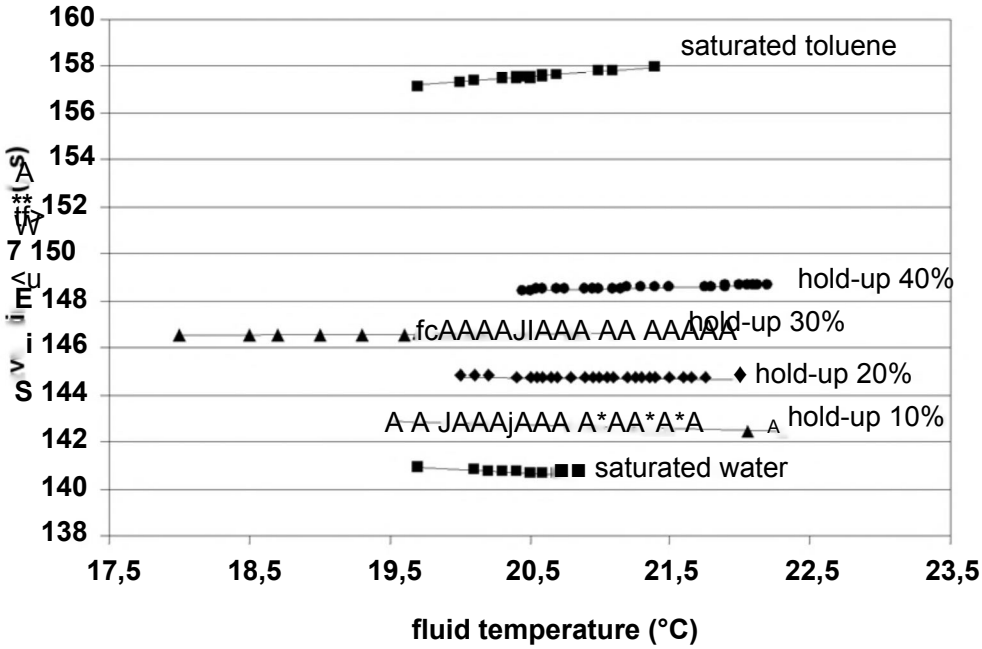


Figure 3 - Variation of the travel time (t_2s%) with temperature for different vessel contents.

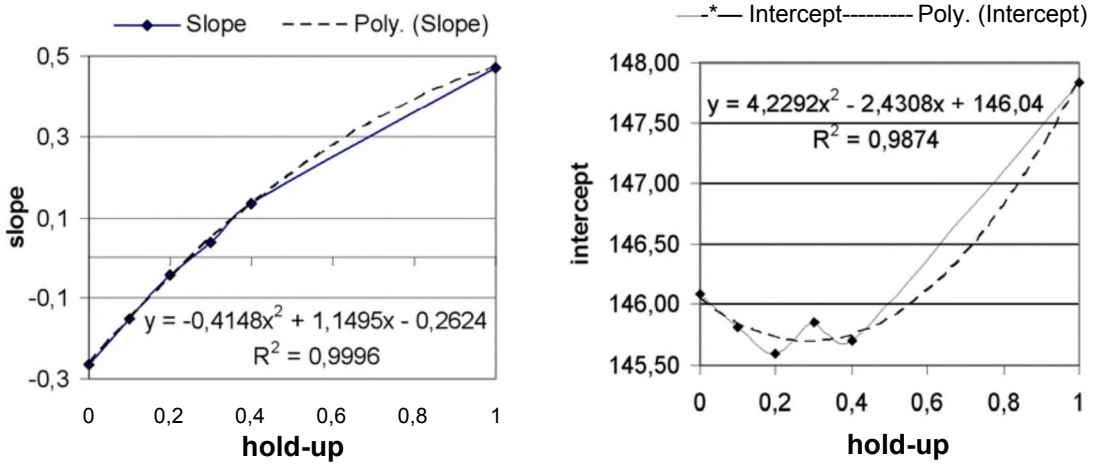


Figure 4 — Regressions of the slope and intercept with dispersed phase hold-up

As previously mentioned, the slope of the regression line has opposite signs for the two saturated phases. Consequently, for low hold-ups, the water effect predominates and the slope is negative. At 20% hold-up the temperature influence is the lowest and exhibits positive slope for high hold-ups.

Although with different slope and intercept values, these linear regressions always offer excellent fit. Thus, further correlations for slope and intercept as functions of the hold-up were obtained (Figure 4), which gives a useful generalization for the travel time dependence on temperature (T) and hold-up (0):

$$125\% = (-0.4148\ xO^2 + 1.1495x0 - 0.2624)xT + 4.2292\ xO^2 - 2.4308x0 + 146.04$$

CONCLUSIONS

1- A clear dependence of ultrasound travel-time *vs.* temperature in toluene and water pure phases as well as in toluene dispersed in water, has been identified. The dependence is direct in toluene and inverse in water. At low hold-ups, the water behaviour prevails.
2- Due to the scattering of the ultra sound signal, four possible travel-time definitions were studied and t_{25}% was chosen, due to its highest precision (least standard deviation).
3- Correlations of travel-time *vs.* temperature for hold ups from 5% to 40% were established, all of them clearly exhibiting linear dependence, although with different parameter values. A general correlation was easily established for travel-time *vs.* temperature and hold-up, which may be used as a calibration equation.

REFERENCES

1. Havliček A. and Sovová H., (1984). "Measurement of Liquid Hold-Up of the Dispersed Phase by an Ultrasonic method", *Coll Czech. Chem. Commun.,* **Vol. 49,** 378-385.
2. Bonnet J.C. and Tavlarides L.L., (1987). "Ultrasonic Technique for Dispersed-Phase Holdup Measurements", *Ind. Engng. Chem. Res.,* **Vol. 26,** 811-815.
3. Jongheop Y., Tavlarides L. L. (1990). "Model for Hold-Up Measurements in Liquid Dispersions Using an Ultrasonic Technique", *Ind. Engng. Chem. Res.,* **Vol. 29,** No.3, 475-482
4. Tsouris C. and Tavlarides L.L., (1993). "Volume Fraction Measurements of Water in Oil by an Ultrasonic Technique", *Ind. Eng. Chem Res.,* **Vol. 32,** 998-1002.
5. Gongalves, C., Ribeiro, M.M.M., Regueiras, P.F., Guimarães M.M.L., Cruz Pinto, J.J.C. (2004). "A New Implementation of the Ultrasonic Measurement of the Dispersed Phase Hold-Up Fraction in Liquid-Liquid Dispersions" *ISMIP 5 - 5th Inter. Svmposium on Mixina in Industrial Processes* - (oral presentation) June 1-4 Seville, Spain.
6. Ribeiro, M.M.M., Guimarães M.M.L., Madureira, C.M.N., Cruz Pinto, J.J.C. (2004). "Non-lnvasive System and Procedures for the Characterization of Liquid-Liquid Dispersions" *Chemical Engineering Journal,* **Vol. 97,** 173-182.

Acknowledgements:
This work was carried out under the gratefully acknowledged financial supports of the European Community Fund FEDER , IPP F. Apoio à Investigagão - Project P/11/98 and of the CIEA-ISEP.

EXTRACTION ON DIFFERENT SCALES: FROM MOLECULES TO COLUMNS

Andreas Pfennig

Department of Chemical Engineering, Thermal Unit Operations
RWTH Aachen University, Germany
www.tvt.rwth-aachen.de, secretary@tvt.rwth-aachen.de

Molecules determine the behaviour of technical equipment. Thus an approach is presented which links the different size scales ranging from molecular behaviour over that of interfaces and drops to that of technical equipment. It is shown how the knowledge on one size scale can fruitfully lead to more reliable models on the higher size scales. Finally it is shown that this way leads to an excellent prediction of the behaviour of pulsed sieve-tray columns.

INTRODUCTION

The behaviour of separation equipment is a consequence of the molecular interactions in the mixtures to be separated. Between the technical and the molecular scale various intermediate levels can be realized which are shown in Fig. 1. To derive reliable models for the description of technical equipment we seek to base the description on one level on the detailed understanding and modelling on the next lower level. In this way the knowledge on the smaller scales is reflected in the structure of the relations on each higher level. In this way it is possible to obtain models for the technical process which incorporate the relevant insight into the smaller scales and thus are reliable in that sense that extrapolations beyond the region to which the model coefficients were fitted are possible.

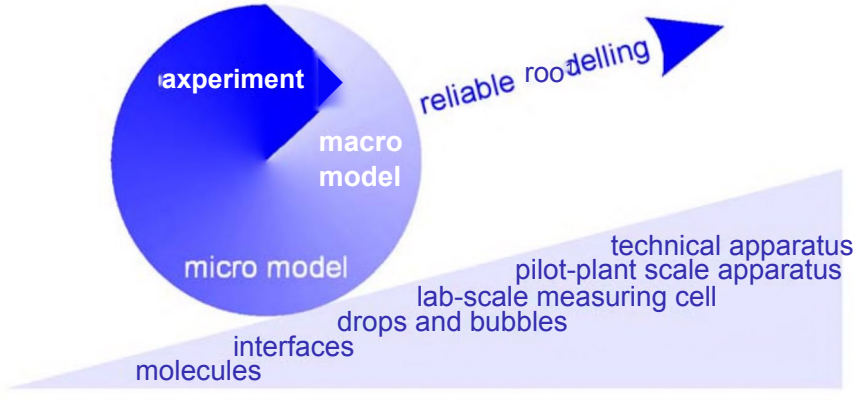


Figure 1: Different levels of size scales to be taken into account in modelling.

That this approach can lead to significant improvement over customary design strategies has been shown e.g. for extraction equipment. As an example for this strategy solvent extraction in a pulsed sieve-tray column has been chosen.

MOLECULAR AND INTERFACIAL LEVEL

If mass transfer takes place across an interface it has been shown that instabilities can occur which result from the specific thermodynamic and diffusive properties of the system. Marangoni convections have been known for a long time. But it was found recently that mass transfer may induce thermodynamic instabilities of the system close to interface [1, 2], These instabilities lead to the formation of nano droplets which behave as individual entities interacting with the major interface. This interaction may lead to different types of instabilities as depicted in Fig. 2. We investigate the stability criterion for the onset of these instabilities as well as the influence of the local convections on mass-transfer rates.

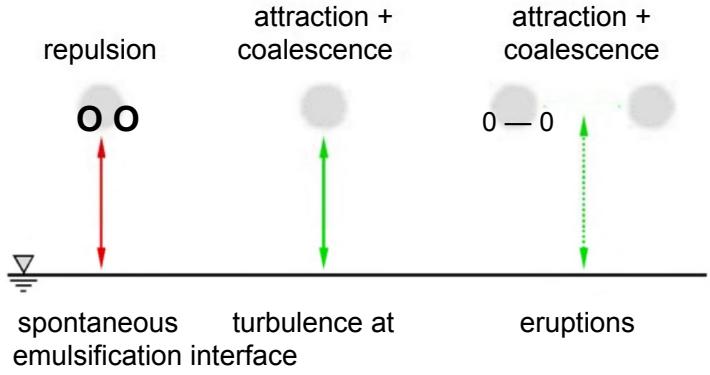


Figure 2: Interaction of nano droplets among each other and with the major interface.

DROP AND LAB-SCALE LEVEL

The finding of these local convections explains the results obtained on the drop level. Here measurements were performed in a lab-scale levitation cell which has been developed in collaboration with Bayer AG [3], The results obtained with this cell are shown in Fig. 3 in comparison with various simulations and models. The experimental data could not be modeled with the model of Kronig and Brink [4], This is astonishing, since their model corresponds to the fastest mass-transfer rate that can be imagined according to conventional concept. The outer mass-transfer resistance has been neglected completely in this calculation and the circulation inside the drops has been assumed to be infinitely fast. Thus the only remaining mass-transfer resistance is the diffusion between the stream lines of this circulation. These calculations have been verified with a CFD simulation where diffusion was depicted by the random motion of discrete particles. Thus an additional mechanism has to improve mass transfer. Such a model is that proposed by Hensche and Pfennig [3] which takes local convections and turbulences into account by an appropriate parameter. This model can represent the experimental data with good accuracy. The reason for this mass-transfer improvement has been found on the molecular and interface level as described above. Also detailed investigations are under way on the drop level where the fluid dynamics inside the drop are investigated by NMR techniques which in turn allow to deduce the behaviour of the interface.

DROP AND LAB-SCALE LEVEL

Based on these investigations on drops and drop swarms the behaviour of an entire solvent extraction column can be modeled. Here various approaches are possible. One is solving the drop-population balances with appropriate mathematical methods. Our approach is rather to solve these equations with a Monte-Carlo type method. This ReDrop model (representative drops) follows a significant number of drops through the solvent-extraction column and moni-

tors their behaviour which is modeled based on the correlations found in the lab-scale measuring cells on sedimentation, mass transfer, splitting, and coalescence. This algorithm is schematically shown in Fig. 4 [5, 6], It turns out that roughly 1000 drops per meter of column are sufficient for significant results. The advantage of this method is that further parameters characterizing the drops like lifetime since last splitting or coalescence event can be included without mathematical difficulty whereas this poses a significant complication in the direct solution of the drop-population balances. Also e.g. reactions in reactive extraction can be modeled with manageable effort.

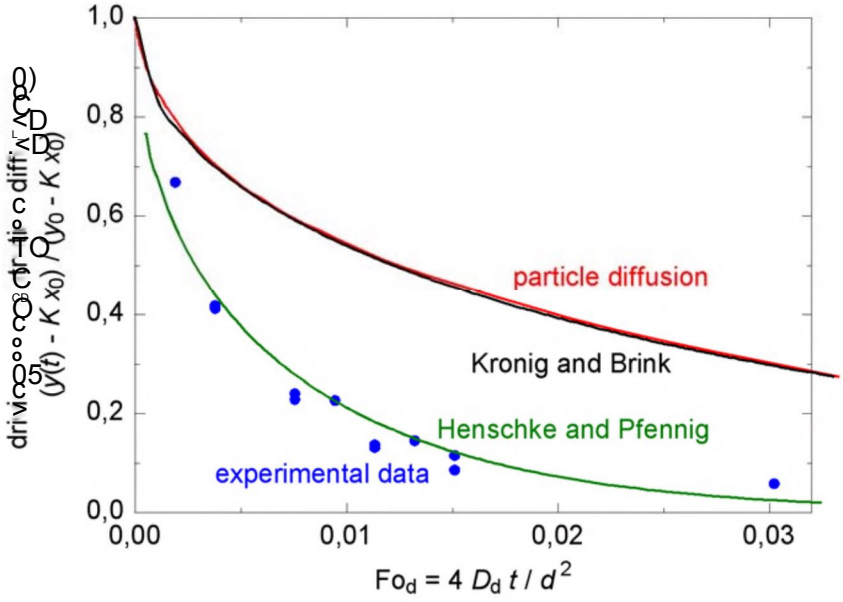


Figure 3: Dimensionless driving concentration difference as function of dimensionless time.

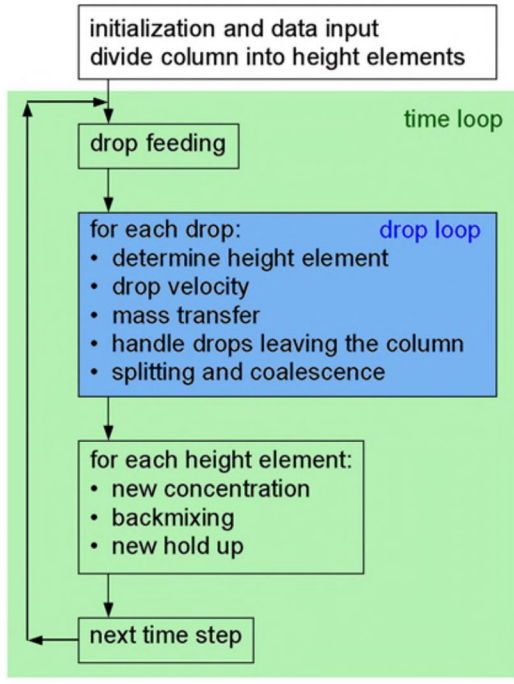


Figure 4: Schematic representation of the ReDrop algorithm.

The ReDrop model has been first used to describe pulsed sieve-tray columns by Henschke [6], Results are shown in Fig. 5 and 6. It can be seen that the efficiency of the extraction column can be modeled with an accuracy of better than 15% which is generally fully sufficient for technical applications. What is surprising is that the flooding can be modeled with high accuracy as well. Thus this kind of modeling is capable of predicting the limits of operability simultaneously. This is a feature few correlation methods show.

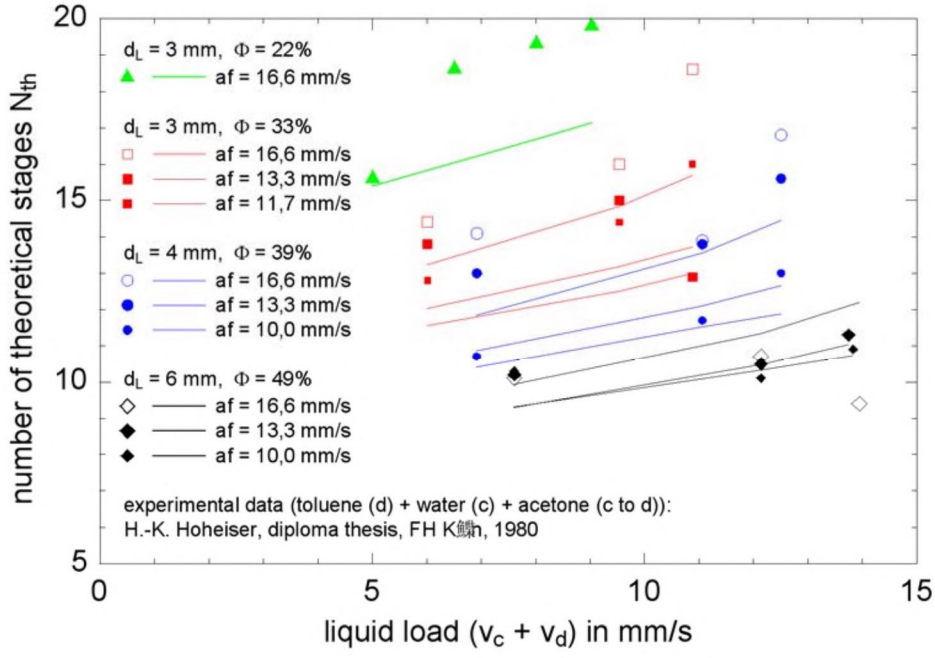


Figure 5: Efficiency of pulsed sieve-tray columns fora variety of geometries and operating conditions.

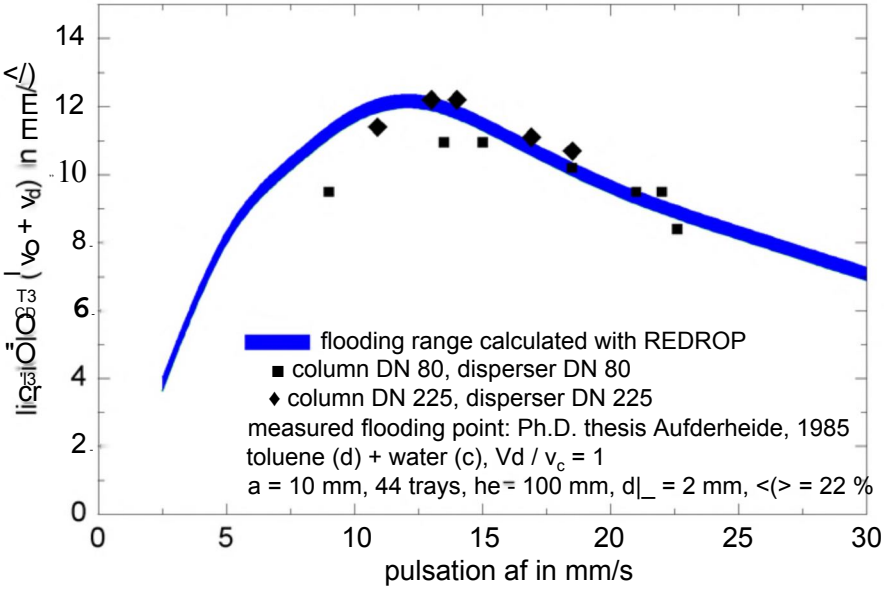


Figure 6: Flooding point of pulsed sieve-tray columns.

This approach is currently followed by joint projects in Germany. The groups collaborating are that of Prof. Dr. H.-J. Bart in Kaiserslautern, that of Prof. Dr. J. Stichlmair in Munich and

our group. The interaction between these groups is shown in Fig. 7. In Munich the interactions between the drops among each other and with the internals are investigated, in Kaiserslautern columns with rotating internals are taken care of an in Aachen pulsed columns are dealt with. As a result of this joint project a reliable simulation tool will be available which is based on models for which the parameters are determined solely from lab-scale experiments and the behaviour of the extraction column is then predicted.

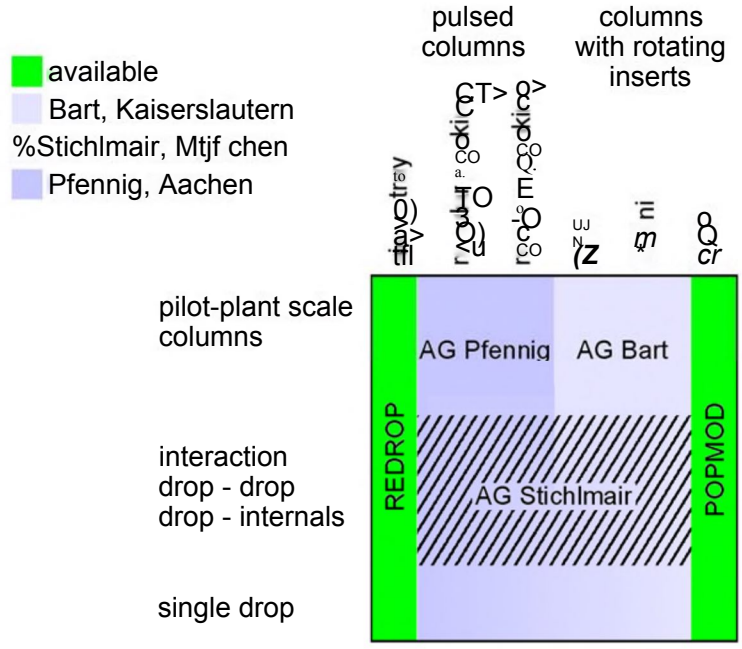


Figure 7: Schematic representation of joint projects.

ACKNOWLEDGEMENTS

This work has been supported in part by the AiF - German Federation of Industrial Cooperative Research Associations "Otto von Guericke" - under contract 40 ZN. Part of this work has been funded by the German Science Foundation.

REFERENCES

1. A. Pfennig: Mass Transfer Across an Interface Induces Formation of Mikro Droplets in Lattice Systems. *Chem. Eng. Sci.* 55(22), 5331-5337 (2000)
2. R. Schott, A. Pfennig: Modelling of mass-transfer induced instabilities at liquid-liquid interfaces based on molecular simulations. Mol. Phys. **102(4),** 331-339 (2004).
3. M. Henschke, A. Pfennig: *Mass-Transfer Enhancement in Single-Drop Extraction Experiments. AIChEJ.* 45(10), 2079-2086 (1999)
4. R. Kronig, J.C. Brink: *On the theory of extraction from falling droplets. Appl. Sci. Res.* **A2,** 142-154 (1950).
5. M. Henschke, A. Pfennig: Simulation of packed extraction columns with the REDROP model. *Proc. 12th International Congress of Chemical and Process Engineering,* Chisa '96, Praha, Czech Republic, ISBN 80-02-01106-6 1130 (1996).
6. M. Henschke: Auslegung pulsierter Siebboden-Extraktionskolonnen. Habilitation, RWTH Aachen University, (2002).
7. E. Aufderheide: Hydrodynamische Untersuchungen an pulsierten Siebbodenextraktionskolonnen. Ph.D. thesis, TU Clausthal, Germany (1985).
8. K.H. Hoheiser, Einflufl der freien Siebfläche auf die Wirksamkeit einer pulsierten Siebbodenextraktionskolonne, diploma thesis, FH Cologne (1980)



PREDICTION OF SEPARATION BEHAVIOUR OF LIQUID-LIQUID DISPERSIONS IN SETTLERS WITH INTERNALS BASED ON SIMPLE SETTLING EXPERIMENTS

Nils Hülswitt*, Andreas Pfennig**

'Filter- und Pumpentechnik, Klaus Hülswitt
Industriegebiet Birten, Bruchweg 18, D-46509 Xanten, Germany
www.FilterUndPumpen.de

"Department of Chemical Engineering, Thermal Unit Operations
RWTH Aachen University, Germany
www.tvt.rwth-aachen.de, secretary@tvt.rwth-aachen.de

Internals lead to a reduction of settler volume by at least a factor of 2. Nevertheless design strategies for horizontal settlers with internals are scarce. Thus a design method was derived which is based on lab-scale settling experiments which are fast and need only a small amount of original two-phase system. This design strategy has been validated with various measurements in this lab-scale cell as well as pilot-plant scale experiments.

INTRODUCTION

It is known that internals in horizontal settlers lead to a reduction of the settler dimension by a factor of at least 2, even 5 in some cases. Simultaneously trace impurities in liquid dispersions strongly influence the settling behaviour. Thus for the design of liquid-liquid settlers experiments with the original two-phase system are required. The goal of this work was to develop a reliable method for the design of horizontal liquid-liquid settlers with internals which is based on lab-scale experiments. The basis for the design method was the standard settling experiment for settlers without internals designed by Henschke [1, 2] who also proposed a corresponding model for its description. A variety of results from related project form the basis of this extension of the simple and reliable design strategy [3, 4, 5],

LAB-SCALE SETTLING CELL

The standard lab-scale cell for settlers with internals which was developed is shown in Fig. 1. The two-phase system to be characterized is first filled into the upper vessel which is supplied with a thermostated jacked. Here the two phases are equilibrated by repeated stirring and settling. Temperature stabilization takes roughly half an hour depending on the temperature. Then the actual measurement starts. The stirrer is switched on for 30 s at 800 min^{-1}. Then the stirrer is switched off and at the same moment the time measurement starts. It is observed how long it takes until the dispersion has settled, the settling time without internals $t_{s,without\ internals}$ is determined. Since the coalescence of the very last drops displays a strongly stochastic behaviour, the end of the settling time is characterized by half

of the interface between the clear phases still being occupied by a drop-layer. This value can easily be reproduced with high accuracy. Simultaneously the entire settling experiment is recorded on video which is evaluated later. From the video the settling and the sedimantation curves are determined. From the curves the behaviour of a technical settler without internals can be calculated e.g. with the help of the Henschke model [1, 2] yielding a length of the settler $/_{Si}$without internals required for the settling task.

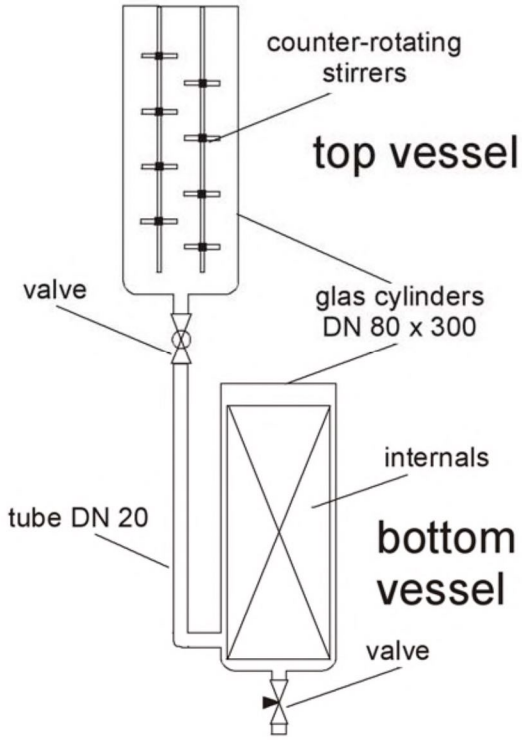


Figure 1. Lab-scale settling cell for measurement with and without internals.

Then the settling experiment with internals is performed. The dispersion is again generate in upper vessel by stirring for 30 s with 800 min'[1]. Then the valve between the two vessels is opened and the dispersion transferred to the lower vessel which contains the internals. It has been verified that this transfer, which takes at most 2 s, does not influence the settling behaviour. The settling is again monitored with a stop watch and recorded on video for detailed evaluation. The settling time $f_{s,}$with internals ''s obtained from this experiment. The observation of this settling time may be difficult, depending on how translucent the internals are. If e.g. a stainless-steel random packing is used only the dispersion at the outer glass wall can be observed. Also the evaluation of the video may become difficult. It turned out though that the settling time could be measured directly in the experiment with a stop watch for all internals used in the project.

The systems investigated were cyclohexanone + water, toluene + water, tridecanol + water and butanol + NaCI + water. In the latter system the settling time can be adjusted in a wide range by appropriate choice of the salt concentration. The concentration was chosen to be roughly 4-10'[2] g_{NaC}i/lH2o which result in a settling time of 170 s, whereas the settling time without salt addition is around 35 s.

Each experiment was repeated at least three times and the settling times obtained averaged. Generally the individual settling times for one system and phase ratio did not vary significantly. The phase ratio was varied for the systems investigated. Performing these experiments with a given system for all interesting phase ratios takes roughly one day

including the preparation and cleaning the settling cells. The evaluation of the videos together with evaluation based on the Henschke model [1, 2] takes between half a day and an entire day depending on the number of videos evaluated.

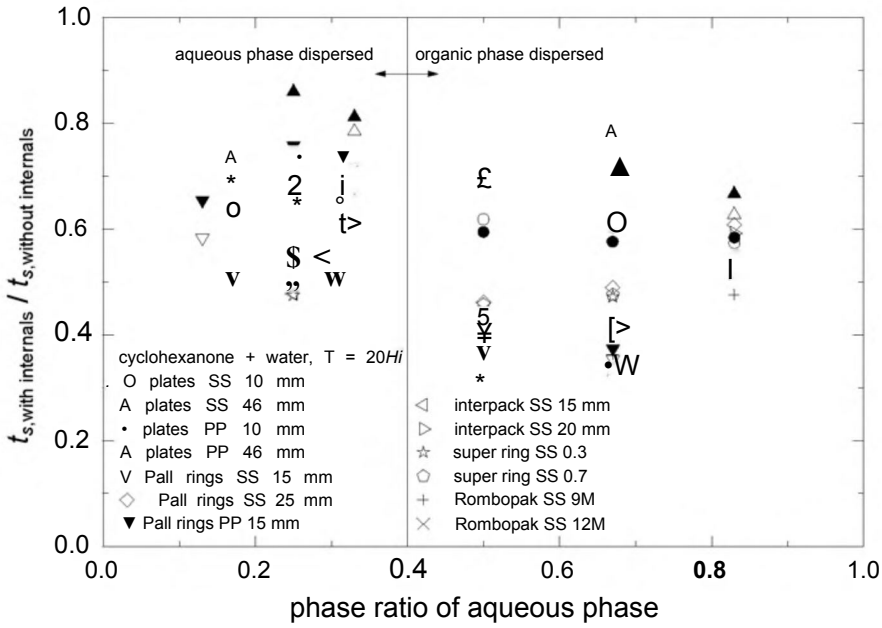


Figure 2. Relative settling time fora variety of internals (PP - poly propylene, SS - stainless steel).

PILOT-PLANT SETTLING EXPERIMENTS

In a pilot-plant scale settling equipment the settling length was investigated simultaneously. The equipment is described in detail in [3, 4], It contains two settler with 200 mm diameter of which one is equipped with internals while the second is left empty for reference. This way both settlers can be run without opening the equipment, since opening of the equipment might introduce trace impurities which effect the settling behaviour significantly. The settling length was determined in both settlers for a variety of systems, phase ratios and volume flow rates.

RESULTS

It turned out that the following relation holds for a wide range of conditions:

$$\frac{\text{^s,with internals}}{\text{^s,without internals}} = K \frac{\text{^s,with internals}}{\text{^.without internals}}$$

is unity, if the internals are inclined horizontal plates and roughly 0.5 for random packings. This difference is due to the different flow behaviour in the different internals. The flow of the dispersion is not hindered between the horizontal plates. Thus the behaviour in the settler with plates can be regarded as being directly related to the phenomena in the lab-scale settling experiments. As the dispersion flows through the settler the behaviour is the comparable to that occurring in the lab-scale settling experiment. The spatial resolution in the settler directly corresponds to the time resolution in the settling experiment. The comparison is shown in Fig. 3.

If there is a difference in the interaction with the internals between the homogeneous phases and the close packed band of dispersion floating on the major interface, is reduced. For the packings investigated was found to be 0.5. This indicates that the close-packed dispersion is held back in the settler with packings relative to the homogeneous phases more strongly by a factor of roughly two as compared to the settler with horizontal plates.

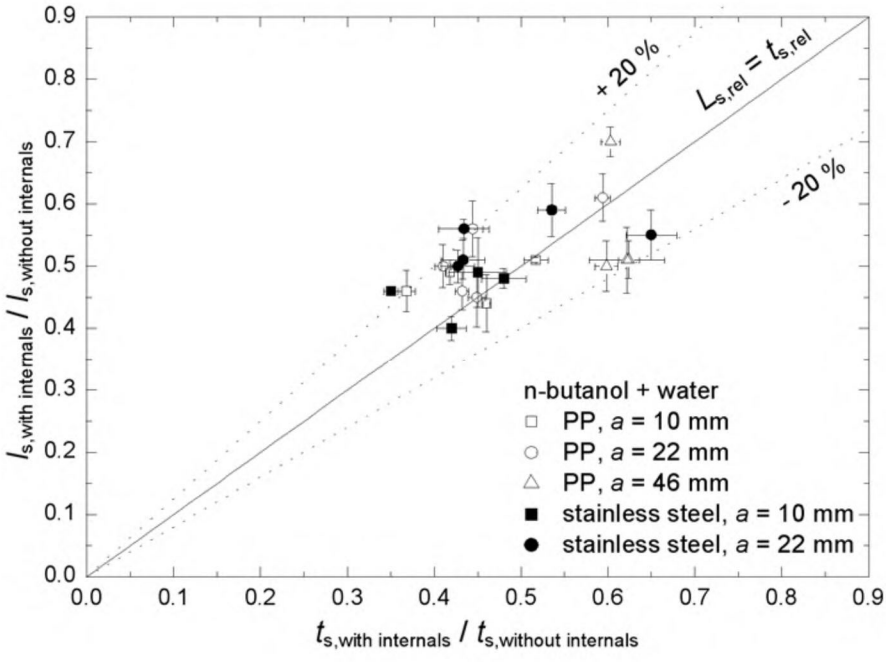


Figure 3. Short-cut method for design of settlers with internals.

CONCLUSION

The design method presented is a short-cut method for the design of horizontal settlers with internals. First lab-scale settling experiments are performed without internals. The settling curves obtained are evaluated with the model of Henschke [1, 2], This description is then used to predict the behaviour of the technical settler without internals. Then the lab-scale experiments are performed to characterize the influence of the internals. The reduction factor is then transferred to the settler behaviour. A value of unity for is used, if the internals do not hinder the flow of the close-packed dispersion. This constitutes a conservative estimate of the settler design. If the internals have a strong influence on the flow of dispersion, =
0.5 can be used. This factor has been found for random packings. In the future this coefficient will be determined for a variety of other common internals.

ACKNOWLEDGEMENTS

This project (AiF-FV-Nr. 12962 N/1) was funded by the Federal Ministry of Economics and Labour via the German Federation of Industrial Cooperative Research Associations "Otto von Guericke". We also thank the members of the steering committee, namely Dr.-Ing. E. Aufderheide, Dipl.-Ing. W. Bäcker, Dr.-Ing. M. Chatterjee, Dr.-Ing. P. Deckert, Dr.-Ing. G. Müller, Dr.-Ing. M. Weber.

REFERENCES

1. M. Henschke: Dimensionierung liegender Flussig-Flussig-Abscheider anhand diskontinuierlicher Absetzversuche. Fortschritt-Berichte VDI, Ser. 3, No. 379, VDI-Verlag, Düsseldorf (1995).
2. M. Henschke, L. Schlieper, A. Pfennig: *Determination of a coalescence parameter from batch-settling experiments. Chem. Eng. J.* 85, 369-378 (2002).
3. MR. Chatterjee: Dimensionierung liegender Flussig-Flussig-Abscheider mit Platteneinbauten. Fortschritt-Berichte VDI, Ser. 3, No. 558, VDI-Verlag, Düsseldorf (1998).
4. L. Schlieper: Trennung von Flüssig-Flüssig-Dispersionen in liegenden Abscheidern mit Platteneinbauten. Fortschritt-Berichte VDI, Ser. 3, No. 700, VDI-Verlag, Düsseldorf (2001)
5. N. Hulswitt, A. Pfennig: Dimensionierung liegender Flüssig-Flüssig-Abscheider mit Einbauten auf der Basis von Laborversuchen. AiF-Abschlu&bericht, Lehrstuhl für Thermische Verfahrenstechnik, RWTH Aachen University (2004).

PERFORMANCE OF A PERFORATED ROTATING DISC CONTACTOR IN THE DEACIDIFICATION OF RICE BRAN OIL: II. THE INFLUENCE OF THE MINOR COMPOUNDS IN THE FREE FATTY ACID MASS TRANSFER

Christianne Elisabete da Costa Rodrigues[1], Cintia Bernardo Gongalves[2] and Antonio José de Almeida Meirelles[3]

Universidade Estadual de Campinas (UNICAMP), Faculdade de Engenharia de Alimentos, Laboratório de Separagões Fisicas, Campinas, SP, Brazil
e-mail: [1]chrisc@fea.unicamp.br, [2]cintiabg@fea.unicamp.br, [3]tomze@fea.unicamp.br

The deacidification of rice bran oil by continuous liquid-liquid extraction, using as solvent ethanol containing approximately 6 mass % of water, was investigated in a rotating disc column (PRDC). The influence of the presence of acylglycerols and minor compounds in the free fatty acids mass transfer was observed. The experimental results obtained proved that the total deacidification by solvent extraction is feasible presenting low level of neutral oil loss.

INTRODUCTION

Rice bran oil presents functional and nutraceutical properties that provide several unique food applications. These properties are associated with the high level of unsaponifiable matter presented in the oil that contains natural antioxidants such as vitamin E and y-oryzanol [1], Notwithstanding, the rice bran oil world production is very low due to some difficulties in processing. The high level of free fatty acids, induced by intensive enzymatic activity, makes difficult the deacidification by alkali or physical refining [2], These traditional processes cause high losses of neutral oil, high-energy consumption and losses of nutraceutical compounds [2,3]

An alternative refining process, performed under more mild conditions (room temperature and atmospheric pressure) is the deacidification by liquid-liquid extraction. This process is based on the difference of polarity between triacylglycerols, the principal component of the oil, and the solvent, ethanol, which guarantees the formation of two phases and permits the removal of free fatty acids [4], Deacidification by liquid-liquid extraction may produce vegetable oils with low acidic levels and simultaneously can minimize the loss of neutral oil and nutraceutical compounds. Some researchers report the decreasing of the rice bran oil acidic value [5,6] using this approach with several solvents such as isopropanol and methanol.

To make possible the use of liquid-liquid extraction as a substitute of chemical deacidification or steam distillation, the study of performance of equipment, hydrodynamic behaviour and mass transfer phenomena, are required. With this purpose, this paper presents an

investigation about mass transfer in a perforated rotating disc column (PRDC) for the rice bran oil deacidification process. The influence of the presence of partial acylglycerols and phosphorus in the free fatty acid mass transfer was evaluated. The experimental results obtained proved that the total deacidification by solvent extraction is feasible. The loss of neutral oil was significantly lower than the results reported in the literature for alkali or physical refining of rice bran oil.

EXPERIMENTAL APPARATUS

The perforated rotating disc contactor (PRDC) was made of glass, jacketed, presenting 50 mm internal diameter, 1300 mm column height and 1000 mm extraction zone height. Perforated discs (total of 33, with 47 mm diameter, drilled with holes of 3 mm diameter presenting 20 % of flow free area) were placed at constant spacing distances (25 mm) in the column. They were mounted on a central shaft, which was rotated at different velocities (50 to 300 rpm). A schematic drawing of the PRDC used in this work is shown elsewhere [7], The apparatus was maintained at (298 ± 1) K and local atmospheric pressure (727 mmHg). The equipment was feed with the continuous phase (ethanol food grade containing approximately 6 mass % of water) through the bottom of the column and its flow rate was maintained at the desired constant value. The rotor was started and the rotating speed was measured by a digital tachometer 1726 (Ametek, Largo, FL). The dispersed oil phase was feed to the top of the column with flow rate maintained at the desired value. Both phases were pumped into the column by peristaltic pumps (Cole Parmer, Chicago, IL).

For the mass transfer experiments the operational variables were rotor speed (50-300 rpm), phase ratio (*VdA/c* = 0.70 to 1.19 - where *Vd* and *Vc* are the superficial velocity of the dispersed and continuous phases, respectively. These values are very close to a mass ratio oil to solvent 0:S=1), and fatty acid content in the oil feed stream (5.5 to 11.7 mass %). Inside the column, steady state was achieved after approximately 120 min of continuous operation. This was verified by the constant position of the interface level at the bottom of the equipment. After achieved the steady state five samples of outlet phases, extract and raffinate, were taken (every 15 minutes) and analysed to determine the alcohol, water, and acid concentrations of each phase.

MATERIAL AND METHODS

To evaluate the influence of the fatty raw material kind in the volumetric mass transfer values three kinds of rice bran oils were used, refined oil (RBOr) with addition of acidity, crude (RBOc) and degummed (RBOd) oils. Refined rice bran oil (Blue Ville) was purchased from Santalúcia, Brazil, and crude and degummed rice bran oils were kindly supplied by Helmut Tessmann, Brazil. The fatty acid source used in the experiments with refined oil was a commercial oleic acid (Merck, Germany). The solvent used in all experimental runs was neutral aqueous ethanol, food grade, purchased from Usina Ester, Brazil.

All fatty reagents used in this work were analysed by gas chromatography of fatty acid methyl esters according to official method 1-62 of the American Oil Chemists' Society (AOCS) [8] to determine the fatty acid composition. The fatty samples were prepared in the form of fatty acid methyl esters according to the official method (2-66) of the AOCS [8], A HP5890 gas chromatograph with a flame ionisation detector was used under the following experimental conditions: fuse silica column of cyanopropylsiloxane 0.25 mm, 60 m x 0.32 mm id; hydrogen as the carrier gas at a rate of 2.5 ml/min; injection temperature of 548.2 K;

column temperature of 448.2 - 498.2 K (rate of 1.3 K/min); detection temperature of 578.2 K. The FAMEs were identified by comparison with external standards purchased from Nu Check Inc. (Elysian, IL). The quantification was accomplished by internal normalization.

In addition, the fatty samples were characterized in terms of concentration of phosphorus (colorimetric method AOCS Ca 12-55); mono-, di-, triacylglycerols and polymerized triacylglycerols by gel permeation HPLC (AOCS Cd 22-91; HPLC system Perkin Elmer model 250, refractive index detector Sicon Analytic, columns Jordi Gel DVB 300 mm x 7.8 mm id, 0.01 and 0.05 mm, mobile phase tetrahydrofurane, sample solution 1% (w/v) in tetrahydrofurane). For all experiments the concentration of free fatty acids was determined by titration [9] with an automatic burette (Metrohm, model Dosimat 715). The total solvent concentration was determined by evaporation at 338.15 K in a vacuum oven (Napco, model 5831). The water concentration was determined by Karl Fischer titration, according to AOCS method Ca 23-55 [8], with a KF Titrino (Metrohm, model 701). In this work all measurements were performed at least in triplicate. Table 1 summarizes the experimental runs accomplished.

Table 1. Experiments Description

Oil	Acidity in the Feed (mass %)	Rotor Speed (rpm)	Phase ratio vyv_c	Experiment number	K_ra-10 [kg fatty acids / m^3s(kg fatty acids /kg oil phase)l
RBOr	5.53	150	0.70	1	4.60
		200		2	4.69
		250		3	4.75
		300		4	5.04
	6.42	50	1.18	5	2.64
		150		6	4.67
	11.67	200	1.19	7	5.15
RBOc	7.66	200	0.82	8	3.93
RBOd	8.52	150	0.81	9	3.52

RESULTS AND DISCUSSION

In order to evaluate the deacidification experiments, the volumetric overall mass transfer coefficients for the fatty acids were estimated based on the units of concentration of dispersed phase. The calculation of an overall coefficient applicable to entire column requires that the film coefficients for each phase be approximately constant and that the equilibrium curve be a straight line [10], Both approximations are valid in the present case. It should be further considered that the effect of axial mixing and the influence of the mass transfer of other compounds were not taken into account, so that the calculated values should be better considered as apparent overall coefficients. Despite this fact, the obtained results can undoubtedly help in the design of liquid-liquid extractors for edible oil deacidification.

The equilibrium curve was obtained from equilibrium data determined according to the procedure described by [11] for the rice bran oil / commercial oleic acid / ethanol / water system. The equilibrium curve is a straight line with a correlation coefficient of 0.9998 for a fatty acid concentration range of 0 to 25 mass %. This line is given by equation:

$$w'_{E2} = 0.9462 w'_{R2} \quad (1)$$

where w'_{E2} and w'_{R2} are the concentration of fatty acids in the extract and raffinate phases, respectively. These concentrations were the mass fractions on a fatty acid-free basis, calculated using the following equation:

$$w'_2 = \frac{w_2}{1 - W_2} \quad (2)$$

where w_2 is the mass fraction of fatty acids in each phase. The overall mass transfer coefficients can be calculated using equation 3:

$$R'(2-w^*,2) = K_R a V A V_{R2M} \quad (3)$$

where R' is the dispersed phase mass flow on a fatty acid free-basis in kg/s; w'_{F2} and w'_{R2} are the fatty acid concentrations in the feed and raffinate streams, respectively; K_R is the overall mass transfer coefficient in Kg fatty acids/[m^2.s.(kg fatty acids/ kg oil phase)]; a is the mass transfer area per unit of extraction zone volume in m^2/m^3; V is the volume of extraction zone in m^3; and Aw'_{R2M} is the logarithmic average of the concentration differences at the ends of the column based on the units of the concentration of the oil phase. Aw'_{R2M} was calculated by taking into account the equilibrium concentrations given by equation 1 [11], In the evaluation of mass transfer coefficients the systems were treated as composed by pseudocomponents as a fatty acid equivalent to commercial oleic acid, in the case of systems with refined rice oil, or a fatty acid equivalent to free fatty acids presented in crude or degummed rice oil, and a triacylglycerol equivalent to rice bran oil, ethanol and water. The volumetric mass transfer coefficients are given in Table 1 above. Their values increased as the rotor speed and the oil phase flow increased, as a consequence of the higher turbulence level in the apparatus.

The values of volumetric mass transfer coefficients of this work are in accordance with the values obtained by Pina and Meirelles [7] for the deacidification of corn oil. The experiments 8 and 9 accomplished with crude and degummed rice oils, respectively, presented the lowest values of volumetric mass transfer coefficients. These results can be a consequence of the presence of high contents of phosphorus in the degummed and crude oils (55.19 and 121.33 ppm, respectively, while for refined rice oil the level of phosphorus quantified was lower than 1 ppm). These compounds cause the formation of an emulsion between oil and solvent that difficults the Dhase seoaration at the bottom of the column as shown bv the hiah content of solvent in the raffinate stream (22.56 mass % for experiment 8 and 13.19 mass % for experiment 9). For all the others experiments the content of solvent in the raffinate stream is not higher than 11 mass %, a value that is in accordance with the solubility of aqueous ethanol in oil which varies from 8 to 11 mass % as the fatty acid content changes from 0 to 10 mass % [11],

Figure 1 shows a linear dependence of the solvent content in the raffinate stream in relation to the phosphorus content in the oil. In addition, it can be seen that the content of solvent in the raffinate stream is not influenced by the discs rotating speed. In the other hand the solvent content increases with the increasing of the continuous phase velocity and the acidity in the oil.

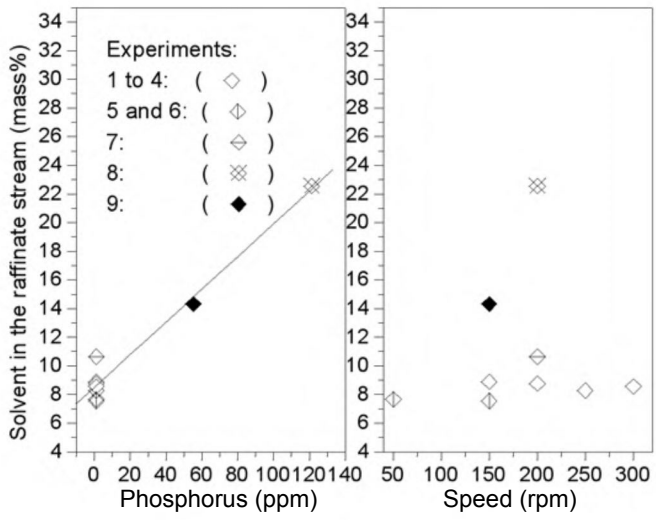


Figure 1. Solvent content in the raffinate stream as function of phosphorus content in the oil and of discs rotating speed

Furthermore, the presence of phospholipids can cause a backflow of continuous phase; in other words, the continuous phase is dragged by dispersed phase diminishing the mass transfer efficiency. The backflow is only one of many effects that compose the axial mixing. This phenomenon reduces the extraction efficiency, and its value, given by the coefficient of axial mixing, increases as the increase of the rotor speed. In this work the influence of the axial mixing in the mass transfer calculations were not taken into account. To include such effect in mass transfer calculations, it would be necessary to accomplish special experiments for measuring the coefficient of axial mixing for each phase.

Table 2 shows the transfers of phosphorus, diacylglycerols and monoacylglycerols during the liquid-liquid extraction process for RBOd, RBOr and RBOc. This evaluation was based on the level of MAG, DAG or phosphorus measured in the extract phase of the refining step. The transfer levels were calculated according to equation 4.

$$T_i = \frac{[E \times w_{fatty,i} \times W_{E,fatty} \times 100]}{F \times w_{FJ}} \quad (4)$$

where /' is MAG, DAG or phosphorus, w_{Fi} is the mass fraction of MAG, DAG or phosphorus in the feed, $w_{E}.r_{a}tty$ is the mass fraction of fatty material in the extract stream and, $w_{fatty}i$ is the mass fraction of MAG, DAG or phosphorus in the fatty material present in the extract stream. In the same way, *F* and *E* are the total mass flow rates of the feed and extract.

Table 2. Transfer of MAG, DAG and phosphorus

	Transfer (%)		
	RBOr[3]	RBOd	RBOc
MAG	5.47	5.97	4.95
DAG	5.39	5.67	4.50
Phosphorus	-	13.21	14.06

[a] experiment number 1

It can be seen in Table 2 that the contents of MAG, DAG and phosphorus on the oils were

reduced during the liquid-liquid extraction process. The transfer of mono (MAG) and diacylglycerols (DAG) were very similar for RBOr, RBOc and RBOd. In the same way, the phosphorus transfer from degummed or crude oils to the alcoholic phase was around 14 %. It can be concluded that raw material characteristics do not influence significantly the extension of phosphorus, MAG and DAG transfers.

From a technological point of view, it is also important to discuss the results of the mass transfer experiments in relation to the total amount of extracted fatty acids (T_2) and the loss of neutral oil in the extract stream (L_f). The values for T_2 and Li were calculated by performing mass balances for both types of fatty compounds. In the case of fatty acids, the following equation can be derived:

$$T_2 = \frac{[(F \times w_{F.2}) - (R \times w_{R.2}) \times 100]}{F \times w_{F,2}} \quad (5)$$

where w_{F2} and w_{R2} are the mass fractions of fatty acids in the feed and raffinate, respectively. In the same way, F and R are the total mass flow rates of the feed and raffinate. Figure 2 shows the values of the total amount of extracted fatty acids (T_2) and the loss of neutral oil in the extract stream (Lj) for the experiments accomplished. The values of T_2 varied in the range of 70 to 90 %. The values increased with increasing rotor speed. The values for L, showed a slightly increasing with increasing of discs speed and varied in the range of 0.80 to 3.13 %.

It should be emphasized that these values for loss of neutral oil are significantly lower than the results reported in the literature for alkali or physical refining of rice bran oil [2], In liquid-liquid extraction, the loss of neutral oil is largely determined by the oil solubility in the solvent. According to the equilibrium data, the oil solubility in aqueous ethanol varies from 2.14 to 3.10 mass % as the fatty acid content changes from 0 to 12 mass % [11], In this case, using an oil/solvent flow ratio of 0.8, the loss of neutral oil due to its solubility in the extract stream must be approximately 3.9 %.

Since all experimental values for the loss of neutral oil were lower than or in the range of the oil solubility in the solvent, it can be concluded that the mechanical entrainment of oil phase droplets by the extract phase was negligible.

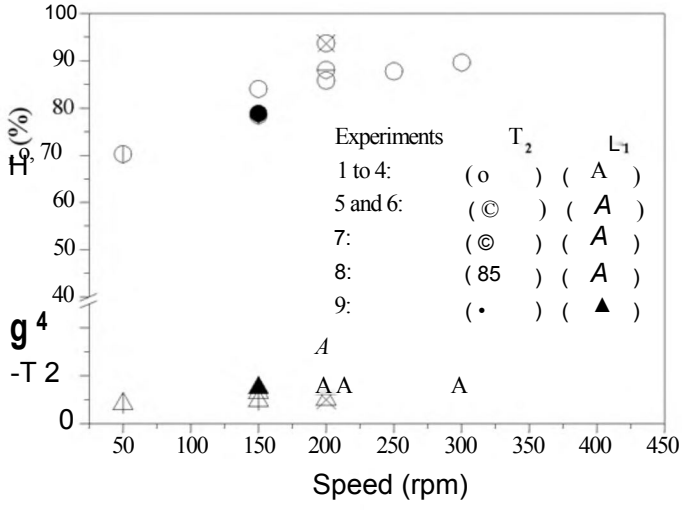


Figure 2. Transfer of free fatty acids and loss of neutral oil as function of discs rotating speed.

CONCLUSIONS

The experimental results of the present work show the feasibility of the total deacidification of edible oils by solvent extraction. The loss of neutral oil was significantly lower than the results reported in the literature for alkali or physical refining of rice bran oil.

ACKNOWLEDGEMENTS

The authors wish to acknowledge FAPESP (Fundagão de Amparo à Pesquisa do Estado de São Paulo - 01/10137-6 and 03/13927-3), CAPES, FINEP and CNPq (Conselho Nacional de Desenvolvimento Cientifico e Tecnológico - 521011/95-7), for the financial support.

REFERENCES

1. Deckere, E. A M.; Korver O. (1996). *Nutr. Rev.,* 54, 120S-126S.
2. Orthoefer, F. T. (1996). *Food Tech.,* 50, 62-64.
3. Krishna, A.G.G.; Khatoon, S.; Shiela, P.M.; Sarmandal, C.V.; Indira, T.N.; Mishra, A. (2001). *J. Am. OilChem. Soc.,* 78, 127-131.
4. Thomopoulos, C. (1971). *Rev. Fran, des Corps Gras,* 18, 143-150.
5. Kim, S., Kim, C., Cheigh, H.; Yoon, S. (1985). *J. Am. Oil Chem. Soc.,* 62, 1492-1495.
6. Kale, V.; Katikaneni, S. P. R., & Cheryan, M. (1999). *J. Am. Oil Chem. Soc.,* 76, 723-727.
7. Pina, C.G.; Meirelles, A.J.A. (2000). *J. Am. Oil Chem Soc.,* 77, 705-712.
8. A.O.C.S. (1988). Official methods and recommended practices of the American Oil Chemists' Society, Press, 3 ed., Champaign, v. 1-2.
9. IUPAC. (1979). 6 th edition, part 1 (sections I and II). PAQUOT, C. editor, Pergamon Press.
10. Treybal, R.E. (1980). Mass Transfer Operations, 3° ed., McGraw Hill Book Co., New York.
11. Rodrigues, C. E. C., Antoniassi, R., Meirelles, A. J. A. (2003). *J. Chem. Eng. Data,* 48, 367-373.

CONCEPTION OF A NEW TYPE OF PULSED COLUMN APPLIED TO SOLID-LIQUID CONTACTING : DESIGN METHODOLOGY BASED ON EXPERIMENTAL STUDY

Léna Brunet, Laurent Prat, Gilbert Casamatta and Philippe Carvin*

Laboratoire de Génie Chimique, Toulouse, France
*Rhodia Recherches, Lyon, France

INTRODUCTION

Pulsed columns are an interesting tool among a wide variety of solid liquid contactors. Its main advantages lean on the continuous functionning, the counter-current mode and the suspension of particles.

However, the operation of these columns remains difficult as they often meet flooding problems, fines driving and too short residence times. In a general way, solid circulation is not well controlled, or is narrowly linked to the liquid flow [1],

When the kinetics of mass transfer or reaction occuring in the column is rather long (above a few minutes), a too short residence time of solid will either be compensated by the conception of a high column, or either by enhancing the liquid flow, which will increase the consumption of solvent and the quantity solid losses because of fines driving.

The perceived benefits of the technology developped here are appropriate for the processing industry which aims to reduce the size of its units and improve control of flows [2],

PROCESS DESCRIPTION

Experiments were performed in an apparatus that is shown in figure 1. The active zone of the column is composed of stacked compartments, which are separated by a filtering cloth and a pneumatic valve. The filtering cloth allows the solvent flow and retains solid particles. The solid suspension is only enabled to circulate through the valve pneumatically controlled. Solids and mother liquid enter continuously at the bottom of the column, whereas the purified suspension overflows at the top through an outlet tube. The washing solvent is injected at the top of the column and flows downwardly.

The column operates on a cycle mode with two sequences :

- A mixing step ; a classic sinusoidal pulsation is used to mix the two phases in each compartment ; the valves are closed and the particles are trapped between two trays while the liquid phase is flowing downwardly on average ; this step is characterized by the amplitude **A** and the frequency **f** of the pulsation which has to be intensive enough to generate high speed vortices, able to drive dense particles. This step is programmed with a timer, during a fixed duration Taxing-

- An impulsion step ; this second step allows for a brief upward flow of high velocity while the valves are opened and the pulsation is still generated. This impulsion is destinated to transport the solid from one compartment to the next. It is characterized by its flow rate $\mathbf{Q_{imp}}$, the duration $\mathbf{T_{imp}}$. The volume injected is written $\mathbf{V_{imp}}$.

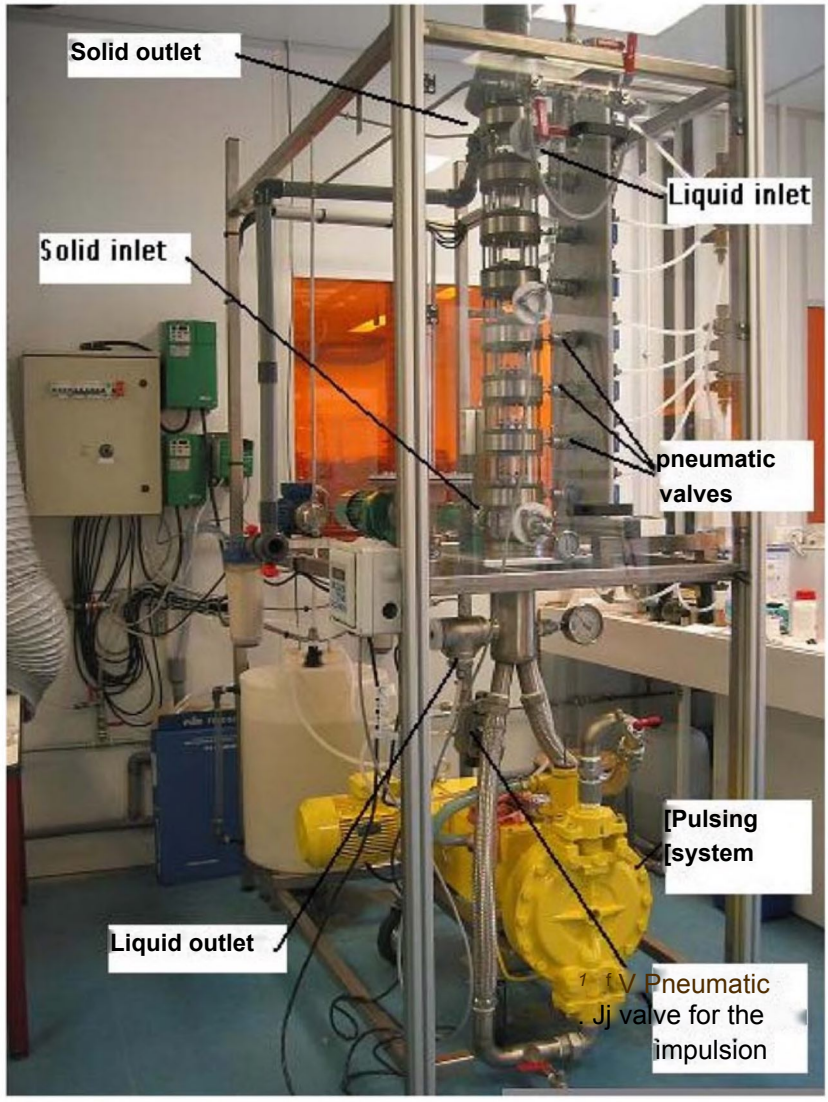


Figure 1 : Process developped

STUDY OF SOLID BEHAVIOUR

Description of experiments

The objective of this study on the solid phase is to determine the pulsation and impulsion parameters leading to a plug-flow transport of the solid. With the device described before, experiments have consisted in introducing a mass of solid in the lowest compartment of the column. The cake thickness is approximately equal to 2 cm in each trial set. Pulsation sets in suspension the particles. Here, the column does not operate on a cycle mode : an upward flow produced continuously has been prefered to characterise the transport of the solid during the impulsion step. The slurry is then recovered continuoulsy at the top of the column

while the valves are permanently opened. Series of samples are finally filtered, dried and weighed.

In the present study, the solid tested was polystyrene powder (p=1050 kg/m^3) distributed in two classes of particles : 200 and 900 pm. At the end of each test, the dried solid is sieved to separate fines and coarse particles.

Various pulsation intensities, duration and flow rate impulsions are tested. The variation ranges are the following :

- Amplitude A : 0.6 - 3 cm
- Frequency f: 0.39 - 1.35 hz
- $Q_{,mp}$: 400 - 700 L/h

Separating particles of different sizes could provide the distinct residence time distributions (RTD) of fines and coarse particles. In order to compare experimental data, each mass of solid is normalized by the total mass of the solid recovered at the outlet. The fraction of outlet solid is a percentage. Then, the solid mean residence time (Ts) and the number of Peclet (Pe) are calculated by the classical momentum method.

Role of pulsation

The absence of oscillations or small oscillations were found to segregate the flow of the bimodal population. For example, a pulsation with A=2.4 cm and f=1Hz superimposed on an unidirectional flow at 400L/h was sufficient to allow a synchronous outlet of particles of all sizes. These oscillatory conditions correspond to an oscillatory flow velocity of 2.4 cm/s, compared to the terminal velocity of coarse particles 1.4 cm/s and fine particles 0.3 cm/s. The fraction of outlet solid is reported in figure 2. On the contrary, at 0.75 Hz and 1.8 cm, the measurement of mass fractions showed that fines particles were transported faster than coarse ones. And it was observed visually that a part of solid, mostly 900 pm, stayed towards the base end of the column. These results are shown on figure 3. At high oscillatory velocities, the pulsation causes the apparition of intense recirculations occupying the whole volume of the compartment, and reducing dead volumes. When the velocity in such vortices is equivalent to several times the terminal velocity, the particles are driven in recirculations, and maintained in suspension. The solid phase form a nearly uniform slurry that will be transported upwardly thanks to the impulsion. These results are in good agreement with the study performed by Mackley et al. who determined that pulsation was a powerful tool to control segragation in closed pulsed columns [3],

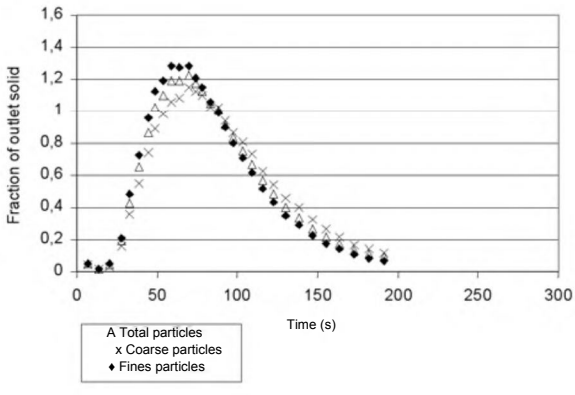


Figure 2 : Fraction of outlet solid in function of time for Q_{imp}=400L/h ; Af= 2,3 cm/s ; V_{imp}=0,771-

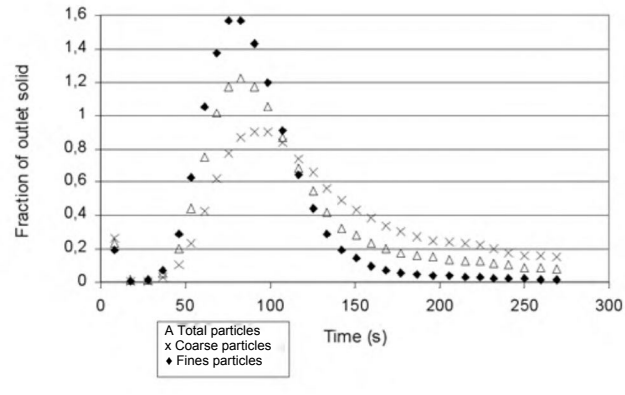


Figure 3 : Fraction of outlet solid in function of time for $Q_{,mp}$=400Uh ; V_{imp}=0,77 L ; with no pulsation

Role of impulsion flow rate

The same kind of behaviour was observed concerning the influence of the impulsion flow rate. The figure 4 shows that the system operates closer to a plug flow for greater upward flowrate. Experiments carried with bimodal populations also demonstrated that granulometric dispersion was reduced for high flowrate (figure 5). Enhancing the unidirectionnal flow destinated to the transport of the solid tends to increase the size and the intensity of recirculations.

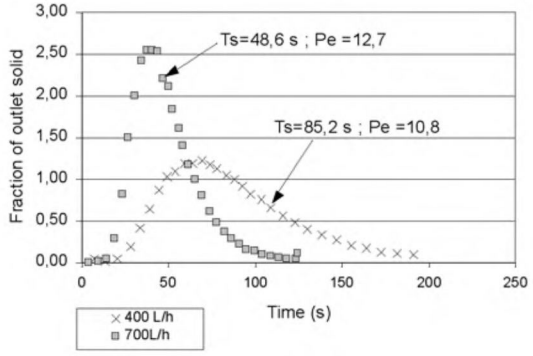


Figure 4 : Fraction of outlet solid in function of time forAf=2.3 cm/s and two flow rate

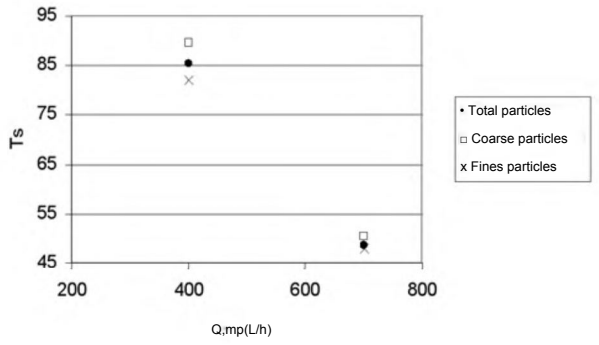


Figure 5 : residence time of fines coarse and all particles as a function of impulsion flowrate (Af=2.3 cm/s)

Not enough experiments have been performed to define a precise criterion which will characterize the impulsion flow rate and the intensity pulsation necessary to allow a plug flow transport of the solid. It is also too early to uncouple the role of both parameters. However, it results from these experiments that it is essential to generate an intensity pulsation and impulsion flow rate superior or equal to the terminal velocity of the heaviest particles.

In the operation mode of the column, pulsation is the base for mixing the particles in the compartment and enhance mass transfer between the suspension and the solvent, during the mixing step. It is now established that pulsation is also a precious tool to improve RTD performance and to allow more flexibility in the practical choice of the impulsion flowrate.

A series of experiments designed to test the role of the volume injected on the solid flow found no influence for a range between one third and one compartment and a half, provided impulsion and the pulsation are powerful enough.

STUDY OF LIQUID BEHAVIOUR

Procedure

The residence time distribution experiments were performed by injecting 15 mL of sodium hydroxide in a by-pass added to the liquid inlet. Two three-way valves are turned simultanuously in order to let the liquid feed sweep the volume occupied by the tracer. Injections take approximately 15 s, to be as close as possible to a perfect pulse injection in comparison to the time scale of the experiment (1500-2500 s). The conductivity probe versus timeis then measured directly at the exit by means of a conductivity probe.
The ouput concentration decuced from the conductivity is normalized :

$$C_\infty = \int_0^\infty C(t).dt$$

The exit age distribution is then defined as :

$$E(t) = \frac{C(t)}{C_\infty}$$

Role of pulsation

The specific effects of frequency and amplitude of pulsation on the liquid behaviour was examined. A partial set of RTDs performed for different frequencies are presented in figure 6. From figure 7, a net decreasing tendency of Peclet number in function of the intensity pulsation can be observed.

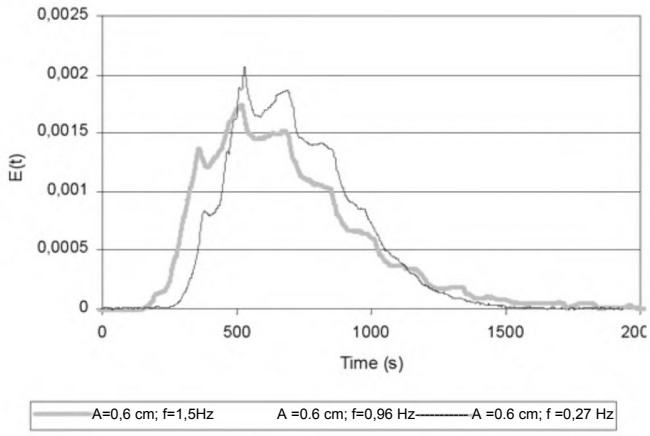


Figure 6 : Measurement of the normalized concentration in tracer at the liquid outlet; Qimp= 700 L/h ; V_{imp}=830mL / T_{mixing}= 160s / Influence of the pulsation intensity.

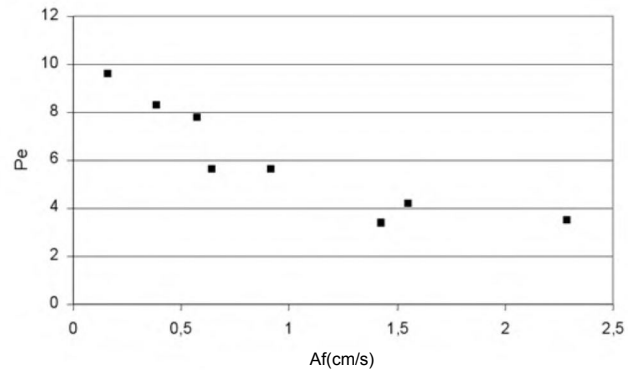


Figure 7; The dependency of the Peclet number on the pulsation intensity Af (cm/s)

Indeed, pulsations enhance axial mixing in the liquid phase, by increasing the size and the intensity of the vortices, all the more so as the radial convection is limited by tube walls. The opposite results were shown ealier concerning the solid phase. Based on our observations and experiments on bimodal populations, the physical explanation is provided by the fact that particles need a minimum velocity to be transported. Solid suspension need intense recirculations occupying the whole compartment to be driven. Furthermore and unlike the liquid phase, solid phase back-mixing is limited because particles are trapped between two trays.

Role of impulsions (frequency and volume and flowrate)

It is obvious that the introduction of the impulsion step will have a negative impact on the liquid flow. The upward flow is opposite to the average counter-current and downward liquid flow . Back-mixing is inherent to our system. This phenomenon can be observed on figure 8. The tracer concentration was followed at the liquid outlet for different mixing time. One experiment was also performed with no impulsion at all (T_{mixing}=infinite). It is interesting to notice the peaks due to the repeated impulsions. And, as expected, the dispersion of residence time distribution is increased when impulsions occurs more frequently.

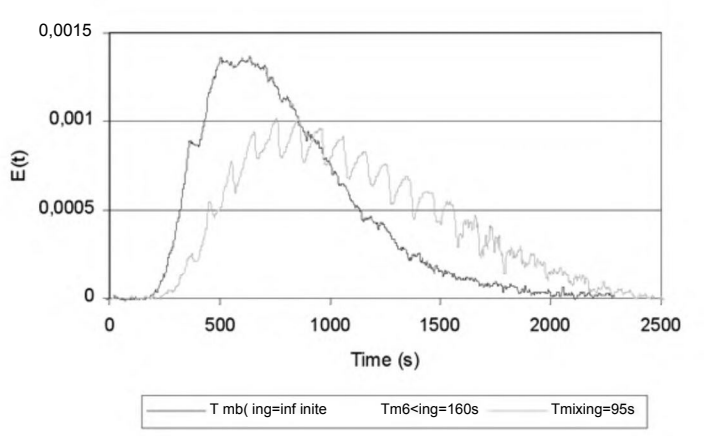


Figure 8 : Measurement of the normalized concentration in tracer at the liquid outlet; Qimp=600Uh ; Vimp=840 mL ; Af=2.3 cm/s ; Influence of the duration of the mixing step.

An equivalent series of experiments has also been performed to examine the effect of the volume impulsed. The results are not shown here, but, in the same way, it demonstrated that the increase of volume impulsed enhanced back-mixing.

Lastly, the investigation on the impulsion flowrate found no influence on the liquid behaviour.

OPTIMISATION OF PARAMETERS FOR COLUMN DESIGN

The optimisation of the RTD response leads to the column design and to the determination of operating conditions. The selection of the pulsation and impulsion parameters follows a methodology which will depend on the application set up in the new technology.
For a particular solid-liquid system, preliminary tests have to be realized with a cake of solid injected in the closed column only submitted to the pulsation. This will allow to characterize the solid behaviour in function of pulsation intensity and to choose the amplitude and the frequency able to set and maintain in suspension the particles. As a minimum pulsation is essential to transport upward heaviest particles, the parameters A and f will be choosen in function of these criteria, even if it is incompatible with a plug-flow convection of liquid phase.
Batch kinetics studies will provide a contact time, assuming an ideal mixing. Based on this contact time for the residence time in the continuous column, the mixing time $\mathbf{T_{mixin}g}$ would then be determined. Indeed, in closest conditions to plug-flow, solid residence time is near to (Tmixing $^{+}$ T_{imp}) times the number of compartments.

As the impulsion flowrate has no influence on liquid behaviour and as it reduces solid axial mixing, high values for $Q_{,mp}$ will be prefered. $Q_{,mp}$ will not have to be too important either because the impulsed volume is around one volume compartment and the duration of the impulsion must be superior to a few seconds for inertial reasons.

The impulsion volume is arbitrarily choosen equivalent to one compartment.

Solid throughput will depend on process objectives and will be limited by the maximal solid holdup that can be achieved. Further experiments with high concentration of particles will be performed to determine this criterion. It is expected that the pressure drop and the minimum velocity able to well mix the solid suspension will increase with the solid holdup.

Finally, with the device described, the liquid feed is not dependent anymore on solid residence time. Then, this parameter will first be choosen in order to ensure the condition of a counter-current between solid and liquid phases :

$$Q_L > Q_{imp.} \frac{T_{imp}}{(Timp+Tmixing)}$$

One should notice that the longer the mixing time is, the less forcing is the contraint. Once this condition met, Q_L is selected according to solvent consumption considerations.

CONCLUSIONS

A new technology has been set up in order to improve continuous columns used in solid-liquid contacting. An important aspect of the innovation is the introduction of a step mixing which allows to almost control the solid residence time. Another aspect is the role of pulsation in an homogeneous transport of the solid suspension, in particular, the reduction of the granulometric dispersion.

Based on the experiments presented, this column would be valid for dense particles presenting a low difference density with the liquid phase. The column has also been tested for floating particles and applications can possibly be extended to more dense solids, provided a powerful system of pulsation can ensure high velocities in the column.

For the column used in this study, mixing time ranges between 2 and 3 minutes and impulsion time between 5 and 10 seconds, which corresponds to residence times around 20 minutes. But, the counter-current condition makes the use of the new technology suit the type of system where a long residence time is needed.

A wide scope of potential applications is apparent: heterogeneous reactions, washing limited by diffusion. Of course, for high concentrations and dense particles, added complications of having to maintain in suspension the particles will be considered.

REFERENCES

1. L. Brunet, L. Prat, R. Wongkittipong, C. Gourdon , G. Casamatta and S. Damronglerd (2005), *CET,* **Vol. 28, 1,** under press.
2. Patent application under progress
3. M.R. Mackley, K.B. Smith and N.P.Wise (November 1993), *Trans IChemE*, **Vol. 71,** Part A.



Comparison of Disk & Doughnut vs. Sieve Tray internals on the operation of a pulsed column

Eyal Coleman, Keren Fadlon, Yigal Man, Baruch Grinbaum', Geoff Stevens**

Bateman SX, POB 15, Yokneam 20692, Israel

* - TAMI(IMI) Institute for R&D, POB 10140, Haifa Bay 26111, Israel

** -Department of Chemical & Biomolecular Engineering, the University of Melbourne, Victoria, Australia 3010

This research deals with the comparison of different internals in a pulsed extraction column and their effect on the column efficiency. The two internals studied were Disk & Doughnut and Sieve Tray. The system tested is Zinc Sulphate and DEPHA. Two identical pilot columns with different internals were operated under identical parameters in different configurations and the performance and recovery of the columns was calculated and compared. The flooding curves were obtained from hydraulic testing and mass transfer tests were held in mutual no flooding zones of these curves. It was found that there is no major difference between both types of internals, with small advantage to the Disk & Doughnut. Further research, applied to larger columns, is needed in order to determine the preferred internals.

INTRODUCTION

Bateman Solvent Extraction (BSX) has conducted research in order to compare the performance of Disk & Doughnut (D&D) and Sieve Tray (S.T.) internals for pulsed columns. The system of extraction of Zinc Sulphate with DEHPA (di-(2-EthylHexyl) Phosphoric Acid) as extractant was chosen for this research. This specific system is widely used as a standard in hydrometallurgy and as a base for comparison. In former studies Bateman showed that the Bateman Pulsed Column (BPC) could be applied successfully to Zinc Sulphate extraction and stripping [3][4][6],

BASIS OF COMPARISON

Three main parameters were compared:

1. The maximum flux - obtained at a given phase ratio and temperature as a function of the energy input.

2. *The composition of the outlet streams and the recovery.* The recovery of a column is defined as the percentage of the solute that was extracted or stripped in the column.

3. Holdup through the column. The holdups are used to calculate the residence time of each phase and the slip velocity, and may help predicting the flooding.

PROCESS DESCRIPTION

The extraction and stripping took place in two 40 mm pilot columns, identical in all aspects except for the internals being tested. The Zn was extracted from a Zinc Sulphate solution using DEHPA diluted with an aliphatic hydrocarbon diluent as an extractant. The extent of extraction is a function of pH and is accompanied by a decrease in pH. This is to be expected as the extractant acts as a liquid ion exchanger, substituting H^+ for Zn^{++} in the extraction process and vice versa in the stripping process. The chemical equilibrium is:

$$Zn^{2+}_{(Aq)} + 2HY<Org) <=> ZnY_2(Org) + 2H^+_{(A}q)$$

The subscripts Aq and Org refer to the aqueous and organic phases respectively [8] (HY is the DEHPA).

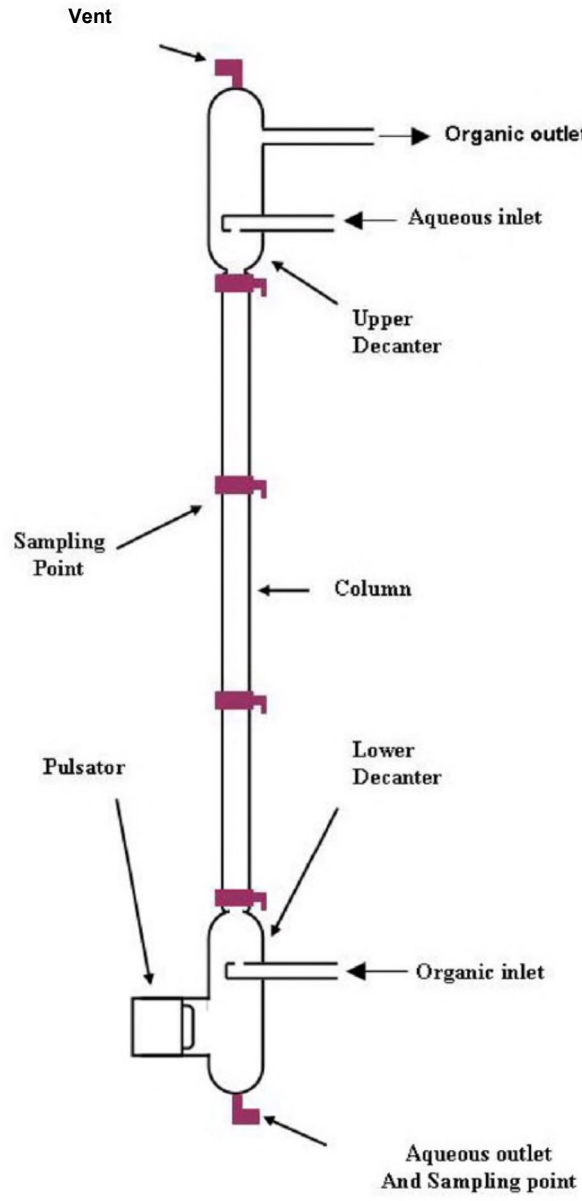
PILOT-PLANT EQUIPMENT AND PROCEDURES

The pilot plant consists of two 40 mm diameter glass columns, with an active height of 3000 mm. Sampling points are present at 1000 mm intervals along the active section. The sampling points are numbered from bottom to top. Glass settlers with a diameter of 80 mm are situated at either end of the active section. Pulsation is provided by a mechanical pulsator with a diameter of 70 mm and a maximum stroke of 15 mm. Frequency is controlled by a frequency converter in the range 0-150 CPM. Fig. 1 presents an unsealed sketch of BPC.

Piston metering pumps are used to feed the solutions to the column. The aqueous phase is fed to the top of the column and the organic to the bottom. Two heat exchangers are used for heating the fluids in the column by hot water. Suitable insulation is provided in order to reduce heat loss to the atmosphere.

The internals are made of PVDF. The column with the D&D internals is a standard BPC that consists of alternating discs and doughnuts. The doughnut internal diameter, disc diameter and distance between discs and doughnuts are 19.5 mm, 34.5 mm and 8.4 mm respectively, giving a free area of 25%. The trays of the S.T. internal are of 40 mm diameter and are spaced 50 mm apart. They have 34 drilled holes of 3.2 mm diameter, evenly spaced on each with 6 mm between the centers of the holes, giving a free area of 22%. Fig. 2a and 2b present unsealed design sketches of the internals.

At the pilot the pulsation is provided mechanically. A piston is given the required frequency (F) and amplitude (A). The product 'A·F' is the Pulsation intensity (PI) supplied to the column.



Fie. 1: Design sketch of BPC

EXPERIMENTAL PROGRAM

The solutions used in the experiments are similar to those used in typical industrial plants: the feed contains 35 g/L Zinc Sulphate and the stripping solution - 50 g/l.
During the experiments the pulsation frequency was kept at a constant 120 CPM.
The amplitude was changed between 2 mm to 14 mm. The volumetric 0:A flow ratio was constant at 1.6:1 for extraction and 3.2:1 for stripping. The temperature was kept around 45°C.
Two sets of tests were done: hydraulic tests and mass transfer tests.



Fig 2a: sieve tray internals

The Hydraulic Tests

The hydraulic tests are performed in order to find the flooding curve and the hold up characteristics for all configurations. The tests were carried out with both O/A and A/O dispersions.



Fig 2b: Disk & Doughnut internals

Mass Transfer Tests

Mass transfer tests were performed for every configuration at a specific flux and pulsation intensity under conditions of no flooding, which provide acceptable dispersion.

RESULTS & DISCUSSION

HYDRAULIC TEST RESULTS

The resulting flooding curves of the eight hydraulic tests are summarized in table 1.

Table 1: flooding curves summary table

				Stable Operation Range	
	TEST PARAMETERS			Flux Range	Pulse Intensity Range
Test No	Process	Dispersion	Internals	[$m^3/m^2/hr$]	[A x F, mm/sec]
1	Extraction	A/O	D&D	20-25	700-1000
2	Extraction	A/O	S.T.	20-25	500-1000
3	Extraction	O/A	D&D	20-25	1200-1700
4	Extraction	O/A	S.T.	20-25	1200-1500
5	Stripping	O/A	S.T.	20-35	250-1700
6	Stripping	A/O	S.T.	20-55	500-1700
7	Stripping	O/A	D&D	20-35	800-1500
8	Stripping	A/O	D&D	20-50	1200-1700

Discussion on Hydraulic Test Results

The mutual no flooding zone, for both types of internals, is at fluxes of 20-25 $m^3/m^2/h$ for extraction and 20-35 $m^3/m^2/h$ for stripping. The pulse intensities range is higher for the organic continuous (A/O) dispersion and slightly higher for D&D internals than for S.T.

Fluxes below 20 $m^3/m^2/h$ were not tested, as this range is of small practical interest. Also, fluxes above 55 $m^3/m^2/h$ was not investigated, as it is known experimentally to be too high for efficient mass transfer.

The results show the operational zone is larger for stripping than for extraction.

In extraction the stable operation range is similar for both dispersions. In stripping, the maximum flux for organic continuous dispersion was 50% higher than for aqueous continuous (O/A), with both types of internals.

D&D internals required higher minimum pulse intensity than S.T. internals.

MASS TRANSFER TEST RESULTS

The four configurations, i.e. extraction and stripping at both A/O and O/A, were tested for both types of internals. For each pair an optimum no flooding point was chosen.
At all configurations the column was operated for two hours at a steady state before taking samples. This corresponds to 2-8 residence times of the continuous phase - see Table 2.

Table 2: Operating conditions in mass transfer experiments

Configuration	Flux [$m^3/m^2/h$]	Amplitude [mm]	Flow Rate(L/h)	Residence time[h]
Extraction, A/O	25	10	19.4	0.36
Extraction, O/A	25	11	12.1	0.75
Stripping, A/O	30	8	28.7	0.25
Stripping, O/A	30	11	9	1

Tables 3 and 4 present the inlet and outlet concentrations of each phase measured by Atomic Absorption spectrometry, and the calculated recovery.

Table 3: Mass transfer test results for Extraction

No.	1	2	3	4
Internals	D&D	D&D	S.T.	S.T.
Dispersion	A/O	O/A	A/O	O/A
	Concentration of Zn [cJ/L]			
Loaded Solvent	13.9	13.5	15.1	15
Barren Solvent	2.2	2.4	6.6	3.7
Feed	33.4	37.5	31.0	37.5
Raffinate	14.2	17.5	17.1	20
Recovery (%)	57	53	45	47

Table 4: Mass transfer test results for Stripping

No.	5	6	7	8
Internals	D&D	D&D	S.T.	S.T.
Dispersion	A/O	O/A	A/O	O/A
	Concentration of Zn [cJ/L]			
Loaded Solvent	12.7	14.4	13.1	13.1
Barren Solvent	5.2	1.26	6.2	2.25
Strong Elect.	72.5	116.9	70.2	100
Weak Elect.	47.5	55.5	60.2	60
Recovery (%)	59	91	53	83

DISCUSSION OF MASS TRANSFER RESULTS

The recovery calculations for extraction are based on the concentrations measured in the aqueous phase, and for the stripping - on the solvent.

Extraction

In both cases, i.e. organic continuous (experiment 1 & 3) and aqueous continuous (experiment 2 & 4), the recovery with the D&D internals was higher by a few percent. Although this number is within the experiment error, the fact that in both experiments the D&D internals gave higher recovery shows that, at the given configuration, hints that the D&D internals are slightly superior.

Stripping

In stripping the results were similar; i.e. the recovery in the D&D internals was slightly higher, in both dispersions.

It is interesting to note that while for extraction both dispersions yielded similar recovery, in stripping there is significant advantage of running aqueous continuous dispersion.

The results for both batteries are different from those obtained by Jahya [7], who found the S.T. internals slightly more efficient.
It may be due to the different system that he analyzed, but also due to the different dimension of the tested columns.

It is important to note that the relative dimensions of the tested column were not exactly to scale: the distance between the sieve plates was 50 mm, just as in the 72.5 mm column used by Jahya [7], while in the D&D it was only 17 mm for the full compartment, to compare with 25 mm in the experiments of Jahya. More dense internals improve the mass transfer, and this is probably why in the present work the D&D internals performed better than in the case of Jahya. Actually in a large (above one 1 m) industrial column the mass transfer in the S.T. column may be as good as in the D&D or even better.

This would mean that for reliable comparison larger pilot columns are needed.

At the scale and configuration of the present work, there is a slight advantage for the D&D internals.

CONCLUSIONS

The main conclusion is that there is no major difference between both types of internals. This conclusion is similar to the work of Jahya [7],

Both types of internals yielded similar maximum flux.

There was a slight preference for the D&D internal regarding mass transfer.

The plate spacing of the S.T. internals is far larger than the plate spacing of the D&D. Further tests with larger diameter of columns are needed in order to determine which internals are superior for this system.

BIBLIOGRAPHY

1. R. L. Movsowitz, R. Kleinberger, E. M. Buchalter, B. Grinbaum, S. Hall, “Comparison of the performance of full scale pulsed columns vs. mixer-settlers for uranium solvent extraction”, in Cox, Hidalgo, Valiente, (eds.), *"Solvent Extraction for the 21st Century", 2* 1455-1460, 2001, SCI, London, UK
2. B. Grinbaum, “An integrated method for development and scaling up of extraction processes”, in Y. Marcus, A. Sangupta, *"Ion exchange and solvent extraction"* **vol.** 15, 1-106, Marcel Dekker, 2002
3. Bateman Inc., *“Zinc Sulphate solvent extraction, Bateman pilot pulse column test work”,* report no. 32262/1, August 1999.
4. Bateman Inc., *“Zinc Sulphate extraction using Bateman pulse column 40 mm pilot unit for Tecnicas Reunidas S.A.”,* report no. 32485/TR/01, July 2000.
5. I. A. Siddiqui, S. V. Kumar, *“Solvent extraction studies in a pulsed perforated plate column",* Symp. Solvent Extr. Met. (1979), Dep. Atomic Energy, Bombay, India.
6. R. Kleinberger, *“Zinc Sulphate extraction by Bateman pulsed column technology",* Copper, Cobalt, Nickel and Zinc Recovery, Conference, Victoria Falls, Zimbabwe, July 16-18, 2001, South African Institute of Mining and Metallurgy, Johannesburg, S. Africa.
7. Ali Budijoyo Jahya, *“Performance of the pulsed disk and doughnut solvent extraction column",* Ph. D. Thesis, Department of Chemical Engineering, University of Melbourne, Australia (2002).
8. D. F. Peppard, G.W. Mason," Some mechanics of M(II),(III),(IV), and (VI) metals extraction by acidic organophosphorus extractants”, *Nuclear science and engineering* , 16,382-384 (1963).

EXPERIMENTAL SETUP FOR INVESTIGATION OF THE KINETICS OF NON-EQUILIBRIUM PROCESSES

A. Kopyrin, M. Afonin, A. Fomichev

Department of Rare Earth, Saint-Petersburg State Institute of Technology, Saint-Petersburg, Moskovsky ave. 26, 190013, Russia; kopyrin@tu.spb.ru

The experimental setup for investigation of kinetics of non-stationary processes was created. The software for automation of the setup devices calibration, controlling of the process during the experiment and for experiment results processing is developed. A number of experiments were carried out with this setup. The system was deflected from stationary state by chemical and electrochemical method, and the method using alternative current with determined frequency.

INTRODUCTION

Almost all modern processes of elements and isotopes separation are based on achievement by a system stationary or near to it condition. In these conditions the separation of elements with similar properties is difficult. Today's problem state of separation and isolation of lanthanides and other elements with similar properties requires to search new methods of elements separation. These investigations are carrying out in the world, devoted to looking-for new ways of element separation using non-stationary non-equilibrium processes, based on differences in kinetics of chemical reactions of being separated elements.

Realization of the process in non-stationary non-equilibrium conditions using phenomena of oscillating extraction allows to use the differences in kinetics of ion complexation and extraction, their transport through the boundary area in both directions to separate elements [1. Oscillating extraction allow to use new coordinate - evolution of chemical system in time. For achievement of high elements separation factors using oscillating extraction it ispossible to use multiple repetition of process similar to those described in literature "parametric pumping" [2, 3, 4], This can change and essentially enrich exist methods of isolation and separation of elements and isotopes. For adequate description of elements oscillating extraction it's necessary knowledge of extraction and stripping rate constants of rare earth elements (REE) and its mass transfer coefficients. There are no data in literature about the extraction kinetics of REE at their mutual presence in extraction system (3 and more elements). During the studies of extraction kinetics of individual rare earth it's impossible to achieve the absolutely identical conditions to obtain the comparable rate constants of different REE. The potential problem for adequate simulation of the kinetics of multicomponent extraction system is the possible interference of rate constant of one element with the presence of another element(s). That is why the use of such constants to describe the kinetics of multicomponent extraction systems should be inadequate.

In present work the set up which was design in Saint-Petersburg State Institute of Technology is presented. This set up and procedure allow to find the rate constants of element in their mutual presence in extraction system. This approach has advantages in comparison with traditional extraction kinetics methods.

SETUP DESCRIPTION

Flow sheet of the setup (fig. 1.) is following: the emulsion is pumped from thermostatic extractors 16, 17 to centrifugal separators 5, 6 through the turbidimeters 11, 12 by peristaltic pump 10. After separation from the first separator 5 organic phase flow to the second extractor 17 and from the second separator 6 organic phase is analyzed in spectrophotometer 8 and come to the first extractor 16. In this way circulation of organic phase between two extractors is provided. Passing through spectrophotometers 7, 9 aqueous phases come back to their corresponding extractors. A number of devices register behavior of extraction system: pH, red/ox potential of aqua phase, temperature and emulsion turbidity, which are recorded to the computer 18 with frequency above 1 Hz using DAQ board and specially designed software.

SETUP EQUIPMENT AND PROCEDURES

Thermostatic extractors, each 300 ml, are filled with aqueous and organic phases, each 150 ml correspondingly. Aqueous phase 6M NaN03, and organic phase - 0,5M n-tributylphosphate (TBP) in kerosene or tetradecane used.

One of possible variants: in aqueous phase 6M NaN03 of the first extractor where target components (difficulty separable neodymium and praseodymium) are situated - extraction, organic phase circulates between two extractors - like a pseudo membrane, and aqueous phase of second extractor is 0,1M HN03 - stripping. Other variant: both aqueous phases 6M NaN03 content target components at the beginning of the experiment.

A number of experiments were carried out with this setup. As factor, deflecting the system from stationary state chemical method, electrochemical and alternative current with determined frequency were used.

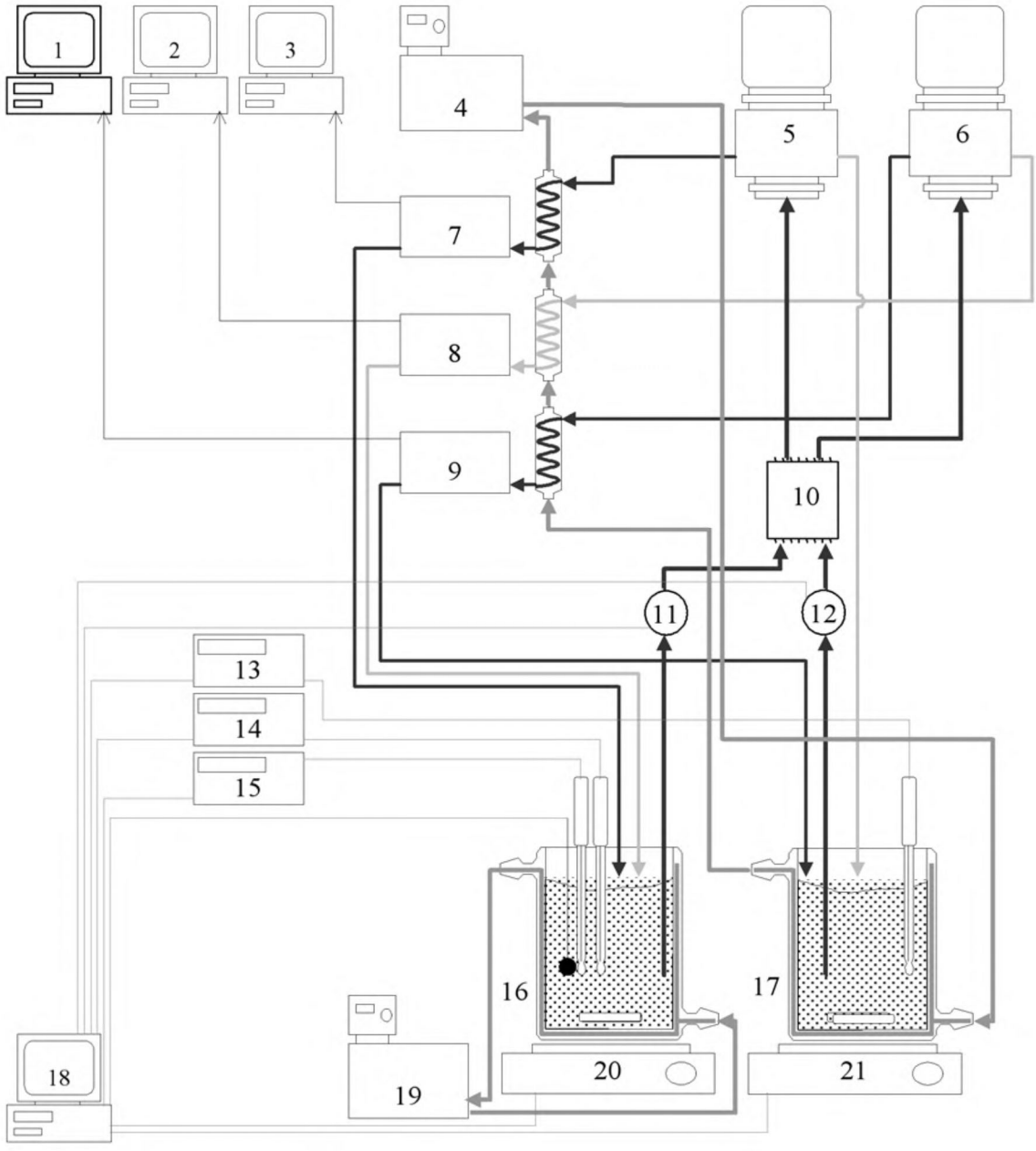
Diode-array spectrophotometers get spectra every 6-15 seconds. By deconvolution of each spectrum, using especially designed software we can get concentration of several elements.

DYNAMICS OF CONVENTIONAL EXTRACTION OF CHEMICALLY SIMILAR ELEMENTS PR AND ND

Studying of conventional extraction of Nd and Pr (Fig. 2.) give us extraction and stripping rate constants of elements and its mass transfer coefficients (1) for it's further using in modeling of oscillating extraction.

$$\begin{aligned} k_e(Nd) &= 7{,}685?\ O'^{3}\ M'min^{1} \\ k_r(Nd) &= 8{,}0?\ O'^{3}\ M\ 'mm^{1} \\ k_e(Pr) &= 4{,}831?\ O'^{3}\ M\ 'min'^{1} \\ k_r(Pr) &= 8{,}38?\ O'^{3}\ Mimin' \end{aligned} \qquad (1)$$

k_e - extraction mass transfer coefficient;
k_r - stripping mass transfer coefficient



---------- ▶ - heat-transfer flow
---------- ▶ - emulsion flow
---------- ▶ - organic phase flow
---------- ▶ - aqueous phase flow
---------- > - data flow
- analog signals collected by data acquisition board

Fig. 1. Experimental setup: 1-3, 18 computers; 4, 19 - thermostats; 5, 6- centrifugal separators EC-33 NIKIMT; 7,9- spectrophotometers SF-2000 OKB Spectrum; 8 - spectrophotometer PMR-11 LOMO; 10 - peristaltic pump Watson Marlow; 11, 12- turbidimeters Orbecko-Flellige Model 966 Kernko; 13 -phi-meter pFI-673; 14 - potentiometer 1-120; 15 - potentiometer Thermo Orion Model 720A; 16, 17- extractors; 20, 21 - magnetic stirrers HANNA Instruments

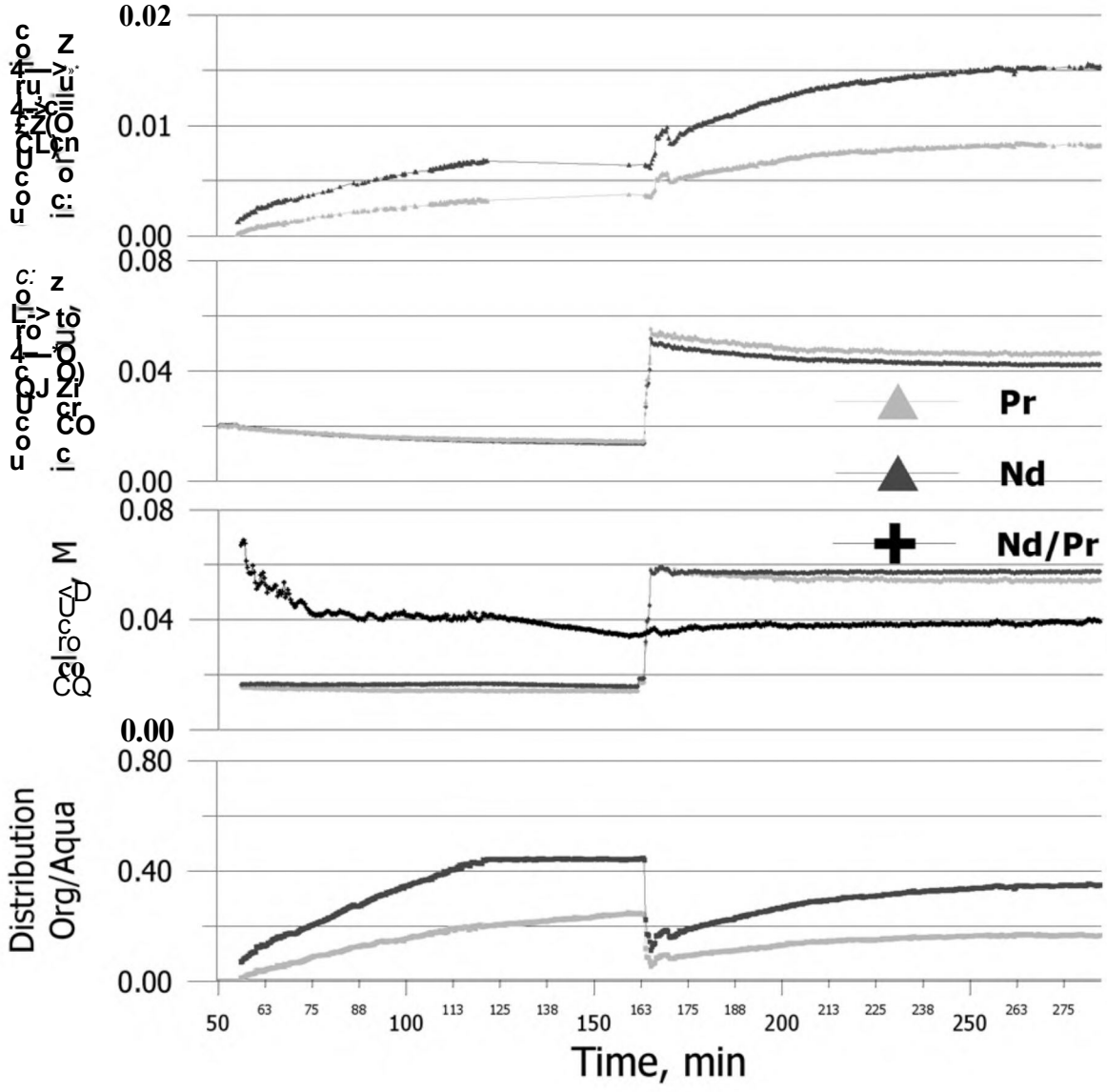


Fig. 2. Extraction of Nd and Pr.

BEHAVIOR OF EXTRACTION SYSTEM IN NON-STATION ARY OSCILLATING CONDITIONS

Besides concentration, distribution and separation factor of the elements it's necessary discus about non-stationary oscillating extraction also on such parameters as temperature, red/ox potential, stirrer speed and emulsion turbidity (fig. 3.).

It's possible to estimate effective boundary area on the emulsion turbidity. It depends on numerous factors: stirrer rotation speed, emulsion rate, organic to aqueous phase volume ratio, extractor diameter, stirrer unit diameter and many others. It's very difficult work and search of this dependence is going on at this time.

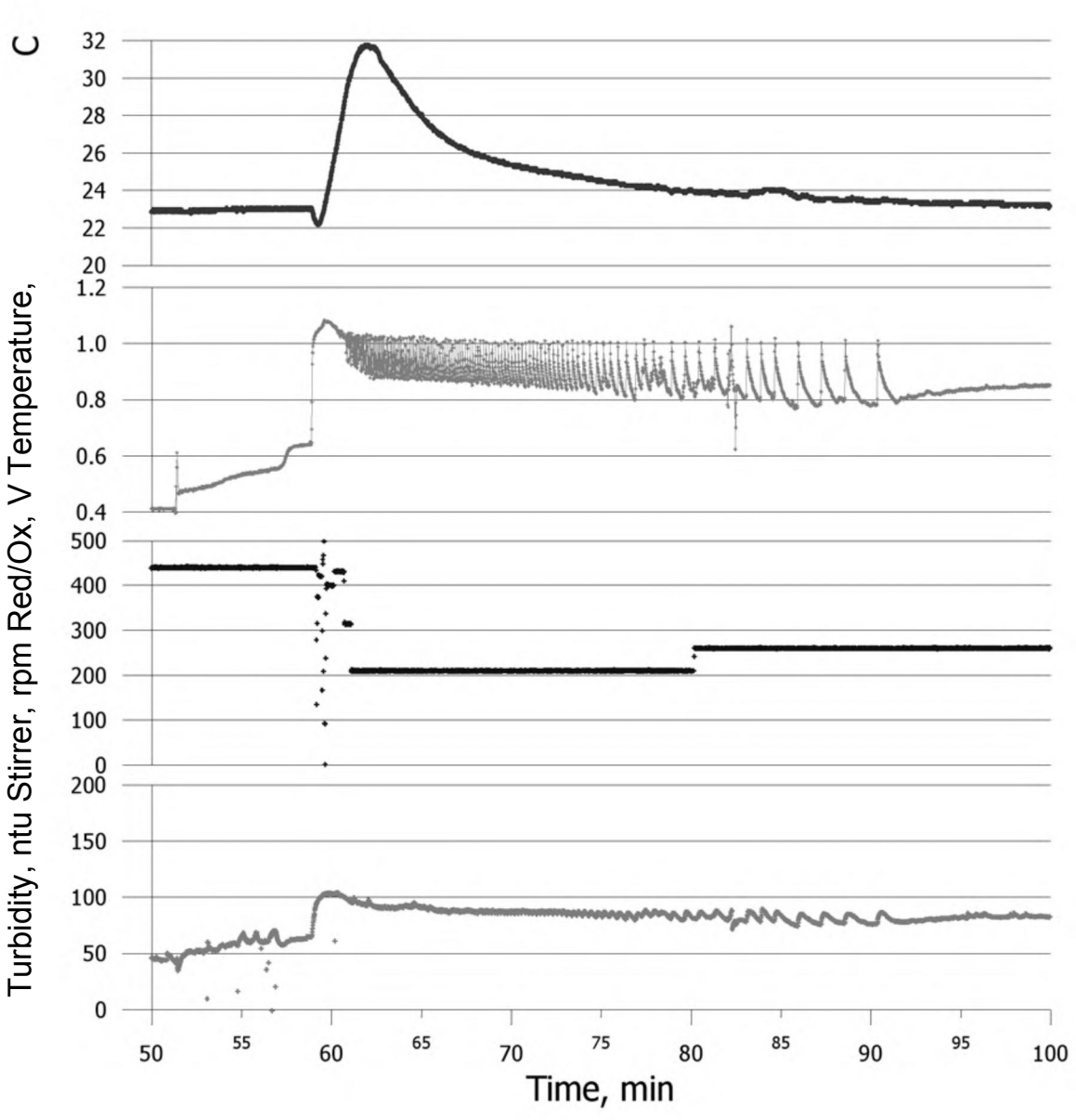


Fig. 3. Parameters of the system in non-stationary oscillating conditions.

CONCLUSIONS

Using the oscillatory Belousov-Zhabotinsky reaction in extraction system gives advanced increasing of effective separation coefficients of chemically similar elements in comparison with classical methods in case of two extractors, coupled by bulk liquid membrane. After two hours after lunching of oscillation reaction effective separation coefficient of pare Pr/Nd exceeded 3.

Electrochemical method of initiating of oscillation allows reaching high separation coefficients of elements in organic phase. Concentration ratio of Pr with respect to Nd in organic phase during the experiment was reached 5. Usage of this method for element's separation requires further research.

Such factor deflecting the system from stationary state as temperature and behavior of the system and difficulty separable elements using so called “thermal parametric pumping” is being investigated at this time.

The main advantages of the setup: 1. chemical composition simultaneous analysis in all phases; 2. quick and simultaneous determination of several elements by deconvolution of UV-VI spectra; 3. online system behavior monitoring using DAQ board and developed software; 4. flexibility - easy to modify of the setup for different tasks.

ACKNOWLEDGEMENTS

This work was supported by the U.S. Department of Energy, Office of Basic Energy Sciences, under grant RC0-20000-SC14 administered by the Civilian Research and Development Foundation.

REFERENCES

1 M. A. Afonin, A. A. Kopyrin, A. I. Shvalbe, A. A. Baulin, A. S. Petrov, Chemical and electrochemical oscillatory extraction of F-elements-new procedure development, *Journal of Alloys and Compounds,* Vol. 374 (2004) pp. 426-430

2 N. Nikolaev, D. Muraviev, M. Mamoun, Dual-temperature ion-exchange separation of copper and zinc by different techniques, *Separation Science and Technology*, Vol. 32, Issue 1-4 (1997), 849-866

3 R. Alan Gregory and Norman H. Sweep Parametric Pumping: Behavior of Open Systems. Part II. Experiment and Computation, *The Chemical Engineering Journal,* 139-149

4 C. Stöhr, C. Bartosch, R. Kiefer, W. H. Höll Separation of Mixtures of Heavy Metals by Parametric Pumping with Variation of pH, *Chemical Engineering & Technology,* Vol. 24, Issue: 9 (2001), 879-883



Local Coalescence Effect on Extraction Column Performance

X.J. Tang, G.S. Luo*, J.D. Wang

(State Key Laboratory of Chemical Engineering, Tsinghua University, Beijing 100084, China)

Coalescence-dispersion pulsed-sieve-plate extraction column (CDPSEC) is an improvement of traditional pulsed-sieve-plate extraction column (PSEC), whose mass transfer efficiency is much better than that of standard PSEC under certain operating conditions because of the interface renewal effect led by the local coalescence of droplets in CDPSEC. In this work, a method is developed to quantitatively calculate the influence of local coalescence of droplets. The calculated results show that higher energy input can keep better dispersion of droplets with suitable coalescence, where the fraction of the droplets which coalesce to form the local continuous phase is less than 10% of the total dispersed phase, to reach perfect mass transfer performances in CDPSEC over PSEC. Lower energy input drives excessive coalescence of droplets, which leads the serious lowing of mass transfer efficiency in CDPSEC.

INTRODUCTION

Drop size distribution of the dispersed phase strongly influence the mass transfer performances of extraction equipments, which makes the differences in residence times and mass transfer rates of droplets with different size. It was proved that coalescence and redispersion of the droplets could reduce the influences of drop size distribution and the axial mixing [1,2], A multistage mixer-settler extraction column was applied to the extraction of rare earth metals to restrain the axial mixing by introducing the local coalescence effect of the droplets [3], But the structure of the column was very complex, especially for those contaminated systems. A coalescence-dispersion pulsed-sieve-plate extraction column (CDPSEC) was another kind of improved pulsed-sieve-plate extraction column (PSEC), where a special kind of plates, wetted by the dispersed phase, were inserted into to replace the standard steel plates. Thus, the droplets coalesced under the coalescence plates and then redispersed when the droplets passed throuqh the standard plates. This behavior of the dispersed phase resulted in the repeated interface renewal to improve the mass transfer performance. The structure of CDPSEC was simple but efficient, whose mass transfer efficiency increased by 20% and throughput increased by 100% over PSEC [4-6], although the mean drop size was larger in CDPSEC than that in PSEC [7,8], From above, it could be concluded that introducing the local coalescence effect into extraction columns was quite helpful to overcome the bad effect of drop size distribution. Thus, to design the higher efficiency extraction columns, investigations in the coalescence of droplets are very necessary. Many researchers paid their attentions to the coalescence of one droplet with a phase interface, two droplets, and droplet swarms [9-13], In the sense of industrial practice a lot of empirical equations have been suggested, but they are complicated and unsatisfactory. An accurate quantitative method, which is not only simple but also close to practice, to

* Corresponding author, E-mail:gsluo@tsinghua.edu.cn

calculate the influence of coalescence on the mass transfer performances is still unavailable.

In this work, the local phase separation caused by the coalescence of droplets during the droplets passing through the coalescence plates was observed. A method applying the 'area principle' [14] to calculate quantitatively the fraction of droplets, which coalesced under the coalescence plates, was developed.

Experimental set-up

The extraction column was composed of a glass section, with 150mm in diameter and 225mm in settlers, and an effective height of 2m as shown in figure 1. Two combinations of the plates were applied in this work, which were dispersion plates completely with 50mm in plate spacing, called PSEC, and one coalescence plate every four plates with 25mm in plate spacing, called CDPSEC. The detail information of the column and the plates has been provided elsewhere [8],

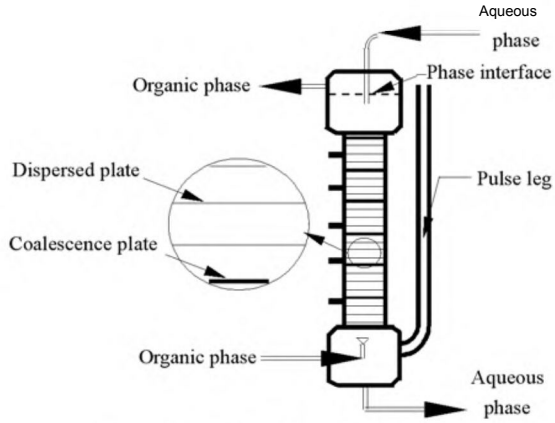


Figure 1 Experimental set-up

The experimental system was 30% tributyl phosphate (TBP) (in kerosene)-nitric acid-water, and the organic phase as the dispersed phase. All the chemicals were purchased from Beijing chemical plant, and used directly without any further purification. The holdup of the dispersed phase was measured by the volumetric replacement method. The average drop size and its distribution were determined by taking photographs with a Sony DSC-S50 digital camera.

Model to calculate the fraction of coalescence

Figures 2 and 3 are the photos of two-phase flow behavior in the CDPSEC respectively. It can be seen that there is a layer of the dispersed phase under the coalescence plate, but it does not exist under the dispersion plate. As mentioned in our previous paper [5, 6], this is because the two kinds of plates are made from the different materials with different wetting abilities to the dispersed phase. The droplets of the dispersed phase coalesce and redisperse periodically along the column in CDPSEC, while the coalescence of droplets can be ignored in PSEC. Furthermore, it can be found that the layer of dispersed phase beneath the coalescence plate can be divided into two layers. The upper is an organic film covering the coalescence plate and the lower is a swarm of droplets. This point indicates that the droplets coalesce under the coalescence plate resulting the local phase separation. The situation is similar to that in the upper settler to some extent, where the droplets coalesce completely and form the continuous organic phase, shown in Figure 5.

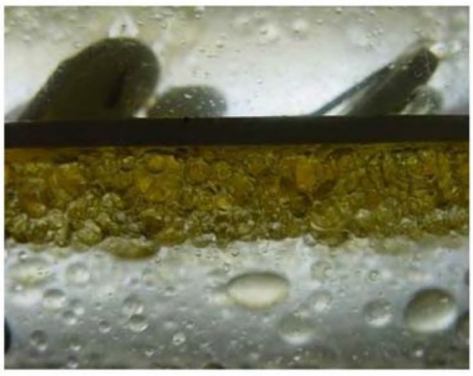


Figure 2 Dispersed phase passing a coalescence plate

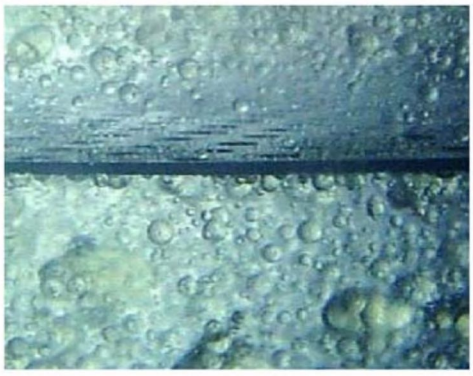


Figure 3 Dispersed phase passing a dispersion plate

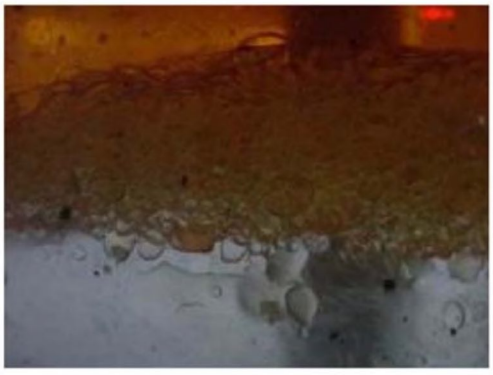


Figure 4 Phase separation in the upper settler of CDPSEC

Comparing with Figure 4, the situation shown in Figure 2 can be assumed as a partial settler, where part of the droplets coalesce and form a local continuous organic phase. Thus, the droplets above the coalescence plate contain two parts of droplets, which are the smaller droplets and those larger ones generated from the local organic continuous phase. And the local organic continuous phase is the decisive factor in the formation of interface renewal to enhance the mass transfer efficiency in CDPSEC over PSEC. If the thickness of the local continuous phase is thinner, the interface renewal effect is too weak to increase the mass transfer efficiency. Otherwise, thicker local continuous phase due to excessive coalescence of droplets may lead to the poor interface area with larger mean drop size and the lowing of mass transfer efficiency. In this sense, a quantitative method applied to obtain the operating conditions, where the suitable thickness of the local continuous phase is formed, should be developed as follows.

As mentioned above, in CDSEC there is a similarity between the upper settler and the partial settler beneath the coalescence plate although the diameters of them are different. According to the 'area principle' [14], the heights of middle layer with different cross-sectional area can be calculated by Equation (1).

$$H = \frac{K(0}{A}^{Y} \qquad \text{(D}$$

where H is the height of the middle layer in the settler, Q is the flow rate of the continuous organic phase discharged from the settler, A is the cross-sectional area of the settler, and K and y are the parameters in the equation. Assumed that the parameters K and y for the upper settler and Equation (3) for the partial settler beneath the coalescence plate are the

same, then equations (2) and (3) are obtained.

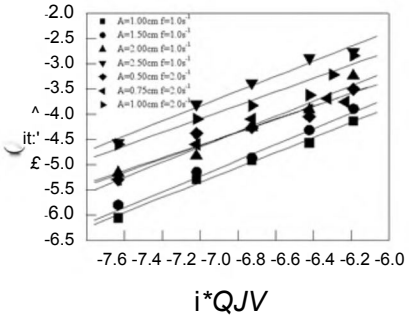
$$H_d = K\&\text{-}y \quad (2)$$

$$H_p = K\,AL_{-Y} \quad (3)$$

H_d and H_p are the height of the middle layer in the upper settler and in the partial settler respectively. The parameters K and y can be obtained by measured values of H_d at different operating conditions. Thus, parameter Q_p in Equation (3) can be calculated by measured values of H_p.

Results and discussions

In this section, the influence of the flow rate of the continuous phase Q_c on the dispersion of the droplets is ignored. This is because the drop size distribution mainly depends on the holdup of the dispersed phase, the pulse amplitude and the pulse frequency. The influence of Q_c on the holdup is much weaker than other operating conditions, so the ignorance of Q_c on the dispersion of the droplets is reasonable. Figure 5 shows the relation between H_D and Q_d/A_d.



i*QJV

Figure 5 Relation between H_d and Q_d/A_d

From Figure 5 the relation between H_d and Q_d/A_d fits with Equation (2) very well and the parameters K and y can be express as Equations (4) and (5). Figure 6 illustrates the comparison of Hd between experimental values and calculated results. It can be seen that the results are satisfactory.

$$\ln AT = \backslash 5.9A^{025}f\sim^{\circ 032} \quad (4)$$

$$y = \begin{cases} [1.5 & (/\text{-}1.05\text{-}^{1}) \\ [1.29 & (/ = 2.0s^{1}) \end{cases} \quad (5)$$

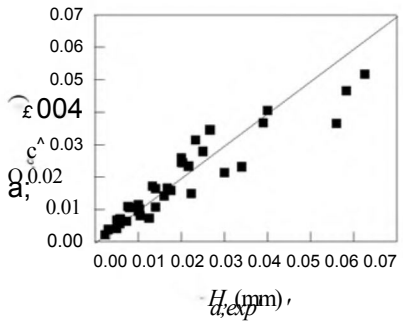
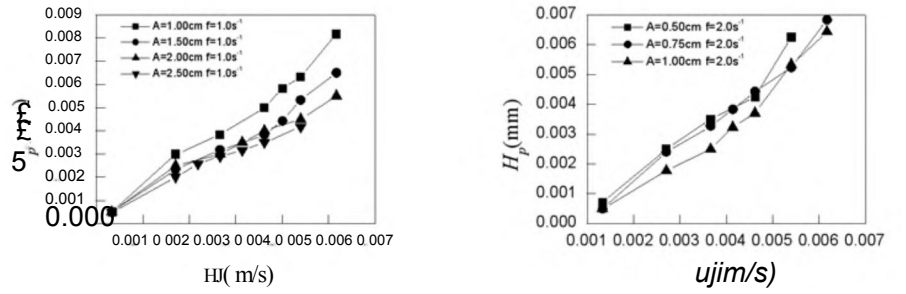


Figure 6 Comparison between $H_{d\,exp}$ *and* $H_{d\,cal}$

The influence of the operating conditions on H_P is shown in Figure 7. Hp increases with the increase of u_d or with decrease of Af. Equation (6) is a relationship to calculate H_p and Figure 8 is the comparison between $H_{pexp}$and H_{pcal}.



(a) *(b)*

Figure 7 Influence of operating conditions on H_p

$$H_p = 1.6(Af)^{0.11} u_d^{x} f^{-} \qquad (6)$$

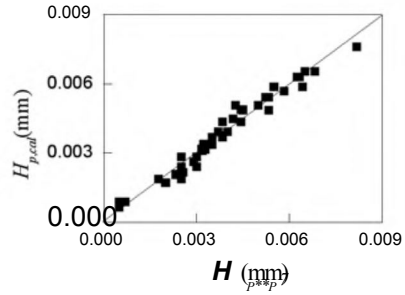


Figure 8 Comparison between H_{pexP} *and* $H_{p\,cal}$

The relationship between u_d and (Q_d/A_d) is given as Equation (7).

$$u_d = \frac{9}{4}\frac{Q_d}{A_a} \qquad (7)$$

With Equations (3)-(7) Q_p can be obtained as shown in Figure 9. And the fraction of local separated phase (Q_p/Q_d) due to the coalescence of droplets is shown in Figure 10.

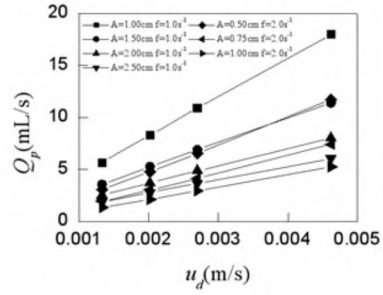


Figure 9 Flow rate of local phase separation

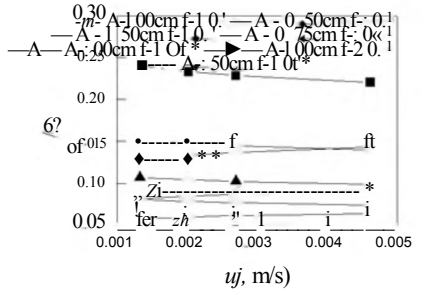


Figure 10 Fraction of local separated phase

According to the results above, a quantitative method to describe the local phase separation led by the coalescence of droplets in CDPSEC is developed. To obtain the optimized operating conditions in CDPSEC of higher mass transfer performances over PSEC, experiments were carried out. Figure 11 illustrates the mass transfer performances in CDPSEC.

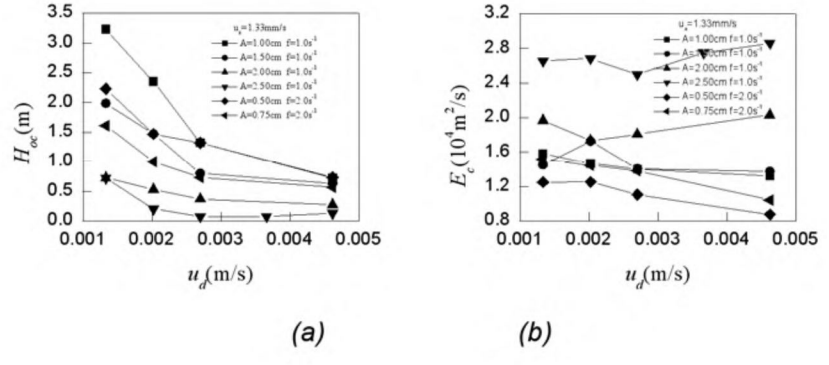
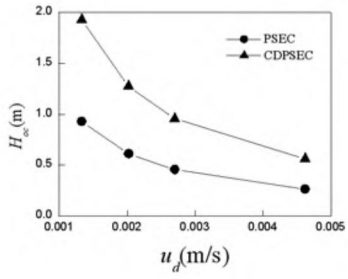


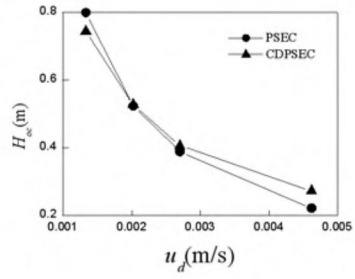
Figure 11 Mass transfer performances in CDPSEC

Under the same Af, (Qp/Q_d) is lower with higher f than that with higher A for the conditions of lower u_d as shown in Figures 10. It can be concluded that the dispersion of droplets with higher f is better than that with higher A under the same Af. Thus in this situation, the mass transfer performances with higher f is much better than that with higher A in CDPSEC as

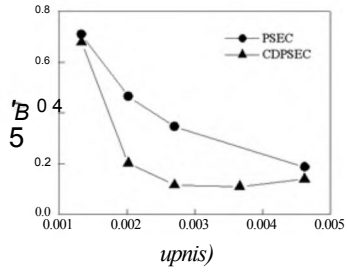
shown in Figure 11. On the other hand, with the increase of u_d (Qp/Q_d) grows when f is higher, while (Qp/Q_d) reduces when A is higher under the same Af. As the result, Hoc mainly depends on higher Af, neither on higher f nor on A.
Figures 12 and 13 are the comparison of mass transfer performances between CDPSEC and PSEC.



(a) A=1.0cm, f=1.Os-1, u_c=0.00133m/s

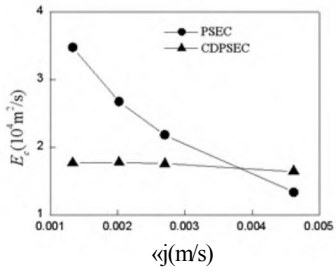


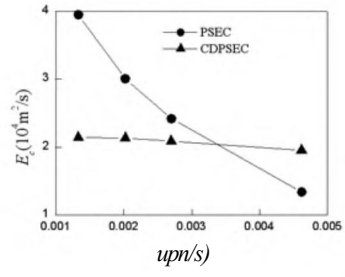
(b) A=1.5cm, f=1.Os-1, u_c=0.00133m/s



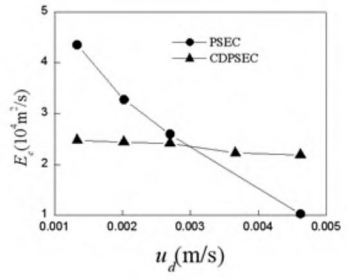
(c) A=2.0cm, f=1.0s-1, u_c=0.00133m/s

Figure 12 Comparison of Hoc between CDPSEC and PSEC





(a) A=1.0cm, f=1.0s-1, u_c=0.00133m/s (b) A=1.5cm, f=1.0s-1, u_c=0.00133m/s



(c) A=2.0cm, f=1.Os-1, u_c=0.00133m/s

Figure 13 Comparison of E_c between CDPSEC and PSEC

From Figures 13, it can be seen that the axial mixing in CDPSEC is quite low comparing with that in PSEC, and varies little with the change of u_d for its low plate spacing. But Hoc is strongly influenced by Af as shown in Figure 12. When Af is lower than 2.0cm/s Hoc in CDPSEC is higher than that in PSEC, which means the mass transfer efficiency in CDPSEC is lower than PSEC with lower Af. When Af is higher than 2.0cm/s the mass transfer efficiency in CDPSEC is better than PSEC. When Af is 2.0cm/s the mass transfer efficiencies of CDPSEC and PSEC are almost equal. As shown in Figure 10, this can be explained by that when Af is lower than 2.0cm/s the dispersion of droplets is bad because of the serious coalescence of droplets corresponding to **(Q_p/Q_d)** higher than 10%, and when Af is higher than (or equal to) 2.0cm/s the dispersion of droplets becomes better and better with suitable coalescence corresponding to **(Q_p/Qd)** lower than 10%, where the interface renewal effect plays an important role to enhance the mass transfer efficiency in CDPSEC. According to the discussions, the mass transfer efficiency in CDPSEC can be increased markedly with interface renewal effect due to suitable local coalescence of droplets, whose fraction is less than 10% of the total flow rate of the dispersed phase.

Conclusions

The local phase separation due to the coalescence of droplets exits beneath the coalescence plates in CDPSEC, which can enhance the mass transfer performances efficiently. The 'area principle' is applied to calculate the influence of local coalescence of droplets quantitatively. This method can be used to explain the mass transfer experimental phenomena in CDPSEC very well. According to the calculated results, higher energy input is important to keep better dispersion of the droplets with suitable coalescence. In this situation, the local phase separation fraction of the dispersed phase is less than 10%, where the interface renewal effect can enhance the mass transfer efficiency in CDPSEC over PSEC. Lower energy input drives excessive coalescence of droplets, which leads the serious lowing of mass transfer efficiency in CDPSEC even worse than PSEC.

Acknowledgements

We acknowledge the support of the National Natural Science Foundation of China(20490200) on this work.

Symbols used

A	=pulse amplitude, (cm)
Ac	=cross-sectional area of upper settler, (m^2)
A_p	=cross-sectional area of partial settler, (m^2)
E	=diffusion coefficient of solute, (m^2/s)
f	=pulse frequency, (s'^1)
H	=height of dispersion band, (mm)
Hoc	=true' height of mass transfer unit, (m)
K	=parameter in Equation (1)
Q	=flow rate, (m^3/s or mL/s)
u	=superficial velocity, (m/s)
y	=parameter in Equation (1)
Greek symbols	
d>	= holdup of dispersed phase
Subscripts	
c	= refer to continuous phase
cal	= refer to calculated value
d	= refer to dispersed phase or upper settler
exp	= refer to experimental value
P	= refer to partial settler

References

1. Chartres, R. H., Korchinsky, W. J., "Modelling of liquid-liquid extraction columns: Predicting the influence of drop size distribution", *Trans. Inst. Chem. Eng.,* 53, 247-254 (1975)
2. Cruz-Pinto, J. J., Korchinsky, W. J., "Experimental conformation of the influence of drop size distribution on liquid-liquid extraction column performance", *Chem. Eng. Sci.,* 35, 2213-2219 (1980)
3. Katsuroku Takahashi, Ahmed Abdel-Sattar Abdel-Tawab, Susumu Nii; Toshihiro Yajima, Fumio Kawaizumi, "Extraction of Rare Earth Metals with a Multistage Mixer-settler Extraction Column", *Chem. Eng. Sci.,* 57, 469-478 (2002)
4. Rouyer, H., Lebouhellec J., Henry E., Michel P., "Present study and development of extraction pulsed columns", In: *Proceedings of Int. Solv. Extn. Conf. (ISEC'74),* Jeffreys, G. V., ed., Soc of Chem. Ind., London, UK (1974).
5. Lei, X., Dai, Y.Y., Shen, Z.Y., Wang, J.D., "Study on tow-phase flow characteristics and mass transfer in pulsed column with dispersion-coalescence type cartridge", In: *Proceedings of CIESC/AICHE Joint Meetings of Chem. Eng.,* Chemical Industry Press ed., Beijing, China (1982).
6. Li, H. B., Luo, G.. S., Fei, W. Y., Wang, J. D., "Mass transfer performance in a coalescence-dispersion pulsed sieve plate extraction column", *Chem. Eng. J.,* 78(2-3), 225-229 (2000).
7. Luo G. S., Ph.D. Thesis, Tsinghua University, Beijing (1993)
8. Li H. B., Ph.D. Thesis, Tsinghua University, Beijing (1999)
9. Gourdon C., Casamatta G.., "Population balance based modelling of solvent extraction column", In: *Liquid-Liquid Extraction Equipment,* Godfrey J. C., Slater M. J. eds, John Wiley & Sons, Chichester (1994)
10. Ban Takahiko, Fumio Kawaizumi, Nii Susumu, Takahashi Katsuroku, "Study of drop coalescence behavior for liquid-liquid extraction operation", *Chem. Eng. Sci.,* 55, 5385-

5391 (2000)
11. Tobin T., Ramkrishina D., “Modelling the effect of drop charge on coalescence in turbulent liquid-liquid dispersions”, *Can. J. Chem. Eng.,* 77, 1090-1104 (1999)
12. Rommel W., Meon W., Blass E., “Hydrodynamic modeling of droplet coalescence at liquid-liquid interface”, Sep. *Sci. & Tech.,* 27, 129-159 (1992)
13. Simon M., Stephan A., Bart H., “The droplet population balance model-estimation of breakage and coalescence”, *Chem. Eng. & Tech.,* 26, 745-750 (2003)
14. Ryon A. D., Daley, F. L., Lowire R. S., “Scale-up of mixer-settlers”, *Chem. Eng. Prog.,* 55, 70-75 (1959)



THE INFLUENCE OF DIFFERENT TYPE SURFACTANTS ON THE RATE OF MASS TRANSFER IN LIQUID-LIQUID EXTRACTION

Javad Saien, Maryam Riazikhah' and Seyed N. Ashrafizadeh"

Department of Applied Chemistry, Graduate Faculty, Arak Branch, Islamic Azad University, Arak, Iran
'Department of Applied Chemistry, University of Bu-Ali Sina, Hamadan, Iran
"Department of Chemical Engineering, Iran University of Science and Technology, Narmak, Tehran, Iran

Single drop experimental data were obtained in the presence of three different types of surfactants, each of them with two solute mass transfer directions, for a range of drop size. The effectiveness of surfactants in reducing mass transfer was found to increase in the order: cationic < anionic < non-ionic. Adding contaminants with high concentrations causes a number of small drops to demonstrate rigid behavior. The rate of mass transfer for dispersed to continuous phase direction is greater in all cases. A combined mass transfer coefficient can be used to describe the variations of mass transfer coefficient with the aid of an empirical coefficient, which was developed here.

INTRODUCTION

Although a great deal of effort has been made to identify the range and mechanisms of mass transfer in the presence of surfactants, no consistent conclusion has been drawn in a systematic way. It is still promising to use mass transfer data from single drops in conjunction with a hydrodynamic model.

The change in interfacial movement due to the gradient of interfacial tension along the drop surface has been studied and a model named “interfacial tension variation model” has been offered in a series of works beginning by Lochiel [1], Considering the relationship between interfacial tension and contaminant concentration, an equation has been derived for the continuous phase Sherwood number, in which the effect of contamination is included. Slater and Hughes [2] and Slater [3] have proposed using the ratio of average surface to terminal velocities to link the effect of contamination in continuous and dispersed phases. In this way a “combined mass transfer model” has been provided and has been used by a number of authors [4, 5], In their works, sodium dodecyl sulphate (SDS) has been used as contaminant in mass transfer direction of dispersed phase to continuous phase.

In the present work, the influence of three types of surfactants (as contaminants) on the rate of mass transfer of different drop size was studied. Both directions of mass transfer were applied. This subject, i.e. the influence of mass transfer direction on the retarding effect of contamination, has not been investigated yet. The combined mass transfer coefficient model was assessed in accordance with results to find its adequacy for these conditions.

EXPERIMENTAL

The chemical system of toluene-acetone-water was chosen as a result of high accuracy and repeatability in using GC for analysis. The European Federation of Chemical Engineering (EFCE) [6] has recommended this system. The main specification of this system is its high interfacial tension. Toluene and acetone were Merck products with purities of greater than 99% and 99.5% respectively. Distilled and de-ionised water was produced from a new still and was used for continuous phase. Three different surface-active agents have been used to investigate the influence of different type contaminants: sodium dodecyl sulfate (SDS), dodecyl trimethyl ammonium chloride (DTMAC), and octylphenol decaethylene glycol ether (Triton X-100). These are anionic, cationic and non-ionic surfactants and are products of Merck, Fluka and Merck with purities of more than 99%, 99% and 99.5%, respectively. Each surfactant was used in both mass transfer directions.

The average (with respect to solute concentration) physical properties of the chemical system at 20 C were considered. The physical properties were measured using a self-adjustable temperature density-meter (Anton Parr DMA 4500), a calibrated automatic ring method tensiometer (Sigma 70) and an Ostwald viscometer. Because of the sensitivity of mass transfer equations to the viscosity, this property was measured for continuous phase (surfactants are added to this phase) at the appropriate concentrations. The viscosity of aqueous phase increases by adding surfactants, having a significant variation for SDS. Organic and aqueous molecular diffusivities were applied from those reported by Baldauf and Knapp [7],

A Pyrex glass column was used with different glass nozzles located at the bottom. The toluene phase was held in a glass syringe conducted by an adjustable syringe pump. Each drop size formed at the nozzle tip was influenced by surfactant concentration due to the changing interfacial tension. Experiments were carried out in both mass transfer directions. Mass transfer direction from continuous to dispersed phase provides larger drop sizes. Variation in drop size was achieved by using glass nozzles with different tip diameters.

In order to omit the influence of unsteady mass transfer during drop formation, the initial drop concentration was considered to be at a location of 6.5 cm above the nozzles' tip, since drops are assumed to reach steady movement after this distance. The appropriate concentrations were determined using a short column under same conditions and drop size of the main column.

A small inverted glass funnel attached to a pipette and vacuum bulb was used to catch a sample of 1 to 2 mL of dispersed phase at top of the column with 31.2 cm distance from initial point. Two or three samples were prepared for each concentration and were kept at a cold medium until GC analyzing. The contact time of drops from the initial concentration point to the collection point was measured several times with a stopwatch. Terminal velocity of drops was obtained with respect to these times.

Analysis of acetone in obtained samples was carried out using a GC calibrated with reference substances of toluene and acetone (Merck) for gas chromatography.

THEORETICAL

The range of drops used in this work is within the conditions of circulating drops since the values of dimensionless group *H,* defined by Grace et al. [8] are in the range 11.6- 39.3, i.e. $2 < H < 59.3$ unless the presence of contaminants change them to rigid behavior.

When a drop moves in a contaminated solution, contaminant molecules that adsorb on the interface are convected toward the rear of the droplet, where they reduce the local interfacial tension. At the leading pole of the drop, the contaminant concentration is lower and thus, the local interfacial tension will be higher than those of the surroundings. As a consequence, the mass transfer rate will be decreased. Lochiel and Calderbank [9] developed a model describing the transfer of solute around a spherical drop when the Schmidt number is large (Sc >> 1), in the form:

$$Sh = -\frac{}{-wr} a^{0.5} \mathrm{Re}^{05}\, Sc^{05} \qquad (1)$$

where $a = V_j / V_t$ is the ratio of averaged tangential velocity component at the interface to the terminal velocity, $\mathrm{Re} = p_c V,d / p_c$ is the drop Reynolds number and $Sc = p_c / p_c\, D_c$ is the Schmidt number for the continuous phase.

For contaminated chemical systems, Lochiel [1] assumed that the adsorption of contaminants at the interface provides a contamination concentration gradient. This gradient will provide a tangential velocity gradient at the interface with respect to polar angle, relative to the axis of drop movement. A model like Equation (1) was derived including the parameter, *m,* named by Slater [3] as the "contamination factor", to be determined by fitting:

$$\alpha = \frac{V_i}{V_:} = 1 - \frac{2 + 3\frac{\mu_d}{\mu_c} + m}{\left(\quad\right)_{\backslash 0.5\ r>\ 0.5}} \times \frac{1.45}{1 + \left(\frac{MU'\,\mathrm{Re}}{\vee PcVc\ J}\right)} \qquad (2)$$

Slater [2] proposed an alteration to equation of *a,* to extend the range of usefulness of this equation to a wide range of Reynolds number, using the approximation: $a = 1 - x = (1 + x)^{-1}$ (valid at low values of *x*).

For mass transfer inside a drop, the well-known "Newman equation" is frequently used which is based on the diffusion equation in the spherical drops and in spherical co-ordinates:

$$k_d = \frac{-d}{61} \ln\left[\frac{6}{\pi^2} \sum_{n=1}^{\infty} \frac{1}{n^2} \exp\frac{-4\ 7[^2 n^2 Dt}{d^2}\right] \qquad (3)$$

where *d* is drop size, *t* is contact time and *D* is molecular diffusivity.

It has been attempted to describe the effect of contamination in both phases with a single parameter. This has an industrially significant interest. In this regard and as the "combined model", Slater and his co-workers have used the contribution of effective diffusivity based on that used by Handlos and Baron [10]:

$$D_e = \frac{dv,}{2048(1 + \kappa)} \qquad (4)$$

where $K\text{-}p_d/p_c$ and the molecular diffusivity have been used to give overall effective diffusivity in the form:

$$D_{oe}=D + ccD_e \quad (5)$$

This D_{oe} is used in Equation (3) instead of *D.* So, the term **or,** which represents the effect of interfacial tension gradient together with the retardation effect of contamination, is also applied to the drop side mass transfer coefficient and both coefficient are linked in this way.

Whitman two-film theory is used to add the individual mass transfer resistance in continuous and dispersed phases obtained from appropriate equations and the overall mass transfer coefficient is calculated.

The empirical equation given by Steiner [11] is used to check if drops reach the rigid conditions by adding the contaminants:

$$Sh_r = 2.43 + 0.775\mathrm{Re}^{05}\, Sc^{033} + 0.0103\ \mathrm{Re}\ \text{„}\mathrm{Sc}^{\circ 33} \quad (6)$$

RESULTS AND DISCUSSION

Experimental data series including initial and final concentrations, drop size and contact time were obtained for each mass transfer direction. The experimental overall mass transfer coefficient values are calculated using:

$$K_{od}=\sim Ml\text{-}\frac{d}{6/} \quad (7)$$

where *t* is the contact time and *E* is the extraction fraction, defined by:

$$E = \frac{\text{k } d\text{f}\text{L}\ d,}{C_d^* - C_{di}} \quad (8)$$

where C_a , C_{df} and C_d are the initial, final and equilibrium solute concentrations in drop phase, respectively. For d —> c mass transfer direction C_d is zero, since the solute concentration in the aqueous phase is zero for this case.

Figure 1 shows the variation of overall mass transfer with contaminant concentration typically. The overall mass transfer coefficient decreases rapidly with low amounts of surfactant and reaches nearly a constant value at concentrations from about 12 mg/L depending on the type of surfactant and the drop size. The order of effectiveness of surfactants, acting as contamination increases in the order: DTMAC < SDS < Triton X-100. Chen and Lee [12] have used these surfactants for the chemical system of carbon tetrachloride - acetic acid - water. In their work, the effectiveness of SDS and Triton comes close together with minor effects on the mass transfer coefficient for concentrations greater than about 10 mg/L; however, for the lower concentration, the order of effectiveness is in agreement with the results of our work.

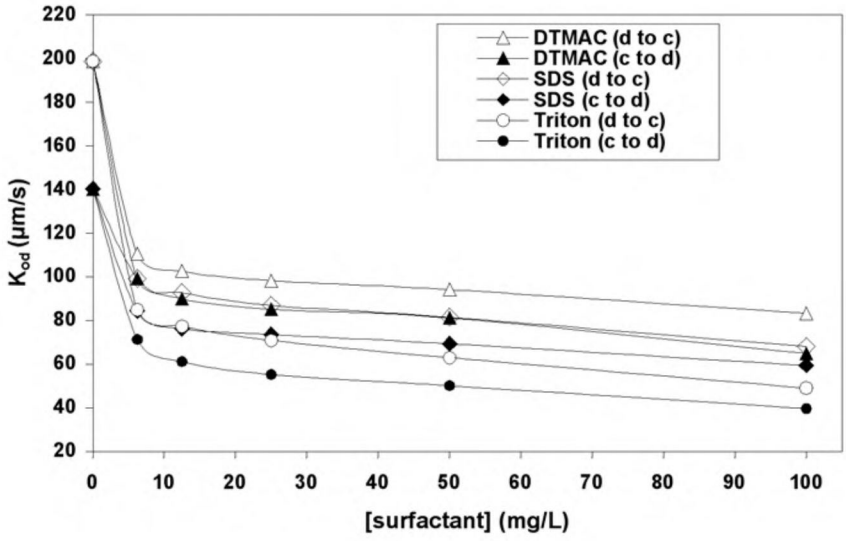


Figure 1. Typical variation of overall mass transfer coefficient with contaminant concentration.

As Figure 2 shows typically, the mass transfer coefficient increases with drop size. Adding contaminants has not changed the trend of increasing with drop size. Similar variation is observed for other contaminant concentrations. Drops tend to higher circulation with increasing their size and enhancing mass transfer.

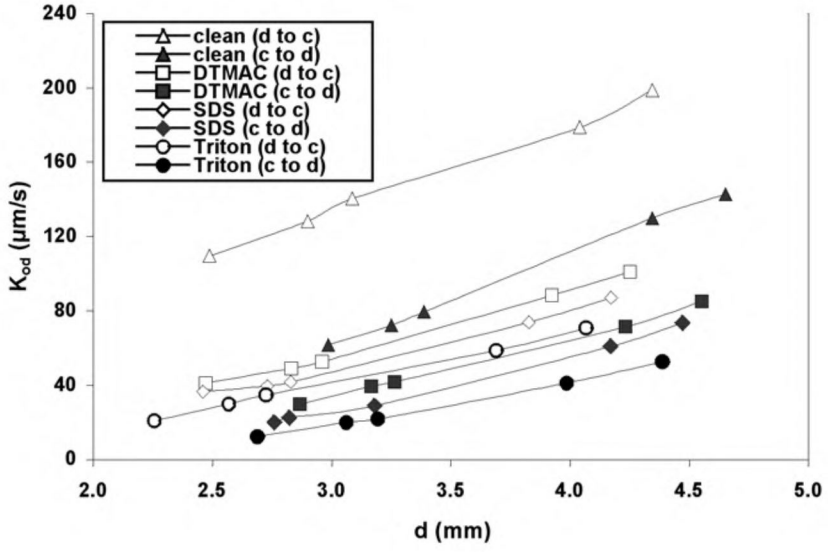


Figure 2. Variation of overall mass transfer coefficient with drop size for surfactant concentration of 25 mg/L.

From Figures 1 and 2 it is obvious that the mass transfer coefficient is greater in d—>c direction for all cases under similar conditions. When investigating the difference between two mass transfer directions, the variation of contact time (hydrodynamic term) and extraction fraction (mass transfer term), included in Equation (7), is useful. Both the contact time and the extraction fraction are higher for d->c direction; however, the influence of extraction fraction is dominant.

The mass transfer model, described above, was applied in accordance with the experimental conditions. The appropriate *a* values were first obtained by adjusting its value until measured and calculated overall mass transfer coefficients agree while everything else is fixed.

The values of *a* required to fit the combined model to experimental data are significantly less than 1 for contaminated systems; thus the alteration proposed by Slater [3] for using the modified Lochiel's equation is not consistent for conditions used in this work.

Some *Kod* values lie below the rigid drop limit at high concentrations of contamination, i.e. *Sh* becomes lower than Sh_r (Equation 6) for them. The number of these drops is more in the c—>d direction, due to the lower mass transfer coefficient.

The trend of variation of *a* versus surfactant concentration and drop size is nearly similar to the variation of K_{od} with the appropriate variables. Dependence on drop size implies dependence on contact time, during which the surface adsorption of the contaminant is continued.

The variation of *a,* under conditions studied, is contributed by the non-linear influences of contaminant concentration (c) and drop size (d). As a simplified correlation, applicable in the combined model, the data are nicely reproduced with:

$$a = \text{ar}, + a_2 c^{n'} + \text{a}_3\text{c}/'' : \qquad (9)$$

to be fitted with experimental data. In this equation $a_{;}$, a_2, a_3, n_1 and n_2 are the parameters. Due to the different level of *a* values for each mass transfer direction and different physical properties for different surfactant types, each series of data were processed separately. The model needs the parameters to be found from experimental results; however, it has the advantage that no mathematical assumption is included and is consistent with both mass transfer directions in the present of different contaminants.

The appropriate obtained values of parameters along with the regression coefficients are given in Table 1, where c is in mg/L and *d* in mm. Equation 10 with the appropriate parameters in Table 1 is applicable for circulating drops when moving in aqueous medium, contaminated with one of the surfactants.

Table 1. Parameters of the Equation (9).

mass transfer direction	surfactant	*ai*	a_2	tfjXIO^3	*ni*	*02*	R^2
d —»c	Triton	-1.051	1.421	6.512	-0.086	2.701	0.98
	SDS	-0.612	1.092	8.489	-0.148	2.678	0.97
	DTMAC	-0.671	1.120	7.812	-0.132	2.865	0.98
c—»d	Triton	-0.471	0.639	6.12	-0.129	2.591	0.98
	SDS	-0.503	0.702	6.511	-0.113	2.588	0.98
	DTMAC	-0.381	0.711	7.014	-0.227	2.738	0.96

Applying the combined model with the help of Equation (9) provides *Kod* values that have relative deviations within ± 8.5% for most of the experiments in both mass transfer directions. This deviation is thought to be sufficient considering an experimental error of approximately

5% in K_{od} values. The combined model in its new form can therefore be used satisfactory to predict the overall mass transfer coefficient.

REFERENCES

1. A. C. Lochiel (1965), *Can. J. Chem. Eng.,* 43, 40-44.
2. M. J. Slater, and K. C. Hughes in *"Proc. Int. Solvent Extraction Conf. ISEC 93,* York, (1993), D. H. Logsdail and M. J. Slater, Eds., Elsevier Applied Science, London.
3. M. J. Slater (1995), *Can. J. Chem. Eng.,* 73, 462-469.
4. J. S. Ghalehchian and M. J. Slater (1999), *The Chem. Eng. J.,* 75, 131-144.
5. M. J. Brodkorb, D. Bosse, C. von Reden, A. Gorak and M. J. Slater (2003), *Chem. Eng. Proc.,* 42, 825-840.
6. T. Misek (1978), Pub. Instn. Chem. Engs, for EFCE,.
7. W. Baldauf and H. Knapp Ber. Bunsenges. (1983), *Phys. Chem.,* 87, 304-309.
8. J. R. Grace, T. Wairegi and T. H. Nguyen (1976), *Trans. Inst. Chem. Eng.,* 54, 167-174.
9. A. C. Lochiel and P. H. Calderbank (1964), *Chem. Eng. Sci.,* 19, 471-484.
10. A. S. E. Handlos and T. Baron (1957), *AIChE J.,* 3, 127-136.
11. L. Steiner (1986), *Chem. Eng. Sci.,* 41, 1979-1986.
12. L. H. Chen and Y. L. Lee (2000), *AIChE J.,* 46(1), 160-168.



MASS TRANSFER OF CONTAMINATED HIGH INTERFACIAL TENSION LIQUID-LIQUID EXTRACTION SYSTEMS IN AGITATED CONTACTORS

Javad Saien and Ali Darayi*

Department of Applied Chemistry, Graduate Faculty, Arak Branch, Islamic Azad University, Arak, Iran
'Department of Applied Chemistry, University of Bu-Ali Sina, Hamadan, Iran

The liquid-liquid extraction process is usually accompanied with a level of contamination in chemical system and processing in agitated equipments. In this work, the influence of contamination and agitation was investigated for the chemical system of toluene-acetone-water with a high interfacial tension. Surfactant was added to the continuous phase. A pilot rotating disc contactor was used providing a uniform agitation. An improvement was made on a combined mass transfer model to be consistent with experimental data without mathematical assumption and a correlation was proposed for the coefficient of this model.

INTRODUCTION

The contamination of chemical systems and agitation of contactors have influence in the rate of mass transfer of single drops. Two separate attempts on theoretical study of the effect of contamination, as the more important factor are developing the stagnant cap model and the interfacial tension variation model.

In the preferred model of interfacial tension variation, a continuous interfacial tension gradient on the surface is considered while the contaminants are present. The continuity equation with shear stress balance at the interface and the analysis of tangential velocity is applied. Considering the relationship between interfacial tension and contaminant concentration, a model is proposed for continuous phase Sherwood number.

There is a need in most industrial mass transfer systems to have a single quantitative description of contamination; i.e. the drop phase could be described using the same criterion of contamination as for the continuous phase. Otherwise, each phase can provide a separate value for the contamination level. In this regard, it has been proposed [1,2] using the ratio of average surface to terminal velocities to link the effect of contamination in continuous and dispersed phases. A number of investigations, on the other hand, have been concerned with the mass transfer coefficient around drops in agitated systems. The objective of this work is to investigate the influence of agitation on the mass transfer rate in the presence of contamination and to correlate mass transfer coefficient based on obtained data using a combined model, without mathematical assumptions. The proposals made here involve keeping the main form of the models, with reference to interfacial tension variation.

EXPERIMENTAL

A rotating disc contactor in a Pyrex glass column was used. The internal diameter of the column is 114 mm with 7 stages, each stage 45 mm height, rotor diameter 69 mm, stator diameter 87 mm, shaft diameter 16 mm, and stator and rotor thickness 3 mm. An electric inverter adjusted the rotation speed of the agitation motor. All internals are made of stainless steel and all valves and pipe-work are of glass, PTFE and stainless steel.

Single drops of dispersed phase were produced from nozzles located at the bottom of the column. Variation of drop size has been achieved by changing glass nozzles with different tip diameters. The dispersed phase was held in a glass syringe fed by an adjustable syringe pump and flowed to the nozzle in the stationary continuous phase to produce single drops. The pump delivers a constant flow-rate for each nozzle. A small inverted glass funnel attached to a pipette and vacuum bulb was used to catch the samples of dispersed phase at the level of collection point, just above the top stage.

The high interfacial tension, toluene-acetone-water chemical system, recommended in the EFCE document [3] was used. It has the advantage of high accuracy and repeatability in using GC for analysis. Distilled water was used as the continuous phase while the droplet phase was toluene. Toluene and acetone with purities of more than 99% and 99.5%, respectively were used. Because of the sensitivity of equations to the viscosity, this property was measured for continuous phase at the appropriate concentrations of added contaminant.

Experiments were carried out in the mass transfer direction of dispersed to continuous phases. Acetone with a concentration of about 5 g/L was dissolved in droplet organic phase. Sodium dodecyl sulphate (SDS), usually used as the contaminant agent, was added to continuous phase with concentrations from 6.25 to 100 mg/L. Toluene drop sizes ranging from 2.71 to 4.20 mm were generated. Due to the decrease in interfacial tension by addition of surfactant, drop size and terminal velocity change, depending on the amount of surfactant and thus these values were measured whenever a new amount of SDS was added.

The range of agitation speed used, is within 15-60 rpm. This range remains in the laminar region with $Re_{jV} < 1.6 \times 10^4$ [4], Higher speeds of agitation cause radial motion of drops and problems in collecting drops, during sampling. Drops move through the rotor / stator gap and a sample of about 1 mL of dispersed phase was caught. Two samples were prepared for every concentration and were kept at cold medium until GC analyzing.

In order to avoid the influence of unsteady mass transfer during drop formation, the initial drop concentration was considered for a location of moving drops at 6.5 cm above the nozzle tip, just below the first stator. To determine this initial concentration, an empty and small column with nozzle location at the bottom was used under the same concentrations and drop sizes of the main column. Sampling in this column was carried out with the same procedure at the same distance from nozzle tip. The ambient temperature was 20 ± 2 °C.

THE COMBINED MASS TRANSFER COEFFICIENT MODEL

It has been attempted to describe the effect of contamination in the mass transfer coefficient of both phases with a single parameter. This has an industrially significant interest especially when the resistance exists in both phases. For clean chemical systems, Lochiel and Calderbank [5] developed a model that describes the transfer of solute around a spherical drop when the Schmidt number is large (Sc>>1).

Lochiel [6] assumed that the adsorption of contaminants at the interface provides a contaminant concentration gradient. This gradient will provide a tangential velocity gradient at the interface with respect to polar angle, relative to the axis of drop movement. A model containing the quantitative effect of contamination was obtained:

$$Sh = \frac{2}{\sqrt{\pi}} a^{0.5}\ \mathrm{Re}^{05}\ Sc^{05} \qquad (1)$$

where:

$$\alpha = \frac{V_i}{V_t} = 1 - \frac{2 + 3\frac{\mu_d}{Mc} + m}{1 + \left(\frac{' Pdf^*_d}{K\ PcPc\ j}\right)^{-05}} \times \frac{1.45}{\mathrm{Re}^{05}} \qquad (2)$$

in which *m* is a dimensionless positive parameter, named by Slater [2] as "contamination factor" and represents the level of contamination. It is a function of some physical properties such as surface and bulk diffusivity of contaminant, film thickness and parameters for adsorption of contaminant. Due to difficulties in measuring these properties, the value of parameter *m* is usually determined from experimental data.

Equations (1) and (2) is suitable for high Reynolds numbers and low contamination factor values. It can fail at low drop Reynolds numbers (order of 10) giving negative values. Slater [2] proposed an alteration to Equation (2) in order to extend the range of this equation's validity where Reynolds number is about 1< Re <1000 , using an approximation:

$a = 1 - x = (1 + x)^{-1}$, valid at low values of *x.*

For mass transfer in drops, the well-known "Newman equation" which is based on the diffusion equation in spherical coordinates, without continuous phase resistance, is generally used:

$$k_d = \frac{-d}{6} \ln\left[\frac{6}{\pi^2} \sum_{n=1}^{\infty} \frac{1}{n^2} \exp\left(\frac{-4\pi^2 n^2 Dt}{d^2}\right)\right] \qquad (3)$$

In this regard, a number of investigators [2,7,8] considered the contribution of effective diffusivity (D_e) derived by Handlos and Baron [9] and the overall diffusivity, D_{oe}, is given in the fornrD^ =*D* + *aD*$_e$. This D_{oe} is used in Equation (3) instead of *D.* The term *a,* which represents the effect of interfacial tension gradient together with the retardation effect of contamination, is also applied to the drop side mass transfer coefficient and the effect of contamination is linked to both film coefficients, providing the "combined mass transfer model". The term *a* was used in its modified form. Whitman's two-film theory is used to combine the mass transfer resistances to obtain the overall mass transfer coefficient.

RESULTS AND DISCUSSION

One hundred and thirty experimental data series were obtained. The experimental values of K_{od} are calculated by:

$$Kod = -4 - M^{-F)} \qquad <4>$$

where / is the contact time, and *E* is the extraction fraction, defined by:

$$E = \frac{C_{dm} - C_{dout}}{C_{dm} - C^{*}_{d}} \qquad (5)$$

for dispersed to continuous mass transfer direction.

There is a good agreement between measured terminal velocity and those predicted by Grace *et al.* [10]. For a specified drop size in the circulating region, the interfacial tension has no significant effect on terminal velocity. It is because all the drops in this work remain in the range of circulating; since the values of dimensionless group *H* defined in Grace's model are in the range of 11 - 30, i.e. 2<H<59.3. The drop Weber numbers *{We)* is also less than 3.58.

The overall mass transfer coefficient increases with drop size and tends to be constant values for large drops. Addition of SDS surfactant, on the other hand, resulted in significantly lower values of overall mass transfer coefficient. Recently, Brodkorb *et al.* [8] have shown similar behavior under non-agitated operation. Mass transfer coefficient increases with agitation even in the presence of contamination. This could be due to the mass transfer enhancement in the continuous phase by agitation. Providing agitation, within the range used, helps to the mass transfer to increase by more than 77% even with contaminant.

The combined mass transfer model proposed by Slater [2] was considered, the values of *a* were first calculated from Equation (2) when *m* is zero. This equation gives *a* values in the range: 0.105-0.957, most of them much less than 1, while drops behave circulating. The values will become smaller if a positive value for *m* is considered. Thus, application of the alteration proposed to the Lochiel's equation is not consistent.

In order to obtain more realistic and consistently positive values of **or,** it is proposed here to apply a correction factor to *a* in the equation by Lochiel and Calderbank [5] for clean chemical systems:

$$a = F\left[1 - \frac{2 + 3\kappa}{' + (PjPd/Pc\ Mc)^{\circ'5}\ \mathrm{Re}} \times \frac{1.45}{0.5}\right] \qquad (6)$$

The significance of *F* is that it is a factor that represents how the ratio of interfacial velocity to the drop terminal velocity *{a)* is changed due to contamination and agitation.

The coefficient *F* was determined by adjusting its value until measured and calculated overall mass transfer coefficients agreed while the other parameters were fixed. Generally, the values of *F* are closer to 1 for large drops and cleaner chemical systems; i.e. the combined model predicts a good agreement of K_{od} for them; however, For most of the experiments, the values of *F* are lower than 1 which means that the model predicts high values of K_{od}.

Examination of the obtained values of *F*, reveals that this coefficient varies with drop size, contaminant concentration and agitation speed. The influence of agitation could lead to the variation in K_{od} due to mass transfer enhancement in continuous phase. Drops move in longer paths through the column with increase of agitation; so, the dependence on agitation could be related to the contact time during which the adsorption of contaminant is continued.

The parameter *F* is considered as a function of drop Reynolds number, rotor Reynolds number (Re^) and fractional surface coverage (C_s/Cj). The latter term is the ratio of contaminant concentration at the surface of drops to its saturation value which are determined from the variation of interfacial tension with SDS concentration according to the Gibbs adsorption equation:

$$C_S = \frac{-d\gamma / d\ln C_B}{2RT} \qquad (7)$$

for charged films in the absence of inorganic salts (assuming activities equal to 1.0). C_s and C_B are the surface and bulk concentration of contaminant in continuous phase respectively. The values of C_s are assumed equilibrium values and a maximum value of the slope of plot of *y* against lnC^ may be presumed to give a "saturation value", *c;* [in.

As a typical variation, Figure 1 shows that *F* increases toward 1 with increasing drop Reynolds number under constant agitation and contamination level; i.e. the combined model predicts a better rate of mass transfer for larger drops. Since the effect of contamination in the combined model appears only through theF, therefore by increasing surfactant, lower values of this coefficient is required (Figure 2). Increasing agitation, on the other hand, causes higher contact times for drops. Increasing time (/) in Equation (6) reducesk_d \ nevertheless, *F* still varies like the variation of K_{od} with agitation. Figure 3 shows that the variation is almost linear.

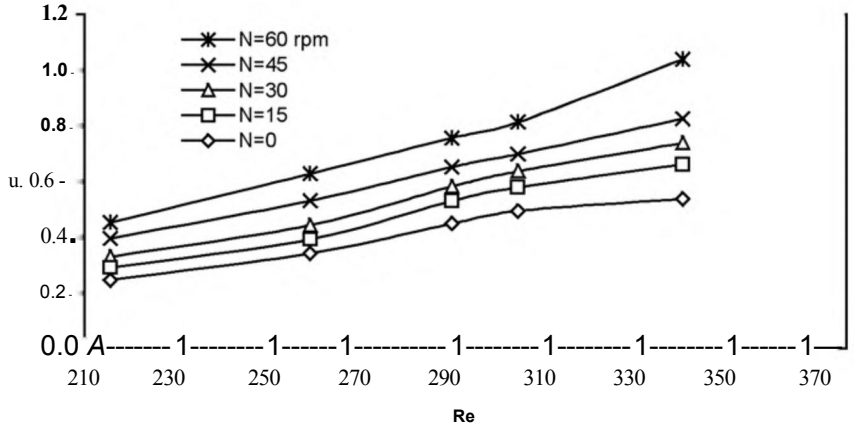


Figure 1. Typical Variation of F with drop Reynolds number. SDS concentration of 12.5 mg/L

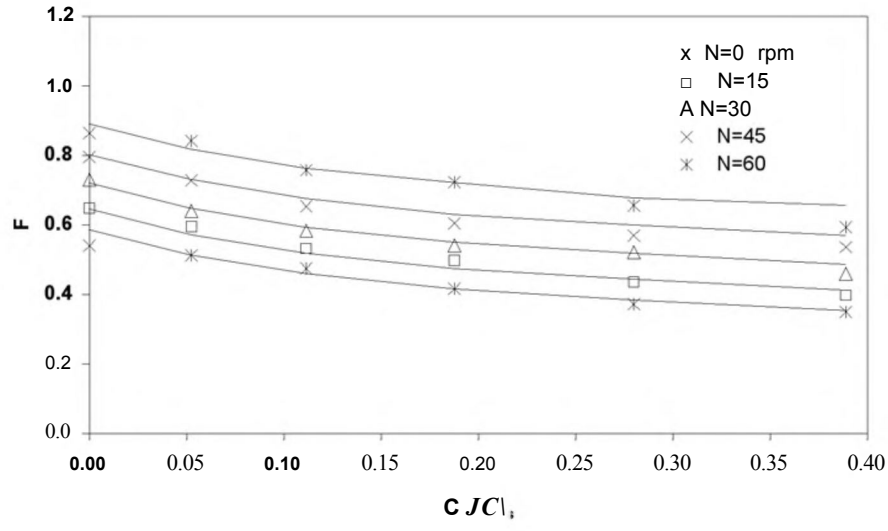


Figure 2. Typical variation of F with contaminant surface concentration. The solid lines are the correlated values.

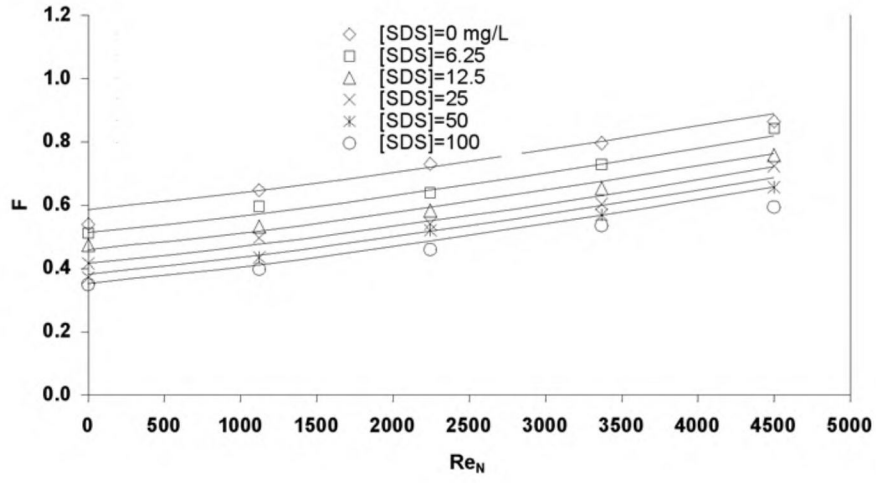


Figure 3. Typical variation of F with rotor Reynolds number. The solid lines are the correlated values.

The above investigation shows that similar to contamination factor, *m,* the coefficient *F* is dependent on physical properties and drop size (through Re and C_s/Cj). The alternative influence of agitation, found in this work, proves that agitation speed (through Re_w) should also be considered.

A procedure was performed for regression of data using the non-linear multivariable regression method. The correlation obtained is:

$$F = 4.52 \times 1(T^5\ Re^{1598} + 1.50 \times 10\sim^5\ (1 + Re_N)'^{179} + 0.1704(1 + C_s / C'_s)''^{4476} \quad (8)$$

with a maximum deviation of ±16% (three experiments with ±19%). The applicability of the above model is limited to the range of variables; i.e. within the approximate ranges of Re:

220 - 350; Re_{jV}: 0 - 4500 and C_s/Cj : 0 - 0.4. The power of the contamination term is higher; due to significant changes at low C_s/C^*_s values and that the mass transfer rate has the most sensitivity to this parameter.

The new combined model with the use of Equation (8) was used to calculate K_{od} with the appropriate operating conditions. The relative deviations are within the range ±6.9% (six experiments within ±9.3%). As it is expected, small drops in the high-contaminated systems provide the highest deviations. The proposed combined model therefore, is able to correlate the data, without using the mathematical assumption and includes the effect of agitation that was not incorporated in earlier works.

CONCLUSIONS

The experimental results showed that agitation in the extraction process can compensate a significant part of the retarding effect of contamination. The simultaneous effect of contamination and agitation in the extraction process can be included in a combined mass transfer model without simplified mathematical assumptions and having consistency with experimental data. The combined model itself has the highest level of agreement for large drops with low contaminant concentrations; however, to apply the model in accordance with other operating conditions, an empirical coefficient for the ratio of surface velocity to terminal velocity of drops is utilized. From experiments carried out for mass transfer with a wide range of drop size, mild agitation and usual contaminant concentration, a correlation is proposed for this coefficient. The model can be used for prediction and design purposes of high interfacial tension chemical systems for extraction.

REFERENCES

1. M. J. Slater and K. C. Hughes (1993), Proceeding of ISEC 93, Vol. 2, 1238-1245.
2. M. J. Slater (1995), *Can. J. Chem. Eng.,* 73, 462-469.
3. T. Misek (1978), Pub. *Instn. Chem. Engs,* for EFCE.
4. V. Cauwenberg, J. Degreve and M. J. Slater (1997), *Can. J. Chem. Eng.,* 75, 1046-1055.
5. A. C. Lochiel and P. H. Calderbank (1964), *Chem. Eng. Sci.,* 19, 47-484.
6. A. C. Lochiel (1965), *Can. J. Chem. Eng.,* 43, 40-44.
7. J. S. Ghalehchian and M. J. Slater (1999), *The Chem. Eng. J.,* 75, 131-144.
8. M. J. Brodkorb, D. Bosse, C. von Reden, A. Gorak and M. J. Slater (2003), Chem. Eng. Proc., 42, 825-840.
9. A. S. E. Handlos, and T. Baron (1957), *AIChE J.,* 3, 127-136.
10. J. R. Grace, T. Wairegi and T. H. Nguyen (1976), *Trans. Inst. Chem. Eng.,* 54, 167-174.
11. M. J. Slater, M. H. I. Baird and T-B. Liang (1988), *Chem. Eng. Sci.,* 43, 233-245.



EVALUATION OF A LEACH-ZINCEX™ SX PROCESS FOR THE RECOVERY OF ZINC FROM ACCUMULATED ELECTROLYTIC ZINC REFINING RESIDUES AT ZINCOR

EHO Meyer[1], GH Howard[1], NM Vegter[1] (Kumba Resources Limited), WH van Niekerk [2](Zincor), G Diaz, MA Garcia, F Sánchez [3](Tecnicas Reunidas)

[1] Kumba Technology - A Division of Kumba Resources Ltd., P O Box 9229, Pretoria, 0001, South Africa (email: gavin.howard@kumbaresources.com)
[2]Zincor- A Division of Kumba Base Metals Ltd., P O Box 218, Springs, 1560, South Africa (email: willem.vanniekerk@kumbaresources.com)
[3] Técnicas Reunidas, S.A., C/Sierra Nevada, 16, 28830 - San Fdo. De Henares, Madrid Spain (email: gdiaz@tecnicasreunidas.com)

A dual need to remediate an existing zinc residue site as well as to build a new one at the Zincor refinery has prompted the development of a process to recover zinc within the intended rehabilitation exercise. At the core of the process lies optimal selective dissolution of zinc followed by concentration and recovery by ZINCEX™ solvent extraction technology licensed by Técnicas Reunidas to Kumba. A demonstration plant comprising a combined leach-iron oxidation step, followed by ZINCEX™ solvent extraction using D2EHPA as extractant, was operated at Anglo American Research Laboratories (AARL) for a period of 6 weeks. Its purpose was to expand the knowledge base and to provide invaluable information for the possible future large-scale implementation of the process. The piloting process pinpointed key processing parameters and confirmed the robustness of the ZINCEX™ solvent extraction technology for the specific application.

INTRODUCTION

The Zincor zinc smelter situated in Springs some 20 km east of Johannesburg in the Gauteng province of South Africa has been in operation since 1968. Prior to this date the infrastructure was used for the recovery of gold and uranium, which with cessation of mining operations was converted to a zinc refinery. In converting to a zinc refinery it was decided to carry on with residue deposition on top of the historical gold residues. This combined gold-zinc leach residue tailings is now approaching the end of its useful life with its maximum storage capacity being reached within the next two years. Consequently Zincor has been obliged to consider construction of a new residue disposal site.

With the need of having to build a new residue disposal site as well as rehabilitate the old residue site the feasibility of using a nearby mothballed gold carbon-in-pulp (CIP) plant as a sequential zinc ion exchange (IX) - gold/silver carbon-in-leach (CIL) process was studied in order to see if base and precious metals could be simultaneously recovered whilst performing an

environmental clean-up operation [1], However exciting the process initially appeared, further pursuit could not be justified as high operating costs, fuelled by resin degradation for zinc extraction, and lime and cyanide costs for gold and silver recovery, adversely affected key profitability criteria.

In a post study appraisal an alternative processing option consisting of hydraulic mining followed by mild leach and iron oxidation, and soluble zinc recovery using ZINCEX™ solvent extraction technology was explored. The process flowsheet is largely based on the Modified Zincex Process applied on zinc oxides as raw material [2],[5], - however in this case the overlying process objective would be to maximise zinc recovery under less aggressive leaching conditions whilst solubilising minimal amounts of iron from the contained iron within the residues.

Key financial modeling outputs from this exercise are illustrated in Figure 1 below where a comparison between the zinc ion exchange option versus a zinc solvent extraction option was conducted respectively for 11 and 20-year treatment periods [3], A sensitivity analysis on the best option indicated the profitability to be highly sensitive to CAPEX and zinc price. Table 1 provides a summary of this sensitivity analysis.

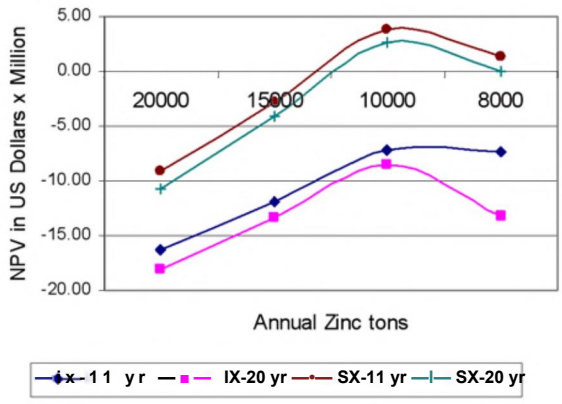


Figure 1. Net Present Value comparisons for residue reclamation options.

Table 1. Summarised results for a sensitivity analysis conducted on the 11 year SX option.

Variable	Change in Variable	Change in Net Present Value
CAPEX	-10%	+51.26 %
	+10%	-51.26%
OPEX	-10 %	+12.43 %
	+10%	-12.43 %
Zinc Price	-10%	-32.84 %
	+10%	+32.84 %

MOTIVATION FOR PILOTING

The Kumba Base Metals zinc extraction and recovery expertise is limited to operation of a zinc-lead concentrator at Rosh Pinah, Namibia, and zinc smelters at Springs, South Africa, and Chifeng, Inner Mongolia, China. In view of Kumba's limited exposure to SX it was deemed

necessary to pilot the leach-solvent extraction circuit as an integrated leach-SX unit in order to develop a primary knowledge base from which further decision making could be made with confidence.

In order to gain the necessary confidence in the process and technology the following would have to be demonstrated and understood :

- o Successful operation of an integrated leach-solvent extraction operation,
- o Selective zinc extraction and efficient impurity rejection,
- o Effect of leach and iron control on SX performance,
- o Operating and design parameter information.

PILOT PLANT

Suitable piloting facilities were identified at the Anglo American Research Laboratories (AARL) situated in Johannesburg. The facilities comprised a suitably sized leach-solvent extraction-electrowinning circuit complemented by a 24 hour/day analytical service.

Following scoping discussions a fit-for-purpose piloting flow sheet and analytical procedure was derived that covered all processing aspects from the blending of dry solids through to the output of residues, bleed solutions, loaded strip liquors and effluents. The downstream electrowinning step was excluded from the campaign as the specific focus was purely on the leach-SX integration aspect. The pilot plant flow sheet was constructed along the overall processing flowsheet as shown in Figure 2 below.

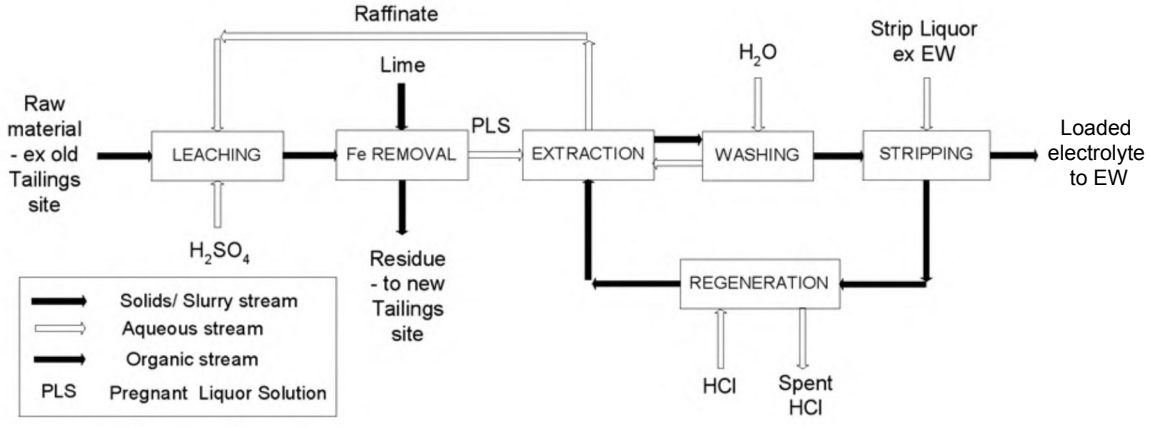


Figure 2. Simplified block flow diagram illustrating the integrated leach-solvent extraction circuit.

Contacting equipment in the leach and iron removal circuit consisted of a series of 150 to 200 liter stirred tanks equipped with air spargers, immersed heaters and pH control. Liquid-solid separation immediately following the leach and iron removal stage was undertaken via a 1,0 m diameter high-rate thickener followed by a 0.1 m^2 horizontal vacuum belt filter. Thickener overflow clarification was made possible with a 1.125 m^2 polishing filter test unit. Conventional mixers settlers with an active mixing volume of 32 litres and a settling area of 0.091 m^2 were used in the solvent extraction circuit. Immersion heaters were also inserted at selected points in the circuit for temperature control. Solution pumping was managed via the use of peristaltic

pumps. Flowrates of all streams entering the respective sections were measured manually and adjusted as necessary on an hourly basis.

LEACHING-IRON REMOVAL

The raw material arising from the Zincor tailings dam consists of a blend of ferritic zinc residues, iron precipitate residues and effluent treatment residues consisting of gypsum and basic zinc hydroxy-sulphates. Intermittent lesser amounts of gold residues contaminated with basic zinc sulphates will also be present and will also require treatment. The total tailings resource, including the gold tailings base is estimated to be 13,9 million tons. The treatable portion in the above-mentioned residues constitutes approximately 4 million tons. The average composition of raw material fed to the leaching step during the pilot campaign is shown in Table 2 below.

Table 2. Pilot plant feed material composition.

Zn(%)	Fe(%)	Ca(%)	Si(%)	Pb(%)	Al(%)	Mn(%)	Mq(%)
8.8	13.4	10.7	4.5	2.6	1.2	1.2	1.0

In the leaching process, tailings solids are contacted with raffinate over the pH range 3 to 4, - where zinc is dissolved by the raffinate which acts as the leachant. In the process it is important to ensure proper leach conditions are maintained so as to minimise iron and aluminium dissolution. Important chemical reactions involved in the leaching process, are shown below.

$$ZnS0_4.3Zn(0H)_2.4H_20 + 3\ H_2S0_4 \leftrightarrow 4\ ZnS0_4 + 10\ H_20 \quad (1)$$

$$2\ Fe(OH)_3 + 3\ H_2S0_4 <- Fe_2(S0_4)_3 + 6\ H_20 \quad (2)$$

$$2\ Al(OH)_3 + 3\ H_2S0_4 \sim Al_2(S0_4)_3 + 6\ H_20 \quad (3)$$

Pilot plant operation confirmed zinc leaching efficiency to be sensitive to pH control and raw material source. Under stable and optimised operating conditions, values of higher than 80 per cent were achieved.

The iron removal step consisted of a simultaneous air oxidation and pH adjustment of the post leach slurry pH to between 3,5 and 4,5 by using lime. Important chemical reactions involved in the iron removal process are the following.

$$2\ FeS0_4 + H_2S0_4 + 0.5O_2 \text{« } Fe_2(S0_4)_3 + H_20 \quad (4)$$

$$Fe_2(S0_4)_3 + 3\ Ca(OH)_2 + 3H_20 \text{«} 3\ CaS0_4.H_20 + 2\ Fe(OH)_3 \quad (5)$$

$$Al_2(S0_4)_3 + 3\ Ca(OH)_2 + 3H_20 \text{«} 3\ CaS0_4.H_20 + 2\ Al(OH)_3 \quad (6)$$

After the leaching and iron removal step a zinc PLS was obtained with compositional ranges as shown in Table 3.

Table 3. Pilot plant PLS composition.

Element and concentration	Minimum	Maximum	Element and concentration	Minimum	Maximum
Zn(g/l)	10	28	Si(mg/l)	27	178
Mg(g/i)	2.2	9.1	Al(mg/l)	80	190
Mn(g/l)	1.3	3.7	Cd(mg/l)	50	200
Ca (g/l)	0.5	0.62	Fe(mg/l)	5	15
Cu(g/l)	0.1	0.4	Co / Ni (mg/l)	3/3	19/23

EXTRACTION & WASHING STEPS

Zinc is extracted from the PLS by using D2EHPA (di-2-ethyl hexyl phosphoric acid) as the extractant reagent in an organic phase. This organic phase (RH) has a high affinity for zinc extraction atZINCEX™ conditions according to the reaction.

$$2\ (R\text{-}H)_{org} + (Zn^{2+})_{aq} \quad \text{«->} \quad (R_2Zn)_{org} + 2\ (H^{+})_{aq} \quad (7)$$

The organic phase exiting the extraction stage includes traces of impurities, mainly consisting of aqueous phase entrainment and a minimum quantity of co-extracted impurities. In the washing stage the organic phase is thoroughly cleansed by means of a water solution so as to avoid any impurities reporting to the stripping stage. The pilot plant results demonstrated the selective extraction of zinc from the PLS and rejection of the main impurities. Average composition of the raffinate solution obtained, is shown in Table 4 below.

Table 4. Pilot plant Raffinate composition.

Element and concentration	Average	Element and concentration	Average
Zn(g/l)	7,7	Si(mg/l)	91
Mg (g/l)	6.6	Al(mg/l)	80
Mn(g/l)	2.1	Cd(mg/l)	134
Ca(g/l)	0.55	Fe(mg/l)	5
Cu(g/l)	0.17	Co / Ni (mg/l)	18/23

STRIPPING & REGENERATION STEPS

As the main objective of the process is to produce a high purity zinc solution for electrowinning, it was decided to rather make use of a synthetic acid solution in the pilot plant instead of Zincor spent electrolyte so that the delta for zinc and impurities arising from the Zincex™ SX circuit

could be better identified. Average results from this stage yielded a AZn of 75.7 g/l, and with all the main impurities yielding results below the analytical detection limit (ppb levels). The piloting campaign rendered a zinc solution capable of producing SHG Zinc, - hence illustrating the robustness of the Zincex ™ process.

As an aside, stripped organic phase from the stripping step is treated in the organic regeneration step with hydrochloric acid in order to avoid a build up of co-extracted impurities (such as Fe) that are difficult to strip in a sulphuric acid media. Chemical equilibrium corresponding to the Fe removal from the organic phased is presented in equation (8).

$$(R_3Fe)_{org} + 3\,(HCl)aq \sim (R_3H)_{org} + (FeCl_3)_{aq} \qquad (8)$$

Results obtained during the piloting confirmed the efficiency of the regeneration step maintaining the organic phase at the appropriate levels of such impurities.

CONCLUSIONS

Within the time constraints and piloting objectives set for the AARL piloting campaign it can be concluded that the outputs from the piloting campaign were of significant value in enhancing the understanding by Kumba Resources of the chosen technology as well as for the supply of key design and operating parameters for any future industrial scale ambitions. Results obtained from the study of the process confirm that the Leach-Zincex™ SX is technically and economically attractive for the clean-up and recovery of zinc from a tailings resource such as that encountered at Zincor.

ACKNOWLEDGEMENTS

This paper is published by permission of Kumba Base Metals Ltd. The successful outcome from the piloting campaign would not have been possible without expert guidance from Doug Alexander and Dr. Kathy Sole from AARL.

REFERENCES

1. Grinaker LTA Process Engineering, *Prefeasibility Report (2003) - Zincor 7L3 Tails retreatment project,* G-LTA-PE No:6594, Johannesburg, South Africa.
2. T.R. Bachmann (2004), *Proc. Anglo American Group Tech. Conf. Technology Adding Value to Natural Resources,* Johannesburg, South Africa.
3. V. Nagel (2004), Internal communication - Kumba Base Metals Ltd, Kumba Resources, Pretoria, South Africa.
4. Anglo American Research Laboratories, *Report No. 3 (2004) - Kumba 7L3 Pilot-Plant Campaign: Technical evaluation of the performance of the zinc solvent-extraction circuit,* AARL PROJECT No. S49197, Johannesburg, South Africa.
5. D. Martin, G. Diaz, M.A. Garcia & F. Sanchez (2002), *Proc. ISEC-2002,* Cape Town, South Africa, pp. 1045-1051.



Investigation of Phase Inversion of Liquid-liquid Dispersions in Agitated Vessels

Bin Hu* ", Lan Liu , Omar K. Matar", Panagiota Angeli*, Geoffrey F. Hewitt**,**

E. Susana Perez de Ortiz **

*: Department of Chemical Engineering, University College London, Torrington Place, London, UK, WC1E 7JE
**: Department of Chemical Engineering & Chemical Technology, Imperial College London, Prince Consort Road, London, UK, SW7 2BY

In this paper, we report results from on-going theoretical and experimental studies carried out at Imperial College London and University College London, respectively. Laser-induced florescence (LIF) is used to investigate phase inversion experimentally and to observe phenomena that accompany the inversion process such as secondary dispersions, drop coalescence and breakup, in great detail. Theoretically, a two-region model together with a criterion based on a dynamic balance between drop coalescence and breakup is employed to predict phase invasion. The concept of a radial distribution function was also utilized in order to better model the interaction of drops at high dispersed phase holdup. The modeling work is capable of predicting the existence of ambivalent ranges which are in good agreement with experimental observations.

INTRODUCTION

Liquid-liquid dispersions in agitated vessels are frequently used in the chemical industry for conducting operations such as extraction, heterogeneous reactions etc. In liquid-liquid two-phase flow systems, usually consisting of an aqueous liquid (e.g. water) and an organic liquid (e.g. oil), there are two general types of dispersions in which either oil drops are dispersed in a water phase (oil-in-water) or water drops are dispersed in an oil phase (water-in-oil). *Phase inversion* is defined as the phenomenon whereby the phases of a liquid-liquid dispersion interchange such that the dispersed phase spontaneously inverts to become the continuous phase and *vice versa*, under conditions that are determined by the system properties and operational conditions, for example, phase volume ratio and energy input. In general, for dispersions formed in agitated vessels phase inversion will take place at a critical impeller speed and for a certain dispersed phase fraction. Phase inversion can be obtained by either increasing the dispersed phase volume fraction or increasing the agitation speed (or power input). In some chemical processes, such as solvent extraction, in mixer-settlers, phase inversion can be extremely undesirable because it can delay the settling process. On the other hand, phase inversion could be desirable in some operations, such as the preparation of waterborne dispersions of polymer resin.

The phenomenon of phase inversion was first reported by Rodger *et at.* in 1956. Since then, it has been the subject of a considerable amount of experimental and theoretical research. However, until now, the precise physical mechanisms driving phase inversion have not been

elucidated. Moreover, there exist very few models that can accurately describe the inversion process. The fundamental difficulty in understanding phase inversion lies in the problem of conceptualising the actual mechanism behind the phase inversion processes. A number of experiments, however, have indicated that phase inversion is affected by a number of physical and physicochemical parameters, such as liquid properties, container geometry and the initial conditions of flow systems.

EXPERIMENTAL STUDIES

Elucidation of the mechanism that drives phase inversion entails the direct observation of the dynamic evolution of concentrated liquid-liquid dispersion before, during, and after the inversion process. A novel technique, laser-induced fluorescence (LIF), which allows direct, *non-intrusive* visualisation of the concentrated dispersion, is employed in the experimental studies at Imperial College London.

A 20-W nominal output copper vapour laser (Oxford Lasers LS20-10), available as a green light source, is used, with an output spectrum of 510.6 nm (green); the laser is pulsed (about 2 mJ/pulse), with an internal clock frequency of 10 kHz. Two precision cylindrical lenses are applied to expand the laser light beam into a 40 mm wide and 1 mm thick laser light sheet. In order to record the high speed dispersed flow, a high-speed digital video camera (Kodak Ektapro HG Imager) is used, which is capable of frame rates up to 2000 frames per second (typically 256x512 pixel resolution). The camera is located perpendicularly to the laser light. A Trigger Box is used to synchronize the laser pulse with a digital camera so that each pulse illuminates one image.

In order to obtain clearer images, liquid pairs with matched refractive indices are chosen. In work described in this paper, the liquid pair-- Exxol D80 Oil and 39 wt.% calcium chloride ($CaCl_2$) was used to carry out the LIF experiments. The refractive index of the liquid pairs is matched at 1.442 at 25°C and 2 ml of the fluorescent dyestuff Eosin Y (5% wt. solution) per litre of calcium chloride solution was used in the experiments. Table 1 gives the properties of the liquids with dyestuff. The test section (shown in Figure 1) was 80mm high and 30 mmx30 mm square cross section cell made of CaF_2 glass. A magnetic stirrer was used as an impeller, which was 20 mm long, with 6 mm diameter cylinder having a PTFE surface, located at the centre of the base of the cell. The configuration of the liquid-liquid dispersions in the cell could be determined by passing the (green) laser sheet through the cell (as shown in Figure 1b), causing the aqueous phase (containing Eosin Y) to fluoresce.

Table 1. Physical Properties of the Selected Liquid Pair

	Exxol D80	39 wt.% *Calcium Chlohde* Solution
Density (20°C)	803kg/m^3	1442 kg/m^3
Viscosity (25°C)	0.00162 Pa.s	0.01184 Pa.s
Interfacial Tension (20°C)	0.0190 N/m	

Phase inversion is experimentally achieved by increasing the power input to the system in this study. For example, to record images of the process of phase inversion, say, from an o/w to a w/o dispersion, the stirrer speed is gradually increased at a fixed phase holdup (e.g. 45% water holdup) until the inversion is observed. The initial emulsion with a given aqueous phase fraction is generated by stirring at a lower stirrer speed for several minutes.

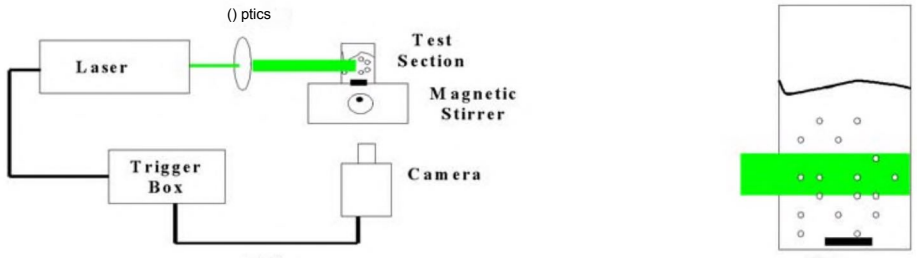


Figure 1. (a) A schematic representation of the experimental setup; (b) The position of the laser light sheet.

THEORETICAL MODELLING

In this paper, a two-region model suggested by Hu et al. (2004) is applied to predict phase inversion. It is assumed in the two-region model that there are two dominant regions in a stirred vessel for the occurrence of drop breakage and coalescence processes, due to the inhomogeneity of the energy input. Drop breakage is assumed to take place in the proximity of the impeller due to the high turbulence level (or high dissipation rate) in that region, while drops prefer to coalesce away from the impeller region which has a low dissipate rate. In the absence of phase inversion, a dynamic balance between drop breakage and coalescence is reached and the population of drops and their size distribution in the system is said to be in an equilibrium state. Phase inversion, therefore, is assumed to result from a disturbance of this state. In other words, phase inversion is expected to occur when the coalescence frequency in the circulation region exceeds the breakage frequency in the impeller region. In order to calculate the critical volume fraction of organic phase at inversion (the phase inversion point), therefore, the drop size distribution and functions of breakage and coalescence frequencies are required.

The breakage function of Luo & Svendsen (1996) and coalescence function of Coulaloglou and Tavlarides (1977) are used in this study to obtain the break-up and coalescence frequencies, which are given by Equation (1) and (2), respectively.

$$*(</)=C,(1-\phi)\left(\frac{\varepsilon_B}{d^2}\right)^{1/3} \text{i} \; \frac{(\text{I+f>*}}{\text{!<„*}} \; 7\text{TT}/3 \; \text{cx}\left(\text{P}\frac{\backslash 2C_f<J}{2.04\rho_c\varepsilon_B^{2/3}d^{5/3}\xi^{11/3}}\right)d\pounds df \qquad \text{(D}$$

$$A(d_l,d_s)=C,h_l,\frac{\varepsilon}{1+<f>}\text{l2_(t7, +</OV,:'3 +}d^{2'3}\text{)''2exp}\left[-\frac{C_3\rho_c\mu_c\varepsilon_O}{<\text{T}^2(1+\text{+})^3}\left(\frac{d_l d_2}{d, +d_2}\right)^4\right] \qquad \textbf{(2)}$$

where C* = 0.4615, C_2 = 2.17xl0'4 and C_3 = 2.28x10'13 are parameters obtained from experiments, *tj>* is the volume fraction of the dispersed phase, e_B and e_0 are the energy dissipation rates of the impeller and circulation regions, pc and p_c are the density and viscosity of continuous phase, respectively, *d* (or d_1 and d_2) is the Sauter mean diameter (d_{32}) which is expressed as follows (Yeo et al., 2002):

$$d_n=C,\{\backslash+C^)We,"D,\left(\frac{\mu_d}{\mu_c}\right)^{\backslash c\text{«}} \qquad \textbf{(3)}$$

Here, C_4, C_5 and C_6 are empirical constants, *We,* is the Weber number, p_d is the viscosity of dispersed phase and D, is the impeller diameter. In order to model accurately the collision of

drops in dense dispersions, in Equation (2) a radial distribution function (h_{12}) is introduced:

$$/2p=\frac{1}{1-\wedge 3}\ +**\&\text{----------}\frac{\chi_2}{d\backslash\ +d i<\backslash -XiY}\wedge +2\left(\frac{d_1 d_2}{d\backslash +d_{,}}\right)^{V}\frac{\chi_2^2}{(l\text{-}J,)^{3}} \tag{4}$$

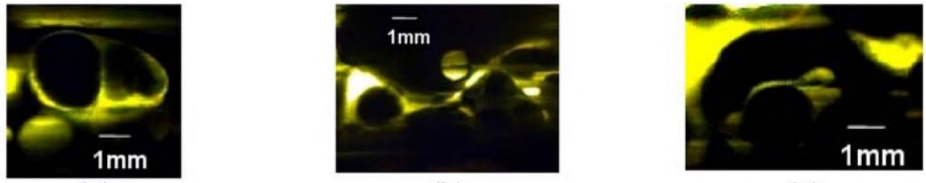
where given number density, *N(k),* for drop diameter d„:

$$\pi_{Z,}=jjN(k)d(d'_k)\ /=\mathbf{2\ and\ 3} \tag{5}$$

Given the fluid properties and system setup, the phase inversion point (or the maximum volume fraction of the dispersed phase) can then be calculated by Equations (1-5) on the basis of the phase inversion criterion discussed above.

RESULTS AND DISCUSSION

The experiments are carried out within a range of impeller speed of 350-1000 rpm for different initial organic phase holdup. Phase inversion is identified visually as the aqueous and 'oil' phases are yellow and black, respectively. The photographic evidence observed prior to, during and after phase inversion process from an o/w to a w/o dispersion clearly show that before phase inversion the coalescence rate becomes increasingly dominant over that of break-up, resulting in an increase of the average drop size. During phase inversion, oil drops deform and elongate severely and the continuous phase is gradually entrapped in the dispersed phase; this leads to a large number of secondary dispersions (oil-in-water-in-oil or water-in-oil-in-water) and even multiple dispersions (shown in Figure 2). We have also found that phase inversion might not occur globally but locally, with the inversion location being dependent on the local phase distribution. In addition, we have also found that the droplets inclusion process of the continuous phase is increased rapidly and happens even more frequently than drop coalescence. The inclusion process results in the formation of extremely large drops containing continuous phase droplets inside; the size of some of the host-drops were found to comparable to the width of the vessel. If the agitation speed is continuously increased (as was in the case in our experiments) or more dispersed phase is added into the system, phase inversion would occur globally. The co-existence of W/O and O/W dispersion also proved that phase inversion happens locally (see Figure 3). More details of the phase inversion process could be found elsewhere (Liu et al., 2005).



(a) (b) (c)

Figure 2. Secondary and multiple dispersions during phase inversion from O/W to W/O for 38% aqueous solution holdup; (a) oil-in-water-in-oil (O/W/O) secondary dispersion; (b) water-in-oil-in-water (W/O/W) secondary dispersion; (c) O/W/O/W multiple dispersion.

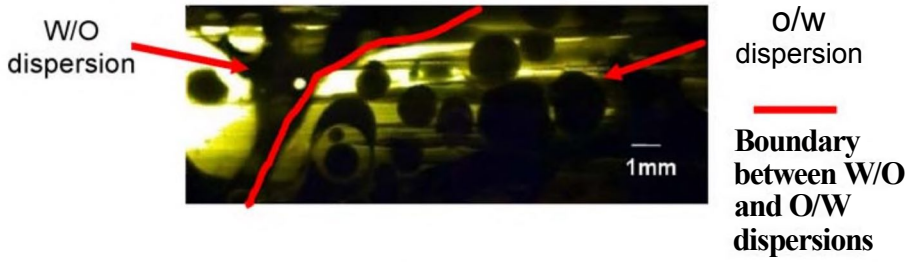


Figure 3. Co-existence of W/O and O/W dispersions during phase inversion of O/W to W/O for 38% aqueous solution holdup.

In this study, we have also found that the drops of the organic phase within a highly concentrated dispersion (say >40%) can stay together for a long period without coalescing, even for the current system which does not include any surfactants. In contrast, water drops in an oil continuous medium were found to coalesce comparatively easily. The resistance to coalescence may be explained by the presence of electric double-layers which are formed because of preferential adsorption of ions from the continuous water phase (Kumar, 1996; Pal, 1993). In the case of a W/O dispersion, however, the continuous oil phase is nonpolar; therefore water drops have a high potential to coalesce due to the absence of the electric double-layer effect. As a result, the electric double-layer effect is suggested as a contributing factor to the existence of an ambivalent range.

Apart from observing the phase inversion process and associated phenomena visually using LIF technique, the critical volume fractions of organic phase at phase inversion are also measured and compared with the predictions of the two-region model postulated by Hu et al. (2004). Figure 4 illustrates the experimental findings and the predictions by using the parameters in Equation (3) as follows:

Table 2. Values of the parameters in Equation (3).

Regions	Impeller region		Circulation region	
Dispersions	O/W	W/O	O/W	W/O
C_4	0.07	0.07	0.07	0.07
C_5	5.0	0.1	4.5	2.0
n	0.6	0.375	3/8	3/8
C_6	0.25	0.25	0.25	0.25

It can be seen in Figure 4 that the experimental results are in good agreement with the predictions for the upper curve of the ambivalent range, which characterises the inversion from O/W to W/O dispersions. The agreement between the predictions of the lower ambivalent range curve (inversion from W/O to O/W dispersions) and the experimental data, however, are not as good and the model overestimates the experimental data. These observations were also found by Hu et al. (2004), who suggested that the disagreement is due to the appearance of secondary dispersion that potentially increases the effective volume fraction of the dispersed phase. As shown in Figure 2, secondary and multiple dispersions have been found to be an important factor contributing to phase inversion. Therefore, to precisely understand and predict phase inversion it is imperative to conduct fundamental studies of secondary and multiple dispersion. In addition, the values in Table 2 are different from the original suggested values by Hu et al. (2004). We assume that the discrepancies could be due to the fact that the vessel used in this study is \ square cell and the impeller is located at the bottom, which are different from the cylindrical systems widely used.

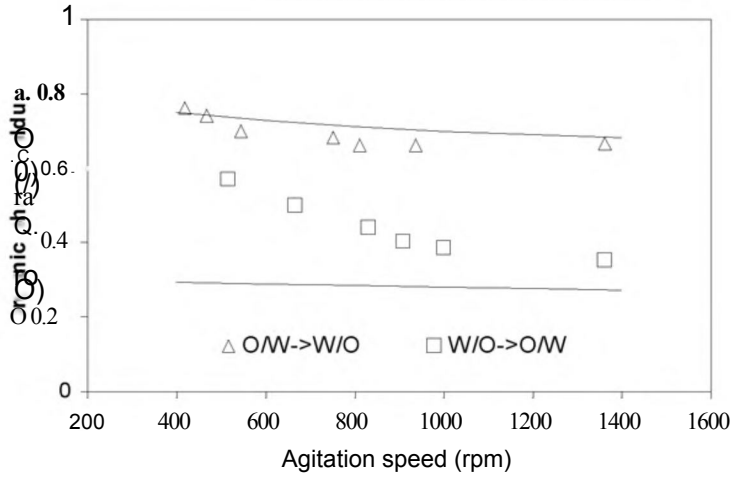


Figure 4. Comparison of the organic phase holdup at inversion between experimental data and the predictions of two-region model (solid lines).

CONCLUSIONS

Phase inversion in an agitated vessel is experimentally and theoretically studied. A laser-induced fluorescence (LIF) technique is applied to visualize the internal structure of the dispersion during phase inversion. Our results indicate that the inversion process is accompanied by the formation of numerous secondary (and even multiple) dispersions. We also suggest that the ambivalent range (or hysterisis effect) characteristic of phase inversion in agitated vessels may be partially due to the presence of electric double-layers, which are present in oil-in-water rather than in water-in-oil dispersions. In order to predict phase inversion, a so-called two-region model is used; good agreement was found between theory and experiment, particularly for the upper curve of the ambivalent region. However, more fundamental studies are required in order to further understand the underlying mechanism of phase inversion.

ACKNOWLEDGEMENTS

The authors would like to acknowledge the financial support of EPSRC (ref. No. GR/R54699/01 and GR/R56044/01). Mrs. L Liu and Mr. B Hu are also grateful to EPSRC and Overseas Research Students Awards Scheme (Universities UK) for providing financial support for the studentships.

REFERENCES

1. C. A. Coulaloglou, L. L. Tavlarides (1977), *Chem. Eng. Sci.,* 32:1289-1297.
2. B. Hu, P. Angeli, O. K. Matar, G. F. Hewitt (2004), *Chem. Eng. Sci.,* Submitted.
3. S. Kumar (1996), *Chem. Eng. Sci.,* 51(5): 831-834.
4. L. Liu, O. K. Matar, E. Susana Ortiz, G. F. Hewitt (2005), *Chem.Eng. Sci.,* 60: 85-94.
5. H. Luo, H. Svendsen (1996), *AIChE J.,* 42, 1225-1233.
6. R. Pal (1993), *AIChE J.,* 39(11): 1754-1764.



Prediction of Ternary Diffusion Coefficients in Liquids by Modified Group Contribution Method

Zhongqi Ren, Weiyang Fei*

Key Lab. Sci./Technol. C.C.R., Beijing Univ. of Chemical Technology, Ministry of Education, Beijing 100029, PR. China
* State key laboratory of chemical engineering, Department of chemical engineering, Tsinghua University, Beijing, 100084, PR. China

ABSTRACT

The modified group contribution method (MGCM) for prediction of diffusion coefficients in liquids was extending to calculate the effective diffusivity of component *i* at infinite dilution in multicomponent solution. The composite algorism of MGCM and the ternary extension of the interpolation scheme can be used to estimate ternary diffusion coefficients for the systems which can be described by Vignes's interpolated equation. The calculated results are consistent with the experimental values.

INTRODUCTION

Multicomponent diffusion coefficients in liquids play an important role in many chemical engineering processes and equipment designs[11'51]. It is essential for application of the non-equilibrium stage model (NESM) for separation column simulation especially [6].

The measurement of multicomponent diffusion coefficients was difficult, and the reliable

experimental data were lack. The concentration dependence of the diffusivities in ternary diffusion is more complicated than in binary diffusion. The estimation of ternary diffusivities is difficult. So far, only a few attempts have been made [7'121. Unfortunately, none of theories predicted well.

Maxwell-Stefan diffusivities were used for the estimation of ternary diffusivities, because these diffusivities are thought to be a less complicated function of composition than the Fick coefficients.

Ren and Fei[13,14] were proposed the modified group contribution method (MGCM) for prediction the binarv diffusion coefficients in liauids based on the arouo contribution methods. The performances of the molecules were regard as the sum of performances of the functional groups which compose the molecules. There are millions of compounds and mixtures but only a limited number of functional groups. It is convenient to estimate functional group parameters from existing data and then predict on that basis the behavior of new compounds.

MGCM is based on the following assumptions:

1) Diffusivity is governed by the diffusion surface area parameter S and volume parameter *V* of molecules and their diffusional activation energy E.

2) All the parameters are the contributions of each group which compose the molecules.

The main correlation of MGCM for self diffusivity in liquids was:

$$D_S = KS_A^{a-b}\sqrt{T}\exp\left(-\frac{E_{AA}}{RT}-\alpha\frac{298.15}{T}V_A^{c-d}\right) \quad (1)$$

for the binary diffusivitity at infinite dilution:

$$D_{AB}^0 = K\frac{S_A^a}{S_B^b}\sqrt{T}\exp\left(-\frac{E_{AB}}{RT}-\alpha\frac{298.15}{T}\frac{V_A^c}{V_B^d}\right) \quad (2)$$

for the ideal binary diffusivity:

$$D^{id}_{AB} = K\frac{(x_A S_B + \text{Vf}\ x_B S_A)^a}{(*A + *A)^b}\exp\left(\pounds - \frac{}{*7'} - {}^{ff}\frac{298.15\ (\text{ArA} + \text{^})^{cA}}{7'\ (x_A V_{A+} x_B V_B)^a}\right) \quad (3)$$

for the binary diffusivity:

$$D_{A,} = D^{id}_{AB}\beta \quad (4)$$

where

$$^{S}. = \sum_{7=1}^{n} 2>A\ (/ = /\text{I.B}) \quad (5)$$

$$\text{^, = } \sum_{7=1} 1>A \qquad (' = 4^*) \quad (6)$$

$$\text{T^.-IB} - \sum_{>=1}^{n}\sum_{7=1}^{n} \text{S S ^4 } {}^{A}B_{,B_j} \quad (7)$$

$$\text{^ } {}^{X}A\text{^}BA\ \text{"*■ } {}^{X}B\text{^}AB \quad (8)$$

$$a = 0.89,\ b = 0.22,\ c = 0.75,\ d = 0.15,\ K = 6\text{x}10'^{9},\ o = 0.58 \quad (9)$$

where S is the diffusion surface area and Vis the volume parameter, which are obtained from Mod. UNIFAC model [1S|, Q is the group surface area parameter, and *R* is the group volume parameter. *E* is the diffusion activation energy in J-mol"[1], E^is the diffusion activation energy between group *7* in component *A* and group *j* in component 6. *x* is the mole fraction. *T* is the temperature in Kelvin, v^is the number of the functional group Q, in molecule /, *n* is the number of the groups in liquid mixture. /3 is the thermodynamic correction factor, which can be calculated by UNIFAC or Mod. UNIFAC model[15>16].

MGCM developed for predicting diffusivities in liquids can be applied to many liquid mixtures in a wide concentration ranae. Even complex commerciallv important systems (DMSO or Sulfolane/aromatics) can be handled successfully.

The purpose of this study was to investigate the diffusivities of ternary systems.

THE EFFECTIVE DIFFUSIVITY OF COMPONENT *i* AT INFINITE DILUTION IN MULTICOMPONENT SOLUTION

MGCM can be extending to estimate the effective diffusivity of component *i* at infinite dilution

in multicomponent solution, which conception was given by Holmes[1171].

Component / is at infinite dilution in multicomponent solution. Molecular of component / was surrounded with molecules of other components. The mixture can be considered a pseudo-binary solution, the component / is the solute A at infinite dilution, all the other components can be considered solvent B. The parameters of the MGCM can be calculated by specially rule of superposition as follows:

$$S_A = S, s_B - \frac{\left(\sum_{7=1}^{m} x_j S_j\right)}{1 - x_{,}} \quad (10)$$

$$K,=K\, v_B \quad = \frac{\left[\sum_{7=1}^{m} l^{*}/,\right]}{1 - x_{,}} \quad (11)$$

$$E_i = \frac{\sum_{j=1}^{m(ñn} \text{XI XXw}^{*}}{1\text{-x,}} \quad (12)$$

Then, the effective diffusion coefficients of component /' at infinite dilution in mixture was:

$$/D_{im}=^5VT\exp\left(-\frac{A.}{RT}\right) \text{-or} \frac{298.15}{r\, v,} \frac{V_A^c}{d_B} \quad (13)$$

The effective diffusion coefficients of toluene at infinite dilution in various multicomponent solvents at 298.15K were used to verify the method. Results are listed in Table 1 and 2. It is seen from the comparison between experimental and calculatina values that the maximum deviation is 13.76% and the average deviation is 5.06%. It is indicated that MGCM can be used for prediction of effective diffusivities at infinite dilution in multicomponent solutions.

Table 1. Diffusivity of toluene in n-hexane and n-tetradecane solvents at 298.15K

mole fraction of n-hexane	Exp.[1171] xIO^9 mV	Calc. xIO^9 mV	deviation %
0.0	1.08	1.068	1.123
0.197	1.37	1.404	2.467
0.328	1.58	1.686	6.732
0.499	1.92	2.145	11.74
0.664	2.38	2.707	13.76
0.785	2.90	3.208	10.60
0.887	3.57	3.692	3.413
1.0	4.62	4.292	7.089

Table 2. Diffusivity of toluene in n-decane and cyclohexane solvents at 298.15K

mole fraction1 of cyclohexane	Exp.[17] xIO^9 mV	Calc. xIO^9 mV^1	deviation %
0.00	1.81	1.625	10.24
0.754	1.87	1.739	7.021
0.492	1.94	1.870	3.600
0.241	2.00	2.008	0.3817
1.00	2.24	2.152	3.934

THE TERNARY DIFFUSION COEFFICIENTS

A simple interpolation can be used for estimation of binary diffusivities of non-associating mixtures. For ideal or nearly ideal mixtures, the diffusivities were well described by the Vignes

or the Darken equation. Mixtures with a larger deviation from ideality require more complicated schemes which require a mixture viscosity. For ternary mixtures, the diffusivities were haven to rely on interpolation schemes. Because of the lack of data on ternary mixture viscosities, only Vignes relation can be used. The ternary Vignes relation in a mixture with species *i,j* and /cwas first suggested by Cullinan[7,91]:

$$D_{ij} = \left(D_{ij}^{i\to 1}\right)^{x_i} \left(D_{ij}^{j\to 1}\right)^{x_j} \left(D_{ij}^{k\to 1}\right)^{x_k} \tag{14}$$

The Eq.(14) requires nine parameters:

- six diffusivities at dilution which are eaual to the binarv diffusivities at infinite dilution and can be obtained from binary measurements or predictions.
- and three diffusivities of a type $D_{ij}^{\to 1}$ which is difficult to obtain from experiment. This can be easily explained from the Maxwell-Stefan equation. As x/ and *x,* are almost zero, all terms with $D_{(J}$ are small (the friction of dilute *i* and dilute *j* in almost pure *k* is negligible in comparison with the total frictional force). The diffusivity D,y in *k* has to be estimated [m].

Wesselingh [41] suggests using the geometrical average of the binary diffusivities of the *'i-f* pair at infinite dilution:

$$o'r' = \sqrt{D_{ij}^{i\to 1} D_{ij}^{j\to 1}} \tag{15}$$

Eq.(15) can easily be improved by a correlation term for the viscosity [7]:

$$\text{/■)*—»•• j7V-}>1\ \sqrt{JU_\ \text{TV-}^{*1}\ HL} \quad \text{V \% } y_k \tag{16}$$

The viscosities in Eq.(16) are pure component viscosities.

Kooijman[1121] suggested an equation similar to Eq.(15) but with the limiting diffusivities of the 7-A[J] and *'j-k'* pairs:

$$D_{ij}^{k\to 1} = pi''^{D}T \tag{<17)}$$

Rutten[?1] improved Eq.(16). The effect of a correlation with the square root of the viscosity

according to:

$$Df^{*} = \left[Dr\text{»}r \quad \frac{\sqrt{\eta_i \eta_j}}{n_k} \right] \text{n] :} \tag{18}$$

The test of the Eq.((15)-(18)) was performed with three different mixtures listed in Table 3-5. The standard deviations of the diffusivities are very larger.

In this study, a composite algorism of MGCM and the ternary extension of the interpolation scheme was derived to estimated ternary Maxwell-Stefan diffusion coefficients. For the diffusivities of type D_{ij}^{k} the mixture can be considered a pseudo-binary mixture too, the main comoonent *k* is reaard as the solvent B. the other two components can be considered solute A, which parameters of MGCM were the geometrical mean of the component *i* and *j.* Then,

$$_{ij}D^{*}\text{-}^{*}\text{'} = \frac{\text{V}_{i}}{S_B^{o}} \text{exp}\left(-\frac{E}{RT} \text{-} a \quad \frac{298.15}{T} \frac{V_A^{c}}{V_B^{d}} \text{y} \right) \tag{19}$$

Where,

$$S_A = \sqrt{S_i S_j} \qquad S,\text{=}S, \tag{20}$$

$$V_{V_A} \text{=} f7, \qquad V_B = V_k \tag{21}$$

$$E = \sqrt{E_{ik} E_{jk}} \tag{22}$$

Three different mixtures were used to test the methods. The first one is the ideal mixture toluene(1)-chlorobenzene(2)-bromobenzene(0)[181, all the species are of about the same size(the van der Waals radii are respectively 0.2422, 0.2399 and 0.2441 nm). The second mixture is the nearly ideal mixture acetone(1)-benzene(2)-CCI_4(0)[191. This mixture was chosen because the three binaries are well described with the Vignes equation. The third system is a mixture with a larger deviation from ideality methanol(1)-isobutanol(2)-propanol(0)[2Q1, this mixture is characterized by a large difference of the viscosity and the diffusivities at infinite dilution. The molar volumes and viscosities are given in Table 3.

First, whether the experimental Maxwell-Stefan coefficients can be described by the Vignes

Eq.(14) was checked. This can be done by fitting the experimental points to the Vignes equation. The standard deviations are used as weighting factors in the optimization. The binary diffusivities D'-D_{ij}^{*1} and $D_{ij}^{j\to1}$ are used as constants, so only one fitting parameters remains: t h$D_{ij}^{k\to1}$. The standard deviation in this optimized parameter and the maximum deviation between the experimental points and the ideal surface of diffusivities determine whether the dataset can be used in the analysis.

Table 3. Pure component properties

Component	Viscosity xlO'³ Pa·s	Molar Volume xlO'⁶ m³mol	Temperature *IK*
toluene	0.526	106.64	
chlorobenzene	0.740	102.67	302.75
bromobenzene	0.985	105.98	
acetone	0.307	73.80	
benzene	0.601	89.56	298.15
CCl4	0.906	97.35	
methanol	0.510	40.97	
i-butanol	2.913	92.65	303.15
1-propanol	1.737	95.58	

The fitted equations for the diffusivities of toluene(1)-chlorobenzene(2)-bromobenzene(0) are:

$$D_n = 2.2168^{X|}1.7024^{X2}1\mathbf{.6032*®} \quad \text{st. dev } 0.013$$

$$D_{J0} = 2.2700^{A'}1{,}8423^{V2}1.410r° \quad \text{st. dev } 0.030 \qquad (23)$$

$$D_{20} = 1.8908'M.6754^{XJ}1.3082^{X°} \quad \text{st. dev } 0.083$$

The values in bold represent the fitting parameters. The maximum deviations of the experimental points from the fitted equations are respectively: 0.023, 0.066 and 0.172.

The diffusivities of the mixture acetone(1)-benzene(2)-tetrachloromethane(0) are fitted to the equations:

D_{l2} = 4.1513$^{x'}$2.7434$^{i'^2}$1.3072$^{x°}$ st. dev 0.061

D_{l0} = 3.6689^{Vl}3.2993^{A}M.7200Vo st. dev 0.036 (24)

D_{20} = 2.3007*^{1}1.9126^{VJ}1.4088$^{X°}$ st. dev 0.088

The maximum deviations are respectively 0.176, 0.089 and 0.131.

The fitted equations for the diffusivities of methanol(1)-i-butanol(2)-1-propanol(0) are:

D_{n} = 1.0400$^{V'}$0.5870^{A2}0.5574$^{A;°}$ st. dev 0.020

D_{l0} = 1.9700$^{V'}$0.6534^{VJ}0.8000$^{';°}$ st. dev 0.030 (25)

D_{20} = 1.2552^{Al}0.5820^{i2} 0.3836*$^{°}$ st. dev 0.030

The maximum deviations are respectively: 0.038, 0.116 and 0.086.

So, all the experimental points of these mixtures can be described by the Vignes Eq.(14).

In order to determine which of the empirical equations describes the fitted parameters most accurately, the next step is to calculate the fitted parameters from the empirical relations ((15) -(19)). The results of the calculations are summarized in Table 4. It is seen that none of the equations is able to predict the diffusivity $D^{\wedge J}$ well. The results of MGCM are the best.

Table 4. Comparison between the fitted parameters D^{*}_{ij} and the calculated parameters

Mixture	Correlation				
toluene-chl.benz.-br.benz*	MGCM	Eq.(15)	Eq.(16)	Eq.(17)	Eq.(18)
Dy' =1.6032(10.013)	1.3585	1.9426	1.2305	1.3582	1.5461
£$■** = 1.8423(10.030)	1.6904	1.7891	1.7403	1.6888	1.7645
Dy' =1.8908(10.083)	2.0506	1.4805	2.4029	2.2432	1.8861
acetone-benzene-CCU					
$D'^{\wedge'}_{i2}$ =1.3072(10.061)	1.5471	3.3747	1.5961	1.4926	2.3209
D£~*^{J} = 3.2993(±0.036)	3.8667	2.4575	2.1141	2.2906	2.2794

D,V = 2.3007(+0.088)	2.3160	1.5852	3.8959	3.8453	2.4851
methanol-i-butanol-propanol					
$D_{12}^{*'''}$ =0.5574(10.005)	0.5638	1.0375	0.7280	0.5548	0.8691
D'o'''*1 = 0.6534(±0.030)	0.5551	1.2632	0.4082	0.5840	0.7180
$D_{20}^{x_1 \to 1}$ = 1.2552(±0.030)	1.7556	0.4703	2.0742	1.9023	0.9877

MGCM can be used to estimate the Maxwell-Stefan diffusivities completely. First, the binary diffusivities $D_{ij}'T^{*'}$ and $D_{ij}^{j \to 1}$ can be calculated by Eq.(2). and $D_{ij}^{k \to 1}$ can use Eq.(19) to estimate. The results are list in Table 5.

Table 5. Comparison of Maxwell-Stefan diffusivities of experimental and calculated values

x_1	*2	Cal xiQ -9 mV			1 D"p - Dfc | /D"p ij × 1		
		Di2	Dio	D20	AD12	AD10	AD20
A: Toluene(1)-Chlorobenzene(2)-Bromobenzen(0) 302.75K							
0.25	0.5	1.7188	1.7391	1.5571	0.0352	0.0109	0.0685
0.26	0.03	1.5534	1.6046	1.9192	0.0063	0.0488	0.0980
0.7	0.15	1.9798	2.0221	1.6640	0.0232	0.0384	0.1522
0.15	0.7	1.7122	1.7194	1.4523	0.0281	0.0101	0.1585
0.45	0.25	1.7917	1.8280	1.6732	0.0585	0.0042	0.0089
0.18	0.28	1.5804	1.6163	1.7432	0.0073	0.0879	0.0356
B: Acetone(1)-Benzene(2)-CCl_4(0) 298.15K							
0.2989	0.349	2.5379	2.8224	1.7946	0.0110	0.0009	0.0572
0.1496	0.1499	1.9541	2.1439	2.0672	0.0751	0.0620	0.0571
0.1497	0.6984	2.6757	3.3699	1.5148	0.2370	0.1676	0.1094
0.6999	0.1497	3.3634	3.2250	1.8609	0.0014	0.0709	0.1294
C: Methanol(l)- i--Butanol(2) ■Propanol(O) 303.15K							
0.4633	0.2406	0.9836	1.1164	0.7284	0.0626	0.0043	0.0092
0.2531	0.1098	0.7635	0.9731	1.1222	0.0216	0.0001	0.1704
0.2781	0.5708	0.8005	0.8359	0.5391	0.0018	0.0015	0.0152
0.8283	0.077	1.5043	1.6427	0.6253	0.0414	0.1305	0.0272

It is seen from the comparison that the calculated results are consistent with the experimental values. Despite the somewhat larger deviation in D^{*}_{ij}, the standard deviations of Maxwell-Stefan diffusivities between experimental and estimated values are not large. It is indication that the effect of *D'p'* is usually small.

CONCLUSIONS

The modified group contribution method (MGCM) for prediction of diffusion coefficients in liquids can be extending to calculate the effective diffusion coefficient at infinite dilution in multicomponent mixture.

The composite algorism of MGCM and the ternary extension of the interpolation scheme can be used to estimate ternary diffusion coefficients completely for the systems which can be described by Vignes's interpolated equation. The method requires nine parameters: six diffusion coefficients at infinite dilution and three diffusion coefficients of a type $\pounds_{ij}$. First, all the parameters were estimated by MGCM. Then, the Maxwell-Stefan diffusivities were estimated by interpolation scheme. The calculated results are consistent with the experimental values. The ternary diffusivities can be estimated by existing binary experimental dataset.

In ternary mixtures, the number of systems for which reliable data is available, is still too small to allow much generalized study.

REFERENCES

1. Cussler E L. Multicomponent diffusion. Amsterdam: Elsevier, 1976
2. Cussler E L. Diffusion: Mass transfer in fluid systems. London: Cambridge University Press, 2000
3. Krishna R, Taylor R. Multicomponent mass transfer. New York: Wiley-Interscience, 1993
4. Wesselingh J A, Krishna R. Mass Transfer. London: Eills Horwood Limited, 1990
5. Sherwood T K, Pigford R, Wilke C R. Mass transfer. New York: McGraw-Hill, 1975

6. Krishnamurthy R, Taylor R. A nonequilibrium stage model of multicomponent separation processes. AIChE J„ 1985, 31(3): 449-465
7. Rutten W M. Diffusion in Liquids. Netherlands: Delft University Press, 1992
8. Wendt R P. The estimation of diffusion coefficients for ternary systems of strong and weak electrolytes. J. *Phys. Chem.,* 1965, 69(4): 1227-1237
9. Cullinan H T, Cusick M R. Predictive theory for multicomponent diffusion coefficients. Ind. *Eng. Chem. Fundam.,* 1967, 6(1): 72-77
10. Mortimer R G, Clark N H. Transition state theory for diffusion coefficients in multicomponent liquids. Ind. *Eng. Chem. Fundam.,* 1971, 10(4): 604-610
11. Bandrowski J, Kubaczka A. On the prediction of diffusivities in multicomponent liquid svstems. *Chem. Ena. Sci..* 1982. 37: 1309-1313
12. Kooijman H A, Taylor R. Estimation of diffusion coefficients in multicomponent liquid systems. Ind. *Eng. Chem. Res.,* 1991, 30(6): 1217-1222
13. Ren Z Q. Dissertation of Ph D. Beijing: *Tsinghua University,* 2004
14. Ren Z Q, Fei W Y. A modified group contribution method for prediction of binary liquid molecular diffusion coefficient. *Chemical Engineering of Chinese,* 2004, 32(1): 60-64
15. Gmehling J, Li J D, Schiller M A, et al. Modified UNIFAC model. 2. present parameter matrix and results for different thermodynamic properties. Ind. *Eng. Chem. Res.,* 1993, 32(3): 178-193
16. Taylor R, Kooijman H A. Composition derivatives of activity coefficient models (for the estimation of thermodynamics factors in diffusion). *Chem. Eng. Comm.,* 1991, 102: 87-106
17. Holmes J T, Olander D R. Diffusion in mixed solvents. AIChE J. 1962, 8(5): 646-649
18. Burchard J K, Toor H L. Diffusion in an ideal mixture of three completely miscible non-electrolvtic liauids-toluene, *chlorobenzene, bromobenzene. J. Phvs. Chem..* 1962. 66(10): 2015-2022
19. Cullinan H T, Toor H L. Diffusion in the three-component liquid system acetone-benzene -carbon tetrachloride. J. *Phys. Chem.,* 1965, 69(11): 3941-3949
20. Shuck F O, Toor H L. Diffusion in the three component liquid system methyl alcohol -n-propyl alcohol-lsobutyl alcohol, ibid. 1963, 67(3): 540-545



ENHANCEMENT OF PLANT PERFORMANCE BY CONTROL OF ORGANIC SURFACTANTS AND POISONS

Gordon M. Ritcey

G.M. Ritcey & Associates Inc., Ottawa, Canada

ABSTRACT

The investigation of numerous operating plants has indicated that most of the problems experienced with the operation can be attributed to the various “organics” present that are not part of the original organic solvent components. These “organic” compounds can act as poisons to the process thereby adversely affecting the process and thus the losses of reagents. In addition, amphoteric compounds are also a major contributing factor in the operational efficiency, adversely affecting the rate of coalescence as well as contribute towards crud formation.

These poisons act as surfactants and influence the surface tension, viscosity and therefore the coalescence rates. The result is high raffinates and decreased solvent loading. Thus the plant production suffers.

INTRODUCTION

There are numerous causes of inefficiency in SX circuits. While many of the causes may be similar from process to process, nevertheless there are often situations where the cause may be unique to the plant as a result of the particular mineralogy; the type of contactor and the mode of operation; the aqueous phase and the contained impurities, or to the extraction system for the particular metal to be recovered. These symptoms of inefficiency include the following: high solvent losses, poor extraction, poor stripping, foam generation, stable emulsions, slow phase disengagement, high entrainment losses, back-eddies in the settler, crud formation, misting, etc.

The author began investigating problems in SX circuits in the mid 1970’s. The perceived problems were soon discovered to be symptoms of a problem occurring elsewhere in the circuit. The challenge then was to determine the causes by examining variables such as shear and droplet formation, surfactants, chemical break-down as affecting the emulsions, cruds, etc. in order to improve on the efficiency and therefore the economics. There was little appreciation by the industry of the importance of droplets caused by the mixing device when the organic and aqueous were mixed. In the original gravity mixer settler plants, mixing was independent of pumping, and it was common to have 100 ppm suspended solids or more.

Over time in these investigations it was recognized that the following could be considered in addressing plant performance with a view to making improvements, based on the evidence obtained from laboratory work. These are: recognizing the symptoms of poor operation; b) determining the source of the problem; and c) assessment of the problem and development of treatment methods

This paper will deal generally with 3 mine types: cobalt-nickel, copper, uranium—all with similar problems. Because of space limitations for such a paper, the subject areas will be covered only briefly, in no specific order. Tests were performed at mines in Australia, Brazil, Canada, Chile, and Norway.

MAJOR PROBLEM AREAS AND TESTS

Emulsions

Stable emulsions can form in most circuits, and are due to manv causes. These include impurities in the system, inorganic or organic surfactants, which adversely affect coalescence Thus, fouling of the solvent by impurities in the water or PLS (pregnant leach solution) result in poor plant performance. This can be exhibited by not only poor coalescence, but also contribute to the formation of cruds, misting and thus high solvent losses.

Foam

Foam has been occurring in many circuits particularly where there has been excessive flocculent or other liquid-solids chemical added. The foam, in some plants, occurs on the surface of the organic throughout the circuit and results in poor phase separation with resultant crud and other solvent losses. The crud accumulates behind the picket fences as a spongy-elastic material, the linear velocity down the settler is affected and much reverse flows result.

By the time a sample of foam from any of the Cu, U, Co circuits was taken to the lab, it appeared to be normal solvent. However when shaken in a separatory funnel for about 30 seconds and compared to another sample of fresh solvent or solvent treated with a dilute NaOH wash, there was a wide difference in the relative rates of phase disengagement: “foam” solvent 215 sec; caustic treated solvent 65 sec Thus there is obviously a surfactant also on the solvent even after the plant acid stripping for metal recovery. Often, only a slight stir of the solvent was sufficient to generate foam.

Crud

There are many types and compositions of cruds. Several may exist in a single circuit. At one cobalt-nickel plant, a sample of crud was allowed to dry in the sun and the diluent evaporated. After a week the material had a composition of a fibrous-elastic substance that could be rolled up like rubber. This polymer-type crud was considered to be the result of flocculent overdosing. Some analyses of crud from circuits containing flocculents assayed as follows, in %: a) Si 20.8, Al 3.79, Mn 0.59, Mg 1.31 .b) Si 10-29 Fe 15 (flocculent added in plant following pressure leaching).c) Si 6.8, Ni 14.0, Co 0.14, Cu 0.01, Mn 0.01, C 12.7, S 12.4

In another Co circuit, the analyses of the crud material indicate that although the Si in the PLS was determined to be <1 ppm, it was one of the major constituents in the crud, at 3.5%. Major was Ni at 16.8%, and Co at 2.4 %. In one uranium plant, the major constituent of the crud was bismuth, at 35% Bi. Other uranium operations had crud analysing 8-10% Zr. Whenever amphoteric metals were the major crud constituent, none of those metals were detected in the

ore or in the PLS. The most common amphoteric in the PLS that has been the major crud constituent has been Si (as a silicate or a colloid).

Because the surfactants cause slow phase disengagement, then stable emulsions and considerable crud appear in each stage. Some of the surfactant is lost during extraction. If there was over-dosing of the flocculent, then it was discovered that plant emulsions could form very stable, rubbery-like crud, that resists easy breakdown. Examination of one crud by microscopy indicated rod material present (bacteria). Following heat treatment, the residue analysed appreciable amounts of C, Fe, Si, Ca

Flocculents / Organic Acids

Degradation of an organic reagent produces organic products that can exist in both the aqueous and organic phases, dependent upon their relative solubilities. These organics can have adverse affects on the entrainment losses, by decreasing the phase separation rates. In addition, the organics present in the leach feed solution to solvent extraction, humic and fulvic acids in the ore, or organics added to improve liauid-solids separation or to improve electrodeposition can have serious effects on the operation. Degradation of the alcohol modifier to the carboxylic acid can result in off-specification product due to the extraction capabilities of carboxylic acids. Any severe retardation of phase separation, by poisons as well as over-mixing, can also lead to misting and losses of the reagent as well as the metal being extracted. A few simple and useful tests were developed to determine the major sources of the problems. These include:

a) wash of the as-received extractant reagent with an alkali
b) wash of the aqueous (water, PLS) with diluent
c) wash of the “stripped plant solvent” with an alkali

In a test, 2 drops of 0.3% flocculent were added to PLS and mixed with diluent vigorously for 2 minutes. Although the phases separated rapidly in 10 seconds, there was an emulsion in the diluent phase that cleared in a couple of minutes to a clear layer. This corresponds to an earlier test in which no flocculent was added and no emulsion in the organic phase. On re-stirring, the emulsion was more difficult to separate, the primary break was again in 10 seconds but the emulsion was still in the organic phase after 5 minutes. The diluent appears capable of extracting the polyacrylamide material, as shown by the very lengthy phase disengagement time when added and mixed

The yellow aqueous resulting from contact of an U-amine solvent with 0.3 M NaOH was slurried with some activated carbon for a few minutes and filtered. The yellow coloration virtually disappeared. Thus, organic compounds constituted the yellow colour and were subsequently removed by passing the solution through activated carbon.

Loading of flocculent onto Cyanex solvent and subsequent contact with the PLS showed decreased selectivity of Co over impurities, particularly that of Ni. Other tests showed that although the diluent was capable of extracting the flocculent, organic acids had to be present for metal chelates to be extracted as impurities.

Water and / or PLS Pre-Treatment

If the PLS contains organic impurities (e.g. surfactants, organic acids, amphoteric metals), and are not removed prior to extraction, they can be extracted by the solvent. The “poisons” that load will result in extraction sites being blocked resulting in decreased extraction. A wash of the PLS with diluent can remove such contaminants.

Washing of Pond Water or the PLS with diluent in Cu, U, Co-Ni plants resulted in “webbing” as well as a dark material at the interface following contact of aqueous with diluent. When 0.05 M NaOH was mixed with the separated diluent wash solution a distinctive organic acid (yellow-light brown) coloration resulted which would indicate humic and/or fulvic acids (organic acids). Thus humic acids (and other impurities) were passing into the PLS and subsequently extracted to poison the solvent.

Laboratory tests at several sites showed that when fresh PLS was mixed with diluent, and agitated, foaming occurred in the diluent and there was a “web” throughout. After sitting for 10 minutes the web still remained. A gel was also often present in these slow phase separating systems, due to the presence of surfactants such as flocculents. Tests have indicated the web to be a polymer (flocculent) plus complexed metals. A “web” at the interface, as an emulsion, can be stable for hours, while a gel may be stable for days.

The extracted poisons or “surfactants” adversely affects the rate of phase disengagement and contribute to crud formation. Also, reduced extraction sites are available for extraction of the desired metal. In addition, there then exists the possibility of such “organic acid” surfactants to behave as “extractants” to extract the undesired impurities. For example, as high as 5 g/L Fe has been obtained through a diluent wash of the PLS in a U plant. In a Co-Ni plant, the washing of the PLS with diluent showed the following elements were extracted into the diluent (no extractant present): Si, Co, Ni, Fe, Cu, Mn. The data suggests the metals are extracted probably as a chelate with organic (humic) acids, and would obviously adversely affect the plant performance.

Pre-treatment of the PLS or Raffinate with H_20_2 appears to have a positive effect on destruction of some of the organic contaminants in the aqueous phase. Treatment of the PLS with activated carbon resulted in the same improvement as that of a diluent wash.
Some characteristics noted for organic acids (including humates) are:

1. blocking of sites on the solvent, thus inhibiting mass transfer, resulting in high raffinates;
2. the process of a diluent wash for removal of organic acids from the PLS followed by stripping with NaOH and re-contact with diluent appears to be reversible, depending upon pH, and the organic acids can be re-extracted into regenerated diluent;
3. most or all of the organic acids in the PLS are extracted by the solvent during the extraction stage in the plant. Their presence on the loaded solvent inhibits stripping and regeneration; and
4. destruction of organic acids occurs at the higher EMF values.
    a) at a ratio of 40/1 PLS / Diluent, in a single contact, about 80% or more of the organic acids were removed from the PLS, dependent upon the amount present, and
    b) the removal of the organic acids is an equilibrium process in which probably a number of stages are required for any particular feed PLS situation.

Treatment of the Plant Solvent

Dependent upon the reagent preparation by the manufacturer, such as the incorporation of specific wash stages, the SX plant may have phase separation problems for a few initial cycles of the solvent. An evaluation technique was developed by the author in the first U plant in 1956. This consisted of the contact of a fresh amine-diluent-modifier solvent with 0.7% Na_2C0_3 for 2 minutes. A “dirty” reagent would be indicated by a yellow aqueous phase after the treatment, as well as possible interfacial white crud. The yellow raffinate was treated with activated carbon, which resulted in the removal of the colour, implying a soluble organic that had been removed, which was later identified by analysis as impurities from the manufacture of the amine. Similar

results were found for oximes and alkylphosporus acids when treated by a similar but more dilute alkali wash.

In many operations examined (Co-Ni, Cu, U, Zr) the organic phase became fouled with recycle. The result was loss of extraction “sites”, poor extraction, low solvent loading, slow phase disengagement, crud formation, high solvent losses, and misting. A procedure for problem assessment or plant clean-up was developed, which was an alkali wash at controlled pH. The impurities will vary with the particular operation, but will contain metals, as well as organic acids or degraded products. NaOH or Na_2C0_3 or a combination can be used provided that the equilibrium pH is not sufficiently high to saponify the reagent. Following are some examples of solvent treatment.

In one Cu plant the phase separation was considered excessive at 120 seconds. Following treatment with 0.05 M NaOH, separation of phases, acidification, and contact with diluent-washed PLS, the phase separation was very rapid, at 20 seconds.

Another Cu plant was experiencing incomplete stripping and high raffinates. Wash of stripped solvent (10% Acorga 5640) with 1-2% Na_2C0_3, resulted in interfacial crud-precipitate and yellow raffinate. The phases were separated, and the solvent acidified. Saturation loading of this treated solvent was compared to an untreated solvent.

Untreated solvent	5.34 g/L Cu Loading	10.0% Acorga (equiv)
Na_2C0_3 treated solvent	7.81	14.6% Acorga (apparent)

Thus the treatment has removed “non-strippable poisons” resulting in the freeing of active sites to result in increased extraction due the now higher solvent concentration.

In another Cu plant with poor recovery and slow phase disengagement, a sample of “plant stripped solvent” was treated with a dilute (0.05 M) NaOH wash and compared to a non-treated solvent and a clay-treatment performed in the plant when contacted with the PLS. The data shows that the dilute caustic wash is more effective than clay treatment for improving the performance.

	Phase Disengagement Time (sec)	% Cu Extracted 1-stage
Non-treated solvent	» 90	28.7
Clay-treated solvent	90	73.5
NaOH treated solvent	45	92.2

In cation exchange systems, such as extractants for Co or Cu, it is also equally important that the equilibrium pH following the alkaline wash is not higher than pH 10 to prevent saponification of the extractant. Thus the combination of phase ratios and alkali type and concentration will be important for the treatment of a specific solvent. By contrast, in anion exchange systems, such as amine extraction for U, or solvating systems such as TBP extraction of Zr, or TBP extraction of U, the extractants can tolerate relatively high (eg. 10 %) concentrations of alkali. Whatever the extraction system, a continuous treatment is recommended. The best physical and chemical performance was always obtained when both the PLS and the solvent were "clean”. Pre-treatment results in increased performance in extraction, scrubbing, and stripping.

Bacteria / Algae

Bacteria and algae appear to be entering many circuits, probably through the bio-leach process. This slimy material coats the walls of the mixer settlers and could be the cause of the blockage in the picket fences. The material that is growing on some of the Cu heaps was examined qualitatively. It was washed with 1 M NaOH, which resulted in the release of a brown (Fe??) material to the wash. This was repeated 3 times before the "material" when washed produced a clear solution The addition of biocide to the PLS or Process water destroyed the bacteria, resulting in increased performance.

Cross-Contamination

If the extractant from one circuit is permitted to enter the 2nd circuit, the result will be an accumulation of the extractant from the first circuit in the solvent in the second circuit. The resultant mixture will act as a synergist, affecting the extraction and discrimination over impurities, particularly Ni in the case of Co-Ni separation in sequential Co-Ni separation circuits. Also, there will be adverse physical affects on the phase separation. In at least one Co-Ni plant the cross-contamination was so serious that both circuits had to be dumped and fresh solvents added. A diluent wash between the circuits improved the subsequent operation as regards cross-contamination.

SUMMARY /CONCLUSIONS

In summary, laboratory tests at numerous plant sites have indicated the major sources of the plant problems that exhibit adverse surfactant effects to be:

1) Return water from the pond (humic and other organic acids)
2) Biocides (bacteria, yeast, moulds)—3rd phase
2) Lignins-phase separation problems resulting in crud
3) Phenols (analysed in cruds and solutions) resulted in slow phase separation
4) Re-use of recovered solvent without pre-treatment for degradation products
5) Humic and fulvic acids in the PLS (from the ore)
6) Degradation products of the solvent system
7) Insects in tankhouse, dissolved in H_2S0_4 (fulvic acids)
8) Cross-contamination (carry-over of solvent from first circuit to next)
9) Other surfactants (eg., coagulants, flocculents, flotation agents)

It is important to remember that the solvent extraction circuit is only part of a larger integrated plant operation, so is interconnected with the “upstream and downstream” sections of mining, leaching and electrowinning. Any impurities arising from the 3 areas act as “surfactants” in the solvent extraction process These surfactants can be very detrimental to not only the chemistry (loading and metals discrimination) but also the physical aspects (phase separation rates, formation of colloids, gels, cruds etc). The ultimate effect is on product purity and economics of the plant.



A PRACTICAL GUIDE TO SX PLANT OPERATION

By: Mark F. Vancas

Bateman Engineering, Tucson, Arizona, USA

INTRODUCTION

This hopefully will be the beginning of an on going series of discussions concerning solvent extraction plant operating practice. The intent is to develop a data base of practical operating procedures and practical solutions to common problems. Similar to the database of World Operating Data for SX and EW plants that has been assembled and updated periodically by Tim Robinson, Jackson Jenkins, and Bill Davenport; this database will be continually updated and may well lead to more conference presentations along the same vein. To create this database, various operators scattered around the globe and throughout the minerals industry solvent extraction plants have been solicited to provide input. These operators have responded with their insight/thoughts about the various questions posed to them. Reagent and equipment suppliers to the industry have also been included because, in many cases, they have been exposed to many more “situations” than a single operator has in his/her respective plant.

The names have been changed to protect the innocent. Actually to avoid any association of the answers to individuals or companies the respondents to the questions have been designated simply as operator 1,2,3, etc. The operator number is assigned by the order in which the responses were received so operator 1 for question number one is not the same person as operator 1 for a different question. The responses are unedited other than spelling, punctuation, and formatting. Some of the terminology will give a hint as to the continent of origin. Specific flow rate becomes flux rate, gpm becomes m^3/h, hp becomes kW, and °F become °C, etc. This just adds an international flare and forces us to realize that there is a world outside our individual plants/offices.

For presentation purposes the intent is to select a few representative questions and lists of responses for review and to “set the stage” so to speak. Following on from that, the audience of the conference session will be expected to add to the review with comments of their own. Eventually enough questions and answers will be assembled to make a fairly comprehensive list. That list may be published in booklet form if deemed advantageous. Time will be our judge as to whether or not the effort is worth continuing. Obviously I believe there is a need for such interaction or I would not be trying to start this ball rolling.

DISCUSSION

Question #1
What do you do to insure that the PLS feed concentration to your plant is uniform and what do you do if and when it varies?

Operator #1
If the feed grade varies to the plant O/A s are adjusted as needed to optimize extraction efficiency. If the feed grade is temporarily high and EW is not maxed and O/As have been increased as much as possible, I've shut the iron bleeds and make up H_20 off to SX so all of the loading capacity of the reagent is used to transfer copper from the leach solution. Then, when the feed grade drops off, increase bleeds and make up H_20 to make up for time they were off. As far as keeping a steady feed grade, working directly with the mine is critical to assure grade does not go to high or low but sometimes such is inevitable.

Operator #2
The areas under leach are rotated to try to maintain a steady feed concentration. Some averaging/blending of solutions occurs in the PLS pond and the SX Feed pond. When that fails, the plant feed rate is adjusted to maintain a steady copper input so the EW circuit is not affected. Internal mixer settler recycling of aqueous or organic is adjusted to hold the total flux rate in the mixers and settlers fairly constant.

Operator #3
Coordination with the mine and adjustments to the leaching schedule keep the PLS grade in a tight enough range that we can maintain steady production by temporarily increasing flows, increasing O/A when the PLS is low. On the high side, we generally slow the flow to the plant thus increasing PLS pond inventories to avoid by-passing to raffinate which we are forced into on occasion.

Operator #4
Noting that we are not operational yet we do not have the practical experience to detail this question. However, the modeling that we have done demonstrates two methods - both interlinked - of controlling PLS. These are adjustment of milled tonnage and leach density. The former, of course, is more of a long term control whilst the latter is short term.

Operator #5
Short term and long term planning models are utilized to forecast PLS grades and flows. The models incorporate short term/long term mine planning models, ore placement schedules, lift height, recovery curves, application rates, ore types, etc. We place a lot of emphasis on and effort in planning to avert variances of this nature. We have four major PLS reservoirs, average operating volume of ~ 12 million gal each, that report to a single SX feed pond. Consequently we have some flexibility with regard to blending and the large volume of solution in the reservoirs tends to minimize spikes in the grade. In the event the PLS grade is above forecast, the organic to aqueous ratio can be increased or additional extractant can be added to the circuit. All unbudgeted organic purchase requests, diluent/extractant, must be accompanied by an economic evaluation supporting the expenditure.

Operator #6
In most cases plant operators try to handle small fluctuations in PLS grade by adjusting the advance organic / aqueous flow ratio across extraction and stripping. Most plants are reluctant to add reagent to handle an increase in the copper in the PLS unless they are convinced the increase in copper will be around for a good bit of time. We think this is the right thing to do and it is the thing we would do if we were operating the plant. Copper solvent extraction is a very flexible process and altering the advance O/A ratio is a good way to use that flexibility to the SX plants advantage. The other thing that can be done on a temporary basis is to alter the acid concentration on the strip side to either increase or decrease the stripped organic. Some plants have built in the ability to change the circuit configuration from series to series parallel or from series parallel to full parallel to handle significant changes in flow and in PLS grade. If there are multiple sources of PLS and multiple SX plants the possibility exists to blend PLS to get a more even grade or perhaps ship PLS to a plant that has excess reagent from a plant with too little reagent or vice versa.

This would be a special case as there are not many operations with that many multiple sources of PLS or multiple SX plants.

Operator #7
In our experience most operators have a good idea of the expected variation in PLS Cu & pH, based on the mineralogy of the ore at the various stages in the leach cycle. Additionally, some operations which have multiple collection ponds will blend PLS to achieve a reasonably steady head grade. Generally speaking +- 10% is considered normal PLS Cu variation and recovery is maintained by making small changes to one or more process variables (most commonly the extract O/A ratio but also the reagent concentration & lean electrolyte acid concentration as required). If a major change is expected (say, >20%), the operators generally carry-out some circuit modeling using software from the reagent suppliers or request the models from the suppliers, based on expected PLS conditions. This may simply require a change in reagent concentration and/or a change to some of the process variables but commonly we are asked to look at reconfiguring the existing circuit to meet the recovery & transfer objectives of the plant.

Operator #8
Question No. 1: What do you do to insure that the PLS feed concentration to your plant is uniform?

- blend separate ore units into large homogeneous stockpiles of average grades, that are sufficient for 4 weeks feed to roasting.
- adjust ore feed rate to roasting to maintain constant extractable nickel throughput
- adjust pregnant liquor flow rate to maintain constant Ni tenor (6 hourly sampling frequency)
- control feed slurry density to leach to maintain target (on line density meter)
- control the strip liquor flow rate to maintain target metal tenor in loaded strip (which is the feed to the next SX circuit)
- control the metal tenor in raffinate to the target using an on-line analyzer (which is the feed to the next SX circuit)

And what do you do if and when it varies?

If the feed concentration is too high:

- add dilution water to achieve the target metal tenor in feed liquor
- recycle raffinate to dilute the feed and achieve the target metal tenor in the feed liquor
- reconfigure the circuit to utilize one of the strip cells as an additional extract cell
- decrease the feed liquor flow rate to give target metal through put
- increase the stripped organic flowrate to maintain the target metal tenor in loaded organic

If the feed concentration is too low:

- decrease the pregnant liquor flowrate
- decrease the stripped organic flowrate to maintain target metal tenor in loaded organic

Question #2
How do you measure 0:A ratio, how do you change/adjust the 0:A ratio, and how often do you do so?

Operator #1
Use a graduated cylinder (approx. 1000 ml) attached to a long pole, if mixer has multiple stage mixing O/A is taken from primary mixer. Solution should be taken from area of mixer where no settling has occurred. Could also use beaker and pour into graduated cylinder if it is easier. All of sample should be used (don't pour off top part of sample if to large of sample is collected as separation occurs immediately and will give a false reading) so an accurate reading can be taken. Can also take several readings and average the difference as there is usually a slight difference between O/As.

O/A measurements are taken as needed, if flow meters are trustworthy O/As only verify the flow meters and are not needed to often. If flow meters are not accurate or if the recycles on strippers do not have any flow meters then O/As would be taken after any major adjustment in flow.

O/A ratios are adjusted by changing the appropriate flowrate depending on what out come you desire. On extractors usually by increasing or decreasing the organic flow rate (not always) on strippers by increasing or decreasing the recycle. Examples: If the raffinate Cu leaving SX is too high; I would increase organic flowrate to increase extraction. If the O/A is too low in the stripper, I would decrease electrolyte recycle to increase the O/A.

Operator #2
O/A ratio can be measured in three ways:

1. Dipping the mixer - e.g. using a 1 liter plastic measuring cylinder attached to a long plastic pole.
2. Basing O/A on relative flow rates of Org, PLS & LE
3. Calculating the O/A from the measured copper concentration of all streams entering and exiting the SX circuit.

The O/A is adjusted either by increasing/decreasing organic, PLS & LE flows. Small changes (say, +- 5%) to all three flows is routine; larger changes much less common - and only in reaction to a specific change in requirements (grade/pH change to PLS; solution availability etc).

Operator #3
I cannot comment on the way the various plants measure O/A, but I can comment on an experiment that a colleague and I did some time ago. We stood on top of a large square primary mixer. With a large graduated cylinder attached to the end of a long pole we pulled samples of dispersion (emulsion) from various places in the mix box, allowed the phases to separate and measured the O/A in the grad cylinder. The O/A ratio was different from each spot we took the sample and the variability was significant. We plotted the O/A ratio on a mao of the mixer surface to see if there was some pattern to the O/A and the surface of the mixer - no such luck. High O/A here, low O/A there, and different O/A everywhere. Dr. Seuss.

Operator #4
For normal day-to-day operations, we measure the O/A ratio by the individual flowrates. If we feel that we have a problem, we use a 1 liter graduated cylinder attached to a pole and dip the primary mix chamber from the support platform.

Operator #5
We use a 250 ml graduate attached to a PVC pipe which is rapidly submerged near the primary mixer impeller. Adjustments are made by changing flow set points for the respective organic or aqueous stream. Then the O/A is checked again by dipping the graduated cylinder. O/A's are changed to settle out crud movement, phase changes or to effect overall

copper extraction. So the answer to how often is highly variable from no changes in excess of a week to several times per day.

Operator #6
How do you measure 0:A ratio?

- IOOmL graduated glass cylinder, filled from a sample point on the side of the tank. The filled cylinder is placed upright inside a purpose built aluminum box with a glass window at the front, and left to coalesce while the operator continues with other tasks. The purpose of the box is to prevent contamination (rain etc) and to prevent the wind from blowing the cylinder over.
- Where both aqueous and organic are opaque so that the interface is not readily visible, a few ml of water is then added to the cylinder. The water passes through the organic and settles on top of the aqueous, because the aqueous density is >1.1. The water allows the interface to be readily located.

How do you change/adjust the 0:A ratio?

- adjust a manual control valve on either the aqueous or organic recycle line

How often do you do so?

- 0:A is checked either 4 hourly or 6 hourly, and adjusted as required.

These are examples of the type of questions and answers that have been asked and given; simple questions, straight answers, a little humor, in some cases conflicting approaches but nevertheless all good stuff and hopefully just the beginning. If anyone not already included on the mailing list is interested in participating in this effort, please contact Mark F. Vancas at bsxtucson@aol.com.

PILOT-PLANT COMPARISON OF BATEMAN PULSED COLUMNS AND MIXER SETTLERS FOR THE EXTRACTION AND STRIPPING OF ZINC IN THE DI(2-ETHYLHEXYL)PHOSPHORIC-ACID SYSTEM

Kathryn C. Sole and Sean A. Scott*

Anglo American Research Laboratories, Johannesburg, South Africa
* Mintek, Randburg, South Africa

A pilot-plant evaluation of the extraction and stripping performances of mixer settlers and a Bateman pulsed column test unit is described. Zinc extraction from a leach liquor containing 24 g/l Zn was accomplished using 45 vol.% di(2-ethylhexyl)phosphoric acid in an aliphatic diluent. The zinc-loaded organic phase was stripped with 150 g/l H_2S0_4. A comparison of the chemical and physical operating performance of the two contactors is presented.

INTRODUCTION

While most hydrometallurgical solvent-extraction (SX) applications rely on the use of mixer settlers as the contacting equipment, an alternative technology is that of columns. In the metallurgical industry, Bateman pulsed columns (BPCs) have been commercialised for uranium [1] at Olympic Dam, Australia, and a decision made to install these units for the two SX circuits in the Goro nickel flowsheet in New Caledonia. Piloting of zinc, cobalt, nickel, and copper systems has been reported [2-8], Some advantages claimed for BPCs are [9]:

- flux rates of 30 to 50 m^3/m^2h, resulting in very small footprint requirements;
- no evaporation losses or air ingress as the units are sealed;
- improved safety of operation and lower fire risk;
- replacement of several mixer settlers by a single column for the equivalent performance;
- operation in either aqueous- or organic-phase continuity (including the possibility of dispersing the major phase in the minor phase);
- inclusion of washing or scrubbing operations in the extraction or stripping columns;
- improved phase separation in the settlers, lower entrainment losses, and reduced crud formation since mixing and mass transfer occur in a very low-shear environment;
- high tolerance of solids or crud in suspension;
- lower maintenance downtime due to few moving parts;
- reduced reagent losses, maintenance costs, and operating costs.

Since columns are particularly appropriate for systems that have rapid kinetics and do not require interstage pH control, the extraction of zinc by di(2-ethyl-hexyl)phosphoric acid (D2EHPA) is ideally suited to this application. The objectives of this study were (i) to determine whether data comparable to the previously optimised results for this system obtained using mixer settlers could be achieved for similar process conditions using a column configuration, and (ii) to validate the claimed advantages of BPCs.

PROCESS DESCRIPTION

The circuit, depicted for a mixer-settler configuration, is shown in Figure 1. Zinc is extracted from a clarified pregnant leach solution (PLS), generating acid that reports to the raffinate:

$$Zn^{+2}_{(aq)} + 2\ H_2A_{2\ (org)} \rightarrow Zn(HA_2)_{2\ (org)} + 2\ H^+_{(aq)}$$

where H_2A_2 represents the dimerised form of D2EHPA. Co-extracted impurities are displaced from the loaded organic (LO) phase by scrubbing. Zinc is stripped from the scrubbed organic phase (ScO), generating a loaded strip liquor (LSL). Co-extracted iron(III) is removed from the stripped organic (SO) using 160 g/l HCl to produce the regenerated organic phase (RO).

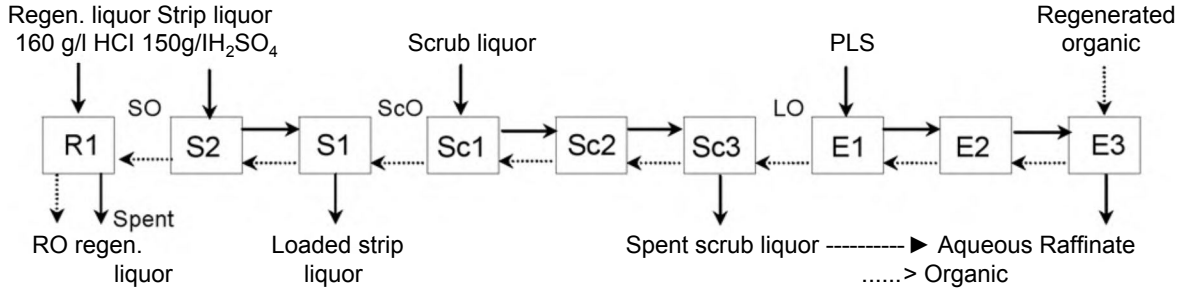


Figure 1. Mixer-settler SX circuit configuration for the purification of zinc using D2EHPA.

PILOT-PLANT EQUIPMENT AND PROCEDURES

Solutions and Reagents

The PLS composition is given in Table 1. The organic phase comprised 45 vol.% D2EHPA in the paraffin diluent SSX 210. The strip liquor contained 150 g/l H_2S0_4. The LO fed to the strip circuit contained 13-14 g/l Zn, and only trace levels of impurities.

Table 1. Typical PLS composition.

Element	Cone. (mg/l)	Element	Cone. (mg/l)	Element	Cone. (mg/l)	Element	Cone. (mg/l)
Al	155	Co	< 5	Fe	< 10	Pb	6
Ca	580	Cr	< 5	Mg	7800	Si	81
Cd	144	Cu	174	Mn	3100	Zn	23 600
Cl	< 5	F	2.0	Ni	19.3	PH	2.0

Mixer Settlers

Each stage of the mixer-settler circuit had a 32 l square mixing box, equipped with a 190-mm diameter flat-vaned pumping impeller, and settling area of 0.091 m^2. To maintain the required temperature (40 °C) in the extraction circuit, the settlers of these stages were fitted with immersion heaters, and the PLS and RO were preheated. Aqueous recycles were used to control the phase continuity in the mixers. Aqueous solutions were fed to the circuit using peristaltic pumps, while the RO was introduced *via* a Bredel pump.

Bateman Pulsed Column

A 4-m high, 40-mm diameter glass BPC was used. Disc-and-doughnut polyvinylidene fluoride internals facilitated the continuous dispersion and coalescence of the dispersed phase. Interfacial contact was achieved by means of pulsation, the frequency (0-150 strokes/min or spm) and amplitude (2-14 mm) of which were varied to alter the energy input. On each pulse, the two phases are mixed, and then coalesce and separate again in contact with the column internals. Using gravity and density differences, the two phases move countercurrently through the column. The column and piping were insulated using fibrefrax to maintain the extraction operating temperature.

The piloting campaign separately assessed extraction and stripping performances. When extraction was carried out using the BPC, the LO produced was fed forward to the scrub, strip, and regeneration stages in mixer settlers, bypassing the mixer settler extraction stages; when stripping was carried out in the BPC, the strip mixer settlers were bypassed. Aqueous- and organic-continuous modes of operation were tested. Appropriate hydrodynamic conditions for operation were first identified (determination of the flooding curves for the column by variation of the energy and flux inputs to the column). Once stable operation was achieved, the circuit was run under constant conditions to obtain mass transfer data and evaluate the chemical efficiency of the operation. The campaign was run 24 h/d for 10 days.

BPC METALLURGICAL RESULTS

Extraction

In aqueous-continuous mode, flooding occurred across a range of energy inputs. The dispersed phase comprised distinct droplets, the diameter of which could be controlled by increasing the energy to obtain fine droplets. Organic hold-ups were uniformly distributed across the column. Zinc recovery increased with increasing energy input (frequency x amplitude), and decreased with increasing flux (Figure 2). The extent of extraction is dependant on the mass transfer surface area (degree of agitation or energy input) and on the contact time between the phases (residence time in the column or flux). The lowest zinc recovery was recorded at the highest energy input, but at a high flux. The extraction reaction was mass transfer-limited under these conditions due to low residence time in the column. The highest zinc recovery (80 %) was achieved at lower fluxes and maximum energy input.

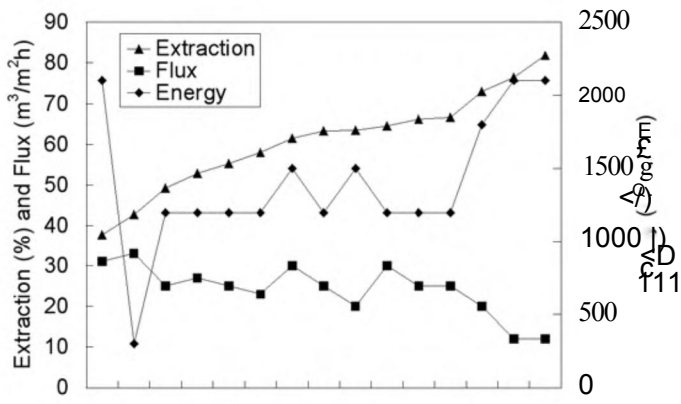


Figure 2. Relationship between zinc extraction, energy input, and solution throughput.

In organic-continuous operation, the aqueous phase could not be dispersed to form distinct droplets in the organic phase, the dispersion was stringy, and widely varying hold-ups in the column were measured. Stable operation was limited, and the maximum zinc extraction measured was 40 %. The energy range of the pulsator was inadequate to achieve good dispersions in organic-continuous mode, and results comparable to the mixer-settler data were achieved only under aqueous-continuous conditions using this size of BPC unit.

Stripping
Aqueous-continuous operation yielded flooding behaviour that was limited by both maximum flux and maximum energy inputs. The dispersion was uniform and a narrow range of hold-ups measured. Under appropriate operating conditions, excellent stripping (> 99 %) was achieved, and it was possible to achieve the target LSL concentration of 80-90 g/l Zn. Figure 3 shows the relationship between stripping efficiency, energy, and flux. Combinations of low flux and high energy gave high stripping efficiencies.

Under organic-continuous conditions, hydrodynamically stable operation was found to be limited by flux rather than by energy; dispersion was poor, with no visibly distinct droplets; and stripping efficiency was poor, primarily due to very low hold-ups.

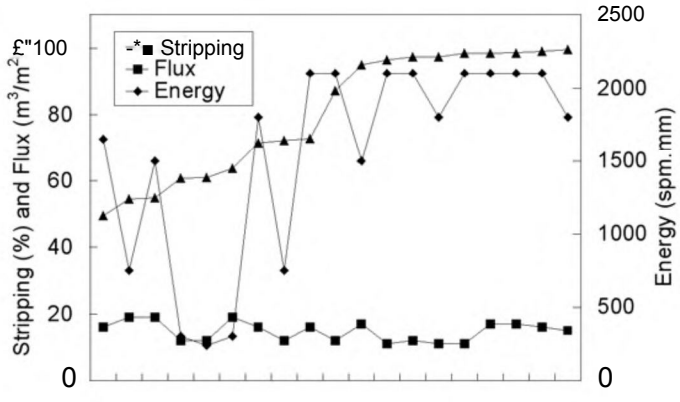


Figure 3. Relationship between zinc stripping, energy input, and solution throughput.

COMPARISON OF BPC AND MIXER-SETTLER PERFORMANCE

Extraction and Stripping Efficiencies
As shown in Table 2, the extraction performances of both circuit configurations were very similar. Zinc extraction of ~70 % was achieved with the organic phase loaded to full capacity.

Stripping results for the two contactors were also very similar (Table 2). The higher LSL zinc concentration for BPC operation is due to the higher LO concentration and is not equipment-dependent. In both cases, it would be preferable to operate at slightly lower LSL zinc tenors to ensure quantitative stripping (< 0.1 g/l Zn on SO), since any zinc remaining on the SO will be removed in the regeneration circuit, representing a waste of regeneration reagent. In this study, the strip liquor acid content was lower than conventional for a zinc electrowinning spent electrolyte; by increasing the acid concentration, it should be possible to achieve both complete organic stripping and concentration of the LSL to a higher value.

The main difference between the two configurations for both extraction and stripping was the flux required to achieve comparable results (Table 2). The column can process a much higher flowrate per unit area than mixer settlers, representing significant capital cost saving. The real estate advantage claimed for BPCs can certainly be validated for this application.

Deportment of Impurities
The average impurity loadings on the organic phase for optimised extraction conditions (Table 3) were very similar for both trials, with the exception of cadmium. It is unclear why transfer of this element was so much higher in the BPC case, but it may be due to the aging of the organic phase, since the BPC trial was carried out subsequent to the mixer-settler trial.

The impurity deportment to the LSL (Table 4) shows a slight advantage to the BPC. It is concluded that the BPC unit matched or exceeded the performance of the mixer settlers.

Table 2. Comparison of extraction and stripping efficiencies.

Extraction	Mixer settlers	BPC	Stripping	Mixer settlers	BPC
Zn recovery (%)	69.3	71.0	Stripping efficiency (%)	98.0	99.0
[Zn] in raffinate (g/l)	7.36	7.25	[Zn] in LSL (g/l)	70.1	77.7'
[Zn] on LO (g/l)	13.9	13.7	[Zn] on SO (g/l)	0.28	0.8
Advance 0:A	1.1	1.1	Advance 0:A	4.5	3.7
Flux (m^3/m^2h)	1.9	20	Flux (m^3/m^2h)	1.2	15
No of stages	3	–	No of stages	2	—
Height of column (m)	—	4	Height of column (m)	—	4

* LO used for stripping contained 21 g/l zinc during stripping tests in BPC.

Table 3. Comparison of impurity transfer in extraction circuits.

Element*	Loaded organic (mg/l)		Element	Loaded organic (mg/l)	
	Mixer settler	BPC		Mixer settler	BPC
Ca	33	36	Mn	27	36
Cd	< 2.5	11.6	Ni	< 2.5	<2.5
Co	< 2.5	< 2.5	Pb	< 2.5	< 2.5
Cu	< 2.5	< 2.5	Si	23.1	15
Mg	5.5	6.3	zn (g/i)	13.9	15.0

* Trivalent cations load irreversibly onto the organic phase. Since regeneration conditions were not comparable for the two trials, these elements have been omitted.

Table 4. Comparison of impurities reporting to the LSL in strip circuits.

Element	Loaded strip liquor (mg/l)		Element	Loaded strip liquor (mg/l)	
	Mixer settler	BPC		Mixer settler	BPC
Al	66	23	Fe	< 5	< 5
Ca	53	32	Mg	< 5	< 5
Cd	6.1	8.1	Mn	< 2.5	< 2.5
Co	< 5	< 5	Ni	< 2.5	< 2.5
Cr	< 2.5	< 2.5	Pb	< 2.5	< 2.5
Cu	< 5	< 5	Si	< 2.5	< 2.5

Entrainment Losses

Table 5 compares the average entrainment losses. Relative aqueous-in-organic entrainment was compared by monitoring chloride deportment to the LSL, since this anionic species will not be complexed by D2EHPA and its transfer through the circuit can be considered to occur by physical means. Organic-in-aqueous losses were assessed by monitoring the total organic carbon (TOC) content of the raffinate and LSL.

Table 5. Comparison of entrainment losses.

Exiting stream	TOC (mg/l)		Cl (mg/l)	
	Mixer settler	BPC*	Mixer settler	BPC*
Raffinate	16.5	2.7	N/D	N/D
LSL	2.4	6.4	8.4	3.4

* Aqueous-continuous mode of operation

The LSL would be expected to have lower organic entrainment because of the enhanced phase disengagement typically encountered for higher aqueous-phase acidity. The mixer-settler data follow the expected trend. While the BPC shows much lower organic entrainment than the mixer settlers for extraction, the opposite effect was recorded for stripping. The aqueous entrainment is indicated to be lower in the BPC circuit. While vendor claims have some validity, confirmation of potential savings due to lower entrainment losses is required.

CONCLUSIONS

Pilot-plant comparison of the performances of the zinc SX extraction and stripping circuits in mixer settlers and BPCs yielded the following main results and conclusions:

- In both contactors, extractions of 70 % could be achieved, with a zinc transfer of > 15 g/l and organic-phase loading of 14 to 15 g/l Zn without pH adjustment.
- For both contactors, zinc stripping efficiency was 98 to 99 %, limited by the availability of acid in the strip liquor. Higher LSL upgrading measured in the BPC trial corresponded to higher LO and SO zinc concentrations, and was not equipment-dependent.
- LSL purity and impurity deportments were comparable.
- Equivalent extraction and stripping results were achieved using a flux an order of magnitude higher for the column configuration.
- Organic-in-aqueous losses were much lower for the BPC operating in extraction mode, but no significant difference was measured in the stripping mode.

This testwork confirmed the potential of column technology for the zinc-D2EHPA system. Although no optimisation of the circuit was undertaken, it was shown that the extraction and stripping performance of the BPC can meet or exceed the performance of an equivalent mixer-settler circuit. A number of operational advantages, including lower fire risks, exist for columns, and capital and operating cost savings may accrue.

ACKNOWLEDGEMENTS

Appreciation is extended to Chemquest and Sasol Wax for their respective donations of Chemorex D2EHPA and SSX 210, and to Kumba Resources for providing the PLS. The significant contributions of Mintek and AARL shift metallurgists, pilot-plant operators, and analysts to the success of the piloting campaigns are also acknowledged.

REFERENCES

1. R. L. Movsowitz, R. Kleinberger, E. M. Buchalter, B. Grinbaum, S. Hall (2000), *Proceedings ISEC '99, Society of Chemical Industry, London, pp.* 1455-1460.
2. R. Kleinberger (2001), *Copper Cobalt Nickel and Zinc Recovery Conference,* South African Institute of Mining and Metallurgy, Johannesburg.
3. V. Nagel, M. Gilmore, S. Scott (2002), *Proceedings ISEC 2002,* South African Institute of Mining and Metallurgy, Johannesburg, pp. 970-975.
4. M. H. Fox, S. J. Ralph, N. P. Sithebe, E. M. Buchalter, J. J. Riordan (1998), *ALTA 1998 Nickel Cobalt Pressure Leaching and Hydrometallurgy Forum,* ALTA Metallurgical Services, Melbourne.
5. V. Nagel, A. Feather, A. Swarfs (2002), *ALTA 2002 Nickel/Cobalt-8,* ALTA Metallurgical Services, Melbourne.
6. D. Parkes, B. Grinbaum, R. Kleinberger, B. Arnall (2000), *ALTA 2002 Nickel/Cobalt-8,* ALTA Metallurgical Services, Melbourne.

7. E. M. Buchalter, R. Kleinberger, B. Grinbaum, C. Nielson (2002), *Proceedings ISEC 2002*, *South African Institute of Mining and Metallurgy, Johannesburg, pp.* 1021-1026.
8. G. Johnson, E. M. Buchalter, R. Kleinberger, R. L. Movsowitz, J. Riordan (1999), *Solvent Extraction and Electrowinning: Basic Principles and Applications,* South African Institute of Mining and Metallurgy, Johannesburg.
9. S. Burks (1999), *Solvent Extraction and Electrowinning: Basic Principles and Applications,* South African Institute of Mining and Metallurgy, Johannesburg.



SOLVENT EXTRACTION IN ZINC PRODUCTION FROM A PRIMARY SOURCE: THE SKORPION ZINC EXPERIENCE

Herman Fuls, Kathryn C. Sole* and Taaf Bachmann

Skorpion Zinc, Rosh Pinah, Namibia
* Anglo American Research Laboratories, Johannesburg, South Africa

The Skorpion Zinc refinery, Namibia, was successfully commissioned during 2003, and is approaching full production of 150 000 t/a of special high grade zinc (> 99.995 % Zn). The orebody presents unique challenges, containing fluorides and chlorides that cannot be processed *via* traditional extraction routes. The process flowsheet represents a radical departure from classical zinc refineries in the use of atmospheric leaching of the high-silica oxide ore, followed by solution purification by solvent extraction, and the electrowinning of zinc cathode. Solvent extraction has proven to be very effective in producing a high-purity electrolyte for the production of high purity zinc on a large scale. Impurities reporting to the leach liquor are reduced to mg/l or pg/l levels in the electrolyte, while the zinc is upgraded from 30 to 105 g/l. This technology has enabled Skorpion Zinc to produce special high grade zinc as a new branded product in the market. The main features of the process are presented, and some experiences during the commissioning and ramp up are discussed.

INTRODUCTION

Anglo American's Skorpion Zinc refinery, located near Rosh Pinah in southern Namibia, produced its first metal in May 2003, and is approaching full production of 150 000 t/a of special high grade (SHG) zinc (> 99.995 % Zn). From the discovery of a sizeable but unconventional orebody in the remote Namib desert, once considered untreatable, to the existence today of a robust world-class operation consistently producing amongst the highest quality zinc at one of the lowest operating costs in the world, the Skorpion Zinc operation represents a world first in the application of solvent extraction (SX) to the production of a primary zinc product directly from ore. Contributing significant economic advantage is that cathode is produced at the mine site—a feature seldom seen for sulphide ore processing [1],

The orebody, a substantial oxide resource averaging 10.9 % Zn, was discovered in 1976. The main minerals are sauconite (a zinc-bearing clay mineral), smithsonite (zinc carbonate), and hemimorphite (zinc silicate) [2], The elevated silica levels and the presence of halides deterred early efforts to develop a processing route but, in collaboration with Reunion Mining, Técnicas Reunidas, and Umicore, the integrated flowsheet was piloted at Anglo American Research Laboratories during 2000. Project approval was announced later that year, at a capital expenditure of US$ 454 million. The feasibility study indicated that Skorpion Zinc would be one of the lowest cost zinc facilities in the world, with an expected production cost of US$ 0.25/lb [3], Bateman and SNC Lavelin were appointed as joint engineering, procurement, construction, and management (EPCM) contractors.

PROCESS DESCRIPTION

A simplified flowsheet of the process is given in Figure 1. Following an atmospheric sulphuric acid leach, Fe, Al, and Si are precipitated from solution. The clarified pregnant leach solution (PLS) is purified by SX with di(2-ethylhexyl)phosphoric acid (D2EHPA), enabling the electrowinning (EW) of SHG zinc. The raffinate is recycled to the leaching circuit so a bleed for removal of impurities is required. Base metals that co-precipitate with zinc (such as Cu, Co, Ni, and Cd) are removed from the bleed by cementation with zinc dust. The halides and magnesium exit in the secondary filtrate that is treated for zinc recovery by the precipitation of basic zinc sulphate ($(Zn0)_3ZnS0_4$). This zinc is returned to the main circuit by recycling the precipitate as a neutralising agent.

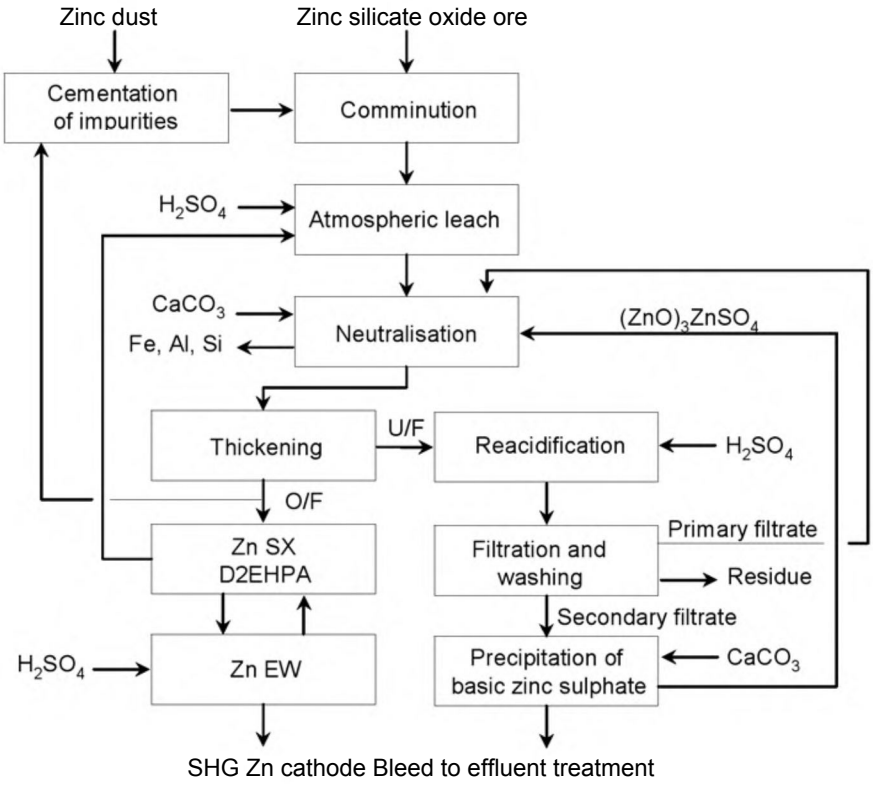


Figure 1. Simplified process flowsheet of the Skorpion Zinc refinery [4],

Técnicas Reunidas were responsible for the provision of the SX technology, which is based on the Modified Zincex Process developed for the treatment of secondary materials [5-7], The selection of SX as the purification step serves several purposes in this flowsheet [4]: D2EHPA is selective for zinc over most base metal impurities (specifically Co, Ni, Cu, and Cd, where only pg/l levels can be tolerated by EW) (Figure 2); the choice of a cation exchanger ensures rejection of the halides released from the ore; and, the dilute leach liquor (30 g/l Zn)—produced by leach conditions dictated by the elevated silica content (~ 26 %) of the ore—ensures that soluble losses of zinc in the filtration step are minimised and that the problematic formation of silica gel is avoided. SX successfully upgrades this PLS to 105 g/l Zn required for EW. The high extractant concentration (40 vol.% D2EHPA) allows high zinc transfer (20 g/l) in the extraction circuit without the need for neutralisation, and the acid generated by the extraction reaction is available for leaching on recycle of the raffinate. Operation at high organic loadings limits the extent of Ca co-extraction, while the washing

stages further reduce impurity transfer to EW. The selectivity of D2EHPA for Zn over Mn poses a disadvantage in that the Mn required for anode conditioning in EW must be added from another source.

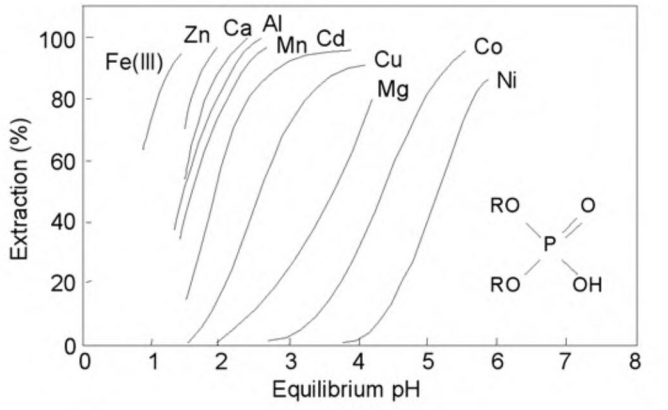


Figure 2. D2EHPA selectivity as a function of equilibrium pH [8],

SOLVENT-EXTRACTION CIRCUIT

The Skorpion plant is the largest yet built for zinc SX, with a PLS flowrate of 960 m^3/h. The circuit (Figure 3) comprises three extraction, three washing, and two strip stages. The first two washing stages use demineralised water to remove physically entrained impurities; diluted spent electrolyte (SE) is employed as a scrub liquor in the third wash stage to remove co-extracted impurities from the loaded organic phase. SE is employed as the strip liquor, and the loaded electrolyte (LE) generated is fed forward to EW for zinc recovery as cathode. Iron build-up on the organic phase is controlled by treating a bleed stream with 6 *M* HCl in the regeneration circuit.

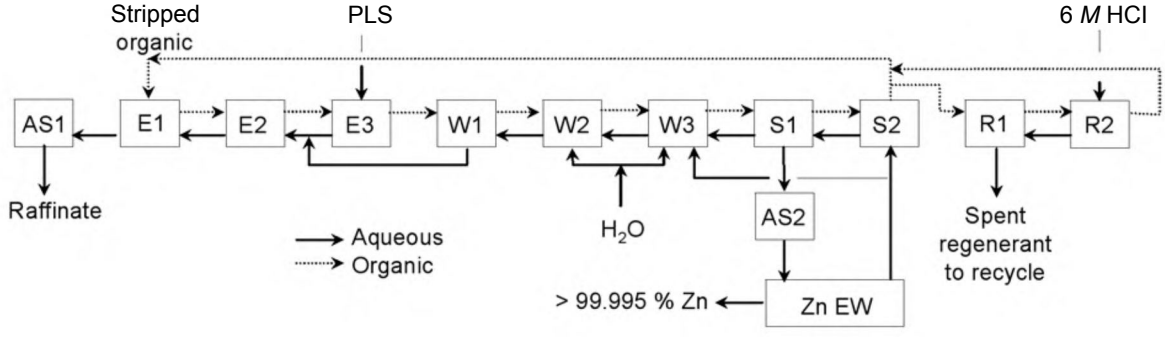


Figure 3. Skorpion Zinc SX circuit configuration [8].

A conventional mixer-settler design has been employed, with settlers of area 390 to 650 m^2. The extraction stages have four mixing compartments, powered by three agitators and a pump mixer, while the washing and stripping stages have three mixing compartments. The concrete cells are lined with high-density polyethylene, and phase separation is assisted by two rows of baffles in the settlers. Two rows of picket fences are installed at the inlet to the settlers to distribute flow evenly through the settlers.

START-UP AND COMMISSIONING

The stringent purity requirements of the electrolyte posed challenges to the refinery start-up and demanded that the SX plant was carefully prepared ahead of processing the first zinc. The entire circuit was flushed with water and hydraulically tested, before adding 10 g/l H_2S0_4 to assist with mild chemical washing of the process equipment and ensure adequate phase disengagement once the organic phase was introduced. Two-phase operation commenced with the addition of the diluent (Escaid 100). Once the settler configurations had been optimised and the organic loop commissioned, the extractant was added. Water in the wash and strip circuits was then replaced with synthetic spent electrolyte (250 g/l H_2S0_4).

Success in commissioning enabled a strong start to the ambitious production ramp-up programme. However, shortly into the ramp-up phase, effects of corrosion by the aggressive plant conditions became evident. Production during the following several months was adversely affected by a variety of materials problems, including the widespread failure of under-specified halar-coated butterfly valves throughout the refinery, corrosion in the glass flake-lined piping in the carbon columns, and failure of rubber-lined piping within reducers on the raffinate line. In general, problems were related to deficiencies in construction quality control and assurance and the selection of the materials, rather than to inherent process issues. A systematic repair and replacement programme was able to restore the ramp-up progression: by April 2004 the SX circuit had exceeded nameplate production capacity.

FULL-SCALE PROCESS PERFORMANCE

The success of the process chemistry can be assessed with reference to the typical compositions of the various process streams (Table 1). In the extraction circuit, zinc transfer of 20 g/l from the clarified PLS is achieved using an advance 0:A of 1.5 and organic loading of 14-15 g/l Zn. Most base metals and other impurities are rejected. Residual Fe(III) and some Al(III) entering the circuit are co-extracted. Extraction selectivity has matched design expectations, and electrolyte purity has consistently remained within specification and independent of PLS characteristics. Although some trace Ni and Co carryover to the strip circuit is evident, the very low levels of other impurities nevertheless ensure that the zinc cathode target specification is maintained.

Table 1. Typical compositions ofSX process streams.

Element	PLS (mg/l)	Raffinate (mg/l)	LO (mg/l)	SO (mg/l)	LE (mg/l)	Target LE (mg/l) [8]
Al	60	55	20	50	220	—
Ca	660	600	50	20	55	–
Cd	210	200	< 5	< 5	0.012	< 0.05
Cl	1700	1600	–	–	56	< 100
Co	13	12	< 5	< 5	0.072	< 0.05
Cu	500	480	< 5	< 5	0.081	–
F	30	29	–	–	3	< 20
Fe	4	2	150	150	5	< 5
Mg	1140	1100	< 5	< 5	26	–
Mn	2040	2000	< 5	< 5	2500	3000
Ni	210	205	< 5	< 5	0.073	< 0.05
Si	70	60	< 5	10	–	–
Zn	35 000	13 000	14 500	500	105 000	> 90 000

Anionic halides are eliminated by washing the loaded organic phase with water to remove and dilute any entrained PLS droplets. The high acid content of the scrub liquor (33 g/l Zn, 100 g/l H_2S0_4) reporting to stage W3 serves to strip the less-strongly complexed impurity cations from the organic phase, while the high zinc content serves a more conventional scrubbing role by 'crowding off these species. Spent electrolyte (50 g/l Zn, 180 g/l H_2S0_4) returned from the cellhouse is passed through carbon columns to reduce any Mn(IV) before entering the strip circuit, where it is upgraded to 105 g/l Zn.

Fe(lll) is more strongly complexed by D2EHPA than zinc and is not stripped at the acidity of the spent electrolyte (Figure 2). Organic-phase iron loading is maintained at < 300 mg/l by treating an organic bleed with 6 *M* HCI. The extent of iron loading is strongly related to iron levels in the PLS (typically < 5 mg/l). While this is generally well controlled, episodes of elevated iron levels have been intermittently experienced. Performance of the organic regeneration circuit has proved adequate to deal with these upsets and no identifiable negative consequences of elevated electrolyte iron levels have been observed. The spent HCI stream is recycled through an acid displacement reaction with H_2S0_4 and salt. Although the chemistry has proven successful, this has to date been the most problematic aspect of the SX section due to initial equipment failures in the HCI regeneration plant.

Crud formation is primarily confined to the extraction circuit, occurring as an interfacial deposit resulting mainly from the carryover of suspended solids in the PLS. The crud is treated by filtration in a press filter to remove solids and the recovered liquid phase is recycled to stage El.

Organic contamination of the up- or downstream processes could lead to dire consequences, so containment of organic entrainment in the aqueous product streams is extremely important. In the leach plant, organic ingress would lead to the generation of large volumes of a tenacious froth, inhibiting settling and solid-liquid separation; in EW, the presence of even trace organics significantly alters the cathode morphology, leading to brittle, adherent deposits that cannot be mechanically processed [10], The raffinate and LE are processed through aftersettlers, flotation columns, and activated carbon filters. The performance of these units has proven adequate in containing organic entrainment to the required levels.

The cellhouse is a Umicore design. The electrolyte characteristics are, however, substantially different from the standard, with low levels of deleterious impurities, the absence of an upstream manganese source, and the closed electrolyte loop. Zinc EW is extremely sensitive to the presence of metal impurities which affect current efficiency, morphology, and associated mechanical handling properties of the plated zinc, and to trace organics which cause brittle and sticky deposits [10], The success of both the SX and acid plants in meeting the required electrolyte purity levels has proven the effectiveness of the process design. Manganese addition is required to replace that lost in anode cleaning and the bleed to SX. The low levels of electrolyte imDurities have enabled conversion from electrolytic manaanese flake to $MnS0_4$, which permits safer operation by eliminating hydrogen generation. Although manganese addition introduces an extra operating cost over the traditional process, the levels required to maintain an effective protective barrier to lead dissolution on the anode surfaces can be optimised: the start-up concentration of 7 g/l Mn has since been reduced to 3 g/l. The low calcium in the electrolyte enables the cellhouse to be essentially free of any scaling within piping and cooling towers. Sludge generation in the EW cells is minimal, and the frequency of anode cleaning is considerably lower than typical .

Cathode quality has consistently exceeded SHG grade due to the high electrolyte purity. The amenity of the cathodes to mechanical stripping has occasionally proven problematic, mainly due to ‘stickiness’ rather than brittleness. These problems were first encountered during release of elevated organic concentrations to the LE, however subsequent episodes occurred in the absence of detectable organic ingress or elevated fluoride levels. Only

isolated cathodes were affected and the deposit ductility was sustained, suggesting that the sticky behaviour arose from factors specific to individual cathode surfaces rather than to bulk electrolyte characteristics. The stripping of zinc is now modulated by routine addition of antimony to the brushing water applied to the freshly stripped blanks. This promotes hydrogen generation on the starting surface, resulting in a reduced area available for zinc attachment. Table 2 shows the specification for SHG cathode [9] and a typical analysis of the Skorpion Zinc product.

Table 2. Comparison of British SHG Standard with typical Skorpion Zinc cathode analysis.

Element	BS SHG spec. (%)	Skorpion cathode (%)	Element	BS SHG spec. (%)	Skorpion cathode (%)
Zn	99.995	99.9956	Cu	0.0010	0.0007
Cd	0.0030	0.0000	Sn	0.0010	0.0000
Fe	0.0020	0.0015	Al	0.0011	0.0001
Pb	0.0030	0.0027			

CONCLUSIONS

Aside from set-backs due to plant engineering and design issues, 18 months of operation at Skorpion Zinc have convincingly proven the soundness of the fundamental metallurgical process. The robustness and success of the SX chemistry in handling impurities have been repeatedly demonstrated by the ability of the process to tolerate various upsets whilst maintaining consistent SHG product output.

ACKNOWLEDGEMENTS

The development, commissioning, ramp-up, and production successes of the Skorpion Zinc SX plant are attributed in no small part to the commitment and enormous contributions of the staff of the Skorpion Project Joint Venture, NamZinc, Técnicas Reunidas, and Anglo American Research Laboratories. This paper is published by permission of Skorpion Zinc, Anglo Base Metals, and Anglo American Research Laboratories.

REFERENCES

1. D. Martin, G. Diaz, M. A. Garcia, F. Sanćhez (2002), *Proc. ISEC 2002, South African Institute of Mining and Metallurgy, Johannesburg,* pp. 1045-1051.
2. Bachmann, T. (2004), *Proc. Anglo American Group Technical Conference,* Anglo American, Johannesburg.
3. M. A. Garda, A. Mejias, D. Martin, G. Diaz (2000), *Lead-Zinc 2000,* The Minerals, Metals & Materials Society, Warrendale, PA, pp. 751-761.
4. K. C. Sole (2001), *Proc. (?h World Congr. Chem. Eng.* (CD-ROM), Melbourne, 10 pp.
5. G. Diaz, D. Martin, C. Lombera (1994), *Res. Conserv. Recyc.,* 10, 43-57.
6. D. Martin, G. Diaz, M. A. Garcia (2001), *World Pat.,* WO 01/44520 A1, June 21.
7. D. Marlin, G. Diaz, M. A. Garcia (2002), *World Pat.,* WO 02/066708, Aug. 29.
8. P. M. Cole, K. C. Sole (2003), *Miner. Proc. Extr. Metall. Rev.,* 24, 91-137.
9. British Standard (1996), BS EN 1179:1996 Zinc and Zinc Alloys - Primary Zinc.
10. M. Niera, T. J. O'Keefe, T. L. Watson (1992), *Miner. Eng.,* 5, (3-5), 521-534.



INTEGRATED APPROACH TO THE DEVELOPMENT OF SOLVENT EXTRACTION FLOW SHEETS

Baruch Grinbaum

IMI(TAMI) Institute for Research and Development

P.O.B. 10140, Haifa Bay 10140, ISRAEL

The objective of the integrated approach is to minimize the cost and duration of the development of the final flow sheet, by optimal allocation of the resources to various steps of the development.

In the integrated approach, the development of a SX flow sheet is done in the following order:

1. Definition of the process: composition of the feed, specification of the product, minimum yield etc. 2. Selection of the solvent(s) and studying its chemical and physical properties. 3. Design of the optimal flow sheet using a computer simulation. 4. Combination of process definition and the results of both the simulation and the laboratory experiments for every battery yields the right type of equipment.

Finally, experimental proof of the recommended flow sheet, in the adequate equipment, follows - first in a bench-scale, and then in a full scale pilot or demonstration plant.

Following of these simple rules ensures a successful development of the process.

INTRODUCTION

The objective of the integrated approach is the development of optimal flow sheet with minimum resources [1], Too often new SX processes are implemented before the development was completed, only to be sent back to the laboratory after the demonstration plant (or yet worse - the industrial plant) fails to deliver. It follows the

Murphy's Law for Process Development: *There is never enough time and money to do the work well but there is always plenty of resources to repeat it* (at double cost).
Design of a *working* plant is based on reliable data, not on timetables. While all possible efforts should be done to finish the job as scheduled, the quality of the process development should never be compromised by considerations of timetable. The overall damage to the project, caused by "shortcuts", may be far heavier than a reasonable delay in the timetable. Topics that were either skipped or done only partially have often to be completed later, because the missing data prevent efficient and safe design, or the bottom line may be malfunction of the plant.
Yet we must accept the basic fact of life that our budget and time *are* limited. While we should not bound to an unreasonable timetable, it is essential to see that the work is done efficiently *in the first iteration*, by optimal allocation of the resources.

THE INTEGRATED APPROACH

The general objective of the integrated approach is to develop an optimal process with minimum resources and within certain time limits. It enables one to eliminate inferior options in the earliest possible stage, and go on to the advanced - and more expensive - stages of development only with the most promising ones.
The development of a SX flow sheet is done in two main steps:

A. Preliminary Research

1. Definition of the process: composition of the feeds, specification of the product, required yield, number of batteries, etc. This is usually either included in the project definition or based on knowledge of the process and theoretical considerations, without experimental work.
2. Literature survey to find recommended solvents, equilibrium and physical data for the relevant process. It includes a thoughtful analysis of all the data available from the client and talk to his staff (if applicable).
3. For a new process, checking the feasibility of the solvents that seem to be suitable, by testing their chemical (liquid-liquid equilibrium) and hydrodynamic (phase separation) properties.
4. For the solvent (or solvents) that seems to be optimal, or that is known to be suitable for the process, the distribution coefficient **D** is derived for every solute. From the value of **D** the phase ratio and the number of stages may be roughly estimated. For a multi-component process, the feasibility of separation between various species may be determined too.
5. For reactive extraction in a new (or unknown) system, kinetic experiments must be carried out, in order to determine the residence time required for completion of the process, as a function of the temperature and intensity of mixing.
6. Hydrodynamic tests: the measurement of density, viscosity and interfacial tension for the various streams, and the determination of the phase separation rate, as a function of the temperature and the continuity.

7. The optimum flow sheet of the process is developed using the computerized simulation. If several solvents are considered, the parametric runs enable finding the best one. It should be emphasized that in the integrated approach *the use of computerized simulation is of crucial importance:* this is the stage at which maximum savings in time and manpower can be achieved.

The results obtained so far enable one to recommend the final composition of the solvent, the operating temperature, dispersion type, the flow sheet (phase ratio and number of stages for each battery) and the equipment to be used. They are sufficient for a rough economical estimate.
In this stage all the inferior processes should be ruled out.

B. Scaling up and Piloting

Only processed that passed successfully through the preliminary research, deserve the high investment needed for testing the equipment and piloting. Every dollar invested in the first step pays itself ten fold in the second one. And every dollar saved in the second step costs tenfold in the industrial plant.

1. The recommended equipment is tested in a dedicated pilot plant, to estimate the mass transfer, entrainment and phase separation, and optionally - for quick accumulation phenomena, e.g. precipitation, foaming etc. (this last point can be checked only by running the pilot plant with real process solutions).
2. Experimental proof of the recommended flow sheet and equipment follows.

This is the longest and most expensive part of the development. It should be used only to discover problems that could not have been detected otherwise.

THE INITIAL PROCESS DEVELOPMENT

This initial stage is the most important for the success of the process. It is also relatively cheap: only a limited team of researchers - both chemists and engineers - is involved. It covers the process definition, literature survey, selection of solvent, preliminary kinetic and hydrodynamic tests, preparation of equilibrium data and simulation.

Definition of the Process and Literature Survey

This is the most crucial step in the process development. If the proposed (or required) process is not fully defined, a lot of work will be wasted. For a new process, detailed literature survey is essential. For an upgrade or modification of existing process all the available data should be collected. If possible, personal contact with the people who developed the process and with those who operated it is very important. During these talks a lot of important and undocumented information is usually delivered. Some projects may be ruled out already in this stage, saving money and frustration.

Initial Experiments

The initial experiments should be done using the *limiting conditions* method [1], i.e. the *loading phase* is in large excess, so that after the contact with the *receiving phase* its composition hardly changes. For extraction, the feed is the loading phase and the solvent is the receiving phase. For stripping and scrubbing/purification the solvent is the loading phase.
The results of the limiting conditions experiments are similar to the maximum concentration in the *receiving phase* that can be obtained in a multistage plant, under the correct phase ratio. So a single experiment gives us fair estimation what can be expected from the examined solvent.

Measurement of basic physical properties like density and viscosity of both phases and their interfacial tension enables reasonable prediction of the phase separation. A simply shaking experiment at various temperatures illustrates this phenomenon yet better.
If the phase separation is problematic (e.g. high mutual solubility, small difference in the density of both phases, high viscosity or very low interfacial tension) the solvent must be modified or ruled out.
For reactive extraction in a new (or unknown) system, kinetic experiments must be carried out, in order to determine the residence time required for completion of the process, as a function of the temperature. In the case of slow kinetics it is an important parameter in determination of the process temperature and the recommended equipment.

Simulation
For the chosen solvent (or solvents) the distribution coefficient D is derived for every solute, using data banks and standard correlations whenever possible, or generating liquid-liquid equilibrium isotherms if no reliable data or correlations are available. For preparation of equilibrium isotherms, the variable phase ratio method, in which the feed is contacted with the solvent at various phase ratios, as recommended by Ritcey and Ashbrook [2], should be applied.

The standard steady state simulator calculates the flow rates and compositions of output streams, for a given plant configuration and operating conditions: number of stages, flow rate and composition of all the input streams, process temperature and pH. In good simulators the expected entrainment and stage efficiency for each stage may be calculated or gave as input. Using parametric runs, the simulation enables the design of the flow sheet, i.e. for given solvent and recovery to determine the number of stages in each battery as a function of the phase ratio, and predict the influence of pH, temperature and variations in feed composition.
Once the equilibrium correlation is prepared, the simulation itself is among the quickest steps of the development. It is important to remember that *the results of a simulator are only as good as the accuracy of the equilibrium data.*

The final result of the simulation, for a given solvent, is the optimal configuration: temperature, pH, phase ratio, number of stages etc. If several solvents are considered, the parametric runs help us to pick the best one.

The results of such an optimization are more accurate than any experimental procedure, and usually need far less manpower. Sometimes the results of the simulation are quite unexpected. Once obtained and understood they seem perfectly logical, but without a simulation it could have been unlikely to think about them, at least not before a pilot plant was run.

How long should all the preliminary research take?

It depends upon the complexity of the process. For extraction and stripping of a single solute, using a known solvent, one-two man month should be enough to carry out all the literature survey, laboratory experiments and simulation and to come out with a well defined flow sheet. For a complex case it may take a man year and above.

It is important to remember that this is the very wrong stage for savings: a week in the library (or on the net) may save a few months of laboratory work that has been done before and published. Just as well *few* month of preparation of equilibrium data and simulation may save a *few* months of piloting.

By the end of the preliminary research, the following data should be known:

1. Composition of the solvent.
2. Process temperature and pH for each battery.
3. Composition of all outlet streams.
4. Approximated flow sheet
5. Phase ratio in each battery.

One should also have a reasonable estimation of the recommended dispersion in each battery and the type of equipment to be recommended for the industrial plant.

It is important to emphasize that all this work must be done by a joint team of chemists and engineers.

Choice of Equipment

At this stage one should determine which type of equipment is recommended for the industrial plant. This is essential, as the pilot plant should be run in the type of equipment that is designated for the industrial one.

Sometimes it is difficult to decide what equipment is optimal. As a mater of fact it may be difficult even after the piloting is over. If two different types of equipment seem attractive in a similar way, testing both of them in the pilot may be the right choice. This is expensive - but cheaper than missing the more efficient equipment. The author participated in three projects where two different types of equipment were tested in the demonstration plant.

A comprehensive study of SX equipment was published by Stevens and Pratt [3], It divides the available equipment to 22 subclasses, and points out a wide range of

criteria to choose from them. Another recent book on liquid-liquid extraction equipment was published by Godfrey and Slater [4],
As a general guideline, mixer-mettles are recommended in each of the following cases:
a. No more than two stages are needed.
b. High phase ratio (above 20).
c. Crud or crystallizing solids are present.
d. Slow kinetics.
e. Very high flow rates.

For more than two stages, moderate flow rates and phase ratio and relatively clean solutions columns are recommended.
If the phase separation is really poor or very quick separation is required, centrifugal separators should be used.

Of course there are exceptions from these rules, and each case has to be analyzed carefully. For example, a battery of Bateman pulsed columns is applied in Olympic Dam uranium extraction, with flow rates above 2000 m^3/h.

PILOTING AND DEMONSTRATION PLANTS

Once the results from the preparatory stage show feasibility of the process, it is the time to test the recommended configuration in a pilot or a demonstration plant.
The pilot has to test mainly the parameters that cannot be predicted by the simulation: preferred dispersion, flux, entrainment, accumulation phenomena, crud formation, precipitation, deterioration of the solvent etc.

A representative pilot should use the real process solutions, and if possible - to be run on the designated site.

A demonstration plant is erected to fully simulate the future plant. Its configuration and type of equipment is similar to the full-scale plant, and it should be run in the designated site, using the real raw materials. Its main purpose is the verification of the results that were obtained in the bench-scale or pilot plant, regarding production rate, recovery, product quality and analysis of accumulation phenomena.

Quick accumulation phenomena can be detected and solved during the running in of the bench or pilot plant. Slow phenomena, which are detected after a few weeks or months, are the more problematic ones. They are caused by solvent decomposition, oxidation, precipitation or extraction of traces of harmful elements. A crucial problem is to decide how long should the running in be.

How long should the run last?

Usually until one of the following happens:
a. No new problem is detected during an agreed period (typically 3-6 month).
b. The period set a *priori* for the piloting passed successfully.
c. The budget for the piloting is exhausted.
d. The plant does not operate well and the project is defined as a failure (sad, but it happens too).

It is important to keep using the simulator during the running in of the pilot or demonstration plant. The routine comparison of the results from the plant with the simulator may help in discovering various problems, like poisoning of the solvent, malfunction of the equipment or analytical problems.

If during the piloting some unexpected problem is discovered, it is recommended to go immediately back to the laboratory and try to solve it on a smaller scale.

CONCLUSIONS

The integrated approach in the development of SX processes is based on sequential process development, with maximum attention to the early stages of the research. These stages are the quickest and the cheapest, so it is reasonable to invest in them as much as necessary, in order to save in the following, and far more expensive steps, e.g. piloting or demonstration plants.

Adequate investment in laboratory experiments and computer simulation enables ruling out of inferior and non economic options, and to invest in piloting only when the feasibility and apparent profitability of the process is proved.
Full cooperation between chemists and engineers during all stages is essential for the success of a project.

In the case that in advanced stage of the process some unexpected problem is discovered, it is recommended to go one step back and try to resolve it on a smaller scale.

REFERENCES

1. B Grinbaum "The integral approach to development of SX processes", in Y. Marcus ed., "Ion exchange & solvent extraction", vol. 15, *Dekker,* N.Y. 2001
2. AW Ashbrook and G Ritcey, *Solvent Extraction,* Part I, Amsterdam, Elsevier, 1984.
3. G Stevens, HRC Pratt, in J.D. Thornton (ed.), *Science & Practice of Liquid-Liquid Extraction*", Clarendon Press, New York, 1992, pp. 492-582.
4. JC Godfrey, DH Longsdail, *Liquid-Liquid Extraction Equipment,* New York, John Wiley and Sons Ltd., 1994



How operating practices and variables affect the Bottom Line

Mark F. Vancas

Bateman Engineering, Tucson, Arizona, USA

INTRODUCTION

For this discussion I will use primarily a copper SX-EW plant as the basis for most of my examples however I will also sneak in an example of cobalt and nickel. What I will try to demonstrate is that because of interactions between different unit processes and unit operations what is good for one specific process or operation may not be good for others and may indeed result in an overall negative effect for the entire processing plant.

An example that, even though is not directly SX related, demonstrates my point rather clearly has to do with mining and leaching. When we did the development work for the San Manuel Oxide project we intended to merely rip and then haul the ore to the leach dumps. We did this for our testing and found that we had a bulk ore that was 90+% minus 4 inch in size. All of our subsequent testing and economics were predicated on this feed stock. Along comes the reality of a production mine needing to drill and blast to recover the ore. Well the miners did as they felt they should, they used the minimum amount of powder to get their job done. As can be predicted, that changed the particle size of the material going onto the leach dump. This, in turn, changed the leaching rate and to maintain the copper production out of the processing plant meant that the mining rate had to be increased for which the miners were not prepared. In the end using a higher powder factor, even though it increased the blasting unit cost, made the particle size smaller, increased leaching recovery, and reduced the overall processing cost.

DISCUSSION

Now let's look at the various unit operations involved in the solvent extraction unit process. The basics are mixing and settling. Mixing can be broken down into primary mixing including droplet formation and mass transfer, auxiliary mixing, phase continuity, and possibly pH control. Settling can include flow distribution, coalescence, horizontal velocities, vertical velocities, interface control, discharge launder control. Just in a simple mixer-settler unit we can see that there are quite a few variables that may or may not interact to affect the overall result. Add to this the effect that the mixer-settler operation has on other plant operations and you begin to see that the matrix continues to get more complex. What makes this whole thing even more difficult is that no two plants are the same. What holds true for one plant may not apply to another. This is why we often say that SX-EW plant operation is as much art as science.

The job of the primary mixer is to produce droplets of one phase, disperse them throughout the other phase and produce sufficient discharge head to cause movement of the feed streams through the primary mixer and into either another mixing compartment or a settler; sounds simple enough. The size of the droplets determines the mass transfer area and

therefore influences the mass transfer per unit time and the size of the mixing compartments. A reasonable approach would be to make lots of small droplets so as to minimize the size of the mixing vessels. However, in the settler these droplets must coalesce back together to make a clean separation between the two phases. Small droplets do not coalesce well. This requires more settling time, and a bigger settler, all of which may negate any savings in costs resulting from making the mixers smaller. These are capital cost issues. What about operating costs?

EXAMPLES

Series Parallel

Let's start with an operating plant with mixers and settlers that are in place and fixed in size. Suppose, for sake of conversation, that the circuit is a standard 2 extraction 2 strip arrangement. More flow is desired through the plant to achieve a higher production rate. Higher flowrates can be achieved by several means. One way to achieve the higher flowrates is to increase the rotational speed of the primary mixers to move more fluid through the mixers and into the settlers. Higher mixer speed also results in finer droplets, faster mass transfer, AND slower coalescence. The settlers are fixed in size so slower coalescence probably means more entrainment of the dispersed phase in the continuous phase. Another way to increase the flow of PLS is to convert the circuit to a series-parallel arrangement. Let's look at each of these options and evaluate the overall impact of each on the SX-EW circuit.

Bear in mind that a truly accurate comparison without actual hard data for the particular operating plant is conjecture. Even though the conclusions at which we will arrive in this case are not supported with any facts, the principles demonstrated are what are important.

As a basis lets say that a doubling of the mixer tip speed from 3 m/s to 6 m/s will double the PLS flow through the plant from 1000 m^3/h to 2000 m^3/h. A series-parallel conversion could also double the flow through the extraction stages. Organic entrainment losses to the raffinate were 50 ppm of a mixture with 10% extractant. Extractant cost is $12 / liter and diluent cost is $0.70 / liter. The initial flux rate was a nominal $3m^3/h/m^2$.

Speeding up the mixers in the first option will decrease the droplet size and increasing the total settler input will increase the flux rate to 6 $m^3/h/m^2$. The combined effect will increase the entrainment losses. The sticky part here is that the entrainment versus flux rate and the entrainment versus droplet size relationships are not linear but rather, exponential. Likewise the relationships between droplet size and tip speed and droplet size and coalescence rate are not linear either. To determine these relationships, one would need to perform a battery of tests in an operating plant. As we know, the managers of operating plants must focus on production so this type of data just does not exist because they are not going to let someone "fiddle" with their production iust for the sake of science. If however the manaaers can be convinced that collection of such data will actually allow the plant to be optimized, then maybe there is a chance of obtaining this critical information.

If the combination of the smaller droplet size and the higher flux rate adds up to a four fold increase in entrainment losses, a 100% increase in production will increase the entrainment from 50 to 200 ppm. The value of these entrainments will increase from $66,000 per month to $528,000 per month, a factor of 8. Production has only increased by a factor of 2.

In the case of conversion to a series parallel configuration, the flowrate of PLS can be doubled but to achieve equivalent extraction, the concentration of extractant must be increased to 25%. Therefore the value of the entrainment increases and because the number of raffinate streams also doubles, the total entrainment is more than double assuming that the increased extractant concentration increases the entrainment losses to 70

ppm due to a change of coalescence rate. So the value of the entrainments will increase from $66,000 per month to $353,000 per month, a factor of a little over 5. Production once again has only increased by a factor of 2.

Comparing these two options, clearly the series parallel option has the lower relative operating cost but there is an associated capital cost for equipment, reagent, and loss of production. Will there be a positive return on investment? That will depend on the total operating cost of which reagents are only a portion.

What if the speeding up the impellers and increasing the flux rate only increases the entrainment to 135 ppm? In that case the economics break even and simply speeding up the impellers would win. Here I must reiterate again that to determine which case is better requires real world operating data and these numbers are not supported with any facts.

Nevertheless, carrying on from here let's look at the ripple effect. In most cases the series parallel option is the best so with that assumption what else will be required? Stripping will be more difficult due to the higher copper content of the organic phase. To achieve the increase in stripping with the same (or reduced equipment) normally requires an increase in the acid concentration of the spent/weak electrolyte used for stripping. The increased acid content will also increase the degradation rate of the organic phase and will affect the reagent requirements from that direction.

The increased concentration of organic and increased phase disengagement time will also influence the amount of aqueous entrainment in organic. Therefore the entrainment of aqueous borne impurities, that constitute direct contamination of the electrolyte, also increase. This leads to a requirement to increase the impurity bleed rate from the electrolyte to keep the impurity concentrations at the desired levels. Replacement of the sulfuric acid and cobalt in the bleed will be required. The increased recycle of copper will increase the operating inventory of metal. If the bleed is recycled to the SX feed stream the effects are minimized, however, if the bleed recycles to the raffinate and goes through the leach dump/pads before returning to the SX feed the impact can be quite large.

For example a simple 0.1 g/l Cu increase in the raffinate copper content applied to a leach dump with a total of 10 million tonnes of wetted material could conceivably lead to an increase in operating inventory of 100 tonnes of copper. This copper is not lost but the delay in production is significant.

The increase in organic entrainment in the raffinate is paralleled with an increase in the organic entrainment in the electrolyte. Here, this will increase the load on the organic removal equipment (filters, coalescers) operating on the electrolyte stream. Inevitably this will lead to increased organic in the EW tankhouse. This in turn will lead to increased organic contamination of the cathode product. As Iona as this is kept to a reasonable level there mav not be any impact on the sale price of the cathode. If contamination increases to the point that the LME "A" grade copper is no longer produced then there will be a loss of income.

Back to the increased acid content of the electrolyte used for stripping of the organic. That increase in acid content also affects the EW tankhouse. Assuming the amount of mist generation does not change, the increased acid content of the mist will therefore increase the amount of acid in the atmosphere. This will increase the rate of deterioration of the EW building and the contained equipment not to mention health and safety considerations. Accordingly, an increase in ventilation of the EW building will probably be required.

So, in review, we have looked at a simple change in the configuration of the SX plant which leads to an increase in production but at the same time has the potential of increasing operating and maintenance costs of not only the SX plant but also the EW plant along with a

potential increase in the amount of copper in inventory. The web that is spun from a simple change may have far reaching affects on the overall plant economic performance and the point being made here is that what may seem like the logical decision from one point of view may not, in fact, be the best overall decision.

Dispersion Band Thickness

Let's look at another example that is a little simpler and easier to verify in an operating plant. Science tells us that increasing the thickness of the phase band in a settler actually decreases the entrainment or allows more flow for the equivalent entrainment. The information shown in Figure 1 is taken from the Handbook of Solvent Extraction and clearly shows a logarithmic relationship between dispersion band width and allowable flux rate. Not shown is the requirement to retain the same depth of clear organic phase above the dispersion band. This means that the total inventory of organic phase in the settler must increase. Consequently, an adjustment of the organic weir height will be required as well as a potentially large investment of operating capital. If such a change can be made in a particular plant will depend on the design of the settlers and, if so, an attempt should be made to convince the plant managers to purchase the estimated organic quantities required for current operations in advance. That inventory can then be placed in the settlers as increased organic depth and data kept on the entrainment losses. Once the managers see that the increased organic inventory actually decreases operating costs then further increases may be possible depending on the mechanical design of the settlers.

Coalescing Media

Addition of coalescing media to the settler is normally an easier method of achieving an increase in the allowable flux rate because of the lower capital cost. Coalescing media comes with an associated operating cost for installation and replacement of the media as required by fouling of the media with debris, etc. In the classification of coalescing media I am also including additional mechanical equipment installed in the settler such as horizontal baffles, etc., that aid in increasing the coalescence rate. Many of the currently operating SX plants use something other than "picket fences" in the settlers and most of those plants do not "advertise" that fact.

Whether increasing the organic inventory or adding coalescing media to a settler, the affect can be easily measured and an economic evaluation performed. In this case the ripple effect is not too great but the logic of spending more money now to save over the long term must be applied.

Phase Continuity

Another simple example is the general rule of thumb that tells us to operate a plant with organic as the continuous phase in those stages where aqueous leaves the circuit and can carry organic away as a loss (i.e. raffinate and rich electrolyte). Likewise, to operate with aaueous as the continuous chase where oraanic exits to storaae or transfers between extraction and stripping. While this general rule applies in most cases, there are plenty of operating plants that find the opposite may be true because of other conditions that do not apply in most plants. A particular combination of extractant, diluent, temperature, and mixing conditions may lead to an overall scenario where not following the general rule is actually better for that particular plant.

Nickel/Cobalt

I promised a nickel/cobalt example. In one particular project, cobalt was being extracted with Cyanex 272. The extraction of cobalt and nickel is pH dependent. If a good separation of the two is desired then the pH at which the cobalt extraction is conducted is critical. As the pH increases, the likelihood of co-extracting nickel also increases. This also required addition of more base to raise the pH. The client insisted on keeping the consumption of base to a minimum and set the pH criteria on the low side of the good operating range. This

did reduce the consumption of base but the other effect of restricting the loading of cobalt then created a loss of cobalt to the subsequent nickel recovery circuit which not only resulted in loss of revenue for cobalt but also created problems in the nickel recovery circuit. The net result being that the savings of base were outweighed by the downstream operating costs. This lesson was learned quite quickly by the client.

We can carry on with many more examples of how the apparent economic affect of changes on a plant may not be as originally envisaged. I am sure everyone knows of several examples but there is no real reason to belabor the point further. The simple fact is that the affect of changes is not always what is expected and changes in one area can affect what may seem to be a totally unrelated part of an operating plant.

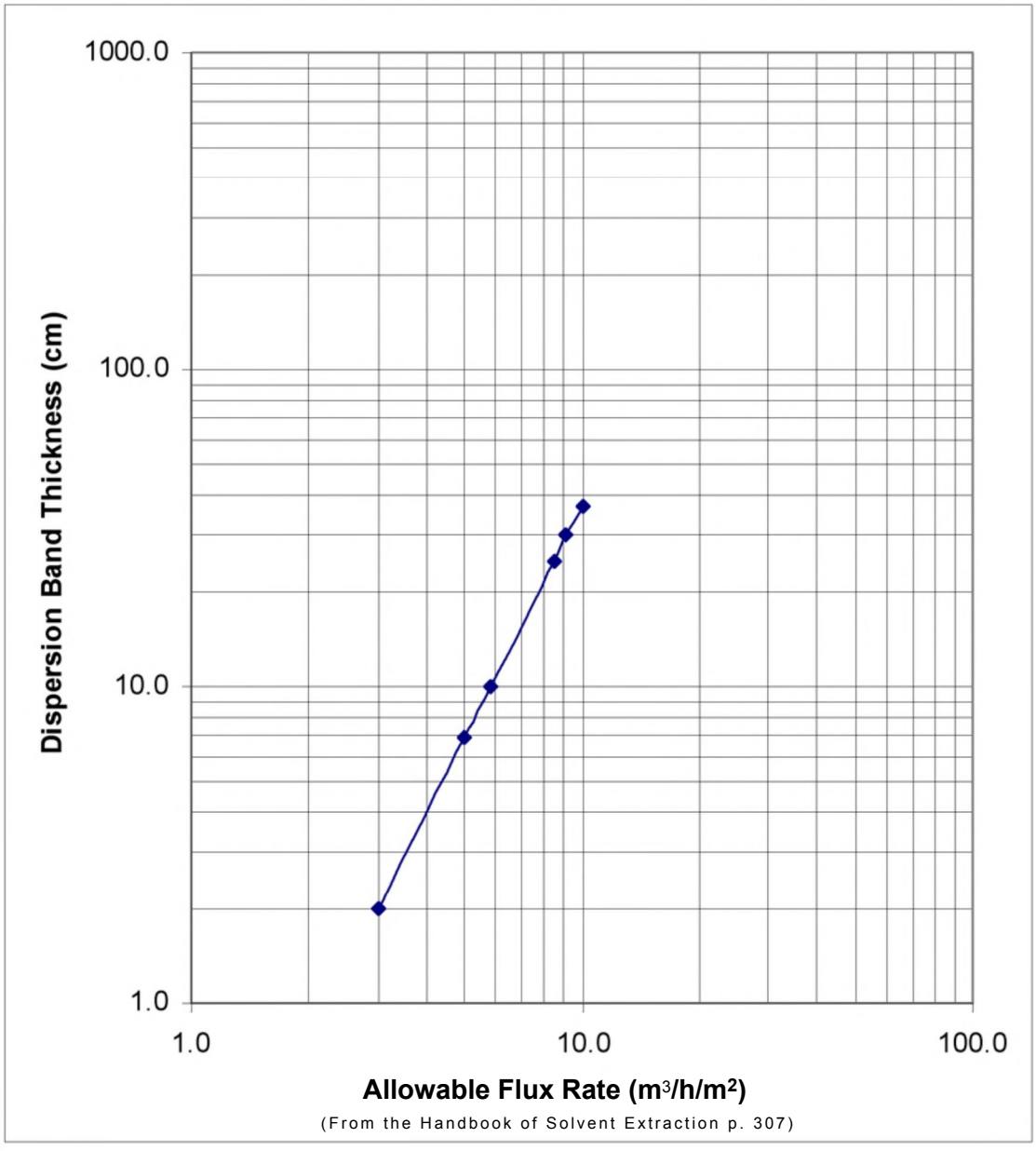


Figure 1.



VARIATION OF PROPERTIES OF AQUEOUS PHASE IN SOLVENT SUBLATION FOR BUTYL ACETATE RECOVERY FROM PENICILLIN WASTEWATER AND SYNTHETIC SOLUTION

Xinghua Sun' ", Zhidong Chang, Mingmei Wang , Shufeng Shen ", Xin Hu ", Zhi Xie , and Huizhou Liu*

* Laboratory of Separation Science and Engineering, State Key Laboratory of Biochemical Engineering, Institute of Process Engineering, Chinese Academy of Sciences, Beijing, China
** Graduate School of the Chinese Academy of Sciences, Beijing, China

Solvent sublation is effective to the recovery of butyl acetate (BA) from the wastewater of penicillin plant, but its efficiency in synthetic solution is much less. Experiment results on the variation of properties of the aqueous phase showed that the surface tension and electrical conductivity of the wastewater increased during the sublation. However surface tension of synthetic solution first increased, then decreased, and increased again or decreased a little during the sublation. Viscosity of the wastewater also decreased during the sublation. Chemical oxygen demand (COD) of the wastewater decreased after the sublation, and such variation compared with that in conventional azeotropic distillation (stripping) was discussed. It shows that the properties of wastewater are different from the synthetic solution because of various biological materials, surfactants and polymers in the wastewater.

INTRODUCTION

Solvent sublation, suggested first by Sebba, is a novel adsorptive bubble separation method based on interface property of solute. In the separation process, organic compounds, ions or particles are adsorbed or attached to the air-water interfaces of ascending bubbles, and then collected into an immiscible and stagnant organic solvent layer floating on top of the aqueous phase [1], It is a process combining the conventional transport extraction and bubble separation, and a promise separation process with a number of advantages. Many studies on solvent sublation have been carried out for removing inherent hydrophobic compounds from simulated wastewater [2-5], In recent years, it has been explored to remove trace organics from industrial wastewaters [6, 7],

Penicillin is usually extracted from its filtered ferment broth with solvent of butyl acetate (BA).

In the extraction operation, BA dissolves into the aqueous phase to cause wastewater with BA of about 1% by weight [8], Subsequent recovery of BA from the wastewater is obligatory from ecological and economical point of view. Conventional recovery of the BA is by azeotropic distillation (or stripping) [9], Distillation is not only costly and energy consuming, but also BA can hydrolyze to butanol and acetic acid at high temperature, leading to the corrosion of apparatus. The distillation facilities are usually clogged by filth after a period of operation because of the diverse materials dissolved in the wastewater.

In our previous work, the recovery of BA from the wastewater of penicillin plant by semi-batch solvent sublation was studied [10], It is an efficient process for such recovery in spite of poor effect with air stripping. In order to understand the process better, solvent sublation was carried out with synthetic solution in laboratory. But sublation efficiency in synthetic solution is much less than that in the wastewater. The wastewater contains various biological materials. In addition, commercial de-emulsifier and flocculants composed of surfactants and polymers should be added into the broth to fulfil the extraction of penicillin. Some of them will be left in the wastewater after solvent extraction [11], All of them made it unnecessary to add additional surfactants to assist the sublation. It is difficult to simulate a solution like industrial wastewater of penicillin plant completely. In previous studies on solvent sublation, few of them were focused on the variation of properties of the aqueous phase. Therefore the aim of our paper will be to examine such variation, especially to compare the wastewater of penicillin plant with synthetic solution.

EXPERIMENTAL

Materials

Wastewater samples after solvent extraction of penicillin were supplied by North China Pharmaceutical Corporation Limited (Shijiazhuang). n-Nonane, butyl acetate, n-hexane, sodium dodecyl sulfate (SDS) and hexadecyltrimethyl ammonium (CTAB) were purchased from Beijing Chemical Reagent Company, China. They were all of analytical grade purity. Commercial de-emulsifier was supplied by East Green Process Engineering Company, Beijing.

Apparatus and Method

Semi-batch sublation experiments were performed in a glass cylindrical column with sample ports at 10, 45, 80, 115, 150 and 185 cm from the bottom, respectively. The glass column was 200 cm high with inner diameter of 10 cm as described in the literature [10], Cylinder nitrogen was dispersed by a sintered titanic plate (Beijing General Research Institute for Nonferrous Metals) with the mean pore size of 20 pm at the bottom of sublation column. Five plates with sieve pores of 3-5 mm diameters were located in the glass column.

Synthetic solution was prepared using tap water mixed BA and various surfactants. During the sublation process, 15 L wastewater or synthetic solution was pumped into sublation column by peristaltic pump. 300 ml/min cylinder nitrogen measured by manometer and rotameter was introduced into the column bottom through the titanic plate. Experiments were all done with a stagnant aqueous layer and a stagnant solvent layer while gas was used in a

once pass through mode. Liquid samples (about 20 ml) were taken from the ports along the column for analyses at different setting time.

Aqueous sample of 5 ml was taken and diluted two times and mixed with 2 ml n-hexane, then stirred with electric stirrer for 2 min. After that, the sample was centrifuged (3000 r/min) for 2 min. Finally the organic phase was collected and analyzed by gas chromatography (GC). A sample of 0.3 pi was injected into GC with Flame Ionization Detector (FID), and the capillary column is HP-5 (30 mx0.32 mmx0.5 pm) (HP6890 Agilent Technologies, USA) [12], Surface tension of liquid sample was measured by ring method with a ZL-2 auto-tensiometer (Kesen, Zibo, China). Viscosity of the wastewater was measured by DV-E Viscometer (Brookfield, USA). Chemical oxygen demand (COD) of wastewater was determined by North China Pharmaceutical Corporation Limited. Electrical conductivity of the wastewater was measured using DDS-302 digital conductivity (Shengbang, Tianjin, China).

RESULTS AND DISCUSSION

The wastewater processed in experiments was directly collected from industrial discharged water with residual concentration of BA of around 1% by weight. The concentration of BA was stable in each experiment relatively. For the sake of comparing data, the sublation efficiency at time *t* is defined as:

$$E_{\text{„}} = \frac{c_{wi} - c_w}{c_{wi}} \text{x} 100\% \qquad (1)$$

where

c_{wi} = the initial solute concentration in water, v/v.

c_w = the solute concentration in water at time *t, v/v.*

Sublation Efficiencies of Wastewater and Synthetic Solution

The sublation efficiencies of wastewater of penicillin plant and synthetic solutions with different surfactants are showed in Figure 1. Solvent sublation in wastewater is more effective than that in synthetic solution. Synthetic solution with cationic surfactant and de-emulsifier had a little better sublation efficiencies than that with anionic surfactant, but the improvement was very limited. It is shown that the electric effect between BA and surfactant is very weak. An important point should be mentioned that wastewater was directly collected from industrial process, therefore the concentration of BA varied according to difference batch and difference taken time in the same batch. The concentration of BA was almost among 0.7-1.5% (v/v). With larger concentration of BA, some of organics would be separated out automatically. But the sublation efficiency and properties change little. Such results showed that there were some common properties in the wastewater.

In addition, some properties of the wastewater were different from those of synthetic solution. Synthetic solution was a true solution of BA, but to some extent, the wastewater was not a true solution of BA when the concentration of BA was large. Sometimes the wastewater was an emulsified system. The mutual effect of various biological materials, surfactants and polymers could result in the stability of the emulsified solution in a period. The small droplets of BA in wastewater could be sublated into the solvent layer by spreading or attachment on the air-water interface of rising bubble, which could improve the effect of solvent sublation. Another reason for the better efficiency in the wastewater may be that the smaller bubbles in it than those in synthetic solution, resulting in more air-water interface of the equal gas volume. Larger air-water interface area would also lead to a better sublation efficiency because more BA could be adsorbed or attached, and sublated into the solvent layer.

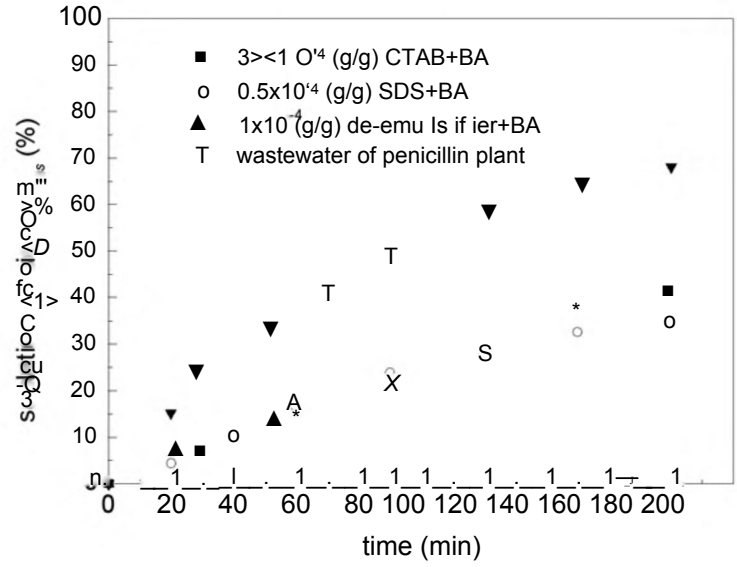


Figure 1. Sublation efficiencies of wastewater and synthetic solution.

Variation of Surface Tension

Surface tension is an important property of solution. Its variation during solvent sublation can assist us to understand better the mechanisms of the sublation. Variation of surface tensions of wastewater of penicillin plant and synthetic solution are shown in Figure 2. Compared with synthetic solution, the surface tension of the wastewater was much lower, which could make smaller bubbles in the wastewater. Furthermore, smaller bubbles would give larger air-water interface, resulting in better sublation efficiency. In addition, as concentration of BA in the wastewater increased, the surface tension of wastewater decreased as shown in Figure 2. During the sublation, it increased, showing that the organics in the wastewater were sublated into the organic layer.

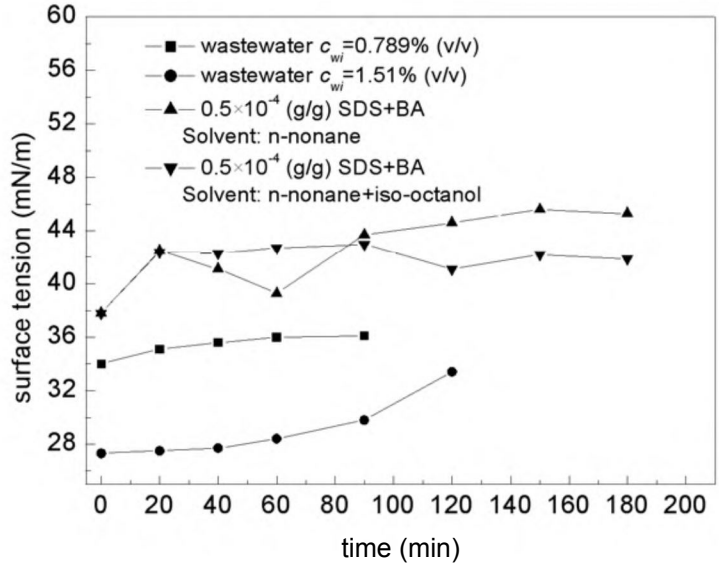


Figure 2. Variation of surface tensions during the sublation.

During solvent sublation of synthetic solution, the variation of surface tension was complex and different from that in solvent sublation of the penicillin wastewater. If n-nonane was used as organic solvent, the surface tension of synthetic solution first increased, then decreased, and increased again during the sublation. It might be elucidate that the back mixing of n-nonane into water, leading to the decrease of surface tension. When the sublation was steady after a period, the back mixing was reduced, and the surface tension would increase again with the decrease of organics in the solution. But if n-nonane and iso-octanol were used as mixed organic solvents, the surface tension of synthetic solution increased, then almost maintained unvarying, and decreased a little. Iso-octanol has a much larger solubility in water than n-nonane and it is hard to be again sublated into the solvent layer because of its hydrophilic property, therefore a little dissolved iso-octanol would make the surface tension of synthetic solution decrease. In previous studies, the better effect of dissolved methanol or ethanol on solvent sublation was also explained by their resulting in much smaller bubbles in aqueous phase.

Electrical Conductivity, COD and Viscosity of Wastewater

Variation of electrical conductivity of the wastewater of penicillin plant during the solvent sublation was shown in Figure 3. The pH of the wastewater was usually about between 1.0 and 2.0 because penicillin was extracted in acid conditions, and there were salts in the wastewater, so its electrical conductivity was larger than tap water (565pS/cm). As sublation time increased, the electrical conductivity of the wastewater increased, which could be elucidated that the properties of the wastewater varied as dielectric organics, such as BA and macromolecule, were sublated into the solvent layer. The rheology of the wastewater was changed. In addition, the pH of solvent layer also decreased a little, which showed a little acid ion was sublated into it.

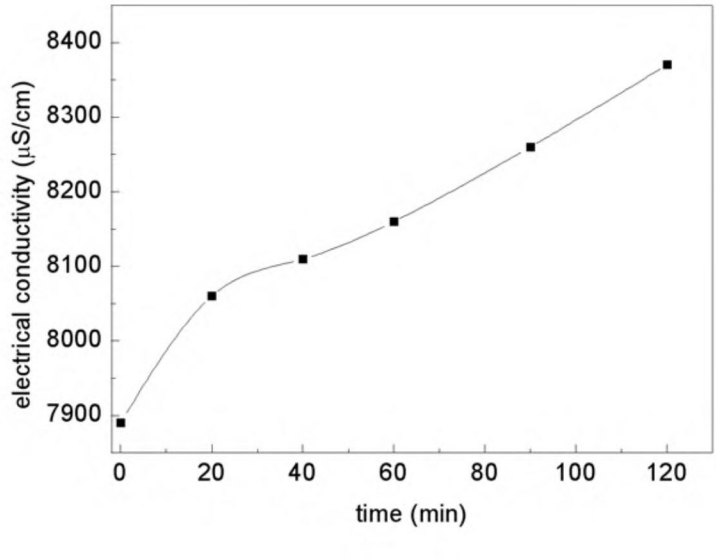


Figure 3. Variation of electrical conductivity of wastewater.

Different from the variation of electrical conductivity of the wastewater, the viscosity of the wastewater decreased during the sublation. The initial viscosity of wastewater stuff was about 12.6cP, and it decreased to about 10.2cP at the end of the sublation. Such decrease of the viscosity showed that some organics with high molecular mass were also sublated into the solvent layer. Emulsification at he solvent-water interface or in solvent layer, sometimes occurred under high gas flow rate, which could be explained by the effects of such materials with high viscosity.

Chemical oxygen demand (COD) usually indicates the quantities of chemical polluters in wastewater. Solvent sublation was ever carried out to decrease the COD of the textile wastewater [13]. But in our work, as the aim is to recover BA from the wastewater, the sublated or distilled wastewater should be again treated before being let out. COD of the wastewater was also measured in our sublation. It was shown that the COD was decreased from 23375mg/L to 19550mg/L during the sublation. But the COD of the wastewater after solvent sublation was still higher than that after conventional azeotropic distillation (stripping) (12538mg/L). The reason may be that azeotropic distillation is a thermo-physical chemical process, in which most of organics are stripped from the wastewater. Some of them will get tar in the distillation column at high temperature. Therefore, the distillation facilities are usually clogged by filth at high temperature as discussed above. It also showed that the behind treatment of sublated wastewater is more important than that of distilled wastewater.

CONCLUSIONS

The wastewater discharged from penicillin production is different from the synthetic solution to some extent. Biological materials, surfactants, and polymers in flocculants have a conjunct effect on the solvent sublation, so it is more effective than that in synthetic solution for the recovery of butyl acetate (BA). There is no use to make experiments on sublation with synthetic solution to study the effects of operational parameters. The surface tension of wastewater was much lower than that in synthetic solution, resulting in much smaller bubbles in the wastewater and better efficiency. The surface tension and electrical conductivity of the wastewater increased during the sublation because the organics were sublated into solvent layer. The different variation of surface tension of synthetic solution from the wastewater during the sublation was caused by the removal of organics and the back mixing of solvent, especially as iso-octanol was used. Viscosity and chemical oxygen demand (COD) of the wastewater also decreased after the sublation.

ACKNOWLEDGMENTS

This work was supported by a grant from North China Pharmaceutical Corporation Limited. We would like to thank the National Natural Science Foundation of China for financial support (No. 20406021, No. 20236050 and No.20221603).

REFERENCES

1. F. Sebba (1962), *Ion Flotation,* American Elsevier, New York, pp. 112-117.
2. A. N. Clarke, D.J. Wilson (1983). *Foam Flotation-Theory and Application,* Dekker, New York, pp. 317-353.
3. Y. J. Lu. X. H. Zhu (20011. Sea *Purif. Meth..* 37 (21. 157-189.
4. G. J. Thoma, M. L. Bowen, D. Hollensworth (1996), Sep. *Puhf. Technol.,* 16 (2), 101-107.
5. B. G. Bryson, K. T. Valsaraj (2001), *J. Hazard. Mater.* 82 (1), 65-75.
6. T. Lionel, D. J. Wilson, D.E. Pearson (1981), *Sep. Sci. Technol.,* 16 (8), 907-935.
7. J. S. Smith, K. T. Valsaraj, L. J. Thibodeaux (1997), *Ind. Eng. Chem. Res.,* 36 (3), 903-914.
8. Z. D. Chang, X .F. Wei, H. Z. Liu, J. Y. Chen (2002), *Sep. Sci. Technol.,* 37 (4), 981-991.
9. N. Kolev, R. Darakchiev, Kr. Semkov (1996), *Water Res.,* 30 (5), 1312-1315.
10. X. H. Sun, Z. D. Chang, H. Z. Liu, W. F. Wang, Y. X. Zhang (2005), *Sep. Sci. Technol.,* 40 (4), 927-940, in press.
11. H. Z. Liu, G. A. Han, J. Y. Chen (1996), *Chem. Ind. Times,* 10 (4), 3-7. (in Chinese)
12. Z. D. Chang, N. Yao, H. Z. Liu, J. Y. Chen (1999), *Chinese J. Anal. Chem.,* 27 (1), 118. (in Chinese)
13. **S. H. Lin, C. C. Lo (1996),** *Environ. Technol,* **17 (8),** 841.



SEPARATION OF METALS FROM SPENT PORTABLE BATTERIES BY LIQUID-LIQUID EXTRACTION WITH CYANEX 272

Danuza Pereira Mantuano, Germano Dorella and Marcelo Borges Mansur

Departamento de Engenharia Quimica, Universidade Federal de Minas Gerais
Belo Horizonte, MG, Brazil

A hydrometallurgical route consisting of classification, dismantling, sulphuric acid leaching and liquid-liquid extraction steps has been proposed to recover metals from spent portable batteries. In this work, the liquid-liquid extraction step with Cyanex 272 is highlighted in order to separate Zn, Mn, Ni, Cu, Al, Cd, Li and Co which were found as main metal content of NiCd, NiMH and lithium batteries. Equilibrium tests were carried out by contacting a synthetic aqueous solution containing 0.1 mol/L of each metal with an organic solution of 0.3 mol/L Cyanex 272 dissolved in commercial kerosene (Escaid 110) at 50°C. Analysis of metal extraction at different pH values have shown that $pH_{1/2}$ = 2.5-3.0 for Zn and Al, $pH_{1/2}$ = 4.0-4.5 for Mn, Cd, Cu and Co, pHic = 6.5 for Ni and pHi/2 = 8.0 for Li. Data fitting to an equilibrium model proposed to the test system by the EFChE (European Federation of Chemical Engineering) have indicated that $MR_2(RH)_2$ and MR_2 complexes (where M = Zn, Mn, Co, Cd and Cu) with Cyanex 272 co-exist in the organic phase depending on loading conditions.

INTRODUCTION

The annual consumption of portable batteries in the USA and Europe is estimated to range around 8 billion units while the Japanese production of primary and secondary batteries was over 6 billion units last year [1], In Sweden the number of mobile phones has surpassed its population. The demand for portable batteries is constantly growing around the world. Safe disposal followed by adequate treatment of this kind of residue may avoid the release of potentially hazardous metals to the environment. In addition, the reuse of waste products could lead to the preservation of raw materials. These actions are essential to guarantee the existence of future generations. Hence the increasing importance of recycling and the related issue of sustainable development have prompted society to seek processes to treat spent batteries. The most common batteries for mobile phones are nickel-cadmium (NiCd), nickel-metal-hydride (NiMH) and lithium-ion (Li-ion). Because of the high toxicity of cadmium, NiCd batteries have been progressively replaced by NiMH and Li-ion types.

In comparison to existing pyrometallurgical routes, hydrometallurgical treatment of spent batteries seems more adequate to meet principles of sustainable development at lower operational costs. Hydrometallurgical routes require lower energy consumption compared

to other routes and there is no atmospheric emission of toxic gases. The proposed route for spent battery treatment consists of classification, dismantling, sulphuric acid leaching and liquid-liquid extraction steps. This paper focuses the use of extractant Cyanex 272 [bis(2,4,4-trimethylpentyl)phosphinic acid] for the separation of metals found in higher quantities in batteries. Cyanex 272 has provided to be a very efficient extractant to separate Co and Ni from both sulfate and cloride media [2], These metals are found in all types of mobile phone batteries and have a relatively high price in the market place. Data from London Metal Exchange from January to October 2004 have shown that the price of Ni is about eight times greater than Al and five times that of Cu, for example. The price of Co is even higher around three times more valuable than Ni.

EXPERIMENTAL

Reagents

The extractant Cvanex 272 was kindlv supplied bv Cvtec Canada. The extractant was used as received (without further purification) and the average content of active reagent was 85%. The commercial kerosene Escaid 110 was used as diluent. The aqueous phase was prepared by dissolving sulfate salts of the respective metals Zn, Mn, Ni, Co, Al, Cd, Li and Co in distilled water. No modifier was used since no problem concerning the formation of a third phase was observed.

Procedure

Firstly, NiCd, NiMH and Li-ion batteries from three different manufacturers (A, B and C) were dismantled manually. Each sample (total of 9) was dissolved in aqua regia and analysed by atomic absorption spectrometry in order to quantify the metallic content.

Aqueous solutions containing 0.1 mol/L of each metal found in the batteries (Zn, Mn, Ni, Cu, Al, Cd, Li and Co) was contacted with an organic phase consisting of 0.3 mol/L Cyanex 272 (monomeric base) dissolved in Escaid 110. The experiments were carried out at 50°C in reactors of 250 and 400 mL provided with a glass impeller, a thermometer and a pH electrode (Digimed DM 20). Both phases were contacted by mechanical stirring for 20 minutes (time enough to reach equilibrium as verified in preliminary tests). The pH was controlled by addition of small quantities of NaOH and H_2S0_4. After phase separation, the concentration of metal in the aqueous phase was analysed by atomic absorption spectrometry. The concentrations in the organic phase were determined by mass balance. Experiments were carried out to determine: (1) the pHi/2 values at constant A/O volume ratios of unity and (2) equilibrium isotherms at changing A/O ratios (5/1, 3/1,2/1, 1,5/1, 1/1, 1/1,5, 1/3, 1/5). Data were fitted to an equilibrium model proposed for the reactive test system ZnS04/D2EHPA by the European Federation of Chemical Engineering (EFChE) and valid over a wide concentration range of extraction and stripping conditions [3],

RESULTS AND DISCUSSION

Metallic content of the spent batteries

The average content of metals in NiCd, NiMH and Li-ion batteries from three different manufacturers (A, B and C) is shown in Table 1, including the interval of 95% of confidence level in order to show their variability. Metal composition differs only accordingly to the battery type but not significantly between manufacturers [4], This result points out that batteries of the same type can be treated together independently of

manufacturer, so they must be sorted by type in the classification step. Metals found in more significant quantities for each type of battery are shown in gray scale on Table 1. Metals Ni, Co and Cd were found in quantities relatively higher compared to other metals analyzed.

Table 1. Average metal composition of NiCd, NiMH and Li-ion batteries from three different manufacturers (A, B and C) *(% by weight).*

	NiCd				NiMH				Li-ion			
	A	B	C	average	A	B	C	average	A	B	C	average
Al	0.01	0.02	0.03	0.02 ±0.01	0.81	0.94	0.85	0.9 ±0.1	10.0	6.5	6.6	8 ± 3
Cd	394	35.3	284	34 ±8	0.01	n.d.	n.d.	< 0.01	0.03	0.01	0.03	0.02 ±0.02
Co	2.08	2.56	1.43	2.0 ±0.8	5.64	6.16	6.64	6.1 ±0.7	42.9	30.8	34.2	36 ±9
Cu	0.03	-	-	0.03	0.02	-	-	0.02	13	-	-	13
Fe	0.01	0.03	0.04	0.03 ±0.02	0.09	0.06	0.15	0.10 ±0.07	0.03	0.06	0.10	0.06 ±0.05
Li	0.05	0.07	0.04	0.05 ±0.02	0.05	0.07	0.10	0.07 ±0.04	8.88	2.48	2.45	5 ± 6
Mn	n.d.	0.01	n.d.	< 0.01	1.11	1.37	2.62	2 ± 1	n.d.	n.d.	0.01	< 0.01
Ni	14.3	19.8	33.3	22 ± 14	46.8	52.8	47.9	49 ±5	0.02	0.02	0.02	0.02
Pb	n.d.	n.d.	n.d.	n.d.	0.08	n.d.	n.d.	0.03 ±0.07	n.d.	n.d.	n.d.	n.d.
Zn	0.90	0.01	0.03	0.3 ±0.8	1.56	0.01	1.13	1 ± 1	0.01	n.d.	n.d.	≤0.01

* n.d. = not detected

Effect of pH on the extraction with Cyanex 272

The influence of pH on the extraction efficiency with Cyanex 272 of metals found in higher quantities in portable batteries is shown in Figure 1. The $pH_{1/2}$ values obtained are 2.5-3.0 for Zn and Al; 4.0-4.5 for Cu, Mn, Co and Cd; 6.3 for Ni and 8.0 for Li. Again, these results point out batteries that must be leached by type. Different treatment routes depending on the type of battery have to be considered, so a very flexible plant is necessary.

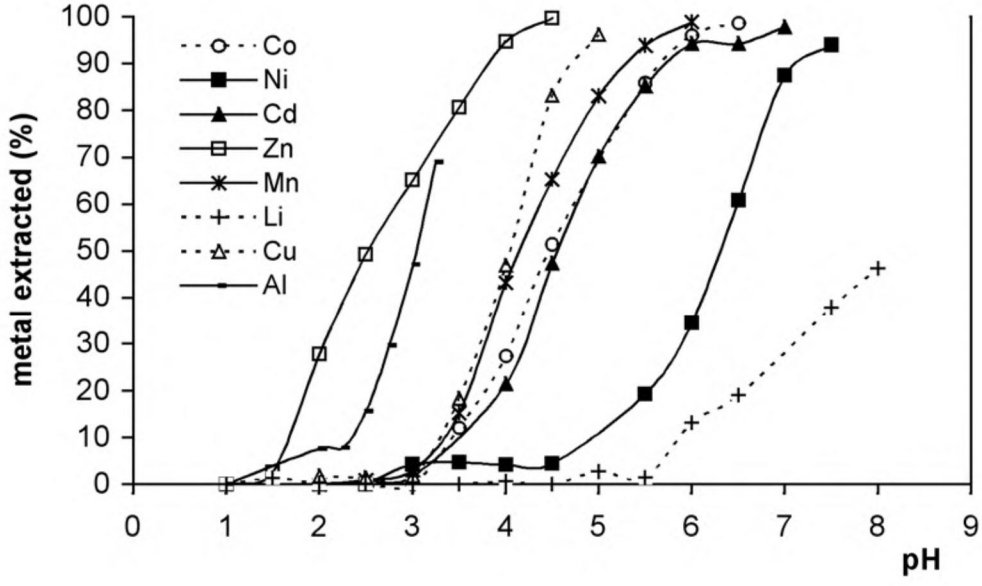


Figure 1. Extraction efficiency of metals (initial metal concentration = 0.1 mol/L) against equilibrium pH (0.3 mol/L Cyanex 272, A/O = 1, T = 50°C).

For NiCd batteries, the results shown in Figure 1 point out that Cyanex 272 can efficiently separate Cd from Ni which are present in major proportion in this type of battery (see Table 1). A scrubbing step may wash co-extracted Co from Cd but it seems to be more appropriate to use a selective extractant to separate Co-Cd if recovery of cobalt is desirable. For example, Co can be easily separated from Cd using D2EHPA (di-2-ethylhexyl phosphoric acid) as extractant [5],

For NiMH batteries, Zn and Al are extracted together, the same occurring to metals Co and Mn. Nickel remains in the aqueous solution. Since Zn, Al and Mn are present in very small quantities (see Table 1), the recovery of Ni and Co seems to be more attractive for NiMH batteries. In the particular case of Mn, its content can be significantly reduced in the aqueous phase if leaching with sulphuric acid occurs in the absence of a reductive agent [6], Therefore, Co and Mn can be partially separated in the leaching step.

For the Li-ion batteries, Al, Co/Cu and Li can be separated as shown in Figure 1. Li-ion batteries are constituted of two thin electrode films, one made of metallic Cu and other of Al. Both films are covered by the active material of battery, containing Li and Co (fine powder of $LiCo0_2$ aggregated with a polymeric binder) [7] and rolled up in a cylindrical shape. Therefore, metals can be separated in a three-step process: (1) batteries are firstly washed to remove the active material (Li and Co) from the metallic films (Al and Cu), (2) the active material is filtered and leached by sulphuric acid solutions and, finally, (3) Li and Co are separated by liquid-liquid extraction with Cyanex 272.

Extraction model

Extraction isotherms for Cd, Co, Cu, Mn and Zn were obtained experimentally in order to find the stoichiometric reaction of these metals with Cyanex 272. Plots of equilibrium concentration in the organic phase *versus* equilibrium concentration in the aqueous phase have shown a typical curvature presented by systems requiring a minimum number of theoretical extraction stages using McCabe-Thiele method for all metals considered in the study. Figure 2 shows the isotherm of zinc with Cyanex 272; similar curves were obtained for metals Cd, Co, Cu and Mn.

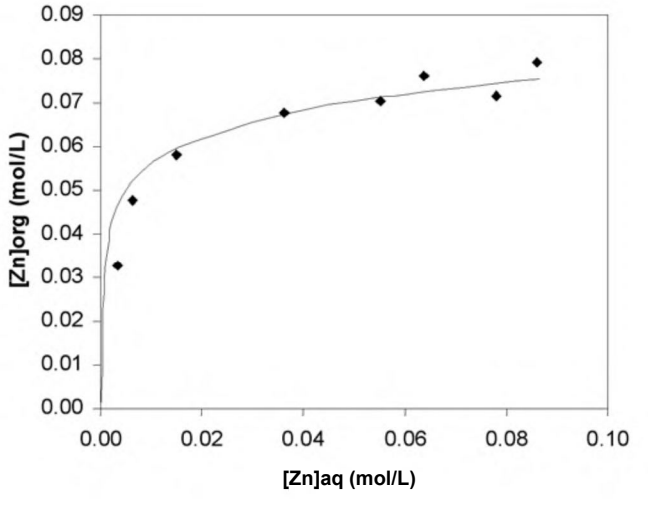


Figure 2. Equilibrium isotherm of zinc with Cyanex 272 (0.1 mol/L Zn, 0.3 mol/L Cyanex 272, T= 50°C, pH = 2.5).

Experimental data were fitted to an equilibrium model assuming two stepwise reactions [3], the first reaction occurring at the liquid-liquid interface:

$$M^{2+} + n(RH)_2 \Leftrightarrow MR_n(RHV_n| + 2H^+ \quad (1)$$

$$K_D = \frac{C_{GD}C_H^2}{C_M C_{BD}^n} \quad (2)$$

and the second reaction occurring in the bulk of the organic phase considering that the complex $\mathbf{MR_2(RH)_2(n\text{-}i)}$ formed at the interface breaks down as its concentration increases:

$$MR_n(RH)_{2(n-1)} \text{ o } MR_2(RH)_r \quad m\text{-}2 + \left(n \frac{m}{2} \right) (RH); \quad (3)$$

$$K_C = \frac{C_{CM}C_{BD}^{n-m/2}}{C_{CD}} \quad (4)$$

The stoichiometric constants (n and *m)* and equilibrium coefficients (K_D and K_c) were found for each metal by data fitting using a computational procedure [3], The equilibrium model including mass balances of metal and extractant was solved using the Newton-Raphson method while the estimates of *n,* m, K_c and K_D were obtained by the Hooke-Jeaves optimization method. It was verified that both stoichiometric constants converged to value 2. The equilibrium coefficients K_D and K_c shown in Table 2 were obtained by fixing $n = m = 2$, including 95% confidence levels for the error.

Table 2. Stoichiometric constants and equilibrium coefficients for the extraction reaction of main metals present in batteries with Cyanex 272 (T = 50°C)

Metal	n	m	K_D	K_c(mol/L)
Cadmium	2	2	(2.6 ± 0.2) x 10‘7	(1.6 ± 0.1) x 10‘2
Cobalt	2	2	(6.3 ± 0.3) x 10"7	(8.1 ± 0.2) x 10‘3
Copper	2	2	(8 ± 1) x 10'7	(1.3 ± 0.3) x 10'1
Manganese	2	2	(1.6 ± 0.1) x 10'6	(1.4 ± 0.1) x 10'2
Zinc	2	2	(6.88 ± 0.01) x 10-3	**(6.19 ± 0.01)** x **icr3**

Information on the equilibrium constants as shown in Table 2 is very helpful for guiding plant design procedures in order to calculate the number of theoretical stages for a given separation level or even to simulate best operational conditions for scrubbing and stripping steps, for example.

CONCLUSIONS

The problem caused by spent mobile phone batteries is widely known due to its environmental repercussions. A hydrometallurgical plant using liquid-liquid extraction step with Cyanex 272 has been proposed to treat such kind of residue. Based on the chemical composition of NiCd, NiMH and Li-ion batteries considered in this study, it has been found that such batteries must be firstly sorted by type in order to be efficiently treated by

leaching and liquid-liquid extraction with Cyanex 272. Ni and Co appear as the main metals to be recovered from spent mobile batteries because of their quantity in the batteries considered and their market price. Cyanex 272 can separate Cd from Ni ($ApH_{1/2}$ = 2) of the NiCd batteries, Ni from others metals ($ApH_{1/2}$ = 2) present in NiMH batteries and Co from Li ($ApH_{1/2}$ = 3) of the Li-ion batteries. The plant has to be flexible enough in order to accommodate each type of battery to be treated. Isotherms of the metals Zn, Mn, Co, Cd and Cu have been obtained at changing loading conditions in order to estimate the value of the stoichiometric constants and equilibrium coefficients assuming the breakage of organo-complexes in more concentrated extract phases.

List of symbols

C	concentration (mol/L)
K_c	equilibrium coefficient defined by Eq. (3) $(mol/L)^{m/2}$
K_D	equilibrium coefficient defined by Eq. (1) $(mol/L)^{2n}$
m	stoichiometric constant for the homogeneous reaction
n	stoichiometric constant for the heterogeneous reaction

Subscripts

BD	dimer-Cyanex 272
CD	organo-metallic complex formed according to Eq. (1)
CM	organo-metallic complex formed according to Eq. (3)
H	hydrogen ion
M	metallic ion

ACKNOWLEDGEMENTS

This work has been carried out with the financial support from CNPq (Edital Universal 2003, n° 474577/2003-1) and FAPEMIG (Grant PROBIC/2003). The authors wish to thank technician Fernando Silva Magalhães for the atomic absorption spectrophotometric analysis and Eng. Ricardo Capanema (Cytec Brazil) for the kind supply of Cyanex 272.

REFERENCES

1. A. M. Bernardes, D. C. R. Espinosa and J. A. S. Tenorio (2004), *Journal of Power Sources,* 130, 291-298.
2. B. K. Tait (1993), *Hydrometallurgy,* 32, 365-372.
3. M. B. Mansur, M. J. Slater and E. C. Biscaia Jr. (2002), *Hydrometallurgy,* 63, 117-126.
4. D. P. Mantuano, G. Dorella, F. S. Magalhaes, S. D. F. Rocha and M. B. Mansur (2004), *Proc. of Congresso Brasileiro de Engenharia Quimica, Curitiba, Brazil.*
5. C. A. Nogueira and F. Delmas (1999), *Hydrometallurgy,* 52, 267-287.
6. M. Bartolozzi, G. Braccini, P. F. Marconi and S. Bonvini (1994), *Journal of Power Sources,* 48, 389-392.
7. M. Constantible, S. Panero and B. Scrosati (2001), *Journal of Power Sources,* 92, 65-69.

IONIC LIQUIDS AS EXTRACTANTS OF PHENOLIC COMPOUNDS AND METAL IONS: INFLUENCE OF THE TYPE OF IONIC LIQUID

M. Joana Neiva Correia, M. Matilde Marques, M. Rosinda Ismael, M. Teresa A. Reis

Chemical Engineering Department, Instituto Superior Tecníco, Av. Rovisco Pais, 1049-001 Lisboa, Portugal.

ABSTRACT

This work presents some results concerning the use of 1-(n-alkyl)-3-methylimidazolium- ($C_n$mim), 1-(2-ethoxyethyl)-3-methylimidazolium- (C_2OC_2mim), and 1,3-bis(2-ethoxyethyl)-imidazolium-derived [$(C_2OC_2)_2$im] ionic liquids (IL) in liquid-liquid separation processes. For this purpose, a series of methylimidazolium and imidazolium tetrafluoroborate and hexafluorophosphate ILs were prepared by standard synthetic methods and characterized by 'H NMR. The density and viscosity of the water-equilibrated ILs were also determined. Equilibrium studies on the extraction of copper and zinc ions (300 mg/L) from chloride solutions and of some phenolic compounds (tyrosol and p-hydroxybenzoic acid) from aqueous media were performed. High extraction efficiencies of both metal ions were attained with BF_4 ILs, while the corresponding values with PF_6 ILs were in some instances about 50% lower. Concerning the extraction of the organic compounds it was found that the BF_4 ILs are also more efficient than the corresponding PF_6 derivatives. Furthermore, for the PF_6 ILs, the substitution of the alkyl group by an ether in the methylimidazolium structure resulted in increases of about 10% in the extractions of p-hydroxybenzoic acid and tyrosol. Finally, the ILs containing BF_4 were the most efficient to extract zinc (extraction>90%). In addition, $(C_2OC_2)_2$imPF_6 was also capable of removing more than 80% of the zinc from a 4.5 M NaCl solution. The same IL, $(C_2OC_2)_2$imPF_6, extracted 82% of the copper from a 4.5 M NaCl solution, while a value of 44% and 21% was obtained with the BF_4 ILs and with C_4mimPF_6, respectively.

INTRODUCTION

Liquid-liquid extraction of metal ions from an aqueous phase using toxic organic solvents as extractants or diluents is common in several industrial processes. However, the use of toxic, flammable, and volatile organic compounds (VOCs), and the problems associated with disposal of spent extractants and diluents, have stimulated the search for safe and environmentally benign separation processes, among which the use of room temperature ionic liquids (ILs) is an appealing alternative. These liquids represent a new class of solvents with ionic character. They consist entirely of ions and can be fluid at temperatures as low as -96°C, are colorless, easily handled, and capable of dissolving a wide range of organic and inorganic compounds to very high concentrations [1],

Many common ILs consist of nitrogen-containing organic cations and inorganic anions. Their chemical and physical properties can be tuned for a range of applications by varying the cations and anions. Within the IL class of compounds, 1-(n-alkyl),3-methylimidazolium

cations are among the most commonly used [1-4]. Moreover, PF_6 and BF_4 based ILs are historically the most thoroughly investigated. Typical syntheses of some ILs [5] have been reported and currently there are a number of companies offering hundreds of ILs and reportedly ready to produce them in ton quantities upon demand [6],

Several possible IL applications in separation processes [7] and the partition of several organic solutes in IL-water systems have also been published [3,5], Other studies addressed the use of ILs in antibiotic production [8], the extraction of alkaline and alkaline-earth cations by crown ethers in ILs [2,9], and the use of ILs in metal catalysis [1], The extraction of Cd and Hg with ILs where the cation contains metal ion-binding components such as sulfur atoms has also been described [4], Improvements in the extraction of metal ions by ILs were observed by changing the hydration environment of the metal, using either organic ligands or inorganic anions [7,10,11], In a previous study [12], we have reported some promising results concerning the usefulness of 3-methylimidazolium-derived ILs in the extraction of certain phenolic compounds and heavy metal ions from aqueous solutions.

The present work further explores the ability of selected ILs to extract heavy metal ions and phenolic compounds from aqueous solutions. For this purpose, a series of 1-(n-alkyl)-3-methylimidazolium, 1-(2-ethoxyethyl)-3-methylimidazolium- and 1,3-bis(2-ethoxyethyl)-imidazolium-derived tetrafluoroborates and hexafluorophosphates were prepared and their extracting performances compared. Very encouraging extraction efficiencies were obtained for zinc and copper (> 80%). High extraction efficiencies were also attained for phenolic compounds.

MATERIALS AND METHODS

All chemicals used were of analytical grade. The aqueous solutions were prepared with deionized water. The aqueous media consisted of solutions (300 mg/L) of tyrosol, and p-hydroxybenzoic acid (PHBA), or salt solutions of copper and zinc as chlorides, with 4.5 M sodium chloride. Sodium hydroxide was used for pH adjustments.

1-(n-Alkyl)-3-methylimidazolium- ($C_n$mim), 1-(2-ethoxyethyl)-3-methylimidazolium- (C_2OC_2mim) and 1,3-bis(2-ethoxyethyl)-imidazolium-derived [$(C_2OC_2)_2$im] ILs were synthesized by standard nucleophilic substitutions, using alkyl chlorides or the appropriate alkoxyalkyl chloride and commercially available 1-methylimidazole or imidazole [5], The counter-ions tested were PF_6' and BF_4\ 'H NMR analyses in deuterated acetone were used to characterize the synthesized ILs. Measurements of the density and viscosity of the synthesized ILs were performed at 25°C, after equilibration with water, using an Anton Paar DMA 5000 density meter and a Brookfield DV-II+ programmable viscometer, respectively.

Distribution data of solutes were determined by mixing 2 mL of the water-equilibrated IL and 4 mL of the aqueous phase, containinq the solute, in an orbital shaker (100 rom). with temperature control, for at least 12h at 22°C. The phases were separated by settling, and aqueous phases were analyzed. The organic compounds were analyzed in a Hitachi U2000 double beam ultra-violet/visible spectrophotometer, while heavy metal ions were analyzed by atomic absorption spectroscopy (Perkin Elmer 3100). The concentrations of the organic solutes in the aqueous phase were determined using Beer's law, after testing the analytical method for each compound, namely for potential interference by the IL. Each experiment was carried out, at least, in duplicate and the results agreed to within 5%.

RESULTS AND DISCUSSION

Experiments were performed to assess the influence of the substituent in the imidazolium ring and of the anion on the viscosity and density and the results are presented in Table 1.

This table shows that the anion affects the properties of the ionic liquid. In fact, the BF_4 salts have lower densities, lower viscosities, and higher water solubility compared to the corresponding PF_6 salts [12], Furthermore, increasing the length of the alkyl chain also increases the viscosity and hydrophobicity of the ionic liquid. The substitution of the alkyl groups in the C_4mimPF_6IL by the ether groups does not significantly affects the viscosity of the IL.

Table 1. Physical properties of the tested ionic liquids after equilibration with water (T=25°C)

	C_4mimPF_6	C_8mimPF_6[a]	C_8mimPF_6[a]	$C_2OC2mimPF_6$	$(C_2OC_2)2imPF6$	C_8mimBF_4[a]
$10^{'3}$ p (kg m ^{3})	1.335	1.285	1.232	1.366	1.333	1.084
F (mPa s)	58.0	164	290	43.5	50.7	26.5

[a] Values presented elsewhere [12 .].

Extraction of Phenolic Compounds

Previous work [12] showed that the extraction of p-hydroxybenzoic acid (PHBA) with PF_6 salts decreases from 51% (for C_6mim) and 43% (for C_8mim - not shown in Figure 1) to 7 and 1%, respectively, when the initial pH increases from 3.7 (natural pH of the solution) to 9. This fact presumably reflects the contribution of the ionized form (pKa1=4.5; pKa2=9.3) in basic media. By contrast, tyrosol is a weaker acid (pKa=10) and neither its ionization state nor the extent of extraction are expected to change substantially within the same pH range. In the present work, we have analyzed further the influence of pH on tyrosol extraction. The results show that at pH 12.4, where ionization of the phenolic hydroxyl is anticipated, the extraction of tyrosol is also greatly affected. In fact, at pH 6.3 (natural pH) it was possible to remove 51% of tyrosol from a 300 mg/L solution using C_6mimPF_6 while at pH 12.4 this value decreased to 9%. These results suggest that ILs preferentially extract the neutral forms of the organic solutes.

The influence of the type of IL on PHBA and tyrosol extraction is presented in Figures 1 and 2, respectively.

As previously reported [12], Figures 1 and 2 show that ILs containing the BF_4 anion are very efficient in removing phenolic compounds from an aqueous phase. For the PF_6 ILs, the replacement of an alkyl chain (C_4mimPF_6) by an ether substituent (C_2OC_2mimPF6) has a positive effect on the removal of this type of compounds.

Another relevant aspect is related to the kinetics of the extraction process. In fact, even using mild agitation during the contact stage, more than 45% of the final extraction are attained in the first 10 minutes. Thus, for example, in 10 minutes the C_6mimPF_6 IL extracted about 45% of the PHBA in solution and after 12h the final extraction was 51%.

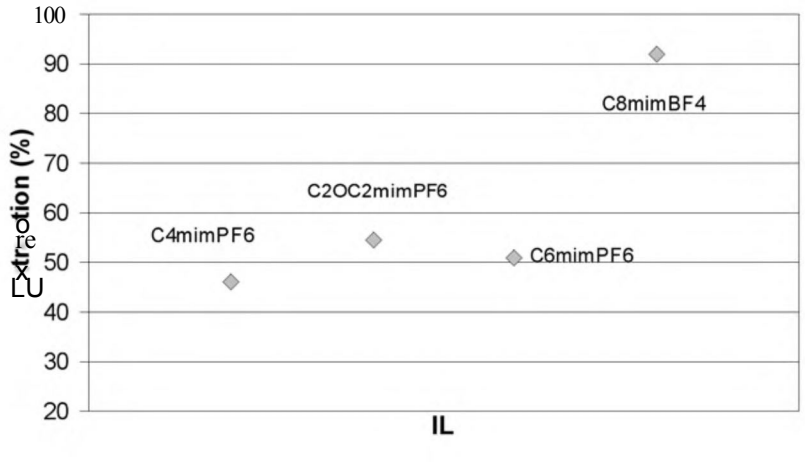


Figure 1- Extraction of p-hydroxybenzoic acid (PHBA) from aqueous solutions with several ILs. Aqueous phase: PHBA- $pH_{ini}u_{ar}3.7$. Data for C_6mimPF_6 and C_8mimBF_4 are from [12]

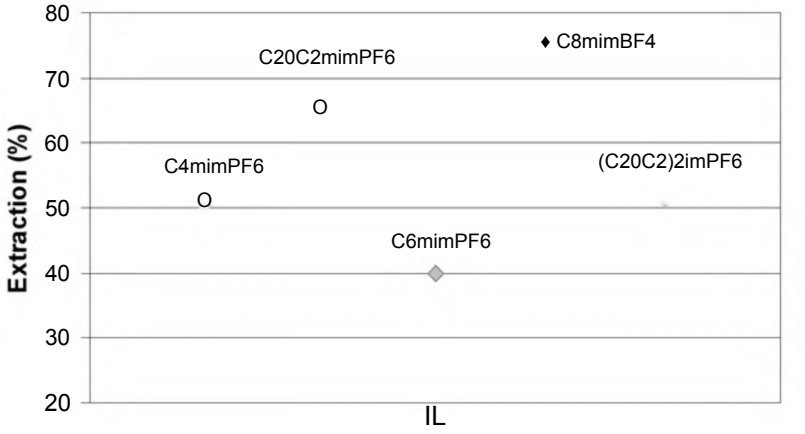


Figure 2- Extraction oftyrosol from aqueous solutions with several ILs. Aqueous phase: tyrosol- pHi_niti_ai-6.3. Data for C_6mimPF_6 and C_8mimBF_4 are from [12]

Extraction of Heavy Metals

We showed previously [12] that zinc extraction by C_6mimPF6 is highly affected by the addition of sodium chloride to the aqueous phase, whereas the effect on copper extraction is marginal. This difference in behavior was attributed to the differences in the affinity for chloride ions presented by these two metals. In fact zinc is a stronger chloride acceptor and so in chloride solutions, zinc in mainly distributed between two negative chloro complexes. On the contrary, copper is mainly distributed between the positive and neutral complexes. The above mentioned results concerning the influence of sodium chloride on metals extraction apparently indicate that the anionic species of the metals are easily extracted by the 1-(n-alkyl)-3-methylimidazolium- ILs.

The influence of the type of IL on copper and zinc extraction from 4.5 M NaCl solutions is presented in Figures 3 and 4, respectively. In this case the replacement of the alkyl chain by an ether-containing substituent did not favor copper or zinc extraction. When compared to the results obtained for the organic solutes (Figures 1 and 2), these results indicate that the

mechanism associated with the extraction of heavy metals from solution is different from the one associated with the extraction of phenolic compounds.

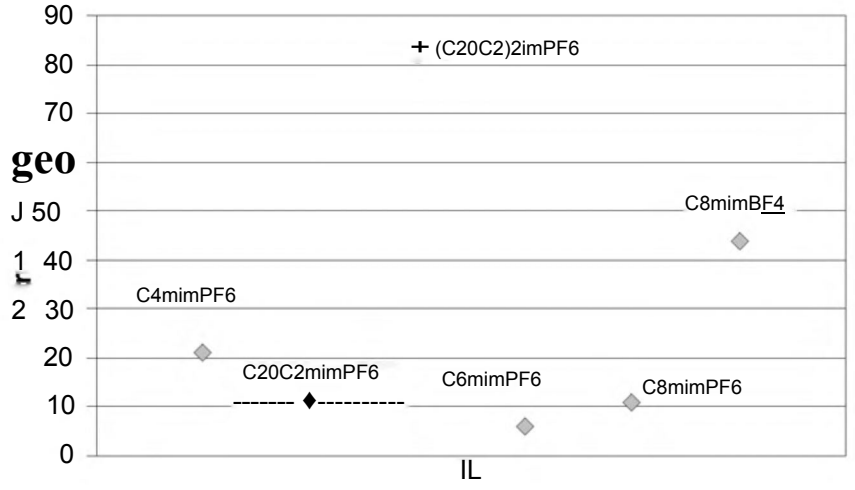


Figure 3- Extraction of copper from 4.5 M Nad solutions with several ILs. Data for C_6mimPF_6 is from [12]

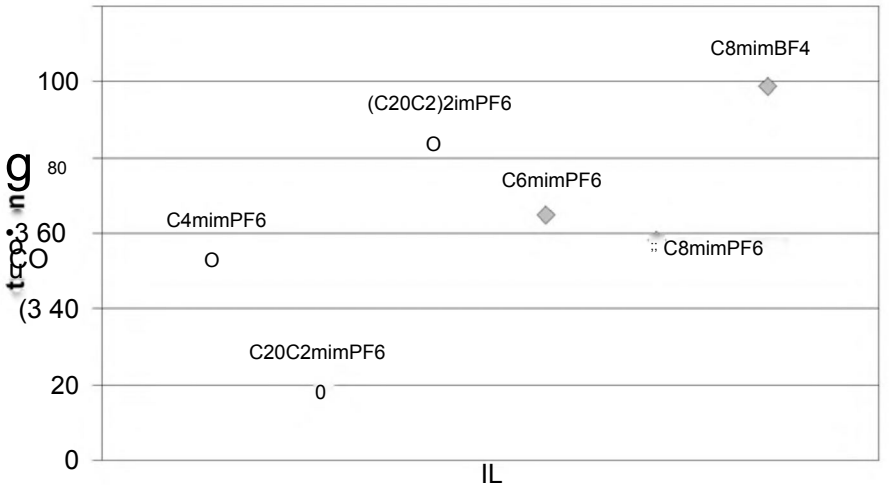


Figure 4- Extraction of zinc from 4.5 M Nad solutions with several ILs. Data for C_6mimPF_6 and C_8mimBF_4 are from [12]

Figures 3 and 4 further show that the introduction of two ether-containing substituents in the imidazolium structure increased the affinity of the IL phase for the heavy metals, to the extent that the extraction efficiencies were comparable (for zinc) or superior (for copper) to those obtained with the representative BF_4 IL, C_8mimBF_4. Although further studies are needed to elucidate this remarkable effect, it is plausible that the two oxygen-containing substituents in the imidazolium ring provide a chelating and / or solvating effect that is absent from alkyl groups and may not be reached with a single oxygen-containing substituent.

CONCLUSIONS

In the present work we have extended previous observations concerning the usefulness of (methyl)imidazolium-derived ILs as extractants of phenolic compounds and metal ions (zinc and copper) from aqueous solutions. Very encouraging results were obtained in both instances. In particular, remarkable extraction efficiencies (up to ca. 80%) were obtained for both copper and zinc with the imidazolium-based IL, $[(C_2OC2)2im]PF_6$, containing two ethoxyethyl substituents. This effect, which requires further investigation, may be related to a chelating and / or solvating effect provided by the two oxygen atoms in the IL.

ACKNOWLEDGEMENTS

Ana Jesus and Guadalupe Rodrigues are thanked for their help in part of this work.

REFERENCES

1. K.R. Seddon (1997), *J. Chem. Tech. Biotechnol.,* 68, 351-356.
2. A.E. Visser, R.P. Swatloski, W.M. Reichert, S.T. Griffin and R.D. Rogers (2000), *Ind. Eng. Chem. Res.,* 39, 3596-3604.
3. J.G. Huddleston, A.E. Visser, W.M. Reichert, H.D. Willauer, G.A. Broker and R.D. Rogers (2001), *Green Chem.,* (3), 156-164.
4. A.E. Visser, R.P. Swatloski, W.M. Reichert, R. Mayton, S. Sheff, A. Wierzbicki, J.H. Davis Jr. and R.D. Rogers (2001), *Chem. Commun.,* 135-136.
5. J.G. Huddleston, H.D. Willauer, R.P. Swatloski, A.E. Visser and R.D. Rogers (1998), *Chem. Commun.,* 1765-1766.
6. G. Parkinson (2004), *Chem. Eng. Progress,* 100 (9), 7-8.
7. A.E. Visser, J.D. Holbrey and R.D. Rogers (2002), Proc. Int. Solv. Extr. Conf. ISEC'2002, *Johannesburg, South Africa,* pp. 474-480.
8. S.G. Cull, J.D. Holbrey, V. Vargas-Mora, K.R. Seddon and G.J. Lye (2000), *Biotechnol. Bioeng.,* 69 (2), 227-233.
9. S. Dai, Y.H. Ju, C.E. Barnes (1999), J. *Chem. Soc. Dalton Transact.,* 1201-1202.
10. A.E. Visser, R.P. Swatloski, S.T. Griffin, D.H. Hartman and R.D. Rogers (2001) *Sep. Sci. Technol.,* 36 (5-6), 785-804.
11. G.T. Wei, Z. Yang, C. J. Chen (2003), *Anal. Chim. Acta,* 488, 183-192.
12. S.T. Vidal, M. J. N. Correia, M. M. Marques, M. R. Ismael, M. T. A. Reis (2004), Sep. *Sci. Technol.,* 39,2155-2161.



Methyl tert-pentyl ether (TAME) - a new solvent for phenol extraction from wastewater

Florin Oprea, Mihaela Petre

Universitatea Petrol-Gaze din Ploie§ti, Romania
Chemical Engineering Department

Methyl tert-pentyl ether [1, 2, 3] is a new solvent, usable for the phenol extraction from the wastewater. Liquid-liquid experimental data in the system water-phenol-TAME show a much higher distribution coefficient for this solvent than for other solvents. The liquid-liquid equilibrum data, obtained with low prices in an extremely simple laboratory installation, have allowed the design of an industrial installation for phenol recovery from the wastewater in an industrial plant of a Romanian phenol producer. The process has been initially tested using a laboratory extraction column, provided with different packings.

Along with the liquid - liquid extraction column, the suggested installation is endowed with a solvent recovering system from (1) the extract phase, respectively TAME-phenol mixture, and (2) refined phase, respectively water-TAME mixture.

Because the solubility of TAME in water is lower than the one of the other suggested solvents (methyl f-butyl ether - MTBE), its recovery from the refined phase is easier.

The phenol extraction from acid water is another usage direction for proving the possibilities of also using it in this field of activity.

INTRODUCTION

In the industrial phenol-production, there surely is waste water with a phenol content varying between 0.5 and 3% weight, no matter what the used technology was. There are other industrial processes (novolac production, coal and wood distillation, thermocatalytic processes in refineries) where this kind of water with different phenol concentration is produced. The necessity of the phenol removal up to an acceptable level is obvious, for avoiding the pollution of the surface water and also of the available ground water. Knowing that there still are older phenol installations which are using a special procedure of dilluating the waste water up to a level which it allows the use of depolluting biological processes (with high waste of phenol), it is indeed necessary for them to be provided with phenol removal/recovery installation, in order to conform with the latest standards regarding the pollution limits.

There are several processes for phenol removal from wastewater, depending on the initial and required final phenol contents: (1) liquid-liquid extraction with several solvents, (2) distillation in presence of electrolytes, (3) adsorption on active carbon, and (4) biochemical process.

It is also good to mention that the recovery of this phenol from the wastewater is a clear way of covering the depollution costs. Our team has high knowledge in solving this kind of problems [4, 5], the value of the recovered phenol has successfully covered the investment and the operating costs, due to using the suggested installations.

A previous achievement was using MTBE as a solvent, but considering the latest studies regarding its toxicity, it was decided that it should be replaced by TAME, which is also available on the considered industrial platforms. At first sight, using TAME is even more favourable considering that its solubility (1.2 g TAME/100 g water) is four times lower than that of MTBE(4.8 g MTBE/100 g water), which reduces the effort of recovering it from the wastewater. Actually, the project has to decide upon the necessary conditions for the present installation (that is using MTBE like solvent) to be adjusted for using the suggested solvent.

The proposed process implies the study of two problems: (1) the actual extraction and (2) the recovery of the solvent. Considering that the processing capacity of this kind of installation is quite low and that there are few available installations, the research and design effort was not too high. A relatively simple, quick and cheap solution was chosen, which, on the other hand, does not diminish the performance required by this kind of process.

EXPERIMENTAL CONCERNING LIQUID-LIQUID EXTRACTION DATA IN THE SYSTEM WATER - PHENOL - TAME

Different solvents are used in the liquid-liquid extraction of the phenol: aromatics (benzene, toluene, xylenes, cumene [4]), diisopropylether, butylacetate, and methyl f-butyl ether (MTBE) [5, 6], The most important property of a solvent is its extraction power for the component that is extracted, in our case phenol. This power can be expressed by the distribution coefficient, *K,* defined as the ratio of solute concentrations in both liquid phases:

$$K = \frac{Y}{X} \quad (1)$$

where *Y* represents the phenol concentration in solvent (kg phenol/kg solvent or kg phenol/m^3 solvent);
X is the phenol concentration in wastewater (kg phenol/kg water or kg phenol/m^3 water).

As the distribution coefficient increases, the solving power of the solvent improves, and the performance of the process is better, requiring fewer equilibrium stages, a lower solvent ratio, and giving a higher degree of extraction. From this point of view, the solvents like diisopropyl ether butyl acetate, MTBE and TAME, having higher distribution coefficients, are better than aromatics. The advantage of these solvents is even more obvious, considering the toxicity of benzene.

For the water-phenol-TAME system, the liquid-liquid equilibrium experimental data was obtained using an extremly simple equilibrum cell, presented in *Figure 1.* The first studied aspect was the phenol distribution coeficient's temperature variation, between the two phases, the experimental data showing an unsignificant variation, considering the industrial use.

In the case of phenol extraction with TAME, liquid-liquid equilibrium data, obtained at 40°C, are presented in *Figure* 2, compared to the data for the water-phenol-MTBE system. Experimental values were fitted according with Nerst-Shilov equation and both (experimental data and regression curve) are presented in *Figure 3:*

$$Y = a \cdot X^{b}, \quad (2)$$

where a = 3993.99435 and 6 = 1 . 59158.

The distribution coefficient of phenol in TAME (65 to 104) is higher than the distribution coefficient of phenol in benzene, which has the value 3, and is comparable to those of butyl acetate, diisopropyl ether and MTBE (80 to 110). On the other hand, the price of TAME is much lower than that of the others solvents.

THE DESIGN OF THE LIQUID-LIQUID PHENOL EXTRACTION COLUMN

Knowing the equilibrum data in the water-phenol-TAME system, the liquid - liquid extraction column can be design, in order to obtain the solvent ratio and the number of equilibrums. This is the right moment to mention that, even though the TAME solvent and the water are partially soluble, their low mutual solubilities allow the design of the extraction column as a liquid-liquid extraction column with nonmiscible solvents, the design procedure being noticeable simplified. The mutual solubilities of the two substances are taken into account during the design of the solvent recovery system.

In the extraction column presented in *Figure 4,* S-i represents water flow rate (kg/h); S_2 - TAME flow rate (kg/h); Xi, X_0 - phenol content in aqueous solution, input and output from the column (kg phenol/kg water); Yj, Y_0- phenol content in TAME stream, input and output from the column (kg phenol/kg TAME).

For a practical example it can be considered that, in order to reduce phenol content in stream Si from an input value X_i = 0.031 kg phenol/kg water to output value between X_0 = 0.0001 and X_0 = 0.0002 kg phenol/kg water, the TAME stream S_2 enriches from the input concentration Y_i = 0.002 kg phenol/kg TAME (value from the solvent recovery system, see next section) to several output concentrations Y_0 depending of solvent ratio (0.0308 to 0.0616 kg phenol/kg TAME). Using a simplified graphical method in rectangular diagram [7] the solvent ratios, S_2/S_U were calculated for different numbers of necessary equilibria (number of theoretical trays), N_{tt}. The value of N_{tt} increases from 1.9 to 2.4 for S_2/Sj varying from 1:1 to 0.5:1 .

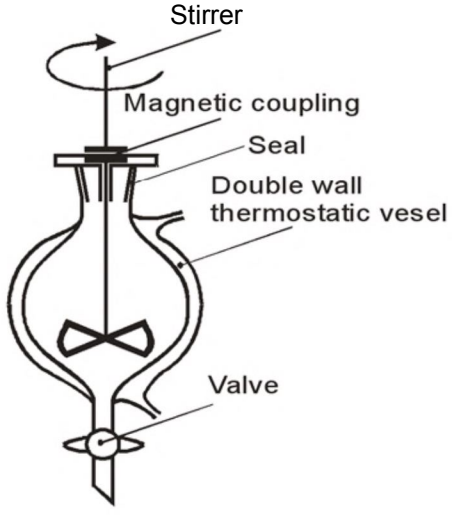
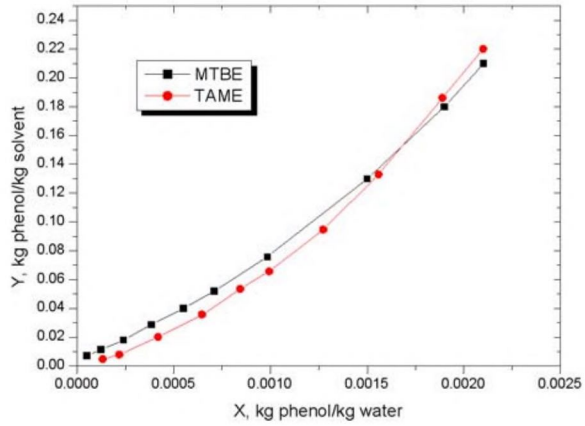


Figure 1 Laboratory cell for study of the liquid - liquid equilibrium



Fiaure 2 Eauilibrium data for the systems water-phenol-solvent for solvents MTBE and TAME

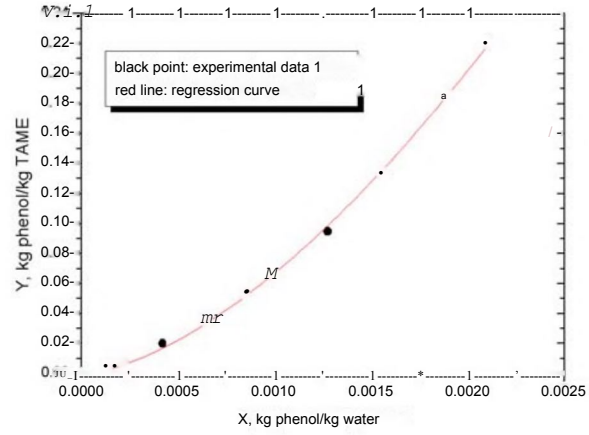


Figure 3 Liquid-liquid equilibrium data and regression data for the water-phenol-TAME system.

The checking of the liquid-liquid equilibrum data was made by testing the extraction on a laboratory column, provided with (1) Raschig or (2) structured Sulzer packing. The calculations based on the experimental data obtained from the two types of columns proved that there are no noticeable efficiency differences, the low price leading to choosing the Raschig packing for the industrial column.

Considering the economic consequence, the solvent ration of 1:1 was chosen as a solvent ratio for the industrial installation. In this way, the height of the packing has a reasonable value. The diameter of the extraction column does not cause any problems during the design.

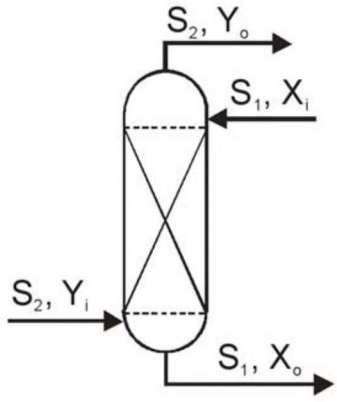


Figure 4. Extraction column configuration

DESIGN OF THE SOLVENT RECOVERY SYSTEM

The design of an installation such as the one in *Figure* 5, requires, besides the actual extraction, the recovery of the extracted phenol, concomitently with the regeneration of the solvent, and also the recovery of the solvent (TAME) from the water phase, due to the TAME solvent's solubility in water. Any appreciations regarding the extraction step are irrelevant if this phase is not studied along with the solvent's regeneration steps.

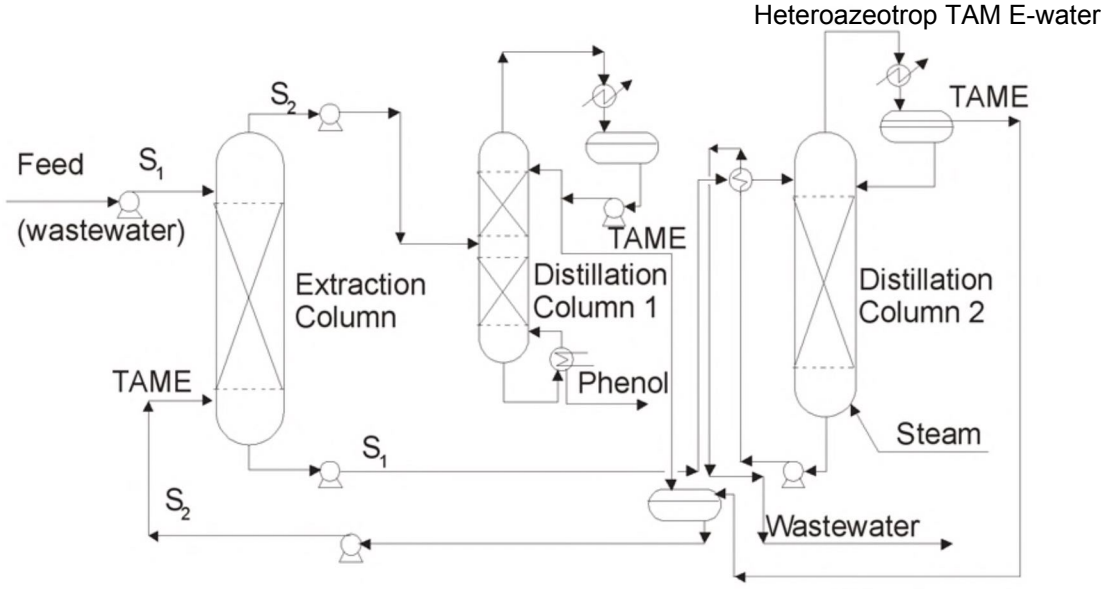


Figure 5 Industrial Installation for phenol extraction with TAME

The two components (TAME and phenol), from the extract stream which leaves the extraction column, are separated in the distillation column 1 *(Figure* 5), the phenol obtained at the bottom of the column being returned for purrifying in the installation which produces it, and the TAME solvent (obtained at the top of the column) goes back to the extraction column.

The recovery of the solvent from the refined stream (wastewater) is made by stripping it in the column 2 *(Figure* 5). The heat supply in the bottom of the column is brought by the steam and a part of the used heat is recovered in the heat exchanger with the refined stream which feeds the stripping column. The wastewater is evacuated to the biological purrification stage,

having a low phenol content.The TAME - water azeotrop is obtained at the top of the column, and by condensing it, two phases are obtained: the water phase which is used like reflux in the column, and the solvent phase which goes back to the extraction column, the latest being saturated with water from this very moment. The adapted system leads to minimizing the loss of (1) solvent in water, (2) solvent in phenol and, of course, (3) phenol in wastewater, all these with lowest possible heat consumption.

Considering the low flowrate of wastewater, the chosen alternative for practice was the one of using the same distillation column for both (1) the recovery of TAME from the extract phase, and (2) the recovery of TAME from refined phase, only one industrial column functioning with the two purposes. The result is the obvious decrease of the investment costs, even if there may be certain difficulties in operating it.

Computer simulations have been done, using our own software, in order to obtain the optimum for the separation system, considering the total annual costs. The vapor-liquid equilibrium data necessary for the stimulation were taken from literature [8],
Utilities consumptions obtained in simulations are presented in *Table 1.*

Table 1 Main utilities consumption.

Utility	Annual consumption
Steam (tonne)	2000
Cooling water (m^3)	30000
Electric power (kWh)	7000

A preliminary economic calculation for suggested installation which processes almost 1500 kg/h wastewater with a phenol content of almost 3% weight and which removes the phenol up to a level of almost 200 ppm weight, enough for supplying the biological treatment stage but also for a high recovery of the phenol, shows that the operating costs rise to the level of 10-30% of the value of the recovered phenol (depending of phenol and energy price).

REFERENCES

1. Tert-amil Methyl Ether, ChemicalLand21.com, http://www.chemicalland21.com/arokorhi/industrialchem/solalc/tert-AMYL%20METHYL%20ETHER.htm
2. EPA, CAMEO, http:/www.epa.gov/ceppo/cameo/help/chapt15d.htm
3. EPA, Office of Research and Development, Oxygenates in Water, http://water.usgs.gov/pubs/wri/wri024276/pdf/WRI024276.pdf
4. *Romanian patent* 00109191/1994 - Proces unitar de recuperare a fenolului din apele fenolice §i din produsele secundare rezultate din procesul de fabricare a fenolului (Process for simultaneous recovery of the phenol from phenolic water and secondary products from industrial phenol installation.
5. Costică Strătulă, Florin Oprea, Ca§en Panaitescu, Mihaela Petre and Gheorghe Boțoc, Methyl tert - butyl ether - a new solvent for phenol and acetic acid extraction from wastewater, *ISEC 2002,* Cape Town, march 2002.
6. Process for phenol/recovery from wastewater, RELANSIN project, National Agency for Research, 2001.
7 C. Taran, and C. Strătulă (1978), *Procese difuzionale de separare, volume II, IPG Ploie§ti.*
8. Gmeling, J., Vapor - Liquid Equilibrium Data Collection, Dechema

SELECTIVE RECOVERY OF PHENOLS FROM PHENOLIC RESIN PLANT EFFLUENT BY LIQUID-LIQUID EXTRACTION

Paulo F.M.M. Correia, Licinio M. Ferreira, Jorge M.R. de Carvalho

Instituto Superior Técnico
CPQ - Chemical Processes Centre
Av. Rovisco Pais, 1049-001 Lisboa, Portugal

In this work the recovery of phenols from a phenolic resin plant effluent by liquid-liquid extraction has been studied. Several extractants were tested. The selected organic phase allowed a selective recovery of phenols towards formaldehyde by this technology. Concentration of phenols from 46 g/L in the phenolic resin wastewater to 28 wt. % was obtained. The stripping concentrate can be reused for phenolic resin production.

INTRODUCTION

Phenolic resins are polymeric compounds of phenols and aldehydes characterised by their high shear and heat resistance. These resins are produced by a batch process consisting on the loading of a reactor with a phenol and formaldehyde mixture in certain proportions, catalyst addition, pre-heating or continuous heating to achieve polymerisation conditions and consequent resin formation and drying until the desired resin water content is reached. Phenolic resins are mostly used in moulding compounds, coatings and industrial bond resins for grinding wheels, coated abrasives, brake lining, clutch facing, laminates, plywood adhesives, glass-wool thermal insulation, bonded organic-fibre padding, foundry-sand bonding, wood-waste and cork bonding, among other miscellaneous applications (1).

In this work, the recovery of phenols and formaldehyde from an effluent resulting from phenolic resins production by using liquid-liquid extraction has been studied.

Despite of the process of liquid-liquid extraction applied to simple phenols has been extensively studied, most of the studies concentrated on its application to extraction with volatile and water-soluble solvents (2-4) and mixtures of solvents (5).

As an alternative to these conventional solvents, extractants with low solubility in the aqueous phase have been developed, such as tertiary amines and trialkylphosphine oxides. The extractant reacts with phenols during the extraction stage, forming a complex soluble in the organic phase. Due to phenols' high boiling point (181.4°C for phenol (6)), chemical stripping by contacting the extract with a concentrated aqueous solution of a strong base is more interesting economically than distillation. Studies with salts of tertiary amines (namely chlorides and sulphates) (7-9) and with Cyanex 923 (a mixture of four trialkylphosphine oxides) as extractants for phenols (10-13) have been presented in the literature. Up to now

no work has been published considering the application of Cyanex 923 to the recovery of phenols from an industrial effluent.

EXPERIMENTAL

Liquid-liquid extraction equilibrium studies at several temperatures were performed by agitation of rigorous volumes of the aqueous and organic phases in an orbital agitator Aralab Agitorb 160E, with temperature and agitation speed control, connected to a cooling unit Aralab Refri 320E.

Liquid-liquid extraction kinetic studies were performed by dispersing the organic phase in the aqueous phase in a 1 L cylindrical glass reactor (85 mm internal diameter, round bottom) immersed in a water bath (that also allowed cooling). Agitation was performed through a stainless steel paddle and provided by a Heidolph RZR1 driver. During permeation samples were taken at known times since organic phase half addition time (taken as time zero).

Organic phases were prepared by diluting the intended extractant in the isoparaffinic hydrocarbon solvent ShellSol T (paraffin content higher than 99 wt.%, Shell Chemicals Ltd .). Aromatic hydrocarbon solvent ShellSol A (aromatic fraction higher than 99.5 wt. %, Shell Chemicals Ltd.) was also tried out. The following extractants were tested in this study: Hostarex A327 (mixture of tri-n-octylamine and tri-n-decylamine, Clariant Chemical Co.), Cyanex 923 (a mixture of 4 trialkylphosphine oxides, Cytec Co.), Aliquat 336 (water insoluble quaternary ammonium salt made by the methylation of mixed tri-octyl/decyl amine, Cognis Co.), Primene JM-T (mixture of f-alkyl isomeric primary amines in $C_{16\cdot22l}$ Rohm and Haas). 1-decanol (Riedel-de-Haën), methylisobutylketone (MIBK) (J.T. Baker) and diethylether (MERCK p.a.) were also used for preparing some organic phases. All chemicals were used as received.

For preparing the aqueous stripping solutions, sodium hydroxide (MERCK p.a.), HCl (MERCK p.a.), NH_4OH (MERCK p.a.) were used.

Analysis of phenols in the aqueous phase samples was made by 4-aminoantipyrine reaction colorimetric method (14). Formaldehyde analysis was done by the Hantzsch reaction colorimetric method by using acetylacetone reagent (14). Both analyses were performed in a double beam ultraviolet/visible spectrophotometer Hitachi U2000. Both phenol and formaldehyde used for standards preparation were analytical grade (MERCK p.a.).

pH measurement was performed by using a Metrohm 632 pH Meter with a Metrohm combined electrode.

RESULTS AND DISCUSSION

The composition of phenolic resin plant effluent used in this study is presented in Table 1.

Table 1. Characteristics of phenolic resins effluent used in this study.

Parameter	Effluent
Appearance	Transparent liquid
Colour	Light violet
PH	3.5
Phenols cone, (as phenol)	46 g/L
Formaldehyde cone. (mg/L)	41 g/L

Extraction Studies

Several extractants typically used in liquid-liquid extraction for phenols removal were tested, in order to evaluate both their efficiency and selectivity towards formaldehyde. The obtained results are presented in Figure 1. Cyanex 923 presented both the highest extraction degree for phenols and the highest selectivity towards formaldehyde among the tested extractants.

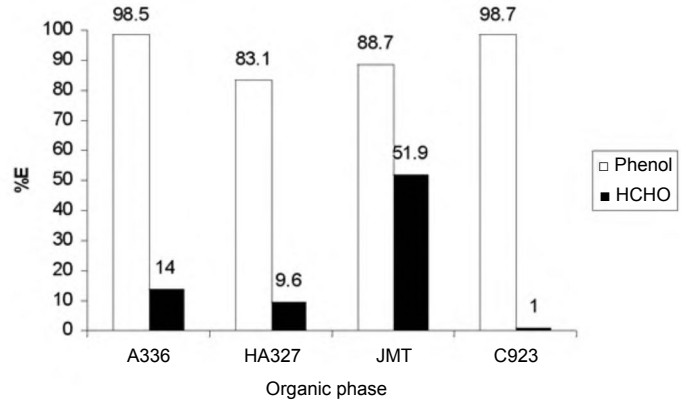


Figure 1. Comparison of different organic phases composition for extractant choice (Organic phases composition: A336 - Aliquat 336 0.6 M in ShellSol T + 10 vol. % 1-decanol; HA327 - Hostarex A327 0.6 Min ShellSol T + 10 vol. % 1-decanol; JMT - Primene JM-T 0.6 M in ShellSol T + 10 vol. % 1-decanol; C923 - Cyanex 923 0.6 M in ShellSol T; Operating conditions: V_{aq} $A/_{org}$ = 1; agitation speed: 130 rpm; temperature: 298 K; agitation time: 18 h).

With a second extraction of the raffinate with Cyanex 923 0.6 M in ShellSol T, most of the phenols were removed, resulting a raffinate with most of the formaldehyde formerly contained in the effluent (as shown in Figure 2).

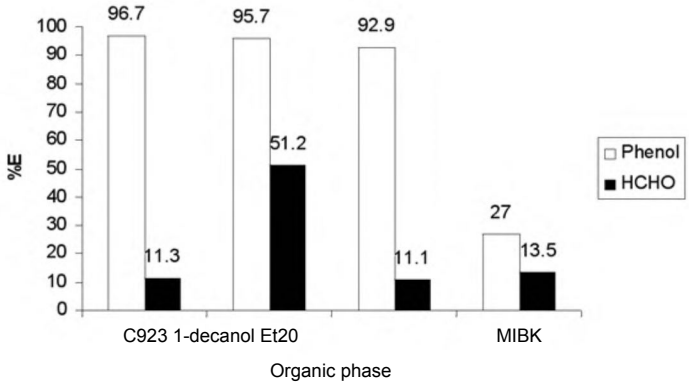


Figure 2. Studies with the raffinate of the extraction of phenolic resin plant effluent with Cyanex 923 in ShellSol T (Organic phases composition: C923 - Cyanex 923 0.6 M in ShellSolT; 1-decanol; Et20 - diethylether; MIBK; Operating conditions: $V_{aq}A/_{org}$ = 1; agitation speed: 150 rpm; temperature: 298 K; agitation time: 16 h).

The kinetics of phenol extraction by Cyanex 923 was very fast. Equilibrium was reached in less than 1 minute (as shown in Figure 3). This allows the use of liquid-liquid extraction columns in continuous mode operation. Temperature had a slight deleterious effect in the extraction rate and also in the extent of mass transfer.

In order to select a solvent, with a reasonable capacity to extract formaldehyde and, at the same time, to observe its behaviour towards phenols extraction, studies were undergone using the raffinate obtained from the 1st. extraction with Cyanex 923 0.6 M in ShellSol T as the aqueous phase. Results are presented in Figure 2. From these results and from the tests presented in Figure 1, it was verified that, among the tested solvents, the only ones that allow some extraction capacity for formaldehyde are 1-decanol and the organic phase composed by the primary amine Primene JM-T 0.6 M, diluted in ShellSol T and using, as modifier, 10 vol. % 1-decanol.

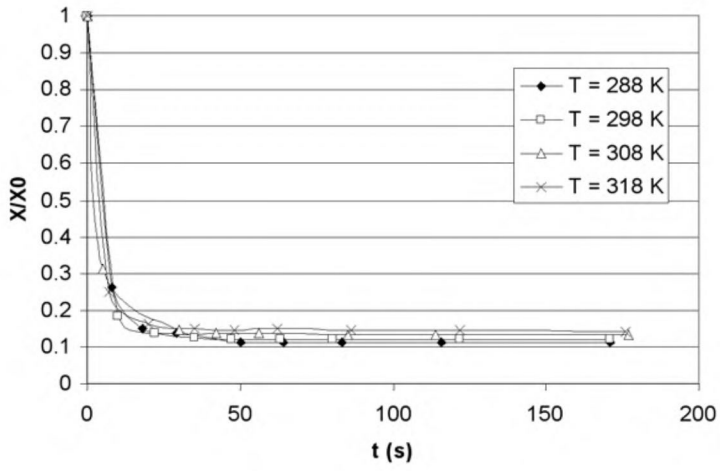
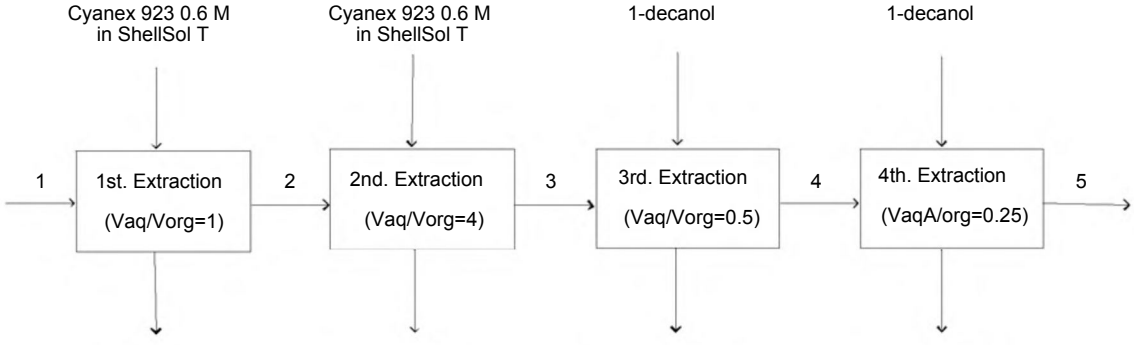


Figure 3. Kinetics of phenol extraction
(Operating conditions: $V_{aq}A/_{org}$ = 2; agitation speed: 300 rpm; organic phase: Cyanex 923 0.6 M in ShellSol T; aqueous phase: 46 g/L phenol aqueous solution).

It is also verified that all the organic phases that extracted formaldehyde also extracted phenols. Thus, any integrated process for the treatment of phenolic resin effluent should pass first for a stage of selective removal of phenols and their concentration and later to the concentration of the formaldehyde that remained in the effluent after phenols removal.



Stream	1	2	3	4	5
Phenols (g/L) **(%E)**	46 –	0.576 (98.7%)	0.023 (96.0%)	0.005 (78.3%)	0.0015 (70.0%)
HCHO (g/L) **(%E)**	41 –	40.6 (1.0%)	39.4 (3.0%)	11 (72.1%)	2 (81.8%)
PH	3.5	3.0	2.9	3.0	3.1

Figure 4. Integrated process for the treatment of phenolic resin plant effluent (Operating conditions: agitation speed: 150 rpm; temperature: 298 K; agitation time: 10 h).

Due to the difficulties in the stripping with NaOH of the loaded organic phase containing Primene JM-T (1), further tests of liquid-liquid extraction with 1-decanol, of the phenolic resin effluent after two extractions with Cyanex 923 were performed. The obtained results, for the sequence of the process, are presented in Figure 4. It was verified that, with successive extractions with 1-decanol, some degree of formaldehyde extraction was obtained and at the same time the effluent was being further purified towards phenols.

Stripping Studies

The kinetics of phenol stripping with NaOH 5 M was very fast. Equilibrium was reached in less than 2 minutes (as shown in Figure 5). Temperature had a notorious positive effect in the extraction rate and also in the extent of mass transfer.

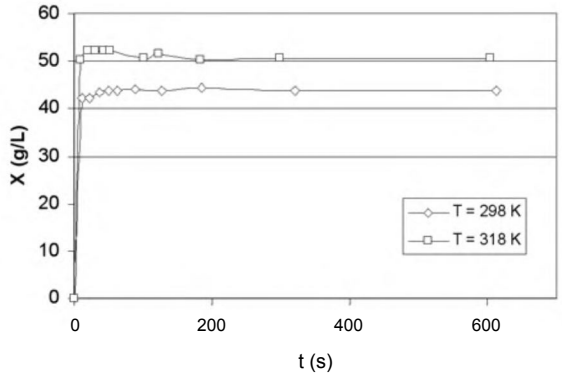


Figure 5. Kinetics of phenol stripping
(Operating conditions: $V_{aq}A/_{org}$ = 0.5; stirring speed: 300 rpm; organic phase: Cyanex 923 0.6 M in ShellSol T loaded with phenol; aqueous phase: NaOH 5 M).

From the results of the stripping tests presented in Table 2, as the phase ratio $V_{aq}A/_{org}$ lowers and NaOH concentration increases, the stripping percentage of the organic phase decreases, because of the increase in both the aqueous phase viscosity and in the salting-out effect due to the increase of the aqueous phase ionic strength. Thus a compromise solution is needed: a stoichometrically enough concentration (taking the phenols present in the effluent as phenol) to strip the phenols of the organic phase to the wanted limit - a solution of about 30 wt. % in phenol - was used. Due to this reason, NaOH 5 M was used as stripping solution.

Table 2. Stripping of loaded organic phase containing Cyanex 923
(Operating conditions: agitation speed: 150 rpm; temperature: 298 K).

Stripping solution	$\mathbf{v_{aq}/v_{org}}$ (agitation time)	Aqueous phase composition after stripping (pH > 14 in all cases)
NaOH 2 M	15 mL/15 mL (15 h)	40.4 g/L phenol (%Stripping = 90%) 530 mg/L formaldehyde
NaOH 4 M	10 mL/50 mL (4 h)	105 g/L phenol (%Stripping = 46%) 2360 mg/L formaldehyde
NaOH 3M	10 mL/100 mL (24 h)	150 g/L phenol (%Stripping = 33%) 3865 mg/L formaldehyde
NaOH 5M	10 ml_/200 mL (9 h)	173 g/L phenol (%Stripping = 19%) 3713 mg/L formaldehyde
NaOH 8 M	7 mL / 70 mL (7 h)	71.6 g/L phenol (%Stripping = 16%) 2372 mg/L formaldehyde

Considering the formaldehyde recovery and concentration, taking the affinity of formaldehyde for the molecular nitrogen groups (that justifies its use in tanning industry (15)) into account, the stripping of the formaldehyde loaded organic phase with ammonia was tested. Agitating the organic phase resulting from the 2nd. extraction with 1-decanol of phenolic resin effluent in the orbital agitator, at 150 rpm, during 6 h, with an aqueous solution of ammonia 6 M in a phase ratio $V_{aq}A/_{org}$ = 0.5, a stripping extent of 87% was obtained.

Process Improvements

The possibility of already getting a partial concentration of the phenols in the extraction stage was tested. When the phase ratio $V_{aq}A/_{org}$ = 0.5 was tried out, an insoluble phenols-Cyanex 923 complex was obtained in the aqueous phase. The aromatic solvent ShellSol A was used to solubilise it. In a test were the phenolic resin plant effluent was contacted with an organic phase composed by Cyanex 923 0.6 M in 70 vol. % ShellSol T and 30 vol. % ShellSol A in a phase ratio V_{aq}/V_{org} of 5 and the extract was stripped with NaOH 5 M in a phase ratio $V_{aq}A/org$ of 1/5, a concentration of the order of 28 wt. % phenols was obtained in the concentrate. According to the phenolic resin company, this allows the extract to be reused for phenolic resin production.

CONCLUSIONS

A brief description of phenolic resins and of their production process was presented. Liquid-liquid extraction was applied to an effluent resulting from their production. Several extractants were tested. Cyanex 923 allowed a high phenols removal and selectivity towards formaldehyde. From the results presented, this technology allowed recovery and re-use of the phenols present in phenolic resin plant wastewater. Concentrations of the order of 28 wt. % of phenols in the stripping phase were obtained. According to the phenolic resin company, these concentrations allow the reuse of phenols concentrate for phenolic resin production. Pilot plant studies are however needed to evaluate the actual performance of this technology considering phenols removal. Considering formaldehyde removal and recovery by liquid-liquid extraction, further studies are still needed for its improvement.

ACKNOWLEDGEMENTS

The authors would like to thank Cytec Inc., Rohm and Haas Co., Clariant Chemical Co. and Cognis Co. for providing the reagent samples and the company FUNDIPOR, Lda. (Oporto) for the phenolic resins effluent. The financial support of FCT (Portuguese Government Funding Agency) is also acknowledged.

REFERENCES

1. P.F.M.M. Correia (2002), PhD Thesis, Instituto Superior Tecnico, UTL, Lisbon, Portugal.
2. P.R. Kiezyk and D. Mackay (1971), *Can. J. Chem. Eng.,* 49, 747-752.
3. J.P. Earhart, K.W. Won, H.Y. Wong, J.M. Prausnitz and C.J. King (1977), *Chem. Eng. Prog.,* 73(5), 67-73.
4. R.L.P. Alvarez, J.A.V. Chamosa, M.A.A. Sanchez, J.E. Pascual and L.I. Hernandez (1998), *Span. ES* 2,112,095.
5. M. Medirand D. Mackay (1975), *Can. J. Chem. Eng.,* 53, 274-277.
6. *Perry's Chemical Engineers' Handbook,* 6th. Ed., R.H. Perry, D.W. Green and J.O. Maloney (eds.), McGraw-Hill, New York, 1984.
7. G. Braun, W. Grunbein, M. Mayer and B. Wojtech (1986), *ISEC'86 - Preprints,* DECHEMA, München, Federal Republic of Germany; Vol. III, 885-891.
8. B. Wojtech, G. Braun and R. Steiner (1988), *ISEC'88 - Conference papers,* Moscow,

USSR, 1988; Vol. III, 370-373.
9. H. Tetzlaff and S. Ritlner (1992), *Solvent Extraction 1990,* T. Sekine (ed.), Elsevier Science Publishers, 1992, 479-484.
10. E.K. Watson, W.A. Rickelton, A.J. Robertson and T.J. Brown (1988), *ISEC'88 - Conference papers,* Moscow, USSR, 1988; Vol. III, 370-373.
11. A.M. Urtiaga and M.I. Ortiz (1997), *Sep. Sci. Technol.,* 32(6), 1157-1162.
12. W. Cichy, S. Schlosser and J. Szymanowski (2001), *Solvent Extr. Ion Exch.,* 19(5), 905-923.
13. W. Cichy and J. Szymanowski (2002), *Environ. Sci. Technol.,* 36, 2088-2093.
14. ASTM (1999), 1999-Annual Books ofASTM Standards, ASTM, Philadelphia, Vol. 11.
15. J.F. Walker (1975), Formaldehyde, 3rd. Ed., Robert E. Krieger Publishing Company, New York, 483-660.



RECOVERY OF ZINC FROM SULPHATE AQUEOUS SOLUTIONS USING HOLLOW FIBRE CONTACTORS

M. Rosinda Ismael, M. Teresa A. Reis, L. Gameiro, T. Cabrita, Jorge M. R. Carvalho

Chemical Engineering Department, Instituto Superior Tecnico,
Av. Rovisco Pais, 1049-001 Lisboa, Portugal

ABSTRACT

This work aims to study the extraction of zinc from sulphate aqueous solutions using a hydrophobic propylene membrane contactor. The organophosphorus compounds bis(2-ethylhexyl)phosphoric acid (D2EHPA) and bis(2-ethylhexyl)thiophosphoric acid (D2EHTPA) were used as extractants. The influence of the initial pH of the feed phase on the overall mass transfer coefficient was determined for both systems. The effect of the aqueous and organic throughputs on the overall mass transfer coefficient was also analysed. Integration of the extraction and stripping stages was carried out using different volume phase ratios. Concentration ratios of about 18-fold with 90% recovery were obtained. The results were finally compared with the ones obtained by applying the Emulsion Liquid Membranes separation technique.

INTRODUCTION

The extraction of zinc from sulphuric media has experienced a renewed interest because of the use of this process on a commercial scale for treating waste streams and secondary materials [1], Several papers concerning the extraction of zinc with organophosphorus compounds such as bis(2-ethylhexyl)phosphoric acid (D2EHPA) have been published [1-4], However, the problems associated to the formation of a third phase and crud formation at the interface as well as solvent loss due to aqueous solubility of D2EHPA are reported in literature [5], These drawbacks and other shortcomings (e.g. flooding and loading in conventional contactors) may be eliminated using so-called nondispersive solvent extraction (NDSX) [6], NDSX is shown as an alternative to the classical extraction in mixer-settlers and columns. NDSX is carried out using microporous membranes to immobilise the aqueous-organic interface within the porous structure. One of the two phases wets the membrane and a slight overpressure must be applied to the other phase to stabilise the interface and to avoid the mixing of fluids. The solute is thus transported from the feed to the extractant phase, through the membrane, without phase dispersion. Membrane extraction processes have been applied in a large number of systems including the extraction of metals [5,7-9], organic pollutants [10-12], pharmaceutical and fermentation products [13-15], etc.

NDSX processes using hollow fibres as contactors are of particular interest because of the versatility and the high surface area/volume associated with these devices. Thus, these processes can also allow the use of extractants that are not common in solvent extraction

because of its low kinetics of stripping. One example is the equivalent form of D2EHPA with a sulphur atom, bis(2-ethylhexyl)thiophosphoric acid (D2EHTPA). This liquid ion exchanger is able to extract zinc at lower pH values [16] but exhibits slower stripping kinetics [17].

The present work aims to study the extraction of zinc from sulphate solutions using D2EHPA and D2EHTPA, as extractants, and hollow fibres as contactors. It is also intended to carry out simultaneous extraction and stripping to recover zinc with a high content in the final acidic stripping solution. The results are then compared with the ones obtained by applying the Emulsion Liquid Membranes (ELM). ELM is other membrane based process, where a primary emulsion is dispersed in a continuous phase, which is the phase to be treated. The details of this separation technique are described elsewhere [18].

MATERIALS AND METHODS

Chemicals in the aqueous phase ($ZnS0_4$, H_2S0_4, and Na_2S0_4) were of high-purity analytical grade (Merck). The content of zinc in the feed phase was 300 mg L'^1 (4.59x1 O'^3 M) and the concentration of the sodium salt was 20 g L'^1. The pH values of the aqueous solutions were varied by adjusting the amount of H_2S0_4 added and were measured on a Metrohm 682 Titroprocessor at 298 K with a combined electrode. A sulphuric acid aqueous solution (2.0 M) was used as stripping solution. The extractant bis(2-ethylhexyl)phosphoric acid (D2EHPA) was purchased from BDH Chemicals Ltd and its purity was 96%. The extractant bis(2-ethylhexyl)thiophosphoric acid (D2EHTPA) was kindly supplied by Hoechst AG and used without purification. Its purity was determined to be 79% by potentiometric titration in 2-propanol with 0.1 M tetrabutylammonium hydroxide (Merck). Shellsol T (Shell Chemical Ltd.) was used as diluent. The concentration of extractant (D2EHPA or D2EHTPA) in all the organic phases was determined to be 0.1 M. The organic phases were washed with deionised water to remove the soluble impurities. In the tests with emulsion liquid membranes, the surfactant ECA4360J (Essochem Europe Inc.) was used to stabilise the emulsions (2 wt.% in the organic phase).

Extraction runs were carried out using one hollow fibre module, while two modules were used to carry out the extraction and stripping stages forming a closed loop cycle. The hollow fibre modules (Liqui-Cel 2.5 x 8 Extra-Flow) were purchased from Celgard Inc. (USA). The contactors used had 10,800 polypropylene fibres (X-50 fibres) with a porosity of 40% and an effective length of 155 mm. The internal diameter of the fibres was 220 pm and the wall thickness was 40 pm. The internal area of mass transfer was 1.16 m^2. The aqueous phases flowed trough the tubes of the modules. The organic phase flowed counter-currently on the shell side. The overpressure of the aqueous phase was 0.5-1.0 bar to stabilise the interface in the pores. Pumping of the phases was achieved by using gear pumps (DDS.38, Tuthill). Flow meters were used to monitor the flow rates of the phases. The hollow fibre set-up is similar to the one presented by Cichy et al. [11], The experimental procedure of the emulsion liquid membranes is described with detail elsewhere [19], All the experiments were carried out at 298 K. The concentration of zinc in the aqueous phases was measured by atomic absorption (Perkin-Elmer AAnalyst 200).

For the equilibrium experiments to obtain partition data, the aqueous solutions were contacted with the organic phases using different volume phase ratios, for at least 12 h. The agitation of the phases was performed by an orbital shaker with temperature control (298±0.1 K). After extraction, the phases were allowed to settle for more than 2 h and subsequently separated. The concentration of zinc in the aqueous phase was measured by atomic absorption, as stated before, as well as in the organic phase after extraction (Perkin-Elmer 373).

RESULTS AND DISCUSSION

Experiments were performed to assess the influence of hydrodynamics as well as the pH of the aqueous phase on the overall mass transfer coefficient. Before the membrane contactor experiments, equilibrium conditions should be determined as a basic study for mass transfer calculations. Partition data were thus obtained using D2EHPA and D2EHTPA as extractants by varying the initial pH of the aqueous phase. The results obtained are presented in Table 1. The distribution ratio for the extraction with D2EHPA was found to be constant in the range of zinc concentration tested for each initial pH. On the other hand, the distribution ratio for the extraction with D2EHTPA is dependent on the solute concentrations at equilibrium. The functions listed in Table 1 were used in mass transfer calculations with the extractant D2EHTPA.

Table 1 Equilibrium data, at 298 K, for the systems under investigation. Initial aqueous phase: Zn=300 mg L'¹, pH=1.50-3.50, Na_2SO_4=20 g L'¹. Initial organic phase: 0.1 M D2EHPA or 0.1 M D2EHTPA in Shellsol T.

	pH=1.50	pH=2.00	pH=3.50
D2EHPA	distribution ratio 0.383	distribution ratio 2.11	distribution ratio 36.5
D2EHTPA	$[Zn]_{aq} = 1.83xlO^{-4}[Zn]^{\wedge}{}_{Ig} + 8.02xl0_^{3}[Zn]_{org}$	$[Zn]_{aq} = 3.58xl0^{-5}[Zn£_g + 1.67xlO^{-3}[Znl_{org}$	$[Zn]_{aq} = 1.94xlO^{-6}[Zn]^{\wedge} + 1.18xlO^{-4}[Znl_{OTg}$

To calculate the overall mass transfer coefficient, the variation of zinc concentration with the length of the hollow fibre module was taken into account. The set of equations describing the mass transfer in this type of process is published by González-Muñoz et al. [12], The differential equations related to the concentrations of zinc in both phases in the contactor were solved by the subroutine DBVPFD simultaneously with the ordinary differential equation of the aqueous phase tank by the subroutine DIVPAG, both from IMSL Math Library. The value of the overall mass transfer with respect to the aqueous phase coefficient was calculated from the experimental data by the least-squares method.

Figure 1 shows the effect of the flow rates on the extraction rate. The organic throughput, Q_{org}, was maintained at 310 mL min'¹ (Reynolds number=2.0) and the aqueous throughput was varied in the range of 155-600 mL min'¹ (Reynolds number=1.4-5.4). The organic throughput was then varied (Reynolds number=1.0-4.0) and maintaining the aqueous throughput, Q_{aq}, at « 300 mL min'¹ (Reynolds number=2.7). It is observed that increasing the aqueous flow rate slightly increased the extraction rate. The augment in the throughput of the organic phase did not influence the extraction rate. The overall mass transfer coefficient, K_{aq}, was evaluated to be 5.0x1 O'⁶ m s'¹ under those operating conditions. Thus, the resistance of mass transfer in the aqueous and organic phases had practically no contribution to the overall resistance of mass transfer. Thus, it is concluded that the transport of zinc should be dominated by the membrane phase resistance. It is worth mentioning that the chemical reaction between the extractant and the solute is assumed to be very fast at pH 3.5. The effect of the aqueous flow rate on the overall resistance was confirmed to be negligible using D2EHTPA as extractant. Since the equilibrium with D2EHTPA is more favoured than with D2EHPA, the diffusion in the organic layer is also not expected to play an important role in the overall transport process.

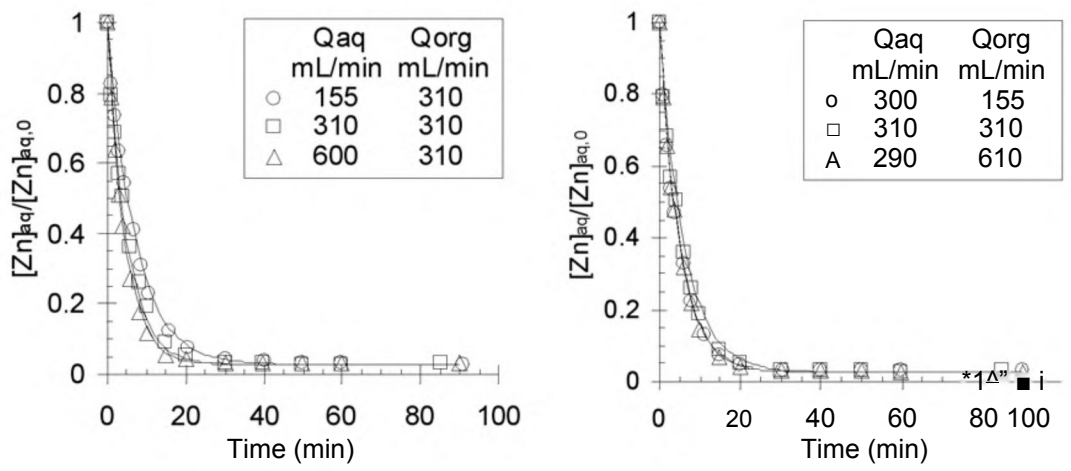


Figure 1- Influence of flow rates on the extraction rate of zinc with D2EHPA (one membrane contactor). Initial aqueous phase: Zn=300 mg L'\ pH=3.50, Na_2SO_4=20 g L'1. V_{aq}=V_{org}=1 L. Solid lines: calculated profiles with K_{aq}=5.0x10'6 m s'1 (aq: aqueous feed, org: organic phase).

Figure 2 depicts the effect of the initial pH on the extraction rate of zinc for both extractants. As expected, the overall mass transfer coefficient increased with pH and the values are higher for the system with D2EHTPA. This latter ion exchanger is more acidic than the other due to the sulphur atom, which is less electronegative than oxygen. Thus, according to the hard-soft acid-base principle [20], the extraction of the soft acid Zn^{2+} will be favoured with D2EHTPA. Thus, the membrane phase resistance decreases with the substitution of oxygen by sulphur in that alkylphosphoric acid. As presented in Figure 2, the overall mass transfer coefficient is very high for the extraction with D2EHTPA, even at pH 1.5. Nevertheless, at this low value of pH, the extraction reaction resistance might contribute to the overall resistance of mass transfer.

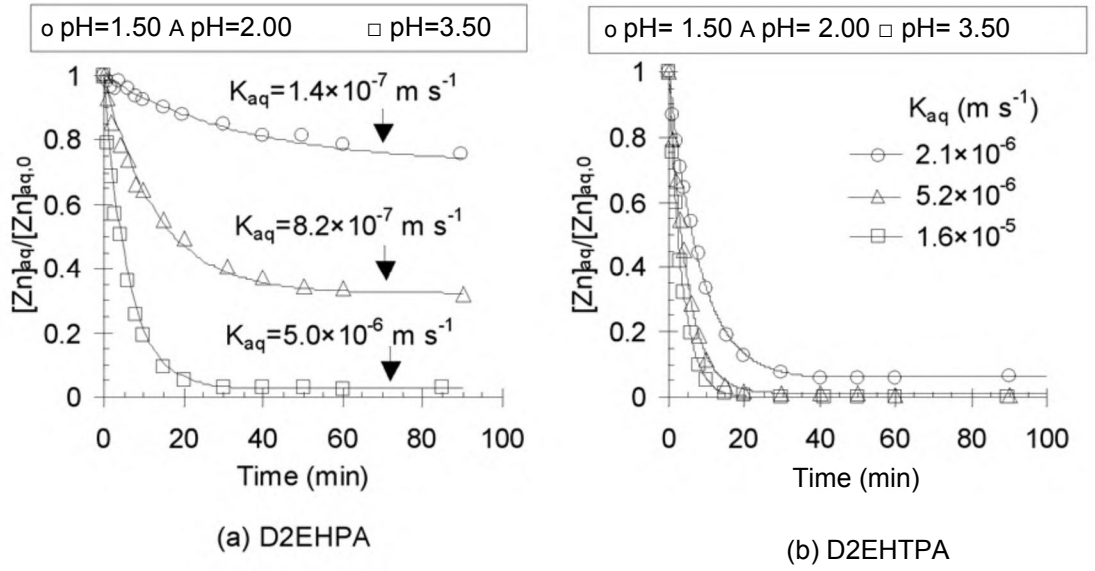
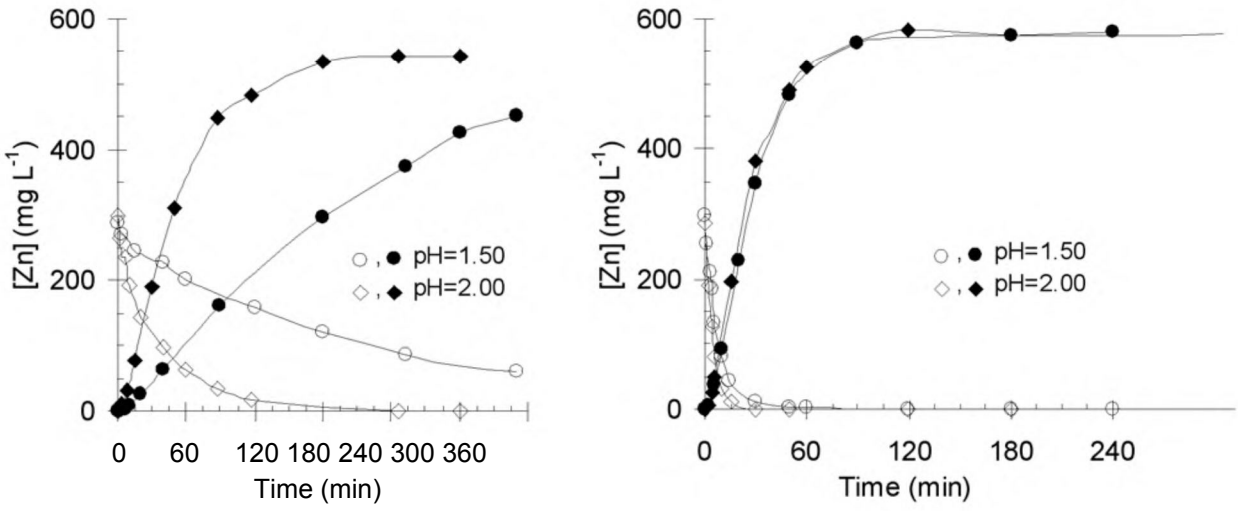


Figure 2- Influence of the initial phi and extractant on the extraction rate of zinc using one membrane contactor. Initial aqueous phase: Zn=300 mg L'1, pH=1.50-3.50, Na_2SO_4=20 g L'1. V_{aq}=V_{0f}g=1 L, Q_{aq}=Q_{org}=310 mL min'1. Solid lines represent calculated profiles.

In an integrated extraction-stripping process, zinc is extracted to the organic phase and is simultaneously transferred to a stripping solution, using two contactors. This scheme permits continuous regeneration of the organic phase and if the volumetric ratios are properly adjusted, a stripping solution with a high content of zinc may be attained. Figure 3 presents the aqueous concentration profiles obtained with simultaneous extraction and stripping experiments, at pH 1.5 and pH 2.0. Values of zinc recovery and the concentration ratio reached in several experiments are summarised in Table 2. As observed in Figure 3, the kinetics is faster using D2EHTPA as extractant. Moreover, at pH 1.5, only this extractant allowed obtaining satisfactory results. The extraction of zinc attained 99.9% and the recovery exceeded 97%. The extraction and recovery of zinc with D2EHPA were low as 80% and 75%, respectively, after 5 h of operation. At pH 2.0, the use of D2EHPA led to 99.8% of extraction for a concentration ratio of 1.8 being the results closer to the ones with D2EHTPA. As presented in Table 2, concentration ratios of about 18-fold with 90% recovery were obtained for both extractants at pH 2.0 by varying the volume ratio of feed phase to stripping phase, V_{aq}/V_s.



(a) D2EHPA (b) D2EHTPA

Figure 3- Zinc concentration vs time during simultaneous extraction and stripping runs. Feed phase (o,), *stripping phase* (•,♦). *Initial aqueous phase: Zn=300 mg L'¹, pH=1.50, 2.00, Na_2SO_4=20 g L'¹. $V_{aq}=V_{org}$=1 L, V_s=0.5 L, $Q_{aq}=Q_s$=310 mL min'¹, Q_{org}=300 mL min'¹ (aq: aqueous feed phase, org: organic phase, s: aqueous stripping phase).*

Table 2 Zinc recovery and concentration ratio reached in simultaneous extraction and stripping stages using two hollow fibre contactors. Initial aqueous phase: Zn=300 mg L'¹, pH=2.00, Na_2SO_4=20 g L'¹. $V_{aq}=V_{ol}$g=1 L, V_s=0.5 L, $Q_{aq}=Q_s$=310 mL min'¹, Q_o^=300 mL min'¹.

	Extractant D2EHPA		Extractant D2EHTPA	
v_{aq}/v_s	Recovery (%)	Concentration ratio	Recovery (%)	Concentration ratio
2	91.7	1.8	97.0	1.9
8	87.0	7.0	93.8	7.5
20	87.3	17.5	92.4	18.5

Finally the ELM separation technique was applied to compare the performance of other membrane-based process. Table 3 shows the results obtained using D2EHPA and D2EHTPA as extractants. It is observed that the concentration in the raffinate increased with

permeation time above 2-3 min. This is because of the occurrence of non-ideal phenomena, such as water transport and leakage of the internal stripping phase to the feed phase. These deleterious phenomena reduce the efficiency of the process and must be minimised. High recoveries were therefore obtained after 3 min of permeation, which could be further optimised. The recovery of zinc with the ELM tests is similar to that obtained in hollow fibre modules. The difference between the two processes is mainly due to the kinetics. For instance, the fluxes of zinc were evaluated for the ELM experiments by measuring the Sauter

Table 3 Results of the experiments with emulsion liquid membranes. Initial aqueous phase: Zn=300 mg L'¹, pH=2.00, Na_2SO_4=20 g L'¹ ($V_{aq}A/_s$=20, V_{org}/V_s-2, $V_{aq+o}g_{+s}$=1 L; aq: aqueous feed phase, org: organic phase, s: aqueous stripping phase)

Extractant	$[Zn]_{aq}$ (mg L'¹)					$[Zn]_s$ (9 L'¹)	Recovery (%)	Concentration ratio
	60 s	120 s	180 s	360 s	600 s	180 s		
D2EHPA	49.0	11.5	6.8	70.0	116	5.25	87.5	17.5
D2EHTPA	4.1	2.6	10.0	38.0	56.0	5.20	86.7	17.3

mean diameter of the emulsion globules (0.46 and 0.48 mm for D2EHPA and D2EHTPA, respectively). It was found that the average flux of extraction during the first minute is about one order magnitude higher than the one obtained in hollow fibres module. This is mainly because of the additional mass transfer resistance offered by the pores of the membrane, which is the most important drawback of those contactors [10,12], However, the results show that hollow fibres are adequate to the systems studied and allow obtaining a very low content of zinc in the raffinate besides concentrating.

CONCLUSIONS

The use of hydrophobic hollow fibre modules showed to be adequate for the extraction and stripping of zinc with the extractants D2EHPA and D2EHTPA. Concentration ratios of about 18-fold with 90% recovery were obtained in simultaneous extraction and stripping stages. The use of D2EHTPA is more promising because of its higher acidity and faster kinetics. The recovery and concentration ratios obtained in the tests with emulsion liquid membranes were similar, regardless the occurrence of non-ideal phenomena.

ACKNOWLEDGEMENTS

This work was conducted in the “Centro de Processos Quimicos do 1ST” (“Centre for Chemical Processes”), Instituto Superior Tecnico (1ST), Technical University of Lisbon (UTL), Portugal. Financial support of the equipment (hollow fibre modules) by Fundapão para a Ciência e a Tecnologia (FCT, Portugal) with European Community (FEDER) and national funds is gratefully acknowledged. Eng. Ondina M. de Freitas is thanked for her help in part of the experimental work. We also thank Eng. Remigio Machado for fruitful discussions.

REFERENCES

1. C.I. Sainz-Diaz, H. Klocker, R. Marr and H.-J. Bart (1996), *Hydrometallurgy,* 42, 1-11.

2. H. Klocker, H.-J. Bart, R. Marr and H. Mullër (1997) *AlChE J.,* 43 (10), 2479-2487.
3. M. Mörters and H.-J. Bart (2000), *J. Chem. Eng. Data,* 45, 82-85.
4. M.B. Mansur, M.J. Slater and E.C. Biscaia Jr. (2002), *Hydrometallurgy,* 63 (2), 117-126.
5. R.-S. Juang and H.-L. Huang (2002), *J. Memb. Sci.,* 208, 31-38.
6. A. Gabelman and S.T. Huang (1999), *J. Memb.* Sci., 159, 61-106.
7. A. Alonso, A. Urtiaga, A. Irabien and I. Ortiz (1994), *Chem. Eng. Sci.,* 49 (6), 901-909.
8. I. Ortiz, B. Galan, F.S. Roman and R. Ibanez (2001), *AlChE J.,* 47, 895-905.
9. J. Haddaoui, D. Trébouet, J.M. Loureiro and M. Burgard (2004), *Sep. Sci Technol.,* 39 (16), 3839-3858.
10. M. Rodrigues, R.M.C. Viegas, S. Luque, I.M. Coelhoso, J.P.S.G. Crespo and J.R. Alvarez (1998), J. *Memb. Sci.,* 137, 45-53.
11. W. Cichy, S. Schlosser and J. Szymanowski (2001), *Solv. Extraction and Ion Exchange,* 19, 905-923.
12. M.J. González-Muñoz, S. Luque, J.R. Alvarez and J. Coca (2003), *J. Memb. Sci.,* 213, 181-193.
13. R. Prasad and K.K. Sirkar (1989), *J. Memb. Sci.,* 47 (3), 235-259.
14. I.M. Coelhoso, P. Silvestre, R.M.C. Viegas, J.P.S.G. Crespo and M.J.T. Carrondo (1997), *J. Memb. Sci.,* 134 (1), 19-32.
15. M.M. Cardoso, R.M.C. Viegas and J.P.S.G. Crespo (1999), *J. Memb. Sci.,* 156, 303-319.
16. H.-J. Bart, R. Marr, J. Draxler and J. Hartl (1990), *Chem. Eng. Technol.,* 13, 313-318.
17. J. Draxler and R. Marr (1990), Poc. *ISEC'*90, 37-48.
18. W.S.W. Ho and N.N. Li, in Membrane Handbook, Eds. W.S.Winston Ho, K.K. Sirkar, *Van Nostrand Reinhold,* New York, 1992, 597-610.
19. M.T.A. Reis and J.M.R. Carvalho (2004), *J. Memb. Sci.,* 237, 97-107.
20. Choppin G.R., in Principles and Practices of Solvent Extraction, Eds. J. Rydberg, C. Musikas, G.R. Choppin, Dekker Inc: New York, 1992, 88-91.

STUDY OF PARAMETERS IMPORTANT IN THE PROCESS OF BIOSORPTION TO THE REMOVAL OF HEAVY METALS

Albina da Silva Moreira*, Julio Nandenha, Marcia Maria Lima Duarte and Gorete Ribeiro de Macedo

*UFRN - Dept, de Engenharia Quimica - PPGEQ/NT - Natal - RN - Brasil - 59072-970
('E-mail: albina@eq.ufrn.br)

The increase of the concern with the ambient question and of the severity of the legislation in the discarding of industrial and domestic containing metals has motivated the inquiry of new technologies for the recovery and metal removal. The removal of you put heavy for microbial biomass has been investigated as an alternative to the traditional methods. Thus it was studied removal of metals has copper and iron of discarded lubricating oil having used as biosorbent the seaweed Sargassum sp

INTRODUCTION

The capacity of certain microorganisms to concentrate metals well is known. However during the last decades only it is that the microorganisms are being used as an alternative for the removal and metal. The term "biosorption" is defined as a process in which solids of natural origin or its derivatives are used in the metal retention heavy of a watery environment [1], The biosorption process already is being studied in watery systems, therefore, the interest in studying the metal removal appeared heavy of organic systems using used lubricating oil

A factor that has stimulated research of new biosorbents materials from help biomasses is its great availability. Although thousands of seaweed species have been identified during last the 200 years, much little has been investigated to determine its relative ability to hold back ions metallic toxics [2],

In the present work the used automotive oil of a fleet of bus of the city of Natal -RN-Brazil was chosen, after that this oil with the objective was characterized to characterize and to quantify metals heavy gifts. The metals Fe and Cu had been study object. For the biosorption process it was used the seaweed Sargassum sp. Studied the effect of the protonation in the seaweed aiming at to improve the efficiency of removal of these metals. The time of contact between oil was determined and necessary biomass so that the balance between the phases was reached and the influence of the amount of biomass was finally studied.

MATERIALS AND METHODS

The used automotive lubricating oil, Rimula-D-Shell SAE 40, **was kindly provided by a bus fleet from Natal- Rio Grande do Norte - Brazil,** was used in the present study

Biosorbent used was the seaweed *Sargassum* sp., collected in the Areia Preta beach in the city of Natal -RN-Brazil, during the April month.

Characterization of the lubricating oil with relationship to the presence of heavy metals

A sample of the oil was characterized its burned and after that acidified until complete solubilization of ashes. It was characterized by flame atomic absorption spectroscopy (FAAS), using a Spectrometer Varian AA 12/1475 Gemin, in order to determine which heavy metals were present and their concentrations.

Biosorbent

The seaweed Sargassum sp. was collected at Mãe Luiza beach to be used as biosorbent. It was applied in two different conditions: protonated and non-protonated. The protonation was made with the purpose to remove metals such as Na, Ca and Mg from its structure cell. It was carried out by washing 15 g of dried seaweed (60 °C - 12h) in 400 mL of 0.06 M HCl solution during 3 hours, under agitation and at room temperature. After that, the seaweed sample was thoroughly washed with distilled water until the pH of the wash solution reached 4.5 and then dried again at 60° C during 12 hours. After drying, the sample was powdered using mortar and pestle and stored in a hermetic container to avoid its contact with air because it is a highly hygroscopic material.

Study of kinetic and the effect of the amount of biomass

The evaluation of kinetic of biosorption of the iron and copper by the biomass *Sargassum* sp. Was performed in erlenmeyer flasks of 1000 mL containing 500 mL of discarded lubricating-oil and about 0,5 g of biomass. The biomass was put in contact with the lubricating-oil and agitated at 150 rpm in a rotational shaker. The oil samples were taken in different time intervals, vacuum filtered using quantitative filter of 12,5 cm <j> - pore 8 pm and analyzed to the concentration of copper and iron by atomic absorption spectrometry.

The same conditions were used to the biosorbent protonated and non-protonated. All experiments were perfomed in duplicate and the average was used in the analysis of the results.

The sorption experiments to evaluate the effect of biomass amount in the biosorption efficiency were performed in erlenmeyer flasks of 1000 mL. In each flask, a certain quantity of biomass, varying between 0,2 a 5 g, was contacted with 500 mL of used lubricating-oil and was agitated during 10 hours at 150 rpm in a rotational shaker.

Figure 1 illustrates the used experimental procedure for the biosorption process

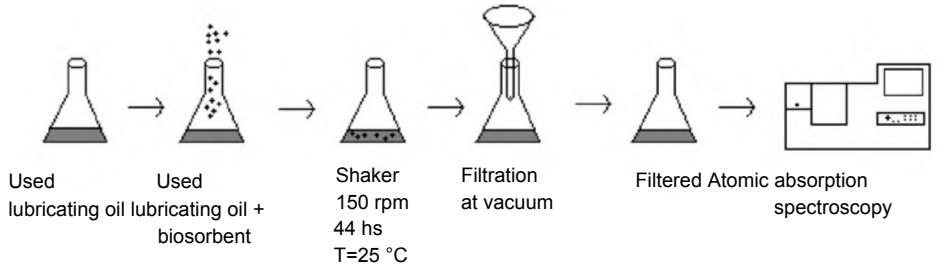


Figure 1. Experimental system for the process of biosorption of used lubricating oil.

RESULTS AND DISCUSSIONS

The data of the characterization of the used automotive oil, with the identification of the present metals and its respective concentrations are presented in Table 1.

Table 1. Characterization of the used lubricating oil how much to the presence.

Element	Concentration (ppm)
Fe	43,95
Cu	3,75

The data of the assays of biosorption with biosorbent protonated and *in natura*, in order to verify its efficiency in the removal of metals heavy presents in the oil, are presented in Tables 2 and 3.

Table 2. Concentration of the metals after the biosorption process (biosorbent protonated).

Element	Concentration(ppm)	Removal (%)
Fe	27,45	37,54
Cu	2,56	31,53

Table 3. Concentration of the metals after the biosorption process (biosorbent in natura).

Element	Concentration (ppm)	Removal %
Fe	33,70	23,32
Cu	2,95	21,33

The kinetic study of the process of removal of the iron and copper for the *Sargassum* sp. was carried through with the intention of if observing the evolution of the process until the system to reach the balance and thus to establish the necessary. The assays had been carried through in rotational shaker the 25 °C and 150 rpm using 0,5 g of biosorbent and 500 mL of used lubricative oil. The biosorption of the iron in function of the time is presented in Figure 2, in which the concentration of the iron mentions the phase to it oil

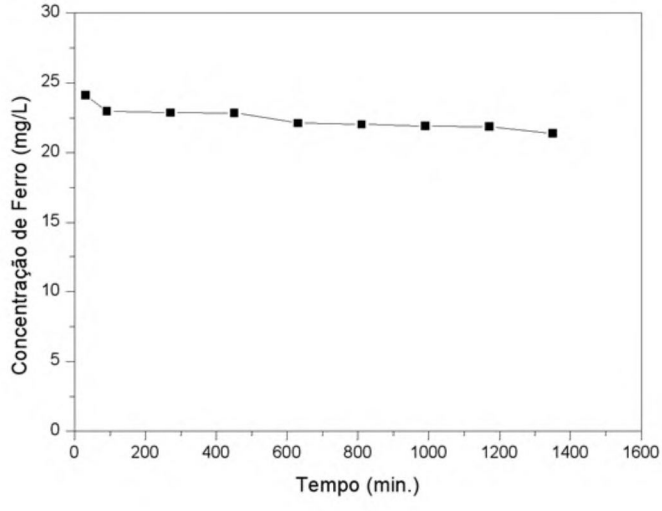


Figure 2. Kinetic of biosorption of the Iron for the Sargassum sp.

The concentration of the iron in the oil diminishes meaning that the biosorption increases with the contact time and reaches the balance after approximately 10 hours. The necessary

time so that the balance between the phases is reached is function of some factors, between them the type of biomass (amount and types of involved active small farms in the biosorption), size and form of the biomass (active or inactive, it exempts or immobilized), beyond the involved material in the biosorption system.
The biosorption of copper in function of the time was carried through in the same conditions that the biosrption of the iron and is presented in the illustration Figure 3

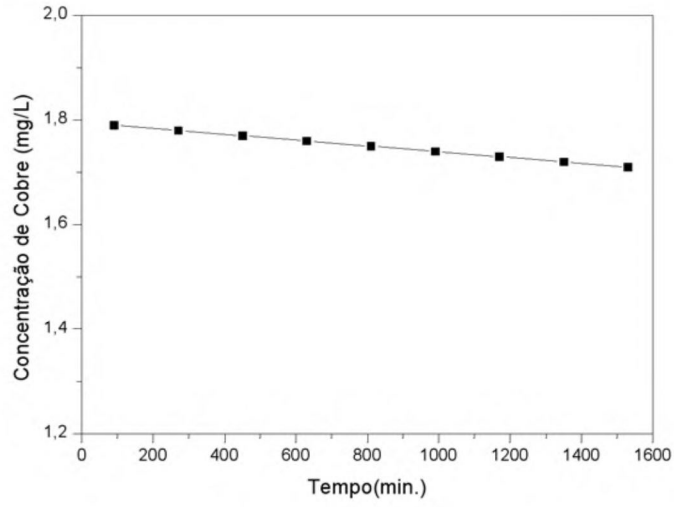


Figure 3. Kinetic of biosorption of the Copper for the Sargassum sp.

The concentration of copper in the oil diminishes meaning that the biosorption increases with the contact time, however in the studied conditions is not obtained to need a point where the balance was reached.

For the determination of the influence of the amount of biomass in the process of biosorption of the iron and copper for the *Sargassum* sp. had been carried through assays in rotational shaker (25 °C and 1500 rpm) using a time of contact among the phases of 10 hours with the oil used lubricating. The results obtained for these experiments are shown in the Illustrations 4 and 5..

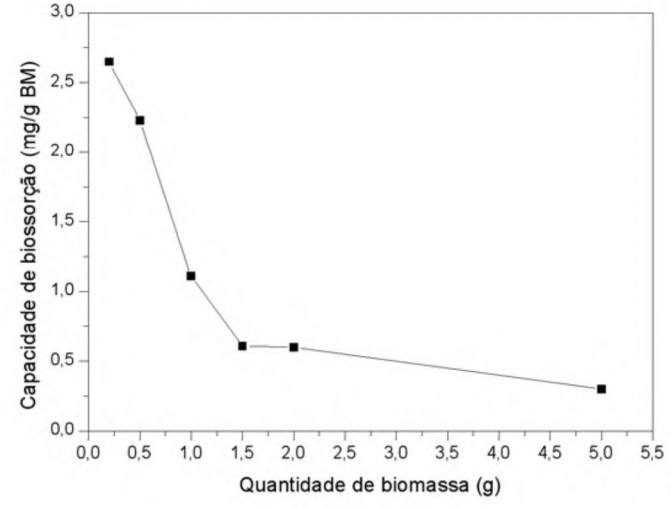


Figure 4. Biosorption of the Iron in function of the amount of biomass

For the analysis of Figure 4 it is observed that it has a decrease of the capacity of sorption of the iron to the measure that if increases the amount of biomass, probably in result of the interfacial area of contact when works with bigger amount of biomass.

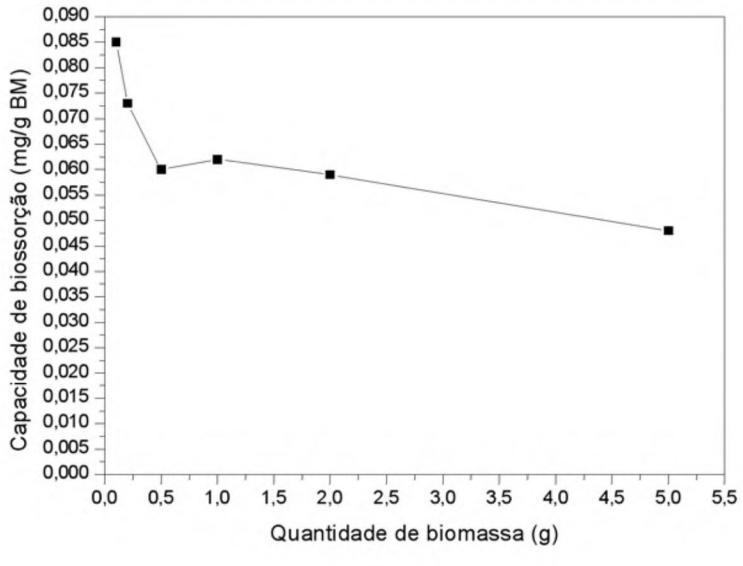


Figure 5. Biosorption of Copper in function of the amount of biomass *biomass*

The figure 5 shows a decrease in the sorption capacity of copper when the amount of biomass is increased.

CONCLUSIONS

The biosorbent *Sargasum* sp, abundat in our area, was shown efficient in the process of removal of these metals. The protonated seaweed was more efficient in the removal of Fe and Cu.

The biosorption kinectics of iron by *Sargassum* sp. is relatively fast. The contact time of 10 hours was enough to reach the equilibrium. The biosorption kinectics of copper was more fast, however, the equilibrium was not viewed.

It was observed a decrease in the biosorption capacity of the metals studied when the biomass amount was increased.

ACKNOWLEDGEMENTS

The authors would like to thank National Petroleum Agency - Brazil (ANP) for their financial and support to carry out this work.

REFERENCES

1. T. R. Muraleedharan, L. Iyengar and C. Venkobachar (1991), Biosorption: an attractive alternative for metal removal and recovery. *Current Scienc.,* v.61, n.6,379-385.

2. G. Qetinkaya, Z. Donmez, Z. Aksu, A. Ozturk, and T. Kutsal (1986b), A comparative study on heavy metal biosorption characteristics of some algae. *Process Biochem.,* v.34, 885-892.
3. A. M. Hayashi (2001), Remogao de cromo hexavalente através do processo de biosorption em algas marinhas. Tese (Doutorado). Universidade Estadual de Campinas. Faculdade de Engenharia Quimica, Unicamp, Campinas, SP, Brasil.



Separation Propionic Acid/Acetic Acid with Basic Polymeric Sorbents

Shaokai Huang, Wei Qin*and Youyuan Dai
State Key Laboratory of Chemical Engineering, Department of Chemical Engineering,
Tsinghua University, Beijing 100084, China

Propionic acid is an important carboxylic acid applied in pharmaceutical, pesticide and foodstuff. During recovery of product propionic acid from the fermentatiOon broths, it is important to maximize the selectivity for the desired acid to the additive acetic acid. In this work, three types of weakly basic resins, D301R, D301G, D392 and one neutral phosphine resin, TBP resin, were selected as the adsorbents, the uptakes of single component of propionic acid and acetic acid, as well as competitive uptakes of propionic acid and acetic acid have been measured. The dependence of pH values on the adsorption equilibrium was studied also. The results showed that Langmuir equation could be used to describe the sorption isotherms for both single carboxylic component (propionic acid and acetic acid) and two components of propionic and acetic acid. Despite of low uptake capacity, TBP resin gives a higher selectivity in the pH 3~5 range than D301R, D301G and D392.
Key Words: propionic acid, acetic acid, weakly basic resin, composite uptake

INTRODUCTION

Carboxylic acids are readily made by fermentation and are among the most attractive substances that can be manufactured from biomass.[1,2] Recovery of carboxylic acids from fermentation broths presents a challenging separation problem. Historically, the conventional technique for recovering nonvolatile carboxylic acids from aqueous solutions has been precipitation of the calcium carboxylate salt, e.g. citric and lactic acids.[3] The major disadvantage of the calcium carboxylate salt process, however, is that for every mole of carboxylic acid produced, 1 mol each of an acid (e.g., sulfuric acid) and the calcium base are consumed, and 1 mol of waste calcium salt (e.g., calcium sulfate) is created. This calcium sulfate poses a major disposal problem, especially as environmental controls tighten.

Methods of recovery that utilize reversible chemical complexation with polymeric sorbents, that are selective for carboxylic acids are attractive.[4"6] Important characteristics of solid sorbents are a high capacity and selectivity for the acid, and depending upon the process configuration, biocompatibility with microorganisms. Many fermentation processes, e.g. propionic acid, are subject to end-product inhibition. If a solid sorbent can be used *in situ,* higher overall yields can be achieved.

For most separation techniques, the mass transfer driving force is the concentration of the

---

*Corresponding author, E-mail: qinwei@tsinghua.edu.cn .
Fax: +86 10 62770304.
Tel: +86 10 62782748

unionized form of the acid.[7'10] Many fermentation producing carboxylic acids operate most effectively at pH above $pK_a$of the acid product, [11-13] e.g., propionic acid (pK_a=4.87), is typically produced at pH 4-5.[14] One approach for recovering carboxylic acids from such solutions is to use agents that are sufficiently basic sorbent to retain a substantial capacity at several pH units above the pK_a of the carboxylic acid, and was strongly dependent upon the basicity and capacity of the agent. [5"6,15'16]

Propionic acid and acetic acid, the most important chemicals intermediate, are widely used for manufacturing medicine, pesticide and foodstuff, [17] and can be produced by fermentation and chemical synthesis.[14,18'1&] In this work, three types of weakly basic resins, D301R, D301G, D392 and one neutral phosphine resin, TBP resin, were selected as the adsorbents, the uptakes of single component of propionic acid and acetic acid, as well as competitive uptakes of propionic acid and acetic acid have been measured. The dependence of pH values on the adsorption equilibrium was studied also.

EXPERIMENTAL

Four types of sorbents are washed successively with water, methanol, NaOH solution (5%), and HCI solution (5%), and then dried to the constant weight in a vacuum oven at 60”C and 60 kPa. All four sorbents were initially in the dry form, and their properties are listed in Table 1.

Table 1. The Properties of Sorbents

properties	D301R	D301G	D392	TBP
functional group	$-N(CH_3)_2$	$-N(CH_3)_2$	$-NH_2$	TBP
particle diameter (mm)	0.315-1.25	0.6-1.6	0.315-1.25	0.105-0.245
porosity (mL/mL)	0.45	0.55	0.45	0.40

Propionic acid and acetic acid (Arcros Corp.) were analytical reagents and were used to prepare the aqueous solutions of various concentrations.

Sorption isotherms for propionic acid and acetic acid onto various sorbents were conducted in 20 mL flask sealed with foil-line caps. The sorbent (typically 0.25g, 0.5g, I .Og, dry basis) and acid solutions (typically 10ml) were added to a flask without or with adjustment of the solution pH by NaOH or H_2S0_4 solution. The flask was shake for about 4 h in a shaker bath with a vibration rate of 120 rpm, which was demonstrated to be at equilibrium by preliminary tests. The aqueous solution was separated with the sorbents by a vacuum filtration, an aqueous phase sample was taken for pH and solute concentration (C) analyses, and the impregnate sorbents sample was obtained for weighting.

The aqueous samples were analyzed for solute concentration by using a high- performance liquid chromatography (HPLC) system (Waters), with each measurement being performed in duplicate, and the pH value of the solution was measured with an Orion Model 601A pH-meter.

THEORY

Langmuir Model

Adsorption of carboxylic acids onto basic polymeric sorbents occurs by the formation of complexes between undissociated acid molecules and functional group on the sorbent. Assuming that only (1,1) stoichiometric acid- functional group complexes exist, the Langmuir isotherm is described mathematically as

$$\frac{Q}{Q_m} = \frac{KC}{\text{i+^c}} \qquad \text{(D}$$

Where Q (mmol/g) represents the uptake of the acid, Q_m (mmol/g) represents the acid adsorption capacity of the sorbent for monolayer coverage. K (L/mol) is the apparent sorption equilibrium constant, and C (mol/L) is the concentration of the acid in the aqueous phase.

When more than one acid is present in solution, the resulting adsorbed phase will consist of free basic sites and complexes for each acid. The relative amounts of each of these species will depend on the apparent equilibrium constants for adsorption of each acid, with competition between the acids for the functional group. Assuming independent 1:1 complexation, a competitive Langmuir adsorption isotherm for each acid result:

$$\frac{Q_i}{Q_m} = \frac{K_i C_i}{1 + KC_{i\ i}} \qquad (2)$$

The Values of Q_m and Ki for each acid can be obtained from a nonlinear least-squares fit of the experimental data for single-acid adsorption to eq (1), and then these Kj and Q_m were used to verify the feasibility and reasonability of predicting adsorption equilibria for multiple-acid adsorption using single-acid adsorption data.

RESULTS AND DISCUSSION

Equilibrium Behavior for Single-Acid Adsorption Isotherms

Figure 1-2 show adsorption isotherms for acetic and propionic acid onto the four polymeric sorbents at 25”C. The data of carboxylic acid adsorption isotherms were fitted to the Langmuir model using a nonlinear least-squares regression to determine the best fitting values of Q_m and K, the fitting results were listed in Table 2, and the predicting adsorption isotherms shown in the Fig. 1-2 in line also. For amine adsorbent, D301R, D301G and D392, the lines was approach to the experimental data, i.e., Langmuir model can be used to describe the adsorption isotherms for acetic and propionic acid very well. For the TBP adsorbent, the predict line on basis of Langmuir model is nearly a beeline, fitting to the experimental data very well at the low acid concentration in the aqueous phase (< 0.5 mol/L). In comparison, the apparent equilibrium constant K for both acids were D301G D301R >D392>TBP.

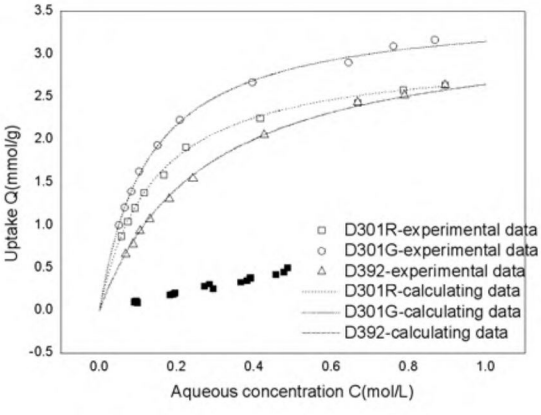


Figure. 1 Composite sorption isotherm for acetic acid onto sorbnts at 25°C

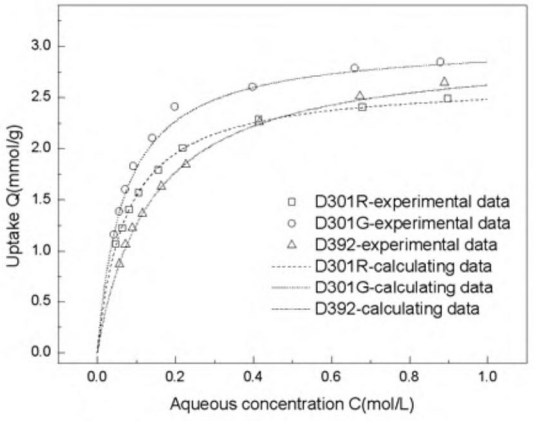


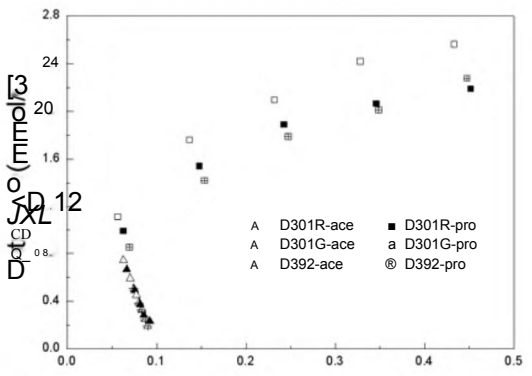
Figure.2 Composite sorption isotherm for propionic acid onto sorbents at 25°C

Table 2. The Fitted Parameters of Sorption and Extraction

	Acetic acid				Propionic acid			
	D301R	D301G	D392	TBP	D301R	D301G	D392	TBP
Qm	3.03	3.54	3.36	2.5	2.66	3.04	2.98	2.2
K,i	7.30	8.00	3.71	0.46	13.78	14.66	7.28	1.51

Equilibrium Behavior for Multiple-Acid Adsorption Isotherms

Figure 3-4 show the experimental isotherm for acetic acid/propionic acid onto four polymeric sorbents at 25°C. With increasing the acid concentration, the uptakes of propionic acid increase, but the uptakes of acetic acid decrease, which resulted from the competitive adsorption between acetic acid and propionic acid. When the solute consists of acetic and propionic acid, propionic acid is adsorbed preferentially from the mixtures as propionic acid, being the more hydrophilic acid, has a lower aqueous-phase activity coefficient than acetic acid. With the uptake of propionic acid increasing, more of the functional groups are occupied by propionic acid, making less sites available for acetic acid to be adsorbed, then, the uptake of acetic acid decrease.



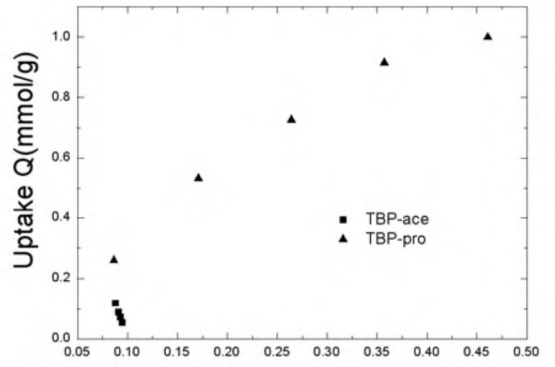
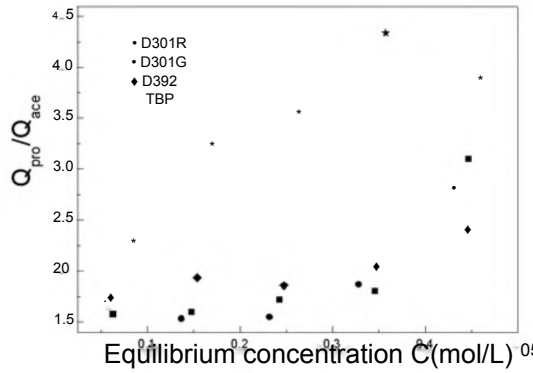


Figure 3 Competitive sorption isotherms for acetic/propionic acid onto D301R, D301G, D392 at 25 "C

Figure 4 Competitive sorption isotherms for acetic/propionic acid onto TBP at 25°C

The selectivity is compared between acetic acid and propionic acid of four resins in Figure 5. The results show the selectivity of TBP is better than that of other three amine resins, therefore, TBP resin is fitter to separate acetic acid/ propionic acid than relatively strong basic resin, D301R, D301G and D392.

Using the fitted parameter of Kiand Q_m for single acid, the typical predicted isotherms by the competitive Langmuir model with the experimental data for uptake of acetic acid/propionic acid onto TBP resin was shown in Figure 6, and the predicted curves superimpose the experiment data very well. Thus, it is believable to predict the uptake value for multiple-acid with the fitted parameters obtained from single acid system.



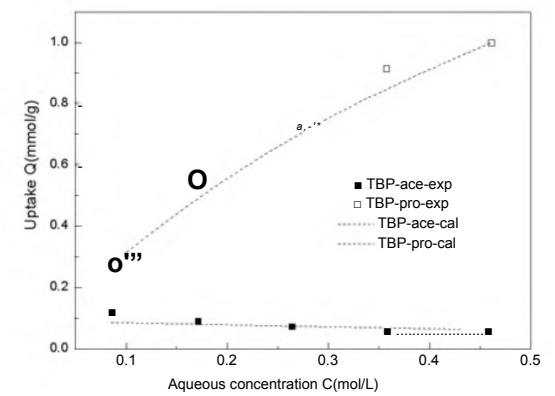


Figure 5 the selectivity between acetic acid/propionic acid of D301R, D301G, D392 and TBP at 25"C

Figure 6 the prediction isotherm for acetic acid/propionic acid onto TBP at 25”C

Effect of pH for Adsorption of Single Acid

TBP associate most Lewis acid functional groups from the aqueous phase by forming a complex with the neutral molecule. Because the undissociated acid concentrations are functions of pH, the uptake of the two acids will greatly depend on the pH of the aqueous phase. As is already shown in Fig. 7, the uptake of acetic acid or propionic acid with the TBP resin is greatly affected by the pH. The uptake value decreased with an increase in the pH value.

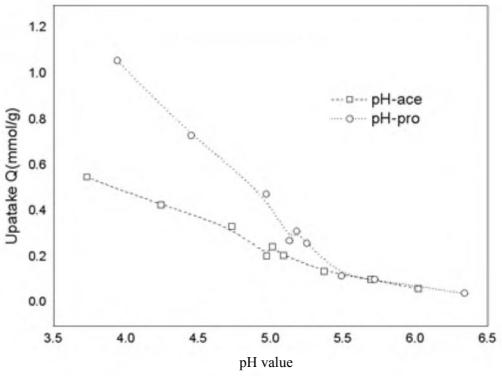


Figure **7** Effect of pH on composite uptakes of acetic and propionic acid onto TBP **(C_{0a}ce=0.5577** mol/L; **Co_{pro}=0.4712** mol/L; **$W_{0/m}$=20** ml_/g)

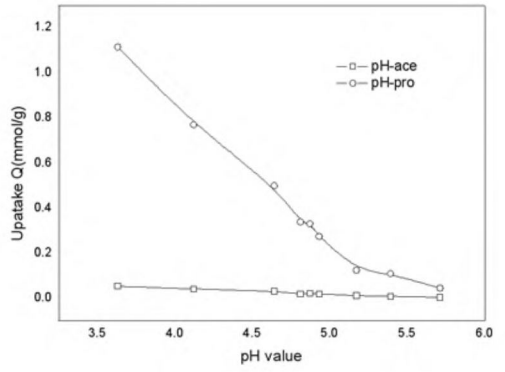


Figure 8 Uptake-pH isotherm for adsorption of acetic acid/propionic acid onto TBP from mixture **(C_{0ace}=0.5577** mol/L; **C_{0p}ro=0.4712** mol/L; **$W_{o/m}$=20** mL/g)

Effect of pH for Adsorption of Multiple-Acid

Figure 8 shows the uptake-pH isotherms for adsorption of acetic and propionic acid onto TBP resin from an aqueous acid mixture at 25 °C. With increasing solution pH, the acetic and propionic acid uptake isotherms decrease. This result is consistent with the idea that acid uptake is through adsorption of the undissociated forms of the acids. This fact is attributable to the pK_a of acetic acid being about equal to that of propionic acid. As the pH rises above the pK_a of acetic acid, the concentration of undissociated acetic acid and propionic acid decrease, and the uptake of acetic acid decrease accordingly as well as propionic acid.

Figure 9 shows the pH influence upon the selectivity of the TBP resin between acetic and propionic acid. The selectivity P_{pro}/aceOf propionic acid to acetic acid decrease with increasing pH. The result show lower pH has an advantage for separating the mixture of acetic and propionic acid.

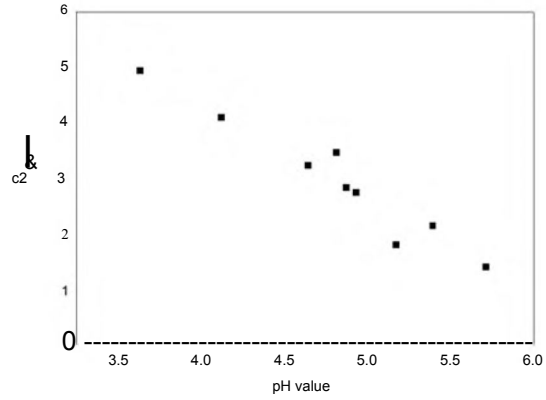


Figure.9 Selectivity-pH isotherm for adsorption of acetic acid/propionic acid onto TBP **(C_{0a}ce=0.5577** mol/L; **C_{0p}ro=0.4712** mol/L; **$W_{0/m}$=20** mL/g)

CONCLUSIONS

The experiments for uptake single and binary systems of acetic acid and propionic acid were conducted. The adsorption isotherms of single systems were fitted to the Langmuir model using a nonlinear least-squares regression. The ability to adsorb organic acids is in the order DSOIG^DSOI R>D392>TBP. However, TBP was fitter to separate propionic acid and acetic

acid. And it is feasible to predict the adsorption isotherms of binary system to use the fitted parameter of single system and competitive Langmuir model.
Furthermore, the influence of ph value of the aqueous solute upon the uptake and selectivity of TBP resin were investigated. The results show that low pH has an advantage for separating the mixture of acetic and propionic acid.

ACKNOWLEDGMENTS

This research was supported by the State Key Lab of Chemical Engineering, Tsinghua University, Beijing, China.

REFERENCES

[1] T.K. Ng, R.M. Busche, K.C. McDonald, R.W.F. Hardy, *Production of Feedstock Chemicals, Science.* 219(1983) 733-740.

[2] M.K. Jain, R. Datta, J.G. Zeikus, High-Value Organic Acids Fermentation-Emerging Processand Products, in: T.K. Ghose(Ed.), Bioprocess Engineering: The first Generation, Ellis Horwood Limitd, Chichester, 1989, pp. 366-389.

[3] R. Datta, Hydroxycarboxylic Acids, in: I. Kroschwitz, M. Howe-Grant(Eds.), Kirk-Othmer Encyclopedia of Chemical Technology, Vol. 13, John Wiley & Sons, New York, 1995, pp. 1042-1062.

[4] C.J. King, Separation Process Based on Reversible Chemical Complexation, in: R.W. Rousseau(Ed.), Handbook of Separation Process Technology, Wiley, New York, 1987, pp. 760-764.

[5] L.A. Tung, C.J. King, Sorption and Extraction of Lactic and Succinic Acids at pH>pKa1. I. Factors Governing Equilibria, Ind. Eng. *Chem. Res.* 33(1994) 3217-3223.

[6] R.L. Evangelista, A.J. Mangold, Z.L. Nikolov, Recovery of Lactic Acid by Sorption , Appl. Biochem. *Biotechnol.* 45/46(1994) 131-144.

[7] A.S. Kertes, C.J. King, Extraction Chemistry of Fermentation Product Carboxylic Acids, Biotechnol. *Bioeng.* 28(1986) 269-282.

[8] J.A. Tamada, A.S. Kertes, C.J. King, Extraction of Carboxylic Acids with Amine Extractants. I Equilibria and Law-of-Mass-Action Modeling, Ind. Eng. *Chem. Res.* 29(1990) 1319-1326.

[9] J.A. Tamada, C.J. King, Extraction of Carboxylic Acids with Amine Extractants. II Chemical Interactions and Interpretation of Data, Ind. Eng. *Chem. Res.* 29(1990) 1327-1333.

[10] J.A. Tamada, C.J. King, Extraction of Carboxylic Acids with Amine Extractants. III Effect of Temperature, *Water Co-Extraction and Process Considerations, Ind. Eng. Chem. Res.* 29(1990) 1333-1338.

[11] F.W. Getzen, T.M. Ward, A Model for the Adsorption of Weak Electrolytes on Solids as a Function of pH. 1. Carboxylic Acid-Charcoal Systems, J. *Colloid Interface* Sci. 31(1969) 441-451.

[12] R.L. Gustafson, H.F. Filius, R. Kunin, Basicities of Weak Base Ion Exchange Resins, *Ind. Eng. Chem. Fundam.* 9(1970) 221-229.

[13] M.H. Scott, C.J. King, Carbon Dioxide-Sustained Adsorption of Lactic Acid at pH>pKa of the Acid, Ind. Eng. *Chem. Res.* 38(1999) 1625-1632.

[14] V.M. Yabannavar, D.I.C. Wang, Bioreactor System with Solvent Extraction for Organic Acid Production Ann. N. Y. Acad. *Sci.* 506(1987) 523-535.

[15] V.M. Yabannavar, D.I.C. Wang, Extractive Fermentation for Lactic Acid Production, Biotechnol. *Bioeng.* 37(1991) 1095-1100.
[16] C. Cotellessa, T. Manunta, I. Ghersetich, *The Use of Pyruvic Acid in the Treatment of Acne, J. Eur. Acad. Dermatol.* 18 (3)(2004) 275-278.
[17] R. Miyata, T. Yonehara, Improvement of fermentative production of pyruvate from glucose by Torulopsis glabrata IFO 0005, J.Ferm. Bioeng. 82 (5)(1996) 475-479.
[18] M.H. Scott, C.J. King, Multiple-acid equilibria in adsorption of carboxylic acids from dilute aqueous solution, *Ind. Eng. Chem. Res.* 38(1999) 501-511.

MIXED SOLVENTS AS ENVIRONMENTALLY BENIGN REPLACEMENT FOR BENZENE IN CAPROLACTAM EXTRACTION

M. L. van Delden, N. J. M. Kuipers, A. B. de Haan

University of Twente, Enschede, The Netherlands

Because of the strict legislation for currently applied solvents in the industrial extraction of caprolactam, being benzene, toluene and chlorinated hydrocarbons, a need exists for alternative, environmentally benign solvents. As replacement solvent mixtures containing a polar solvent and an alkane were proposed, in order to combine the favourable and eliminate the negative properties of both solvent types. In a screening procedure it was found that the caprolactam distribution ratio increased with increasing solvent (mixture) polarity, characterized by a more polar active group (ether, ester, ketone and alcohol), decreasing carbon chain length (C_{12}-C_6) or increasing polar solvent fraction in the mixture. Based on a high capacity and a low mutual solvent solubility the mixture methylcyclohexane-heptanol (40 mass %) was selected as replacement solvent. Calculating the solvent to feed ratio and NTS needed to reach the required raffinate concentrations for the industrial DSM extraction process lay-out, it was found that in the forward extraction *S/F* = 3.0 for both the mixed solvent and benzene, whereas NTS = 5 and 10, respectively. In the back-extraction *S/F* = 0.75 and 0.50 and the NTS = 10 and 6 for the mixed solvent and benzene, respectively.

INTRODUCTION

Caprolactam, the monomer of Nylon-6, is recovered after the Beckmann rearrangement by neutralizing the reaction mixture with aqueous ammonia, which results in the formation of two phases. The crude caprolactam top phase, containing 65-70 mass % caprolactam and 1 mass % ammonium sulfate, is in equilibrium with a nearly saturated aqueous ammonium sulfate solution. After separation of the phases caprolactam is industrially recovered by extraction with an organic solvent like benzene, toluene or chlorinated hydrocarbons [1,2].

Because of the negative effects on health and environment of currently applied solvents and the resulting strict legislation [3,4], the need exists for an environmentally benign solvent as replacement. Thereby a solvent is needed with a comparable capacity towards caprolactam and comparable mutual solvent solubility [2], Literature on alternative solvents is limited to 1-heptanol and 2-heptanone, where the influence of caprolactam and ammonium sulfate concentrations and temperature on phase compositions is described [5,6], For cyclohexanol the binodal is determined at 20 °C [7], The caprolactam distribution is investigated as function of the carbon chain length at limited experimental conditions for a series of linear alcohols (C_5-C_8) [8], These polar systems show a favourable distribution ratio, but also a relatively high mutual solvent solubility. Non-polar solvents possess a low mutual solubility, but show a non-favourable capacity towards caprolactam. It was therefore proposed to apply a mixture of a polar and a non-polar solvent in order to optimise the capacity and mutual solubility by changing the mixture composition in order to obtain a suitable green solvent [9]

In this research the caprolactam distribution ratio between the aqueous and mixed solvent phase was investigated at 20 °C for an initial 10 mass % aqueous caprolactam solution as function of the active group of various polar compounds (alcohol, ketone, ester, ether), their carbon chain length (C_6-C_{12}) and their concentration in a mixture with methylcyclohexane (MCH). Solvent mixtures showing favourable capacities for caprolactam were selected based on the determined distribution ratios compared to benzene and toluene. For these mixtures the capacity and mutual solvent solubility were determined as function of the aqueous caprolactam concentration ($w_{CPL,aq}$ = 0.0 to 0.6) and the temperature (77°C = 20, 40 and 60). Based on these results the final mixture was selected and its composition optimised.

EXPERIMENTAL PROCEDURE

Chemicals

All chemicals were used as received. The are: s-caprolactam (purity 99 %), di-propyl-ether (purity > 99 %), propyl-butyrate (purity 99%), 2-heptanone (purity 99%), 5-nonanone (purity 98%), methylcyclohexane (purity > 99 %) by Sigma-Aldrich (USA), butyl-butyrate (purity > 98%) by Merck (Germany), di-hexylether (purity > 97%), di-butylether (purity > 99%) by Fluka (Germany) and di-pentylether (purity 99%), 3-octanone (purity 99%), 2-methylcyclohexanol (purity 99%) and 1-heptanol (purity 98%) by Acros (Belgium). MiliQ water was used in all experiments.

Experimental set-up and procedure

To obtain experimental data the following procedure was followed. A stirred glass vessel, which was surrounded by a jacket for temperature control within 0.1 °C, was used. For each experiment an aqueous feed mixture, consisting of the desired amount of caprolactam in water, was prepared. After adding the organic solvent (mixture) and obtaining the desired temperature, the cell was stirred continuously for at least 45 min to ensure that equilibrium was attained. The stirring was stopped and the mixture was allowed to settle for at least 1 hour, to obtain full separation into two completely clear liquid phases. Samples were taken from both phases and analysed. Gas chromatography was used to determine the caprolactam and organic solvent concentration in both the aqueous and organic phase. Karl-Fisher titration was used to measure the water concentration in the organic phase and ion chromatography was applied for the determination of ammonium sulfate in the aqueous phase. The amount of water in the aqueous phase was determined from mass balance. The concentrations determined with GC, 1C and K-F analysis were obtained with an average absolute error < 0.2 mass %, < 0.01 mass % and 0.005 mass %, respectively [10],

Data analysis

The distribution ratio of a solute /', K_D./, is defined as the ratio of the determined solute mass fraction in the organic phase, **w**$_{/i0r}$**g,** to the one in the aqueous phase, **w,,**$_a$**q,** at equilibrium:

$$K_{D,i} = \frac{w_{i,org}}{w_{i,aq}} \qquad (1)$$

This distribution ratio represents the capacity of a solvent system in the extraction of caprolactam and was used for interpretation and evaluation of the experimental results.

EXPERIMENTAL RESULTS

In Figure 1 the results are shown for the caprolactam distribution ratio of the systems water + caprolactam + mixed solvent at 20 °C for an initial 10 mass % aqueous caprolactam solution as function of the equilibrium polar solvent concentration in the organic phase. The data

measured are compared with the equilibrium distribution ratio for benzene and toluene at comparable conditions [10], The amount of caprolactam extracted was increased with increasing polarity of the organic phase. This was shown by an increase of the distribution ratio at higher polar solvent concentrations, at shorter carbon chains, which trend was observed in literature before [8], and a more polar active group. The distribution ratio with toluene as solvent, presented as the dashed line in Figure 1, was used as minimal required capacity for a system. From Figure 1 it could be concluded that several solvents or solvent mixtures showed an acceptable to favourable distribution ratio. These solvents were heptanone, which was already known to possess a too high mutual solvent solubility [6], propyl-butyrate, octanone and the solvent mixtures with methylcyclohexanol and heptanol. The latter three solvents were further investigated. The equilibrium distribution ratio and mutual solubility for the solvent systems octanone, MCH-heptanol (15 mass % initially) and MCH-methylcyclohexanol (12 mass % initially) were investigated at 20 °C and aqueous caprolactam concentrations up to 50 mass % at equilibrium. The distribution ratio for these systems as function of the aqueous caprolactam concentration at equilibrium compared to the values for benzene and toluene is shown in Figure 2.

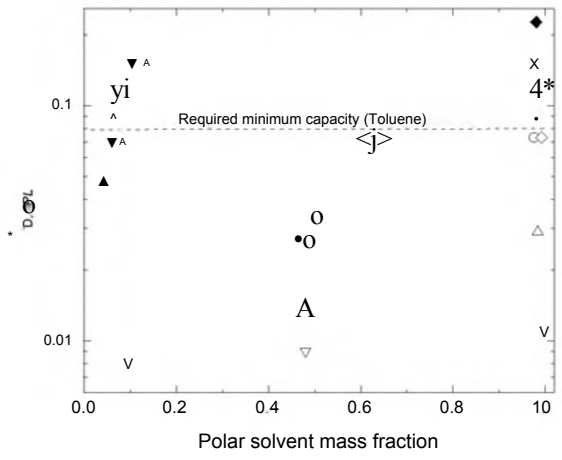


Figure 1. K_{DCPL} as function of the polar solvent fraction in MCH for: V, *di-hexylether;* A, *di-propylether;* O, *butyl-butyrate;* •, *propyl-butyrate;* O, *nonanone,* ■$>, *octanone;* ♦, *heptanone;* ▼, *methylcyclohexanol;* ▲, *heptanol;* x, *benzene and toluene as reference at 20 °C and* $w_{CPL,aq}$ *= 0.10 initially.*

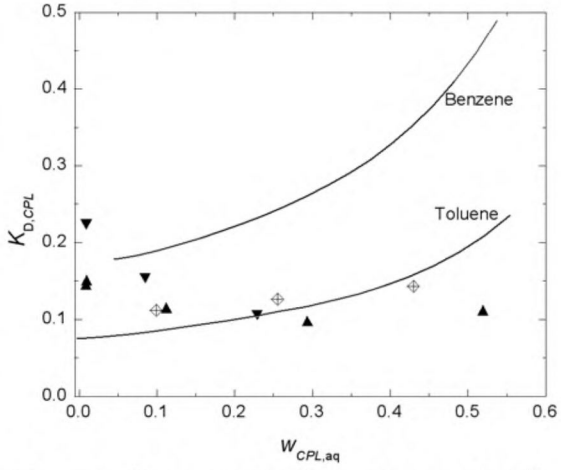


Figure 2. $K_{D,CPL}$ *as function of* $w_{CPL,aq}$ *for:* ⊕, *octanone;* ▲, *MCH-heptanol (15 mass % initially);* ▼, *MCH-methylcyclohexanol (12 mass % initially) at 20* °C.

From Figure 2 it was concluded that, although the selected solvent systems showed favourable capacities at low caprolactam concentrations, the capacity at high caprolactam concentrations was below that of toluene. For the solvent mixtures, however, it was known that the caprolactam distribution ratio was increased for increasing alcohol concentrations in the organic phase. It was therefore investigated whether the alcohol concentration could be increased such that at high caprolactam concentrations a capacity comparable to benzene and toluene was obtained, without increasing the mutual solvent solubility too much. Since the loss of alcohol to the aqueous phase for the MCH-methylcyclohexanol system was already 0.02 at $w_{C}pL_{,aq}$ = 0.2 and an alcohol fraction of 0.1 in the organic phase, it was expected that at higher alcohol and caprolactam concentrations, the mutual solubility would be increased too much. It was therefore investigated if in the system MCH-heptanol the alcohol content could be increased in order to obtain a suitable solvent for aqueous caprolactam concentrations up to 50 mass % at equilibrium. The caprolactam distribution as function of the aqueous caprolactam concentration at initial organic alcohol concentrations of 5, 15 and 40 mass % and 20 °C is shown in Figure 3.

From Figure 3 it could be concluded that the amount of caprolactam extracted to the organic phase increased strongly with the amount of alcohol in the organic phase, as already expected from Figure 1. In comparison to the distribution ratio in toluene at 20 °C a mixed solvent with initially 40 mass % alcohol shows a higher extraction capacity. For benzene the distribution ratio is only larger at high caprolactam concentrations ($w_{CPL,aq}$ > 0.4). The temperature influence on the distribution ratio for the MCH-heptanol (40 mass %) mixture is shown in Figure 4. From this figure it follows that increasing the temperature results in an increase of the distribution ratio for all systems. However, the trends relatively do not change.

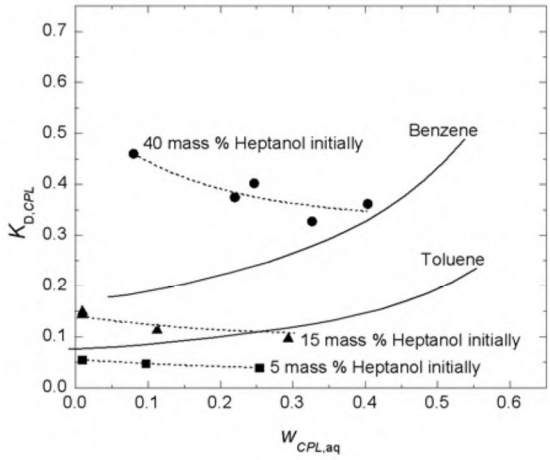


Figure 3. $K_{0,i}$ as function of the aqueous caprolactam concentration for MCH-heptanol mixtures having different equilibrium heptanol concentrations at 20 °C.

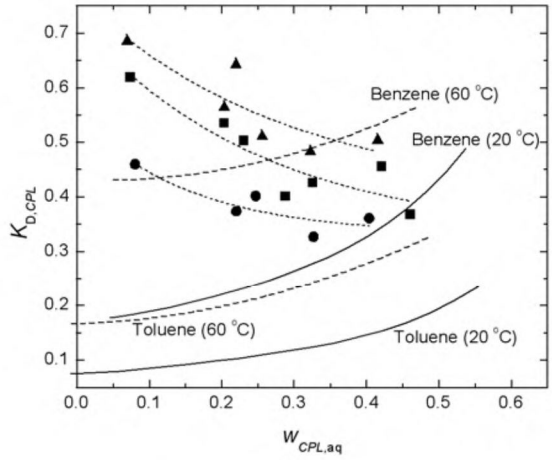


Figure 4. $K_{D\,i}$ as function of temperature and the aqueous caprolactam concentration for MCH-heptanol (40 mass % initially) at: •, 20 °C; ■, 40 °C; ▲, 60 °C.

The mutual solvent solubility of the solvent mixture MCH-heptanol (40 mass %) was determined and compared with the mutual solvent solubility in the system with benzene as solvent at 20 °C (Figure 5). In this diagram the mixed solvent was assumed to be a single component ('solvents') and the mass fractions of heptanol and methylcyclohexane were added in order to acquire the solvent fraction.

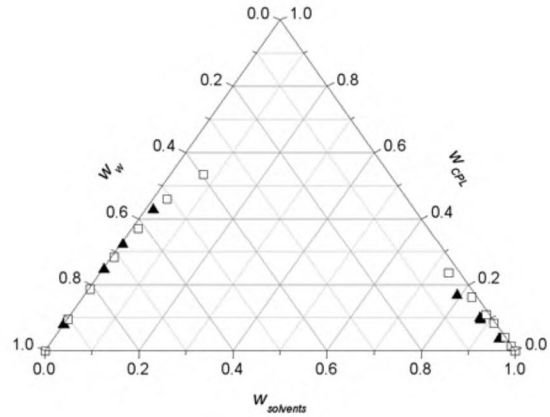


Figure 5. Phase compositions at 20 °C of: ▲, MCH-heptanol (40 mass % initially) and □, benzene as reference.

From Figure 5 it can be concluded that the amount of water extracted to the organic phase is slightly higher for the mixed solvent compared to benzene. The values at high caprolactam concentrations are almost comparable, however. The amount of solvent lost to the aqueous phase is always lower for the solvent mixture than for benzene.

EQUILIBRIUM STAGES CALCULATION

Using the presented results in Figure 1 to 5, the solvent to feed ratio (S/F) and the number of equilibrium stages (NTS) needed for the extraction of caprolactam according to the industrial DSM process lay-out [1,13] with the mixture MCH-heptanol (40 mass % initially) was calculated and compared to benzene.

In the forward extraction of caprolactam a 70 mass % aqueous caprolactam phase is extracted at 40 °C with an organic solvent. The solvent to feed ratio for both benzene and the mixed solvent was chosen at *S/F* = 3.0, since the minimum solvent to feed ratio for the mixed solvent and benzene was calculated as $(S/F)_{min}$ = 1.7 and 1.5, respectively. The fraction of caprolactam remaining in the raffinate after extraction is shown in Figure 6a as function of the amount of equilibrium stages used. It was thereby assumed that there was no mutual solubility of the solvents and the extraction of the aqueous ammonium sulfate layer, which is present in the industrial process [1,9] was not considered. In the back-extraction the caprolactam rich organic phase from the forward extraction is re-extracted at 40 °C with water as solvent. Using the extract concentration from the forward extraction, w_{CP}L,extract = 0.189, the minimum solvent to feed ratio needed for the back-extraction process at 40 °C was calculated for both the mixed solvent and benzene at $(S/F)_{mm}$ = 0.3. Therefore *S/F* = 0.5 was selected for both solvents. However, since it was known from Figure 4 that the caprolactam distribution ratio for the mixed solvent is higher at low caprolactam concentrations than for benzene, the solvent to feed ratio for the back-extraction of caprolactam from the mixed solvent system was chosen at *S/F* = 0.75. The fraction of caprolactam remaining in the raffinate after extraction is shown in Figure 6b as function of the amount of equilibrium stages used.

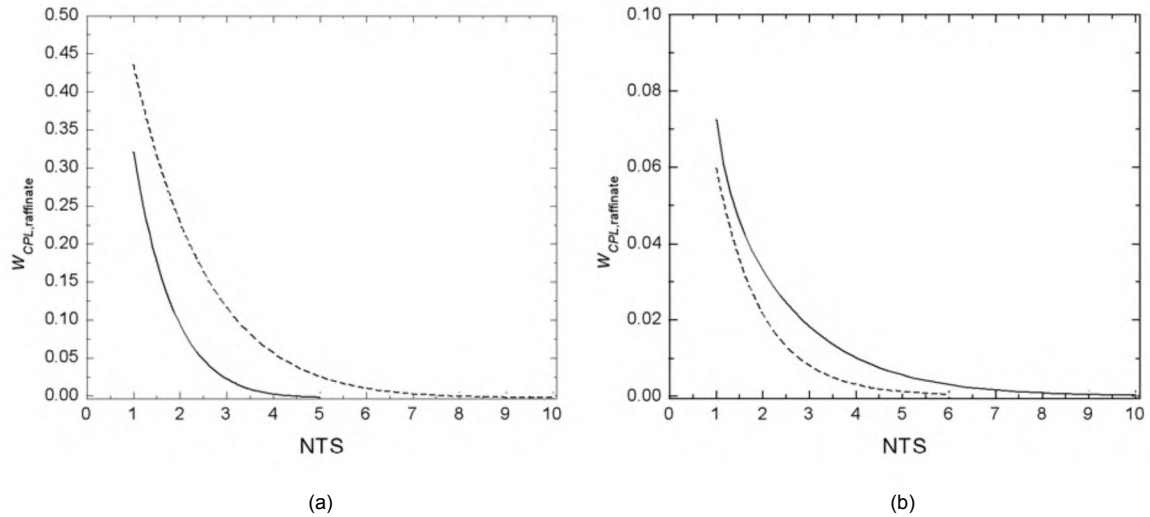


Figure 6. Caprolactam raffinate fraction at 40 °C as *function of NTS used in the forward extraction (a) and back-extraction with water (b) for: — mixed solvent and --, benzene.*

From Figure 6a it was concluded that in the forward extraction the mixed solvent needs only half of the NTS in order to reach the required raffinate concentration of w_{CP}*i*_.raffinate = 5 x 10'4 relative to benzene under comparable conditions. From Figure 6b it could, however, be concluded that this trend is reverse, while the mixed solvent system also needs a slightly higher solvent to feed ratio. This behaviour can be understood from Figure 4. In this figure it can be seen that at high caprolactam concentrations the behaviour of both solvents is more or less comparable, whereas at low concentrations the caprolactam distribution ratio is higher for the mixed solvent compared to benzene. This results in the mixed solvent being

favourable in the forward extraction at low caprolactam concentrations, but benzene being favourable in the back-extraction at low concentrations.

CONCLUSION

As replacement solvent for benzene and toluene in the caprolactam extraction process mixtures containing a polar and a non-polar solvent were investigated. It was found that the caprolactam distribution ratio increased with increasing solvent (mixture) polarity, characterized by a more polar active group (ether, ester, ketone and alcohol), decreasing carbon chain length (C_{12}-C_6) or increasing polar solvent fraction in the mixture. Based on a high capacity and a low mutual solvent solubility the mixture methylcyclohexane-heptanol (40 mass %) was selected as replacement solvent. This mixture appears to be a good alternative for benzene as solvent, based on the calculated solvent to feed ratios and NTS needed to reach the required raffinate concentrations for the industrial DSM extraction process lay-out.

LITERATURE

1. A. J. F. Simons and N. F. Haasen. Extraction of Caprolactam; from T. C. Lo, M. H. I. Baird and C. Hanson (1983), Handbook of Solvent Extraction, Wiley, New York, pp. 557-566.
2. F. Ullmann (2004), Ullmann's Encyclopedia of Industrial Chemistry; Wiley-Interscience: New York, Electronic version.
3. European Environment Agency, Report No 22 *[Internet],* Available from: <http://reports.eea.eu.int/environmental_issue_report_2001_22/en>. *[Accessed 24 September 2004],*
4. EUR-Lex, The portal to European Union law *[Internet],* Available from: <http://europa.eu.int/eur-lex/en/com/pdf/2004/com2004_0320en01 .pdf>. *[Accessed 24 September 2004],*
5. M. Wijtkamp, G. H. van Bochove, Th. W. de Loos and S. Niemann (1999), *Fluid Phase Equilibria*, 158-160, 939-947
6. G. H. van Bochove, G. J. P. Krooshof and Th. W. de Loos (2002), *Fluid Phase Equilibha,* 194-197, 1029-1044.
7. K. Tettamanti, M. Nogradi, J. Sawinsky (1960), *Periodica Polytechnica,* 4, 201.
8. M. Poraicu, C. Davidescu, and C. Pacurariu (1997), *Chem. Bull. Politehnica,* 42, 139-143
9. M. L. van Delden, N. J. M. Kuipers, A. B. de Haan and O. Lerner (2002), *Proc. Int. Solvent Extraction Conf.,* Cape Town, South Africa, pp. 668-673.
10. M. L. van Delden, N. J. M. Kuipers, and A. B. de Haan (2004), *J. Chem. Eng. Data*, web ed.



EXTRACTION OF ZINC(II) AND IRON(III) FROM SPENT PICKLING SOLUTIONS OF HIGH ZINC(II) CONTENT

Marta ROZENBLAT, Magdalena REGEL-ROSOCKA*, Jan SZYMANOWSKI

Institute of Chemical Technology and Engineering, Poznan University of Technology,
Pl. M. Sklodowskiej-Curie 2, 60-965 Poznan, Poland

Zinc(II) or iron(III) extraction with tributyl phosphate (TBP) from spent pickling solutions containing high zinc(II) concentration is studied. Two technological approaches for the separation are considered: the selective extraction of iron(III) over zinc(II) with small portions of TBP, and zinc(II) selective extraction with an excess of TBP after iron(III) reduction to iron(II). None of the both versions enables selective extraction of iron(III) orzinc(II). The total removal of iron(III) needs several successive extractions with fresh TBP portions. Zinc(II) can be quantitatively recovered in the presence of iron(II) using 5-10 volume excess of TBP.

INTRODUCTION

Hot-dip galvanizing in 96.5-99% purity zinc, carried out at 445-465°C, needs the pure surface of iron goods. The rust is removed by the pickling with 20% HCI carried out at room temperature.

Spent pickling solutions from steel pickling contain zinc(II). The metal cation originates from dissolution of zinc(II) coated materials such as racks, chains and baskets used to transport galvanized elements. Poor zinc coatings are usually removed in different pickling baths. As a result, zinc(II) concentration increases even up to 130 g/L, while iron content does not exceed 10 g/L in spent pickling solutions [1],

Pickling solutions are considered as spent solutions when the concentration of hydrochloric acid decreases to 75-85%, and the metal content increases up to 150-250 g/L [1, 2], The spent pickling solution content depends on the plant and the pickling method applied there.

The use of several techniques for regeneration of spent pickling solutions was proposed but they were not implemented into industrial practice [3], Multistage solvent extraction is an alternative for pyrohydrolysis (the Ruthner process) in the case of pickling solutions containing high concentrations of zinc(II). Detailed studies on an effective extractant for zinc(II) recovery from spent pickling solutions and on the application of zinc(II) extraction with tributyl phosphate (TBP) and stripping were described in our works [4-9],

It is the aim of the work to study the effect of phase ratio on selectivity of zinc(II) or iron(III) extraction with tributyl phosphate (TBP) from spent pickling solution containing high zinc(II) concentration. Moreover, efficiencies of stripping and scrubbing with water from loaded TBP are studied.

EXPERIMENTAL

Tributyl phosphate (TBP) (Merck, Germany) was used as an extractant. The reagent was used as delivered without any purification and was applied as undiluted and diluted (80% v/v) with low aromatic kerosene Exxsol D 220/230 (ESSO A.G., Germany).

Extraction was carried out in a small scale (separatory funnels) using different volume ratios equal to (organic/water) 1/10, 1/5, 1/1, 5/1, 8/1, 9/1 and 10/1. Phases were mechanically shaken for 10 minutes and left for phase separation. Contents of the model aqueous feed was near to a real solution from “Belos” galvanizing plant in Bielsko-Biala and contained 100 g/L Zn(II), 29 g/L Fe(II), 1 g/L Fe(III) 2.5 M HCI, 6.5 M Cl^-. The content of a real spent pickling solution was as follows: 120 g/L Zn(II), 30 g/L Fe(II), 0.79 g/L Fe(III), 2.5 M HCI, 6.5 M Cl". Stripping from loaded TBP was carried out with deionized water at volume ratio 1/1. Scrubbing of loaded TBP was carried out with deionized water at w/o ratio 1/5 and 1/10.

In the second part of the experiments the aqueous phase containing 120 g/L Zn(II), 30 g/L Fe(III), 4 M HCI, 6.5 M Cl (FeedI) was extracted with 80% TBP in several stages until iron(III) was removed completely. Three volume ratios were used o/w 1/2, 1/5, 1/10. After first extraction, the organic phase was contacted with the fresh aqueous feed (Feed2: 120 g/L Zn(II), 30 g/L Fe(III), 4 M HCI, 6.5 M Cl^-) and after each further extraction the organic phase was contacted with raffinate (R2,) to load TBP with iron(III) and to push up zinc(II) from the organic phase. The way of carrying out the experiment is shown in Fig. 1.

Zn(II) concentration in the aqueous phase was determined by amperometric titration with 0.05 M $K_4[Fe(CN)_6]$, HCI content in the aqueous phase was determined by potentiometric titration (702 SM Titrino, Metrohm, Switzerland) with 0.1 M NaOH. The content of Fe(II) and Fe(III) was determined by titration with $K_2Cr_20_7$ (Fe(III) was reduced to Fe(II) with 5% solution of $SnCI_2$). The content of water in the organic phase was determined by the Karl - Fischer titration.

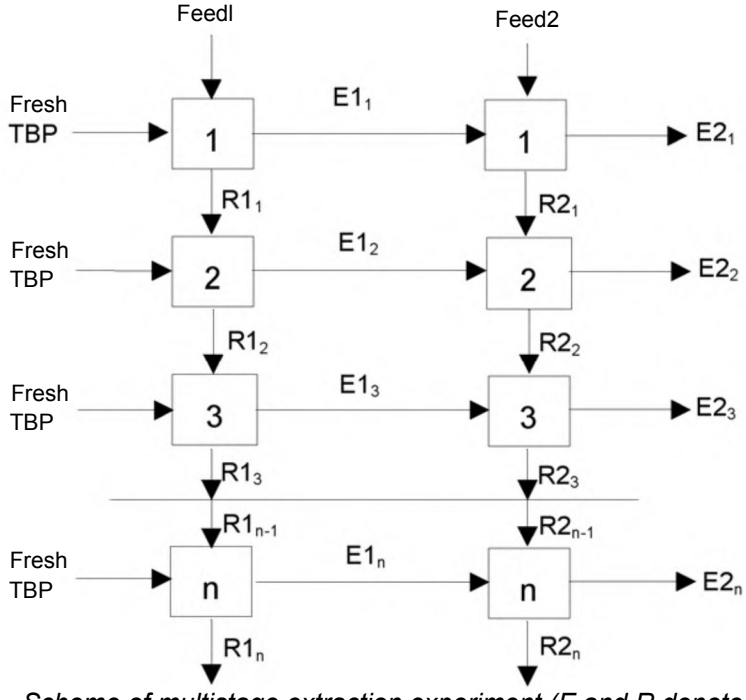


Figure 1. Scheme of multistage extraction experiment (E and R denote extract and raffinate, respectively; capital digit succeeding R or E stands for feed 1 and 2; subscripts denote extraction step).

RESULTS AND DISCUSSION

Two technological approaches for the separation were considered. Firstly, the selective extraction of iron(III) over zinc(II) with small portions of TBP. Thus, it was assumed that prior to the extraction iron(II) would be oxidized to iron(III), e.g., with hydrogen peroxide. Secondly, iron(III) reduction to iron(II) with iron wool followed by zinc(II) selective extraction with an excess of TBP.

Extraction with small portions of TBP

The separation of iron(III) over zinc(II) is enhanced by an excess of the aqueous feed due to the crowd effect, i.e. when the organic phase is saturated with metal species then weaker complexes are replaced by the stronger ones. Such a phenomenon takes place in case of the second extraction (see Fig. 1 with extraction scheme), where raffinate after the extraction is richer in Zn(II). It is observed especially for o/w ratios 1/5 and 1/10 (Fig. 2).

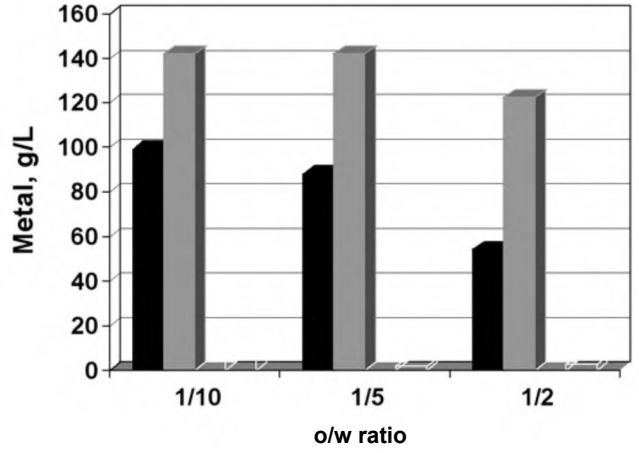


Figure 2. Concentration ofzinc(II) (■) *and iron(III)* (®) *in raffinate R1, and zinc(II)* (Hj *and iron(III)* (S) *in raffinate R2, after last extraction stage for different phase ratios (Feed: 120 g/L Zn(II), 30 g/L Fe(III), 4 M HCI, 6.5 M Cf).*

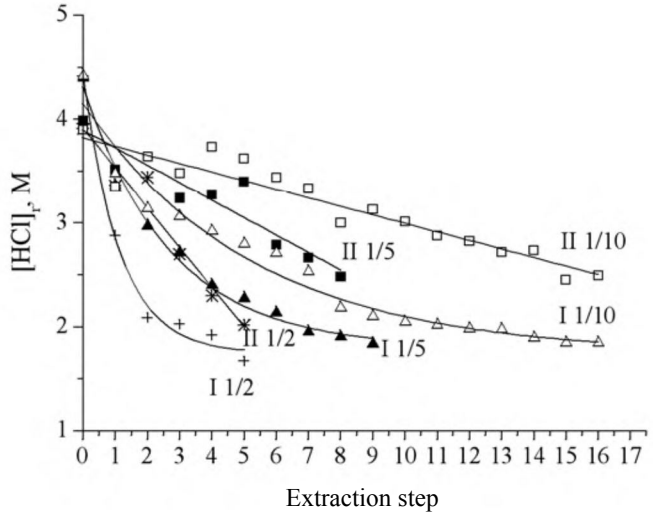


Figure 3. Concentration of HCI in raffinate R1, (+, ▲, A) *and R2, (%,* ■, □) *after each extraction stage for different phase ratios.*

For o/w ratio 1/2, Zn(II) increase in R2, is not significant. Iron(III) concentration in both raffinates (R1, and R2,) decreases almost to 10 g/L. However, zinc(II) concentration in raffinate R1< decreases in each successive step of extraction. It means that Zn(II) is co-extracted to the organic phase. However, after contacting the loaded TBP with the second raffinate R2„ Zn(II) concentration increases in each step and finally amounts to at least initial value in feed. HCI extraction plays important role in zinc(II) and iron(III) extraction. A dramatic decrease of HCI concentration, from over 4 to 2 M, is observed in first three, six and nine steps in raffinate R1 i for o/w of 1/2, 1/5 and 1/10, respectively (Fig. 3). Then, HCI transport is not significant. HCI concentration decreases continuously in the raffinate R2,.

The results indicate that the “double extraction” carried out according to the scheme given in Fig. 1 enables the extraction of iron(III) in the presence of zinc(II) which accumulates in the aqueous phase. Unfortunately, too many stages are needed to remove Fe(III) from the feed completely, that is 5, 9 and 16 for o/w equal to 1/2, 1/5 and 1/10, respectively.

Stripping both of zinc(II) and iron(III) can be effectively accomplished with water which, however, is not selective, i.e., both Fe(III) and Zn(II) are stripped. Prior to stripping, the organic phase can be washed with small amounts of water (Table 1). For w/o = 1/5 near 30% of zinc(II) is scrubbed from loaded TBP with water and almost 40% with Fe(III) solution. Fe(III) solution is used to increase crowd effect and to cause higher zinc(II) transfer to the aqueous phase. However, no visible impact is observed.

Table 1. Zinc(H) and iron(III) scrubbing from two times loaded 80% TBP (E2J (Sc stands for scrubbing, ol and o2 denote organic phase before and after scrubbing, respectively).

Scrubbing phase	w/o	$[Zn(II)]_{01}$ g/L	$[Fe(III)]_{01}$ g/L	**SCzn(II)** %	**SCpe(III)** %	$[Zn(II)]_{o2}$ g/L	$[Fe(III)]_{o2}$ g/L
water	1:5	47.2	16.3	27.5	20.4	34.3	13.0
water	1:5	31.7	42.2	28.4	18.0	22.9	34.6
4.5 g/L Fe(III)	5:1	18.3	23.2	100	71.3	0	6.62
4.5 g/L Fe(III)	1:5	19.4	22.1	39.4	15.8	11.7	18.6

An excess of scrubbing phase causes high Fe(III) washing out. Unfortunately, in case of small water amounts, iron(III) is also scrubbed. Thus, it is impossible to wash out zinc(II) selectively without loss of iron(III). Scrubbing solution is always a mixture of zinc(II) and iron(III) and it must be recycled to the extraction step in continuous process. However, scrubbing is more advantageous than multistage extraction with small volume of TBP.

Extraction with an excess of TBP

Results presented in Table 2 show very effective zinc(II) extraction (over 98%) in the presence of iron(II) at high excess of the organic phase. On the other hand, iron(II) is extracted significantly (over 10%). It probably results from water transfer to the organic phase and physical transport of iron(II). o/w ratio after extraction confirms a dramatic decrease in the aqueous phase volume, especially in case of 100% TBP. Practically, such continuous process can be carried out only with recycling of the aqueous phase from the settler to the mixer of the same contactor to keep the phase ratio in reasonable range o/w = 2/1-1/1.

Scrubbing of TBP solutions containing zinc(II) and iron(II) enables the removal of iron(II) with small amount of zinc(II) (Table 3). 100% of iron(II) is washed out from 80% TBP at w/o volume ratio 1/5. Use of higher volume ratio decreases amount of scrubbed iron(II). Again, the solution must be recycled because some amounts of zinc(II) (5-16%) are washed out. The removal of iron(II) by scrubbing with water supports the idea of unspecific iron(II) transfer in the cores of reverse micelles.

Table 2. Zinc(II) and iron(II) extraction for different volume ratios and TBP concentrations (Feed: 100 g/L Zn(II), 30 g/L Fe(II), 2.5 M HCl, 6.5 M Cf).

[TBP] %	o/w before extraction	Ezn(II) %	Epe(II) %	$[Zn(II)]_0$ g/L	$[Fe(II)]_0$ g/L	o/w after extraction
[illegible]	8/1	99.4	15.9	11.9	0.55	20/1
	9/1	99.8	42.1	10.3	1.3	37/1
[illegible]	8/1	98.3	12.4	11.7	0.44	16/1
	9/1	99.0	14.9	10.9	0.49	20/1

Table 3. Zinc(II) and iron(II) scrubbing with water from loaded 80% TBP (Sc stands for scrubbing, ol and o2 denote organic phase before and after scrubbing, respectively).

w/o	$[Zn(II)]_{0l}$ g/L	$[Fe(II)]_{0l}$ g/L	[illegible]	**SCpefII)** %	$[Zn(II)]_{o2}$ g/L	$[F e(I I)]_{o2}$ g/L
1/5	12.7	0.42	15.3	100	10.7	0
1/5	11.3	0.43	16.1	100	9.4	0
1/10	12.7	0.42	5.1	50.6	12.09	0.21
1/10	11.3	0.43	6.5	78.4	10.56	0.09

Regeneration of a real spent pickling solution

After iron(III) reduction to iron(II), a real spent pickling solution was extracted with an excess of 80% TBP. Results in Table 4 are consistent with these obtained for a model solution. Almost 100% of zinc(II) and some amounts of iron(II) are extracted from the aqueous phase. Thus, theoretical results are confirmed in practice.

Table 4. Zinc(II) and iron(II) extraction for different volume ratios of 80% TBP (Feed: 120 g/L Zn(II), 31 g/L Fe(II), 2.5 M HCl, 6.5 M Cf).

o/w before extraction	Ezn(II) %	**EFe(II)** %	$[Zn(II)]_0$ g/L	$[Fe(II)]_0$ g/L	o/w after extraction
8/1	98.7	18.2	15.6	0.75	21/1
9/1	99.5	16.7	14.4	0.66	23/1

Scrubbing with small amounts of water allows to remove iron(II) from loaded TBP completely and next to recover zinc(II) by stripping with water (Table 5). Though over 10% of iron(II) is extracted, the selective separation of the metal from zinc(II) in spent pickling solution is possible.

Table 5. Zinc(II) and iron(II) scrubbing (Sc) and stripping (R) with water from loaded 80% TBP (ol and o2 denote organic phase before and after scrubbing or stripping, respectively).

Process	$[Zn(II)]_0$i g/L	$[Fe(II)]_{01}$ g/L	Sczn(ii) or Rzn(II) %	Sczn(ii) or Rpe(II) %	$[Zn(II)]_{02}$ g/L	$[Fe(I I)]_{o2}$ g/L
Sc*	15.6	0.75	13.2	100	13.5	0
	14.4	0.66	12.8	100	12.5	0
R**	13.5	0	98.7	-	0.17	-
	12.5	0	99.4	-	0.075	-

* w/o=1/5

**w/o=1/1

Process for regeneration of spent pickling solution

As a result of the studies we propose a technological process shown in Fig. 3. Spent pickling

solution of high zinc(II) concentration is contacted with steel wool to reduce iron(III) to iron(II). Afterwards zinc(II) from the aqueous stream is extracted in one step with 5-10 folded excess of 80% TBP. A raffinate after zinc(II) extraction contains Fe(II) and HCI, thus it can be used to produce coagulants for water treatment plants. Loaded organic phase contains high amounts of zinc(II) and some of iron(II). The latter can be removed from TBP by scrubbing with small volume of water. Scrubbings containing iron(II) with small amount of zinc(II) should be recycled to the reduction step. The loaded TBP phase cannot be stored but must be washed with water immediately to remove HCI and zinc(II) chlorocomplexes which behave as a strong acid and induce hydrolysis of tributyl phosphate. The organic phase loaded with zinc(II) is contacted with water (w/o = 1) to strip zinc(II). Before recycling, TBP is washed with NaOH solution to remove partial esters, mainly dibutylphosphoric acid, and to prohibit in this way the undesired transfer of iron(II) to the recycled TBP.

Aqueous phase after stripping contains zinc(II) and HCI, so it can be used to prepare a fluxing liquor or it can be further concentrated by evaporation to obtain $ZnCl_2$ solution or crystalline salt. Electrowinning of metallic zinc is also possible.

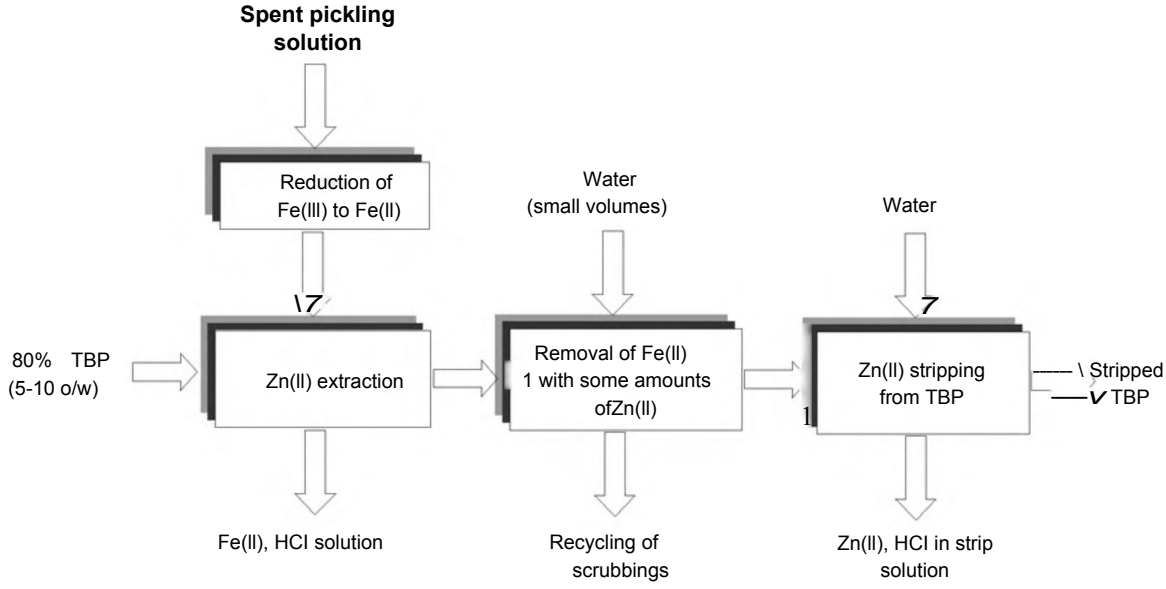


Figure 3. Proposed flowsheet for zinc(II) recovery from spent pickling solution of high zinc(II) concentration.

CONCLUSIONS

Two technological approaches for the separation are considered: the selective extraction of iron(III) over zinc(II) with small portions of TBP, and zinc(II) selective extraction with an excess of TBP after iron(III) reduction to iron(II). None of the both versions enables selective extraction of iron(III) or zinc(II). The total removal of iron(III) needs several successive extractions with fresh TBP portions. Zinc(II) can be quantitatively recovered using 5-10 volume excess of TBP.

Stripping both of zinc(II) and iron(III) can be effectively accomplished with water but is not selective. Prior to stripping, the organic phase can be washed with small amounts of water. Scrubbing of TBP solutions containing iron(III) contaminated with zinc(II) gives always a mixture of zinc(II) and iron(III) which must be recycled to the extraction step in continuous process. Scrubbing of TBP solutions containing zinc(II) and iron(II) enables the removal of iron(II) with some amounts of zinc(II) (5-16%). Again, the solution must be recycled. The

removal of iron(II) by scrubbing with water supports the idea of unspecific iron(II) transfer in the cores of reverse micelles.

Zinc(II) extraction from a real spent pickling solution in the presence of iron(II) with an excess of TBP is as efficient as in case of model solutions.

The following technological concept is proposed: reduction of iron(III) to iron(II), extraction of zinc(II) with 5-10 volume excess of TBP, washing of TBP phase contaminated with iron(II) with small volumes of water and recycling of the scrubbings and stripping of zinc(II) with water from loaded TBP.

ACKNOWLEDGMENT

The work was supported by the grant 32-044/05 DS.

REFERENCES

1. P. Maass, P. Peissker (1998), *Hot-dip Galvanising,* Agencja Wydawnicza Placet, Warsaw.
2. B. Gopfert (1998), Ruckgewinnung von Zink aus zinkhaltigen Abfällen der Feuerverzinkungsindustrie - Ökologische und ökonomische Bewertung, *ABAG Projektbericht.*
3. T. C. Lo, M. H. J. Baird, C. Hanson (1991), *Handbook of Solvent Extraction,* Krieger Publishing Company, Malabar, Florida.
4. M. Regel, A. M. Sastre, J. Szymanowski (2001), *Environ. Sci. Technol.,* 35, 630-635.
5. R. Cierpiszewski, I. Miesi^c, M. Regel-Rosocka, J. Szymanowski (2002), *Ind. Eng. Chem. Res.,* 41, 598-603.
6. M. Bartkowska, M. Regel-Rosocka, J. Szymanowski (2002), *Physicochem. Problems Min. Proc.,* 36, 217-224.
7. M. Regel-Rosocka, P. Zawistowski, A. M. Sastre, J. Szymanowski (2003), *Pol. J. Appl. Chem.,* 67, 83-94.
8. M. Regel-Rosocka, K. Alejski, A. M. Sastre, J. Szymanowski (2003), *Chemical Industry and Environment IV,* Macias Machin A., Umbria J. (Eds), Universidad de Las Palmas de Gran Canaria, vol. 1, pp. 377-386.
9. K. Alejski, S. Gorzelanna, M. Regel-Rosocka, J. Szymanowski (2002), *Chemistry for Agriculture,* Gołecki H., Dobrzahski Z. and Kafarski P. (Eds), Prague - Bruxelles - Stockholm, CZECH-POL TRADE, vol. 4, pp. 709-717.

EXTRACTION OF ZINC(II) AND IRON(III) FROM SPENT PICKLING SOLUTIONS OF HIGH ZINC(II) CONTENT

Marta ROZENBLAT, Magdalena REGEL-ROSOCKA*, Jan SZYMANOWSKI

Institute of Chemical Technology and Engineering, Poznan University of Technology,
Pl. M. Sklodowskiej-Curie 2, 60-965 Poznan, Poland

Zinc(II) or iron(III) extraction with tributyl phosphate (TBP) from spent pickling solutions containing high zinc(II) concentration is studied. Two technological approaches for the separation are considered: the selective extraction of iron(III) over zinc(II) with small portions of TBP, and zinc(II) selective extraction with an excess of TBP after iron(III) reduction to iron(II). None of the both versions enables selective extraction of iron(III) orzinc(II). The total removal of iron(III) needs several successive extractions with fresh TBP portions. Zinc(II) can be quantitatively recovered in the presence of iron(II) using 5-10 volume excess of TBP.

INTRODUCTION

Hot-dip galvanizing in 96.5-99% purity zinc, carried out at 445-465°C, needs the pure surface of iron goods. The rust is removed by the pickling with 20% HCI carried out at room temperature.

Spent pickling solutions from steel pickling contain zinc(II). The metal cation originates from dissolution of zinc(II) coated materials such as racks, chains and baskets used to transport galvanized elements. Poor zinc coatings are usually removed in different pickling baths. As a result, zinc(II) concentration increases even up to 130 g/L, while iron content does not exceed 10 g/L in spent pickling solutions [1],

Pickling solutions are considered as spent solutions when the concentration of hydrochloric acid decreases to 75-85%, and the metal content increases up to 150-250 g/L [1, 2], The spent pickling solution content depends on the plant and the pickling method applied there.

The use of several techniques for regeneration of spent pickling solutions was proposed but they were not implemented into industrial practice [3], Multistage solvent extraction is an alternative for pyrohydrolysis (the Ruthner process) in the case of pickling solutions containing high concentrations of zinc(II). Detailed studies on an effective extractant for zinc(II) recovery from spent pickling solutions and on the application of zinc(II) extraction with tributyl phosphate (TBP) and stripping were described in our works [4-9],

It is the aim of the work to study the effect of phase ratio on selectivity of zinc(II) or iron(III) extraction with tributyl phosphate (TBP) from spent pickling solution containing high zinc(II) concentration. Moreover, efficiencies of stripping and scrubbing with water from loaded TBP are studied.

EXPERIMENTAL

Tributyl phosphate (TBP) (Merck, Germany) was used as an extractant. The reagent was used as delivered without any purification and was applied as undiluted and diluted (80% v/v) with low aromatic kerosene Exxsol D 220/230 (ESSO A.G., Germany).

Extraction was carried out in a small scale (separatory funnels) using different volume ratios equal to (organic/water) 1/10, 1/5, 1/1, 5/1, 8/1, 9/1 and 10/1. Phases were mechanically shaken for 10 minutes and left for phase separation. Contents of the model aqueous feed was near to a real solution from “Belos” galvanizing plant in Bielsko-Biala and contained 100 g/L Zn(II), 29 g/L Fe(II), 1 g/L Fe(III) 2.5 M HCI, 6.5 M Cl^-. The content of a real spent pickling solution was as follows: 120 g/L Zn(II), 30 g/L Fe(II), 0.79 g/L Fe(III), 2.5 M HCI, 6.5 M Cl". Stripping from loaded TBP was carried out with deionized water at volume ratio 1/1. Scrubbing of loaded TBP was carried out with deionized water at w/o ratio 1/5 and 1/10.

In the second part of the experiments the aqueous phase containing 120 g/L Zn(II), 30 g/L Fe(III), 4 M HCI, 6.5 M Cl (FeedI) was extracted with 80% TBP in several stages until iron(III) was removed completely. Three volume ratios were used o/w 1/2, 1/5, 1/10. After first extraction, the organic phase was contacted with the fresh aqueous feed (Feed2: 120 g/L Zn(II), 30 g/L Fe(III), 4 M HCI, 6.5 M Cl^-) and after each further extraction the organic phase was contacted with raffinate (R2,) to load TBP with iron(III) and to push up zinc(II) from the organic phase. The way of carrying out the experiment is shown in Fig. 1.

Zn(II) concentration in the aqueous phase was determined by amperometric titration with 0.05 M $K_4[Fe(CN)_6]$, HCI content in the aqueous phase was determined by potentiometric titration (702 SM Titrino, Metrohm, Switzerland) with 0.1 M NaOH. The content of Fe(II) and Fe(III) was determined by titration with $K_2Cr_20_7$ (Fe(III) was reduced to Fe(II) with 5% solution of $SnCI_2$). The content of water in the organic phase was determined by the Karl - Fischer titration.

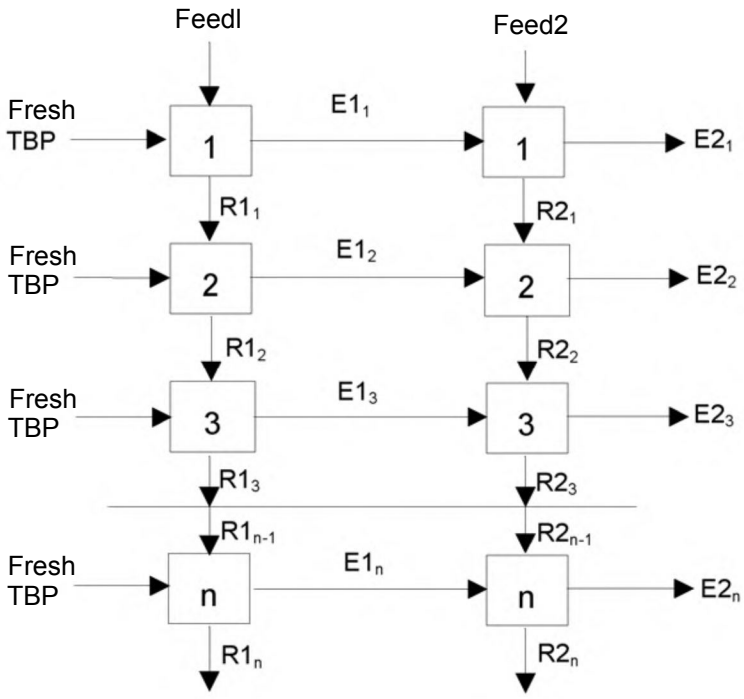


Figure 1. Scheme of multistage extraction experiment (E and R denote extract and raffinate, respectively; capital digit succeeding R or E stands for feed 1 and 2; subscripts denote extraction step).

RESULTS AND DISCUSSION

Two technological approaches for the separation were considered. Firstly, the selective extraction of iron(III) over zinc(II) with small portions of TBP. Thus, it was assumed that prior to the extraction iron(II) would be oxidized to iron(III), e.g., with hydrogen peroxide. Secondly, iron(III) reduction to iron(II) with iron wool followed by zinc(II) selective extraction with an excess of TBP.

Extraction with small portions of TBP

The separation of iron(III) over zinc(II) is enhanced by an excess of the aqueous feed due to the crowd effect, i.e. when the organic phase is saturated with metal species then weaker complexes are replaced by the stronger ones. Such a phenomenon takes place in case of the second extraction (see Fig. 1 with extraction scheme), where raffinate after the extraction is richer in Zn(II). It is observed especially for o/w ratios 1/5 and 1/10 (Fig. 2).

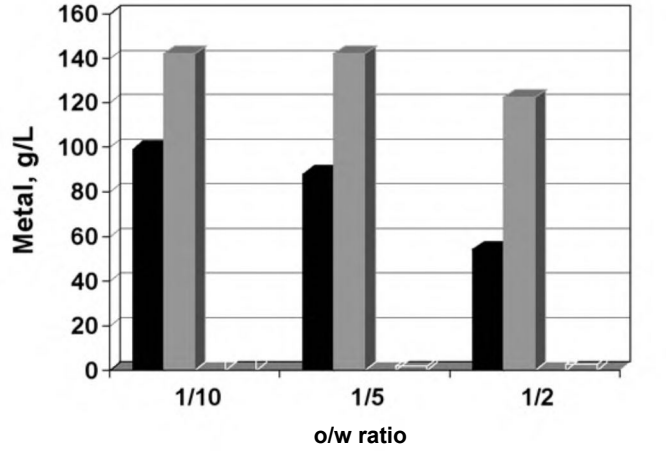


Figure 2. Concentration ofzinc(II) (■) *and iron(III)* (®) *in raffinate R1, and zinc(II)* (Hj *and iron(III)* (S) *in raffinate R2, after last extraction stage for different phase ratios (Feed: 120 g/L Zn(II), 30 g/L Fe(III), 4 M HCI, 6.5 M Cf).*

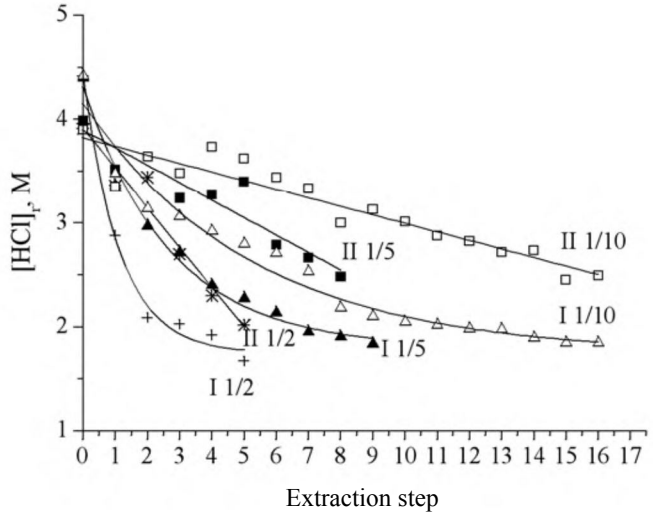


Figure 3. Concentration of HCI in raffinate R1, (+, ▲, A) *and R2, (%,* ■, □) *after each extraction stage for different phase ratios.*

For o/w ratio 1/2, Zn(II) increase in R2, is not significant. Iron(III) concentration in both raffinates (R1, and R2,) decreases almost to 10 g/L. However, zinc(II) concentration in raffinate R1< decreases in each successive step of extraction. It means that Zn(II) is co-extracted to the organic phase. However, after contacting the loaded TBP with the second raffinate R2„ Zn(II) concentration increases in each step and finally amounts to at least initial value in feed. HCI extraction plays important role in zinc(II) and iron(III) extraction. A dramatic decrease of HCI concentration, from over 4 to 2 M, is observed in first three, six and nine steps in raffinate R1 i for o/w of 1/2, 1/5 and 1/10, respectively (Fig. 3). Then, HCI transport is not significant. HCI concentration decreases continuously in the raffinate R2,.

The results indicate that the “double extraction” carried out according to the scheme given in Fig. 1 enables the extraction of iron(III) in the presence of zinc(II) which accumulates in the aqueous phase. Unfortunately, too many stages are needed to remove Fe(III) from the feed completely, that is 5, 9 and 16 for o/w equal to 1/2, 1/5 and 1/10, respectively.

Stripping both of zinc(II) and iron(III) can be effectively accomplished with water which, however, is not selective, i.e., both Fe(III) and Zn(II) are stripped. Prior to stripping, the organic phase can be washed with small amounts of water (Table 1). For w/o = 1/5 near 30% of zinc(II) is scrubbed from loaded TBP with water and almost 40% with Fe(III) solution. Fe(III) solution is used to increase crowd effect and to cause higher zinc(II) transfer to the aqueous phase. However, no visible impact is observed.

Table 1. Zinc(H) and iron(III) scrubbing from two times loaded 80% TBP (E2J (Sc stands for scrubbing, ol and o2 denote organic phase before and after scrubbing, respectively).

Scrubbing phase	w/o	$[Zn(II)]_{01}$ g/L	$[Fe(III)]_{01}$ g/L	**SCzn(II)** %	**SCpe(III)** %	$[Zn(II)]_{o2}$ g/L	$[Fe(III)]_{o2}$ g/L
water	1:5	47.2	16.3	27.5	20.4	34.3	13.0
water	1:5	31.7	42.2	28.4	18.0	22.9	34.6
4.5 g/L Fe(III)	5:1	18.3	23.2	100	71.3	0	6.62
4.5 g/L Fe(III)	1:5	19.4	22.1	39.4	15.8	11.7	18.6

An excess of scrubbing phase causes high Fe(III) washing out. Unfortunately, in case of small water amounts, iron(III) is also scrubbed. Thus, it is impossible to wash out zinc(II) selectively without loss of iron(III). Scrubbing solution is always a mixture of zinc(II) and iron(III) and it must be recycled to the extraction step in continuous process. However, scrubbing is more advantageous than multistage extraction with small volume of TBP.

Extraction with an excess of TBP

Results presented in Table 2 show very effective zinc(II) extraction (over 98%) in the presence of iron(II) at high excess of the organic phase. On the other hand, iron(II) is extracted significantly (over 10%). It probably results from water transfer to the organic phase and physical transport of iron(II). o/w ratio after extraction confirms a dramatic decrease in the aqueous phase volume, especially in case of 100% TBP. Practically, such continuous process can be carried out only with recycling of the aqueous phase from the settler to the mixer of the same contactor to keep the phase ratio in reasonable range o/w = 2/1-1/1.

Scrubbing of TBP solutions containing zinc(II) and iron(II) enables the removal of iron(II) with small amount of zinc(II) (Table 3). 100% of iron(II) is washed out from 80% TBP at w/o volume ratio 1/5. Use of higher volume ratio decreases amount of scrubbed iron(II). Again, the solution must be recycled because some amounts of zinc(II) (5-16%) are washed out. The removal of iron(II) by scrubbing with water supports the idea of unspecific iron(II) transfer in the cores of reverse micelles.

Table 2. Zinc(II) and iron(II) extraction for different volume ratios and TBP concentrations (Feed: 100 g/L Zn(II), 30 g/L Fe(II), 2.5 M HCl, 6.5 M Cf).

[TBP] %	o/w before extraction	**Ezn(II)** %	**Epe(II)** %	$[Zn(II)]_0$ g/L	$[Fe(II)]_0$ g/L	o/w after extraction
[illegible]	8/1	99.4	15.9	11.9	0.55	20/1
	9/1	99.8	42.1	10.3	1.3	37/1
[illegible]	8/1	98.3	12.4	11.7	0.44	16/1
	9/1	99.0	14.9	10.9	0.49	20/1

Table 3. Zinc(II) and iron(II) scrubbing with water from loaded 80% TBP (Sc stands for scrubbing, ol and o2 denote organic phase before and after scrubbing, respectively).

w/o	$[Zn(II)]_{0l}$ g/L	$[Fe(II)]_{0l}$ g/L	[illegible]	SCpefII) %	$[Zn(II)]_{o2}$ g/L	$[F e(I I)]_{o2}$ g/L
1/5	12.7	0.42	15.3	100	10.7	0
1/5	11.3	0.43	16.1	100	9.4	0
1/10	12.7	0.42	5.1	50.6	12.09	0.21
1/10	11.3	0.43	6.5	78.4	10.56	0.09

Regeneration of a real spent pickling solution

After iron(III) reduction to iron(II), a real spent pickling solution was extracted with an excess of 80% TBP. Results in Table 4 are consistent with these obtained for a model solution. Almost 100% of zinc(II) and some amounts of iron(II) are extracted from the aqueous phase. Thus, theoretical results are confirmed in practice.

Table 4. Zinc(II) and iron(II) extraction for different volume ratios of 80% TBP (Feed: 120 g/L Zn(II), 31 g/L Fe(II), 2.5 M HCl, 6.5 M Cf).

o/w before extraction	Ezn(II) %	**EFe(II)** %	$[Zn(II)]_0$ g/L	$[Fe(II)]_0$ g/L	o/w after extraction
8/1	98.7	18.2	15.6	0.75	21/1
9/1	99.5	16.7	14.4	0.66	23/1

Scrubbing with small amounts of water allows to remove iron(II) from loaded TBP completely and next to recover zinc(II) by stripping with water (Table 5). Though over 10% of iron(II) is extracted, the selective separation of the metal from zinc(II) in spent pickling solution is possible.

Table 5. Zinc(II) and iron(II) scrubbing (Sc) and stripping (R) with water from loaded 80% TBP (ol and o2 denote organic phase before and after scrubbing or stripping, respectively).

Process	$[Zn(II)]_0$i g/L	$[Fe(II)]_{01}$ g/L	**Sczn(ii)** or **Rzn(II)** %	**Sczn(ii)** or **Rpe(II)** %	$[Zn(II)]_{02}$ g/L	$[Fe(I I)]_{o2}$ g/L
Sc*	15.6	0.75	13.2	100	13.5	0
	14.4	0.66	12.8	100	12.5	0
R**	13.5	0	98.7	-	0.17	-
	12.5	0	99.4	-	0.075	-

* w/o=1/5

**w/o=1/1

Process for regeneration of spent pickling solution

As a result of the studies we propose a technological process shown in Fig. 3. Spent pickling

solution of high zinc(II) concentration is contacted with steel wool to reduce iron(III) to iron(II). Afterwards zinc(II) from the aqueous stream is extracted in one step with 5-10 folded excess of 80% TBP. A raffinate after zinc(II) extraction contains Fe(II) and HCI, thus it can be used to produce coagulants for water treatment plants. Loaded organic phase contains high amounts of zinc(II) and some of iron(II). The latter can be removed from TBP by scrubbing with small volume of water. Scrubbings containing iron(II) with small amount of zinc(II) should be recycled to the reduction step. The loaded TBP phase cannot be stored but must be washed with water immediately to remove HCI and zinc(II) chlorocomplexes which behave as a strong acid and induce hydrolysis of tributyl phosphate. The organic phase loaded with zinc(II) is contacted with water (w/o = 1) to strip zinc(II). Before recycling, TBP is washed with NaOH solution to remove partial esters, mainly dibutylphosphoric acid, and to prohibit in this way the undesired transfer of iron(II) to the recycled TBP.

Aqueous phase after stripping contains zinc(II) and HCI, so it can be used to prepare a fluxing liquor or it can be further concentrated by evaporation to obtain $ZnCl_2$ solution or crystalline salt. Electrowinning of metallic zinc is also possible.

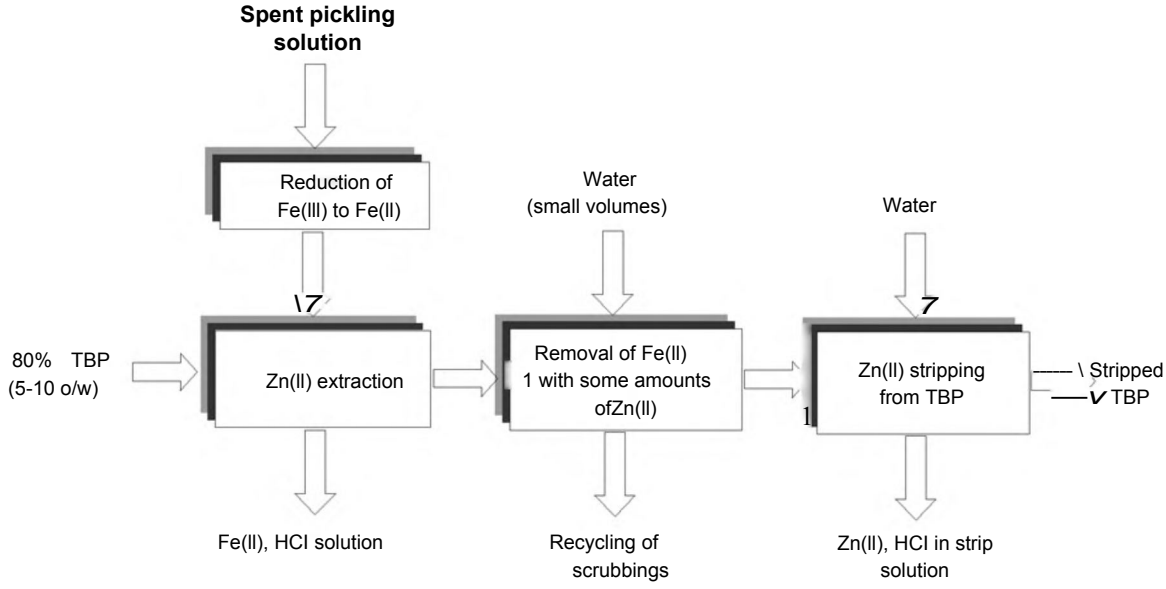


Figure 3. Proposed flowsheet for zinc(II) recovery from spent pickling solution of high zinc(II) concentration.

CONCLUSIONS

Two technological approaches for the separation are considered: the selective extraction of iron(III) over zinc(II) with small portions of TBP, and zinc(II) selective extraction with an excess of TBP after iron(III) reduction to iron(II). None of the both versions enables selective extraction of iron(III) or zinc(II). The total removal of iron(III) needs several successive extractions with fresh TBP portions. Zinc(II) can be quantitatively recovered using 5-10 volume excess of TBP.

Stripping both of zinc(II) and iron(III) can be effectively accomplished with water but is not selective. Prior to stripping, the organic phase can be washed with small amounts of water. Scrubbing of TBP solutions containing iron(III) contaminated with zinc(II) gives always a mixture of zinc(II) and iron(III) which must be recycled to the extraction step in continuous process. Scrubbing of TBP solutions containing zinc(II) and iron(II) enables the removal of iron(II) with some amounts of zinc(II) (5-16%). Again, the solution must be recycled. The

removal of iron(II) by scrubbing with water supports the idea of unspecific iron(II) transfer in the cores of reverse micelles.

Zinc(II) extraction from a real spent pickling solution in the presence of iron(II) with an excess of TBP is as efficient as in case of model solutions.

The following technological concept is proposed: reduction of iron(III) to iron(II), extraction of zinc(II) with 5-10 volume excess of TBP, washing of TBP phase contaminated with iron(II) with small volumes of water and recycling of the scrubbings and stripping of zinc(II) with water from loaded TBP.

ACKNOWLEDGMENT

The work was supported by the grant 32-044/05 DS.

REFERENCES

1. P. Maass, P. Peissker (1998), *Hot-dip Galvanising,* Agencja Wydawnicza Placet, Warsaw.
2. B. Gopfert (1998), Ruckgewinnung von Zink aus zinkhaltigen Abfällen der Feuerverzinkungsindustrie - Ökologische und ökonomische Bewertung, *ABAG Projektbericht.*
3. T. C. Lo, M. H. J. Baird, C. Hanson (1991), *Handbook of Solvent Extraction,* Krieger Publishing Company, Malabar, Florida.
4. M. Regel, A. M. Sastre, J. Szymanowski (2001), *Environ. Sci. Technol.,* 35, 630-635.
5. R. Cierpiszewski, I. Miesi^c, M. Regel-Rosocka, J. Szymanowski (2002), *Ind. Eng. Chem. Res.,* 41, 598-603.
6. M. Bartkowska, M. Regel-Rosocka, J. Szymanowski (2002), *Physicochem. Problems Min. Proc.,* 36, 217-224.
7. M. Regel-Rosocka, P. Zawistowski, A. M. Sastre, J. Szymanowski (2003), *Pol. J. Appl. Chem.,* 67, 83-94.
8. M. Regel-Rosocka, K. Alejski, A. M. Sastre, J. Szymanowski (2003), *Chemical Industry and Environment IV,* Macias Machin A., Umbria J. (Eds), Universidad de Las Palmas de Gran Canaria, vol. 1, pp. 377-386.
9. K. Alejski, S. Gorzelanna, M. Regel-Rosocka, J. Szymanowski (2002), *Chemistry for Agriculture,* Gołecki H., Dobrzahski Z. and Kafarski P. (Eds), Prague - Bruxelles - Stockholm, CZECH-POL TRADE, vol. 4, pp. 709-717.

CLOUD POINT SEPARATION OF PHENOLS

Katarzyna Materna*, Achim Schaadt'*, Hans-Jörg Bart** and Jan Szymanowski*

'Poznan University of Technology, Poznan, Poland
"Technical University of Kaiserslautern, Kaiserslautern, Germany

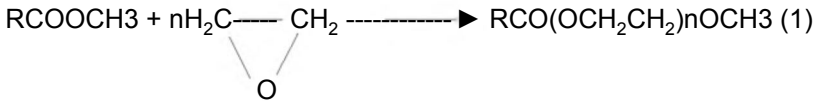
The removal of phenols from aqueous streams by the cloud point extraction technique was studied. New oxyethylated methyl dodecanoates with various average degrees of oxyethylation (n) were used as nonionic surfactants. The effect of surfactant hydrophobicity, electrolyte content, the hydrophobicity of solutes on recovery of phenols was determined. The overheating of 20°C over CP was selected as sufficient. It was found that the recovery of phenols depended mainly on the hydrophobicity and proton donor acidity of solutes. The recovery of phenols was enhanced by the electrolyte presence. The obtained results could be explained by the linear solvation energy relationship (LSER) proposed by Abraham for micellar systems.

INTRODUCTION

The removal of pollutants from aqueous industrial streams and wastewaters remains an important challenge. In the perspective of the development of new separation methods based on innovative concepts. The cloud point (CP) extraction technique is a promising method of separation based on the concept of one-phase system.. The cloud point phenomenon occurs when micellar solutions of nonionic or zwitterionic surfactants are heated. Surfactants separate from aqueous solutions above the cloud point - after some time the second surfactant rich phase separates. The surfactant rich phase and a micellar phase can co-exist in equilibrium. These phases differ in their hydrophilicity and hydrogen bond basicity and acidity. As a result, organic solutes can be transferred to the surfactant rich phase. The concentration of surfactants in the initial aqueous feed is only few percent. As a result, the separated surfactant-rich phase has a relatively small volume in comparison to the volume of the initial feed. Thus, the method permits both the separation and enrichment of the solute [1],

Up to now polyoxyethylated alkylphenols were usually used, and only in a few cases polyoxyethylated alcohols were applied. It is obvious that polyoxyethylated alkylphenols are not surfactants for the 21st century. Therefore we decided to carry out our studies using

oxyethylated fatty acid methyl esters. They seem to be prospective surfactants as they are synthesized by a direct reaction of fatty acid methyl esters with ethylene oxide:



avoiding one step of the synthesis, i.e. hydrogenolysis of fatty acids or their methyl esters to fatty alcohols.
Oxyethylated fatty acids exhibit similar surface activity as typical nonionic surfactants [3], They are biodegradable surfactants which hydrolyze easily in sewage systems to non-toxic and non-surface active components [2],

The aim of work was to study the separations of selected phenols (phenol, 4-chlorofenol, 2,4-dichlorophenol, 4-fluorophenol, 4-methylphenol, 4-methoxyphenol, 4-nitrophenol) by the cloud point technique using oxyethylated methyl dodecanoates as environmental friendly surfactants. The effect of surfactant hydrophobicity, electrolyte content, the hydrophobicity of solutes on recovery of phenols was determined.

EXPERIMENTAL PART

Reagents

The following phenols were used: phenol, 4-chlorofenol, 2,4-dichlorophenol, 4-fluorophenol, 4-methylphenol, 4-methoxyphenol, 4-nitrophenol, al pure, Aldrich, Germany. Oxyethylated methyl dodecanoates with the average degree of oxyethylation from 5 to 14 were obtained from the Institute of Heavy Organic Synthesis, Kedzierzyn-Kozle, Poland. The abbreviation OMD-i will be further used for oxyethylated methyl dodecanoates, where “i” denotes the average degree of oxyethylation. Sodium chloride was used as an electrolyte, and water from reverse osmosis as a solvent.

Separation Procedure

Cloud Point, abbreviated as CP, was determined in the classical way by the heating of the solution above the cloud point, i.e., when the solution became turbid, and then its slowly cooling with an intensive mixing. The procedure was repeated few times to check the reproducibility and to obtain the average value. The error did not exceed 1 deg. The concentrations of surfactants and sodium chloride were changed up to 5 and 20%, respectively. The temperature at which the solution became transparent was assumed as the cloud point.
2.5% solutions of oxyethylated methyl dodecanoates were used for separations. The concentration of phenols was changed from 0.05 to 0.25 g/L. The concentration of sodium chloride was zero or 1 mol/L. pH of the aqueous solutions was below 3.5.

Analytical procedure

The concentration of phenols was determined spectrophotometrically. The continuous spectra were obtained using a SHIMAMADZU 215 spectrophotometer, Japan. The quantitative measurements at the wavelength corresponding to the maximum absorption were maid using a SECOMAM spectrophotometer type S.750, France. The concentrations of phenols were calculated analytically from the calibration data.

RESULTS AND DISCUSSION

Oxyethylated methyl dodecanoates as being nonionic surfactants show the cloud point phenomenon. The clouding occurs at lower temperature in comparison to oxyethylated alcohols. As a result, even in the case of surfactants having a long polyoxyethylene chain, e. g. for the average degree of oxyethylation equal 14, the cloud point in deionized water is below 75°C [publikacja]. Thus, these surfactants are very convenient for separations. The cloud point depends mainly upon the degree of oxyethylation and decreases with a decrease of the polyoxyethylene chain length. The effect of surfactant concentration is observed only in the region of low concentrations (below 1%) [4],

The separation of the surfactant rich phase is a slow process and about 12 hours is needed to achieve complete and reproducible separations [4, 5],

Effect of electrolytes

Salting-out electrolytes such as NaCl and $NaHC0_3$ cause a dehydration of the polyoxyethylene chain resulting in a significant decrease of the cloud point according to eqs. 2 and 3:

$$CP = -0.7n^2 + 20.6\,n - 9.2\,C_{Naa} - 81.8 \qquad R^2 = 0.985 \qquad (2)$$

$$CP = -0.7n^2 + 21.2/7\text{-}19.9\,C_{WaHC}03 - 87.4 \qquad R^2 = 0.985 \qquad (3)$$

Salting-in electrolytes, e .g., KSCN, increase the CP, but the effect is smaller in comparison to the addition of salting-out electrolytes. The effect is caused by a decreased association of water molecules resulting in an increased hydration of the polyoxyethylene chains with non-self-associated water molecules according to eq. 4.

$$CP = -0.6n^2 + 19.5/7 + 10.2\,C_{KSCW} - 77.1 \qquad R^2 = 0.989 \qquad (4)$$

The effects of salts can be separated on the effects of individual ions. Both cations (Na^+ and K^+) decrease CP in the same way causing a similar dehydration of the polyoxyethylene chain. The effect is strengthened by an increased self-association of water molecules occuring in the presence of Cl^- and $HC0_3^-$. However, SCN^- destroys the structure of water, increasing in this way the possibility of monomer water molecules to form hydrogen bonds with oxygen atoms of the polyoxyethylene chain. As a result, an increase of the cloud point is observed.

Water activity

The cloud points of oxyethylated methyl dodecanoates of various hydrophilicity was correlated with water activity. It were found linear relationships between log *CP* and log a_w (Figure 1).

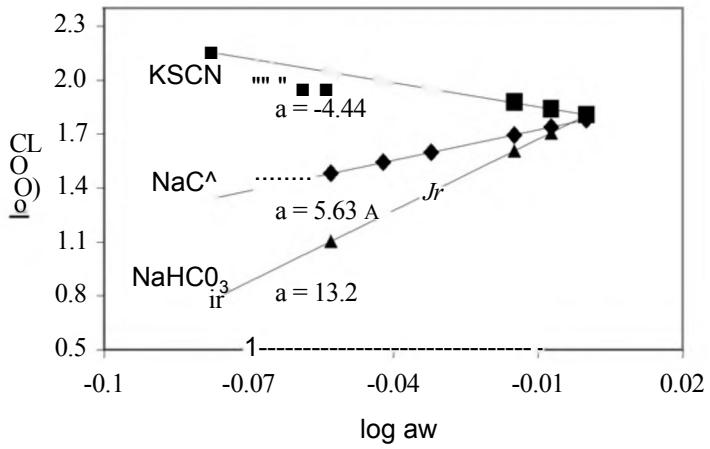


Figure. 1. Relationship between log CP and log a_w (C_0MD-n = 1%) in the presence of electrolyte.

Finally, the values of cloud points can be correlated with length of polyoxyethylene chain and water activity. For a given electrolyte the following relationships were obtained:

– for 1 M NaCl $CP = [165.5\log n - 112.0](aw)^{5'63}$ (5)

– for 1 M $NaHC0_3$ $CP = [165.5\log n - 112.0](a_w)^{13'2}$ (6)

– for 1 M KSCN $CP = [165.5\log n\text{-}112.0](a_w)^{'4\,4}$ (7)

The exponents of water activity in eqs. 5-7 accepted the characteristic positive values for salting-out electrolytes (NaCl, $NaHC0_3$) and negative value for salting-in electrolyte (KSCN). The different effects of salting-out and salting-in electrolytes on the cloud points were confirmed.

Recovery of phenols

The overheating of 20°C was selected to compare the efficiencies of separations.

Percent separation (%E) of pollutant is defined by eq. 8:

$$\%E = \frac{V_F \cdot C^0_F - V_M \cdot C_M}{V_F \cdot C^0_F} \cdot 100\% \qquad (8)$$

when V_F denotes the volume of the feed, V_M is the volume of the separated micellar phase 0°_F and and C_M stand for the pollutant concentrations in the feed and separated micellar phase, respectively.

The recovery percents (*%E)* for solutions containing solutes with and without electrolyte are given in Table 1. They change in the following order: 4-methoxyphenol < 4-fluorophenol < phenol < 4-methylphenol < 2,4-dichlorophenol < 4-nitrophenol < 4-chlorophenol. The recovery of phenols is increased in the presence of sodium chloride.

Table 1. Recovery percent (%E) for solutions with and without electrolyte ([OMD-nf = 2.5%, [iPollutantf = 0.1 g/L), ACP = 20°C.

Pollutant	Deionized water		With 1 M NaCl	
	%E	s.d.	*%E*	s.d.
Phenol	52.0	1.4	65.1	1.3
4-Chlorophenol	80.9	1.9	89.6	1.4
4-Fluorophenol	38.0	3.2	71.1	3.2
4-Methoxyphenol	21.4	3.6	61.3	1.7
4-Methylphenol	64.9	1.6	69.1	1.5
4-Nitrophenol	72.2	2.5	79.6	2.3
2,4-Dichlorophenol	70.4	5.5	90.2	3.1

Linear solvation energy relationship (LSER)

Separation by cloud point technique can be explained by the linear solvation energy relationship (LSER) introduced by Abraham [6]:

$$\log (sp) = c + rR_2 + sI_2 + aZa_2 + bip_2 + vV_x \quad (9)$$

where: *c, a, b, s, r, v* denote numerical coefficients; Sa£ - the solute hydrogen-bond acidity; $\Sigma\beta_2^H$ - the solute hydrogen-bond basicity; π_2^H the solute dipolarity /polarizability, R_2 - the solute excess molar refraction; V_x - the McGowan characteristic volume; sp - *%E.* The value of la_2 , ip" , π_2 and R_2 can be found in literature, and the value of V_x can be calculated from solute structure [6, 7],

The following relationships were obtained for a series of studied solutes (after elimination of least important terms):

- separations in the absence of sodium chloride

$$\%E = 4.40Ea_2^H - 85.03Sp_2^H - 29.21n£ + 97.02R_2 + 35.41V, \quad (10)$$

$R^2 = 0.995$; s.d. = 4.01; F = 326.3.

– separations in the presence of 1 M NaCl

$$\%E = 40.02£a_2^H - 116.1Zp_2^H - 90.65V, \quad (11)$$

R^2 = 0.992; s.d. = 6.12; F = 359.1.

The surfactant rich phase shows a higher hydrogen bond accepting ability than the aqueous phase. As a result, an increase of the solute hydrogen bond donating power increases the transfer of solute to the surfactant rich phase. The effect of the solute hydrogen bond ability is opposite, i.e. negative as the aqueous phase has a significantly higher ability to donate proton than the surfactant rich phase. That ability depends upon the water content in the aqueous and surfactant rich phase. The aqueous phase contains the surfactant in the concentration near cmc. The content of water in the surfactant rich phase depends upon the temperature (i.e., the overheating over the cloud point - A *CP)* and the electrolyte content.

CONCLUSIONS

The cloud point phenomenon can be successfully used to recovery toxic pollutants (phenols) from aqueous solutions. Oxyethylated methyl dodecanoates are convenient nonionic surfactants for such separations. Separation by cloud point technique can be explained by the linear solvation energy relationship (LSER) proposed by Abraham.

ACKNOWLEDGEMENTS

The work was supported by a grant from the Polish State Committee for Scientific Research, KBN No. 3 T09D 055 26.

REFERENCES

1. W. L. Hinze and E. Pramauro (1993), *Crit. Rev. Anal. Chem.,* 24, 133-177.
2. I. Szwach, W. Hreczuch and P. Fochtman (2002), *5th World Conference on Detergents, Reinventing the Industry: Opportunities and Challenges*, A. Cahn (Ed), AOCS Press, Champain, Illinois, 163.
3. K. Alejski, E. Bialowas, W. Hreczuch, B. Trathnigg and J. Szymanowski (2003), *Ind. Eng. Chem. Res.,* 42, 2924-2933.
4. K. Materna, I. Milosz, I. Miesiac, G. Cote and J. Szymanowski (2001), *Environ. Sci. Technol.,* 35, 2341-2346.
5. K. Materna and J. Szymanowski (2002), *J. Colloid Interface Sci.,* 255, 195-201.
6. M.H. Abraham (1993), *Chem. Soc. Rev.,* 22, 73-83.
7. M.H. Abraham, H.S. Chadha, J.P. Dixon, C. Rafols and C. Treiner (1995), *J. Chem. Soc. Perkin Trans. 2, 5,* 887-894.

SEPARATION OF PHENOLS BY MICELLAR ENHANCED ULTRAFILTRATION

Katarzyna Materna and ^Jan Szymanowski

Poznan University of Technology, Poznan, Poland

Micellar enhanced ultrafiltration (MEUF) of solutions containing phenols was studied. Oxyethylated fatty acid methyl ester (OMD), alkylpolyglucoside (APG), sodium dodecylsulfate (SDS) and hexadecyltrimethylammonium bromide (CTAB) were used as representatives of nonionic, anionic, cationic surfactants. It was found that MEUF enable high recovery of phenols without using any hydrocarbon solvents. CTAB and SDS are appropriate surfactants for this technique. The recovery of phenols could be estimated by the micelle binding constants or from linear solvation free-energy relationships according to the Abraham model.

INTRODUCTION

Phenols are toxic pollutants, frequently found in waste streams, but also in surface and tap waters. They are listed in the US Environmental Protection Agency priority list of pollutants and in the 76/464/EEC Directive of the European Union, related to hazardous substances discharged into the aquatic environment. Solvent extraction is the most often used technique to recover phenols from various aqueous effluents. Classical extraction exhibits important drawbacks, connected with discharge of wastes containing dissolved solvents, or even dispersion or emulsion of solvents in water. These problems can be eliminated using membrane processes. Direct removal of phenols by ultrafiltration of aqueous solutions is not possible. Such separation can be achieved using surfactant solutions in which organic pollutants are solubilized in surfactant micelles.

The effectiveness of micellar enhanced ultrafiltration (MEUF) in removing organic compounds from aqueous stream owes to the fact that surfactant micelles containing these contaminants are too large to pass through the pores of the ultrafilter. In this process a surfactant is added to the aqueous stream and forms micelles which solubilize pollutants, so that the subsequent ultrafiltration step produces a permeate stream, passing through the membrane nearly free from impurities, while most of the target solutes and the added surfactant are retained in the retentate [1],

The aim of the work was to study ultrafiltration of surfactant solutions containing different phenols (phenol, 4-chlorophenol, 2,4-dichlorophenol, 4-fluorophenol, 4-methylphenol, 4-methoxyphenol and 4-nitrophenol). Oxyethylated fatty acid methyl esters (OMD), alkylpolyglucoside (APG), sodium dodecylsulfate (SDS) and hexadecyltrimethylammonium bromide (CTAB) were used as representatives of nonionic, anionic, cationic surfactants. These surfactants seem to be non-hazardous for the environment.

Oxyethylated methyl fatty acid methyl esters are new biodegradable surfactants which hydrolyze easily in sewage systems to non-toxic and non-surface active components [2], Generally, aquatic toxicity of oxyethylated fatty acid methyl esters is one order lower compared to that of oxyethylated alcohols. Biodegradability tests performed on activated sludge following the OECD Confirmatory Test procedure No. 82/242/EEC at the certified laboratory show the biodegradation level of oxyethylated fatty acid methyl esters and oxyethylated alcohols equal to 88.4-93.3 and 83.2-90.4%, respectively [3].

APG is non-toxic and is easy biodegradable as it contains an oligoglucose moiety. SDS hydrolyzes quickly in aqueous solutions giving dodecanol, especially in acidic and neutral solutions. Cationic surfactants are used in small quantities, compared with anionic surfactants present in detergent compositions, and they precipitate in the form of salts with anionic surfactants.

EXPERIMENTAL PART

Chemicals

The following surfactants were used: hexadecyltrimethyl ammonium bromide - CTAB (purum), Chemapol, Czech Republic, sodium dodecyl sulphate - SDS (purum), BDH, Great Britain, alkylpolyglucoside Glucopon 215 CS UP abbreviated further as APG, Henkel, Germany and oxyethylated methyl dodecanoate (OMD) of an average oxyethylation degree equal to 11 (OMD-11), Institute of Heavy Organic Chemicals, Kedzierzyn-Kozle, Poland. Phenols (pure): phenol, 4-chlorophenol, 2,4-dichlorophenol, 4-fluorophenol, 4-methylphenol, 4-methoxyphenol and 4-nitrophenol were obtained from Aldrich, Germany.

GLUCOPON 215 CS UP is an alkaline 50% aqueous solution. The surfactant contains 8-10 carbon atoms in the alkyl group. The oxyethylated methyl dodecanoates were obtained in the presence of calcium based catalyst under the conditions similar to those used for the oxyethylation of alcohols and alkylphenols .

Ultrafiltration experiments were carried out at 22 ± 1°C, with an Amicon 8010 (USA) stirred cell having a volume of 10 ml. A nitrogen pressure of 0.35 MPa was applied. The hydrophilic Millipore membrane (PLGC type) with a micellar weight cut-off of 10,000 Da was made of regenerated cellulose. Equal volumes of pollutant and surfactant solutions (5 ml each) were introduced into a filtration module and pH was adjusted to 3. The solution present in the module was stirred for 5 minutes with a magnetic stirrer and then it was filtered until 5 ml of

permeate was obtained while stirring vigorous. The concentrations of the surfactants amounted to 9.7-1CT^2, 9.2-10'^{3}, 1.1-10'^{2}, 9.8-IO^M for SDS, CTAB, APG and OMD and were equivalent to 10 cmc in distilled water. The concentrations of pollutants in the permeate and retentate were determined by UV at the maximum wavelength, using surfactant solutions of appropriate concentrations (1 cmc and 19 cmc for permeate and retentate, respectively) as a reference. A Secomam 750 (France) spectrophotometer was used. Continuous UV/VIS spectra were recorded on a Shimadzu 215 spectrophotometer (Japan).

RESULTS AND DISCUSSION

Phenols are week acids. pK_a values for considered phenols are in the range 7.23 - 10.28 in water. It means that at the pH values considered in this paper (pH = 3), phenolic pollutants in pure water are present only in nonionic forms. The situation is different in micellar solutions containing CTAB and SDS. The charged micelles of the cationic surfactant accumulate hydroxyl groups in the Stern layer. Thus, the local pH at the micelle interface is higher, compared with the one measured in solution. As a result, the apparent K_A value increases and enhanced dissociation of week acids (phenols) is observed. The opposite effect is observed in micellar solutions of anionic surfactants [4, 5],

In acidic media, which are very convenient from the point of view of the pollutant acid-base equilibrium, the hydrolysis of SDS and APG can occur [6, 7], To eliminate the hydrolysis, separation was made directly after pH adjusting.

Recovery of phenols

Recovery of phenols (Table 1) can be characterized by rejection R_{AlUF} and micelle binding constant $K_{A,UF}$:

$$K_{AUF} = \frac{H}{\text{“lAMs]-cmc)}} \qquad (1)$$

$$R_{A.UF} = \left(1 - \frac{HI}{HJ}\right) \cdot 100\% \qquad (2)$$

where A and S denote the pollutant and the surfactant respectively, and the subscripts P, R, M and W stand for the permeate, retentate, micellar pseudophase and aqueous pseudophase, respectively. [S] - cmc is the concentration of the surfactant which contributes to the surfactant pseudophase, and $[A]_M$ and $[A]_w$ are the concentrations expressed in the total volume of the solution.

The values of R_{AlUF} and log K_{AUF}, calculated from ultrafiltration experiments (Table 2), indicate that satisfactory rejections of phenols are observed for SDS and CTAB solutions. The exception is the rejection of phenol and 4- methoxyphenol for CTAB. Alkylpolyglucoside is not an appropriate surfactant for the recovery of the considered pollutants. The rejection up to 50% were obtained only for 4-nitrophenol and 4 chlorophenol. In teh case of OMD-11 the best rejection were obtained for 2,4-dichlorophenol and 4-nitrophenol.

Table 1. Rejection $R_{A,UF}$ (%) and binding constant K_{AUF} calculated from ultrafiltration experiments.

Pollutant	CTA B		SDS		APG		OMD-11	
	$R_{A.UF}$	log $K_{A.UF}$	$R_{A.UF}$	log $K_{A.UF}$	$R_{A.UF}$	log $K_{A.UF}$	$R_{A.UF}$	log $K_{A.UF}$
4-methylphenol	72.8	2.20	86.2	1.55	39.8	1.52	51.2	1.76
phenol	33.6	1.49	66.2	1.05	20.3	1.11	43.4	1.59
4-fluorophenol	64.0	2.03	74.9	1.23	19.4	1.09	31.2	1.31
4-methoxyphenol	44.7	1.69	71.1	1.15	20.3	1.11	26.7	1.21
4-chlorophenol	91.1	2.79	92.7	1.86	53.3	1.76	72.3	2.24
2,4-dichlorophenol	96.5	3.22	88.5	1.64	39.8	1.52	80.1	2.41
4-nitrophenol	99.4	4.00	78.0	1.31	60.3	1.89	78.5	2.37

All this means that CTAB or SDS solutions are preferred for recovery of phenols.

Abraham model

Linear solvation free energy relationship (LSER) has proven to be useful for understanding processes that involve the transfer of solutes between two phases. The following linear model was proposed by Abraham [8, 9]:

$$\log SP = c + aZ\,cx_2^{H} + bZ\,(3_2^{H} + sn_2^{H} + rR_2 + vV_x\,/100 \qquad (4)$$

where *SP* refers to the property of interest for a series of solutes, Sou and lp, account for solute hydrogen bond acidity and basicity, respectively, TT_2 stands for solute dipolarity, R_2 is excess molar refraction and V_x is solute molar volume; *c, a ,b, s, r*, and v are regression coefficients. The value of Xocj , Zp? ■ TT_2 and R_2 can be found in literature, and the value of t/xcan be calculated from solute structure [8, 10],

The following equation for $R_{A,UF}$ is obtained:

- for CTAB

$$R_{A.UF} = -72.3 + 53.55xx" - 193.4Zp£ - 14.3i£ + 36.3f?_2 + 182.4t/_x/1$$

- for SDS

$$R_{AUF} = 12.3\ 0.31XCX?\ 78.6SP? - 25.1TI" + 11.2R_2 + 137.4V_x\ /100 \qquad (6)$$

The dominant contributions to the solute binding and then rejection in ultrafiltration experiments arise from the terms in V_x and Zp_2^n • The former reflects the hydrophobic effect. As a result, more hydrophobic solutes are better bound by micelles and better rejected in ultrafiltration. The high negative coefficients at the Xp_2 terms imply that solute hydrogen bond basicity strongly favors partitioning to the aqueous pseudophase, i.e. that bulk water is a much better hydrogen bond donor that the solubilization sites in the micelles.

The values of Ea“ and Xp^ depend upon the substituent and they change in a typical way,

i.e., Sot” increases and Xp“ decreases in the presence of electron withdrawing

substituents. The strongest effect is observed for the nitro group. The molar volume is sensitive upon the substituent and it increases in the presence of any substituent.

The effect of solute dipolarity is negative but relatively weak, indicating that the dipolarity of the bulk water is only slightly lower than that of micelles solubilizations sites. The effect of solute excess molar refraction is positive but also week in CTAB and SDS solutions. This means that neither water nor the micelles of these surfactants provide a polarizable solubilization environment. The parameter is important for nonionic surfactant because polyoxyethylene chain contributes to the polarizability of micellar solubilizations sites.

Hydrogen bond acidity makes little or no contribution to micellar solubilization in SDS, indicating that hydrogen bond basicity of the micellar solubilization environment is comparable to that of bulk water. Thus, the hydrogen bond acidity of the solute makes little or no contribution to micellar solubilization and then rejection in ultrafiltration. The effect is positive and relatively strong for CTAB and nonionic surfactant solutions, i.e., solute hydrogen bond acidity favors pollutant incorporation into micelles and rejection in ultrafiltration.

All this means that strongly hydrophobic pollutants can be easily bound by micelles and their high rejections can be achieved in ultrafiltration, irrespective of the choice of micelles. Low hydrophobic pollutants can be also rejected in ultrafiltration but only in the presence of attractive electrostatic interactions. Thus, the use of cationic and anionic surfactants is favored for rejections of pollutants having acidic and basic group(s), respectively.

CONCLUSIONS

It was found that micellar enhanced ultrafiltration enable high recovery of phenols without using any hydrocarbon solvents. CTAB and SDS are appropriate surfactants for this technique. The recovery of phenols could be estimated from the micelle binding constants or from linear solvation free-energy relationships according to the Abraham model. The efficiency of separation increased with an increase of pollutant hydrophobicity and excess molar refraction. Hydrogen bond acidity of pollutants improved separation from systems containing nonionic surfactants and CTAB, but it did not affect the separation in the presence of SDS. Hydrogen bond basicity and dipolarity of pollutants decreased the recovery. The derived models enable the selection of pollutants, which can be efficiently removed from aqueous streams by micellar enhanced ultrafiltration.

ACKNOWLEDGEMENTS

The work was supported by a grant from the Polish State Committee for Scientific Research, KBN No. 3 T09D 055 26.

REFERENCES

1. J.F. Scamehorn and J.H. Harwell (Eds.) (1989), *Surfactant-Based Separation Processes,* Marcel Dekker, New York, pp. 3-28.
2. K. Alejski, E. Bialowas, W. Hreczuch, B. Trathnigg and J. Szymanowski (2003), *Ind. Eng. Chem. Res.,* 42, 2924-2933.
3. I. Szwach, W. Hreczuch and P. Fochtman (2002), *5th World Conference on Detergents, Reinventing the Industry: Opportunities and Challenges,* A. Cahn (Ed), AOCS Press, Champain, Illinois, 163.
4. E. Pramauro, A.B. Prevot, P. Savarino, D. Viscardi, M. de la Guarda and E.P. Cardells (1993), *Analyst,* 118, 23-27.
5. S.D. Christian, G.A. Smith, E.E. Tucker and J.F. Scamehorn (1985), *Langmuir,* 1, 564-569.
6. K. Hill, W. Rybinski and G. Stol (Ed.) (1996), *Alkyl Polyglycosides, Technology, Properties and Application,* VCH Publisher Inc., Weinhem.
7. M. Muramitsu and M. Inove (1976), *J. Colloid Interface Sci.,* 55, 80-84.
8. M.H. Abraham (1993), *Chem. Soc. Rev.,* 22, 73-83.
9. F.H. Quina, E.O. Alonso and J.P. Farah (1995), *J. Phys. Chem.,* 99, 11708-11714.
10. M.H. Abraham, H.S. Chadha, J.P. Dixon, C. Rafols and C. Treiner (1995), *J. Chem. Soc. Perkin Trans. 2,* 5, 887-894.

THE USE OF IONIC LIQUIDS IN SOLVENT EXTRACTION PROCESSES

Kelly K. L. Yung,[a] Jilska M. Perera,[3] Craig Smith[15] and Geoffrey W. Stevens[3]

[3] Department of Chemical and Biomolecular Engineering, The University of Melbourne, VIC, 3010, Australia.
[b] GlaxoSmithKline Australia Ltd., Port Fairy, VIC, 3284, Australia.

In this study, room temperature ionic liquids (RTILs) have been investigated as an alternative to volatile organic solvents (VOSs), in solvent extraction processes. The RTILs have been used in a range of applications by various researchers due to their very low vapour pressure, ability to dissolve a range of organic, inorganic and organometallic compounds, and their immiscibility with water and ability to form biphasic systems. This research work has focussed on determining the physical properties of two ionic liquids, namely 1-butyl-3-methylimidazolium hexafluorophosphate [bmim][PF_6] and 1-hexyl-3-methylimidazolium bis((trifluoromethyl)sulfonyl)imide [hmim][Tf_2N] and comparing these properties to the conventional organic solvents, xylene/benzyl alcohol (BA) and xylene/tributylphosphate (TBP) to determine their potential as replacements solvents. Physical properties such as the interfacial tension, viscosity and density were determined. Also, the solubility of water in these solvents was measured. Distribution ratio versus pH were obtained for four systems [bmim][PF_6]/water, [hmim][Tf_2N]/water, xylene/TBP/water and xylene/BA using amine containing compounds as solutes.

INTRODUCTION

Many applications such as those in the pharmaceutical, insecticide and fragrance industries use volatile organic solvents (VOSs) for extracting natural products or compounds of interest. However, many of these VOSs are essentially toxic and flammable leading to safety concerns in operating plants and potential to contaminate the final product. Over recent years, room temperature ionic liquids (RTILs) continue to draw attention as solvents for green technology [1,2]. Viscosities of RTILs range from less than 10 to over 400cP [3,4], which are significantly higher than traditional VOSs and therefore make these solvents more difficult to handle and perhaps require the re-engineering of the contacting equipment. The viscosity amongst other physical properties may be affected by water solubility [5], Water miscibility is largely dictated by the anion and ionic liquids with anions such as the halide, ethanoate, nitrate, dicyanamide and trifluoroacetate are generally miscible with water [6-8] and those with anion hexafluorophosphate or bis((trifluoromethyl)sulfonyl)imide can readily form a biphase with water [9-12],

In this research, ionic liquids (ILs) that can form biphasic systems with water were investigated for solvent extraction applications. Hence, two different dialkylimidazolium ionic liquids, one containing anion hexafluorophosphate and the other containing

bis((trifluoromethyl)sulfonyl)imide were studied. These are compared to some of the conventional VOSs.

EXPERIMENTAL SECTION

Tyramine (99% pure) and 2-methoxyphenethylamine (MPEA) (98% pure), anhydrous methanol (99.8% pure) from Sigma-Aldrich were used as received in this work. Chemicals used for the synthesis of [bmim][PF_6] were either AR grade or HPLC grade and were also obtained from Sigma-Aldrich, except for the high purity nitrogen from BOC and silver nitrate from MERCK. Xylene, benzyl alcohol (BA) and tributylphosphate (TBP) were all LR grade and [hmim][Tf_2N] (AR grade) were from MERCK. Hydranal®-Composite 5 from Riedel-de Haen was used as received.

A Karl Fischer titrator (Metrohm 701 KF Titrino, Switzerland) was used with Hydranal®-Composite 5 and anhydrous methanol for the titrations to determine the water content of [bmim][PF_6], [hmim][Tf_2N], xylene/BA and xylene/TBP. Densities were determined directly from the pycnometer volume and the mass of the sample. Interfacial tensions were measured using the First Ten Angstrom (FTA200) instrument (USA), which was operated with the FTA Video Drop Shape Software, and viscosities were determined using the Rheometric Scientific SR5 rheometer.

The distribution ratios were obtained by performing shake-up tests, which involved the mixing of equal volumes of the aqueous phase of known pH containing the solute and the solvent on an orbital shaker (OM6 Orbital Mixer, Ratek Instrument Pty. Ltd., Australia) at 130 rpm until the system reached equilibrium (3-4 hours). The aqueous phase pH was re-measured at 20 ± 1°C after separation of the two phases, the concentration of solute in the aqueous phase was determined using HPLC. The solute in the solvent from all systems was back extracted into 10%v/v glacial acetic acid in one wash, which was then analysed quantitatively by HPLC. The equipment consisted of a Waters Model 590 pump, Waters 712 WISP injector, Waters M-490 programmable multi-wavelength detector and a Varian 4270 integrator. The column used was a Waters Symmetry® C_{18} 5pL 3.9 x 150 mm and the sonicator for degassing the mobile phase was a Soniclean 120HT. The mobile phase was made up of Milli-Q® water, acetonitrile (HPLC grade from EM Science), glacial acetic acid (HPLC grade from Science Supply), trifluoroacetic acid (100%HiPerSolve from MERCK) and ammonium acetate (AR grade 98.0% pure from MERCK). All chemicals were used as received without further purification. The flow rate of the mobile phase was 1 mL/min and detection for both tyramine and MPEA was at 280 nm.

COMPARISON BETWEEN IONIC LIQUIDS AND COVENTIONAL VOLATILE ORGANIC SOLVENTS

The physical properties of [bmim][PF_6], [hmim][Tf_2N], xylene/BA and xylene/TBP are compared in Table 1. In liquid-liquid extraction systems, high interfacial tension is desired as it enhances coalescence and reduces loss of the aqueous phase in the solvent and vice versa [13]. Comparing the four systems studied, [hmim][Tf_2N] had the highest interfacial tension (14.0 mN/m) followed by xylene/TBP (13.3 mN/m), [bmim][PF_6] (10.6 mN/m) then xylene/BA (7.2 mN/m), which implied phase separation between [hmim][Tf_2N] and water would occur quickest. The viscosity of [bmim][PF_6] was approximately 200 times that of xylene/BA (1.85 cP) and xylene/TBP (1.61 cP), which made the IL more difficult to handle. Even though [hmim][Tf_2N] (89 cP) is significantly lower than [bmim][PF_6], it is still considerably (about 50 times) more viscous than the VOSs.

It was important to determine the water content of the solvents since the presence of water can effectively change their physical and chemical properties, especially in the case of [bmim][PF_6] due to its hygroscopicity. The water content in [bmim][PF_6] was found to be 0.17 wt.% after synthesis but after saturation, the water content increased to

2.04 wt.%. This was in agreement with Marsh et. al. [14]. The water content in [hmim][Tf_2N] as received from MERCK was an order of magnitude less than that of [bmim][PF_6] but when saturated with water, the water content was half that of [bmim][PF_6j. The two organic solvent systems also increased in water content after saturation. It was observed that of the four systems, [hmim][Tf_2N] absorbed the least amount of water.

Table 1. Physical properties of [bmim][PF_6], [hmim][Tf_2N], xylene/BA and xylene/ TBP systems. (T = 20 ± 1°C.)

Physical Property	[bmim][PF_6]	[hmim][Tf_2N]	xylene / BA	xylene / TBP
Density (g/ml_)	1.353	1.364	0.943	0.910
Viscosity (cP)	312* *	89 @ 25°C#	1.61*	1.85*
Interfacial Tension (mN/m)	10.6	14.0	7.2	13.3
Water Content before shaking with water (wt.%)	0.17	0.02	0.55	0.05
Water Content after shaking with water (wt.%)	2.04	0.97	2.59	1.72
Maximum Distribution Ratio (tyramine as solute) (D_{max})	0.5 (pH 9.4)	0.2 (pH 9.0)	3.2 (pH 9.9)	1.1 (pH 10.1)
'Distribution Ratio (MPEA as solute) (D) @ ~pH 12.5 ±0.9	14.6	16.3	349	15.3

* D_{max} cannot be determined when MPEA is the solute for the pH range studied.
* Viscosity data supplied by MERCK.

The partitioning behaviour of tyramine and MPEA as a function of pH was determined in the four different liquid-liquid systems and this was expressed in terms of the distribution ratio (D) and is defined as follows:

$$D = \frac{\text{Concentration of solute in solvent phase}}{\text{Concentration of solute in aqueous phase}}$$

Tyramine and MPEA (see Figures 1 & 2 for structures) were used as solutes because they are representative of compounds used in some of the natural products industries. The systems studied were [bmim][PF_s], [hmim][Tf_2N], xylene/BA and xylene/TBP as the non-aqueous phase and water. The results are summarised in Table 1 and Figures 1 and 2.

Tyramine Extraction

In the organic systems using tyramine as solute, the maximum distribution ratio, D_{max} = 3.2 in xylene/BA and D_{max} = 1.1 in xylene/TBP occurred at about pH 10. In [bmim][PF_6] and [hmim][Tf_2N], D_{max} = 0.5 and 0.2 respectively were displayed at around pH 9. In

* cone and plate (Since |bmimJ[PF_6| was much more viscous that VOSs, it w as possible to avoid using bob and cup, w hich required a larger sample to obtain accurate measurements.)

* bob and cup

both xylene/BA and xylene/TBP systems, the distribution ratio decreased to essentially zero in pHs below 7 and pHs above 13. This was due to tyramine having two ionisable groups, an amine group and a phenolic group. The pK values to the groups are around 9.3 and 10.9 [15-18], When the pH is 9.3 or lower and 10.7 or higher the tyramine molecule is ionised, and thus has a high solubility in the aqueous phase, resulting in decreasing distribution ratios.

The inability to load tyramine appreciably into the ILs, and the tendency for tyramine to remain dissolved in the ILs at pH < 7, make them unsuitable for extracting tyramine. Figure 1 shows a comparison of all the solvent systems using tyramine as solute. The error bars in the plots from Figure 1 were obtained from triplicate HPLC readings for each of the shake-up tests for the varying pHs.

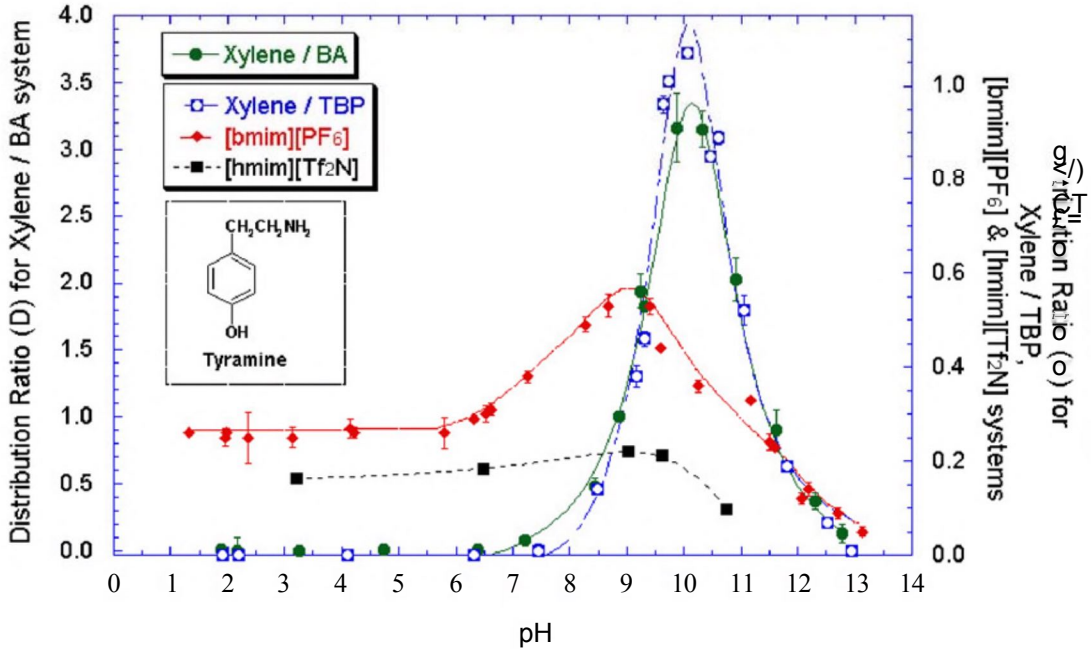


Figure 1. Distribution ratio versus pH with tyramine as solute in xylene/BA/water, xylene/TBP/water, [bmim][PF_6]/water and [hmim][Tf_2N]/water systems.
The lines have been added for clarity and do not represent a theoretical fit.

2-Methoxyphenethylamine Extraction

When MPEA was used as a solute, like tyramine, some partitioned into the ILs in the acidic pHs. However, since MPEA has only one ionisable group, as the pH is increased it is less ionised and partitions into the non-aqueous phase. The pK value of MPEA is reported as 10.20 at 25°C [18], Hence, with all systems studied, MPEA displayed increasing distribution ratios as the pH is increased, especially when pH > pK ~10. From Figure 2, it can be observed that in the IL systems, MPEA cannot be completely back extracted into the aqueous phase with only one wash because of its solubility in the ionic liquid at pH < 7. Several washing stages will be necessary to recover the MPEA from the loaded ionic liquid systems, compared to the VOS systems.

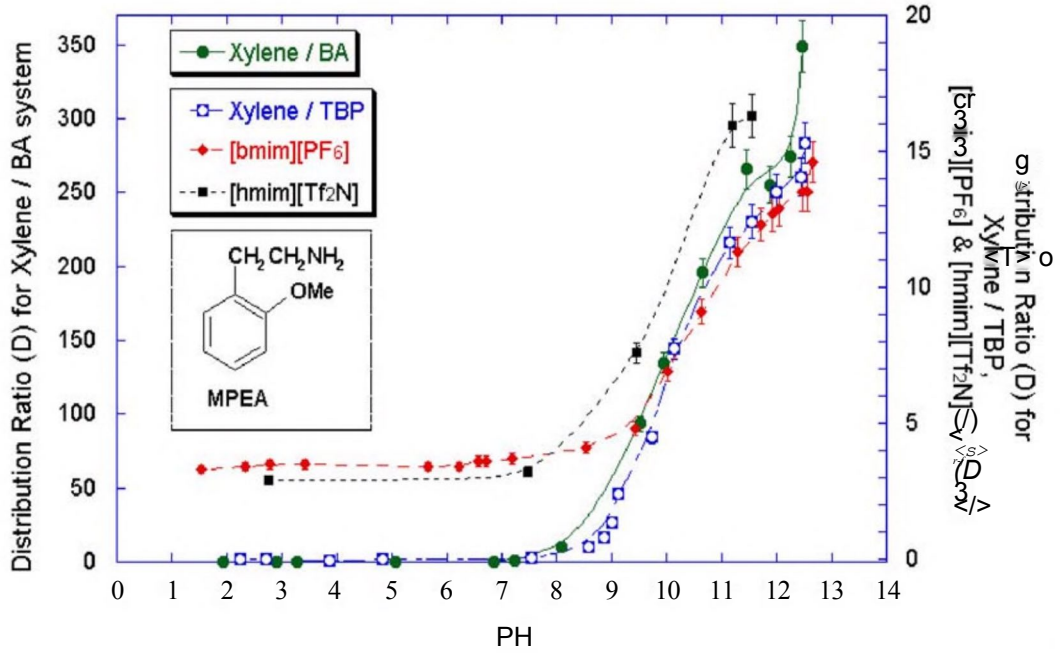


Figure 2. Distribution ratio versus pH with 2-methoxyphenethylamine (MPEA) as the solute in xylene/BA/water, xylene/TBP/water, [bmim][PF_6]/water and [hmim][Tf_2N]/water systems.
The lines have been added for clarity and do not represent a theoretical fit.

CONCLUSION

Using tyramine as the solute, the following systems seemed most effective for solvent extraction in decreasing order: xylene/BA > xylene/TBP > [bmim][PF_6] > [hmim][Tf_2N]. With MPEA as solute, all four systems displayed higher distribution ratios than the tyramine with the [hmim][Tf_2N] system proving slightly more effective than [bmim][PF_6]. Stripping of tyramine and MPEA from xylene/BA and xylene/TBP systems were attained with a 0.1 - 7.4 % error in the material balance.

It was found that even though the viscosity of [hmim][Tf_2N] was appreciably lower than [bmim][PF_6], both ionic liquids are still significantly more viscous than conventional VOSs. This can lead to difficulty in handling, especially the bulk quantities required for industrial scale. Hence, cosolvents to reduce viscosities may be necessary but this could lead to changes in the physical, chemical properties and solvent extraction capabilities of the ionic liquids, which would then need to be investigated. Even if the cosolvents are VOSs, if the combination of ionic liquid and VOS displays high extraction abilities, the fact that the use of VOSs is reduced, is a start to a more environmental approach to solvent extraction.

ACKNOWLEDGEMENTS

This work was made possible with the financial support of the Australian Research Council (ARC), GlaxoSmithKline Australia Ltd. (GSK) and the Particulate Fluids Processing Centre (PFPC). The assistance from Dr. Peter Scammels and co-workers at Victorian College of Pharmacy at Monash University in synthesising the ionic liquid, [bmim][PF_6], was greatly appreciated.

REFERENCES

1. R.D. Rogers, K.R. Seddon (2003), *Ionic Liquids as Green Solvents: Progress and Prospects*, ACS Symposium Series 856, American Chemical Society, Washington, DC, 599 pp.
2. R.D. Rogers, K.R. Seddon (2002), *Ionic Liquids: Industrial Applications for Green* Chemistry, ACS Symposium Series 818, American Chemical Society, Washington, DC, 474 pp.
3. A.B. McEwen, H.L. Ngo, K. LeCompte, J.L. Goldman (1999), *J. Electrochem. Soc.*, 146, 1687-1695.
4. H. Matsumoto, H. Kageyama, Y. Miyazaki (2001), *Chemistry Letters,* 2, 182-183.
5. K.R. Seddon, A. Stark, M-J. Torres (2000), *Pure Appl. Chem.,* 72, 2275-2287.
6. P. Bonhote, A-P. Dias, M. Armand, N. Papageorgiou, K. Kalyanasundaram, M. Grätzel (1996), *Inorg. Chem.,* 35, 1168-1178.
7. C.F. Poole, B.R. Kersten, S.S. Ho, M.E. Coddens, K.G. Furton (1986), *J. Chromatogr.,* 352, 407-425.
8. S. Pandey, K.A. Fletcher, S.N. Baker, G.A. Baker (2004), *Analyst,* 129, 569-573.
9. U. Schroder, J.D. Wadhawan, R.G. Compton, F. Marken, P.A.Z. Suarez, C.S. Consorti, R.F. de Souza, J. Dupont (2000), *New J. Chem.,* 24, 1009-1015.
10. D.S.H. Wong, J.P. Chen, J.M. Chang, C.H. Chou (2002), *Fluid Phase Equilib.,* 1194, 1089-1095.
11. J.L. Anthony, E.J. Maginn, J.F. Brennecke (2001), *J. Phys, Chem. B.,* 105, 2879-2885.
12. L. Cammarata, S.G. Kazarian, P.A. Salter, T. Welton (2001), *Phys. Chem. Chem. Phys.,* 3, 5192-5200.
13. R.W. Cusack, P. Fremeaux, D. Glatz (1991), *Chemical Engineering,* Feb, 66-76.
14. K.N. Marsh, A. Deev, A.C-T. Wu, E. Tran, A. Klamt (2002), *Korean J. Chem. Eng.,* 19, 357-362.
15. A.G. Ogston (1936), *J. Chem. Soc.,* 1713.
16. G.P. Lewis (1654), *Brit. J. Pharmacol.,* 9, 488-493.
17. S. Riegelman, L.A. Strait, E.Z. Fischer (1962), 51, 129-133.
18. T. Kappe, M.D. Armstrong (1965), *J. Med. Chem.,* 8, 369-374.

A CONTINUOUS SOLVENT EXTRACTION PROCESS FOR THE VALORIZATION OF ZINC FROM SLUDGE LEACHING LIQUORS

D.-L. Tambwe, D. Pareau, G. Durand and M. Stambouli

Ecole Centrale Paris/LGPM, Châtenay-Malabry 92295, France

CYANEX 301 dissolved in n-dodecan and modified by octanol-1 was used to extract zinc from a strong acidic sulphate ferrite's leaching liquor. From thermodynamics and kinetics studies, conditions for a selective and quantitative extraction were found. Cementations onto the leaching liquor prior to solvent extraction proved to be useful for both environmental sight and effective long term process running. Zinc was quantitatively stripped from its extracted organic complex using aqueous NaOH. Laboratory scale mixer-settlers tests achieved the required level of zinc separation within only two single extraction stages, confirming Me Cabe & Thiele predictions. The global hydrometallurgical process flowsheet developed represents an adding value to ferritic zinc resources with an environmental clean option.

INTRODUCTION

As primary zinc resources are becoming scarce and the associated mining costs increasing, industrial interest has been prompted to the investigation and development of suitable new routes for processing the large amounts of metallic scrap, as well as metallurgical residues that are available all around the world.

The present issue has taken advantage of the association of liquid-liquid extraction technique and solution chemistry to investigate and then design a simple process to quantitatively recover zinc in presence of large amounts of iron dissolved in the acidic leaching solution to produce a suitable electrolyte for an industrial electrowinning. Chemical composition of the fresh leaching liquor was as follows [1]:

Table 1. Typical composition of a fresh sulphuric leaching liquor (\SO^]$_{lot}$=\ ,6M).

Element	Concentration (g/l)	Element	Concentration (g/l)
Al	0.20	Fe(II)	38.82
As(III)	0.21	Fe(III)	4.19
Ca	0.09	Mn(II)	0.45
Cd	0.14	Ni(II)	0.02
Co	0.02	Zn	14.39
Cu	2.03	pH	0.3-0.5

CYANEX 301, whose active component is the bis(2,4,4-trimethylpentyl)dithiophosphinic acid (98,5-99,0%), has been chosen as the main extractant, diluted in dodecan. This dialkyl-dithiophosphinic acid supersedes CYANEX 272, its non sulphured analogue known for years

to very effectively extract Zn from sulphate acid media, working at even lower pH [2,3,4], Recent studies has shown the good stability of CYANEX contacted with 3 mol/l sulphuric acid for 3000 hours at 60°C [5], Moreover, the extractant allows an excellent extraction selectivity for Zn(II) versus calcium and the others earth elements at the considered liquor pH [6], Octanol-1 has been used as a modifier for its interfacial properties allowing better and quicker settlings of the organic and aqueous phases.

A preliminary series of tests conducted on a synthetic solution similar to the leaching liquor having shown the most likely co-extraction of Co^{2+}, Cd^{2+} and Ni^{2+} (*Figure 1),* a zinc powder cementation was decided onto the liquor [1], This step intended also to comply with the environmental aspects of the process development, especially regarding its outflows and final residues which had to obey drastic constraints. Deadly environmental As and Cd were thus removed from the leaching solution, avoiding harmful off-streams rejections from the process.

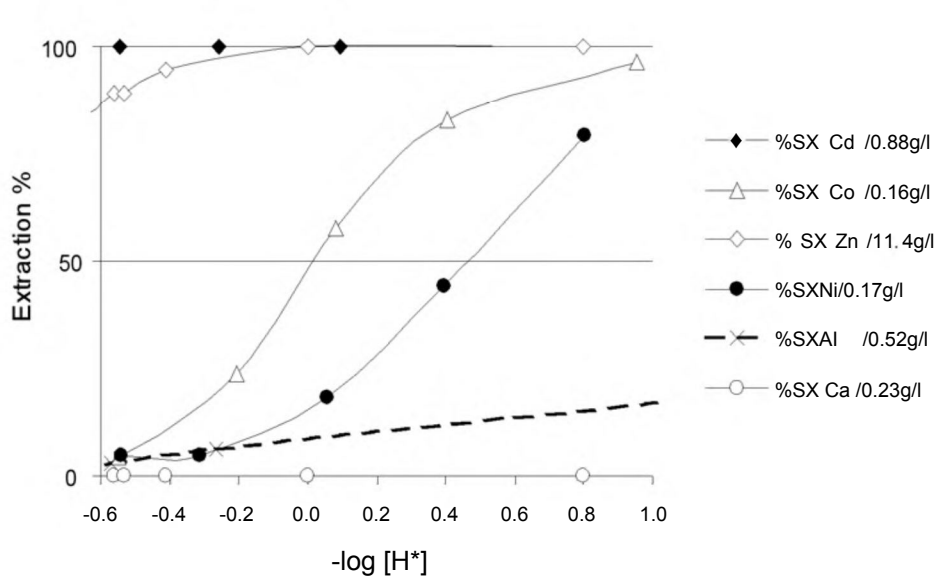


Figure 1. Metal extraction by CYANEX 301 /octanol-1/n-dodecan system versus acidity (total sulphate concentration = 1.6mol/l; phase's contact time= 20min; T=21±1 °C).

Apart of Zn(II), only iron(III) remained the species mostly to be up-taken at equilibrium by CYANEX 301 for pH ranges below 0.5 and thus every effort has been made to keep as low as possible the latter's concentration, regarding the slow atmospheric oxidation of ferrous iron readily occurring. An ultimate reduction by iron powder onto the liquor, prior to its entering liquid-liquid extraction section, allowed a lowering of the residual concentration of ferric iron below 100 mg/l. While the so-called ferric iron pre-extraction problem could hopefully be fixed in this way, drastic savings in organic solvent inventories were also expected, especially regarding the alternative strategy coupling the ferric iron extraction with the reductive stripping of iron used for D_2EHPA extraction system [7,8,9,10],

EXPERIMENTAL

Materials and reagents

The original samples of neutral leaching residues were supplied by *GECAMINES (Générate des Carrières et de Mines)* from its zinc plant, *UZK (Usines à Zinc de Kolwezi),* in Democratic Republic of Congo. Composition of the leaching solution after iron and zinc powder cementations is shown below [1] :

Table 2. Typical composition of the leaching solution after cementations ($[SOI]_{to}$,=\.6M).

Element	Concentration (g/l)	Element	Concentration (g/l)
Al	0.20	Fe(ll)	41.89
As(lll)	ND	Fe(lll)	< 0.10
Ca	0.09	Mn(ll)	0.47
Cd	ND	Ni(ll)	ND
Co	ND	Zn	13.73
Cu	ND	PH	0.5

Except for the n-dodecan which was of technical purity (>35% v/v) all the other chemicals used were of analytical grade (sulphuric acid, oxalic acid, iron(ll) sulphate, iron(lll) sulphate, sodium sulphate and zinc sulphate from Fisher Scientific, sa., tributyle phosphate and octanol-1 from Merck, and CYANEX 301 from Cytec Industries).

Batch experiments have been conducted to investigate metal extraction kinetics and thermodynamics. For each experiment 25 to 100 ml of organic solvent were added to the appropriate volume of aqueous solution. The mixture was stirred at constant temperature. The organic extract was then contacted with an aqueous NaOH solution for zinc back-extraction. Chemical analysis were done on both aqueous and organic samples after extraction and stripping and mass balances verified.
A series of continuous counter-current extraction experiments have been performed onto a laboratory mixer-settler pilot according to the Me Cabe & Thiele settings to prove the technical feasibility of the designed solvent extraction process.

RESULTS AND DISCUSSIONS

Separation selectivity and speciation

Kinetics of both metals extracted by CYANEX 301 from the synthetic solution are presented hereafter *(figure 2).* Running global kinetic experiments ensured for similar interfacial and settling areas.

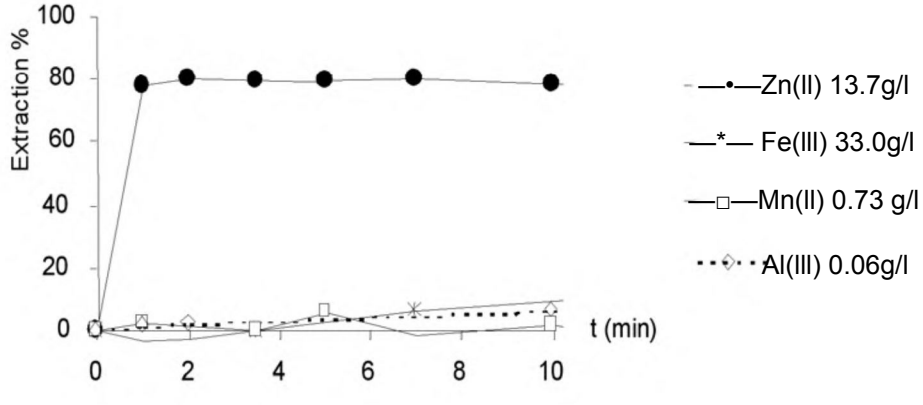


Figure 2. Global kinetic extraction with CYANEX® 301 (0.36M)/octanol-1 (20% vA/)/n-dodecan (v_{stirr} =930rpm; T=30 ±1°C)

While Zn(ll) extraction equilibrium was reached after one minute, Mn(ll) and Al(lll) being extracted to less an extent than 0.2%, Fe(lll) extraction equilibrium requires 4 hours to be reached. The ratio of Zn (II) and Fe(lll) initial extraction rate, $k£^{*,n)}/k\%^{*n)}=0.0$ showed out that a good extraction selectivity was attainable by taking advantage of the process kinetics. An optimal contact time for the aqueous and organic phases was found to be 30 to 45s.

Slope analysis has been used for the identification of the thermodynamic mechanism of zinc extraction according to a cationic exchange equilibrium :

$$Zn^{2+} + (m+n)\overline{HA} \rightleftharpoons \overline{ZnA(HA)_m} + nH^{+} \qquad (1)$$

Due to the higher octanol-1 concentration, CYANEX 301 was considered as being mainly a monomer species [11], The Zn distribution factor can be written in a logarithmic form as :

$$\log D_{Zn} = \log K + n\log[H^{+}] + (m+2)\log[\overline{HA}] \qquad (2)$$

The successive derivations of expression (2), respective to pH (at constant CYANEX concentration) and log$[\overline{HA}]$ (at constant pH), are graphically displayed in *figures 3* and *4.*

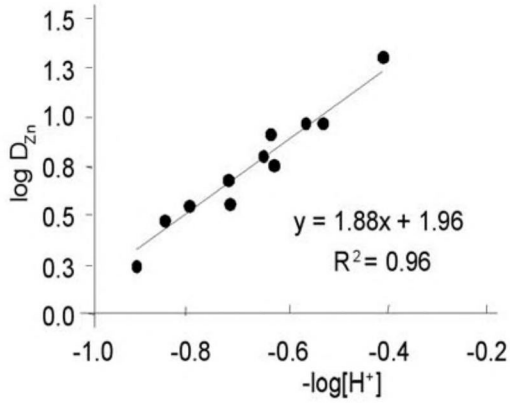


Figure 3. Extraction of Zn^{2+} by CYANEX® 301 (0.36M) / octanol-1 (20% v/v) /n-$C_{12}H_{26}$ (Vstirr =930rpm; t_{CO}ntact=5min ; T=21±1°C)

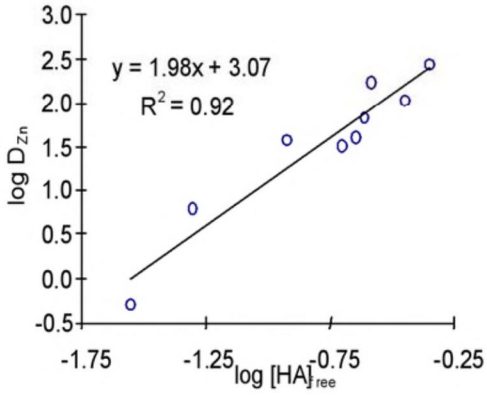


Figure 4. Extraction ofZn^{2+} as a function of CYANEX 301 concentration (Vstirr = 930rpm; t_{CO}ntact=5min ; T= 21 ±1°C)

Thus, the extracted metallic complex is ZnA_2 (n=2 ; m=0) and the equilibrium constant, ^/"=$10^{307\pm0.2}$.

The extraction isotherm of *Zn²** has been compared to the simulated curve computed after the assumed mechanism *(fig.* 5).

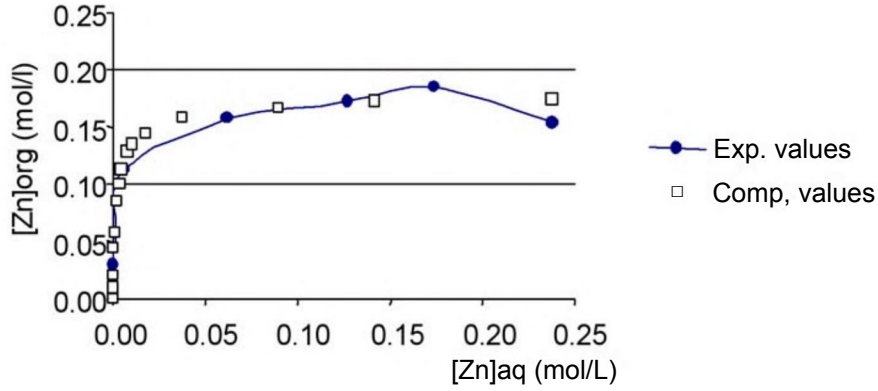


Figure 5. Extraction isotherm of Zn² by CYANEX 301 (0.36M) at pH=0.5 ([$S0_4^{2'}$]=1.6M; v_{st}in^930rpm; t_{CO}ntact=5min ; T=21±1°C)*

The fairly good similarity between the two curves fully supported the proposed extraction reaction. It is worth to notice that at saturation loading two moles of CYANEX 301 (i.e. 0.36 mol/l) reacted with one mole of *Zn²** (0.18 mol/l).

Me Cabe & Thiele diagram

The Me Cabe & Thiele construction for zinc extraction is illustrated *(fig. 6)* for a volume phase ratio (A:0) of 0.7 and pH=0.5 to recover 99.9% of the metal with less than 10.0 mg/l of co-extracted iron. Two stages were expected to reach the goal.

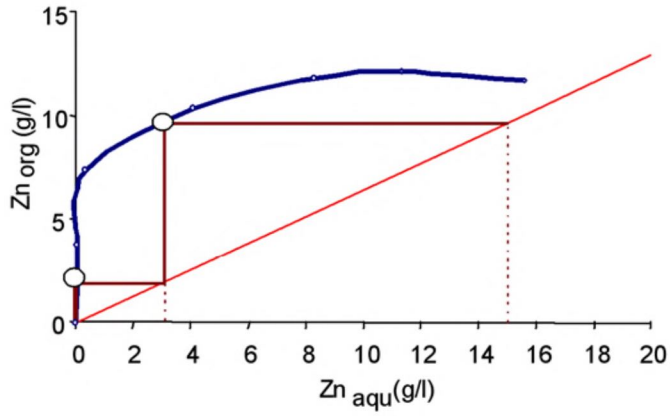


Figure 6. Me Cabe & Thiele diagram forZn² extraction by CYANEX 301 (0.36M)/ octanol-1 (20%) in n-dodecan*
(^{v}aqi/^{v}org = 0.7; v_{stirr} = 930 rpm; $t_{conlact}$=5 min ; T=22±1°C)

Zinc stripping

Zinc was quantitatively stripped from organic phase in only one contact using NaOH 4M with a phase ratio v_{aqu}/v_{org}= *V₂* . Organic and aqueous phases settling was optimal for less than 10

mg/l of iron loaded within the initial extract. More organic iron dramatically increased settling time (*figure 7).*

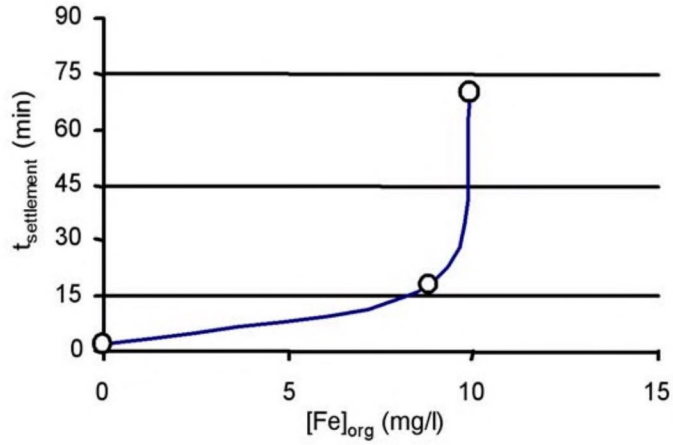


Figure 7. Settlement times after zinc stripping from CYANEX® 301 by NaOH as a function of organic Fe(III) content (T=38 ±1°C)

Continuous counter-current tests

The results of the laboratory scale piloting onto mixer-settlers units operated counter-currently with two extraction stages were the following (*Table 4).*

Table 4. Solvent extraction process efficiency onto the industrial liquor

	Extraction(pH=0.5;A/S=0.7;v_{stir}=600rpm)				Stripping(A/S=0.5;$v_s$ti,=300rpm;40°C)			
Element	Zn (II)	Al(III)	Fe(III)	Mn(II)	Zn (II)	Al(III)	Fe(III)	Mn(II)
Organic (g/l)	9.7	< 0.0005	< 0.006	<0.0002	0.26	-	< 0.001	-
Yield (%)	> 95.0	0.0	0.0	0.0	> 97.5	-	> 85.1	-

These results proved the feasibility of the solvent extraction process with CYANEX 301/n-dodecan system to quantitatively and selectively recover zinc from a strong acidic leaching liquor even in presence of large amounts of iron (III) and both alkaline and earth elements.

Loaded iron readily precipitated from its organic phase as $Fe(OH)_{Hs)}$ during stripping. The slow precipitation of iron has been thought to be responsible of the poor phases settling.

CONCLUSIONS

Analytical physical-chemistry of solutions has been associated to hydrometallurgical operations, to rationally design a solvent extraction process for zinc recovery from a strong acidic leaching liquor. The process was designed with most environmental requirements concern and, such that, represents an adding value to ferritic zinc resources with an environmental clean option. The global hydrometallurgical flowsheet process is presented hereafter.

ACKNOWLEDGEMENTS

D.-L. Tambwe wishes to thank both French Ministry of Cooperation for scholarship granted him under ref. N°EGIDE 256180H, together with GECAMINES (GCM/Centre, GCM/Géo) for both material supplied and expert level discussions.

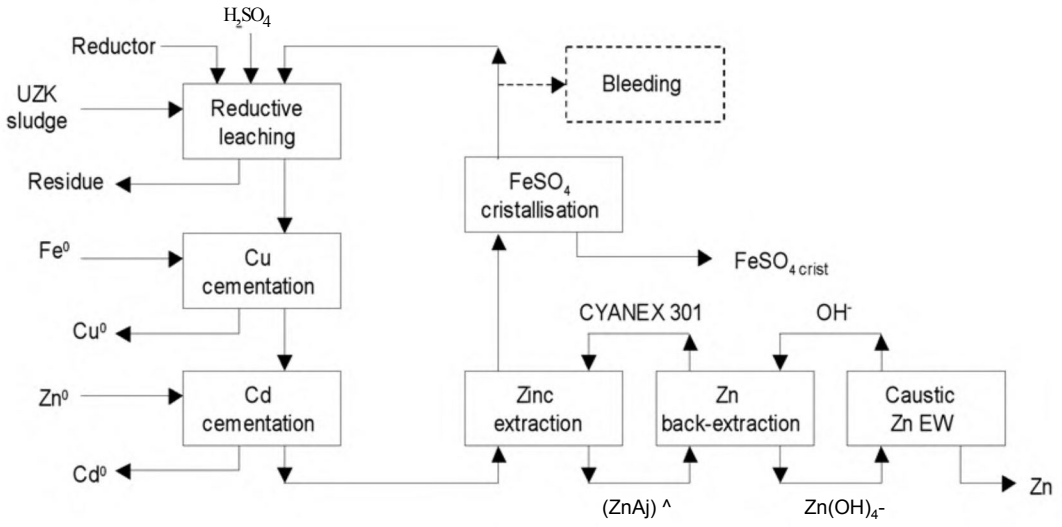


Figure 8. SX based hydrometallurgical flowsheet for valorising metals from residues

REFERENCES

1. D.-L., Tambwe (2004), *Ph D Dissertation,* Ecole Centrale Paris, 92295, France, 216p.
2. W.A., Rickelton, R.J., Boyle (1990), *Solvent Extraction & Ion Exchange* 8, 783-97
3. A. Nayak, et al. (1995), *Indian J. Chem. Technoi,* 2, 2.
4. C., Wang, D., Li (1995), *Solvent Extraction & Ion Exchange*, 13, No. 3, 502-523
5. K.C., Sole, J.B. Hiskey, T.L., Ferguson (1993), *Solvent Extraction & Ion Exchange,* 11, 783-796
6. CYANEX® Solvent Extractant Database, Cytec Industries Inc., West Paterson, NJ, USA
7. J., Sun, T.J., O'Keefe (2002), *Environmental Minerals Engineering* 15, 177-185
8. H„ Majima, T., Izaki, S., Sanuki (1985), *Metall. Trans. B* 16B, 187-194
9. B., Belew, J.R., Harlamovs, T.J., O'Keefe et al.(1993), *Hydrometallurgy Fundamentals: Technology and Innovation,* AIME, Littleton CO, pp. 817-830
10. M.S., Moats, T.J., O'Keefe (1996), *Second International Symposium on Extraction and Processing for the Treatment and Minimization of* Wastes, TMS, Warrendale PA, pp. 673-684
11. G., Cote, J.-V., Martin, D., Bauer, Y., Mottot (2002), *Proceedings of ISEC 2002,* Johannesburg, RSA, pp291-298

APPLICATION OF BLOCK COPOLYMER IN THREE-LIQUID-PHASE EXTRACTION SYSTEM

Shufeng Shen, Zhidong Chang, Xinghua Sun, Xin Hu and Huizhou Liu

Laboratory of Separation Science and Engineering, State Key Laboratory of Biochemical Engineering, Institute of Process Engineering, Chinese Academy of Sciences, Graduate school of the Chinese Academy of Sciences, Beijing, 100080, PR China

A novel three-liquid-phase extraction system (TES) composed of butyl acetate (BA), block copolymer [polyethylene oxide-polypropylene oxide-polyethylene oxide (PEO-PPO-PEO)] and ammonia sulphate aqueous solution [$(NH_4)_2S0_4$] as top, middle and bottom phase respectively has been developed. The copolymer recycling and partitioning behaviour of penicillin V has been studied in this system. Results showed that the copolymer could be purified and recycled and penicillin V of the filtrated ferment broth could be partitioned unevenly among the phases and purified in the top phase of this TES. About 90% (weight percent) of penicillin V could be distributed into the top phase around pH2.5 and only less than 0.1% left in the bottom phase.

INTRODUCTION

Polyethylene oxide-polypropylene oxide-polyethylene oxide (PEO-PPO-PEO) block copolymers are non-ionic surfactants and include hydrophilic PEO and hydrophobic PPO segments. Due to the presence of PPO central block, PEO-PPO-PEO copolymers have lower cloud point than poly (ethylene glycol) (PEG) with same molecular mass. Therefore, thermoseparation is one of important properties of block copolymers. [1, 2]

Three-liquid-phase extraction system (TES) is considered as an exploring-worthy, promising method of separating and purifying complex systems. It offers the possibility of separation of two or more compounds or groups by single step extraction [3, 4], Chen et al. [5] developed a TES contained butyl acetate (BA), PEG, ammonia sulphate ($(NH_4)_2S0_4$) and water for one-step extraction and purification of penicillin G in 2002. However, separation and recycling of PEG is a tough work, which limits this system further application and development. Therefore, how to solve the recycling of components forming phases has been the focus in the three-liquid-phase extraction field recently.

Phenoxymethyl penicillin (penicillin V) is an important oral antibiotic. Partition behaviour of penicillin V is not clear in the TES because of the polymer phase introduction. Furthermore, deep understanding about distribution of Penicillin V in TES will be greatly helpful for individual and selective separation from penicillin V and phenoxyacetic acid mixture.

In this study, we has applied block polymer to form a novel TES. The aim is not only to separate effectively objective substances, but also to offer a probable solution to realize recycling of polymers forming phase. Moreover, Phase behaviour of the TES contained block copolymer and effects of pH on the partition behaviour of penicillin V among the phases were

investigated.

EXPERIMENTAL

PEO-PPO-PEO, a block copolymer (average molecular weight 2,200) of 60% ethylene oxide and 40% propylene oxide, was obtained from Sigma-Aldrich Inc. Potassium penicillin V and filtrated ferment broths were obtained from North China Pharmaceutical Corporation limited. Other chemicals were of analytical reagent grade. All the concentrations of compositions were calculated as percentage of weight (w/w). Stock solutions of sulphate salt 40% and the copolymer 40% were previously prepared to be used in TES.

The three-liquid-phase systems, composed of 8.35% polymers, 8.35% ammonia sulphate and 30.45% BA, were prepared with a final mass of 28.70 g at room temperature. All the phase-forming compositions, the filtrated ferment broth or solution of Potassium penicillin V were added from stock solutions. Then 10% (v/v) H_2S0_4 solution was added to adjust the pH which was controlled by pH meter (pH211, HANNA, Italy). Then, the phase separation was enhanced by centrifugation for 10 min at 2,000r/min. Three phase volumes and the concentration of penicillin V in each phase were determined accurately.

The concentration of penicillin V was analyzed by high performance liquid chromatography (HP1100 Agilent Technologies, USA) with UV at 254nm as detector [6], A Cl8 column (250mmx4.6mmx5pm, Agilent Technologies, USA) was used. Samples were eluted isocratically with water-acetonitrile-glacial acetic acid (64.5:35:0.5, v/v) at a flow rate of I.Oml/min. The concentration of ammonium sulphate was measured by the formaldehyde method [2], The copolymer was determined by drying portions of sample solution in an infrared oven at 70°C [7], The copolymer concentration can be obtained by subtraction the weight of the salt which is calculated from the method mentioned above. BA was analyzed by gas chromatography among the phases with FID as detector [8], A sample of 0.3pl was injected, and the capillary column is HP-5 (30mx0.32mmx0.5(.im) (HP6890 Agilent Technologies, USA).

Distribution ratios of penicillin V are defined by the concentration ratio between the phases as follows:

$$D_{tb} = \frac{C_t}{C_b}, \quad D_{mb} = \frac{C_m}{C_b}, \quad D_{tm} = \frac{C_t}{C_m}$$

Where C_t, C_m, C_b is the concentration of penicillin V in the top, middle and bottom phase, respectively.

Mass fractions of penicillin V in each phase are defined as follows:

$$w_t = \frac{C_t \times V_t}{m_0}; \quad w_m = \frac{C_m \times V_m}{m_0}; \quad w_b = \frac{C_b \times V_b}{m_0}$$

Where V_t, V_m, V_b is the volume of the top, middle and bottom phase respectively, and m_0 is the total mass of penicillin V added.

RESULTS AND DISCUSSION

Phase behaviour

A three-liquid-phase system with BA/PE0-PP0-PE0/$(NH_4)_2S0_4$/water could be formed and the compositions of equilibrated phase in the TES with 30.45% BA, 8.35% PEO-PPO-PEO and 8.35% $(NH_4)_2S0_4$were shown in Table 1. BA, copolymer and $(NH_4)_2S0_4$ was enriched in the top, middle and bottom phase, respectively (Table 1).

Table 1. Compositions of the equilibrated phases in the TES[a].

Phase	Concentration of compositions, % w/w			
	BA	PEO-PPO-PEO	$(NH_4)_2S0_4$	Water
Top	87.18	11.85	0.22	0.75
Middle	0.50	36.76	2.43	60.31
Bottom	0.13	4.56	12.98	82.33

[a] The TES contained 30.45% w/w BA, 8.35% w/w PEO-PPO-PEO and 8.35% w/w $(NH_4)_2S0_4$ at 298.15K

The copolymer predominates in the middle phase that contained 36.76% (w/w) PEO-PPO-PEO, and the top phase contained 11.85%, and the bottom phase less than 5%. Most of salt was partitioned into the bottom phase. The middle phase was more hydrophobic than the bottom phase but less than the top phase. Hydrophobic or hydrophilic nature of the middle phase may be adjusted by changing average molecular weight of copolymer and compositions of system. Therefore, the system can produce hydrophobic or hydrophilic gradient, and compounds with different properties probably can pass to different phases.

This TES mentioned above was used for extraction of the filtrated broth of penicillin V, as shown in Fig. 1.



Figure 1. Three-liquid-phase extraction of the filtrated broth of penicillin V.

Similar to the BA/poly(ethylene glycol)(PEG)/salts sulphate three-liquid-phase system [5], no emulsion phenomenon took place with demulsifer cancelled and most of the pigments and other biological residues could be left in the middle phase.

Effects of pH on partition behaviour of penicillin V

Concentration of the filtrated ferment broth of penicillin V was about 20 mg/ml. The used TES contained 30.45% BA, 8.35% PEO-PPO-PEO and 8.35% $(NH_4)_2S0_4$ was prepared at 298.15K. The extraction profiles of penicillin V with changing pH and contrast between TES and conventional two-liquid-phase extraction system (CTES) were presented in Figure 2 and Figure3.

Distribution ratio and mass fraction of penicillin V in each phase had greatly changed in the range of pH were investigated in the TES at 298.15K.

Dt/b, $D_{m/b}$ increased sharply with the decreasing pH and go up to 213 and 118, respectively at pH2.6. However, $D_{m/b}$ improved slightly, as shown in Figure 2. $D_{t/b}$ was significantly higher in the TES than that in the CTES and $D_{t/b}$ ratio between two systems was more than 10 at pH3.5. It can be seen from Figure 3 that penicillin V was enriched gradually in the top phase similar to the CTES with decreasing pH. The affinity of penicillin V for the other phases was successively lessened, first for the bottom phase, and then for the middle phase. While

penicillin V favoured in the middle phase at higher pH. w_m and w_b equalled and each accounted for about 45% at pH4.3 and w_m exceeded 65% and little was partitioned into the top phase above pH5.5. As pH was decreased, Penicillin V in the middle phase was transferred to the top phase. About 90% of penicillin V could be found in the top phase around pH2.5 and only less than 0.1% left in the bottom phase.

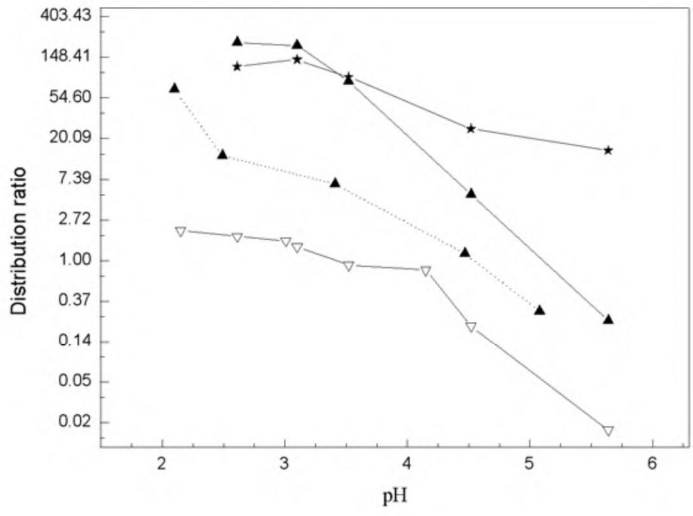


Figure 2. Effect of pH on distribution ratio of penicillin V in each phase at 298.15K.
The TES (—) contained 30.45% w/w BA, 8.35% w/w PEO-PPO-PEO and 8.35% w/w $(NH_4)_2S0_4$. The CTES (...) were composed of BA and water and volume ratio of aqueous to organic phase is 2:1.
V — $Dt/_m$; A — Dt/b; — $D_m/_b$

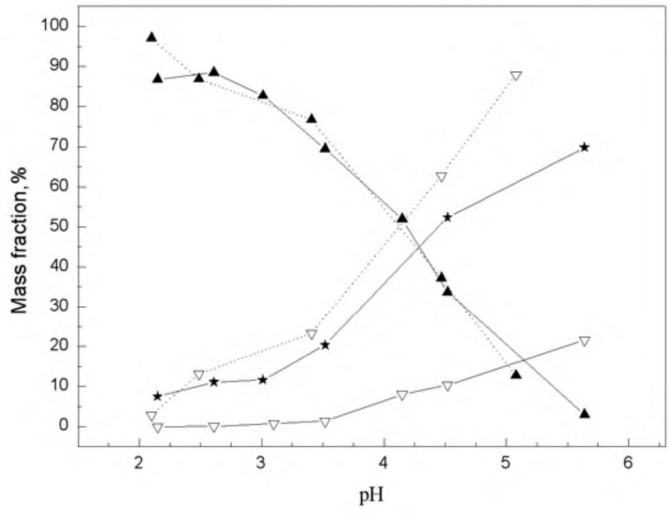


Figure 3. Effect of pH on mass fraction of penicillin V in each phase at 298.15K.
The TES (—) contained 30.45% w/w BA, 8.35% w/w PEO-PPO-PEO and 8.35% w/w $(NH_4)_2S0_4$. The CTES (...) were composed of BA and water and volume ratio of aqueous to organic phase is 2:1.
▲ — w_t; V — w_b; — w_m

It can be deduced that penicillin V (pKs=2.70) with carboxylate functionality exists two states in the aqueous solution: dissociated form and neutral or free acid form, and the concentration of neutral form of penicillin V is related to the total concentration and the pH by the Henderson-Hasselbach relationship [9], Neutral form of penicillin V shows low water solubility and has a relatively strong affinity for hydrophobic compositions. At higher pH, much penicillin V molecular exists as dissociated form in aqueous solution. With decreasing pH, more penicillin V would rather stay in the more hydrophobic top or middle phase. Therefore, penicillin V was almost not found in the strong polar bottom phase and unevenly partitioned into the weakly hydrophobic middle phase, and then was transferred into the top phase.

However, effects of interaction between objective matters, copolymers, etc on partition mechanism need to be further studied. We are now conducting experiments to investigate other polymers, microstructure mechanism and develop new three-liquid-phase systems.

Copolymer recovery

After three-liquid-phase extraction of the filtrated broth of penicillin V, the block copolymer recovery was shown in Fig.4.

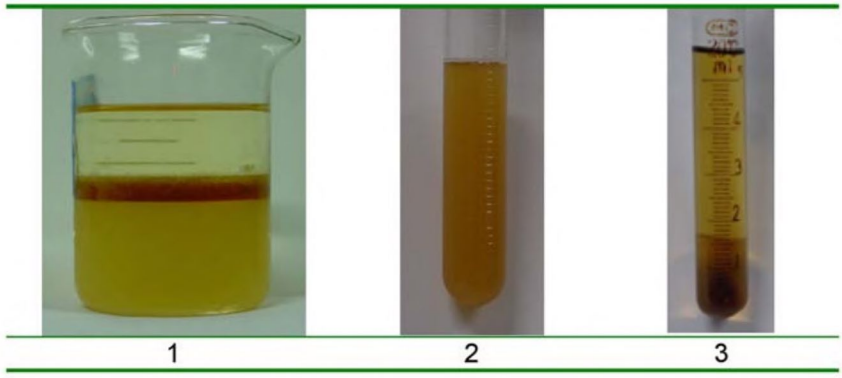


Figure 4. Pictures of three-liquid-phase extraction of the filtrated broth of penicillin V[3] and thermoseparation of the middle phase[b].

1: three-liquid-phase system; 2: the middle phase; 3: thermoseparation of the middle phase

[a] Three-liquid-phase system composed of 30.45% w/w BA, 8.35% w/w PEO-PPO-PEO, 8.35% w/w $(NH_4)_2S0_4$ and the filtrated broth of penicillin V.

[b] Thermoseparation was performed at 75°C for 30 min in a water bath

The middle phase enriched in the copolymer was taken out. After temperature-induced phase separation at 75°C for 30 min, the middle phase could be clearly separated into one upper copolymer-enriched phase and one lower water phase. Most of impurities and residues of broths were squeezed into the interphase or the lower phase. So the copolymer could be purified and recycled.

CONCLUSIONS

A new TES composed of 30.45% BA, 8.35% PEO-PPO-PEO and 8.35% $(NH_4)_2S0_4$ has been developed and the copolymer in the middle phase of TES can be concentrated and purified by thermoseparation.

Penicillin V of the filtrated broth could be partitioned unevenly and purified in the TES. $D_{t/b}$, $D_{m/b}$ increased sharply and $D_{m/b}$ improved slightly with the decreasing pH. $D_{,/b}$ was significantly higher in the TES than that in the CTES. With decreasing pH, more penicillin V would rather stay in the more hydrophobic top or middle phase and only little left in the

bottom phase.

ACKNOWLEDGEMENTS

This work was financially supported by Innovative Research Group Science Fund (No. 20221603) National Natural Science Fund (No. 20406021) and National Natural Science Key Fund (No. 20236050).

REFERENCES

1. J. Persson, A. Kaul and F. Tjerneld(2000), *J. Chromatogr. B,* 743, 115-126.
2. P. Martinha, W. You-Ting, V. Armando and T. José(2003), *Biochem. Eng. J.,* 15, 131-138.
3. M. Mojski and I. Gluch(1996), *J. Anal. Chem.,* 51(4), 329-342.
4. P. A. Albertsson(1986), *Partition of cell particles and macromolecules :* separation and purification of biomolecules,cell organelles,membranes, and cells in aqueous polymer two-phase systems and their use in biochemical analysis and biotechnology , 3rd ed., New York :Wiley
5. J. Chen, H. Z. Liu, B. Wang, Z. T. An and Q. F. Liu(2002), /SEC, Cape Town, 602-606
6. The United States Pharmacopoeias XXIV (2000), Washington, DC: The board of trustees, 1287-1288.
7. A. Salabat(2001), *Fliuld Phase Equilibra.,* 187-188, 489-498.
8. Z. D. Chang, N. Yao, H. Z. Liu and J. Y. Chen(1999), *J. Anal. Chem.,* 27 (1), 118 (in Chinese).
9. V. C. Mahesh, F. P. Gregory, H. R. Charles and L. A. Robert(1995), *Biotechnol. and Bioeng.,* 47(2), 215-226.



EXTRACTION BEHAVIOR AND MECHANISM OF ORGANIC SOLUTES FROM DILUTE SOLUTION BY GREEN SOLVENT DIMETHYL CARBONATE

Jingtao Zhang, Xianglan Piao, Shenlin Zhu
State Key Laboratory of Chemical Engineering, Tsinghua University, Beijing 100084, China

Dimethyl carbonate(DMC) was selected as green extractant to prevent pollution existed in current liquid-liquid extraction process. An experimental investigation of the distribution of organic solutes between DMC and water was carried out and the extraction mechanism of it was studied in this work. Distribution coefficients of 13 substances between DMC and water were determined by experiments. Also comparisons of the distribution coefficients with substance structures were made. Vanillin was selected as an example solute to study the extraction behavior of DMC in detail. Molecular structure of DMC and the interaction of DMC with other molecules were analyzed. Solute distribution coefficient between Octanol and water(P) was proposed as an auxiliary parameter to study extraction mechanics of DMC. Correlation results of the logarithmic form of distribution coefficients (logD) with hydrophobic parameter (logP) showed that they had a quite good linear relationship. This provided one good guide for the application of DMC as a green extractant.

INTRODUCTION

As a highly effective and selective separation technique, liquid-liquid extraction is widely used in petrochemical, pharmaceutical industry and waste water treatment to recover organic solutes from dilute aqueous solution. However, extractants now in use are most solvents with phosphorus, nitrogenous or phenyl group, which are toxic to human body and resist to degradation. During the contact of two phases, extractants dissolve in the second phase or are carried away by it and in turn make pollution to the environment. With strict regulations over environment being established and more attention being paid to environmental protection, these extractants must be replaced by green solvent to eliminate pollution in liquid-liquid extraction process.

Currently, many researchers have carried out such researches and employed supercritical

fluids[11'31], room temperature ionic liquids[14'71] etc. as green extractants. Though these solvents all have very promising futures, lots of work should be done before they can meet the industry requirements due to the higher energy or money input involved. So organic solvents with little or very small toxicities are good alternatives to this problem. Green solvent dimthyl carbonate(DMC) is among chemicals with the safest toxicological and ecotoxicological data. Table 1 showed that DMC is not only safe to human body but also easy to degrade and has little pollution to the aqueous body. Due to this, it registered as "non-toxic substances" in Europe in 1992 and aroused more and more interests in researchers afterwards[1®1].

Table 1 Toxicological and ecotoxicological properties of DMC, MIBK and Toluene

Substances	Acute toxicity		Subchronic toxicity	Irritation properties	Aerobic biodegradation	Acute toxicity on fish
	LD_5o(Oral, Rat)	LCjoOnh.. Rat. 4h)	NOAEL(Ora 1. Rat. 13 Weeks)	Skin, Rabbit	Mod. MITI(28dd)	NOEC(Golden Orfe)
	8 * kg^{-1}	G • m"^{3}	mg • kg' • d'^{1}			EC$_{50}$ • L^{-1}
DMC[181]	13.8	140.0	500	Not irritant	90%	1000
MIBK	2.1	23.3	250	Irritant	NA	460
Toluene	5.0	15.0	223	Slight irritant	NA	57.7

DMC. Dimethyl carbonate: MIBK. Methyl isobuty l ketone

In our former work[19'101,] aqueous solution of phenol and aqueous solution of vanillin were chosen as experimental systems to study extraction characteristics of DMC. The extraction equilibrias of phenol (or vanillin) between DMC and water were compared with those between MIBK (or Toluene) and water. Compared with original extractants, extraction processes utilizing DMC could recover these substances successfully and had little pollutions on the environment. Present work will extend the former work and focus on the extraction mechanism of the DMC system.

EXPERIMENTAL

Dimethyl carbonate was obtained from Acros Organics. Propanoic acid and p-aminophenol were of chemical grade and all the other reagents were of analytical grade. All reagents were used without further purification.

Measured volumes of aqueous solutions and DMC were brought together into lOOmL flasks with stopper. All experiments were carried out in a thermostatic bath shaker(GFL 1086) maintained at temperatures of 20°C and 190 r-min'^{1} shaking frequency. After shaken for 60 minutes, samples were transferred to centrifuge and settled in it for 10 minutes under 4000 r-min"^{1} frequency. Samples of each layer were removed with syringes for collection and analysis.

Aqueous concentrations of most acids were determined by titration with NaOH solution except that p-aminobenzoic acid was determined by UV spectrophotometer. Other solutes were also determined by UV spectrophotometer(HP-8452). The amount of solute in organic phase was determined by mass balance.

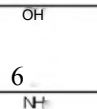
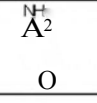
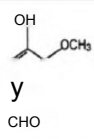
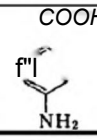
EXPERIMENTAL RESULTS AND DISCUSSION

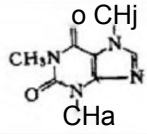
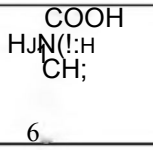
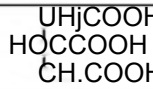
Distribution of Organic Solutes between DMC and Water

We defined distribution coefficient to be the solute concentration in organic phase at equilibrium divided by the counter-part in aqueous phase. Table 2 listed the distribution results between DMC and water, structures and logP of 13 substances. The substances included fatty acid, inorganic acid, phenol, aniline, caffeine and vanillin etc. Results showed that LogD ranged from -1.1 to 1.4, which meant D has a change of 200 times.

We could divide the 13 substances into two groups for the sake of mechanism analysis. The first 7 substances all had phenyl or cyclo- structures and the two substances(phenol and vanillin) that had the highest distribution coefficient were among them. The left 6 substances were all acids which had lower distribution coefficients. This showed that phenyl group seemed to have great contribution to the distribution results. From the comparison of propanoic acid and acetic acid, we could find that fatty acids with longer carbon length would have higher distribution coefficients. However, this was not true for citric acid and oxalic acid. Oxalic acid had much lesser carbon length than citric acid but the difference between distribution coefficients was not that apparent. It seemed that the carboxyl group had some contribution to the whole coefficients.

Table 2. Solute structures, DM CAN ate r distribution coefficient and logP

Solute CAS No.	Structure	Aqueous concentration ($g\text{-}L^{-1}$)	Distribution coefficient *(D)*	LogD	LogP
Phenol 108-95-2		0.198	23.7	1.375	1.46
Aniline 62-53-3		0.443	3.29	0.517	0.90
Vanillin 121-33-5		0.288	12.91	1.111	1.21
p-aminobenzoic 1^ acid 150-13-0		0.109	3.59	0.555	0.83

p-aminophenol 123-30-8		1.707	0.64	-0.193	0.04
Caffeine 58-08-2		12.22	0.62	-0.207	-0.07
a-amino-p-phenylpropionic acid 63-91-2		0.556	0.08	-1.097	-1.44
Propanoic acid 79-09-4	CH_3CH_2COOH	14.94	1.67	0.223	0.33
Acetic acid 64-19-7	CH3C00H	24.10	0.66	-0.180	-0.17
Phosphoric acid 7664-38-2	H3PO4	40.50	0.21	-0.678	-0.77
Succinic acid 110-15-6	$HOOCCH_2CH_2COOH$	15.87	0.26	-0.585	-0.59
Oxalic acid 144-62-7	HOOC-COOH	17.66	0.11	-0.959	-2.22
Citric acid 77-92-9		36.79	0.12	-0.796	-1.64

Extraction of Vanillin from Aqueous Solution

Among 13 substances in table 2, we selected vanillin as an example solute to study the extraction behavior of DMC in detail. Vanillin was an important flavor in daily life and an important chemical in industry. During the purification process of it, toluene was used as extractant to recover vanillin in water[111'121]. Due to the high toxicity of it, great pollution was produced in this process. We used hexane as diluent and DMC as extractant to replace toluene and eliminate the original pollution.

Fig. 1 showed the liquid-liquid equilibrium of vanillin between aqueous phase and organic phase. Initial organic phase composition was DMC, 60%(v/v)DMC-40%(v/v)hexane, toluene, 50%(v/v)DMC-50%(v/v)hexane respectively. We could know that the slope of the equilibrium line almost equal to constant, which meant that the distribution coefficient did not change with the aqueous phase vanillin concentration. With the rise of DMC volume fraction in initial organic phase, the slope also increased. Organic phase with more than 60%(v/v) DMC could acquire higher distribution coefficient than toluene and was able to replace toluene as extractant.

Fig. 2 showed the extraction efficiency after three cross-current stage extractions. Initial organic phase composition was 50%(v/v)DMC-50%(v/v)hexane. Phase ratio ranged from 0.75 to 1.25. Results showed that one stage extraction efficiency was about 75% and it rose when the phase ratio increased. With the increase of stage numbers, the extraction efficiency increased fast. After three stages, the extraction efficiency would approach to 100%, which meant vanillin could be recovered through these means successfully.

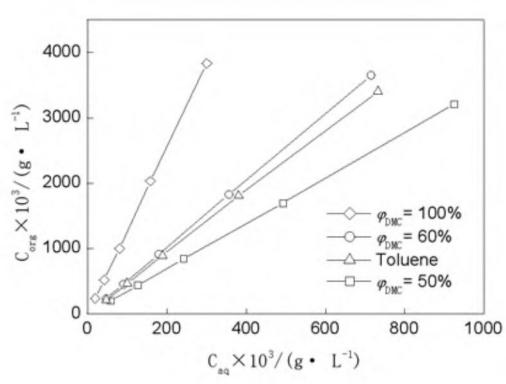


Fig. 1 liquid-liquid equilibrium of vanillin(t=25 °C)

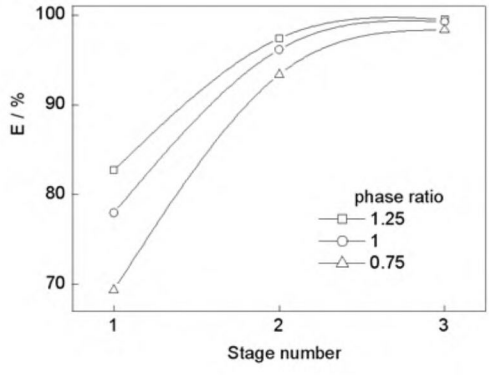


Fig. 2 Influence of cross-current stage numbers and phase ratio on the extraction efficiency

EXTRACTION MECHANISM

Distribution of a substance between extractant and water depends on the molecular interaction of this substance with extractant and water. So extraction mechanism study depends on the analysis of molecular interactions between solute and extractant. From analysis of the molecular structure of DMC, we can know that molecular interaction of DMC with solute can only be Van der Waals force and hydrogen bond. If we use parameters to reflect these forces, we can then derive out the extraction mechanism through the comparison between these parameters and the distribution results.

Hydrophobic parameters are important data in studying the toxicology of organics. Organics with higher hydrophobic parameters are easy to dissolve in fat and harm organisms. It is now widely used in Quantitative-structure-activity-relationship (QSAR) study. Currently, hydrophobic parameter adopts octanol/water partition number(P) recommended by Hansch as its value and often takes the ten based logarithmic form(logP).

$$P = \frac{\textbf{\textit{Solute concentration}} \text{ in the octanol phase at equilibria}}{\textbf{\textit{Solute concentration}} \text{ in the aqueous phase at equilibria}} \quad \textbf{(D}$$

While two liquid phases are reaching phase equilibrium, we can get

$$\mu_i^{org} = \mu_i^{aq} \quad (2)$$

Since $=\mu_i^{\circ} + RTln(y_i x_j)$, we then get

$$P = \frac{x_s^{org}}{\gamma^{\circ} s} = \frac{\gamma_s^{aq}}{\cdot s} \quad \textbf{(3)}$$

$$\log P = \log\left(\frac{\gamma_s^{aq}}{\gamma_s^{org}}\right), \text{ s means the solute.} \quad \textbf{(4)}$$

logP mostly takes the partition result while solute is infinitely diluted. Then we come to

$$\log P = \log\left(\frac{\gamma_s^{aq,\infty}}{\gamma_s^{org,\infty}}\right) \quad \textbf{(5)}$$

Infinite dilution activity coefficient can be expressed by solution parameter with the following relation[1131].

$$RTlny? = F,[(\hat{} - Xj + (r,-\tau J - 2<p_n] + RT[\backslash n\{V_2 !V_X) + (l - V_2 /F,)] \quad (6)$$

A and τ are non-polar and polar solubility parameter. 1 represents the solvent and 2 represents the solute. From the definition of solubility parameter, we know it reflects the inner energy of the substance. So logP can reflect the interaction energy of solute with octanol and water. Since forces existed between solute and octanol can only be Van der waals forces, logP is one good parameter to represent it. In this work, we will take logP as the parameter to study the extraction mechanism of DMC.

Fig. 3 was the relationship of logD with logP. Correlation results of the logarithmic form of distribution coefficients (logD) with hydrophobic parameter (logP) showed that they had a quite good linear relationship. This revealed that the molecular interactions of DMC with solute were similar with those existed in octanol and solute. So we could know that extraction by DMC was mainly through the Van der waals forces between DMC and solute. This meant that hydrophobicity played an important part in the final distribution results. There were also some exceptions in Fig. 3. For citric acid and oxalic acid, the logDs were higher than the whole trend. This meant that some specific interaction forces other than Van der waals forces must exist between DMC and them.

Fig. 3 could be easily used to predict the distribution coefficients of one solute between DMC and water since logP was very widely used in environmental science and every substance had its own number. We could forecast the results of experiment through logP. Results in Fig. 3 also showed that solutes with higher hydrophobicity and octanol/water number were easy to be extracted by DMC. The relationship of logD and logP could be one good guide to the application of DMC as an extractant.

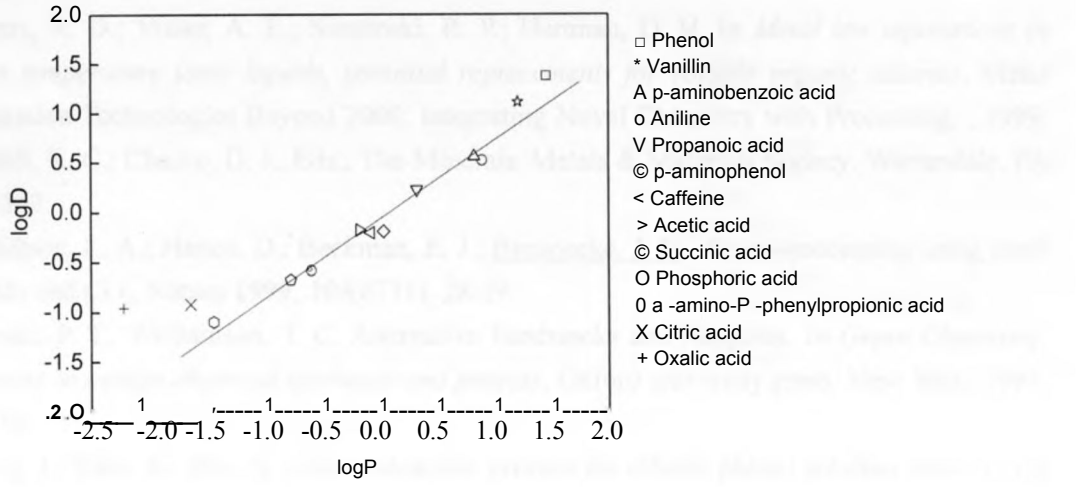


Fig. 3 Relationship oflogPand logD

CONCLUSIONS

Distribution coefficients of 13 substances between DMC and water were determined by experiments. Results showed that phenyl group had greater contribution to the distribution coefficients and fatty acids with longer carbon length would have higher distribution coefficients. Distribution coefficient of vanillin between DMC and water did not change with the aqueous phase vanillin concentration. Organic phase with more than 60%(v/v) DMC could acquire higher distribution coefficient than toluene and was able to replace toluene as extractant. After three cross-current stages, the extraction efficiency would approach to 100% and vanillin could be recovered through these means successfully. Octanol/water number(P) was proposed as an auxiliary parameter to study extraction mechanics of DMC. Correlation results of the logarithmic form of distribution coefficients (logD) with hydrophobic parameter (logP) showed that they had a quite good linear relationship. Extraction by DMC was mainly through the Van der waals forces between DMC and solute. Solutes with higher hydrophobicity and octanol/water number were easy to be extracted by DMC. The relationship of logD and logP could be one good guide to the selection of extraction system.

REFERENCES

1. M. Roth(1996). Thermodynamic Prospects of Alternative Refrigerants as Solvents for Supercritical Fluid Extraction. *Anal. Chem*., 68, 4474.
2. A. V. Yadi, E. J. Beckman(1996). Design, Synthesis, and Evaluation of Novel, Highly $C0_2$-Soluble Chelating Agents for Removal of Metals. *Ind. Eng. Chem. Res.,* 35, 3644-3652.
3. A. I. Cooper, J. D. Londono, G, Wignall, J. B. McClain, E. T. Samulski, J. S. Lin, A.

Dobrynin, M. Rubinstein, A. L. C. Burke, J. M. J. Frechet, J. M. DeSimone(1997). Extraction of a hydrophilic compound from water into liquid $C0_2$ using dendritic surfactants. *Nature,* 389(25), 368-371.

4. K. R. Seddon(1997). Ionic liquids for clean technology. *J. Chem. Tech. Bitechnol.,* 68(4), 351-356.
5. J. G. Huddleston, H. D. Willauer, R. P. Swatloski, A. E. Visser, R. D. Rogers(1998). Room temperature ionic liquids as novel media for clean liquid-liquid extraction. *Chem. Commun.,* 16, 1765-1766.
6. R. D. Rogers, A. E. Visser, R. P. Swatloski, D. H. Hartman(1999). Metal ion separations in room temperature ionic liquids, potential replacements for volatile organic diluents, Metal Separation Technologies Beyond 2000: Integrating Novel Chemistry with Processing, 139-147.
7. L. A. Blanchard, D. Hancu, E. J. Beckman, J. F. Brennecke(1999). Green processing using ionic liquids and $C0_2$. *Nature* , 399(6731), 28-29.
8. P. T. Anastas, T. C. Williamson(1998). Alternative Feedstocks and Reagents. *Green Chemistry: frontiers in benign chemical syntheses and process.* Oxford university press: New York, 87-100.
9. J. Zhang, X. Piao, S. Zhu(2002). Green extraction process for diluent phenol solution recovery (in Chinese). *Journal of Tsinghua University,* 42(5), 633-637.
10. J. Zhang, X. Piao, S. Zhu(2002). Novel Green Extraction Process for Vanillin Production (in Chinese). Proceedings of the Eleventh National Conference on Chemical Engineering. Hunan, China, May 17-20; China Chemical Engineering Society: Xiangtan; 285-288.
11. D. G. Diddams, N. E. Renaud. Process for purifying vanillin. *US patent,* 3686322, 1972-08-22.
12. F. W. Major, F. M. A. Nicolle. Vanillin recovery process. *US patent,* 4021493, 1977-05-03.
13. A. F. M. Barton(1983). Cohesion Parameters and Liquid Thermodynamic Data. In *CRC Handbook of Solubility Parameters and Other Cohesion Parameters.* CRC press: Florida, 121-126.
14. J. Sangster(1989). Octanol-water partition coefficients of simple organic compounds. *J. Phys. Chem. Ref. Data.,* 18(3), 1111-1229.
15. W. M. Meylan, P. H. Howard(1995). Atom/fragment contribution method for estimating octanol-water partition coefficients. *J. Pharm. Sci.,* 84(1), 83-92.

BATH LIFE EXTENSION DURING ELECTROLESS NICKEL PLATING BY SOLVENT EXTRACTION

Mikiya Tanaka, Yukinori Saiki*, Kazuhiro Hagisawa* and Hirokazu Narita

National Institute of Advanced Industrial Science and Technology (AIST), Japan
*Jaoan Kaniaen Co.. Ltd.. Jaoan

For the electroless nickel plating onto aluminum alloys, nickel preplating (strike plating) is necessary after zincate treatment to improve the adhesion of the nickel deposit. However, the life of the strike plating bath is short due to the accumulation of zinc in the bath. We have applied solvent extraction using acidic organophosphorous extractants, such as PC88A and Cyanex272, in order to extend the bath life by selectively removing zinc ion from the baths. This process has been in actual operation at a plating plant using a mixer-settler extractor for more than one year. Since the introduction of this process, the bath life has been extended 5-7 times longer when compared to the standard process.

INTRODUCTION

Electroless nickel plating is an indispensable surface finishing technology in the electronic and automobile industries, because it enables plating with a uniform thickness onto both regularly and irregularly-shaped conducting and nonconducting objects.

Before the electroless nickel plating is done on an aluminum alloy substrate, its surface is initially coated with zinc due to cementation (zincate treatment). In most cases, this coating is done twice (double zincate treatment). Pre-nickel plating (nickel strike plating) is then carried out. The zincate treatment improves the nickel adhesion on the substrate due to the coating film formation of zinc which has an ionization tendency between aluminum and nickel.

During this nickel strike plating, zinc is dissolved by cementation with nickel and accumulates in the bath as an impurity. When the zinc concentration exceeds 100 g/m^3, the plating rate is reduced, and the quality of the product decreases. Therefore, in order to avoid this situation,

the nickel strike plating bath must be disposed of after some repeated use. The average bath life for the strike plating after the double zincate treatment is 0.5 MTO, where MTO denotes the metal turn over, and 1 MTO means that the amount of nickel supplied after the initiation of the plating is equal to that at the beginning.

From this viewpoint, a new method of bath life extension for the nickel strike plating was proposed [1], in which the time for the zincate treatment is adjusted. This method, however, is not an essential solution of the zinc accumulation in the bath, although the accumulation is retarded.

We have applied the solvent extraction technique to remove zinc ion from the nickel strike plating bath and succeeded in extending the bath life 5-7 times as well as maintaining the aualitv of the Droduct. This Drocess is now in Dractical ooeration in the Tokvo Plant of the Japan Kanigen Co., Ltd.

SELECTION OF THE EXTRACTANT AND THE LOADING CAPACITIES

In our previous studies, the extraction properties of zinc, iron, and nickel ions in the electroless nickel strike plating bath with the acidic organophosphorous reagents (AOR), such as D2EHPA, PC88A, and Cyanex272, were investigated [2,3], It was found that AOR removes zinc and iron leaving nickel in the aqueous raffinate without adjusting the pH of the bath. In particular, PC88A and Cyanex272 are preferable, because the amount of the coextracted nickel is reduced.

In order to assess the loading capacities of zinc on PC88A and Cyanex272, a loading test was carried out, where 1 vol% extractant dissolved in Shellsol D70 and the real spent strike bath containing 140 g/m^3 zinc (pH 5.4) were used as the organic and aqueous phases, respectively. The 1 vol%PC88A and Cyanex272 contained 32 and 30 mol/m^3 AOR as monomers, respectively. The organic phase was vigorously mixed with the aqueous phase in a separatory funnel at the phase ratio of 1:2 for 10 min at room temperature (298-300K). After phase separation, the aqueous raffinate was removed from the funnel, and its zinc concentration was determined by ICP-AES. The organic phase was then mixed again with the fresh aqueous phase. This operation was repeated until the saturation of the organic phase occurred.

As the result, the maximum zinc concentrations by PC88A and Cyanex272 were 800 g/m^3 (12 mol/m^3) and 530 g/m^3 (8.1 mol/m^3), respectively. Thus, the molar ratios of Zn:AOR at saturation are 1:2.6 and 1:3.7 for PC88A and Cyanex272, respectively. A gelatinous phase appeared in the PC88A and Cyanex272 organic phases when the zinc loadings exceeded

60% and 98%, respectively, of the saturation and increased with the approach to saturation.

PROCESS DESCRIPTION

The conceptual diagram of our bath life extension process is shown in Figure 1. In the plating tank, the aluminum alloy substrate after zincate treatment is immersed in the nickel strike bath, where zinc on the solid surface is replaced by nickel and dissolved in the solution as Zn^{2+}. A part of the bath is withdrawn and sent to the extraction section in order to selectively extract Zn^{2+}. The aqueous raffinate is filtered with the lipophilic material such as polypropylene, polyethylene, and Teflon to remove the entrained organic phase and then returned to the plating tank. The loaded organic phase is sent to the stripping section, and the zinc is stripped with sulfuric acid which is recirculated and periodically replaced. The organic phase is reaenerated bv striDoina and then sent back to the extraction section.

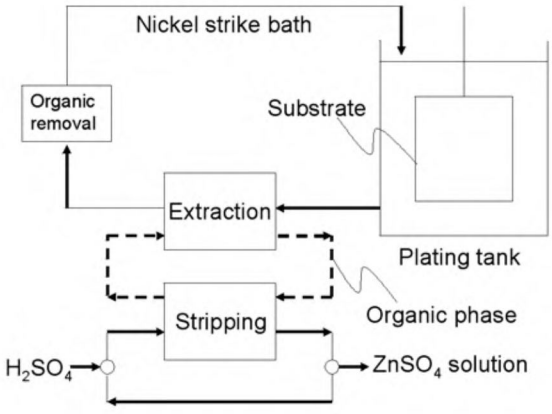


Figure 1. Conceptual diagram for the bath life extension process.

CONTINUOUS EXTRACTION TEST AND PLATING PROPERTIES MEASUREMENT

A mixer-settler extractor, which had a 0.01 m^3 mixer and 0.03 m^3 settler, was used in the continuous test. The number of stages was three for extraction and two for stripping. The plating tank was filled with 1 m^3 of a Ni-P plating bath (Japan Kanigen, SC-93). The bath was sent to the extractor at the flow rate of 0.1 m^3/hr, and the raffinate was returned to the plating tank after passing through a polypropylene filter (Advantec, pore size 0.2 pm). Plating was executed on the aluminum alloy after the double zincate treatment by supplying nickel sulfate, sodium phosphinate, and sodium hydroxide under the following conditions: temperature, 363K; bath ratio, 10 cm (bath volume /surface area of the substrate); time, 6 min. Zincate treatment to the aluminum alloy was done using a zincate solution (Japan Kanigen, K-102) at 298K for 30s.

The adhesion of the coating films to metallic substrates was evaluated by the crosscut adhesion tape test. Four horizontal and four vertical cuts were made in the coating by a diamond stylus in one steady motion at the pressure of 4 kg/cm^3 while maintaining a distance of 2 mm between parallel cuts. The crosscut areas were covered with an adhesive tape that was then rapidly removed and visually inspected. The adherence level was rated as follows: 3 when no coating square was removed (excellent adhesion), 2 when some of the squares were removed, and 1 when all the coating squares were removed (poor adhesion).

Extraction was carried out using 10 vol% PC88A or Cyanex272 dissolved in Shellsol D70 as the organic phase, in which the flow rate of the organic phase was 0.12 m^3/hr. Stripping was carried out using 0.4 kmol/m^3 sulfuric acid as the aqueous phase, in which the flow rate of the aaueous Dhase was 0.06m^3/hr.

Figures 2 and 3, respectively, show the zinc concentration in the bath and the plating rate as a function of the MTO. When zinc was extracted by PC88A or Cyanex272, the zinc concentration was constant at 20-30 g/m^3, and the plating rate only slightly decreased with the increasing MTO. In contrast, when zinc was not extracted, the zinc concentration and the plating rate rapidly increased and decreased, respectively.

Table 1 lists the results of the adhesion test. When zinc was extracted, a good adhesion was maintained even at 3.5 MTO, whereas the adhesion rapidly became poorer without the zinc extraction. At 0.7 MTO, the adhesion was degraded to an unacceptable level, at which point the bath cannot be used any more and has to be disposed.

Based on these results, it is clear that the bath life can be extended by removing zinc in the bath using solvent extraction.

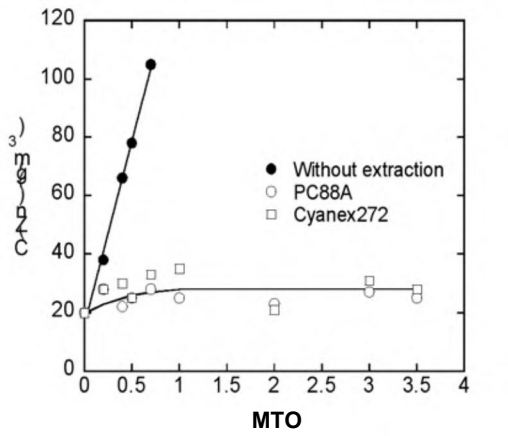


Figure 2. Zinc concentration in the bath, C(Zn), as a function of MTO.

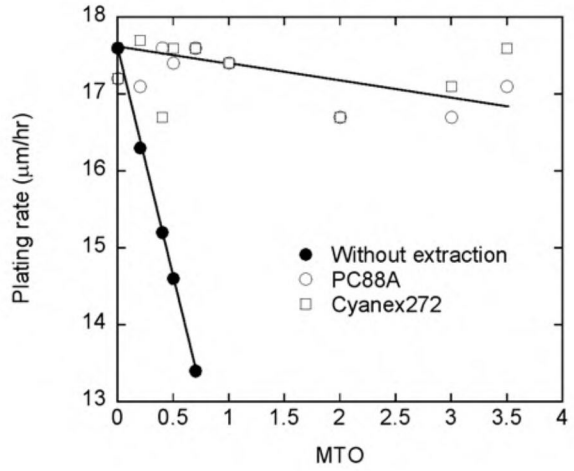


Figure 3. Plating rate as a function of MTO.

Table 1. The results of the adhesion test.

MTO	Extracted with PC88A	Extracted with Cyanex272	Without extraction
0	3	3	3
0.2	3	3	3
0.4	3	3	2
0.5	3	3	2
0.7	3	3	1
1.0	3	3	
2.0	3	3	
3.0	3	3	
3.5	3	3	

LONG-TERM PRACTICAL OPERATION

By using the same mixer-settler extractor as previously mentioned, a practical operation was started in November, 2002, at the Tokyo Plant of the Japan Kanigen Co., Ltd. in order to extend the bath life for the strike platina after the double zincate treatment. Fioure 4 is the bath life and the plating rate during the strike plating as a function of time (day) during the first 360 working days after the initiation of the practical operation, showing that the plating rate is fast enough and the bath life is extended 5-7 times. Initially, PC88A was used as the extractant; however, the process suffered from crud formation during stripping with sulfuric acid. Since it was found that the crud consisted of calcium sulfate due to the transfer of calcium from the bath by the coextraction with zinc, the extractant was changed to Cyanex272 in February, 2004, because Cyanex272 is known to have a lower calcium extractability than PC88A [4], Since this change, there has been no crud formation.

Since the beginning, this process has been contributing to the emission reduction and the improvement of the cost-performance during the electroless nickel plating, although we recognize that further improvements can be achieved by optimizing the operating conditions during the extraction-stripping circuit.

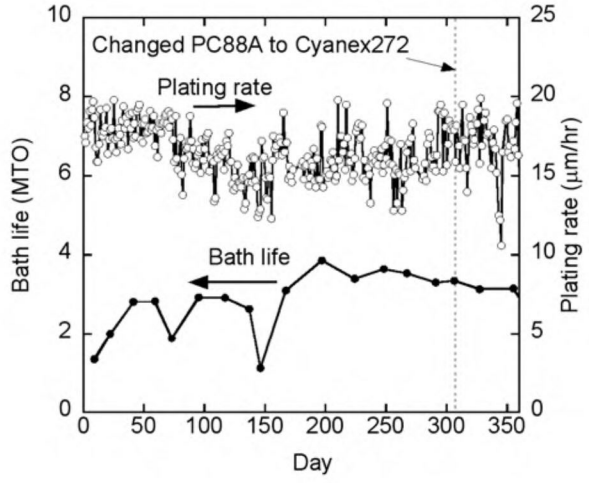


Figure 4. The bath life and plating rate during the strike plating since the initiation of the practical operation.

ACKNOWLEDGMENT

A part of this work was financially supported by a Grant-in-Aid for Scientific Research from the Ministry of the Environment, Japan.

REFERENCES

1. F. Matsui, M. Saito, Y. Shimomura, H. Takami and I. Nakayama (2000), *Japanese Pat.,* No. P3033455 (Feb. 18V
2. M. Tanaka, M. Kobayashi and T. Seki (2002), *Proc. ISEC2002,* South African Institute of Mining and Metallurgy, Johannesburg, South Africa, 787 pp.
3. M. Tanaka, M. Kobayashi and T. Seki (2002), *Shigen-to-Sozai, 118,* 751-755.
4. W. A. Rickelton, D. S. Flett and D. W. West (1984), *Solvent Extr. Ion Exch., 2,* 815-838.



SOLVENT EXTRACTION AND SEPARATION OF PALLADIUM FROM RECYCLED AUTOCATALYSTS WITH A NEW-BRANCHED DIALKYL SULPHIDE

Jianmin Yu* Xianzhi Hu Xiaotang He

(*Kunming University of Science and Technology,
Kunming 650093,Yunnan Province, P.R.China)

The experiment conditions of solvent extraction and separation of palladium from recycled autocatalyst with DIAS have been studied.The results shown that the extraction percentage in four cross-current extraction stages and stripping percentage in three counter-current stripping stages of palladium is 99.95%,99.9% respectively.The recovery and purity of palladium are all 99%.The results indicated that the method has many advantages including high kinetics,continuous process,wide acidity range,high selectivity and recovery,short work flow, friendship work environment,and so on.

Keywords:palladium, solvent extraction,separation,recycled autocatalyst,a new-branched dialkyl sulphide(DIAS).

INTRDUCTION

The spent autocatalyst is an important secondary resource of precious metals.The amount of palladium recovery from spent autocatalysts in the world is up to 41000 ounces in 2003 [1]. There are more and more spent autocatalysts in china have to be treated to recovery precious metals in the future.

The main chemical composition of palladium in the acidity chloride medium is $PdCl_4^{2-}$.The traditional recovery method(precipitation) has many disadvantages,for example, low recovery, long processing periods,high labor-intensity,and so on.

There are many extrantants thant can extract $PdCl_4^{2-}$ from acidity chloride medium,but the extrantants which have good selectivity for palladium are mainly sulphide,sulphoxide and oxime.

The extraction kinetics of oxime for palladium is slow, and it's selectivity is decreased with the addition of amine which acts as accelerators.Sulphoxides including synthesized sulphoxide and petroleum sulphoxide are used for palladium extraction, but it also can extract platinum and iridium.So the best extractant to separate palladium from platinum rhodium and iridium is sulphide.For example,dioctyl sulphide(DOS) and di-n-hyptyl sulphide(DNHS) are used to produce palladium in Acton refinery and the National Institute for Metallurgy of South Africa(NIM) respectively[121].However,the extracting speed of the above two sulphides is so slow that 1-3 hours are required for complete extraction of palladium,therefore,the production have to be a batch process.Moreover.the symmetrical sulphide can be easily oxidized to sulphoxide and the sulphoxide also is an effictive extractant of platinum,Iridium and ferric,so the extraction selectivity of palladium would be decreased.However,the extraction kinetics of iso-alkyl sulphide is so fast that only 5 minuets are required for palladium complete extraction and it can be used in continuous process of palladium extracting separation.A new-branched dialkyl sulphide(DIAS) has been used in this experiment.The conditions of extraction and separation of palladium from recycled autocatalyst have been systematic investigated.

EXPERIMENTS

Main reagents and apparatus

Extractant:dialkyl sulphide (DIAS)(99%), The chemical composition [$CH_3CH2(CH3)CH_2CH2$]2S,molecular weight 174.34,boiling range 85-88°C/15mmHg,specific gravity (d_4^{25}) 0.8283,viscosity 1.702 cp (25°C),refraction(n_D^{25}) 1.4512, flashing point 74-78 *C.
Dilute: n-dodecane(98%).
Other reagent:hydrochloric acid (CP), nitric acid (CP), ammonia water (CP), sodium chloride (CP), hydration hydrazine(CP).
Main apparatus:vibrator, 1000 ml separating funnel.

Feed of extraction experiment

Smashed spent autocatalyst which contains palladium 100-300g/t,platinum 800-1500g/t,rhodium 100-800g/t is leached with mixed solution of sulphuric acid and sodium chlorate.The precious metals in leaching solution are replaced by zinc powder,and the sediment is leached by sodium hydroxide solution to remove silicon and then it is washed by hydrochloric acid solution to neutralize the base.The residue(precious metals) is dissolved by hydrochloric acid-hydrogen peroxide into liquor, and the liquor is the feed of solvent extraction of palladium.The qualitative analysis results of spectrum of the feed are(%):Pt, Pd and Rh great quantity, Mg 0.8,Ag 0.003,Pb 5,Cr 0.1,Si 0.1,Fe 1,Cu 0.1,Ti 0.1,Al 0.5,Zn 0.005,Au 0.001 ,Bi 0.001;The chemical quantitative analysis results of it are (g/l): Pd 5.85,Pt 10.02,Rh 1.63,Ag 0.003,Fe 3.56,Cu 1.83,Pb 1.48,Zn 0.31 .acidity [H^+] 1.2 mol/l.

Experiment methods

The feed containing palladium, platinum, rhodium is mixed 5 minuets with equal volume organic phase (which is balanced with same acidity solution of hydrochloric acid in advance)

on the vibrator at room temperature (0/A=1:1 ,t=5min,T=25°C).The time of phase separation is about lOmin.Palladium is extracted in four cross-current extraction stages.The palladium concentration in raffinate is analyzed by DbDO colorimetry[131] and the palladium concentration in organic phase as well as the extraction percentage of palladium are calculated.The loaded organic phase is scrubbed in three counter-current stages by hydrochloric acid solution and stripped in three counter-current stages by dilute ammonia solution respectively (0/A=2:1,t=5min,T=25 °C).The distribution percentage of palladium, platinum,rhodium in scrubbing liquor and stripping percentage of palladium in stripping liquor are calculated.The stripped organic phase is regenerated by dilute NaCI solution and balanced by dilute HCI solution.The regenerated organic phase can be reused repeatedly.

RESULTS AND DISCUSSION

The fundamental extraction properties of palladium by a new-branched dialkyl sulphide (DIAS)

The fundamental extraction properties of gold, palladium, platinum in acidity chloride medium by 10 different structure of dialkyl sulphide has been studied and comparated in literature[141]. The results shown that DIAS is the optimum extractant for extract palladium in the following conditions:liquor acidity 0.1-6 mol/L HCI or 0.1-6 mol/L (HCI+H_2S0_4),the concentration of DIAS 10%-40% (V/V),the concentration of palladium 0.5-1 Og/I,extraction time 90 seconds.The extraction percentage of palladium is 99.99%.The research [5]also indicated that the extraction capacity of palladium can be greatly increased by adding a little aromatic hydrocarbon into the organic phase.The saturated capacity of palladium is larger than 30 g/L in organic phase including 30% DIAS(V/V)-10%aromatic hydrocarbon(V/V)-dodecane.

DIAS has very high selectivity for palladium because it has a tertiary-carbon atom and the distance of the branched chain to active group(-S-) is 3 carbon atoms[141],The separation coefficient of palladium (II) and platinum (IV) is larger than 1000 in the medium of hydrochloric acid.The extraction reaction of palladium is a coordination reaction:

$$[\ PdCI_4]^{2-}{}_{(A)}+2R_2S_{(0)}\text{—}[PdC1_2 \bullet 2\ R_2S]_{(O)}+2C|-_{(A)} \qquad (1)$$

The mixed solution of dilute ammonia and suitable quantity of salt is the ideal stripping agent for palladium,The stripping process have many advantages such as quickly speed of phase separation,distinctly interface,highly quality of stripping liquor which is easy to join refining palladium process and get 99.99% sponge of palladium.The stripping extraction reaction of palladium is as following:

$$[PdC1_2 \bullet 2\ R_2S]\ _{(0)}+4NH_3H_20_{(A)}\text{^=Pd}\ (NH_3)_4CI_{2\ (A)}+2R_2S\ _{(}o)+4H_20_{(A)} \qquad (2)$$

The concentrations of gold,palladium,platinum,rhodium and iridium in the regenerated organic phase are 0.0006,0.0011,0.095,0.0025,0.037g/L respectively after the organic phase was reused twelve times. Evidently,there is no metal accumulation in the organic phase.The infrared spectrum of a new and reused organic phase have been analysed.The main infrared absorption of a new organic phase are(cm–1): v_{as},cH3 **2957,$v_{s>CH3}$** 2870,5_{as},cH3 1467, 8 as.cH3l384,$(CH_2)_n$,744 respectively and the main infrared absorption of the reused organic phase are(cm'1):v_{as}.cH32958,v_s,cH328 54,$5_{as,C}$H3l466, $5_{as,CH}$3l380,$(CH_2)_n$,744 respectively, There is no sulphoxide absorption peak in the reused organic phase(this absorption peak should be

in 1060-1040 cm'[1]).The results shown that DIAS has very good chemical stability and it would not be oxidized to sulphoxide in the experiment conditions.

Solvent extraction palladium by DISA from spent automobile catalysts
The flowsheet (shown in Fig.1)

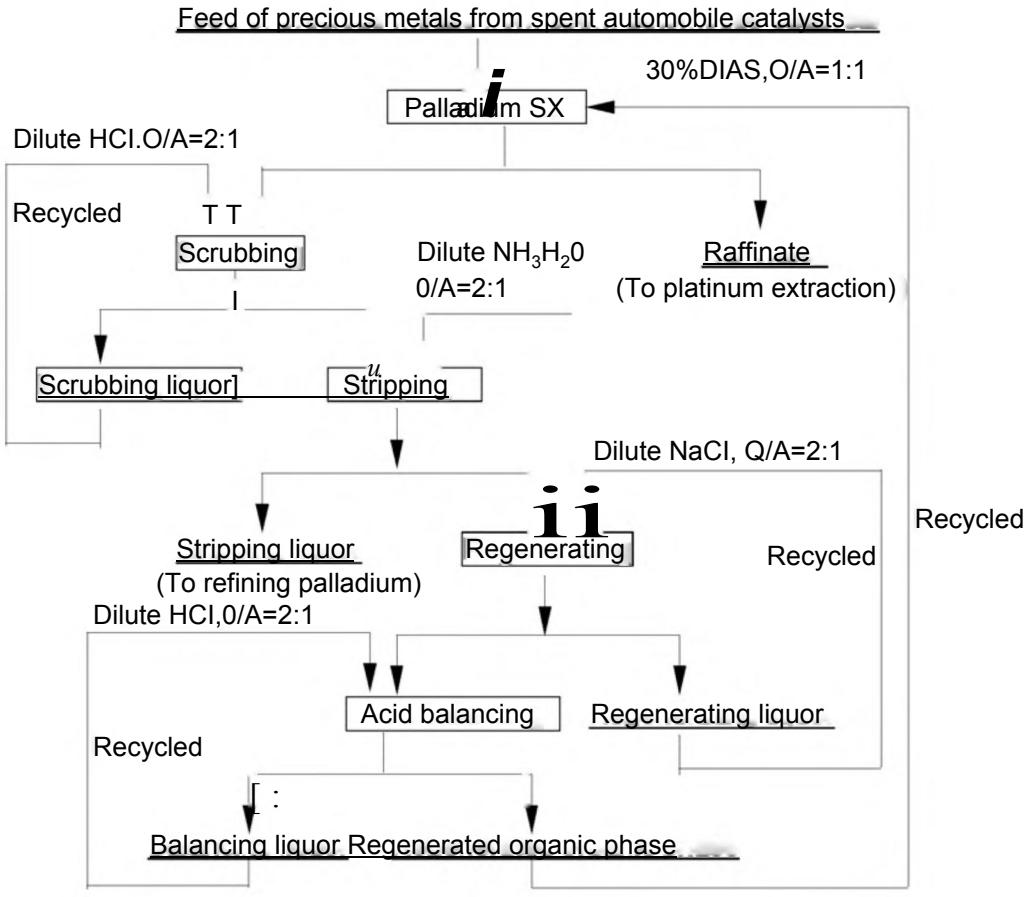


Fig. 1. The flowsheet for the recovery of palladium from spent autocatalysts

The main experiment conditions

The palladium is extracted in 4 stages by 30%DIAS(V/V)-10%aromatic hydrocarbon(V/V)-dodecane(0/A is 1:1,feed acidity is 1.2 mol/l HCI),The loaded organic phase is scrubbed in 3 stages by dilute HCI solution (O/A is 2:1),and then stripped in 3 stages by dilute NH_3H_20 solution (O/A is 2:1),The stripped organic phase is regenerated in 3 stages by dilute NaCI solution(0/A is 2:1),and balanced in 1 stages by dilute HCI solution (O/A is 2:1).The regenerated organic phase can be reused repeatedly.

The experiment results of the extraction of palladium

Extraction of palladium has been tested according to above principle flowsheet (see fig. 1). 5 batches samples have been totally carried out in every batche of 1000 ml liquor. Experiment results (see tablel) shown that the extraction percentage of each batch of palladium is larger

than 99.9%.The total extraction percentage of palladium in 5 batches is up to 99.95%.

Table 1. extraction percentage of palladium

Batch number	Palladium concentration in extraction raffinate (g/l)	Palladium extraction percentage(%)
1	0.0026	99.96
2	0.0020	99.97
3	0.0045	99.92
4	0.0038	99.94
5	0.0029	99.95
5 batches samples	0.0032	99.95

Precious metals(Pd, Pt, Rh) distribution in the scrubbing,stripping,regenerating and balancing liquor during extraction of the palladium

The palladium concentration in scrubbing,stripping,balancing liquor and regenerated organic phase in all tests have been analysed,The results shown that the palladium distribution (%) in scrubbing,stripping and balancing liquor are only 0.0002,0.0007 and 0.0014.There is nearly no palladium in these liquors.The total distribution (%) of platinum,rhodium in these liquors are only 0.48, 0.38 respectively (see table 2).The lost of platinum and rhodium are mainly in scrubbing liquor which can be merged into the raffinate of palladium for recovery of platinum and rhodium.The scrubbing liquor can also be reused and then replaced by zinc powder.The stripping percentage of palladium is up to 98.94%.

Table 2. Precious metals(Pd, Pt, Rh) distributions in the scrubbing,stripping, regenerating and balancing liquor during extraction of the palladium

The name of liquor	Concentration (g/l)			Distribution percentage (%)		
	Pd	Pt	Rh	Pd	Pt	Rh
Scrubbing liquor	0.00020	0.093	0.015	0.00020	0.38	0.37
Stripping liquor	14.47	0.013	0.0057	98.94	0.050	0.00014
Regenerating liquor	0.00020	0.016	0.00055	0.0007	0.030	0.0069
Balancing liquor	0.00040	0.0075	0.0003	0.0014	0.015	0.0037
The total				98.94	0.48	0.38

Palladium metal equilibrium

There is 29.25 g palladium in the feed,0.56g palladium is used sample analysis.Therefor,there are 28.69 g palladium to be recovered from the feed.The sponge palladium obtained from the feed is 28.67g, so the direct recovery of palladium is 99.93%.There are 0.02g palladium in the raffinate,and there is nearly no palladium in scrubbing,regenerating and balancing liquor.The total recovery of palladium is about 100%.

CONCLUSION

The solvent extraction process is the optimum methods to recovery precious metal from spent autocatalysts.The extraction and separation of palladium using a new branched dialkyl sulphide(DIAS) have many advantages including high kinetics,continuous process,wide acidity range,high selectivity and recovery,short work flow, friendship work environment,and so on.The process is easy to be operated automatically.The experiment results indicated that the branched dialkyl sulphide (DIAS) for palladium extraction is better than dioctyl sulphide(DOS) used in Acton refinery and di-n-hyptyl sulphide(DNHS) used in the National Institute for Metallurgy of South Africa(NIM).A pilot plant whose prodution capacity is about 600kg/a of palladium,platinum and rhodium using this process from spent autocatalyst has been set up in China.

REFERENCES

1. T.Kendall(2003),*Platinum 2003(Interim Review),*Johnson Matthey Publish Ltd,London. 6

2. M B Mooiman(1*993).The solvent extraction of precious metals-a review.Precious Metals,Proceedings of 17,hIPMI.*USA. pp.411

3.Shuxing Cai, Chao Huang(1985).*Precious metals analysis(in* C/7//7ese/)..Beijing:Metallurgy Industry Publish House.pp204

4. Hengli Ma.Chengye Yuan et al(1989*),The chemical structure of diaalkylsulphide and extraction of gold and palladium,Precious metals(in Chinese),10(2):']*

5. Jianmin Yu.Zhengfen Yang.Shijie Liu et al(1997).*Solvent extraction and separation palladium by diisoamylsulphide.Precious metals(in Chinese),18(4).45*

6.Shijie Liu.Zhengfen Yang.Jianmin Yu et al(1996).*Separation and refining of gold and pgms by continuous solvent extraction. Precious Metals,* Proceedings of 20[lh]I PM I, Newport Beach,California,USA. pp451

EXTRACTION OF THE *CALENDULA OFFICINALIS* L. ESSENTIAL OIL AND IT'S CHEMICAL COMPOSITION

Franceli da Silva[1], Kil Jin Park[1], Pedro Melillo Magalhães[2]

School of Agricultural Engineering, State University of Campinas. P.O. Box 6011, 13083-970, Campinas, SP, Brazil, E-mail: franceli@agr.unicamp.br; kil@agr.unicamp.br
[2]Chemical, Biological and Agricultural Research Centre, State University of Campinas, P. O. Box6171.ZIP 13081-970, Paulinia, SP, Brazil. E-mail: pedro@cpqba.unicamp.br

The use of the vegetable raw material as medicinal herbs has been increased in national and international companies. The oil of *Calendula officinalis* stimulates the granulocytosis and the fagocitosis helping the fight against the infections. The extraction of the oil was made through the adapted method that use water vapor. The indentification of the compound was done by comparing the mass spectums obtained with the ones of the data bank and by the Kovats index of each component. The results show that the lower drying temperature results in more oil extraction of this species, with the preservation of the monoterpenoes.

INTRODUCTION

The use of medicinal plants for the worldwide population has been very significant in the last times. It is esteemed that about 80% of the worldwide population makes use of some phytoterapy medicine [1,4]. Many plants possess economically important composites, such as, essential oils, alkalis, resins, tanning barks, waxes and others [2], Parallel to the expansion of the research and application of these plants in practical therapeutical, it is observed the increase of essential oil demand to confer special aromas and odors to products, such as cosmetic, condiments, candies, etc. Some components of these oils have pharmacological properties, being used in the medicine composition.

The essential oils are oily volatile liquid endowed with pleasant and strong aroma, almost always proceeding from the secondary metabolism, existing in almost two thousands species of plants distributed in 60 families. The biochemist routes and the corresponding metabolism are specific and unique, characterizing themselves as elements of differentiation and specialization of the specie [1], It is used to define this metabolic set as secondary metabolism, whose products, even so not necessarily essential to the producing organism, guarantee advantages in their survival and perpetuation of the species, in its ecosystems [4], The secondary metabolism can be divided into three main groups: terpenoes, phenolic composites and nitrogenous composites (Figure 1) [3], The metabolism of Acetil-CoA generates, structurally, the diversified group of secondary metabolism, the isoprenoes or terpenoes [6] that represent the second class with bigger number of active constituents, where the essential oils are found.

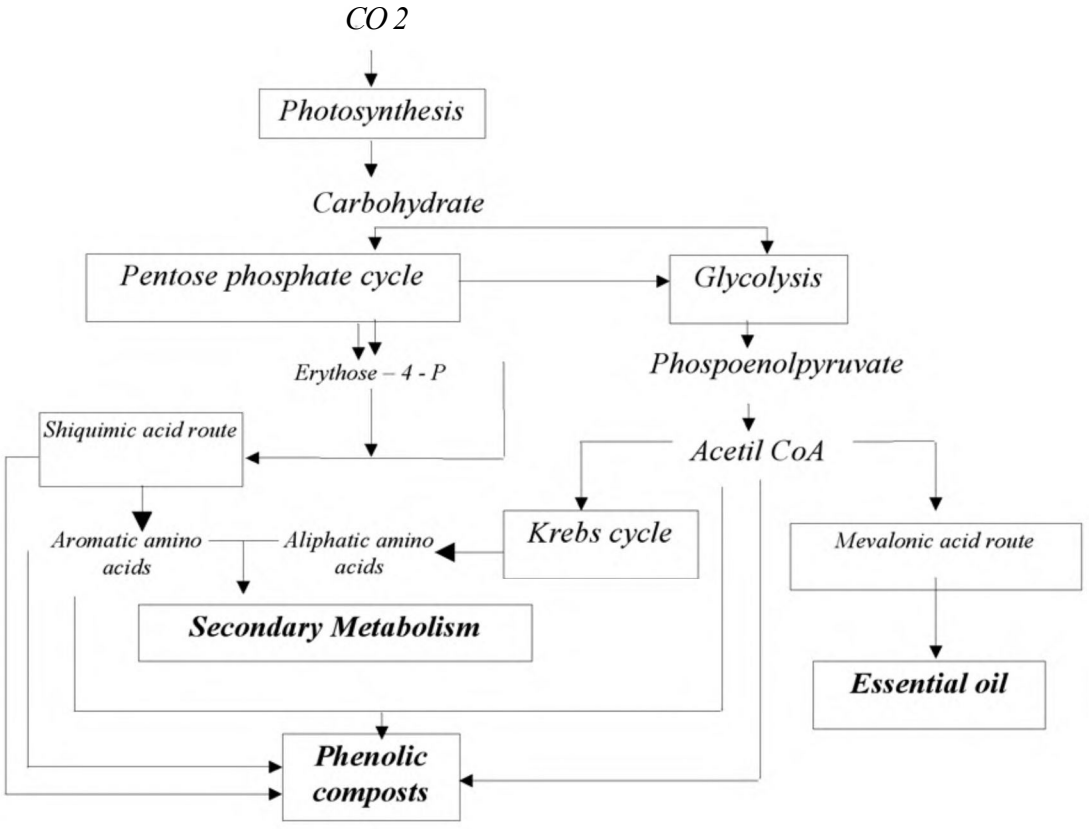


Figure 1 - Metabolic route

Terpenoes are constituted of five carbon units (isoprene units), and the nomenclature and classification reflect the number of isoprene units present and the cyclical form, presenting diverse cyclical skeletons or not. The monoterpenoes constitute the simple class of isoprenoes with alO-carbon structure, constituted of 2 isoprene units, being a component of essential oils and particularly accumulated in certain Umbelliferae and Pinaceae. They constitute a subclass that includes very common composites such as citral, linalol, camphor, carvacrol, amongst others of wide use in the cosmetic and food industry, besides presenting important pharmacology properties. Many of these metabolites are responsible for qualities attributed to vegetables along time, mainly medicinal attributes, what it being authenticated for the research, becoming each time bigger the interest of understanding and controlling these processes of synthesis of secondary metabolites, on the scientific community side and the industry [6] as well. These oils are normally elaborated in leaves, being stored in extra cell spaces, between the cut and the wall of the cell, and compound basically by terpenoes, synthesized bv the route of the acid mevalonic. In the ohvtoteraDv. the volatile oils are distinguished for their antibacterial, stimulant and other characteristics. The parts of calendula that can be used therapeutically can be either the leaves or the flower. They are indicated for skin treatment and mucous membranes inflammation, healing of wounds and light burns. The following pharmacological properties of calendula: it stimulates the granulocytosis and phagocytosis to help the combat against infections, diminishes gastritis and duodenal ulcer, and clinic tests have proved its anti-tumor action.

PROCESS DESCRIPTION

Cultivation

Calendula officinalis L. (Calendula) was cultivated in the experimental field of CPQBA (Centro Pluridisciplinar de Pesquisas Quimicas Biológicas e Agricolas - *Multidiscilplinar Center of Chemical, Biological and Agrarian Research)* in the city of Paulinia - SP. The plant was spread by seeds in PVC tubes with a substrate consisting of soil, sand and manure in the proportion 2:1:1. The seedlings remained in a greenhouse for 54 days. The seedlings were planted in the definitive place with a spacing of 0.20 x 0.50m (Figure 2 and 3).





Figure 2. Experimental field of calendula culture. Figure 3. Partial view of some plants.

Processing

After the harvest, the flowers were sent to a drying process in convective vertical column drier, in temperatures of 30, 45 and 60°C, in which had been placed 145g samples of approximately 145g of the product, with the accompaniment of the similar weight in order to observe the behavior of the curves of drying in three different temperatures. The system is composed for fan, heater and ducts. The airflow, to supply the desired speed, was controlled in the entrance of the fan, by a wooden device similar to a mobile door and its speed measured for an anemometer with digital reading in the air exit of the dryer.

Extraction of the essential oil

The extraction of the essential oil was made through the adapted method that uses steam (Figure 4). The methodology recognizes: 120 minutes of extracting time; use of lOOg of dried fresh plant in the extraction, and 1L of volume of the collected hydrolyte.

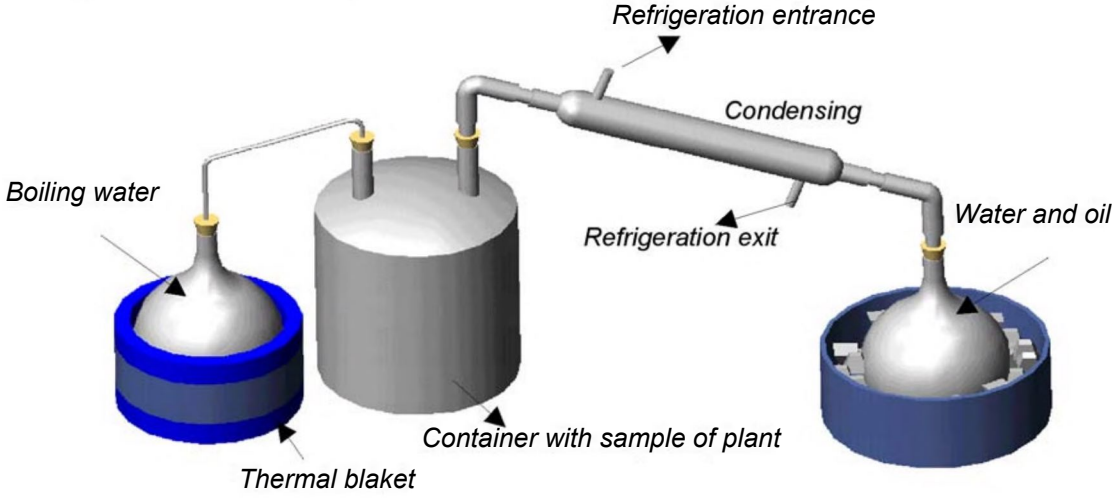


Figure 4 - Extracting device of essential oil.

The essential oil was extracted with dichloromethane. The organic phase was dried with filtered anhydrous sodium sulfate, and a rotary evaporator operated in reduced pressure conducted the remotion of the solvent. The chromatography in a gaseous phase and the spectrometry of masses were done in a Shimadzu QP 5000. The operational conditions used in the chromatography were: column DB 5 (length 30 m and 0,25 mm of internal diameter), temperature of the injector 220° C; temperature of the detector 240° C; program of temperature: 60 - 240° C for 3° C/min, 240° C for 15 minutes; inert gas He (lmL/min); split proportion, 1:20; volume injected 1 pL; electronic impact energy 70 and V; fragments collected of 45 to 650 Da; constituents with concentration under 1% were not considered. The identification of the compound was done by comparing the mass spectrums obtained with the ones of the data bank of the machine Willey 140.000 and by the Kovats index of each component.

RESULTS AND CONCLUSIONS

The oil incomes in relation to the dry substances were calculated in each sample submitted to the extraction, using the final moisture content (dry mass) gotten after the drying of the sample in 105°C for 24h, generating the value of dry mass of the vegetable substance. This way, the oil mass gotten in the extraction was related to the dry substance of the sample (table 1).

$$\text{Oil text (\%)} = \frac{\text{mass of oil (o) x 100}}{\text{mass of plant (g)}}$$

Table 1 - Averages of the oil income in relation to the dry substance, gotten in the treatment of drying process of calendula, in function of the temperature and the type of dryer.

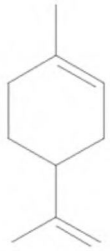
Temperature of air (°C)	Type of drying	Moisture content of the product (dry mass)	Income of the oil in relation to dry substance (%)
30	Convective drier of column vertical	0,11 ± 0,003	0,13
45	Convective drier of column vertical	0,13 ±0,004	0,12
60	Convective drier of column vertical	0,14 ±0,009	0,10
	Fresh plant	5,64 ± 0,371	0,27

Chemical composition

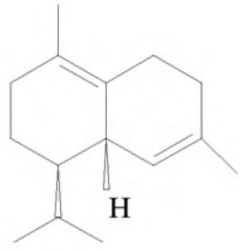
The variation was observed in the chromatographic profile in different temperatures. Considering composites with percentage of area over 10%, it was identified as majority component, the following composites (table 2).

Table 2 - Chemical composition of calendula in function of the temperature and type of drier. .

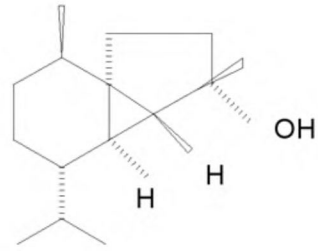
Temperature of air (°C)	Component majority	Retention indice	Area (%)
30	limonene [a]	1031	11,75
45	cubebol [b]	1514	10,82
60	candinene <delta-> [c]	1524	8,62



a - Limonene



b - Cubelol



c – Candinene <delta->

The influence of the relative humidity of drying air when volatilizing the oil, intensifies the process of making the monoterpenoes volatile, such affirmation can be proven as the temperature increases. There is loss of more volatile substances; with lesser molecular weight that indicates this loss. With the increase of the temperature there are preservation of the components with bigger molecular weight, case of diterpenos and sesquiterpenos. Therefore, if the objective will be to keep the substances more volatile, due to the intense aroma of the flowers, it is recommended to dry them in lower temperatures, in this case, 30°C. If the objective will be to keep substances less volatile, those of bigger molecular weight, however less aromatic, the temperature can vary between 45 and 60°C. What dictate such choice; in the truth it is the necessity of these substances in the production of phytotherapy.

ACKNOWLEDGEMENTS

FAPESP, CNPq, CPQBA, FEAGRI/UNICAMP.

REFERENCE

1. F. M. Andrade, V. W. D. Casali (1999). *Plantas Medicinais e aromáticas: Relagão com o ambiente, colheita e metabolismo secundario*, Dept, de Fitotecnia, UFV, 1. Ed.,139pp.
2. M. F. Balandrin, J. A. Klocke, E. S. Wurtele (1985). *Natural plant chemical-source of industrial e medicinal materials,* Science, v.228, p. 1154-1160.
3. E.J. Kays (1991). *Postharvest physiology of perishable plant products.* New York: AVI Book, 532pp.
4. F. Silva, V. W. D. Casali (2000). *Plantas Medicinais e aromáticas: Pós colheita e óleos essenciais,* Dept, de Fitotecnia, UFV, 2. Ed.,153pp.
5. C. M. O. Simões, V. Spitzer (1999). *Óleos voláteis.* In: Farmacognosia da planta ao medicamento. Porto Alegre, Florianopolis: Ed. Universidade UFRGS, Ed. UFSC, 821pp.
6. P.G. Waterman (1993). The chemistry of volatile oils. In: Hay, R.K.M., Waterman, P.G. ed. *Volatile oil crops: their biology, biochemistry and production.* Avon: Logngman Group, p.47-62.

OPTIMIZATION OF INULIN EXTRACTION FROM CHICORY ROOTS

Rafael Augustus de Oliveira, Kil Jin Park and Kil Jin Brandini Park

School of Agricultural Engineering, State University of Campinas - Campinas, SP, Brazil.

Chicory root is the most important tuberous root for industrial production of inulin which has a high fructose content. Inulin is a storaged carbohydrate which can be found in more than 30,000 vegetable products. It is a fructooligosaccharide that is not digestible but is selectively utilized by bifidobacteria in the large intestine, making inulin-type fructans the prototype prebiotic. Recently, inulin was identified as an ingredient that substitutes fat or sugar. In this work, inulin samples were extracted from chicory roots by a hot water diffusion process. The methodology consisted of the election of two levels of bath temperature and water:root ratio (water mass/root dry mass) and their combinations in a experimental design to execute the experiments. Second order polynomial model, response surface and contour plot were generated and allow the choice of temperature and water:root ratio that gives the extraction condition with highest inulin concentration.

INTRODUCTION

Chicory *(Cichorium intybus* L.) is a plant whose tuberous roots store inulin, with a high fructose content (about 94%). Recently, inulin was identified as an ingredient that substitutes fat or sugar, but there is still no commercial production of the roots as an inulin source in Brazil.

Inulin has specific technological assets, being soluble upon heating and bland in taste. It can be blended into a large number of different food products, which retain their intrinsic flavour without alteration of texture. Furthermore, inulin helps to provide body, good mouthfeel and improve appearance, thus it can be used as a fat replacer for the emerging sector of lower energy food products. Thanks to its water-binding capacity, it displays gelling and thickening properties [1],

Inulin is a polydisperse fructan commercially extracted from the chicory root by extraction with water, followed by refining and spraydrying. Inulin-type fructans or (3[2—1] fructans are non-digestible in the upper intestinal tract, and reach the large intestine, where they are fermented selectively (prebiotic property) by the local microflora [2, 3, 4], They stimulate the growth of bifidobacteria (bifidogenic) in the intestine, which has been proposed to be connected with health-promoting functions. Many other health-beneficial effects for fermentable fructans have been reported, concerning diabetes, lipid metabolism and cancer prevention [2, 5], Several investigations have demonstrated that rats fed the prebiotic fructans absorbed more Ca and Mg than control rats [4],

An important physico-chemical property of pure inulin is that it is almost insoluble in cold water, but easily soluble in hot water [1],

The objective of this work is to study the solid-liquid extraction of inulin from chicory roots. The first part deals with the central composite experimental design applied in an inulin extraction lab process. Then, in a second part, hot water extraction experiments are performed in order to identify the influence of the operating parameters. In the third part, a empirical Second order polynomial (SOP) model is proposed, taking into account the temperature of bath, watenroot ratio used in experiments and the concentrations of the soluble solids in extracted solution.

From a global point of view, this work will allow us to choose the significantly parameters and to identify the influence of the main operating parameters in an inulin extraction process.

EXPERIMENTAL DESIGN AND RESPONSE SURFACE METHODOLOGY

Experiments are frequently performed to measure the effects of one or more variables on a response. Factorial designs are extremely useful for this purpose. These designs are economical and easy to use and can provide a great deal of valuable information [6],

The RSM technique is frequently used for the optimization of process models based on determination of the coefficients of a low order polynomial by regression analysis. It uses these simple polynomial models to develop a statistically precise predictive knowledge about the process [7],

This methodology, associated with experimental design, is used to optimize several unit operations in food process engineering. The central composite experimental design with five variation levels is very useful when it is desired to verify if there is influence of the independent variable (factor) on the dependent variable (response). A mathematical model and the response surface can be obtained with this design.

A statistical technique, analysis of variance (ANOVA), enables the less significant terms in the polynomial approximation to be identified, as well as shows the adequacy of adjustment. Based on adjusted polynomial model, the response surface can be built and the optimum range of parameters (factors) can be determined.

MATERIALS AND METHODS

Materials

Chicory plants were cultivated in Experimental Produce Field of School of Agricultural Engineering, Campinas, SP, Brazil, The roots were harvested and immediately washed and cut in small pieces. Then, samples were stored at -10 °C. The frozen material was stored for approximately 9 months, when it was used in experiments.

Moisture content

Roots initial moisture was determined by the oven drying method at 105°C for 24 hours [8],

Extraction

The process of diffusion by water was the method employed for extracting inulin from chicory roots.

To apply the RSM methodology, a preliminary test was conducted and the central point for the experiments programming was defined (70°C and 8.5 kgw/kg_{DM}). This planning consisted of the election of two levels for bath temperature and waterroot ratio, the construction of central composite experimental design with the possible combinations and the execution of experimental runs. The design is shown in Table 1.

For each experimental run, samples were collected and grated in a food processor. Then, a portion of grated roots was weighed according to waterroot ratio on experimental design. It was immersed on water in a becker (250 ml) and put in a circulated bath with fixed temperature.

The time for extraction was set at 30 min.

Table 1. Coded and uncoded variable levels and extracted soluble solids.

Run		Coded variables		Uncoded variables		Extracted soluble solids [%]
		X!	X2	T [°C]	W:R [kg_w/kg_DM]	
Factorial points	1	-1	-1	50	6.0	51.5
	2	-1	+1	50	11.0	52.3
	3	+1	-1	90	6.0	71.0
	4	+1	+1	90	11.0	76.1
Central points	5	0	0	70	8.5	60.2
	6	0	0	70	8.5	57.4
	7	0	0	70	8.5	59.5
Axial points	8	-1.41	0	42	8.5	45.1
	9	+1.41	0	98	8.5	74.4
	10	0	-1.41	70	5.0	61.7
	11	0	+1.41	70	12.0	66.0

RESULTS AND DISCUSSION

The average initial moisture content of the samples was 2.39 ± 0.13 kg_w/kg_{DM} for the frozen roots.

The amount of soluble solids in final extract was determined by measurement using a benchtop refractometer.

The influence of the extraction conditions on the amount of extracted inulin was evaluated by building a response surface of this parameter as function of bath temperature and waterroot ratio, using the Experimental Design of the Statistica v.5.0 software. The model that best represented extracted soluble solids amount is given by Equation 1, shown in Figure 1, where the linear effects of bath temperature and waterroot ratio were significant at 5% level.

The model is evaluated through the analysis of variance (ANOVA) in Table 2. The first model coefficient correlation (R^2) was equal the 0.994, which means that 99.4% of the variations in the results obtained can be explained by the empirical model [7], The second-order polynomial equation that correlates the extracted soluble solids (SS) as a function of the bath temperature (T) and waterroot ratio (WR) is indicated as follows:

$$SS = 59.016 + 21.310T + 1.159T^2 + 3.005WR + 5.364WR^2 + 2.167T*WR \quad (1)$$

The trend of increasing the amount of extracted soluble solids along with the increase in bath temperature is coherent with the literature, where solubilization of inulin increases as water temperature increases.

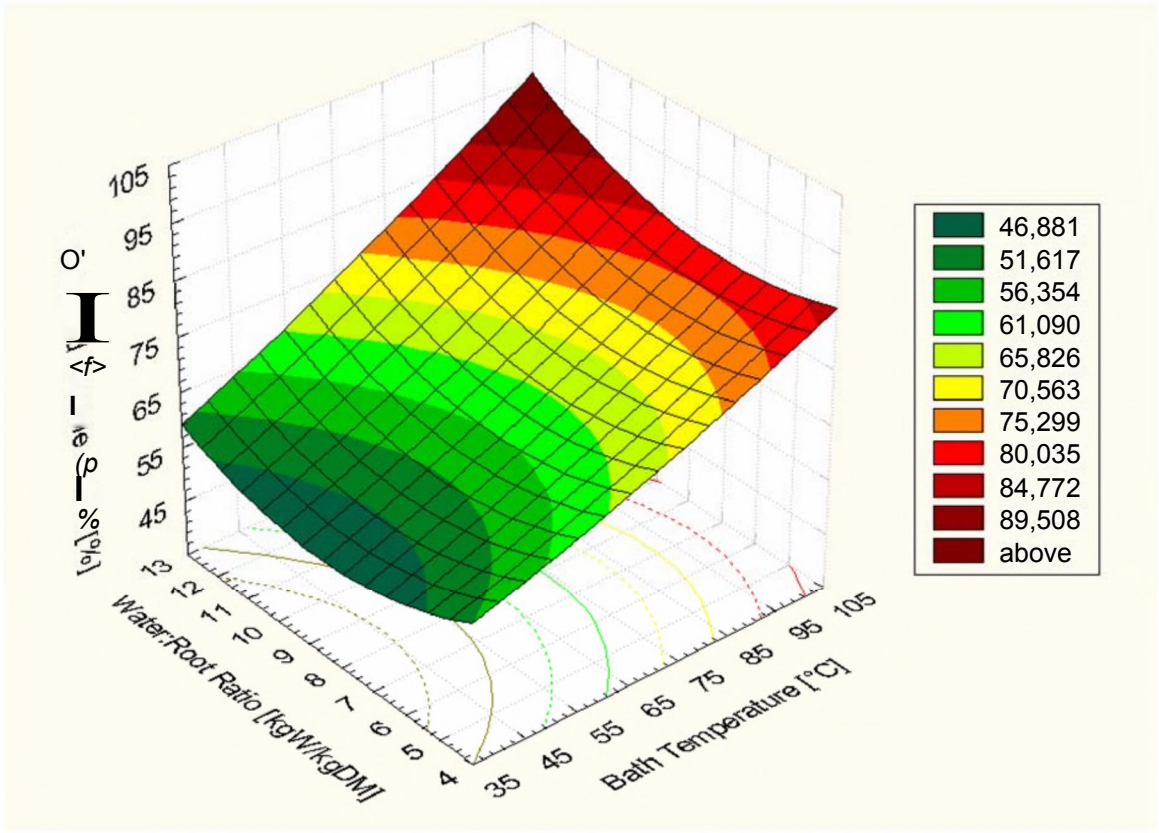


Figure 1. Response surface of inulin extraction for first Model.

Table 2. Analysis of variance (ANOVA) of the extraction for first Model.

Source of variables	Sum of squares	Degree of freedom	Mean squares	F-value	Significant level (p value)	R^2
T (linear)	899.17	1	899.17	413.56	0.002	0.994
T (quadratic)	1.85	1	1.85	0.85	0.454	
W:R (linear)	17.88	1	17.88	8.22	0.103	
W:R (quadratic)	39.54	1	39.54	18.18	0.051	
T by W:R	4.69	1	4.69	2.16	0.279	
Lack of fit	1.79	3	0.60	0.27	0.843	
Pure error	4.35	2	2.17			
Total sum of squares	967.61	10				

The second model was built through the removal of some of the sources of variable that seemed less significant according to the statistical analysis. The results are shown in Figure 2 and Table 3:

$$SS = \mathbf{46.248 + 0.5337 - 6.245fTft + 0.403ff7\text{^}2} \quad (2)$$

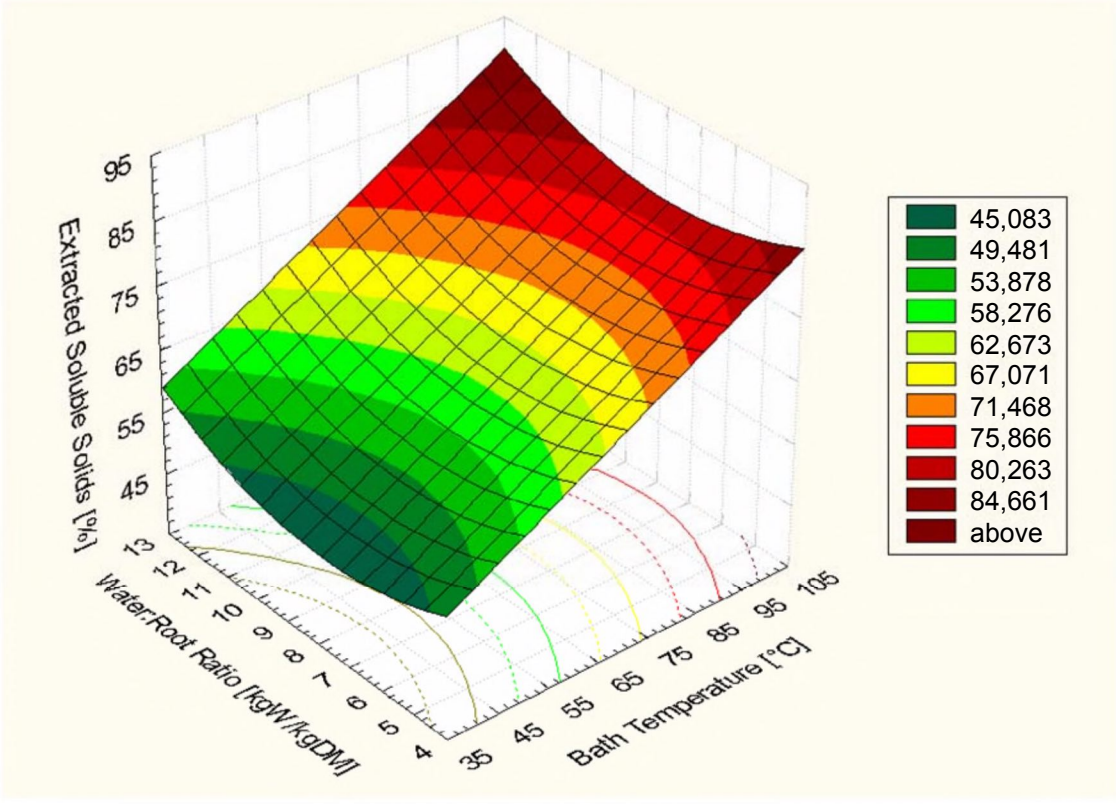


Figure 2. Response surface of inulin extraction for second Model.

Table 3. Analysis of variance (ANOVA) of the extraction for second Model.

Source of variables	Sum of squares	Degree of freedom	Mean squares	F-value	Significant level (p value)	R^2
T (linear)	899.17	1	899.17	413.56	0.002	0.987
W:R (linear)	17.88	1	17.88	8.22	0.103	
W:R (quadratic)	37.89	1	37.89	17.43	0.053	
Lack of fit	8.33	5	1.67	0.77	0.650	
Pure error	4.35	2	2.17			
Total sum of squares	967.61	10				

The mean relative deviation modulus, criterion used to evaluate the aualitv of the fit. achieves 0.99% for the first model and 1.38% for the second model.

The values of Lack of fit and $R^2$of the second model, compared with those of the first model, show that the first model results a better fit of the experimental data.

CONCLUSION

The obtainment of inulin by hot water extraction can be evaluated by a response surface method. The extraction of inulin is function of bath temperature and water:root ratio. The model that best represent extracted soluble solids amount is given by polynomial equation, where the linear effects of bath temperature and waterroot ratio are significant at 5% level.

ACKNOWLEDGEMENTS

We acknowledge the support of The State of São Paulo Research Foundation (FAPESP), The National Council for Scientific and Technological Development (CNPq), Coordenagão de Aperfeigoamento de Pessoal de Nivel Superior (CAPES) and Campinas State University (UN I CAMP).

REFERENCES

1. S. Vendrell-Pascuas, A.I. Castellote-Bargalló and M.C. López-Sabater (2000), *Journal of Chromatography A,* .881, 591-597.
2. M. Roberfroid (1993), *Critical Reviews in Food Science and Nutrition*, 33 (2), 103-148.
3. J. Van Loo, P. Coussement, L. De Leenheer, H. Hoebregs and G. Smits (1995), *Critical Reviews in Food Science and Nutrition*, 35 (6), 525-552.
4. C. Coudray, J. C. Tressol, E. Gueux, Y. Rayssiguier (2003), *European Journal of Nutrition*, 42 (2), 91-98.
5. G. Flamm, W. Glinsmann, D. Kritchevsky, L. Prosky and M. Roberfroid (2001), *Critical Reviews in Food Science and Nutrition,* 41 (5), 353-362.
6. G. E. P. BOX, W. G. HUNTER and J. S. HUNTER (1978), Statistics for experimenters: an introduction to design, data analysis and model building, 1. ed., John Wiley & Sons, New York, 653 p.
7. B. Barros Neto, I.S. Scarminio, *R.E. Bruns* (2002), Como fazer experimentos: pesquisa e desenvolvimento na ciência e na indústria, Editora da UNICAMP, Campinas,SP, 401 pp.
8. Association of Official Analytical Chemists - AOAC. (1990), Official Methods of Analysis: 930.04, 1,949.

Extraction of Succinic Acid with Trialkylamine

Guofeng Guan, Chen Xu, Hui Wan, Huqing Yao

College of Chemistry and Chemical Engineering, Nanjing University of Technology, Nanjing, 210009, People's Republic of China

Abstract

The extraction of succinic acid from aqueous solution by trialkylamine dissolved in binary mixed solvent of n-octanol and toluene was studied. In addition to the influence of single factor on extraction, equilibrium experiments were designed by orthogonal experiment. By the treatment of the orthogonal experimental data, the main influence factor was obtained. Using mass action law, the liquid-liquid equilibrium model of complex extraction of polybasic acid has been induced, and physical extraction was also considered in the model. Comparing experimental data with model value, it could be held that the regression precision of model was high. IR spectrum was performed for information on the complexes and extraction mechanism, which confirmed the concurrence of hydrogen-bond and ionic-bond between succinic acid and amine. Combined the complex constant value of model with the spectrum, four kinds of complex compounds synthesized by succinic and trialkylamine were determined.

Keyword: Trialkylamine; Succinic acid; Complex Extraction; Equilibrium; Orthogonal Experiment

1.Introduction

The extraction based on reversible complexing reaction of carboxylic acid with long-chain aliphatic tertiary amines has been discussed for many publication (e.g. Tamada, J. A.[M1], Kirsch, T[121], Ziegenfu(3, F. A[131], Poposka, M[141], OtonoT. [15]and Matsumoto M. [61]etc). Many authors[17'101] have investigated all kinds of effects on the extraction of carboxylic, such as temperature, the complexing agent concentration, the initial concentration of carboxylic acid etc.

Foundation Item: Supported by education department natural science foundation of Jiangsu (NO: 03KJB530042)

Biography: Mr. Guan Guo-feng (1962-), born in Jiangdu, Jiangsu province, professor, Ph. D., field of research: transfer and separation, E-mail: guangf@njut.edu.cn, Tel: 025-83587198

It is the committed step to obtain the chief influence factor and better operational conditions in the complex extraction process. It is the better choice to use the orthogonal experiment design to draw up experimental plan and mathematic method for interpretation and analysis of experimental data.

Succinic acid was chosen as one of the important raw material used in organic synthesis, which is frequently considered as solute with multiple functional groups in extraction process. Trialkylamine was chosen as the reactive extractant, n-octanol as hydrogen-bond-donating and toluene as non-polar solvent respectively. Like other carboxylic acid, succinic acid with Lewis acidity functional group is representative to be separated by complex extraction with trialkylamine, which has Lewis basic functional group. In this work, on the basis of orthogonal experiment, equilibrium data of succinic acid extraction were analyzed and interpreted by mathematic method. On the same time with mass action law universal mathematical models of polybasic acid considering physical extraction has been induced. Infrared (IR) spectroscopic studies for information on the complexes and extraction mechanism were reported.

2. Experiment

2.1. Materials and Apparatus

Table 1 gives information on supplier and the purities of reagents used in the experiments.

Table 1 Reagents used in the experiments

Chemical		Supplier
Succinic acid	analytically pure	Easter-China Reagent Industrial Supply and Marketing Corporation
Trialkylamine	industrially pure	Oil and Fat Chemical Plant of Dalian
N-octanol	chemically pure	BASF company in Germany
Toluene	analytically pure	Yi-Di Chemical Industry Limited Company

2.2 Liquid-Liquid Phase Equilibrium Measurements

For liquid-liquid phase equilibrium measurements, equal volumes of aqueous succinic acid solution and organic solution mixture with trialkylamine dissolved in n-octanol and toluene were stirred in glass flask for 1 hour with temperature constant(uncertainty:±0.1 °C). Then, both phases were separated by separating funnel. The pH of the aqueous was measured (uncertainty: ±0.01 pH units). The concentration of the succinic acid in the aqueous phase was determined by titration with aqueous solution of sodium hydroxide (relative uncertainty: 1%). The concentration of the succinic acid in the organic phase were determined by matter balance (relative uncertainty less than 1%).

IR spectrum of the organic solvent loaded with succinic acid was carried out to analyze the extraction mechanism by the stretching vibration of characteristic peak.

3. Results and discussion

3.1 Factors and plan of orthogonal experiment

It is known that the distribution coefficient (D) of the succinic acid between aqueous phase and organic phase depends on all kinds of factors, including the initial concentration of succinic acid, the concentration of n-octanol and trialkylamine and temperature and so on. The results of the extraction of succinic acid dependent on these factors are shown in Figures 1-3 respectively.

Figurel shows the results for the extraction of succinic acid varying the initial concentration by 20%(v/v) trialkylamine dissolved in mixed diluents, in which n-octanol comprised 30%, 50%, 70%(v/v) of the total diluent's volume and toluene made up the remaining volume. The decrease of D value with the increase of succinic acid concentration indicates that the decreasing concentration of succinic acid resulted in higher D value. Figure2 shows at higher n-octanol and trialkylamine concentration in the organic phase, distribution coefficient increases. The effect of temperature on the distribution coefficient of the extraction of succinic acid obtained from Figure 3 shows that extraction distribution coefficient decreases with the increase of temperature. On the basis of above experimental research, four factors with three levels were chosen in order to design the orthogonal experiment shown in table 2.

The array chosen was the $L_27(3^4)$ which has 27 rows corresponding to the number of test, as shown in table 3.

From the above research, the condition preferable to complex extraction of succinic acid could be decided. The preferred conditions were that the temperature was 25°C, the volume percent of trialkylamine and n-octanol was 30% and 50% and the initial concentration of succinic acid was 0.01604mol L^{-1} on the experimental scale.

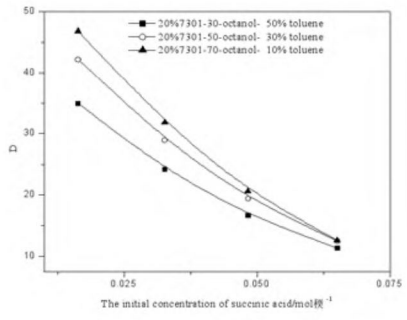


Fig. 1 Effect of different initial concentration of succinic acid on extraction distribution coefficient

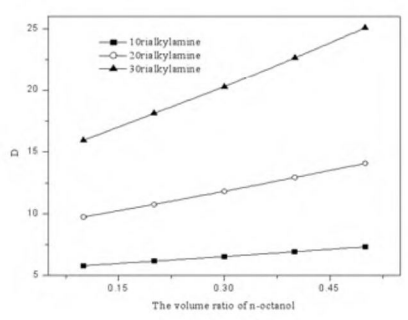


Fig. 2 Effect of concentration of n-octanol on extraction distribution coefficient of succinic acid (0.0651mol-L-1)

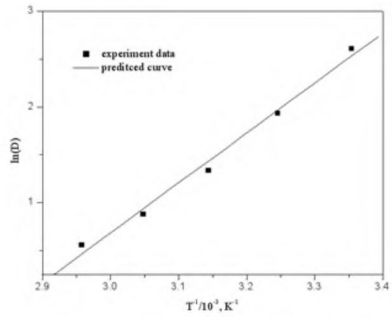


Fig. 3 Effect of temperature on extraction distribution coefficient of succinic

acid(0.0651mol- L-1)

trialkylamine: n-octanol: toluene=20:50:30(in volume)

Table2 Assignment of the levels to factors

factors	Level 1	Level 2	Level 3
The initial concentration of succinic acid /mol-L⁻¹ A	0.01604	0.04056	0.06508
Volume percent of trialkylamine B	10	20	30
Volume percent of n-octanol C	10	30	50
Temperature/!? T	25	40	55

3.2 Liquid-liquid equilibrium model

As a particularly important aspect, the mathematical model of extraction of polybasic acid from the aqueous with trialkylamine was established for interpretation and analysis of equilibrium data by the mass action law. Equilibrium constant K was shown in Eq.(1), where the species concentrations are denoted by square brackets and expressed in molar terms, and the organic-phase species are marked with an overbar. The complex, polybasic acid and trialkylamine is denoted by NA, A and X respectively.

$$H_nA + n\bar{X} \; f \; ^{\wedge} \; H\bar{A}_n'X, \; K = \frac{[\bar{NA}]}{[A][\bar{X}]^n} \qquad (1)$$

Most polybasic acids are weak acids. They will partially ionize in aqueous according to Eq.(2)

$$H_nA \xrightleftharpoons{Ka1} H^+ + H_n.iA''$$

$$H_n\text{-}iA \xrightleftharpoons{Ka2} H^+ + H_{n\cdot 2}A^{2'}$$

...

$$_{HA}(n\sim i)\sim \xrightleftharpoons{Kan} H^+ + A^{n'} \qquad (2)$$

The concentrations of dissociated ($H_{n\cdot 1}A'...A^{n'}$) and undissociated acids (H_nA... HA^'1*') are affected by the concentrations of hydrogen ion(H^+) or pH, and are subject to equilibrium constant, Ka!... Ka_n, equal to

$$Ka, = \frac{[A\sim][H^+]}{[A]}$$

$$Ka_2 = \frac{[A^2J[H*]}{[A]}$$

...

$$Ka_n = \frac{[A^nJ[H]^+}{[A^{(n_,)}\text{“}]} \quad (3)$$

Ka_n is usually called the dissociation constant of weak polybasic acid which is function of temperature on the basis of Gibbs-Helmhoze formula.

Table3 Orthogonal experiment results of extraction of succinic acid with trialkylamine

Serial number	A	B	C	T	D
1	0.01604	10.0	10.0	25.0	14.76
2	0.01604	10.0	30.0	55.0	2.72
3	0.01604	10.0	50.0	40.0	6.61
4	0.01604	20.0	10.0	55.0	3.95
5	0.01604	20.0	30.0	40.0	10.41
6	0.01604	20.0	50.0	25.0	32.65
7	0.01604	30.0	10.0	40.0	11.21
8	0.01604	30.0	30.0	25.0	41.06
9	0.01604	30.0	50.0	55.0	7.33
10	0.04056	10.0	10.0	55.0	2.21
11	0.04056	10.0	30.0	40.0	3.76
12	0.04056	10.0	50.0	25.0	9.30
13	0.04056	20.0	10.0	40.0	4.98
14	0.04056	20.0	30.0	25.0	19.33
15	0.04056	20.0	50.0	55.0	3.21
16	0.04056	30.0	10.0	25.0	23.04
17	0.04056	30.0	30.0	55.0	3.20
18	0.04056	30.0	50.0	40.0	13.69
19	0.06508	10.0	10.0	40.0	1.62
20	0.06508	10.0	30.0	25.0	4.11
21	0.06508	10.0	50.0	55.0	2.14
22	0.06508	20.0	10.0	25.0	13.04
23	0.06508	20.0	30.0	55.0	2.48
24	0.06508	20.0	50.0	40.0	5.66

25	0.06508	30.0	**10.0**	**55.0**	**2.51**
26	0.06508	30.0	**30.0**	**40.0**	**6.96**
27	0.06508	30.0	**50.0**	**25.0**	**26.27**
Ki	130.70	47.23	**77.32**	**183.56**	
K_2	82.72	95.71	**94.03**	**64.90**	
K_3	64.79	135.27	**106.86**	**29.75**	
ki (=K_1/9)	14.52	5.25	**8.59**	**20.40**	
K_2 (=K_2/9)	9.19	10.63	**10.45**	**7.21**	
K_3 (=Ka/9)	7.20	15.03	**11.87**	**3.31**	
Range	7.32	9.78	**3.28**	**20.37**	
Preferred plan	A,	B_3	**c_3**	**Ti**	

$$K=\exp(\frac{\Delta H}{RT}+C) \tag{4}$$

Physical extraction of polybasic acid in the diluent has something with equilibrium constant.

$$H_n A <\xrightarrow{m}> \overline{H_n A}$$

$$m=\frac{[\overline{A}]}{[A]} \tag{5}$$

The distribution coefficient D is defined as the total concentration of acid (all forms) in the organic phase divided by that in the aqueous, so D is determined by the extraction behavior parameters as follows.

$$D=\frac{[\overline{NA}]+cb[\overline{A}]}{[A]+[A^-]+[A^{2-}]+[A^{3'}]+...+[A'''']}$$

$$=\frac{K[A][\overline{X}]^n+<X>m[A]}{[A]+[A-]+[A^{2}-]+[A^{l}]+...+M"-]}$$

$$=\frac{K[\overline{X}]^n+Om}{1+\frac{[A^-]}{[A]}+\frac{[A^-HA^-]}{[A][A^-]}+\frac{[A^3][A^2]}{[A^2][A^-][A]}+\frac{[AH[A^{(n-1)}]}{[A^{(n-1)}][A]}[A-]}$$

$$=\frac{K[\overline{X}]^n+<Dm}{1+10^{pH-pKal}+10^{pH-pKa2}10^{pH-pKal}+...+10^{pH-pKan}10^{pH-pKa(n-1)}...10^{pH-pKal}} \tag{6}$$

O is defined as the diluent volume fraction. Replace the K with Eq.(4) and Eq.(6) can be obtained as follow.

$$D=\frac{\exp(\frac{\Delta H}{RT}+C)nX]^n+cDm}{1+10^{pH-pKal}+10^{pH-pKa2}10^{pH-pKal}+...+10^{pH-pKan}10^{pH-pKa(n-1)}...10^{pH-pKal}} \tag{7}$$

Namely universal mathematical equilibrium models of polybasic acid considering physical extraction is obtained, where [X] is denoted the initial concentration of extractant.

Some parameters in the model had to be known and fitted to the results of the liquid-liquid equilibrium. The dissociation constants of succinic acid are well known. Succinic acid can ionize with two steps, shown in Eq.(8)

$$HOOCCH_2CH_2COOH \text{<-^.} HOOCCH_2CH_2COO^- + H^+$$

$$HOOCCH_2CH_2COO^- \xleftrightarrow{Ka2} {}^-OOCCH_2CH_2COO' + H^+ \quad (8)$$

Eq.(7) can be transformed into Eq.(9) according to the character of succinic acid.

$$D = \frac{\exp(-\frac{AH}{RT} + c) * [R,N]^n + 0,111, + 0,m,}{1 + [QpH-pKal] + [QpH-pKa2][QpH-pKal]} \quad (9)$$

$[R_3N]$ is denoted by the initial concentration of trialkylamine, Φ_1 and 0_2 are the volume fraction of n-octanol and toluene, respectively. pKal and pKa2 of succinic acid are 4.19 and 5.45 in turn.

The model shown in Eq.(9) was used to correlate the orthogonal experimental data shown in table 3. The model parameters were obtained shown in table 4.

Table 4 Model parameters of extraction of succinic acid by trialkylamine

AH/J-mol'[1]	C	n	R
-43648.0	-12.15	1.56	0.990

Some comparisons between the experimental results and the correlation are shown in table 5.

Table5 Comparison of experimental data of extraction of succinic acid into trialkylamine with predicted value

[AJ/molL"[1]	$[R_3N]$ /mol-L"[1]	d>i	02	T/°C	pH	Dexp	Deal	Relative error
0.01604	0.6881	0.1	0.6	40	4.70	11.21	11.72	4.57%
0.04056	0.4587	0.3	0.5	25	4.55	19.33	19.47	0.73%
0.06508	0.2294	0.5	0.4	55	4.26	2.14	2.16	1.12%

Comparing experimental data with model value, it could be held that the regression

precision of model was high.

3.3 IR Spectrum

To investigate the extraction mechanism, IR spectrum of the organic samples loading succinic acid was taken, shown in Figure 4.

1 and 2 of figure4 showed the IR spectrum of extraction of succinic acid with the initial concentration of 0.0166 mol-L'¹ and 0.0644 mol-L'¹ by 30% trialkylamine -70%tolune(v/v). Band at 1450 cm'¹ results from the COO'¹ stretching vibration in a carboxyl group of succinic acid bonded to an amine molecule, so do bands between 2700 cm'¹ and 2800 cm'¹ which is NH^+ stretching vibration. Both of the phenomena account for the concurrence of an ionic bond between succinic acid and trialkylamine. Band at 2398 cm'¹ arises from the v(0-O)+ $5(0\text{-}H)_{i\ p}$ combination vibration. In the wave number range, the C=0 stretching vibration transferring from 1700 cm'¹ to 1620 cm'¹ might indicate the concurrence of hydrogen-bond between an succinic acid molecule and an amine or two. Carbonyl complexes (hydrogen-bond between succinic acid and amine) and carboxylate complexes might exist. There was a little difference in the peak areas at 1450 cm'¹ and 1620 cm'¹ of 1 in comparison to 2 of figure 4.

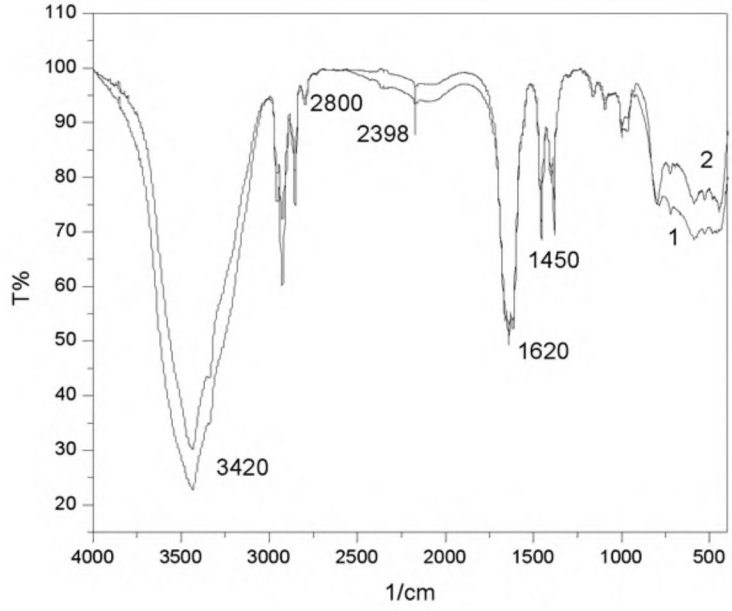


Fig. 4 IR spectrum of 30%trialkylamine-70%toluene loading succinic acid

On the basis of model parameters the stoichiometric proportion namely n between succinic acid and trialkylamine was *obtained from complex formation, which is 1.56. So (1,1) and (1,2) acid-amine complexes were formed in some proportion. Figure 6 shows some examples of possible succinic acid /amine complexes.*

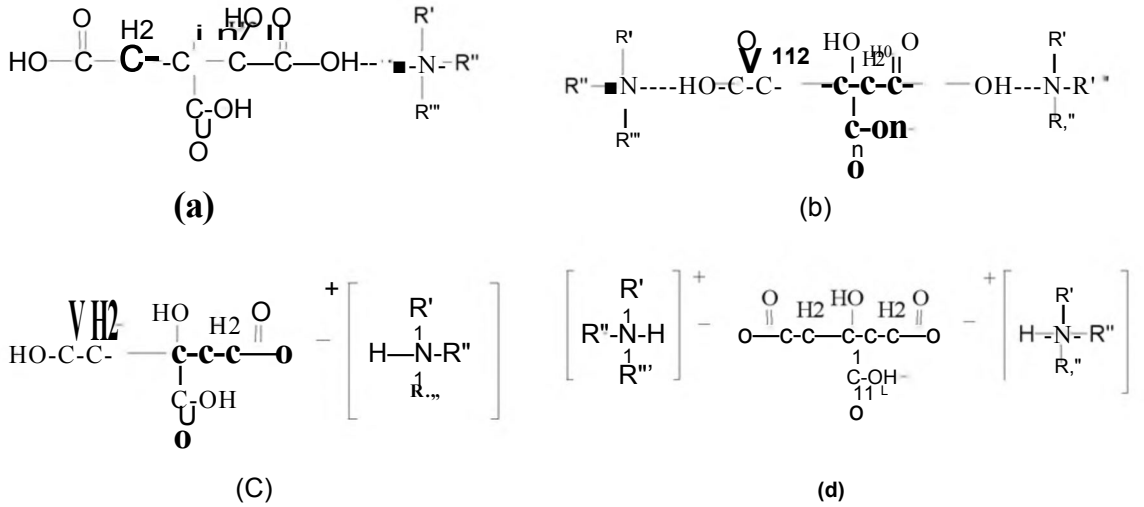


Fig. 6 Examples of complexes between tertiary amine and succinic acid
(q) 1:1 complex in carbonyl form; (b) 1:2 complex in carbonyl form;
(c) 1:1 complex in carboxylate form; (d) 1:2 complex in carboxylate form.

4 Conclusions

4.1 The extraction distribution coefficient increases with the decrease of the concentration of succinic acid and temperature, or with the increase of n-octanol and trialkylamine concentration in the organic phase.

4.2 On basis of orthogonal experimental design, equilibrium of succinic acid extraction from aqueous solution with trialkylamine dissolved in n-octanol and toluene were studied. The conditions preferable to complex extraction of succinic acid were that the temperature was 25°C, the volume percent of trialkylamine and n-octanol is 30% and 50% and the initial concentration of succinic acid is 0.01604mol L^{-1} on the experimental scale.

4.3 Using mass action law, the liquid-liquid equilibrium model of complex extraction of polybasic acid has been induced, and physical extraction was also considered in the model. Comparing experimental data with model value, it could be held that the regression precision of model was high.

4.4 IR spectrum was performed for information on the complexes and extraction mechanism, which confirmed the concurrence of hydrogen-bond and ionic-bond between succinic acid and amine. Combined the complex constant value of model with the spectrum, four kinds of complex compounds synthesized by succinic and trialkylamine were determined.

Nomenclature

D — Distribution coefficient

H_nA —Polybasic acid

[A'"]—Concentration of dissociated polybasic acid radical in the n step, mol-L'[1]

[X] [R_3N] —The initial concentration of trialkylamine, mol-L^{-1}

K—Equilibrium constant

Ka_n — The dissociation constant of weak polybasic acid in the n step, mol-L'[1]

m — Partition of physical extraction

O— Volume fraction of diluents in organic phase

AH— Enthalpy of complex reaction, J-mol'[1]

References

[1] J.A. Tamada, A.S. Kertes, C.J. King, Extraction of carboxylic acids with amine extractants. 1. Equilibria and Law of Mass Action Modeling, *Industrial and Engineering Chemistry Research,* 29(1990):1319-1326

[2] T. Kirsch, G. Maurer, Distribution of Oxalic Acid between Water and Organic Solutions of Tri-n-octylamine, *Industrial and Engineering Chemistry Research,* 35(1996) :1722-1735

[3] H. Ziegenfu(3, G. Maurer Distribution of acetic acid between water and organic solutions of tri-n-octylamine, *Fluid Phase Equibrium* 120(1994):211-255

[4] F. A. Poposka, et al. Extraction of tartaric acid from aqueous solutions with tri-iso-octylamine(HOSTAREX A 324). Equilibrim and Kinetics, *Chemical Engineering Science* 55(2000): 1591-1640

[5] M. Matsumoto, T. Otono, K. Kondo, Synergistic extraction of organic acids with tri-n-octylamine and tri-n-butylphosphate, *Separation and Purification Technology* 24(2001) 337-342

[6] M. Matsumoto. Extraction kinetics of organic acid with tri-n-octylphosphine *Chemical Technology and Biotechnology,* (3)1996 :260-264

[7] G. M. Sadaka, The Temperature on Forward/Back Extraction Using an Amine Extraction for the Recovery of Cyclic Hydroxy Carboxylic Acids, *Separation Science and Technology,* 11(1998): 1667-1680

[8] J.Zigova, D.Vandak, S.Schlosser, et al. Extraction equilibria of butyric acid with organic solvents *Reparation Science and Technology,* 19(1996): 2671-2684

[9] A. Senol. Extraction equilibria of formic and levulinic acids using alamine 308/diluent and conventional solvent systems, *Separation and Purification Technology*, (1-2)2000: 165-179

[10] J. Prochazka, A. Heyberger, V. Bizek, et al. Amine extraction of hydroxycarboxylic acids. 2. comparison of Equilibria for actic, malic, and citric acids, *Industrial and Engineering Chemistry Research,* (6)1994: 1565-1573



STUDY ON LIQUID-SOLID EXTRACTION FLOTATION SEPARATION OF MERCURY (II) BY THE SYSTEM OF SODIUM CHLORIDE-AMMONIUM THIOCYANATE-CETYLPYRINIUM BROMIDE-WATER

Xinrong Wen and Changqing Tu

Department of Chemistry, Jiaying University , Meizhou , Guangdong 514015,China

The liquid-solid extraction flotation separation of mercury (II) from other metal ions using the system of sodium chloride-ammonium thiocyanate-cetyl pyrinium bromide-water was studied. The results showed that with the amount of 1,0g NaCl and 0.5ml_ of a solution of O.lmol/L NH_4SCN and I.OmL of a solution of 1.0xi0"^{2}mol/l_ cetylpyrinium bromide(CPB),Hg^{2+} could be extraction floated quantitatively,and Cd^{2+},Ni^{2+},Mn^{2+},Co^{2+}, Fe^{2+},Al^{3+} could not be extraction floated,so Hg^{2+} could be separated successfully from those metal ions by extraction flotation at pH5.0. This method has been used for the extraction flotation separation of Hg^{2+} in the sample of synthetic water and the results were satisfactory.

INTRODUCTION

The separation of metal ions using the liquid-solid extraction system without organic solvents has been re ported [1-3], In this work, the liquid-solid extraction flotation separation behaviour of mercury(ll) from other metal ions using the system of sodium chloride-ammonium thiocyanate-cetylpyrinium bromide-water was studied. The results showed that with the amount of I.Og NaCI and 0.5mL of a solution of O.lmol/L ammonium thiocyanate and I.OmL of a solution of 1.0x10‘^{2}mol/L cetylpyrinium bromide(CPB), the precipitation $(CPB)_2[Hg(SCN)_4]$ could be formed by Hg(II) reacted on I" and the cation of cetylpyrinium bromide (CPB^+) at pH5.0.The precipitation $(CPB)_2[Hg(SCN)_4]$ stayed above the salt-water phase and formed the extraction flotation phase(solid phase). In the course of forming liquid phase and solid phase, Hg^{2+} could be extraction floated quantitatively, and Cd^{2+}, Ni^{2+}, Mn^{2+}, Co^{2+}, Fe^{2+}, Al^{3+} could not be extraction floated, so Hg^{2+} could be separated successfully from those metal ions without any masking agent by extraction flotation at pH5.0. Hg^{2+} and Cd^{2+} cannot always be separated easily because of similar properties, but Hg^{2+} and Cd^{2+} could be separated perfectly by using this system. This system has the advantages of being poison-free, environmental-friendly, operation-safe, and fast. Compared with the references [1-3],this system used less reagent and was economical. Comparing this system with the extraction flotation of organic solvent[4,5] and the forth flotation separation^],the operation of liquid-solid extraction flotation separation can be completeed in the absence of the toxic organic solvents and complicated instrumentation.

EXPERIMENT

Reagents and instruments

Analytical-reagent grade chemicals were used. Dissolving 7.613 g of ammonium thiocyanate in distilled water and diluting it to 1 L prepared a stock of standard solution of O.lmol/L ammonium thiocyanate. A stock of standard solution of O.OImol/L cetylpyrinium bromide(CPB) was prepared by dissoliving 0.4025g of CPB in distilled water and diluting it to lOOmL. A stock of standard solution of 1 $g \cdot L'^{1}$ Hg(ll) standard solution was prepared by dissolving 1.354g $HgCl_2$ in distilled water and diluting it to 1L, a working standard solution was prepared by appropriately diluting the stock standard solation.
Buffer solutions of different pH were prepared by referring the reference^].

A Model 722S spectrophotometer was used for photometric measurements.

Methods

Add 50g of Hg(ll), 0.5mL of 0.1 mol/L NH_4SCN and I.OmL of 0.01 mol/L CPB to a 25mL ground color comparison tube. Then adjust the pH with buffer solutions and dilute the mixture to 10mL. Add I.Og of solid NaCI and shake the mixture for 2 min before allowing it to stand for 4 min. Take I.OmL of salt-water phase and place it in another 25mL ground color comparison tube. Add 1.5mL of 0.001 mol/L 2-(5-bromo-2-pyridylazo)-5-diethylaminophenol (5-Br-PADAP) (dissolved in ethanol) and 3.0mL of 0.1 mol/L sodium borate and 0.5mL of 10% TritonX-100 to the tube. After dilution to volume, determine the amount of the metal ion at 565nm against a reagent blank, or determine the amount of the metal ion after dissolving(by using ethanol) the precipitation derived from filtrating.
Photometric analysis of other metal ions was referring the reference^].

RESULT AND DISCUSSION

Influence of the amount of NH_4SCN and CPB and extraction flotation mechanism

Using 50ug of Hg(ll) and 2.5mL of 0.01 mol/L CPB, when the amount of 0.1 mol/L NH_4SCN was 0.5mL resulted in the extraction flotation yield of 100% for Hg(ll). Hence, 0.5mL of 0.1 mol/L NH_4SCN was selected for all further studies.

Influence of CPB amount on extraction flotation yield of Hg(ll) is shown in Figure 1 .Using 50ug of Hg(ll) and 0.5mL of 0.1 mol/L NH_4SCN, when the amount of 0.01 mol/L CPB was I.OmL or more, Hg(ll) was extraction flotated perfectly. Hecen, 1 .OmL of 0.001 mol/L CPB was selected.

The experimental results showed that only when NH_4SCN and CPB were present together could the Hg(ll) be extraction flotated. So, the extraction flotation machanism of Hg(ll) is:

$$Hg^{2+} + 4SCN' \text{ — } [Hg(SCN)_4]^{2'} \qquad (1)$$

(water phase) (water phase)

$[Hg(SCN)_4]^{2'} + 2CPB^+ \text{ — } (CPB)_2[Hg(SCN)_4]$ (2)

(water phase) (extraction flotation phase)

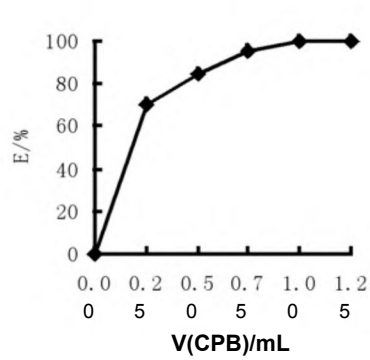


Figure 1. Influence of CPB amount on extraction flotation yield of Hg(II)
Hg(II):50jjg; NH_4SCN(0.1mol/L):0.5mL;
CPB: 0.01 mol/L

Influence of amount of different salts

Different amounts of NaCI, $NaN0_3$, $(NH_4)_2S0_4$ and KBr were added, in turn, to solutions of 50pg of Hg(ll), 0.5mL of 0.1 mol/L NH_4SCN,and 1.OmL of 0.01 mol/L CPB,the results showed that these salts all could form the liquid-solid phase.In these salts, NaCI is most effective. When the amount of NaCI is 1.0, 2.0 and 3.0g, the extraction flotation yield of Hg^{2+} was 100%, 100% and 98.8%,respectively. These data allowed us to conduce that 1.0g of NaCI can make liquid-solid phase separation perfectly, therefore, 1,0g of NaCI was selecteld

Influence of pH on extraction flotation yield of metal ions

The results showed that the extraction flotation yield of Hg(ll) was 100% in the pH range 1.0-7.0,and none of the following--Cd^{2+}, Ni^{2+},Mn^{2+}, Fe^{2+}, and Al^{3+} - could be extraction flotated in this pH range,in the pH range 1.0-5.0, the extraction flotation yield of Co^{2+} was 0, and when pH was 6.0 and 7.0, the extraction flotation yield of Co^{2+} was 7.0% and 11.3%. Hence, in the pH range 1.0-5.0, Hg(ll) can be separated perfectly from those metal ions by extraction flotation.

Sample separation

The extraction flotation separation results of Hg(ll) from Cd^{2+}, Ni^{2+},Mn^{2+}, Co^{2}\ Fe^{2+}, Al^{3+} are given in Table 1 and Table 2, under the conditions of this experiment, when the pH was 5.0.

CONCLUSION

In this paper, the extraction flotation separation of mercury (II) from other metal ions was reported. When the pH was 5.0,in the system of NaCI-NH_4SCN-CPB-H_20, the precipitation $(CPB)_2[Hg(SCN)_4]$ could be formed and stayed above the salt-water phase forming the extraction flotation phase, while Cd^{2+}, Ni^{2+},

Mn^{2+}, Co^{2+}, $Fe^{2\backslash}$ Al^{3+} still stayed in the salt-water phase, so Hg^{2+} could be separated successfully from those metal ions.This method was successfully applied to the extraction flotation separation of Hg^{2+} in the sample of synthetic water.

Table 1. Separation results of binary- mixed ions (pH=5.0)

Mixed ions	Metal ions added (pig)		Metal ions found in water phase (pig)		Extraction flotation yield(%)	
	Hg	Me	Hg	Me	Hg	Me
Hg'^{+}- Cd'^{+}	50	30	0.1	32.8	99.8	9.3
	50	50	0	46.8	100	-6.4
	50	200	0.2	216.8	99.6	8.4
Hg^{2+}- Ni^{2+}	50	30	0	27.7	100	-7.7
	50	50	0	49.2	100	-1.6
	50	200	0.2	200.4	99.6	0.2
Hg^{2+}- Mn^{2+}	50	30	0	28.0	100	-6.7
	50	50	0	49.2	100	-1.6
	50	200	0	197.6	100	-1.2
Hg^{2+}- Co^{2+}	50	30	0.3	32.7	99.4	9.0
	50	50	0	49.9	100	-0.2
	50	200	0	204.9	100	2.5
Hg^{2+}- Fe^{2+}	50	30	0.1	32.0	99.8	6.7
	50	50	0	47.2	100	-5.6
	50	200	0	200.9	100	0.5
Hg^{2+}- Al^{3+}	50	30	0	32.5	100	8.3
	50	50	0	46.6	100	-6.8
	50	200	0.2	215.6	99.6	7.8

Me represents the other metal ions except Hg^{2+}

Table 2. Separation results of Hg2+ from multiple-mixed ions (pH=5.0)

	1	2	3	4
Hg^{2+} added (pig)	50.0	100.0	200.0	400.0
Cd^{2+},Ni^{2+},Mn^{2+},Co^{2+},Fe^{2+},Al^{3+} each ion added (pig)	30.0	50.0	100.0	200.0
Hg^{2+} found in solid phase (pig)	54.2	92.6	188.6	426.8
Extraction flotation yield of Hg^{2+} (%)	108.4	92.6	94.3	106.7

REFERENCES

1. Sun X, Li B, Fu K. Mikrochim.Acta, 1990, 111:101.
2. Horath W J. Talanta, 1992,39(5):487.
3. Xingguo Chen, Xiaojuan Wang, Zhide Hu. Anal Leet, 1996,29:1003.
4. Karger B L, Pinfold T A, Palmer S E. Sep.Sc/., 1970,5:603.
5. Elhanan J, Karger B L. *Anal.Chem.,* 1969,41:671.
6. Somasudaran P. *Sepn.Sci.,* 1975,10(1):93.
7. Wenbao Chang, Kean Li. The Concise Analytical Chemistry Handbook, *Beijing:Peking University Press,* 1981:262.
8. Jiaomai Pan, Yasen Chen, Hengtai Yan . Chromogenic Agent and Its Application in Metallurgical Analysis,Shanghai: *Shanghai Scientific and Technical Publisher,* 1981: 116

EXTRACTION WITH SUPERIMPOSED CHEMICAL REACTION IN COMPRESSED $C0_2$ BY MEANS OF ESTERIFICATION OF ACETIC ACID WITH METHANOL

Stephan Schwinghammer, Rolf Marrand Matthäus Siebenhofer*

Graz University of Technology, Austria
*Fa. VTU Engineering, Grambach/Graz, Austria

Investigation of esterification of acetic acid with methanol was conducted with and without heterogeneous catalyst in compressed carbon dioxide. In the first part of this project the autocatalytic effect of the compressed $C0_2$ on this equilibrium reaction was investigated. Conducting this esterification reaction in this alternative operating condition of high-pressure carbon dioxide, an environmentally benign solvent, will shift the yield towards the desired product methyl acetate. The influence of temperature, pressure and water content of the feed composition on the reaction yield was studied. Temperature of operation was varied between 298.15 K and 328.15 K. The pressure of operation was up to 9.1 MPa. Catalytic esterification was investigated with Amberlite IR-120, a strongly acidic ion exchanger. The yield of reaction differed significantly from esterification without catalyst.

INTRODUCTION

Supercritical fluids (SCFs) are widely used in industrial and environmental processes. In particular carbon dioxide is a perspective solvent for supercritical extraction of natural materials, mainly in food and pharmaceutical industry. That is due to its environmental benefits and favorable operating conditions. SCFs can either act as active component of a reaction or act as solvent for reactants, catalysts and products. The chemical as well as physical properties of supercritical fluids open a wide range of application, not only in the field of extraction but also in chemical reaction engineering. With a supercritical fluid it may be possible to increase the selectivity of a reaction while maintaining high conversion, to dissolve reactants and catalysts in a single fluid phase and carry out the reaction homogeneously, and to capitalize on the solvent characteristics of the supercritical fluid to separate the product species from the reactants, catalyst, and unwanted by-products.

The supercritical fluid which gained the most attention throughout the chemical and materials research community is carbon dioxide ($C0_2$). It is non-flammable, non-toxic, fairly inert, economical and environmentally benign. The adjustable solvating power of $scC0_2$ is an outstanding advantage in chemical synthesis. The physical properties of $scC0_2$ are highly dependent on pressure and temperature. This specification of $scC0_2$ enables fine-tuning of the reaction environment and as a result optimization of the rate and selectivity of reaction [1], Investigations on equilibrium reactions such as esterification reactions in compressed carbon dioxide have not been performed comprehensively until now [2], [3], In particular the catalysed/non-catalysed acetic acid esterification with methanol in compressed $C0_2$-medium has not been discussed in literature yet. The fact, that esterification of carboxylic acids with

alcohols has been widely studied in conventional media, has motivated us to transfer this reaction from the liquid phase to the alternative environment of supercritical conditions in an effort to increase the yield. Therefore, the evaluation of the use of compressed CO_2 for esterification of acetic acid with methanol in the presence of a heterogeneous catalyst and without any catalyst has been subject of this study (equation 1).

$$CH_3OH + CH_3COOH \Leftrightarrow CH_3COOCH_3 + H_2O \quad (1)$$

EXPERIMENTAL METHODS AND ANALYSES

Chemicals

Carbon Dioxide with purity of >99.94 volume% was purchased from Linde (Graz). Acetic acid and methanol, both of p.a. quality, and the solvent tetrahydrofuran (THF) of p.a. quality were supplied by Fluka (Buchs). Amberlite IR-120, a strongly acidic cation exchanger, used for the investigation of esterification with heterogeneous catalysts was provided by Fluka (Buchs). The chemicals were used without any further purification.

Apparatus and procedure

Investigation of the esterification reaction of acetic acid with methanol was performed in a static apparatus (figure 1). The cell is designed for an operating pressure of 40 MPa at maximum temperature of 373.15 K. Volume of the cell is 140 mL. Two inspection glasses are installed at front and back side of the cell over the whole height enabling permanent visual control of experiments. The CO_2-rich phase is withdrawn on top and is fed back at the bottom of the cell by a gear pump. The apparatus is placed in a temperature controlled water bath to prevent separation of substances due to temperature gradients. Pressure and temperature are measured with an accuracy of ± 0.1 K and ± 0.01 MPa respectively.

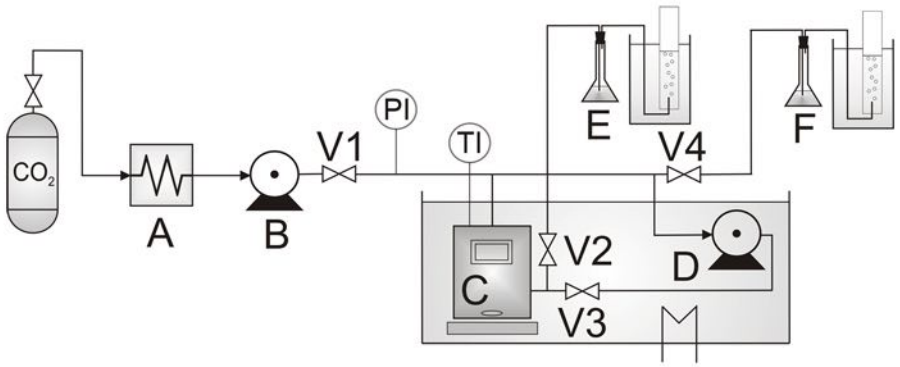


Figure 1. Schematic diagram of the experimental set up: (A) cryostat, (B) membrane pump, (C) high-pressure cell, (D) gear pump, (E) liquid phase sample flask, (F) gas phase sample flask.

In each series of experiments a sample of 15 to 30 mL was placed in the cylindrical equilibrium cell. The samples consisted of an equimolar ratio of acetic acid and methanol. Amberlite IR-120 as heterogeneous catalyst, and in selected experiments water was added to the reaction mixture at the beginning of each experiment. The composition of the liquid phase was determined by expanding a sample of liquid phase from the bottom of the cell into a glass vial. The CO_2 stripped from the sealed top of the glass vial was collected in a volume-calibrated glass cylinder which was filled with acidified water of pH-value 0.5. At pH 2 the loss of CO_2 by dissolving in water is negligible. From the volume of CO_2 gas collected in the glass cylinder and the weight of substance in the glass vial the amount of CO_2 in the liquid phase was calculated. The density of pure carbon dioxide was derived from Bender equation [4]. THF was used as solvent for preparing the liquid sample for gas chromatographic analysis. The gaseous phase was withdrawn from the cell on the top and

was expanded into a solvent flask (tetrahydrofuran) according to the liquid side sampling procedure. About 2-3 mL of THF were prepared in a calibrated 5 mL flask, which was placed in ice water in order to collect all of the sample. After sampling the pipe was washed with THF and purged with compressed air. The final sample volume was 5 mL. The so prepared sample was analyzed by gas chromatography.

Gas chromatographic analyses

All samples were analyzed with a gas chromatograph, type Hewlett Packard 6890N with flame ionisation detector (GC-FID) and a capillary column (DBVRX, 30 m x 0.32 mm x 1.8 µm). The temperature of the capillary column was kept constant at 353.15 K for 1 minute, followed by ramp of 3 K min^{-1} to a temperature of 403.15 K, and a second ramp of 10 K min^{-1} to a final temperature of 443.15 K and held constant for 2 minutes. For calibration the substances were dissolved in tetrahydrofuran.

RESULTS AND DISCUSSION

Esterification of acetic acid with methanol was investigated in two different modes of operation. A first series of experiments was performed in compressed carbon dioxide without catalyst to examine the enhancement effect of carbon dioxide on this esterification reaction. The effect of the heterogeneous catalyst Amberlite IR-120 on the esterification reaction was investigated in a second series of experiments. Reaction yield of the target product methyl acetate was compared with the results obtained in the first series of experiments. Four our means, the esterification yield of methyl acetate is defined as the ratio of the formed methyl acetate to the reaction equilibrium yield of methyl acetate (according to equation 1).

Esterification without catalyst

In the first series of experiments, influence of compressed carbon dioxide on esterification of acetic acid with methanol was investigated. Esterification was investigated at a temperature of 298.15 K, 308.15 K and 328.15 K. Pressure was varied up to 9.1 MPa. In all series of experiments conversion increases with temperature. Without feed water the yield of esterification (at an operating pressure of 6.1 MPa) increases from 0.1 % at 298.15 K, 1.9 % at 308.15 K to 2.8 % at 328.15 K (figure 2).

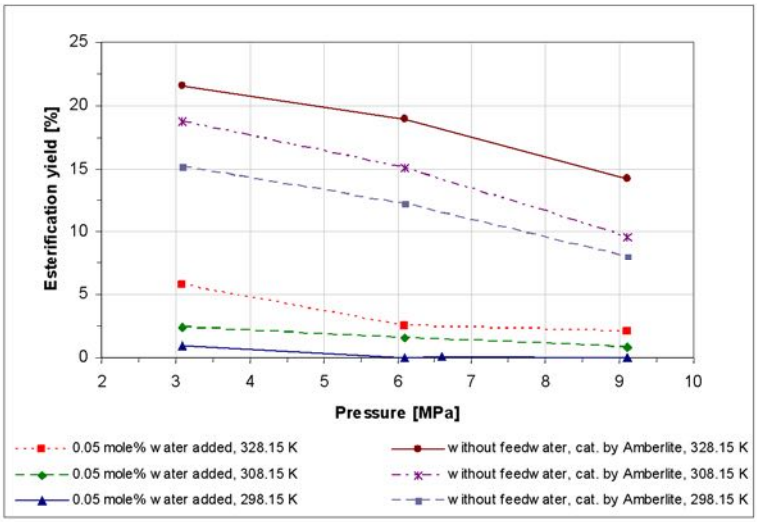


Figure 2. Comparison of esterification yield with and without catalyst vs. pressure; temperatures: 298.15 K, 308.15 K and 328.15 K.

The results are in accordance with the expected temperature dependence of the solvent power of carbon dioxide. The solvent power of carbon dioxide strictly depends on the density which is controlled by both the temperature and the pressure of operation. Particularly in the vicinity of the critical point the influence of the pressure is important. Density of carbon dioxide increases with increasing pressure and decreasing temperature. At low pressure the solvent
power of CO_2 decreases with increasing temperature, while at elevated pressure the opposite effect is observed (Cross-Over-Point) [5]. An increase in temperature results in a decrease in density and an increase of the vapor pressure. In the low pressure range the decrease in solvent density predominates. At elevated pressure the exponential increase of the vapor pressure with temperature is the predominating effect. As a consequence the solvent power of carbon dioxide increases with temperature. This phenomenon is responsible for the raise of the esterification yield shown in figure 2. At a temperature of 328.15 K the equilibrium solubility of pure methyl acetate in CO_2 is favored over acetic acid, methanol and water [6].

According to equation 1, water is expected to have a negative effect on the yield of esterification. Nevertheless the effect of feed water on the rate of reaction due to proton formation from carbon dioxide was investigated. The amount of water in the feed solution was varied up to 0.08 mol%. In the investigated temperature range an increase of water in the feed mixture will decrease the yield of esterification. Enhancement of the rate of esterification by adding water to the feed mixture due to protonation of carbon dioxide was not observed.

In the investigated pressure range an increase in pressure results in a decrease of the esterification yield. This phenomenon is more distinct at higher temperature, but was also observed at a temperature of 298.15 K. Since in accordance with equation 1 the total number of moles does not change during esterification the observed pressure sensitivity was not expected. The molar fraction of methyl acetate in the solvent phase corresponds with Dalton's law. Specific solvent-solute interaction may also explain the increased esterification yield at lower pressure. There is evidence in literature that the local density of a solvent in the vicinity of the solute is greater than the bulk density [7].

Effect of heterogeneous catalyst

In the second part of this project the effect of heterogeneous catalysts on esterification of acetic acid with methanol was investigated and compared to the non-catalyzed experiments. The catalyst Amberlite IR-120, a strongly acidic cation exchanger in H^+-form, was used in these series of experiments. The same tendency in the pressure and temperature dependence of catalytic esterification of acetic acid with methanol compared to the non-catalyzed cases was observed. With the heterogeneous catalyst Amberlite IR-120 a significant improvement in esterification yield was observed. At a temperature of 308.15 K and a pressure of 6.1 MPa the yield increased from 1.9% to 15.1%. This increase in the yield was achieved by adding 4.1 g of Amberlite IR-120 to an equimolar feed mixture of 30 mL which is equivalent 2.7 wt% of catalyst related to the amount of methanol in the feed mixture. As shown in figure 2, catalytic esterification does not differ from non catalytic esterification except the yield.

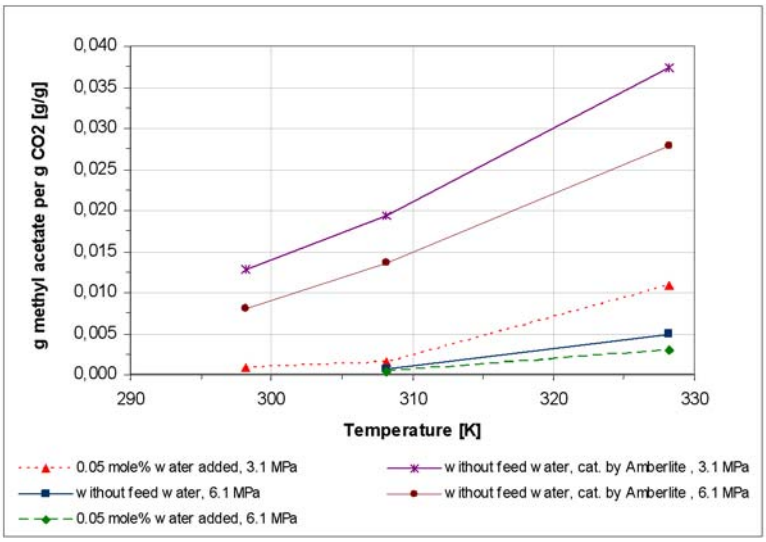


Figure 3. Methyl acetate load of the carbon dioxide phase versus temperature; parameters: operating pressure and water content of the feed for the catalyzed and non-catalyzed case.

In figure 3 the temperature and pressure dependence of the methyl acetate load of the carbon dioxide vapor phase is shown. The results of catalytic esterification with Amberlite are compared with non catalytic esterification. Catalytic esterification was again based on 2.7 wt% of catalyst related to the amount of methanol in the feed. In catalytic esterification as well as non catalytic esterification an increase of the methyl acetate load of the carbon dioxide phase with increasing temperature is observed.

CONCLUSIONS

The effect of compressed carbon dioxide on the esterification reaction of acetic acid with methanol was investigated. The first part of the experiments focused on the influence of compressed CO_2 alone on the esterification reaction. In several experiments the influence of temperature, pressure and water content of the feed mixture was studied. Experimental results showed an increase in esterification yield with increasing temperature and a decrease in the yield with increasing pressure. As expected, feed water has a negative effect on the yield and it does not accelerate the rate of conversion due to protonation of carbon dioxide. In the second part of the project the influence of a heterogeneous ion exchange catalyst on the esterification of acetic acid with methanol was investigated. Experiments carried out with Amberlite IR-120 as a heterogeneous catalyst showed a significant improvement of the esterification yield compared with the non catalytic reaction.

ACKNOWLEDGEMENTS

The authors wish to thank H. Luttenberger, Department of Chemical Engineering and Environmental Technology, Graz University of Technology, for carrying out the gas chromatographic analyses.

REFERENCES

1. P.G. Jessop, W. Leitner (1999), *Chemical Synthesis Using Supercritical Fluids*, Wiley VCH, Weinheim, Germany.
2. Z. Hou, B. Han, X. Zhang, H. Zhang, Z. Liu (2001), *J. Phys. Chem. B*, **105**, 4510-4513.
3. C. Vieville, Z. Mouloungui, A. Gaset (1993), *Ind. Eng. Chem. Res.*, **32**, 2065-2068.
4. E. Bender (1970), *Proc. 5th Symp. on Thermophysical Properties of American Society of Mechanical Engineering*, 227.
5. G. Brunner (1994), *Gas Extraction*, Springer, Darmstadt, Germany.
6. S. Schwinghammer, T. Gamse, R. Marr, M. Siebenhofer (2004), *Proceedings 9th Meeting of Supercritical Fluids*, Triest, Italy, 57.
7. J. Ellington, K. Park, J. Brennecke (1994), *Ind. Eng. Chem. Res.*, **33**, 965-974.

EXTRACTION OF METAL CATIONS BY COMPLEXONE SOLUTIONS IN SUPERCRITICAL AND LIQUID CARBON DIOXIDE

A.Yu. Shadrin, A.A. Murzin, V.A. Babain

V.G. Khlopin Radium Institute, St.Petersburg, Russia

The study is concerned with comparison of the extraction processes of macro- and microquantities of metals by complexone solutions in supercritical CO_2, liquid CO_2 and in organic solvents. It has been demonstrated that in most cases the regularities of liquid-liquid extraction are also retained in CO_2 extraction, but it should be taken into account that CO_2 is not an inert diluent and may interact with metal complexes, to form carbonates. Allowance must be also made for the fact that the aqueous phase being in equilibrium with CO_2 has pH = 2,8. It is shown that the other differences are mainly of kinetic character and are explained by much lower viscosity of liquid and supercritical carbon dioxide.

INTRODUCTION

One of the basic advantages of extraction by supercritical fluids or liquefied gases is the possibility for regeneration of "solvent" without the use of aqueous solutions, enabling dramatically to reduce secondary waste volume. Therefore, the specialists in management of radioactive wastes express interest to processes of supercritical fluid extraction (SFE). In the recent ten years the investigations in different countries have been aimed at extraction and leaching the traces of different radioactive [1-5] and heavy metals [6,7] as applied to purification and decontamination of solids, including soils, and to extraction and leaching of actinide macroquantities for spent nuclear fuel reprocessing [8-12]. Radiochemical directionality of research has led to the conclusion that the radioactive elements and uranium fission products are the most extensively studied. In the world a great body of non-systematized data is accumulated on metal extraction by supercritical fluids and liquid gases. The present work is devoted to analysis of main regularities of metal extraction (leaching) in media of supercritical or liquid carbon dioxide.

MATERIALS AND EXPERIMENTAL PROCEDURE

In order to demonstrate the observed regularities, use was made of the data obtained by the Radium Institute (see below) and the available literary data. For conducting the experiments a syringe high-pressure pump with cooled head and an extraction stainless-steel cell (3.5 ml) coated with pyrolytic chrome were employed. The samples containing on the surfaces the microquantities of uranium and plutonium or weighed portions of actinide oxides, as well as the aliquots of complexone, modifier and water, were placed into the extraction cell. Then the cell was filled with CO_2, was thermostatically controlled and kept for 20 min under preset pressure and temperature - static extraction; thereafter carbon dioxide was passed through the cell under the same pressure and temperature during 40 min - dynamic extraction. Extract was collected into methanol through a capillary restrictor. Block-diagram of the experimental setup is shown in Fig. 1. Procedures for samples preparation, experiments and

analysis are comprehensively described in [1,13].

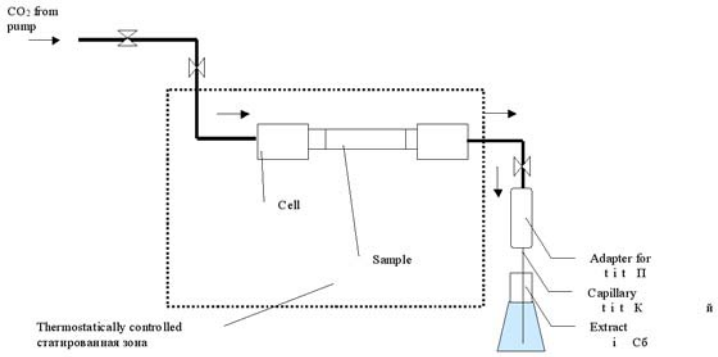


Fig.1. Block-diagram of laboratory setup

RESULTS AND DISCUSSION

To extract metals from different surfaces, β-diketones [14-17], tributylphosphate (TBP) and its mixtures with β-diketones [14,16-19], mixtures of TBP and dialkyldithiocarbamates [20,21] and alkylphosphoric acids [22-24] are applied. Extraction by β-diketones, TBP, TBP-diketone mixtures is the most extensively studied area. Analysis of literary data shows that all extractants have practically the same characteristics as compared with liquid-liquid extraction.

Although the processes proceeding in CO_2 medium and in medium of organic solvents share the common properties, they are also characterized by the following features:

- diffusion rate in organic solvent phase and penetrating ability of solutions in organic solvents are ten times lower than the same parameters in supercritical carbon dioxide (SC-CO_2), and are much lower than in liquid CO_2;
- carbon dioxide may affect pH value of liquid phase being in equilibrium with it;
- carbon dioxide may lead to formation of insoluble metal carbonates.

However, there exist differences in extraction of micro- and macroquantities of metals by complexone solutions in carbon dioxide. These differences are considered by the example of extraction of actinides and fission products.

Extraction of actinide microquantities

The first experiments on supercritical fluid extraction of actinides were conducted with the use of actinide microquantities. Investigation on dissolution and recovery of uranium nitrates and oxides in solutions of different complexones in carbon dioxide was first carried out by C. Wai's groups at University of Idaho (USA) [8,17]. The first experiments on supercritical fluid extraction of plutonium and neptunium from their oxides and nitrates were performed by Radium Institute [5,13].

From among investigated systems, the solutions of tributylphosphate (TBP), trifluoroacetylacetone (TFA) and di-2-ethylhexylphosphoric acid (D2EHPA) are most efficient for radionuclide removal under conditions of supercritical fluid decontamination [16,18,19,22]. Using these compounds as an example, the extraction processes of uranium traces from solutions in supercritical (300 atm., 60 °C) and liquid (70 atm., 25 °C) carbon dioxide were compared. The results obtained are presented in Table 1.

Table 1. Removal of uranium microquantities from stainless-steel surface by some complexone solutions in liquid CO_2 (60 atm.; 25^{0}C; 50 μg U in form of $UO_2(NO_3)2*6H_2O$; 0,55 mM H_2O)

Amount of complexone, mM	Uranium recovery by different complexone solutions, %								
	Supercritical CO_2, (300 atm., 60 °C) 20 min static extraction			Liquid CO_2, (70 atm., 25°C)					
				20 min static extraction			20 min static extraction		
	TBP	D2EHPA	TFA	TBP	D2EHPA	TFA	TBP	D2EHPA	TFA
0	< 0.5								
0.5	31 ± 7	11 ± 4	17 ± 6	12 ± 5	44 ± 11	18 ± 6	22 ± 4	41 ± 8	16 ± 8
1.0	47 ± 3	36 ± 7	29 ± 7	22 ± 4	76 ± 14	24 ± 4	29 ± 7	78 ± 7	22 ± 5
1.5	57 ± 5	57 ± 8	32 ± 6	2 ± 1	6 ± 3	9 ± 3	44 ± 6	86 ± 3	29 ± 4
3.0	68 ± 4	61 ± 9	34 ± 5	4 ± 2	---	9 ± 2	59 ± 4	---	29 ± 7
5,0	71 ± 4	82 ± 9	---	4 ± 3	----	---	---	----	---

It is established that in extraction by complexone solutions in liquid CO_2 it takes 40 min of static extraction to attain equilibrium, while in extraction in SC-CO_2 it will suffice 20 min according to many literary data. Non-monotony in dependence of metal recovery on complexone concentration in liquid carbon dioxide testifies that with increasing the added complexone volume the complexone concentration in carbon dioxide increases, the viscosity of medium increases and the diffusion rate decreases, resulting in recovery decrease. It may be also noted that the TFA extraction ability decreases as compared to expected value in accordance with the data on liquid-liquid extraction. This is due to the fact that pH of aqueous phase being in equilibrium with CO_2 comes to 2,8, which is not very good for complexformation with diketones. On adding some modifiers (TBP, DMSO, pyridine, amines) into the system the recovery of uranium increases. The conducted investigations show that the introduction of an organic base capable of forming more stable complexes with acid permits to bind HNO_3 released in the course of complexformation and thus results in growth of extraction efficiency [5]. Effect of amines is also observed in uranium extraction by solutions of fluorocarboxylic and phosphoric acids in carbon dioxide [26].

In Table 2 there are the data on Pu, Np and Am extraction by solutions of hexafluoroacetylacetone (HFA) and pyridine in SC- and liquid CO_2. Differences in metal recovery are observed only in the case of neptunium and plutonium extraction from their oxides. In this case the higher recovery of Pu and Np seems to be connected with the high penetrating ability of supercritical carbon dioxide.

Table 2 Extraction of Pu, Np and Am by HFA and pyridine solutions in SC and liquid CO_2 (0,07 mM HFA, 0,55 mM H_2O, 0,125 mM Py, 25 °C, 40 min)

Element	Chemical form	Recovery of element, %	
		300 atm., 25 °C	70 atm., 25 °C
Pu	nitrate	97 ± 1	77 ± 1
	oxide	76 ± 16	18 ± 2
Np	nitrate	99 ± 1	94 ± 1
	oxide	84 ± 6	16 ± 1
Am	nitrate	98 ± 6	97 ± 1
	oxide	85 ± 7	90 ± 5

The needed presence of water traces for efficient recovery is the characteristic property of metal cation extraction by complexone solutions in carbon dioxide. The data given in Table 3 reveal that there is the limiting concentration of water (0,3 % vol.); below this value the

extraction proceeds moderately and further growth of water concentration does not practically affect the extraction efficiency. Such property of extraction system suggests two main mechanisms of water effect in complexone solutions in CO_2 as follows:

- water is necessary to provide dissociation of β-diketone and metal salt;
- water forms stable micelles (colloid solution) in SC-CO_2 and metal complexes are extracted into SC-CO_2 just in the form of micelles.

Table 3. Influence of water on extraction efficiency of $Am(NO_3)_3$ by HFA-TBP or HFA-Py solutions in SC and liquid CO_2 (0,07 mM HFA, 0,55 mM H_2O, 70 atm., 25 °C, 40 min)

Complexone	Recovery of Am^{241} depending on water presence, %			
	0 mM	0,275 mM	0,55 mM	1,65 mM
Supercritical CO_2 (300 atm, 60°C)				
Pyridine, 0.125 mM	38 ± 4	54 ± 3	62 ± 3	61 ± 2
TBP, 0.035 mM	34 ± 5	59 ± 3	60 ± 6	59 ± 5
Liquid CO_2 (70 atm., 25°C)				
Pyridine, 0.125 mM	11 ± 3	79 ± 1	77 ± 1	82 ± 3
TBP, 0.035 mM	21 ± 10	76 ± 3	80 ± 4	77 ± 2

Hence, the main distinction of liquid-liquid extraction of metal microquantities from extraction into SC- or liquid CO_2 media lies in the fact that (i) diffusion rate in complexone solutions in CO_2, especially in supercritical carbon dioxide, is much higher than in organic solvents and thus the efficient extraction in CO_2 can be conducted without forced stirring, and that (ii) carbon dioxide may affect pH of liquid phase being in equilibrium with it.

Extraction of actinide macroquantities

Somewhat different regularities are observed in extraction of actinide macroquantities. So, the microquantities of U, Pu and Np oxides may be extracted by HFA solutions in CO_2 in the presence of water and TBP or pyridine (Table 3 and [13]); at the same time the efficient extraction of the macroquantities of actinide (IV) oxides is possible only in the presence of an oxidant like nitric acid [8]. The data in Table 4 show that, In contrast to the systems based on β-diketones, the solutions of TBP-HNO_3 complex in carbon dioxide can dissolve uranium dioxide, because HNO_3 is a quite strong oxidant. Pure Pu(IV) and Np(V) oxides are practically not dissolved even in the presence of HNO_3. But the homogeneous mixtures of actinide oxides efficiently dissolve in CO_2 containing TBP-HNO_3 complex (Fig. 2).

Table 4. Recovery of actinides from their individual oxides by complexone solutions in liquid and supercritical CO_2

Oxide	10 % vol. TBP-HNO_3, [Me] : [extractant] = 1: 2		10 % vol. HFA-TBP [Me] : [extractant] = 1: 2	
	250 atm, 60 °C	70 atm, 25 °C	250 atm, 60 °C	70 atm, 25 °C
PuO_2 (20 mg)	< 0.1	< 0.1	< 0.1	< 0.1
NpO_x (20 mg)	< 0.1	< 0.1	< 0.1	< 0.1
UO_2 (200 mg)	69 + 11	63 + 8	< 0.1	< 0.1

Thus, the differences in extraction of actinide macroquantities in CO_2 as compared to «classical» are determined by faster extraction kinetics, on the one hand, and possible decomposition of extractable complexes, on the other hand [27].

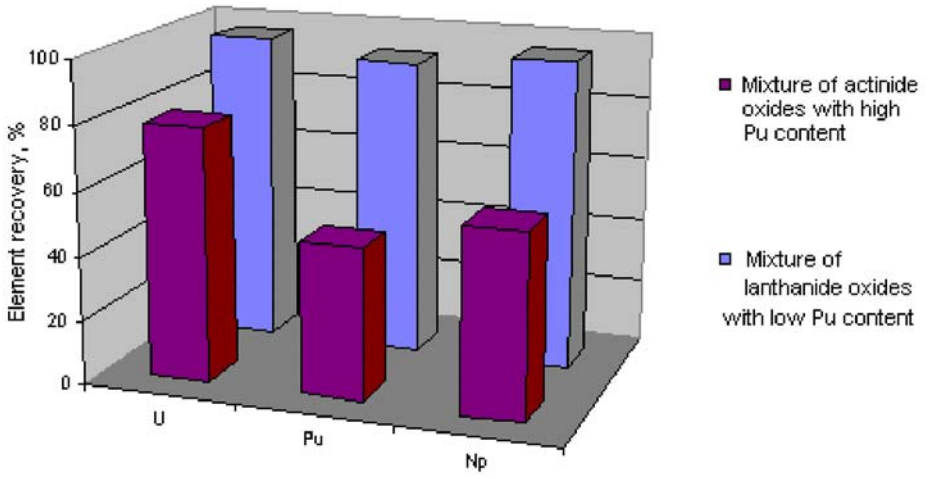


Fig. 2. Extraction of actinides from mixture of their oxides by TBP-HNO_3 solutions in liquid CO_2 (200 mg of oxide mixture, [U]:[TBP]:[HNO_3]=1:3:6)

Extraction of microquantities of heavy metals and fission products

The fundamental regularities of metal extraction by complexone solutions in liquid carbon dioxide are considered by the example of extraction (leachability) of metal cations from Cambrian clay. The obtained data show that lead can be efficiently extracted (by more than 70% in a single operation) by HFA-pyridine or HFA-TBP solutions in CO_2 and solutions of alkylphosphoric acids - di-2ethylhexylphosphoric acid (D2EHPA), dioctafluoroamylphosphoric acid (DOFAPA), di-2-ethylhexyldithiophosphoric acid (D2EHTPA). The solutions of organophosphoric acids in CO_2 may also extract cadmium, and the D2EHTPA solutions can be used for removal of antimony and arsenic [7]. The data given in Table 4 indicate that the DOFAPA and D2EHTPA solutions in CO_2 may be used for efficient extraction of such elements as cesium, strontium, americium and antimony, i.e. no other essential differences between liquid-liquid extraction of metal microquantities and extraction into CO_2 medium are observed, except for pH effect of equilibrium liquid phase.

Table 5. Extraction of some fission products by solutions of phosphorus-containing acids in liquid CO_2 (70 atm., 25 °C)

Composition	Recovery, %				
	Cs^{137}	Sr^{90}	Am^{241}	Sb^{125}	Ru^{106}
0.09 mM DOFAPA, 0.075 mM OctOH, 0.55 mM H_2O, 0.105 mM TBP	$86_{\pm 16}$	$83_{\pm 12}$	$90_{\pm 11}$	$4_{\pm 2}$	$67_{\pm 15}$*
0.09 mM D2EHPA, 0.0075 mM OctOH, 0.55 mM H_2O, 0.105 mM TBP	$86_{\pm 16}$	$83_{\pm 12}$	$90_{\pm 11}$	$81_{\pm 13}$	$2_{\pm 1}$

* - 20 % aqueous solution of H_2O_2 was used instead of H_2O.

CONCLUSION

The extraction of metal cation microquantities by complexone solutions in liquid and supercritical CO_2 differ little from the liquid-liquid extraction processes. At the same time it should be noted that

- low viscosity and high diffusion rate allow to conduct the extraction into CO_2 without phase stirring;
- CO_2 may affect the pH value of liquid phase being in equilibrium with it.

ACKNOWLEDGEMENTS

This study was performed under financial support of International Science and Technology Center (ISTC project 2055), RosAtom (Russia) and JNC (Japan).

REFERENCES

1. Shadrin, A. Murzin, N. Smart et al., (1998), *Proc. 5th Meeting on Supercritical Fluids*, ISASF, France, 155-160.
2. J. Mincher, R.V. Fox, R.G.G. Holmes et al.. (2001), *Radiochim. Acta*, **89**, 613-619.
3. K. Park, M. Koh, H. Kim et al., (2004), Proc. 11th *Meeting on Supercritical Fluid Chromatograhy,* USA, 113-114.
4. Y.Meguro, J. Ougiyanagi, O. Tomioka et al..(2003), *Proc. 2nd Meeting on Supercritical Fluid Technology for Energy, Super Green,* Japan, 175-179.
5. A. Murzin, V. Babain, A. Shadrin et al.. (1998), *Radiochemistry*, **40**, 47-54.
6. C. Kersh, M.J.I. van Roosmalen, G.F. Woglee, C.J. Witkamp (2000), *Ind. Eng. Chem. Res.*, **12**, 4670-4674.
7. A. Shadrin, V. Kamachev, A. Murzin et al.. (2003), *Proc. Int. Conf. SIS'03*, Bratislava, Slovakia, 66.
8. C.M.Wai, N.G.Smart, C.Phelps (1998), *US Pat.* 5606724 A /
9. M. Samsonov, T. Trofimov, S. Vinokurov et al.. (2001), *Proc. Int. Conf. Actinides 2001*, November 4-9, Hayama, Japan, 263-266.
10. T. Shimada, S. Ogumo, N. Ishihara et al. (2001), *Proc. Int. Conf. Actinides 2001*, November 4-9, Hayama, Japan, 757-760.
11. Y.Enokida, K. Savada, I. Yamamoto (2004), Proc. 11th *Meeting on Supercritical Fluid Chromatography,* USA, 111-112.
12. A. Shadrin, A. Murzin, V. Babain et al. (2002),., *Abstracts 9th Meeting on Supercritical Fluids*, ISASF, Italy, 52.
13. A. Shadrin, A. Murzin, V. Babain et al., (1998),., *Proc. 5th Meeting on Supercritical Fluids*, ISASF, France, 791-796.
14. Y. Lin, C.M. Wai, F.M. Jean, R.D. Brauer (1994), *Environ. Sci. Technol.*, **6**, 1190-1193.
15. N. Saito, Y. Ikushima, T. Goto (1990), *Bull. Chem. Soc. of Japan*, **5**, 1532-1534.
16. C.M. Wai, (1995), *Anal. Sci.*, **11**, 165-167.
17. Y. Lin, R.D. Brauer, K.E. Laintz, C.M. Wai (1993), *Anal. Chem.*, **65**, 2549-2551.
18. K.E. Laintz, E. Tachikawa (1994), *Anal. Chem.*, **13**,2190-2193.
19. Y. Lin, H. Wu, N. Smart, C.M. Wai (1998), *Journal of Chromatography A*, **793:1**, 107-113.
20. Y. Lui, V. Lopez-Avila, M. Alcaraz et al.. (1993), *J. of Chromatographic Science*, **31**, 310-316.
21. E. Laintz, C.M.Wai, C.R. Yonker, R.D. Smith (1991), *J. Supercritical Fluids*, **4**, 194-198.
22. A. Shadrin, A. Murzin, V. Starchenko (1998), *Proc. Int. Conf. Spectrum'98*, ANS Inc, USA, 94-98.
23. S.N. Joung, S.J. Yoon, J.U. Park et al.. (1999), *J. Chem. Eng. Data*, **44**, 1034-1039.
24. A. Shadrin, A. Murzin, D. Shafikov et al. (2004), *Abstracts 9th Meeting on Supercritical Fluids*, ISASF, Italy, 180.
25. A. Shadrin, A. Murzin, V. Romanovsky (2002), *Proc. Int. Conf. Spectrum'2002*, ANS Inc, USA, on CD.
26. A. Shadrin, A. Murzin, S Podoinitsin, (2002) *Proc. Int. Conf. Supergreen'2002, Suwon, Korea pp 42-47*.
27. A. Murzin, V.Babain, A. Shadrin et al. (2002) *Radiochemistry, Engl Ed,* **44**.467-471

LARGE ENHANCEMENT EFFECT OF HYDROGEN-BOND DONORS AS MODIFIER ON THE SOLUBILITY OF TRIS(β-DIKETONATO)-CHROMIUM(III) IN SUPERCRITICAL CARBON DIOXIDE

Akira Ohashi, Hirobumi Hoshino, Hisanori Imura and Kousaburo Ohashi

Department of Environmental Sciences, Faculty of Science, Ibaraki University, Mito, Japan

The solubilities of tris(pentane-2,4-dionato)chromium(III) ($Cr(acac)_3$), tris(trifluoroacetylacetonato)chromium(III) ($Cr(tfa)_3$) and tris(benzoylacetonato)chromium(III) ($Cr(bzac)_3$) in supercritical carbon dioxide ($Sc\text{-}CO_2$) with various modifiers of hydrogen-bond donor were investigated by UV-vis spectrophotometry. The modifiers used were methanol (MeOH), ethanol (EtOH), 2,2,2-trifluoroethanol (TFE), 1,1,1,3,3,3-hexafluoro-2-propanol (HFP), and 3.5-bis(trifluoromethyl)phenol (BTMP). The solubility enhancement of $Cr(acac)_3$ by the addition of the modifiers became larger in the following order: BTMP > HFP > TFE > MeOH > EtOH. This order is consistent with that of the ability of hydrogen-bond among these modifiers, showing that the solubility enhancement of $Cr(acac)_3$ by the addition of these modifiers is ascribed to the formation of the ternary complexes between $Cr(acac)_3$ and modifiers through hydrogen bonding in $Sc\text{-}CO_2$. The solubility enhancement by the addition of TFE became larger in the following order: $Cr(acac)_3$ > $Cr(bzac)_3$ > $Cr(tfa)_3$ among these Cr(III)-β-diketone complexes,.

INTRODUCTION

The supercritical fluid extraction (SFE) of organic compounds and metal complexes from solid and aqueous media has become a feasible alternative separation method to solvent extraction [1,2]. In particular, a supercritical carbon dioxide ($Sc\text{-}CO_2$) has been widely used as an extraction solvent [3,4], because it is non-toxic, cheap, and environmentally acceptable, and has a relatively mild critical point. Unfortunately, the solubility of a solute in $Sc\text{-}CO_2$ is generally much lower than that in conventional organic solvents. Therefore, modifiers, such as methanol and acetonitorile, have been employed for increasing the solubility of a solute in $Sc\text{-}CO_2$. There are several studies on the solubility of metal chelates in modified $Sc\text{-}CO_2$ [2]. However, an understanding about the interaction between metal chelate and modifier in $Sc\text{-}CO_2$ is not still enough, regardless of the fundamental significance for SFE.

Recently, we found that TFE drastically enhanced the solubility of $Cr(acac)_3$ in $Sc\text{-}CO_2$ much more than methanol that had generally been used as a modifier [5]. From IR measurement, the remarkable solubility enhancement effect of TFE could be ascribed to the formation of an association complex of $Cr(acac)_3$ with TFE through hydrogen bonding in $Sc\text{-}CO_2$. This effect is promising to overcome the disadvantage of the lower solubility of a solute in $Sc\text{-}CO_2$. Therefore, the investigation on the interaction between metal complex and modifier in $Sc\text{-}CO_2$ is very attractive.

In this study, we investigated the effect of various modifiers which were hydrogen-bond donors on the solubility of $Cr(acac)_3$ in Sc-CO_2 by UV-vis spectrophotometry. Moreover, the solubilities of tris(trifluoroacetylacetonato)chromium(III) ($Cr(tfa)_3$) and tris(benzoylacetonato)-chromium(III) ($Cr(bzac)_3$) in Sc-CO_2 modified with TFE were also investigated and the difference in the solubility enhancement among these Cr(III)-β-diketone (CrA_3) complexes was revealed.

EXPERIMENTAL

Reagents

$Cr(acac)_3$ (97.5%, Dojindo) and $Cr(bzac)_3$ (97%, Kanto Kagaku) were recrystallized from a benzene and hexane mixture. $Cr(tfa)_3$ (99.9%, Aldrich) was used as purchased. Methanol (MeOH, HPLC grade, Wako), ethanol (EtOH, HPLC grade, Kanto Kagaku), TFE (>95%, Daikin), 1,1,1,3,3,3-hexafluoro-2-propanol (HFP, 99%, Central Glass), and 3.5-bis(trifluoromethyl)phenol (BTMP, >95%, Tokyo Kasei) were used as modifiers. Liquid CO_2 (99.99%, Nippon Sanso) were also used.

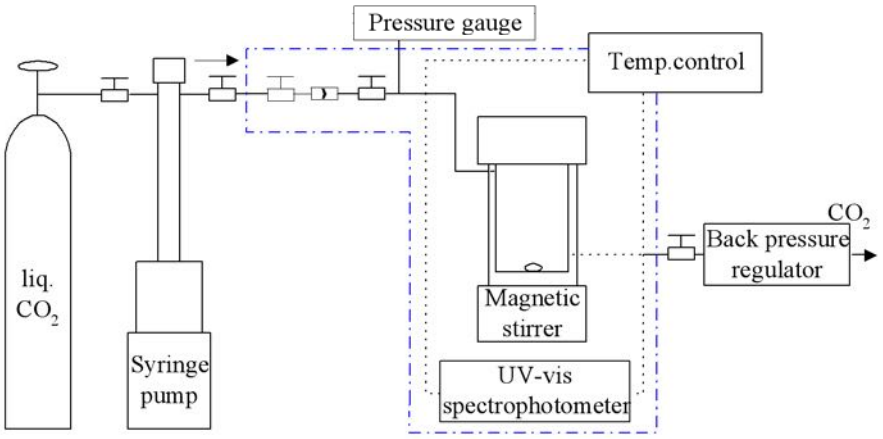


Figure 1. Schematic drawing of apparatus for measuring solubility of CrA_3 in Sc-CO_2.

Procedure

The apparatus for measuring the solubility of CrA_3 in Sc-CO_2 is illustrated in Figure 1. A stainless-steel cell (Jasco) of 2.20 cm^3 inner volume, consisting of a pair of sapphire windows (10 mm in diameter and 6 mm thick), was installed in a UV-vis spectrophotometer (Jasco, V-550). The optical path length was 10 mm. The temperature of the cell was controlled at 318 - 338 K using a water-jacket-type thermostat with a water circulator. After excess CrA_3 and a given amount of modifier were taken into the cell, CO_2 compressed to 10.1 - 20.3 MPa by a syringe pump was introduced into the cell. After stirring with a magnetic stirrer for 60 min and left standing for 5 min, the absorption spectra of CrA_3 dissolved in Sc-CO_2 were measured. The absorbance was constant after the prolonged stirring.

The molar absorptivity of $Cr(acac)_3$ in Sc-CO_2 was also measured in the same manner as described above, except for the addition of known amounts of $Cr(acac)_3$. The concentration of $Cr(acac)_3$ in Sc-CO_2 was varied from 1.25×10^{-3} to 1.12×10^{-2} mol dm^{-3}. The molar absorptivities of CrA_3 in various organic solvents were also measured with a Jasco 560 spectrophotometer at 298 K.

The CO_2 density, ρ (g dm^{-3}), at a given temperature and pressure was calculated using the freeware EOS-SCx ver. 0.2 [6], which is the program calculating density and thermodynamic properties by the equation-of-state for water, methanol, and CO_2.

RESULTS AND DISCUSSION

Molar absorptivity of CrA_3

The molar absorptivities of $Cr(acac)_3$ in Sc-CO_2 with and without 0.278 mol dm^{-3} TFE were determined using the Lambert-Beer law. The absorption band with a maximum absorbance at 562 nm, which is assigned to the d-d ($^4T_{2g} \leftarrow {}^4A_{2g}$) transition [7], was measured both in non-modified and modified Sc-CO_2 systems. The molar absorptivities, ε, of $Cr(acac)_3$ at 562 nm in non-modified and modified Sc-CO_2 with 0.278 mol dm^{-3} TFE at 318 K and 20.3 MPa were obtained as 69.1 $\pm$ 1.4 and 67.1 $\pm$ 1.3 dm^3 mol^{-1} cm^{-1}, respectively. These molar absorptivities were close to the values obtained from benzene (ε = 70.7 $\pm$ 0.3 dm^3 mol^{-1} cm^{-1}) and TFE (ε = 69.2 $\pm$ 1.4 dm^3 mol^{-1} cm^{-1}) solutions. This result implies that the molar absorptivity of $Cr(acac)_3$ at 562 nm is hardly changed by the solvation. Therefore, the value of ε in non-modified Sc-CO_2 was used for the calculation of the solubility of $Cr(acac)_3$ in the modified and non-modified Sc-CO_2.

The molar absorptivities of $Cr(tfa)_3$ and $Cr(bzac)_3$ in toluene were obtained as 73.3 dm^3 mol^{-1} cm^{-1} at 566 nm and 85.8 dm^3 mol^{-1} cm^{-1} at 563 nm, respectively. Since it was thought that these values were hardly changed in other solvents, these values were used for the calculation of the solubilities of $Cr(tfa)_3$ and $Cr(bzac)_3$ in Sc-CO_2.

Solubility of $Cr(acac)_3$ in modified Sc-CO_2

The Dependency of the $Cr(acac)_3$ solubility in Sc-CO_2 on the concentration of the modifier of hydrogen bonding donor was investigated at 318 K and 20.3 MPa (Figure 2). *S* in Figure 2 denotes the solubility of $Cr(acac)_3$ in modified Sc-CO_2. As shown in Figure 2, the solubility of $Cr(acac)_3$ was enhanced by the addition of the modifier in all cases. In particular, BTMP demonstrated a remarkably solubility enhancement of $Cr(acac)_3$. The solubility enhancement of $Cr(acac)_3$ by the addition of the modifier became larger in the following order: BTMP > HFP > TFE > MeOH > EtOH. This order is consistent with that of the ability of hydrogen-bond among these modifiers. (Each value of pK_a is 7.7 for BTMP [8], 9.3 for HFP [9], 12.4 for TFE [9], 15.2 for MeOH [9], and 15.9 for EtOH [9].) Previously, we found the ternary complex formation of $Cr(acac)_3$ with TFE through hydrogen bonding in Sc-CO_2 by FT-IR measurement [5]. This suggested that the solubility enhancement of $Cr(acac)_3$ by the addition of TFE resulted from the interaction between $Cr(acac)_3$ and TFE molecules through hydrogen bonding. Therefore, in the present study, most of the solubility enhancement effect by the addition of the other modifiers should be explained for the same cause.

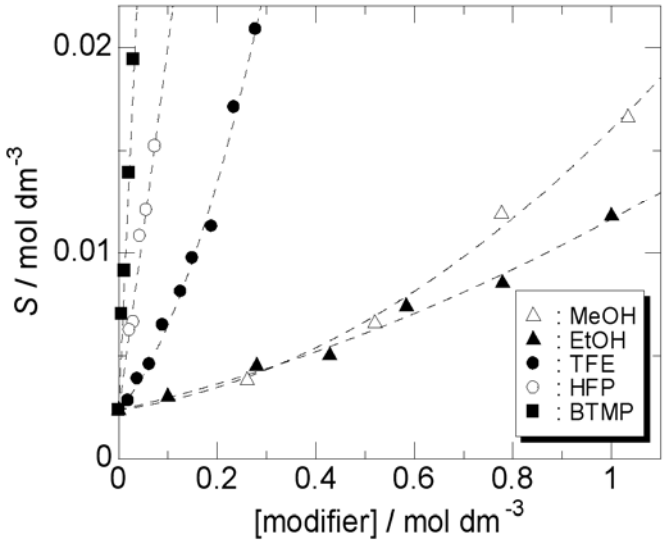


Figure 2. Dependency of the $Cr(acac)_3$ solubility on the concentration of modifier in Sc-Co_2. Pressure 20.3 MPa, temperature 318 K.

Effect of β-diketone on the solubility of its Cr(III) complex in modified Sc-CO_2

To begin with, the solubility, S_0, of CrA_3 in pure Sc-CO_2 was investigated using $Cr(acac)_3$, $Cr(tfa)_3$, and $Cr(bzac)_3$. In the absence of modifiers, the solubility of CrA_3 in Sc-CO_2 became larger in the following order: $Cr(tfa)_3$ > $Cr(acac)_3$ > $Cr(bzac)_3$. The solubilities of $Cr(acac)_3$ and $Cr(bzac)_3$ in Sc-CO_2 at 318 K and 20.3 MPa were 2.4 x 10^{-3} mol dm^{-3} and 6.9 x 10^{-5} mol dm^{-3}, respectively. The solubility of $Cr(tfa)_3$ in Sc-CO_2 was measured at 338 K and 10.1 MPa, since it dissolved too much to measure with Uv-vis spectrophotometer at 318 K and 20.3 MPa. The solubility of $Cr(tfa)_3$ at 338 K and 10.1 MPa was 1.0 x 10^{-3} mol dm^{-3}.

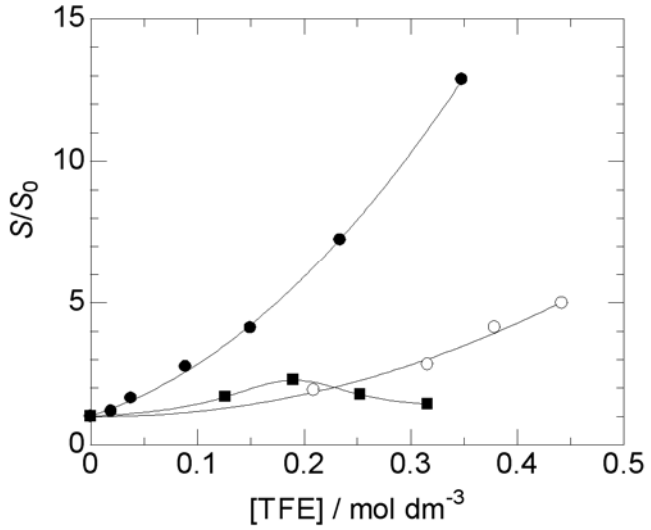


Figure 3. Dependency of the solubility enhancement of CrA_3 on the concentration of TFE in Sc-CO_2.
●, $Cr(acac)_3$ (318 K, 20.3 MPa); ○, $Cr(bzac)_3$ (318 K, 20.3 MPa);
■, $Cr(tfa)_3$ (338 K, 10.1 MPa).

Figure 3 shows the dependency of the solubility enhancement, S/S_0, of CrA_3 on the concentration of TFE in Sc-CO_2. The solubility enhancement by the addition of TFE became larger in the following order: $Cr(acac)_3$ > $Cr(bzac)_3$ > $Cr(tfa)_3$. The solubility of $Cr(tfa)_3$ was hardly enhanced by the addition of TFE. The association complex of CrA_3 with TFE through hydrogen bonding is probably formed between the hydroxyl hydrogen atom of TFE and the oxygen atoms of CrA_3 on an open octahedral face [10]. Therefore, the basicity of the oxygen atom of β-diketone affects the interaction between CrA_3 and TFE through hydrogen bonding. The pK_a values of β-diketones used are 8.67 for acetylacetone, 8.39 for benzoylacetone, and 6.13 for trifluoroacetylacetone in 0.1 mol dm^{-3} sodium perchlorate solution [11]. As the pK_a value of β-diketone is larger, the solubility enhancement of its Cr(III) complex become larger. This implies that the solubility enhancement in this system is also ascribed to the formation of the association complex through hydrogen bonding. The basicity of the oxygen atoms of $Cr(tfa)_3$ may be too low to form the hydrogen bonding with TFE.

CONCLUSIONS

In this study, we investigated the solubility of CrA_3 in Sc-CO_2 in the absence and presence of the modifiers donating hydrogen bonding by Uv-vis spectrophotometry. In the present system, most of the solubility enhancement of CrA_3 upon the addition of the modifier should be ascribed to the formation of the association complex through hydrogen bonding between CrA_3 and the modifier molecules in Sc-CO_2. Therefore, as the acidity of the hydroxyl

hydrogen atom of modifier and the basicity of the oxygen atom of β-diketone were larger, the solubility enhancement became larger. The technique developed in the present study is promising to overcome the disadvantage of the lower solubility of a solute in Sc-CO_2, and will be widely applicable to the SFE of various organic compounds and metal complexes from solid and aqueous media.

ACKNOWLEDGEMENTS

This work was partially supported by the REIMEI Research Resources of Japan Atomic Energy Research Institute and Mitsubishi Chemical Corporation Fund.

REFERENCES

1. F. V. Bright and M. E. P. McNally (1992), *Supercritical Fluid Technology*, ACS, Washington DC.
2. L. T. Taylor (1996), *Supercritical Fluid Extraction*, John Wiley & Sons, New York.
3. N. G. Smart, T. Carleson, T. Kast, A. A. Clifford, M. D. Burford and C. M. Wai (1997), *Talanta*, **44**, 137-150.
4. C. Erkey (2000), *J. Supercrit. Fluids*, **17**, 259-287
5. A. Ohashi, J. Niida, H. Hoshino, H. Imura and K. Ohashi (2003), *Proc. Super Green 2003*, Nagoya, Japan, 289-292.
6. T. Ohmori, EOS-SCx Ver. 0.2 *[Internet]*. Available from: <http://hp.vector.co.jp/authors/VA030090/>.
7. A. M. Fatta and R. L. Lintvedt (1971), *Inorg. Chem.*, **10**, 478-481.
8. S. Hayashi and H. Imura, unpublished data.
9. E. P. Serjeant and B. Dempsey (1979), Ionisation Constants of Organic Acids in Aqueous Solution, Pergamon Press: Oxford, New York.
10. S. Katsuta, H. Imura, and N. Suzuki (1991), *Bull. Chem. Soc. Jpn.*, **64**, 2470-2474
11. T. Sekine, Y. Hasegawa and N. Ihara (1973), *J. Inorg. Nucl. Chem.*, **35**, 3968-3970.

EXTRACTION OF BAUHINIA UNGULATA L. USING SUBCRITICAL CO_2 AND ETHANOL

Elisa M. B.D. Sousa; Ana P. C. Câmara; Wallace.A. Costa; Auberan. V. Souza; C.P.Souza; Elisângela L. Galvão

Universidade Federal do R.G.Norte-Departamento de Engenharia Química
Campus Universitário s/n,CT/ DEQ/PPGEQ, Lagoa Nova – 59072970 -Natal, RN- Brazil
E-mail: Elisa@eq.ufrn.br

Brazil is considered the country with the greatest biodiversity, including aromatic, medicinal and spice plants. In some processes, traditional solvent extraction can be replaced by supercritical fluid extraction (SFE). In this study, experimental results of extraction of *Bauhinia ungulata* are presented. The effect of the temperature and packing diameters on the total yield, and chemical composition were determined. Comparative analysis was performed between SFE extraction and liquid extraction, using ethanol. The solubility was calculated by using the dynamic method. Characterization of the obtained extracts was performed using GC/MS system, and the results showed that chemical composition is influenced by the method of extraction used.

INTRODUCTION

The extraction of solute from solids consists of a solubilization process and posterior separation of the mixture of solute and solvent. The extraction with pressurized fluids uses a fluid in conditions which are close or superior to critical area in order to extract the oil contained in the solid matrix. It is an advantageous method, because it provides products of high purity (without solvent residues and with excellent sensorial properties, flavor and aroma), conserving the therapeutic and nutritious qualities.

Bauhinia ungulata L. is characterized as a wild, small tree, of hard stem, fibrous peels and split leaves, forming two lobes whose form reminds the trace of a paw of bovine. In Brazil, it receives the name of "Mororó" or “pata de vaca" popularly. It is quite common in the region of the Brazilian northeast, especially on the seashore [1]. Although it is still not widely studied chemically, its hypoglycemic activity has been tested in several experiments, besides in including in clinical trials. According to the obtained results, it was observed that it acts reducing blood glucose. Some authors [2] submitted several species of *Bauhinia* to extraction of volatile components by steam distillation. The varieties: *forficata, aculeata, brevipes, longifólia, pentandra, rufa* and *variegata* were studied. It was detected the presence of several monoterpenes and sesquiterpenes as the caryophylene, germacrene, humulene, copaene, elemene, fenchene, etc, depending on the analyzed species. The phytochemical analysis of *Bauhinia manca* was evaluated [3]; about 63 components have been identified in an extraction performed with organic solvent. The most representatives

were the gallic acid, cinnamic acid, ß sitosterol and ß-D-glucoside. Some constituents of *B. guianensis* were also identified: ß-sitosterol, stigmasterol and naphtoquinone lapachol [4].

MATERIALS AND METHODS

Raw material characterization and preparation

The *Bauhinia ungulata* L.was from Fortaleza (State of Ceará, Brazil). The leaves were dried naturally in the shadow. After harvesting, the raw material was cleaned, conditioned in plastic bags under vacuum, and stored in a domestic freezer (Consul, model 280, Brazil). The humidity of the leaves was determined using the xylol distillation method [5]. For each experimental test, the frozen raw material was triturated in a domestic food processor (ARNO, model PRO, Brazil) for 15 seconds. Afterwards, the triturated solid was sifted using a shaker with sieves of the Tyler series (Produtest, no. 3614) for 15 minutes. The particle size distribution adopted for the extraction experiments was a mixture composed of particles of 28, 35 and 48 mesh.

Experimental equipment and procedure

The device used for the SFE experiments is presented in Figure 1. For each test about 120 g of *Bauhinia ungulata* L. were used to form the fixed bed. The material was weighed and placed inside of the equilibrium cell with the aid of a funnel and compressed by means of a stem in order to obtain a complete and uniform bed accommodation.

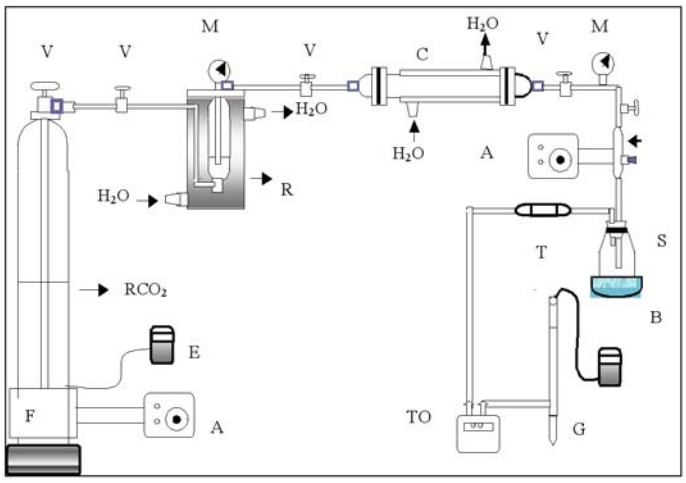


Figure 1 Experimental- Extraction unit: RCO_2= CO_2 reservoir containing a siphon and capacity of 25 kg; C = Jacketed equilibrium cell or extractor made of stainless steel with length of 0.60 m, diameter of 0.0216m and wall thickness of 0.028 m; M = Manometer type Bourdon (RECORD, 004-99, 0 – 100 bar, Brazil); H_20 = Water bath (TECNAL, model TE 184); R = Jacketed cylinder to keep the solvent as a sub cooled liquid with capacity of $0.5x10^{-3}$ m^3; T = capillary glass tube filled with porapak-Q (Supelco, 80/100 mesh, 75CC, lot 113, USA); S = glass flask, capacity for 5 mL; B = glass recipient with ice-cubes and water; A = voltage regulator (VARIAC, STP - Societies Technical Paulista, model -ATV-215 M, Brazil); E = digital thermometer (LUTRON, model TM-905); F = heating tape (FISATON, model 5, Brazil); V = needle type valves (HOKE, model 3712G2Y, USA); VM = micrometric valve (HOKE, model 1335G2Y, USA); G = glass bubble meter; TO = flow totalizer (LAO, model G1, Brazil).

Initially the stabilization of the system was promoted regulating it to operate at the desired temperature and pressure. Once these conditions were attained, the experimental run began

by opening the valve placed before the equilibrium cell, with the downstream valves previously opened. The experiment timing started with the appearing of the first oil drop in the collector flask placed just after the micrometric valve. Each minute the flow rate of CO_2 was recorded, both in the totalizer and in the bubble meter. Samples were collected at pre-determined time intervals. The collector flasks were closed and stored in the freezer for posterior analysis.

Ethanol extraction

The oleoresin from *Bauhinia ungulata* L was obtained using ethanol (MERCK, 99.8%) and the procedure of Povh (2000): 30 g of triturated *B. ungulata* was added to 180 mL of ethanol in an erlenmeyer (250 mL), which was covered with rubber corks, weighed and kept under agitation (190 opm) for 8 hours in a refrigerated incubator (Tecnal, model TE-421, Brazil) at 15°C. Afterwards, the mixture was vacuum filtered. The micelle (solvent + oleoresin) was placed in a dark flask, covered, weighed, and kept under refrigeration for 24 hours. The oleoresin quantification was made gravimetrically (Spricigo, 1998, cited by Povh, 2000): 20 mL of the filtered micelle was weighed using an analytical balance (AND-HR-120, Japan) in Petri plates and allowed to rest for 48 hours in a room with the air conditioning set at 18°C. The amount of solvent evaporated was then determined. The Petri plates were taken to an oven with air circulation (Marconi, model MA035, Brazil) and temperature was set at 165°C for 6 hours. Afterwards, the plates were allowed to cool in a desiccator (30 minutes) and weighed. The Petri plates returned to the oven for additional periods of 30 minutes up to constant mass.

The chemical composition of the extracts

The chemical composition of the *Bauhinia ungulata* extracts was determined using a gas chromatographer coupled to a mass spectrometer system (GC-MS, Shimadzu, model QP 5000, Japan) equipped with a capillary column DB-5 (30m *x* 0.25 mm *x* 0.1μm). The carrier gas was helium. The temperature programming 35-180°C, 4°C/min; 180-280°C, 20°C/min; 280°C (5min). The split ratio was 1/20. The injected sample was 1.0 μL of extract diluted in ethyl acetate. The identification of the substances was based on *i*) comparison of substance mass spectrum with GC/MS system data bank (Nist 62 Library); *ii*) comparison of mass spectrums with data in literature [6], and *iii*) retention index [7].

Calculation procedures

Using the experimental data, the overall extraction curves were fitted to a spline using two straight lines. The first line represented the constant extraction rate period (CER). From the spline, the mass-transfer rate for the CER period (M_{CER}) was computed, as well as the time corresponding to the interception of the two lines (t_{CER}). The spline fit was done using multiple-regression analysis (STATISTICA 5.5). MS Excel 2000 was used to determine the interception of the two lines. The mass ratio of solute in the supercritical phase at the equilibrium cell outlet (Y_{CER}) was obtained dividing M_{CER} by the mean solvent flow rate for the CER period ([8] and [9]).

RESULTS AND DISCUSSION

The table 1 presents the samples and the particles bed characteristics used in all the experiments. The figure 2 shows the extraction kinetics curves obtained for the two temperature levels analyzed. It is observed that, for the initial phase of the process, the extraction rate at 20ºC is superior to the rate at 15ºC, which doesn't happen for the intermediate and final phases, where the inversion of this behavior is verified with the increase of the extraction rate at 15°C. The final result showed that the amount of extracted oil in the established total time (around 220 minutes) was larger in temperature of 15ºC. This

can be confirmed in the figure 3 where is observed that the increase of 15ºC to 20ºC resulted in a reduction of 11% in the extraction yield values and of approximately 9.38% in the solubility values.

Table 1- Characterization of the samples

Bauhinia ungulata		
Humidity (%)	7.0	
Bed apparent density (g/cm^3)	0.48	
Granulometry (mesh)	Fine	Medium
	28 mesh (49.98%); 35 mesh (33.34%); 48 mesh (16.68%)	28 mesh (70.38%); 35 mesh (22.22%); 48 mesh (7.40%)

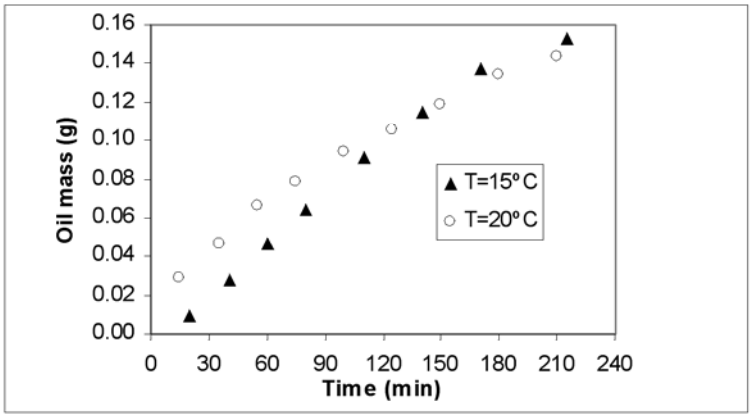


Figure 2- Extraction kinetics curves. P=66.7 bar; Q_{CO2}=0.95 g CO_2/min

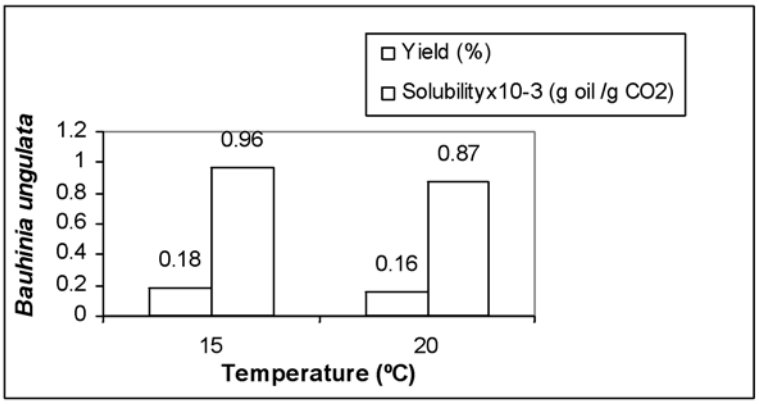


Figure 3- Influence of the temperature on the extraction yield and on the oil solubility.

The influence of the sample granulometry on the extraction yield and oil solubility in carbon dioxide was also evaluated, and the results are presented in the figure 4. Two granulometry types were used. They are named medium and fine granulometry. A strong influence of the particle size was observed on the yield and the solubility. It was concluded that working with particles of very fine granulometry would not be viable because this fact caused a considerable reduction in the yield as well as in the solubility. This influence was very strong on the experiments accomplished with the *Bauhinia ungulata*, because the results presented a decrease of 29.17% and 65.8% in the yield and in the solubility, respectively, when the samples granulometry was reduced. Probably, a certain amount of extract has been lost during the phase of preparation of the samples, in function of excessive triturating to reduce the size of the particle.

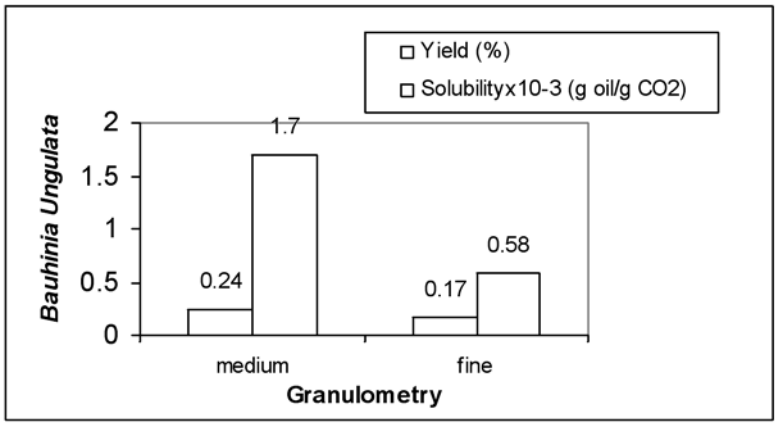


Figure 4- Influence of the granulometry on the extraction yield and on the oil solubility.

The influence of the crop period about the yield and the solubility was also investigated (figure 5). The crops were accomplished in the rains (April) and in the dry season (September). It was verified that the results were superior to the samples picked in September. The differences were significant, because there was a considerable increase of 5.9% and 65.5% for the yield and the solubility, respectively.

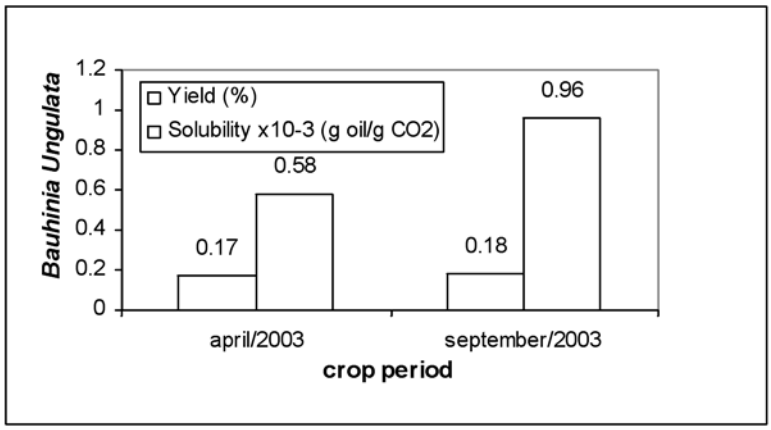


Figure 5- Influence of the crop period on the extraction yield and on the oil solubility.

The yield results and chemical composition of the extract obtained from using the technique of extraction with CO_2 were compared to the results obtained from the conventional technique using organic solvent (ethanol). The yield for the extraction with ethanol was shown very superior (3.54%), as table 2 demonstrates. However, in that value of total extract, besides the essential oil there are pigments, waxes, resins, etc. In that way, it is more viable to compare the results obtained only in relation to the essential oil content. Even so, the extraction with ethanol presented results superior (0.74%) with relation to extraction with CO_2 (0.24%).

Table 2- Extraction yield versus extraction technique

Extraction technique		Yield (%)
CO_2		0.24
Ethanol	Total extract	3.54
	Essential oil	0.74

The chemical composition of the obtained extracts presented significant differences in relation to the two techniques used (table 3). The extraction with CO_2 obtained 15 components, corresponding to 92.31% of the identified components. The extraction with

ethanol obtained just 10 components and the percentage of identified components was 81.75%. The following components stood out: trans-pinene and stigmast 5-en-3-ol (ethanol) and neophytadiene and squalene (CO_2).

Table 3- Influence of the extraction technique on the chemical composition of the Bauhinia ungulata extract

% (Area)					
Components	Ethanol	CO_2	Components	Ethanol	CO_2
α-copaene	-	2.61	vitamin E	6.05	2.75
β-elemene	2.27	1.50	neophytadiene	8.73	22.5
trans-caryophylene	-	4.67	hexadecanoic acid	-	2.73
β-selinene	-	1.88	squalene	8.90	36.4
caryophylene oxide	-	2.70	δ-fenchane	6.48	
4-stigmasten-3-one	5.74		Stigmast-5-en-3-ol	14.7	
δ-cadinene	-	3.70	hexadecane	5.47	
palustrol	-	5.31	γ- muurolene	-	3.23
α-muurolene	-	3.38	Identified total	81.75	92.31
trans-pinene	23.41	1.65			

CONCLUSIONS

The extraction process of the *Bauhinia ungulata* with pressurized CO_2 seemed to be viable for offering a larger variety of components than the extraction technique with ethanol, even so, new operational conditions should be investigated, with the objective of rising the yield values and oil solubility, as well as new temperature strips, pressure and solvent flow rate and the operational time. The crop period and the granulometry of the samples interfered a lot in the yield values and solubility observed. Among the samples analyzed, the ones which stood out were picked in dry season and they had intermediate granulometry. From the identification of the components present at the extract, the therapeutic activity might be discovered and compared to the oil obtained by steam extraction which is a traditional process of essential oil extraction.

REFERENCES

1. Matos, F.J.A. Farmacias vivas, (1988) Edições UFC, Fortaleza, Brazil
2. Almeida, J.M.D.; Negri, G.; Salatino, A. (2004) Biochemical systematics and ecology (article in press- available online at www.sciencedirect.com).
3. Achenbach, H.; Stocker, M.; Constenla, M. (1988) *Phytochemistry*, **27,** 6, 1835-1841.
4. Viana, E.P.; Santa Rosa, R.S.; Almeida, S.S.M.S.; Santos, L.S. (1999), *Phytochemical communication*, Fitoterapia**, 70**, 111-112.
5. Jacobs, M. B., (1973), *The Chemical Analysis of Food Products*. 3ª ed., Robert Krieger, Publishing Co., New York.
6. McLaferty, F.W.; Stauffer, D.B. (1989), The wiley/NBS Registry of mass spectral data. Vol. 1-2, John Wiley and sons, New York, 3139 p.
7. Adams, R.P. (1995), Identification of essential oil components by gas chromatography/mass spectroscopy 1st Ed. Allured Publishing Corporation, 468 p.
8. Rodrigues, V.M.; Sousa, E.M.B.D.;Monteiro, A.R.; Chiavone-Filho, O.; Marques, M.O.M.; Meireles, M.A.A. (2002), *J. Supercritical Fluids* **22**, 21-36.
9. Sousa, E.M.B.D.; Chiavone Filho, O; Moreno, M.T.; Silva, D.N.; Marques, M ; Meireles, M A.A. (2002), *Brazilian Journal of Chemical engineering*, **19,** 2, 229-241



Supercritical CO_2 extraction of green chemicals from Przewalsk Sage Root

Song Qihuang[1], Yao Yudong[2], Zhou Jiahua[1], Lin Huicong[1]

1 Faculty of chemical engineering and light industry, Guangdong University of Technology, Guangzhou, 510090, China
2 Guangzhou Light Industry Institute, Guangzhou, China

CO_2 is stateless, odorless, non-toxic and chemical inertness and would not contaminate environment and products. Conforming to more and more higher requirement of the modernized industrial productive process and product quality and high-grade product such as herbal medicine. CO_2 and co-solvent ethanol was used in the extraction of tanshinone II_A from przewalsk sage root. Controlling pressure, temperature, and amount of co-solvent tuned the solubility of supercritical fluid, and hence the extraction ratio of tanshinone II_A. It was revealed that the optima operation condition was 25Mpa, 45degree, ethanol 600mL/h, and granule size 40 mesh in term of extraction ratio and operation cost. The highest extraction yield was 98.9%

Keywords: Tanshinone II_A, supercritical extraction, przewalsk sage root

INTRODUCTION

Chinese herbal medicine has been employed in Chinese for thousands of years and has made great contribution to the development of the entire human beings. However, the development of Chinese herbal medicine has encountered great challenge in maintaining its market share in China and opening new market outside China. The major difference between Chinese herbal medicine and western medicine is that the composition of the Chinese herbal medicine is largely unknown. No data is available on the mechanism of the active ingredients and the toxicity and side effect of other chemicals in the medicine. To solve this, the active components of herbal medicine must be extracted and characterized properly.

Modern medical research shows that przewalsk Sage Root has the effects of resisting bacteria, diminishing inflammation, improving cardiovascular system considerably, avoiding oxygen deficit of cardiac muscle, protecting liver, inhibiting tumor and stabilizing nervous system[1]. However, the active material tanshinone II_A is not stable under heat in the presence of water. The aqueous extraction ratio was 55.55%[2]

Supercritical fluid extraction is a nontoxic state-of-the-art technology originally commercialized for the food, fragrance, and environmental industries. Supercritical CO_2 is an excellent solvent for many substances. The solvent properties of supercritical CO_2 can be tuned over a wide range to provide an optimal extraction. This is done by finding the exact combination of temperature and pressure in the extraction chamber to yield an extract with the desired profile. The solubility profile of CO_2 can be extended further with the introduction of polar solvent[3,4].

The aim of this research was to development a better process to extract the active ingredient tanshinone II_A of Przewalsk Sage Root using supercritical CO_2 extraction.

EXPERIMENTAL

Equipment and reagents

Supericritical Fluid extractor (Extractor volume 0.5L, Guangzhou Light Industry Institute,Guangzhou, China).

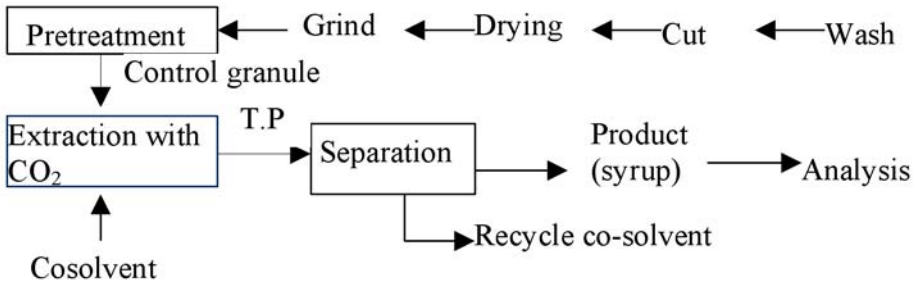
Rotational vacuum evaporator (Shanghai Instruments, Shanghai, China)

HPLC (HP1100, Dalian Elite Instruments, Liaoling, China)

CO_2 and ethanol(99.99%) were of analytical grade.

Przewalsk sage root was bought from Jiangzhong county, Sichuan province. The content of tanshinone II_A was 1331.3μg/g. Samples were ground to different size before extraction. The original size was denoted as 0 mesh. The samples that passed 40 and 20 mesh were denoted 40 mesh and 20 mesh, respectively.

Extraction



Przewalsk sage root was extracted as follow:
Przewalsk sage root was ground to pre-selected size and extracted with CO_2 using 95% ethanol as co-solvent under different temperature and pressure. The extract was then concentrated with rotary vacuum evaporator to recycle the used ethanol. The product was then weighted and analyzed with HPLC. The extraction ratio was calculated as the content of tanshinone II_A in the product /the content of tanshinone II_A × 100%. 50 gram of sage root was used in each bath. The flow rate of carbon dioxide was 15 kilogram per hours. The extraction time was three hours per batch.
To optimize the extraction parameters, a four-factors three-levels orthogonal experimental design was used based on a series of preliminary experiments[5]. Table I show the extraction the range of pressure, temperature, co-solvent, and granule size of raw material used in our research. The experimental result was shown in Table 2.

Table 1. Parameters investigated in the experiment

Level	Factors			
	A Pressure, MPa	B Temp, ℃	C Co-solvent, mL/h	D Granule size, mesh
1	15	35	200	0
2	20	45	400	20
3	25	55	600	40

Results and Discussion

The effect of granule size

Table2. The extraction result of tanshinone II_A

No.	A Mpa	B ℃	C Ethanol mL/h	D Granule size	Extraction ratio %
1	15	35	200	0	67.2
2	15	45	400	20	42.7
3	15	55	600	40	94.8
4	20	35	400	40	98.9
5	20	45	600	0	91.7
6	20	55	200	20	31.9
7	25	35	600	20	53.8
8	25	45	200	40	96.9
9	25	55	400	0	84.8
R_1	204.7	219.9	196	243.7	
R_2	222.5	230.9	226	128	
R_3	235.5	211.5	240.3	290.6	
$R_1/3$	68.23	73.3	65.33	81.23	
$R_2/3$	74.17	76.97	75.33	42.67	
$R_3/3$	78.50	70.50	80.10	96.87	
R (range)	10.27	6.47	14.77	54.20	

The order of the effect was D>C>A>B. The optimum condition was $A_3B_2C_3D_3$
Tanshinone II_A is located at the cortex of przewalsk sage root, granule size had a mixed affect on extract efficiency. The reduction in granule size increased surface area moderately and increased the contact of supercritical fluid with part of root carrying very low level of tanshinone II_A. The 40-mesh granule had the highest extraction efficiency while the 20-mesh granule had the lowest extraction efficiency. As the finer the granule size, the higher the processing cost and the more likely the fine powder clogs the filtration cloth, 40 mesh was considered suitable for extraction.

The effect of co-solvent

As carbon dioxide has a solubility index close to that of alkane, it is hard to extract polar materials with carbon dioxide alone. When ethanol was used, it increased the solubility of tanshinone II_A and hence, could reduce the extraction pressure and
the requirement for carbon dioxide. The results show that the extraction ratio increase with ethanol input. However, increase ethanol concentration also increase the recycling cost.

The effect of pressure

The capacity of the Supercritical CO_2 extraction depends upon the density of the liquid, and the conditions of controllable manipulation (pressure and temperature) can change its solubility and realize the selective extraction. Pressure increased the density, and hence, the solubility of carbon dioxide. However, the effect of pressure leveled off at high pressure and high pressure increased the operation cost and the requirement for equipment.

The effect of temperature

The overall effect of temperature was relatively small due to the double role played by temperature in the capacity of carbon dioxide and co-solvent. High temperature increased the diffusion coefficient at constant pressure on the one hand, it reduced the density of carbon dioxide on the other hand. To avoid the decomposition of active material relatively low temperature is preferred.

CONCLUSION

Extracting tanshinone II_A from przewalsk sage root with supercritical carbon dioxide was superior to traditional organic solvents. Supercritical CO_2 possessed the characteristics of normal temperature, none toxin, making a good environment, and use safely and simple, and the extraction time was short, and the product quality was high etc. Of cause, it was also has its limitations when comparing with the traditional organic solvents, such as a lower dissolving capacity for polar components. This was solved by introduction of polar co-solvent. The optima operation condition is 25Mpa, 45degree, ethanol 600mL/h, and granule size 40 mesh. The highest extraction ratio was 98.9%.

REFERENCES

1. Dong X W, The extract of active ingredients from sage root and its anti-oxidation effect. *Journal of Yintai University,* 1997,**28**,3-7
2. Yin M. Studies on the extraction ratio of Chinese herbal medicine. *Chinese Medicine*, 1995, **17**, 45-46
3. Zhang R C, *Supercritical Fluid Extraction,* Chemical Industry Press, Beijing, 2000, 106-108
4. Brennecke, J F, Eckert C A, Phase equilibrium for supercritical fluid process design, *AIChE,* 1989,**35**,1409-1420
5. Yin J., *Experimental design*, Shanghai Jiaotong University Press, Shanghai, 1986, **30-35**

AN ENZYME-FACILITATED LIQUID MEMBRANE BASED ON IONIC LIQUIDS FOR THE OPTICAL RESOLUTION OF (S)-IBUPROFEN

Masahiro Goto*, Eijiro Miyako and Tatsuo Maruyama

Department of Applied Chemistry, Graduate School of Engineering,
Kyushu University, PRESTO, JST, Fukuoka, Japan

We have succeeded in the enantioselective transport of our target (*S*)-enantiomer from racemic ibuprofen through a lipase-facilitated supported liquid membrane (SLM) based on ionic liquids. (*S*)-Ibuprofen was selectively esterified by CRL lipase in the feed phase, and the resulting ester dissolved into the ionic liquid phase of the SLM and diffused across the SLM. In the receiving phase, a different lipase (PPL) catalyses the ester hydrolysis to produce the initial ibuprofen and ethanol, which are water soluble. Finally, the target (*S*)-ibuprofen was selectively transported through the SLM, based on the enantioselectivity of biocatalysts. A control experiment performed without the lipases resulted in no ibuprofen transport through the SLM. This is the first report that successfully demonstrates that enzyme-facilitated SLM based on ionic liquids can be utilized for the optical resolution of racemic ibuprofen.

INTRODUCTION

A Liquid membrane technique is an advanced membrane separation technique, which combines forward and backward extraction in solvent extraction operation. In the present study, a biological function was introduced to the liquid membrane phase, which shows a high selectivity to a target compound.

Room-temperature ionic liquids (RTILs), especially those based on the *n*-alkylimidazolium cation, are emerging as novel alternatives for the conventional organic solvents used in chemical processes [1,2]. These environment-friendly solvents have many useful properties such as thermal stability, high ionic conductivity, negligible vapor pressure and a large electrochemical window. They also attract much attention as green solvents, as a reaction medium or an extraction solvent. In particular, recent studies have demonstrated that enzymes (lipases) are catalytically active in RTILs without considerable denaturation [3,4]. The use of RTILs as an immobilized phase in a supported liquid membrane (SLM) is interesting due to the non-volatile character of the RTILs which makes it possible to obtain a very stable SLM without any loss of the membrane phase to the atmosphere.

Rethwisch *et al.* reported enzyme-facilitated transport of organic acids through a bulk liquid membrane [5,6]. They employed lipase-catalyzed reactions to promote the transport of substances through the bulk liquid membrane. Enzymes usually have high substrate specificity and high enantioselectivity. In particular, lipases have been studied as biocatalysts for enantiospecific or substrate-specific reactions [7]. An enzyme-facilitated liquid membrane has the potential to be a highly selective liquid membrane. In the present study, we have

succeeded in the enantioselective transport of the (*S*)-enantiomer from racemic ibuprofen through a lipase-facilitated SLM based on ionic liquids.

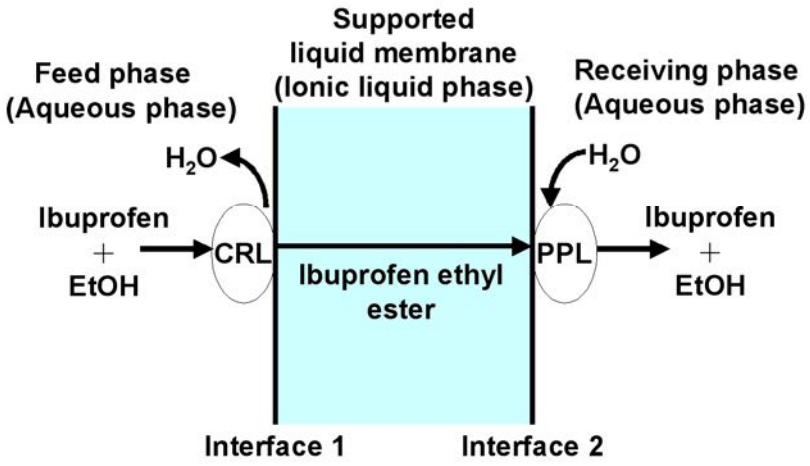
MATERIALS AND METHODS

Ionic liquids, 1-n-butyl-3-methylimidazolium hexafluorophosphate (abbreviated to C4mimPF_6), 1-n-hexyl-3-methylimidazolium hexafluorophosphate (C6mimPF_6), 1-n-octyl-3-methylimidazolium hexafluorophosphate (C8mimPF_6) and 1-n-butyl-3-methylimidazolium hexafluorophosphate (C4mimTF_2) were prepared according to the procedure described in the literature (Huddleston et al. 1998). The lipase from Candida rugosa (abbreviated to CRL) and that from porcine pancreas (PPL) were purchased from Sigma Chemical Co., St Louis, MO. Microporous polypropylene film (Celgard 2500) was obtained from Celgard Co., Tokyo. The thickness of the film was 25 μm and the maximum pore size was 0.2×0.05 μm. All other reagents were of guaranteed reagent grade.

A typical experimental procedure for the ibuprofen transport through a lipase-facilitated SLM based on an ionic liquid was as follows: the SLM was prepared by immersing a hydrophobic poly(propylene) film (Celgard 2500) into C4mimTF_2N. The ibuprofen transport experiment was performed at 37^{0}C using a pair of glass cells (Each cell had a volume of 55 mL and a 5 cm^2 cross-section). The SLM separates the two aqueous phases. The feed phase consisted of 65 vol% ethanol, 10 mM racemic ibuprofen and 35 vol% McIlvaine buffer (pH 6.3) containing 30 mg/mL lipase from *Candida rugosa* (CRL). The receiving phase consisted of McIlvaine buffer (pH 6.3) containing 20 mg/mL lipase from porcine pancreas (PPL). The concentrations of (*S*)- and (*R*)-ibuprofen in the feed and receiving phases were determined by HPLC analysis.

THEORY OF SELECTIVE PERMEATION OF CHIRAL COMPOUNDS

Lipase-facilitated transport of (*S*)-ibuprofen through an SLM based on ionic liquids is illustrated schematically in Figure 1. Lipase from *Candida rugosa* (CRL) is good at catalyzing esterification in the feed phase (at Interface 1), and another lipase from *porcine pancreas* (PPL) is an ester hydrolysis catalyst in the receiving phase (at Interface 2). Lipases are usually known as ester-hydrolysis catalysts, however, some of them, such as CRL, are able to catalyse ester synthesis. (*S*)-Ibuprofen is selectively esterified by CRL in the feed phase, and the resulting ester dissolves into the ionic liquid phase of the SLM and diffuses across the SLM.



CRL: lipase to promote esterification reaction
PPL: lipase to promote hydrolysis reaction

Fig. 1 Schematic illustration of enzyme-facillitated liquid membrane

At Interface 2 in the receiving phase, PPL catalyses the ester hydrolysis to produce the initial ibuprofen and ethanol, which are water soluble.

Finally, the (*S*)-ibuprofen is selectively transported through the SLM, based on the enantioselectivity of lipases.

RESULTS AND DISCUSSION

Figure 2 depicts the transport of (*S*) and (*R*)-ibuprofen through the SLM based on the water immiscible ionic liquid 1-*n*-butyl-3-methylimidazolium bis(triflylmethylsulfonyl)imide (abbreviated as C4mimTF_2N). A control experiment performed without the lipases resulted in no ibuprofen transport through the SLM. When the lipases were present in the feed and receiving phases, the (*S*)-ibuprofen concentration in the receiving phase increased with time, and that in the feed phase decreased correspondingly, meaning that the lipase-catalyzed reactions drove the transport of (*S*)-ibuprofen through the SLM, as interpreted in Fig. 1.

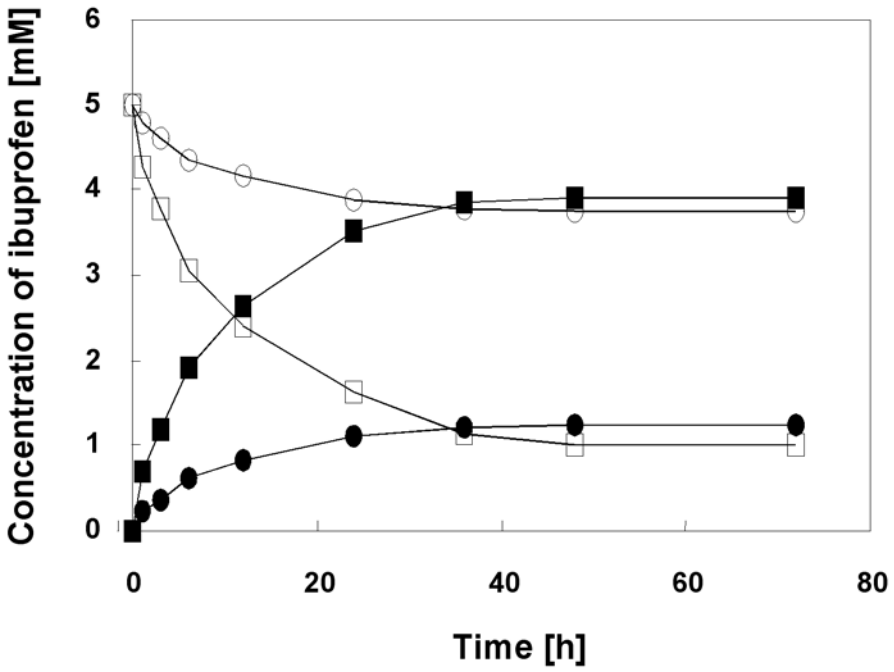


Fig. 2 Time courses of ibuprofen permeation through the liquid membrane
Open circle: R-ibuprofen in feed phase, open square: S-ibuprofen in feed phase, closed circle: R-ibuprofen in receiving phase, closed square: S-ibuprofen in receiving phase.

(*R*)-Ibuprofen was also transported through the SLM, however, the permeate flux of (*R*)-ibuprofen was much less (one-third) than that of (*S*)-ibuprofen. This result indicates that the enantioselectivity of the lipases induced the difference between the transport behaviors of (*S*)- and (*R*)-ibuprofen. Indeed, the lipase CRL has been studied as an enantioselective biocatalyst in esterification and hydrolysis reactions [8].

Figure 3 shows the effects of different solvents used as liquid membranes in the SLM. Four ionic liquids (C4mimTF_2N, C4mimPF_6, C6mimPF_6 and C8mimPF_6) and six different water-immiscible aliphatic hydrocarbons (pentane, hexane, heptane, octane, isooctane and dodecane) were tried as the liquid membrane phase in the lipase-facilitative SLM. The SLM based on the ionic liquids provided a high initial-permeate flux of ibuprofen. In particular, employing C4mimTF_2N as the liquid membrane resulted in the highest permeate flux. The differences in the permeate flux among the organic solvents and the ionic liquids could be

explained by the solubility of the ibuprofen ethyl ester in the SLM phase and by the lipase activity at the interfaces. The lipase activity at the liquid-liquid interface is significantly influenced by the kinds of organic solvents involved [9].

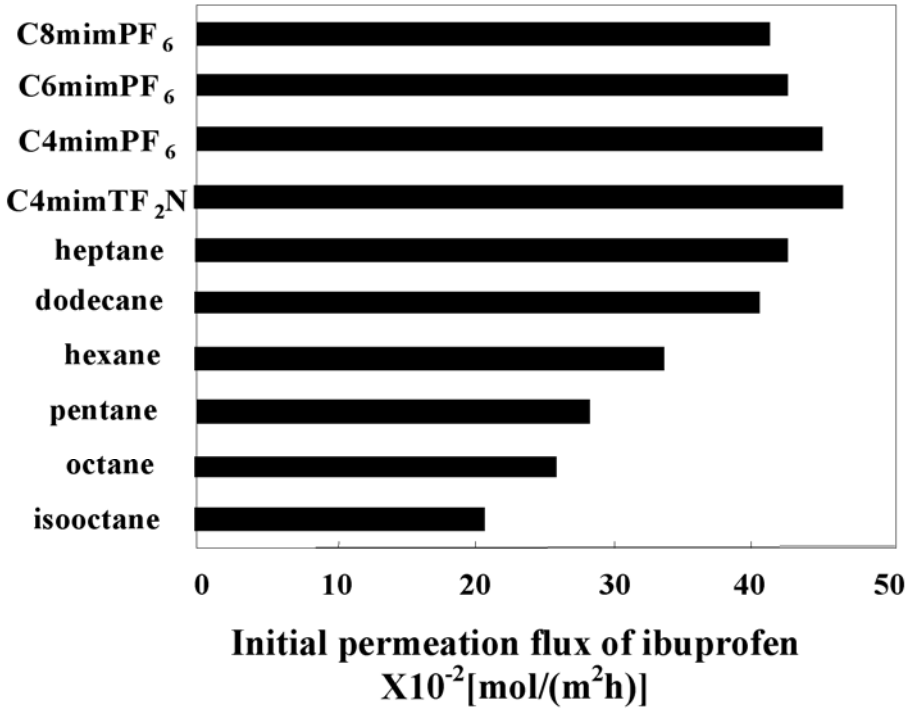


Figure 3. Effect of liquid membrane solvent on the permeation fluxes of ibuprofen

The solvent used in the SLM is one of the most critical factors for determining the membrane function for the transport of organic acids [9]. Hence, we employed three different RTILs, C6mimPF_6, C8mimPF_6 and C4mimTF_2, in addition to C4mimPF_6 as the liquid membrane phase, and compared the initial permeate fluxes of the substrates to those with typical organic solvents (*n*-dodecane and isooctane). In the case of C6mimPF_6 and C8mimPF_6, the permeate fluxes were similar to those of C4mimPF_6. The use of C4mimTF_2 as the liquid membrane phase resulted in a relatively higher permeate flux of 4-PBA than those with the other RTILs. All the fluxes in the RTILs were, however, higher than or similar to those of dodecane, while obviously smaller than those of isooctane.

The differences in the permeate fluxes among the solvents can be explained by the following two reasons. The first is the solubility of each esterified substrate in the solvents. Indeed, the ionic liquids used in this study have a variety of chemical properties. The second is the lipase activity at the interfaces. It is well-known that lipases adsorb at an oil-water interface and the lipase activity at a liquid-liquid interface is considerably influenced by the kinds of organic solvents involved [4].

Next, we turned our attention to the stability of the SLM based on the RTILs compared with that using isooctane. In the case of C4mimPF_6, the 4-PBA concentration in the receiving phase did not change after it reached 6 mM for up to 120 h. On the other hand, in the case of isooctane, the 4-PBA concentration in the receiving phase reached a maximum value at 50 h, but then began to decrease around at 75 h and finally fell to 5 mM (data not shown). This means that the liquid membrane based on isooctane was broken at around 75 h and that the 4-PBA in each phase was allowed to move freely to the opposite phase. These results indicate that the replacement of isooctane with the RTIL improves the stability of the liquid membrane [10].

Our findings demonstrate that the use of RTILs as the liquid membrane phase enables a long-term SLM operation for the separation of organic acids. Design of the liquid membrane phase and the enzymes will allow control of the permeation selectivity of the supported liquid membrane system.

Table 1 Initial permeate flux of (S)- and (R)-ibuprofen (J_S and J_R [10^{-2} mol/(m^2/h)] and the optical resolution ratio (α) using lipases of diverse origin in the feed and receiving phases [a)]

Lipase in the feed phase[b)]	J_S	J_R	α [c)]	Lipase in the receiving phase[d)]	J_S	J_R	α
CRL	38.4	9.9	3.9	PPL	38.4	9.9	3.9
Novo	14.3	9.5	1.5	A	10.2	6.2	1.7
PS	11.8	8.8	1.3	QL	14.3	9.9	1.5
QLM	14.5	11.1	1.3	F	13.9	10.2	1.4
AK	13.5	11.9	1.1	CRL	18.2	14.7	1.2
F	15.1	13.4	1.1	SL	11.4	9.4	1.2
PPL	4.5	4.5	1.0	Novo	17.5	17.4	1.0

(a) Origin of lipases; CRL (*Candida rugosa*), Novo (*Aspergilus oryzae*), PS (*Burkholderia cepacia*), QLM (*Burkholderia gradiloi*), AK (*Pseudomonas fluorescence*), F (*Rhizopus oryzae*), A (*Aspergillus niger*), SL (*Pseudomonas cepacia*), PPL (poricine pancreas), QL (*Alcaligenes sp.*)
(b) The lipase in the receiving phase was fixed on a lipase PPL., (c) Optical resolution ratio: α was defined as J_S/J_R., (d) The lipase in the feed phase was fixed on a lipase CRL.

Finally, we examined the effect of lipase origin in both aqueous phases on the enantioselectivity of the racemic ibuprofen transport. Table 1 summarizes the initial permeate flux of (*S*)- and (*R*)-ibuprofen (J_S, J_R, respectively) and the optical resolution ratio ($\alpha$was defined as J_S/J_R). As seen from Table 1, J_S, J_R and α depended strongly on the kinds of lipases in both aqueous phases. In the feed aqueous solution, we found that the CRL was the best selection, because the lipase was good at synthesizing the ester compound from ibuprophen and ethanol. On the other hand, the PPL was the suitable biocatalyst in the receiving phase. The lipase showed a high hydrolysis activity to the ibuprophen ester.

CONCLUSIONS

We carried out selective permeation of the target (s)-ibuprophen by using the liquid membrane technique. In the transport system, a biocatalyst lipase was utilized to recognize the optical active compound. The maximum α, which means the highest selectivity, was obtained when lipase CRL and lipase PPL were used in the feed and receiving phases, respectively. These results suggest that the combination of lipases CRL and PPL is appropriate for the facilitative and selective permeation of (S)-ibuprofen. In conclusion, a lipase-facilitated SLM based on ionic liquids showed enantioselective transport of (*S*)-ibuprofen. This is the first report that successfully demonstrates that enzyme-facilitated SLM based on ionic liquids can be utilized for the optical resolution of racemic ibuprofen.

ACKNOWLEDGEMENTS

This work was partly supported by a Grant-in-Aid for Scientific Research (No. 13129205) from the Ministry of Education, Science Sports and Culture of Japan. We are grateful to Amano Pharmaceutical Co., Ltd., Novozymes Japan, and Meito Sangyo Co. Ltd. for generously providing the lipases.

REFERENCES

1. K. R. Seddon (1997), *J. Chem. Tech. Biotechnol*. **68,** 351-356.
2. T. Welton (1999), *Chem. Rev.* **99,** 2071-2083.
3. R. M. Lau, F. van Rantwijk, K. R. Seddon, and R. A. Sheldon (2000), *Organic Letters*. **26**: 4189-4191.
4. T. Maruyama, M. Nakajima, S. Ichikawa, H. Nabetani, S. Furusaki, and M. Seki (2000), *J. Am. Oil. Chem. Soc.* **77**: 1121-1126.
5. D. G. Rethwisc, A. Subramanian, G. Yi, and J. S. Dordick (1990), *J. Am. Chem. Soc.* **112**: 1649-1650.
6. D. G. Rethwisc, S. Parida, G. Yi, J. S. Dordick (1994), *J. Membrane. Sci.* **95**: 83-91.
7. A. M. Klibanov (1990), *Acc. Chem. Res.* **23**, 114-122.
8. M. Goto, S. Noda, N. Kamiya, F. Nakashio (1996), *Biotechnol. Lett.*, **18**, 839-834.
9. E. Miyako, T. Maruyama, N. Kamiya and M. Goto (2003), *J. Biosci. Bioeng*., **96**, 370-374.
10. E. Miyako, T. Maruyama, N. Kamiya and M. Goto (2003), *Biotechnol Lett.*, **20**, 805-810.



THREE-PHASE (PSEUDO LIQUID MEMBRANE) MULTI-STAGE EXTRACTION

Artak E. Kostanian

Kurnakov Institute of General & Inorganic Chemistry of Russian Academy of Sciences, Moscow, Russia

A theory of three-phase multi-stage extraction has been developed. The process is performed sequentially in a series of pseudo liquid membrane stages. In each stage the extractant circulates in a closed circuit and alternately contacts a donor (feed) phase and an acceptor (stripping) phase. Special cases (phases in the chambers move countercurrently in the plug-flow mode; contact chambers represent perfectly-mixed cells; contact chambers consist of series of theoretical stages; each contact chamber represents a theoretical stage) have been analyzed. Some new constructions of multi-stage three-phase extraction (pseudo liquid membrane) apparatuses in which circulation of continuous phase of extraction agent between contact chambers takes place due to the difference in emulsion density in the chambers have been described.

INTRODUCTION

Three-phase extraction is a technology for the extraction and purification of a wide range of pharmaceutical and chemical substances (including radionuclides) by transferring the compounds from one (first) phase into another (second) phase through a mass-transfer medium (extraction agent). It allows the separation of species on their partition between two miscible solvent phases. The mass-transfer liquid medium is held stationary in the operating system while the first and second miscible solvent phases are eluted through it as the mobile phases. The process enables the purification of an aqueous solution and / or the concentration of solute in the second aqueous solution. It includes the steps of contacting a feed solution, an aqueous feed solution for instance, from which it is desired to extract metal ions for example, with an organic extraction agent containing a chemical having high affinity for the metal ions to be removed. The extraction agent enriched in metal ions is then brought into contact with a stream of an aqueous "stripping" solution which has a higher affinity for the metal ions than the organic liquid. The aqueous feed solution is thus purified of the metal ions which are concentrated into the aqueous stripping solution.

Three-phase multi-stage extraction process is carried out in a cascade of N mass-transfer stages (which can also be called pseudo liquid membrane stages), each comprising two interconnected contact chambers - one extraction chamber and one stripping chamber. The extraction agent contacts with a feed stream (or donor phase) in the extraction chambers and with a stream of acceptor (or stripping) phase in the stripping chambers and recycles between the chambers within the same stage building N closed circuits. The extraction agent is thus drawn in a cross-flow with the acceptor and donor phases within the same stage, while the donor and acceptor phases are drawn through all of the stages in the counterflow.

THREE-PHASE MULTI-STAGE EXTRACTION

General Case

The flowsheet of the three-phase multi-stage extraction is shown in Figure 1.

The extraction process is carried out in a cascade of N mass-transfer stages, each comprising two interconnected contact chambers - one extraction chamber and one stripping chamber. The extraction agent (liquid membrane) contacts with a feed stream in the extraction chambers and with a stream of stripping phase in stripping chambers and recycles between the chambers within the same stage building N closed circuits.

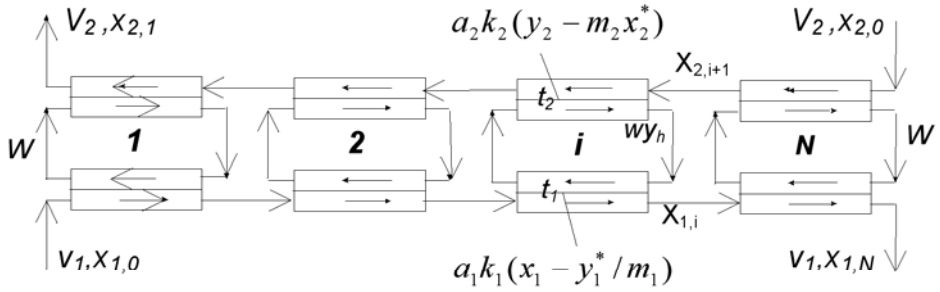


Figure 1.Fflowsheet for multi-stage three-phase extraction: general case.

To analyze mass transfer in the described system, we make the following assumptions:

1. The contacting phases in the chambers move countercurrently in the plug-flow mode;
2. Mass transfer between the phases and the extraction agent is described by the mass-transfer equations as in the case of conventional extraction;
3. Equilibrium-distribution coefficients $m_1 = y^*/x_1^*$ and $m_2 = y^*/x_2^*$ of the passing component are constant.

The material-balance and mass-transfer equations for the current stage *i* are

$$v_1 \frac{dx_1}{dz} = a_1 k_1 (x_1 - y_1^*/m_1) = -w \frac{dy_1}{dz} \quad (1)$$

$$v_2 \frac{dx_2}{dz} = a_2 k_2 (y_2 - m_2 x_2^*) = -w \frac{dy_2}{dz} \quad (2)$$

$$v_1 x_1 + w y_h = v_1 x_i + w y_1 \quad (3)$$

$$v_2 x_{2,i+1} + w y_2 = v_2 x_2 + w y_h \quad (4)$$

where a_1 and a_2 are specific surface area of phase contact in extraction and stripping chambers, respectively; k_1 and k_2 - mass-transfer coefficients in the chambers; v_1, v_2 - specific flow rates of the phases, w is the specific flow rate (circulation rate) of the extraction agent; x_1 and x_2 are the concentrations of the passing component in the donor and acceptor phases, respectively and the symbol * stands for equilibrium conditions; z is the coordinate over the phase contact surface in the chambers ($0 \le z \le h$).

For simplicity, we put $x_{2,0} = 0$. The solution of equations (1) – (4) for *N* stages is given by:

$$\frac{x_{1,N}}{x_{1,0}} = \frac{1 - F_1 F_2}{\left[\dfrac{1-\phi}{1-\phi/(F_1 F_2)}\right]^N - F_1 F_2} \quad (5)$$

where

$$\phi = \frac{F_1 F_2 S_1 S_2}{S_2 + F_1 S_1 (1 - S_2)} \tag{6}$$

$$S_1 = \frac{1 - \exp[t_1 (F_1 - 1)]}{1 - F_1 \exp[t_1 (F_1 - 1)]} \tag{7}$$

$$S_2 = \frac{1 - \exp[t_2 (F_2 - 1)]}{1 - F_2 \exp[t_2 (F_2 - 1)]} \tag{8}$$

$F_1 = v_1 / (w m_1)$, $F_2 = w m_2 / v_2$ are the mass-transfer factors in extraction and stripping respectively; $t_1 = a_1 k_1 L_1 / v_1$, $t_2 = a_2 k_2 L_2 / w$ are the numbers of transfer units at the extraction and stripping steps respectively; L_1 and L_2 are the lengths of contact chambers (phase contact lengths); $x_{1,0}$ is the concentration of solute in the feed and $x_{1,N}$ the concentration of solute in the raffinate.

Special Cases

1. The contact chambers represent perfectly-mixed cells

The flowsheet of the extraction process is shown in Figure 2.

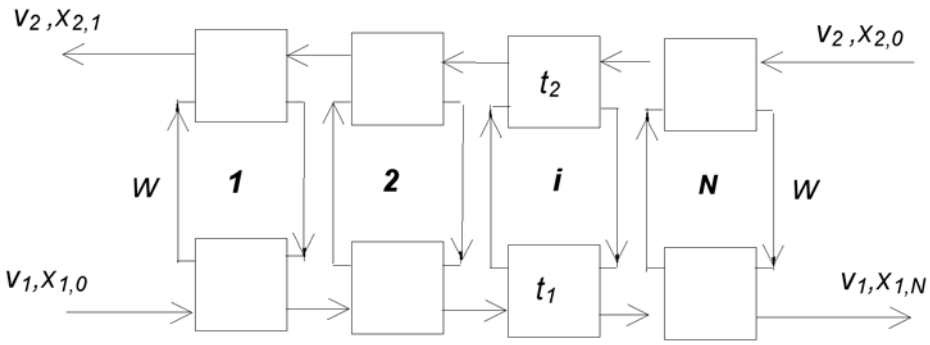


Figure 2. Flowsheet for multi-stage three-phase extraction: the contact chambers are perfectly-mixed cells.

The relative end concentration in the raffinate is given by the equations (9) and (10)

$$\frac{x_{1,N}}{x_{1,0}} = \frac{1 - F_1 F_2}{\left[\frac{1 + A F_1}{(A + F_2) F_1}\right]^N - F_1 F_2} \tag{9}$$

$$A = 1 + 1/t_2 + 1/(F_1 t_1) \tag{10}$$

where $t_1 = a_1 k_1 V_1 / v_1$, $t_2 = a_2 k_2 V_2 / w$ are the numbers of transfer units in the extraction and stripping well-mixed cells respectively; V_1 and V_2 are the volumes of contact cells and v_1 , v_2 , w – volumetric flow rates.

2. The contact chambers consist of series of theoretical stages

Each mass-transfer stage includes n_1 theoretical (or equilibrium) stages at the extraction step and n_2 theoretical stages at the stripping step as shown in Figure 3.

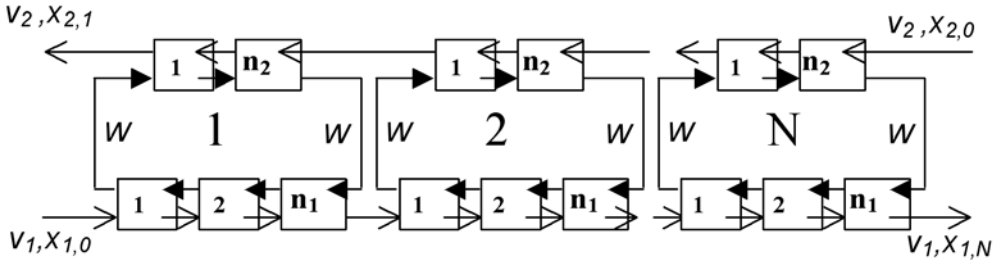


Figure 3. Flowsheet for multi-stage three-phase extraction: the contact chambers are series of theoretical stages.

The relationship between the variables can be represented by equations (5) and (6) with values of S_1 and S_2 expressed by the following equations:

$$S_1 = \frac{1 - F_1^{n_1}}{1 - F_1^{n_1+1}} \qquad S_2 = \frac{1 - F_2^{n_2}}{1 - F_2^{n_2+1}}$$

3. Each contact chamber represents a theoretical stage

The process is performed sequentially in a cascade of N mass-transfer stages, each consisting of two contact chambers, where the liquid membrane alternately interacts with the initial solution and the receiving phase and the equilibrium distribution of the passing component is attained. The flowsheet of the process is similar to that shown in Figure 2 with $t_1 \to \infty$ and $t_2 \to \infty$. The outlet (end) concentration of the solute in the raffinate is given by the following expression:

$$\frac{x_{1,N}}{x_{1,0}} = \frac{1 - F_1 F_2}{\left[\dfrac{1 + F_1}{(1 + F_2)F_1}\right]^N - F_1 F_2} \tag{11}$$

As the rate of circulation of extraction agent between the contact chambers at each of the mass-transfer stages rises, the solute concentration ratio in the phases approaches a certain limiting (equilibrium) value equal m_1 / m_2. Under these conditions ($w \to \infty$), expression (11) is reduced to

$$\frac{x_{1,N}}{x_{1,0}} = \frac{F^N - F^{N+1}}{1 - F^{N+1}} \tag{12}$$

where

$$F = \frac{v_1 m_2}{v_2 m_1} \tag{13}$$

For the conventional countercurrent two-phase extraction (x and y, $y^* = mx^*$) in a cascade of N theoretical stages, the outlet concentration of solute in the raffinate is

$$\frac{x_N}{x_0} = \frac{f^N - f^{N+1}}{1 - f^{N+1}} \tag{14}$$

where $f = \frac{v_x}{v_y m}$ is the extraction factor.

A comparison of expressions (12) and (14) implies that F in formula (12) is the three-phase extraction factor and that relationship (12) defines the efficiency of this process in a cascade of N theoretical three-phase mass-transfer stages.

For co-current three-phase mass transfer the outlet concentration of the solute in the raffinate phase is given by the expression:

$$\frac{x_{1,N}}{x_{1.0}} = \frac{F_1 F_2 + \left(1 + F_2 + 1/F_1\right)^{-N}}{1 + F_1 F_2} \tag{15}$$

When $w \to \infty$, equation (15) becomes

$$\frac{x_{1,N}}{x_{1,0}} = \frac{F}{1 + F}$$

Thus, as in the case of simple two-phase mass transfer, a co-current flow of phases in three-phase mass transfer can, in the limit, ensure the extraction efficiency only of a single theoretical stage of three-phase mass transfer.

The three-phase multi-stage extraction described above can be considered as the stagewise embodiment of supported liquid membrane technique. The conventional implementations of liquid membrane method (film pertraction and processes with emulsion and supported membranes) due to the complexity are hard to apply and have low capacity. These disadvantages can be bypassed by implementation of three-phase multi-stage extraction, which can be called pseudo liquid membrane technique. This technique can be realized either in a series of mixer-settler combination or in special two- or multi-chamber extraction apparatuses [1-10]. Some of these new apparatuses for conducting the three-phase multi-stage extraction processes are briefly described below.

THREE- PHASE MULTI-STAGE EXTRACTION APPARATUSES

In Fig. 4 are shown three schematic arrangements of the three-phase multi-stage extraction apparatus indicating the basic operation and flow patterns of the liquids. The circulation of the continuous liquid membrane phase between the extraction and stripping chambers in each mass-transfer stage takes place due to the difference in emulsion density in the chambers.

ACKNOWLEDGEMENTS

The author is grateful to the Russian Foundation for Basic Research (grant No 04-03-32584) and to the Russian President (grant No NSH-1577.2003.3) for the financial support of this work.

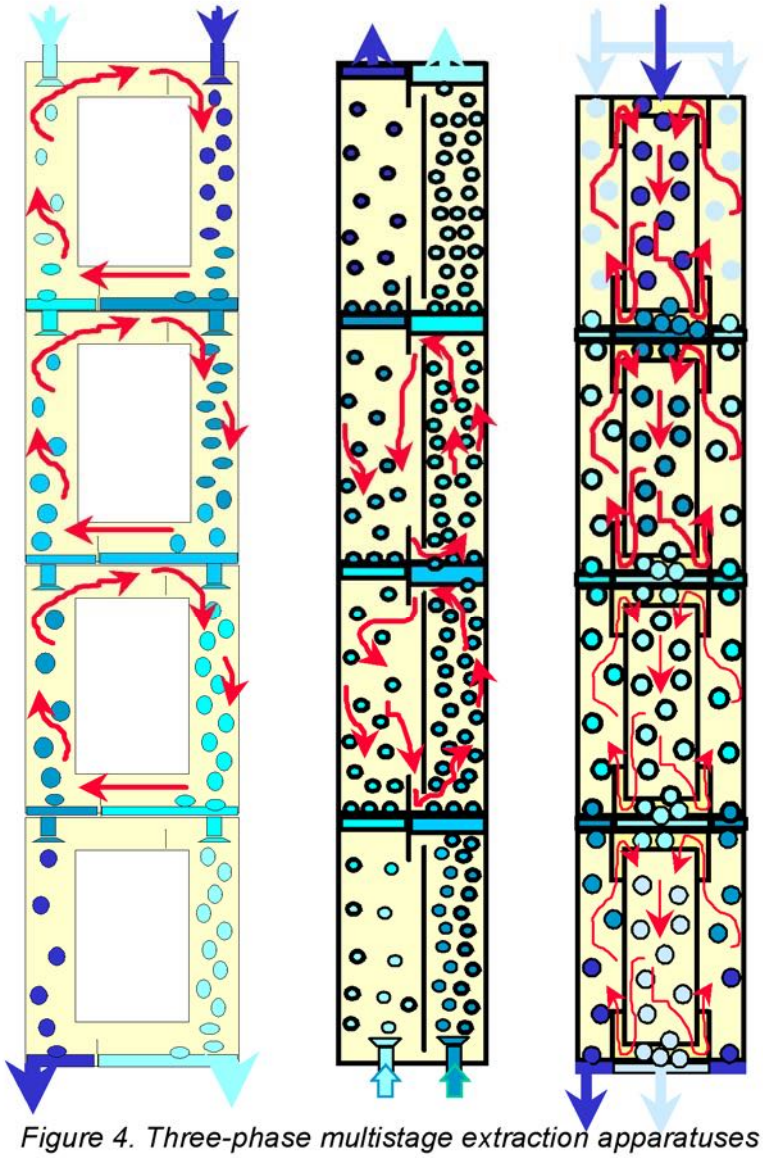


Figure 4. Three-phase multistage extraction apparatuses

REFERENCES

1. A. E. Kostanian (1997), *Russian* Pat., No. 2080162 (27 May).
2. A. E. Kostanian (1997), PCT Application, No. WO 97/14486 (April 24).
3. W. Baecker and A. E. Kostanian (1998), PCT Application, No. WO 98/45014 (Okt. 15).
4. A. E. Kostanian and W. Baecker (1998), PCT Application, No. WO 98/37939 (Sept. 3).
5. A. E. Kostanian (1998), *Euro.* Pat., No. 0858363 (August 19).
6. A. E. Kostanian (1998), *Euro.* Pat., No. 0862487 (Sept. 9).
7. A. E. Kostanian (1998), CZ. *Pat.*, No. 9801183 (Oct. 14).
8. A. E. Kostanian (2000), *US. Pat.*, No. 6,143,178 (Nov. 7).
9. A. E. Kostanian (2000), *US. Pat.*, No. 6,090,352 (Jul. 18).
10. A. E. Kostanian (2000), *US. Pat.*, No. 6,129,842 (Oct. 10).

AN EXPERIMENTAL STUDY ON IRON EXTRACTION WITH BINARY EXTRACTANTS IN A PSEUDO LIQUID MEMBRANE DEVICE

Andrey A. Voshkin, Artak E. Kostanian, Vera V. Belova, Natalia S. Egorova, Anatoly I. Kholkin

Kurnakov Institute of General & Inorganic Chemistry, Moscow, Russia

Binary extractants based on monocarboxylic acids are used in the study of iron extraction in a pseudo liquid membrane device. The device represents a three-phase extractor comprising an extraction and a stripping chamber. The chambers consist of contacting and separation zones and are connected together by overflows for circulation of the continuous phase. In the extraction chamber, the raffinate phase (initial solution) is brought into contact with a extractant phase from which extracted species are stripped in the second chamber with a stripping phase. The initial solution and the stripping phase are each dispersed into droplets in the appropriate chamber by means of a dispersing device. Owing to the difference in density between the emulsions in the first and second chamber, circulation of continuous phase, which is the extractant phase, occurs through the upper and lower overflows, resulting in transfer of the substances to be extracted from one chamber to the other and from the first dispersed phase into the second.

INTRODUCTION

There are two ways to improve the efficiency of extraction processes: the choice of extractants providing high distribution coefficients and the application of high effective apparatuses.

Binary extraction has been established [1 – 6]. Binary extractant systems represent the salts of organic acids and organic bases. These systems combine the properties of anion-exchange and cation-exchange extractants. By different combinations of organic cations and anions a great number of binary reagents with various properties can be produced. Since interphase distribution of cations and anions in the binary extractant systems are interconnected, the use of combination of organic cations and anions with different properties in composition of binary extractants offers new possibilities for conducting extraction processes. Further advantages of the application of binary extractants are high velocities of extraction and back-extraction(stripping), linearity of extraction isotherms, high-resolution due to the particularly large difference between the distribution ratios of the salts with different anions and cations. In some cases pure water can be used as the stationary phase.

In systems involving binary extractants such as salts of quaternary ammonium bases (QAB) with phosphorus containing organic acids (dialkylphosphinic, dialkylphosphoric) some non-ferrous and rare metals form stable extracted complexes that provide effective application of binary extractants for separation of these metals from other accompanying species (Fe and

others) [7]. Binary extractants based on cheap monocarboxylic acids (for example, caprylic) appear to be effective reagents for recovery of iron from waste solutions [8]. In binary extractants systems stripping of metals from the organic phase is simpler and more effective with water or dilute mineral acids.

Pseudo liquid membranes are a relatively new type of extraction devices in which a transfer medium (liquid membrane) is held stationary in the operating system consisting of two interconnected chambers while the feed and stripping phases are eluted through it as the mobile phases. This technique can be realized either in a series of mixer-settler combination or in special two- or multi-chamber extraction apparatuses [9]. In our laboratory several designs of multi-chamber devices have been developed and studied [9].

EXPERIMENTAL

Experimental Methods and Extractants

The binary extractant, R_4NA, was prepared by mixing equimolar amounts of trioctylmethylammonium chloride (R_4NCl) and caprylic acid (octanoic acid) (HA) in hexane and with subsequent washing of an organic solution with 1 M NaOH for 10 min:

$$R_4NCl_{(o)} + HA_{(o)} + OH^-_{(a)} \Leftrightarrow R_4NA_{(o)} + Cl^-_{(a)} + H_2O_{(a)} \qquad (1)$$

To improve the stripping a binary extractant, trioctylmethylammonium caprylate, was used with a two-fold excess of caprylic acid.

The concentration of iron in aqueous solutions was determined by EDTA titration using xylenol as the indicator and by a photometric method using sulphosalicylic acid as the reagent. The differences in Fe concentration between the initial and final aqueous solutions were used to calculate the concentration of iron in the organic phase. In some experiments iron in the organic phase was stripped with 1 M hydrochloric acid and then Fe concentration was determined by the photometric method.

Apparatus

The laboratory plant represents a stage of the three-phase extractor with natural convective circulation of the continuous liquid membrane phase – a pseudo liquid membrane (PLM) device (Figure 1).

The PLM device includes an extraction and a stripping chamber. Each chamber has contacting and separation zones and is equipped with a dispersing device (we have used needles with different diameters). The chambers are connected at their upper and lower parts by overflows for circulation of the continuous organic phase containing an extractant (the liquid membrane phase). The apparatus is filled with the liquid membrane and the two aqueous phases (feed and stripping) are each dispersed into small droplets in the appropriate chamber. In the extraction chamber, the stream of initial solution is brought into contact with the extractant phase from which the extracted species are stripped in the second chamber with the stripping phase. Owing to the difference in density between the emulsions in the first and second chamber, circulation of continuous phase occurs through the upper and lower overflows, resulting in transfer of the substances to be extracted from one chamber to the other and from the first dispersed phase (feed) into the second dispersed phase (stripping). The circulation of the continuous phase is influenced by the density of the dispersed phases and the values of hold-up in the chambers. The hold-up is controlled by the flow rate and the size of the droplets. The plant is equipped with peristaltic pumps for supply of aqueous phases. We have used two three-phase extractors: 1) a large apparatus - chamber diameter 30 mm, chamber height 400 mm; 2) a small apparatus - chamber

diameter 15 mm, chamber height 200 mm. Most experiments were carried out in the small apparatus.

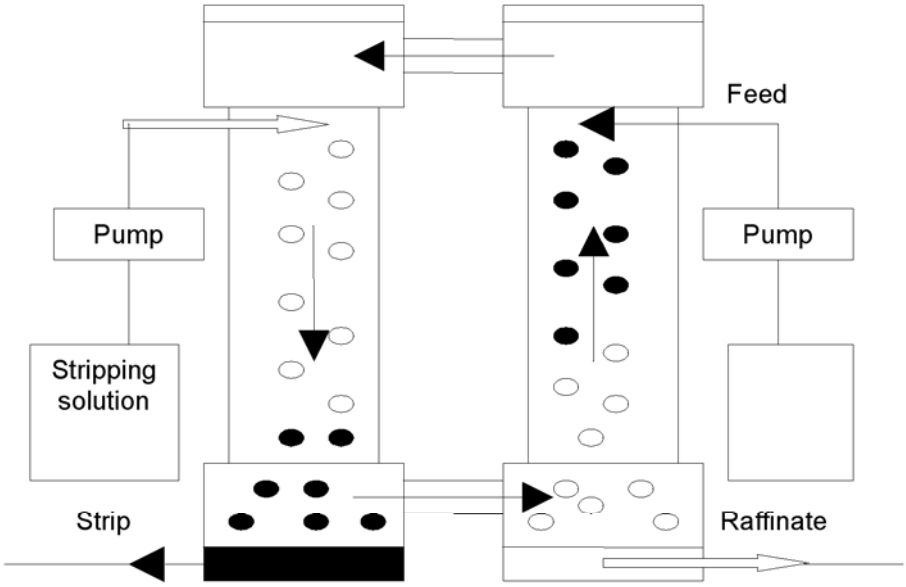


Figure 1. Experimental apparatus set-up.

Extraction of Fe(III) from acidic chloride solutions

Extraction of Fe(III) from acidic chloride solutions with trialkylmethylammonium caprylate in hexane with 10 % hexanol addition can be described by the following equations [8, 10]:

$$H^{+}_{(a)} + FeCl_4^{-}{}_{(a)} + R_4NA_{(o)} \Leftrightarrow R_4NFeCl_{4\,(o)} + HA_{(o)} \qquad (2)$$

$$Fe^{+3}_{(a)} + 3Cl^{-}_{(a)} + R_4NCl_{(o)} \Leftrightarrow R_4NFeCl_{4\,(o)} \qquad (3)$$

Kinetic studies on iron extraction and stripping with QAB caprylate showed that stripping is a faster process compared to extraction. A few experiments were conducted on the large apparatus.

To determine the effect of various parameters on the process of iron recovery from acidic chloride solutions with trioctylmethylammonium caprylate using the PLM device the experimental studies were carried out in the small apparatus. Efficiency of extraction and stripping was estimated by using a parameter of relative efficiency, E, which was determined as follows:

$$E_{ex} = C_{Fe\,(raff.)} / C_{Fe\,(init.)} \qquad E_{str} = C_{Fe\,(str.)} / (C_{Fe\,(init.)} - C_{Fe\,(raff.)}) \cdot V_{str.} / V_{feed.},$$

where V are the flow rates of stripping and feed (raffinate) phases.

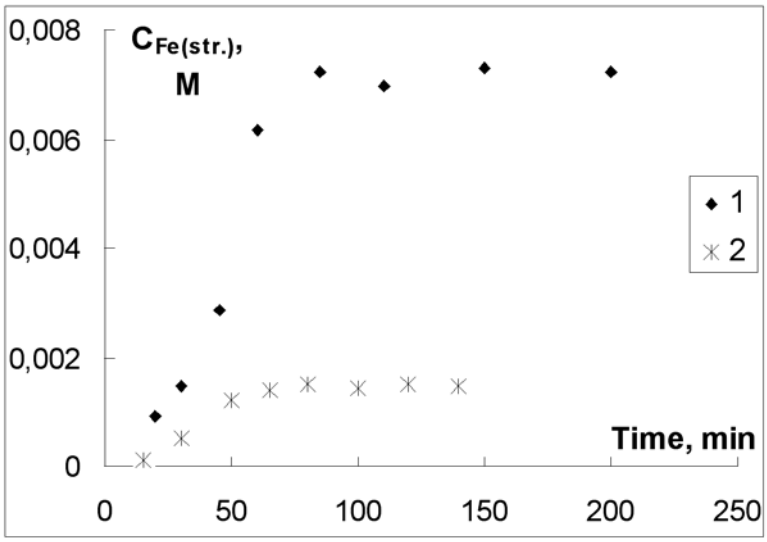


Figure 2. Time-dependent Fe-concentration in the strip phase

(C_{R4NA} = 0.02 M, $C_{capr.}$ = 0.04 M, solvent – hexane + 10 % hexanol, feed C_{Fe} = 0.023 M, C_{HCl} = 2.5 M) 1 – needle diameter 0.8 mm, $V_{str.}$ = 8 ml/min, V_{feed} = 15 ml/min; in extraction – co-current , in strip – countercurrent. 2 – needle diameter 0.8 mm, $V_{str.}$ = 12 ml/min, V_{feed} = 5 ml/min; in extraction– countercurrent, in strip. – co-current.

RESULTS AND DISCUSSION

It was established that the steady-state mode in the small apparatus is reached in 60 – 70 minutes (Figure 2).

The results of experiments on the small PLM-device are given in Table 1. In spite of the fact that the flow rates of strip solution were larger than those of feed we observed co-current flow in the extraction chamber and countercurrent flow in the strip chamber. This can be explained as follows: in the extraction chamber the droplet size was considerably smaller than in the strip chamber and as a result the hold-up in the extraction chamber was larger than in strip chamber which caused the observed direction of circulation.

Table 1. Data obtained on the small apparatus
(C_{ex} = 0.02 M, C_{HA} = 0.04 M, solvent – hexane + 10 % hexanole)
extraction – countercurrent, stripping – co-curent

N	Needle Diameter mm	$V_{str.}$, ml/min	V_{feed} ml/m	$V_{str.}/V_{feed.}$	$C_{Fe\ (init.)}$, M	$C_{Fe\ (raff.)}$ M	$C_{Fe\ (str.)}$, M	E_{ex}, %	$E_{str..}$, %
1	0.8	12.0	5.0	2.4	0.023	0.0175	0.0015	24	65
2	0.6	13.0	6.0	2.2	0.022	0.0150	0.0023	29	78
3	0.3	12.5	5.5	2.3	0.018	0.0100	0.0026	44	71
4	0.3	7.0	4.5	1.6	0.023	0.0110	0.0070	52	90
5	0.3	4.5	3.5	1.3	0.020	0.0170	0.0018	15	77

The efficiency of the process in the PLM-device is determined by the interphase contact area in the chambers and the flow ratio of the phases.

Table 2. Data obtained on the large apparatus (C_{ex} = 0.5 M) extraction – co-current, stripping – countercurrent

N	Parameter	Initial solution	Stripping agent	Final org. phase	Raffinate	Stripping phase
Binary extractant – trioctylammonium carboxylate, Solvent – carboxylic acid + 10 % hexanol						
1	V, ml/min C_{Fe}, M C_{HCl}, M	50 0.506 3.0	25 0 0.3	- 0.100 -	50 0.310 2.0	25 0.028 0.3
Binary extractant – trioctylammonium carboxylate, C_{HA} = 1 M Solvent – hexane + 10 % hexanol						
2	V, ml/min C_{Fe}, M C_{HCl}, M	40 0.506 3.0	20 0 0.1	- 0.310 -	40 0.155 -	20 0.122 0.1

To determine the effect of the nature of a solvent on the process parameters we have used a carboxylic acid and hexane as solvents for preparing a binary extractant solution. The experimental results on the purification of an acidic chloride solution from iron using trioctylammonium carboxylate, obtained with the PLM-device, are given in Table 2. The data (Table 2, test N 1) showed that efficiency of the extraction and the stripping is lower than that in the previous extraction studies (Table 1). This is because iron carboxylate, Fe_3A_9, is mainly formed in the organic phase in these experiments [10]. Such change in the extraction mechanism is obviously connected with peculiarities of the given extraction device. The initial aqueous solution dispersing into the extractant phase exists under conditions of a significant excess of the binary extractant and carboxylic acid. At a low volume ratio of the aqueous and the organic phases in the extraction stage, the activity of organic acid is much higher than that of QAB resulting in the changing composition of the extracted species. When the mixer-settler apparatus is used as an extractor, the mechanism does not change. Thus, composition of the extracted species changes due to construction peculiarities of the PLM-device. The formation of iron(III) carboxylate resulted in decreasing efficiency in the stripping in the system studied. Using a solution of QAB carboxylate as the extractant, activity of carboxylic acid decreases and efficiency of extraction and stripping processes improves (Table 2, test N 2) because of the predominant binary extraction according to Equation (2).

ACKNOWLEDGEMENTS

The authors are grateful to the Russian Foundation for Basic Research (grant No 04-03-32584) and to the Russian President (grant No NSH-1577.2003.3) for the financial support of this work.

REFERENCES

1. C Deptula (1967), *J Inorg Nucl Chem*, **43**, 100.
2. RR Grinstead et al (1969) / (1970), *Ind Eng Chem Prod Res Develop.* **8**, 218 / **9**, 66.
3. A.M. Eyal, E. Bressler, R. Bloch (1994), *Ind. Eng. Chem. Res.*, **33**, 1067 - 1075.
4. A.M. Eyal, E. Bressler, R. Bloch (1994), *Ind. Eng. Chem. Res.*, **33**, 1076 - 1085.
5. A.I. Kholkin, G.L. Pashkov, I.Yu. Fleitlikh and et al. (1994), *Hydrometallurgy,* **36**, 109-125.
6. A.I. Kholkin, G.L. Pashkov and V.V. Belova (2000), *Min. Pro. Extr. Met. Rev.,* **21**, 217-2468.

7. A.A. Voshkin, T.I. Zhidkova, V.V. Belova, V.I. Zhilov, Yu.Yu. Brenno and A.I. Kholkin (2004), *Zh. Neorg. Khim.,* **49**, 1384-1389.
8. A.A. Voshkin, V.V. Belova, A.I. Kholkin and A. Agrawal (2003), *Khim. Tekhnol.*, **11**, 28-32.
9. A.E. Kostanian (2000), *US Pat.,* No 6129842.
10. A.A. Voshkin, A.I. Kholkin and V.V. Belova (2002), *Proc. Int. Solvent Extr. Conf., ISEC'02*, Cape Town, South Africa, p.p. 341-346.



A NEW APPROACH TO MODELLING OF MASS TRANSFER OF ZN^{2+}_{aqu} THROUGH SUPPORTED LIQUID MEMBRANES

Christian Huber[*], Rolf Marr[*], Matthäus Siebenhofer[**]

[*]Department of Chemical Engineering and Environmental Technology, Graz University of Technology, Graz, Austria
[**]VTU-Engineering GmbH, Grambach/Graz, Austria

ABSTRACT

Research on mass transfer in liquid membrane permeation has still left some challenging aspects to be solved. Although discussed very intensively the published models are rarely comparable and suffer from a lack of accuracy.

The program was started with research on the widely investigated and very common test system Zn^{2+}_{aqu} / Bis(2-ethylhexyl) phosphoric acid/ sulphuric acid. Based on the experimental investigation and the modelling of mass transfer in liquid/liquid extraction the target of this project has been detailed analysis of mass transfer through rigid membranes.

Besides variation of the chemical potential the influence of the composition of the mobile solvent phase on mass transfer has been determined. Several transport properties such as composition dependence of the dynamic viscosity of the solvent phase have been recorded. For modelling of the experiments an analytical model with consideration of transport and thermodynamic properties has proven advantageous over several mass transfer models.

INTRODUCTION

Liquid membranes have been investigated since more than 30 years and various types of applications have been proposed. Although liquid membranes are highly efficient, difficult handling and stability of liquid membranes have yet hindered successful industrial application.

Competing technologies such as precipitation or solvent extraction are not satisfying either and do suffer from different problems and limitations as well. Recent developments of new base materials and new ways of configuration allow new approaches in application of liquid membranes and offer the possibility of feasible application. Target of this project is to investigate mass transfer through supported liquid membranes and to develop appropriate tools for process and plant design.

EXPERIMENTAL METHODS AND ANALYSES

Membrane Module

Investigation of mass transfer was carried out in a circular cell separated into two compartments with the membrane. The mass transfer area of the membrane was $1.38*10^{-3}$ m^2. Membrane thickness was 100 µm at a porosity of ε=0.25.

As shown in Figure 1 each compartment was equipped with a flow barrier in the center. The size of the barrier was evaluated through CFD optimization. The membrane was stabilized with the framed gasket and the central flow barrier. Correspondingly a very narrow velocity distribution of both electrolytes without dead zones was available for mass transfer experiments.

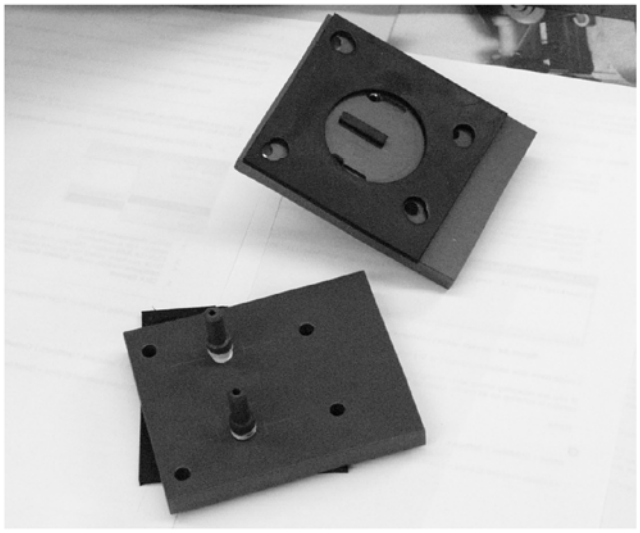


Figure 1: Membrane module

The membrane was prepared by impregnating PTFE base material of 25% porosity and a pore size of 45 µm with solvents of different composition by evacuation of the base material and saturation with solvent during pressurization.

Chemicals

The feed solution was prepared by dissolving zinc sulfate of 99.5% purity (Merck, No 108883) in distilled water. For preparing the membrane bis(2-ethylhexyl) phosphate (Merck, No 814181) of 98% purity was dissolved in the diluent dodecane (Aldrich, No 489131) of 99% grade. The strip phase was prepared with distilled water and sulfuric acid (Roth, No 4623.5) of 95 % purity.

Apparatus and Procedure

The experiments were carried out in the batch mode. Both electrolytes, the feed phase and the strip phase, were fed into the corresponding membrane chamber with a peristaltic pump. The extract phase and the raffinate phase exited the membrane module on top and were discharged into the corresponding storage tanks again to provide a batch electrolyte loop for each phase. The experimental setup is shown in the schematic of figure 2. The schematic also shows the sensors for temperature, flow rate and pH-value.

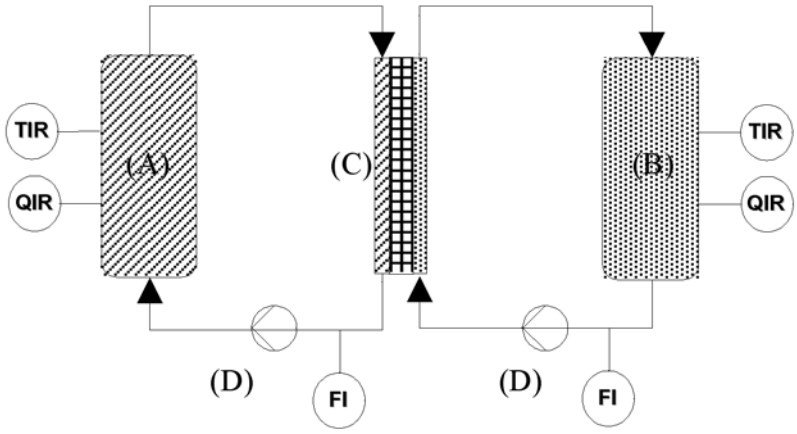


Figure 2: Schematic of the experimental set up: (A) feed vessel, (B) strip vessel, (C) membrane module with membrane, (D) peristaltic pumps; Sensors: FI (flow indicator), TIR (temperature indicator and recorder) , QIR (pH value indicator and recorder)

In order to minimize (exclude) concentration gradients in the boundary layer of the electrolyte and the membrane the shear rate was optimized prior to performing the measurement series by increasing the flow rate of both electrolyte loops. As shown in Figure 4 rate of mass transfer was constant above pump rates of >35%.

Thus it was concluded that the resistance of the boundary layers was to neglect above this rotational speed and advancing it was decided to operate the pumps at maximum speed to avoid influences of the aqueous phases.

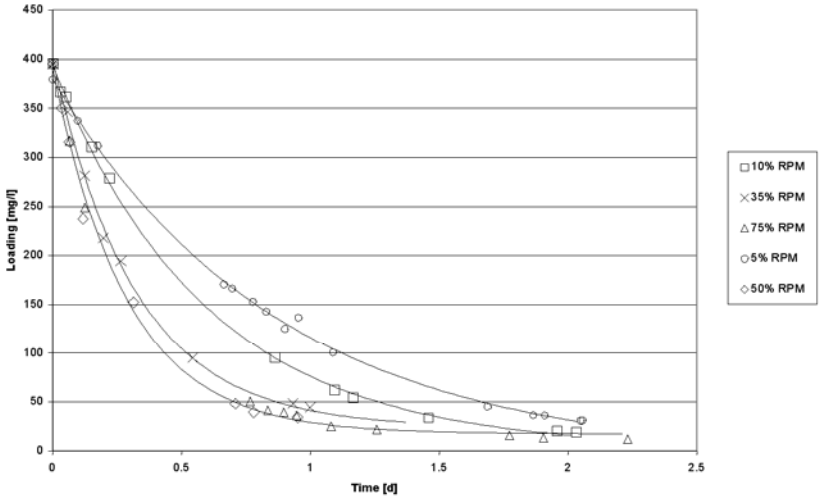


Figure 3: Influence of the pump rate on mass transfer

Mass transfer experiments were performed for several concentration levels of the aqueous feed phase, the organic membrane phase and the aqueous strip phase. During each experiment samples of the extract loop and the raffinate loop were collected for analysis. Analysis was carried out by atomic absorption spectroscopy with a Perkin Elmer AAS, model 5100. Zinc absorption was recorded at wavelength λ = 210 nm.

MODELING OF MASS TRANSFER

The basic idea behind industrial application of liquid membranes is the advantage of combined extraction and reextraction. The process schematic of the process is shown in Figure 4. Number III indicates the raffinate phase, number II indicates the membrane phase and number I indicates the extract (or strip) phase. Further Figure 4 schematically shows the concentration levels of Zn^{2+} and H^+ in both aqueous phases and the concentration gradient of Zn^{2+} in the membrane phase. The driving force for mass transfer of zinc from the raffinate phase into the extract phase is qualitatively indicated by the concentration difference of H^+ between phase I and phase III.

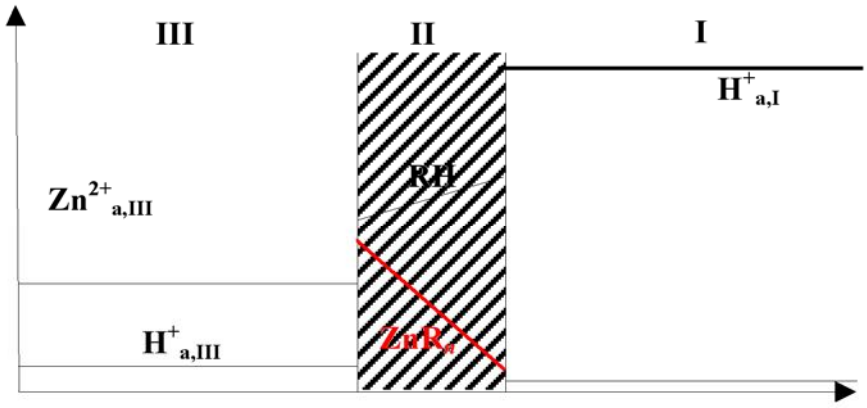


Figure 4: Mass transfer model

At both interfaces, interface II-III and interface II-I Zn^{2+} undergoes ion exchange with the solvent according to equation 1. The laden solvent is forced to diffuse through the membrane due to the difference of the chemical potential between phase I (extract phase) and phase III (raffinate phase). At the strip interface I-II the laden solvent undergoes ion exchange in the reverse direction according to equation 1 again.

$$\mathrm{Zn}_a^{2+} + n \cdot \mathrm{HR}_\mathrm{o} \Leftrightarrow \mathrm{ZnR}_{n,o} + n \cdot \mathrm{H}_\mathrm{a}^+ \qquad (1)$$

In equation 2 the equilibrium constant K according to the Law of Mass Action is mentioned

$$K = \frac{\gamma_{\mathrm{ZnR}} \cdot [\mathrm{ZnR}_n]_o \cdot \gamma_H^n \cdot [\mathrm{H}^+]_a^n}{\gamma_{\mathrm{Zn}} \cdot [\mathrm{Zn}^{2+}]_a \cdot \gamma_{RH}^n \cdot [\mathrm{RH}]_o^n} \qquad (2)$$

The concentration profile in the membrane at equilibrium can be considered as independent from diffusion coefficients and the concentration profile across the membrane can be assumed to be linear [1]. The boundary conditions are not determined by mass transfer but by the surrounding fluids.

Therefore modeling of mass transfer can be based on Fick's 1st law:

$$\dot{J} = k \cdot \varepsilon \cdot A \cdot \Delta c \qquad (3)$$

The governing concentration difference of the laden solvent can be written as

$$\Delta c = [\mathrm{ZnR_n}]_{o,II-III} - [\mathrm{ZnR_n}]_{o,II-I} \qquad (4)$$

Unfortunately the interface concentrations II-III$_o$ and II-I$_o$ at the membrane are not accessible, but supposing an excess of acid in the strip phase the carrier concentration at the interface II-I$_o$ can be neglected as far as mass transfer is far off equilibrium.

$$\Delta c = [\mathrm{ZnR_n}]_{o,II-III} \qquad (5)$$

Under the same conditions it can be considered that the distribution of zinc between the two phases is constant as the concentration of complexed carrier is very low due to the excess of carrier (5 times the concentration of zinc). With the rearrangement of equation 2 according to equation 6 and

$$k_{equ} = \frac{[\mathrm{ZnR_n}]_{o,II-III}}{[\mathrm{Zn^{2+}}]_{a,III}} = K\frac{[\mathrm{RH}]^n}{[\mathrm{H^+}]^n} \qquad (6)$$

combination of equations (3) and (6) to the solute flux can be expressed in terms of solute concentration in phase III as expressed in equation (7).

$$\dot{J} = k \cdot \varepsilon \cdot A \cdot k_{equ} \cdot [\mathrm{Zn^{2+}}]_{a,III} \qquad (7)$$

Equation (7) combines two constants, the mass transfer coefficient *k* and the equilibrium constant k_{equ}. Both constants can not be determined independently and they are summarized in the permeation coefficient *k* . [2] as expressed in equation (8).

$$\dot{J} = k_{\pi} \cdot \varepsilon \cdot A \cdot [\mathrm{Zn^{2+}}]_{a,III} \qquad (8)$$

RESULTS AND DISCUSSION

As expected from equation 8 proportional dependency of solute flux and zinc concentration in the raffinate phase can be observed. Figure 6 shows the result of several tests. Parameter of these tests was the concentration of the carrier DEHPA.

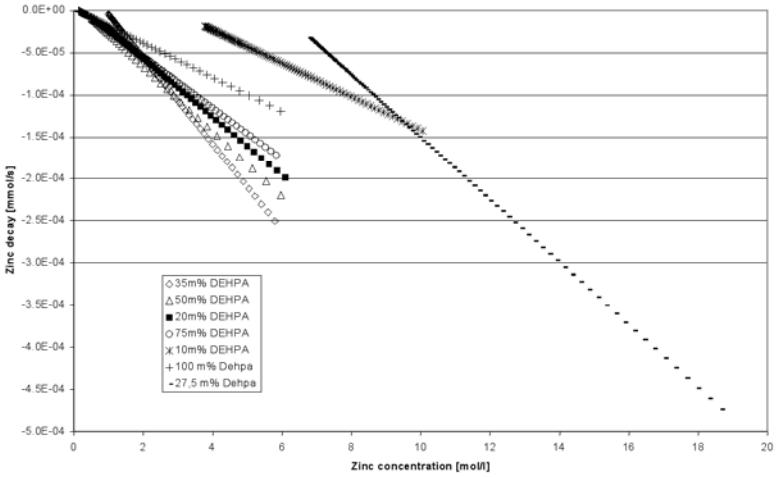


Figure 5: A dependency of the Zinc decay to the zinc concentration
in the feed phase can be observed; parameter: DEHPA content of the diluent n-dodecane

According to equation 8 the permeation coefficient k can be calculated from the slope of the graphs shown in Figure 5.

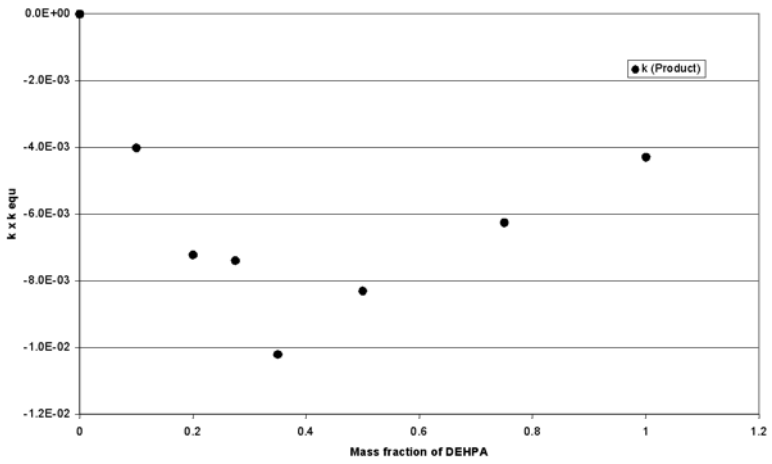


Figure 6: Dependency of k on the DEHPA content of the solvent

At low DEHPA content of the solvent mass transfer is limited by the DEHPA content. After passing a maximum mass transfer is increasingly limited by the transport properties.

SUMMARY

Mass transfer of Zn^{2+} through plane supported liquid membranes was investigated. For that purpose a mass transfer cell was constructed and tested. From preliminary investigation of mass transfer the optimum operation conditions were deduced.

Finally the influence of the solvent composition on mass transfer was investigated and modeled. The apparent mass transfer coefficient, deduced from experiments passes a maximum at specific solvent composition.

REFERENCES

1 Cussler, E.L., *Diffusion – Mass transfer in fluid systems*, Cambridge University Press, 1984

2 Van de Voorde, I., et al., Recovery of nickel ions by supported liquid membrane (SLM) extraction, *Journal of membrane Science*, (**234**), 2004

EFFECT OF ELECTROLYTES ON STABILITY OF EXTRACTING EMULSIONS

Marina Yu. Koroleva, Evgeny V. Yurtov*

Mendeleev University of Chemical Technology,
Miusskaya Sq., 9, Moscow, 125047, Russia

The influence of different electrolytes on extracting emulsion stability has been investigated. There is a small difference in emulsion stability dependence on electrolyte type at very low ionic strength in the internal aqueous phase. This is a result of isothermal distillation, when water diffusion from smaller water drops to larger ones takes place. In the middle concentration range the emulsion stability depends strongly on electrolyte medium. At high ionic strength emulsion stability is influenced by electrolyte concentration to a limited extent. In this case emulsion stability is affected mainly by the influence of electrolyte type on the strength of surfactant adsorption layers, on water structure near the interface, etc.

For the case of the extraction of surface active compounds, restrictions on multiple emulsion stability were analyzed. The total pressure in the extracting emulsion and the osmotic pressure in the external aqueous phase should be equalized to prevent the mass transfer of water in multiple emulsions. Necessary changes in electrolyte concentrations in the internal water phase should be made. These changes are especially high in fine emulsions with small drops.

INTRODUCTION

Extracting emulsions with different electrolytes are used at the extraction in multiple emulsions. In many cases the external aqueous solution contains electrolytes in much lower concentration than the internal water phase in the extracting emulsion. The difference in electrolyte concentration may reach 10 and more times. As a result, mass transfer of water between the aqueous phases takes place, which leads to swelling of the extracting emulsion. Water can be transported through the liquid membrane mainly by inversed micelles [1] or nanodispersion droplets. The structure of micelles and water solubility are dependent on the composition of the extraction system [2].

The type and valence of the electrolyte influence the breaking of the extracting emulsion at extraction and the long-time stability at rest [3]. Usually extracting emulsions are polydispersed systems. In the case of a low ionic strength in the internal phase of the emulsion, isothermal distillation takes place, i. e., water diffusion from smaller water drops to larger ones. As a result, drop size distribution changes and average drop diameter increases. The stability of such emulsions is much lower than emulsions, which do not undergo any significant isothermal distillation. Increasing ionic strength in the internal water phase of the extracting emulsion retards isothermal distillation, but the influence of different cations and anions is not the same.

INFLUENCE OF ELECTROLYTE TYPE AND VALENCE

The extracting emulsions studied were of the W/O type stabilized by Span 80. The internal phases were aqueous solutions of salts consisting of different cations and anions: Na^+, K^+, Ca^{2+}, Mg^{2+}, Fe^{3+}, Cl^-, SO_4^{2-}, PO_4^{3-}, etc. Extracting emulsions were made by homogenization and then after preparation were allowed to rest at 20°C.

The following parameters were used for the stability tests:

- the time not separating of the oil phase (t^0_{oil}), that is the time when a visible separation of the oil phase was not observed;
- the half-separation time of the water phase ($t_{1/2}$), that is the time when the half of water phase volume was separated.

The value of t^0_{oil} characterizes the sedimentation stability of the extracting emulsion, the value of $t_{1/2}$ shows emulsion stability towards coalescence.

Figure 1 illustrates the influence of different electrolytes on the emulsion stability. The sedimentation and coalescence rates are extraordinarily high at low electrolyte concentrations. There is a small difference in emulsion stability dependence on electrolyte type at very low ionic strength in the internal aqueous phase. The increase in salt concentration results in a rise in the emulsion life-time. t^0_{oil} and $t_{1/2}$ are enhanced rapidly up to approximately 0.2 M salt concentration and then become weakly dependent on electrolyte concentration. Extracting emulsions with $FeCl_3$ has an acidic medium in the internal phase; emulsions with Na_3PO_4 contain a basic solution. These emulsions are unstable towards coalescence and sedimentation because of surfactant hydrolysis. The incorporation of Na_3PO_4 in the extracting emulsion leads to a dramatic decrease of emulsion life-times. The break-up time of emulsions with 0.1 M Na_3PO_4 is less than 1 day.

It is of interest to note that the sedimentation rate in emulsions with Na_2SO_4 or $MgSO_4$ concentration above ~0.3 M is vanishingly small, the oil phase does not separate from these emulsions till the on-set of the separation of the water phase.

The examined electrolytes can be arranged according to their influence on emulsion stability towards coalescence:

$$Na_2SO_4 > MgSO_4 > CaCl_2 > NaCl \sim KCl > FeCl_3 > Na_3PO_4$$

and with reference to the sedimentation stability:

$$Na_2SO_4 > MgSO_4 > CaCl_2 > NaCl > KCl > FeCl_3 > Na_3PO_4$$

Thus, the type of electrolyte has a slight effect on the stability of the extracting emulsion at low salt concentrations because of the high rate of isothermal distillation. In the middle concentration range emulsion stability depends strongly on the electrolyte medium. At high ionic strength emulsion stability is influenced by electrolyte concentration to a limited extent. In this case emulsion stability is affected by such factors as the influence of electrolyte type on the strength of surfactant adsorption layers, on water structure near the interface, etc.

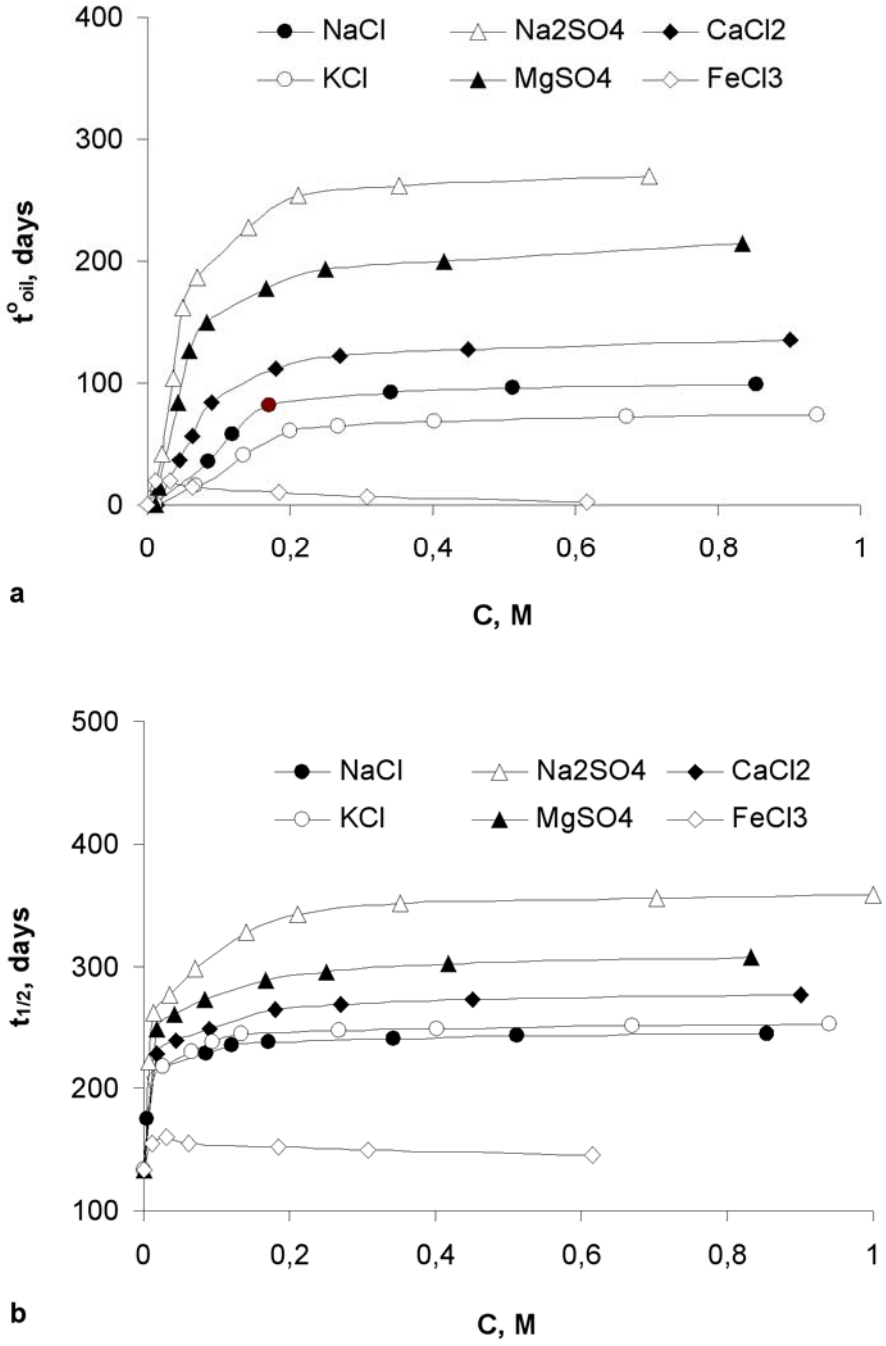


Figure 1. Stability of extracting emulsions. The time not separating of the oil phase (a) and the half-separation time of the water phase (b) as functions of electrolyte concentration.

EXTRACTING EMULSION STABILITY IN A THREE-PHASE SYSTEM

Emulsion swelling as a result of water transfer is the unfavorable process at the extraction in multiple emulsions. In many cases it is impossible to prevent water diffusion because of the significant difference in water activities between the internal and the external water phases.

Nevertheless extraction of surface active compounds may be carried out under conditions of the same water activities. A typical example is the extraction of cholesterol from human blood, when cholesterol adsorbs at the interface in the extracting emulsion. The equality of the total pressure in the extracting emulsion and the osmotic pressure in the blood prevents water transfer out of extracting emulsion into the blood, and vice versa. At quasi-equilibrium

$$P_{os}^{III} = P_{os}^{I} - \frac{1-\phi}{\phi} \Pi - 2 \frac{S}{S_0} \frac{\sigma}{R} \qquad (1)$$

where P_{os}^{III} and P_{os}^{I} are the osmotic pressures in the external phase of the multiple emulsion and in the internal water phase, respectively; Π is the osmotic pressure of water drops in the extracting emulsion; ϕ is the internal phase ratio; σ is the interfacial tension between the oil phase and the aqueous phase in the emulsion; S/S_0 is the ratio of the surface area of the deformed drops and that of the spherical drops of the same volume; R is Sauter mean radius of these drops in the polydisperse emulsion.

The second term of this equation shows the influence of drop deformation in a highly concentrated emulsion. If the internal phase concentration in the extracting emulsions is less than 0.74, Π is equal to zero. The third term is the capillary pressure (P_{cap}). The capillary pressure is caused by the curvature of water drops and is dependent on size distribution in the extracting emulsion. Increasing the internal phase ratio and diminishing the drop sizes, which are preferable for cholesterol recovery because of high values of the specific interface, lead to the alteration of the terms of the total pressure in the extracting emulsions (Table 1). The presented data correspond to average drop diameters equal to 100, 200, and 300 nm. Values of the reduced osmotic pressure ($\Pi / (\sigma / R)$ and S/S_o were obtained from Princen [4].

Table 1. The influence of the internal phase ratio on the terms of the total pressure in the extracting emulsion for cholesterol recovery.

ϕ	P_{os}^{I}, kPa			P_{cap}, kPa			Π, kPa		
	100 nm	200 nm	300 nm	100 nm	200 nm	300 nm	100 nm	200 nm	300 nm
0.70	498.08	426.08	402.08	144.00	72.00	48.00	0	0	0
0.75	498.73	426.41	402.30	144.07	72.04	48.02	1.73	0.86	0.58
0.80	499.67	426.88	402.61	144.22	72.11	48.07	5.47	2.74	1.82
0.85	500.89	427.49	403.02	144.65	72.32	48.22	12.24	6.12	4.08
0.90	502.55	428.32	403.57	145.51	72.76	48.50	26.57	13.28	8.86
0.95	505.28	429.68	404.48	147.24	73.62	49.08	75.24	37.62	25.08
0.99	508.24	431.16	405.47	151.34	75.67	50.45	277.99	139.00	92.66

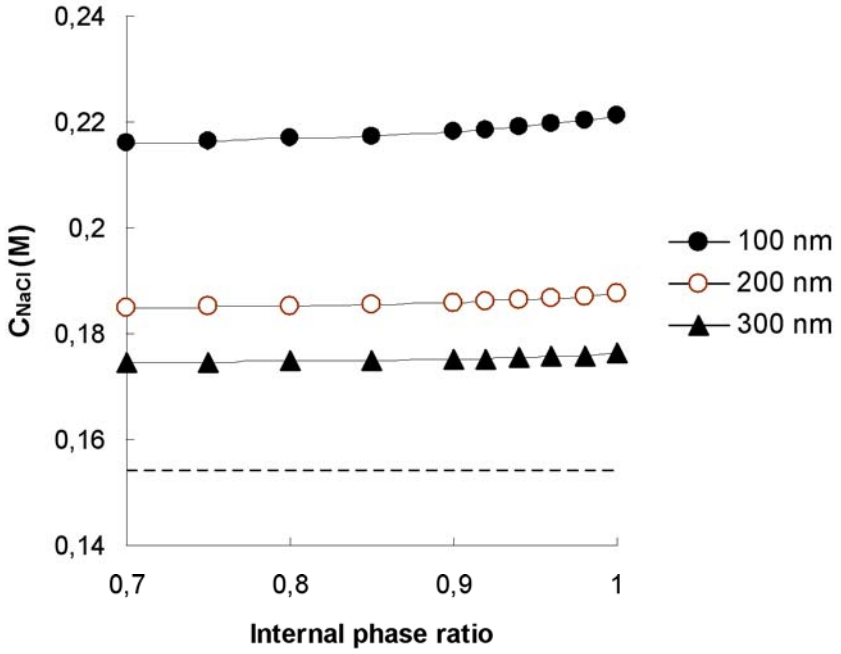


Figure 2. The necessary NaCl concentration in water drops with different diameters as a function of the internal phase ratio.
Dashed line corresponds to NaCl concentration in the external water phase.

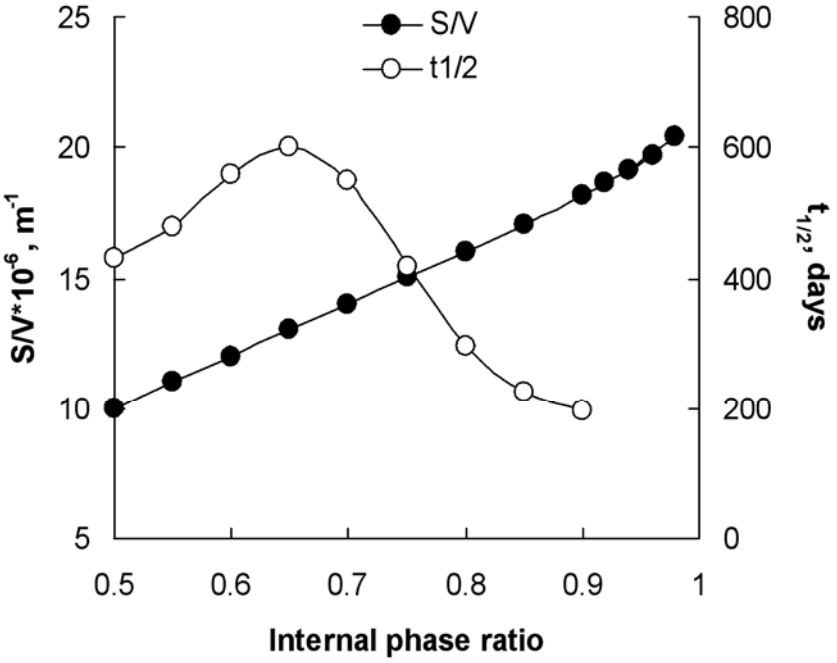


Figure 3. Specific interface area in extracting emulsions with drop diameter equal to 300 nm and half-separation time of the water phase as a function of the internal phase ratio.

The smaller drop size and higher internal phase concentration, increases the values of capillary and osmotic pressures in the emulsion. As a consequence, the osmotic pressure in the internal water phase should be enhanced to equalize the pressures inside and outside the extracting emulsion. Salt concentration in the internal water phase should be also increased, as shown in Figure 2. The dashed line in Figure 2 corresponds to NaCl concentration in the external aqueous solution, which gives the osmotic pressure equal to the osmotic pressure of human blood. There is a marked difference in NaCl concentration in water drops and in the external water phase. This difference is especially significant in fine extracting emulsions. In the main this is caused by the capillary pressure due to water drop curvature. The influence of the osmotic pressure in emulsion because of water drop deformation is much lower.

Values of specific interface area are greatly enhanced by the rising internal phase ratio (Figure 3). Specific interface area in an emulsion with $\phi = 0.75$ is 1.5 times larger than in an emulsion with $\phi = 0.50$. Nevertheless the stability of the extracting emulsion has a maximum value at $\phi = 0.65$. An increase in the internal phase ratio beyond this limit leads to a decrease in the half-separation time of the water phase.

CONCLUSIONS

Thus, the type and the valence of electrolytes have a marked effect on the long-time stability of an extracting emulsion. At very low ionic strength in the internal aqueous phase the rate of isothermal distillation is high. As a result, the emulsion break-up time is short and emulsion stability is scarcely influenced by electrolyte type. In the middle concentration range the emulsion stability depends strongly on electrolyte medium. At high ionic strength emulsion stability is influenced by electrolyte concentration to a limited extent.

The necessary changes in electrolyte concentrations should be made to prevent mass transfer of water in multiple emulsions. The size distribution in the extracting emulsion, and consequently, capillary pressure due to drop curvature has a marked influence on such changes. The influence of water phase ratio is negligible and its effect can be not taken into account.

ACKNOWLEDGEMENTS

This material is based upon work supported by Russian Foundation of Fundamental Investigations (Grant 04-03-32789) and by Russian Federal Program "Integration" (Project I0420).

REFERENCES

1. H. J. Bart, H. Jüngling, N. Ramaseder, R. Marr (1995), *J. Membr. Sci.*, **102**, 103-112.
2. I.Abou-Nemeh, H.J. Bart (1998), *Langmuir*, **14**, 4451-4459
3. E.V. Yurtov, M.Yu.Koroleva (1996), *ACS Symposium Series No 642: Chemical separations with liquid membranes,* Washington, DC, 89-102.
4. H. M. Princen (1988), *Langmuir*, **4**, 164-169.

EXTRACTION OF URANIUM IN A PSEUDO LIQUID MEMBRANE DEVICE BY MEANS OF AN ORGANIC SOLVENT BASED ON TRIBUTYL PHOSPHATE

Alfia M. Safiulina, Artak E. Kostanian*, Ivan G. Tananaev and Boris F. Myasoedov

Vernadsky Institute of Geochemistry and Analytical Chemistry, Moscow, Russia
Kurnakov Institute of General & Inorganic Chemistry of RAS, Moscow, Russia

The extraction of uranium with an organic solvent based on tributyl phosphate and the separation of uranium and thorium have been investigated using pseudo liquid membrane devices.

INTRODUCTION

The conventional versions of liquid membrane method (film pertraction and processes with emulsion and supported membranes) due to the complexity are hard to apply and have low capacity. These disadvantages can be bypassed by implementation of three-phase or multi-phase extraction processes called also pseudo liquid membrane methods [1-14]. This technique can be realized either in a series of mixer-settler combination or in special two- or multi-chamber extraction apparatuses.

The general flowsheet of the three-phase multi-stage extraction is shown in Figure 1 (a). The extraction process is carried out in a cascade of N mass-transfer stages, each comprising two interconnected contact chambers - one extraction chamber and one re-extraction chamber The extraction agent contacts with a feed stream (or donor phase) in the extraction chambers and with a stream of acceptor (or stripping) phase in re-extraction (or stripping) chambers and recycles between the chambers within the same stage building N closed circuits. The extraction agent is thus drawn in a cross-flow with the acceptor and donor phases within the same stage, while the donor and acceptor phases are drawn through all of the stages in the counterflow.

In Figure 1 (b) is shown a schematic arrangement of the three-phase extraction apparatus indicating the basic operation and flow patterns of the liquids. The circulation of the continuous phase of extracting agent between the contact chambers takes place due to the difference in emulsion density in the chambers. When the apparatus is being operated to concentrate a dilute feed solution, the feed flow rate is much grater than the flow rate of the acceptor phase. This causes circulation between the chambers which is co-current on the feed side and countercurrent on the strip side. It is possible to change the circulation direction by operating the strip side at high levels of reflux.

With regard to the most efficient extraction of the desired species the flow directions of both the aqueous feed and stripping solutions are to be generally opposed to the flow direction of the extracting agent within the contact chambers. Where there are two or more species in the feed solution which can be extracted by the continuous phase, the product in the stripping solution will be contaminated by the unwanted species extracted from the feed solution.

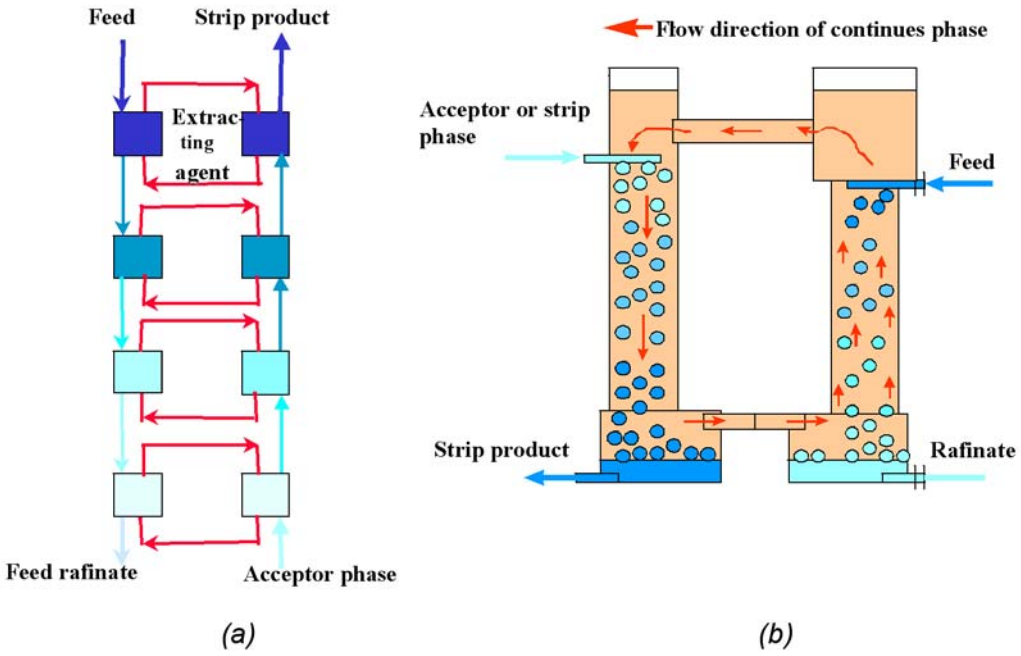


Figure 1.The schemas of the three-phase multi-stage extraction (a) and the three-phase extraction apparatus (b).

To promote countercurrent mode simultaneously in both the extraction and re-extraction chambers and to minimise the stripping stream contamination by feed stream and vice versa, the apparatus shown in Figure 2 is provided with the third (scrubbing) chamber situated between the former two ones. In scrubbing contact chamber the stream of loaded continuous phase (in considered case it is the organic phase) moving from the feed side and the stream of continuous phase denuded of the extracted
species by the stripping solution join and
are contacted by the scrubbing stream.
It is clear that the flow rate of the

scrubbing stream must be greater than the flow rates of the feed and stripping streams.
In order to minimise the volume of scrubbing solution employed the scrubbing liquid can be recycled back through the continuous organic phase as shown in Figure 2.

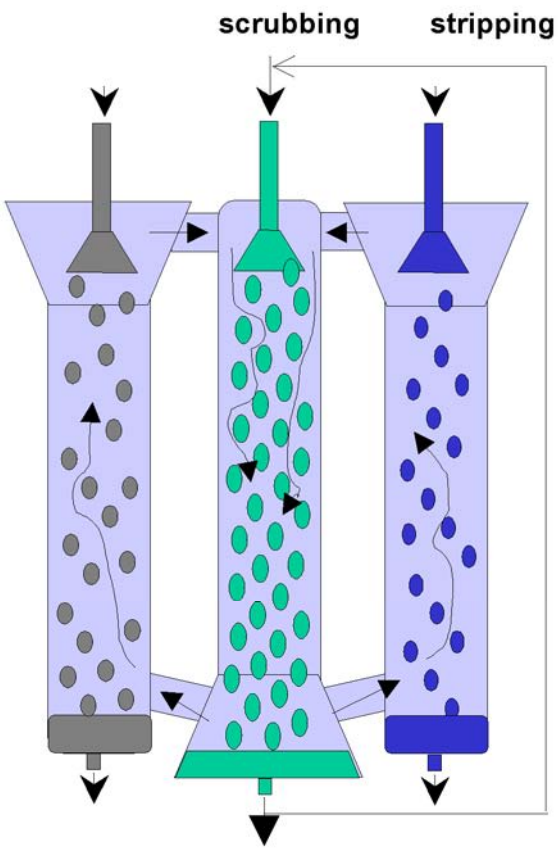


Figure 2. Multi-phase extraction apparatus.

EXPERIMENTAL

Apparatuses and Experimental Methods

Two pseudo liquid membrane devices according to Figures 1 and 2 were constructed and tested: a three-phase extractor and a multi-phase extractor. The apparatuses are filled with a continuous phase through which two dispersed aqueous phases are passed in the form of droplets. Mass transfer is thereby effected from one dispersed phase (the raffinate phase), through the continuous phase (extracting agent or liquid membrane phase), into the other dispersed phase (the extract or strip phase). The circulation of liquid membrane phase, which is the continuous phase, between the contact chambers takes place due to the difference in emulsion density in the chambers. The circulation rate can be changed by changing the droplets size and / or the flow rates of dispersed phases.

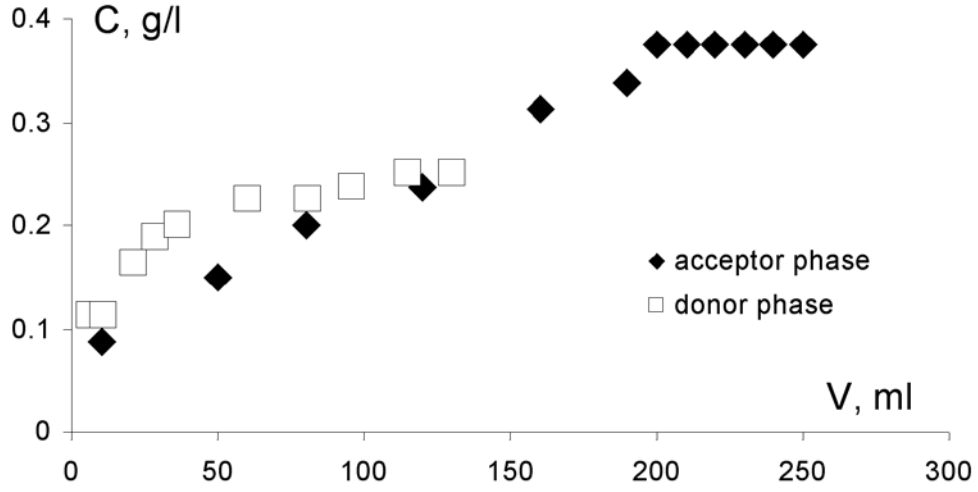
The three-phase apparatus (chamber diameter 10 mm, chamber height 200 mm) was used to extract uranium ^{238}U (VI) from acidic nitrate solutions (3 M HNO_3): liquid membrane phase - 30% thriisobutylphosphate in decane, strip phase – 0.01 M HNO_3, uranium concentration in feed solution – 2 g/l.

The multi-phase apparatus (chamber diameter 10 mm, chamber height 300 mm) was used to separate uranium ^{238}U (VI) and thorium: feed phase - acidic nitrate solutions (3 M HNO_3) containing 0.95 g/l U (VI) and 0.81 g/l Th (IV), liquid membrane phase - 30% thriisobutylphosphate in decane, scrub phase – 0.01 M HNO_3, strip phase – 0.3 M HNO_3 .

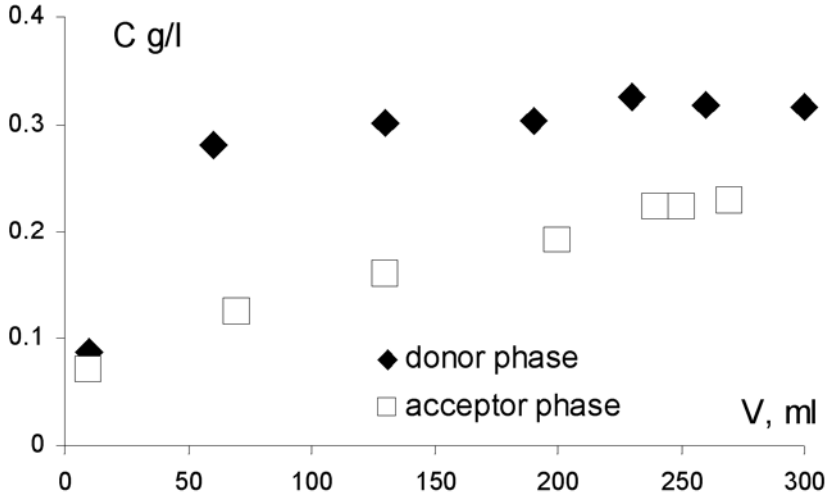
Th (IV) and U (VI) were determined in the aqueous phase with Arsenazo III at 663 nm and 655 nm, respectively. The amounts of Th (IV) and U (VI) were computed from the calibration curve.

RESULTS

Figure 3 illustrates the attainment of the steady-state mode in the three-phase pseudo liquid membrane device.



Flow rates: acceptor phase – 0,8 ml/min., donor phase – 0,18 ml/min.



Flow rates: acceptor phase– 2 ml/min., donor phase – 1.43 ml/min.

Figure 3. Values of concentrations in the raffinate and strip phases vs. total passed through volume of raffinate: three-phase apparatus.

In experiments on multi-phase apparatus the steady-state conditions were attained for uranium only, for the extraction of thorium by thriisobutylphosphate appeared to be irreversible for the scrub and strip solutions applied. Experiments are to be conducted by using new extractants and / or new scrub and strip solutions.

ACKNOWLEDGEMENTS

The authors are grateful to the Russian Foundation for Basic Research (grant No 04-03-32584) for the financial support of this work.

REFERENCES

1. Gu. Zhong-Mao (1990) *J. of Membrane Science*, **52**, 77.
2. X. J. Yang et al. (1995) *J. of Membrane Science*, **106**, 131.
3. Ch. J. Broan (1997) *PCT Application,* No. WO 97/18880
4. Ch. J. Broan (1998) *PCT Application*, No. WO 98/45016
5. Ch. J. Broan (2000) *US Pat.,* No 6051112.
6. M.A. Afonin, V.V. Esimantovskii, V. N. Romanovskii (1996), *Russian Pat.*, № 2.053.308.
7. M. A. Afonin., V. V. Romanovsky.,Esimantovsky and V. M. Romanovsky V. N. (1997), *Proceedings of 6th Intern. Conf. on Radioactive Waste Management and Environmental Remediation ICEM* '97. ASME, NY. V.1, p. 277.
8. A. E. Kostanian (1997), *Russian Pat.*, No 2.080.162.
9. A. E. Kostanian (1999), *Eur. Pat.,* No 0858363.
10. A. E. Kostanian (1998), *Eur. Pat.,*No 0862487.
11. A. E. Kostanian (1999), *Eur. Pat.,* No 0873167.
12. A. E. Kostanian (2000), *US. Pat.,* No 6,090,352.
13. A. E. Kostanian (2000), *US. Pat.,* No 6,129,842.
14. A. E. Kostanian (2000), *US. Pat.,* No 6,143,178.

EFFECTS OF GAS-DISTRIBUTOR CONFIGURATION ON LIQUID-PHASE BACK-MIXING IN A PILOT-SCALE EXTERNAL-LOOP AIRLIFT REACTOR

LI Tian-Cheng [*1,2], XIN Feng [2], ZHU Shen-Lin [1]

1 State Key Laboratory of Solvent Extraction, Department of Chemical Engineering, Tsinghua University, Beijing, 100084, China

2 School of Chemical Engineering and Technology, Tianjin University, Tianjin 300072, China

The back-mixing characteristics of the liquid phase in a pilot-scale external loop airlift reactor (2.5 m height, 0.47 m riser inner diameter and two downcomers of 0.08 m inner diameter) with gas distributors of different hole numbers and opening directions was investigated for the gas-liquid and gas-liquid-solid systems, using an axial dispersion mathematical model. It was that the Peclet number (*Pe*) sharply decreased with the increase of the air flow rate (Q_g) whereas it was less affected by the liquid velocity (u_L) in the downcomers. Upward holes and more holes in the gas distributor lead to increased values of the *Pe* values for the same liquid velocity in the downcomers. Conversely, the influence of opening direction and the number of holes in the gas distributors on *Pe* values was insignificant in the relationship between *Pe* number and air flow rate. The *Pe* values in the gas-liquid-solid system were relatively higher than those in the gas-liquid system at the same operating conditions.

Key words: external loop airlift reactor; pilot-scale; axial dispersion model; gas distributor; liquid phase back-mixing

Corresponding author: Tel: 010-62785524, E-mail: litiancheng@tsinghua.edu.cn

INTRODUCTION

External loop airlift reactors have been extensively studied in recent years owing to their obvious advantages such as simple construction, well-designed flow path, high gas holdup, low shear stress, good temperature control and low power input, among others [1]. Furthermore, the external loop reactors combine the advantages of both the bubble column and the fluidized bed reactors. The circulation flow in an external loop reactor intensifies the mass and heat transfer and favors the mixing of reactants [2]. In addition, the short path and

slugging regimes are also significantly reduced [3]. Due to the injection of gas at the riser bottom, the liquid phase circulates between one riser and two downcomers. And this can promote the suspension of solid particles.

Although many studies on the external loop airlift reactors have been reported in literature [4-7], most were conducted in bench-scale devices. In the present work, the authors investigated the flowing dynamics in a pilot-scale external loop airlift reactor for the both an air-water system and an air-water-active carbon system. The influence of different types of gas distributors on the fluid dynamics was also investigated so as to provide a basis for their industrial applications.

MATHEMATICAL MODEL

In an external loop reactor, the mass transfer efficiency and the chemical reactions rate if any taking place can be promoted by turbulent back-mixing in the liquid phase. Therefore, a better understanding of the liquid phase back-mixing is of great importance in the development of commercial reactors. There are two main factors inducing the liquid phase back-mixing [8]: one is the axial mixing induced by the loop flow; and the other is the formation of eddies in the loop flow. Because of the molecular and eddy diffusions, as well as the liquid velocity profiles, the liquid phase flow often deviates from the ideal flow models so that the axial dispersion model is often used. The following assumptions are made to develop a mathematical model for the external loop reactor flow used in our experiments.

(1) The liquid flows through the riser at a constant velocity u_{L0};
(2) The radial distribution of the tracer concentration is neglected;
(3) The diffusions induced by the turbulent mixing, i.e. molecular diffusion and flow velocity distribution, only exist in the axial direction and can be described by the axial dispersion coefficient D_a;
(4) D_a is a function of reactor configuration, operating conditions and fluid flow type and independent of time and location in the reactor.
(5)

The axial dispersion equation in the riser of the external loop reactor can be expressed as

$$\frac{\partial C}{\partial t} = D_a \frac{\partial^2 C}{\partial Z^2} - u_{L0} \frac{\partial C}{\partial Z} \tag{1}$$

The initial and boundary conditions are

$$t = 0, \quad Z = 0: \quad C(0,0) = C_0 \tag{2}$$

$$t > 0, \quad Z = 0: \quad C(t,0) = 0 \tag{3}$$

$$t > 0, \quad Z = L: \quad C(t,L) = C_0 \delta(t) \tag{4}$$

The above equations can be transformed into their dimensionless forms by introducing the following dimensionless variables

$$\theta = \frac{tu_{L0}}{L},\ \psi = \frac{C}{C_0},\ \xi = \frac{Z}{L},\ Pe = \frac{u_{L0}L}{D_a} \tag{5}$$

Therefore, the axial dispersion equation becomes

$$\frac{\partial \psi}{\partial \theta} = \frac{1}{Pe}\frac{\partial^2 \psi}{\partial \zeta^2} - \frac{\partial \psi}{\partial \zeta} \tag{6}$$

Correspondingly, the initial and boundary conditions are

$$\theta = 0,\quad \xi = 0:\quad \psi(0,0) = 1 \tag{7}$$

$$\theta > 0,\quad \xi = 0:\quad \psi(\theta,0) = 0 \tag{8}$$

$$\theta > 0,\quad \xi = 1:\quad \psi(\theta,1) = \psi(\theta) \tag{9}$$

The above model equation is a parabolic partial differential equation. Because of the non-analytic function in the boundary condition, it can only be solved numerically. Thus, it is necessary to transform it first into algebraic equations based on the six-point difference formula and then to solve the system using the Thomas algorithm.

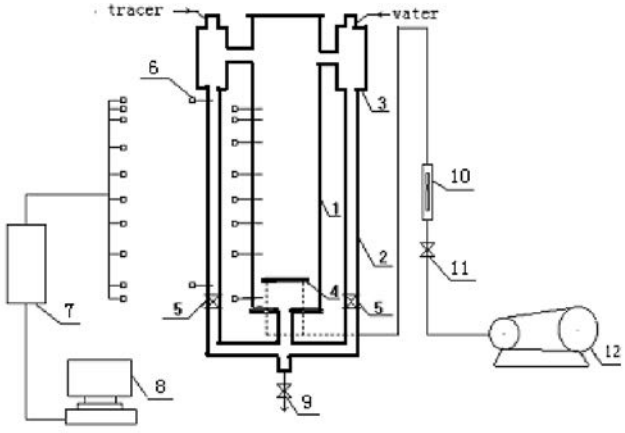
The *Pe* number can be obtained by the least square optimization method of the calculated value $\psi_{cal}(\theta_n, \xi_n)$ and experimental data $\psi(\theta_n, \xi_n)$

$$\min F(Pe) = \sum_{i=1}^{M} (\psi_{cal} - \psi)^2 \qquad Pe \geq 0.0 \tag{10}$$

,

EXPERIMENTAL

The external loop airlift reactor consists of two downcomers and one riser. The height and



1-Raiser 2-Downcomer 3-Separator 4-Gas distributor
5-Butterfly valve 6-Pt electrodes 7-Conductivity device 8-Computer
9-Drain valve 10-Air Flow meter 11- Air inlet valve 12-Air blower

Fig.1 Schematic diagram of experimental apparatus

the internal diameter of the riser are 2.2m and 0.47m respectively, whereas the height and the internal diameter of two downcomers are 2.4m and 0.08m. Fig.1 shows the schematic diagram of the experimental apparatus.

The perforated gas distributors consisted of two concentrically arranged stainless steel. The inner diameters of the two rings were 240mm and 410mm, respectively. Six types of gas distributors with different number of holes and opening directions (Table 1 and Fig.2) were tested.

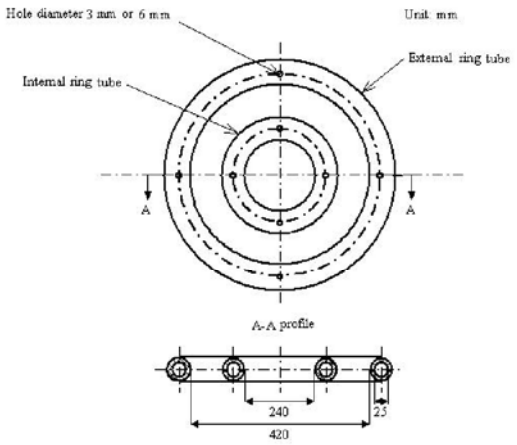


Fig.2 Gas-distributor configuration

Table 1 Gas distributors used in the experiments

Structural parameter	I	II	III	IV	V	VI
Hole opening direction	Down	Down	Down	Up	Down	Up
Hole diameter /mm	6	3	3	3	3	6
Hole number	80	70	140	140	21	46
Total area of holes / cm^2	2.3	0.5	1.0	1.0	1.5	1.1

The conductivity probes were made of platinum wire of 0.5 mm diameter. The length of the exposed parts of the two probes was 5 mm and the distance between them was 3 mm. Two butterfly valves were installed at the bottom of the two downcomers to regulate the liquid velocity in the downcomers. The operating conditions are listed in Table 2.

Table 2 Operational conditions of the tracer experiments

T /℃	P/kPa	ξ/%	Liquid volume /L	C_0/g·mL^{-1}	D_a /mm	active carbon /g
25	100	20 -100	350	0.25	10-38	250

Both an air-water and an air-water-active carbon system were investigated. A tracer was introduced into the system from the top of one of the downcomers and its concentration was measured at different axial positions and time by using the conductivity apparatus connected to a microcomputer for data processing.

The liquid velocity in the downcomer, u_L, was obtained by measuring the responding time difference (τ) of the conductivity signals from two electrodes at different locations in the downcomer according to the following formula [9]

$$u_L = \frac{L_d}{\tau} \tag{11}$$

Here, L_d stands for the distance between the two electrodes in one of the downcomers.

RESULTS AND DISCUSSION

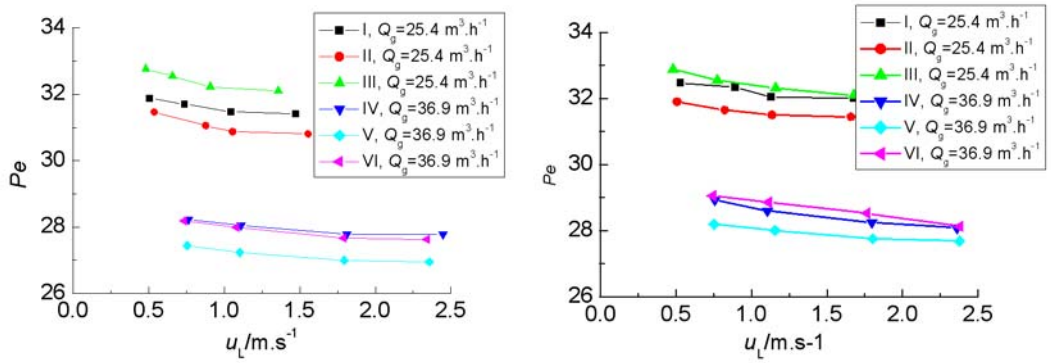
Effect of u_L and holes' opening direction on *Pe* at fixed Q_g

Fig.3 shows the effect of u_L and gas distributor configuration on *Pe* at fixed Q_g in the gas-water and gas-water-solid systems.

Fig.3a shows that *Pe* values were significantly affected by the number and opening direction of holes in the gas-liquid system, whereas their effect of the liquid velocity in the downcomer was relatively insignificant. In the cases of gas distributors I, II and III with the hole opening downward but of different number of holes, the *Pe* values were greatly changed by the number of holes. As the number of holes affected the size of the gas bubbles produced, it also affected the *Pe* values, which are a reflection of the liquid phase back-mixing. In contrast, in the cases of gas distributors IV and VI with hole opening upwards, the *Pe* values were much larger than that in the case of gas distributor V with the hole opening downward. These phenomena have been explained in terms of the different flowing characteristics for different gas distributors. The reason was that the gas phase passed through the upward-holes gas distributors in the same direction as the liquid flow, while the gas phase penetrated through the downward holes' gas distributors in a reverse direction to that of the liquid flow. This showed that the airlifting force to the liquid fluid was larger in the former case than that in the latter case, leading to less severe liquid phase back-mixing.

Fig.3b shows that *Pe* values slightly decreased with the increase of u_L in the gas-liquid-solid system. However, *Pe* values were affected by both the opening direction of holes and the number of holes of the gas distributors, too. Compared with gas-liquid system, the effects of both the holes number and opening direction of the gas distributors on *Pe* values were decreased because the back-mixing of the liquid phase was less severe as active carbon was added. The solid particles played a role to promote break-up of large bubbles and prevent coalescence of small ones. Consequently, the back-mixing of the liquid phase became relatively smooth, leading to larger *Pe* values.

Fig.4a shows that *Pe* value sharply decreased with Q_g below a Q_g value of $17 m^3 \cdot h^{-1}$ and the decrease became smooth above it, but the effect of the holes opening direction was insignificant in gas-liquid system. At lower gas rate, the airlifting interaction with the liquid was small and the liquid phase moved in a manner near to a plug flow; while at larger gas rate, the increased airlifting interaction with the liquid made liquid back-mixing severer and liquid phase circulated in a manner similar to continuously stirred flow. For gas distributors with upward



a Air-water b Air-water-solid

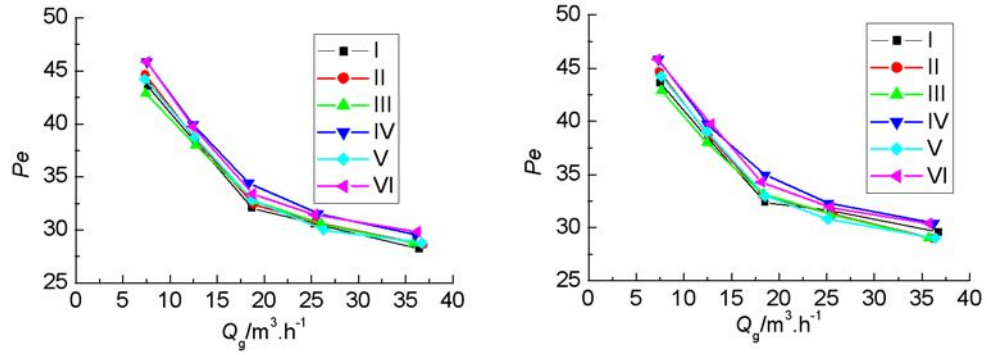
The active carbon concentration added was 0.7 g·L^{-1}

Fig.3 Effects of u_L and holes' opening direction on Pe at fixed Q_g in different system

4.2 Effect of Q_g on Pe at fixed opening degree of the butterfly valves

holes, larger *Pe* values were observed at lower gas rates.

Fig.4 illustrates the effect of Q_g on Pe at a fixed opening degree of the butterfly valves in gas-water system and gas-water-solid system.



a Air-water system b Air-water-solid system

ξ=100 %, the active carbon concentration added was 0.7g·L^{-1}.

Fig. 4 Effects of Q_g on Pe at fixed opening degree of butterfly valves

Fig.4b depicts that the effect of Q_g on *Pe* was very similar to that in the gas-liquid system, and the effect of the holes opening direction was also insignificant in gas-liquid-solid system. However, under the same conditions the *Pe* values in the gas-liquid-solid system were slightly higher than those in the gas-liquid system, especially at larger Q_g. This may be attributed to the more average distribution of solid particles at larger Q_g leading to the formation of more bubbles of smaller sizes.

CONCLUSIONS

Based on an axial dispersion model, liquid phase back-mixing in a pilot-scale external loop airlift reactor with different gas distributors was investigated for both a gas-liquid and a gas-liquid-solid system. The *Pe* values sharply decreased with the increase of gas flow rate

but were only slightly decreased with increasing liquid flow rate. The opening direction and the number of holes in the gas distributors had obvious effect on *Pe* within the relationships between *Pe* values and liquid velocity in the downcomers. However, the effect of hole opening direction and number of holes was insignificant in the relationships between *Pe* values and gas flow rate. The *Pe* values in the cases of upward holes were larger than those in the cases of downward holes. Compared with gas-liquid system, the effects of both opening direction and number of holes in the gas distributors on *Pe* values were decreased in gas-liquid-solid system. In addition, the *Pe* values in gas-liquid-solid system were slightly higher than those in gas-liquid system, especially at larger Q_g under the same conditions. This phenomenon was attributed to the enhancement of large bubbles break-up and small bubbles coalescence in the presence of the solid particles, this leading to slight liquid back-mixing and higher *Pe*.

REFERENCES

[1] H Dhaouadi, S Poncin, J M Hornut, G Wild, et al. Mass transfer in an external-loop airlift reactor: experiments and modeling, *Chem. Eng. Sci.* **52** (1997) 3909-3917

[2] E Delnoij, J A M Kuipers, W P M van Swaaij. Dynamic simulation of gas liquid two-phase flow: effect of column aspect ratio on the flow structure, *Chem. Eng. Sci.* **52** (1997) 3759-3772

[3] R S Douek, A G Livingston, G F J Hewitt. Instability phenomenon in an external-loop three-phase gas-liquid-solid airlift reactor. *AIChE.* **41** (1995) 2508-2511

[4] J B Snape, J Zahradnik, M Fialova, et al. Liquid-phase properties and sparger design effects in an external-loop airlift reactor, *Chem. Eng. Sci.* **50** (1995) 3175-3186

[5] B I Tarmy, C A Coulaloglou. Alpha-omega and beyond industrial view of gas/liquid/solid reactor development, *Chem. Eng. Sci*. **47** (1992) 3231-3246

[6] B Glennon, W Al-Masry, P F Macloughlin, et al. Hydrodynamic modeling in an air-lifted loop reactor, *Chem. Eng. Comm.* **121** (1993) 181-192

[7] M Y Chisti, B Halard, M Moo-Young. Liquid circulation in airlift reactor. *Chem. Eng. Sci.* **43** (1998) 451-457

[8] H J Wang, M L Fei, D W Chen. Liquid back-mixing characteristics and gas-liquid mass transfer coefficient of three phases external-airlift loop reactor, *Chemical reaction engineering and technology*. **8** (1992) 178-184

[9] J P Zhang, J R Grace, N Epstein, et al. Flow regime identification in gas-liquid flow and three-phase fluidized beds, *Chem. Eng. Sci.* **52** (1997) 3979-3992

NOTATION

C	Concentration of tracer	uL	Liquid velocity through downcomers
C0	Base concentration of tracer	Z	Axial position of riser Greek letters
Da	Axial dispersion coefficient	δ (t)	Delta function of impulse response
Ds	diameter of active carbon particles	ζ	Dimensionless distance
L	Riser height	θ	Dimensionless time
Ld	Distance between two electrodes	ξ	Opening degree of butterfly valves
Qg	Air flow rate	τ	Time difference in pulse response
t	Time of tracer pulse response	Ψ	Dimensionless concentration



REACTIVE EXTRACTION OF L-PHENYLALANINE WITH ANION EXCHANGER IMPREGNATED RESINS

Albena Kostova, Hans-Jörg Bart

Institute of Thermal Process Engineering / University of Kaiserslautern
67663 Kaiserslautern, Germany

The objective of our work is to apply the advantages of the Solvent-Impregnated Resins (SIR) for the amino acid separation from aqueous solutions. The impregnation and the advantages of this process are discussed. The amino acid L-phenylalanine is chosen as a model substance. The resin XAD1180 was impregnated with the liquid ion exchanger tricaprylylmethylammonium chloride (TCMAC) and tested for its sorption properties. The equilibrium experiments at different conditions and their modelling are presented.

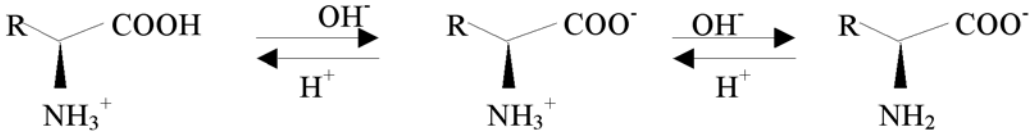
INTRODUCTION

The SIR's are known as novel and effective media for selective separation of metal ions and carboxylic acids from aqueous solutions [1, 6]. The concept of SIR is based on the physical impregnation of a liquid ion exchanger into a macro porous polymer. The breakthrough of this idea was in the 60s. The extractant LIX 64 was immobilised on paper or cellulose powder and used for the analytical separation of cobalt, nickel and magnesium [7]. For the preparative use it was a problem to find a good carrier for the impregnation. A good possibility for this is when macro porous resins efficiently immobilise the liquid ion exchanger thus offering a big mass transfer area [8,9].

The reactive sorption with impregnated resins combines the high selectivity of the liquid ion exchangers and the high throughput flexibility of the fixed bed adsorption. The SIRs have a high adsorption capacity, because the ion exchanger is impregnated without dilution. The substance, which must be separated from the aqueous solution, reacts with the impregnated ion exchanger and adsorbs onto the solid phase. With an appropriate desorption it is possible to obtain this substance in a high purity. Another advantage in comparison with conventional ion exchange resins is in a broad availability of cheap liquid ion exchanger. The reactive sorption avoids the entrainment of the extractant, which is a problem in rigorously stirred mixer-settler extractors. The bleeding loss of an impregnated ion exchanger is in contrast to this negligible [10,11].

Very important for the technical application is the mass transfer rate. New resin structures with micro and macro pores (reaction and transfer pores) give the opportunity to new applications. The structure of the used polymer has a markedly influence on the mass transfer kinetics and on the sorption capacity. Evidently, the bigger transport pores have a faster mass transfer and the smaller micro pores give rise to a higher capacity.

Till now only little is known in the area of separation of amino acids with reactive sorption [11-16]. This separation process uses the property of the amino acid to have a different ionic form. Amino acids exist at the intermediate pH range as zwitterions in aqueous solutions. At low pH they behave as cations and at high pH as anions:



(1)

The amino acid should be present in the correct ionic form for appropriate ion exchange. It is possible to extract or to strip the amino acid from a liquid ion exchanger with pH control by adding an acid or a base. L-phenylalanine (L-phe) was chosen due to its economical importance as bench mark to test this separation technology.

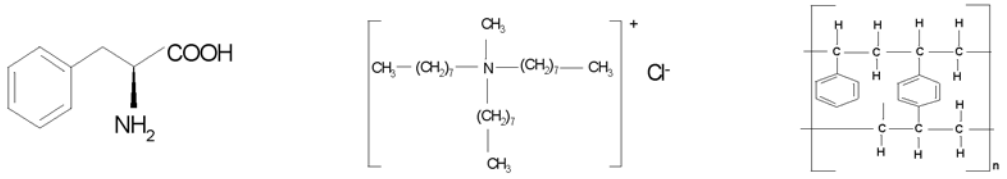
TCMAC is a well-known carrier for the extraction of amino acids [17-19] and has already been successfully impregnated on macro porous resins [12]. The objective of this paper is to investigate the reactive sorption of amino acids with the anion exchanger impregnated resins. In this paper we present the impregnation method, the equilibriums experiments and modelling.

EXPERIMENTAL AND MATERIALS

The dissociation constants of acidic and basic groups of L-phe (Figure 1a) in aqueous solution are pK_1 = 1.83 and pK_2 = 9.13 respectively. This shows that the L-phe can be extracted at its anionic form from aqueous solutions at high pH. The liquid anion exchanger TCMAC (Figure 1b) was impregnated in the neutral resin XAD 1180 (Figure 1c). The properties of this resin are summarised in Table 1. Other reagents such as n-hexane and sodium hydroxide were of analytical grade and were used without purification.

Table 1. Properties of the resin XAD1180 (Fluka)

	XAD1180
Surface area, m^2/g	>500
Porosity, ml/ml	0,6
Particle diameter, mm	0,25-0,85
Pore diameter, nm	40-45



a) *b)* *c)*

Figure 1. Chemical structure of a) phenylalanine, b) TCMAC, c) XAD1180

Impregnation

The impregnation was carried out by shaking an impregnation solution (TCMAC in n-hexane) together with the XAD 1180 resin. After this the SIR was filtered and dried at a temperature of 65°C. The impregnation Langmuir like isotherm is shown on Figure 2. With increasing concentration of the ion exchanger in the impregnation solution the maximal saturation is approached, which will be the case when all pores are filled with the ion exchanger.

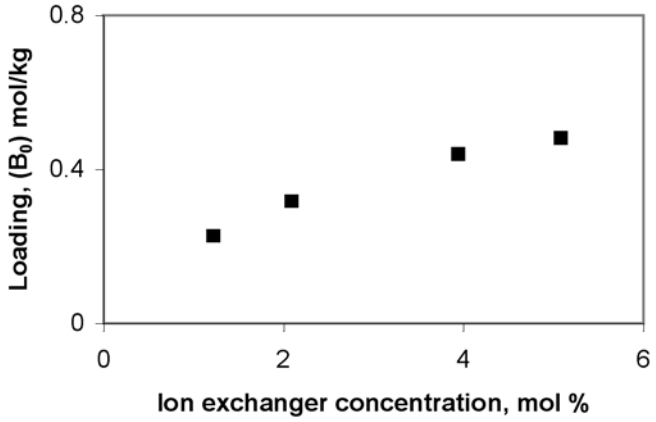


Figure 2: Loading of SIR (B_0) in dependence of the initial ion exchanger concentration in the impregnation solution.

The used impregnation method provides a stable adsorption of the ion exchanger on the resin surface. In [16] we show that the SIR can be used multiple times without leaching of the impregnated ion exchanger.

Equilibrium experiments

The sorption equilibrium data were measured in batch experiments at 25°C. The pH was adjusted with NaOH. The equilibrium concentration of L-phe in the aqueous solution was determined with a UV-VIS spectrophotometer (UV-160A Shimadzu). The concentration of L-phe in the SIR at equilibrium q^*_{Phe} was determined from the mass balance:

$$q^*_{Phe} = \frac{V_L}{m_{SIR}}(C_0 - C^*_{Phe}) \qquad (2)$$

with

q^*_{Phe} concentration of phenylalanine in SIR [mol/kg]

C_0 initial concentration of phenylalanine in the aqueous solution [mol/l]

C^*_{Phe} equilibrium concentration of phenylalanine in the aqueous solution [mol/l]

m_{SIR} mass of SIR [kg]

V_L volume of the aqueous solution [l]

The efficiency of the process is defined as:

$$E\% = \frac{q^*_{Phe}}{C_0}\frac{m_{SIR}}{V_L}100 \qquad (3)$$

L-phe must be present in an anion form in the aqueous solution to be extracted with an anion exchanger. At high pH the OH-ions in the aqueous solution are also extracted from the anion exchanger. Figure 3 shows the dependence of the sorption efficiency from the initial pH of the solution. Is can be seen, that the optimal pH region is between 10 and 11. At pH lower than 10 there are not enough amino acid anions, which can be extracted, and at pH higher than 11 the co-extraction of OH-anions is dominant.

The influence of the ion exchanger concentration on the efficiency of the process is shown for two initial amino acid concentrations in the aqueous solution on Figure 4. With increasing ion exchanger the efficiency of the process is increasing, too. The lower initial amino acid concentrations in the aqueous solution are recovered at a higher efficiency.

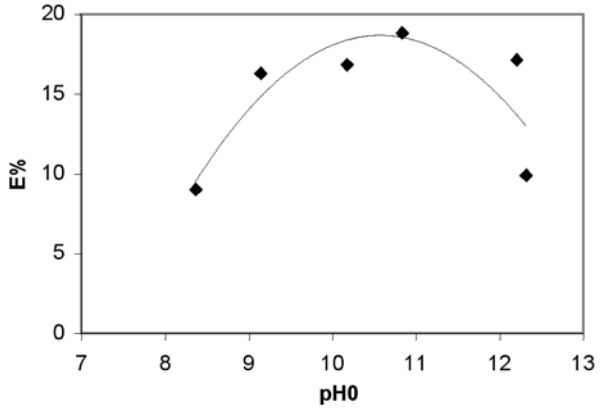


Figure 3: Efficiency of the sorption process in dependence of the initial pH

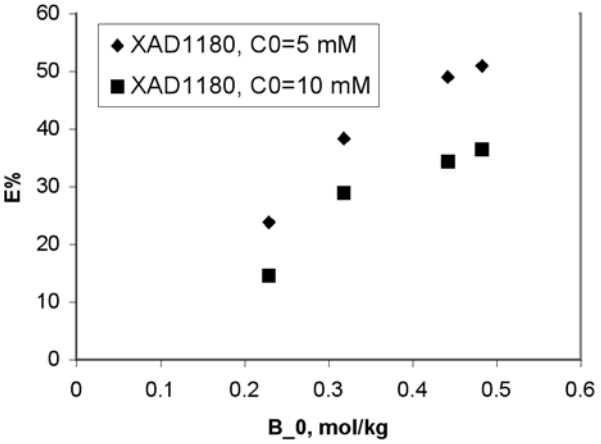


Figure 4: Efficiency of the sorption process in dependence of the ion exchanger concentration (initial L-phe of 5 and 10 mM).

EQUILIBRIUM MODEL

The following assumptions were made:

- L-phe anions and OH anions can be adsorbed simultaneously;
- TCMAC in the pores has the same chemical behaviour as in liquid extraction.

The sorption reaction between the L-phe anions and the impregnated resin (RCl) is:

$$L-phe^- + RCl \xleftrightarrow{K_1} RL-phe + Cl^- \qquad (4)$$

The co-extraction of OH anions during the sorption process must be taken into account too:

$$OH^- + RCl \xleftrightarrow{K_2} ROH + Cl^- \qquad (5)$$

Here RL-phe and ROH are the concentrations of amino acid and OH in the resin phase, respectively. The equilibrium constants of these reactions are defined as:

$$K_1 = \frac{[RL-phe][Cl^-]}{[L-phe^-][RCl]} \quad (6) \qquad K_2 = \frac{[ROH][Cl^-]}{[OH^-][RCl]} \quad (7)$$

At a given total concentration of L-phe (C) and OH in the aqueous solution the concentration of the L-phe anion is:

$$L-phe^- = \frac{C(OH)^2 K_{p1} K_{p2}}{K_{p1} K_{p2} (OH)^2 + K_{p1} OH\, 10^{-14} + 10^{-28}} \quad (8)$$

Taking into account the mass balances for L-phe, OH and Cl between the aqueous and the resin phase than equations (6) and (7) are:

$$K_1 = \frac{V_L * (C_0 - C) * (C_0 - C + OH_0 - OH) * (Kp_1 * Kp_2 * OH^2 + Kp_1 * OH * 10^{-14} + 10^{-28})}{m_{EIP} * C * OH^2 * Kp_1 * Kp_2 * \left(B_0 - \frac{V_L}{m_{EIP}} (C_0 - C) - \frac{V_L}{m_{EIP}} (OH_0 - OH) \right)} \quad (9)$$

$$K_2 = \frac{V_L (OH_0 - OH) * (C_0 - C + OH_0 - OH)}{m_{EIP} * OH * \left(B_0 - \frac{V_L}{m_{EIP}} (C_0 - C) - \frac{V_L}{m_{EIP}} (OH_0 - OH) \right)} \quad (10)$$

In comparison to experimental data shown on Figure 4 for the equilibrium constants were found K_1=1,21 and K_2=2,6.

Model validation

To prove these constants experiments were made at different initial concentration of L-phe in the aqueous solution (Figure 5a) and varying the ratio of the volume of the aqueous phase to the mass of the SIR (Figure 5b). From the comparison of the experiments with the calculations it can be seen, that the supposed equilibrium model offers a very good description of the experimental data.

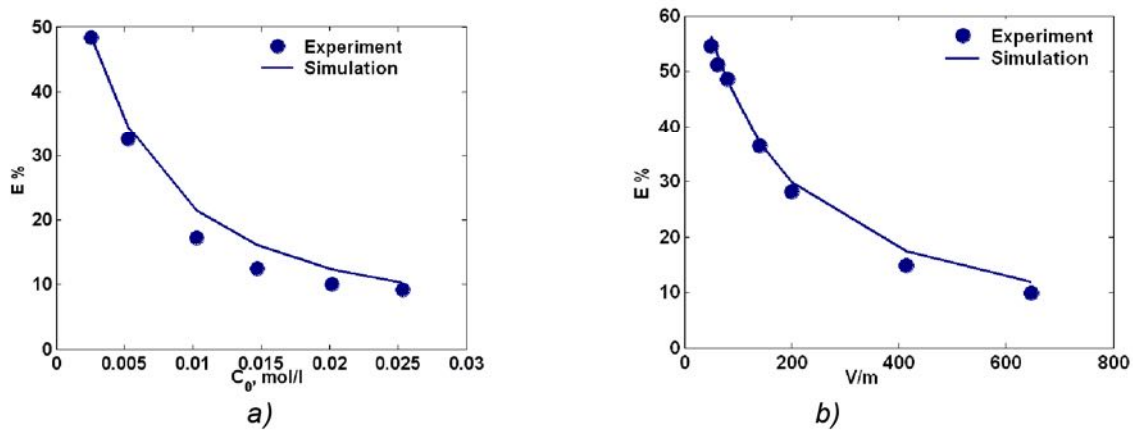


Figure 5: Comparison between experiments and calculations a) V/m=80, B_0=0,32 mol/kg, pH_0=10, C_0=var; b), B_0=0,48 mol/kg, pH_0=10, C_0=5,3 mmol/l V/m=var

CONCLUSIONS

A macro porous resin was impregnated with the anion exchanger TCMAC and the impregnation isotherm shows a Langmuir character. This impregnated polymer was successfully used for the sorption of the amino acid L-phenylalanine from aqueous solution. The optimal pH region was determined between 10 and 11. It was found that the efficiency could be increased with increasing the ion exchanger concentration in the SIR. The equilibrium experiments were modelled taking into account the adsorption of phenylalanine anions and the co-adsorption of OH-anions. The equilibrium constants were fitted on the experiments by varying the anion exchanger concentration in SIR and used for the calculation of the experiments at different L-phe concentrations in the aqueous phase and different volume to mass ratio. A satisfying agreement between calculation and experiment was found.

ACKNOWLEDGEMENTS

The authors wish to thank the German Research Foundation, DFG (Deutsche Forschungsgemeinschaft), for supporting this work.

REFERENCES

1. A. Warshawsky (1981), *Solv. Extr. Ion Exch.*, **8**, 229-311.
2 R. S.Juang, M. L. Chen (1997), *React. Funct. Polym.,* **34**, 93-102.
3. R. S.Juang, H. C. Lin (1995), *J. Chem. Technol. Biotechnol.,* **62**, 141-147.
4. R. S.Junag, H. L. Chang (1995), *Ind. Eng. Chem. Res.,* **34**, 1294-1301.
5. M. Traving, H. J. Bart (1998), *Chem. Ing. Techn.,* **70**, 1152
6. M. Traving, H. J. Bart (2001), *Proc. ISEC'99*, *Solvent Extraction for the 21st Century*, ed M. Cox, M. Valiente, M. Hidalgo, Society of Chemical Industry, London, **1**, 125-129
7. E. Cerrai, G. Ghersini (1969), *Analyst*, **94**(1120), 599-604.
8. R. Kroebel, A. Meyer (1971), *West German Pat. Appl.,* No. 2162951 (18.12.1971).
9. A. Warshawsky (1971), *S. Afr. Patent Appl.*, No. 71/5637 (23.8.1971).
10. Traving M. (2000), *Diss. Universität Kaiserslautern*, ISBN 3-8265-7927-5.
11. A. Kostova, H. J. Bart (2004), *Proc. of IEX 2004*, Ed: M. Cox, Churchill College, Cambridge, 4-8.07.2004, 251-258.
12. M. O. Ruiz, J. L. Cabezas, I. Escudero, J. R. Alvarez, J. Coca (2002), *Trans IChemE.*, **80**, Part A, 537-542.
13. M. O. Ruiz, J. L. Cabezas, I. Escudero, J. R. Alvarez, J. Coca (2002), *Trans IChemE.,* **80**, Part A, 529-536.
14. A. Kostova, H. J. Bart (2004), *Chem. Ing. Tech. 76 (11), 1743-1748.*
15. A. Kostova, H. J. Bart (2004), *Proc. of 10th International Summer School of Chemical Engineering*, Varna, Bulgaria, Ed. Ts. Sapundzhiev, R. Popov, 230-233.
16. A. Kostova, H. J. Bart (2004), *Ion Exchange Technology for Today and Tomorrow*, Ed. M. Cox, 251-258.
17. M. R. Pursell, M. A. Mendes-Tatsis, D. C. Stucky (2003), *Biotechnol. Bioeng.*, **82**, 5, 533-542.
18. H. Escalante, A. I. Alonso, I. Ortiz, A. Irabien (1998), *Sep. Sci Technol.*, **33**, 1, 119-139
19. R. Haensel, W. Halwachs, K. Schügerl (1986), *Chem, Eng. Sci*, **41**, 7, 1811-1815

FUNCTIONALISED SOLVENT IMPREGNATED RESINS FOR THE REMOVAL OF ALDEHYDES FROM AQUEOUS STREAMS

Katarina Babić, A. G. J. van der Ham, A. B. de Haan

University of Twente, Enschede, The Netherlands

The performance of Solvent Impregnated Resin technology for extraction of aldehydes from aqueous solutions has been investigated. The extraction capabilities of several different aliphatic and aromatic primary amines towards aldehydes were tested and compared. Aliphatic amines showed higher affinity. The most promising extractant, Primene® JM-T, was immobilized in a porous particle. As a solid support two different macroporous adsorbents were used, namely XAD16 and MPP. Their capacities for removal of aldehydes were compared with the non-impregnated resin and the resin impregnated with the non-reactive solvent. It was shown that the addition of a reactive extractant can significantly increase the adsorption capacity of an otherwise poor adsorbent. Capacity for removal of aldehydes was increased with the increase of amine loading on the particle.

INTRODUCTION

Aldehydes cause contamination of the environment. Therefore their presence in wastewater streams should be reduced to very low concentrations (ppb-level), rendering conventional reactive extraction unfeasible due to the high excess of solvent/reactant needed. On the other hand, adsorption is very often not selective enough, has very low capacity or is very expensive when resins containing functional groups are used.

Therefore it is necessary to design a process that will overcome these disadvantages, but maintain the advantages of both mentioned separation techniques. This can be achieved by Solvent Impregnated Resin (SIR) technology, a synergistic combination of adsorption and reactive extraction that combines a high capacity and selectivity with relatively simple equipment and operation. Already a lot of research has been done in this field for removal of traces of metals from aqueous streams [1,2]. Lately, the SIR technology has been applied for recovery of organic compounds, like flavonoids [3], carboxylic acids [4,5,6] and amino acids [7,8]. In the present research we investigate the removal of aldehydes from diluted aqueous streams using SIR technology.

The concept of SIRs is based on the incorporation of a selective extractive reagent into a porous particle by physical impregnation. In order to apply this technology to water treatment it is necessary to fill the pores with a water-insoluble organic phase. However, aldehydes do not show a strong tendency to transfer from an aqueous to an organic phase. To improve their affinity for the organic phase it is functionalised with a complexing agent capable of forming a complex with aldehydes, which remains in the organic phase (Figure 1). This reaction should be reversible but sufficiently strong to increase the aldehyde's affinity for the organic phase by several orders of magnitude to obtain an economically feasible process.

As complexing agents primary amines can be used because they form stable Schiff bases in reaction with aldehydes (Figure 2). By choosing an amine with a large apolar organic tail it can be assured that it is insoluble in water.

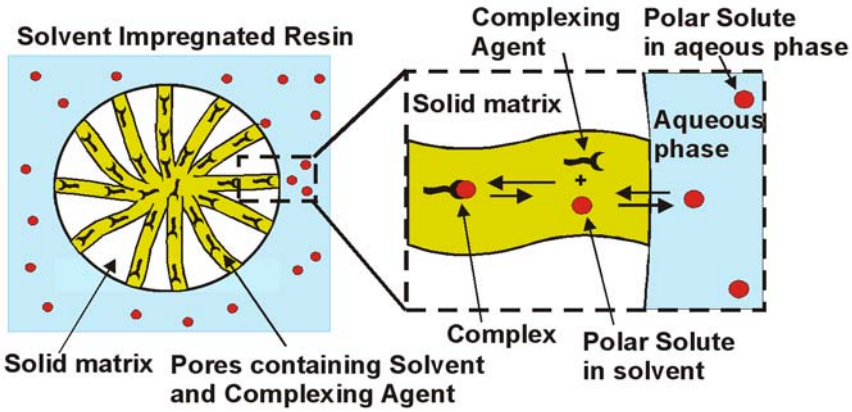


Figure 1. Solvent Impregnated Resins



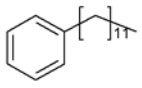
Figure 2. Schiff base formation

According to the mentioned criteria some aliphatic and aromatic amines were selected and experimentally tested. The performance of two different polymeric resins, Amberlite XAD16 and Macroporous polypropylene (MPP) was investigated.

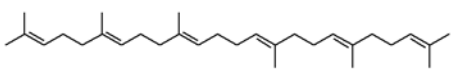
EXPERIMENTAL

Reagents

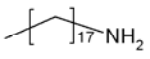
Benzaldehyde, 1-phenyldodecane (1-PD), squalene (SQ), dodecylamine (DDA), octadecylamine (ODA), n-hexane and acetone were purchased from Merck, Germany. 4,4'-Methylenebis-(2,6-diisopropylaniline) (MBDIPA) and 4,4'-Methylenebis(2-isopropyl-6-methylaniline) (MBIPMA) were purchased from Acros, Belgium. All chemicals were used as received. A sample of Primene® JM-T was received from Rohm and Haas, Europe. Amberlite XAD16 (porosity 0.6, particle size 0.75 mm) was purchased from Sigma Aldrich. Macroporous polypropylene (MPP) particles (porosity 0.5, particle size 1 mm) were donated by Akzo Nobel, the Netherlands.



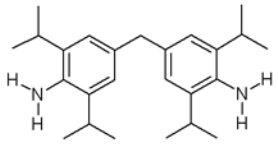
1-phenyldodecane
1-PD



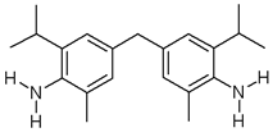
squalene
SQ



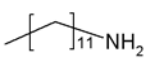
octadecylamine
ODA



4,4'-methylenebis-
(2,6,-diisopropylaniline)
MBDIPA



4,4'-methylenebis-
(2-isopropyl-6-methylaniline)
MBIPMA



dodecylamine
DDA

Figure 3. Structures of used extractants

Liquid-Liquid Equilibria

Liquid-liquid equilibrium experiments were conducted on a fully automated workstation, described by Kuzmanović et al. [9]. The extraction was done in closed 2-ml glass vials that were agitated for 24 h to ensure equilibrium. After agitation, the vials were transferred into thermostated (25°C) trays, and a settling time of at least 2 h was allowed and shown to be sufficient. After settling, 70 µl samples of the aqueous phase were taken and diluted with 255 µl of ethanol to prevent phase separation and the evaporation of benzaldehyde. Finally, 25 µl of an internal standard solution (0.025 M dibenzofuran in ethanol) was added to the vial and quantitative analysis was done using a gas chromatograph, Varian CP-3800 system equipped with a capillary CP–FFAP–CB column (25 m, 0.15 mm; 0.25 µm packing) and a FID detector. The distribution ratio of benzaldehyde was calculated as the ratio of its concentration in the organic phase over its concentration in the aqueous phase. The concentration of benzaldehyde in the organic phase was calculated from the mass balance.

Impregnation Procedure

The impregnation procedure is based on the procedure published by Juang et al. [4]. Amberlite XAD16 was first cleaned with acetone and n-hexane and then dried under vacuum at 60°C, while MPP did not require any pre-treatment. Dry resin was then contacted with a mixture of n-hexane and amine or 1-PD. Dilution of the amine and 1-PD in n-hexane was done only to assure a homogeneous loading of the particles. After a contact time of at least 3 hours [6] n-hexane was removed by drying under vacuum.

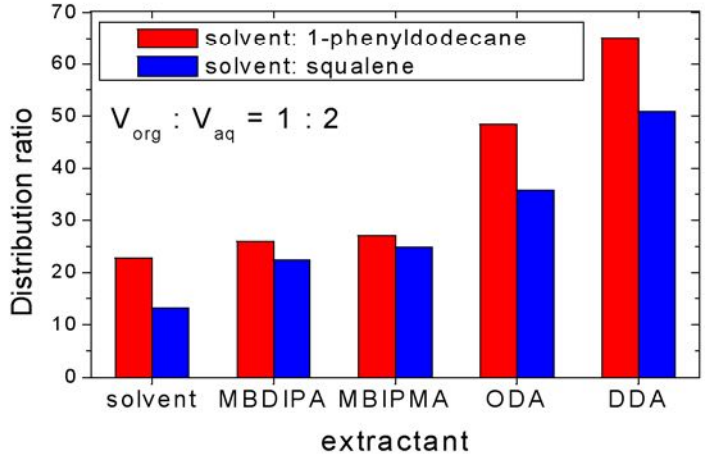
Solid-Liquid Equilibria

Batch adsorption experiments were used to determine the capacity of the SIRs. In each experiment equal volumes of SIR (0.5 ml) and an aqueous solution of benzaldehyde (15 ml) were placed in a 50 ml glass-stoppered flask and shaken at 200 rpm and 25°C for at least 24 h using the thermostated shaking bath (Julabo Shake Temp SW23). Finally, a 2-ml sample of the aqueous phase was removed using a 2-ml syringe fitted with a filter (Schleicher&Schuel, Spartan 30/0,45 RC), and transferred to a 2-ml amber vial. Preparation and analysis of the samples were in parallel with the liquid-liquid experiments. The amount of benzaldehyde in the SIR particles was calculated from the mass balance.

RESULTS AND DISCUSSION

Extractant Screening

Different amines were tested in order to find the most suitable extractant for further use in SIR technology. Selection was based on amine affinity for benzaldehyde recovery, but also on certain physical properties, like solubility in water and being a liquid at room conditions. Figure 4 shows the results of the extractant screening.



amine	solvent	saturation concentration mol/l
MBDIPA	1-PD	0.3680
	SQ	0.4890
MBIPMA	1-PD	0.1810
	SQ	0.2110
ODA	1-PD	0.0240
	SQ	0.0225
DDA	1-PD	0.0684
	SQ	0.0399

Figure 4. Distribution ratio of benzaldehyde for different solvent and extractant combinations

The first two selected extractants, MBDIPA and MBIPMA are aromatic amines with two amino groups. As shown in Figure 4 they do not give a significant increase in the capacity compared to the pure solvent, although their saturation concentrations are much higher than the amines ODA and DDA. Apparently, the aromatic ring stabilizes the amino groups through the delocalization of the unshared electron pair of the nitrogen over the ortho and para positions of the ring [10]. Additionally, there might be some steric hindrances as well. Consecutively, it becomes much less reactive. On the other hand, aliphatic amines (ODA, DDA) show some increase in the capacity towards benzaldehyde. The difference between DDA and ODA is due to the difference in concentration. Although trends are the same, squalene shows lower capacities in all cases.

It can be concluded that for this application the extractant should be an aliphatic amine, insoluble in water, and, for a feasible process, should be present in high concentrations. Primene® JM-T fulfils these criteria. It is a mixture of isomeric primary aliphatic amines in the C16-22 range, with a highly branched alkyl chain in which the amino nitrogen atom is linked to a tertiary carbon. It is a liquid and not very viscous at room conditions ($13.9 \cdot 10^{-6}$ m^2s^{-1} at 22.8°C [11]), therefore it does not require an additional solvent. That it is indeed a promising extractant can be seen in Figure 5 where distribution ratios are presented as a function of Primene® JM-T concentration. The concentration of amine was varied by dilution with n-hexane and the last point represents distribution ratio obtained with pure amine. It also shows an increase of the distribution ratio with the increase of the amine concentration, which proves the need of high amine concentrations. The obtained experimental data can be satisfactorily explained with a simple equilibrium model presented with equations 1 – 4 and Figure 6.

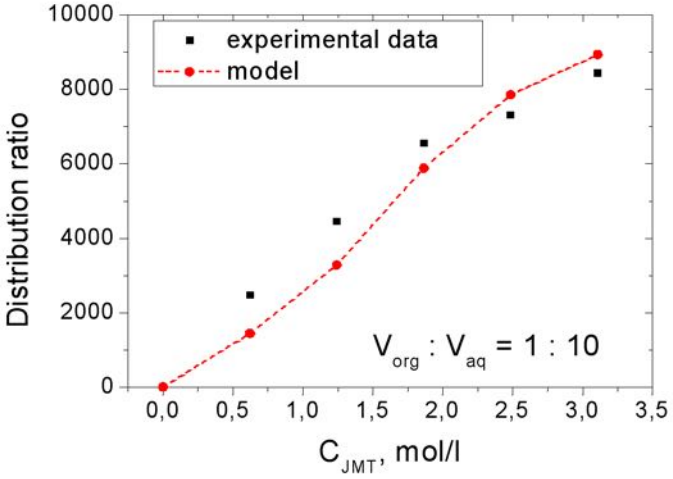


Figure 5. Distribution ratio of benzaldehyde as a function of Primene® JM-T concentration in n-hexane at 25 °C

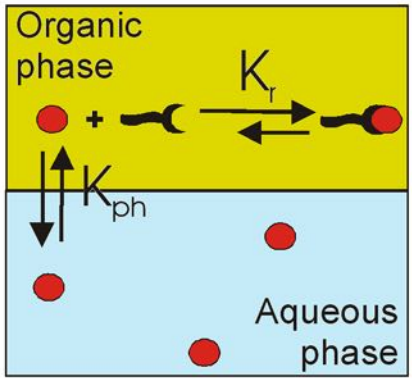


Figure 6. Schematic representation of the reactive liquid-liquid equilibria

The reaction equilibrium constant is defined with eq. 1. C represents the concentration in mol/l. Subscripts Ald and Am stand for aldehyde and amine, respectively, while AldAm stands for the complex formed by aldehyde and amine (Schiff base). Superscripts org and aq indicate organic and aqueous phase, respectively. It was assumed that the concentration of water is constant and therefore does not influence the equilibrium.

$$K_r = \frac{C^{org}_{AldAm}}{C^{org}_{Ald} \cdot C^{org}_{Am}} \qquad (1)$$

The physical partitioning ratio of aldehyde is given by eq. 2.

$$K_{ph} = \frac{C^{org}_{Ald}}{C^{aq}_{Ald}} \qquad (2)$$

The overall equilibrium, as a consequence of physical and reaction equilibria, is expressed with the overall distribution ratio of the aldehyde (eq. 3).

$$D = \frac{C_{Ald}^{org} + C_{AldAm}^{org}}{C_{Ald}^{aq}} \qquad (3)$$

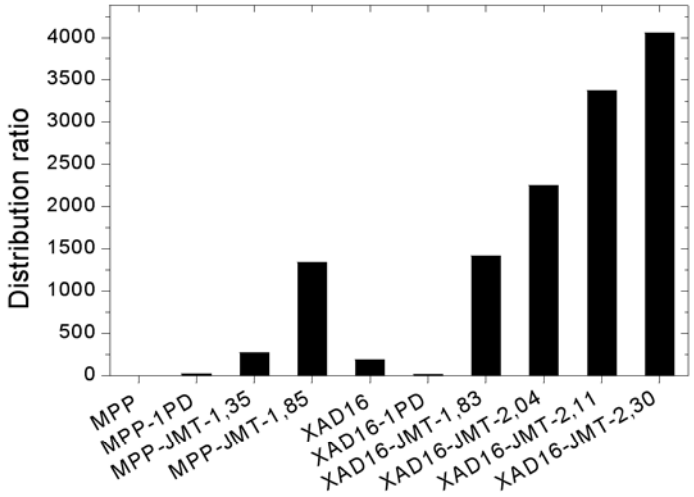
By combining equations 1–3 and applying mass balances for all the species present in the system, the overall equilibrium of aldehyde in the system as a function of the initial concentration of amine in the organic phase for the known initial concentration of aldehyde was obtained (eq. 4).

$$D = K_{ph} \cdot \left[1 + K_r \frac{C_{Am,o}^{org} \cdot \left(1 + \frac{V_{org}}{V_{aq}} D \right)}{1 + \frac{V_{org}}{V_{aq}} D + K_r \cdot K_{ph} \cdot C_{Ald,o}^{aq}} \right] \qquad (4)$$

Eq. 4 was used to fit experimental data. By minimizing the sum of squares of the deviations of the fitting curve from the experimental points, the unknown reaction equilibrium constant was obtained (253±15 $l \cdot mol^{-1}$).

SIR performance

The most promising extractant, Primene® JM-T, was immobilized. Resins impregnated with the amine were compared with non-impregnated resins and resins impregnated with a non-reactive solvent. Results are presented in Figure 7. For comparison of different SIRs, the distribution ratio was defined as the ratio of benzaldehyde concentration in the SIR particle over its concentration in the aqueous phase. Equal volumes of SIR (0.5 ml) were compared. The SIR volume was defined as the total volume of particles.



resin	extractant	concentration mol/l SIR
MPP	-	n.a.
	1-PD	2.02
	JM-T	1.35
	JM-T	1.85
XAD16	-	n.a.
	1-PD	2.51
	JM-T	1.83
	JM-T	2.04
	JM-T	2.11
	JM-T	2.30

Figure 7. Distribution ratios of benzaldehyde for different SIRs at 25 °C

The affinity of unimpregnated MPP towards benzaldehyde is very poor. As can be seen from Figure 7, by adding only a non-reactive solvent, in this case 1-phenyldodecane, the distribution ratio is increased seven times. If, instead, the reactive amine Primene® JM-T is added the capacity improvement is much higher. The distribution ratio can be increased up to 440 times compared to the unimpregnated MPP to a level of 1400 for a fully impregnated particle (3.71 molJMT/kgMPP).

Amberlite XAD16 is a polystyrene-divinylbenzene particle, thus being aromatic it has some affinity towards aromatic compounds like benzaldehyde. Impregnation with a non-reactive solvent, such as 1-phenyldodecane, results in a decrease of its capacity. Possibly all the

adsorption sites are blocked with 1-phenyldodecane and the solvent can not compensate this loss. Simple physical solubility of benzaldehyde in 1-phenyldodecane is not sufficient enough. On the other hand, if XAD16 is impregnated with Primene® JM-T, its capacity is increased significantly up to a distribution ratio of 4000 for a fully loaded particle.
If the MPP and XAD16 with similar loading of extractant are compared, it can be seen that the distribution ratios are similar. Actually, the distribution ratio of XAD16 impregnated with Primene® JM-T is slightly higher than that of MPP. Probably XAD16 is not fully impregnated and some active adsorption sites are left. Since they show affinity towards benzaldehyde they can increase the capacity.
With the increase of the amine loading on the particle the distribution ratio is increased, which is shown for both MPP and XAD16. Therefore, it is desirable to have as much amine inside the particle as possible to increase the distribution ratio.

CONCLUSIONS

Branched aliphatic amines are high capacity extractants for aldehydes and being liquid at room conditions, suitable for application in SIR technology. Immobilized in macroporous particles (SIRs) they still keep their favourable complexation properties resulting in very high distribution ratios.
Addition of an extractant can significantly increase adsorption capacity of otherwise very poor adsorbents, which is shown for the case of MPP particles. Particles with a higher porosity (Amberlite XAD16) have the ability to immobilize a higher amount of extractant, which leads to a higher capacity.

ACKNOWLEDGEMENTS

The authors would like to acknowledge Akzo Nobel, the Netherlands and Rohm and Haas, Europe for providing chemicals used in this research.

REFERENCES

1. J. L. Cortina and A. Warshawsky (1997), Developments in Solid-Liquid Extraction by Solvent Impregnated Resins, Ion Exch. Solvent Extr., Vol.13, J. A.Marinsky and Y. Marcus (Eds.), Dekker, New York, pp. 195-293.
2. C. A. Bowe, D. D. Pooré, R. F. Benson and D. F. Martin (2003), *J. Environ. Sci. Health, Part A,* **A38** (11), 2653-2660.
3. H. Kitazaki, M. Ishimaru, K. Inone, K. Yoshida and S. Nakamura (1996), *Proc. ISEC'96*, Melbourne, Australia, pp. 1667-1672.
4. R.-S. Juang and H.-L. Chang (1995), *Ind. Eng. Chem. Res.*, **34**, 1294-1301.
5. R.-S. Juang and T.-C. Chou (1996), *Sep. Sci. Technol.*, **31** (10), 1409-1425.
6. M. Traving and H.-J. Bart (2002), *Chem. Eng. Technol.*, **25** (10), 997-1003.
7. M. O. Ruiz, J. L. Cabezas, I. Escudero, J. R. Alvarez and J. Coca (2002), *Trans IChemE*, **40** (A), 529-536.
8. A. Kostova and H.-J. Bart (2004), *Proc. IEX 2004*, Churchill College, Cambridge, UK, pp. 251-258.
9. B. Kuzmanović, M. L. van Delden, N. J. M. Kuipers and A. B. de Haan (2003), *J. Chem. Eng. Data*, **48** (5), 1237-1244.
10. T. W. G. Solomons (1998), *Fundamentals of Organic Chemistry*, Third Edition, John Wiley & Sons, New York, pp. 775-776.
11. Primene Amines, Physical Properties, Rohm and Haas *[Internet]*. Available from: <http://www.rohmhaas.co./Primene/physical_prop.html>. *[Accessed 14 October 2004].*



FRACTIONAL REACTIVE EXTRACTION FOR CHIRAL SEPARATION OF AMINO-ALCOHOLS AND AMINES: A PILOT PLANT STUDY

Maartje Steensma, Rob J.G.W. Stoffele, Margriet J. Rouhof, Norbert J.M. Kuipers, André B. de Haan, Gerard Kwant*

University of Twente, Enschede, The Netherlands
* DSM Research, Geleen, The Netherlands

Fractional reactive extraction is studied as a promising chiral separation technique for the commerical production scale. In this work, a previously developed enantioselective extractant system is tested for the separation of phenylglycinol and phenylethylamine in a pilot set-up consisting of two membrane modules. It was shown that more than one equilibrium stage could be realised in the pilot. The role of the solvent/feed ratio and the wash/solvent ratio was studied experimentally and compared with the equilibrium stages model. The model was shown to be qualitatively correct for some of the experimental trends, but to clarify all behaviour in the pilot, the development of a rate-based differential model is recommended.

INTRODUCTION

Chiral amino-alcohols and amines are important chiral intermediates in the pharmaceutical industry. It is desirable to obtain the pure enantiomers by a cost-efficient chiral separation technique [1]. Fractional reactive extraction (fig. 1b) is studied as a promising and flexible alternative to existing chiral separation techniques for the industrial scale. In previous work [2], an azophenolic crown ether was identified as a very promising versatile enantioselective extractant to separate various chiral amines and amino-alcohols. The single-stage physical and chemical equilibria of this extractant system (fig. 1a) were studied experimentally and modelled. Both the capacity and selectivity in the single stage can be controlled by the choice of process parameters such as temperature, pH and concentrations for enantiomers and extractant.

The aim of the present paper is the practical demonstration of the chiral separation of phenylglycinol and phenylethylamine (figure 2a,b) by fractional reactive extraction in a pilot set-up, and comparison of the experimental observations with multistage equilibrium model predictions. Because only a limited amount of the azophenolic crown ether was available, a hollow-fiber membrane module was selected as contactor (figure 2c). This type of experimental set-up has been used by several authors to study fractional reactive extraction [3,4], because a relatively large number of transfer stages can be realised at small scale: HTU ~ 2-10 cm. The focus will be on the influence on the extraction performance of the flow rate ratios (solvent-to-feed and wash-to-solvent) and on the influence of the absolute flow rates.

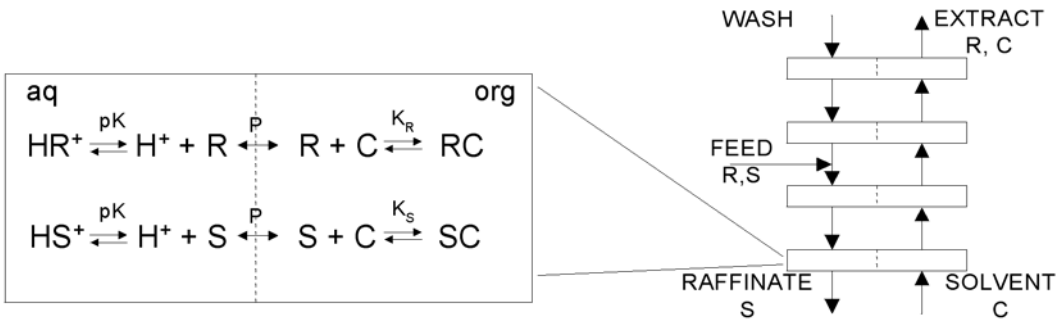


Figure 1: (a) single extraction stage: main equilibria between enantiomers 'R' and 'S' and enantioselective extractant 'C'; (b) fractional extraction scheme, $K_R > K_S$

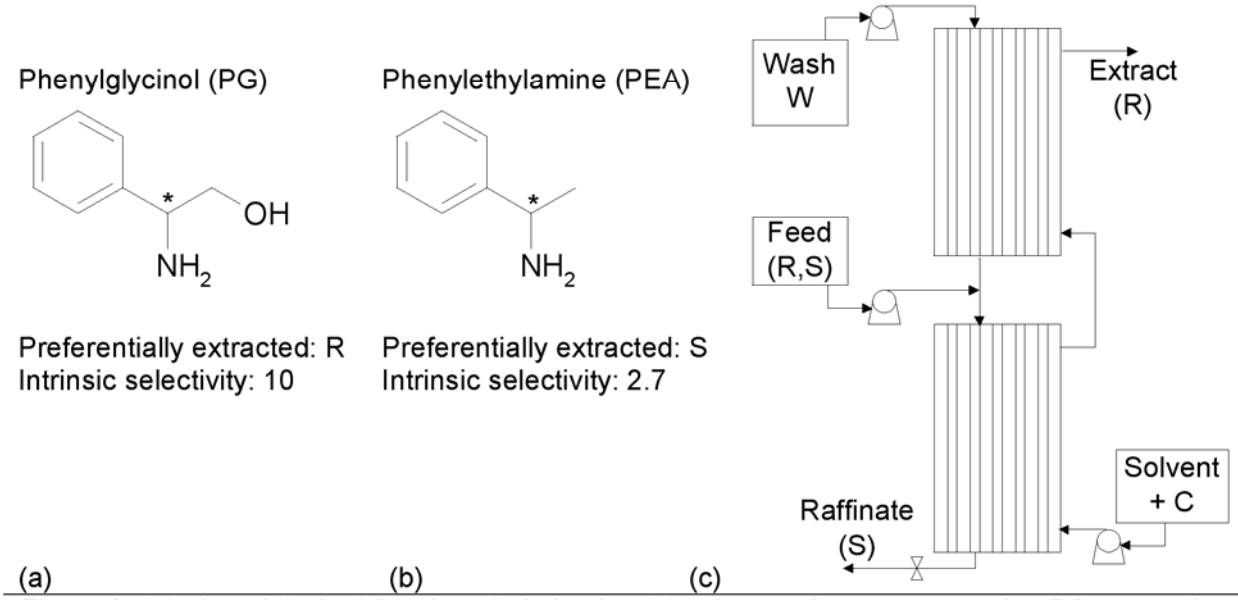


Figure 2: (a) phenylglycinol (b) phenylethylamine (c) scheme of set-up, assuming PG separation.

Multistage equilibrium model

The single equilibrium stage was modelled successfully [2] by solving the relevant chemical and physical equilibria and mass balances simultaneously (fig. 1a). All model parameters are obtained from independent experiments. For a single stage, the capacity is characterised by the distribution ratios D for each enantiomer (equation 1 and 2) and the selectivity α_{op} is defined as the ratio of distribution ratios (eq. 3). The intrinsic selectivity α_{int} is determined by the complexation constants (K_R, K_S) between the crown ether and enantiomers.

$$D_R = \frac{[R]_{org,allforms}}{[R]_{aq,allforms}} = \frac{[R]_{org} + [RC]_{org}}{[R]_{aq} + [HR^+]_{aq}} \quad (1) \qquad D_S = \frac{[S]_{org,allforms}}{[S]_{aq,allforms}} \quad (2) \qquad \alpha_{op} = \frac{D_R}{D_S} \quad (3) \qquad \alpha_{\text{int}} = \frac{K_R}{K_S} \quad (4)$$

A multistage equilibrium model was defined based on this single-stage description by assuming that the exiting streams of each stage are in equilibrium. The multistage model was solved with the program gPROMS (Process Systems Enterprise, UK). The two liquid phases flow countercurrently through the column (fig. 1b). At the feed stage, the feed is mixed with the aqueous stream. The function of the wash section is to remove the co-extracted undesired

component from the extract stream. The extraction performance is characterised by the yield (eq. 5) and the product purity as enantiomeric excess e.e. (eq. 6). Similar equations as (5) and (6) are defined for each enantiomer in the raffinate and extract stream.

$$yield_{R,EXTRACT} = \frac{total \quad R \quad extract}{total \quad R \quad feed} \quad (5) \qquad e.e._R = \frac{[R]-[S]}{[R]+[S]} \quad (6)$$

EXPERIMENTAL METHOD

The enantioselective extractant was manufactured by Syncom BV (Groningen, The Netherlands) in a custom synthesis according to Naemura *et al* [5]. R- and S-phenylglycinol were obtained from Fluka (Buchs, Switzerland). Rac-phenylethylamine was obtained from Sigma-Aldrich (Milwaukee, WI, USA) and toluene was obtained from Merck (Darmstadt, Germany). A scheme of the membrane pilot is given in figure 2c. The two membrane modules were obtained from SolSep BV (Apeldoorn, The Netherlands). Each module has 15 cm effective membrane length, 16 mm inner diameter and contains 150 polypropylene fibers of 0.33/0.63 mm ID/OD (Membrana, Wuppertal, Germany), that are potted with a proprietary solvent-resistant potting. The porosity of the membrane material was determined at 0.78, the (calculated) tortuosity is 1.90 and the material is wetted by the toluene phase. To prevent toluene leakage to the aqueous phase, a pressure difference of 100 mbar between the aqueous and organic side is maintained by adjusting a valve in the raffinate exit. The modules are jacketed to enable temperature control with a thermostat bath (Julabo F-32). The feed and solvent streams are delivered by a Stepdos 08 S pump (KNF FLODOS AG, Sursee, Switzerland) and the wash stream by a Watson Marlow 101U/R pump (Watson Marlow Limited, Cornwall, UK). All experiments were carried out with the aqueous phase in the fibers and the toluene phase at the shell side. The feed concentration of the racemic mixture was 2 mM (unbuffered) in MilliQ water (Millipore, Billerica, USA), the extractant concentration was 3 mM in toluene and the wash stream was milliQ water. In each experiment, the module is flushed during 2-5 times the residence time of the solvent flow at the shell side. After that, samples are taken from the aqueous raffinate stream and organic extract stream. The organic phase sample is extracted with dilute acid to obtain an aqueous sample for analysis. All samples are analysed by chiral HPLC for amine/amino alcohol enantiomer concentration. Experiments in which the mass balance did not close within 10% were discarded. The HPLC set-up consisted of a Varian 2510 HPLC pump, a Daicel Crownpak (+) chiral column in a column oven, a derivatization coil and a Jasco FP-2020 *plus* fluorescence detector operated at 325 nm excitation and 465 nm emission. Post-column derivatisation with o-phtalic aldehyde/mercaptoethanol reagent is carried out according to [6].

RESULTS

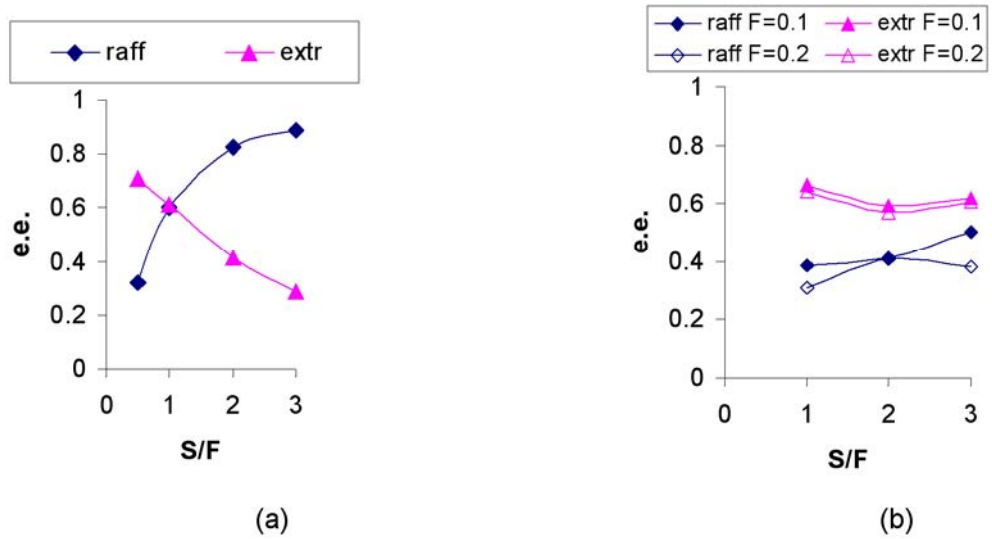
Estimation of number of stages

To characterise the mass transfer in the membrane module, the physical extraction of phenylethylamine from water to toluene was studied. The experimental results were interpreted in terms of NTU/HTU [7], because a 'number of stages' is required as input in the simulations. It was concluded that HTU is about 7.5 cm, so 2 stages can be realised in one membrane module. This value is comparable to the results in literature [3,7].

Reactive extraction: solvent-to-feed ratio

The influence of the solvent-to-feed (S/F) ratio for reactive extraction of phenylglycinol was studied in one membrane module, corresponding with one extraction section. The predicted and

experimental effect on enantiomeric excess is presented in figure 3, the effect on the yield is shown in figure 4. According to the simulation (fig. 3a and 4a), increasing the S/F ratio results in a higher yield in the extract but a lower purity. Because this is an equilibrium simulation, changing the feed flow and solvent flow rate by the same factor while keeping S/F constant does not affect the result. Simulations for separation of phenylethylamine (not shown) show similar trends, but the lower selectivity in one stage compared to PG results in a lower enantiomeric excess.



(a) (b)

Figure 3: Influence of S/F ratio on enantiomeric excess in one module (2 stages) (a) simulation pH 8.6 (b) experimental result, feed flow rates F=0.1 and 0.2 ml/min. Phenylglycinol system.

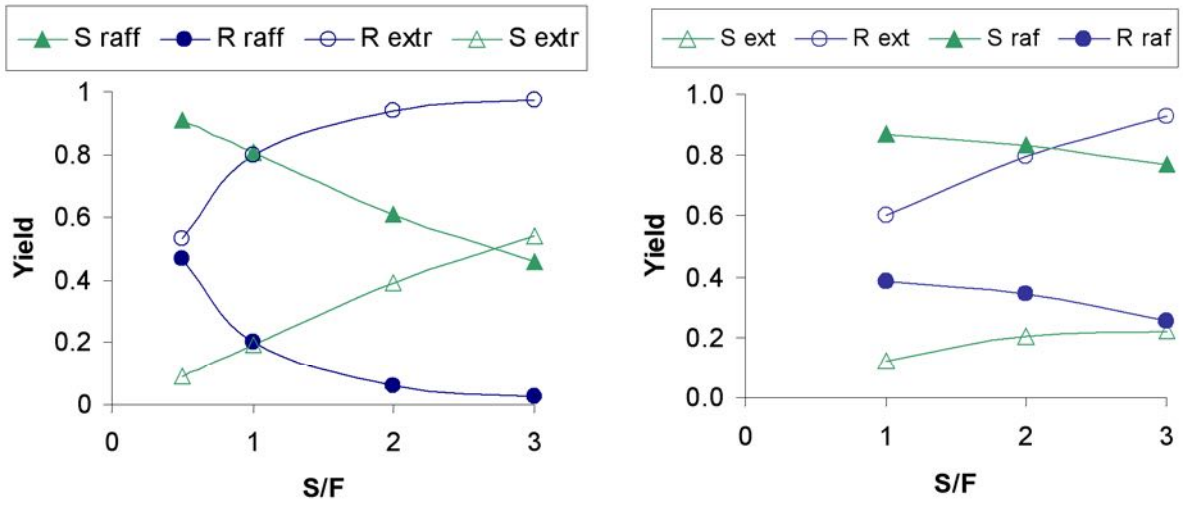


Figure 4: Influence of S/F ratio on yield in one module (2 stages) (a) simulation, pH 8.6 (b) experimental results, data for F=0.1 ml/min. Phenylglycinol system.

First of all, it was observed that the experimental enantioselectivity (expressed as ratio of distribution ratios, equation 1-3) is larger than the single-stage operational enantioselectivity for this system: under suitable circumstances α_{op} = 12 vs. α_{op} = 7 in the single stage. This proves

that indeed more than one equilibrium stage is realised in the module. The result for the yield (fig. 4b) is qualitatively correct: with increasing S/F, the yield in the extract increases and the yield in the raffinate decreases for both enantiomers. Furthermore, it can be seen that the effect of S/F on the obtained enantiomeric excess (e.e.) is rather small. To reach the point in which the e.e. values are the same in both exiting streams, a higher S/F ratio seems to be required. In other words, the solvent flow is not used effectively. It can also be seen in fig. 3b that a change in flow rates at constant S/F has some influence on the obtained results: both e.e. values are slightly lower at higher flow rates. Both these observations cannot be explained from the multistage equilibrium model. It is expected that the residence time in the extractor and the mass transfer and/or reaction rate should be taken into account.

Fractional reactive extraction: influence of wash-to-solvent ratio

Two-module experiments were carried out to identify the influence of the W/S ratio on the chiral separation. To our knowledge, this influence was not studied before, although a number of authors estimate the optimal W/S ratio beforehand based on the extraction factors for each enantiomer [8,9]. The simulated and experimental effect on enantiomeric excess is presented in figure 5, the effect on the yield is presented in figure 6. It can be seen that according to the simulation, W/S has a pronounced effect on yield and product purity: an increase in W/S results in a more pure extract, but a lower yield in the extract. Yield and e.e. in both streams are coupled by the mass balance.

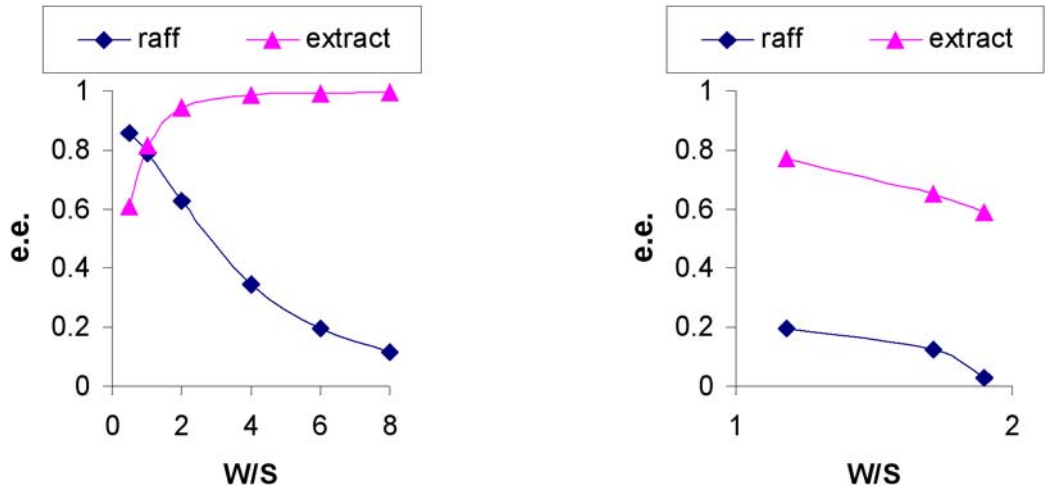


Figure 5: Influence of W/S ratio on e.e. for phenylglycinol separation. S=0.6 ml/min, F = 0.2 ml/min, T = 25 °C, pH 8.6 (a) simulation, 2+2 stages (b) experimental data.

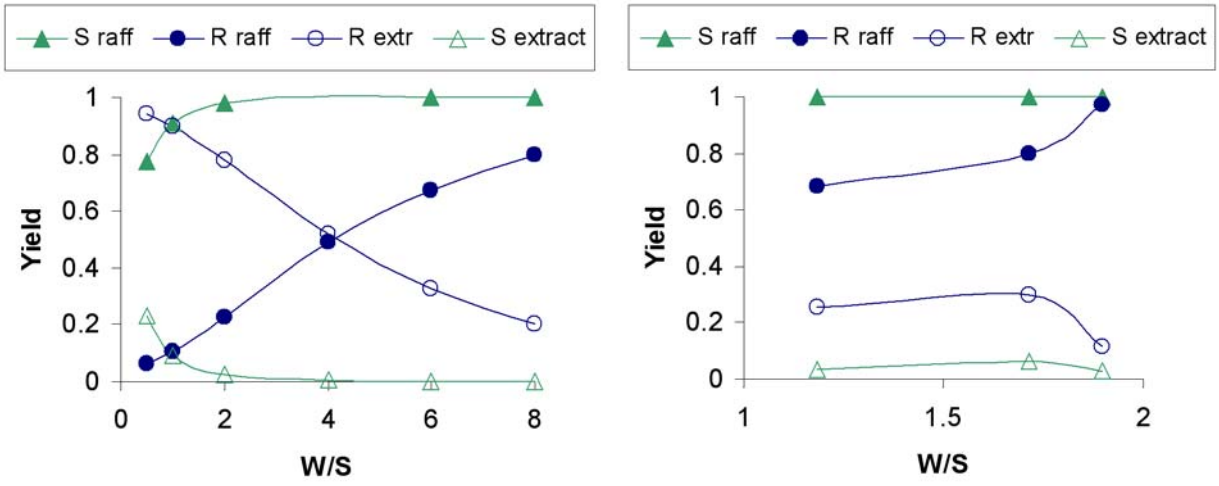


Figure 6: Influence of W/S ratio on yield for phenylglcyinol separation. S=0.6 ml/min, F = 0.2 ml/min, T = 25 °C, pH 8.6 (a) simulation, 2+2 stages (b) experimental data.

Again, the experimental and simulated results for the yield are qualitatively similar, although the pattern found in the experimental data is expected at higher W/S ratio. The influence of W on the e.e. is clearly visible (compare also fig. 3b and 5b). However, the pattern observed in the e.e. in the product streams (fig. 5b) is not expected; the e.e. of the extract is expected to increase further at increasing W/S ratio instead of decrease. It may be that the higher aqueous flow rate and thus shorter residence time at higher W/S is detrimental to the separation, but such an effect cannot be described by the equilibrium model. Secondly, the effect in e.e. may be partly caused by the measuring error: because the yield in the extract is low, the concentrations of both phenylglycinol enantiomers are low as well. Furthermore, it was observed that a data point obtained at the same W/S ratio but at higher overall flow rates did not correspond at all with the data in figure 5b and 6b (not shown). This also indicates that the magnitude of the flow rates influences the separation. Data points at lower W/S ratio may confirm the patterns found in figure 5b and 6b, but measurements at low W/S could not be carried out because of the limited operating range of the wash flow pump. Finally, an excess of enantiomer R was measured in the aqueous stream exiting the wash section. This excess of R is indeed predicted by the model at a large W/S ratio.

Conclusion

Fractional reactive extraction has been demonstrated in a pilot set-up. More than one equilibrium stage could be realised in each module. The W/S and S/F ratio have a large influence on the yield and purity that can be obtained. The multistage-equilibrium model can explain some of the experimental results, but not quantitatively. Therefore, it is recommended to develop a differential rate-based model that gives a more realistic description of the reactive extraction process in a membrane module. In this way, the time-dependent processes can be taken into account, and the use of 'number of theoretical stages' is circumvented.

ACKNOWLEDGEMENT

This project is financially supported by the Institute of Mechanics, Processes and Control Twente (IMPACT) and by DSM Research. The authors would like to thank Bert Vos for technical

assistance and Wytze Meindersma and Antoine Kemperman for advice regarding the membrane modules.

REFERENCES

1. R.A. Sheldon (1993), *Chirotechnology*, Industrial synthesis of optically active compounds. Marcel Dekker Inc.
2. M. Steensma, N.J.M. Kuipers, A.B. de Haan, G. Kwant (2004), submitted
3. H.B. Ding, P.W. Carr, E.W. Cussler (1992), *A.I.Ch.E.J.*, **38(10)**, 1493-1498
4. W.H. Pirkle, W.E. Bowen (1994), *Tetrahedron Asymmetry*, **5(5)**, 773-776
5. K. Naemura, K. Nishioka, K. Ogasahara, Y. Nishikawa, K. Hirose, Y. Tobe (1998), Tetrahedron*: Asymmetry*, **9**, 563-574
6. A.L.L. Duchateau, M.G. Hillemans, I. Hindrikx (1997), *Enantiomer*, **2**, 61-67
7. W.S. Ho, K.K. Sirkar (1992), in Membrane Handbook, New York: Van Nostrand Reinold, 727-763
8. T. Takeuchi, R. Horikawa, T. Tanimura, Y. Kabasawa (1990), *Sep. Sci. Tech.* **25(7&8)**, 941-951
9. H. Nishizawa, K. Tahara, A. Hayashida, Y. Abe (1993), *Anal. Sci.*, **9**, 611-615



UPTAKE OF SILVER BY NEW DEVELOPED STABLE ALGINATE MICROCAPSULES ENCLOSING CYANEX 302

Hitoshi Mimura, Mohammad Outokesh, Yuichi Niibori, Kouichi Tanaka

Dept. of Quantum Science & Energy Engineering, Tohoku University, Sendai, Japan

Uptake properties of stable alginate microcapsules enclosing bis (2, 4, 4-trimethylpentyl) monothiophosphinic acid (Cyanex 302) extractant for Ag^+ ions were examined using batch method. The stable microcapsules were prepared by coating of fresh microcapsules with mono or 4 double layer chitosan or polyethyleneimine. The microcapsules exhibited relatively high uptake ability in a wide range of pH 1 - 6, and in the presence of Na^+ ranging up to 1 M. Up to a definite initial Ag^+ concentration (e.g. 875 ppm for uncoated microcapsules), equilibrium Ag^+ concentration is almost zero. These results suggest that the microcapsules are effective for fully decontamination of effluents polluted by Ag^+ ions.

INTRODUCTION

In the past few years, many attempts have been made to develop a stationary solvent extraction process as simple as ion exchange column by immobilizing extractants into solid matrices. Among many proposed methods, microcapsules, due to suitable physical form and lesser loss of solvent, are more prominent for the extraction - decontamination purposes [1], [2]. Alginates, due to having high acid resistance, simple capsulation procedure and ion exchange properties are among the most attractive biopolymers for the microencapsulation of extractant. In fact, alginate microcapsules may adsorb the metal ions by both matrix and extractant [3].

The aim of this study is to elucidate the uptake properties of new stable alginate microcapsules in order to apply these adsorbents to the decontamination of heavy metal ions.

EXPERIMENTAL

Preparation procedure

Bis(2,4,4-trimethylpenthyl) monothiophosphinic acid (Cyanex 302) with 86% assay was supplied by Cytech Canada Inc., and used without further purification.

For simplicity "MCs" is used hereinafter as an abbreviation for "microcapsules". The MCs were prepared as follows. Cyanex 302 (1.2 g) extractant was fully dispersed in 100 cm^3 of 2.4 % sodium alginate solution (Type 300-400 cP, Wako Pure Chemical Industries, Ltd.). The kneaded sol was injected into 0.05 or 0.1 M Ca $(NO_3)_2$ solutions using a 0.4 mm medical needle to form MCs. After 6.5 hr-stirring, the MCs were then filtrated, washed and dried at 40°C for 14 h. Final MCs were abbreviated as ***Uncoated***.

The coated MCs were prepared as follows. ***Uncoated*** MCs before drying were transferred to either 3 g/L chitosan (*M*w= 17,000) containing 0.3 M Ca^{2+} or 5 g/L PEI solutions, both buffered at pH= 5.6, then gently stirred for 4 - 12 h. These MCs after drying were abbreviated as ***Chit-1*** and ***PEI-1***, respectively.

The 1-double layer extra coating was achieved by transferring ***Chit-1*** before drying to 1 g/L sodium alginate solution (Type 500-600 cP), then to 1.5 g/L chitosan (*M*w=17,000) containing 0.05 M Ca $(NO_3)_2$, in succession. The 4-double layer coated MCs are abbreviated as ***Chit-4D***.

Uptake of Ag^+ ions

In order to clarify distribution of incorporated Ag^+ ion into MCs, between the matrix and extractant phases ,the cross-section of the specimens saturated with Ag^+ ions , was analyzed by electron probe microanalyses (EPMA).

The uptake of Ag^+ ions was examined by batch method. An aqueous solution containing 10 ppm Ag^+ (7cm^3) was contacted with 70 mg of different MCs at 25°C, and Ag^+ concentration in the supernatant was measured by atomic absorption spectrometry (AAS). The effects of following parameters on the uptake of Ag^+ were examined:

(1) Kinetics of Ag^+ uptake up to 48 h.
(2) Effect of HNO_3 concentration from 10^{-4} to 10 M and effect of equilibrium pH,
(3) Selectivity in the presence of Na^+ ions up to 3 M,
(4) Adsorption isotherms by using Ag^+ solution from 10 to 5,000 ppm in the presence of 10^{-3} M HNO_3.

The uptake percentage (*R*, %) and distribution coefficient (K_d, cm^3/g) are defined as:

$$R = \frac{C_O - C_t}{C_O} \times 100\% \quad (1)$$

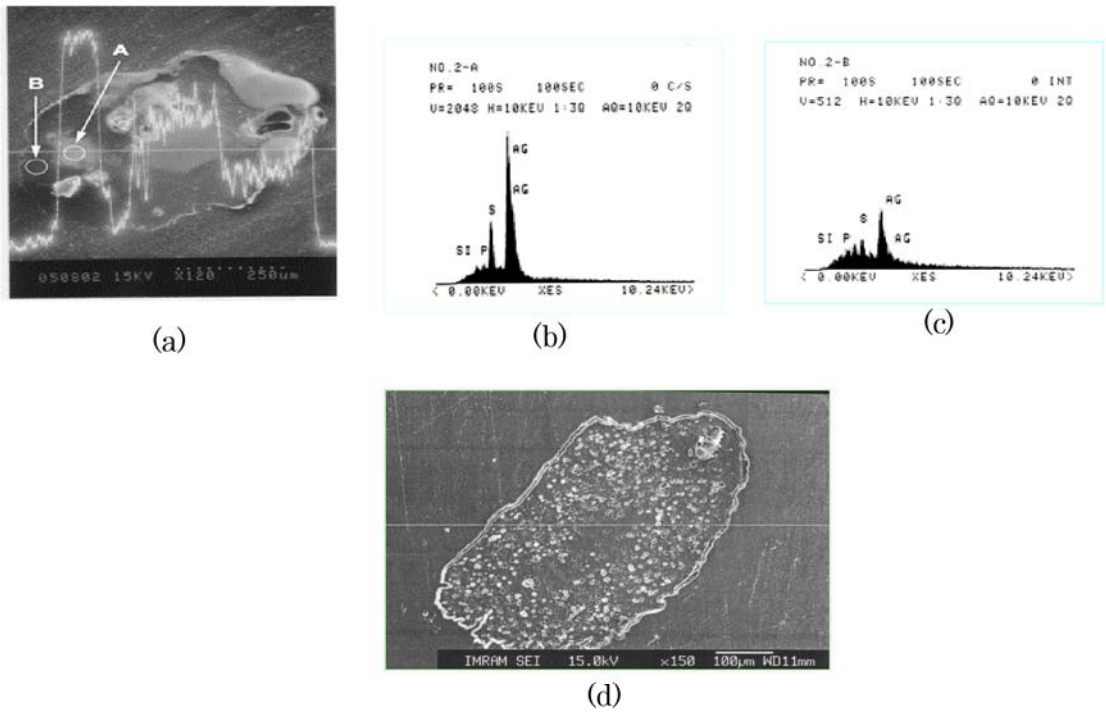
$$K_d = \frac{C_0 - C_f}{C_f} \times \frac{V}{m} \quad (\text{cm}^3/\text{g}) \qquad (2)$$

where C_0 and C_t ,and C_f are concentration (ppm) of Ag^+ at initial, at time *t*, and at equilibrium, respectively ; *m* (g) the weight of microcapsule; *V* (cm^3) the volume of Ag^+ solution.

RESULTS AND DISCUSSIONS

Distribution of Ag^+ ions in MCs

Figures 1 (a)-(c) show the cross sectional SEM images of ***Uncoated*** MCs and energy dispersive spectra (EDS) for both phases of extractant (A) and matrix (B). According to EDS spectra, the Ag^+ ions were mainly incorporated into the extractant phase (A). The microcapsule in Fig. 1 (a) with only two droplets was specially prepared for the EDS study. Normal MCs contained numerous micro-droplets (Fig. 1(d)).



(a) (b) (c)

(d)

Figure 1. (a)Cross sectional SEM image, (b), (c) EDS spectra of extractant (A) and matrix (B) phases respectively, (d) Cross sectional SEM image of normal MCs showing microdroplets.

Uptake rate

Kinetics of Ag^+ uptake in short and long periods is shown in Figs. 2(a) and (b). In short time, at higher Ag^+ concentration (*e.g.*, 750 ppm), ***Uncoated*** showed faster kinetic than the coated MCs. At lower concentrations (*e.g.*, 10 ppm), only Cyanex 302 droplets near to the surface of MCs are participating in the Ag^+ uptake. Hence the effective diffusion length is considerably small in this instance, and the uptake rate is equal for both coated and

Uncoated MCs (Fig 2. (a)). In contrast with coated MCs, on longer time (Fig. 2(b))., ***Uncoated*** MCs, due to instability , loses its Cyanex 302 content, resulting the decrease in *R* value.

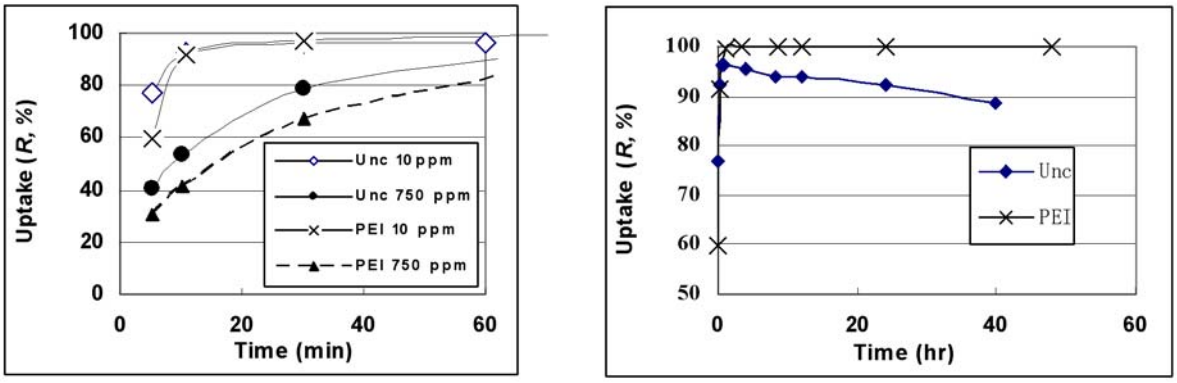
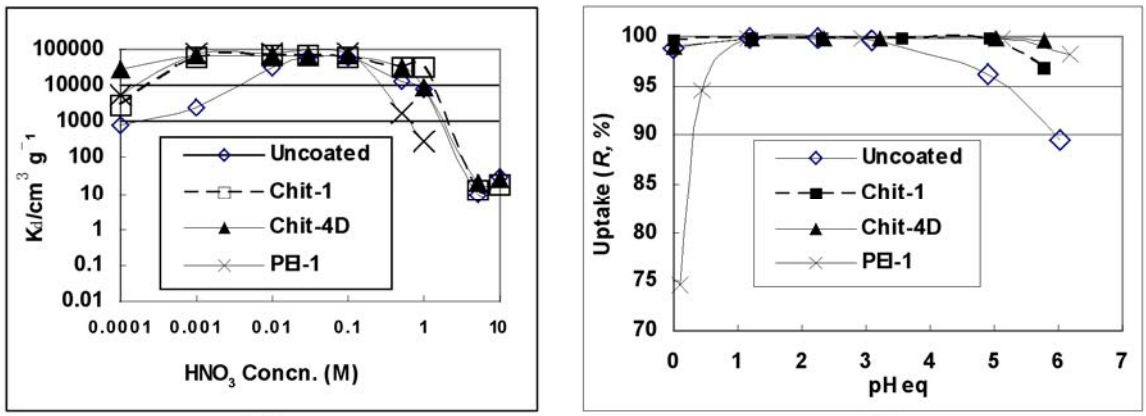


Figure 2. Kinetic of Ag^+ uptake in short time (a) and long term (b), Unc: Uncoated, PEI: PEI-1.

Effect of HNO_3 concentration and equilibrium pH

Figure 3(a) shows the uptake behavior of MCs at different acid concentrations from 10^{-4} to 10 M (up to 1 M for ***PEI-1***). Further, the effect of equilibrium pH on uptake percentage is exhibited in Fig. 3 (b). In mild concentration of HNO_3 ranging10^{-3} to 0.1 M, the K_d value for MCs was almost constant, while it lowered remarkably at higher or lower concentrations.

Quantitative uptake of Ag^+ ions at pH 1 - 5 is arisen from the high selectivity of Cyanex 302 which shows approximately 100% extraction for Ag^+ ions at pHs higher than zero [4]. At higher HNO_3 concentrations above 0.5 M, all the MCs became unstable and tended to loss their extractant contents. In addition, the extractability of Ag^+ by Cyanex 302 was lowered in the presence of HNO_3 higher than 1.5 M. The lowering of uptake ability at pHs >5.5 or [HNO_3] < 10^{-4} M may be due to either swelling of alginate matrices and loss of content, or formation of unstable Ag^+-Cyanex 302 complexes.



(a) (b)

Figure 3. Effects of HNO_3 concentration (a), and equilibrium pH (b) on uptake of Ag^+ ions.

Effect of Na^+ concentration

The uptake of Ag^+ ions by MCs in the presence of Na^+ is shown in Fig. 4. From preliminary

tests, the average relative error was found to be within10 %; when the Ag^+ ion (1-10 ppm) in the presence of 3 M Na^+ ions was measured by using AAS by dilution methods. As evident from Fig. 4, all MCs could selectively adsorb at least 90% of 10 ppm Ag^+ ions in the presence of 3M Na^+ ions.

Effect of Ag^+ concentration

The most significant feature of metal ions uptake by MCs is appeared when the initial

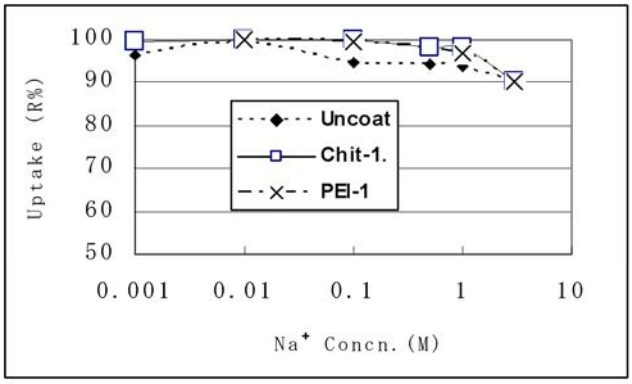


Figure 4. Selectivity of the microcapsules for uptake of Ag^+ ions in presence of Na^+ ions

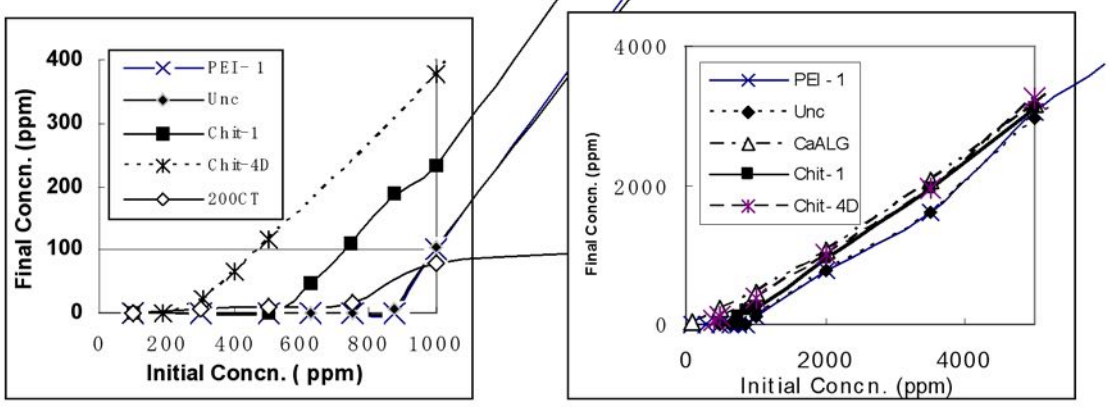
concentration of Ag^+ ions increases from 10 ppm to 1,000 ppm (Fig. 5(a)). Here the uptake by a strongly acidic ion exchanger (200CT) is also shown for comparison. According to Fig. 5 (a). In the above initial concentration range, the final concentration of Ag^+ was almost zero up to a definite initial concentrations which termed "breakpoint". The existence of breakpoints may be attributed to a relatively high affinity of Cyanex 302 for Ag^+ ions [4]. In fact, EPMA analyses of MCs indicated that before reaching breakpoints the Ag^+ ions were preferentially extracted with Cyanex 302 and only minor fraction adsorbed on alginate matrix. Thus, the content of Cyanex 302 can be estimated from the determination of breakpoints. As is evident from Fig. 5 (a), one can drive the following order of extractant content: ***PEI-1 ~ Uncoated > Chit-1 >> Chit-4D***. Coating process itself caused some physical stresses on MCs, which led to extractant losses and the variation of its content in different MCs. The high uptake ability of MCs below 1,000 ppm is practically important because it allows fully decontamination of industrial effluents from Ag^+ ions.

Above breakpoints (*i.e.*, >875 ppm in Fig. 5(a)), the polymeric matrices (calcium alginate) greatly contribute to the uptake of total Ag^+ ions so that the final Ag^+ concentration for all MCs is close to that of calcium alginate (Fig. 5 (b)).

As for the adsorption isotherm, the curves showed a convex profile and the Q_{eq} value tended to approach an asymptotic value, indicating possibly the uptake of Ag^+ ions follows a Langmuir adsorption equation (Fig. 7(a)). As shown in Fig. 7(b), the Langmuir plots give straight lines at higher concentrations, from which the maximum capacity for ***PEI-1***, ***Uncoated*** and calcium alginate was roughly estimated to be 4.4, 4.1 and 3.9mmol/g, respectively.

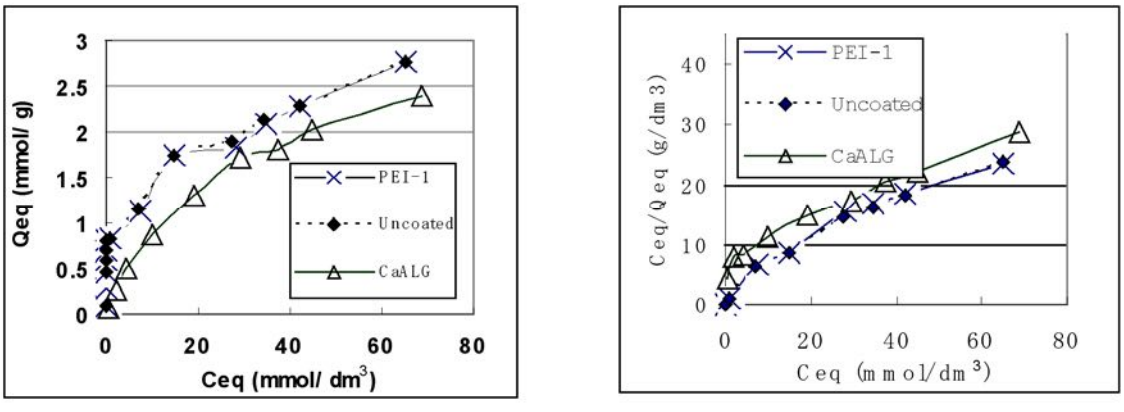
CONCLUSIONS

The MCs exhibited almost constant and relatively high uptake ability in a wide range of pH 1-6 and in the presence of Na^+ ranging up to 1 M. EDS analyses indicated the main active component in MCs was Cyanex 302 extractant. The uptake characteristics of the MCs were classified into two categories. In the first one, there are some properties such as selectivity or pH dependency of uptake, which are in fact reflecting the primary features of the enclosed extractant of Cyanex 302. The second one includes practical properties such as excellent concentrating ability of metal ions from dilute solutions and relatively fast kinetics of MCs, which are to an extent created due to specific uptake mechanisms in MCs. Thus the microencapsulating techniques are found to be effective for the selective removal of heavy metal ions, and the MCs with various shapes such as granule, fiber and film are applicable to the wide fields of environmental remediation.



(a) (b)

Figure 5. Equilibrium Ag^+ concentration vs. initial concentration, Unc: Uncoated.



(a) (b)

Figure 7. (a) Adsorption isotherm and (b) Langmuir plots for the uptake of Ag^+ by MCs.

ACKNOWLEDGEMENTS

The authors express appreciation to Mr. Y. Sato Mr. T. Kamaya and K. Sakata (Tohoku University) for their helpful discussion of SEM, EPMA and ICP analyses.

REFERENCES

1. H. Watarai and S. Hatakeyama (1991), *Anal. Sci.*, **7**, 487-489.
2. E. Kamio, M. Matsumoto and K. Kondo (2002), *J. Chem. Eng. Japan,* **35**(2), 178-185.
3. H. Mimura, H. Ohta, K. Akiba, Y. Onodera (2001), *J. Radioanal. Nucl. Chem.,* **247**(2) , 375-379.
4. K. C. Sole, T. L. Ferguson and J.B. Hiskey (1994), *Solv. Ext. Ion Exch.,**12***(5), 1033-1050.



INVESTIGATION OF METHYL ACETATE PRODUCTION BY REACTIVE EXTRACTION

Christian Rohde, Rolf Marr, Matthäus Siebenhofer* and Stephan Schwinghammer

Department of Chemical Engineering and Environmental Technology, University of Technology, Graz, Austria
*VTU-Engineering GmbH, Grambach/Graz, Austria

Methyl acetate is produced through catalytic esterification of acetic acid with methanol. Catalytic acceleration is induced by sulfuric acid or ion exchange resins respectively. Acceptable product yield is obtained by reactive distillation. Separation and isolation of methyl acetate has to overcome two azeotropes (methyl acetate – water and methyl acetate - methanol).

Scope of this project has been the investigation of methyl acetate formation by reactive extraction and distillative separation of methyl acetate from the solvent.

From reactive extraction an increased yield of product is expected due to immediate separation of the ester from the reaction mixture. Investigation focused on the solvent n-nonane which suffices the needs of appropriate solubility for methyl acetate and excellent vapor/liquid equilibrium data. On account of the selectivity of n-nonane for methyl acetate the formation of aceotropes during distillative separation can be avoided.

Experimental investigation of reactive extraction confirmed both an improved yield of methyl acetate as well as high product quality of 99.3% purity.

INTRODUCTION

In the last decade increasing interest was paid to hybrid processes both in industry and research, especially to reactive distillation and reactive extraction i.e. reported in [1]. Simultaneous chemical reaction and separation of products of hybrid processes is advantageous over the process performance of separate unit operations. As a result of simultaneous operation capital cost and cost of operation are considerably lowered. Application is possible when one of the reaction products has a lower boiling point than the residual substances of a mixture or a higher solubility in the extracting agent. In fact a high selectivity of the solvent for a specific reaction product is needed to decrease its concentration in the reaction mixture, therefore increasing the rate of reaction. As a consequence conversion and rate of reaction are increased.

Esterification of acetic acid with methanol with the homogenous catalyst sulfuric acid suffices the

above mentioned boundaries. Therefore this reversible reaction (equation 1) has intensively been studied and reported in [2]:

$$CH_3OH + CH_3COOH \leftrightarrow CH_3COOCH_3 + H_2O \quad (1)$$

The multicomponent system has an azeotrope of methyl acetate with water (5 weight% water, boiling point = 329.25 K) and an azeotrope of methyl acetate with methanol (18 weight% methanol, boiling point = 327.05 K) (e.g. [3]). Since the boiling point of methyl acetate (330.15 K) is very close to the boiling points of the azeotropes a complex plant design and rigorous process control is required to overcome the two constant boiling mixtures. Target of the present project was to work out an alternative process to reactive distillation design. Reactive extraction was applied to simplify the separation task.

The esterification reaction (equation 1) was chosen as a test system to verify reactive extraction. The program was split into two steps. In the first step methyl acetate was extracted selectively by n-nonane and, in a second step the extract was regenerated in a lab scale distillation column.

EXPERIMENTAL PROCEDURE

Reactive Extraction

Experiments were carried out in a reactor (Heraeus company, type UV-RS-2) in lab scale (equipment: reaction vessel with a volume of 850 ml, diameter 0.1 m, magnetic agitator) equipped with a temperature sensor and a pH-value sensor and two sampling sockets. The reaction vessel was fed with equivalent amounts (2.5 mole) of methanol and acetic acid plus 500 ml of solvent and then mixed at constant temperature. Within each experiment several samples were withdrawn from the reaction vessel mixture for chemical analysis. During sampling the magnetic agitator was switched off and as soon as the two phases were separated a sample was withdrawn from each phase.

Each experiment was started by injecting a specific amount of sulfuric acid into the reaction mixture. Over a period of 180 minutes samples of the reaction mixture and the solvent phase were collected. During operation the temperature of the reaction mixture was held constant at 299±2 K. The samples were analyzed with a gas chromatograph, Hewlett-Packard 5960, equipped with a J&W Scientific DBVRX column. The temperature was held constant at 353 K for 5 min, ramped to 383 at a rate of 5 K/min and then ramped to 523K at a rate of 40 K/min. This temperature was held constant for 10 min. The temperature of the injection port was adjusted at 523 K and the temperature of the FID was kept at 573 K.

Solvent Regeneration

The extract phase was separated by distillation in a batch distillation column in lab scale (reboiler volume: 500 ml, height of column: 320 mm, column diameter: 30 mm). The column was equipped with a temperature sensor at the bottom and the top. A heating jacket of 150 Watt electrical power provided the reboiler with heat. By means of a data logger (Fluke company, type Hydra series II) the temperatures were displayed online on a screen. Distillation was stopped when the temperature on the top of the column started to rise above the boiling point temperature of methyl acetate. The chemical composition of the bottom product and the top product was analyzed by gas chromatography according to the above described guideline.

RESULTS AND DISCUSSION

Every reactive extraction experiment was carried out in two steps by admixing pure solvent to the reaction mixture twice. In the consecutive distillation process the solute methyl acetate was separated from the solvent.

Reactive Extraction

Sulfuric acid was used as a catalyst. An amount of 8 g/l sulfuric acid was fed to the mixture of acetic acid, methanol and n-nonane (Figure 1).

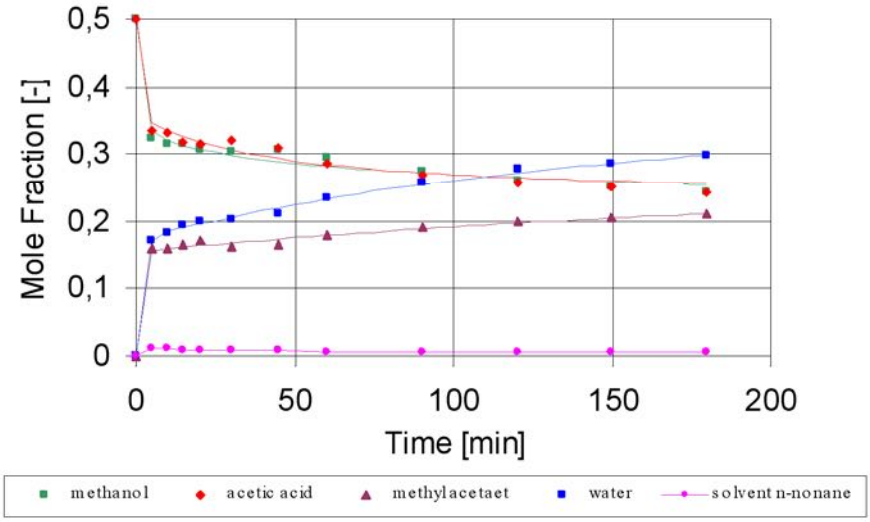


Figure 1. Concentration of the components in the reaction mixture for equimolar start of acetic acid and methanol; concentrations sulfuric acid concentration: 8 g/l, solvent: 500 ml n-nonane.

Figure 1 shows the equimolar decrease of the reactants. Since methyl acetate is partly extracted with n-nonane the amount of water and methyl acetate differ. Due to its low solubility the amount of n-nonane in the reaction mixture is negligible. Figure 2 indicates that n-nonane is a suitable solvent for extracting methyl acetate with sufficient selectivity.

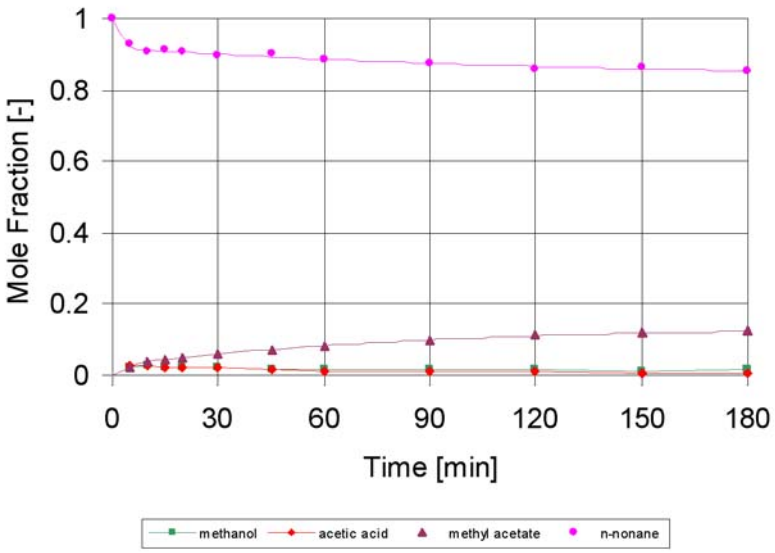


Figure 2. Concentration of the components in the solvent phase.

The load capacity of the solvent n-nonane for methyl acetate in equilibrium with the reaction mixture is limited although methyl acetate is completely miscible with n-alcanes as reported in [4]. Due to the excellent solubility of methyl acetate in the reaction mixture the distribution coefficient for methyl acetate of K = 0.61 at a temperature of 299 K was determined experimentally.

In a second extraction step the solvent phase was replaced. Compared with Figure 1 Figure 3 confirms the increase in rate of conversion.

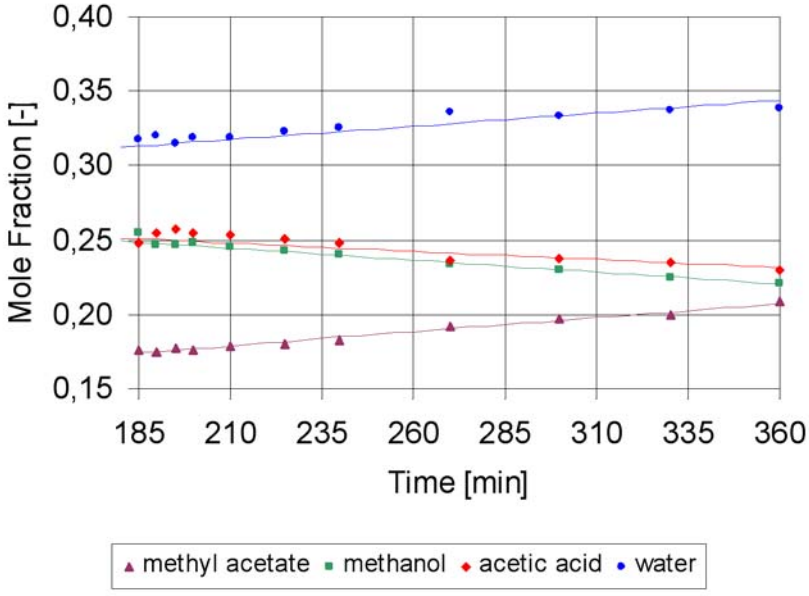


Figure 3: Composition of the reaction mixture during the second extraction step
sulfuric acid concentration: 8 g/l, solvent: n-nonane.

Conversion of methanol and acetic acid was 0.55 after the first step and 0.70 after the second step of extraction.

Solvent regeneration

The solvent mixture was separated by batch distillation in lab scale. According to the solvent composition azeotrope formation was not observed. The temperature of the reboiler was kept constant at the boiling point of methyl acetate. Methyl acetate quality yielded in 99.3 weight%.

SUMMARY

Target of the present project was to verify whether the performance of methyl acetate production from acetic acid and methanol can be improved by combining esterification with liquid/liquid extraction. The results of investigation can be summarized as follows:

- Methyl acetate is extracted from the reaction mixture with n-nonane with high selectivity.
- Rate of conversion of the esterification reaction is improved by reactive extraction.
- The solute methyl acetate can be separated from the solvent n-nonane by distillation.
- Methyl acetate quality of is 99.3 weight% can be obtained.
- Distillative separation of methyl acetate from n-nonane is neither affected by the methanol/methyl acetate aceotrope nor by the methanol/water aceotrope.
- Recycling of the solvent n-nonane after distillation is possible without further upgrading.

ABREVIATIONS AND SYMBOLS USED

AcOH	acetic acid
MeOAc	methyl acetate
MeOH	methanol
T_{bp}	boiling point [K]

REFERENCES

1. V.H Agreda, L. R. Partin and W. H. Heise (1990), *Chem. Eng. Prog.*, **Feb. 1990**, 40-46.
2. L. Bonnaillie, X. M. Meyer and A. M. Wilhelm (2001), *3rd European Congress of Chemical Engineering, ECCE*, Nuremberg, Germany.
4. L. M. Casas, B. Orge, C. Diaz and J. Tojo (2004), *J. Chem. Thermodynamics*, **36**, 237–243.
3. Z. P. Xu and K. T. Chuang (1997), Ind. *Eng. Chem. Res.,* **36**, 2866-2870.



THE APPLICATION OF POLYMER LIQUID MEMBRANES TO THE EXTRACTION OF COBALT(II) FROM AQUEOUS SOLUTIONS

Alexandra H. Blitz-Raith[*], Rohani Paimin[*] and Spas D. Kolev[**]

[*]School of Molecular Sciences, Victoria University of Technology, P.O Box 14428, MCMC, Melbourne, 8001, Victoria, Australia
[**] School of Chemistry, The University of Melbourne, Victoria 3010, Australia

ABSTRACT

Poly(vinylchloride) (PVC)-based polymer liquid membranes incorporating Aliquat 336 (tricaprylylmethyl ammonium) chloride as the liquid ion-exchanger were used to extract Co(II) from aqueous solutions containing different concentrations of HCl or LiCl. The concentration of Aliquat 336 chloride in the polymer membranes was varied between 10 and 50% (m/m) while the concentration of the chloride ion in the feed solution was varied between 1.0 and 7.0 mol L^{-1}. It was found that both the rate and degree of extraction increased with the concentrations of Aliquat 336 chloride in the membrane and the Cl^- in the solution. The Co(II) extracted into the Aliquat 336/PVC membranes was rapidly and completely back-extracted into deionized water.

INTRODUCTION

Current industrial solvent extraction processes (e.g., hydrometallurgy, industrial and domestic wastewater treatment) are of considerable environmental concern because of the use of large amounts of volatile solvents, which then have to be disposed of. In addition, the energy consumption of these processes is substantial and expensive synthetic extractants, which often cannot be fully recovered, are used.

Extraction processes based on liquid membranes require minimal amounts of solvents and therefore have become an attractive alternative to conventional solvent extraction methods. A more recently introduced type of liquid membranes, called polymer liquid membranes, have shown promising results in the extraction of gold(III) [1,2], palladium(II) [3], cadmium(II) and copper(II) [4,5] from hydrochloric acid solutions. These membranes are usually casted from tetrahydrofuran solutions of poly(vinylchloride) (PVC) and a suitable liquid extractant such as Aliquat 336 chloride [1-4] or di-ethylhexyl phosphoric acid [5]. Polymer liquid membranes do not require an additional solid support since they exhibit sufficient mechanical strength. They offer longer lifetime than conventional supported liquid membranes as a result of more efficient immobilization of the liquid extractant within the membrane structure.

Cobalt and nickel are often present together in ores. Their separation based on solvent extraction suffers from the serious drawbacks mentioned above. This paper reports on the extraction of Co(II) from aqueous solutions containing HCl or LiCl into PVC/Aliquat 336 membranes and its back-extraction into deionized water. This study was conducted with view of exploring possibilities for using this type of polymer liquid membranes for the separation of Co(II) and Ni(II) from their chloride aqueous solutions.

EXPERIMENTAL

Reagents

Aliquat 336 chloride (Fluka) was obtained as a mixture of quaternary ammonium chlorides and was used as received. High molecular mass PVC (Fluka Selectaphore) was used in the preparation of the polymer liquid membranes. Tetrahydrofuran, THF, (BDH) was HPLC grade. It was further purified by passing it through an activated alumina column to remove the stabilizer and peroxides. Analytical grade hydrochloric acid, lithium chloride and cobalt(II) chloride were purchased from BDH. Standard Co(II) solutions, used in the membrane extraction experiments, were prepared in HCl (1.0 – 7.0 mol L^{-1}) or LiCl (1.00 – 7.00 mol L^{-1}). Calibration standards of Co(II) were prepared by appropriate dilutions of a 1000 mg L^{-1} spectroscopic Co(II) standard (BDH Spectrosol). All aqueous solutions were prepared in deionized water (18 MΩ cm, Barnstead, USA).

Membrane Preparation

Membranes containing 10, 20, 30, 40 and 50% Aliquat 336 chloride (m/m) were prepared following the procedure described earlier [1]. This procedure involved the dissolving of exact amounts of Aliquat 336 chloride and PVC with a total mass of 800 mg in 5 to 10 ml THF. The homogenous solution obtained was then poured into a glass ring on a flat glass plate. The THF was allowed to evaporate slowly over 12 h to yield a colorless and flexible membrane. The membrane was then peeled from the glass plate, cut into 4 sections and used in the membrane extraction and back-extraction experiments. Membranes with concentration of Aliquat 336 chloride higher than 50% were not used because in previous studies [1] such membranes were found to be soft and sticky and thus unsuitable for membrane extraction.

Membrane Extraction and Back-Extraction Studies

The membrane extraction studies were conducted in a beaker immersed in a water bath thermostated at 25°C. Each extraction experiment involved the use of a 100 ml solution of Co(II) in the presence of HCl or LiCl and a membrane cut in 4 segments of approximately equal size. The solution was stirred mechanically with a magnetic stirring bar at a constant

rate throughout the experiment. The depletion of Co(II) in the solution was monitored by taking 1.0 ml samples at preselected times. The Co(II) concentration was determined by atomic absorption spectrometry, AAS, (Varian Model Spectra AA 400). Solution removed as a result of each sampling was replaced with an equal volume of fresh metal solution.

In each back-extraction experiment a 40% (m/m) Aliquat 336 chloride membrane containing Co(II), extracted from 100 ml solution of 100 mg L^{-1} Co(II) in 7.0 M HCl or 7.0 M LiCl, was stripped in 100 ml deionized water under stirring. The concentration of Co(II) in the stripping solutions was monitored at regular time intervals by AAS.

RESULTS AND DISCUSSION

The Effect of Membrane Composition on Co(II) Extraction

The effect of the membrane composition on the extraction of Co(II) from 7.0 M HCl is shown in Fig.1. Similarly to the solvent extraction of Co(II) from hydrochloric acid solutions by Aliquat 336 chloride dissolved in chloroform [6], the extracted amount of Co(II) into the PVC/Aliquat 336 chloride membranes increased with the membrane Aliquat 336 chloride concentration. The substantially higher degree of extraction at 50% Aliquat 336 chloride composition is consistent with previous studies [1,3,4] and indicates a possible structural change in the membrane occurring at Aliquat 336 chloride concentrations higher than 40%. This conclusion was supported by the fact that the 50% membranes were considerably softer than membranes with lower concentration of extractant which resulted in insufficient mechanical stability. For this reason the optimal Aliquat 336 chloride concentration was selected to be 40% and all further studies were conducted at this concentration.

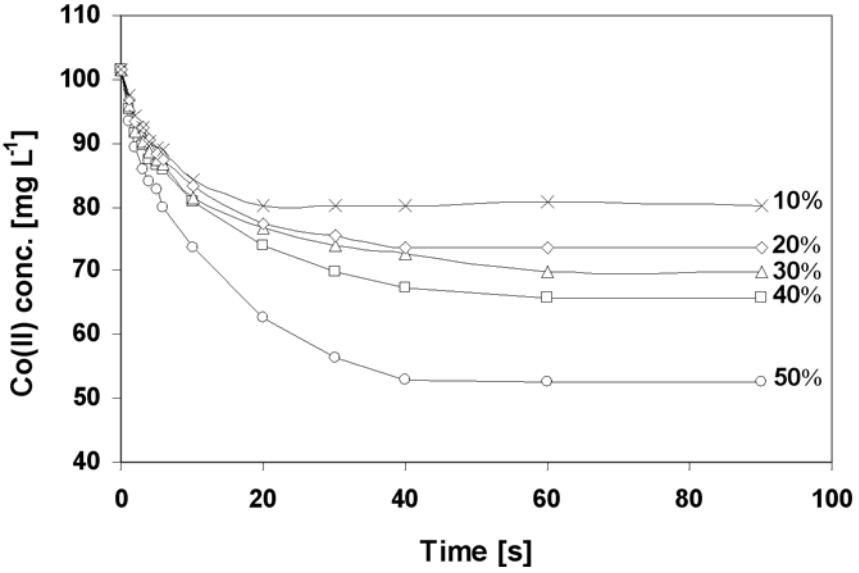


Figure 1: Aqueous Co(II) concentration vs. time of contact for membranes containing 10, 20, 30, 40 and 50% Aliquat 336 chloride (feed solution composition: 100 mg L^{-1} Co(II) in 7.0 M HCl).

The Effect of Solution Composition on Co(II) Extraction

The effect of the chloride ion concentration in the feed solution on the extraction of Co(II) into 40% Aliquat 336 chloride membranes was studied in the presence of HCl and LiCl. The amount of Co(II) extracted was found to increase with increasing hydrochloric acid concentration (Fig. 2) similarly to solvent extraction of Co(II) by Aliquat 336 dissolved in chloroform [6]. The PVC/Aliquat 336 membranes were found to be stable in concentrated hydrochloric acid solutions. However, membrane extraction experiments at hydrochloric acid concentrations higher than 7.0 mol L^{-1} were not conducted because of the health and safety

issues involved in using concentrated HCl in industrial processes. Extraction experiments from LiCl solutions produced extraction curves (Fig. 2) very similar to those obtained with hydrochloric acid. This finding suggested an identical extraction mechanism in both cases.

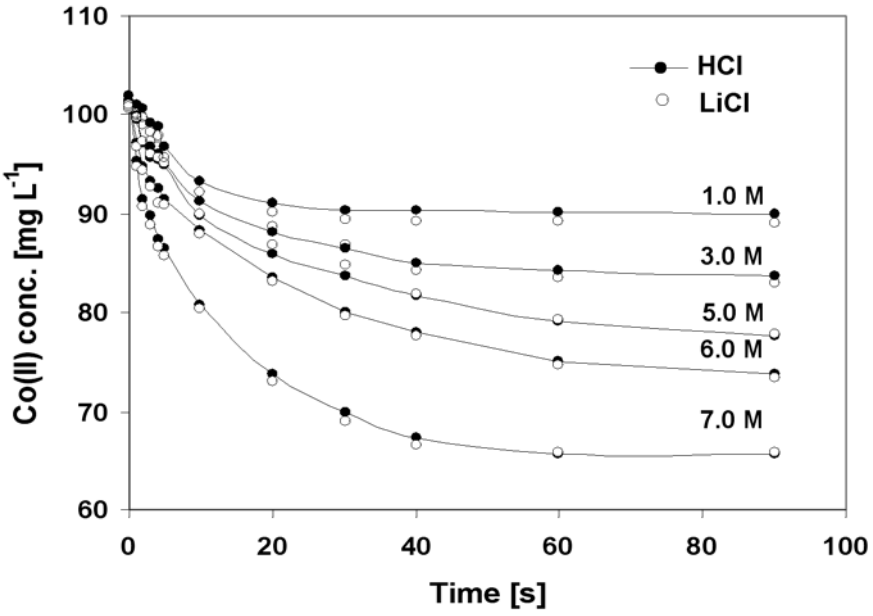


Figure 2: Aqueous Co(II) concentration vs. time of contact for membranes containing 40% Aliquat 336 chloride and feed solutions containing 100 mg L^{-1} Co(II) in 1.0, 3.0, 5.0, 6.0 and 7.0 M HCl or LiCl.

Back-Extraction of Co(II)

Fig. 3 shows the back-extraction curves of 40% Aliquat 336 chloride membranes in deionized water. Co(II) extraction into these membranes was conducted from 100 mg L^{-1} Co(II) in 7.0 M HCl or 7.0 M LiCl solutions. These results indicate that deionized water is capable of rapid and complete stripping of the Co(II) content of PVC/Aliquat 336 chloride membranes.

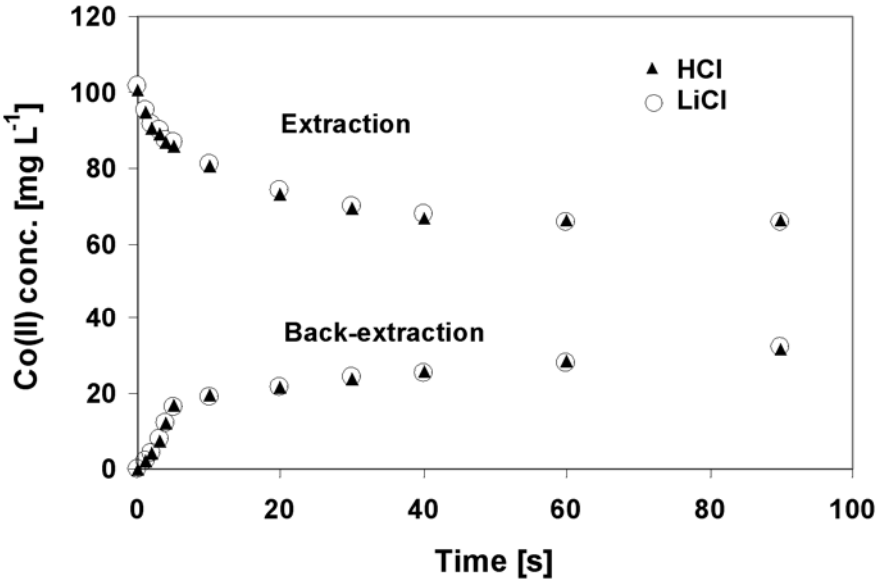


Figure 3: Aqueous Co(II) concentration vs. time of contact during extraction and back-extraction involving membranes containing 40% Aliquat 336 chloride (feed solutions: 100 mg L^{-1} Co(II) in 7.0 M HCl or 7.0 M LiCl; stripping solution: deionized water).

Stability of the PVC/Aliquat 336 Membranes

The PVC/Aliquat 336 membranes were found to retain their extraction properties unchanged after 100 cycles of Co(II) extraction and back-extraction.

CONCLUSIONS

Cobalt(II) was extracted rapidly into PVC/Aliquat 336 chloride membranes from aqueous solutions of high chloride concentrations. The back-extraction of Co(II) in deionized water was found to be fast and complete irrespective of whether HCl or LiCl were present in the feed solution.

On the basis of the results obtained it can be concluded that the PVC/Aliquat 336 chloride membranes offer an attractive alternative to solvent extraction in the separation of Co(II) from its aqueous chloride solutions.

Further investigations are currently being conducted to explore the possibility for separating Co(II) and Ni(II) from their aqueous solutions using PVC/Aliquat 336 chloride membranes and to elucidate the membrane extraction and back-extraction mechanism of these two metal ions.

REFERENCES

1. G Agriropoulos, R W Cattrall, I C Hamilton, S D Kolev and R Paimin (1998), *J. Mem. Sci.*, **138**, 279-285.

2. S D Kolev, G Agriropoulos, R W Cattrall, R Paimin and I C Hamilton (1997), *J. Mem. Sci.*, **137**, 261-269.

3. S D Kolev, R W Cattrall, R Paimin, I D Potter and Y Sakai (2000), *Anal. Chim. Acta*, **413**, 241-246.

4. L Wang, R Paimin, R W Cattrall, W Shen, S D Kolev (2000), *J. Mem. Sci.*, **176**, 105-111.

5. Y Baba, K Hoaki, J M Perera, G W Stevens, T J Cardwell, R W Cattrall and S D Kolev (2001), *Proc. 6th World Congress Chem. Eng.*, *Melbourne*, *Australia*, CD.

6. R Paimin, R W Cattrall (1983), *Aust. J. Chem.*, **36**, 1017-1020.

Cloud Point Extraction of Furosemide by Polyethoxylated Alkyl Ethers

Yan Huang, Wei Qin*,[1]Xiaoping Huo, Youyuan Dai

State Key Laboratory of Chemical Engineering, Department of Chemical Engineering, Tsinghua University, Beijing 100084

A cloud point extraction process (CPE) using the nonionic surfactant polyoxyethylene--10-lauryl ether has been selected to extract and preconcentrate Furosemide in dilute solutions. The CPE process is facilitated at the ambient temperature 20℃ by the reduction of the cloud point temperature of the surfactant with sodium sulfate. The influence of settling time, centrifuge time and centrifuge speed on the extraction efficiency and the behavior of the phase separated was studied. The dependence of extraction efficiency on the concentration of sodium sulfate and the surfactant was also studied. An extraction efficiency higher than 90% with a preconcentration factor larger than 38 was achieved in this work.

INTRODUCTION

Furosemide is classified as one of diuretics, a wide class of drugs eliciting an increase production of urine, which may be misused in sports to achieve acute weight loss or mask the use of other doping agents. A massive, as well as unnecessary, use of Furosemide can lead to dangerous side effects. Furosemide is associated with the reduction of total blood volume, with the risk of hypotension and collapse, and the increase of blood sugar level and blood viscosity, with the risk of thrombosis[1].

Certain surfactant solution exhibits phase separation upon temperature or salinity alteration. Upon phase separation, desired hydrophobic solutes molecules bound to the micelles can be extracted to the coacervate phase whose volume is almost two orders of magnitude lower than that of the original solution, meanwhile, an enormous increase of the concentration of the solutes can be achieved in the coacervate phase. This alternative extraction method is termed as cloud point extraction (CPE)[2].

Historically, CPE has been used in the extraction, preconcentration and analysis of metal chelates and hydrophobic proteins. Watanabe and Tanaka used CPE to concentrate zinc ion in 1978 first with PONPE 7.5, a polyoxyethylene alkyl ether surfactant[3]. In 1981, Brodier used Triton X-114 as the surfactant in the CPE process in which membrane proteins were extracted[4]. Recently, CPE has been extended to the extraction of environmental organics[5], while there is no report of the CPE application in the preconcentration of diuretics according to our survey.

*Corresponding author, E-mail: qinwei@tsinghua.edu.cn.
Fax: +86 10 62770304.
Telephone: +86 10 62773017

The incentive of this work is to investigate the CPE behavior of Furosemide using polyoxyethylene-10- -lauryl ether under different conditions, and the dependence of settling time/centrifuge time, centrifuge speed, salt concentration and surfactant concentration on the CPE. The suitable condition was suggested.

EXPERIMENTAL PROCEDURES

The solutions of surfactant with or without salts were heated to a temperature higher than their cloud point and became turbid. The cloud point of the solutions was determined by observation of the disappearance of the turbidity of the solutions. The solutions were contained in 30 mL screw-capped glass tubes. All cloud points given were the average of triple measurements.

Furosemide solution was prepared by adding weighted Furosemide (about 5 mg) to 0.5 L double distilled water. The solution of $C_{12}E_{10}$ in distilled water (100 $g \cdot L^{-1}$) and sodium sulfate in distilled water (250 $g \cdot L^{-1}$) were also prepared. These solutions were mixed in appropriate amount. and the final solution was insured at 25 mL. Before cloud point extraction. the solutions were in a refrigerator at 2 ℃ for 8 hours.

The cloud point extraction was carried out in 50 mL centrifuge tubes. For centrifuging process, the solutions were poured into the tubes, then were heated in the water bath for 12 minutes at 25 ℃, and then the solutions were centrifuged at 4000 $r \cdot min^{-1}$ in a centrifuger (LD5-2A, Jingli instrument, Beijing). For settling process, the solutions were placed in the water bath at 25 ℃ for 190 hours.

The coacervate phase was transferred to 4 mL screw amber vial and diluted with redistilled water. 0.025mL sample of the diluted coacervate phase was syringed into HPLC. The concentration of the diluted coacervate phase was the average of HPLC results of triplicate samples.

REAGENTS AND APPARATUS

The commercial nonionic surfactant, polyoxyethylene-10-lauryl ether ($C_{12}E_{10}$) was obtained from Sigma. $C_{12}E_{10}$ is a mixture of primary alcohol ethoxylates with an average ethylene oxide number of 10. Reagent grade of Furosemide was purchased from Sigma. The salts, sodium sulfate, sodium chloride, sodium formate, magnesium nitrate and lithium chloride were reagent grade and acquired from Yili Fine Chemicals, Beijing. Water used in all the experiments was deioned and double distilled.

The Furosemide concentrations in the coacervate phase were determined by a HP1050 HPLC with a UV-vis detector and a HP 3395 integrator. The column was Agilent C_{18} column (250×4.6 mm) with an EasyGuard HPLC guard column (Dikma). The eluent was a mixture of acetonitrile (40 vol %) and water (60 vol %). The absorption of the Furosemide was detected at the wavelength of 275nm.

A water bath (Donglian instrument, Harbin) was used to determine the cloud points and heat the solutions before cloud point extraction.

The extraction efficiency (*E*):

$$E = \frac{C_{\mathrm{F,coa}} \times V_{\mathrm{coa}}}{C_{\mathrm{F,ori}} \times V_{\mathrm{i}}}$$

Where $C_{F,\,coa}$ ($mg \cdot L^{-1}$) is the Furosemide concentration of the coacervate phase, V_{coa} (L) is the

volume of the coacervate phase, $C_{F,i}$ (mg·L^{-1}) is the initial Furosemide concentration of the solution before phase separation and V_{ori} (L) is the initial volume of the original solution.
The preconcentration factor:

$$f_C = \frac{C_{F,coa}}{C_{F,i}}$$

RESULTS AND DISCUSSIONS

Cloud Point of $C_{12}E_{10}$

Effects of salts on the cloud point (CP) of $C_{12}E_{10}$ were studied with the concentration of $C_{12}E_{10}$ at 1 wt%. As shown in Fig. 1, Na_2SO_4 had the most dramatic effect among the salts in this work, so Na_2SO_4 was selected to facilitate the manipulation of the cloud point extraction. The introduction of salts may either decrease or increase the cloud point of the surfactant[6]. This alteration varies considerably in magnitude depending on the kind of the electrolyte and its concentration. According to Materna[7] and Schott[8], the influence can be categorized into effects of cations and of anions. Although most cations elevate the cloud point of the solution because of the chelation, the presents of some cations (Na^+, K^+, Cs^+, Rb^+ and NH_4^+) depress the cloud point of the surfactant due to the decrease of the water activity with cations, which favors the dehydration of the polyoxyethylene chain. The decrease of cloud point with the introduction of the "structure forming" anions such as SO_4^{2-} and Cl^- is attributed to the enhancement of the structure of water in bulk solution. This weakens the formation of hydrogen bond between water molecules and the polyoxyethylene chains, which makes the dehydration of the polyoxyethylene chains easier.

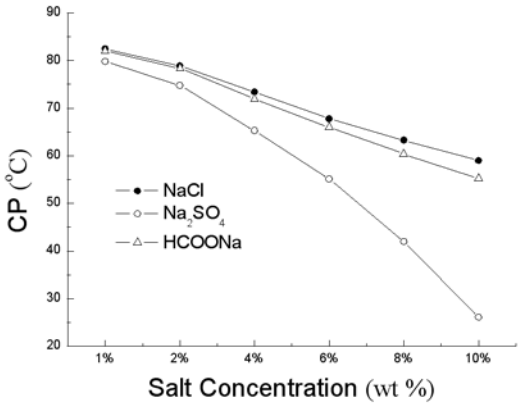


Figure 1-Effects of salts on CP of $C_{12}E_{10}$

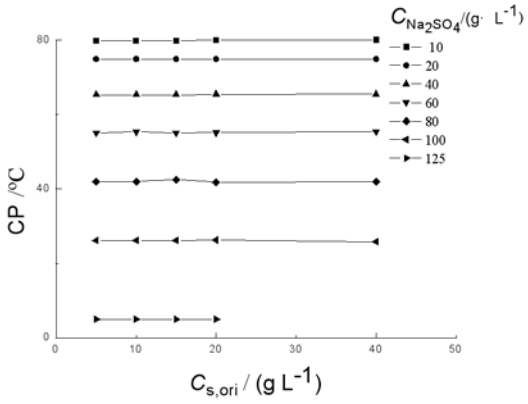


Figure 2-Effects of Na_2SO_4 and $C_{12}E_{10}$ concentration on CP

The effect of Na_2SO_4 concentration and $C_{12}E_{10}$ concentration on the cloud point of the solution is shown in Fig. 2. There was no apparent change of the cloud point of the solution observed with the changing $C_{12}E_{10}$ concentration in the range of 5~40 g·L^{-1}, while the cloud point of the solution decreased with the Na_2SO_4 concentration. The cloud point of the solution was 5 ℃ at the Na_2SO_4 concentration was 125 g·L^{-1}.

Effect of settling time

The extraction efficiency of a CPE system (125 g·L^{-1} Na_2SO_4, 8 g·L^{-1} $C_{12}E_{10}$, 0.2 ~ 5 mg·L^{-1} Furosemide at 25 ℃) is shown in Fig. 3. The extraction efficiency increased up to a constant value at sufficient time (>140 h), and showed a random value for the interface region of coacervate and aqueous phase was not clear in the first 72 hours of settling and it was very difficult to get the sample of the coacervate phase.

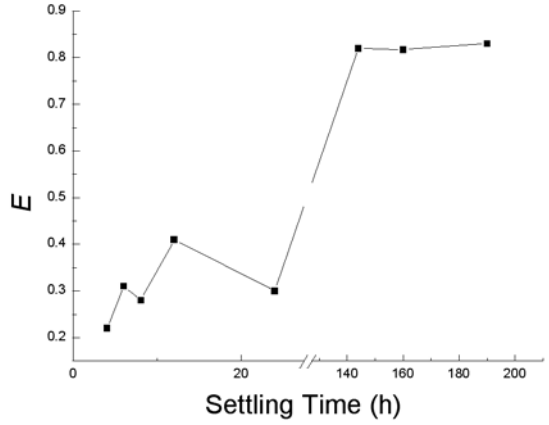


Figure 3-Effects of settling time on the extraction efficiency

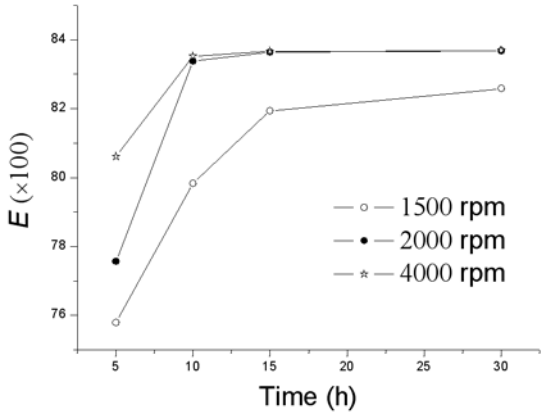


Figure 4-Effects of centrifuge time on the extraction efficiency (C_{C12E10}=8 g·L^{-1}, C_{Na2SO4}=125 g·L^{-1})

Effect of centrifuge time and centrifuge speed

The centrifuge process was carried out in three different centrifuge speeds: 1500 r·min^{-1}, 2000 r·min^{-1} and 4000 r·min^{-1}. The extraction efficiencies in different centrifuge time of these triple centrifuge processes are illustrated in Fig. 4. The results showed that for these three centrifuge speeds, the phase separation almost finished and the extraction efficiency achieved their highest value at about 15 minutes. It is also observed that higher centrifuge speed may result in higher extraction efficiency.

Comparing the centrifuge method to setting, both two methods gave the similar recoveries, but the centrifuged method shortened the time of phase separation (see Table 1).

Table 1 Extraction efficiencies of different process (C_{C12E10}=8 g·L^{-1}, C_{Na2SO4}=125 g·L^{-1})

	$E(\times 100)$
settling (160 h)	81.70
settling(190 h)	83.12
Centrifuge (1500 r·min^{-1}, 15min)	81.94
Centrifuge (2000 r·min^{-1}, 15min)	83.64
Centrifuge (4000 r·min^{-1}, 15min)	83.67

Table 2 Extraction efficiencies of different Na_2SO_4 concentration (C_{C12E10}=8 g·L^{-1})

C_{Na2SO4} /(g·L^{-1})	E×100	V_{coa}	f_C
110	83.00	0.3905	53.14
122	83.67	0.3711	56.36
130	83.16	0.3614	57.53
138	83.39	0.3487	59.79
146	83.66	0.3296	62.69
162	83.39	0.3207	66.59

Effect of Na_2SO_4 concentration

The influence of Na_2SO_4 concentration is shown in Table 2, and extraction efficiency of Furosemide almost kept constant for various Na_2SO_4 concentrations, while the coacervate phase volume decreased due to its water content lost, therefore, the preconcentration factor of the process increased with increasing the Na_2SO_4 concentration.

Effect of $C_{12}E_{10}$ concentration

As shown in Fig. 5 and Table 3, the concentration of surfactant effects on both the extraction efficiency and the preconcentration factor, the volume of the coacervate phase is in linear with the initial $C_{12}E_{10}$ concentration, and f_C and E showed decreasing and increasing tendency with the increase of initial $C_{12}E_{10}$ concentration, respectively. This result is the same as that of the solvent extraction method.

The preconcentration factor achieved the value of 165.30 at $C_{12}E_{10}$ concentration of 2 g·L^{-1} and Na_2SO_4 concentration of 125 g·L^{-1} An extraction efficiency as high as 90.45% can be gained with a cloud point extraction system at $C_{12}E_{10}$ concentration of 12 g·L^{-1} and Na_2SO_4

concentration of 125 g·L^{-1}.

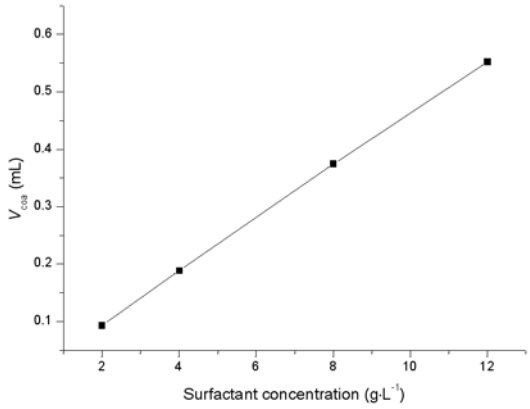


Figure 5-Effects of $C_{12}E_{10}$ concentration on coacervate phase volume and water content (C_{Na2SO4}=125 g·L-1)

Table 3 Extraction efficiencies of different $C_{12}E_{10}$ concentration (C_{Na2SO4}=125 g·L^{-1})

C_{C12E10} /(g·L^{-1})	$E\times100$	V_{coa}	f_C
2	60.47	0.0933	165.30
4	74.11	0.1884	97.27
8	83.67	0.3745	54.96
12	92.23	0.5524	38.46

CONCLUSIONS

The cloud point extraction utilizing polyoxyethylene-10-lauryl ether and sodium sulfate as extractant and auxiliary agent is a simple and efficient method to preconcentrate Furosemide from aqueous solution.

Both settling and centrifuge method can achieve fully separation of the coacervate and aqueous phase. The extraction efficiencies of both methods are almost equal. Centrifugation accelerates the phase separation dramatically.

Decreasing the surfactant concentration and increasing the electrolyte concentration both enhance the preconcentration factor. Higher concentration of surfactant can result in higher extraction efficiency.

Acknowledgement

This work was supported by National Natural Science Foundation of China, Grant No. 29836130

[1] International Olympic Committee, Olympic movement anti-doping code, Prohibited classes of substances and prohibited methods, Appendix A [Z]. Lausanne: International Olympic Committee, 2001.

[2] F H Quina, W L Hinze (1999). *Ind. Eng. Chem. Res*,, **38**, 4150-4168

[3] H Watanabe, H Tanaka (1978). *Talanta,* **25**, 585-589.

[4] C Bordier. (1981) *J. Biol. Chem.,* **256**, 1604-1607.

[5] S R Sirimanne, J R Barr, D G Patterson, et al. (1996) *Anal. Chem.*, **68,** 1556-1560.

[6] S Miyagishi, K Okada, T Asakawa (2001), *J. Colloid Interface Sci.,* **238**, 91-95

[7] K. Materna, J. Szymanowski (2002), *J. Colloid Interface Sci.,* **255,** 195-201.

[8] H. Schott (1997), *J. Colloid Interface Sci.,* **189**, 117-122.



MICROEXTRATION WITH SOLVENT DROPLET TO ANALYZE CAMPHOR IN DILUTE AQUEOUS SOLUTION

Lin Quan, Luo Guang-sheng, Lu Yang-cheng, Dai You-yuan

Tsinghua University, Beijing, China

A fast analysis method for Camphor in dilute aqueous solution has been developed by combining liquid-liquid microextracton technique and gas chromatography. Camphor was extracted from 8mL aqueous samples into 1 μL butyl acetate for 6 min. An enrichment factor up to 70 was achieved in experiments. By using the method, the lowest quantitative analysis concentration was decreased from 0.02 μg/μL to 0.0005 μg/μL. The results prove that this technique has the characteristics of simple equipment, trace solvent cost, easy operability, time saving and high analysis sensitivity.

INTRODUCTION

In the last few years, efforts have been directed towards miniaturizing the liquid-liquid extraction in analysis procedure by reducing the phase ratio, leading to the development of liquid-liquid microextraction (LLME). Like solid phase microextraction (SPME), LLME is not exhaustive and only a small fraction of the analytes is extracted or pre-concentrated for analysis. The general requirements for LLME are the use of an organic solvent (extraction phase) immiscible with water (sample solution), and also analytes are more soluble in the extraction phase than in the sample solution. Jeannot and Cantwell introduced LLME in 1996 firstly, where a micro-drop (8μL) of organic solvent was left suspended at the end of a Teflon rod immersed in a stirred aqueous solution. As the use of Teflon rod was found to be inconvenient, Jeannot and Cantwell later suggested an alternative drop-based extraction technique. According to this revised protocol, microextraction was performed simply by suspending a 1μL drop directly from the tip of a microsyringe needle immersed in a stirred aqueous solution. After extracting for a prescribed period of time, the micro-drop was retracted back into the microsyringe needle and was transferred into the GC for further analysis. Compared to other LLME techniques, the technique is more simple and convenient. Recently, LLME has been applied in environmental analysis and drug analysis.

Camphor is a medical compound and exists in the leech of some herb with low concentration. This study applied single drop microextraction technique introduced by Jeannot and Cantwell combined with gas chromatography to establish the quantitative method of camphor in dilute aqueous solution.

EXPERIMENTAL DESCRIPTION

Camphor was of chemical grade. Chloride, hexane, benzene, butyl acetate, n-butanol

and aether were of analytical grade.

The microextraction apparatus is similar with the one in reference 2, as shown in Figure 1. A 10 mL volumetric flask of 43 mm height, 20 mm inner diameter with a rubber cap is clamped in a water-jackedted vessel and maintained at 25±0.05ºC with a circulating water bath. During an extraction, a 5-μL microsyringe (Model Agilent 5182-9623) is clamped above the flask such that the syringe needle passes through the rubber cap and the needle tip protrudes to a depth of about 5 mm below the surface of stirred 8.0 mL of aqueous sample solution in the flask. A 1 μL drop of the extraction solvent is suspended from the needle tip.

In the type of microsyringe employed here, the plunger is a wire that is inside the needle itself. The liquid in the syringe is contained entirely within the needle. This particular needle has a cone tip.

The Teflon-coated stirring bar of 16 mm length, 5 mm diameter is rotated at a constant rate by means of a magnetic stirrer and motor controller. The stirring controller is inverted, and a rotating magnet assembly from a conventional plate-type magnetic stirrer is mounted in the motor chunk and centered underneath the water-jacketed vessel containing the flask.

Gas chromatographic determination of the amount of camphor extracted into the organic drop was performed on a Model HP 6890 GC (Hewlett- Packard) using Model HP19091F-1127 capillary column（25.0 m×320 μm×0.52 μm）and flame ionization detector. Nitrogen was the carrier gas with a flow rate of 2 mL/min. The injection and detector temperature was 300 ºC, respectively. The GC temperature programm was as follows: initial temperature 100 ºC held for 2 min then an increase at 5 ºC/min to 110 ºC held for 3 min then an increase at 35 ºC/min to 220 ºC.

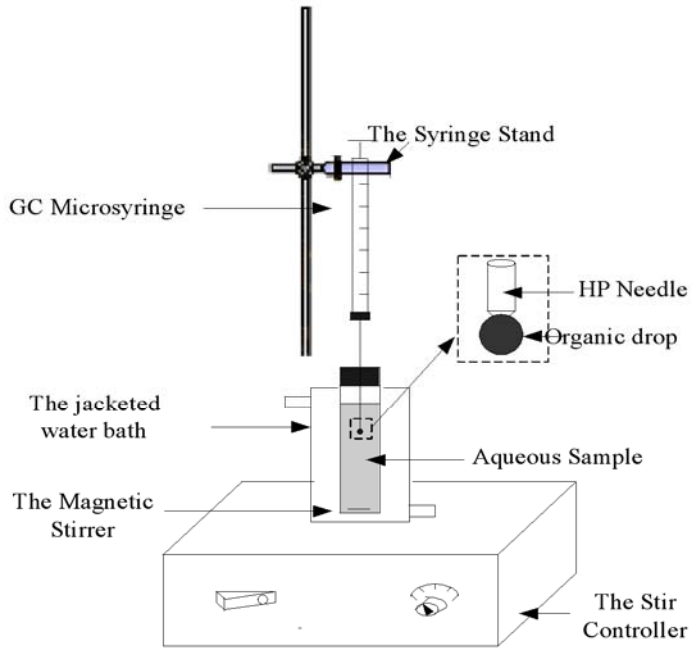


Figure 1. Diagram of Single Drop Microextraction unit

The aqueous phase in the flask was 8mL of one of the following aqueous sample solutions: either 5×10^{-4}, 1×10^{-3}, 2×10^{-3}, 4×10^{-3}, 6×10^{-3}, or 8×10^{-3} g/ L of

Camphor.

The extraction procedure, which follows, was always the same, though extractant, stirring rates, and stirring time were varied in the different studies. Before each extraction, the syringe was rinsed with ethanol and then extractant a total of 10 times to avoid analyte carry-over and air bubble formation. Finally, 1 μL of extractant was drawn into the syringe. The syringe was then clamped above the flask, and the clamped syringe was lowered so that the needle pierced the cap and penetrated into the aqueous solution. The syringe plunger was depressed completely so that the 1 μL of extractant was suspended as a drop at the needle tip, and then the mass transfer between this drop and sample began. Time zero in kinetics experiments was when the stirrer was turned on.

After stirring for the prescribed period of time, the plunger was withdrawn to 1 μL, while the needle was still immersed in the aqueous solution. The microsyringe was then removed from the clamp, and the needle was withdrawn from the flask. Finally, the solvent in the needle was injected into the gas chromatograph for analysis.

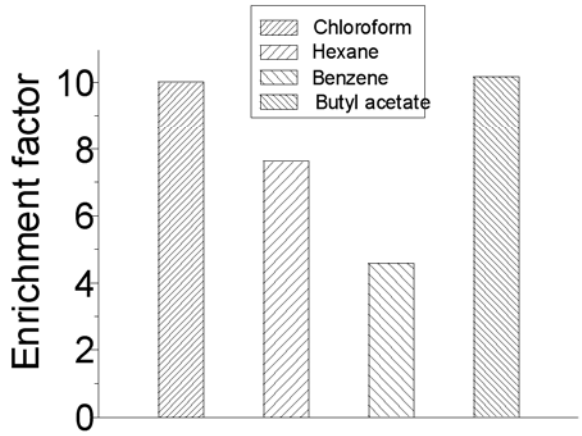
The analytical signal was taken as the area of the analyte peak. A calibration curve was prepared using standard solutions containing camphor in ethanol.

RESULTS AND DISCUSSION

The selection of extraction solvent is a prerequisite to achieveing the highest analytic enrichment factor as the properties related to solvent including analyte solubility and solvent volatility affect extraction efficiency. The enrichment factor E for a diluted sample and extraction solvent was calculated based on the equation

$E = C_o/C_{aq} = C_o V_{aq}/(V_{aq}C_{aq,initial} - V_o C_o)$

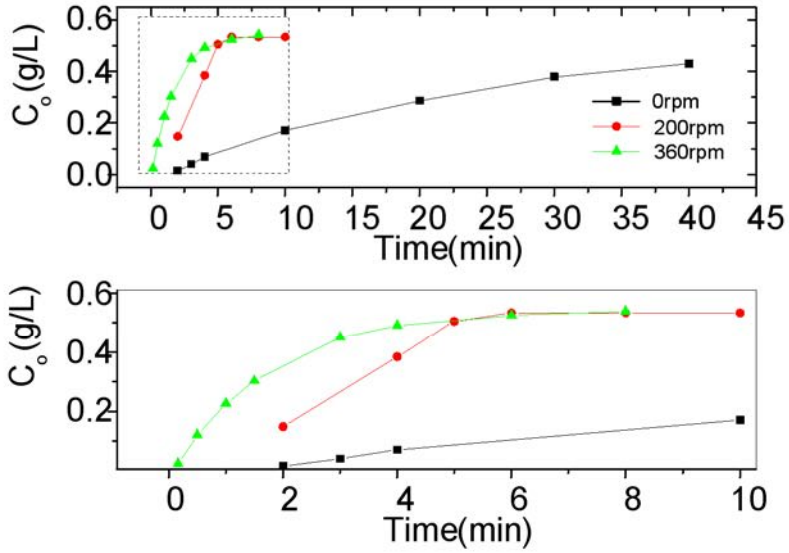
Four solvents were selected for study, according to decreasing polarity, i.e. butyl acetate, chloroform, benzene and n-hexane. Butyl acetate and chloroform gave higher enrichment factors (see Figure 2) for camphor. In contrast, benzene and n-hexane resulted in a relatively lower enrichment factors. Because Butyl acetate has lower toxicity and volatility than chloroform, therefore, butyl acetate was selected as the extraction solvent in following.



$C_{aq,initial}$=7.5 mg/L, V_{aq}=8 mL, V_o=1 μL, N=0 rpm, t=2 min

Figure 2. Comparison of enrichment factor using different organic solvents.

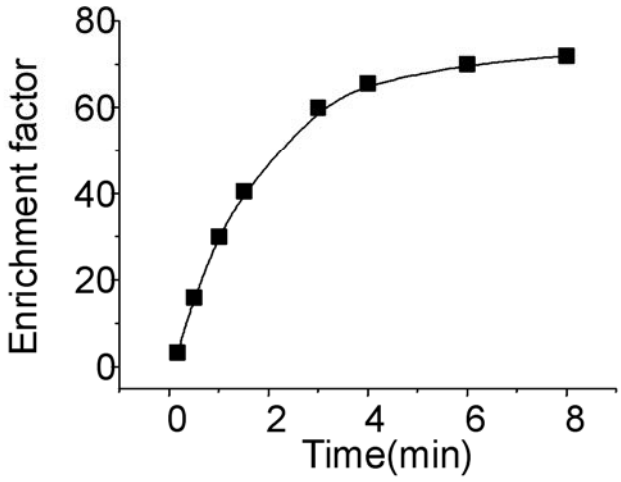
The single drop microextraction set-up was agitated with a magnetic stirrer to facilitate mass transfer of camphor from sample solution to the extraction solvent. Figure 3 shows the plots of camphor concentration in 1 µL butyl acetate versus extraction time at different stir speeds. A higher stirring rate increases the diffusion rate and reduces the time required to reach analyte equilibrium between the sample solution and extraction solvent. An agitation rate of 360rpm was selected for sample analysis since it resulted in the fastest extraction rate in experiments.



$C_{aq,initial}$=7.5 mg/L, V_{aq}=8 mL, V_o=1 µL

Figure 3. Concentration in organic phase vs. time at various stirring rate.

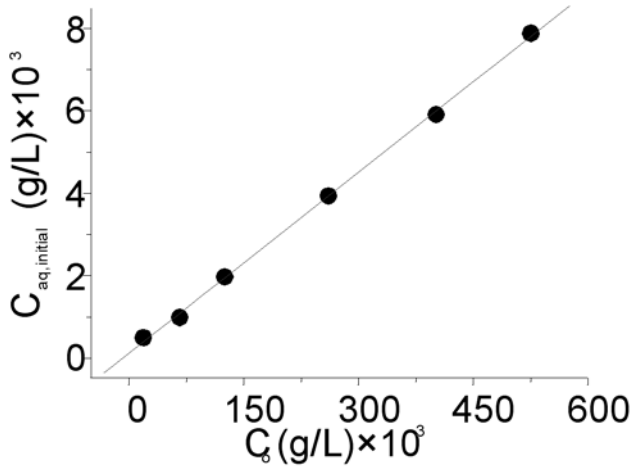
A typical extraction profile of the analyte between the sample and extraction solvent consisted of an initial rapid partitioning phase followed by a slower prolonged uptake, and then steady-state equilibrium. After reaching equilibrium, the amount of analyte extracted becomes a theoretical constant when plotted against extraction time. Figure 4 shows that higher enrichment factor were obtained with an increasing extraction time up to 6 min, after which equilibrium and the maximum enrichment factor of 70 value were achieved. So we selected 6 min as the optimum extraction time for sample analysis.



$C_{aq,initial}$=7.5 mg/L, V_{aq}=8 mL, V_o=1 µL, N=360 rpm

Fig. 4 Enrichment factor vs. time

A calibration curve was constructed using aqueous camphor solution at concentrations between 0.5 and 8 mg/L (see figure 5), which shows an excellent linearity (r=0.9996). As using single drop microextraction, the limits of determination for camphor was 0.5 mg/L. The relative standard deviation for sample with 7.5mg/L (three replicates) was 5.7%. These results demonstrated that single drop microextraction is highly effective for analyzing trace camphor in aqueous sample.



V_{aq}=8 mL, V_o=1 μL, N=360 rpm, t=6 min

Figure 5. Calibration curve of $C_{aq,intial}$ vs. C_o

CONCLUSION

A new method for quantifying a range of camphor in aqueous sample using an optimized single drop microextraction technique has been developed. The microextraction combined GC measurement conditions are 25°C temperature, 1 μL butyl acetate, 8 mL sample, 360 rpm stirring rate and 6 min extraction time. The technique has distinct advantages over conventional methods with respect to small volume of solvent required, low detection limits and high level of precision.

NOTATION

C_{aq}	Concentration of the analyte in the aqueous sample, g/L
C_o	Concentration of the analyte in the microdrop, g/L
$C_{aq,initial}$	Initial concentration of the analyte in the aqueous sample, g/L
E	Enrichment factor，$E=C_o/C_{aq}$
V_{aq}	Volume of the aqueous phase, L
V_o	Volume of the organic solvent phase, L

REFERENCES

1. Jeannot M A, Cantwell F F. Solvent Microextraction into a Single Drop[J]. *Analytical Chemistry*. 1996, **68**(3):2236-2240

2. Jeannot M A, Cantwell F F. Solvent Microextraction as a Speciation Tool: Determination of Free Progesterone in a Protein Solution [J]. *Analytical Chemistry*. 1997,**69**(15):2935-2940
3. Jager L S, Andrews A R J. Development of a rapid screening technique for organochlorine pesticides using solvent microextraction and fast gas chromatography [J]. *Analyst.* 2000,**125**:1943-1948

BACK-EXTRACTION OF CITRIC ACID BY DISPERSED SYSTEM ELECTRO-ELECTRODIALYSIS

Lu Yang-cheng, Yi Sha-sha and Luo Guang-sheng

Tsinghua University, Beijing, China

It is difficult to recovery organic acid from complex extractant by physical extraction. In the paper, dispersed system electro-electrodialysis was applied in back-extraction of citric acid from mixed solvent with trialkylamine and octanol. Factors that have influences on solute flux, recovery and specific energy consumption were studied, including phase ratio in dispersed system, composition of aqueous solution as receptor, and current density. Compared with back-extraction with hot water, dispersed system electro-electrodialysis is an energy-saving process producing much richer citric acid solution, which provides fundamentals for the application of complex extraction in water treatment and fermentation broth extraction.

INTRODUCTION

Solvent extraction is a widely used separation technology in the field of material purification, chemical production, pollution treatment, etc. Classified by separation mechanism, it includes physical extraction and chemical extraction. To polar organic compound in dilute aqueous solution, which is common for waste water, fermentation broth and fine chemical intermediates, complex extraction as chemical extraction exhibits highlighted advantage in special selectivity and high distribution ratio contrasting to physical extraction.

While, since there exists relative strong chemical interaction between solute and separating medium, it is difficult to recovery polar compounds like organic acid from complex extractant by physical extraction. Back-extraction by adjusting solvent composition or pH will bring sequential environmental and cost problems.

To the demand on extracting ionizable or polar compounds from organic solvent and preparing acidic or basic compounds with low solubility in water, electro-separation processes concerning with non-aqueous phase such as two phase electrophoresis and two phase electro-electrodialysis emerge recently. These processes presenting excellent separation effect and realizing simultaneous extraction and concentration are painful for exorbitant energy consuming and poor processing capability in common.

Wherefore, emulsion electro-electrodialysis with an emulsion as anolyte instead of bulk organic phase has been developed in our laboratory. It shows relatively low electro-osmosis, back diffusion, operating voltage and specific energy consuming in concentrating citric acid from aqueous solution.

In the paper, we present dispersed system electro-electrodialysis, which uses transient oil-water dispersion without surfactant as anolyte or catholyte, and expect to reach separation effect similar with emulsion electro-electrodialysis and avoid end-product pollution and

difficult phase separation in sequence.

EXPERIMENTAL DESCRIPTION

Reagent and instruments

Citric acid and sodium hydrate were purchased from Beijing Fine Chemical reagent Ltd. and n-octanol was bought from Tianjin Bodi Chemical Company Ltd. They were all of AR grade, and used without further purification. Trialkylamine (TAA) was kindly provided by Shuzhou Organic Solvent Company. IPE-AM-203 anion-exchange was purchased from Shanghai Qiulong Chemical Company, Ltd. The mono-sodium citrate aqueous solutions were prepared in our laboratory.

The experimental set-up and procedure

Figure 1 is a schematic diagram of the experimental setup. The electro-electrodialyzer was divided into two compartments by an anion-exchange membrane, the thickness of which was 5 mm each. The effective membrane area was 60 cm^2. Two electrodes connected to the electrophoresis apparatus were made of platinum. Two pumps were used for continuously delivering anolyte and catholyte into the electro-electrodialyzer with flow rate of 0.012 m^3h^{-1} respectively.

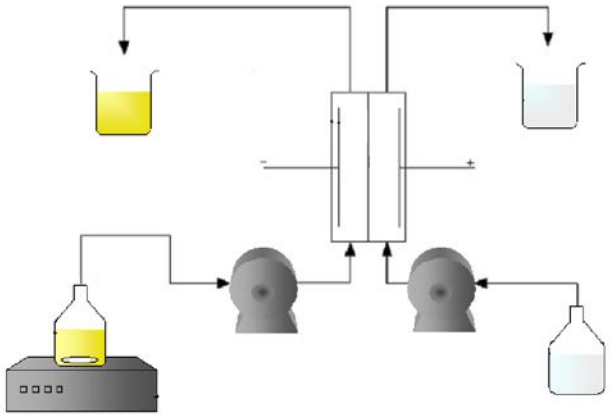


Figure 1. The setup of experimental apparatus

The extractant used in this work was 3:7 (v/v) mixing solvent of TAA and n-octanol. After extracting citric acid from a citric acid aqueous solution, the loading extractant was mixed with a mono-sodium citrate aqueous solution to form the dispersed system, which was used as catholyte and maintained stable by a magnetic stirrer.

When the steady state operation at different conditions reached, samples of the concentrated phase were collected and the citric acid concentration was analyzed by titration. Solute flux J, recovery E, concentration ratio R and specific energy consumption W_t are defined as follows.

$$J = \frac{C_{O1}v_{O1} - C_{I1}v_{I1}}{At}$$

$$E = \frac{(C_{O1}v_{O1} - C_{I1}v_{I1})\cdot(r+1)}{C_{I2}v_{I2}r}$$

$$R = \frac{C_{O1}}{C_{I1}}$$

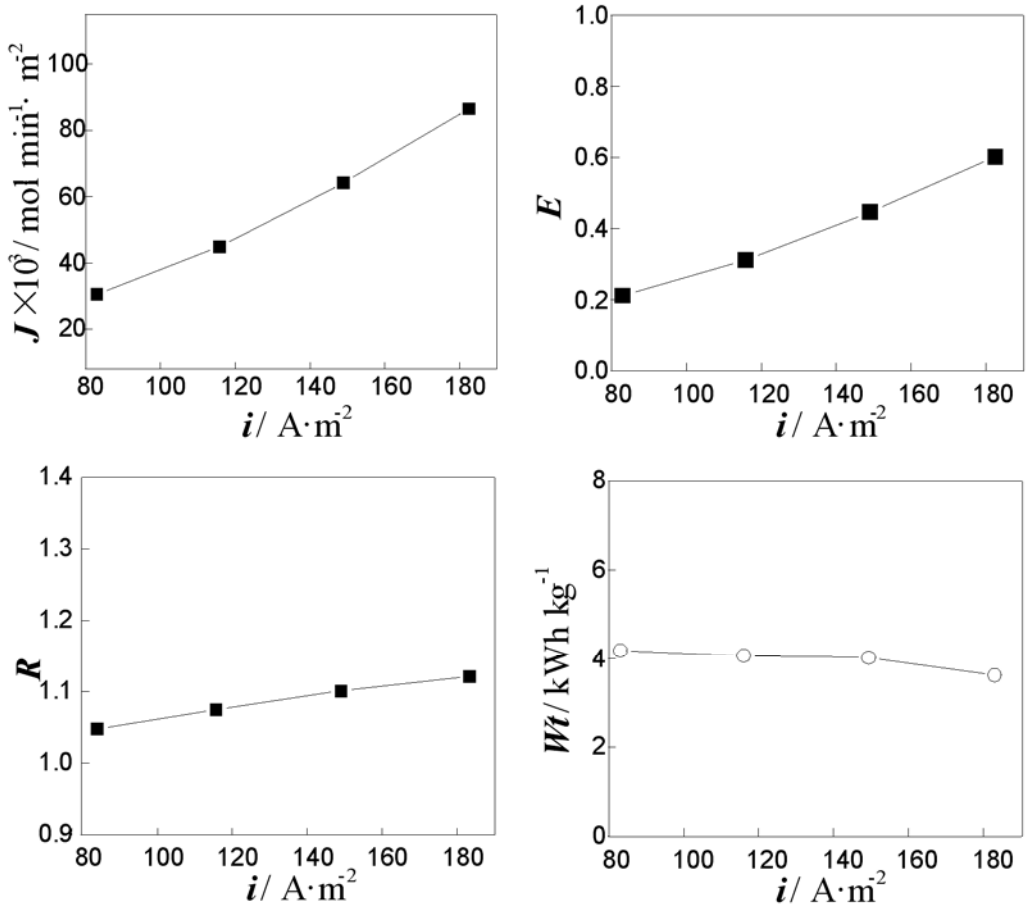
$$W_t = \frac{\int_0^t IUdt}{(C_{O1}v_{O1} - C_{I1}v_{I1}) \cdot M}$$

where t is time, r is phase ratio (v/v) in the disperse system, I is current, A is effective membrane area, U is average cell voltage, and M is molecular weight of citric acid. C_{O1} and C_{I1} are the citric acid molarity of anolyte at outlet and inlet respectively, C_{I2} is the citric acid molarity of the loading extractant at inlet. v_{O1} and v_{I1} are the volume flow rate of anolyte at inlet and outlet respectively, and v_{I2} is the volume flow rate of the concentrated phase at inlet.

RESULTS AND DISCUSSION

Influence of current density on back-extraction

Figure 2 shows the influence of current density on the solute flux, recovery, concentration ratio and specific energy consuming. An increase in current density resulted into the increasing of solute flux, concentration ratio and recovery. This result is similar to that in most of electro-electrodialysis process. As the current density reached 180 A·m^{-2}, the solute flux was over 0.92 kg·m^{-2}h, and the concentraction ratio approached to 1.10. These results showed that citric acid was not only back-extracted from the organic phase to the aqueous phase successfully, but also concentrated in this process.



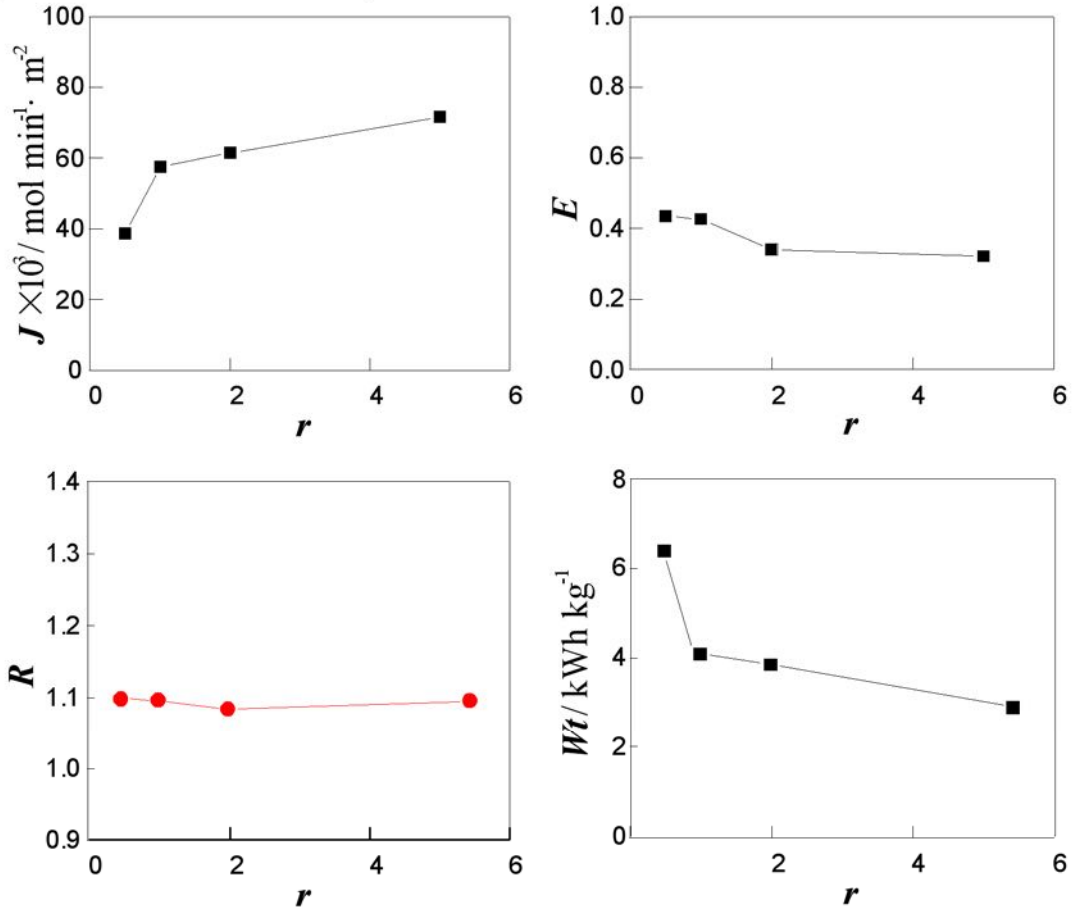
$c_W = 0.73\text{mol}\cdot\text{L}^{-1}$, $c_O = 0.56\ \text{mol}\cdot\text{L}^{-1}$, $c_S = 0.72\ \cdot\text{L}^{-1}$, $r=1$

Figure 2. Influence of current density on the separation process

Since the maximum current density and specific energy consuming in experiments is already close to common electro-electrodialysis process reported in literature, these two kinds of electro-electrodialysis technology probably have comparative capability. Based on the successful application of common electro-electrodialysis on related field, the specific energy consuming of this new technology is acceptable.

Influence of phase ratio on back-extraction

Figure 3 shows the influence of the phase ratio in dispersed system on solute flux, recovery, concentration ratio and specific energy consuming. It tells us that with the phase ratio increasing the solute flux is increased, but the recovery is decreased. Herein, the former is the embodiment of apparent current efficiency changing, and the latter is dependent on the total solutes flow in donor. In experiments, the cell voltage was decreased gradually with the phase ratio increasing, which means the dispersed system structure and its stability is an even more critical factor for electric conductivity. Affected synergistically by resistance and efficiency, the specific energy consuming is increased with phase ratio increasing. When phase ratio equalled to 5, W_t was 2.60 kWh·kg^{-1}, which is a low value even for common aqueous electro-elctrodialysis. In general, it is contribute to efficient separation to increase phase ratio and elongate resistance time to some extent. Different with other parameters, the changing of concentration ratio is little, because the citric acid concentration in receptor is too large for solute transfer in set-up.



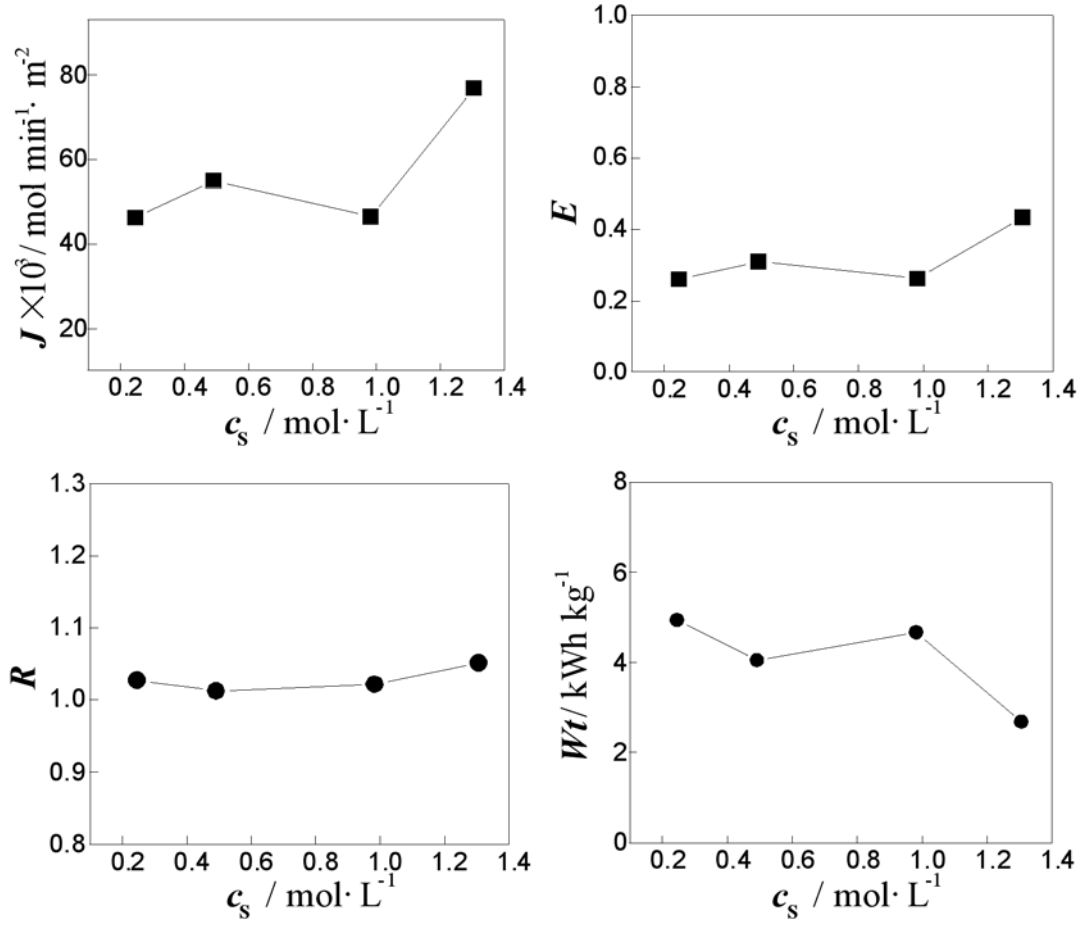
c_W = 0.6995mol·L^{-1}, c_O = 0.5258 mol·L^{-1}, c_S = 0.9822 mol·L^{-1}, i=150 A·m^{-2}

Figure 3. Influence of phase ratio on the separation process

Influence of salt concentration in dispersed system on back-extraction

Figure 4 shows the influence of the salt concentration in dispersed system on solute flux,

recovery, concentration ratio and specific energy consuming. It is seen that when the concentration of mono-sodium citrate in aqueous phase of catholye is less than 1.0 M, its change has no typical influence on all the parameters. While increasing c_S in further, solute flux jumps up for apparent current efficiency improvement related to species taking on current transport across ion exchange membrane. Accordingly, the recovery and concentration ratio increase, and the specific energy consuming cuts down.



c_W= 1.11mol/L, c_O= 0.51 mol/L, r=2, i=150 A/m^2

Figure 4. Influence of salt concentration on the separation process

Influence of citric acid concentration of receptor on back-extraction

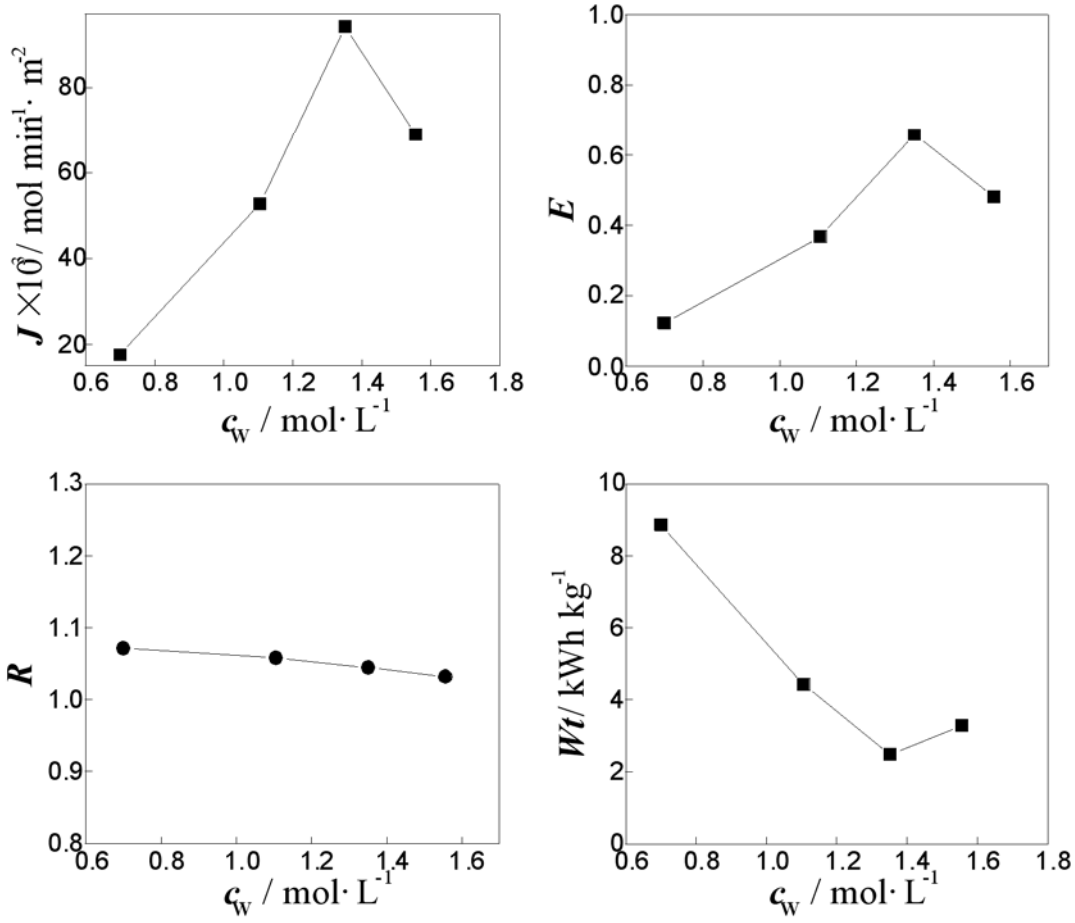
The initial concentration of receptor was another important influence factor in electrodialysis. As shown in Figure 5, there existed a maximum value for the solute flux, recovery when the c_W was changed. In experiments, the cell voltage was nearly kept constant. When the initial concentration was higher than 1.35 mol/L, the solute flux, the recovery began to decrease. The possible reason was the back diffusion to abate directional mass transfer. Just on the contrary, the specific energy consuming had a minimum value in the interval of c_W. Although the concentration ratio will decrease with the increasing of receptor concentration, considering to convenience and avoiding problems in enrichment, it is worth adjusting c_S to obtain citric acid aqueous solution with expected concentration directly.

CONCLUSION

Dispersed system electro-electrodialysis was successfully applied in back-extraction of citric

acid from mixed solvent with trialkylamine and octanol. A possible recovery ratio of 81.1% at suitable operation condition could be reached. The average cell voltage could be obviously decreased, and the energy consumption was limited and satisfying. And also our experimental results showed that the major factors to influence the performance of the process were the current density, phase ratio in dispersed system, the salt concentration in dispersed system, and the initial citric acid concentration in the concentrated solution. The increase in these experimental parameters resulted in an increase of the mass transfer flux. But when the initial citric acid concentration was larger than 1.35 mol/L, the mass flux decreased.

Compared with back-extraction with hot water, dispersed system electro-electrodialysis is an energy-saving process producing much richer citric acid solution, which provides fundamentals for the application of complex extraction in water treatment and fermentation broth extraction.



$c_O = 0.4163$ mol·L^{-1}, $c_S = 0.9822$ mol·L^{-1}, r=2, i=150 A/m^2

Figure 5. Influence of citric acid concentration in receptor on the separation process

REFERENCES

1. Filimena, A. P., K. Nikolovski and R. Tomovska, “Kinetics, Mechanism and Mathematical Modelling of Extraction of Citric Acid with Isodecanol/n-paraffinum Solution of Trioctyl Amine,” *Chem. Eng. Sci.*, **53** , 3227 (1998).
2. Siebold, M., P. V. Frieling, R. Joppien, D. Rindfleisch, K. Schugerl, and H. Ropper, “Comparison of the Production of Lactic Acid by Three Different Lactobacilli and Its Recovery by Extraction and Electrodialysis,” *Process Biochem.*, **30, 31** (1995).
3. Luo, G. S., J. G. Liu, Y. C. Lu, S. Pan and J. D. Wang, “Two-Phase Electro-Electrodialysis with an Emulsion as Anolyte,” *Sep. Sci. Technol.*, **39**, 1267 (2004).

Extraction and separation of caprolactam with microcapsules containing n-octanol

X.C. Gong, G.S. Luo*, W.W. Yang

(State Key Lab of Chemical Engineering, Department of Chemical Engineering, Tsinghua University, Beijing 100084, China)

Polysulfone (PSf) microcapsules (MCs) containing n-octanol were prepared with the phase inversion method, and the extraction process of caprolactam with the MCs was carried out. Their mean diameter was 1.86mm with narrow distribution. They have digital structure wall and compact surface. The extraction to caprolactam of the MCs is much higher than liquid-liquid extraction. After reused for 5 times, the loading capability gradually became unchanged. Using the temperature swing, the MCs can be regenerated very well. Caprolactam could be extracted using the MCs from its crude product effectively. The loading ratio reached 1422mg/g-dry-MC.

INTRODUCTION

Caprolactam is one of important industrial chemicals. It is mainly used to manufacture nylon 6 and resins. Nylon 6 is widely used in rag trade. Resins are widely used in carrying trade and food industry for their heat endurance and chemical stability. Because caprolactam polymers have many merits, the demand and price of caprolactam continue rising these years.

Several different processes can obtain caprolactam[1]. Though some new methods to produce caprolactam have been invented, conventional processes are still used in industry. The conventional methods like DSM/HPO method, BASF-NO reduction method, SNIA toluene method have some similar characteristics. The technological processes of these methods are complex, working operation and equipments used are excessive, the byproducts and waste are in large amounts. Subtractive process is

* Corresponding author, gsluo@tsinghua.edu.cn

the committed step to achieve high quality caprolactam. At most occasions, extracting caprolactam from its crude product and the following water stripping are the core of subtractive process. In industry, benzene and toluene are the most commonly used extractant. But benzene and toluene are not only carcinogenic chemicals, but also have low capability in extraction of caprolactam. The distribution coefficient of caprolactam between benzene and water is less than 0.3. The distribution coefficient of toluene is even smaller. Low distribution coefficient results in large phase ratio when extracting caprolactam in industry. It cause high energy cost in regenerating extractants. In fact, some other extractants, such as n-octanol or heptanol[2,3], have much higher capability when extracting caprolactam. The distribution coefficient can be more than 1. But when using them, it is easy to form an emulsion for higher concentration solution. So they can not be used in industry directly.

Microcapsules have very interesting characteristics, and the technology of microcapsulation has been used in various fields such as medicine, medical treatment, agriculture, foods, and the chemical industry. A lot of techniques for preparation of microcapsules containing various functional materials and their application have been reported. Recently, a new application of microcapsules in solvent extraction processes has generated considerable interest. There are several advantages compared to conventional liquid-liquid extraction, such as a large specific interfacial area, high selectivity, minimal use of organic solvents, and easy phase separation. However, the applications of extractant microcapsules are just begun. Most of the applications focus on the recovery of heavy metals. Kondo et al. [4], Nishihama et al. [5], Laguecir et al. [6], Saito et al [7], as well as Yang et al. [8] have applied the extractant microcapsules to extract metal ions from their dilute solutions. And their results prove that the microcapsules have high separation performance with good stability.

Few efforts on the recovery of caprolactam from its crude product with extractant microcapsules have been made. In this work, polysulfone microcapsules containing n-octanol were prepared by the phase inversion method. The separation performance of the microcapsules to caprolactam was determined, and the stability of the microcapsules was examined.

PREPARATION OF POLYSULFONE MICROCAPSULES

Materials and Chemicals

Polysulfone (PSf) with intrinsic viscosity of 0.59 was purchased from BoXiong Chemical Industry (China). Caprolactam (>99.9%) and crude caprolactam were kindly provided by Shijiazhauang Huaxianchang Chemical Plant. Ethanol, methanol, n-octanol, n,n-dimethylformamide (DMF), diphenyl ketone, hexane and other reagents were purchased from VAS Chemical Co., Ltd (China). All materials were used as received without any further purification.

Preparation of Microcapsules

Figure 1 is the experimental set-up for preparing PSf microcapsules. PSf solution was prepared by dissolving 1g polysulfone in 10ml DMF. Then 2ml n-octanol was added into the polymer solution under stirring condition. The mixed solution was dropped into a solidification solvent through a nozzle to form the PSf microcapsules in which n-octanol was enclosed. The solidification solvent was a mixture of 200ml ethanol and 500 ml water. The outside diameter of the nozzle was 0.4mm. The formed microcapsules were kept in the solidification solvent for more than 1h and then rinsed several times with deionized water. Then the microcapsules were conserved in deionized water before application.

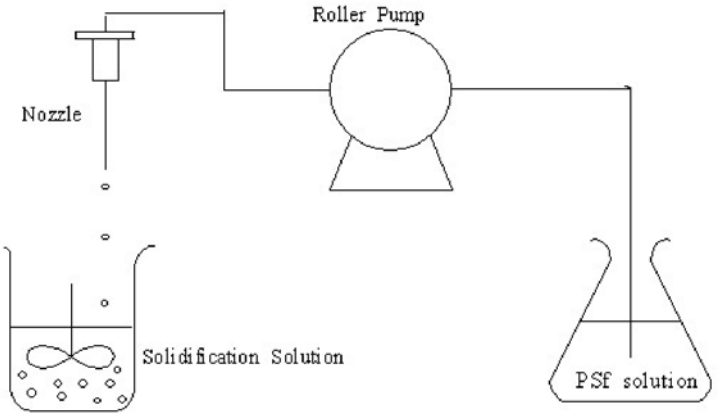


Figure 1 The experimental set-up

Characterization of Microcapsules

The diameter and its distribution of the microcapsules were measured by the imaging method. The extractant loading defined as grams of extractant per gram of dry PS was determined by a solvent extraction method as described below. Add 2g wet microcapsules to 50ml hexane with stirring for 24 hours. Then n-octanol concentration in hexane is measured with gas chromatography. Extraction performance of the microcapsules was determined by contacting them with caprolactam solutions. The amount of extracted solutes by the microcapsules was determined by measuring the solution concentrations with gas chromatography.

RESULTS AND DISCUSSIONS

Microcapsule diameter distribution and extractant loading

Figure 2 shows the MC size and its distribution. The mean diameter is around 1.86mm, and its distribution is narrow. So the microcapsules are suitable to be packed in a column. Table 1 describes the composition of the wet microcapsule.

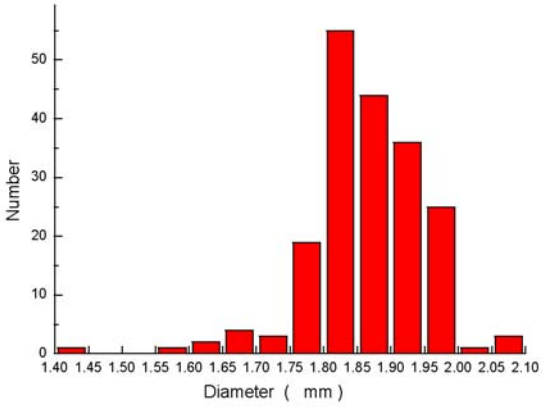
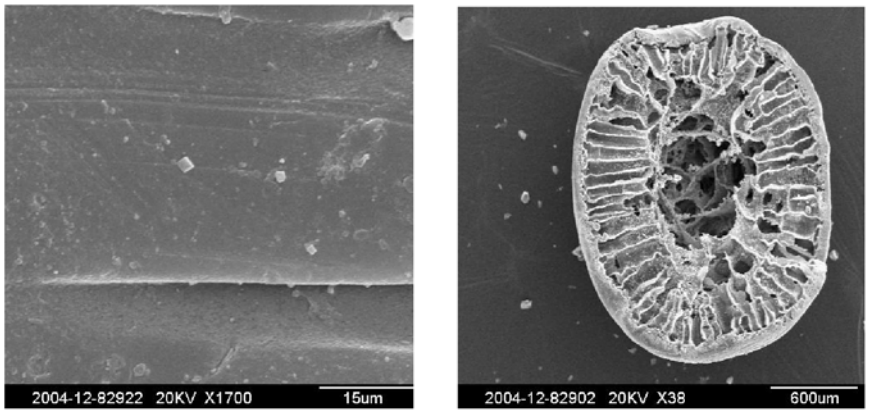


Figure 2 MC size and its distribution

Table 1 Composition of wet microcapsules

Water in wet microcapsule (wt%)	n-octanol loading (g/g PSf)
80.01%	0.811

Surface and Internal structures of microcapsules



(a) (b)

Figure 3 The surface and internal structures of microcapsules

The surface of microcapsules containing n-octanol is compact, as shown in Figure 3 (a). There is no apparent deficiency, but some drapes on the surface. The internal structures of the PSf microcapsules are in digital form, as shown in Figure 3 (b). These structures may help microcapsules to keep the extractant from losing.

Mass transfer characteristics of microcapsules

Extraction of caprolactam

In order to test the mass transfer performance of the microcapsules, 3.95g wet microcapsules was packed in a column. The dry weight of the microcapsules was 0.79g. The length of the column was 5.5cm and the internal diameter was 1.5cm. The flow rate was 2.25ml/min. Figure 4 shows the breakthrough curve for the caprolactam

solution of 0.492g/L.

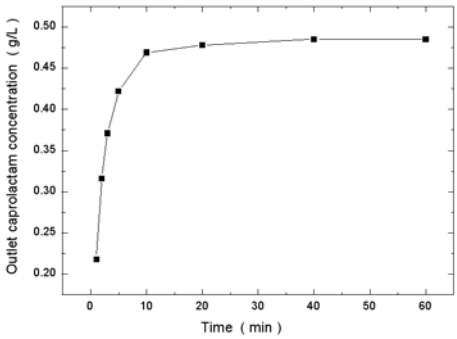


Figure 4 Extraction of caprolactam with n-octanol microcapsules

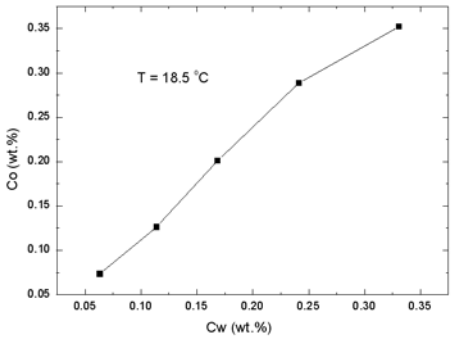


Figure 5 The distribution of caprolactam between water and n-octanol

It took about 10 minutes to reach the complete break-point. By integrating of the breakthrough curve, we found the packed microcapsules absorbed 3.33E-3 g caprolactam. In liquid-liquid extraction, at 18.5℃, the distribution coefficient is about 0.9, as shown in Figure 5. It indicates that the extractants' capacity is improved after encapsulation.

The stability of microcapsules

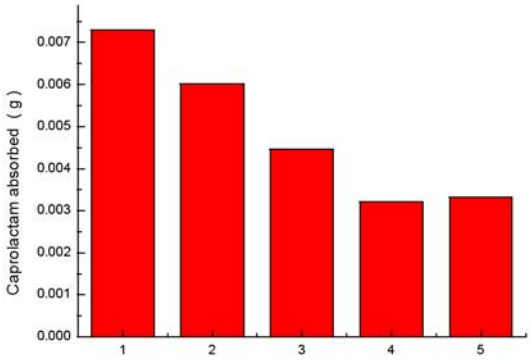


Figure 6 Extraction of caprolactam for 5 times

Extraction of caprolactam using microcapsules in the column mentioned above had been repeated for several times, and the results are shown in Figure 6. After extraction, microcapsules were regenerated by stripping them with 1L deionized water. After 4 times extraction, the microcapsules' capacity became changeless. It indicates parts of n-octanol will lose in preliminary several times.

Influence of temperature on extraction using microcapsules

3g wet microcapsules were put into 10ml 1.042 g/L caprolactam solution. Under different temperatures, caprolactam concentration in the aqueous phase at

equilibrium state was determined, and the results are shown in Figure 7. When the temperature is lower, the microcapsules can absorb more caprolactam. This temperature swing can help to regenerate the microcapsules.

Extracting caprolactam from crude product

3.43g wet microcapsules were contacted with 20ml crude caprolactam product at 20℃ for 1 hour. After being taken out, the microcapsules were rinsed with deionized water. Then microcapsules were put into 5ml deionized water for 2 hours. At 40℃ the concentration of the obtained caprolactam solution reached up to 213 g/L. The calculated loading ratio was 1422mg/g-dry-MC. The concentration is comparative to the striping caprolactam solution in industry process.

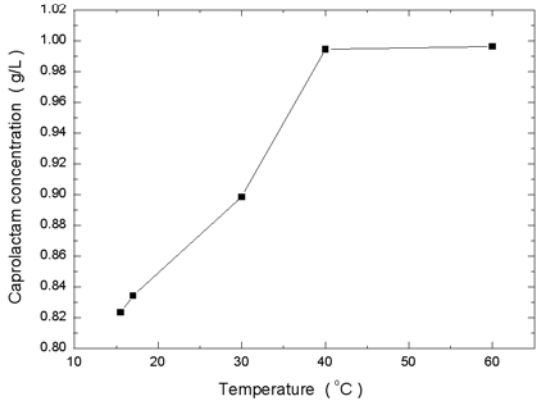


Figure 7 Influence of temperature to extraction

CONCLUSIONS

Polysulfone microcapsules containing n-octanol were prepared with the method of phase inversion successfully. Their mean diameter was 1.86mm with narrow distribution. They have digital structure wall and compact surface. The extraction to caprolactam of the MCs is much higher than liquid-liquid extraction. After reused for 5 times, the loading capability gradually became unchanged. Using the temperature swing, the MCs can be regenerated very well. Caprolactam can be extracted from its crude product effectively. The loading ratio can reach 1422mg/g-dry-MC.

Acknowledgment

We wish to acknowledge the support of the National Science Foundation of China (20176022) on this work gratefully.

REFERENCES

1. A. Romero, A. Santos and P. Yustos (2004), *Ind. Eng. Chem. Res.*, **43**, 1557-1560.
2. M. Wijtkamp, G. H. van Bochove, Th. W. de Loos and S. H. Niemann (1999), *Fluid Phase Equilibria*, **158-16**0, 939-947
3. G. H. van Bochove, G. J. P. Krooshof and Th. W. de Loos (2002), *Fluid Phase Equilibria*, **194-197**, 1029-1044
4. K. Kondo and E. Kamio (2002), *Desalination,* **144**, 249-254
5. S. Nishihama, N. Sakaguchi, T. Hirai and I. Komasawa (2002), *Hydrometallurgy*, **64**, 35–42
6. A. Laguecir, Y. Frere, L. Danicher and M. Burgard (2002), *European Polymer Journal*, **38**, 977–981
7. T. Saito and S. Torii (2002), *Separation Science and Technology*, **37**(1), 77-87
8. W. W. Yang, G. S. Luo, F. Y. Wu, F. Chen and X. C. Gong (2004), *Reactive and Functional Polymers*, **61**(1), 91-99



Adsorption of Chromium(VI) from Aqueous Solutions Using an Imidazole Functionalized Adsorbent, SOL-IPS

Park, H.J., Lee, J.S., Nam, K.H., Tavlarides, L.L.

Department of Chemical Engineering & Material Science
Syracuse University, Syracuse, NY 13244

Abstract

Chromium (VI) separation from aqueous solutions is investigated using an imidazole functionalized sol-gel adsorbent. Batch adsorption equilibrium studies show a decrease in chromium uptake capacity with increase in pH in the range 2 – 9, and the uptake capacity at pH 2.5 is found to be 2.92 mmol/g (152 mg/g). The kinetics study conducted in a batch reactor show a rapid rate of adsorption. The adsorbent shows a high selectivity towards Cr(VI) and negligible adsorption of Cd(II) and Zn(II). Stripping of the chromium-loaded column bed is achieved using 4 M HNO_3. Adsorption tested in a fixed bed column shows a sharp breakthrough curve. The adsorbent shows stability over multiple adsorption/desorption cycle operation, i.e., 95 % of the original capacity is retained after 11 cycles of operation. The imidazole functional adsorbent is demonstrated to be an effective sorbent material for the separation of chromium(VI) from aqueous solutions.

Introduction

The presence of hexavalent chromium in wastewater has received much attention in recent years. Chromium contamination is generated from various industries such as electroplating, pigment manufacture, leather tanning, metal finishing, etc. This metal ion has a significant impact on human health and the other organisms.[1] Chromium has two oxidation states in the aqueous system, Cr(III) and Cr(VI), and their mobility and toxicity are different. Cr(VI) is about 100 times more toxic than Cr(III).[2] The risk of

surface water contamination is greater than ground water contamination.[3] According to the United States Environmental Protection Agency (USEPA), the concentration of chromium in drinking water has been regulated with a maximum allowable level of 0.1 mg/L for total chromium.[4] This problem of chromium ions in the environment is made more prominent by the increased chromium discharge from industrial wastes. It is reported that the USEPA estimates that 97379 lb of chromium from surface water and 29 million lb from land is released[5]. The common concentrations of hexavalent chromium found in typical wastewaters are 50–100 mg/L[6].

The traditional means to separate Cr(VI) from wastewaters are chemical reduction, precipitation, evaporation, and ion exchange. Adsorption is an economically reasonable alternative. Various adsorbents studied for chromium removal from aqueous solutions include activated carbon[7], activated alumina[8], coated silica gel[9], treated sawdust[10], peat moss[11], and feldspar[12]. Accordingly, technologies have been reported for the removal of hexavalent chromium.

The present work is focused on the use of an imidazole functionalized sol-gel adsorbent (namely SOL-IPS[13]) as an alternative material for Cr(VI) removal from aqueous solutions.

Experimental Section

1. Materials, Reagents and Equipment

SOL-IPS is a sol-gel material composed of clusters of imidazole ligands on the pore surface and silica backbone. Details of the adsorbent synthesis are reported elsewhere [13]. A thermostatically controlled shaker bath (Precision Scientific model 50) is used in batch adsorption experiments. Analyses of total chromium concentration are measured with an atomic absorption spectrophotometer (Perkin-Elmer model 2380). Batch adsorption experiments are conducted in a temperature controlled shaker water bath. pH is measured using a Chemcadet pH meter. A 5000 mg/L Cr(VI) stock chromate solution is prepared from chromium (VI) oxide (Sigma Aldrich). All other chemicals used in this study are of reagent grade.

2. Characterization

The effect of solution pH on metal ion adsorption at 25℃ is investigated using 50 mg/L of chromium concentration at pH 2 – 9. A 0.1M acetate buffer is used. Equilibrium

uptake capacities of SOL-IPS are determined using 0.1g of adsorbent with 50 mL of Cr (VI) solution buffered by 0.1M acetate at various initial concentrations (50-1250 mg/L) and pH (2.5, 4.5, 6.0) at room temperature. The amount of adsorbed chromium ions is calculated by a mass balance between the initial and equilibrium concentrations. Kinetics experiments are carried out at constant equilibrium pH (4.5) with various initial metal ion concentrations (50, 200, 750 mg/L), each buffered by 0.1M acetate. Samples are withdrawn at determined intervals to plot C/C_0 versus time. Stripping experiments are carried out in a 0.7 cm ID column using three concentrations of nitric acid (1, 2, 4 M). Volumes of 100 mL of 750 mg/ L Cr (VI) solutions at pH 2.5 are passed through the column bed containing 0.2 g of adsorbent. The volume of stripping agents used is 50mL. A 5mL of DI water is used to wash column before and after stripping steps to ensure discharge of remaining metal ions. The column performance is carried out using an initial chromium concentration (50 mg/L) at a flow rate of 1mL/min through a 0.7 cm ID column packed with 0.5 g of adsorbent. Effluent concentrations are collected at volume intervals for analysis. The stability of the adsorbent is tested by repeated adsorption and desorption experiments (a total of 11 cycles) in a 0.7 cm ID column packed with 0.2 g of adsorbent. Volumes of 100 mL of 750 mg/L Cr (VI) solution at pH 2.5 are used to saturate the column. A 100 mL of 4 M nitric acid is selected as the stripping solution. A 5 mL volume of DI water is used to wash column before and after stripping steps to ensure discharge of remaining metal ions.

Results and Discussion

Equilibrium Studies

The dependency of solution pH on the adsorption of chromium(VI) using SOL-IPS is investigated. The anions of chromium are known to exist as the following forms depending on the pH of the aqueous solution.[14]

$$H_2CrO_4 \Leftrightarrow H^+ + HCrO_4^- \quad (\log K = -0.8) \qquad (1)$$

$$HCrO_4^- \Leftrightarrow H^+ + CrO_4^{2-} \quad (\log K = -6.5) \qquad (2)$$

$$2HCrO_4^- \Leftrightarrow Cr_2O_7^{2-} + H_2O \quad (\log K = 1.52) \qquad (3)$$

$$HCr_2O_7^- \Leftrightarrow H^+ + Cr_2O_7^{2-} \quad (\log K = 0.07) \qquad (4)$$

Chromate ion species in the aqueous solution evaluated using the chemical equilibrium modeling software MINEQL+ show that at pH < 6.5, $HCrO_4^-$ is predominant, whereas at pH > 6.5, CrO_4^{2-} is predominant. Figure 1 shows the removal of Cr(VI) with respect to

the equilibrium pH over the range of 2 – 9. The results show that chromium removal increases with decrease in pH values. The increase in the adsorption capacity at lower pH values is due to the availability of protonated imidazole sites for anionic species adsorption to take place. The following is a general adsorption mechanism describing the protonation of the imidazole site followed by the adsorption of a single charged chromate ion:

$$\overline{RN} + H^+ \leftrightarrow \overline{RNH^+} \quad (5)$$

$$M^- + \overline{RNH^+} \leftrightarrow \overline{RNH^+M^-} \quad (6)$$

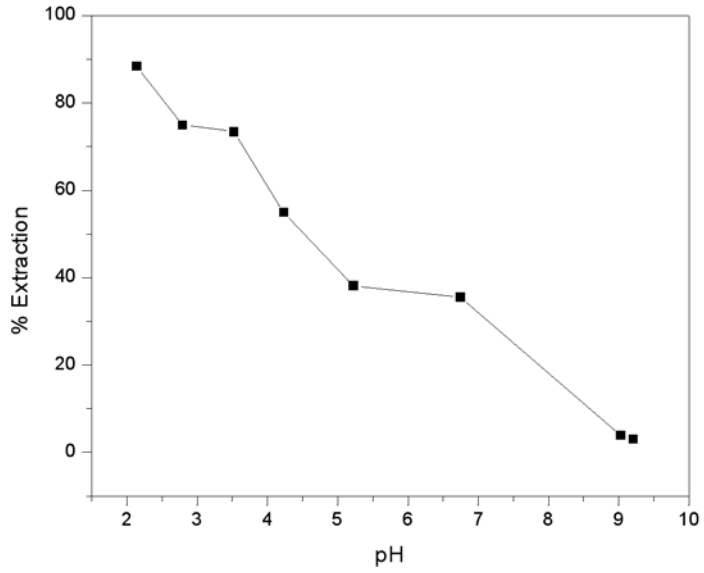


Figure 1. Effect of pH on the removal of Cr(VI): weight of SOL-IPS = 0.1 g; volume = 50 mL; contact time = 24 h; buffered by 0.1 M acetate.

Equilibrium adsorption isotherms conducted in batch at three pH values (2.5, 4.5, and 6) are shown in Figure 2. The maximum Cr(VI) adsorption capacity observed at pH 2.5 is found to be 152 mg/g, whereas that at pH 6 is found to be 94 mg/g. Based on the maximum capacity observed at pH 2.5 (2.92 mmol/g) and the ligand density of 3.0 mmol/g[13], it is expected that the chromium ions are adsorbed on a 1:1 mechanism.

Adsorption Kinetics

Three different initial concentrations of chromium (50, 200, 750 mg/L) of 250 mL at pH 4.5 are placed in contact in a batch mode with 0.5 g of the adsorbent. As shown in

Figure 3, equilibrium is reached within 30 minutes of contact time for the 50 mg/L solution. The rapid adsorption equilibrium is an indication that the surface of the SOL-IPS is readily available for adsorption. In addition, this may also be due to the large open pore channels accompanied by hydrophilic pore surfaces.

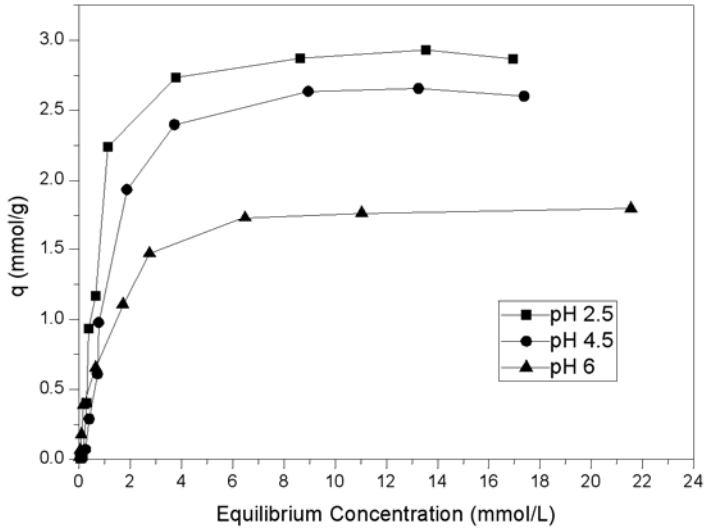


Figure 2. Adsorption equilibrium isotherm of Cr(VI) at pH 2.5, 4.5, 6: weight of SOL-IPS = 0.1 g; volume = 50 mL; contact time = 24 h; buffered by 0.1 M acetate

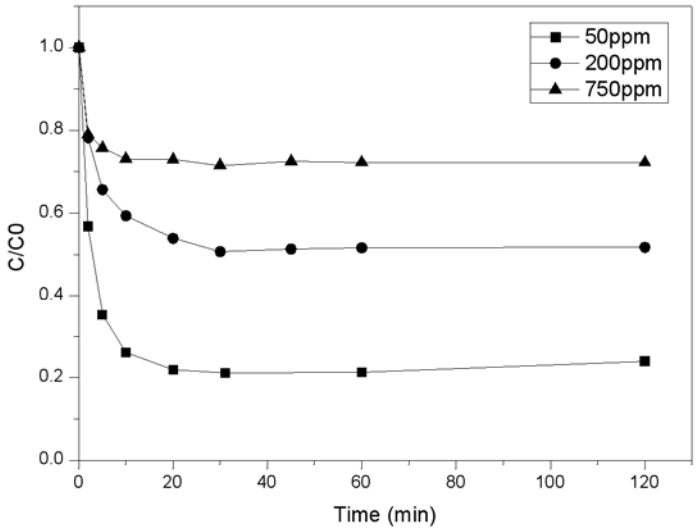


Figure 3. Adsorption kinetics of chromium on SOL-IPS for different chromium concentrations: weight of SOL-IPS = 0.5 g; volume = 250 mL; pH_i 4.5

Selectivity

The selectivity of SOL-IPS for different metals [Cr(VI), Cd(II), Fe(III), Zn(II)] is investigated and the results are presented in Table 1. Results show high selectivity of the adsorbent for Cr(VI) and negligible uptake of Zn(II) and Cd(II). These metal ions can be separated from chromium containing solution using adsorbents with thiol functionality, such as SOL-AD-IV[15, 16]. The adsorption of Fe(III) is approximately half of that of Cr(VI).

Table 1. Equimolar amount of each metal (0.0248 mmol) in 100 mL solution at pH 3.1

metal ion	% extraction	metal ion	% extraction
Cr(VI)	55.6	Cd(II)	0.0
Fe(III)	27.8	Zn(II)	0.11

Fixed Bed Adsorption

The breakthrough experiment is performed with a 0.7 cm ID column packed with 0.5 g of SOL-IPS to evaluate the performance of this adsorbent in a fixed bed column adsorption. This experiment is conducted using a chromium concentration of 50 mg/L, which falls within the concentration range of industrial wastewaters. As shown in Figure 4, the sharp effluent concentration of the breakthrough curve shows that the adsorption of chromate ions with imidazole is fast and that there exists minimal mass transfer resistance in the adsorbent pores. The effluent concentrations are observed to be below 0.1 mg/L up to 560 bed volumes before breakthrough that occurs at 1200 bed volumes.

Although, sodium hydroxide is typically used as the stripping agent in several chromium sorption studies[14, 17], in this work, due to the instability of the adsorbent at high pH conditions (> pH 10), acid solutions are used as stripping agents. Based on preliminary stripping studies, 4 M HNO_3 solutions are chosen as the stripping agent for chromium. The subsequent stripping of the loaded chromium using 4 M HNO_3 is shown in Figure 5. A stripping efficiency of 99.0 % is obtained at 121 bed volumes and 94.1 % at 30 bed volumes. The percent recovery from the total loaded amounts is 99.5 %.

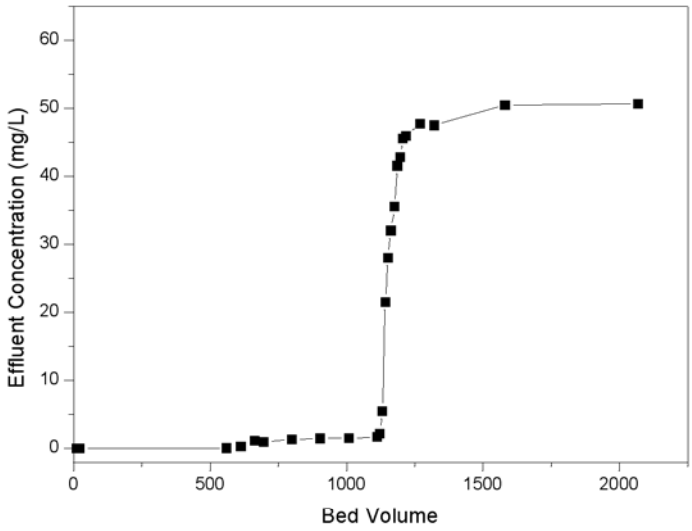


Figure 4. Breakthrough curve of chromium on a SOL-IPS bed: 1 bed volume = 0.9625 mL; $[Cr]_{feed}$ = 50 mg/L at pH 2.6; volume = 2000 mL; weight of SOL-IPS = 0.5 g; Q = 1.1 mL/min ; capacity = 102 mg/g

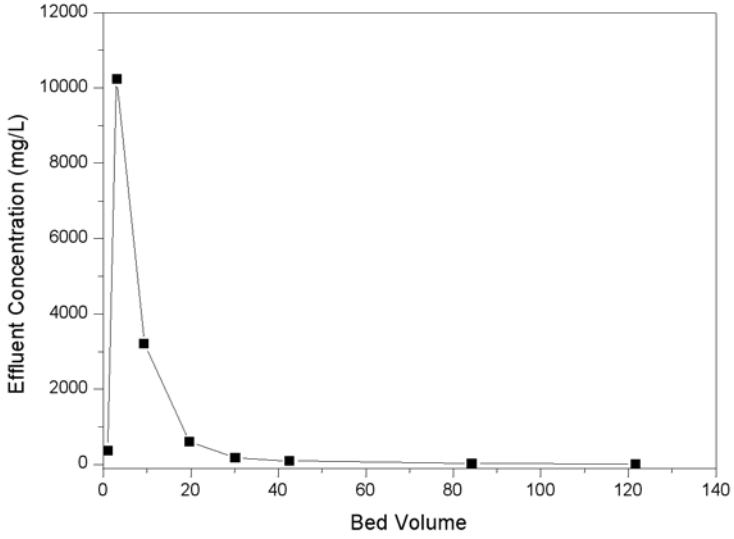


Figure 5. Stripping tests of chromium using 4 M HNO_3: weight of SOL-IPS = 0.5 g; 4 M HNO_3 250 mL; 1 bed volume = 0.9625 mL

Stability Test

The adsorbent stability for multiple adsorption/desorption operation is tested for 11 continuous cycles in a fixed bed scheme. The adsorbent retains 95% of the first chromium adsorption capacity throughout the test period, with stripping efficiencies greater than 90 % (Figure 6). This small fraction of the adsorbent that is not

regenerated is likely due to irreversible chromium binding through strong interaction and oxidation of the imidazole group. These results show stability of SOL-IPS in multi-cycle column operation.

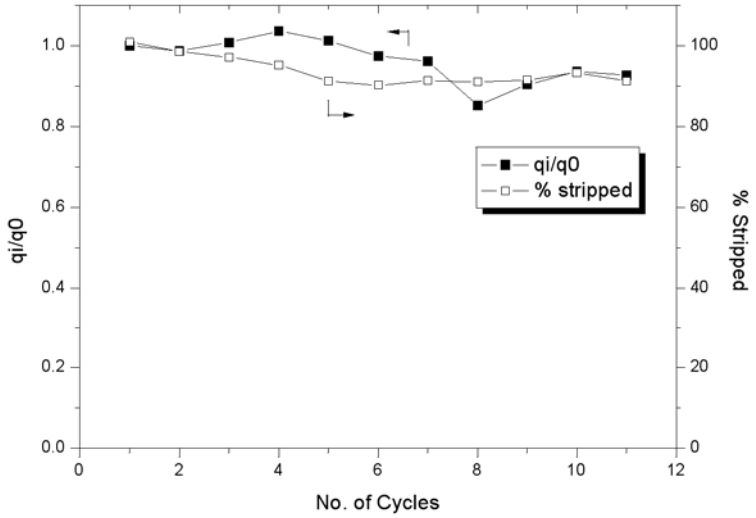


Figure 6. Stability test of SOL-IPS for multiple adsorption and desorption cycles; q_i is the chromium uptake capacity after the i^{th} cycle; q_0 is the chromium uptake capacity after the first cycle; loading with 100 mL of a 750 mg/L Cr(VI) solution at pH 2.5; stripping with 100 mL of 4 M HNO_3

Comparison to Other Adsorbents

Table 2. Comparison to other materials for Cr(VI) adsorption

Material	q (mg/g)	Equil time	pH	Support material	Ref.
SOL-IPS	**152**	**30 min**	**2**	**silica**	**This work**
sawdust	173	2 hr	3	Iron(III) complex	2
LDH	28	2 hr	6	Al, Zr, Zn, Mg	18
Aliquat 336	10	3 hr	5	SIR	19
Activated carbon	459	300 hr	2	Raw material	6

The chromium extraction performance of SOL-IPS is compared to other adsorbents, as shown in Table 2, by means of maximum adsorption capacity and equilibrium time. Among these materials found in the literature, the iron(III) complex of the carboxylated polyacrylamide-grafted sawdust and the activated carbon materials show high adsorption capacities of chromium. However, the time required to reach equilibrium is in the order of hours, whereas that for SOL-IPS is in the order of minutes. This implies that SOL-IPS shows relatively minimal mass transfer resistances and that more

feasible operating conditions can be employed in column adsorption schemes. These characteristics of SOL-IPS together with stability over multi-cycle operation make this adsorbent an attractive alternative for the separation of chromium from aqueous solutions.

Conclusions

Organo-ceramic adsorbents functionalized with imidazole, SOL-IPS, are characterized for chromium(VI) separation from aqueous streams. The adsorbent exhibits a high selectivity towards chromium and negligible adsorption of zinc and cadmium. A high capacity of 152 mg/g is observed at pH 2.5; however, the capacity decreases with increase in solution pH. Chromium separation is found viable using a fixed bed adsorption unit with stripping efficiencies greater than 99 % using 4 M HNO3. Moreover, stability over multiple adsorption/desorption cycles is demonstrated with 95 % of the first capacity retained after 11 cycles.

Acknowledgement

The financial support from the National Science Foundation through Grant CTS-0120204 is gratefully acknowledged.

References

1. Shubo Deng and Renbi Bai, *Water Research*, 2004, **38,** 2423-2431

2. Maya R. Unnithan and T. S. Anirudhan, *Ind. Eng. Chem. Res.,* 2001, **40,** 2693-2701

3. Lazaridis, N. K., Pandi, T. A., and Matis, K. A., *Ind. Eng. Chem. Res.*, 2004, **43**(9), 2209-2215

4. USEPA. *Office of Ground Water and Drinking Water*; EPA 815-R-03-003; EPA: Washington, DC, March 2003.

5. USEPA. *Office of Water*; EPA-815-D-02-006; EPA: Washington, DC, March 2002.

6. Li Chun, Chen Hongzhang, and Li Zuohu, *Process Biochemistry,* 2004, **39**, 541–545

7. Manuel Perez-Candela, Jose M. Martin-Martiez, and Rosa Torregrosa-Macia, *Water Res.,* 1995, **29**(9), 2174—2180

8. Narsi Ram Bishnoi, Mini Bajaj,Nivedita Sharma, and Asha Gupta, *Bioresource Technology*, 2004, **91**, 305-307

9. Dianchen Gang, Wenqing Hu, Shankha K. Banerji, and Thomas E. Clevenger, *Ind. Eng. Chem. Res.* 2001, **40**, 1200-1204

10. V.K.Garg, Renuka Gupta, Rakesh Kumar, and R.K.Gupta, *Bioresource Technology,* 2004**, 92**, 79-81

11. Sharma, D. C. and Froster, C. F., *Water Res.,* 1993, **27**, 1201-1208

12. Singh, D. B., Rupainwar, D. C., and Prasad, G., *J. Chem. Technol. Biotechnol.* 1992, **53,** 127-131.

13. J. S. Lee and L. L. Tavlarides., *Solvent Extr. And Ion Exch*., 2002, 20(3), 407-427

14. Arup K. Sengupta and Dennis Clifford, *Environ. Sci. Technol*., 1986, **20,** 149-155.

15. Nam, K. H., Gomez-Salazar, S., and Tavlarides, L. L., *Ind. Eng. Chem. Res.,* 2003**,** ***42***(9), 1955-1964.

16. Gomez-Salazar, S., Lee, J. S., Heydweiller, J. C., and Tavlarides, L. L., *Ind. Eng. Chem. Res.*, 2003, **42**(14), 3403-3412

17. Mark W. Heiniger and C. E. Meloan, *Solvent Extr. And Ion Exch*., 1992, 10(1), 159-171

18. N. N. Das, J. Konar, M. K. Mohanta, and S. C. Srivastava, *Journal of Colloid and Interface Science*, 2004, **270**(1), 1-8

19. N. Kabay, M. Arda, B. Saha, and M. Streat, *Reactive and Functional Polymers,* 2003,54(1-3),103-115

COUPLED PROCESS OF REACTION AND SOLVENT EXTRACTION

Xin Xu[1] and Tun Zhu[2]

[1]School of Environmental Science, University of East Anglia, United Kingdom

[2] Institute of Process Engineering, Chinese Academy of Sciences, Beijing, China

1 INTRODUCTION

For chemical reactions with small equilibrium constants, it is necessary to remove at least one of the products to another phase to ensure the reaction can be continual, as to evaporate products to a gas phase or to precipitate into a solid phase, which are usually do. To extract the products to a solvent----a liquid phase is another option.

In the industrial process of strontium carbonate from the solution of strontium nitrate or strontium chloride, strontium carbonate is obtained through adding carbonates (Na_2CO_3 or $(NH_4)_2CO_3$). The cost could be reduced as the carbonates are replaced by carbon dioxide (Zhu and Xu, 2000).

The chemical potential of H^+ in the organic phase is:

$$\mu_{\mathrm{H}}^{\mathrm{O}} = \mu_{\mathrm{H}}^{0(\mathrm{O})} + RT \ln C_H^O \gamma_H^O \tag{8}$$

Which is equal to that in the aqueous phase,

$$\mu_{\mathrm{H}}^{\mathrm{O}} = \mu_{\mathrm{H}}^{\mathrm{A}} \tag{9}$$

i.e.

$$\mu_{\mathrm{H}}^{0(\mathrm{O})} + RT \ln C_H^O \gamma_H^O = \mu_{\mathrm{H}}^{0(\mathrm{A})} + RT \ln C_H^A \gamma_H^A \tag{10}$$

Supported by Chinese National Nature Science Foundation (No. 50074028).

Where the superscript (^{O}) and (^{A}) denote the organic and aqueous phase, respectively, and subscript ($_{H}$) represents H^+.

The calculation shows that in order to allow the reaction to proceed, or say, to shift the following reaction equilibrium to the far right side to ensure a high productivity of strontium carbonate, it is necessary to keep $C_H^A \gamma_H^A$ lower than 3.3×10^{-6} (Xu, 2001; Xu, 2004).

Blumberg et al (Blumberg 1974) proposed a process to react carbon dioxide with sodium chloride solution to produce sodium bicarbonate by removing hydrochloride acid with solvent extraction and a tertiary amine was used as the extractant. Three phases (NaCl-NaOH aqueous solution--amine organic solution--gas CO_2) presented in this reaction system.

In present case, it is also possible to remove the produced acid by solvent extraction, as following equation:

$$SrCl_2 + CO_{2(g)} + 2B_{(o)} + H_2O = SrCO_{3(s)} + 2B \cdot HCl_{(o)} \quad (11)$$

or

$$Sr(NO_3)_2 + CO_{2(g)} + 2B_{(o)} + H_2O = SrCO_{3(S)} + 2B \cdot HNO_{3(o)(S)} \quad (12)$$

where B refers to a basic extractant.

In the above system, four phases (aqueous, organic, gas and solid-) are involved, and factors influencing the equilibrium are complicated. Various factors including diluents, concentration of the reactants, temperature and CO_2 pressure at equilibrium were examined, and a new flow sheet for the production of strontium carbonate from celestite is proposed.

2 EXPERIMENTAL

The reaction-extraction experiments were conducted in a conical flask or an autoclave of 100mL volume at room temperature. For flask experiments, 20mL of organic phase were mixed with 20mL of aqueous solution and meanwhile pure carbon dioxide or mixed gas of carbon dioxide and air were sparged into the system at atmosphere pressure. The flow rate of gases containing carbon dioxide was much higher than the reaction consumption, and the outlet gas was virtually

the same as the inlet, thus ensuring a constant gas composition and a constant carbon dioxide partial pressure in the reaction vessel. Samples were taken from the reaction vessel, and centrifuged to separate phases for determination.

For the high pressure experiments, the autoclave was first filled with carbon dioxide under a certain pressure before mixing the two phases.

The concentration of acid in aqueous solution was titrated with a calibrated sodium hydroxide solution, and that in the organic phase was titrated with a potassium hydroxide ethanol solution.

3 RESULTS AND DISCUSSIONS

3.1 Selection of amines

Alkyl amines, including primary, secondary and tertiary amines, are basic extractants. Their ability to extract strong mineral acids is dependent on their basicity and the steric hindrance of the alkyl groups. With the requirement that the extracted acid is to be recycled in the coupled process, it has to compromise the ability for extraction and stripping, in other words, not only the extractant should possess a strong extractive ability, but also the loaded acid should be readily stripped. As has been studied (Xu, 2001; Blumberg 1974), the tertiary amine with three mixed octyl group, N235 is chosen in this coupled process.

3.2 Influence of Diluents

When contacting the aqueous solution of a strong acid, for example, hydrochloric acid, basic tertiary amines (HR_3) is protonated to form ammonium cation (NR_3H^+), which then couple chloride anion to form ion pair extract ($NR_3H^+Cl^-$). $NR_3H^+Cl^-$ has a high polarity, and is strongly hydrated, therefore, polar solvents are expected to be better diluents for such extracts than nonpolar solvents. It was previously reported that acid extraction with tertiary amines usually increases with solubility coefficient of the hydrocarbon diluents (Frolov, 1966).

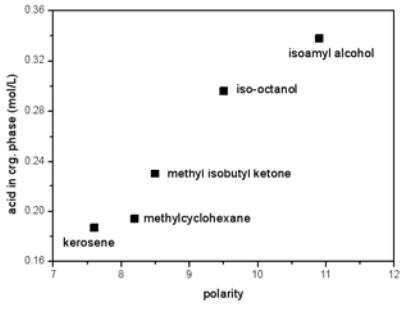


Fig.1 Polarity influence of diluents on HCl extraction with N235 in the reaction-extraction coupling system
N235: 0.487 mol/L; $SrCl_2$: 0.2 mol/L

The comparison of different solvents as diluents for the coupled reaction and solvent extraction of hydrochloric acid with tertiary amine N235 is shown in Figure 1. The concentration of hydrochloric acid in the equilibrium organic phase increased with the polarity of the diluents. Long chain alcohols were much better diluents than kerosene and methylcyclohexane. It is well known that long chain alcohols themselves are weak extractants for HCl, while the extractive ability of methyl isobutyl ketone (MIBK) is relatively stronger. However, as diluents, alcohols are superior to MIBK, due to their greater compatibility with the extract NR_3HCl. It is reported that the extraction ability for tri (2-ethylhexyl) amine could be increased with the addition of octanol to the organic phase (Eyal 1991).

The ammonium salt formed during the coupled precipitation and extraction process with a 0.487mol/L N235 and a 0.2mol/L $SrCl_2$ at a phase ratio of 1:1 in different alcohol diluents is shown in Table 1. It can be seen that iso-amyl alcohol is better than the others longer chains alcohols.

Table 1 Formation of ammonium chloride of the tertiary amine in different diluents

Diluents	$NR_3H^+Cl^-$ formation (%)
isoamyl alcohol	69.8
Isooctanol	60.7
Isododecanol	53.3

$NR_3H^+Cl^-$ formation = [$NR_3H^+Cl^-$] / [initial N235]

3.3 Effect of the concentration of N235

Figure 2 shows that increasing the concentration of N235 raised the acid concentration in the organic phase. It means that the extent of conversion of $SrCl_2$ to $SrCO_3$ increased with the concentration of N235. The conversion could be more than 95% in just one contact, when a 1 mol/L of N235 organic solution was used to extract HCl.

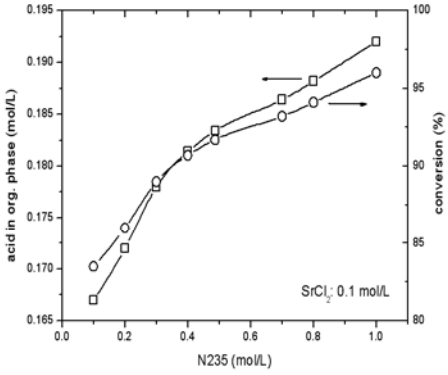


Fig. 2 Effect of the concentration of N235 on reaction－extraction coupled system

3.4 Effect of carbon dioxide pressure

3.4.1 High CO2 Pressure

0.2 mol/L N235 in iso-amyl alcohol and 0.2 mol/L $Sr(NO_3)_2$ were mixed together in an autoclave at a CO_2 pressure of 3.0×10^5 Pa and 5.6×10^5 Pa, respectively. The results in Figure 3 show that under high pressure the time required to achieve equilibrium was shortened a lot. The equilibrium pH of 5.8 was higher than that under normal atmosphere, which indicates that the coupled reaction at high pressure was more efficient.

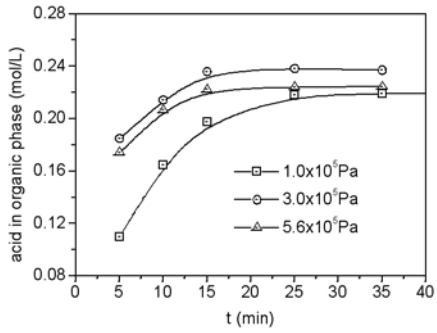


Fig. 3 Effect of pressure of carbon dioxide on kinetics of the reaction－extraction coupled process
N235: 0.2 mol / L; $Sr(NO_3)_2$: 0.2 mol / L

The equilibrium concentration of nitric acid of the mixture solution with initial 0.2 mol / L N235 and 0.2 mol / L strontium nitrate had been investigated under different CO_2 pressure up to 10×10^5 Pa.. The formation of strontium carbonate is linearly and gently increased, with the increasing of pressure of CO_2. At the pressure of 7.0×10^5 Pa, the formation of $SrCO_3$ is increased about 10% than that at the atmosphere pressure. The reason is that the solubility of carbon dioxide in aqueous phase increases with its pressure (Hodgman, 1971), which leads to the reaction forward and results in a higher formation of $SrCO_3$.

3.4.1 Low CO_2 Pressure

To research the possibility of using carbon dioxide from industrial process is not only more economical, but also important for reducing environmental pollution. Under the normal atmosphere, the influence of the partial pressure of CO_2 mixed with air has been examined to the coupled process. It can be seen from Figure 4 when the mole concentration of strontium nitrate was less than that of the extractant N235, as long as there was sufficient carbon dioxide in the system, no matter what pressure was, almost all the nitric ions could be transferred to the organic phase. It means that almost all the strontium nitrate can be precipitated into solid phase as strontium carbonate. While the concentration of strontium nitrate is more than that of the N235, the coupled reaction extent could not be complete as anticipated.

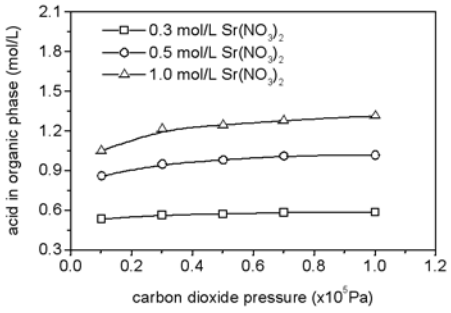


Fig.4 Effect of carbon dioxide partial pressure on reaction － extraction coupled process
N235: 1.4 mol / L

This results show that any industrial process carbon dioxide, even combustion exhaust gas, can be used as precipitant carbon dioxide to produce strontium carbonate.

3.5 A New Flow sheet for the Production of Strontium Carbonate

A well known manufacture method for strontium carbonate is double decomposition process. Following this manufacture, the reaction takes place between the fine celestite powder and sodium or ammonium carbonate solution at a temperature about 90℃. Because the higher thermodynamic stability and lower solubility of strontium carbonate than that of strontium sulfate, during the reaction, the latter transfers to the former, as shown by the equation below,

$$SrSO_4 + Na_2CO_3 = SrCO_3 + Na_2SO_4$$

The formed $SrCO_3$ is a mixed intergrowth with gangue minerals, but can be easily separated from the solid residue by dissolution with hydrochloric acid. After further purification of the strontium chloride solution, strontium carbonate is precipitated through the addition of sodium or ammonium carbonate. Higher consumption of hydrochloric acid and sodium carbonate makes the process uneconomic. Several improvements have been proposed in recent years (Xiong et al. 1988; Chen 1988; Xiong et al 1991), the energy cost is still a problem to these processes. The key to make the double decomposition process economically is to further reduce energy consumption during the recycling of acid and carbonate.

Based on the above coupled process, a new flowsheet has been proposed as shown in Figure 5. In this process, ammonium bicarbonate and ammonia are used to replace expensive sodium carbonate. With the recycling of nitric acid and carbon dioxide, their consumption is much less than that in the traditional process and carbonate consumption is reduced to a half. The coupled precipitation reaction and solvent extraction of acid is conducted at room temperature and the energy cost should be much lower than evaporation of ammonium carbonate.

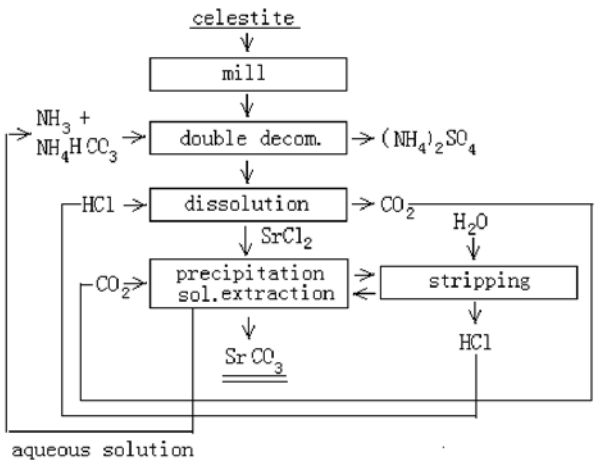


Fig. 4 Process with coupled solvent extraction of acid and precipitation of strontium carbonate

4 CONCLUSIONS

Precipitation of strontium carbonate from neutral solution of strontium chloride or nitrate with carbon dioxide could be done by coupling the reaction with solvent extraction of hydrochloric acid or nitric acid with a tertiary amine. The higher pressure of carbon dioxide benefits the reaction equilibrium, and shortens the reaction time. When there was enough tertial amine N235 and CO_2 in the system, all Sr^{2+} could be transferred to $SrCO_3$ and fulfilled the coupling process, even if the partial pressure of CO_2 was very low. A new flow sheet for production of strontium carbonate has been suggested, with which the consumption of raw materials and energy are much less than the current process.

REFERENCES

1. Blumberg R., Gai J. E. and Hajdu, K., 1974. Interesting Aspects in the Development of a Novel Solvent Extraction Process for Producing Sodium Bicarbonate. *ISEC*. 2789
2. Chen Rongguo and Li Desheng (Chongqing Institute of Chemical Technology), 1988. A Method of Preparation of Strontium Carbonate with no Chloride and Sodium from Celestite. *China Patent* CN 88 106794
3. Eyal A. M., Hazan B., Bloch R., 1991. Recovery and Concentration of Strong Acids from Dilute Solutions through LLX. II. Reversible Extraction with Branched-chain Amines. *Solvent Ex. Ion Exch.*, **9**(2): 2119
4. Frolov Yu. G., et al., 1966. Extraction of Mineral Acids by aliphatic Amines. *Tr. Mhti. Mendeleev*, **51**, 116
5. Hodgman D. Charles, et al. *Handbook of Chemistry and Physics*. 44th edition. Ohio: the Chemical Rubber Publishing Company, 1961
6. Xiong Shangbin and Ling Lu (Tianjin Institute of Chemical Technology), 1988. A Preparation Method of Strontium Carbonate *China Patent* CN 88 108923
7. Xiong Shangbin and Ling Lu (Tianjin Institute of Chemical Technology), 1991 A Preparation Method of Strontium Carbonate. *China Patent* CN 91 102557
8. Xu X. 2001. Separation of Akaline-Earth Metal Ions and the Coupled Four-Phase Process for the Production of Strontium Carbonate. PhD thesis. Institute of Process Engineering, Chinese Academy of Sciences.
9. Xu X. and Zhu T. 2004. Coupled Process of Reaction and Solvent Extraction I. The Reaction Between CO_2 and $SrCl_2$ Coupled With Solvent Extraction of HCl. *Hydrometallurgy* (in press).
10 Zhu T. and Xu X. (Institute of Process Engineering, Chinese Academy of Sciences), 2000. Direct Precipitation of Strontium Carbonate or Barium from Neutral Solutions Containing Strontium or Barium with Carbon Dioxide. *Chinese Patent Appl.* No. 00124604.6.